11th ICARD
IMWA 2018
Annual
Conference
South Africa

INAP | IMWA | MWD

11th ICARD | IMWA | MWD

Volume I

Christian Wolkersdorfer | Lotta Sartz
Anne Weber | Jo Burgess | Gilles Tremblay

RISK TO OPPORTUNITY

Volume 1

in memoriam ____

Paul Younger
Philip Hobbs
Peter Gunther

RISK TO OPPORTUNITY
Volume 1

Proceedings of the
11th ICARD | IMWA | MWD Conference –
"Risk to Opportunity"

10 – 14 September 2018

Pretoria, South Africa

Editors
Christian Wolkersdorfer
Lotta Sartz
Anne Weber
Jo Burgess
Gilles Tremblay

11th International Conference on Acid Rock Drainage (2018: Pretoria, South Africa)
International Mine Water Association
WISA Mine Water Division

Risk to Opportunity
2018, Pretoria, South Africa
Tshwane University of Technology (TUT)

ISBN 978-0-620-80650-3 (2 Volumes)

Editors
Christian Wolkersdorfer, Lotta Sartz, Anne Weber, Jo Burgess, Gilles Tremblay

Cover Design
Karoline Wolkersdorfer, Christian Wolkersdorfer

Layout and Typesetting
Jigsaw Graphic Design

Cover Photograph
Christian Wolkersdorfer – Mine Water discharging from an abandoned mine shaft (18 Wince) in the Westrand.

Papers with the ◎ sign have been peer reviewed. All abstracts were initially reviewed by 2 – 3 experts of the International Scientific Committee.

Printed in South Africa on certified paper

www.INAP.com.au
www.IMWA.info
www.WISA-MWD.org

Organizers

International Network of Acid Prevention

International Mine Water Association

WISA Mine Water Division

11th ICARD
IMWA 2018
Annual
Conference
South Africa

International Scientific Committee (ISC)

Teresa Albuquerque, Portugal
Bert Allard, Sweden
John George Annandale, South Africa
Margarida Horta Antunes, Portugal
Mona Arnold, Finland
Thitiphan Assawincharoenkij, Thailand
Tim Aubel, Germany
Mattias Bäckström, Sweden
Jeff Bain, Canada
M Dolores Basallote, Spain
Melanie Lise Blanchette, Australia
Rob Bowell, United Kingdom
Charlotte Barbara Braungardt, United Kingdom
Jo Burgess, South Africa
Juan Cepriá, Spain
Hana Kirsten Christenson, New Zealand
Henk Coetzee, South Africa
Jacob Grant Croall, United States
Gareth Digges La Touche, United Kingdom
Enrico Dinelli, Italy
Kajetan d'Obyrn, Poland
Catherine Joanna Edward, South Africa
Scott Effner, United States
Nils Eriksson, Sweden
Nuria Fernandez Castro, Brazil
Linda Ann Figueroa, United States
Michael Moore Gabora, United States
Marwan Ghanem, Palestinian Territories
Cleber Jose Baldoni Gomes, Brazil
Bashan Govender, South Africa
Ros Green, Australia
Antti Häkkinen, Finland
Robert S Hedin, United States
Kari Heiskanen, Finland
Amy L Hudson, United States
Andrew Kinnon Hughes, United Kingdom
Andrei Ivanets, Belarus
Ryan Thomas Jakubowski, United States
Ewa Janson, Poland
Tommi Johansson, Finland
Andrew Clifford Johnstone, South Africa
Margarete Maria Kalin, Switzerland
Päivi M. Kauppila, Finland
Anu Kettunen, Finland
Muhammad Kamran Khalid, Finland
Elena Khayrulina, Russia
Duk-min Kim, South Korea
Robert Lawrence Kleinmann, United States
Frans Knops, Netherlands
Ulla Lassi, Finland
Tim Lilley, United Kingdom
Zaibin Liu, China
Jorge Loredo, Spain
Simon Antony Lorentz, South Africa
Paul Joel Lourens, South Africa
Mark Lund, Australia
Maria Mamelkina, Finland
Malibongwe Shadrach Manono, South Africa
Thirumurugan Marimuthu, India
Vhahangwele Masindi, South Africa
Matthew P. McGann, Peru
Thomas Metschies, Germany
Philip Graeme Morgan, United Kingdom
Jacek Motyka, Poland
Ritva Muhlbauer, South Africa
Victor A. Munoz Saavedra, Canada
Kevin Myers, United States
John William Neale, South Africa
Carmen Mihaela Neculita, Canada
Michael Paul, Germany
Steven Richard Pearce, United Kingdom
Daniele Pedretti, Finland
Jaakko Olavi Pellinen, Finland
Nadine Piatak, United States
James Pope, New Zealand
Ana Claudia Queiroz Ladeira, Brazil
Marja-Liisa Räisänen, Finland
Naďa Rapantova, Czech Republic
Carlos Ruiz Cánovas, Spain
Liudmila Rybnikova, Russia
Lotta Sartz, Sweden
Christopher James Satterley, United Kingdom
Ralph Schöpke, Germany
Martin Schultze, Germany
Robert R Seal, United States
Maria Sinche-Gonzalez, Finland
Alison Sinclair, Australia
Sarah Jane Wolfe Skinner, South Africa
Mariette Smart, South Africa
Frank Stapelfeldt, Brazil
Wanghua Sui, China
Piia Katariina Suvio, Canada

International Scientific Committee (ISC) continued

Jouni Torssonen, Finland
Gilles Tremblay, Canada
Sari Annikki Tuomikoski, Finland
Wilfried Uhlmann, Germany
Robert Paul van Hille, South Africa
Danie Vermeulen, South Africa
Ian Watson, United Kingdom
Anne Weber, Germany
Walter Weinig, United States
Helena Wessman-Jääskeläinen, Finland
Roderick David Williams, United States
Christian Wolkersdorfer, Finland
Peter Woods, Austria
Zhenguo Xing, China
Jorge Zafra, Peru

Local Organizing Committee (LOC)

Champion
Richard Garner

Co-Chairs

Christian Wolkersdorfer	*IMWA President*
Gilles Tremblay	*INAP Technical Director*
Jo Burgess	*Water Research Commission*

Members

Henk Coetzee	*Council of Geoscience*
Lester Goldman	*Water Institute of Southern Africa*
Bashan Govender	*Department of Water and Sanitation*
Philip Hobbs†	*CSIR*
Stephinah Mudau	*Chamber of Mines*
Blanché Postma	*Clean Stream Environmental Consultants*
Lotta Sartz	*IMWA General Secretary*
Jaco Seaman	*Water Institute of Southern Africa*
Chris Swartz	*Chris Swartz Water Utilisation Engineers*
John Waterhouse	*IMWA Past President*

Administration

Zicki Joubert	*Tshwane University of Technology (TUT)*
Danielle Henn	*Conference Consultancy South Africa (Pty) Ltd*

11th ICARD | IMWA | WISA MWD 2018
Sponsors and Partners

AngloAmerican

GCS
Water & Environmental
Consultants

GEOSLOPE

INAP

SMI
Sustainable
Minerals
Institute

ITASCA
Africa (Pty) Ltd.

srk

aqualytic
laboratory & environmental

Klohn Crippen Berger

Sovereign
Water Sealing Specialists
www.sovereignhydro.com

3SMEDIA

WATER
RESEARCH
COMMISSION

South Africa
Inspiring new ways

Tshwane University
of Technology
We empower people

Welcome to South Africa!

We, the organisers and the champion of the 11th ICARD, IMWA, INAP and WISA welcome you with a warm Sawubona to Pretoria, South Africa. This is the first ICARD held in South Africa, IMWA returns for a third time and, for the Mine Water Division it is the homeland of WISA's Mine Water Division. We are proud to combine our efforts: instead of having three different conferences in one year, we can offer delegates one mine water conference of the highest calibre, with nearly 350 experts from all around the word.

As you will see from browsing through the programme, the majority of the papers will deal with mitigation, remediation, and responsible mine water management. This falls beautifully within the chosen theme of our conference, which is "Risk to Opportunity". What does that mean? It means that we need to see the risks that are involved in managing or mitigating mine water, and specifically that acid rock/mine drainage must be considered an opportunity. It is an opportunity to learn from each other and to plan for the future. This, exactly, is what this year's conference aims to be: a platform for exchanging ideas and experience from mining operations to remediation of abandoned mine sites in various climatic and cultural conditions.

When in South Africa, one must not forget to speak about transformation. The papers presented by our colleagues clearly show that transformation is an integral part of the work that our community is doing. A lot of students and young professionals are coming from previously disadvantaged communities to present their work, resulting in an increase the number of well-educated local students. Gender equality is another goal, and the fact that nearly one third of the registered delegates are female clearly shows progress to encourage young female students to join the mining environmental community.

Mining is seen as environmentally and ecologically unfriendly. This is primarily caused by examples of unethical mining and the past negative track record of the mining industry. Yet the situation has changed globally with most mining companies now seeing themselves as responsible for the sustainable use of earth resources. Though mining *per sé* cannot be sustainable, the entire production process from exploration to exploitation to closure can be. This combined conference shall therefore be the first "Green" Conference in ICARD's history. This means that carbon offsetting will be achieved by planting an adequate number of trees to compensate for the conference's carbon footprint. In addition, similar to the IMWA 2010 in Sydney, Nova Scotia, Canada, the conference shall avoid plastic containers wherever possible, and the amount of garbage produced shall be kept to the unavoidable minimum. Each item produced and used during the conference shall be from a "Green" perspective. Please help us to keep this conference as green as possible by avoiding waste wherever possible and use the glass bottles provided to get your water from the dispensers.

We hope that you will have a successful conference and we are looking forward to seeing you over the next several days.

Richard Garner, Jo Burgess, Gilles Tremblay, Christian Wolkersdorfer

Contents

Volume 1 Topics 1-8

1 Mining for Closure

2 Water Treatment Processes in Perspective

3 Produced Water

4 Saline and Neutral Mine Water

5 Electrochemical Treatment Options

6 Acceptability of Processed Mine Water

7 Prediction

8 Mitigation

Volume 2 Topics 9-17

9 Geochemistry Hidrogeology

10 Catchment Management

11 Economics of Mine Water

12 Mine Water By Products

13 Best Practice Guidelines

14 Piloting of the Waste Discharge Systems

15 Funding Models for Mine Water

16 Mine Water Hydraulics

17 New Technologies

Lagniappe

1

MINING FOR CLOSURE

Bespoke field columns to assess hexavalent chromium risk for refinement of mine closure plans

Julia Dent[1], Martin Williams[2], Bakary Draba[3]

[1]Senior consultant, WSP UK Ltd., 2 Queen St., Manchester, M2 5JB, UK, Julia.dent@wsp.com
[2]VP for Europe/Africa / Group Chief Geochemist, Piteau Associates, 25 Rudd Rd, Illovo, Johannesburg, Gauteng, South Africa, 2196
[3]Plant Manager, AngloGold Ashanti, Yatela Mine, Mali

Abstract

Yatela mine in Mali operated a heap leach pad (HLP) to recover gold for 20 years until 2017. Ore placed on the HLP was routinely agglomerated using cement. In early operations cement contained around 200 mg/kg of chromium, predominantly as Cr^{6+}. On termination of irrigation in 2017, a solution inventory of >100,000 m3 prevailed containing Cr^{6+} at a concentration of >4 mg/L. The Yatela Closure Plan (YCP) contemplates rinsing of the HLP to remove residual contaminants from the pore solution. However, the risk of long-term mobilization Cr^{6+} from the spent ore is uncertain. An experimental assessment was initiated in 2017 involving six test columns each filled with sub-samples of 80 kg of ore from the HLP. Different solutions were applied to each column with variability in pH, plus in some instances variable levels of $Ba(OH)_2$ as a prospective reagent to induce Cr immobilization. While high concentrations of Cr^{6+} (>1.5 mg/L) were observed in initial column leachate, concentrations declined to <0.01 mg/L within a month of the onset of irrigation. The Cr^{6+} concentration reduction appears partially correlated to pH. Column irrigation at ambient rainfall pH resulted in rapid reduction of Cr^{6+}. Columns irrigated with $Ba(OH)_2$ solution showed Cr^{6+} attenuation trends analogous to those irrigated by near-neutral water. The efficacy of $Ba(OH)_2$ for Cr immobilization appears restricted by difficulties sustaining the compound in solution, competition from SO_4 and increased column ambient pH.

Keywords: Mine closure, Heap leach pads, Hexavalent chromium, Field columns

Introduction

Yatela is an open pit gold mine, located in western Mali approximately 50 km southwest of the regional centre of Kayes. Mining was initiated in 2001 and terminated in 2013, although processing of gold continued to 2017. Throughout operations, gold recovery was undertaken through the crushing, agglomeration and heap leaching of ore using NaCN solution. Pregnant leach solution (PLS) reporting to the base of the heap leach pad (HLP) was stripped using activated carbon. Gold was then recovered in a refinery to produce doré. The HLP consists of a series of cells approximately 850 m long by 80 m wide and up to 24 m high. There are 20 full size cells, some of which are sub-divided. The HLP occupies an area of approximately 175 ha and holds a total rock mass of 36 million tons.

As Yatela entered its closure phase in 2017, a particular complexity was recognized to relate to the potential risk of long-term release of hexavalent Cr from the pad. During the early period of operations, the cement used to agglomerate ore was sourced from a location in Senegal in which the firing kilns for cement production were lined with ferrochrome steel. This resulted in mobilization of Cr^{6+} into the cement during production. Within the HLP, re-mobilization of Cr^{6+} has occurred with attendant generation of high levels of Cr^{6+} (typically around 4 mg/L) n the PLS.

A rinsing plan for the HLP currently forms part of the approved Closure Plan for Yatela, principally with the objective of eliminating residual CN compounds from the pore water inventory. Any continued mobilization of Cr^{6+} from the ore mass during rinsing would, however, significantly undermine the value of rinsing as continued generation of contaminated solution would occur. The Closure Plan currently envisages addition of $Ba(OH)_2$ to the rinse solution as a mechanism for immobilizing Cr as a low-solubility barium chromate compound. This, however, carries a substantial cost and is of unproven efficacy.

Historical monitoring data for the heap leach circuit suggest that elevated Cr^{6+} levels now prevail largely in solution emanating from the more recently stacked and irrigated cells of the HLP. This supports the assertion that either Cr^{6+} has been flushed from the system, or a control on Cr^{6+} mobilization, such as pH, is influential in the older pads. To assess this assertion, and in conjunction to determine the value of supplementation of rinse solution with $Ba(OH)_2$, a series of controlled column tests were initiated at Yatela in 2017, as described in this paper.

Methodology

The Yatela column test program was designed with the central objective of establishing an understanding of the mobilisation controls and exhaustion rates of hexavalent Cr in the spent ore on the HLP. The columns were also designed to determine the extent to which $Ba(OH)_2$ may enhance Cr^{6+} immobilisation within the ore matrix, and any risks of Cr^{6+} remobilisation following the cessation of $Ba(OH)_2$ addition.

Six columns were set-up in the Yatela Metallurgical Laboratory in March 2017. The columns were 300 mm diameter by 1 metre in height and were each filled with 82 kg of spent ore, recovered from Cell 19A on the HLP. The columns were set-up as follows:

- The columns were made from high grade plastic (PTFE) which may be considered extremely unlikely to leach inorganic constituents.
- Spent ore was uniformly crushed to <3 cm.
- The columns were housed under cover (in the metallurgical testing laboratory) to avoid any infiltration of rainfall.
- The columns contained a drainage vent and tubing at the base, through which solution was routed to a collection canister.
- Collection vessels of 10 litres in volume were placed at the base of each column.
- Dripper systems were emplaced to administer solution at a rate of 3 ml/minute to each column. This was confirmed experimentally to allow free solution flow without saturation.

The methodology for column operation is outlined in Table 1. Key points include:

a) All columns were irrigated with identical raw water for the first 72 hours. This was sourced from the Raw Water Pond at Yatela and had a slightly alkaline pH. This common irrigation procedure for the first 72 hours was intended to allow confirmation of the comparability of Cr concentrations emanating from each column.
b) With effect from day 4, each column was irrigated with a unique solution as shown in Table 2. Column YT-2 was acidified to ensure a solution pH (entering) of 5.5. For each column, solution conditions remained unchanged until day 30.
c) A critical aspect of YT-05 was the use of monitoring pond water.
d) From days 31 to 50 the columns were allowed to drain. Solution was collected for analysis at approximately weekly intervals, if present.
e) From days 51 to 60 raw water was applied. Column YT02 used water acidified to pH 5.5. The aim of this phase of the column tests was to simulate leaching by rainfall following a period of rinsing, plus draindown.

Two sample suites were collected to analyse column leachates. The first was used specifically to measure pH, temperature, electrical conductivity (EC), dissolved oxygen and hexavalent chromium (by colorimetry) on site at Yatela. The second was shipped to a laboratory in the UK (Exova Jones) for analysis of hexavalent chromium, major cations, major anions, trace metals and cyanide species. Leachate was sampled daily during Step 1 and weekly during Steps 2 and 3 as defined in Table 1.

***Table 1** Bespoke column test methodology steps*

Column	Test duration (days)	Step 1	Step 2		Step 3	Step 4	
		Days 1 to 3	Days 4 to 30	Reagent addition	Days 31 - 50	Days 51 to 66	Reagent addition
YT01	66	Raw water or tap water (pH <7.8)	Raw water or tap water (pH <7.8)	None	No irrigation	Raw water or tap water (pH <7.8)	None
YT02	66	Raw water or tap water (pH <7.8)	Water (pH 5.5)	HCl (few drops)		Water (pH 5.5)	HCl (few drops)
YT03	66	Raw water or tap water (pH <7.8)	Raw Water or tap water + $Ba(OH)_2$	50 mg/L $Ba(OH)_2$ in solution		Raw water or tap water (pH <7.8)	None
YT04	66	Raw water or tap water (pH <7.8)	Raw Water or tap water + $Ba(OH)_2$	5 mg/L $Ba(OH)_2$ in solution		Raw water or tap water (pH <7.8)	None
YT05	66	Raw water or tap water (pH <7.8)	Monitoring pond + $Ba(OH)_2$	50 mg/L $Ba(OH)_2$ in solution		Raw water or tap water (pH <7.8)	None
YT06	66	Raw water or tap water (pH <7.8)	Raw water or tap water + Fe_2SO_4.	50 mg/L Fe_2SO_4 in solution		Raw water or tap water (pH <7.8)	None

***Table 2** Initial analysed chromium and hexavalent chromium abundances in column test material*

Sample	Hexavalent Chromium (CrVI)	Total Cr	Cr2O3
	mg/kg	mg/kg	%
YAT01	1.75	58	0.02
YAT02	1.61	72	0.02
YAT03	1.70	71	0.02
YAT04	1.79	67	0.02
YAT05	0.44	76	0.02
YAT06	1.01	75	0.02

Results

The results Cr and Cr^{6+} head-grade assays for each column are shown in Table 2. Daily hexavalent chromium analyses of column leachates are presented in Figure 1. These show that Cr^{6+} concentrations in all columns declined from initial levels of >2 mg/L to near zero by around day 10 of initiation, with no significant differentiation evident between columns with and without barium hydroxide addition. The Cr concentration decay curve occurred in response to a pore-volume transfer rate of approximately 0.5 per week, thus equating to slightly less than one full pore volume in total. The persistence of concentrations of Cr^{6+} in the very low part per billion range was then observed throughout the remaining testing period in columns YAT01 and YAT02, which were irrigated with raw water at pH levels of 7.8 and 5.5 respectively.

In contrast, measured hexavalent chromium levels appeared to increase with effect from day 12 in all solutions subject to $Ba(OH)_2$ addition.

The addition of $Ba(OH)_2$ was observed to produce an alkaline irrigation solution. This appears to increase Cr^{6+} stability in solution and overwhelms any potential benefit which could otherwise arise with respect to Cr immobilization through barium chromate precipitation. Further, concentrations of SO_4 in the leachates of columns subject to $Ba(OH)_2$ addition were reported to decline in a sequence inversely correlated to the molarity of reagent addition. This suggests that Ba is preferentially consumed in barite precipitation, with little reactive Ba available for Cr immobilization. This, in conjunction with the persistently low Cr^{6+} concentrations observed in columns YAT01 and YAT02 to which raw water of neutral to weakly acidic pH with no additional reagent was applied, confirms that barium hydroxide addition is unlikely to be warranted in any future field-scale rinsing of the Yatela HLP. This prospectively reduces the cost of Yatela's current Closure Plan strategy for the HLP by more than US$ 1 million.

A key aspect of the column test design was inclusion of a cessation of irrigation at Step 2, a subsequent drain-down period of 20 days (Step 3) and finally the re-initiation of irrigation for a 10 day period using clean water (Step 4). These steps were considered critical for understanding the risk of remobilization of Cr^{6+} following field-scale HLP rinsing by residual long-term rainfall infiltration. In the test columns, recommencement of irrigation in Step 4 produced no apparent Cr remobilization in YAT01 and YAT02, with leachate concentrations remaining close to detection limits.

Simple mass balance calculations for each of the six test columns indicate that the reduction trend of Cr^{6+} is in no way related to exhaustion of the available hexavalent Cr inventory in the ore. Instead, the results of all column tests viewed in conjunction suggest that a primary control is ambient pH. Under strongly alkaline conditions, as occurred in the HLP cells during active irrigation with CN, Cr^{6+} is readily stabilized in solution. With falling pH towards a neutral or acid state, this stability is suppressed.

The WAD-CN concentration in column

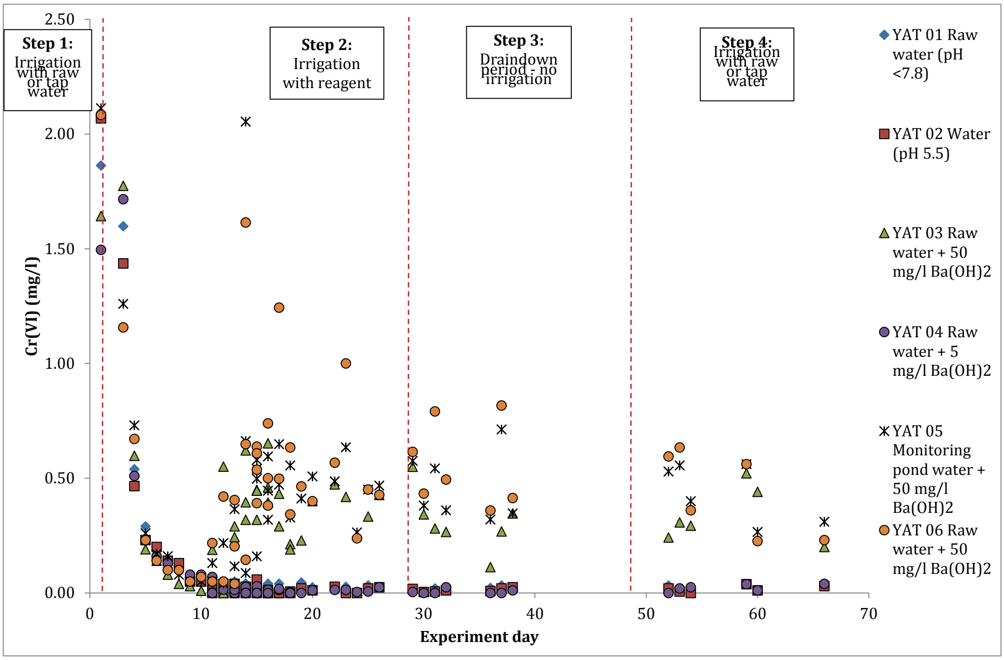

Figure 1 Daily onsite Cr(VI) analyses of column leachates.

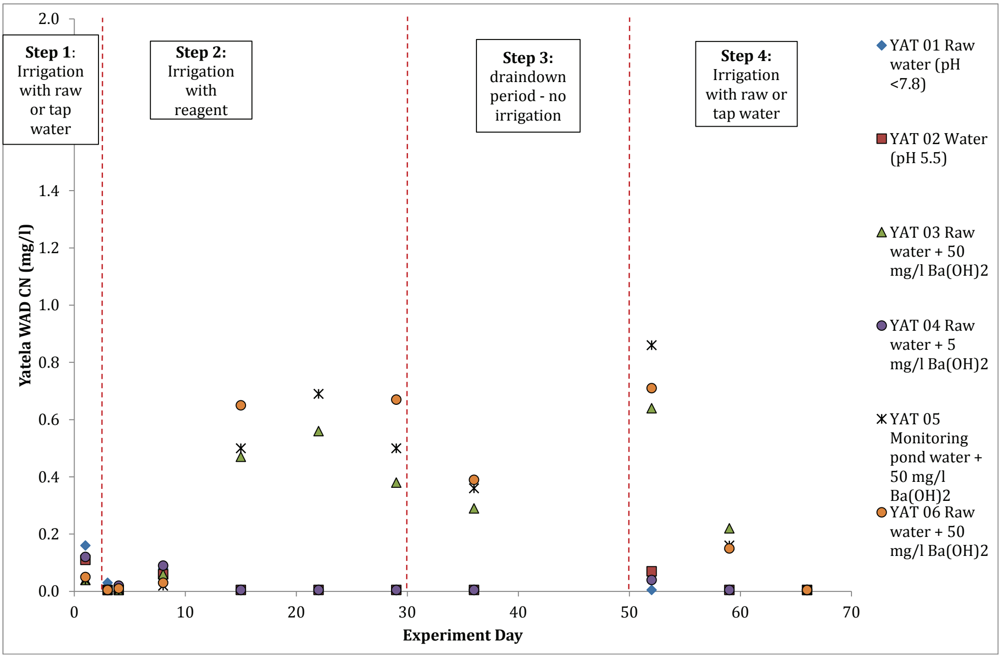

***Figure 2** Weekly WAD cyanide analyses of column leachates*

leachates was not recorded at levels in excess of 2 mg/L in any column. This is positive as Yatela's completion criterion for rinsing of the HLP is the attainment of a sub- 2mg/L CN threshold. The majority of samples were also below the IFC effluent guideline of 0.5 mg/L WAD-CN. Within a week of test commencement, WAD-CN concentrations in leachates from the columns were typically 0.2 mg/L or less. There appears to be mobilisation of WAD-CN from day 15 of the experiment in the leachate samples YAT03, YAT05 and YAT 06, based on the Yatela and external laboratory data. This coincides with the high concentraions of barium and hexavalent chromium remobilisation in these column leachates. WAD-CN in columns where no barium hydroxide is added (YAT01 and YAT02) remain at a low concentration of WAD-CN, often below detection limits, following the initial flush of WAD-CN in the first week of irrigation and sampling. The apparent mobilisation of WAD-CN in columns where barium hydroxide could be related to the high pH caused by the barium hydroxide. However, as the pH of the other columns is also relatively high (Figure 2) it is more likely to be a direct effect of the addition of barium hydroxide and either chemical remobilisation due to this, perhaps from redox effects, or measurement interference. As WAD-CN in column leachates with no barium hydroxide addition is successfully lower than Closure Plan and regulatory requirements the column experiments verify the rinsing plan for this parameter.

Conclusions

The column tests performed at Yatela during 2017 to assess potential long-term risks of hexavalent Cr mobilization from the Yatela HLP have provided valuable guidance in the refinement of a defensible Closure Plan for the facility. The results also suggest that considerable cost-savings may be achieved through elimination of previously held concepts regarding the addition of $Ba(OH)_2$ to irrigation solution during rinsing of the HLP. The experimental scale data suggest that high levels of Cr^{6+} mobilization during active irrigation of the HLP with CN solution were at least in part attributable to the highly alkaline nature of the solution. To some extent, such mobilization may be anticipated to attenuate naturally following rinsing and the establishment of conditions in which infiltrating solution is of a pH approximating rainwater.

The reduction of leachate Cr^{6+} levels to no more than a few parts per billion following only around 1 pore volume of rinsing in test columns subject to raw water irrigation, coupled with the prevalence of CN levels in the leachate which fall substantially below Yatela's HLP closure completion criterion of 2 mg/L, suggest that a similar volumetric approach to rinsing plan design may reasonably be adopted for the full scale HLP. This is extremely encouraging, as the overall timeframe for execution of the rinsing plan may need to extend over only a few months.

Former Galmoy Mines tailings restoration

Cora Devoy[1], Linda Wrong[1], Kevin Collins[2]

[1]Environmental Manager, Lundin Mining Corporation, cora.devoy@lundinmining.com
[1]Director of Sustainability and Regulatory Affairs, Lundin Mining Corporation, linda.wrong@lundinmining.co
[2]Bird Watch Ireland - Tipperary Branch, kevincollins062@gmail.com

Abstract

Galmoy Mines completed the restoration of a tailings management facility (TMF), incorporating an engineered wetland, returning the site to a land use compatible with the surrounding countryside, while efficiently treating surface water runoff and creating an enhanced environment for local and migratory bird species. Increased breeding density of Curlews (IUCN Red List), in addition to nesting Little Ringed Plover and a Glossy Ibis were observed, demonstrating biodiversity support. The wetland system improved post-closure water quality. Ammonia in the revegetated caps of the TMF has stabilised and reductions in the sulphate were noted as the TMF remediation matures.

Keywords: Mine Closure, Wetland, Biodiversity, Little Ringed Plover, Ammonia, Sulphate

Introduction

Galmoy Mines zinc-lead deposit, located in south-central Ireland, discovered in 1986 (Doyle 2016), was owned and operated by the Lundin Mining Corporation since 2005. Most of the underground mine workings were between 100 m and 160 m below surface, hosted in extensively dolomitized and brecciated basal Waulsortian (Lower Carboniferous) "Reef" mudbank limestones Production of concentrates at Galmoy commenced in early 1997, with mine production carried out by room-and-pillar and bench-and-fill methods as reported by Lowther et al. (2003). During the operational phase, the excess non-acid generating tailings from processing ore were disposed of in the TMF, with drainage reclaim water pumped to the mine site, treated and discharged to the licensed discharge point (River Goul). The surface area of the TMF measures 33.64 Ha and is an engineered double HDPE lined ring dam built from local glacial materials with chimney and finger drains of sand (Derham 1999). While the original concept of three adjoining cells remained constant; the numbering, size, and sequence of construction changed due to revisions of the life of mine and discovery of new orebodies, affecting the underlying principles behind the original design. Most of the progressive rehabilitation of Phase 1 (9.36 Ha) and Phase 2 (14.02 Ha) of the TMF was completed during mine operation. TMF drainage design allowed for the safe discharge of water during the operational and post-closure stage. The three main sources of water identified were seepage water from the internal drainage within the cells (potentially contaminated), tailings surface water discharged from the TMF (potentially contaminated), and clean surface water reporting to the perimeter drains (Golder 2011).

The mine operated under an Integrated Pollution Control Licence, Planning Permissions, and State Mining Licences [Environmental Protection Agency (EPA) 2002; Local Authorities (Kilkenny County Council) 1994; Department of Communications, Climate Change, & Environment (DCCAE) SML 1, 6, 8-10 (1994–2005)]. All licenses and permissions referred to the rehabilitation of the TMF as an integral part of the Mine Closure Plan (MCP). In the MCP 1992, the preferred option for rehabilitation was the development of a "general amenity/wildlife sanctuary", with interim and final drainage schemes incorporated into the post-closure periods using a combination of wet/dry landscapes on the surface of the TMF. At that time, the long-term maintenance requirements were envisaged to be minimal and a "walk-away" end-point would not pose a threat to the environment. However, modern legislation, regulators, and Galmoy Mines recognised the retention of water below the crest of the dam wall did not offer a "walk-away" solution. The Second Interim Mine Closure Plan (2005) envisaged a wetland located externally to the southwest of the TMF, however at the announcement of unplanned early closure in 2009 Phase 3 of the TMF remained partially unfilled and the closure design of the TMF required modification.

Methods

TMF rehabilitation at Galmoy Mines began in 2001 with a pilot-scale tailings dam constructed to mimic the conditions in the TMF at closure. Pilot trial cells were established in compliance with planning permission requirements. The trial cells were subdivided, and a variety of grass species and depth of substrate were investigated with a mixture of topsoil and compost assessed. Nine cultivars were selected on the basis of a literature search and the experience gained at Tara Mines, Navan Ireland (Brady 1993). Vegetation trials demonstrated that the grasses selected for the large-scale TMF remediation (Festuca rubra cv. Merlin, *Agrostis castellana* cv. Heriot and *Agrostis capillaris* cv. Hyland) were based on genetic or physiological tolerance to metals, low uptake of lead and zinc to allow for the possibility of grazing animals, and good surface coverage and sustainability of vegetation density.

Based on these trials, capping and revegetation of TMF Phase 1 began in 2001, with subsequent monitoring of the performance of the cover through the collection and analysis of soil and vegetation samples. Calculation of a bioconcentration factor by Perkins et al. (2015) suggests no accumulation of the As, Cd, and Pb studied in the roots of grass growing on the Galmoy TMF. The data would suggest that grass species growing on the Galmoy TMF are relatively successful in excluding metals, taken up by the roots, from transferring to the remainder of the plant. Recent studies by Perkins et al. (2015) have shown that the maximum As, Cd, and Pb in herbage on Phase 1 and the trial cells are within the normal ranges for plants and that all maximum concentrations are below the upper threshold of the concentration ranges that could be considered excessive in leaf tissue. Perkins et al. (2015) suggest low translocation factors, noted at Galmoy TMF, indicate the positive potential future use of remediated TMFs for uses including pastoral agriculture, even where the soil layer is very thin.

Successful sheep grazing trials in 2008 and subsequent cattle trials in 2011 and 2012 were conducted on Phase 1 to confirm the agronomic value of the rehabilitated cap. Analysis was conducted on the grass; the animals' liver, kidney and muscle tissues; and blood samples at the end of each trial. The practical experience and analytical information from the grazing trials demonstrated the ability of the grassed cap to support livestock that, at slaughter, complied with all the relevant regulatory requirements for animals to safely enter the food chain.

A variety of organic materials and glacial till substrates were approved for use by the EPA throughout progressive remediation of Phase 1 and 2 (Figure 1), including black spent grains, limed sewage sludge, kieselguhr (a form of diatomaceous earth used in various manufacturing and laboratory processes), effluent screenings, sludge from Bulmers^{TM} cider production, topsoil from the borrow area, and composted products. The aim was to provide a sustainable growing medium to support a natural and vibrant vegetation cover, however, the organic material cover on Phase 1 and 2 generated effluent with high levels of BOD, COD, ammonia, nitrate, phosphorus and potassium, during the early stages of remediation which would likely require passive treatment presenting a challenge to long-term discharge compliance, due to elevated ammonia concentrations in particular, in the interstitial layer of the vegetation cap.

A wetland trial was designed by Vesi Environmental Ltd., in 2009 whereby two cells were constructed adjacent to the TMF. Both cells were planted with four types of wetland species (*Glyceria maxima* (main species), *Carex riparia, Cladium mariscus* and *Alisma plantago-aquatica*) and irrigated using water from the TMF spillway and surface runoff, to assess the impact on the wetland plants of the parameters of interest.

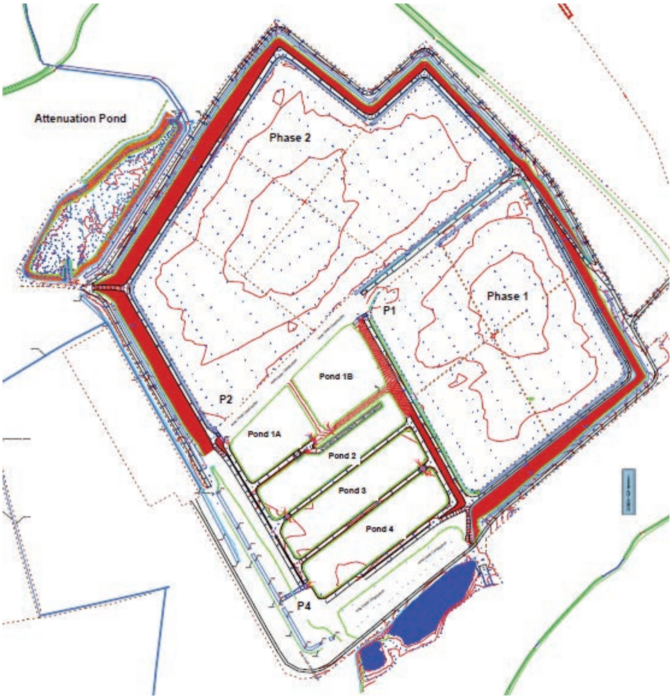

Figure 1 *Final layout and design of TMF, wetland, and attenuation to licensed discharge (oriented North)*

The remediation of partially filled Phase 3 (8.29 Ha) presented an additional challenge in the closure process. Approval was received from the authorities to redesign TMF Phase 3 and develop an integrated constructed wetland (ICW) on the surface area of the partially filled Phase 3 (Figure 1). The innovative location of the ICW within Phase 3, was designed to reduce the footprint of the tailings runoff area and remediate Phase 3 simultaneously. The deposited tails in Phase 3 required resurfacing before the ICW could be constructed on the capped surface. Designed by Golder Associates (2011), Phase 3 was capped with glacial till and HDPE liner derived from the reduction in the height of the dam wall of the partially filled Phase 3. Based on the trial data in 2009, Vesi Environmental Ltd., developed the ICW to treat surface runoff water reporting from remediated Phase 1 (P1) and Phase 2 (P2).

Domed capping profiles for Phases 1 and 2 allowed surface water to migrate to the perimeter interceptor drainage system, thereby directing the surface runoff and interstitial drainage through redesigned spillway systems to the newly established ICW. Golder (2011) notes that very few mine operations considered doming their tailings facility to eliminate the long-term risks associated with containment and spillage of surplus water. Following the passive treatment of Phase 1 and 2 surface waters in the ICW, P4 discharge directed towards the attenuation pond located northwest of Phase 2 is polished, prior to discharge through the post-closure outfall to Glasha stream(Figure1). The surface area of the attenuation pond is approximately 2.4 Ha, with a capacity of 50,000m^3 and varies in depth due to the undulating nature of the limestone bedrock. Construction of the ICW commenced within the boundary of Phase 3 of the TMF in 2013, providing an HDPE lined area in which to locate the ICW. The wetlands were divided into four sequential ponds, Pond 1 to Pond 4, with Pond 1 subdivided into Pond 1A and 1B and were commissioned in October 2014 (Figure2).

Results

Table 1 outlines the results achieved during the wetland trial (2009) indicating large reductions in the concentrations of the chemical species monitored. Based on the trial results, the ICW design was finalised by Vesi. Construction of the full-scale wetland was

Figure 2 *Aerial view of Galmoy Mines constructed wetland (September 2016)*

Table 1. *Trial wetland results in 2009 (Carty 2017)*

Parameter	Inflow (max conc)	Outflow (max conc)	% Removal
Lead µg/L	275	26	91
Zinc µg/L	668	27	92
Sulphate mg/L	595	195	80
Total NH_4 mg/L	3074	36.6	98
Potassium mg/L	421	2.9	99
BOD mg/L O_2	130	50	79
COD mg/L O_2	6600	126	97

Table 2. *Wetland efficiency results in 2015 - 2017 discharge vs % removal (Carty 2017)*

		Discharge quality			% Removal		
Parameter	ELV*	2015	2016	2017	2015	2016	2017
Total NH_4 (as N) mg/L	0.065	0.04	0.03	0.05	99.8	99.8	99.3
Sulphate mg/L	400	105	161	231	82	84	74
Lead µg/L	7.2	1	1	2	85	90	97
Zinc µg/L	100	32	22	56	99	99	98

completed in 2014, with the wetland commissioned sequentially as each pond in the ICW was filled. Discharge through the spillway system from Phase 2 was commissioned in October 2014, with flow commissioned through the spillway at Phase 1 in November 2014. As each stage progressed, the quality of the discharged water was monitored. Discharge from the final pond to the attenuation pond commenced in January 2015. Discharge flow from the Pond 4 to the attenuation pond is managed using a low-flow sensor pump.

Based on the tailings hydrochemistry, wetland pilot trials (2009), and the proposed

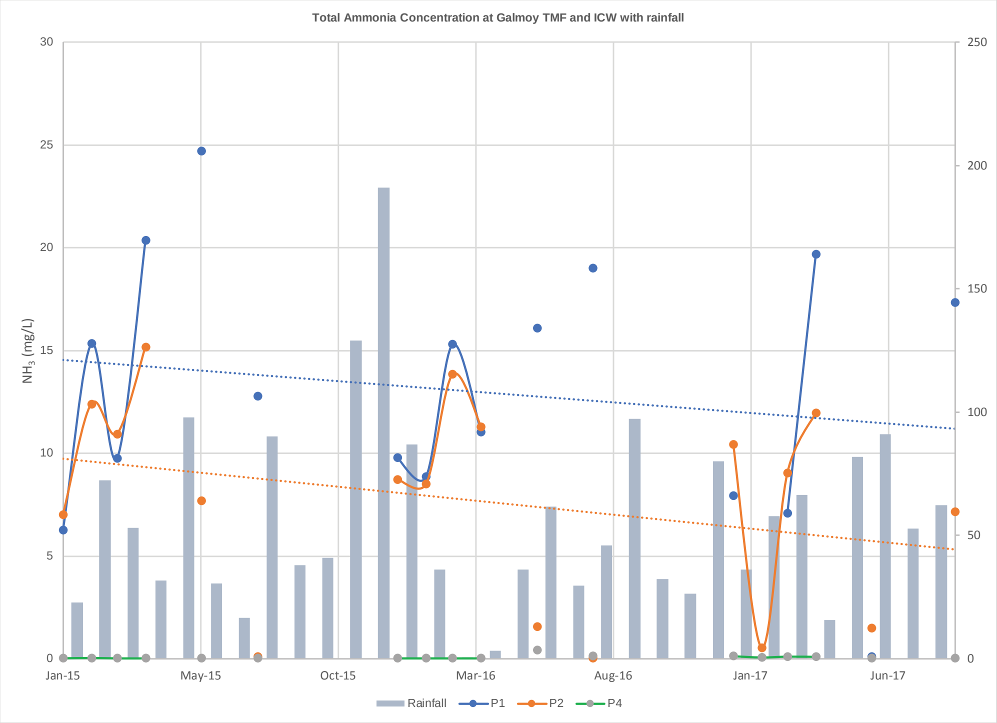

***Figure 3** Total Ammonia concentration discharged from TMF Phase 1 (P1) and Phase 2 (P2) and ICW discharge point (P4) vs rainfall 2015 to 2017*

discharge water quality limits, a number of parameters were selected to monitor the removal efficiency compared to the ELV since the commissioning of the wetland in October 2014 (Table 2).

Historical data shows that ammonia concentrations tended to be elevated above normal background levels at the spillways, with a maximum value of 3074mg/L noted in 2009 to 48.81mg/L in 2014, attributed to the high ammonium content in the various organic materials used to improve the growing medium on the capping layer, particularly on Phase 1. Figure 3 supports this with TMF Phase 1 discharge (P1) reporting consistently higher ammonia concentrations than water emanating from TMF Phase 2 discharge (P2). Figure 3 illustrates the decreasing trends in ammonia concentration at P1 and P2 in recent years (2015-2017) with the trendlines demonstrating the maturity of the remediated cap on Phase 1 and 2. Concentrations of ammonia in the discharge water quality from the ICW are denoted by ICW outfall (P4) demonstrate the effectiveness of the ICW to treat ammonia. The variable nature of the data is most likely due to the impact of rainwater on water quality discharge at the P1 and P2. The gaps in the data provided are explained by no discharge from either the spillways (P1 and P2) or the outfall of the ICW (P4). In addition, low concentrations of nitrate in the runoff water of TMF Phase 1 and 2 indicate reducing conditions in the organic material. Elevated concentrations of ammonium and metals appear to be correlated to lower flows.

Figure 4 illustrates that the sulphate concentrations are elevated during various periods, caused by oxidation of sulphite. Elevated concentrations of sulphate appear to be correlated to lower flows from the P1 and P2. Variations in sulphate concentration in the runoff water quality appear to reflect rainfall patterns, based on the available data. The trendline at P4 demonstrates that the sulphate concentration has stabilised. The reduction in sulphate concentrations between 2015 and 2017 in the ICW system are most

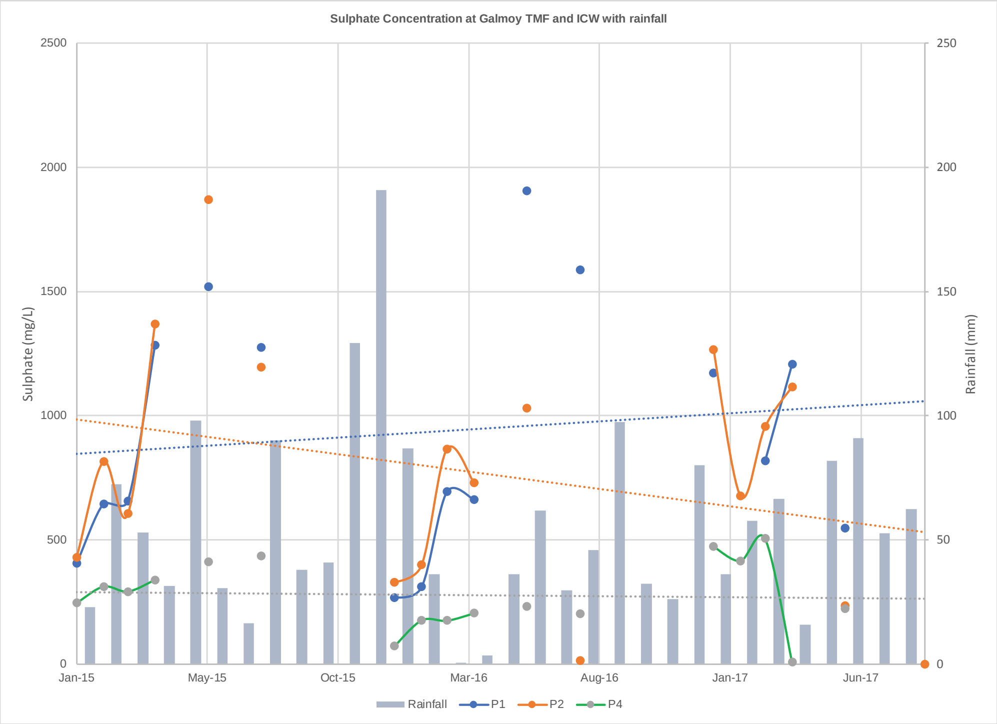

Figure 4 Sulphate concentration discharged from TMF Phase 1 (P1) and Phase 2 (P2) and ICW discharge point (P4) vs rainfall 2015 to 2017

likely attributable to rainfall. Further polishing of the discharge water occurs in the attenuation pond (approximately 50,000m^3) located on the northwest corner of Phase 2. As with Figure 3, the gaps in the data provided in Figure 4 are due to no discharge from either of the spillways or the outfall of the ICW.

Of note and in parallel to the remediation works, since 2008 Galmoy Mines commissioned biodiversity and bird surveys. Studies focussed on the TMF and a reference site located to the northwest of the TMF. During the course of the surveys, Kevin Collins2 noted dramatic increases in breeding density of Lapwings, Swallows, Sandmarks and identified a wide variety of resident and migratory species including the confirmed presence of the Curlew (IUCN Red List, Near Threatened, 2017). Collins also observed a nesting Little Ringed Plover at the wetland (2015) and a Glossy Ibis (2016), rare species in Ireland. Collins (2016) reported "32 species of birds were recorded on the tailing dam subsite and only 17 species recorded on the control site", "with the TMF study site attracting predators such as Merlin and Hen Harrier and the establishment of a Black-headed Gull colony (IUCN Red List, Least Concern, 2017) on the wetland ponds.

Conclusions

The successful restoration of the former mine site, consistent with surrounding land use, and the development of a fully functional ICW system within the TMF, was the first project to complete mine closure activities under the EU Mining Waste Directive since its introduction in 2006. Golder (2011) noted that the revegetation trial work, in addition to the environmental and restoration work is considered to be following and, in part, exceeding current best practice for closure in the metal mining industry. The construction of the ICW on the partially filled Phase 3 provides a sustainable passive wetland within the former TMF footprint, regulating water flow and improving water quality in compliance with regulatory requirements. In addition, the area provides a natural habitat for wildlife and migratory birds, contributing to a balanced and functional ecosystem. The remediated TMF and ICW act as host to both local, rare and migratory birds as noted by Collins (2015) and Collins (2016),

To utilise the natural processes involving wetland vegetation, soils, and their associated microbial assemblages to assist in treating wastewater (USEPA 2000), the Galmoy ICW was designed to take advantage of many of the same processes that occur in natural wetlands but do so within a more controlled environment. Due to the high organic nature of the cover materials on Phase 1 and 2, control systems incorporated into the ICW ensured the optimum removal of ammonia and sulphate from discharge water which had presented challenges at the announcement of early closure. Analysis of metals, suspended solids and arsenic from the surface water were monitored but are not discussed in detail in this paper.

It is important to note that the results at the ICW discharge point (P4) show a 99% reduction in ammonia (2015-2017) and an 82%, 84% and 74% respectively, in sulphate over the same period. The data serves to demonstrate that the ICW is functional, however P4 is not the licensed discharge point. Additional polishing is achieved downstream of the ICW at the attenuation pond prior to discharge to the environment at the licensed discharge point (Glasha stream).

Based on the criteria for success detailed in BREF-MTWR (EC 2009), the attainment of a self-sustaining ecosystem at Galmoy was contingent upon the development of a physically, chemically and biologically stable system founded upon habitat, species and community diversity, as well as the restoration of the mine.

Acknowledgments

The authors thank the Irish Authorities (DCENR, EPA, KCC, LCC), Vesi Environmental (Wetland Design), Golder Associates (TMF engineering), TMB Construction, Aberystwyth University, and support from Tara Mines and Lisheen Mines, in addition to all the Galmoy staff who worked on the progressive remediation.

References

Brady E (1993) Revegetation and environmental management of lead-zinc mine tailings. M.Phil. thesis Univ of Liverpool (unpublished)

Carty A, Harrington C (2017) Integrated constructed wetlands (ICW) for mine drainage Galmoy Mine case study, Soc Wetland Scientist (European Chapter) Annual meeting Faro, Portugal 4-6th May

Collins K (2016) Wintering bird survey at the Galmoy Mine rehabilitated tailings dam facility (unpublished)

Collins K (2015) Bird Survey at Galmoy Tailings Dam 2015, Interim Report August 2015 (unpublished)

Doyle E (2016) Ireland's rehabilitation policy eliminating risk and providing benefits. International Conference Sustainability of Mineral Resources and the Environment, Conference Proceedings. Ministry of Environment of the Slovak Republic, Bratislava Page 51-52 ISBN: 978-80-88833-69-7

Derham J, Dhonau NB, Wright GR (1999) Mine closure planning in Ireland: Water aspects. In: Fernández Rubio R Mine, Water & Environment I. –; International Mine Water Association Sevilla p. 143-148

Environmental Protection Agency (2000) Guiding Principles for Constructed Treatment Wetlands: Providing for Water Quality and Wildlife Habitat, USEPA 843-B-00-003

EUROPEAN COMMISSION (BREF) Reference Document on Best Available Techniques for Management of Tailings and Waste-Rock in Mining Activities January 2009

Golder Associates (2011) Tailings management facility at Galmoy Mines, rehabilitation and closure plan submitted to the EPA (unpublished)

BirdLife International (2017) The IUCN Red List of Threatened Species, Larus ridibundus, (amended version of 2016 assessment) e.T22694420A111823721. http://dx.doi.org/10.2305/IUCN.UK.2017-1.RLTS.T22694420A111823721.en

BirdLife International (2017) The IUCN Red List of Threatened Species 2017, Numenius arquata.: e.T22693190A117917038. http://dx.doi.org/10.2305/IUCN.UK.2017-3.RLTS.T22693190A117917038.en

Lowther JM, Balding A, McEvoy FM, Dunphy S, MacEoin P, Bowden AA, McDermott P (2003) The Galmoy Zn-Pb orebodies: structure and metal distribution - clues to the genesis of the deposits. In: Kelly JG, Andrew CJ, Ashton JU, Boland MB, Earls G, Fusciardi L. Stanley, G (2003) Europe’s Major Base Metal Deposits. Irish Assoc Econ Geol, Dublin 437-454

O’Sullivan AD, McCabe OM, Murray DA, Otte ML (1999) Wetlands for rehabilitation of metal mine wastes, Biology and Environment: Proc R Irish Acad 99B(1):11–17

Perkins WT, Bird G, Jacobs SR, Devoy C (2015) Field-scale study of the influence of differing remediation strategies on trace metal geochemistry in metal mine tailings from the Irish Midlands. Environ Sci Pollut Res, doi:10.1007/s11356-015-5725-7

Strategies for Managing Chemically Reactive Mineral Waste at Rio Tinto Iron Ore Mines

Rosalind Green[1], Steven Lee[1], Lisa Terrusi1, Chris Kleiber[1], Kate Glasson[1]

[1]Rio Tinto, 152-158 St Georges Terrace, Perth, Western Australia 6000, rosalind.green@riotinto.com

Abstract

Effective mineral waste management during mining and process activities is critical for protecting the environment and reducing liabilities and long-term risks. Upfront proactive management of chemically reactive mineral waste can be challenging as the consequences of actions may not be fully understood and may involve immediate extra resources and expense. Conversely, the lack of proactive management can result in high ongoing cost, environmental degradation, and regulator intervention.

The awareness of mineral waste risks is important for empowering those that work with chemically reactive mineral waste to make informed decisions. Rio Tinto Iron Ore's corporate HSE&C standards, management plans and assurance process provide guidance on the strategies and expectations for those that work with chemically reactive mineral waste at the Western Australia Pilbara operations.

Keywords: AMD, ARD, Management Plans, Geochemical Characterisation, Pilbara, Case Studies

Introduction

Chemically reactive mineral waste may prevent the re-establishment of vegetation, contaminate surface and groundwater leading to environmental degradation, as well as pose direct exposure (health) risks. Unless managed appropriately, chemically reactive mineral waste may have the potential to generate Acid and Metalliferous Drainage (AMD), salinity, neutral mine drainage or spontaneous combustion.

Potentially Acid Forming (PAF) material is managed at some of Rio Tinto Iron Ore's (Rio Tinto's) Pilbara mining operations within Western Australia. Fig. 1 provides an indication of the PAF tonnages at each operation on a year by year basis. Significantly more ore (330 Mt in 2017) is mined than PAF waste material (4 Mt in 2017). Although chemically reactive waste represents a small percentage (≈1%) of the waste generated by most of Rio Tinto's Pilbara open cut operations, it can contribute to waste-related environmental, health, reputational and financial risks. Therefore, significant effort is devoted to proactively identifying chemically reactive waste materials, assessing risk, developing management strategies, increasing awareness and providing assurance that the systems are working. This approach is what Rio Tinto undertakes as an internal requirement, which is independent of, but is consistent with, external regulatory requirements and/or national and international guidelines and standards (DITR 2007; INAP 2018).

PAF material can exist in unoxidised Mount McRae Shale, sulfidic banded iron formation and detrital (lignite and siderite) waste rock. Extensive sulfur analysis (Fig. 2) is undertaken on drill hole data which is combined with acid base accounting data (Fig. 3) and assessed in AMD risk assessments (Green and Borden 2011). If necessary, findings from the AMD risk assessment are translated into the development of management strategies, plans and safe work practices.

Management Plans and Strategies

Rio Tinto has six environmental standards with the Chemically Reactive Mineral Waste Management standard representing the most relevant for the management of PAF waste. It applies to the full mine life cycle from exploration through to post-closure, providing expectations for planning, implementation and operation, and performance monitoring.

A Mineral Waste Management Plan (MWMP) is applicable for every Pilbara

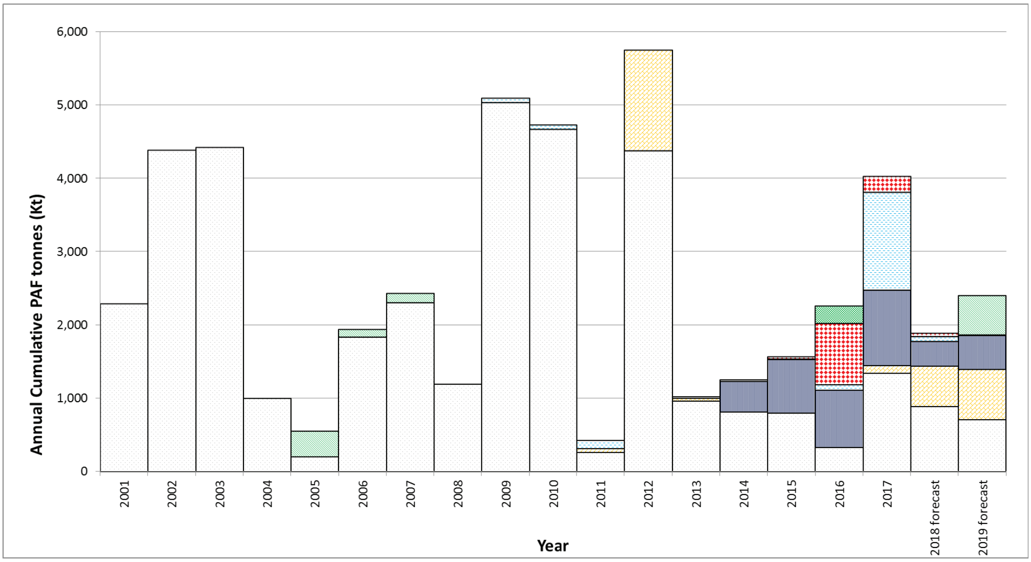

Figure 1 *Indication of yearly PAF tonnages mined at different sites. The different colours and patterns represent different mine sites.*

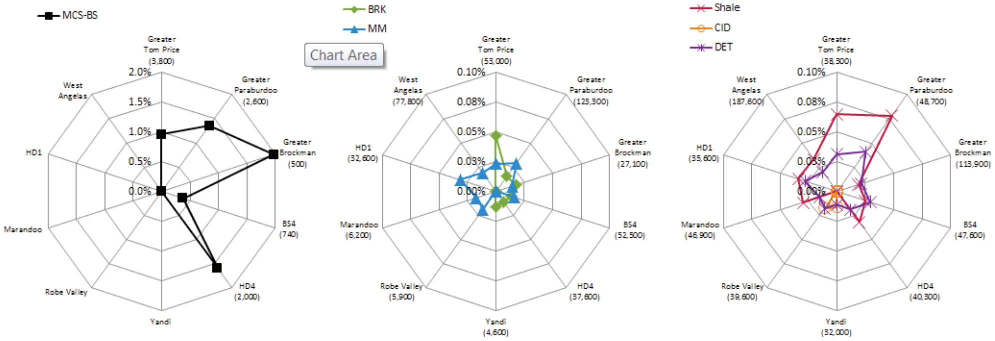

MCS-BS = Unoxidised Black Mount McRae Shale; BRK = Brockman Iron Formation; MM = Marra Mamba Iron Formation; DET = Detrital; CID = Channel Iron Deposits

Figure 2 *Average total sulfur content of drill hole waste samples from Rio Tinto mine sites (both in pit and out of pit). The number of samples analysed are represented next to the site names.*

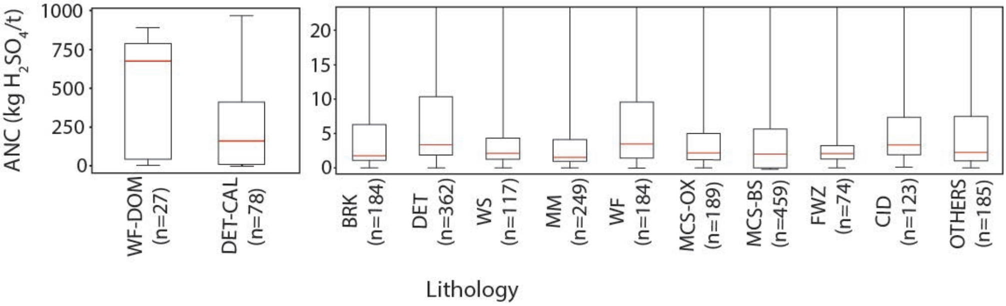

Figure 3 *Acid Neutralising Capacity (ANC) variation (5th percentile, 25th percentile, median, 75th percentile and 95th percentile) in different lithologies (showing the number of samples analysed).*

development project and mining area. The plan describes the actions to be taken during resource drilling, order of magnitude, pre-feasibility and, feasibility studies and mine development.

The MWMP requires the completion of an AMD risk assessment, and if the project is assessed as posing a significant AMD risk, then the Spontaneous Combustion and ARD (SCARD) Management Plan will be implemented. The SCARD plan describes the actions to be taken by long-term planning, site planning, geology, survey, operational planning, blasting, hauling, hydrogeology, environment, health and safety and the mineral waste management team to reduce AMD-related risks at the site. It captures guidance for: dump designs; rehabilitation and closure; and contingency planning.

Easily accessible hyper-links are included in the SCARD plan to relevant technical reports and reference material. Safe work practices, acid water management plans and health guidance notes that are specific to individual operations have also been developed.

Awareness

In addition to site-specific and role-specific training, a general interactive mineral waste training module has been created. The online module provides an engaging approach to self-learning which differs to typical classroom or PowerPoint-type training, and includes case studies and a final interactive assessment. It has been completed 360 times since its rollout in September 2014, primarily by geologists, hydrogeologists and mine planners.

Geographic Information System (GIS) layers have been created for each Rio Tinto operation in the Pilbara that displays:

- AMD risk ratings for pits, including details of lithologies and estimated life of mine PAF tonnages;
- AMD risk ratings for PAF waste dumps, including historically recorded tonnages; and
- PAF pit wall exposures mapping and surface areas relative to catchment areas.

The storage of this information within Rio Tinto's GIS database means this information is readily available for mine planners and other groups that work with mineral waste. This enables informed decisions on rehabilitation, pit backfill and monitoring.

Assurance

Business Conformance Audits (BCAs) are undertaken at all Rio Tinto operations (typically every two years). They assess compliance with the Rio Tinto HSE&C standards (including the Chemically Reactive Mineral Waste Management standard). Auditors external to the operation assess the risks and identify findings for the mine site to implement and track. In addition, the Chemically Reactive Mineral Waste Management standard requires a review of PAF management across a site every four years if the risks are significant. These reviews are undertaken by mineral waste experts that are external to the site and the scope covers the characterisation programs, management strategies, disposal facilities, monitoring and closure plans. The findings are actioned and tracked by each site, and communicated or transferred to other sites in the Pilbara, if relevant.

Case Study 1: Dedicated PAF Study for an Operating Mine

Whilst PAF waste management is a component of many studies, particularly prior to mining, a detailed and dedicated PAF study to inform an existing operation on optimal PAF management is relatively unique. Such a study was undertaken in 2016 for a mine that began mining low tonnages of PAF waste in 2009. Questions were raised on the optimal long-term storage location for this PAF waste (i.e., above the water table or below the water table, in-pit or external). The pit represents a flow-through system that will be backfilled above the water table at closure.

Rio Tinto progressed a dedicated PAF study to assess options. A study manager was assigned, and a team was formed which included representatives from mine operations, business analysis, mine planning, hydrogeology, hydrology, mineral waste management, environment, closure, risk and sustainable development. A management Steering Committee was formed consisting of general managers and managers to review findings and make the final decision. The focus of the study was to identify the optimum storage location for chemically reactive mineral waste to meet both environmental and company objectives.

The study was undertaken over eight months and included:

- Mine designs, option analysis and fatal flaw analysis;
- Hydrogeological and geochemical modelling;
- Geochemical and eco-toxicological testing;
- Closure, legal and environmental approval considerations;
- Mineral waste strategy and constructability reviews; and
- Risk register and decision framework development.

The outcomes of this study meant that Rio Tinto was able to make an informed decision on the future PAF waste storage location based on risk and other business considerations. The strategy developed by the study team had management support and a waste management strategy was developed that is unique within Rio Tinto. This study is an example of developing an upfront informed management strategy to support an effective life of mine plan, rather than placing the material in a sub-optimal location.

Case Study 2: Avoidance of PAF material

During the study phase for three Rio Tinto mine sites, investigations were undertaken to determine the amount of PAF material within proposed pit shells. This included an evaluation of uncertainty due to gaps in drilling data and the potential for any inaccuracies in the geological modelling.

Based on the risk assessment process (Green and Borden 2011) and the confirmation of PAF material exposed on the proposed pit walls, the mine plans for each development project were revised to avoid or minimise exposing PAF material. This reduced the likelihood that acidic pit lakes would need to be managed in perpetuity.

Conclusions

Mining and ore processing unavoidably generates large volumes of mineral waste which may have long-term environmental impacts. Appropriate identification and management of chemically reactive mineral waste can:

- **Ensure accurate valuation of projects, acquisitions, and expansions** by characterising the waste material and assimilative environment to identify and assess the true long-term costs of mineral waste management.
- **Reduce operational costs** over the long-term by minimising the volume of reactive mineral waste that must be selectively managed, and by implementing upfront management of mineral waste rather than management of impacts once they have already occurred.
- **Reduce closure costs** by designing waste disposal facilities with a consideration of rehabilitation requirements.
- **Reduce environmental and health risk** and improve outcomes by on-going monitoring of mineral waste repositories and receiving environments.
- **Enhance business reputation** through better stakeholder relationships that take into account community expectations of the management of mineral waste and by minimising the intensity and duration of mineral waste disposal impacts.

References

DITR (2007) Managing Acid and Metalliferous Drainage, Leading Practice Sustainable Development Program for the Mining Industry produced by the Department of Industry, Tourism and Resources, Canberra (available on DMP website http://www.dmp.wa.gov.au/documents/file_MAMD20070227104556.pdf).

INAP (2018) Global Acid Rock Drainage Guide (GARD Guide), International Network for Acid Prevention (http://www.gardguide.com/).

Green R and Borden R (2011) Geochemical risk assessment process for Rio Tinto's Pilbara iron ore mines. In: Integrated Waste Management, Volume 1 (19), Intech, pp. 365-390.

Mount Isa Mines Rehabilitation Material Sampling and Analysis Program for Closure Planning

Matt Landers[1], Greg Maddocks[1], Candice Nucifora[2], Kristian Mandaran[2],
Jason Jones[2], Amanda Forbes[3], Ward Wilson[4], Steven Newman[5]

[1]RGS Environmental Pty Ltd, PO Box 3091, Sunnybank South, Queensland, Australia, 4109, matt@rgsenv.com

[2]Mount Isa Mines, Glencore Pty Ltd, Australia

[3]Deswik Mining Consultants Pty Ltd, Level 22, Riparian Plaza, 71 Eagle St, Brisbane, QLD 4000, Australia
[4]Unsaturated Soils Engineering Ltd., 960 Massey Court NW, Edmonton, AB, Canada, T6R 3S8

[5]Newman Engineering Pty Ltd, Melbourne, Australia

Abstract

Glencore's Mount Isa Mines Limited (MIM) has completed the second phase of the rehabilitation materials sampling and analysis plan (RMSaAP) to identify and quantify potential materials that can be used to rehabilitate the large tailings storage facility (TSF) with an earthen cover system sourced from adjoining hills. Samples, collected from a test pit/ drilling program, were analysed to evaluate chemical/ physical properties of regolith within major rock/ soil types. Results were used with Deswik software to develop a stratigraphic 3-D overburden model to delineate rehabilitation borrow sources and schedule the TSF cover placement, and to undertake unsaturated zone modelling to evaluate the cover performance.

Keywords: Soil Cover | Deswik | Mount Isa Mines | Rehabilitation | TSF | AMD | Mine planning

Introduction

Glencore's Mount Isa Mines Limited (MIM) operates the Mount Isa open cut and underground copper (Cu) and zinc-lead (Zn/Pb) mines near Mount Isa in Queensland, Australia. Tailings from processed Cu and Zn-Pb ore is contained in a 1,315 ha shallow (< 35 m deep) multi-cell valley fill tailings storage facility (TSF).

Static geochemical testing conducted by MIM over the life of mine (LoM) verifies that the Cu, and Zn-Pb tailings have variable sulfide content and diverse mineralogy with significant acid neutralising capacity (ANC) in some samples. The tailings are predominantly classified as potentially acid forming (PAF) using static analytical methods. Kinetic leach testing using free draining columns and humidity cell tests simulating tailings placed on the surface of the TSF suggest that the tailings samples are likely to remain non-acid forming (NAF) for ≈7 years under aerial exposure, and much longer than this under anoxic saturated conditions within the TSF. During this period of weathering, as ANC is depleted, the neutral pH drainage may contain elevated concentrations of some elements including sulfate, manganese and zinc. Only when the ANC is depleted would the tailings then begin to produce acid drainage.

The main environmental risks posed by the tailings are the potential for (i) the physical movement of tailings or surficial efflorescent salts by aeolian processes, and (ii) the release of acid, major ions, metals and metalloids from the tailings solids and the percolation of these elements in solution into and through the surrounding regolith, and to a lesser degree through the tailings that may result in surface seeps, percolation to basement regolith below the TSF and/or deeper percolation to bedrock. It is assumed tailings solids and solutes would not be released from the TSF in surface water as the TSF is designed with sufficient storage capacity.

The overall management goal for the TSF is to maintain ongoing tailings deposition on the tailings beach and then implement rehabilitation strategies after the final placement of tailings before surficial ANC is depleted in the tailings. This management approach should ensure that potential adverse environmental impacts are minimised as the PAF tailings will continue to produce neutral pH drainage. In practice the decommissioning and rehabilitation of the TSF will occur progressively as TSF cells reach maximum design storage capacity.

Therefore, the current rehabilitation objectives for the TSF are to cover the tailings with an earthen cover system which is (i) safe to humans and wildlife (ii) non-polluting (iii) stable, and (iv) able to sustain native vegetation. The earthen cover system design currently proposed for the TSF comprise the placement of a 1.5 m thick geochemically inert borrow material layer directly on the tailings with a 0.5 m growth media layer overlying the borrow material.

Methods

To achieve the rehabilitation objectives, MIM is implementing a progressive RMSaAP. The work described in this study (Phase 2 of the RMSaAP) aims to identify and quantify the potential materials that can be used for rehabilitation and landform design at MIM: at a broad scale within the project area. The earthen cover system requires soil and regolith to be sourced from adjoining hills that include volcanic, sedimentary and metamorphic units overlain by ferrosol, rudosol and chromosol soil profiles. A test pit and drilling program was undertaken to collect samples to (i) evaluate the variability of the chemical and physical properties of the regolith within the major rock and soil types, and (ii) establish the depth and degree of weathering in the hills (iii) used as input to numerical unsaturated zone modelling to evaluate probable cover performance (iv) map-out potential borrow areas (shallow areas to strip soil) and borrow pits to mine deeper regolith, and (v) to schedule the movement of the soil and regolith onto the TSF.

The drilling and test pit program included 30 test pits and five PQ diamond core drill holes placed within each of the major material types or potential borrow areas. Samples were collected (nominally) from the O, E and A soil horizons for each test pit, and select intervals from the core.

The geochemical analytical methods included continual downhole hyperspectral mineralogy by HyLogger™, pH/ EC, NAPP, CEC/ ESP, metal(loid)s analysis and nutrient and organic carbon content. Physical analytical methods included texture, porosity, density, particle-size-distribution (PSD), point load and abrasion testing, Emerson aggregate analysis, Atterberg limits, hydraulic conductivity and soil water characteristic curves.

The results from physical testing (particle-size-distribution, soil water characteristic curves [SWCC] and saturated hydraulic conductivity) for the material types within the borrow areas were used to undertake finiteelement unsaturated flow modelling using SEEP/W (formerly VADOSE/W) (GEO-SLOPE International, 2016; GEO-SLOPE International, 2008a, b). The SWCC used in the modelling were corrected for particle size according to the Bouwer-Rice correction procedure (Bouwer and Rice, 1984) and fitted with the equation by Van Genuchten (1980). The hydraulic conductivity function (suction [kPa] versus hydraulic conductivity [m/s]) was estimated using the measured ksat and extrapolated using the Fredlund method (Fredlund et al., 1994). A two-dimensional (2-D) slice through the TSF with overlying cover system, including growth medium (Fig. 1), was simulated under transient conditions. The models comprise a climatic flux-boundary on the surface which allows true climatic conditions to be applied (rainfall, evaporation and evapotranspiration), with several flux boundaries within each cover layer (and within the tailings) to determine infiltration (and capillary rise) rates. Since the tailings are de-watered there is no water table within the TSF; therefore, the lower boundary condition of the models was simulated with unit hydraulic gradient. Similarly, lateral interflow of water above the tailings was allowed to exit the model via seepage face. As part of the assessment, the cover material thickness and texture were varied, and runoff and infiltration values provided as performance indicators.

Deswik.CAD software (Deswik.CAD v2017.2) was used to develop a concept level

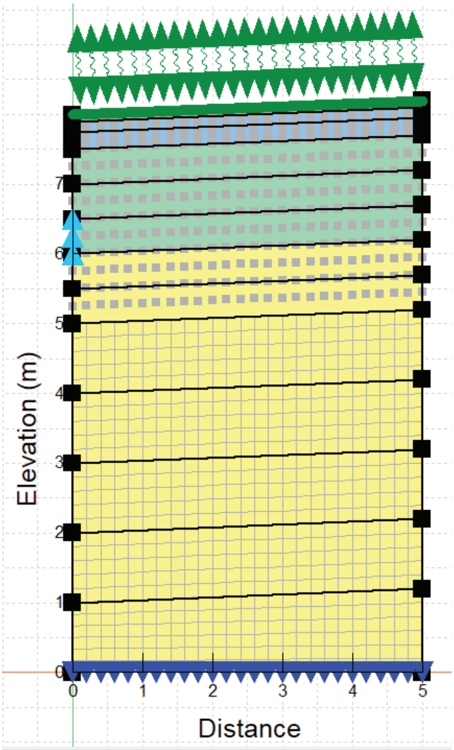

Figure 1 VADOSE/W model geometry and mesh.

stratigraphic 3-D overburden model incorporating a 2 m deep soil profile and underlying regolith. Mining of soil and regolith from borrow areas and borrow pits and scheduling options for placement onto the TSF were evaluated with varying plant and equipment using Deswik.LHS.

Results and Discussion

Geochemical and physical properties of soil and regolith

The results of the analytical program have indicated that there are no fatal flaws related to the chemical and physical properties of the upper profile of the regolith (comprising soil and sub-soil to ≈ 2 m bgl) or the ability to win extremely weathered to weathered material from borrow pits that could extend from the surface of the hills down to ≈ 420 m ASL (nominal elevation selected for the base of the borrow areas as it would be above the final tailings beach and TSF embankments).

There are no geochemical constraints (pH, EC, TS, ANC and soluble and total metal(oids) to using test pit or borrow material for rehabilitation, and no substantial differences in the pH, EC, NAPP or metal(loid) content in topsoil (0 to 0.5 m bgl), subsoil (0.5 to 2.0 m bgl) or deeper soil and regolith below 2.0 m.

There may be issues in the soil cover system relating to chemical imbalances (e.g. CEC) and biological aspects such as nutrient deficiencies, particularly if the upper topsoil layer is diluted with subsoil. Samples that were composited prior to analysis had the following results:

- Soil from 0.to 0.5 m bgl had the following averages pH 6, EC 45 µS/cm, CEC 5.4 meq/100g, ESP 0.5%, TKN 197 mg/kg, Bray P 2.2 mg/kg and TOC 1,283 mg/kg.
- Soil from 0.5 m to 3 m bgl had the following averages pH 7.5, EC 62 µS/cm, CEC 4.9 meq/100g, ESP 0.3%, TKN 78 mg/kg, Bray P 0.8 mg/kg and TOC 766 mg/kg.
- Regolith > 3 m bgl had the following averages pH 8.3, EC 53 µS/cm, CEC 1.3 meq/100g, ESP 0% (n=7) and 25% (n=1), TKN was BDL, Bray P was BDL and TOC was BDL (n=7) and 400 mg/kg (n=1).

From the perspective of the physical material properties, the surface material in all borrow areas is mostly non-dispersive and is dominated by material with low clay content. The fines content decreases substantially with depth in drill core. The physical sampling and analytical program verifies a wide range in measured PSD in the test pit samples. The PSD on the crushed drill core samples provides some qualitative comparison between sample types and was not intended to define the PSD of as-mined rehabilitation units. Whereas it is probable the surficial test pit samples would yield material with a suitable fines content this may not be attained from deeper regolith units. However, because of the low permeability of the underlying tailings water that does percolate through the cover will be stored there in the pore voids. The deeper regolith sampled from drill core may be amenable to use as "general fill" that comprises the 2.0 m layer of geochemically inert material in the concept cover system: the general fill may yield clay, slit and sand to cobble size material in a soil cover system when blasted. This is assumed because of the highly fractured nature of the regolith, low rock strength and measured permeability.

One aspect of the evaluation of the proposed soil cover system which is not able to be modelled is that the soil cover will undergo continual physical and chemical weathering, and a soil profile with increasing fines content will develop within the soil cover over the tailings as fines are leached through the soil cover.

The volume of soil from the designated borrow areas (≈ 485 ha) is in the order of 3 Mlcm (short of the required 9 Mlcm) but this could be increased to the desired 9 Mlcm by increasing the stripping depth from 0.5 m to 1.5 m bgl. Bgl. This would result in "dilution" of the chemical, physical and biological parameters, and functions, of the as-placed soil (as outlined in the above bullet points).

Earthen Soil cover modelling

The placement of a soil cover comprising soil and regolith sourced from borrow pits around the perimeter of the MIM will shed runoff during the large rainfall events (e.g. > 25 mm/day rainfall events) but will generally allow rain to percolate into the soil cover due to the sandy / loam texture soil and the coarse particle size distribution of the weathered to heavily weathered regolith present to a depth of 30 m bgl within the hills around the MIM TSF. The variable surface runoff from the soil cover ranges from: 0% for rainfall events < 10 mm per day; 16.5% for rainfall events > 10 mm and < 30 mm per day; and, 42% for rainfall events > 30 mm per day.

The modelling results verify that the amount of runoff is reduced substantially if the slope of the soil cover is reduced because ponding of water on a flat surface allows more water to percolate into the soil cover. Since average annual evaporation (≈3 m/ yr) exceeds average annual rainfall (≈430 mm/ yr) by a factor of > 7 and since the tailings have very low permeability almost all rain entering the soil cover will leave the cover system as evaporation and or transpiration.

The coarse and blocky nature of the deeper regolith material may act in part as a capillary break reducing upward migration of soluble weathering products but may also allow some lateral movement of water within the cover during large rainfall events.

Rehabilitation scheduling

The material balances for the borrow sources, derived using Deswik.CAD, are presented in Tab. 1. The key results are that approximately 500 ha of borrow areas were identified in the study (Fig. 2), but approximately 1,500 ha of area is required to be rehabilitated. This means that the topsoil (specifically) and underlying subsoil recovered from the 500 ha will need to be diluted i.e. if 60 cm of topsoil is stripped from the borrow areas it would be spread at a depth of 20 cm and it is uncertain if this would enable sustainable growth of vegetation without amendment of the as constructed soil cover. The rehabilitation schedules (in respect to the time over which the cover could be placed) are based on assumptions needing testing and verification, for example the:

- geotechnical properties of the tailings are not known and there are major (untested) assumptions related to the time it will take for the tailings to consolidate so a soil cover can be placed on the TSF; and,
- the time it will take to construct the soil cover (and therefore financial cost) is a function of gaining access to tailings and the fleet that is used, therefore it is necessary to understand the physical properties of the tailings and TSF and determine what type of equipment can (cannot) be used to construct a soil cover on the tailings.

Equipment for sourcing and placing soil and regolith is assumed to include 1 x Komatsu 1250 excavator and CAT 725G (20 t capacity) trucks and requires 14 to 15 years to complete placement of the cover system. The Deswik landform haulage scheduling verifies there are differences in the order of 20,000 to 30,000 hours truck time for the two borrow pit location options (Fig 2) but substantial differences in the order of 200,000 hours for the two sequencing options (Fig 3). The Deswik model can be used to evaluate additional scheduling options including changing borrow area locations, configurations, haul routes, equipment specifications and placement strategies. Similarly, the financial aspects of the current Deswik scheduling model can also be built-in to the model.

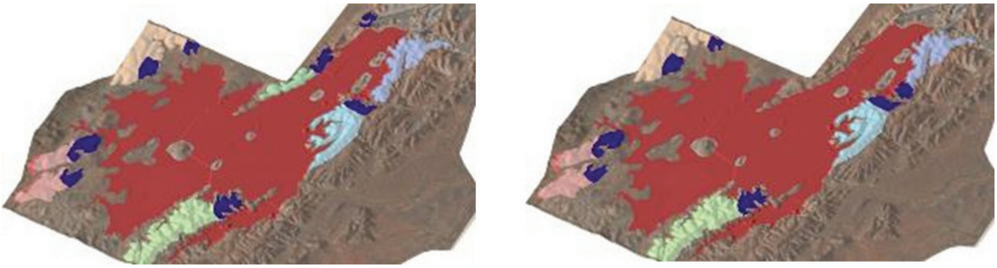

Figure 2 proposed borrow pit locations and scheduling options: Option 1 all borrow areas (left) Option 2 N1 and N2 excluded (right).

Figure 3 Scheduling variations: strip sequence north to south (left) versus no sequence (right).

Conclusions

The findings of the RMSaAP work program informed the work that is scheduled for 2018 and 2019 that includes additional test pits and drill holes in each borrow pit to enable the development of a 3D regolith model that will quantify the volume of each major rehabilitation unit from topsoil through to the partially weathered regolith that could be mined from each borrow pit. When all borrow pits have been drilled, sampled and analysed the detailed regolith models for each borrow area will be used to develop a detailed earthen soil cover system construction schedule to be completed with optimisation around the placement of materials and equipment fleet used to construct the cover system.

The approach being implemented by MIM will provide a robust, reliable and transparent method of calculating the timing and cost of construction and the probable performance of the earthen soil cover system. The overall conclusion of this work is that the soil, sub-soil and extremely weathered to partially weathered regolith in the hills adjacent to the MIM TSF would be suitable to encapsulate the tailings and should support a vegetative cover. Additional detail to support the general conclusion of the work and limitations around this statement are summarised below.

Acknowledgements

The authors thank Tshwane University of Technology (TUT) for hosting the ICARD | IMWA | MWD 2018 Conference.

References

Bouwer H, Rice R (1984). Hydraulic Propertiesof Stony Vadose Zones. Ground Water, 22(6).

Deswik Mining Consultants Australia Pty Ltd (2017) Deswik.CAD v2017.2 software https://www.deswik.com/

Fredlund DG, Xing A, Huang S (1994) Predicting the permeability function for unsaturated soils using the soil-water characteristic curve. Canadian Geotechnical Journal, 31, p 533 - 546

Geo-Slope International Ltd. (2008a) Seepage Modeling with SEEP/W 2007 – An Engineering Methodology. Third Edition, GEO-SLOPE International Ltd., March.

Geo-Slope International Ltd. (2008b) Vadose Zone Modeling with VADOSE/W 2007 – An

Engineering Methodology. Third Edition, GEO-SLOPE International Ltd., March.

Geo-Slope International Ltd. (2016) GeoStudio 2016. Version 8. Online. www.geo-slope.com

van Genuchten M (1980) A Close-form Equation for Predicting the Hydraulic Conductivity of Unsaturated Soils.

Geology, Genetic Processes And Their Consequences On Environmental Impacts At The Abandoned W Mine Of Enguialès, Aveyron, France

Bruno Lemiere, Jérôme Jacob, Gaël Bellenfant

BRGM, F-45060, Orléans, France

Abstract

We investigate arsenic issues at the Enguialès abandoned tungsten mine, relationships with ore genesis model, hydrogeochemical reactions, and consequences on the environmental impact of the site, and on long-term site management.

Acid runoff was monitored, and waste deposits were mapped using pXRF. AMD generates high As concentrations. Runoff drainage was monitored with a multiparameter probe. Heavy rains followed by strong increases in acidity and conductivity can represent a large proportion of cumulated As discharge.

Continuous EC monitoring is more efficient for transfer evaluation and modelling than periodic sampling. Such data are essential for site management and minimise long-term environmental impacts.

Keywords: Arsenic, tungsten, gravity processing, floatation processing, residues, ARD, AMD, site management

Introduction

We investigate here arsenic issues at the Enguialès abandoned tungsten mine, their relationships with the ore genesis model, and the consequences of the hydrogeochemical reactions on the environmental impact of the site, and on the long-term site management plan.

Geological setting and mining history

The former Enguialès mine belonged to the Leucamp – Enguialès regional tungsten district (Cantal - Aveyron region, French Massif Central), hosted in the pre-Hercynian micaschists sequence of “la Chataigneraie” (Bogdanoff et al., 1987). Basal sericite schists (in green on Figure 1) and greso-pelitic schists (in yellow on Figure 1) are in structural contact but do not differ significantly in mineral or chemical composition. Both are affected by similar metamorphic episodes. This sequence was intruded during Silesian times (Monié et al., 1999) by several types of granites and microgranites. The Entraygues porphyritic monzogranite batholith occurs nearby the mine and probably under it. It has a distinctive contact metamorphism aureole of hornfels and spotted micaschists, with abundant cordierite, poikilitic andalusite, biotite, tourmaline and rare sillimanite. It was intruded by a muscovite leucogranite and by microgranitic veins (Figure 1).

The mineralisation is hosted in a cross-patterned quartz vein stockwork covering 1.3 km × 0.3 km. The recognised extension was 300 m long, with 200 m downwards dip. The mine is located between 400 and 700 m elevation at the surface, across a steep slope above the Lot river valley.

The ore-bearing veins paragenesis comprises quartz, wolframite, scheelite, fluorapatite, while the hydrothermal alteration selvages paragenesis comprises tourmaline (schorl), sericite and sulphides in a quartz greisen. Sulphides come as a first phase (pyrite, arsenopyrite) and a second phase (chalcopyrite, molybdenite, bismuthinite, marcasite), followed by a late carbonate phase. Secondary minerals developed through weathering include oxyhydroxides, hydrated sulphates, and arseniates, the most conspicuous being scorodite.

The vein-type, perigranitic nature, and the structural control result in a high arsenopyrite contents in the veins and their host rocks. Late Variscan leucogranitic magmatism and fluid circulation is believed to be the origin of mineralisation (Lerouge et al., 2000; Goer de Herve et al., 2006).

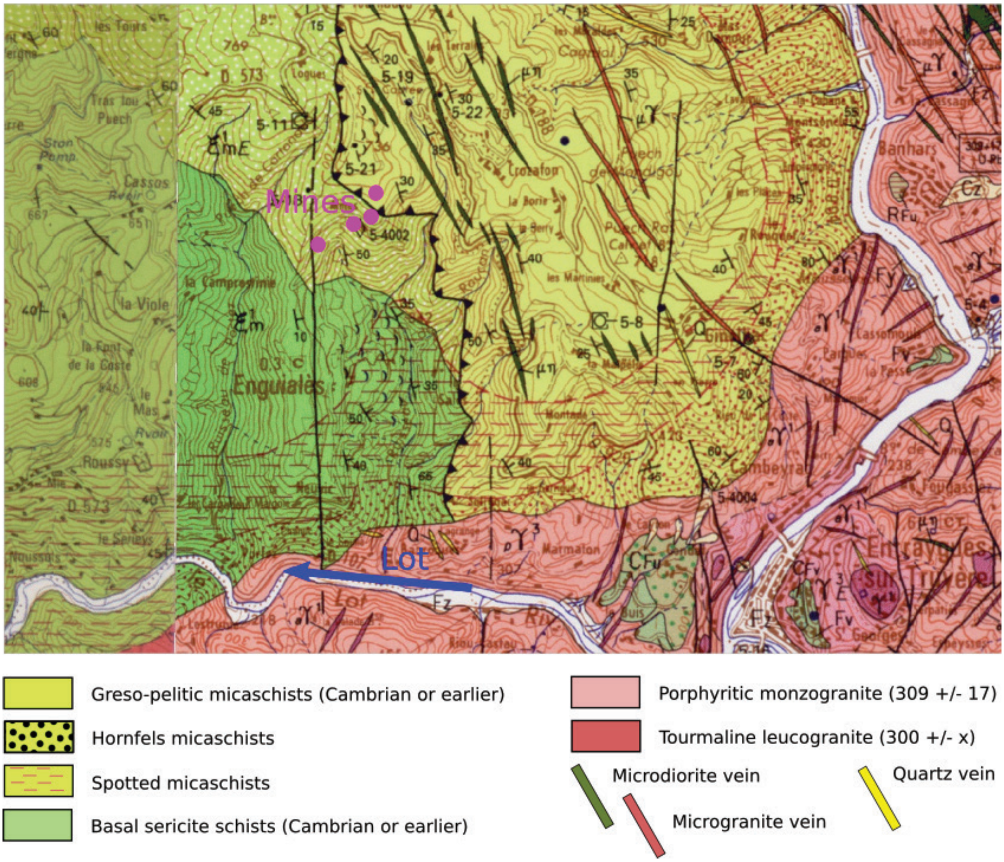

***Figure 1:** Geological map (from the 1:50000 map, Goer de Herve et al., 2006) – colours differ slightly between cations and map due to stitching of two map images, see text for disambiguation.*

The deposit was discovered in 1957 and mined from 1969 to 1978. Irregular distribution, recovery and productivity issues, and W price collapse (1971) led to mine closure in 1979. A total 450,000 t of ore averaging 0.6% WO_3 was mined, yielding 1 300 t of 70% WO_3 concentrates.

Ore beneficiation, according to the 1978 flow sheet, comprised crushing and staged milling (size fractions 5mm, 2mm and 0.8mm), pulp preparation, classification, and gravity sorting using jig concentrators or shaking tables. A last concentration step was later added with froth flotation, using mainly gas oil, and then probably specific reagents such as xanthates.

Processing residues comprised therefore +2-5mm gravel, +0.8-2mm dried sand, <0.8mm thickened sand, and sulphidic decantation sludge. Process waste was dumped down the topographic slope out of the galleries. Most waste rock seems to have been used to build platforms and access tracks.

Environmental impacts

The Enguialès mine site is currently managed as abandoned with no responsible party. The first environmental studies were led in connection with EU mining waste inventories (Cottard et al., 2002). The widespread occurrence of As-bearing phases in waste dumps was recognised by Courtin-Nomade et al. (2003) and confirmed by subsequent studies (unpublished data, 2017).

The structural control still applies to site hydrogeology and the faulted network channelizes the As-rich fluids. Pyrite oxidation provided extensive Fe hydroxide coatings. Mining and beneficiation methods determined waste and residues typology. The underground mine opens on a steep topographic slope, on which waste rock and tailings were disposed. A first generation of gravity sorting on coarse mill feed gave moderately reactive quartz tailings, while later finer mill feeds and floatation techniques gave highly reactive and mobile tailings, with much higher As contents. Fast erosion of the latter, accelerated by the steep topography and the intensity of the rainy episodes, contributes to a high As load of surface water in particulate form. Acidic mine runoff is discharged nearby, favouring As and metals solubility, in the absence of any neutralising host rocks traps. Fe hydroxide fracture coatings behave as natural arsenic retardants through sorption phenomena. This reduces groundwater As migration.

Methods

On-site analyses of waste were performed using portable X-ray fluorescence (pXRF) spectrometers. Both soil (Compton) and mining/geochem (fundamental parameters) modes were used in order to cover a large range of elements (As, Ba, Ca, Cr, Fe, K, Mn, Ni, Pb, Rb, S, Sn, Sr, Ti, V, W, Zn, Zr), with 60 to 120 s counting times. Blanks, duplicates and periodic CRMs measurement ensured relative accuracy. Absolute accuracy was evaluated using laboratory analyses, performed by ICP/AES and ICP/MS after acid digestion of alkali sintered samples.

Water analyses were performed on site for physicochemical parameters (pH, ORP, EC) and by laboratory methods (ICP/AES, ion chromatography) for major ions and trace elements.

Water monitoring on site was performed for 49 days in the (TB 465) runoff using an YSI 6920 multiparametric recording probe. The probe was calibrated offsite using standard solutions and checked onsite with an YSI control solution. It recorded hourly pH, temperature, electrical conductivity (EC), redox potential (ORP), turbidity and dissolved oxygen (DO).

The probe was placed in a pipe retained by a dam of stones between the mine drainage spring and a small pond (Figure 2).

Figure 2 : Mine drainage spring (left) and pipe hosting the multiparametric probe (right)

Figure 3 : The probe as recovered (left) and after gentle wiping (right)

***Table 1.** Results of the verification of the sensors of the probe with standard solutions*

Parameter	Unit	Standard solutions	Measured value at 21°C
Conductivity (EC)	µS/cm	1332	1420
pH		4,01	3,6
Redox (ORP)	mV	220	220
Redox (ORP)	mV	470	500
Dissolved oxygen (DO)	%	100	101
Dissolved oxygen (DO)	%	0	21

At the end of the monitoring period, the sensors were checked to evaluate their response to clogging by iron precipitate (Figure 3). The results of this verification are presented in Table 1.

Sensors show a relatively low drift given the important deposits on their surfaces, with the exception of the DO sensor for low concentrations. If the absolute values provided by the probe require a critical reading, their relative variations reflect the events affecting mine drainage.

In order to compare the variations of the mine drainage physico-chemical parameters with precipitation, rainfall data recorded by a nearby (9 km) weather station were used.

Results and discussion

Detailed site investigations by Cottard et al. (2002) and Courtin-Nomade et al. (2003) showed that the main environmental impact of the former mine was As emission towards surface water, resulting from acid drainage out of the mine galleries and from the meteoric leaching of the waste dumps. Dissemination in host micaschists leads also to locally high As concentrations, usually on iron hydroxide coatings that scavenge As from groundwater (Couture et al., 2013).

In order to understand better the origin of acid drainage, the mine runoff was continuously monitored. The mine drainage reaction to short but intense rainfall events was studied. An inventory of the extent of site contamination and of transport modes of the contaminants (both in solute and in particulate form) were carried out.

Solid waste

The process waste deposits were mapped and analysed using pXRF in order to delineate source areas and to establish a preliminary ranking of their hazardousness. This was based on total As only, as no As speciation

***Figure 4** As-bearing coarse gravity sorting residues in dumps (left) - eroded As-rich floatation residues in gravity dumps (right)*

data could be collected. However, the deeply oxidised erosion profile (Figure 4) suggests that, even if the As leachable fraction differs significantly from the total As, the ranking of source areas and the remediation options remain the same.

Two types of residues occur as separate masses along the slope. Coarse-grained quartz-rich material occurs on the outer sides of the dump. It is believed to be the residue of earlier mechanical gravity sorting processes. Their composition is roughly similar to the hydrothermally altered micaschists (Table 2, Table 3) but with anomalously high As and W. They are partly covered by vegetation.

Fine-grained (<1mm) residues occur in the central part of the dump, near the former plant. They are believed to result from later floatation processes with gas-oil and xanthates. A GC/MS scan confirmed the abundance of heavy petroleum hydrocarbons (C10 to C40), did not identify aromatic hydrocarbons but found S-bearing metabolites, probably from xanthates degradation. Their composition is also roughly similar to the hydrothermally altered micaschists (Table 4) but with anomalously high Zn and Cu, and very high As and W. This part of the dump is severely eroded (Figure 4) and carried away to the river, especially during rainstorms. Almost no vegetation grows on this material.

Significant deviations were observed with ICP/AES analyses after aqua regia digestion for Sn, Ti, W, and Zr. For these elements, pXRF results are often more accurate than aqua regia analyses (Lemiere, 2018).

Mine water

Most of the mine drainage is observed as runoff at the TB465 outlet. It is then discharged to a nearby creek and then to the Lot river, 2km downstream. The outlet and the creek were monitored through sampling programs (Cottard et al., 2002, and later unpublished data).

The probe remained in place for 49 days, but iron hydroxide precipitate heavily clogged its sensors. When the probe was recovered, the pipe in which it was placed was completely clogged. Water was no longer flowing through the pipe, but the probe was still in the pond water. Consequently, the recorded values correspond to the physico-chemical parameters of this pond.

Results of conductivity, pH, temperature, dissolved oxygen concentration and rainfall measurements are presented in Figure 5. The ORP sensor seems to have been particularly affected by precipitates, as it hardly recorded

Table 2. *Statistics of pXRF measurements on host micaschists and derived soil, in mg/kg*

	As	W	Mo	Pb	Zn	Cu	Sb	Sn	S	Fe	Mn	Ti	Ca	K	Ba
nb values	19	5	0	15	18	17	15	15	4	20	19	20	19	20	20
mini	16	49		14	32	31	25	32	2723	29015	221	660	307	3929	200
maxi	2034	488		282	225	370	110	100	4076	152090	1659	5855	5355	29311	1633
median	70	112		28	88	101	56	64	3377	49803	594	2606	678	18761	1026
average	325	178		47	92	118	59	63	3388	62831	688	2906	927	17521	969

Table 3. *Statistics of pXRF measurements on coarse residues, in mg/kg*

	As	W	Mo	Pb	Zn	Cu	Sb	Sn	S	Fe	Mn	Ti	Ca	K	Ba
nb values	11	11	6	11	8	10	3	7	4	11	11	11	11	11	11
mini	432	91	9	34	29	37	25	28	1487	32914	212	1886	485	12441	167
maxi	3122	1898	18	134	50	168	35	56	4811	93991	563	3477	1091	24926	579
median	598	366	11	47	36	49	33	34	2649	44522	257	2531	692	17457	401
average	898	464	12	60	38	66	31	38	2899	47254	300	2554	769	18195	398

Table 4. *Statistics of pXRF measurements on fine-grained residues, in mg/kg*

	As	W	Mo	Pb	Zn	Cu	Sb	Sn	S	Fe	Mn	Ti	Ca	K	Ba
nb values	52	52	14	51	30	42	8	35	22	52	50	52	51	52	51
mini	214	153	10	21	31	37	25	18	1296	13473	128	461	319	1872	180
maxi	212336	9423	35	422	1578	6066	73	87	51361	776331	1527	7592	1823	29131	722
median	830	1031	13	57	52	91	36	30	2246	41606	362	2559	699	18357	422
average	11700	1479	16	81	118	445	41	33	8784	86598	420	2654	762	17725	426

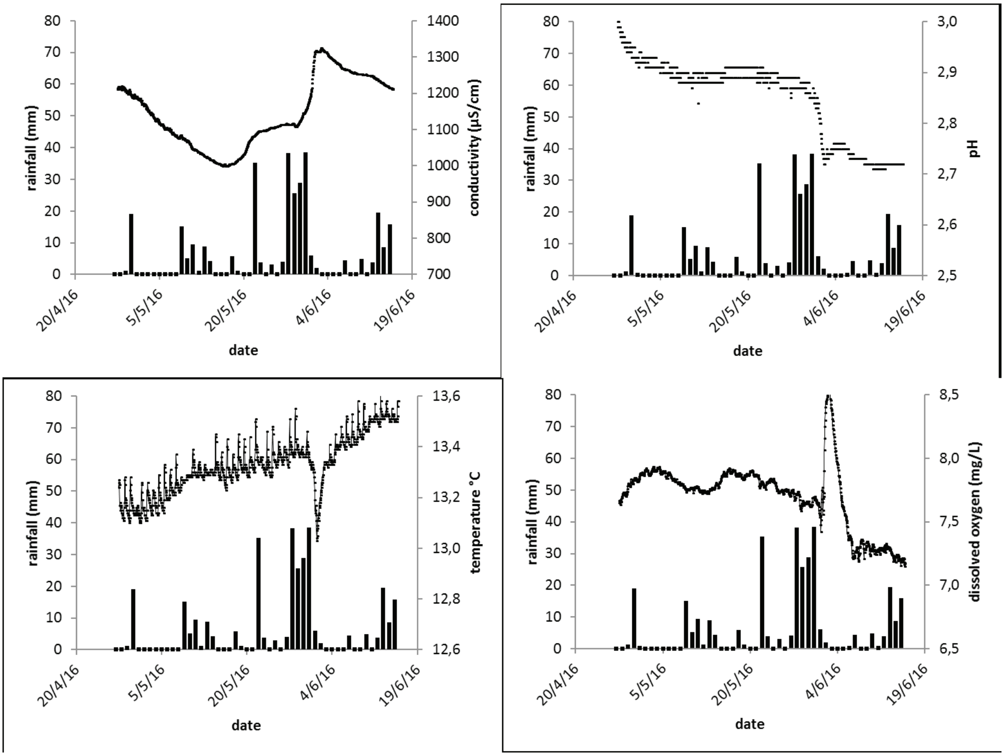

Figure 5 *Conductivity, pH, temperature, dissolved oxygen concentration and rainfall during water monitoring period*

any significant variations. The recorded data are largely unusable and therefore the results of the ORP measurements are not presented.

The monitoring period saw a continuous heavy rain event from May 28 to 31, and an intense but isolated rain event on May 22. The remainder was generally dry with a few days of low rainfall.

EC shows a sharp increase between May 28 and June 1st, followed by a slow decrease until the end of the period. This increase is due to the leaching and dissolution of soluble oxidized minerals in the mine levels above the water table. These minerals were washed during the rain event while they are usually out of the water. pH is globally stable until a sharp acidification episode between May 31 and June 2. This acidification is probably due to the leaching of oxidised sulphides in the mine cavities. When above the water table, they react with air oxygen and with the seepage of oxygenated water. During an intense rain event, they dissolve very quickly, releasing sulphuric acid and soluble metals (Fe, Pb, Zn, etc.).

Water temperature shows a seasonal increase between 13.2 and 13.6°C. Between May 30 and June 2, the temperature drops and then rises sharply, during and after the main rain event. Besides the influx of colder rainwater, it could be due to a decrease in the residence time underground. This is further supported by the time shift between rainfall and temperature change, which would not be observed if the mine aquifer did not play a role.

DO is generally stable except for a sudden increase between May 31 and June 2, followed by a slower decrease until June 6. This increase is probably due to a flowrate drainage increase at the emergence caused by the higher water pressure load due to water inflow. DO variations would therefore indirectly reflect drainage flow variations. DO decrease would represent the progressive drain until the mine returns to its background flow.

Heavy rains were followed by strong increases in acidity and conductivity, As, sulphate and metal contents. The increase in As and metal contents being concomitant with the increase in flow rate, this means that despite their short duration, these events can represent a significant proportion of the As and metal discharge to the environment throughout the year.

Conclusions

The main impact of the abandoned mine is the release of arsenic towards surface water, through process waste erosion and leaching, and through mine runoff. For the former, fine-grained floatation residues are the main source. The steep slopes and the stormy rainfall regime imply that erosion contributes massively to As particular transport, while solute As release could not be precisely located. As leaching is probably active but diffuse. For the latter, water monitoring showed a slowly mitigating As release from the mine runoff but does not allow to investigate in detail the relationships with meteoric events. Continuous monitoring is more efficient for transfer evaluation and modelling than periodic sampling. Such data are essential for site management and to minimise long-term environmental impacts.

References

Bogdanoff S., Cirodde J.L., Ploquin A, Ramboz C (1987) - Recherche du tungstène dans le district de la Châtaigneraie (Cantal, Aveyron - Massif Central français). Géochimie des schistes de la Châtaigneraie. Chronique de la recherche minière, 487, 11-30.

Cottard F., Bouroullec I., Dutartre Ph., Fleury L. (2002) – Audits environnementaux de six mines fermées ou abandonnées de la région Midi-Pyrénées. Rapport BRGM RP-51538-FR. 76 p., 8 fig., 20 tabl., 3 ann.

Courtin-Nomade A, Bril H, Neel C, Lenain J-F (2003) - Arsenic in iron cements developed within tailings of a former metalliferous mine-Enguialès, Aveyron, France. Appl Geochem 18(3):395–408.

Couture, R.M., Rose, J., Kumar, N., Mitchell, K., Wallschläger, D. & Van Cappellen, P. (2013) - Sorption of arsenite, arsenate, and thioarsenates to iron oxides and iron sulfides: a kinetic and spectroscopic investigation. Environ Sci Technol. 4, 47(11):5652-9.

Goër de Hervé A. (De), Bogdanoff S., Couturié J.P. (2006) – Geological map of France (1/50 000), sheet Entraygues-sur-Truyère (836). Orléans : BRGM. Explanatory notes by M. Duguet, S. Bogdanoff, M. Turland, P. Nehlig, P. Lebret, G. Ricodel, R. Simon-Coinçon, M. Thiry (2006), 173 p.

Lemiere, B. (2018) - A review of pXRF (field portable X-ray fluorescence) applications for applied geochemistry. Journal of Geochemical Exploration 188, 350–363.

Lerouge, C., Bouchot, V. & Guerrot, C. (2000) - Fluids and the W(±As,Au) ore deposits of the Enguialès-Leucamp District, La Châtaigneraie, French Massif Central. Journal of Geochemical Exploration 69–70, 343–347.

Monié P., Bouchot V., Faure M., Charonnat X., Najoui K. (1999) - 40Ar/39Ar Laser-Probe Dating of W, Au and/or Sb Deposits and associated granites in the Southern French Massif Central (Cévennes, Châtaigneraie). EUG 10, abstract volume, Strasbourg, France.

Seasonal river flow-through as a pit lake closure strategy: is it a sustainable option in a drying climate?

Mark A. Lund[1], Melanie L. Blanchette[1], Colm Harkin[2]

[1] *Mine Water and Environment Research Centre, Centre for Ecosystem Management,*
Edith Cowan University, 270 Joondalup Drive, Joondalup WA6027 Australia.

[2] *Premier Coal Ltd, Premier Rd, Collie WA6225, Australia*

Abstract

River flow-through has been used to effectively close pit lakes, however much of the evidence for this comes from permanent rather than seasonal rivers. Lake Kepwari (a former open-cut coal mine in Western Australia) was connected to the seasonal Collie River for closure. River water improved lake water quality but the lake caused varying downstream hydrological and chemical changes. Consecutive years of low rainfall resulting in low lake water levels could delay or reduce downstream flows and increase lake acidity. Using seasonal rivers as sources of flow-through presents a riskier scenario than using permanent rivers, particularly in a drying climate.

Keywords: AMD, ecology, salinity, mine water

Introduction

River flow-through – where a river is directed through a pit lake to improve lake water quality – has been successfully used in Germany and Austria to close pit lakes (see McCullough and Schultze 2015). Blanchette and Lund (2016) and Lund et al. (2013) proposed that pit lake catchments could be an important source of carbon for pit lakes, driving natural ecological succession, but that catchments were typically too small to be effective. River flow-through is a way to significantly increase the catchment area of a pit lake, resulting in potentially greater access to carbon, alkalinity, sediment and biological propagules.

River flow into pit lakes can be either 'controlled' (through inlet/outlet structures or pumps) or 'uncontrolled' (where the river flows through the lake unrestricted). However, this closure technique can also result in excessive nutrients, contaminants (e.g., organic pollutants), and unwanted taxa in the lake (McCullough and Schultze 2015). Downstream, the river water may be contaminated by lake decant. Of particular concern in more arid parts of the world, the river's natural hydrological regime below the pit lake may be altered by reductions in peak and base flows, and altered timing of flows (McCullough and Schultze 2015).

Unlike the above examples in Germany and Austria, many Australian rivers are characterised by highly variable flows, with seasonal drying followed by intense flows for short periods during the rainy season (Blanchette and Pearson 2012). Therefore, unlike permanent rivers, we contend that seasonally-flowing/intermittent rivers pose greater challenges for closure based around river flow-through, especially in light of current and projected climate change-related drying (driven by a combination of anthropogenic activities, variations in El Niňo-southern oscillations, tropical Atlantic sea surface temperatures, and Asian monsoons; (Dai 2011)). Further, the spatial extent of intermittent rivers is expected to rise with global increases in drying (Jaeger et al. 2014), suggesting that even current 'permanent' river flow-throughs may be under future threat.

The aim of this paper is to investigate the impacts of seasonal river flow-through on a former acidic coal pit lake in Western Australia on downstream environments, focusing on the hydrological and water quality changes to the river water entering and leaving the lake. We also consider future implications of this technique in the context of an unpredictable future climate.

Methods

Study Site

The Collie pit lake district (Lund et al. 2012) in Western Australia contains over 10 pit lakes formed from open-cut coal mining. Dating back to the 1960s, the water qualities of these pit lakes have remained largely unchanged since filling (e.g., pH mostly 3-4.5, Al-buffered, (Lund and McCullough 2008)). The largest of the Collie pit lakes is Lake Kepwari, around which the Collie River South Branch (CRSB) had been diverted to allow mining to occur. The initial mine closure concept was for Lake Kepwari to become a water ski park, but did not include connection to the seasonally-flowing CRSB. Instead, the lake water level was established under a rapid fill programme whereby river water was diverted to the mine void during periods of high flow. This had the added advantage of managing acidification of the lake by preventing further oxidation of sulphides in the exposed coal seams. The lake water level was then to be maintained by seasonal top-up of the lake under high river flow conditions, with no discharge from the lake. In 2011 the CRSB breached the wall separating the lake from the diversion channel after a large rainfall event, adding river water to the lake (McCullough et al. 2012)Western Australia</pub-location><publisher>IMWA</publisher><urls></urls></record></Cite></EndNote>. A more limited previous study noted few consequences of the breach on the river downstream (McCullough et al. 2013) resulting in government approval to connect the river to the lake, initially as a 3-year trial. The final closure plan includes backfilling of the diversion channel and permanent uncontrolled inlet and outlet structures to allow the river to flow unimpeded through the lake.

Collie is situated in an area of Mediterranean climate, with hot, dry summers (range 11.7–30.5°C) and cool, wet winters (range 4.2–16.3°C) (Commonwealth of Australia, Bureau of Meteorology (BOM) 18/5/2018). Seventy-five percent of the rainfall occurs during the five months from May to September (Figure 1). The 100-year mean annual rainfall for the Collie Basin is 933.1 mm, (BOM) 18/5/2018), although this has decreased to an average of 731 mm over the last 15 years. Evaporation rates for the area are not routinely measured by the BOM weather stations in the region, but it supplies an atlas of potential evaporation rates.

Total annual rainfall in Collie between 2003 and 2016 ranged between 390 mm (2010) and 902.2 mm (2005) (Figure 1). During this study, rainfall was low in 2015 (475.4 mm), while both 2014 and 2016 had average or above average rainfall. The CRSB has a catchment area of 66 047 ha, which is primarily native forest with 24% cleared for farmland and <5% disturbed by mining (Harper et al. 2005). Groundwater is generally lower than river bed, with the exception of a few pools which are groundwater discharge areas. Since 2002 (when Lake Kepwari began filling), the

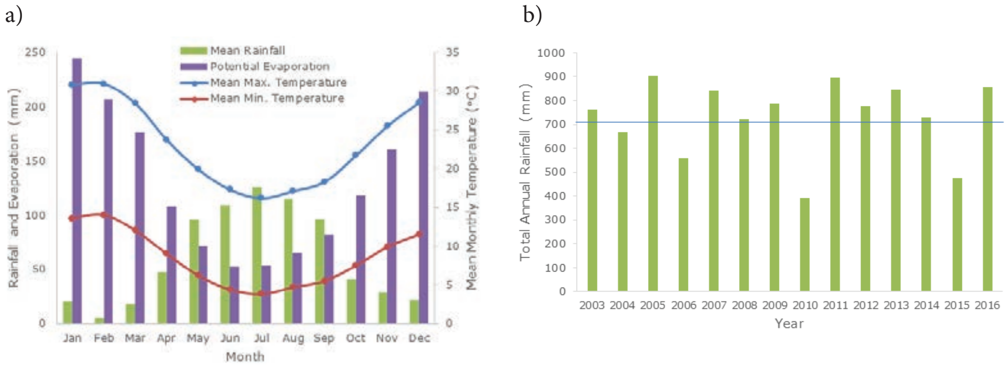

Figure 1. *a) Mean monthly minimum and maximum air temperatures, and mean monthly total rainfall and potential pan evaporation, (Collie East Station, 2002-2016 and Evaporation Atlas) and b) total annual rainfall 2003 to 2016, with average shown (blue line; Collie East, except for 2013 which comes from Collie) Data supplied by the Commonwealth of Australia Bureau of Meteorology.*

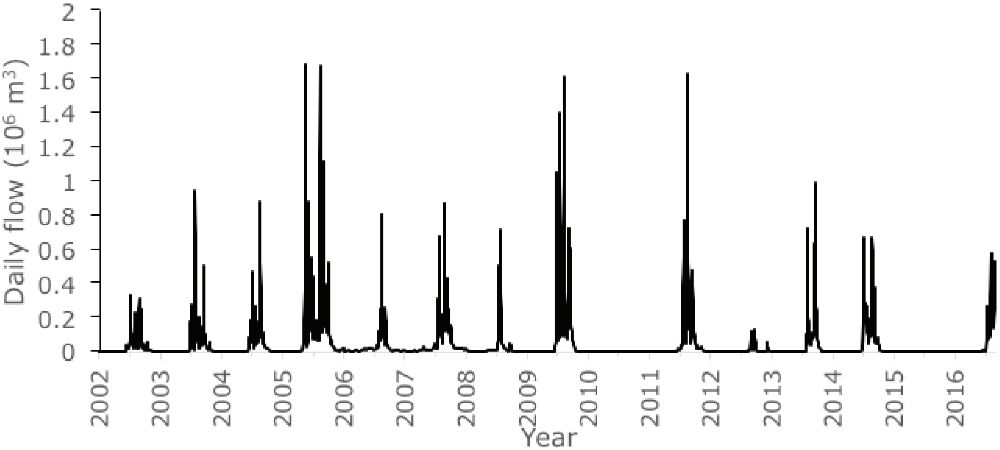

***Figure 2** Total daily flows in the Collie River South Branch 2002 to October 2016 (Shultz Weir Gauging Station, Department of Water (WA)).*

maximum flow at the gauging station downstream of the lake was recorded on 20 May 2005 at 1.69 x 10^6 m3 Figure 1). Total annual flow ranged from zero flow in 1969, 1970 and 2015 to 217.5 x 106 m3 in 1964 (median 20.7 x 106 m3). Average annual flows for each decade (1952-2000) exceeded 28.1 x 106 m3, which has declined over time (2000s; 15.1 x 106 m3 and 2010s currently 10.7 x 106 m3) possibly reflecting declining rainfall (Varma 2002).

Data collection

A water budget was estimated for Lake Kepwari between 2010 and 2016. After the commencement of river flow through in 2013, river inflows and outflows were measured every 15 minutes (2013-2016) using automatic gauging stations, as were select physicochemical data (pH, turbidity, conductivity). Additional measures of water quality (e.g., zinc, net alkalinity, DOC) were sampled monthly by hand (2013-2016; n=35 inlet and n=42 outlet). As the 2011 breach was an unexpected event, inflows and outflows for this breach event were estimated based on McCullough et al. (2012)Western Australia</pub-location><publisher>IMWA</publisher><urls></urls></record></Cite></EndNote>.

Rainfall data for Collie during the study period were sourced from the BOM. There was no pan evaporation data available for Collie or surrounds, however the BOM Climatic Atlas of Australia provided potential evaporation data at Collie as a monthly average. To generate evaporation data for each month of the study period, the potential evaporation data for Collie was adjusted for each month using the ratio of Perth actual monthly evaporation to the Perth long term average monthly evaporation (n.b., Collie is approximately 200 km south of Perth). The lake height data (Australian height datum; AHD) was taken as the value closest to the start of each month (where multiple measurements were available), and linear interpolation was used for missing data. Lake height to lake area and volume was taken from Salmon et al. (2017) and used to develop a hypsographic curve. Polynomial lines of best fit were then applied to calculate the volume and area for any lake water height. Groundwater input and output was estimated from data in Varma (2002). Surface runoff was based on a total catchment area of 150 ha (Lund et al. 2013), and a runoff coefficient estimated at 0.25 (approximating those estimated for the lake by Varma (2002)).

Results and Discussion

Overall, the water budget (Table 1) indicated that *excluding river inflows the lake existed in a slight water deficit, where [(groundwater* *in) + (surface inflow) + (direct rainfall)] < [(evaporation) + (groundwater out)], which has been previously estimated as 0.8 GL per annum* (Platt et al. 2012). Therefore, under most circumstances (c.f., extraordinary scenarios such as extreme direct rainfall over the pit lake or geological or engineering faults – causing the lake to decant without river water inflow), when seasonal river flows commence, the lake will fill first, then an equal or lesser amount of the inflow water volume will flow downstream – either with or without substantial delay after inflows.

There was an error (up to 2.2 GL) associated with the water budget (Table 1), with the greatest error (difference between water inputs and outputs) occurring in years with river inflow, suggesting gauging station error. This error was likely due to unmeasured overtopping of the former breach point in September 2013, 2014 and again in 2016 (increasing river outflow volumes).

Outflows from Lake Kepwari were generally similar in timing and magnitude to inflows, and discharge often continued after inflows ceased (Figure 3). The downstream impact of the lake was most obvious in 2015 when antecedent conditions (low rainfall, high evaporation rates) resulted in low water levels within the lake, delaying outflows by three months as the lake was filled first. In the same way, high lake water levels facilitated outflow from the lake, as small amounts of rainfall across the lake catchment resulted in outflows even when there was no inflow. Future research will examine the impacts of the lake on downstream hydrology in more detail, although these results suggest that if there were several years of low rainfall that resulted in low lake water levels, downstream flows could be substantially delayed.

Changes in water chemistry can occur between inflows and outflows due to chemical interactions and precipitation in the lake (McCullough and Schultze 2015). The pH in the lake was generally lower than the river water flowing in, although lake water did not drop below pH 6 (Figure 4). Conductivity of river water inflows was highly temporally variable (1-6 mS cm^{-1}), although moderated by lake water, and, upon release at outflow, was of similar conductivity (2-3 mS cm-1) throughout the year. Particulates in the river could be expected to settle out in the lake as the river water moved through the larger water body (McCullough and Schultze 2015). However, in Lake Kepwari, the data indicates that turbidity at outflows was not consistently lower than at inflows, although the nature of the turbidity may have changed (e.g., became more algal-dominated). During the study period, acidity was either being produced in or entering the lake via aquifers before being neutralised by river inflows. Therefore, several years of poor rainfall could result in the lake becoming increasingly acidic due to a lack of river water input. Lake Kepwari is a sink for dissolved organic C (DOC), which

Table 1. *Water budget for Lake Kepwari 2010 to 2016 showing inputs, outputs and the error associated with the calculation*

	Inputs				Outputs			Summary		
Years	Rainfall Direct (ML)	Groundwater In (ML)	Surface Runoff (ML)	River Inflow (ML)	Evaporation (ML)	River Outflow (ML)	Groundwater Out (ML)	Total Inputs – Outputs (ML)	Change in Lake Volume (ML)	Error (ML)
2010	396.5	292.0	57.9		1111.1		224.9	-589.6	-538.2	-51
2011	1011.0	292.0	132.5	1900.0	1163.1	600.0	273.8	1298.5	1261.8	37
2012	857.5	292.8	111.5		1125.7		256.2	-120.0	-375.5	255
2013	822.2	292.0	112.0	9473.5	1091.5	8754.1	255.5	598.6	-342.0	941
2014	761.0	292.0	99.5	8682.5	1124.6	10852.9	255.5	-2398.0	-154.2	-2244
2015	511.0	225.2	72.9	28.3	1129.9	3.7	255.5	-551.6	67.9	-620
2016	964.8	219.6	128.9	10793.4	1075.6	12078.1	390.2	-1437.1	68.0	-1505

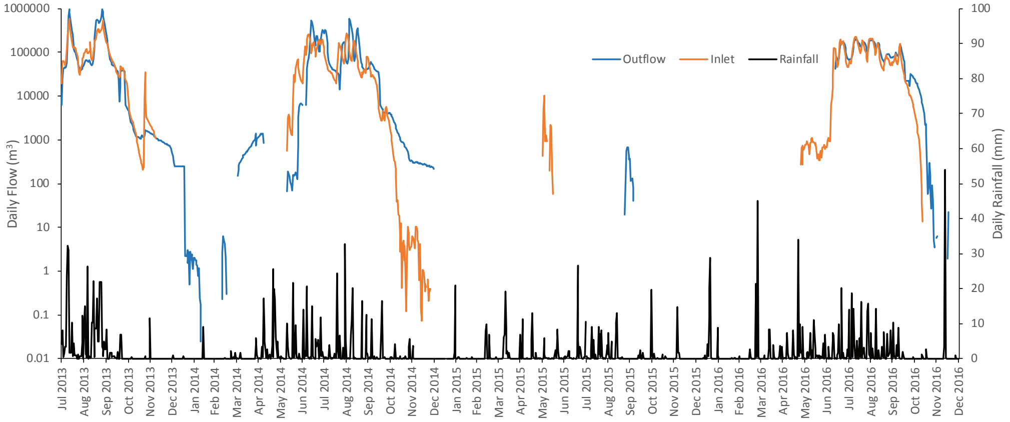

Figure 3 *Collie River inflows and outflows through Lake Kepwari compared with rainfall (2013-2016). Rainfall for 2013 provided by BOM (for Collie), other years use rainfall data provided by PCL as fewer missing dates.*

a) pH

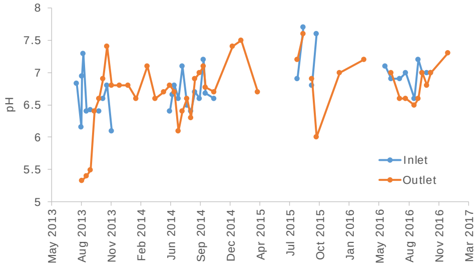

b) Conductivity

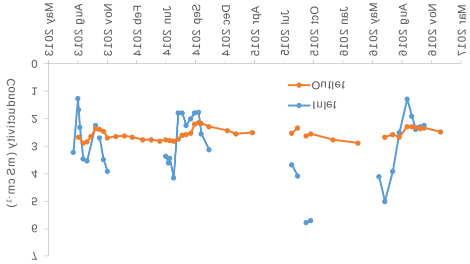

c) Turbidity

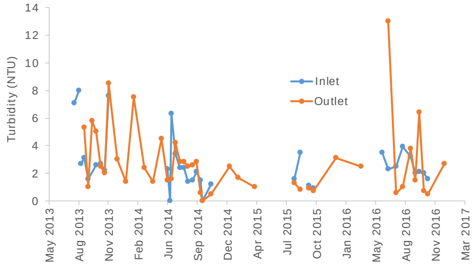

d) Nett Alkalinity

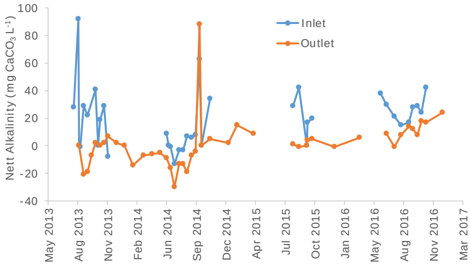

e) DOC

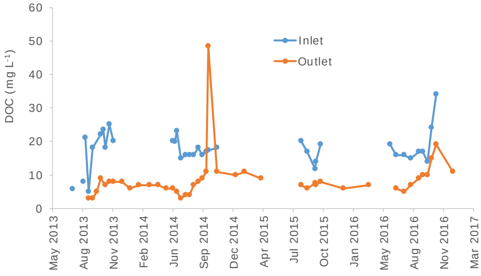

f) Zinc

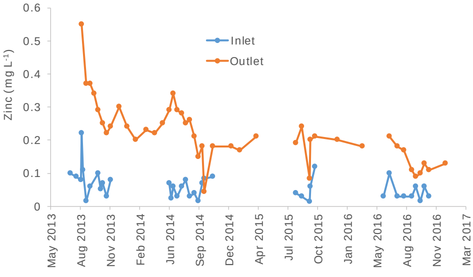

Figure 4 *Physico-chemical parameters for the river inflow and outflow from Lake Kepwari (2013-2016).*

likely benefits ongoing ecological evolution of the lake (Blanchette and Lund 2016). Zinc concentrations (initially high in the river) increased approximately three fold in the outflow, although the high hardness of the waters ameliorated exceedances of trigger values (>0.28 mg L-1 for the outflow) for the protection of aquatic ecosystems (moderately disturbed, 80%)(ANZECC/ARMCANZ 2000).

River flow-through has improved the water quality in Lake Kepwari (e.g., C storage, neutralised pH, increased net alkalinity) to the extent that permanent flow-through has been accepted and agreed by government as an appropriate mine closure strategy. However, flow-through has had a statistically significant effect on the downstream environment by: changing the hydrology of the river, increasing zinc, reducing EC variability, and reducing overall DOC. The Collie River downstream of Lake Kepwari is relatively short (≈15 km) and already highly modified. Therefore, the downstream impacts from the flow-through may be an acceptable trade-off compared to the social and economic benefits associated with the lake's proposed future use for recreation. Our research suggests that using seasonal rivers as sources of flow-through to close acidic pit lakes presents a riskier scenario than using permanent rivers, particularly in light of climate change projections (Dai 2011). However, given the predictions that even permanently flowing rivers may become intermittent (Jaeger et al. 2014), the application of this strategy may be limited. Clearly, careful planning based on projected water volume and acceptance of any downstream impacts is required before river flow-through is used to close pit lakes.

Acknowledgements

This research was funded by Australian Coal Association Research Program C23025, Premier Coal Ltd (managed by Yancoal Australia) and Lanco-Griffin Coal. The authors thank Digby Short (formerly of Premier Coal Ltd) and at Edith Cowan University, C.D. McCullough, Naresh Kumar, Michelle Newport, Jahir Gonzalez Pinto, Mark Bannister and a range of volunteers.

References

ANZECC/ARMCANZ (2000) Australian and New Zealand guidelines for fresh and marine water quality, Volume 1. The guidelines (chapters 1 – 7). Australian and New Zealand Environment and Conservation Council and Agriculture and Resource Management Council of Australia and New Zealand, Canberra

Blanchette ML, Lund MA (2016) Pit lakes are a global legacy of mining: an integrated approach to achieving sustainable ecosystems and value for communities Current Opinion in Environmental Sustainability 23:28-34 doi:http://doi.org/10.1016/j.cosust.2016.11.012

Blanchette ML, Pearson RG (2012) Macroinvertebrate assemblages in rivers of the Australian dry tropics are highly variable Freshwater Science 31:865-881

Dai A (2011) Drought under global warming: a review. Wiley Interdisciplinary Reviews: Climate Change 2:45-65

Harper RJ, Smettem KRJ, Tomlinson RJ (2005) Using soil and climatic data to estimate the performance of trees, carbon sequestration and recharge potential at the catchment scale Australian Journal of Experimental Agriculture 45:1389-1401

Jaeger KL, Olden JD, Pelland NA (2014) Climate change poised to threaten hydrologic connectivity and endemic fishes in dryland streams. Proceedings of the National Academy of Science USA 111:13894-13899

Lund MA, McCullough C Limnology and ecology of low sulphate, poorly-buffered, acidic coal pit lakes in Collie, Western Australia. In: Rapantova N, Hrkal Z (eds) Mine Water and the Environment, Karlovy Vary, Czech Republic, 2008. VSB – Technical University of Ostrava, pp 591-594

Lund MA, McCullough CD, Kumar RN The Collie Pit Lake District, Western Australia: An Overview. In: McCullough CDL, M.A.; Wyse, L. (ed) International Mine Water Association Symposium., Bunbury, Australia, 2012. IMWA, pp 287 – 294

Lund MA, Van Etten EJB, McCullough CD Importance of catchment vegetation and design to long-term rehabilitation of acidic pit lakes. In: Brown A, Figueroa L, Wolkersdorfer C (eds) Reliable Mine Water Technology – International Mine Water Association, Denver, Co, 2013. Publication Printers, pp 1029-1035

McCullough C, D., Schultze M Riverine Flow-Through of Mine Pit Lakes: Improving both Mine Pit Lake and River Water Quality Values? In: Agreeing on solutions for more sustainable mine water management – 10th ICARD & IMWA Annual Conference, Santiago, Chile, 2015. GECAMIN, p Paper 199

McCullough CD, Ballot E, Short D (2013) Breach and decant of an acid mine lake by a eutrophic river: river water quality and limitations of use. Paper presented at the Proceedings of the Mine Water Solutions 2013 Congress, Lima, Peru.,

McCullough CD, Kumar RN, Lund MA, Newport M, Ballot E, Short D Riverine breach and subsequent decant of an acidic pit lake: evaluating the effects of riverine flow-through on lake stratification and chemistry. In: International Mine Water Conference, Bunbury, Western Australia, 2012. IMWA,

Platt J, Tingey W, Sparks TC (2012) Collie River salinity recovery – improving water resource outcomes in a competing environment. Paper presented at the 15th International RiverSymposium 8-11 October, Melbourne, Australia,

Salmon SU, Hipsey MR, Wake GW, Ivey GN, Oldham CE (2017) Quantifying Lake Water Quality Evolution: Coupled Geochemistry, Hydrodynamics, and Aquatic Ecology in an Acidic Pit Lake Environmental Science & Technology doi:10.1021/acs.est.7b01432

Varma S (2002) Hydrogeology and groundwater resources of the Collie basin, Western Australia. Water and Rivers Comminission, Perth

Modelling Complex Mine Water Closure Challenges using a Coupled FEFLOW-GoldSim™ Model

Nick Martin[1], Michael Gabora[1]

[1]*DHI Water & Environment, Inc., 141 Union Blvd., Suite 250, Lakewood, CO 80228, USA, nick.martin@ stanfordalumni.or*

Abstract

A current limitation in modelling pit lake evolution from active mining through closure to optimise management strategies is the separation between physical process and operational modelling tools. To overcome this limitation, a GoldSim™ water balance model of pit operations is dynamically coupled with a FEFLOW, physically-based, model of groundwater inflow to the pit. This approach can be used as part of mine project planning to provide robust estimates of conditions at closure, including an improved representation of the pit lake system physical response, closure cost analysis, and risk assessment through uncertainty analysis.

Keywords: GoldSim™, FEFLOW, dynamic coupling, risk assessment, uncertainty analysis

Introduction

Mine water management strategies can be complex and composed of multiple facets, which depend on operating, physical site, and climatic conditions. Pit lake water management concerns include operational components like: diversions to and from the lake as part of ore processing and management of water at other site facilities; and, maintenance of target lake levels to provide for storage of excess storm water and to limit pumping head. Physical site concerns include groundwater inflow, near-surface, and surface water runoff. Lake evaporation and direct precipitation are often important meteorological conditions for pit lake management strategies.

One of the current limitations in modelling pit lake evolution from active mining through closure to optimise management strategies is the separation between physical process and operational modelling tools. To overcome this limitation, a GoldSim™ water balance model of pit operations is coupled with a FEFLOW, physically-based, model of groundwater inflow to the pit. The combined modelling approach allows detailed and realistic operations, physical site, and climatic representation.

GoldSim™ is Monte Carlo simulation software for dynamic systems modelling in engineering, science and business. It specialises in simulating future performance and representing uncertainty and risk in complex systems (GoldSim Technology Group 2018). A dynamic simulation model is created in GoldSim™ by manipulating graphical objects representing system components; these graphical objects are called "elements" (GoldSim Technology Group 2017). External elements (i.e. a GoldSim™ logical building block) provide dynamic linkage to external computer programs and require specification of outputs of other elements in the GoldSim™ model that will be passed to the external program as well as specification of what the external program will return to the GoldSim™ model (GoldSim Technology Group 2017).

FEFLOW is a comprehensive program for the simulation of flow, groundwater age, mass- and heat-transport processes in porous media (MIKE by DHI 2018). It uses the finite element analysis to solve saturated and unsaturated groundwater flow equations in two- and three-dimensions. FEFLOW provides an open programming interface controlled by the Interface Manager (IFM) to allow coupled simulations with other software programs (MIKE by DHI 2018).

FEFLOW is used to simulate groundwater – lake interaction including groundwater – pit lake interaction. A FEFLOW - lake interaction plugin, IfmLake (DHI WASY GmbH

2018), is freely available that provides for interaction of groundwater and lakes in a FEFLOW model. Wingle and Sinton (2015) created a pit lake module for FEFLOW and used it in simulations of a mine site in the western USA. GoldSim™ has been used extensively in the mining industry to address mine water management and evaluation of mine closure options (GoldSim Technology Group 2018).

Although FEFLOW, and similar physical process models, are commonly used for modelling pit lake evolution, these models tend to be rudimentary in terms of operations-related process representation. Existing operational models, like GoldSim™ water management models, tend to provide limited physical-process simulation abilities. Dynamic coupling of a FEFLOW groundwater flow model of a pit lake system with a GoldSim™ pit lake management model addresses the limitations of each modelling framework.

Methods

FEFLOW and GoldSim™ provide facilities for dynamic coupling to external software programs. Coupling requires creation of communication channels combined with logic to transform the information from each program into useable formats for the other program. GoldSim™ models are completely flexible in structure; the user completely determines the model logic and structure, and each GoldSim™ pit water management model will have different computational structures and logic implementation. The flexibility of the GoldSim™ modelling framework means that the overall communication and logic structure presented here provides a general template that requires customization for each implementation.

One communication channel option would be to use files. Files are computationally inefficient because one program would write a file; the other program would read the file, process the information in the file, and write the file with the return information. File manipulation and management is considerably slower than inter-process communications through memory.

A better communication channel option is to use queues. A queue is a First In/First Out (FIFO) data structure in memory (Lee, Hubbard 2015). The complete communication structure between GoldSim™ and FEFLOW is handled with three queues as shown in **Figure 1**. Queues provide for inter-process communications, which is communication between the processes owned by GoldSim™ and the processes owned by FEFLOW.

Figure 1 *Coupled program structure using queues.*

This queue-centric work pattern that uses queues to pass information among processes, or services, is a common cloud programming pattern (Guthrie, Simms, and others 2014). This type of coupled program structure, requiring consistent and reliable communication between processes or services, would ideally be implemented in a cloud environment as these environments are built specifically for inter-process communication (i.e. communication among services) and provide the communications infrastructure (e.g. queues, distributed cache, and distributed storage). Implementation in a desktop environment is presented here and is achievable with additional communication structure creation and configuration, relative to what would be needed in a cloud environment.

Python programming language modules provide the coupling between GoldSim™ and FEFLOW. Python is used for three reasons: 1) Python DLL for the External element provides integration between GoldSim™ and Python (Martin 2017); 2) Python is integrated with FEFLOW and the FEFLOW IFM (MIKE by DHI 2018); and, the multiprocessing module in the Python Standard Library includes a robust queue implementation (Python Software Foundation 2018).

Coupling of GoldSim™ and FEFLOW for modelling pit lake evolution is implemented using Python modules to link the programs following the procedure provided in **Table 1**. This coupling is dynamic because the programs communicate, or pass information back and forth, for each coupled model time step. Coupling of GoldSim™ and FEFLOW can be extended so that GoldSim™ provides time varying values for recharge, based on a stochastic meteorology model or precipita-

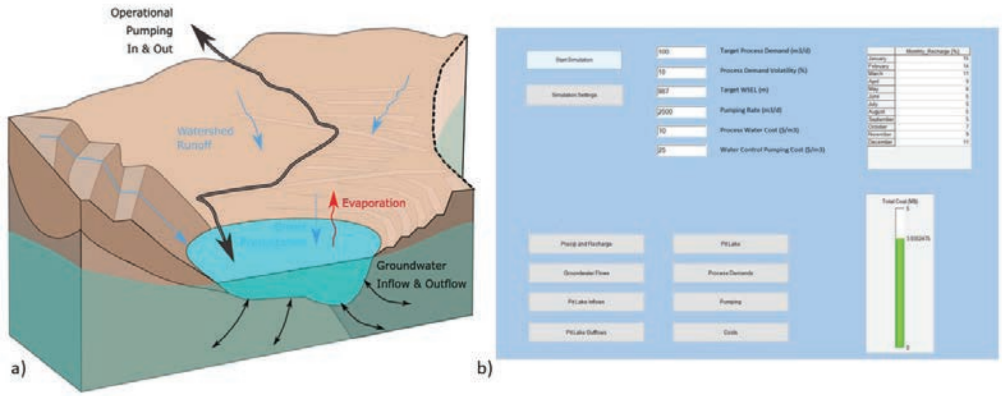

100 Target Process Demand (m3/d)
10 Process Demand Volatility (%)
987 Target WSEL (m)
2500 Pumping Rate (m3/d)
10 Process Water Cost ($/m3)
25 Water Control Pumping Cost ($/m3)

***Figure 2** a) Pit lake water balance schematic and **b)** example application dashboard.*

tion data sets, and elemental Transfer Rates to FEFLOW (Transfer Rates can be set dynamically during a FEFLOW simulation to represent formation of a clogging layer over time (MIKE by DHI 2018)).

***Table 1** GoldSim™ - FEFLOW coupling procedure.*

Step	Component	Description
1.0	GoldSim	Create pit lake water balance and operations management model for the site. **Figure 2a** displays typical lake/reservoir water balance components.
2.0	FEFLOW	Create, calibrate and validate a FEFLOW model of the groundwater flow system including the pit.
3.0	Coupled Model	Couple the models using Python and the three queues so that the FEFLOW model simulates the groundwater inflow and outflow components of the lake water balance shown on **Figure 2a**.
3.1	Coupled Model - GoldSim	GoldSim™ provides the pit lake water surface elevation to FEFLOW at the beginning of the coupled time step using the “From GoldSim” queue on **Figure 1**. Then, GoldSim™ waits to receive the return information from FEFLOW via the “From FEFLOW” queue in **Figure 1**.
3.2	Coupled Model - FEFLOW	FEFLOW uses the water surface elevation to set boundary conditions representing the pit lake.
3.2.1	Coupled Model - FEFLOW	A node selection is identified and stored in FEFLOW that represents the land side of the land – water interface. The IFM is used to go through these nodes and set two types of boundary conditions.
3.2.1.1	Coupled Model - FEFLOW	Fluid Transfer (Type III) boundary conditions with minimum head constraints (MIKE by DHI 2018) for nodes where the node elevation in the model is less than or equal to the water surface elevation.
3.2.1.2	Coupled Model - FEFLOW	Seepage Face (Type I with maximum flux constraint of 0.0 m3/d) (MIKE by DHI 2018) boundary conditions for nodes where the node elevation is larger than the water surface elevation.
3.3	Coupled Model - FEFLOW	FEFLOW simulates forward in time until the end of the coupled time step. The FEFLOW simulation is paused using the IFM and net groundwater inflow to boundary condition nodes is calculated using the IFM.
3.3.1	Coupled Model - FEFLOW	Net groundwater inflow is the total simulated flux to the boundary condition nodes where inflow to the pit lake is negative and outflow from the pit lake would be positive.
3.4	Coupled Model - FEFLOW	FEFLOW sends the net groundwater inflow for the pit lake to GoldSim using the “From FEFLOW” queue on Figure 1. Then, FEFLOW waits to receive the next water surface elevation via the “From GoldSim queue on Figure 1.
3.5	Coupled Model - GoldSim	GoldSim™ uses the net groundwater inflow for the pit lake in its water balance calculation for the coupled time step. The result of this calculation is the water surface elevation for the next coupled time step.

Example Application

A hypothetical implementation of a coupled GoldSim™ and FEFLOW, pit water management model is presented to illustrate the coupling process and to highlight the advantages of the coupled model approach. The example application examines the filling of a pit from the start of closure and management of the pit water levels for operational concerns and stormwater control.

A FEFLOW groundwater model of the open pit system is constructed as shown in **Figure 3**. This model is assumed to be calibrated and validated and ready for use in forecasting applications. It is the end of active mining in the pit (i.e. at the start of closure for the pit) and so the initial water table level is just below the bottom of the pit (**Figure 3b**). The model is transient and uses five (5) layers with constant head boundary conditions along the model edges that enforce the hydraulic gradient shown in **Figure 3b**. It is variably saturated and uses the Modified Van Genuchten formulation with spatially uniform parameterization (Unsaturated flow porosity = 0.439; S_s = 1.0; Sr=0.0233, α=0.0314, n=1.1804, m=0.1528, δ=2.2).

A complimentary GoldSim™ pit water management model is also constructed. The GoldSim™ model has the water balance components shown in **Table 1**. It uses a Markov process precipitation simulator (GoldSim Technology Group 2018) to generate daily precipitation depth and a linked stochastic potential evaporation estimator to provide meteorological forcing. A GoldSim™ Dashboard is included in the model (**Figure 2b**) to provide for results visualization and setting of custom operations parameters. **Table 2** provides a description of the operations parameters.

The coupled model is designed for Monte Carlo simulation over a 5-year period. It uses a 1-day time step which means that FEFLOW simulates a day and then passes groundwater inflow information to GoldSim™ and GoldSim™ simulates a day with groundwater inflow rate to update the pit lake water surface elevation for the start of the next day. The stochastic meteorological forcing generates different time series of precipitation and lake evaporation for each realisation.

Each coupled time step, GoldSim™ passes FEFLOW values for pit lake water surface elevation, Inflow and Outflow Transfer Rates for the elements adjacent to the pit lake in FEFLOW, and uniform recharge rate. Recharge rate is calculated using the percentage specification on the dashboard (Figure 2b) and the simulated precipitation rate. A single transfer rate is used for both Inflow and Outflow Transfer Rates, and this transfer rate is sampled from a uniform distribution between 0.01 1/d and 50.0 1/d for each realisation. It is assumed in our hypothetical example that model calibration was not sensitive to Inflow and Outflow Transfer Rates in the 0.01 to 50.0 1/d range; this constrained, but random, se-

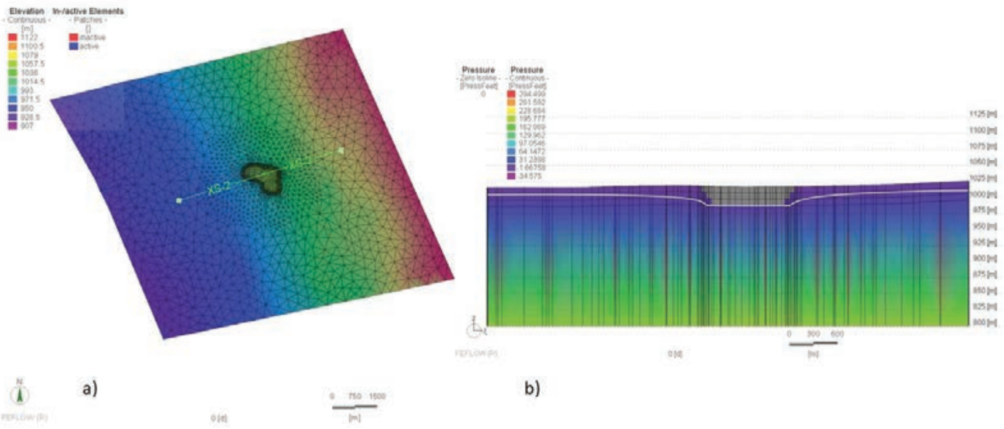

*Figure 3 Example FEFLOW open pit system groundwater model **a)** plan view **b)** Section XS-2.*

Table 2 *GoldSim™ model - pit water balance components.*

Component	Type	Notes
Direct precipitation	Inflow	Current pit lake surface area ✲ precipitation rate
Surface runoff	Inflow	Precipitation rate ✲ runoff coefficient ✲ watershed area
Groundwater inflow	Inflow	Calculated by FEFLOW
Lake evaporation	Outflow	Calculated with stochastic potential evaporation ✲ pan coefficient ✲ current pit lake surface area
Groundwater outflow	Outflow	Calculated by FEFLOW
Operations - process demand pumping	Outflow	Operations specified pumping rate to meet process water demands
Operations - water level maintenance pumping	Outflow	Pumping to maintain the pit water surface elevation within a target range to provide for stormwater storage

Table 3 *Operations specifications available on the dashboard.*

Dashboard Item	Descriptions
Target Process Demand	History Generator element used to generate process demands. This item provides the target value for the generator.
Process Demand Volatility	Volatility specification for the History Generator element
Target WSEL	Target pit lake water surface elevation which is used to control pumping to maintain stormwater storage.
Pumping Rate	Pumping rate to use when pumping for maintaining target water surface elevation
Process Water Cost	Cost allocation for process water demand
Water Control Pumping Cost	Cost allocation for pumping to maintain target water surface elevation
Operations - water level maintenance pumping	Pumping to maintain the pit water surface elevation within a target range to provide for stormwater storage

lection of Transfer Rates provides one avenue to incorporating FEFLOW model uncertainty into the coupled model representation. Each coupled time step, FEFLOW returns the net flux to the boundary condition nodes that represent the pit lake.

Figure 4 displays select results for 25 realisations. Figure 4a shows the simulated, probabilistic time history of pit lake water surface elevation. Water surface results provide the integrated solution for all lake water balance components shown on Figure 2a and described in Table 2, including groundwater inflow and outflow. Figure 4b provides the simulated cumulative distribution function (CDF) of total operations cost which provides an estimate of the risk, in terms of possible cost range, provided by the uncertainty in coupled model results.

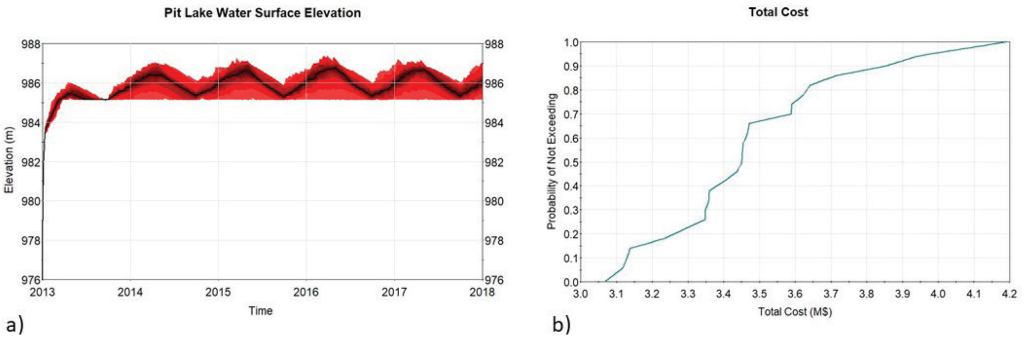

Figure 4 *Coupled model results a) probabilistic pit lake water surface elevation history b) total cost CDF.*

Conclusions

The dynamically-coupled FEFLOW and GoldSim™ pit lake water management model provides a combined operational and physically-based model. This combination allows prediction and examination of the impacts of different operational practices and protocols on the underlying physical site. This approach can be used as part of mine project planning to provide robust estimates of conditions at closure and an improved representation of the pit lake system, physical response, post-closure. The combined pit lake management modelling tool provides for risk assessment via uncertainty analysis, using the built-in uncertainty analysis features of both GoldSim™ and FEFLOW, and for detailed operational cost analysis and comparison, via the built-in financial tools in GoldSim™. Advanced FEFLOW uncertainty analysis could be included in this approach by using a different, calibrated Null Space Monte Carlo distributed parameter representation of system hydrostratigraphy (MIKE by DHI 2018) for each realisation in a coupled model analysis.

The primary drawbacks of the dynamically-coupled FEFLOW and GoldSim™ pit lake water management model approach are complexity and the technical knowledge and skill required to implement the coupling. Dynamic-coupling of computational models is always complicated; in this case the main impediment to a functioning coupled model is impacts of dynamic internal forcing, especially extreme scenario forcing, on FEFLOW model stability during simulations. Technical requirements of coupled model implementation are significant. The need to create custom communication structures for dynamic coupling can be partially alleviated using cloud environments.

Acknowledgements

The authors thank Tshwane University of Technology (TUT) for hosting the ICARD | IMWA | MWD 2018 Conference. Callie Maher provided invaluable editorial and formatting assistance.

References

DHI WASY GmbH (2018, May 5) IfmLake Plug-In. https://www.mikepoweredbydhi.com/download/mike-by-dhi-tools/groundwaterandporousmediatools/

GoldSim Technology Group (2018, May 4) GoldSim: Making Better Decisions in an Uncertain World. https://www.goldsim.com/Web/Home/

GoldSim Technology Group (2017) GoldSim Users Guide, Version 12.0. GoldSim Technology Group LLC, Issaquah, WA, 1183 pp

Guthrie S, Simms M, and others (2014) Building Cloud Apps with Microsoft Azure: Best Practices for DevOps, data storage, high availability, and more. Microsoft Press, Bellevue, WA, 201 pp

Lee KD, Hubbard S (2015) Data Structures and Algorithms with Python. Springer, New York, 363 pp

Martin N (2017) HOWTO: GoldSim Interface to Python Interpreter through an External Element and a DLL. GoldSim Technology Group LLC, Issaquah, WA, 37 pp

MIKE by DHI (2018, May 4) FEFLOW 7.1 Documentation. http://www.feflow.info/html/help71/

Python Software Foundation (2018, May 5) multiprocessing - Process-based "threading" interface. https://docs.python.org/2/library/multiprocessing.html

Wingle WL, Sinton PO (2015) A Pit-Lake Module for FEFLOW (Poster Presentation). FEFLOW 2015 Conference: Modelling the World of Groundwater with Mike by DHI

Determination of acid rock drainage from underground coal gasification at a pilot plant in Majuba

Lehlohonolo Mokhahlane[1]

[1]*University of The Free State, Institute for Groundwater Studies, Bloemfontein, 9100, South Africa, sehaimokhahlane@gmail.com*

Abstract

Underground coal gasification is an unconventional mining method that gasifies coal in situ to produce a synthetic gas that can be used for electricity generation. Residue products from underground coal gasification (UCG) have the potential to leach into groundwater. The products include char, ash and the surrounding in-situ rocks. The acid generation capacity of these products are explored in this study using acid base accounting (ABA). ABA results that the gasification zone in UCG operations will be a mixture of acid producing and acid neutralizing species, hence it is possible that the overall conditions might be neutral to weakly acidic as seen in the final pH.

Keywords: Acid base accounting | Underground coal gasification | Acid rock drainage

Introduction

Underground coal gasification (UCG) is an unconventional mining method that converts coal into gas by in-situ gasification. This process uses a panel of injection and production wells that are drilled to the coal seam to achieve gasification and transportation of the gas to the surface. Oxidants in the form of a mixture of oxygen and steam are injected into the gasification zone via injection wells and take part in UCG reactions. The gasification process converts solid coal into gaseous phases composed mainly of methane, hydrogen, and carbon monoxide known collectively as synthetic gas. The synthetic gas escapes through production wells to the surface where a number of gas scrubbing plants are installed to achieve the desired subsequent gas that can be used for electricity production. The mass transfer of solid coal to gaseous phases leaves a void or cavity in the coal seam which gets partly filled with residue products, ash and char (Figure 1).

Underground coal gasification has less environmental impact than conventional coal mining as most of the waste handling and

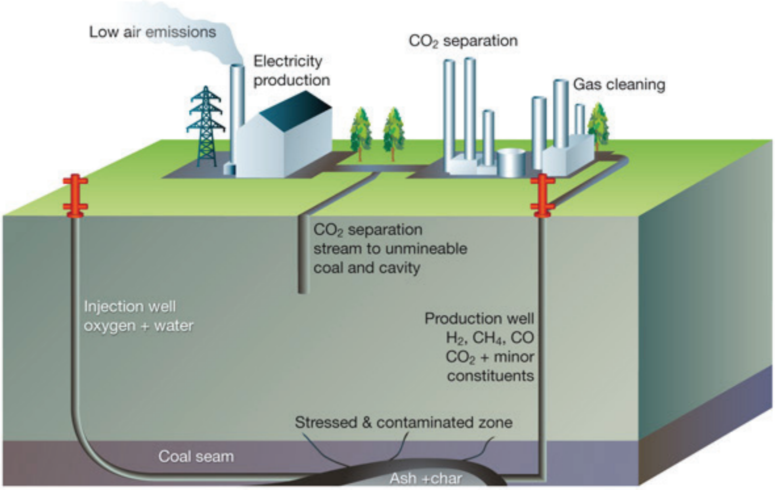

***Figure 1** Dipiction of underground coal gasification (Adapted from Burton et al, 2006)*

coal processing is eliminated (Imran et al., 2014). In traditional coal mining techniques, coal is mined and transported to the point of use where it is stockpiled before processing. All this processes have negative impact on the environment such as groundwater contamination, subsidence, surface disturbance and atmospheric pollution. At the tail end of the coal value chain is the waste handling of ash which also add to the environmental risk and cost. UCG technology has advantages that include improved health and safety of mining, reduction in coal processing and waste handling and less surface damage from mining activity. Carbon capture and sequestration technology can be incorporated into UCG by utilizing the cavity as a Carbon dioxide storage chamber hence further reducing the environmental effects from UCG activities (Bhutto et al., 2013).

Underground coal gasification offers a number of environmental solutions to coal exploitation, however groundwater contamination remains the main environmental risk (Kapusta and Stańczyk, 2011). Reports of groundwater pollution have been documented from the UCG test site in Hoe Creek, where product gas comprising of phenols and condensed vapours penetrated the overlying hydraulic units due to high pressures in the UCG reactor (Imran et al., 2014). Contaminants can migrate and penetrate the surrounding rocks as a result of an outward pressure from the gasification zone. It is widely accepted that operating the gasification zone at a pressure lower than the hydrostatic pressure in the immediate aquifer will cause all groundwater movement towards the gasification zone (Imran et al., 2014). This ensures that no outward pressure is exerted in the aquifer and hence containing the organic products within the gasification zone where there is constant decomposition and removal via the production wells. Most of the inorganic contaminants remain in the cavity as ash and char (Liu et al., 2007). These residue products interact with groundwater after the gasifier shutdown when natural groundwater head rebounds and water starts to fill the cavity. The natural flow of groundwater will leach the residue products leading to groundwater pollution (Bhutto et al., 2013).

Study area

The Eskom underground coal gasification pilot plant near Majuba Power Station in Mpumalanga, South Africa, is the first UCG plant in Africa and has already produced synthetic gas and successfully co-fired around 6-MW into Majuba Power Station by 2010. Gasification has ceased and five verification boreholes were drilled into the gasification zone. The aim of the verification drilling was to determine the impact of gasification and hence the boreholes were sited at strategic locations within the gasification panel. Five boreholes were drilled with two off-cavity and three targeted within the gasification zone. The location of the verification boreholes is shown in Figure 1.

The topography of the area is characterized by regular hills attributed to the erosion of the underlying dolerite sill. Four different intrusive dolerite rocks (T1 to T4) that intersect the Karoo sediments in the Majuba Colliery have been identified (de Oliveira and Cawthorn, 1999). The dolerites intrusions have been found to have displaced the targeted Gus seam by over 70 meters in some places. This has led to limitations in effective extraction of the coal seam by conventional mining. The targeted coal seam is the Gus seam that forms part of the Vryheid Formation of the Ecca Group in the Karoo Supergroup. The Gus seam varies from 1.8 to 4.5 m in thickness and in the Majuba UCG site it is encountered at a depth of around 280 m. The coal zone has also been found to bear several thin (5 – 20cm) laterally impersistent bright coal layers below the Gus seam (de Oliveira and Cawthorn, 1999). There are three other identified coal seam above the Gus seam, namely Eland, Fritz and Alfred seams. These coal seams act as marker seam in the Majuba UCG site and are not targeted for gasification. The location of verification boreholes G1VTH1, G1VH2, G1VH3, G1VH4 and G1VH6 are displayed in Figure 2.

Methods

The residue products of UCG will interact with groundwater after the shutdown of the gasifier and the interfaces in the cavity have the potential for acid rock drainage (ARD) especially if the sulphide quantities are ade-

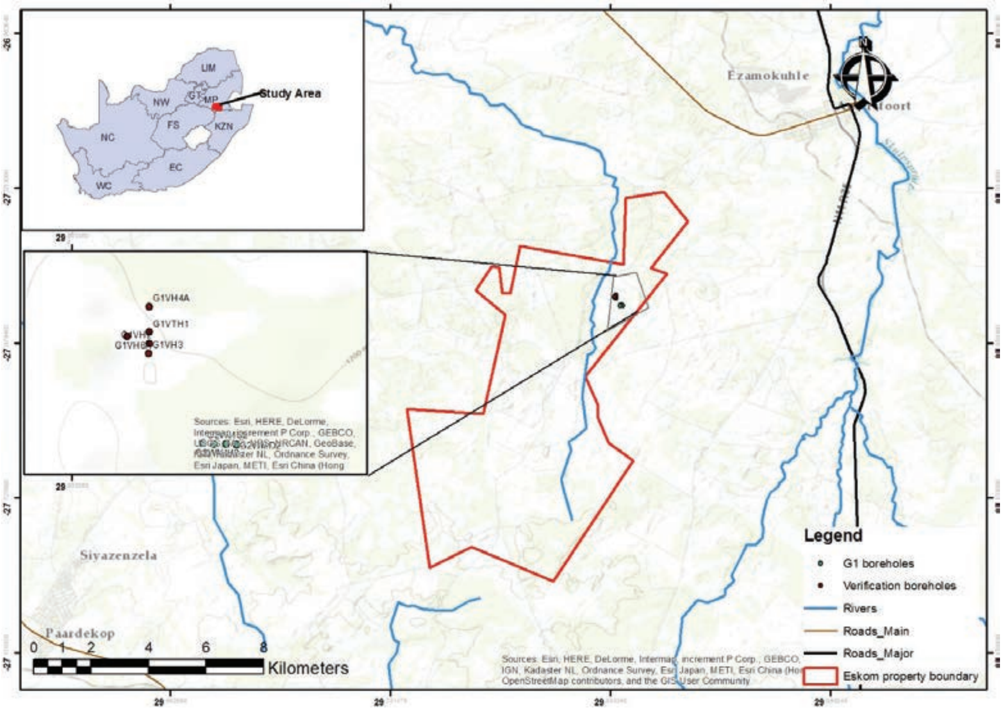

***Figure 2** Aerial view of the Majuba UCG site showing the location of groundwater monitoring boreholes with the verification boreholes encircled in red*

quate for acid generation. The reaction below shows the oxidation of pyrite which leads to acid generation:

2FeS2(s) + 7O2(g) + 2H2O(l) = 2Fe2+(aq) + 4SO42−(aq) + 4H+(aq) [1]

The reaction produces ferrous iron, sulphate ions and acid. While oxidation of sulphide minerals contribute to the acidity of rock drainage, dissolution of carbonate minerals play a role in neutralizing the acid from the following reaction:

CaCo3(s) + H+(aq) = 3HCO-(aq) + Ca2+(aq) [2]

There are two types of laboratory test that can be used for the prediction of acid rock drainage, static and kinetic tests. Static tests like acid base accounting (ABA) and Net Acid Generation(NAG), are relatively simple to carry out while the kinetic tests usually take longer periods to complete. Due to the limitation in sample size only one method (ABA) could be used in this study. Acid base accounting are described by Sobek et al. (1978) as predictive tool that accounts for the balance between the acid producing potential (AP) and the neutralising potential (NP) of geological material and the difference is calculated as the net neutralising potential (NNP). The acid producing material is generally the sulphide minerals as seen in Eq (1), while the acid neutralising minerals are carbonate minerals such as calcite, dolomite and magnesite, Eq 2.

NNP = NP – AP

The AP is based on the theoretical oxidation of all sulphur in the sample to sulphuric acid. The total sulphur in the samples was determined using a LECO (Laboratory Equipment Corporation of St. Joseph, Michigan) sulphur analyser. AP is generally expressed in kg $CaCO_3$ per tonne of material, the conversion factor is 31.25 kg CaCO3/tonne:

AP = Sulphur content (%) * 31.25Kg CaCO3 per tonne

The dissolution of acid neutralizing minerals such as carbonates contribute towards the neutralization potential (NP). Hydrochloric acid is used to sufficiently digest these minerals and it is expressed in Kg CaCO3 per tonne but can also be converted into Acid Neutralising Capacity (ANC, expressed as kg H2SO4/ tonne) by multiplying the NP with 0.98.

The Eskom Majuba UCG pilot plant was successfully commissioned at Majuba coalfield in January 2007 with product gas being co-fired into the nearby Majuba Power station by October 2010 and was successfully operated through to September 2011 when decommissioning commenced with the shutdown of the gasifier (G1). The successful performance and shutdown of the Majuba UCG pilot plant is a significant step towards full commercialization of UCG technology as this is the first UCG plant in Africa. The successful shutdown of G1 presents an opportunity to investigate some of the key environmental questions regarding groundwater contamination. The project has successfully embarked on a drilling exercise to recover residue samples from the gasification zone through what is termed verification drilling. Verification drilling is diamond core drilling from surface to the gasification zone with the aim of retrieving core samples. The successful recovery of ash, char and heat-affected strata provides key insights into the geochemistry of the gasification chamber as these products are regarded as potential sources of groundwater contamination. Samples were taken from the roof and floor of four verification boreholes including the ash and unburned coal.

Results

The ABA results are shown in Figure 3.

The ABA results of show a mixture of acid producing species and also acid neutralizing species. There is one outlier, a sample with a high net neutralization potential of 141.7 kg $CaCO_{3.}$ This inconsistency will have to be investigated by repeating the analysis in order to eliminate possibility of equipment failure or human error. The majority of the samples plot in the uncertainty region of +20 to -20 NNP and will be processed further with kinetic tests to determine their acid potential. In general the results show that the gasification zone in UCG operations will be a mixture of acid producing and acid neutralizing species, hence it is possible that the overall conditions might be neutral to weakly acidic as seen in the final pH.

Conclusion

The ABA results show a mixture of acid producing and acid neutralizing species. Since groundwater will be the leaching medium for the residue products of UCG therefore considerably the leaching behaviour will depend on the chemistry of the local groundwater.

References

Bhutto, A. W., Bazmi, A. A. and Zahedi, G. (2013) 'Underground coal gasification: From funda-

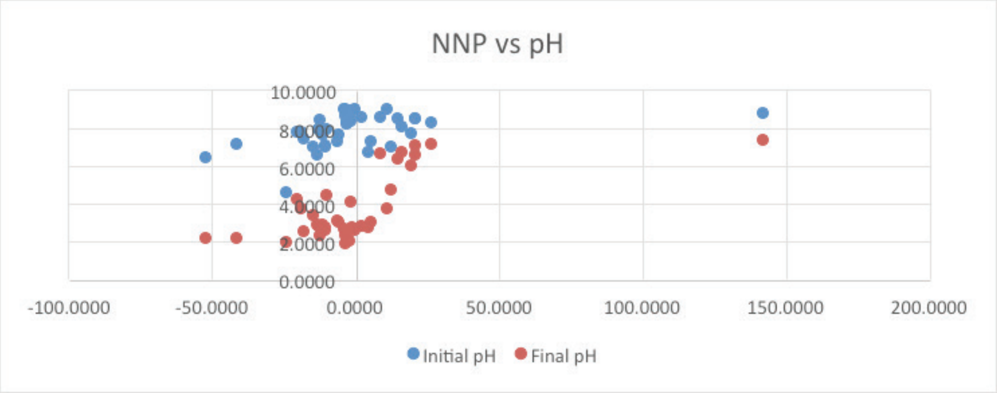

Figure 3 *ABA results, NNP vs pH*

mentals to applications', Progress in Energy and Combustion Science, 39(1), pp. 189-214.

Blinderman, M. S. and Klimenko, A. Y. (2018) '1 - Introduction to underground coal gasification and combustion', in Blinderman, M.S. & Klimenko, A.Y. (eds.) Underground Coal Gasification and Combustion: Woodhead Publishing, pp. 1-8.

Intergrated Energy Plan (40445).

Imran, M., Kumar, D., Kumar, N., Qayyum, A., Saeed, A. and Bhatti, M. S. (2014) 'Environmental concerns of underground coal gasification', Renewable and Sustainable Energy Reviews, 31, pp. 600-610.

Kapusta, K. and Stańczyk, K. (2011) 'Pollution of water during underground coal gasification of hard coal and lignite', Fuel, 90(5), pp. 1927-1934.

Liu, S.-q., Li, J.-g., Mei, M. and Dong, D.-l. (2007) 'Groundwater Pollution from Underground Coal Gasification', Journal of China University of Mining and Technology, 17(4), pp. 467-472.

Mocek, P., Pieszczek, M., Świądrowski, J., Kapusta, K., Wiatowski, M. and Stańczyk, K. (2016) 'Pilot-scale underground coal gasification (UCG) experiment in an operating Mine "Wieczorek" in Poland', Energy, 111, pp. 313-321.

Pershad, S., Pistorius, J. and van der Riet, M. (2018) '14 - Majuba underground coal gasification project', in Blinderman, M.S. & Klimenko, A.Y. (eds.) Underground Coal Gasification and Combustion: Woodhead Publishing, pp. 469-502.

Strugała-Wilczek, A. and Stańczyk, K. (2016) 'Leaching behaviour of metals from post-underground coal gasification cavity residues in water differing in mineralization', Fuel, 173, pp. 106-114.

de Oliveira, D. P. S. and Cawthorn, R. G. (1999) 'Dolerite intrusion morphology at Majuba Colliery, northeast Karoo Basin, Republic of South Africa', *International Journal of Coal Geology, 41(4), pp. 333-349*.

Managing ARD in a Gold Mine in the Vicinity of Paracatu Town, MG State, Brazil

Alessandro L. Nepomuceno[1], Marcos A. Morais[2], Gustavo O. Castro[3]

[1]*Sustainability and Permitting Director, Kinross Brazil Mining*
[2]*Environmental Manager, Kinross Brazil Mining*
[3]*Environmental Senior Engineer, Kinross Brazil Mining*

Abstract

This paper outlines the ARD control program conducted by Morro do Ouro Site, located in the municipality of Paracatu, Northern region of Minas Gerais State in Brazil. The program was an essential piece of the site strategic planning to approve the mining of a sulphide ore near to environmental authorities. The site early understanding of the potential environmental risks and integration of the ARD control actions in the mine planning process has been a significant differential that has allowed the site keeping its environmental license for the last 20 years with the additional benefit of significantly reducing closure costs.

Key words: managing, acid rock drainage, integration, mine planning, sulphides, acid forming, segregation, control of contaminant migration, acid neutralization capacity, planning, savings, closure costs.

Introduction

In the municipality of Paracatu, which is located in the Northern region of Minas Gerais State in Brazil, a carbonaceous phyllites rock hosts a gold mineralization, which originated the Morro do Ouro mine. The mineralized zone is formed by a package that varies between 80 and 100 m in the presence of stretched quartz veins, called “boundins”. Gold is associated with carbonates (mainly Anquerite and Siderite) and some sulfides (Pyrite, Pyrrhotite, Arsenopyrite and lower concentrations of Sphalerite, Galena, and Chalcopyrite) that are associated with these quartz venules. 03 main types of ore have been characterized by the mine: CTBI oxide ores located on the top and B2, the sulphide ore on lower zones of the geological body.

The challenge of managing ARD at Morro do Ouro site is significant as the mine occupies an extensive area of 2,484 ha: mine pit with 931 ha operating less than 500 m of some neighboring communities and the two tailings dams (named Santo Antonio and Eustaquio) occupying 1,553 ha in total. This paper outlines the ARD research program implemented by Morro do Ouro site, how this research was translated into on the ground implemented solutions and the benefits of the implementation of this program.

The Morro do Ouro ARD Research Program

Since 1991, Morro do Ouro mining has been conducting research applied to the control of the acid rock drainage (ARD). By decision of the company’s corporate technical group, the mining of the sulfide ore, named B2, could not be conducted if the process route that took into account environmental controls in the ARD process had not been previously defined. So that a dedicated team effort was initiated including the mine, process, dam and environmental areas to manage the issue.

By the end of 1991, the mine set its first program of static tests aiming to provide a preliminary identification of the acid generation potential on the sulfide ore. Preliminary ABA tests were conducted and results indicated that this potential existed.

In 1994, a dedicated laboratory was installed on site to conduct kinetic tests to evaluate the long-term acid generation potential and investigate potential covers and the required environmental controls (Figure1). The key objectives of these tests were:

Figure 1 *Laboratory built to conduct kinetic tests*

- To investigate different sulfide (sulfur) content in the final tailings and their potential for acid generation;
- Evaluate the possibility of addition of neutralizing material easily available in nearby areas of the site like calcite and dolomite limestone;
- Investigate the need for segregating the sulphides and their safe disposal.

In 1998, Morro do Ouro site started mining the B2 sulphide ore and had already its processing and environmental integrated route defined from the ARD research program. This included the use of a geological model with PAF and NAF materials information to manage the waste and sulphur grade in the ores fed in the plant, the segregation of the sulphides in the flotation process and stoichiometric addition of limestone to prevent acid generation from residual sulphides contained in the final tailings to be discharged in the dams.

In 2002, Ladeira et al. conducted a specific study to confirm the adsorption capacity of a local soil (red clay), which was previously tested in the lysimeter kinetic tests, to be used as a seal in the sumps bearing the sulphur concentrate. Maximum adsorption capacities of the samples were determined by a Langmuir type equation. Chemical and mineralogical characterization was carried out in order to determine the main minerals responsible for the adsorption process. The adsorption process proved to be high and was correlated with the presence of Al and Fe oxides.

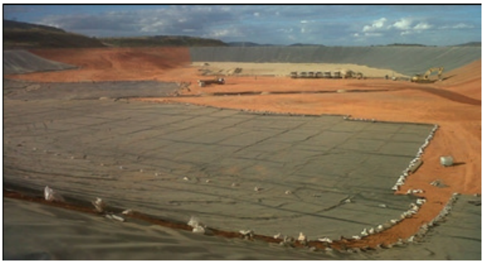

Figure 2 *Red clay used in construction of Specific Tanks*

Figure 2 illustrates the implementation of the local red clay as a seal in the specific tanks.

In 2015 the site initiated a field experiment with the purpose of evaluating the adequate cover for the Santo Antonio Tailings Storage Facility. The pilot-scale experiment consists in four 100-m2 cells which were installed with a trafficability layer of 1.5 m in both experiments and a storage and release layer with and without a hydraulic barrier. Monitoring of moisture profile and oxygen concentration trends within the cover trial plot commenced in May 2016. The instrumented trial cover plot is composed of four experimental cells that simulate two different covers. Two of the cells are embedded by lysimeters, which are lined by geomembrane so that percolated water is collected for flow measurement. The other two cells were installed without geomembrane so there is an interaction between tailings and the cover material, simulating the real scenario (control test). Data indicate the possibility of reducing the cover from the previously designed 3 m to 2.0 m with significant savings in closure costs. Refer to section 4.2 for other details.

Key ARD Control Management Actions Defined from the Research Program

Mine Pit Modelling to Identify NAF and PAF Ores

Initially, a detailed assessment of geochemical data was conducted using the geological database. Approximately 40,200 sulphur assays were conducted for individual 3m depth intervals and 4,500 acid neutralizing capacity (ANC) assays on 12m composite depth interval samples. These data indicated that the future mine rock (waste and ore) was of a low to moderate S and low to moderate ANC type.

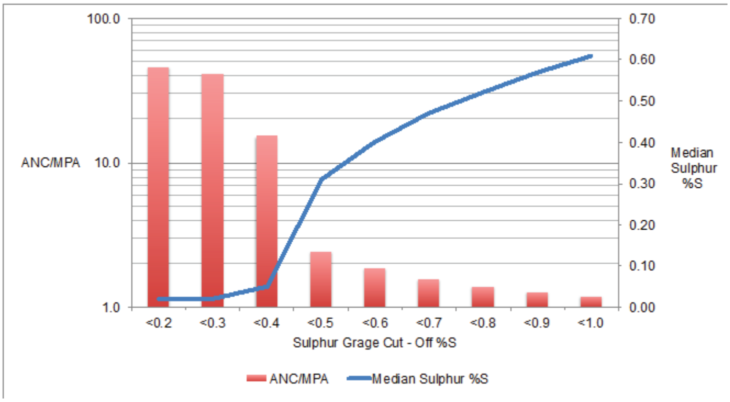

Figure 3 ANC/MPA value and average sulphur content with increasing grade cut-off

In addition, acid-base analyses using the Net Acid Producing Potential (NAPP) approach indicated that about 50% of mine rock was likely to be PAF and 50% was likely to be NAF. These data also demonstrated that the operational classification of waste rock for segregation was better based on NAPP, but in areas where ANC data was not available, a sulfur grade approach needed to be developed.

Figure 3 provides the basis for applying a risk-based approach to defining a workable and realistic S grade cut-off for NAF and PAF in the absence of ANC data. Since the ratio of ANC to MPA* (ANC/MPA) provides a measure of the factor of safety (FOS), it can be used in combination with NAPP to define the ARD risk associated with selected S cut-off values.

The ANC/MPA and median S grade clearly identify a step decrease in the FOS between a cut-off value of 0.4%S and 0.5%S. This indicates a far greater risk of PAF hot spots developing in the dump using a 0.5%S cut off compared to 0.4%S. Unlike process tailings or individual samples, a run-of-mine mixed waste rock dump requires a greater excess in ANC to minimize the risk of ARD.

From this assessment, Morro do Ouro site established the following criteria for the classification of waste rock in order to enable segregation and selective handling to minimize the risk of ARD during operations and post-closure:

- Non-Acid Forming (NAF): Total S ≤ 0.4%S or NAPP <0 KgH2SO4/t
- Potentially Acid Forming (PAF): Total S > 0.4%S or NAPP >5 KgH2SO4/t
- Potentially Acid Forming low capacity (PAF_LC): NAPP 0 to 5 KgH2SO4/t (Note that PAF_LC can not be identified using S only).
- *MPA = maximum potential acidity

These criteria were included in geology block model in order to proceed with the ARD management system at the Morro do Ouro site. This allowed the site to consider the segregation of wastes into the strategic business plan developed for the life of mine.

Plant Design to Ensure Recovery and Segregation of Sulphides

Segregation of Sulphides

The decision of separately store sulfide-rich carbon in leach (CIL) hydrometallurgical tailings from the lower sulfide bulk flotation tailing was one of the most important taken by Morro do Ouro site to control ARD. In this circuit, the flotation tailings are discharged to conventional tailings dams while the CIL tailings are discharged into engineered excavated sumps locally nominated as "specific tanks".

The flotation tailings are classified as non-hazardous waste according to Brazilian legislation (ABNT-NBR 10,004 Standard). The sulfide content of the flotation tailings is controlled within the Beneficiation Plant where gold and sulfide are recovered in the concentrate. Generally, about 40 to 60% of the sulfide in the ore is recovered resulting in flotation tailings containing generally less than 0.5%S.

The base and sides of the specific tanks are excavated into bedrock and lined with about 0.5 m of the local red clay. A low permeability geomembrane (HDPE - high-density polyethylene) is placed over the clay. The clay is naturally rich in Fe and Al oxides and provides a good attenuation capacity to any potential seepage passing through the HDPE liner. Additionally, a seepage collection system and monitoring wells were installed beneath the specific tanks to early identification of any seepage through the structure.

CIL tailings are rich in sulfide sulfur (approximately 20% S) and contain other contaminants such as metal and metalloids, in particular arsenic. These tailings are disposed at a rate of 300 m3/h and maintained under water to minimize exposure to atmospheric oxygen and avoid ARD generation during operation.

Limestone Addition to Final Tailings

Morro do Ouro site implemented a limestone addition program at the Beneficiation Plants to minimize the risk of developing acid generating zones across exposed beaches and to control the solubility of arsenic. The acid-base characteristics of mill tailings are routinely monitored. In the case of Santo Antonio dam, this procedure was optimized to benefit ANC a couple of years before the tailings discharge ceased in that dam in order to increase the target ANC/MPA factor of safety to 1.5 and facilitate closure. Geochemical data of exposed tailings shows that the carbonate addition (as dolomite) has met its goal during the operational period and prepared the dam for a lower cost and more conventional closure (no complex cover required) (see detail in section 6). By avoiding acidic zones in the tailings, the solubility of metals and metalloids has been properly controlled.

Management Commitment to the ARD Control Program

The Morro do Ouro site management commitment to the ARD Control Program has been outstanding. Since the early stages of the program, management has proactively positioned supporting the control requirements. The ARD topic has been integrated in the site business planning and into the decision making process. The topic has been periodically discussed during routine meetings and provisions made accordingly. Around 95.3 Million Dollars have been spent with the ARD control program at Paracatu site including the construction of the specific tanks, reagents to recovery sulphides, consultancy support, geochemical assays and field trial tests in the last 6 years.

***Figure 4** Water quality of tailings dam downstream Santo Antonio and Eustaquio creeks*

Benefits arising from the Morro do Ouro ARD Program

Among the various benefits arising from the Morro do Ouro program, the preservation of water quality and the closure cost reduction should be highlighted.

Preservation of Water Quality

In the State of Minas Gerais (Brazil) the water quality limits are considered conservative (Class II Waters, Brazilian Federal Law CONAMA n° 357/2005) although the legislation recognizes that some regions might have higher limits due to the local geological background as long as scientific based studies are conducted to demonstrate it.

Morro do Ouro site has been very successful in managing its effluents and ensuring water quality within the conservative Class II limits adopted in Brazil or keeping them at least below the background referential limits established for the region and accepted by the agencies (refer to figure 4).

Reduction of Closure Costs

The Morro do Ouro ARD program has been able to considerably reduce costs associated with closure. The Morro do Ouro tailings dams ponds occupy 1,553 ha together, this corresponds to 62 % of the overall area to be closed. Considering that the closure test trials installed at Santo Antonio tailings facility - SATF (refer to item 02) indicate the possibility of reducing the cover thickness from 3 to 2.0 m, this means 23.8MUS$ of closure cost savings. If this is applied to Eustaquio (under current evaluation), the cost savings can be even higher, around 41MUS$. Recent data indicate further potential reduction on cover thickness to just 1.5 m (refer to figure 5).

Conclusions

Morro do Ouro site has implemented an ARD management program in the earlier stages of planning to mine its sulphide ores. This approach demonstrates that the ARD and its potential impacts should be considered in the early stages of mine planning and be integrated to site operations and management decisions in order to be successful. The Morro do Ouro ARD program has also demonstrated that although of significant costs, these can be compensated or even surpassed by the benefits arising from the site keeping a good water quality in a sensitive environment very close to the local community and by achieving significant reduction on closure costs.

References

Brazilian Association of Technical Standards - ABNT 10.004: Classification of solids waste, Rio de Janeiro, 2004

Federal Council for the Environment - Resolution CONAMA 357: Establishes classification of water resources and environmental guidelines for their classification, as well as establishes the conditions and standards for the discharge of effluents, and provides other measures, Brasília 2005

Ladeira, A. C. Q., Ciminelli, V. S. T., Nepomuceno, A. L. Selection of soils for arsenic immobilization. Escola de Minas, Ouro Preto, v.55(3), 2002

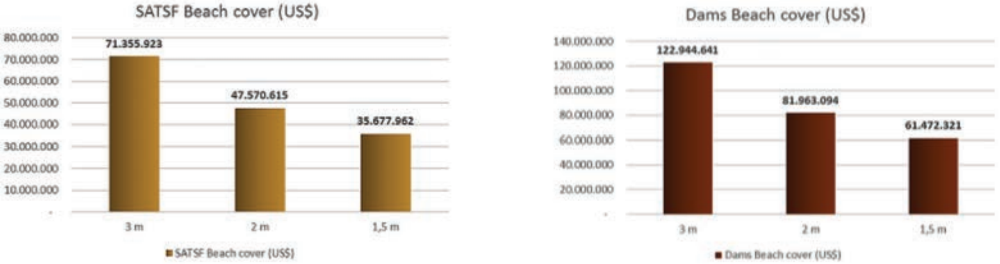

Figure 5 *Closure cost reductions arising from the potential reduction of cover thickness indicated by the test plot at SATSF and total estimated savings for both dams*

Monitoring a field application of a Green Liquor Dregs-till mixture in a sealing layer on top of sulfidic mine waste

Susanne Nigéus[1], Christian Maurice[1,2]

[1]Luleå University of Technology, Department of Civil, Environmental and Natural Resources Engineering, 971 87 Luleå, Sweden, susanne.nigeus@ltu.se
[2]Ramböll Sverige AB, Kyrkogatan 2, Box 850, SE-97126 Luleå, Sweden

Abstract

Sulfidic mine waste left unattended and in contact with oxygen oxidize and have potential to produce acid rock drainage (ARD). A typical method in Sweden to stop sulfide oxidation is to apply a dry cover on top of the mine waste. Using the non-hazardous industrial residue Green Liquor Dregs (GLD) in the cover is useful for the mining industry and the industry providing the residue and a large benefit for the environment. In this study, the effectiveness of a mixture of till and 10 wt. % of GLD in a dry cover was studied by monitoring temperature, oxygen- and moisture content. The conclusion is that the sealing layer in unaffected by frost, the oxygen concentrations are decreasing with time, but not in depth and the sealing layer with GLD-till mixture seem to be nearly saturated.

Keywords: Mine waste, ARD, Industrial residues, Green Liquor Dregs, Field application, Monitoring

Introduction

Mining industry generates massive amounts of mine waste worldwide, e.g. 110-million-ton mine waste in Sweden 2017, which accounted for 77 % of the annual waste produced (Swedish EPA 2018). 70 % of the Swedish mine waste contains sulphide minerals (SGU and Swedish EPA 2017) that if left unattended and in contact with oxygen oxidize and have potential to produce acid rock drainage (Saria, et al. 2006). ARD is a major long-term threat to the environment as metals and metalloids may become mobile (Saria et al. 2006). The GARD guide (Global Acid Rock Drainage guide; Verburg et al. 2009) categorize different methods to prevent ARD, after closure, into two main categories; engineered barriers and water covers. Engineered barriers can be divided into liners and dry covers, where liners are typically designed to act as a barrier for contaminant flow from the overlying waste into the receiving environment. Dry covers are typically designed to limit the ingress of water and oxygen into the underlying waste (Verburg et al. 2009). Under the relatively humid climatic conditions in Sweden a soil cover can be used to reduce oxygen flux to the underlying reactive wastes, and thus can reduce ARD (Collin and Rasmuson 1990; Bussière et al. 2003; Dagenais et al. 2006). The soil cover is a dry cover which usually consists of a sealing layer placed on top of the mine waste and above this, a protective layer. The sealing layer is made of a fine grained compacted material to preventing oxygen to diffuse to the waste underneath by keeping it close to saturation. The purpose of the protection layer is to protect the sealing layer from erosion and frost- and/or root penetration. Sealing layers in Sweden are usually made of a till, ideally a clayey till. However, the availability of clayey till nearby a mine is often limited and the need for alternative solutions are great, e.g. bentonite amendment to till. However, bentonite production is costly both economically and environmentally due to time- and resource consuming production. A suitable alternative material as an amendment to till could be a fine grained industrial residue. Previous studies have shown that the inert residue of pulp production, Green Liquor Dregs (GLD), has properties suitable as a sealing layer i.e. it is fine-grained (d100 < 63µm), commonly has an HC in the range of 10^{-8} and 10^{-9} m/s and a higher water retention capacity (WRC) compared to materials with similar particle size, such as clayey/sandy silt (Mäkitalo et al. 2014). To use the material in its own is however not technically possible due to its low shear strength and high water-content which makes it instable (Mäkitalo et al. 2014). Previous studies have however shown that mixing approximately 10 wt. % GLD with till keeps its positive properties and improve the drawbacks of the material (Mäkitalo et al. 2015). Using an industrial residue in a mine remediation program would serve as a large benefit for the environment, especially for the mining industry and the industry providing the residue.

The oxygen concentrations and water content are important factors to monitor for evaluating the function of the soil cover and if that the sealing layer is kept close to saturation to limit the oxygen diffusion to the mine waste. In humid environments, the general functions of a soil cover system are to reduce the transport of oxygen to the waste material and minimize the water infiltration fluxes. However, the oxygen fluxes through the soil cover is the key issue to control ARD generation (O'Kane 1995; Yanful 1993). This as oxygen together with pH and bacterial activity is the main driving factor in the oxidation process of sulfidic mine waste (Akcil and Koldas 2006). At a relatively low degree of saturation, most oxygen transport occurs through the partially air-filled pores (Aachib et al. 2004), due to the 10 000 times higher diffusion coefficient in the air than in water (Yanful 1993). The effective diffusion coefficient (De) can be explained by the average cross-sectional area open to diffusion and the distance traveled by molecules in the pores of the soil. In addition to a higher diffusion coefficient, the dissolved O2 concentrations in the air is around 20 000 times higher than in water (Höglund et al. 2004; Verburg et al. 2009). The transport of gaseous oxygen through fine-grained materials are mainly by molecular diffusion (Yanful 1993) and in general, the oxygen flux rates are at a minimum when the degree of saturation is greater than 85-90 %, this as the air-phase at a saturation greater than 85 % becomes discontinuous (Corey 1957). The oxygen is then transported through the water phase (Aubertin and Mbonimpa 2001; Aachib et al. 2004) and in a layer that is kept close to saturation, the De can be comparable to the De in water. It is small enough to reduce the oxygen flux to a level comparable to that of a water cover (Yanful 1993; Aachib et al. 2004). In addition to oxygen and moisture content the temperature is another important factor to monitor, especially in the northern Swedish climate with long winters. The low air temperature freezes the pore water in the soil and can create cracks which can increase the hydraulic conductivity of the soil and the oxygen diffusion as the sealing layer dries out.

In this study, the effectiveness of a sealing layer made of a mixture between till and 10 w. % of GLD was studied. An instrumented experimental area within a cover application of the waste rock dump of Näsliden mine was constructed in October 2017. The experimental area consists of sealing layers made of two different materials. One is a mixture of till and 10 wt. % GLD. The other a till and 4 wt. % bentonite. The objective of the study was to evaluate the effectiveness of the sealing layer made of the till-GLD mixture by measuring soil moisture content and oxygen concentrations in the sealing layer and temperature in the protection layer. Another objective of the study is to compare the results from the GLD-till area with the sealing layer made of till-bentonite to see if GLD works as well as the well-studied bentonite in a sealing layer. There is much work done on the evaluation and monitoring of mine waste covers, but no published work yet done on the evaluation of the use of a GLD-till mixture in mine waste remediation.

Methods

An instrumented test area within a cover application of Näsliden mine was constructed in August 2016 and October 2017. The experimental area consists of sealing layers made of two different materials. One is a mixture of till and 10 wt. % GLD, which was constructed in August 2016. The other is a till and 4 wt. % bentonite and was constructed in October 2017 (**Figure 1**).

An observation well and a pit was installed in each monitoring surface and from these four temperature probes (PT1000, EMS Brno) and two soil moisture probes (SM150T, Delta T-devices) were drilled into the different layers at various depth. In addition, 8 oxygen probes (SO110, Apogee instruments)

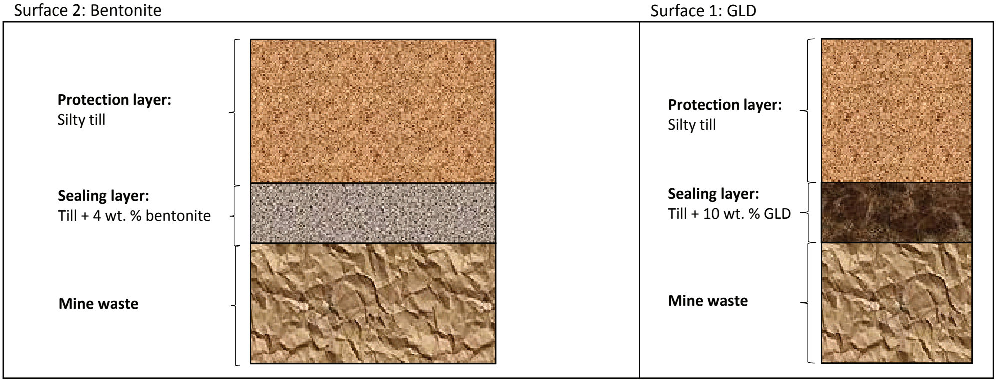

***Figure 1.** Overview of the monitoring surfaces.*

were installed under and on top of the sealing layers. Air pressure measurements to compare to the oxygen concentration were collected from the Swedish Meteorological and Hydrological Institute (SMHI). Unlike the other probes, the oxygen probes were installed vertically before the sealing- and the protection layers were applied to prevent leachate from oxygen through the cables. The probes were connected to two data loggers (Railbox RB32P4, EMS Brno) that were installed in the observation wells. The probes to measure temperature and soil moisture were installed in four vertical profiles, two in observation wells and two in pits, both in the GLD-surface and the bentonite-surface. The observation-wells of 2.7 m height and 1.5 m diameter were placed on the mine waste before the cover was constructed. After installation, the cover was and compacted around the wells by hand-driven machinery. After the cover was applied the pits were dug to a depth of approximately two decimeters on top of the sealing layer. After installation of probes, the pits were backfilled with the same material. The probes were drilled with a machine-driven drill of 40 mm diameter (⌀) and 800 mm lenght. When the soil moisture probes with ⌀ 50 mm were installed a hand-driven drill of ⌀ 60 mm was used. The hand driven drill was also used for bore-holes more than 800 mm long. The cables from all probes were collected to tubes that were led to the observation wells and connected to the loggers there. The loggers are powered by solar panels. The boreholes in the observation wells and tubes were sealed with sealing foam to prevent air and water to pass through the tubes to the probes. The part of the observation well above ground was isolated to prevent the atmospheric temperature to influence the temperature measurements.

Results and discussion

The winter in northern Sweden stretches from October to April and is associated with minus degrees and a thick snow layer. This leads to frost penetration into the soil and a dry period considering water percolation through the soil cover.

The results from the monitoring show that temperature has, as expected, declined and leveled out as the winter approaches and continues (**Figure 2:A-D**). The temperature is also, as expected in winter, lowest closest to the surface and warmer further down the cover. Only the probes closest to the surface (0.3-0.5 m depth) seems to be affected by frost, expect from in the observation well in the bentonite surface where frost seems to have reached 0.8 m depth in early spring (**Figure 2:D**). Comparing the temperatures in the pit and the observation wells, the temperatures in the observation well is lower further down than in the pit (**Figure 2:A-B**), both in the GLD and bentonite surface (**Figure 2:C-D**). This indicates that the observation wells are not fully isolated from the cold air. The conclusion is that the protection layer has protected the sealing layer from frost penetration, which was its purpose.

The purpose of the sealing layer is to act as a barrier towards oxygen diffusion and decrease the oxygen levels close to 0 % un-

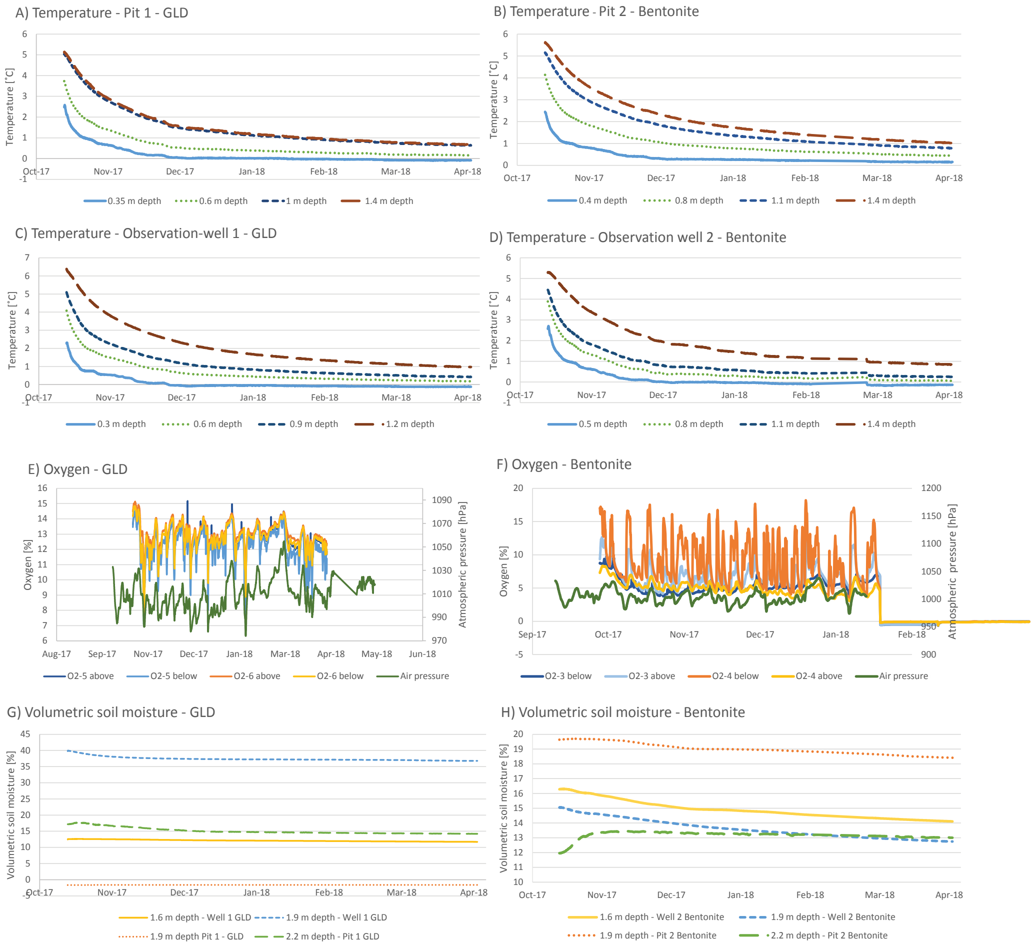

Figure 2. *Temperature, soil moisture and oxygen measurements in the pits and observation wells in the GLD and bentonite-surfaces. Atmospheric air pressure is presented together with the oxygen measurements.*

derneath the sealing layer. It was therefore expected that the concentrations below the sealing layer would be lower than above the sealing layer. No trends comparing concentrations below or above the sealing layer can however be seen in this study (**Figure 2:E-F**). The oxygen concentrations in the different places studied here varies between 3-18 % (**Figure 2:E-F**), where the lowest values can be seen in the bentonite layer (**Figure 2:F**). Comparing the results with oxygen measurements done under the cover of the Storgruve dump in Sweden (Lundgren 2001), the results in this study are higher. The variation in oxygen concentrations is great and attuned in most of the probes (**Figure 2:E-F**). Even though cover system behaviour is known to be dynamic and rarely reaching stable conditions in field under a relatively humid climate (Ricard et al. 1997; Ricard et al. 1999; Bussière et al. 2003; Dagenais et al. 2006), the variations was not expected to be attuned. The explanation for the attuned variation is in the atmospheric pressure, which has been found to affect the gas diffusion in a soils vadose zone (Massmann and Farrier 1992). The atmospheric pressure and the oxygen concentrations varies in the same way (**Figure 2:E-F**). The strong variations in oxygen concentrations in the O_2-4 below probe in the bentonite can likely be explained by leakage of atmospheric oxygen through where the cables were connected to the observation well. Some decreasing trends in oxygen measurements can be detected in the oxygen probes in the bentonite layer (**Figure 2:F**). This decrease is seen in Lundgren's (2001) study as well and was expected as the oxygen derived from when the material was exposed to the atmosphere is depleted. In summary a slight decreasing trend with time can be seen in the oxygen concentrations, but not in depth. The oxygen concentrations are greatly affected by the atmospheric pressure and at least one probe seems to be affected by leakage of oxygen from the atmosphere.

The volumetric soil water content show how much of the total volume of the soil is water and the value depend on the pore volume. The more compacted the material, the less pore volume and possibility of water in them. If the total pore volume is filled with water, the material is saturated. The volumetric soil moisture content in this study varies between 12 and 20 % in the bentonite and 0-40 % in the GLD cover. When the material was compacted in laboratory with a standard proctor compaction method (SS-EN 13286-2:2010) a volumetric water content of 30 % was reached. A pilot study with a similar cover made of till and 10 wt. % of GLD in the sealing layer, constructed three years ago, (not published data) shows a volumetric soil moisture of 3-4 %. The pilot cell with only a half meter of protection cover on top of the sealing layer shows a volumetric soil moisture of 8-10 % in the bottom of the layer and 0.5-18.5 % in the surface of the sealing layer that is more exposed to the precipitation. Greater variation is expected in a sealing layer with closer contact to the atmosphere. However, a volumetric soil moisture 3-4 % is a low value and indicate drying of the sealing layer. This might be due to the design of the pilot cell that with its elongated form supports surface runoff rather than infiltration. Bussière et al. (2006) studied a compacted till under topsoil in Ontario, Canada and measured volumetric soil moisture contents of 10-37 %, which corresponds well with the values in this study. The value of 40 % volumetric moisture content measured in the GLD-till mixture, 1.7 m from the observation-well, is higher than the value reached in laboratory (30 %) and indicate saturation. Two other studies that also show volumetric soil moisture levels of approximately 40 % is clay layers constructed at 20-30 cm depth in New Brunswick, Canada (Yanful 1993) and a moisture retaining layer in an oxygen-limiting cover in Quebec, Canada (Simms and Yanful 1999).

The soil moisture in the sealing layers in this study has generally decreased somewhat with time (**Figure 2:G-H**), this might be due to the dry winter period where the water is frozen. In the GLD layer, the soil moisture was higher in the lower parts of the sealing layer (Figure 2:G). However, it seems unlikely that the level in the upper part of the sealing layer reaches under 0 % and might be a instrument error or that the probe is measuring towards a rock. High soil moisture levels in the GLD-mixture is expected due to the high WRC of the GLD (Mäkitalo et al. 2014), which means that the water that percolates through the protection layer is retained in the sealing layer. This trend is also seen in the pilot study discussed above with a similar cover system. In the bentonite layer, the soil moisture content is somewhat lower at depth (**Figure 2:H**). The high WRC and the higher wt. % of GLD in the sealing layer is likely the reason of the higher soil moisture contents in this layer compared to in the bentonite layer. It is however too early to draw any conclusions between the data, as the bentonite layer was constructed this year and the GLD layer a year before. The GLD layer has therefore had a year more for water to penetrate through the protection layer, compared to the bentonite layer.

In summary the soil moisture content is decreasing with time, likely due to the dry winter period. The GLD has a higher moisture content with depth and the bentonite layer a lower content with depth. The GLD-layer indicate saturation in one of the measuring points.

Conclusions

The conclusion of the data set so far is that the protection layer work as a protection from frost penetration and has kept the sealing layer intact. The oxygen concentrations show no decrease in concentrations comparing measurements under and on top of the sealing layer. A decreasing trend in oxygen concentrations is seen in the bentonite layer with time, but the oxygen concentrations are still too high for a sealing layer. At least one of the probes seem to be affected by leakage and the cable-well-connections need improvement in the sealing. The atmospheric pressure is affecting the oxygen concentrations greatly which makes it difficult to detect trends. The soil moisture data indicate that the sealing layer of GLD-till mixtures is nearly saturated at parts. The collected data indicate a slight difference between the data from the bentonite- and GLD surfaces, with higher moisture levels in the GLD. More data and a longer monitoring time are needed to detect any trends between seasons and sealing layer materials.

Acknowledgments

The study is financed by Boliden Mineral AB, Vinnova, Swedish Energy Agency, The Swedish Research Council Formas and Mistra's program "Closing the loop" (Project GLAD) and the European Union's Horizon 2020 research and innovation program under the grant agreement Nº 730305 (Project Paperchain).

References

Aachib M, Mbonimpa M and Aubertin M (2004). Measurement and Prediction of the Oxygen Diffusion Coefficient in Unsaturated Media, with Applications to Soil Covers. Water, Air, and Soil Pollution 156 (1): 163-193.

Akcil A and Koldas S (2006) Acid Mine Drainage (AMD): Causes, Treatment and Case Studies. Journal of Cleaner Production 14 (12): 1139-1145.

Aubertin M and Mbonimpa M (2001) Diffusion of Oxygen through a Pulp and Paper Residue Barrier: Discussion. Canadian Geotechnical Journal 38 (3): 658-660.

Bussière B, Maqsoud A, Aubertin M, Martschuk J, McMullen J, and Julien M (2006) Performance of the Oxygen Limiting Cover at the LTA Site, Malartic, Quebec. CIM Bulletin 1 (6): 1-11.

Bussière B, Maqsoud A, Aubertin M, Martschuk J, McMullen J, and Julien M (2003) Results from the Monitoring Program at the LTA Site: Hydraulic Behavior of the Cover.

Collin M and Rasmuson A (1990) Mathematical Modeling of Water and Oxygen Transport in Layered Soil Covers for Deposits of Pyritic Mine Tailings. Vancouver, BC, Canada.

Corey A T (1957) Measurement of Water and Air Permeability in Unsaturated Soil 1. Soil Science Society of America Journal 21 (1): 7-10.

Dagenais A, Aubertin M, Bussière B, and Cyr J (2006) Performance of the Lorraine Mine Site Cover to Limit Oxygen Migration. Transactions-Society for Mining Metallurgy and Exploration Incorporated 318: 190.

Guide, GARD (2012) Global Acid Rock Drainage Guide. The International Network for Acid Prevention.Available at: Www.Gardquide.Com. (Accessed 12 June 2013).

Höglund LO, Herbert R, Lövgren L, Öhlander B, Neretniks I, Moreno L, Malmström M, Elander P, Lindvall M, and Lindström B (2004) MiMi-Performance Assessment: Main Report.

Lundgren T (2001) The Dynamics of Oxygen Transport into Soil Covered Mining Waste Deposits in Sweden. Journal of Geochemical Exploration 74 (1-3): 163-173.

Mäkitalo M, Maurice C, Jia Y, and Öhlander B (2014) Characterization of Green Liquor Dregs, Potentially Useful for Prevention of the Formation of Acid Rock Drainage. Minerals 4 (2): 330-344.

Mäkitalo M, Macsik J, Maurice C, and Öhlander B (2015) Improving Properties of Sealing Layers made of Till by Adding Green Liquor Dregs to Reduce Oxidation of Sulfidic Mine Waste. Geotechnical and Geological Engineering 33 (4): 1047-1054.

Massmann J and Farrier D F (1992) Effects of Atmospheric Pressures on Gas Transport in the Vadose Zone. Water Resources Research 28 (3): 777-791.

O'Kane M (1995) Aspects on the performance or the till cover system at Equity Silver Mines Ltd.

Ricard JF, Aubertin M, Firlotte FW, Knapp R, McMullen J and Julien M (1997) Design and Construction of a Dry Cover made of Tailings for the Closure of Les Terrains Aurifères Site, Malartic, Québec, Canada.

Ricard JF, Aubertin M, Pelletier P, Poirier P, and McMullen J (1999) Performance of a Dry Cover made of Tailings for the Closure of Les Terrains Aurifères Site, Malartic, Québec, Canada.

Saria L, Shimaoka T, and Miyawaki K (2006) Leaching of Heavy Metals in Acid Mine Drainage. Waste Management & Research: The Journal of the International Solid Wastes and Public Cleansing Association, ISWA 24 (2): 134-140.

Simms P H and Yanful E K (1999) Some Insights into the Performance of an Experimental Soil Cover Near London, Ontario. Canadian Geotechnical Journal 36 (5): 846-860.

Swedish EPA (2018). In Swedish: Avfall i Sverige 2016. Bromma, Sweden: Arkitektkopia AB.

Verburg R, Bezuidenhout N, Chatwin T, and Ferguson K (2009) The Global Acid Rock Drainage Guide (GARD Guide). Mine Water and the Environment 28 (4): 305-310.

Yanful E K (1993). Oxygen Diffusion through Soil Covers on Sulphidic Mine Tailings. Journal of Geotechnical Engineering 119 (8): 1207-1228.

Managing uncertainty in planning opencast coal final void closure and relinquishment

David A Salmon[1]

[1]*Amanzi Consulting, 44 Lakeside Drive, Peregian Springs, Queensland 4573, Australia*

Abstract

Coal mining companies face uncertainty when selecting appropriate management measures during planning for closure and relinquishment of opencast coal mine final pit voids.

Existing guidelines generalise mine water management and mine rehabilitation practices. Coal mine specific needs may not be met. Guidance can be misinterpreted, and inappropriate, unacceptable measures applied, such that mine water, closure and relinquishment goals are not achieved, making business decisions uneconomic and ineffective. This is a causal factor in the lack relinquishment of opencast coal mine final voids.

ACARP project C25030 researched this dilemma in the eastern coalfields of Australia. The guidance material produced is described.

Keywords: AMD, mine water, guideline, coal mine, opencast, pit void, pit lake, mine closure, mine relinquishment

Introduction

Emphasis on closure planning by Australian coal mines has increased as these mines mature and as some mines face early closure. A common strategy that mines adopt when planning closure is relinquishment of the mining lease to the State. In opencast coal mines this strategy could include leaving open pit final voids that are commonly recharged to form a pit lake. Public concerns apropos water filled coal mine voids in Eastern Australian coalfields have been increased by recent media articles and published documents by stakeholder groups (Walters 2016). These articles have driven stakeholder expectations regarding post mining use, which are not always practical or economically feasible. Backfilling of final voids with mining waste, changing final void pit lakes storing mine water to a backfilled pit containing mine water as groundwater within the backfill, is now the regulator's preferred option.

When assessing and planning water management, rehabilitation and closure options, and implementing designs, the overarching goal is to ensure post closure water and land uses are safe, stable, sustainable, and non-polluting. Existing guidance on the subject of mine water management and closure and relinquishment practices to achieve these goals is generic (DRET 2006, 2007, GARD 2012, ICMM 2008, DISS 2016). Guidelines for pit lakes and mine voids are frequently based on experience in hard rock mines and quarries; coal mine specific needs are not covered. Therefore, available guidance can be misinterpreted resulting in inappropriate and unacceptable measures being applied to coal mines that have their own unique characteristics. In these situations, mine water, mine closure and relinquishment goals may not be achieved, and the business decisions made can prove uneconomic and ineffective. Furthermore, such guidance has lead to misunderstanding by regulators and other stakeholders as to the practices and management measures that can be appropriately applied to coal mine sites.

Application of inappropriate management options financially impacts mining companies wanting to expend effort and resources on workable and acceptable actions leading to relinquishment. This has resulted in uncertainty occurring during planning and implementing coal mine closure activities. Unsurprisingly, uptake of existing guidance, by coal mines, has been limited.

These challenges in the closure of the

opencast coal mine void domain are such that relinquishment of mine sites, in the Queensland (QLD) coalfields of Australia, has not been achieved.

An Australian Coal Association Research Program (ACARP) project C25030 report (Salmon, 2017) provides guidance material to address the uncertainty during water management planning, closure and relinquishment of opencast coal mine final pit voids. The project was supported for ACARP funding by six mining houses; Anglo American, BHPBilliton, New Coal, Peabody Energy, Premier Coal and Qcoal. This paper presents a very brief overview of this work.

Project objectives

At the outset, the project had eight key objectives; to document examples of practices applied to coal pit voids; to provide a reference list of examples of practice; to identify and confirm challenges to pit closure; to provide a list of findings; to identify gaps in knowledge that could increase residual water environmental risk post-closure; to identify stakeholder perceptions of risks associated with void closure; to record regulator understanding and requirements for void closure including scientific and engineering studies and methodologies needed for relinquishment application; and to develop a guideline and a process for opencast coal pit void closure.

The overarching goal of the project was the provision of guidance to support decisions made by coal mine staff planning and implementing closure activities, and which enables residual risk reduction, lists the aspects needing assessment by mines preparing relinquishment applications, and provides assurance to regulators and other stakeholders that residual risk is minimised or removed.

Guidance given in the report is applicable to hard bituminous thermal and coking coal pits, brown coal and lignite mines, and coal pit voids that are dry or contain mine water. Some approaches may be applicable to other types of opencast mining and commodities, but this was not the focus of the project.

Methods

Information was collected through global literature searches, meetings with mining company representatives and site visits to thirteen coal mine sites. The coal mine sites visited were located in the north, central and southern parts of the Bowen Basin coalfield and in the West Moreton coalfield of QLD, and in the Hunter Valley and the Newcastle coalfields of New South Wales (NSW).

Thirteen criteria were used to assess the suitability of sites visited including; mine site geographic location, geological location, coal type, climatic, mining methods employed, surface water regimes, groundwater regimes, rehabilitation methods used or planned, backfilling, final void type, landform design, planned final land use, stakeholder and community engagement and the closure criteria in place.

Guideline development was based on mine site practices and those found in the literature.

Findings

Twelve findings, common to all coal mines were determined and included;

- Uncertainty in acceptable water management and rehabilitation practice occurs throughout the industry
- Void terminology has not been adequately defined leading to confusion amongst practitioners and stakeholders
- Variability in geology and mining methods creates differing pit void geometries
- A variety of water and rehabilitation management measures are employed
- A variety of different planned final land and water uses occur
- Planning and implementing water management and rehabilitation measures for the final pit cannot be considered in isolation from the rest of the void because they are hydraulically interlinked
- Stakeholder engagement gives a better outcome
- Mines have been overly optimistic in stating final water and land use
- External stakeholders may have inappropriate expectations of open pit void post-closure water and land uses
- Safety and health are important aspects of closure and relinquishment of voids
- Final void management plans are being requested more frequently by regulators.

Gaps in information needed for void closure management planning were found and included the lack of or inadequate, water monitoring data, geochemical characterisation of mine materials, characterisation and classification of voids, and development of void water balances and mine waste material balances. A further twenty-six additional constraints and issues that could affect void closure and relinquishment are listed in the report (Salmon 2017).

Aspects to consider in planning void closure measures

General guiding principles in planning coal mine void closure measures were developed. These provide confidence that correct process is being followed. For coal mine voids these general principles include:

- Definition and quantification of the total void area, including the backfilled areas as well as any final pit void
- Determination of the final land use of the total void area (catchment) and the final void taking into consideration the type, amount and extent of the backfill used and the surface landform created, as these factors impact both surface water and groundwater regimes
- Definition of the geology including geochemical assessment and geotechnical testing of all materials mined and placed in the void to allow understanding of the hydrogeological regime
- Development of a void water balance
- Development of a mine waste material balance
- Investigation and trials of any planned measures
- Development of the geometries of the coal mine pits such as the basic cross section for a coal mine pit void given in Figure 1. Water flows into and out of coal pits are described in Salmon (2000).

The guideline report (Salmon 2017) contains examples of existing practice. Some of these include:

- Investigation of the impacts of mining methods and development of void geometry
- The development of void water balances and modelling
- The development of mine waste material balances and impact on final void geometry including surface water drainage and the water holding capacity of the void
- Pit void backfilling methods and backfill material types both solid and liquid waste such as overburden, coal processing coarse discards and wet and dewatered tailings, reactive waste materials, water storage and water treatment waste
- Descriptions of high wall and low wall treatments for stability and development of final landforms slopes, including the methodology and practice of leaving highwalls and side walls in place, reprofiling highwalls and sidewalls to shallower slopes and blending these into the adja-

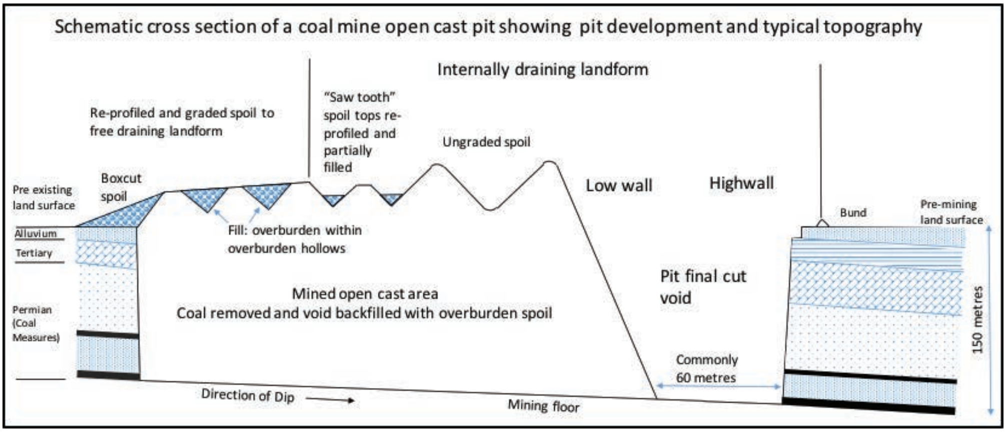

Figure 1 *A cross section showing the geometry of a coal mine pit void (modified from Salmon, 2017)*

cent void backfilled landforms and the effects on surface water and groundwater water
- Final land uses and impact on water resources
- Final void water uses
- Description of options analysis methods
- Description of risk assessment methodology based on source, pathway and receptor analysis and the impacts to water resources
- Environmental risks to water resources associated with the landforms implemented
- Land rehabilitation and closure strategies, specifically actions to achieve safe, stable and sustainable and non-polluting landforms
- Development of final void management plans.

A process for closure and relinquishment

A number of decision making processes were produced for the guideline. The process considers discussion of benefits and challenges of relinquishment, an analysis of alternative water management and closure options and a risk assessment for pit voids.

An overarching fourteen-step process from closure of coal mining operations to the relinquishment application is described (Salmon 2017). These steps include:

- Site assessment
- Regulatory assessment
- Stakeholder participation
- Assessment and strategy for void land and water use
- Backfilling solid or liquid backfill and effects on water regimes and land form (slope) design and water runoff and usage
- Geotechnical stability and impact of groundwater on this aspect
- Classification of the void based on water balance
- Final void environmental impact statement
- Rehabilitation of the watershed land surface
- Care and maintenance of the watershed and pit lake
- Closure criteria and water monitoring
- Residual water risks specifically AMD and mine water hydrochemistry
- The financial assurance estimation
- Relinquishment application.

Within these overarching process steps there are other processes such as the actions to characterise void type. This process is shown in Figure 2. Voids are divided into three distinct types; dry voids, seasonal pit lakes and permanent pit lakes. Pit lakes are further classified, according to their water balance, into terminal sinks, through flow, recharge or overflow systems.

Conclusions

Existing guidance on open pit coal mine voids has not met the business needs of the coal mining sector in the Eastern coalfields of Australia. Guidance is too generalised and based on hard rock mine pit needs and experience. This has resulted in poor business decisions by applying inappropriate water management and void closure strategies or being requested of coal mines by regulators and stakeholders. In eastern Australian coal mines this is illustrated by demands for internally drainage void systems and the later reversal to demands for free draining landforms.

Unsurprisingly, uncertainty continues to exist on what is required to be done to achieve relinquishment due to the generic nature of existing guidelines and lack of regulatory process.

Open pit coal strip mining will, for most pits, end in a permanent void which, if mined below the water table, will fill as groundwater rebounds and surface runoff inflows to form a pit lake. In eastern Australian coal strips mines the void will commonly be a terminal sink unless it is backfilled with solid material to above the water table rebound elevation.

The unique characteristics of each coal mine requires site specific approaches to mine water in void landform surface and groundwater drainage. There is no one size fits all guideline or a single strategy, package of practices or set of methodologies and techniques that can be applied across all mine sites since each mine has unique issues reflecting site-specific characteristics.

Any application of generic water manage-

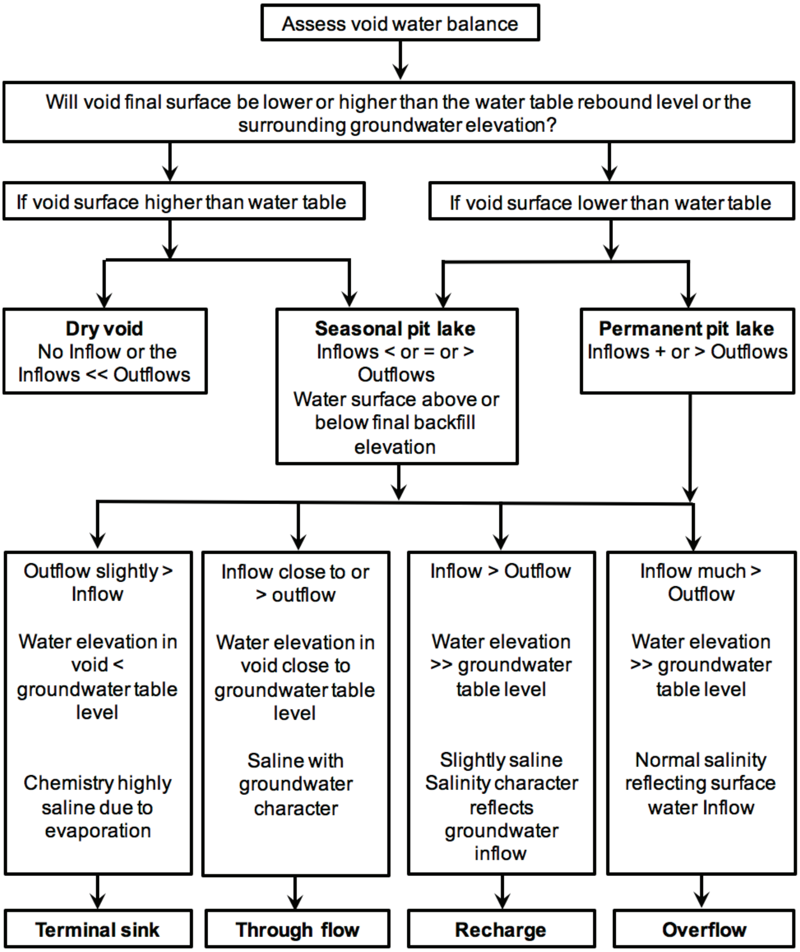

Figure 2 Characterising pit voids and lakes (modified from Salmon 2017)

ment and rehabilitation and closure measures or those used by different mines and mines in different geographies must be trialled to ensure practical relevance to a mine site.

A lack of appropriate guidance limits regulator and community understanding of opencast coal mine closure. It can result in demands for coal mines to apply inappropriate rehabilitation measures that can raise community expectations on what can reasonably be achieved. Mine staff should engage with stakeholders and demonstrate to them appropriate water management measures to prevent such demands.

Mining company statements have historically overstated potential post mining water uses. Such statements raised stakeholder expectations and created distrust of mines by regulators and communities when expectations are not achieved. Scientifically based assessment of water management practice applicable to mine site conditions is needed.

Final void post- closure uses are highly dependent on the geographic location of the mine; its proximity to urban areas, transport routes or its location in remote areas. Successfully implemented mine water uses post mine closure are those that match the surrounding landscape and have received endorsement by local communities and regulators.

Planning and implementing rehabilitation measures for the final pit cannot be considered in isolation from the rest of the void because they are intimately interlinked, hydrologically and hydrogeologically. Knowledge on aspects of backfill spoil hydrogeology and pit void wall geotechnical stability are inadequate to provide confidence about post - closure residual risks to the environment and safety. These aspects require further investigation.

Information on existing practices combined with knowledge sharing between mines can provide confidence to operators that they are planning or implementing the right mine water management practice to achieve the best possible outcomes and gain acceptance by regulators and stakeholders.

Acknowledgements

ACARP staff Keith Smith and Nicole Youngman and the ACARP industry mentors Jason Fittler, Hayden Leary and Pieter Swart provided direction for this project. The staff at the mines visited provided valuable information on the respective sites and willingly gave up time from their work schedules to do this. To all these people I would like to express my gratitude and thanks.

References

DRET (2006) Mine Completion and Closure. Leading Practice Sustainable Development Program for The Mining Industry.

DRET (2007) Managing acid and metalliferous drainage. Leading Practice Sustainable Development Program for The Mining Industry

Department of Industry, Innovation and Science (DIIS). (2016a) Mine closure. DIIS, Canberra

ICMM (2008) Planning for integrated Mine Closure Toolkit. International Council on Mining and Metals 2008.

INAP (2012)) Guideline on Acid Rock Drainage (GARD).

Salmon DA (2000) Management of coal mining impacts on water resources in South Africa. In Sililo, O. (Ed). Past Achievements and Future Challenges. Proceedings of the XXX IAH Congress on Groundwater. Cape Town, South Africa. Published by A.A. Balkema, Rotterdam.

Salmon DA (2017) Guidelines for coal mine open pit final void closure and relinquishment. ACARP Project C25030 Report 169pp June 2017. ACARP Brisbane Australia

Walters A (2016) The Hole Truth: The mess coal companies plan to leave in NSW. Energy and Resources Insights Report for the Hunter Communities Network. http://www.erinsights.com/research/hole-truth.

Facing Challenges of Closure Boom of Underground mines in the Permo-Carboniferous coalfields of the North China: a Medium-size Hydrogeochemical Simulation Experiment ◎

Changshen Wang[1], Haibo Bai[2], Shucai Liu[1]

[1]*China University of Mining and Technology, School of Resources and Geosciences, Daxue Rd 1, Xuzhou 221116, China, cougar3wcs@163.com*

[2]*State Key Laboratory for geomechanics and deep underground engineering, China University of Mining and Technology, Daxue Rd 1, Xuzhou 221116, China*

Abstract

With the shift of coal mining industry from the east Permo-Carboniferous coalfields to the west Jurassic coalfields, there would inevitably appear a boom in coal mine closure in China. However, from the extraordinary mine water problems occurring in the active coal mines, we could anticipate that the hydrogeochemical issues in those abandoned coal mines will also be another case. The paper constructed two medium-size cells to simulate abandoned coal mines with open and close water system respectievly to investigate the hydrogechemical process. The results showed that, after being flooded, the simulated open and close system was medium to light alkaline and had obviously different evolving process for Na+, SO42-, HCO3-, TDS, Sr, Mo, Li and Sb. Most of future abandoned underground coalmines in North China are concealed and would end in relative close water systems and result in a depth-varied hydrogeochemical regime.

Keywords: closure, China, simulation experiment, Permo-Carboniferous coalfields, hydrogeochemistry

Introduction

Nowadays China's coal industry has still been shifting from the eastern Permian-Carboniferous coalfields to the western Jurassic coalfields (National Development and Reform commission 2016), which means more than 3/4 of Permian-Carboniferous underground coalmines in the east China will have to be closed in a very near future. However, there are still no enough experience on mine closure in favor of China to ensure what hydrogeochemical regime would be in those abandoned mining areas and to further answer whether, what extent and when the groundwater in flooded coal mines could be utilized again.

Even for those active coal mines, apart from being notorious for the hazardous inrush accidents (Kailuan Mining Bureau 1986, Bai 1998, Wu 2013), they have also showed the extraordinarily typical mine water features of neutral pH, high TDS, high sulphate, and high alkaline, which is definitely different from those having been widely concerned and investigated in Europe (Wolkersdorfer 2005), North America (Wildeman 2007, Diehl 2012), Australia (Department of Industry Tourism and Resources 2007) and South Africa. So, it can be reasonably imagined that the forthcoming abandoned coalmines would be running on a different track and the closure experience in Europe, North America, etc. might not be simply applicable to China. It is imperative to invest some fundamental investigations to characterize the specific hydrogeological features of flooded Permo-Carboniferous coalmines in north China.

As reported, the methods to investigate the hydrogeochemical features of abandoned mine pool mainly include static methods and dynamic methods. Most popular static methods are ABA and NAG. Dynamic methods are column test and standards HCT test. Considering the representatives, there are also some medium simulation.

Located in the extensive North China alluvial plain, most of the future abandoned coal mines will finally end up as relatively close ground water cycle systems, which controls the process and destiny of the hydrogeochemical environment. This paper is aimed to simulate a pair of flooded closed coal mines with and without consistent water cycle, as open and close system respectively, and to monitor the hydrogeochemically process occurring.

Sampling and Methods

Samples: collected from the Zhangshuanglou coal mine in the Xuzhou Permian-Carboniferous coalfield near eastern side of the North China alluvial plain; made up of coal gangue and overburden dump of the coal bearing Shanxi Formations of the early Permian which are unconformably underlain by the Ordovician-Cambrian marine carbonate deposits; consisting chiefly of typical terrestrial sediments of coal, mudstone, siltstone, quartz sandstone, feldspathic sandstone, lithic sandstone, etc.; and crushed into fragments of grains < 26mm in diameter.

Simulating system: aimed to simultaneously simulate a concealed flooded coalmine with an overall closed water cycle and a half-concealed flooded coalmine with an open water cycle respectively(fig. 1); using two medium size cylinder cells (Φ1.5m × height 2.0m) with built-in dynamic and hydrogeochemical sensing systems which include sensors of water head, temperature, pH, dissolved oxygen (DO), conductivity, Redox, etc.; loaded each with 4≈5 metric tons of crushed samples; initially flooding both of the simulating cells with the chemically known tap water at a flow rate which was determined on the basis of estimated flooding recharge to the Zhangshuanglou coal mine and then only consistently recharging the open system while stopping recharging the close system; at the same time, leachate being periodically collected from the pre-built-in outlets and chemically assayed by ICP-AES.

Figure 1 the medium-size hydrogeochemical simulation platform

The simulating system has been in operation since January of 2017 and will run for at least two years.

Results

Flooding process: The two simulated abandoned coal mines were flooded in about two months and therefore it is estimated that the future abandoned Zhangshuangji coal mine will be flooded within 5-6 months.

After being flooded, the simulating open and close systems showed a different hydrogeochemical process and trend in terms of physical parameters of pH, Dissolved Oxygen (DO), Redox and conductivity: (1) after 34 day since the simulating systems were set up on Jan. 18, 2017, the pH value of the open and close systems firstly soared from 7.7 to the peak of 8.61, then gradually sloped down to the lowest point of 7.6 in Aug. 2017, and finally mounted again to 8.0 in April 2018; in general, the pH of the open system is a little higher than that of the closed system; (2) so far, in terms of the average DO of the leachate collected through the pre-built-in outlets at the height of 1.5m, 1.0, and 0.5m in the cylinder cells, while the open system showed in turn a downward trend from 3.47 mg/L, 3.11mg/L to 2.51mg/L respectively, the close system with an overall lower DO, which are 3.12mg/L, 3.19mg/L and 2.14mg/L respectively, presented a relatively higher DO at the medium height; (3) the redox of the leachate in the two simulating system linearly slowed down from the initial +300 mv to the present -200mv in the first four months, then the redox in the open system mount slowly to +100mv again and the redox in the close system fluctuate between +100 to -150mv; (4) initially in a month, the conductivity of the leachate in the open and close systems synchronously rose up to a peak value of 2600 us/cm on April 9, 2017 and then synchronously descend to 2100 us/cm on May 25, 2017; from then on, the conductivity in the open system continuously descended to 1300 us/cm, while the conductivity in the close system rose up again to about 2600us/cm. It proved that the insistent recharge after flooding made the hydrogeochemical difference.

The water quality of the leachates periodically sampled from the open and close systems showed a main difference in the concentrations of Na^{2+}, SO_4^{2-} and HCO^{3-}: (1) the Na^+ in the two simulating systems fairly synchronously rose from the initial concentration of 205mg/L to the peak value of 508 mg/L on April 26, 2017 and then on June 4, 2017 the close system deviated from the downward trend, as the open system was developing, to mount again instead; (2) after being flooded, the SO42- in the two simulating system quickly went up to the highest value of 650 mg/L on April 10, 2017 and then turned into a linearly downward trend to 200mg/L with the close system changing its evolving tendency away from that of the open system on May 18, 2017 to stay around 480mg/L; (3) till May 18, 2017, the concentrations of HCO3- of the two simulating systems were insistently rising from 300 mg/L to 500 mg/L, afterward the HCO3- in the open system reached a plateau around 500mg/L, while the HCO3- in the close system continuously mounted up to 760 mg/L.

There were 16 kinds of metals, including V, Cr, Mn, Fe, Co, Ni, Cu, Zn, As, Sr, Ba, Pb, Mo, Sb, Li and Al , being tested for the leachate. In comparison, the open and close systems showed an obvious common or distinct release features for the trace metals of Sr, Mo, Li and Sb: (1) though, at the early stage, the open and close system released the metal of Sr, Mo and Li in an almost synchronous way, while, after June of 2017, the release process obviously diverted into two trend;(2) since the beginner, the open and the close system showed an ideally simultaneous Sb release process; (3) the concentrate of Mn, Fe, Ni and Sb exceeded the drinking water standards (China).

Conclusions

It is concluded that (1) after being flooded, the abandoned underground coalmines in Permo-Carboniferous coalfield would mainly experience reactions of dissolution, adsorption, etc. of sulfate, Ca, Na and K rather than the oxidation-reduction reactions of Fe, Mn, etc.; (2) the flooded groundwater pool would be medium to light alkaline; (3) most of future abandoned underground coalmines in North China are concealed and will end in relative close water systems and result in a depth-varied hydrogeochemical regime; (4) Sr, Mo, Ni and Sb could be the main potential pollutants; (5) the trend and fate of abandoned coalmines would closely related with the genesis of Permo-Carboniferous coalfield themselves.

Acknowledgements

The study presented in this paper was supported by the grant of the National Basic Research Program of China (Grant No 2013CB227900).

References

National Development and Reform commission (2016) the 13th Five-Year Plan for the development of China Coal Industry.

Kailuan Mining Bureau (1986) Salvage from gigantic karst water inrush through sinkhole. Coal Science Technology, (1): 6-14,64

Bai HB, Cheng ZS, Zheng BL, et al. (1998) Extra-large water inrush through concealed karst sinkhole: Identifying water sources and salvaging. Coal Engineer (6): 34-36

Wu Q, Cui FP, Zhao SQ, et al. (2013) Type classification and main characteristics of mine water disasters. Journal of China Coal Society 38(4): 561-565

Wolkersdorfer Ch, Bowell R. (2005) Contemporary reviews of mine water studies in Europe. Mine Water and the Environment 24: 1-76

Wildeman T.R., Smith K.S., Ranville J.F. (2007) A simple scheme to determine potential aquatic metal toxicity from mining wastes. Environmental Forensics (8): 119-128

Diehl S.F., Goldhaber M.B., Koenig A.E., et al. (2012) Distribution of arsenic, selenium, and other trace elements in high pyrite Appalachian coals: evidence for multiple episodes of pyrite formation. International Journal of Coal Geology (94): 238-249

Department of Industry Tourism and Resources, Australian Government (2007) Managing acid and metalliferous drainage

Safety Management of Producing Coalmines Adjacent to Closed Coalmines: Case Study of a Coalmine Closure in Xuzhou Mining Area, China◎

Zhimin Xu, Yajun Sun, Mengfei Zhang

School of Resources and Geosciences, China University of Mining and Technology, Xuzhou 221116, China

Abstract

This paper selects Pangzhuang Coalmine in Xuzhou mining district as a case study, and carries out two detailed technical measures: the post-closure safety evaluation and the safety management measures. The safety evaluation includes: the volume calculation of the mining goaf, the prediction of water levels rising, the prediction of local groundwater level recovery and the assessment of adjacent coalmines' boundary coal pillars stability. On the other hand, the safety management measures include: the monitoring of water level ascending in the goaf, the monitoring of local groundwater level recovery, the construction of the water-block wall in connected mining lanes and the pre-closure drainage in surrounding coalmines.

The research and practice results show that, the local groundwater level will recover to its initial state after 9 years by the predicting and the water level rising in the mining goaf after the mine closure by the real time monitoring, it is very important for the adjacent coalmines to take the initiative safety management and measures to prevent and control the goaf water.

The results of the paper has proved the evaluation and management measures as the most cost-effective approach for post-closure safety, and also bring sustainable benefits to the mining stage before the mine closure. The practical experience obtained in this paper is of great significance for China's coalmine to prevent and control the goaf water after closing a large number of adjacent coalmines.

Keywords: mine closure, goaf water, water level recovery, monitoring, mine drainage

Introduction

In recent years, due to the increasing depletion of coal resources in eastern China, the macro-economic control of the country's energy policy and implementation of capacity reduction policies, a large number of coalmines in China's eastern region have gradually closed. Xuzhou mining area has 140 years of mining history, and all coalmines has been closed by the end of 2016. The coalmines in Xuzhou mining area were mainly distributed around the urban areas, and most of the coalmines were located adjacent to each other. During the closure of each coalmine, a series of problems related to hydrogeology and environmental effects arose, the resulting rising water levels affected the deeper producing coalmines. Rising groundwater level in the closed coalmines flowed into the neighboring coalmine in production through some fractures or other water-conducting passages, including breaking through boundary pillars.

Nowadays, the developed countries have begun to research the ecological problems to solve the series of hydrogeological and environmental effects after mine closure since the last century. Dogaru et al. (2009) studied the balance of mining and the environmental risks caused by mining from the perspective of socio-economic and environmental. Lghoul et al. (2014) investigated the characteristics and evolution of mine water and its impact on regional water resources. Khalil et al. (2013) performed the ecological impact and acid toxicity study of acid mine water. With the large number of coalmines closed in China, Huang et al. (2017) proposed the technical system framework of mine closure, Wu and Li et al. (2018) analyzed the positive and negative eco-environmental effects of closed coalmines and proposed corresponding countermeasures. For the safety problem after mine closed, Xiao et al. (2014) conducted experimental research and analysis on the stability of the boundary pillars, Zhou et al. (2010, 2013) analyzed the environmental and safety hazards caused by rising water level of abandoned mine, Li (2014) studied the risk assessment of underground water pollution in abandoned mines, Chen et al. (2015) studied the technical approaches to the geologic environment treatment in closed mines. Although a large amount of basic work was done on the problem of closed mines, there was still a lack of relevant, systematic research.

In this paper, using the example of the threat caused to the Jiahe Coalmine after the closure of the adjacent Pangzhuang Coalmine, the safety management of producing coalmines adjacent to closed coalmines was studied.

Hydrogeological conditions of the study area

The Pangzhuang Coalmine is located in the Jiuli District of Xuzhou , 13 km from the city's center. Formally commissioned on May 1, 1965, the originally designed production capacity of the mine was 450,000 t/a, but after transformation, the approved production capacity was increased to 1.4 million t/a. The main mining coal seams in Pangzhuang Coalmine are No. 7 and No. 9 coal seams, and there are four production levels at–370m,–520m,–620m,and–850m. Due to the exhaustion of the resource, the Pangzhuang Coalmine closed in August, 2013.

The Jiahe Coalmine is located in the southwest of the Pangzhuang Coalmine and the production level is lower than the goaf of the Pangzhuang Coalmine. With the groundwater level rose continuously after the closure of Pangzhuang Coalmine, the groundwater flow transferred from the original mine drainage to a weak section along the coal pillars, faults, and other channels into the Jiahe Coalmine. The Shitun Coalmine is located in a shallow area of Pangzhuang Coalmine and connected by a roadway at the −370m level to the Pangzhuang Coalmine. When the recovering groundwater level rising at —262m, the groundwater of Pangzhuang Coalmine will drain through the connecting roadway and threaten safe production at the Shitun Coalmine. The Wangzhuang Coalmine is also located in a shallow area of the Pangzhuang Coalmine, but there is a natural water-resistant boundary and no hydraulic connection between the two coalmines.

Analysis of the groundwater storage space and flow route

The groundwater storage volume of Pangzhuang Coalmine

The total mine water inflow in Pangzhuang Coalmine is 93m^3/h: the −370m level is 18m^3/h, the −520m level is 26m^3/h and the −620m level is 49m^3/h. Since the mine closure, the rising groundwater formed four catchments at −850m, −620m, −520m and −370m levels (Fig. 1).

In the mine safety evaluation, the calculation of the volume of the mine water in the goaf is particularly important. This article distribute the amount of water in the mining area to each area according to the area of the Pangzhuang Coalmine . The water line is delineated every 20m according to the contour line, of which −370m catchment recharges the -520 catchments and the two catchments are unified into a single catchment area. A preliminary estimation of the volume of water storage for each catchment area was obtained by the following formula from China's

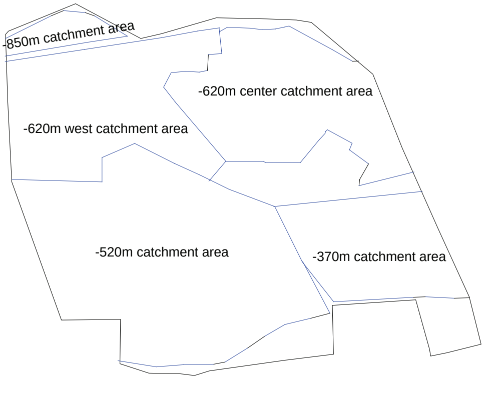

Figure 1 The four catchments of Pangzhuang Coalmine.

National Regulations on Prevention and Control of Mine Water in Coalmines:

$$Q = KMF\frac{1}{\cos a}$$

where Q is the goaf water accumulation (m3), α is the coalseam inclination (°), K is the water-filling coefficient (0.25 was used in this study), M is the mining thickness (m) and F is the horizontal projection area of the goaf water area (m^2).

By calculation, after the Pangzhuang Coalmine closed, there is a lot of mine water storage space below the level of -370m, and the amount of water that can be accommodated is $4522905m^3$.

Stability analysis of the boundary coal pillar

According to the width of the coal pillars at the boundary of the Pangzhuang and Jiahe Coalmines, the gap between the pillars at each level is relatively different: the narrowest boundary of the No.7 coal seam is at the −440m level, where is only 14m; the narrowest boundary of the No.9 coal seam is at the −530m level. The deepest elevation of the No.7 coal seam goaf adjacent Jiahe Coalmine is −685m, where the width of the boundary pillar is 36m. The deepest elevation of the No.9 coal seam adjacent Jiahe Coalmine is −670m, where the width of the boundary pillar is 38m.

According to the national technonigical regulations, the following formula from China's National Regulations on Prevention and Control of Mine Water in Coalmines is derived to calculate the head pressure that the coal pillars can withstand:

$$P = \left(\frac{2L}{KM}\right)^2 \frac{K_P}{3}$$

where L is the width of coal pillar (m), K is the safety factor, generally take 2-5, M is the mining thickness (m), and P is the water head pressure (MPa), Kp is tensile strength of the coal seam(MPa).

By calculation, when the water level rises to -441m, the water pressure on the boundary coal pillars of -685m and -670m levels reach a critical value; when the water level rises to -403m, the -440m horizontal boundary pillar reaches a critical value. As the water level continues to rise, the goaf water of Pangzhuang Coalmine will inrush into the Jiahe Coalmine.

Prediction of water level rising in the goaf

As the water level in the goaf of Pangzhuang Coalmine continues to rise, the volume of water in the goaf will gradually decrease. After about 9 years, the regional groundwater level will reach a new equilibrium and the water level will recover to −370m (Fig. 2).

The goaf water control measures of Pangzhuang Coalmine

In order to achieve effective safety management of Pangzhuang Coalmine, the time required for the water level to reach the weak pillars will win time for safe production to Jiahe Coalmine. This paper proposes prevention and control measures for the goaf water hazard (Fig. 3).

The first line of deep defense

1,600 days after the Pangzhuang Coalmine closed, the water level in the goaf area rises to −441m and the boundary pillar located at −685m is damaged. At this time, the amount of water contained in the goaf area was about $3,817,149m^3$. Therefore, we can use the goaf area to store water and take the real-time monitoring. After investigation, two monitoring holes were installed (Fig. 4). Monitoring hole 1 is located in the No. 7541 panel of Pangzhuang Coalmine −620m level mining area near the boundary; monitoring hole 2 is located in the No. 7433 panel of a mining area to the west of the Jiahe Coalmine near the boundary.

The second line of deep defense

If the mine water in Pangzhuang Coalmine breaks through the boundary pillars as the water level rises and drains into the Jiahe Coalmine, It can use the goaf area of the west mining area of Jiahe Coalmine to store mine water (the volume is 389,000 m^3) and building necessary water retaining walls at the main water leakage point (Fig. 5) to prevent the goaf water from draining into the deep part of the Jiahe Coalmine.

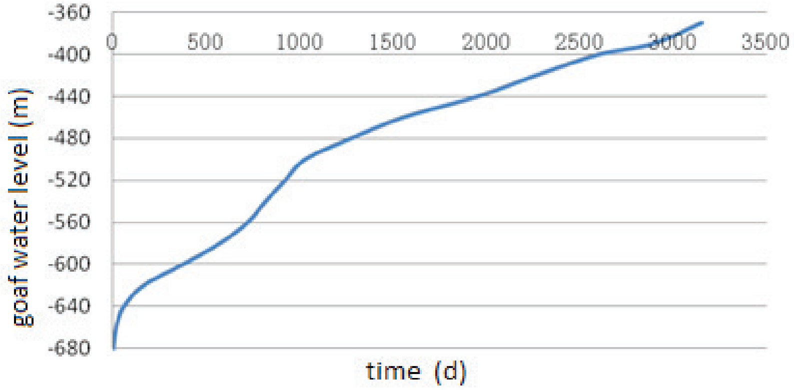

Figure2 Water level recovery and time curve.

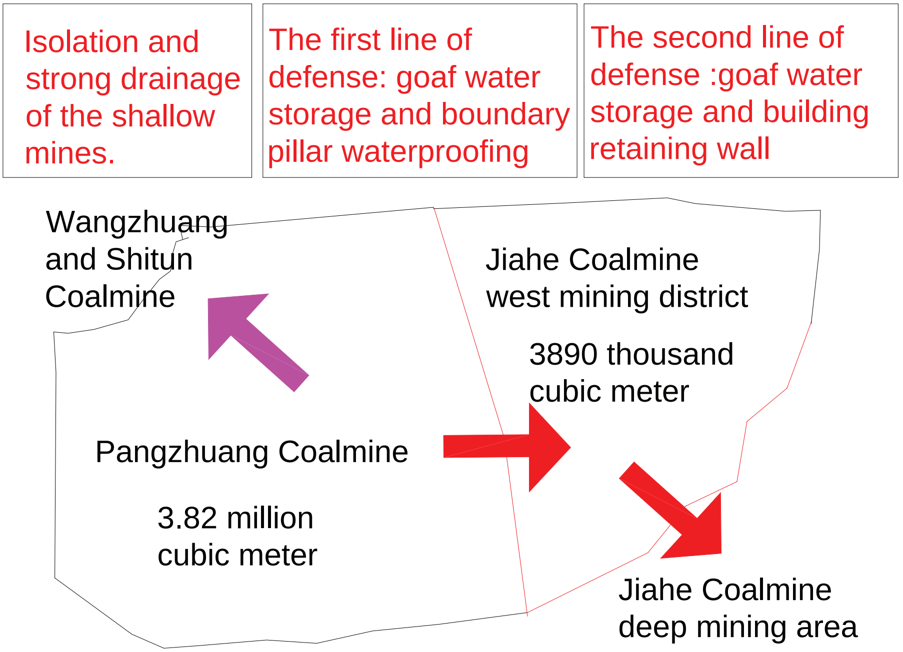

***Figure 3** Prevention and control measures for the goaf water.*

Shallow mine control measures

If the coal pillar is not broken, the goaf water of the Pangzhuang Coalmine doesn't enter the west mining area of Jiahe Coalmine and the water level will continuously rising in the Pangzhuang Coalmine, which poses a threat to the Shitun and Wangzhuang Coalmines.

The Shitun Coalmine contains an artificial boundary between it and the Pangzhuang −370m level roadway and the upper exit at −262m. It is only when the Pangzhuang Coalmine goaf water level rises to over −262m that it can flow through the connecting roadway. However, water in the Shitun Coalmine can be drained using an existing drainage system.

The Wangzhuang Coalmine and the Pangzhuang Coalmine contain natural water-repellent boundaries that cut off the hydraulic connection between the two mines. An inrush of water into the Pangzhuang Coalmine goafs poses little threat to the Wangzhuang Coalmine. However, due to the uncertainty of water passing through the goaf areas, the

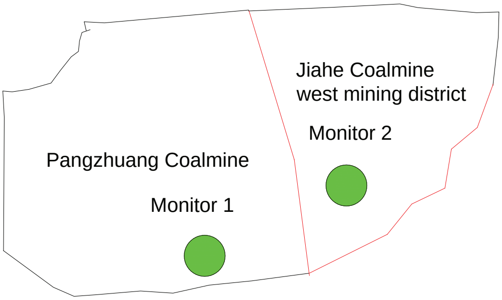

Figure 4 Position of monitoring hole

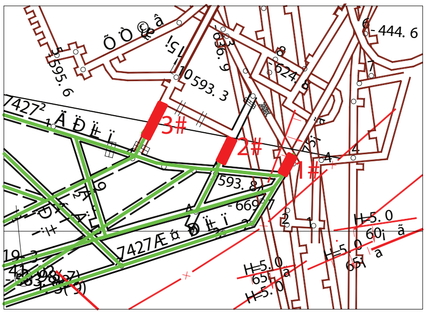

Figure 5 Position of retaining wall

Wangzhuang Coalmine needs to formulate emergency plans for protection against an inrush of water.

Conclusion

(1) In Pangzhuang Coalmine, the goaf below the −370m level can hold 4,522,905m^3 of mine water. When the water level rising to −441m, the water pressure that the boundary pillars at the −685m and −670m levels will reach a critical value; when the water level rising to −403m, the water pressure that the −440m boundary pillar can withstand will reach the critical value.

(2) As the water level in the goaf of Pangzhuang Coalmine continues to rise, the volume of water in the goaf will gradually decrease. After about 9 years, the regional groundwater level will reach a new equilibrium and the water level will recover to −370m.

(3) This paper proposed prevention and control measures for the management of the goaf water hazard created after the Pangzhuang Coalmine closure. The first line of defense at depth is goaf water storage and boundary pillar waterproofing in Pangzhuang Coalmine, and the second line of defense at depth is goaf water storage and building the retaining wall in Jiahe Coalmine.

Acknowledgements

This research was financially supported by The National Basic Research Program of China (No.2013CB227901), the National Key Research and Development Program of China (No.2017YFC0804101) and the National Natural Science Foundation of China (No. 41502282). The authors thank the editors and reviewers for their constructive suggestions.

References

Chen Yuehui, Chen Zhongsheng, et al..Technical approach to geological environmental control in closed mine area[J].Coal Science & Technology,2015(1):81-83.

Dogaru D, Zobrist J, Balteanu D, et al. Community perception of water quality in a mining-affected area: a case study for the Certej Catchment in the Apuseni Mountains in Romania.[J]. Environmental Management, 2009, 43(6): 1131-1145.

Huang B, Liu J, Nan L I, et al. Framework of the theory and technology for mine closure[J]. Journal of China University of Mining & Technology, 2017, 46(4): 715-729 and 747.

Hu Weiyue, Zhou Jianjun, et al . Analysis of environmental and safety hazards caused by rebound of water level in abandoned Mines[J]. Journal of Xian University of Science and Technology, 2010, 30(4): 436-440.

Khalil A, Hanich L, Bannari A, et al. Assessment of soil contamination around an abandoned mine in a semi-arid environment using geochemistry and geostatistics: Pre-work of geochemical process modeling with numerical models[J]. Journal of Geochemical Exploration, 2013, 125(3): 117–129.

Lghoul M, Maqsoud A, Hakkou R, et al. Hydrogeochemical behavior around the abandoned Kettara mine site, Morocco[J]. Journal of Geochemical Exploration, 2014, 144: 456-467.

Li ting. Study on Groundwater Pollution Risk Assessment of Abandoned Coal Mine[J]. Journal of China University of Mining & Technology.

Wu Qiang, Li Songying. Positive and negative environmental effects of closed mines and its countermeasures[J]. Journal of China Coal Society, 2018, 43(1): 21-32.

Xiao Hua, Yang Zhiyang, et al. Influence of water accumulation in the goaf of closed mine on the stability of waterproof coal pillar[J]. Coal Science & Technology,2014(4).

Zhou Jianjun. Risk Analysis on adjacent mine water inrush caused by groundwater rebound of abandoned coalmine[J]. Safety in Coal Mines, 2013,44(7).

The Influence of Rainfall on the Characteristics of Historic Acid Mine Drainage on the Denniston Plateau, New Zealand

Carrie Jewiss[1], James Pope[2], Dave Craw[1]

[1]*University of Otago, PO Box 56, Dunedin, New Zealand*
[2]*CRL Energy Ltd, 97 Nazareth Avenue, Christchurch, New Zealand*

Abstract

Stream flow rates and water chemistry of legacy AMD from pyritic coalmines have been quantified via continuous flow measurement and intermittent water chemistry sampling over a 16-month period. Data show an overall dilution effect in response to rainfall, but high intensity rainfall events lead to an acid flush effect. Precipitates identified mineralogically with scanning electron microscopy, paired with geochemical modelling, has defined the processes of natural amelioration of the discharges. Calculated discharging acid load is 463 t $CaCO_3$ yr^{-1}, with downstream decrease in the total metal load occurring via dilution and precipitation in stream mixing zones.

Keywords: Acid mine drainage, dilution, precipitation, schwertmannite, dissolved metals

Extended Abstract:

The Eocene Brunner Coal Measures on west coast of New Zealand are pyritic and there is low neutralisation capacity in the coal measures, so there is high acid producing potential. Historic mines located on the elevated high-rainfall Denniston Plateau left a legacy of acid mine drainage (AMD). A series of adits created by modern mining now drain the workings and exude AMD into nearby water courses. The aim of this study is to characterise and quantify the AMD discharges from the historic mines, in order to facilitate downstream water quality management and ecosystem recovery.

Characterisation of the water flow rates and water chemistry has been undertaken with continuously-operating data-loggers at strategically-placed V-notch monitoring points. Chemical parameters from data-loggers have been calibrated with periodic water sampling and laboratory analysis over a 16-month period. Response of the water chemistry to rainfall events was a particular focus of the study.

Increases in stream flow rates in response to rainfall events initially causes some dilution of dissolved load and increase in pH from ≈3.3 to ≈3.6. However, as stream flows decrease during waning rainfall, there is a lag of AMD discharge over 1-2 hours because of enhanced flushing of historic mine workings by infiltrating rain. This flushing results in persistence of low pH and elevated dissolved load. Some of this enhanced flushing is attributable to secondary minerals acting as stored acidity in historic workings.

As acid waters evolve to higher pH in the stream discharge system, a series of precipitates form on the streambeds. Scanning electron microscope (SEM) imagery and associated semiquantitative analysis of precipitates has shown that most consist of ferric oxyhydroxide and/or schwertmannite that form agglomerations of nanometre scale particles. These precipitates form at pH > 3. In waters with pH near 5, aluminium rich precipitate is also visible with the ferric oxyhydroxide. Geochemical modelling of mineral saturation levels in the waters are consistent with the SEM mineralogical observations.

The combination of rainfall dilution and dilution by incoming sidestream waters is effective at raising the pH of the AMD discharges and the resulting precipitates facilitate removal of dissolved metals and sulphur. There is a total discharge acid load of 463 t $CaCO_3$ yr^{-1}, and total metal load is lowered by precipitation and dilution from up to 30 g/m^3 Al, 15 g/m^3 Fe and 360 g/m^3 SO_4^{2-}, down to ca. <3 g/m^3 Al, <1 g/m^3 Fe and <75 g/m^3 SO_4^{2-}.

2

WATER TREATMENT PROCESSES IN PERSPECTIVE

Use of ceramic nano-filtration membranes with high specific surfaces for the processing of bio-leachate and the treatment of saline mine water

Tim Aubel, Eberhard Janneck, Eugen Kober, Jessica Rolle

G.E.O.S. Ingenieurgesellschaft mbH, Germany,
email: t.aubel@geosfreiberg.de, e.janneck@geosfreiberg.de

Abstract

Mine water with high salinity occurs through many mining activities in huge quantities. Its treatment can be very challenging because of the high solubility of salts like magnesium and sodium sulfates and chlorides. The application of ceramic membranes with high specific surfaces is a relatively new engineering approach for treatment of high saline mine water and for processing of bio-leachate as well. The great advantages of those membranes are their high temperature and chemical resistance. Therefore they allow longer operating life, better maintenance and cleaning characteristics. They can be used for nano-filtration and membrane distillation.

The first investigation of an alumina ceramic membrane with 0.9 nm pore width was executed by a partner of the joint research project. This test reached high permeate flow and the results with bio-leachate ($c(SO_4^{2-})$=18 g/L) and treated mining water ($c(SO_4^{2-})$=2.4 g/L) were promising. Based on this test results, the production process for the ceramic membranes was improved in terms of increasing permeate flow and selectivity. For that objective a thin and stable membrane support (nano-membrane tube: diameter about 10 mm; flat membrane distillation: thickness of 1 mm) was developed to reduce wall resistance by the permeate flow. The membrane selectivity was optimized by changing the surface material (TiO_2/ZrO_2) which influences the hydrophobicity and the zeta-potential.

The new membranes have a high specific membrane surface area and will be tested as tube modules and in flat form. The up-scaling of the laboratory test of 4 waters from various mining processes with the improved membrane is in preparation:

- treated mine water, $c(SO_4^{2-})$=2.4 g/L, pH: 7
- bio-leachate, $c(SO_4^{2-})$=18 g/L, pH: 2.2
- industry cooling-water, c(Cl-)= 84 g/L, $c(Ca^{2+})$= 31 g/L, $c(Na^+)$=21 g/L, pH: 6-9
- leachate of a mining plant, $c(SO_4^{2-})$=4.3 g/L, pH: 8

These lab-scale tests (membrane area of 0.005 m²) will allow the membrane characterization with normal solutions (pure water, defined saline solution) and with industrial water.

The next test scales will be different pilot plants with membrane areas of 0.25 m² and 1.3 m², each at a length of 1.2 m and with 19 or 152 membrane tubes, respectively. In addition, the implementation of an industrial scale plant with a ceramic nano-filtration membrane is in preparation. The active membrane area will be 4.5 m² and 10 m² which spread of 559 and 1500 tubes, each in one membrane module.

Keywords: ceramic membrane; nano filtration; mine water; bio leachate; saline water

Performance and Review of Passive Minewater Treatment Sites, Pelenna Valley, Wales

Alyson Bannister[1,2], Peter Brabham[2], Tim Jones[2], Rob Bowell[3]

[1]*SRK Consulting (South Africa), Illovo House 2146, Johannesburg, South Africa*
[2]*Department of Earth Sciences, Cardiff University CF10 3AT, Cardiff, United Kingdom*
[3]*SRK Consulting (UK), Churchill House CF10 2HH, Cardiff, United Kingdom*

Abstract

A series of five constructed passive wetlands were constructed between 1995-1999 in the Pelenna valley, South Wales to treat various minewater discharges from abandoned coal mines. Two of the wetlands, Whitworth No.1 and Garth Tonmawr, have been compared to assess their long-term performance over their 20-year design life as well as their individual cell performance. The wetlands have not performed exactly as designed but over the long-term they have achieved the required remediation targets of pH 6-9 and dissolved iron of less than 1 mg/L in the Afon Pelenna downstream of the wetlands. It is concluded that the more complex the cell design the less likely the cell will operate for its design life and more maintenance will be required.

Keywords: oxidation | hydrolysis | aerobic | anaerobic | reducing and alkalinity producing system

Introduction

Coal mining in the United Kingdom (UK) has gone through a full rise and fall cycle, output rose constantly through the 18th century reaching a zenith output around 1913. The 20th century saw a continual decline until the last deep coal mine closed in 2015. In 1994, it was estimated that 200 km of UK rivers and streams were affected by coal minewater discharge (NRA 1994).

During active coal mining, the underground workings are "dewatered" to maintain a safe working environment, and to reduce water ingress creating mostly dry conditions which prevent the mobilisation of contaminants. Once pumping ceases and the water table rebounds, pyrite is exposed to oxygen, water and bacterial catalysts, and the oxidation of pyrite is stimulated producing acid mine drainage. Ideal conditions are created in abandoned workings for the oxidation products, ferrous iron (Fe^{2+}), sulfate (SO_4^{2-}) and free acidity, to be dissolved and carried out of the mine as minewater discharge into the surrounding watercourses.

Minewater discharge from pyrite oxidation may have serious environmental consequences for aquatic ecosystems as it did in the Pelenna valley in the South Wales Coalfields. Following the cessation of active mining operations, the coal workings flooded and minewater discharged into the river system, Nant Gwenffrwd and Nant Blaenpelenna, tributaries of the Afon Pelenna. The two tributaries were stained orange with iron concentrations elevated for approximately 7 km downstream to the confluence with the River Afan (Edwards *et al*. 1997). The aquatic species were thought to be impoverished from a combination of increased acidity, toxic effects of metals and from the smothering effect of ochre on the benthic zone of the watercourse (Wiseman 2002).

In 1992, a study was initiated to establish the impact that minewater discharge was having on the environment. The recommendations from the study were to reduce iron concentrations by 95% and 50% in the Nant Gwenffrwd and Nant Blaenpelenna respectively, so that iron concentrations would be below the required 1 mg/L and the pH would be between 6-9 in the Afon Pelenna. This was expected to provide suitable conditions for recolonisation by salmonid fish (Ishemo and Whitehead 1992). It was decided that the most suitable and cost-effective remediation of the tributaries would be to passively treat the minewater discharge through constructed wetlands.

Between 1995 and 1999, a three-phase passive wetland scheme was constructed to treat five minewater discharges; this was one of the first passive minewater treatment wetlands within the UK and Europe. Different passive constructed wetland configurations were implemented based on the incoming minewater discharge.

The configurations used were considered novel as they were mainly based on work at the time in the USA of Hedin *et al.* (1994) and Kepler and McCleary (1994). The scheme was known as the River Pelenna Minewater Project before the Coal Authority took over management of the scheme that is now known as the Coal Authority Pelenna Minewater Treatment Sites (MWTS).

Site Description

The Pelenna MWTS consist of five constructed wetlands, Whitworth No.1, Garth Tonmawr and Whitworth A, B and Gwenffrwd, located near Tonmawr village, South Wales approximately 11 km northeast of Port Talbot. Tonmawr lies within the Pelenna valley through which the Nant Gwenffrwd and Nant Blaenpelenna flow into the Afon Pelenna. The Afon Pelenna is a tributary of the river Afan, which flows into the sea at Port Talbot.

The three-phase passive wetland scheme was constructed to treat minewater discharge in the Pelenna valley. This paper only discusses Whitworth No.1 and Garth Tonmawr as they have comparable constructed wetland designs and are of similar age.

Whitworth No.1

Whitworth No.1 was the first phase, completed in October 1995 and comprised of four parallel cells. The incoming discharge was split into each cell of which two were aerobic and two were anaerobic. The aerobic cells were expected to remove iron by oxidation and hydrolysis while iron was expected to be reduced by sulfur reducing bacteria (SRB) in the anaerobic cells. Different substrates and vegetation types were utilised for each cell; this was largely due for experimental purposes with the results used to inform the construction of phase II and III. The wetland is constructed in precast concrete with a geosynthetic basal liner (SRK 1994).

The design of Whitworth No.1 changed between 2006 and 2009 to allow the cells to flow in series from cell 4 to cell 1, due to a reduction in wetland performance. Cell 1 and 4 became settlement ponds while cell 2 and 3 became aerobic wetlands as illustrated in Figure 2.

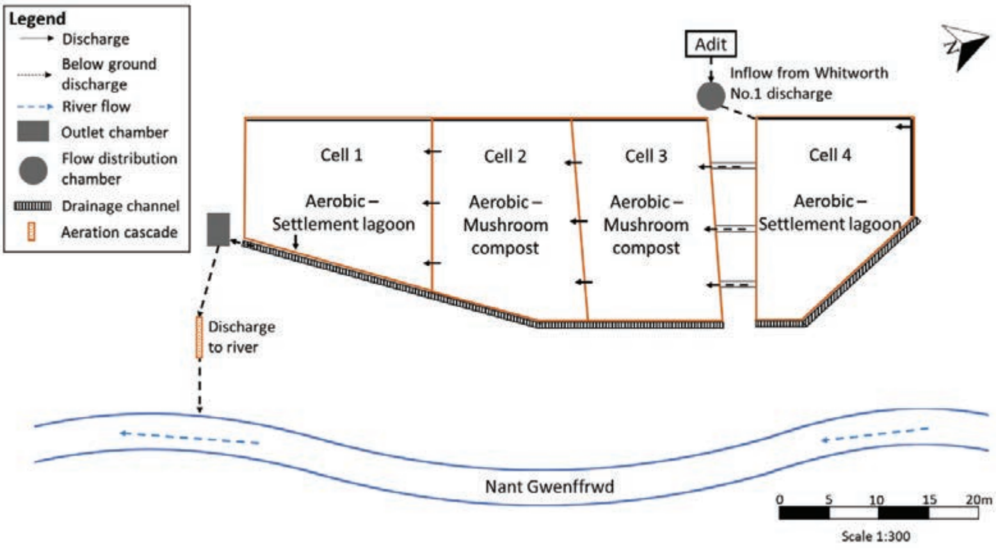

***Figure 1** Schematic of Whitworth No.1 in 2017*

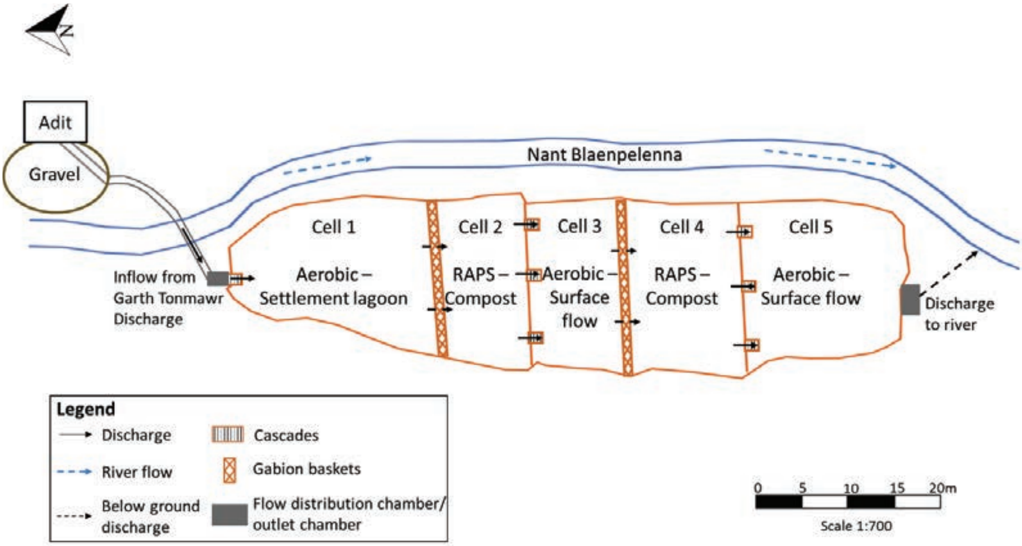

Figure 2 *Schematic of Garth Tonmawr in 2017*

The Garth Tonmawr constructed wetland is illustrated in Figure 3 and consists of a settlement lagoon, two reducing and alkalinity producing systems (RAPS) cells and two anaerobic cells. The settlement lagoon promotes iron oxidation and hydrolysis and allows heavier particles to settle out before being further treated. The RAPS cells are anaerobic and make use of a limestone bed overlain with substrate. The water moves through the substrate, which allows some precipitation of metals before the limestone buffers the acidity of the minewater.

Methods

Water quality data analysis

Natural Resources Wales (NRW) provided long-term water sampling data for the Pelenna MWTS. This included data from river samples up and downstream, and the inlet and outlet of the wetlands.

Using the statistical programme R, the data was standardised by making box and whisker plots and removing any outliers in the data before processing with Excel. The data was reduced to 5 years prior to construction of each wetland until January 2017. Access was used to align the months of the long-term data at each monitoring station to plot long-term trends and determine the removal rate in and out of each wetland.

PHREEQC was used to determine the redox potential (Eh) of the minewater at the inlets and outlets. The initial run produced a list of possible species present within the water and an estimated concentration of each species that included Fe^{3+} and Fe^{2+}, which were subsequently used in the redox calculations to determine the Eh (Appelo and Postma 2006).

Ochre sampling and analysis

Three ochre samples were collected from the four cells at Whitworth No.1. The samples were prepared by drying and crushing before elemental composition was analysed using an Olympus Innov-X X-ray Fluorescence (XRF) analyser.

The samples were also acid leached and the leachate analysed using an Inductively Coupled Plasma Mass Spectrometry (ICP-MS) to determine the mobile elements released from the ochre under acidic conditions.

Results and Discussion

Performance Assessment

When the Whitworth No.1 cells operated in parallel, there was an apparent increase in acidity and a decrease in the sulfate removal efficiency, which may be explained by a reduction in SRB due to unfavourable conditions; SRB occur under anaerobic conditions at medium to high pH (Bass Becking et al. 1960). Whitworth No.1 made use of a flow distribution chamber to distribute the incoming minewater to each of the four cells; this likely increased the acidity at the inlet. It is thought that the decrease in pH at the inlet and the decreased performance of the anaerobic cells was the reason for the change in design to series cells.

The dissolved iron removal rate has remained high and variable throughout the monitoring period (Table 1) although the total iron removal rate has decreased to 76% in the current period. The iron Eh-pH diagram created for Whitworth No.1 indicates that the conditions are suitable for iron oxidation (Bass Becking *et al*. 1960), with $Fe(OH)_3$ deposition. The iron is susceptible to spikes in acidity within the wetland and according to the Eh-pH diagram this would create conditions for the $Fe(OH)_3$ to be reduced to Fe^{2+}. From the 2010-2014 period, the wetland appears to be a source of sulfate rather than a sink.

This decrease in performance at Whitworth No.1 may be from a combination of factors. Firstly, reduced hydraulic retention due to the system short-circuiting through preferential flow paths potentially created during blockages or periods of high rainfall.

Secondly, the lack of specific oxidation and reduction conditions needed to remove iron. The change in Cell 2 from anaerobic to aerobic may have caused the pyrite formed during bacterial sulfate reduction, to be oxidised. This requires ferric iron to be available, which may be the case as not all the ferrous iron will be converted through cells 4 and 3. This is supported by the XRF results, which show that cell 2 is only retaining 28% iron within the ochre while cells 4 and 3 are retaining above 50% and cell 4 is retaining above 40%. The ICP-MS results are an indication of what would be released from the ochre under acidic conditions. This also supports the above suggestion as 7.1 mg/g was released from the sediment in cell 2 while 6.9, 6.6 and 6.5 mg/g were released from cells 3, 4 and 1, respectively.

The difference in filtered and total iron removal also supports this suggestion as the iron particulates may be released from cell 2 and are not fully settling out in cell 1 before the discharge is released into the Nant Blaenpelenna. These reactions also explain the increase in sulfate in the wetland as sulfate is released during pyrite oxidation and during release of previously bound metal sulfides.

It should be noted that aluminium and manganese concentrations are low but appear to be sufficiently removed from the wetland. The removal rate of both constituents increased with the change in design, which may be due to an increased retention time. Aluminium precipitation occurs around pH 5 and under the net acidic conditions aluminium oxidation is expected (Hedin et al. 1994). This is supported by the Eh-pH diagram where aluminium is in the oxidised form $Al(OH)^3$. According to the Eh-pH diagram, manganese is in Mn^{2+} form suggesting that the manganese is being precipitated as metal sulfides rather than oxidised. Oxidation of manganese occurs at around pH 8 (Stumm and Morgan 1981).

The discharge from the outlet at Whitworth No.1 has been within the pH 6-9 range required for the Afon Pelenna. The dissolved iron concentrations represented by the filtered iron was supposed to be reduced by 95% in the Nant Gwenffrwd to be below 1 mg/L in the Afon Pelenna. This means that the filtered iron concentrations at the outlet should be approximately 1.98 mg/L; this has been achieved in the last two years but not over the 22-year life, with an average of 2.34 mg/L. The dissolved iron would therefore be expected to be around 1 mg/L in the Afon Pelenna due to dilution in the Nant Blaenpelenna.

At Garth Tonmawr, iron oxidation and hydrolysis are occurring as designed (Table 2), as evidenced by surface ochre on the first three cells. The dissolved iron removal rates show a small decrease over time to about 90% in the current period with oxidising conditions.

Garth Tonmawr has a net-acidic minewater discharge and so it was decided to implement RAPS cells within the wetland. The RAPS cells seem to have decreased in efficiency quite quickly as the acidity in the discharge is progressively less buffered in the wetland.

Table 1. Summary of the long-term data at Whitworth No.1

Date	Whitworth N0.1	Flow (m^3/s)	pH	Total Fe (mg/L)	Filt Fe (mg/L)	Filt Mn (mg/L)	Filt Al (mg/L)	SO_4 (mg/L)
1995-1999	Inlet	-	6.3	22.97	20.99	1.97	0.065	346
	Outlet	0.003	7.0	3.95	3.23	1.08	0.010	298
	Removal Rate (%)	-	-	83	85	45	85	14
2000-2004	Inlet	-	6.0	24.27	22.13	1.88	0.091	334
	Outlet	0.004	6.3	2.38	2.21	0.86	0.015	313
	Removal Rate (%)	-	-	90	90	54	83	6
2005-2009	Inlet	-	5.8	25.63	-	-	-	332
	Outlet	-	6.0	0.67	-	-	-	274
	Removal Rate (%)	-	-	97	-	-	-	17
2010-2014	Inlet	0.004	6.2	19.40	17.51	1.65	0.098	271
	Outlet	0.005	7.0	2.40	2.08	0.63	0.011	273
	Removal Rate (%)	-	-	88	88	62	88	-0.6
2015-Present	Inlet	-	6.2	19.32	18.55	1.72	0.116	279
	Outlet	-	6.8	4.60	1.84	0.68	0.010	281
	Removal Rate (%)	-	-	76	90	61	91	-0.9
1995-Present	Inlet	0.004	6.1	22.32	19.79	1.80	0.092	312
	Outlet	0.004	6.6	2.80	2.34	0.81	0.012	288
	Removal Rate (%)	-	-	86.8	88.3	55.5	86.8	7.1

The decreased performance in the RAPS cells may be due to changed water levels affecting flow through the substrate and limestone beds. The overflow means that some water is bypassing the cell and will not be buffered by alkalinity.

The performance of the wetland has still been maintained, which may be due to the increase in pH at the Garth Tonmawr discharge to above pH 6, which is suitable for microbiological catalysts to increase iron oxidisation and buffer the pH (Bass Becking *et al.* 1960).

The sulfate removal rates in Garth Tonmawr have been poor because conditions to promote sulfate reduction were not implemented during the construction of the wetland. Aluminium concentrations of the discharge are low, but the removal rate has remained high (85%) even though it has decreased over time, this may be due to a reduced hydraulic retention time. The manganese removal rate is low due to poor oxidising conditions in the wetland. Metal sulfides are unlikely to precipitate out of the water as the conditions do not favour SRB and therefore the manganese would not be expected to co-precipitate to manganese sulfide.

The discharge from the outlet at Garth Tonmawr has been within the pH 6-9 range required in the Afon Pelenna. The dissolved iron concentration is required to be reduced by 50% in the Nant Blaenpelenna to reach the 1 mg/L standard in the Afon Pelenna; this would require a dissolved iron concentration of 14.5 mg/L, which has been consistently reached over each 5-year period.

Effect of wetland design on performance

Both wetlands had high iron removal rates and a similar capacity to buffer acidity indicating that both parallel and series cells can perform well if designed correctly and maintained. Whitworth No.1 showed an initial increase in performance when the wetland design changed to operate in series, this may be due to an increased practical hydraulic retention time, which allows for further chemical and biological processes to take place.

Wiseman (2002) showed that the aerobic cells were performing better than the anaerobic cells at Whitworth No.1. Anaerobic cells are more sensitive to fluctuations in water level from blockages than aerobic cells because the water will flow under higher pressure and may move to the surface of the cell or create openings in the substrate which are likely to become preferential flow paths or alternatively, the cell may completely dry up affecting the microbes in the cell. The limiting factor for anaerobic cells will be carbon if the

Table 2. *Summary of the long-term data at Garth Tonmawr*

Date	Garth Tonmawr	Flow (m^3/s)	pH	Filt Fe (mg/L)	Filt Mn (mg/L)	Filt Al (mg/L)	SO$_4$ (mg/L)
1999 - 2003	Inlet	-	5.9	32.45	0.66	0.123	281
	Outlet	0.019	6.7	1.20	0.48	0.010	274
	Removal Rate (%)	-	-	96	27	92	2.3
2004 - 2008	Inlet	-	5.6	-	-	-	290
	Outlet	-	6.1	-	-	-	287
	Removal Rate (%)	-	-	-	-	-	0.9
2009 - 2013	Inlet	0.016	6.2	26.43	0.58	0.088	217
	Outlet	0.019	6.5	2.11	0.52	0.010	214
	Removal Rate (%)	-	-	92	10	88	1.3
2014 - Present	Inlet	0.024	6.2	28.11	0.55	0.068	213
	Outlet	0.025	6.6	2.43	0.44	0.010	207
	Removal Rate (%)	-	-	91	20	85	2.9
1999 - Present	Inlet	0.020	6.0	29.00	0.60	0.093	250
	Outlet	0.021	6.5	1.91	0.48	0.010	246
	Removal Rate (%)	-	-	93	19	88.3	1.9

anaerobic and redox conditions are preserved to support SRB while the limiting factor for the aerobic cell appears to be space rather than the cell becoming exhausted.

The change in design at Whitworth No.1 has altered the anaerobic cell to an aerobic cell. This has changed the cell from reducing conditions to oxidising conditions and consequently there is evidence for pyrite oxidation and release of iron sulfides once sorbed in the cell. Cell 4, which was an anaerobic bed was cleared of substrate and is now a settlement lagoon which appears to be promoting iron oxidation and hydrolysis as ochre is floating on the surface.

Conclusions

Even though these wetlands are not performing as designed they are still removing the dissolved iron and buffering the pH to suitable concentrations. This indicates that these wetlands are resilient to change and that they may be somewhat over designed. It appears that more simplistic designs would have produced similar results and that the more complex the cell configuration the less likely they are to last the design life. This is mostly due to higher maintenance requirement for more complex cells. It is therefore concluded that regular maintenance is essential for efficient performance.

Acknowledgements

I thank the Commonwealth Scholarship Commission, which funded my Cardiff University Master's thesis on which the paper is based. In addition, I thank the Coal Authority and Severn Trent Services for allowing me to access and collect samples from the Coal Authority Pelenna Minewater Treatment Sites and the Natural Resources Wales for providing the long-term water database. A special thank you to Peter Brabham, Tim Jones and Rob Bowell for their supervision of my thesis and for their contribution to the paper.

References

Appelo CAJ, Postma D (2006) Geochemistry, groundwater and pollution, 2nd Ed. A.A Balkema Publishers, Leiden, Netherlands, p 415—488

Baas Becking LGM, Kaplan IR, Moore D (1960) Limits of the natural environment in terms of pH and oxidation-reduction potentials. The Journal of Geology 68:243—285

Edwards PJ, Bolton CP, Ranson CM, Smith AC (1997) The River Pelenna minewater treatment project. In: Younger PL ed. Minewater treatment using wetlands, Proceedings of a national conference. London Chartered Institute of Water and Environmental Management, Newcastle, p 17—33

Hedin RS, Nairn RW, Kleinmann RLP (1994) The passive treatment of coal mine drainage. US Bureau of Mines Information Circular 9389

Ishemo CAL, Whitehead PG (1992) Acid mine drainage in the River Pelenna: modelling and pollution control. Wallingford: Institute of Hydrology

Kepler DA, McCleary EC (1994) Successive Alkalinity Producing Systems (SAPS) for the Treatment of Acid Mine Drainage. Proceedings of the International Land Reclamation and Mine Drainage Conference and the 3rd International Conference on the Abatement of Acidic Drainage, Pittsburgh, p 195—204

National Rivers Authority (NRA) (1994) Abandoned mines and the water environment. HMSO Water Quality Series No 14

SRK (1994) Pelenna Minewater Treatment Project: Design Review of Proposed Wetland Whitworth No. 1 Discharge for West Glamorgan County Council. Report No. U497/1, SRK (UK) LTD, Cardiff

Stumm W, Morgan J (1981) Aquatic Chemistry, 2nd Ed. John Wiley & Sons, New York

Wiseman I (2002) Constructed Wetlands for Minewater Treatment. R&D Technical Report P2-181/TR, Environmental Agency, Bristol

Assessment of Scorodite Precipitation from Mine Waters

R. J. Bowell

SRK Consulting, Churchill House, Churchill Way, Cardiff CF102HH, Wales, UK

Abstract

Arsenic release from mine waters is often predicted to be limited by precipitation of scorodite ($FeAsO_4.2H_2O$). Although scorodite is often cited as the most stable form of arsenic in supergene environments its actual stability field in terms of redox potential and pH is highly limited and is sensitive to variations in trace element chemistry, redox potential, temperature and pH.

Several schemes have been developed to precipitate scorodite with the key features being oxidizing solution of ferrous iron reacting with high concentrations of arsenic (V). Limitations on the reaction in producing scorodite have been identified and include the presence of competing elements such as copper, zinc, barium, sodium, sulfate and chloride, all of which are common in mine waters. In this study, the precipitation of scorodite was assessed on a natural mildly acidic to neutral pH mine water with a high concentration of arsenic (20 mg/L). The reactions were carried out over a pH range of pH values from pH 2.5 to the natural pH of the mine water at pH 6. The mine water was acidified by ferrous sulfate, sulfuric acid and CO_2 injection to mimic components typical of the mine water environment.

The results were that in all tests below a temperature of 80^{o}C and in all tests where pH was greater than 3, no scorodite phase was produced as determined by X-Ray Diffraction (XRD). In all these tests a ferric hydroxide, ferric arsenate and/or ferric arsenate-sulfate was precipitated that showed variable solubility in a leach test. Where agitation and oxygen were introduced, at low pH (<3) then scorodite crystals up to 50 µm.

In tests at the natural pH of the mine water where natural air was used to agitate, the addition of ferrous sulfate produced Ferrihydrite ($Fe^{3+}{}_{10}O_{14}(OH)_2$), amorphous ferric arsenate-sulfate, Olivenite ($Cu_2(AsO_4)(OH)$) and Dussertite ($BaFe_3{}^{+3}(AsO_4)(AsO_3OH)(OH)_6$) scavenging barium from the mine water although scorodite was formed at low pH. Where oxygen/air was used at pH above 6, arseniosiderite ($Ca_2Fe_3{}^{+3}(AsO_4)3O_2 \cdot 3H_2O$) was precipitated along with kolfanite ($Ca_2Fe_3{}^{3+}O_2(AsO_4)_3 \cdot 2H_2O$), goethite and hydrous ferric oxide. These phases demonstrated low solubility in leach tests although by mineralogical assessment some arsenic was associated with the hydrous ferric oxide phase indicating a strong degree of adsorption in addition to precipitation as arseniosiderite. Without the addition of an oxidant, arsenic removal efficiency was generally less than 30%.

This study clearly demonstrates that under the correct conditions scorodite can be formed from mine waters, however the range of conditions is extremely narrow and formation restricted to highly oxidized highly acidic environments. Critical issues are to ensure all arsenic is oxidized to arsenate, high iron:arsenic ratio in the mixing vessel and a low pH, high oxygen content is maintained in the reactor tanks.

Keywords: Arsenic treatment, precipitation

Introduction

Arsenic contamination of mine and metallurgical waters has long been recognized as a global problem (Matschullat 2000, 2011; Craw and Bowell, 2014). More stringent guidelines based on demonstration of potential toxicity to humans and ecological receptors have motivated regulators and operators to address arsenic levels in discharges from operating mines as well as legacy sites (Craw and Bowell, 2014). An important aspect in the evaluation of arsenic removal from waters is the characterization of the oxidation state of arsenic and its mineral speciation (Bowell et al 2014).

Arsenic can occur in several oxidation states in natural waters although the trivalent arsenite (As(III)) or pentavalent arsenate (As(V)) are the most common (Campbell and Nordstrom, 2014). The most thermodynamically stable species over the natural range of groundwater redox conditions (150-500 mV, Bass-Becking et al. 1960) and pH (4-7, Baas Becking et al. 1960) are H_2AsO^{4-}, $HAsO^{4-}$ and in acid rock drainage waters (pH below 5) H_2AsO^{4-} in more reduced waters, $As(OH)_3$ is the most common species, in highly reducing environments. The kinetics of arsenic reduction-oxidation (redox) reactions is not rapid, so the predicted proportions of arsenic species based on thermodynamic calculations do not always correspond to analytical results. An Eh-pH diagram showing the thermodynamically stable regions for arsenic species is shown in Figure 1.

For this study the removal of arsenic by precipitation methods was assessed as this approach is generally the most common and potentially the most cost effective method of arsenic removal (Bowell, 2003; Nazari et al 2017).

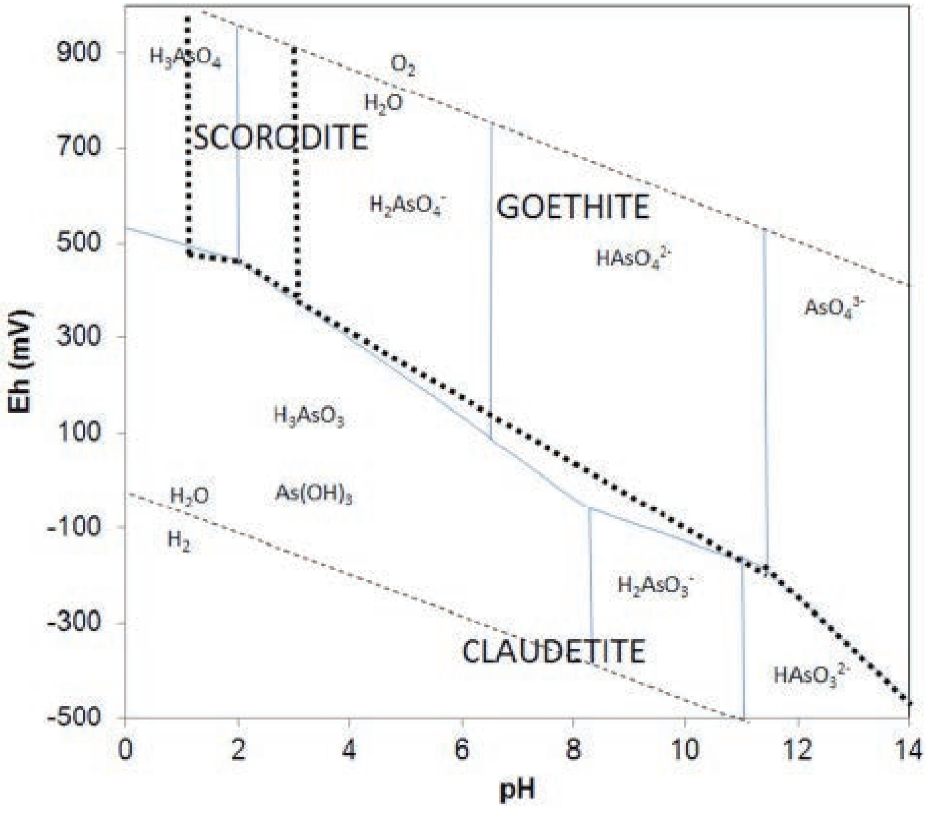

__Figure 1:__ Eh-pH diagram for system Fe-As-H2O at 298 K

Methods

The methodologies applied to precipitate arsenic that were assessed in this paper and references are summarized in Table 1.

All testwork was completed as bench scale tests on site in Tanzania. The feed solution water for this work was a mine water collected in Tanzania from a gold mine. The analysis of the water is shown in Table 2. The water reflects typical mine water from a low sulphide mesothermal gold deposit. Analysis was through Analabs, Tanzania using ICPAES for cations, kone analyser for chloride and sulfate and titration for bicarbonate. The pH was measured using a HACH meter.

The solids produced in this study were subject to a 2:1 dissolved water to solid leach test using a similar methodology to the EPA1312 test. Essentially the precipitate samples were agitated with deionised water for 24 hours. The solution was then filtered and analysed.

Mineralogy

The mineralogical examination was undertaken using p scanning electron microscopy (SEM) and fine powder X-Ray Diffraction (XRD). Samples were prepared from the testwork material as dry powders (for SEM). XRD analysis was carried out on pulverised samples of the precipitates.

Bulk analyses were carried out on the samples. Scans were run using the Philips PW1710 Automated Powder Diffractometer using Cu Kα radiation at 35kV and 40mA, between 2 and 70° 2θ at a scan speed of 0.04 °2θ/s. From the scans, phases were identified using Philips PC-Identify software and from the peak areas, semi quantitative analysis was performed and a percentage of each phase present calculated. Weighting factors were applied where necessary.

Semi-quantitative energy dispersive analysis of precipitates was carried out using a Zeiss Sigma HD Analytical Field Emission Gun SEM with INCA wave-and energy-dispersive X-Ray spectroscopy at the Department of Earth Sciences, Cardiff, UK. This method allows micro-chemical data to be collected that reports the chemical composition of the surface of the mineral phase. The electron beam utilised to gather the information required is approximately 1 to 5 µm in diameter, so even very small phases can be quantified. An accelerating voltage of 20 kV was used with a probe current of 5.0 nA.

Table 1. *Summary of Arsenic Precipitation Approaches*

Method	Reference	Approach	Proposed precipitate	Arsenic
Scorodite process	Fujita et al 2008;Caetano et al 2009	Peroxide addition, Temp 30-95oC, excess ferrous, sulfuric acid	Scorodite	
HDS process	Dey et al 2009; Salokannel et al 2013	Ambient temperature, pH buffer with lime, hydrogen peroxide, ferric sulfate	Ferric Arsenate	

Table 2. *Geochemical analysis **of Mine Water feed***

Parameter	Concentration, mg/L	Parameter	Concentration, mg/L
pH	5.8	Arsenic, arsenite	10.8
Sulfate	220	Arsenic, arsenate	8.6
Chloride	65	Iron, ferrous	0.05
Sodium	56	Iron, ferric	0.97
Magnesium	15	Aluminium	1.58
Calcium	52	Manganese	0.33
Potassium	10	Barium	2.12
Bicarbonate	65	Copper	1.13

Results

Scorodite Process

Using the methodology of Caetano et al (2009) that was similar that applied by Fujita et al (2008a) the reaction of hydrogen peroxide, sulfuric acid, ferrous sulfate and mine water was followed over temperatures ranging from ambient to 95°C and variable levels of Fe/As ratio (Table 3).

Results shown in Table 3 demonstrate that at high acid concentration (low pH) and high Fe/As ratio (3/1 and 5/1) scorodite was produced after 4 hours of reaction. At lower Fe/As ratios, ferric hydroxide and a hydrated ferric arsenate, possibly similar to the Type I salt ($Fe_2(HAsO_4)^3.xH_2O$ where X<4 or HFA) reported by Swash and Monhemius (1995) was produced along with Dussertite ($BaFe_3+3(AsO_4)(AsO_3OH)(OH)_6$) and a ferric-arsenate-sulfate salt (HFAS) with similar chemistry to that reported by Swash and Monhemius (1995) as a type II precipitate ($Fe_4(AsO_4)_3(OH)x(SO_4)y$ where x+2y=3).

In addition, where longer time period was applied dussertite and olivenite was observed at low pH, high temperature along with scorodite and a copper bearing HFAS phase. The complexity of treating mine waters with arsenic and cation metals has been reported as potentially interfere with scorodite formation and intermediate copper (and zinc) bearing HFA phases have been reported in testwork by other studies (Fujita et al., 2008; Gomez et al., 2011).

The agitated tank shows improvement in arsenic removed when compared to static tanks (Bowell, 2003) or when reactions are executed in a chloride-dominated system (Demopoulos et al. 1995). This is most likely reflecting a stronger oxidant in the testwork, more efficient mixing and arsenic oxidation and possibly also reflect lower sodium impurity in the acid medium. Sodium has been shown to inhibit scorodite formation (Gomez et al 2011).The formation of dussertite was only seen in one test and is possibly an anomaly of high Ba in the mine water but does open the possibility that $BaCO_3$ addition to mine waters could also represent a possible removal mechanism.

HDS approach

Following the methodology of Dey et al (2009) a small batch reactor comprising of three reactor vessels allowing for flocculation, thickening and precipitation. The low iron/arsenic ratio in the mine water meant that ferric sulfate was required along with lime to form a high-density sludge. The testwork was completed at ambient temperature (approximately 20-25°C in the on-site laboratory)

Table 3. *Results of Batch Method with Sulfuric acid*

Test #	Test pH	Fe/As ratio	Temp, oC	Length reaction (mins)	Arsenic removed, %	Arsenic minerals
SP1	1.5	3/1	95	60	98	Scorodite
SP3	2.5	3/1	95	60	96	Scorodite, HFA
SP4	2.5	2/1	95	60	71	Scorodite, HFA
SP5	2.5	1/1	95	60	50	HFA
SP6	2.5	1/1	30	60	14	HFO, HFA
SP7	2.5	3/1	95	120	86	Cu-HFAS, olivenite, dussertite, scorodite, HFA
SP11	4	3/1	30	60	67	HFO, HFA
SP13	4	1/1	95	60	84	HFO, HFA, HFAS
SP15	4	3/1	95	60	83	HFO, HFA
SP18	4	5/1	80	60	90	HFO, HFA
SP19	4	5/1	95	60	96	Scorodite, HFO, HFA
SP22	5.8	3/1	95	60	46	HFO, HFA
SP31	6.5	3/1	95	60	40	HFO, HFA
SP42	7	3/1	95	60	28	HFO, HFA

and hydrogen peroxide was added to oxidize arsenite to arsenate in the first tank. This approach is similar to conventional plants currently in operation, such as the Boliden Harjavalta plant (Salokannel et al. 2013).

Throughout all testwork scorodite was not formed and the main phase observed was HFA phase comprised of As-bearing HFO phase (Table 4).

Environmental Testwork

To compare the suitability of the different methods applied here a 2:1 distilled water to precipitate 24-hour leach was undertaken on all the samples and selected results are shown below in Table 5. The required concentration was discharge of the mine water was an arsenic concentration less than 0.05 mg/L. In the testwork this was met in some of the tests, particularly where scorodite was formed but also where the HFAS phase was observed (Table 5). The leach concentration reflects the portion of arsenic initially precipitated as well solubility of the precipitate.

Table 4. *Results of HDS treatment*

Test #	Test pH	Fe/As ratio	Arsenic removed, %	Arsenic minerals
HDS2	2.5	3/1	69	HFA,Jarosite
HDS5	4	3/1	58	HFO, HFA
HDS6	4	2/1	37	HFO, HFA
HDS9	5.8	1/1	9	HFO, HFA
HDS10	5.8	1/1	8	HFO
HDS12	5.8	3/1	28	HFO
HDS15	6.5	1/1	13	HFO
HDS18	6.5	3/1	53	HFO, HFA
HDS23	7	5/1	54	HFO, HFA
HDS24	7	5/1	53	HFO, Arseniosiderite, Kolfanite
HDS30	8	3/1	26	HFO, HFA Kolfanite
HDS32	8 (NO H2O2)	3/1	6	HFO

Table 5. *Results of Bleach Tests on Arsenic Solids*

Test #	Test pH	Arsenic in leach, mg/L	Arsenic minerals
SP1	1.5	<0.002	Scorodite
SP3	2.5	<0.002	Scorodite, HFA
SP4	2.5	<0.002	Scorodite, HFA
SP5	2.5	0.17	HFA
SP6	2.5	0.12	HFO, HFA
SP7	2.5	0.014	Cu-HFAS, olivenite, dussertite, scorodite, HFA
SP11	4	0.22	HFO, HFA
SP13	4	0.013	HFO, HFA, HFAS
SP19	4	0.007	Scorodite, HFO, HFA
SP22	5.8	0.19	HFO, HFA
SP42	7	0.38	HFO, HFA
HDS2	2.5	21.8	HFA,Jarosite
HDS5	4	19.7	HFO, HFA
HDS6	4	20.2	HFO, HFA
HDS10	5.8	39.6	HFO
HDS18	6.5	33.6	HFO, HFA
HDS24	7	42.1	HFO, Arseniosiderite, Kolfanite
HDS30	8	44.3	HFO, HFA Kolfanite
HDS32	8 (NO H_2O_2)	12.3	HFO

Conclusions

This study clearly demonstrates that under the correct conditions scorodite can be formed from mine waters, however the range of conditions is extremely narrow and formation restricted to highly oxidized highly acidic environments. Critical issues are to ensure all arsenic is oxidized to arsenate, high iron:arsenic ratio in the mixing vessel and a low pH, high oxygen content is maintained in the reactor tanks.

Complexity occurs with other competing cations that can lead to the formation of other arsenates such as those of barium or copper in low temperature or calcium-bearing arsenates at high pH. This leads potentially to more leachable phases in environmental tests. The formation of hydrous ferric arsenate sulfate phases present potentially another stable solid for arsenic disposal and they appear also to form suitable materials for arsenic mitigation.

Acknowledgements

The author would like to acknowledge the assistance given in Tanzania by Analabs and company environment department for whom this work was undertaken.

References

Baas Becking LGM Kaplan IR Moore D 1960: Limits of the natural environment in terms of pH and oxidation-reduction-potentials. J. Geol. 6:243-284

Bowell RJ 2003 The influence of speciation in the removal of arsenic from minewaters. Journal of Land Contamination and Remediation. 11, 231-238

Bowell RJ Craw D 2014 The management of Arsenic in the Mining Industry. Reviews in Mineralogy and Geochemistry, volume 79,507-532

Bowell RJ, Alpers CN, Jamieson HE, Nordstrom DK, Majzlan J 2014 The Environmental Geochemistry of Arsenic: An Overview. Reviews in Mineralogy and Geochemistry, volume 79, 1-16

Caetano ML Ciminelli VST Rocha SDF Spitale MC Calderia CL 2009 Batch and continuous precipitation of scorodite from dilute industrial solutions. Hydrometallurgy 95, 44-52.

Campbell and Nordstrom 2014 Arsenic speciation and sorption. Reviews in Mineralogy and Geochemistry, volume 79, 185-216

Craw D Bowell RJ 2014 The Characterization of Mine Waste. Reviews in Mineralogy and Geochemistry, volume 79,473-506

Demopoulos GP Droppet DJ van Weert G 1995 Precipitation of crystalline socordite (FeAsO4.2H2O). Hydrometallurgy 38, 245-261.

Dey M Williams K Coulton R 2009 Treatment of arsenic rich waters by the HDS process. Journal of Geochemical Exploration 100, 160-162.

Gomez MA Becze L Celikin BM Demopoulos GP 2011 The effect of copper on the precipitation of scorodite under hydrothermal conditions. Journal of Colloid and Interface Science 360, 508-518.

Fujita T Taguchi R Abumiya M Masmoto M Shibata E Nakamura T 2008 Novel atmospheric socrodite synthesis by oxidation of ferrous sulfate solution. Part 1. Hydrometallurgy90, 92-102.

Matschullat J, 2000, Arsenic in the geosphere – a review, Science of the Total Environment 249, 1-3: 297-312.

Nazari AM Radzinski R Ghahreman A 2017 Review of arsenic metallurgy: Treatment of arsenical minerals and the immobilization of arsenic. Hydrometallurgy 174, 258-281

Salokannel A Nevatalo LM Martikainen M Meer T McCullough J 2013 Technology selection in the removal of contaminants. Proceedings of Metallurgical Plant Design, Perth, Australia. 3p.

Swash PM Monhemius AJ 1995 Synthesis, characterization and solubility testing of solids in the Ca-Fe-AsO$_4$ system. Sudbury'95- Mining and the Environment CANMET, 17-28.

Material flow analysis for spatiotemporal mine water management in Hon Gai, Vietnam

Katrin Broemme, Viet Quoc Trinh, Sandra Greassidis, Harro Stolpe

Institute of Environmental Engineering and Ecology (eE+E), Faculty of Civil and Environmental Engineering, Ruhr-University Bochum, Universitaetsstrasse 150, 44801 Bochum, Germany, katrin.broemme@rub.de

Abstract

Hon Gai peninsula is a coal mining area in Quang Ninh, Vietnam. The peninsula has limited water resources while the water demand of mines and other users is increasing. As deficits in dry sea-sons occur, recycling and reuse of mine water are solution approaches for the area. Material flow analysis (MFA) was applied to understand the complex linkages of water related elements and processes with regards to mine water flows, treatment and reuse, and to develop a mine water management tool to ensure efficient water treatment and reuse. The tool uses MFA to model different spatiotemporal situations to support management and investment decisions.

Keywords: mine water, recycling and reuse, material flow analysis, Hon Gai mining area

Introduction

The R&D project WaterMiner funded by the Federal German Ministry of Education and Research (BMBF) focuses on a need-based and efficient reuse and recycling of mine water for mining pur-poses as well as for other purposes, i.e. urban, industrial or agricultural.

The R&D project WaterMiner consists of the following work packages: project coordination (eE+E, RUB); baseline and system analysis (eE+E, RUB); GIS water infrastructure (Disy Informationssysteme Ltd., Karlsruhe); monitoring information system (ribeka Ltd., Bornheim); material flow analysis (MFA) (eE+E, RUB); technical concepts (DGFZ); economic concepts (Environ-mental Economics, Koblenz-Landau); exemplary implementation of technical solutions (DGFZ; LUG Engineering Ltd., Cottbus; VINACOMIN Vietnam National Coal and Mineral Industries Hold-ing Corporation Ltd.).

Hard coal mining by VINACOMIN in Hon Gai is taking place since many decades and has nega-tively affected the water resources. The open pits in Hon Gai are scheduled to be closed over the next 10 years or shift to underground mining (GoV 2016). As a result, mining impacted waters will change according to location, quality and quantity.

The R&D project WaterMiner investigates under different considerations how and to what ex-tent the existing water demand in the mining area and parts of the water demand in the sur-rounding area can be covered by treated mine water. The project develops a management tool for mine water reuse with the following components: material flow analysis (MFA), surface wa-ter and sediment management (Ulbricht et al. 2018) as well as economic investigations (Do et al. 2018) accompanied by data management (ribeka, Disy) and exemplary implementation of moni-toring and waste water treatment (DGFZ, ribeka, LUG Engineering and VINACOMIN)

Study area

The project is located on the Hon Gai peninsula (Fig. 1A). Coal is exploited in the central and north-western part. Both open pit and underground mining technologies are applied with a gradual reduction of open pits. Basic investigations and the development of environmental con-cepts for the mining area including mine water treatment have been performed by the R&D pro-ject RAME (Broemme and Stolpe 2011; Broemme et al. 2014) in the period from 2005-2015.

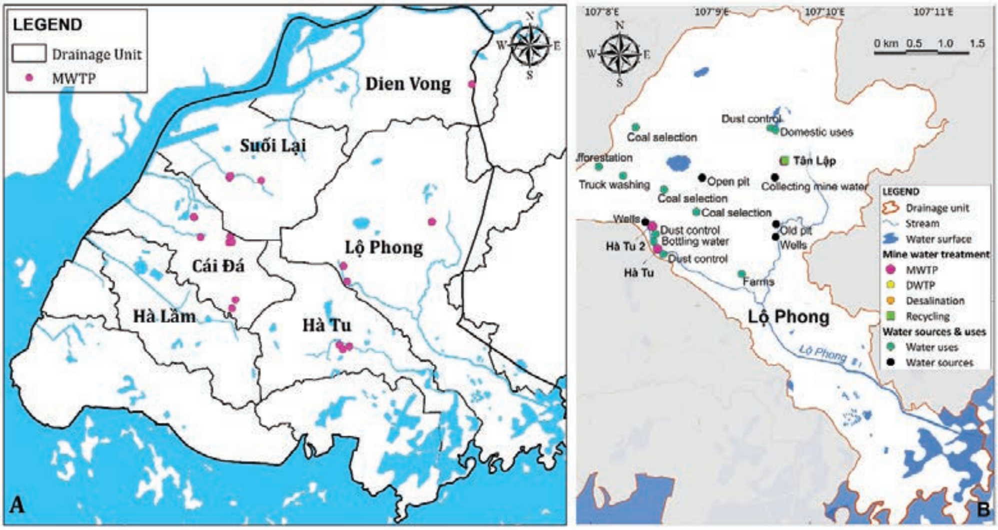

Figure 1 *(A) WaterMiner study area and (B) Example area Lo Phong Drainage Unit*

Five small streams with lengths from 2.2 to 7.1 km drain water into the Halong Bay. The hydro-logical regime is characterised by 80% of annual rainfall during rainy season (May – October) and 20% during dry season (November – April). The lower rainfall in summer leads to water shortages (DONRE, 2016). In recent years water shortages intensified and additional water sources are needed to cover the increasing water demand in the region.

To facilitate an improved mine water management, five drainage units (Fig. 1) were defined based on topology, hydrology features, mine operation and ownership.

The Lo Phong Drainage Unit (Fig. 1) consists of two open pits: Tan Lap and Ha Tu. In its final extension, Ha Tu open pit will be the largest on the peninsula. The open pits are intended to be converted to pit lakes after mining. This provides a possibility to create additional water storage as source for external using purposes in the dry season. Therefore, the focus of the MFA was primarily on this area.

The conceptual model (Fig. 2) shows the main system elements of mine water management: mine water sources, Lo Phong river, mine water treatment, internal uses of mine water and po-tential external uses.

The mine water sources include clean water from the water supply system, discharge from up-stream catchment parts, surface runoff and water withdrawal from wells and ponds. In addition to mine water from open pits or underground mines (mine drainage water, process water e.g. from coal screening) also domestic wastewater (e.g. from pitheads baths) accumulates.

The mine water flows via regulating basins to the mine water treatment plants (MWTP). In the rainy seasons and especially during heavy rainfall events mine water is only partially treated or discharged into the surface waters without treatment. There is also a large amount of surface runoff discharging directly into the rivers.

The treated mine water is partially reused inside the mines (internal uses). Additionally, there is a large water demand in the surrounding urban area of Ha Long City, especially during dry sea-son (external uses).

Spatiotemporal changes in mine water sources, mine water treatment plants, internal uses and external uses are the significant factors determining changes in mine water management in the region.

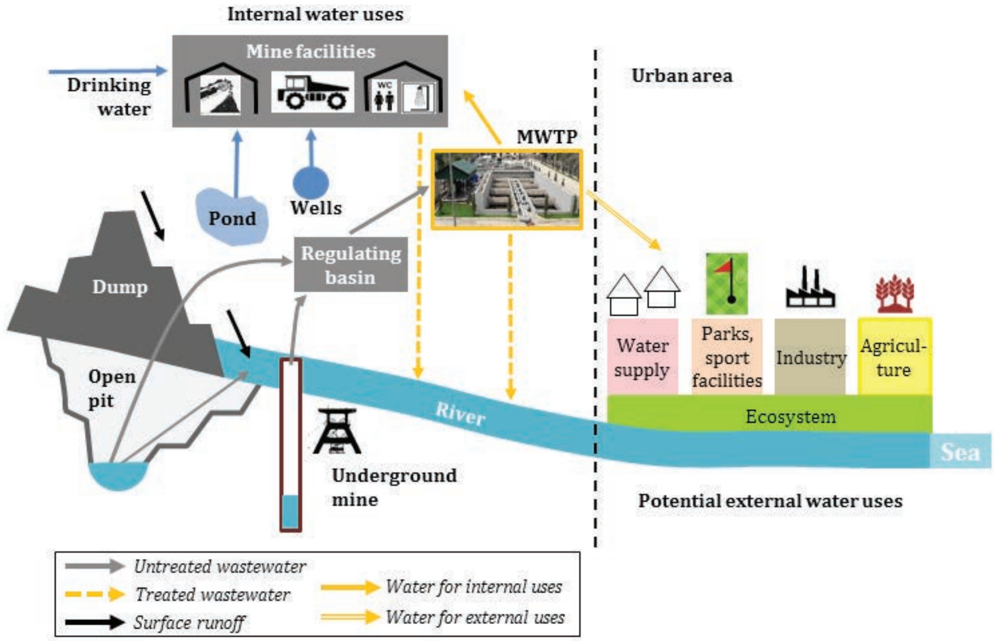

Figure 2 Conceptual model of the mine water management

As mining sites are closed, mine drainage water will decrease, mine water treatment plants will reduce or stop their operation and the water consumption for mining purposes will reduce. At the same time, along with the expansion of industry, urban areas and tourism, water extraction will increase to provide adequate water and satisfy higher demands.

Methodology

Data acquisition

As basis for the WaterMiner project as well as for the MFA comprehensive data on coal mining, meteorology and hydrology, geology, river morphology, water uses and land use have been ob-tained from VINACOMIN, provincial authorities, companies and by own field measurements.

Material flow analysis (MFA)

The Umberto NXT Efficiency software is applied to identify, quantify and assess the potential for the reuse of mine water and to improve the mine water management regarding the different situations of the spatial and temporal development of the mining area.

The development and application of the MFA is conducted through three consecutive steps: (1) Definition of relevant spatiotemporal situations; (2) Assembling the material flow model; (3) Modelling and improving the defined spatiotemporal situations.

Development and application of the MFA

The mentioned three steps have been performed with the following specifications.

The relevant spatiotemporal situations for the example drainage unit Lo Phong are defined as following:

- Situation 1: existing situation of mine water sources, mine water treatment and mine water reuse with Ha Tu and Tan Lap mines in operation (2016)
- Situation 2: future situation of mine water sources, mine water treatment and expected mine water reuse after the planned closure of Ha Tu mine (approx. 2025)
- Situation 3: final situation of mine water sources, mine water treatment and mine water re-use after the planned closure of Tan Lap mine (approx. 2035)

The Lo Phong drainage unit covers mining activities in both Ha Tu and Tan Lap mine. The water balance of each mine is prepared and analysed separately. The outflows drain to the Lo Phong River.

According to the conceptual model (Fig 2.) water flow pathways are divided into four phases: sources, treatment, internal uses, and external uses.

Table 1 gives an overview of the 3 defined spatiotemporal situations and defines which components have to be considered in each phase. For each situation, a material flow model is devel-oped which is used to develop and compare different options for each situation and to create improved situations.

The components of each phase are used in Tab. 1 for the definition of temporal situations:

- Sources: 1) mine drainage water from open pits, 2) mine drainage water from underground mines, 3) groundwater extracted from wells, surface water extracted from ponds, lakes, 4) discharge from upstream catchment parts outside the mining area, 5) surface runoff due to rainfall inside the mining area, 6) clean water from the water supply company QUAWACO
- Treatment: 1) upstream regulating basin for pre-sedimentation and homogenization of the MWTP inflow; 2) mine water treatment plant; 3) additional treatment step for domestic wa-ter quality; 4) reverse osmosis filtration step for drinking water quality; 5) former open pit with reservoir function, storage and sedimentation of rain water and surface runoff
- Internal use: 1) water for drinking (bottling station), water for canteen kitchens; 2) water for laundries, pithead baths, sanitary facilities; 3) water for wet coal screening; 4) water for irri-gation of recultivated areas; 5) water for dust control, industrial cleaning, truck washing
- External use: 1) water for irrigation of agricultural areas; 2) water for industrial users; 3) water for irrigation of public parks, urban greens, golf courses; 4) water for the clean water production; 5) minimum water volume in the river to maintain aquatic life and river ecosystems equal to 10% of the average flow (Tuan, 2015)

The material flow model was developed for an average month of the dry season. In the following, the basic modelling results of 2 defined spatiotemporal situations (Situation 1: existing situation, Situation 3: final situation) are shown (Fig. 3).

The defined spatiotemporal situations are the starting point for further improvement and opti-misation by changing and adaption of treatment components, water allocation, water distribu-tion, other technical issues etc. The direction of optimisation is identified based on water de-mands, cost and benefit, mine planning and acceptance.

Figure 3 (left) shows the results of simulated water flows for the existing situation in the form of a Sankey diagram.

***Table 1.** Three situations of mine water management exemplary for Ha Tu mine, Lo Phong drainage unit: (1) existing situation, (2) situation 2025, (3) final situation*

Sources	Situation			Treatment	Situation			Internal use	Situation			External use	Situation		
	(1)	(2)	(3)		(1)	(2)	(3)		(1)	(2)	(3)		(1)	(2)	(3)
1) Open pit	☒	☒	☐	1) Regulating basin	☒	☒	☐	1) Drinking, cooking	☒	☐	☐	1) Agriculture	☐	☐	☒
2) Underground mining	☐	☐	☐	2) MWTP	☒	☒	☐	2) Domestic uses	☒	☐	☐	2) Industry	☐	☐	☒
3) Wells, others	☒	☐	☐	3) Secondary treatment	☒	☐	☐	3) Coal screening	☒	☐	☐	3) Park, sport facility	☐	☐	☒
4) Upstream flow	☒	☒	☒	4) RO filtration	☒	☐	☐	4) Recultivation	☒	☒	☒	4) Raw water	☐	☐	☒
5) Surface runoff	☒	☒	☒	5) Pit lake	☐	☐	☒	5) Other mining purposes	☒	☒	☐	5) Ecological flow	☒	☒	☒
6) Clean water	☒	☐	☐												

☒ relevant for the situation ☐ not relevant for the situation

- Sources: The main mine water sources originate in the open pits of Ha Tu and Tan Lap mine and are pumped to the regulating basin. The surface runoff flows directly into Lo Phong river. In addition, clean water is supplied via the urban water supply system. Another mine water source is groundwater which is pumped from wells.
- Treatment: The water is flowing from the regulating basin to the MWTP. In Ha Tu area the treated water is partly used for internal water users. The other part flows into Lo Phong river. The clean water is treated by reverse osmosis filtration to reach the quality standards for drinking and cooking purposes. Groundwater is treated in a secondary treatment. Although a MWTP is available and ready to use in Tan Lap mine, the mine water is just pumped to the regulating basin and then drained to the river.
- Internal uses: A large proportion of treated water is used for internal uses like coal screening or truck washing, the rest is discharged to the river. Water for domestic uses is abstracted from wells located within the mine. The water needed for mining processes is abstracted from streams and wells.
- External uses: Under the existing situation, the water volume for external uses is zero due to the lack of related water infrastructure to ensure adequate water quality and quantity.

Figure 3 (right) shows the results of simulated water flows for the final situation:

- Sources: The only mine water sources in Ha Tu are the water from the open pits and the surface runoff. Rainwater and surface runoff are collected in the pit lake. In Tan Lap still groundwater is pumped via wells.
- Treatment: The only remaining treatment function is the pit lake for sedimentation and reduction of turbidity. There is no treatment by a MWTP anymore.
- Internal uses: A small amount of water is still required for recultivation.
- External uses: In this scenario, the water stored in the pit lake is provided as raw water for the urban water supply system. The final distribution of the additional water source depends on the demand of other users, costs and prioritization of decision makers.

Discussion

The reported results have to be further processed by a quasidynamic analysis of the water flows, by worst case assessment and a modellike implementation of measures for an improved water management.

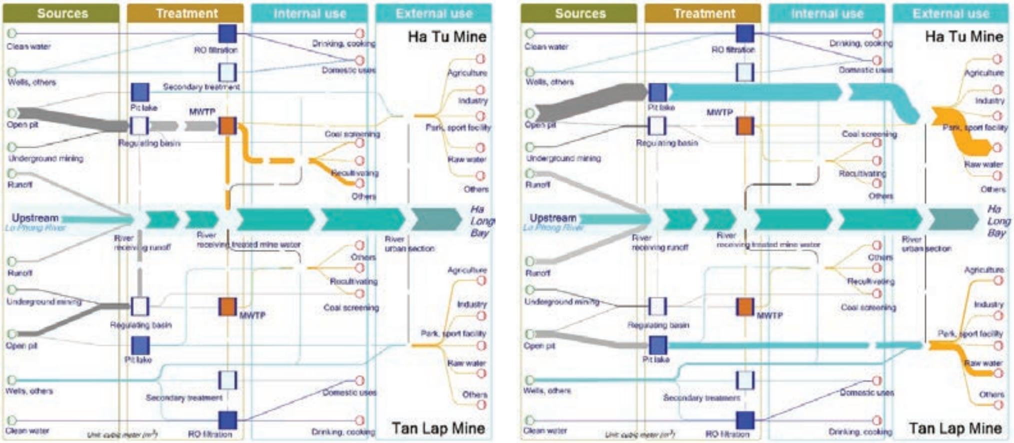

Figure 3 Material flow analysis of the water flow for the existing situation (left) and the final situa-tion (right) (widths of arrows proportionally to flow quantity)

The already applied model is a static model. Dynamic processes over time can be realized through the use of several models in succession where each model describes a short period of time, for instance one month.

Worst case assessments regarding the annual rainfall distribution and extreme variations of the internal and external water demands will be established using the model. Their results help the local decision makers to distinguish between so-called regret and no-regret measures.

The main task of the material flow models is the testing of potential measures for an improved water management. They include improved mine water treatment, additional treatment modules, distribution systems and the use of basins or reservoirs for water storage.

Conclusions

Mining operations and their water management often underlie fast spatial and temporal changes. Therefore, a material flow analysis is a very suitable instrument for the analysis and the management of mine impacted waters.

The developed material flow models describe all relevant components from the various water sources via the treatment steps to the internal and external users. The model is focusing on the water flows but also includes other relevant material flows like energy, supplies, sludges. Furthermore, it supports an economic analysis which is usually the most important factor for decision makers.

The selected Umberto NXT Efficiency software is suitable for the modelling tasks as it is flexible in setting up the model, the resulting Sankey diagrams are a good basis for further analysis and assessments. The lack in dynamic modelling can be solved through the use of several models for small time periods in succession.

Through variations of the water allocation, worst case analyses etc. improved spatiotemporal situations are generated which are the basis for management and investment decisions.

Acknowledgements

The project is sponsored by the German Federal Ministry of Education and Research (FKZ 02WAV1410A). The authors thank all project partners.

References

Broemme K, Stolpe H (2011) Mining and Environment in Vietnam. Research Work of the Research Association Mining and Environment (RAME), Status Report 2011. In: Advances in environmental engineering for natural resources mining, the first International Conference Hanoi, 22-24 June 2011

Broemme K, Stolpe H, Jolk C, Greassidis S, Borgmann A, Zindler B, Mien T (2014) Development of methods for post-mining land use planning for coal mines in urban areas in Quang Ninh, Vietnam. In: Hu, Zhenqi: Legislation, Technology and Practice of Mine Land Reclamation. Beijing International Symposium LRER. Leiden: CRC Press/Balkema, p 517-526

Do HH, Trinh VQ, Froer O (2018) The Economic Benefit Of Mine Water In Halong Peninsula, Vietnam. Proceedings of the International Mine Water Association Congress IMWA, 10-14 Sept. 2018. Pretoria, (in publication)

DONRE (2016) Report on environment status in Quang Ninh Province during 2011-2015 period, Halong (in Vietnamese).

GoV (2016) Decision No. 403/QĐ-TTg dated 16 March 2016, on Adjusted master plan for Vi-etnam's coal industry development by 2020, with perspective to 2030, Vietnam

Tuan ND (2015) Assessment of the minimum flow in Vietnam (in Vietnamese). Technical Science Hydrology and Environment 48, p 45-49

Ulbricht A, Bilek F, Broemme K, (2018) Development of a technical concept of spatial and temporal coordinated mine water recycling exemplified by a mining area with urban influence. Proceedings of the International Mine Water Association Congress IMWA, 10-14 Sept. 2018. Pretoria, (in publication)

Speciation Analysis of Colloidal Silica in Acidic Conditions

Ewa Cukrowska, Levi Ochieng, Hlanganani Tutu, Luke Chimuka

School of Chemistry, University of the Witwatersrand, P. Bag X3, 2050 Johannesburg, South Africa

ewa.cukrowska@wits.ac.za

Abstract

Dissolved silica speciation is of great importance in mining as it interferes in the various metals extraction/removal processes especially in electro-winning. Analytical methods have been devised to identify species in colloidal silica in acidic conditions. Total silica was determined after microwave acid digestion by ICP-AES. Monosilicic acid was determined using molybdic method; alpha and beta isomers were quantified. Silicon dioxide was determined after precipitation as potassium fluorosilicate by titrimetric method. Various interfering ion species which can co-precipitate with silicon dioxide were investigated.

Keywords: colloidal silica, acidic conditions, speciation

Introduction

Silicon is the second most common element found in the earths crust and mantle. It is most abundant in the form of silicates and occurs throughout the mineral realm complexed to metals such as magnesium, calcium, iron and aluminium (Ning 2002; Holleman-Wiberg 1995).

Many different techniques have been adapted to extract minerals from ores. The first step of processes is the milling or crushing of ores followed by a dissolution step. A method of metal extraction is electro-winning, once the sample is completely dissolved.

Silica dissolves from the ore samples, both under acidic or alkali conditions. Various species of silica and its complexes undergo polymerization to form colloidal suspensions. The colloidal silica then interferes with electrodes, complexes with metal ions and metal extraction processes cannot occur (Ning 2002).

There are two types of colloidal systems formed by silica. Silica sols are poly-silicic acids in spheroid, amorphous forms. When sodium silicate (Na_4SiO_4) is acidified a sol is formed. Addition of a base causes deprotonation and a negative overall charge of the molecules that prevent bonding and results in a sol. Under very specific conditions, a sol can convert itself to a gel (Holleman-Wiberg 1995; Govett 1961). If the pH is acidic or if a base does not stabilize the silica, the subunits fuse to form interlinking chains. The aggregation of subunits due to van der Waals forces results in a soft then hard gel.

Most literature on silica analysis focus on the determination of monomeric form of silica using colorimetric technique where a molybdate solution reacts with monomeric silicic acid to produce silicomolybdic acid as proposed by Dienert and Wandenbulkcke (Govett 1961; Roa 1992).

Silicic acid is a tetravalent weak acid with a strong tendency to eliminate water during condensation reactions with other silicic acid molecules (Ning 2002; Holleman-Wiberg 1995). The acid is most stable at a low pH of 1 - 3 and least stable at pH 5 - 6. The solubility of silicic acid increases in the presence of acids such as hydrofluoric acid (HF) and reacts with it to form silicoflouride anions (Govett 1961). Polymerization of silicic acid results in large polymers that form a colloidal solution. The molecules condense to produce a Si-O-Si bond between two molecules. Silicic acid polymerization is strongly dependant on pH (Ning 2002). Below pH 3.2, the polymerization reactions result in linear or openly branched polysilicic acids. Above pH 3.2, the polymerization results in cyclic or cross-linked polymer arrangements. Polymerization is rapid in alkaline or neutral environments and in acidic pH it is much slower. The condensations eventually result in a 3-D structure with the repeating units of $(SiO_2)n$.

Monomeric as well as polymeric silica species exists in dissolved ore samples. It is imperative that their concentration is determined. It is therefore not substantial to just know the total concentrations of silica but more importantly, its speciation (Holleman-Wiberg 1995).

The objective of this study was to develop methods for the analysis of various silica species in colloidal matrix under acidic conditions and to apply the developed methods to carry out silica speciation in electro-winning processes.

Experimental

Determination of silica in this study followed the following procedure: standard sample preparation, determination of total silica content (ICP-AES), monomeric silica determination (Molybdate reagent) and SiO_2 determination by titrimetric method.

Preparation of colloidal silica standard samples

Analytical grade silica gel was milled to a fine powder using Fritsch Planetary mono mill GmbH 'Pulverisette 6' at a speed of 130 rpm for 6 hours, sulphuric acid solution of known pH was added and the mixture shaken for 16 hours to prepare colloidal solutions of known concentration (Saccone et al. 2006) .

Acid digestion and determination of total silica by ICP-AES

Acid digestion was used to convert samples into solution for determination of total silica (Multiwave 3000 digestion Anton Paar GmbH). 0.1 g of ground sample masses were weighed into reaction vessels and 5 mL HNO_3, 5 mL HF and 0.5 mL HCl added. The digested samples are then placed in a 100 mL volumetric flask and mixed with boric acid in the ration of 6 mL : 1 mL of hydrofluoric acid [Roa 1992; May and Rowe (1965). Total silica was determined by spectral analysis using Spectro ICP-AES Genesis.

Determination of soluble silica (monosilicic acid complexation).

Preparation of a stable solution of ammonium molybdate. 100 g of $(NH_4)6Mo_7O_{24}.4H_2O$ and 47 g of concentrated (28% NH_3) ammonium hydroxide was dissolved in 1 L of deionised water.

Preparation of molybdate acidic reagent. A mixture of 100 mL of ammonium molybdate solution, 500 mL of deionised water and 200 mL of 1.5% (H2SO4) were mixed to give a concentration of 0.0707M MoO4-2, 0.375M SO4-2 and 0.148M NH+4, with a pH of 1.2.

Alpha Monosilicic acid analysis

A mixture of 20 mL of molybdate acidic reagent with no more than 5 mL of sample solution was prepared containing about 0.01 to 1.0 mg of SiO_2 and the total volume was then diluted to 25 mL with deionised water. The absorption was measured at a wavelength of 410 nm. Fresh reagent mixtures were made daily (Govett 1961).

Beta Monosilicic acid analysis

Sample solution was diluted to silica concentration of between 0.5 - 4 mg/L. All dilutions preformed were with 1.5 % $H2_SO_4$. 10 mL of each sample was then into 50 mL flasks. 2 mL of a 10% w/v solution of ammonium molybdate was added. The solutions were mixed and allowed to react for 20 minutes. 2 mL of 8% w/v solution of tartaric acid was added to the reagent mixture to prevent ferric (III) ion reduction, followed by 1 mL of reducing agent (4-amino-3-hydroxy-1-naphthalene-sulfonic acid/sodium metabisulfite/sodium sulfite solution). The sample was allowed to stand for 20 minutes to react before reading the absorbance on a UV-Vis spectrometer ((UV- 1201) at 820 nm).

Determination of silica dioxide (SiO_2)

To a 1 mL of sample, 5 mL of 20% calcium chloride and 1 g of sodium fluoride was added; the solution was stirred. Solid potassium chloride was added until an excess of 2 - 3 g over saturation point was attained. The precipitate was filtered and washed with a solution containing 70 g of potassium chloride in 1 L of 1:1 ethanol-water to ensured effective removal of excess acid. The washed precipitate, filter paper were transferred to a 1 L beaker containing 500 mL of boiled deionised water. The solution was titrated with 0.15M sodium hydroxide and 1% phenolphthalein (Lewis-Russ A, Ranville J and Kashuba AT (1991).

Results and discussion

Total silica

The concentration of Si determined for the prepared colloidal solution is shown in table 1. The measurements were done in triplicate and taken at a wavelength of 251.612 nm.

Percentage of silica in the solution was determined as 99.4% with a good precision of 0.15 % RSD.

Monomeric silicates

Monomeric silicates were quantified using UV-Vis spectroscopy. The acidic molybdate reagent forms two compounds when reacting with the Monosilicic acid; Molybdenum heteropolyacid (MHA) $(SiMo_{12}O_{40})^{-4}$ and heteropoly anion $(SiMo_{12}O_{40})^{-5}$ complexes. These ions are commonly known as the alpha (MHA) and beta (anion) forms. The alpha form is the most stable while the beta form converts spontaneously to the alpha form at pH above 2.5. The MHA complex forms a yellow solution that was measured at 410 nm while the reduced beta species forms a blue complex that was measured at a wavelength of 815 nm. The alpha isomer is very stable at pH 3.5 - 4.5 while beta formation occurs more readily at pH 0.8 - 2.5. When the environment is at a low pH the conversion of the beta form is very slow (Govett 1961; Maybodi and Atashbozorg (2006). If the reduction of beta molybdosilicic acid occurs at a low pH of 1.2 the heteropoly blue anion (beta- $(SiMo_{12}O_{40})^{-5}$) results.

Three colloidal solutions were prepared of pH ranges of between 0.8 – 1.0, 1.2 – 1.4 and 1.8 -2.0. They were left to stand and sampled at the top, middle and bottom for analysis to assess the stability of the colloidal solutions and to get a representative fraction of the colloid samples. The means and percentages of monosilicic acids were calculated (table 2) for beta and alpha monosilicic acid values, respectively.

The values obtained are all time dependant as the beta isomer is continually converting into the stable alpha isomer. The two silicic acids differ due to variation in their ionic charges.

Beta molybdosilicic acid predominates during maximum colour formation at pH 1.2 -1.4 and below. Both beta and alpha acids are formed at pH 1.8 − 2.0. The absorbance of alpha acid increases with time at any pH value. The time dependence is minimized under strongly acidic conditions. Therefore the results obtained in acidic media are accurate.

Above a pH value of 3.6 the alpha form dominates and can be purely alpha. The alpha molybdosilicic acid absorbance increases with time at any given pH. This occurs due to the conversion of the unstable beta monomer to it.

The precision of the process is indicated by the RSD values. Generally the higher the pH of the system the lower the RSD value and the greater the precision. The rate of conversion of the beta isomer to the alpha isomer is greatly reduced due to the acidic medium and the ROOM temperatures in which the experiments were done.

Table 1. *Concentration of total silica by ICP-AES*

Solution #	Concentration of silica (ppm)
1	0.994
2	0.993
3	0.996
Mean	0.994
SD	0.002
RSD (%)	0.15

Table 2. *Beta and alpha monosilicic acid concentration in µg L^{-1} determined by UV-vis spectroscopy at different acidic pH ranges*

Sampled region of colloidal solution	pH range of the solution analyzed		
	0.8 - 1.0	1.2 - 1.4	1.8 - 2.0
Beta monosilicic acid			
Top	47.4	43.8	39
Middle	48.6	49.2	37.8
Bottom	50.4	52.8	38.4
X (mean)	48.8	48.6	38.4
SD	1.5	4.5	0.6
RSD	1.2	3.7	0.5
Total Beta %	87.1	86.8	68.6
Alpha monosilicic acid			
Top	3.4	5.45	14
Middle	8.0	8.5	11.9
Bottom	6.6	6.8	13.4
X (mean)	6.0	6.8	13.0
SD	2.4	1.6	1.2
RSD	1.9	1.3	0.9
Total Alpha %	10.7	12.2	23.3

Table 3. *SiO_2 (%) in colloidal solution determined by precipitation and titration method (titre volumes are given in mL)*

Sampled region of colloidal solution	pH range of the solution analyzed		
	0.8 - 1.0	1.2 - 1.4	1.8 - 2.0
Top	1.4	1.6	0.4
Middle	1.5	1.8	0.7
Bottom	1.6	1.4	4.1
X (mL)	1.5	1.6	1.7
SD	0.1	0.2	2.1
% SiO_2	80.4	85.7	92.9

Silica dioxide (SiO_2)

Titrimetric method was used to determine the amount of silica dioxide by alkaline fusion. The titrimetric values were multiplied by a fraction that is dependant on the experimental conditions to determine percentage. The experiment must be done as quick as possible as the longer it takes the more errors occur due to co-precipitation by other metal species Glaso O and Patzauver G (1961).

Three colloidal solutions were prepared in pH ranges of between 0.8 – 1.0, 1.2 – 1.4 and 1.8 – 2.0. They were left to stand and sampled at the top, middle and bottom and analysed for SiO_2 by precipitating it out of solution then titrating with NaOH.

Percentage of SiO_2 in solution was calculated as follows: % SiO_2 = 0.150 × mL NaOH/g of sample

Hence for the top sample: 1.4 mL NaOH titre, (Dilution factor × 500) % SiO_2 = (0.015 × 1.4/1.4) = 105/1.4 = 74%.

The stability of a system greatly affects the accuracy of the results obtained. For the pH region of 1.8 - 2.0 silica stability in solution reduces and the percentage of the compound increases. Therefore, the system exists at a meta-stable equilibrium with its monomer.

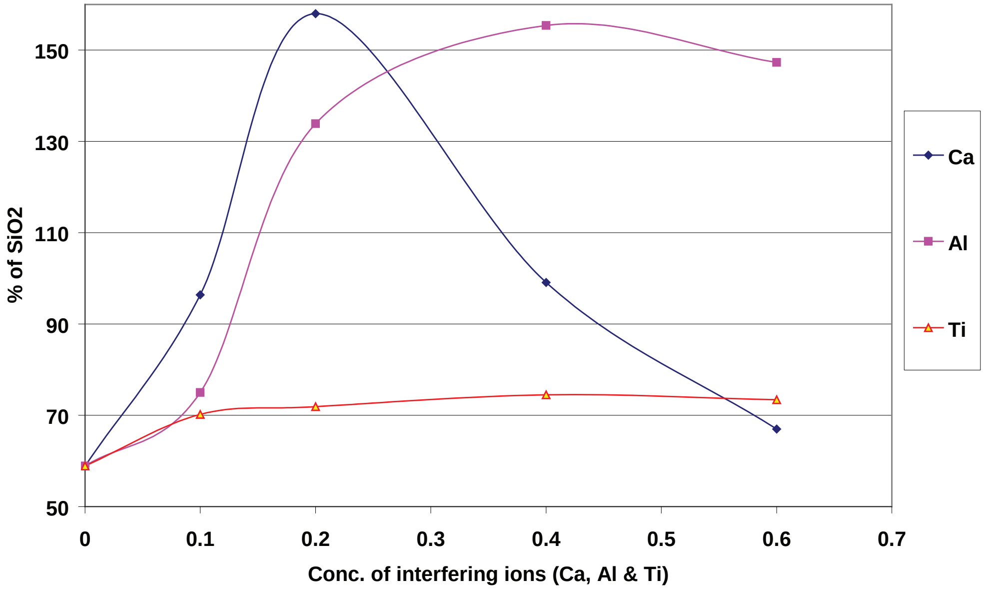

Figure 2 *Change in SiO2 percentage with increasing interfering ions concentrations*

Interferences

Metal ions present in solutions can cause interferences as they complex with silica dioxide and precipitate out as colloid. The positively charged ions electro-statically interact with the negatively charged surface of the colloid. Once the metal co-precipitates with silica it is incorporated into the colloidal structure and becomes difficult to extract during mining.

Silica solutions were spiked with various concentrations of interfering ions and then analysed. Calcium aluminium and titanium exhibited different trends as shown in fig. 2.

Calcium: Calcium causes an immediate exponential increase in the silica dioxide concentrations right from the start. It is the most reactive interfering ion. It appears that in any competition for fluoride ions, calcium is stronger than aluminium and titanium (fig. 2). There is a drastic decrease in % SiO_2 after 0.2 ppm for the calcium curve and this could be due to reversible attachment.

Aluminium: Initially aluminium causes a small increase in percentage silica dioxide but exponentially shots up at a concentration of about 0.1 ppm. At a slightly higher Al ion concentration of 0.2 ppm, % SiO_2 approaches a maximum value and stays constant with continued increase concentration.

Titanium: Of all the three metal ions investigated, titanium has the least influence in increasing silica dioxide concentration by co-precipitation. Initially there is a gradual increase in % SiO_2 and a maximum is rapidly reached. % SiO_2 stays relatively constant after an increase in titanium ion concentration of about 0.15 ppm.

Co-precipitation of SiO_2 occurs with calcium, aluminium and titanium in solution. This is due to the solubility constants of these compounds that are minimal. Calcium ions suppress the co-precipitation of aluminium and titanium. The lowest complexation occurs with titanium.

All the graphs show an increase the colloidal silica percentage to a maximum value and then decreases gradually as no more metal ions can complex by binding due to saturation of the binding sites. The calcium interference reached a maximum value and then decreased which indicates a reversible attachment to the colloidal silica.

Table 4. Mean, standard deviation and relative standard deviation for various species analysed in the Skorpion leachate samples

Sample	pH	Alpha	Beta	Silica ioxide (mg/L) dioxide	*Total Si (ICP-AES) (mg/L)
T1 Mean					
SD		0	0	0.26	0.27
RSD		0	0	0.21	1.26
T2 Mean					
SD		0	0	0.45	0.34
RSD		0	0	0.37	1.96
T3 Mean					
SD		0	0	0	0.31
RSD		0	0	0	1.77

Percentages (%) given in parenthesis, * Total Si after acid digestion

Silica speciation in leachate samples

Acid leachates of Skorpion samples at different pH values ranging from 0.8 – 2.0 obtained from Anglo Research Lab. were analyzed for alpha, beta and total silica, table 4.

Conclusions

Speciation of colloidal silica in acidic conditions was successfully achieved in this study. Various interfering ion species that co-precipitate with the silicon dioxide and increase the titrimetric values such as Ca (II), Ti (II) and Al (III) were assessed.

Good percentage recoveries, accuracy and precision were obtained for the methods used and they were applied to analyze leachates from acid leaching of silica at different pH values.

References

Ning RY (2002) Discussion of silica speciation, fouling, control and maximum reduction. Desalination 151, 67-73

Holleman-Wiberg (1995) Inorganic chemistry. Academic press. Berlin and New York, 822-936.

Saccone L, Conley DJ and Sauer D (2006) Methodologies for amorphous silica analysis. J. of Geochem. Exploration, 88, 235-238.

Govett GJS (1961) Critical factors in the colorimetric determination of silica. Anal. Chim. Acta, 25, 69-80

Roa CRM Reddi GS and Rao TAS (1992) Acid decomposition procedure for the spectrophotometric determination of silica in rocks and minerals at room temperature. Anal. Chim. Acta, 268, 357-359

Glaso O and Patzauver G (1961) Determination of silica in iron ore. Anal. Chim. Acta, 25, 189-192.

May I and Rowe JJ (1965) Solution of rocks and refactory minerals by acids at high temperatures and pressures. Determination of silica after decomposition with hydrofluoric acid. Anal. Chim. Acta, 1965, 33, 648-654.

Lewis-Russ A, Ranville J and Kashuba AT (1991) Differentiation of colloidal and dissolved silica: analytical separation using spectrophotometry and inductively coupled plasma atomic emission spectrometry. Anal. Chim. Acta, 204, 509-511.

Maybodi AS and Atashbozorg E (2006) Quantitative and qualitative studies of silica in different rice samples grown in north of Iran using UV-vis, XRD and IR spectroscopy techniques. Talanta, 70, 756-760.

Experimental Study of Removal of Organic Matters from Alkaline Uranium Leaching Solution with Ultrafiltration

Jinxun Deng, Ying Xu, Hong Cheng, Jianhua Li, Genmao Zhou, Chong Zhang

Beijing Research Institute of Chemical Engineering and Metallurgy, CNNC, Beijing 101149, China

Abstract

Organic matters in alkaline uranium leaching solution during CO_2+O_2 in-situ leaching process will make ion-exchange resins polluted and resin beds hardened. Experimental study is carried out to remove the organic matters from leaching solution with an ultrafiltration device. The organic matters can be removed efficiently with ultrafiltration and resin pollution and bed harden can be reduced which makes resin adsorption more stable and continuous.

Keywords: CO_2+O_2 in situ leaching; organic matters; ultrafiltration

Introduction

CO_2+O_2 in-situ leaching uranium mining technology has been successfully applied in sandstone type uranium deposits in Xinjiang and Inner Mongolia, China. A fixed bed ion exchange adsorption method is widely used in the application of uranium recovery. The impurities in the leaching solution will cause resin pollution and resin bed hardened, affecting the followed operation. Through the analysis and test of the burning-loss amount, total carbon, total organic carbon and infrared spectrum of the related resin contaminants and the hardened samples, it is found that the humic organic matter is the main cause of the resin pollution and hardening. Generally, the indicators of organic matter pollution are chemical oxygen demand (COD) and total organic carbon (TOC). COD is a chemical measure of the amount of reductive substances that need to be oxidized in water. It is an important and fast measuring parameter of organic matter. The greater the COD value, the higher the content of organic matter in the water. TOC, or total organic carbon, is a comprehensive indicator of the total amount of organic matter in water. By comparing the COD and TOC in the tail liquid of the bag filter and the resin tower (Fig. 1 and 2), it is found that both COD and TOC in the tail liquid of the adsorption tower are less than the bag filter solution, and the organic matter that causes the resin pollution is determined from the leaching solution formed by the groundwater. The organic matter in the leaching solution is adsorbed by the resin and enters the interior of the resin particles, causing the pollution of the resin. The deposition of organic matter leads to the adhesion of the resin particles to each other, resulting in the hardening of the resin bed. Cleaning and detoxification cannot fundamentally eliminate resin contamination and resin bed hardening problem. It is preferable to remove organic matters before adsorption.

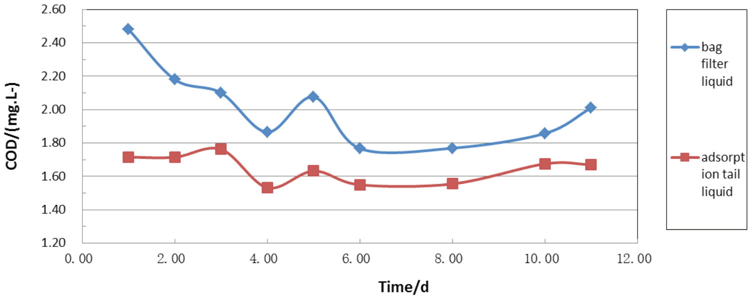

Figure 1 COD test results

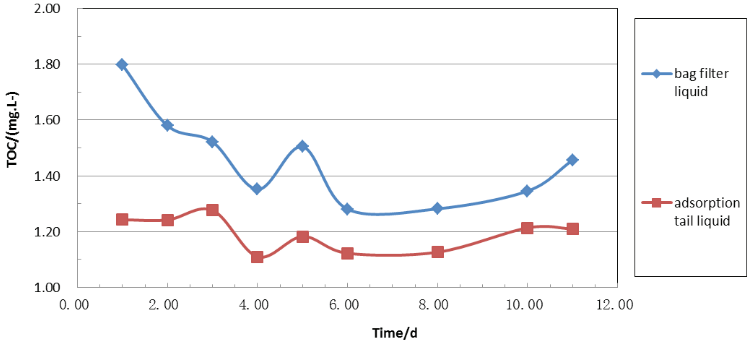

Figure 2 TOC test results

Selection of removal method of organic matter

The ordinary methods of removing impurity from water include adsorption, microfiltration, ultrafiltration and nanofiltration. Compared with other methods, the ultrafiltration has the advantages of less operating pressure, larger water production and higher separation precision. It is more suitable for removing the organic matter in the colloid state, that is, the high suspended organic matter with a particle size below 0.1 μm (<100nm) [1]. The principle of ultrafiltration is that, under the action of external force, the separated solution flows along the surface of the ultrafiltration membrane at a certain velocity, and the solvent in the solution, the low molecular weight material and the inorganic ion, enter the low pressure side through the ultrafiltration membrane from the high pressure side and discharge as the filtrate; The polymer, colloid particles and microbes in the solution are intercepted by the ultrafiltration membrane, and the solution is concentrated and discharged in the form of concentrated solution to achieve the purpose of separation of large and small molecules[2-3]. In conclusion, the ultrafiltration method is used to remove organic matter from uranium leaching solution.

Ultrafiltration test device

The ultrafiltration device used in the experiment is based on field test condition, commissioned by professional manufacturers. The core of ultrafiltration device design is ultrafiltration membrane material and membrane module selection. Ultrafiltration membrane materials include cellulose and its derivatives, polycarbonate, PVC, polypropylene, modified acrylic polymers, etc. Polyacrylonitrile (PAN) has good water permeability, good pressure resistance, stable retention of molecular weight, and a wide range of acid and alkali resistance. It is suitable for low organic matter content and poor water quality in water, and is also a kind of low price among many membrane materials. Referring to the previous analysis and testing of pollutants and the characteristics of the test site, polyacrylonitrile (PAN) was selected as an ultrafiltration membrane material, and a preliminary selection of polyacrylonitrile (PAN) membrane material with a molecular weight of 100 thousand was selected in the explored test. In order to ensure the continuous and stable operation of the ultrafiltration test, self-cleaning ultrafiltration test device is adopted and two membrane components are used in parallel to realize automatic flushing and backwashing. Figure 3 is a picture of a self-cleaning decontamination and impurity removal device. Fig. 4 is a normal working flow chart for self-cleaning, decontamination and impurity removal devices. The test parameters of the ultrafiltration device: membrane module diameter: 90mm; water production: 8L/min; cleaning cycle: 3 months; interception of molecular weight 50 thousand; 4 membrane components, single area 2m^2, single membrane flux 125L/ (m^2/h).

Figure 3 *Ultrafiltration device*

Methods

At the same time, resin adsorption and ultrafiltration were used to compare the removal efficiency of organic matter in the processing plant in Inner Mongolia. Two main branches are separated from the main pipe of bag filter after bag filtration. A branch directly connected with an ion exchange column 1 (as column 1) is used to evaluate the removal of organic matter by adsorption; The other branch is first connected with the ultrafiltration device, and then the ultrafiltration device is connected to the ion exchange column 2 (as column 2), which is used to evaluate the ultrafiltration method for removing organic matter. The evaluation test procedure is shown in Figure 6. The test conditions are as follows:

1) D231 type strong basic anion exchange resin was used for tests, which is same as the resin used for ion exchange adsorption in the uranium mine. The volume of the column 1 bed is 1L, 20L of column 2.
2) The original sorbent used in the test is the feed liquor of the bag filter, of which the uranium concentration is 19mg/L$_0$Initial inlet velocity of column 1 is 0.3L/min, as to column 2 the velocity is 6L/min.
3) The samples were collected from the feed liquor, column 1 tail fluid and ultrafiltration tail liquid respectively, and the relevant water quality parameters were analyzed and tested. The sampling period was 24h.

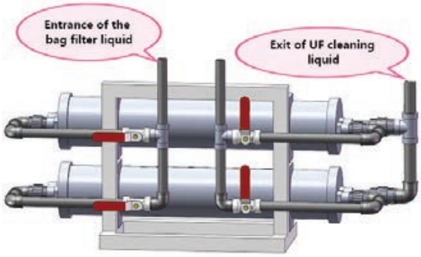

Figure 4 *Flow in the ultrafiltration device in working condition*

Change of water quality parameters

The analysis of COD and TOC were carried out in the feed liquor, tail liquid of column 1 and UF to evaluate the effect of two means of removing the organic matter in the leach solution by adsorption and ultrafiltration. The results of the COD test are shown in Figure 7. The results of the TOC test are shown in Figure 8.

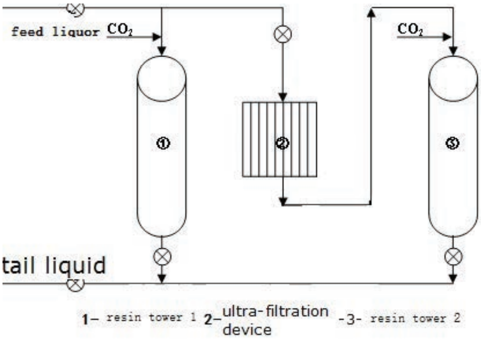

Figure 5 *Evaluation tests process*

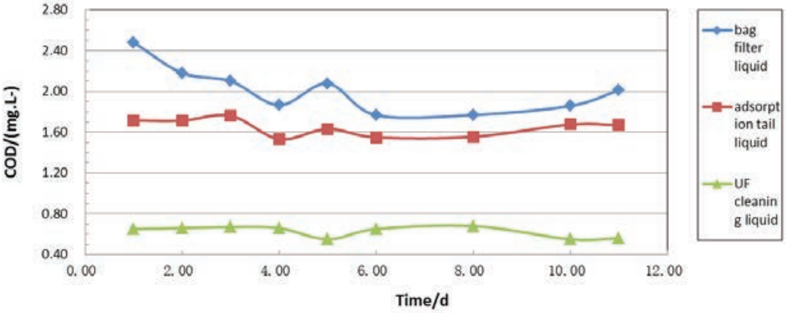

Figure 6 *Results of COD test*

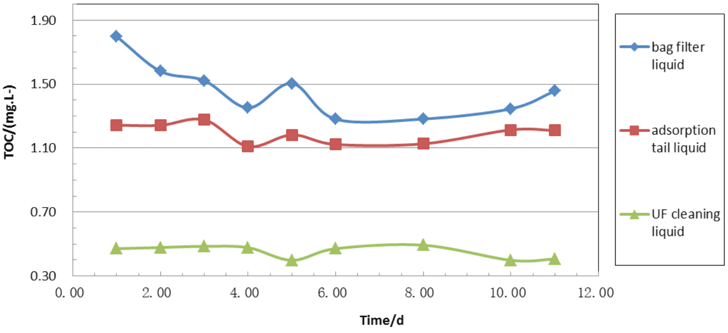

Figure 7 Results of TOC test

According to Figure 7 and figure 8, the values of COD and TOC in the column 1 tail liquid and the ultrafiltration liquid are lower than that in the feed liquor, indicating that the organic matters in the feed liquor can be removed by adsorption and ultrafiltration. Comparing the COD and TOC curves, the values of COD and TOC in ultrafiltration solution were much lower than those in the 1 column tail solution. Ultrafiltration can remove organic matter in leaching solution better than resin adsorption.

Comparison of characters of resin beds

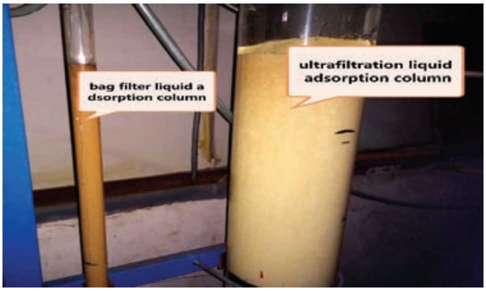

***Figure 8** View of resin beds before adsorption*

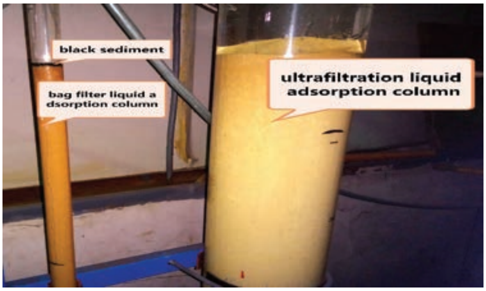

***Figure 9** View of resin beds after 5 times adsorption*

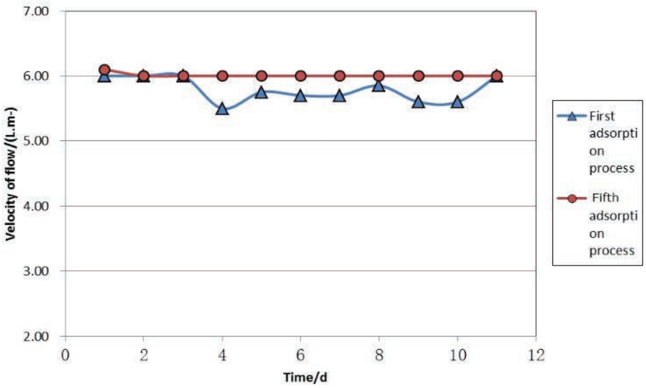

Figure 10 Change of flowrate after several times of adsorption

Figure 10 shows the appearance of the resin adsorption columns before the start of the experiment. Fig. 11 shows the appearance of the columns when the resin is saturated for the fifth time. From the figure, no black solid is found in the adsorption column 2 (right tower), while the adsorption column 1 (the left tower) has a black layer on the top. Analysis shows that the black thing is hardened organic matter. Compared with figures 10 and 11, ultrafiltration can remove organic matter from the feed liquor and reduce resin contamination and hardening. Fig. 12 shows the change of flow rate of the two adsorption process of ultrafiltration resin. It shows that after the treatment of leaching solution the resin in the adsorption column does not have the phenomenon of pollution and hardening. The adsorption process can maintain a very stable continuous operation without the need for the back flushing operation.

Conclusion

The evaluation test shows that both resin adsorption and ultrafiltration can remove the organic matter in the leaching solution. In contrast, the removal efficiency of the ultrafiltration method is more obvious. After ultrafiltration, 2 adsorption cycles were run without resin contamination and resin bed hardening. Ultrafiltration has obvious effect on removing organic matter from leaching solution, eliminating resin pollution and resin bed hardening. The ultrafiltration treatment can improve the continuity and stability of adsorption operation.

References

Jianqiu Ding, Yanan Zhu, Xiaoqin Cai Research and development of UF in treatment of micro polluted water sources treatment, J Guizhou Chemical Industry 2009, 34 (3): 39-43.

Xuehua Duan (1976), Lihong He Application of Ultrafiltration Technology in Treatment of Wastewater,J Environmental Science and Technology, 2010, 23 (1): 36-39.

Jianxin Ren – Membrane Separation Technology and Its Application – 2003: 50-61. Chemical Industry Press, Dongcheng District, Beijing, China.

The Impact of Sulphide Concentration on Microbial Activity in a Biological Sulphate Reduction Process

Kerri du Preez, Mariekie Gericke, Dheepak Maharajh

Mintek, South Africa, kerrid@mintek.co.za

Abstract

Mine impacted water includes all water impacted by mining activities, from process effluents to polluted water courses due to mining activities. In South Africa, mine impacted water has caused severe and long term degradation of the environment. As a result, much research is focused on treating mine impacted water, specifically increasing or neutralising the pH of the water and decreasing the sulphate and metals concentrations. South African mine impacted water generally contains high levels of sulphate, often in excess of 3g/L, and stringent regulations enforce low sulphate discharge limits of 200 600 mg/L. Biological sulphate reduction has been demonstrated as a feasible treatment technology for removal of sulphate and precipitation of metals from mine impacted water. Sulphate is biologically converted to sulphide in this process, which is either released as hydrogen sulphide gas, or remains in solution. There is much discrepancy in the literature regarding the nature of sulphide inhibition and its impact on microbial communities and sulphate reduction activity. This study aims to quantify the impact of increasing sulphide concentrations on an established biological sulphate reducing system.

Most of the available data on sulphide inhibition in anaerobic systems was obtained from studies where sulphide was added to a system, and excluded sulphate, thereby neglecting the interactions of sulphate reducers with other microbial communities. This study used a continuously operated reactor at steady state, with a neutralised mine water feed, consisting of high sulphate concentrations and low levels of metals. Sulphide, in the form of sodium sulphide, was added to the feed in increasing concentrations over the study period. Microbial activity was determined measuring the changes in sulphate reduction rates with increased sulphide concentrations. Variations in the microbial communities in response to the changing feed conditions, were determined using metagenomics techniques.

This study is ongoing, and the results concerning the impact of increasing sulphide concentrations on microbial activity, community dynamics and sulphate reduction rates will be analysed and presented in a full paper.

The results from the study will provide a clearer understanding of the effect of sulphide concentration on microbial activity and community dynamics. This would inform the development and optimisation of active and passive processes for treatment of mine impacted water, resulting in higher sulphate reduction rates.

Keywords: Biological Sulphate Reduction, Sulphide Inhibition

Reuse of Treated Mine-Impacted Water as a Potential Resource for Accelerated Carbon Sequestration

Tamsyn Grewar

Mintek, South Africa, TamsynG@mintek.co.za

Abstract

Mine impacted water (MIW) can refer to any water impacted by a mining process including AMD and brines all of which pose a major environmental threat. The vast quantities of MIW present in South Africa has created serious problems in the water cycle. However this has also provided opportunities where these waste streams could be considered resources under the right conditions. South Africa is not only water scarce but also one of the top 20 CO_2 polluters, world-wide. Average global monthly temperatures are now cresting at 1 °C above pre-industrial levels while atmospheric CO_2 levels seem to have permanently breached 400 µmol/mol. These levels are projected to increase to over 800 µmol/mol by the end of the century if no action is taken. The work presented here provides a potential CO_2 sequestration mechanism using MIW.

Carbon sequestration is defined as a natural/artificial process by which CO_2 is removed from the atmosphere and held in solid/liquid form. Carbon mineralisation for carbon sequestration involves the leaching of Ca-Mg-Fe cations from silicate minerals which are then reacted with CO_2 to form inert carbonate minerals, sustainably trapping CO_2. However, due to the slow kinetics of the initial dissolution step the research focus has shifted to speeding up the dissolution of the target minerals, and identifying more reactive mineral resources. Alternatively, we investigated through batch tests under varying conditions of pH and temperature, the potential of a variety of Ca-Mg-Fe-rich MIWs to function as resources for carbon sequestration where the costly, rate-limiting mineral dissolution step was bypassed altogether. In addition, we investigated the water treatment potential of the carbonation reaction, to co-precipitate and encapsulate other elements present in the MIW into the stable carbonate products, to lead to cleaner effluents.

The work conducted was designed to answer questions relating to; a) how to cost-effectively maintain the alkaline pH required for carbonation, b) the effect of other MIW components on the carbonation reaction, c) how this in turn affected the final carbonate product and d) the effect of elemental encapsulation on MIW quality.

New regulations being imposed worldwide aiming to mitigate the risks of global warming necessitates the R&D of new technologies for carbon sequestration. Linking these technologies to the use of the vast MIW resources present in South Africa that could themselves be treated in the process provides an attractive opportunity on two fronts.

Keywords: Mine-Impacted Water, Carbon Sequestration, Treatment, Encapsulation

Comparison of diversion well substrates for the treatment of acid mine drainage Bellvue Mine, West Coast, New Zealand

Emma Forbes[1], Dave Trumm[2], James Pope[2], David Bell[1]

[1]Department of Geological Sciences, University of Canterbury, Christchurch, New Zealand
[2]CRL Energy Ltd, PO Box 29 415, Christchurch, New Zealand

Abstract

Bellvue Mine, an abandoned coal mine north of Greymouth, West Coast, is discharging AMD into Cannel Creek, resulting in low pH conditions and high dissolved metal concentrations. A diversion well is a form of passive treatment of AMD. This research aimed to test the efficiency of a diversion well using mussel shells in treating AMD at Bellvue, in comparison to the more traditional diversion well using limestone. Results indicate that limestone is more effective at improving water chemistry. Greater increases in the pH level of treated water and greater decreases in dissolved metal concentrations were achieved using the limestone substrate.

Keywords: Acid mine drainage, Bellvue Mine, diversion well, mussel shells, semi-passive treatment

Introduction

A long history of coal mining on New Zealand's West Coast has resulted in the production of acid mine drainage, having a negative effect on the quality of fresh water streams. Bellvue, an abandoned coal mine north of Greymouth, is discharging acidic run-off into Cannel Creek. Past studies have shown sections of the creek, downstream of the mine site, have pH levels as low as 3.55 (Trumm and Cavanagh, 2006). Acidic discharge is also causing high dissolved metal concentrations (West, 2014). As a result, stream water quality is poor, leading to low ecosystem health and a loss of aquatic biodiversity.

Bellvue Mine is approximately 12 km north of Greymouth, West Coast, situated on Cannel Creek (fig. 1). Bellvue Mine operated over several decades beginning in 1927 until production ceased in 1970. The mine was opened as an extension to the larger James Mine, further northwest of Bellvue, along the same Brunner Coal seam. Extraction of coal has exposed minerals, specifically pyrite, allowing the formation of AMD, which flows into the nearby Cannel Creek. Bellvue Mine adit is located at the top of a 50 m cascade. Contaminated water pools at the mine adit as the mine entrance has collapsed over time, damming water behind it. Acid mine drainage flows down the cascade, over a flat, non-vegetated area and into Cannel Creek.

Figure 1 Red square indicating location of Bellvue Mine site, West Coast, New Zealand (adapted from Google Maps (2017) and Land Information New Zealand (2016)).

Passive treatment of AMD is a favourable method of treating contaminated waters at sites similar to Bellvue. These treatment systems are low maintenance, low cost and take advantage of the naturally occurring processes at the given site. Limestone diversion wells are a common form of passive treatment of acid mine drainage. Basic design and system function of a diversion well is described by Arnold (1991) and Schmidt and Sharpe (2002). A typical well consists of a circular casing, often sunk into the ground at a shallow level alongside a stream. Water is forced into the well by having an elevation difference that creates hydraulic head. This often involves damming water upstream. The water is flushed into the centre of the well through a pipe and exits the pipe near the bottom of the well. The water then flows upwards, fluidizing the limestone substrate. Calcium carbonate reacts with the contaminated water to raise the pH and increase alkalinity, thus allowing for the removal of metal contaminants. Treated water is then piped from the well back into the stream (fig.2) (Arnold, 1991; Schmidt and Sharpe, 2002). A diversion well is usually 2/3 full of limestone, which needs to consist of greater than 85% of calcium carbonate for optimal results (Schmidt and Sharpe, 2002). This form of passive treatment is effective in that it treats AMD quickly, without long residence time, and it does not require large amounts of space to install and is of low cost. However, regular maintenance is required to replace limestone and to clear any vegetation debris that can block the well intake (Arnold, 1991; Schmidt and Sharpe, 2002).

This research aimed to determine the efficiency of a diversion well using mussel shells for the treatment of AMD at Bellvue, in comparison to the more traditional diversion well using limestone.

Methods

The system setup consisted of an 800 × 400 mm well (110L blue barrel), linked to two intermediate bulk containers (IBC's: fig 3). Acidic water was siphoned from pooled mine waters using three pre-existing 25 mm alkathene pipes, to a 50 mm PVC pipe, which fed vertically to the bottom of the well. This inlet pipe rested on the base of the well and was perforated with 10 mm holes, equalling the cross-sectional area of the pipe. This increased the velocity of the water flowing into the well, increasing the ability for grains to fluidize towards the outer edges of the well. From the well, IBC 1 was connected down gradient using a 50 mm PVC pipe, and another 50 mm PVC pipe connected IBC 2 to IBC1. This set up allowed siphoned acidic water to flow down into the bottom of the well, up through the substrate, out of the well and through the connected IBCs, exiting the system through a 50 mm hole in IBC 2, which allowed treated water to flow back into Cannel Creek. The use of the IBC's was to increase residence time of water flowing through the system.

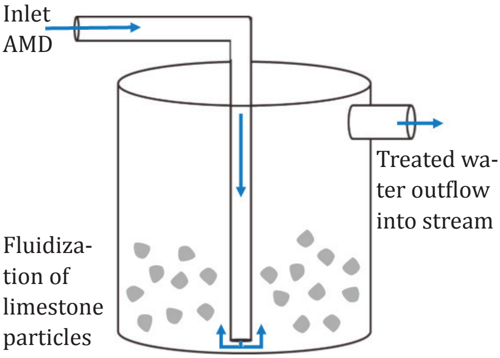

Figure 2 *Schematic diagram of a diversion well.*

Figure 3 Diversion well setup at Bellvue Mine site. Inlet AMD enters the well where fluidization of substrate occurs. Treated water then flows through each IBC, where further dissolution of substrate and neutralisation reactions occur. Treated water then flows into Cannel Creek.

The residence time of water in the system was measured by simply timing how long it took the whole system to fill with water, with the diversion well containing substrate. On average, the system took 10 minutes 3 seconds to fill. Initial sampling took place as soon as water started flowing out of the IBC 2 outlet, back into Cannel Creek, that is 10 minutes, 3 seconds after the valves were turned on allowing water flow through the system. The 15-minute sampling then took place 15 minutes following the initial sample, and so on. Flow rates were taken throughout the experiments using a bucket and stop watch method. Average flow rates of water flowing out of IBC 2 was 2.4 L/second, the same as for inflowing water.

Limestone and mussel shells were tested individually as diversion well substrates. The limestone used was 0-5 mm aggregate and was sourced at size from Springfield Lime Company Ltd. The mussel shells were sourced whole, as a waste product, from United Fisheries, and were crushed using a garden mulcher to and sieved to 0-4.5 mm. Sixty litres of substrate was used in the well during each test, equating to just over half the well volume.

Each test consisted of running the system and collecting data over several hours to observe changes in water quality and chemistry over time. Inlet and outlet samples were collected for total and dissolved Al, Fe, Mn, Ni and Zn and sulphate analysis, for each time interval. The sample time intervals were: at the start (inlet and outlet), 15 minutes, 30 minutes, 1 hour and 18 hours (outlet only). This was repeated four times for limestone treatment and three times for the mussel shell treatment. Water samples were sent to Hills Laboratories for chemical analysis. Previous analysis of acidic drainage at Bellvue indicated elevated levels of Al, Fe, Mn, Ni and Zn. These metals were therefore, chosen for analysis in this project. The pH level, electric conductivity and dissolved oxygen levels for each sample were measured using a YSI probe.

Results

Initially, dissolved metal concentrations rapidly decrease for both substrates compared to the inlet AMD (tables 1 and 2). The pH levels rapidly increase, allowing metals to precipitate. However, over time, improvements in water chemistry and quality decrease. This is likely a result of all the finer substrate material having already been consumed in early stages of diversion well operation, and only the larger grains remain, which take longer to break down and dissolve. Also, precipitated iron hydroxides start to coat the remaining substrate after 18 hours, reducing further dissolution.

The limestone shows greater decreases in dissolved metal concentrations and greater increases in pH levels compared to that of the mussel shells, indicating the limestone is a more favourable diversion well substrate (fig. 4, 5 and 5). Limestone is a much softer, brittle material than the shells. Therefore, it is likely easier to break up and dissolve in the system compared to the shells, resulting in more effective treatment.

Table 1. Average dissolved metal concentrations for treatment using limestone

Metal	Inlet AMD	Initial	15 min	30 min	1 hr	18 hr
Al	37	0.55	23.7	31.3	36	31
Fe	54.2	15	53	33.3	29.5	32.5
Mn	0.71	0.78	0.89	0.73	0.71	0.62
Ni	0.12	0.12	0.14	0.12	0.12	0.11
Zn	0.31	0.24	0.335	0.29	0.30	0.26

*Table 2. Average dissolved **metal concentrations for treatment using mussel shells***

Metal	Inlet AMD	Initial	15 min	30 min	1 hr	18 hr
Al	37	26.3	36.5	35	36.3	39.7
Fe	54.2	41.1	75.5	64.3	67.7	73.7
Mn	0.71	0.73	0.82	0.74	0.73	0.72
Ni	0.12	0.12	0.136	0.124	0.126	0.127
Zn	0.31	0.29	0.34	0.31	0.31	0.323

*Table 3. Average water **quality parameters for treatment using limestone***

	Inlet AMD	Initial	15 min	30 min	1 hr	18 hr
pH level	2.7	5.9	3.3	3.2	3.1	2.8
Sulphate (g/m3)	717.1	1008	800	685	697.7	600
DO (%)	42.3	52.8	55.1	45.9	41.9	58.2
EC (µs/cm)	1472	934	1047	911	889	1068

*Table 4. Average water **quality parameters for treatment using mussel shells***

	Inlet AMD	Initial	15 min	30 min	1 hr	18 hr
pH level	2.7	3.8	3.1	3.0	2.9	2.8
Sulphate (g/m3)	717.1	746.7	780	750	756.7	770
DO (%)	42.3	46.7	48.7	39.4	35.5	54.8
EC (µs/cm)	1472	1412	2030	1550	1603	1793

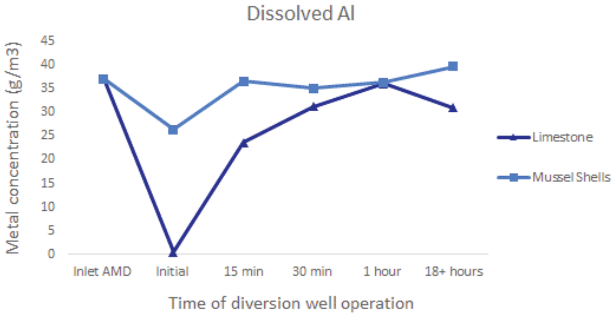

***Figure 4** Graph showing comparison of dissolved Al concentration for limestone and mussel shell treatment. Limestone shows greater decrease in concentrations, indicating it is more effective at treating AMD in a diversion well compared to the mussel shells.*

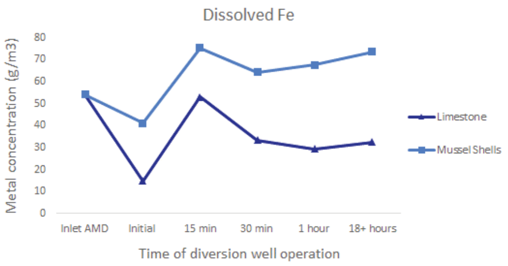

Figure 5 Graph showing comparison of dissolved Fe concentration for limestone and mussel shell treatment.

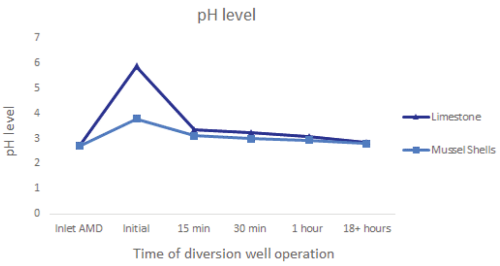

Figure 6 Graph showing comparison of pH levels for limestone and mussel shell treatment.

Conclusions

The efficiency of limestone as a diversion well substrate was compared to that of mussel shells in a diversion well setup at Bellvue Mine. Comparing the water chemistry and quality for treated waters showed that limestone is a more effective diversion well substrate. Greater decreases in dissolved metal contaminants and greater increases in pH levels were seen using the limestone substrate compared to the shells. This system set up was unable to achieve effective long-term function. Having a larger well and thus more substrate is necessary for future semi-passive treatment at Bellvue.

Acknowledgements

This research was financed by the Ministry for Business, Innovation and Employment, Contract CRLE1403. Access to the mine site was provided by MBD Contracting and Solid Energy New Zealand.

References

Arnold, D.E. (1991). Diversion wells- A low cost approach to treatment of acid mine drainage. Proceedings of 12th Annual West Virginia surface mine drainage task force symposium, WV Mining and Reclamation Association, Charleston, WV, USA, pp 39-50.

Google Maps. (2017). Northern South Island of New Zealand. Retrieved from https://www.google.co.nz/maps

Land Information New Zealand. (2016). Topo250 Map 17 Greymouth. Retrieved from http://www.linz.govt.nz/land/maps/linz-topographic-maps/

Schmidt, K. and Sharpe, W. (2002). Passive treatment methods for acid water in Pennsylvania. Penn State College of Agricultural Sciences, Agricultural Research and Cooperative Extension. Retrieved from http://extension.psu.edu/publications/uh157

Trumm, D. and Cavanagh, J.E. (2006). Investigation of remediation of acid-mine-impacted waters at Cannel Creek. Land Care Research Report: LC0506/169, prepared for West Coast Regional Council.

West, R. (2014). Trialling small-scale passive systems for treatment of acid mine drainage: A case study from Bellvue Mine, West Coast, New Zealand (Master's thesis, University of Canterbury, Christchurch, New Zealand). Retrieved from https://ir.canterbury.ac.nz/handle/10092/10907

Pilot Study of *In Situ* Biological Treatment at the Silver King Mine, Keno Hill, Yukon

Andrew G. Gault[1], Jim. M. Harrington[2], Cameron Robertson[3], Monique C. Simair[4] and Vanessa P.M. Friesen[4]

[1]*Alexco Environmental Group, 400-36 King St E, Toronto, ON, M5C 3B2, Canada, agault@alexcoresource.com*
[2]*Alexco Resource U.S. Corp., 7720 East Belleview Avenue, Suite B – 104, Greenwood Village, CO 80111, USA*
[3]*Alexco Environmental Group, 1225-555 Burrard St, Vancouver, BC, V7X 1M9, Canada*
[4]*Contango Strategies, 104-411 Downey Road, Saskatoon, SK, S7N 4L8, Canada,*

Abstract

As part of a pilot test of *in situ* microbiological-based treatment, soluble organic carbon was periodically introduced to the flooded Silver King mine workings (Yukon, Canada), producing sulphate-reducing conditions and the precipitation of zinc and cadmium. Genomic analysis confirmed the presence of sulphate-reducing bacteria, which were dominated by members of the *Desulfosporosinus* genus. Following carbon injection, zinc and cadmium concentrations declined by >90%. Despite rising slowly over time, zinc and cadmium concentrations remained below both their pre-treatment concentrations and the effluent quality standards such that carbon injections on an annual (or longer) basis may maintain low metal concentrations.

Keywords: Biological treatment, in situ treatment, microbial sulphate reduction, zinc, cadmium

Introduction

Biologically driven metal treatment systems have received increasing attention in recent years as potential options to remediate contaminated industrial and mining sites. A common approach adopted by many bioremediation strategies involves the application of soluble organic carbon to stimulate the activity of sulphate-reducing bacteria (SRB). These microorganisms are capable of coupling the oxidation of organic carbon to the reduction of sulphate, producing soluble sulphide which reacts with chalcophile metals (e.g., zinc, cadmium, lead, copper) to precipitate low solubility metal sulphide phases. Furthermore, under such reducing conditions elements such as selenium, chromium, and uranium may be transformed to less soluble reduced phases, providing additional treatment routes that do not rely on metal sulphide precipitation. As such, the exploitation of SRBs, which are ubiquitous in the subsurface environment, offers a promising avenue for metals treatment in subsurface waters. Indeed, injection of soluble organic carbon into contaminated groundwater has been documented to promote removal of chalcophile metals (e.g., Saunders et al., 2005, 2008) and this approach has also been adopted to treat metal concentrations in flooded mine workings (e.g., Harrington, 2002; Bilgin et al., 2007; Harrington et al., 2015).

The historical United Keno Hill Mines (UKHM) site in central Yukon (Canada) is undergoing closure planning, which includes evaluating options for long term treatment of a number of flowing adits in which cadmium and zinc are the principal contaminants of concern. In situ treatment is an attractive closure option given its lower cost, maintenance and power requirements compared to conventional water treatment plants (WTP). Although bench-scale studies have demonstrated the potential for sustained in situ metals treatment at Keno Hill (Nielsen et al., 2018), there are few long term, field-scale studies of in situ treatment at such a cold climate site. Therefore, an in situ treatment pilot test was initiated at the UKHM Silver King mine to evaluate the potential of this closure strategy to treat cadmium and zinc concentrations over the long term. This paper reports the results of the initial 3.5 years of this ongoing pilot study.

Methods

Site Configuration

An overview of the Silver King site is displayed in fig. 1. Prior to starting the in situ treatment pilot test, water discharged from the Silver King mine via the 100 level (SK100) adit (2 to 20 L/s, median 7.4 L/s). Zinc is the primary constituent of concern (0.8 to 1.0 mg/L) in the adit discharge, which requires treatment by a lime-based WTP to meet the site effluent quality standard (0.5 mg/L). Between Oct 2014 and Dec 2016, the mine was dewatered below its static water level, preventing discharge from the SK100 adit. Water pumped from the mine was directed to the WTP for discharge during this time. Dewatering was halted in Dec 2016 allowing the mine to fully flood and discharge via the 100 level adit.

Organic carbon was periodically introduced into the underground mine workings by mixing a portion of the pumped mine water with molasses or methanol and re-injecting via a historical borehole that intersects the workings, or an open pit that infiltrates into the mine workings below. Such reinjection forms a recirculation loop, helping to mix the organic carbon throughout the mine workings. Four molasses injection events were performed in 2015 (Jan to Feb, Feb to Mar, Apr to May and Nov to Dec), each lasting between 24 and 42 days. Two additional injections of methanol followed in 2016 (Jan to Mar and Nov to Dec; total of 105 days).

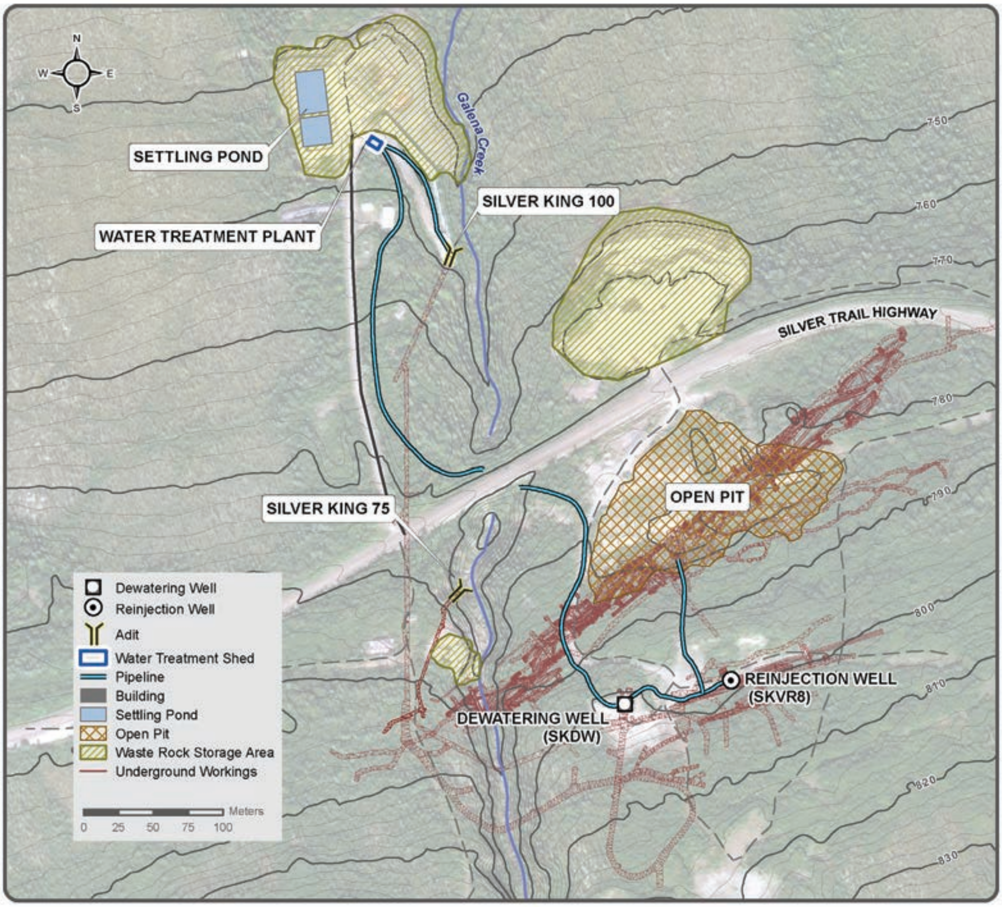

***Figure 1** Plan view of Silver King mine and in situ treatment infrastructure*

Aqueous Sampling and Analysis

During mine dewatering, mine water discharge samples were collected from the Silver King dewatering well (SKDW), whereas samples from the SK100 adit were collected when the mine was fully flooded. In situ measurements of pH, conductivity, temperature and oxidation-reduction potential (ORP) were made at the time of sampling using a YSI multimeter. Samples were submitted to ALS Environmental (Burnaby, BC) for the analysis of major anions, dissolved organic carbon (DOC), and total and dissolved major and trace elements. Dissolved ferrous iron was analysed between May and Jul 2015, but was discontinued since all samples showed 100% of the dissolved iron comprised ferrous iron. Total sulphide was also measured periodically for samples collected since May 2015. Where data are presented graphically and a constituent is below the limit of detection, a value of half the detection limit has been used, evident as a plateau on plots.

Microbial Sampling and Analysis

Two litre samples of unfiltered water were collected periodically from the dewatering well in sterile HDPE bottles. The pumped water collects free-floating or unattached microbes, which are only a subset of the total microbial population that also includes microbes attached to the mine rock surfaces that cannot be easily access for sampling. An aliquot (0.5 – 1 L) was centrifuged (4,696 × g, 10 min, 4°C) and the resulting pellet was used for DNA extraction using a MoBIO PowerLyzer PowerSoil DNA isolation kit. The v3/v4 regions of the 16S rRNA gene were targeted for sequencing, and similar sequences (97% similarity or higher) were grouped together into operational taxonomic units (OTU) and compared against a database for taxonomic classification.

Results

Aqueous Geochemistry

Trends observed for key parameters throughout the in situ pilot test are displayed in fig. 2. Periods of organic carbon injection to the mine workings are indicated in fig. 2, alongside periods that the mine was dewatered (Oct 2014 to Dec 2016), unintentionally flooded due to dewatering pump failure (May/Jun 2015, Oct/Nov 2015 and Jul – Sep 2016), and intentionally flooded to its static water level when dewatering ceased [Jan 2017 to time of writing (May 2018)].

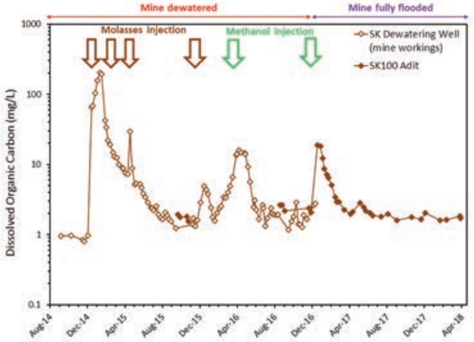

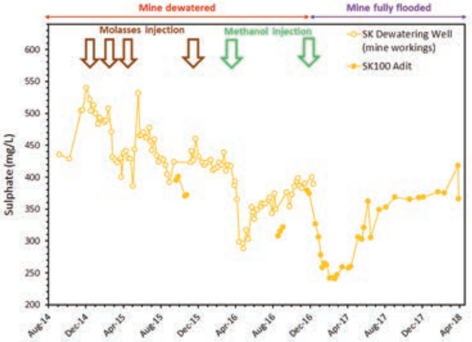

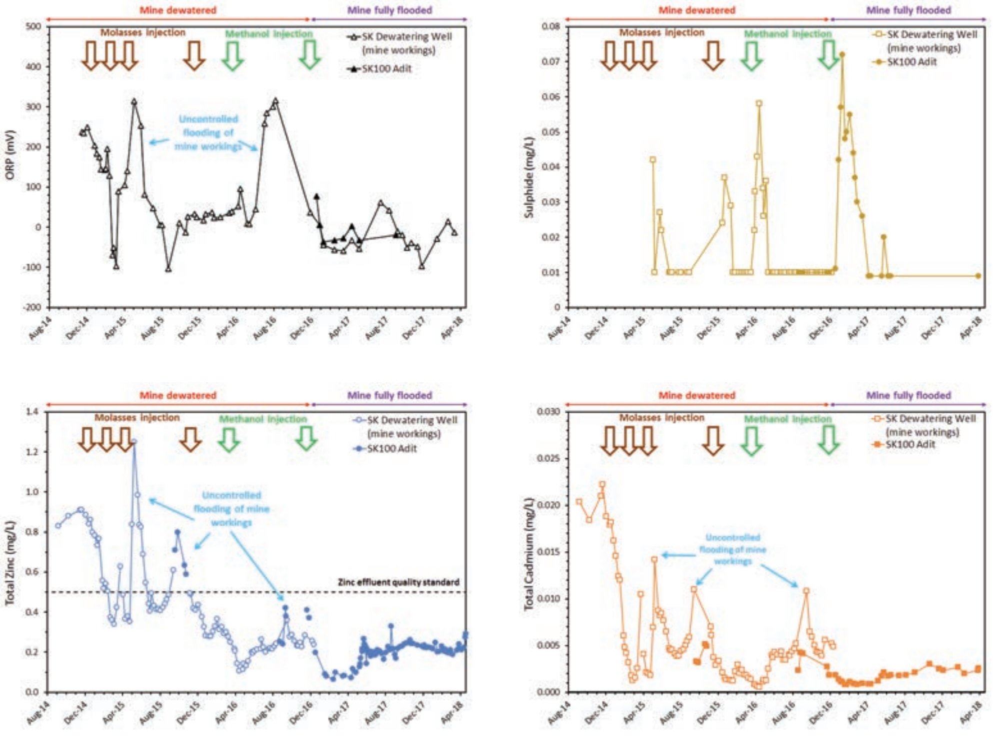

Figure 2 *Change in ORP and concentrations of DOC, sulphate, sulphide, zinc, and cadmium measured in Silver King mine water during in situ treatment pilot test*

Throughout the *in situ* treatment pilot, the Silver King subsurface water has remained circumneutral (pH 5.9 – 7.4, median 6.5). As expected, sharp increases in DOC were observed initially in SKDW samples, and later the SK100 adit discharge, shortly after injection of molasses or methanol into the mine workings via the open pit, confirming that the organic carbon is mixing into the mine workings as planned. The DOC concentration typically declined to baseline levels within five months of the end of carbon injection as it was consumed by resident microorganisms and flushed from the workings. Within a few weeks of the start of organic carbon injection, ORP declined markedly indicating that conditions within the mine workings were successfully becoming more strongly reducing (fig. 2).

Within weeks of the start of organic carbon injection, sulphide was detectable in Silver King mine water (0.02 to 0.07 mg/L), indicative of targeted sulphate-reducing conditions within the mine workings. Indeed, sulphate concentrations exhibited a noticeable dip concomitant with the appearance of detectable sulphide as the sulphate was reduced by native sulphate-reducing bacteria within the mine workings. Sulphate concentrations typically rebounded within a few months as excess sulphide was re-oxidized or removed by reaction with influent metals. Rapid declines in cadmium and zinc concentrations were observed in Silver King mine waters within one month of organic carbon amendment, coincident with the appearance of sulphide, indicating that these metals were likely precipitated as metal sulphides. Concentrations of thallium, another chalcophile element, also displayed similar behaviour (data not shown). Occasional peaks in cadmium, zinc, and ORP levels were observed during high recharge events (spring freshet and following prolonged precipitation events) when uncontrolled reflooding of the mine workings occurred due to failure of the dewatering pump. These peaks may be due to rinsing of soluble oxidation products from the previously unsaturated workings surfaces or a decline in the hydraulic residence time of the workings, resulting in shorter periods over which more oxidizing recharge water may be treated. Interestingly, in each case the cadmium, zinc, and ORP levels declined rapidly following the restoration of dewatering and without further carbon injection, suggesting the system re-established itself following this shorter hydraulic retention time period.

Within two months of the last organic carbon injection in Dec 2016, total cadmium and zinc concentrations declined to 0.0008 and 0.07 mg/L, respectively (representing 96% and 92% removal, respectively), before slowly increasing. Indeed, total zinc concentrations in Silver King mine water have remained below its effluent quality standard (0.5 mg/L) since Dec 2015 (i.e., after approximately one year of pilot in situ treatment). Furthermore, this has included the 16-month period (Jan 2017 to Apr 2018) since the most recent organic carbon injection, indicating the treatment of the Silver King workings may be achieved with organic carbon amendments on an annual, or longer, basis under full-scale in situ treatment conditions.

Cadmium and Zinc speciation

Although ORP is a useful qualitative indicator of changes in redox conditions over time, it is known to be unreliable when determining the actual redox state. This is due to uncertainties in the redox couple to which it is responding and the relative insensitivity of the platinum electrode in the ORP device to some redox couples (e.g. SO^{42-}/HS^{-}). As such, the Nernst equation was used to calculate the in situ Eh for Silver King mine water samples. The ferrihydrite/Fe^{2+} redox couple was used to calculate the Eh for Silver King mine water samples collected before Jan 2015 (i.e., prior to any organic carbon injection). The elevated levels of dissolved iron (median 9 mg/L), sizeable fraction of particulate iron, and absence of sulphidic odour in these samples suggests that iron reduction was the chief redox process that governed the Eh of the mine pool prior to the in situ test. The Eh for samples where sulphide was detected during the in situ treatment pilot was calculated using the SO^{42-}/HS^{-} redox couple, since the presence of detectable sulphide is indicative of sulphate-reduction and use of the redox couple with the lowest potential has been shown to yield more accurate Eh measurements in past work examining groundwater redox geochemistry (Jackson and Patterson, 1982). These sample groups were plotted in Eh-pH space using PHREEPLOT (Kinniburgh and Cooper, 2011) calculated using PHREEQC and based on the Minteq (v4) thermodynamic database, although hydrozincite data were sourced from the LLNL database. It is apparent that prior to carbon amendment both zinc and cadmium were stable as their divalent metal species (fig. 3). Following carbon injection and the development of sulphate-reducing conditions in the Silver King mine waters, precipitation of zinc sulphide and cadmium sulphide was favoured as these samples plotted within the stability fields for these phases (fig. 3).

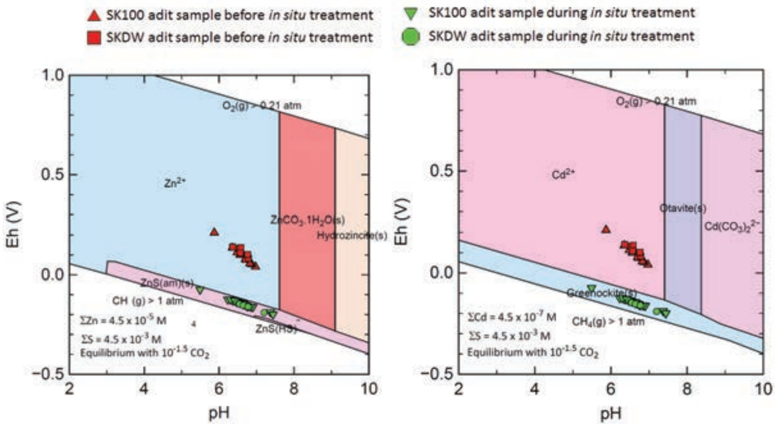

Figure 3 *Eh-pH predominance plots for zinc and cadmium in Silver King mine water*

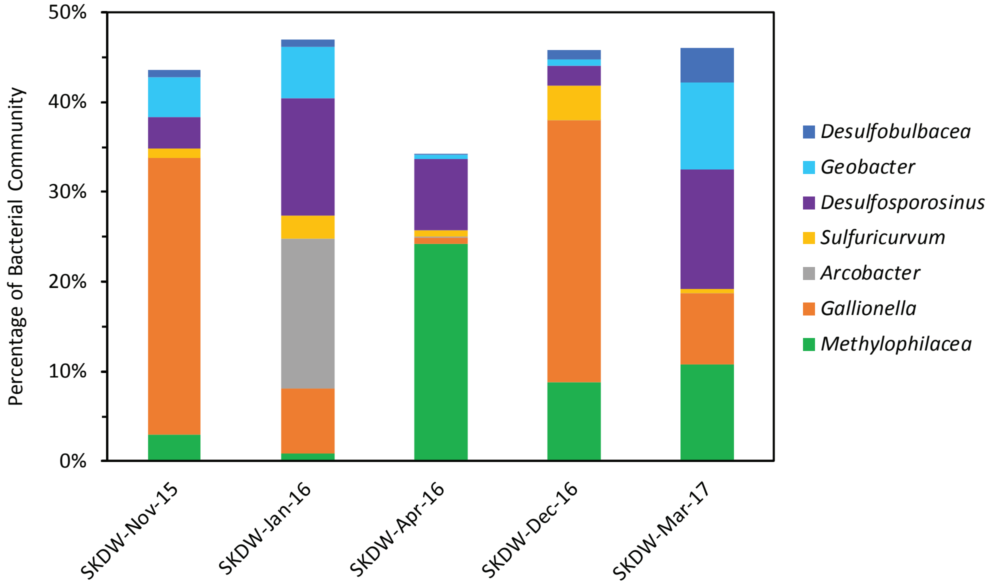

Figure 4 *Change in precentage of methylotrophs and bacteria capable of mediating iron and sulphur redox transformations in Silver King mine water during in situ treatment pilot test*

Microbial Community Structure

Further evidence for the stimulation of sulphate-reducing bacteria by in situ treatment of the Silver King mine workings is provided by microbial community analyses (fig. 4). OTUs with close similarity to microbes capable of sulphate- and sulphur-reduction were present in the SK flooded workings for all five sampling events. Members of the *Desulfosporosinus* genus comprised the bulk of putative sulphate-reducing bacteria detected for most samples, ranging between 2.2% and 13% of the OTUs in each sample (fig. 4). OTUs with a high genetic similarity to *Geobacter* species (0.4% to 9.7% of OTUs) and members of the *Desulfobulbaceae* family (0.05% to 3.9%) also represented more minor members of the sulphur- and sulphate-reducing microbial community. Interestingly, the relative abundance of OTUs with close resemblance to known sulphate-reducing bacteria increased following carbon injection, with peak proportions observed in the Jan 2016 (21% of OTUs) and Mar 2017 (28% of OTUs) sampling events. Additional evidence that the carbon amendment directly influenced the microbial population of the Silver King mine water is provided by the change in relative abundance of OTUs placed within the *Methylophilaceae* family which represents methylotrophic (methanol-using) bacteria. The abundance of OTUs closely related to *Methylophilaceae* family members was low during the period when molasses was used as the carbon source (2.9% and 0.9% of OTUs for the Nov 2015 and Jan 2016 samples, respectively), but increased considerably for the Apr 2016 sampling event (24.3% of OTUs) following the switch to methanol as the carbon source. Although the relative abundance of *Methylophilaceae* family members in the subsequent Dec 2016 and Mar 2017 samples declined (8.8% and 10.9%, respectively), it was still higher than prior to the use of methanol in the in situ pilot test. In addition to sulphate-reducers, a significant proportion of OTUs were linked to iron-reducing, iron-oxidizing, and sulphur oxidizing genera. Indeed, species from both the *Geobacter* and *Desulfosporosinus* genera are also capable of iron-reduction. The detection of OTUs closely related to known sulphur- (*Arcobacter*, *Sulfuricurvum*) and iron-oxidizing genera (*Gallionella*; fig. 4) suggests that a closely coupled redox cycle of iron and sulphur exists within the flooded Silver King mine workings.

Conclusions

- Injection of soluble organic carbon into the Silver King mine workings resulted in microbially-mediated removal of cadmium and zinc via metal sulphide precipitation
- Genomic analyses confirmed an increase of sulphide-producing bacteria following carbon addition, which were dominated by microbes closely related to *Desulfosporosinus* and *Geobacter* genera
- Since the last carbon injection, zinc concentrations in the SK100 adit discharge have been maintained below the effluent quality standard, suggesting annual (or longer) injections may be sufficient for long term treatment mine waters at the UKHM site.

Acknowledgements

The authors are grateful to Indigenous and Northern Affairs Canada, Elsa Reclamation and Development Company Ltd., and Alexco Resource Corp. for their funding and support. Peter Johnson, Grant Ewing, Eric Lancaster, Rob Schneider, Denis Tremblay, Andrew MacPhail, and Mitch Heynen are thanked for their assistance in establishing, operating, and sampling the in situ treatment pilot test at Silver King.

References

Bilgin AA, Harrington JM, Silverstein J (2007) Enhancement of bacterial iron and sulfate respiration for in situ bioremediation of acid mine drainage sites: a case study. Miner Metallurg Process 24(3):139—144

Harrington JM (2002) In situ treatment of metals in mine workings and materials. Tailings and Mine Waste ’02. CRC press, Swets and Zeitflinger, Lisst, The Netherlands, pp 251—261

Harrington JM, Harrington JG, Lancaster E, Gault AG, Woloshyn K (2015) Bioreactor and in situ mine pool treatment options for cold climate mine closure at Keno Hill, YT. Proceedings of the 10th ICARD & IMWA Annual Conference. Santiago, Chile

Jackson RE, Patterson RJ (1982) Interpretation of pH and Eh trends in a fluvial-sand aquifer system. Water Resour Res 18:1255—1268, doi:10.1029/WR018i004p01255

Kinniburgh DG, Cooper DM (2011) PhreePlot. Creating graphical output with PHREEQC. http://www.phreeplot.org/ Accessed 2018-05-08.

Nielsen G, Janin A, Coudert L, Blais JF, Mercier G (2018) Performance of sulfate-reducing passive bioreactors for the removal of Cd and Zn from mine drainage in a cold climate. Mine Water Environ 37(1):42—55, doi:10.1007/s10230-017-0465-1

Saunders JA, Lee MK, Wolf LW, Morton CM, Feng Y, Thomson I, Park S (2005) Geochemical, microbiological, and geophysical assessments of anaerobic immobilization of heavy metals. Bioremed J 9(1):33—48, doi:10.1080/10889860590929583

Saunders JA, Lee M-K, Shamsudduha M, Dhakal P, Uddin A, Chowdury MT, Ahmed KM (2008) Geochemistry and mineralogy of arsenic in (natural) anaerobic groundwaters, Appl Geochem 23(11):3205—3214, doi:10.1016/j.apgeochem.2008.07.002

Pilot Scale Test Of Compact (Short Retention Time) Passive Treatment Process for Acid Mine Drainage Using Agri-Waste in Japan

Takaya Hamai[1], Yuki Sato[1], Kazuhiro Kojima[1], Yusei Masaki[2], Kentaro Hayashi[2],
Mikio Kobayashi[2], Nobuyuki Masuda[2], Masahiro Sowanaka[2], Takeshi Sakata[2]

[1]Metals Technology Center, Japan Oil, Gas and Metals National Corporation, Furudate 9-3, Kosaka-kouzan, Kosaka, Akita, Japan, hamai-takaya@jogmec.go.jp
[2]Metals Environment Management Department, Japan Oil, Gas and Metals National Corporation, Toranomon 2-10-1, Minato-ku, Tokyo, Japan

Abstract

A biological passive mine water treatment system, which is environment-friendly and energy saving, has been developed by JOGMEC (Japan Oil, Gas and Metals National Corporation). In this "JOGMEC process", contaminated mine water is treated in a vertical-flow anaerobic bioreactor that utilizes sulfate reducing bacteria (SRB). It is necessary to introduce compact passive treatment system with a higher flow rate (shorter hydraulic retention time (HRT)).

Keywords: AMD, Passive Treatment, Sulfate Reducing Bacteria

Introduction

Japan Oil, Gas and Metals National Corporation (JOGMEC) has been conducting survey research on passive treatment since 2007 and has focused on treatment methods to remove metals contained in acid mine drainage as sulfide by utilizing of sulfate reducing bacteria (SRB).

Field tests have been conducted with anaerobic reactors filled with "rice bran" in addition to "rice husk" for acid mine drainage since 2014. Continuous removal of metals for more than 300 days has been confirmed with the hydraulic retention time (HRT) of 50 hours under the conditions close to natural environment that the temperature in the winter drops to around -10 degrees. Besides, continuous removal for more than one year has been confirmed with the HRT of 25 hours.

As described above, IT has been confirmed that AMD can be treated for a long period under 12.5 HRT to 50 HRT conditions by "JOGMEC process" which removes metals as sulfide using an anaerobic reactor filled with agricultural waste such as rice husk and rice bran. Then, since November 2016, the pilot scale demonstration test for AMD containing iron, zinc, copper, and cadmium was started.

Methods

1) *Summary of equipment of pilot scale test*

The pilot scale test equipment was installed at abandoned mine site. "Iron oxidation and removal reactor" which oxidizes and precipitates iron ions in AMD utilizing the function of iron oxidizing bacteria and "Anaerobic reactor" which precipitates various metals as sulfide utilizing the function of SRB was installed. The appearance and treatment flow of this test facility are shown in Fig.1.

2) *Structure and Contents of reactor*

Iron oxidation and removal reactor

The iron oxidation reactor is made of PVC and its dimensions are W 1.6 m × D 1.3 m × H 1.0 m. Since the iron oxidation reactor utilizes the function of iron oxidizing bacteria which is aerobic bacteria, it is structured to raise the dissolved oxygen concentration by introducing raw water into the reactor like a shower. The iron oxidation reactor was filled with rice husk as carrier of iron oxidizing bacteria and capturing material of precipitated iron oxihydroxide. Rice husk was filled to a thickness of about 0.5 m, a volume of about 1 m^3.

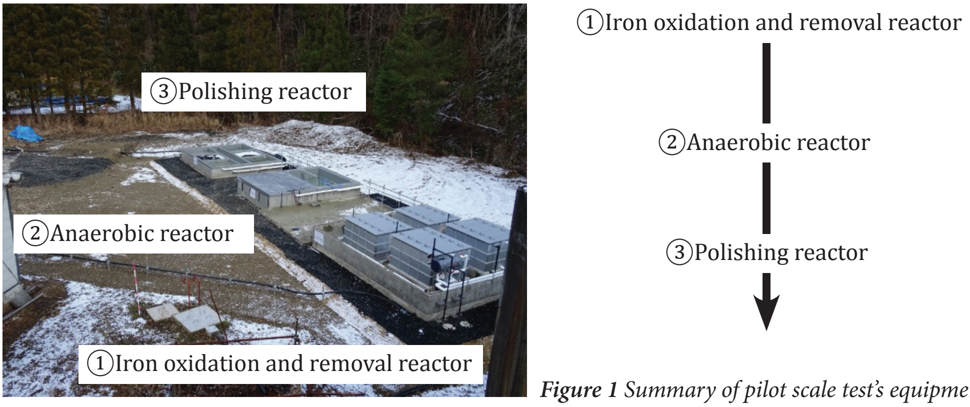

***Figure 1** Summary of pilot scale test's equipment*

Anaerobic reactor
In the anaerobic reactor, sulfate ion is reduced by SRB and metal ions contained in AMD are precipitated mainly as sulfide. The reactor is made of concrete and its dimensions are W 3 m × D 2 m × H 2.5 m. The reactor is buried in the semi-underground, 1.8 m out of 2.5 m in height is installed in the ground.

As the contents, at the bottom of the reactor, limestone (φ 20 mm to 40 mm) was filled to a thickness of about 0.15 m to prevent clogging of the perforated drain pipe, and whole of reactor, rice husk for substrate, limestone for pH buffering and soil for resource of bacteria were mixed and filled to a thickness of 1 m. Each weight is 600 kg of rice husk, 2400 kg of limestone (φ 20 mm to 40 mm), 60 kg of soil. Furthermore, rice bran as organic matter was filled in the upper layer. In order to ensure permeability inside the reactor, rice bran was divided into mesh bags and filled in consideration of maintainability such as additional filling and removing. The anaerobic reactor was set at 4 ports in the depth direction (1st port: 0.25 m from the top of the rice husk layer, 0.5 m at the 2nd port, 0.75 m at the 3rd, 4th port: 1. 0 m) can be sampled.

3) *Condition of Experiments*

Quality of Raw Water
Table 1 shows the quality of the raw water to be treated in this test.

Analysis of items
The raw water to be treated and the water after treatment were periodically sampled and analyzed. Items for testing were temperature, pH, Oxidation-Reduction Potential (ORP), metal concentrations (such as iron, copper, zinc, and cadmium), sulfate ion concentration, sulfide ion concentration (hydrogen sulfide, hydrogen sulfide ion, and other sulfide ion were fixed as sulfide ion in strong alkaline condition, and analyzed with a spectrophotometric method using methylene blue), and chemical oxygen demand (COD).

Water Flow rate
The treated raw water was passed through the iron oxidation and removal reactor at a flow rate of about 5.2 L/min, the HRT is 2.5 hours. About anaerobic reactor, at a flow rate of about 2.6 L/min. and the HRT in the anaerobic reactor is 25 hours.

Results

1) *Performance of iron oxidation and removal reactor*

Fig.2 shows iron concentration of treated water divided into ferrous and ferric iron. For about 5 months from the start of the test, the ferrous concentration of treated water was low but the ferric iron concentration was slightly high and the total iron concentration

Table 1. *Average Quality **of Treated Water (Unit : mg/L)***

	pH	T-Fe	Zn	Cu	Cd	SO_4^{2-}
Drainage	3.5	38	15.4	4.9	0.06	310

was slightly less than 10 mg / L. After April, the ferric iron concentration was decreasing and the total iron concentration gradually decreased, dropping to less than 4 mg / L. Thereafter, although the ferric iron concentration increased in winter, the ferrous iron concentration remained at a low value, the total iron concentration has been remained at only 8 mg / L at a high level, stably lower than 10 mg / L.

2) *Performance of anaerobic reactor*

Fig.3 shows the transition of each depth of the anaerobic reactor and pH of treated water, and Fig.4 shows the transition of ORP. According to Fig. 3, the pH is below 5 at the 1st port of the anaerobic reactor (25 cm deep from the top of the rice husk layer), and it exceeds 6 at the second and subsequent ports. It has thought that the pH has been rising inside the anaerobic reactor by limestone mixed in the rice husk. According to Fig. 4, the ORP in the anaerobic reactor was positive in 1 month from the start of water flow in the first port, also shows an upward trend in the second and subsequent ports, after 2 months the ORP in the third port was a positive value. Fig.5 shows the transition of sulfate ion concentration of raw water and treated water of anaerobic reactor. According to Fig. 5, it is found that the sulfate ion concentration in the treated water decreased by about 100 mg / L or more in the anaerobic reactor immediately at the initial period of the test. As the test progresses, the sulfate ion concentration of the treated water showed an upward trend.

Fig. 6 shows the transition of the total zinc concentration in the treated water of the anaerobic reactor and the zinc ion concentration in filtered with the 0.45 μm syringe filter.

According to Fig. 6, the zinc ion concentration of the treated water in the anaerobic reactor is very low, and zinc ions contained in the treated raw water of about 15 to 18 mg / L are removed inside the anaero-

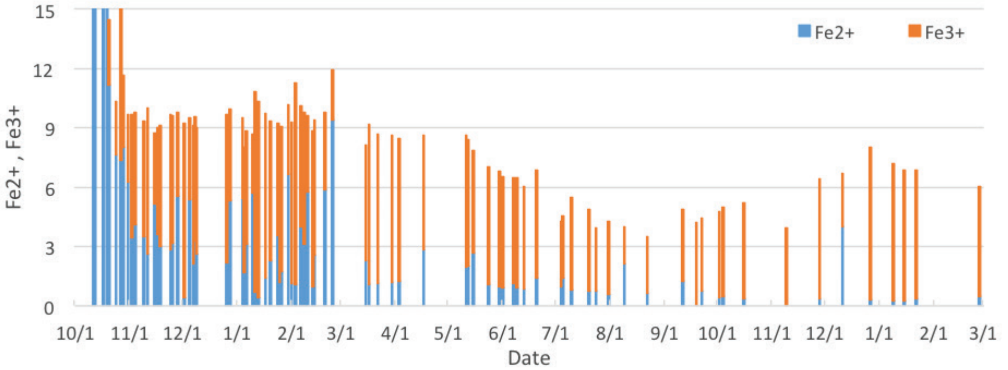

***Figure 2** Changes of iron concentration of treated water*

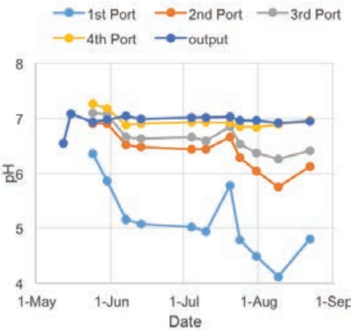

***Fig.3 Changes** of pH*

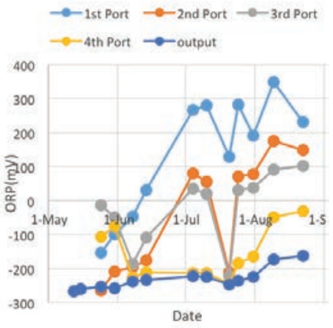

***Fig.4 Changes** of ORP*

bic reactor. However, it can be confirmed that the total zinc concentration in treated water tends to rise gradually. It is presumed that sulfate ion reduction by SRB occurs in the anaerobic reactor, and metal ions contained in raw water have been precipitated mainly as sulfide in the anaerobic reactor. However, since the total zinc concentration in the treated water is high and the zinc ion concentration is low, suspended particles such as sulfide of zinc precipitated have not been captured in the anaerobic reactor and flow out of the system.

Discussion

In the anaerobic reactor, it is strongly suggested that sulfate ion reduction by SRB occurs and metal ions precipitate mainly as sulfide. However, it is also confirmed that a phenomenon in which suspended metal flows out into treated water has occurred. In the anaerobic reactor, reduction of sulfate ion by SRB occurred, metal ions precipitated as sulfide, and it was assumed that the sulfide was trapped by filled rice husk, but as shown in Fig.6, it is conceivable that the suspended particles are not trapped sufficiently.

According to Fig.4, from the beginning of July, ORP of the 1st to 3rd ports of the anaerobic reactor shows positive value, indicating that it is an oxidizing condition. Generally, when SRB is activated, ORP would be indicated about -200 to -400 mV.

In this test, it is considered that SRB is not activated at the first to third ports of the anaerobic reactor, and it is considered that the SRB is activated in the third to fourth ports.

Thus, it is considered that the sulfate ion reduction of SRB is occurring in the limited area of the anaerobic reactor, and there might be a possibility that the area where precipitated sulfide particles are captured is not sufficient.

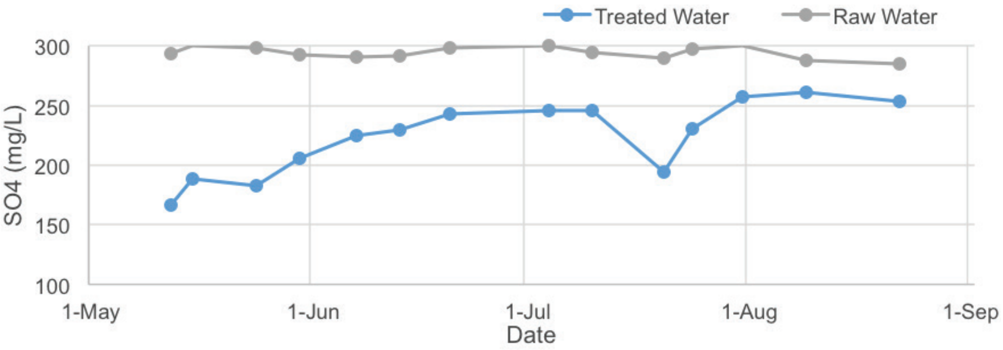

Figure 5 Changes of sulfate ion concentration of raw water and treated water

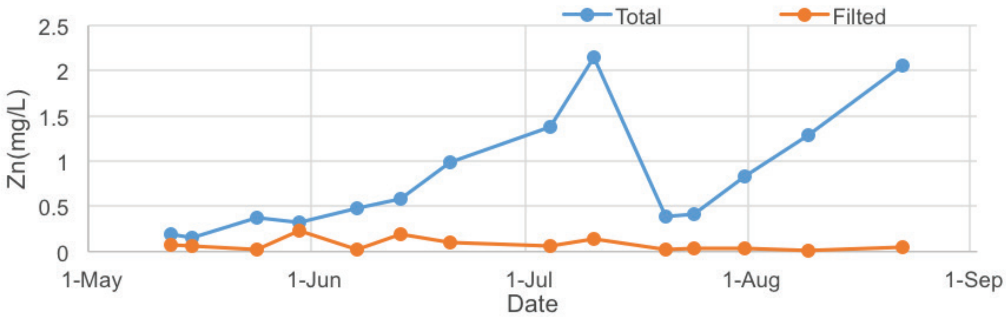

Figure 6 Changes of zinc concentration of raw water and treated water

In order to trap the precipitated sulfide particles in anaerobic reactor, it is estimated that it is important to supply low molecular organic matter with high palatability of SRB at a sufficient concentration so that SRB tends to be activated.

It may be considered to increase the layer thickness of the anaerobic reactor to enlarge the area for capturing precipitated particles. As a result, with regard to the construction of the reaction tank, it is possible to make use of the depth and possibly make the facility area more compact.

References

Furuya et al. (2012) Research on the applicability of anaerobic passive bioreactor for mine water treatment in Japan. IMWA2012 proceedings, Bunbury

Hamai et al. (2013) Research on the applicability of anaerobic passive bioreactor to acid mine drainage treatment in Japan. IMWA2013 proceedings, Colorado

Hamai et al. (2015) The sequential experiments of passive treatment system using bioreactor for acid mine drainage in Japan. ICARD2015 proceedings, Santiago

Hamai et al. (2014) The metal removal performance of anaerobic bioreactor in passive treatment for mine drainage. The Mining and Materials Processing Institute of Japan

Hamai et al. (2014) The field experiments of passive treatment using bioreactor for acid mine drainage. The Mining and Materials Processing Institute of Japan

Hamai et al (2015). The metal removal performance of anaerobic bioreactor in passive treatment for mine drainage. The Mining and Materials Processing Institute of Japan

Hamai et al. (2015) The bench scale field tests of passive treatment for acid mine drainage. The Mining and Materials Processing Institute of Japan

Hamai et al. (2015) The bench scale field tests of passive treatment for acid mine drainage (process compactification). The Mining and Materials Processing Institute of Japan

A critical review on the performance of the gypsum precipitation reactors on hipro® amd plants at ewrp, owrp and mwrp©

Andrew Hammond

Aveng Water, 1 Jurgens Road, Jet Park, Aveng Park, Gauteng, 1459, South Africa, Tel: +27 10 205 1800 Andrew.hammond@avenggroup.com

Abstract

Three Aveng Water designed HiPRO™ plants have been operating for a number of years. A key component of the process is Stage 2 and Stage 3 Precipitation reactors that allow for the additional recovery of water. The paper examines the Stage 2 gypsum reactor performance using statistical methods. The metric used was the outlet calcium sulphate saturations. The deviation of the $CaSO_4$ saturation impacts directly on the availability of the plant. Poor operation will result in RO membrane failure. The variation in the outlet was presented and a regression was done to determine the effect of certain parameters on performance. It was found that temperature variation is a major factor in the outlet saturations but the overall fit was still poor with the data available.

Keywords: ICARD | IMWA | HiPRO™ | Gypsum Reactors | Mine Water Treatment

Introduction

One of the consequences of certain mining activities is the inevitable formation of mine impacted waters. These waters are characterised by high levels of sulphate, calcium, magnesium and often alkalinity, other heavy metals and monovalent ions. The ratio of these contaminants varies from one mining area to another. The resulting effluent is a complex solution and requires treatment prior to being discharged to the environment. One such active treatment process that can be used to remedy the mine impacted waters and produce potable water is Aveng Waters HiPRO™ process. This process combines chemical precipitation with advanced membrane processes. The configuration of the plant allows for large scale treatment of mine impacted waters. Currently four major installations use this technology and were all funded and owned by the senior coal miners in the Mpumalanga province. The four plants are the eMalahleni Water Reclamation Plant (EWRP) – (Phase I and Phase II), The Optimum Water Reclamation Plant (OWRP) and the Middleburg Water Reclamation Plant (MWRP).

HiPRO™ Process

Figure 1 gives a summarised view of the HiPROTM process. Simply, the process comprises of a three stage process where water is recovered sequentially by stage-wise precipitation and thereafter desalinating with Reverse Osmosis (RO) Membranes to produce a product that is of exceptional quality. A more detailed explanation of the process can be found Hutton et al (2009)

As can be surmised, a key aspect of the process is the performance of the precipitation steps, which reduce scaling potential and allow for further recovery of water through RO membranes. Poor control of these reactors will result in rapid and irreversible scaling of the RO membranes which directly compromises production quantity and quality. Due to the nature of water being processed, the precipitation reactors on Stage 2 and Stage 3 are gypsum reactors. Owing to the importance of these units in the process the performance of these reactors will be the focus of this paper. Since the Stage 3 sections of the plant are duplication of the Stage 2, only Stage 2 information will be shown

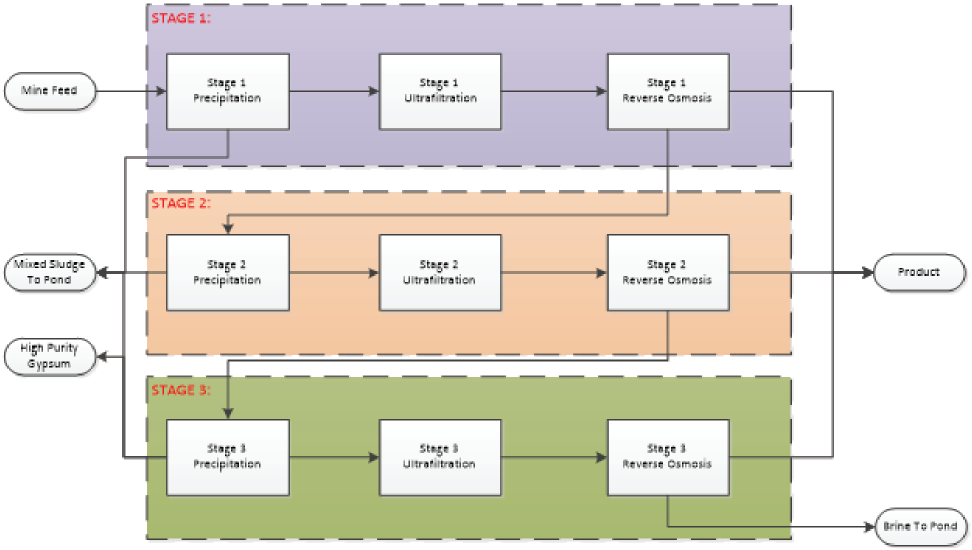

Figure 1 Basic Process Flow of HiPRO™

Feed Water Quality

Table 1 summarises the design capacity of each plant, the year of commissioning, the plant owner, the plant designer and the typical feed water quality (major components only) currently being processed by the plant. It can be seen that the feed water quality differs substantially between plants. It must be pointed out that currently only one of the four plants is currently processing highly acidic mine impacted water – EWRP Phase II but all except OWRP was designed to cater for a degree of acidic mine feeds.

Stage 2 Reactor Performance at EWRP (Phase I and Phase II), MWRP and OWRP

The Stage 2 reactor performance of EWRP Phase I, MWRP and OWRP was evaluated over periods of 2 years. Due to the limited amount of data on the Phase II EWRP operation, only a small segment of information is available but this is also presented. The metric of measure of reactor performance is based on the effluent Calcium Sulphate Saturation and the practical RO cut off that can be set to allow for sustainable operation of the RO mem-

Table 1. Summary of Major Aspects of the plant installations

	EWRP Phase I	OWRP	MWRP	EWRP Phase II
Plant Owner	Anglo American Thermal Coal	Optimum Colliery	South 32	Anglo American Thermal Coal
Plant Designer	Aveng Water	Aveng Water	Aveng Water	Aveng Water
Year Commissioned	2008	2011	2015	2017/2018
Design Capacity	25 Ml/day	15 Ml/day	25 Ml/day	25 Ml/day
Feed Water -Typical				
Calcium (mg/L)	520	414	460	440
Sulphate (mg/L)	2500	3000	3400	4500
Magnesium (mg/L)	180	450	650	210
Acidity (mg/L as CC)	80	0	0	2000
Alkalinity (mg/L as CC)	10	180	180	0
pH	6	8.0	7.5	2.3
TDS (mg/L)	3500	5021.6	5000	6000

branes (no membrane scaling). Antiscalant is dosed upstream of the RO membranes and the efficacy of the product is paramount in protecting the RO membranes from scaling. The saturations reported here are that which is calculated from the antiscalant dosing software. The water quality on each Stage of the plant is measured four times daily for all major constituents namely; Calcium, Sulphate, Magnesium, pH and monovalent species. The resulting vector determines what the calcium sulphate saturation is and based on the specified practical RO cut-off, the RO can or cannot be operated. Consequence of not adhering to these cut-offs is rapid membrane failure of the membrane modules. Figure 2 shows the Stage 2 $CaSO_4$ saturations for the four plants over the periods specified in Table 2.

There are periods where the calcium sulphate exceeds the practical RO cut-off. This is especially true of the EWRP operation in the early part of the period. Although periods of instability can be seen on all trends. This can be shown explicitly by looking at the summary statistics of each plant – Table 2. Owing to the nuances of Phase II, the practical cut off differs from the other plants.

Table 2 shows clearly that the most stable reactor of the four plants is MWRP while EWRP Phase I is the most unstable – Phase II is excluded as the data set is limited due to it being early in its operation phase. The performance of EWRP was of major concern to the designers and although the plant was able to operate through these transients, it was clear that better control was needed to approach that of MWRP and OWRP. Through targeted interventions, it was possible to narrow the normal distribution and variation of the calcium saturations that have been observed. Figure 3 shows the histogram and normal distribution for MWRP and EWRP for the years 2017 and YTD 2018. It can be seen from the histogram that the normal distribution assumption of the saturations is not completely valid as there is both excess kurtosis and a negative skewness. Both indicate a high degree of upside risk to membrane operation or plant availability (if the shut off is exceeded the RO unit is taken offline) at these high saturations. The vertical line indicates the same practical shut off of the membranes as Figure 2. Similar trends are observed for the other installations. Table 2 shows the summary statistics for each installation.

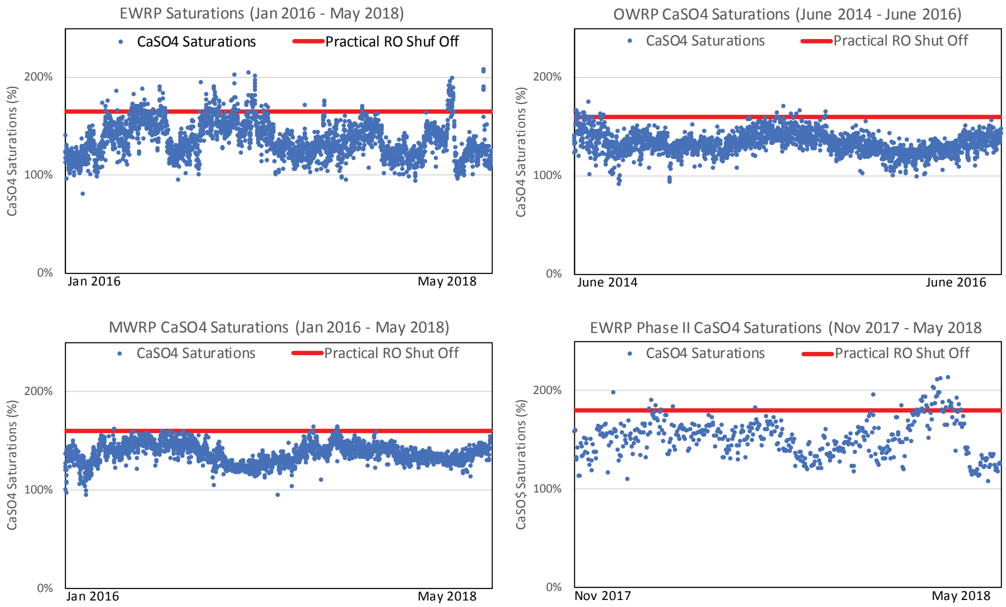

Figure 2 Measured performance of the Stage 2 Calcium Sulphate Saturations at the four installations

Table 2. Summary Statistics of reactor performance of the four installations.

	EWRP Phase I	OWRP	MWRP	EWRP Phase II
Time Period	Jan16-May18	June14-June16	Jan 16–May18	Nov17-May18
Average	135.45%	131.58%	136.53%	151.96%
Standard Deviation	18.4%	10.35%	9.6%	19%
No. Data Points	2918	2068	4098	482
Excess Kurtosis	0.0853	0.283	0.0607	-0.013
Skewness	0.480	-0.00185	-0.178	0.309

Any interesting nuance on Figure 3 is the changing of sign of the skewness on the MWRP sample in 2017 and followed through to 2018. This indicates more data points on the left side of the average, implying less upwards risk at MWRP through 2017 and 2018 than there was in 2016. The second implication of this is that there is a potential to shift the normal distribution left if the greater downward clustering can be intensified. The YTD 2018 information suggests that this shift has occurred but this data set is limited. Shifting the normal distribution in this manner will allow for an adjustment of the practical RO shut off and thereby a direct increase in the capacity of the plant., it is therefore critical to understand what shifts the normal distribution so that that parameter may be controlled. Ideally, one would want a leptokurtotic distribution that is characterised by a peaked mean, narrow shoulders and thin tails. A final comment on the EWRP standard deviation for 2018. Although the standard deviation has increased in 2018, this was in fact due to a single prolonged operational incident that stalled the process. The cluster of data points to the right of the shut-off indicates. A detailed root cause analysis was done

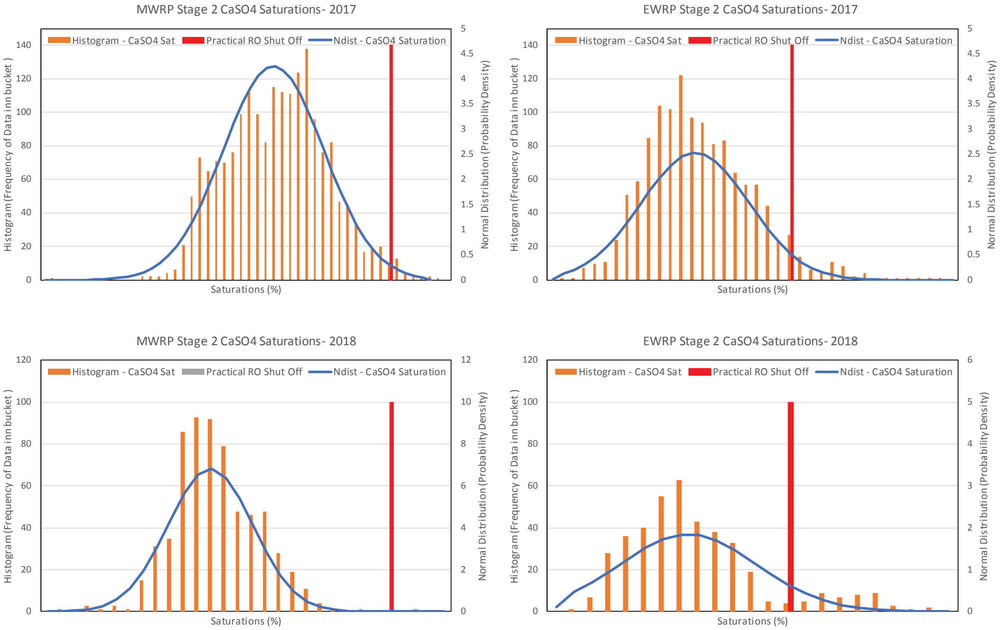

Figure 3 Histogram and Normal Distribution for EWRP Phase I and MWRP 2017-May 2018

and it was found that this related to a change on the plant. The implication of engineering change management is incredibly important in operating a plant of this nature. Baring this incident, the normal distributions have in fact narrowed through 2018.

Stage 2 Reactor Performance – Quantitative Effects

As discussed above, the factors that affect the performance of the gypsum reactors on each of the plants need to be clearly understood. Since this is a precipitation reactor, it obvious that endogenous factors such as feed water quality to the reactor and seeding material are important for controlling the outlet conditions. However, there are other exogenous factors such as temperature which may also be significant. Two separate regressions were run on the information. The first using the controllable variables and the second compensating for temperature. The entire data sample was used for the regression on each plant. The phase II EWRP has been excluded owing to the limited data sample available.

Control Variable Impact

There are a number of variables controlled within the plant but only three are going to be used here, namely the percentage solids of the reactor/clarifier complex and the feed water quality to the reactor. The latter will be represented as the calcium sulphate saturations of the previous stage. It is expected that the solids control will have a substantial effect on the performance. The solids measurement can be regressed against the measured saturations according to:

$$CaSO_4\_Sat = A + B*Reactor\_Solids\% + C*Clarifer\_Solids\% + D*Stage\_1\_CaSO_4\_Sat\%$$

The measure of fit from these variables can be seen by the adjusted R2 value. All three plants show a similar fit with respect to the explanatory variables used. What is surprising is how poor the fit is. An interesting nuance is that the EWRP phase I reactor solids measurement is not statistically significant but this does not mean it is practically insignificant.

Temperature Effect

A regression was performed on the entire sample for each plant to compensate for the impact of water temperature on the $CaSO_4$ saturation. Table 4 Shows the results of the regression. EWRP Phase I and II was not shown owing to the limited amount of seasonal data available. The expectation would be that one would see a reduction in $CaSO_4$ Saturation as the solubility of $CaSO_4$ decreases with decreasing temperature. However, theoretically this will be a function of how dominant the temperature component is in the rate of reaction equation and the sign. The determination of the rate equations for this system is out of the scope of this paper. The following Equation formed the basis of the regression.

$$CaSO_4\_Sat = A + B*Reactor\_Solids\% + C*Clarifier\_Solids\% + D*Stage\_1\_CaSO_4\_Sat\% + E*Temp$$

It can be seen from Table 5 that the calculated R2 (the measure of fit) is similar across both plants. In addition, coefficient A,B and E are highly significant, are of the same order and have the same sign. The dominance

Table 3. *Regression output control variables of the four installations.*

	EWRP Phase I		OWRP		MWRP	
Coefficients	Coeff	P-Value	Coeff	P-Value	Coeff	P-Value
A	1.567	5.7E-52	1.233	5.5E-97	0.964	9.7E-86
B	-0.256	0.639	-1.356	1.2E-06	-0.996	4.4E-24
C	-2.89	7.0E-16	-1.255	2.8E-17	0.760	3.9E-08
D	0.288	5.8E-09	0.459	2.0E-40	0.301	1.1E-19
Adjusted R^2	0.207		0.189		0.127	

Table 4. Regression output addition of temperature of the four installations.

	OWRP		MWRP	
Coefficients	Coeff	P-Value	Coeff	P-Value
A	1.495	7.7E-215	1.662	1.7E-292
B	-1.015	3.9E-07	-0.090	0.208
C	0.091	0.414	-0.159	0.111
D	0.282	1.6E-29	0.129	4.3E-08
E	-0.019	3.9E-203	-0.020	7.2E-257
Adjusted R2	0.584		0.5683	

of the temperature in the fit is clear with it increasing the fit substantially. The implication is that a large proportion of the reactor outlet CaSO4 saturations are statistically not dependent on the controllable variables presented. The second implication is that the rate equation is negatively affected by temperature i.e. the reaction rates slows with decreasing temperature and the rate equation dominates the equilibrium solubility in this system or conversely, the residence time within the system is not sufficient to allow the system to get to complete equilibrium. The lower the temperature the further away from equilibrium. However, it must be noted that it would be impractical to build a reactor system that has unreasonably long residence times as it will cause a substantial ballooning of capital costs. The residence time selection by the designers was a compromise to get as close to equilibrium as possible while minimising reactor size.

In addition, the coefficients "B" and "C" are not statistically significant for MWRP. However, this does not prove the practical significance of the solids control on the performance of the reactors. In fact operational experience has shown that should the solids percentage not be operated in the correct range, there is a substantial and immediate shift in the saturations. This causes particular problems during initial commissioning of the plant. However, since these are operational plants and strict control of the solids is required, the standard deviation of solids control may be too narrow to show the response to incorrect solids positioning. To illicit this point, the standard deviation for the three systems stands at 1.32%, 0.97% and 2.2% respectively.

Conclusions

The performance information from the four operational HiPRO™ plants has been shown and analysed from a statistical point of view. The findings show that the EWRP Installations have a substantial greater deviation in saturations than that of OWRP and MWRP.

The impact of feed water quality and sol-

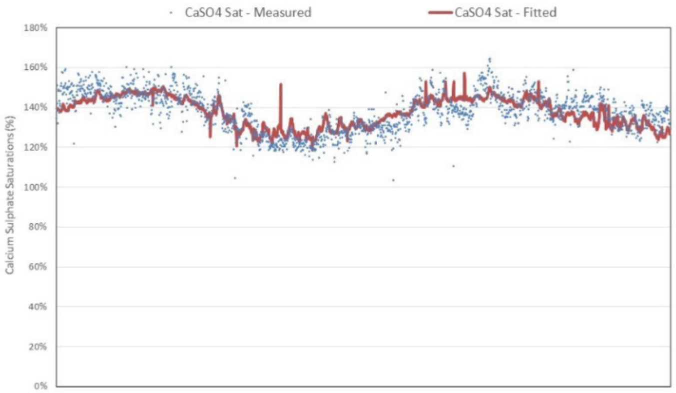

Figure 4: *The Fit of CaSO4 Saturations compensating for temperature for MWRP*

ids control statistically only counts for ≈20% of the deviation in the measured calcium sulphate saturations. This is a smaller contribution than what one may expect for a precipitation reaction. This is in contrast to the substantial effect that the feed water temperature has on the regression, where the temperature increases the fit to ≈58% on both cases investigated. The implication of such a change is that the rate of reaction equation slows with decreasing temperature and the residence times chosen for the design of the plant is not sufficient to get to equilibrium. However, the residence time selection is clearly sufficient as al four plants have operated sustainably over a long period.

The solids percentage was not statistically significant for the combined regressions. However, it does not practically make sense for this to be the case. This may highlight a limitation in only using statistical analysis in evaluating the factors that effect the reactors or highlight that the current measure of solids control is not sensitive enough to show the expected effect.

Further investigations are required following this paper which may include other explanatory variables within the process system as well as a determination of the cointegration between these explanatory variables to be able to develop a theoretical model that is better able to predict the performance of the calcium sulphate reactors.

References

Hutton B, Kahan I, Naidu T , Gunther P, (2009) Operating and Maintenance experience at the eMalahleni Water Reclamation Plant. IMWA 2009.

The Effect of Temperature on the Kinetics of Sulphate Reduction and Sulphide Oxidation in an Integrated Semi-Passive Bioprocess for Remediating Acid Rock Drainage

T.S. Marais[1], R.J. Huddy[1], R.P. van Hille[1,2], S.T.L. Harrison[1]

[1]*Centre for Bioprocess Engineering Research, Department of Chemical Engineering,*
University of Cape Town, Private Bag X1, Rondebosch, 7701, South Africa
[2]*The Moss Group, 13 Bell Crescent, Westlake Business Park, Tokai, 7945, South Africa*

Abstract

A hybrid linear flow channel reactor (LFCR), capable of simultaneous sulphate reduction and partial sulphide oxidation leading to elemental sulphur recovery, was developed and optimised for the semi-passive treatment of acid rock drainage. Under field conditions, seasonal temperatures vary substantially, impacting the sulphate reduction and sulphide oxidation kinetics and therefore the overall performance. Decrease in temperature across the range 10 to 30°C resulted in decreased volumetric sulphate reduction rates, sulphate conversion and sulphur biofilm recovered. Acetate proved an efficient, alternative carbon source to lactate. This work will contribute toward development and implementation of the integrated process for ARD treatment.

Keywords: semi-passive bioprocess, biological sulphate reduction, partial sulphide oxidation

Introduction

The generation and discharge of acid rock drainage (ARD) as a result of mining activities in South Africa (SA) has significant implications on the receiving ecosystems (McCarthy, 2011). ARD is generally characterised as acidic water containing high concentrations of sulphate and heavy metals. The long-term environmental and socio-economic effects associated with ARD discharge in SA have been further exacerbated by the prolonged drought. This has resulted in the need for the development of new and efficient ARD treatment technologies.

In SA, the primary focus on remediation of ARD-contaminated water has been on high volume discharges, using established active technologies. Mostly overlooked, the continuous ARD discharge from diffuse sources (waste rock dumps and discard heaps), associated with coal mining, has substantial impact on the environment, due to the large number of sites and their geographic distribution over rural areas. Under these circumstances traditional passive treatments (wetlands) may be used; these require less maintenance and have lower operating costs. However, typical passive systems are governed by slow, unpredictable kinetics and require extended hydraulic residence times (Skousen *et al.*, 2017), necessitating large land areas. Semi-passive ARD treatment systems present an attractive alternative for addressing these low-flow sources, with lower capital and operational costs than active systems and better control and greater predictability than conventional passive systems. This has led to the development of an integrated semi-passive process, based on a hybrid linear flow channel reactor (LFCR) which enables simultaneous sulphate reduction and partial oxidation of sulphide to elemental sulphur (van Hille *et al.* 2016 and Marais *et al.*, 2017). The operation of the integrated process relies on the formation of niche environments within the LFCR, partitioning a distinct aerobic zone at the air liquid interface and an anaerobic zone within the bulk volume of the reactor. The sulphate reducing bacteria (SRB) in the bulk volume reduce sulphate, in the presence of a suitable electron donor, to sulphide. The sulphide is partially re-oxidised by sulphur oxidising bacteria (SOB) under oxygen limiting conditions at the air-liquid interface, forming a floating sulphur biofilm.

Previous studies by van Hille *et al.* (2016) and Marais *et al.* (2017) have reported on the initial proof of concept, development and characterisation of the integrated process under different operating parameters, such as the effect of HRT, electron donor and reactor size. The findings from the initial development have resulted in the commissioning of the process at pilot scale. This has driven the need for further investigation to address key challenges that are expected at pilot scale. These include the upscaling of the process from lab to demonstration scale (aspect ratio and operating reactor volume), the use of a cost effective electron donor, and the effect of seasonal temperature fluctuation on the performance of the process. The potential use of acetate as an alternative carbon source to lactate in the integrated process as well as the effect of reactor geometry has been tested previously as a function of hydraulic residence time (Marais *et al.*, 2017). Further development of the process requires investigation into the effects of temperature on these parameters.

The effect of temperature fluctuations on system performance is likely to be a key challenge during the larger scale implementation of the integrated process. The effect of temperature on sulphate reduction and sulphide oxidation has been described previously for the separate systems under different reactor configurations, including continuously stirred-tank reactor (CSTR) (Moosa *et al.*, 2005; Buisman et al., 2010)), fluidised bed reactor (FBR) (Sahinkaya *et al.*, 2007) anaerobic side-stream reactor (Ferrentino et al., 2017), and expanded granular sludge bed reactor (EGSB) (Sposob *et al.*, 2017). However, the effects of temperature on the integrated process has not yet been reported. Microbial activity in response to temperature is characterised by upper and lower limits of temperature for growth (Ferrentino et al., 2017). Most SRB and SOB have been characterised as mesophilic bacteria where their active temperature range is between 10 and 50°C with an optimum temperature at 30°C (Greben *et al.* 2002 and Tang *et al.*, 2009).

In this study the primary focus was to simulate a range of temperatures that a typical passive wastewater process would be exposed to, particularly in a SA environment. The research evaluated the effect of temperature on the performance of the integrated process. Additionally, key objectives that ran in parallel were to assess the effect of reactor geometry on system performance as well as the potential of acetate as an alternative carbon source to lactate.

Material and Methods

Microbial cultures and reactor operation

The sulphate reducing mixed microbial community has been maintained at the University of Cape Town (UCT) on modified Postgate B medium (van Hille *et al.*, 2013; Marais *et al.*, 2017). The sulphide oxidising bacteria (SOB) culture was obtained from van Hille, UCT (van Hille et al., 2013). The reactors were operated continuously at a defined hydraulic residence time (HRT) with a feed sulphate concentration of 1000 mg/L and supplemented with either lactate or acetate to maintain a chemical oxygen demand (COD) to sulphate ratio of 0.7.

Linear Flow Channel Reactor (LFCR)

Three lab-scale Perspex LFCRs (2 and 8L) were operated throughout the study. The 8L reactor variation simulated the relative dimensions of the pilot scale reactors. The reactor is distinctly different, compared to the 2L LFCR design, in aspect ratio. The 2L LFCR is fully detailed by van Hille et al. (2016). The standard hybrid LFCR configuration (Fig. 1) includes carbon microfibers as support matrices for enhanced biomass retention, a heat exchanger (4 mm ID) for temperature control, sampling ports along the front of the reactor and a mesh screen to harvest the floating S biofilm.

Analytical methods

Dissolved sulphide was quantified using the colorimetric N,N-dimethyl-p-phenylenediamine method (APHA 2005). Residual sulphate concentrations were measured by the barium sulphate method (APHA 2005). Volatile fatty acid (VFA) analysis was conducted to quantify the concentration of lactic, acetic and propionic acids in the feed and reactor samples. The concentration of each VFA was determined using HPLC on a Waters Breeze 2 HPLC system with a Bio-Rad Aminex HPX-87H column and a UV (210 nm wavelength)

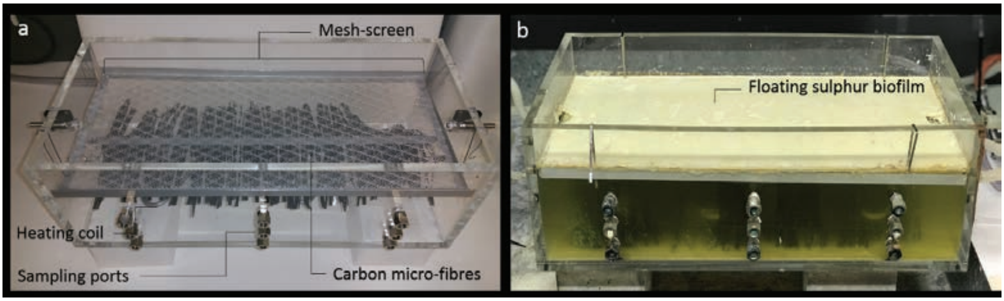

Figure 1: Images illustrating the 8L LFCR a) design prior to inoculation fitted with strips of carbon micro-fibers, heat-exchange coil, harvesting mesh screen and sampling ports b) the inoculated LFCR with a well-developed sulphur biofilm at the surface.

detector (van Hille et al., 2013). Redox potential and pH were measured on a Metrohm pH lab 827 redox meter relative to a Ag/AgCl reference electrode and a Cyberscan 2500 micro pH meter, respectively.

Floating sulphur biofilm collapse and harvesting

The floating sulphur biofilm (FSB) is not attached to a solid surface; instead it develops at the air-liquid interface (surface) of the bulk fluid relying on surface tension for support. The biofilm "scaffold" consists of extracellular polymeric substances (EPS). This imparts structural integrity and retains the biomass and elemental sulphur (Mooruth, 2013). The FSB was collapsed by physically disrupting the biofilm and collecting settled fragments onto the submerged mesh-screen (termed collapse). The sulphur product was recovered by removing the mesh-screen and collecting accumulated biofilm (termed harvesting). The biofilm was dried at 80°C and weighed.

Effect of temperature on the integrated process

This study evaluated the effects of temperature on the integrated system across temperatures of 10, 15, 20, 25 and 30°C. The temperature was controlled by passing either heated or cooled liquid through the submerged heat exchanger. The study began by gradually adapting the reactor to a 2 d HRT, previously shown to be optimum (Marais *et al.*, 2017) at 30°C, after which the temperature was reduced stepwise to 10°C. The system was run for a total of 12 HRTs at each temperature, with a biofilm collapse after 6 HRTs and a biofilm harvest at the end of each run. The sulphur content of the harvested biofilm was determined by elemental analysis. It was hypothesised that a decrease in operational temperature will result in a decrease in overall system performance.

Results and discussion

Results from the study, shown in Fig. 2, reveal that the decrease in operating temperature across both 2L and 8L LFCR configurations resulted in a decrease in volumetric sulphate reduction rate (VSRR) (2L: 13.48 - 10.88 mg L-1 h-1; 8L: 12.46 - 7.86 mg L-1 h-1) and sulphate conversion efficiency (2L: 66.73 to 53.86 %; 8L: 61.68 to 38.91 %) on decreasing temperature over the range 30 to 10°C. As expected, the highest VSRR and sulphate conversion output was achieved at 30°C. Studies by Greben *et al.* (2002) and Ferrentino *et al.* (2017) reported that biological sulphate reduction was relatively stable under temperature perturbations between 20 – 15°C which was found to only account for 3 and 13% decrease in specific sulphate reduction rate, respectively. Similar conclusions can be drawn from the current study where a 5°C reduction in operational temperature from 25 to 20°C resulted in a 7 and 15% decrease in VSRR in the 2L and 8L LFCR respectively. Based on these findings the 2L LFCR outperformed the 8L LFCR, achieving higher VSRR and sulphate conversion throughout the study. Additionally, the 2L LFCR was less sensitive to temperature perturbation compared to the 8L LFCR, which may be a result of higher relative biomass retention in the 2L LFCR, a result of longer system operation.

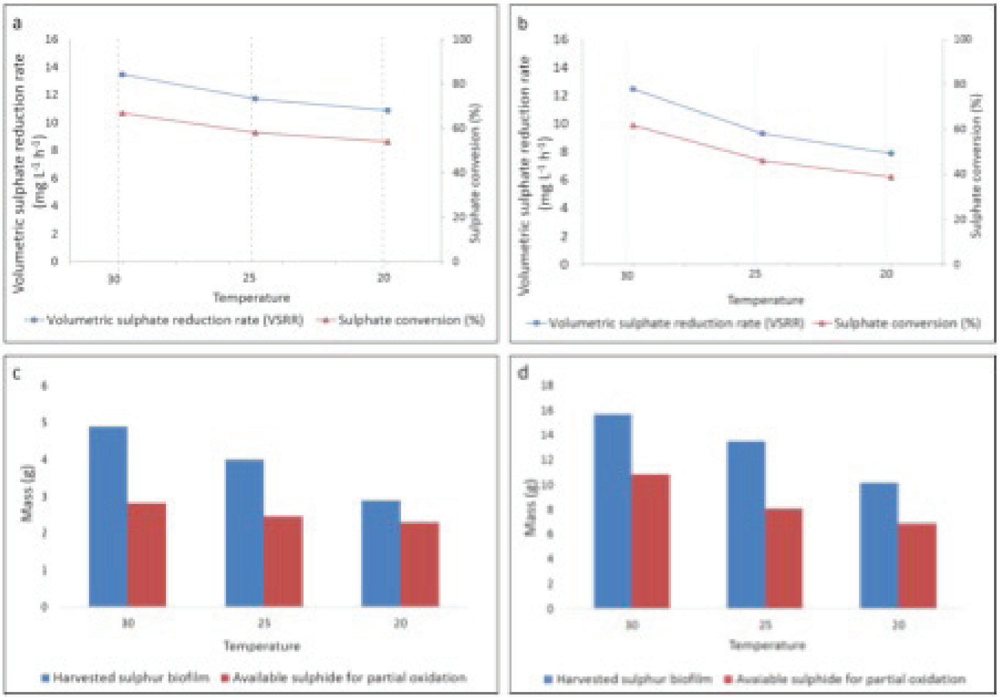

Figure 2: *Effect of residence time on system performance showing volumetric sulphate reduction rate and sulphate conversion efficiency as a function of temperature a) 2L lactate fed LFCR, b) 8L lactate fed LFCR, and partial sulphide oxidation via floating sulphur biofilm showing the mass of biofilm recovered and the total sulphur (grams) in the form of dissolved sulphide available for partial oxidation c) 2L lactate fed LFCR d) 8L lactate fed LFCR.*

Due to the nature of temperature regulation through a submerged heat exchanger, a slight variation in temperature across the reactor was observed. The air-liquid interface, where sulphide oxidation occurs, was exposed to the controlled temperature from below and ambient temperature from above. Thus, the effect of temperature may have had less impact on the performance of the sulphide oxidation component compared to the sulphate reduction efficiency.

The partial oxidation of sulphide to elemental sulphur occurs under oxygen limiting conditions. This can be achieved through limiting the supply of oxidising agent (oxygen or nitrate) or high concentrations of sulphide in the medium. Most active sulphide removal processes promote partial sulphide oxidation by creating oxygen limiting conditions that require fine process control (DO levels). However, the integrated process relies on the sulphide generated through sulphate reduction in the bulk volume of the reactor and the oxygen diffusion barrier created by the biofilm to maintain oxygen limiting conditions within the biofilm. Results from the current study (Fig. 2c and d) showed a decrease in sulphur biofilm recovery (2L: 4.9 – 2.9 g; 8L: 15.7 – 10.2 g) and available sulphide-S for partial oxidation (2L: 2.84 – 2.29 g; 8L: 10.85 – 6.85 g) as temperature decreased from 30 to 20°C. This was consistent across both 2L and 8L lactate-fed LFCR configurations. Studies by Sposob et al. (2017) and Xu et al. (2016) investigated the effect of temperature on the removal of sulphide for elemental sulphur production between 10-25°C. The studies showed that a decrease in temperature caused a decrease in elemental sulphur production. Similar findings in relation to the reduction in recovered biofilm mass strongly suggests that the partial sulphide oxidation in the floating sulphur biofilm was similarly affected by decreasing temperature. The decrease in available sulphide-S was directly proportional to the sulphate reduction activity, as temperature decreased the availability of the substrate (sulphide) for partial oxidation. Previous studies have shown that the floating sulphur biofilm is predominantly comprised of elemental sulphur (Mooruth, 2013). This suggests that partial oxidation through the floating sulphur biofilm was efficient but was most likely limited by the availability of sulphide, given that the temperature change at the surface may not have been as significant as that within the bulk volume of the reactor.

A parallel study assessed the effect of temperature on the use of acetate as an alternative electron donor to lactate. Results (Tab. 1) revealed the similar performance in sulphate reduction obtained through the use of either electron donor at 30 and 25°C. The decrease in temperature (30 -20°C) resulted in the decrease in VSRR (lactate-fed: 13.48 to 10.88 mg L-1 h-1; acetate-fed: 12.36 to 7.18 mg L-1 h-1) and sulphate conversion (lactate-fed: 67 to 54 %; acetate-fed: 61 to 36 %). The lactate-fed LFCR proved more efficient at 20°C and was capable of maintaining sulphate conversion >50 %. The sulphate reduction conversion in the acetate-fed LFCR was significantly reduced to 36 % at 20°C. A previous study by Marais et al. (2017) assessed the effect of hydraulic residence time on the integrated process and revealed that after exposure to perturbations (HRT and biofilm collapse), a lactate-fed system recovered rapidly with negligible effect on VSRR while an acetate-fed LFCR was more sensitive and required longer periods to recover. This is most likely attributed to the lower growth rate of acetate oxidisers (doubling time 10-16 h) compared to that of lactate oxidisers (doubling time 3-10 h) (Celis et al., 2013).

At 30°C, all the lactate was utilised via partial oxidation by SRB, resulting in the accumulation of acetate. This contributed to relatively high residual COD measured in the effluent (results not shown). In the 2L lactate-fed LFCR, the decrease in temperature to 20°C resulted in an increase in residual lactate, an indication of incomplete carbon source utilisation and reduced microbial activity. Similarly, an increase in residual acetate was observed within the 2L acetate-fed LFCR. This revealed that temperature had a direct effect on the consumption of both carbon sources.

The amount of biofilm recovered as temperature decreased was inconsistent across the lactate-fed and acetate-fed LFCR. During the operation of the acetate-fed LFCR at 25°C, premature collapse and incomplete formation of the sulphur biofilm was observed, a result of tearing and spontaneous collapse. This resulted the regeneration of the biofilm outside of the studies’ parameters of inducing collapse after every 6 HRTs. Hence, a greater mass of biofilm was recovered (20 and 25°C) from the acetate-fed LFCR than the lactate-fed LFCR where biofilm collapse was controlled. At 20°C biofilm formation was affected and could not maintain its structure, often disintegrating or prematurely collapsing. This could reflect the effect of temperature on the microbial community responsible for EPS production that form part of the floating sulphur biofilm. It may also indicate that the reduced SRB activity did not generate sufficient sulphide to sustain the development of a structurally sound biofilm.

Table 1. *Effect of carbon source on VSRR and sulphate conversion efficiency.*

Carbon source	Temperature (°C)	Sulphate loading rate (mg L^{-1} h^{-1})	Volumetric sulphate reduction rate (mg L^{-1} h^{-1})	Sulphate conversion (%)	Sulphur biofilm recovered (g)
Lactate	30	20.2	13.48	67	4.9
	25	20.2	11.70	58	4.0
	20	20.2	10.88	54	2.9
Acetate	30	20.2	12.36	61	4.6
	25	20.2	11.50	57	5.0
	20	20.2	7.18	36	3.6

Conclusions

This study confirmed that temperature plays a critical role in the overall activity of the sulphate reducing and sulphide oxidising components in the integrated process. Based on these findings, the system may require operation at a longer residence time in order to compensate for the loss in performance at lower temperatures. The reduction in performance at low temperature was more pronounced in the acetate-fed system. At 20°C, the significant decrease in biological sulphate reduction and poor biofilm formation affected the stability and robustness of the 2L acetate-fed LFCR. The increased recovery of sulphur biofilm observed as a result of increased biofilm collapse and regeneration, highlights the importance of regulating the sulphur biofilm in order to facilitate optimal sulphate reduction and sulphur recovery in the integrated process. On-going work is currently focused on investigating temperatures below 20°C and to define the critical temperature, beyond which system performance is significantly reduced.

Acknowledgments

The authors acknowledge the Water Research Commission (WRC), the Department of Science and Technology (DST), and the National Research Foundation (NRF) of South Africa for funding. STLH holds the South African Research Chair in Bioprocess Engineering (UID 64778). RJH is funded by a DST/NRF Research Career Advancement fellowship (UID 91465). TM acknowledges studentship support from the NRF. The CAF at Stellenbosch University for biofilm analysis.

References

APHA (American Public Health Association) (2005) Standard Methods for the Examination of Water and Wastewater, 21st Edition. American Public Health Association, Washington, D.C.

Buisman, C., Post, R., Ijspeert, P., Geraats, G. & Lettinga, G. (2010). Engineering in Life Sciences 9, 255–267

Celis LB, Gallegos-Garcia M, Vidriales G, Razo-Flores E (2013). J Chem Technol Biotechnol 88: 1672–1679.

Ferrentino R, Langone R, Andreottola R (2017). J Environ Bio Res. 1(1)

Greben HA, Bologo H, Maree JP (2002). The effect of different parameters on the biological volumetric and specific sulphate removal rates, Biennial Conference of the Water Institute of Southern Africa (WISA).

Marais TS, Harrison STL, Huddy RJ, van Hille RP (2017):. – In: Wolkersdorfer, C.; Sartz, L.; Sillanpää, M. & Häkkinen, A.: Mine Water & Circular Economy (Vol I). – p. 262 – 269

McCarthy TS (2011). South African Journal of Science, 107 (5/6): 1-7.

Mooruth N (2013) An investigation towards passive treatment solutions for the oxidation of sulphide and subsequent removal of sulphur from acid mine water. PhD thesis, University of Cape Town, South Africa.

Moosa S, Nemati M, Harrison STL (2005). Chemical Engineering Science 60(13): 3517–3524.

Sahinkaya E, Ozkaya B, Kaksonen AH (2007) Water Res 41: 2706-2714.

Skousen J, Zipper CE, Rose A, Ziemkiewicz PF, Nairn R, Mcdonald LM, Kleinmann RL (2017). Mine Water Environ. 36, 133–153

Sposob M, Bakke R, Dinamarca C (2017) Bioresource Technology, 233 209–215

van Hille R, Mooruth N, Marais T, Naidoo N, Moss G, Harrison S, Muhlbauer R (2016) Proceedings IMWA 2016. 957-964.

Xu, Y., Chen, N., Feng, C., Hao, C., Peng, T., 2016. Environ. Technol. 37, 3094–3103.

Younger PL, Banwart SA, Hedin RS (2002). Mine water: hydrology, pollution, remediation. Dordrecht, Netherlands, Kluwer Academic Publishers

Tang K, Baskaran V, Nemati M. (2009). Biochem Eng J, 44:73–94.

Metal removal from mine water using integrated passive treatment system at Witkrantz discharge point in the Ermelo Coalfields, Mpumalanga

Tlou Betty Mashalane[1], Obed Ntshengedzeni Novhe[1], Bisrat Yibas[1, 3], Henk Coetzee[1, 4], Christian Wolkersdorfer[2, 5]

[1]Council for Geoscience, 280 Pretoria Road, Silverton, Pretoria, South Africa, tmashalane@geoscience.org.za
[2]Department of Environmental, Water & Earth Sciences, Faculty of science, Tshwane University of Technology, Acardia Campus, Pretoria, South Africa
[3]Department of Environmental Sciences, College of Agriculture and Environmental Sciences, University of South Africa, Florida Campus, Johannesburg, South Africa
[4]Department of Geosciences/ Africa Earth Observatory Network, Nelson Mandela Metropolitan University, Summerstrand Campus, Port Elizabeth, South Africa
[5]Lappeenranta University of Technology, Laboratory of Green Chemistry, Sammonkatu 12, 50130 Mikkeli, Finland

Abstract

Passive treatment technology has been used successfully worldwide for treatment of contaminated mine water, but its applicability in South Africa is limited. To help understand it's applicability in the South Africa's context, a pilot plant consisting of integrated anaerobic and aerobic units, was operated in Carolina, Mpumalanga. The main objective was to raise pH levels and remove the contaminants. An overall removal rate of at least 90% was achieved for contaminants such as Fe, Al, Zn, Ni. Overall sulphate was removed up to 30%, with no Mn removal. Deterioration of treated water was due to sludge clogging and depletion of treatment materials. Future investigations will focus on characterisation of organic and alkaline substrates.

Keywords: AMD, SRB, Passive treatment, Contaminants, Anaerobic and Aerobic Units

Introduction

Passive treatments uses natural, chemical and biological processes and requires regular but low maintenance, it is relatively low in capital and operational cost, and can provide long-term water management and treatment based on potential for lower overall costs (Hedin et al., 1994; Younger et al., 2002; Wolkersdorfer, 2008). This technology offers justification of raising pH, lowering acidity, reducing toxic metal concentration, sulphate concentration and salinity. Passive treatment is used as a long-term sustainable solution in many parts of the world and it has been globally successful in United State of America, United Kingdom, Germany and France (Hedin and Nairn, 1992; Kleinmann and Hedin, 1993; Hedin et al., 1994; Wolkersdorfer, 2008). However, in South Africa there are still knowledge gaps in terms of passive treatment applications for remediation of AMD. Witkrantz discharge point has high volume of water with an estimated average flow rate of 30 L/min (fig. 1a) and an oxidation pond was constructed as water controlled dam to reduce Fe concentration (fig. 1b). Over 76 samples were collected and characterised showing low pH of 3 to 3.5, elevated metals and sulfate concentrations.

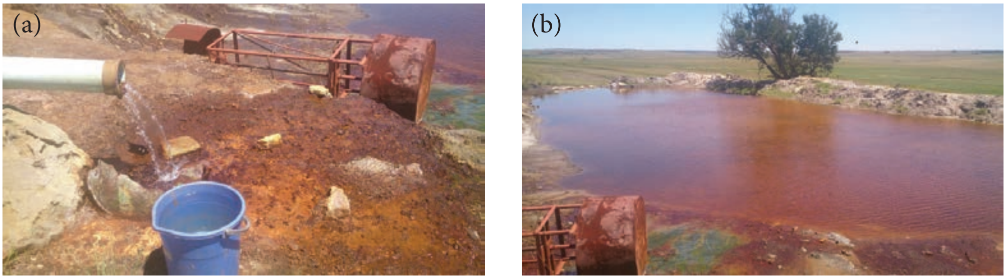

Figure 1 *(a) AMD discharging from Witkranz coal mine (b) AMD pond adjacent to the Witkranz discharge (Photographs by Obed Novhe).*

A pilot passive treatment plant was constructed to treat 1440 L of contaminated mine water discharging from abandoned Witkrantz coal mine and operated for 15 months (Novhe et al., 2016). The treated water was discharged to the nearby stream and eventually to Boesmanspruit dam. The study area is located on the farm Witkrantz 53 IT, portion 11 in Mpumalanga Province approximately ±60 km from the town of Ermelo. The area forms part of Ermelo Coalfield and all seams occur within Vryheid Formation of Ecca Group, Karoo Supergroup. The purpose of this study is to determine the overall metal removal rates from integrated passive treatment system at Witkrantz discharge.

Methodology

Experimental design

The system consisted of two Reducing and Alkalinity Producing System (RAPS), an oxidation pond and cascading trench. As indicated by Novhe et al., (2016), the RAPS consisted of 1.5 t limestone (85% of $CaCO_3$) at the bottom of 1000 L tank, 0.3 t of organic substrates (cow and chicken manure, sewage sludge and powdered limestone) above the limestone and for vertical flow of water a layer of 0.3 m was maintained. Slightly steep and shallow cascading trench consisted coarse limestone was also constructed for further Fe removal.

Water sampling and analysis

Water samples were collected in pre-cleaned and pre-contaminated 100mL and 200mL polyethylene bottles. For anions and cations, filters of 0.45µm were used to remove particulates from suspension. Samples for major and trace cations were preserved using the 2M of Nitric Acid (HNO_3) and kept at a temperature of below 6°C prior chemical analysis. ICP-MS and IC technique was used to analyse the samples. On-site parameters such as pH, temperature, dissolved oxygen, redox and electrical conductivity were conducted with the aid of WTW 3430 Digital Multimeter. Hach DR 1900 meter was used to measure alkalinity, aluminium, manganese and iron concentrations. Bucket and stopwatch method was used to measure the flow rate.

Removal rates or loads

Concentration difference between two sampling points was calculated using a formula developed by (Wieder 1993) to determine the removal rates. The average load removal (ΔL, L/d) was determined by subtracting effluent loads from influent loads, dividing by influent load and multiplying by 100%.

$\Delta L\% = (L_{inf} - L_{eff})/L_{inf}*100\%$ *(eq. 1)*

Where: ΔL% is the average load removal expressed in %, Linf is the influent load expressed in L/d and Leff is the effluent load expressed in L/d. Results were analysed and presented in multiple variables scatterplots using Statistica software.

Results

Table 1 summarises water quality of the influent and effluents from the anaerobic and oxidizing units, as mean and standard deviation (SD). The contaminants (Fe, Al, Zn, Ni and SO_4) removal rates are presented against pH and time in Fig 2, 3, 4 and 5 for RAPS1, RAP2, Oxidation Pond and Cascading Trench, respectively.

Table 1. Water quality of the influent and effluents from the anaerobic and oxidizing units.

	Influent		RAPS1		RAPS2		Oxidation Pond		Cascading Trench	
Parameter	Mean	SD	Mean	SD	Mean	SD	Mean	SD	Mean	SD
pH values	3.3	0.3	6.2	0.6	6.2	0.6	6.4	0.8	7.1	0.7
Ec (mS/cm)	2.1	0.1	2.1	0.1	2.1	0.1	1.8	1.0	1.9	0.9
Fe (mg/L)	225.7	53.6	181.8	43.1	181.8	43.1	80.1	64.9	15.7	27.1
Mn(mg/L)	29.9	8.7	32.5	4.9	32.5	4.9	31.3	9.0	28.0	12.1
Al (mg/L)	28.2	6.8	2.1	5.8	2.1	5.8	0.4	1.0	0.1	0.2
Ni (mg/L)	2.1	1.3	1.1	1.2	1.1	1.2	0.5	0.8	0.0	0.1
Zn(mg/L)	3.0	4.3	0.4	0.6	0.4	0.6	0.2	0.4	0.1	0.2
SO_4 (mg/L)	1098.4	177.8	1041.2	251.4	1041.2	251.4	971.5	237.3	971.5	237.3

The role of alkalinity on pH

Many authors reported cases of successfully treating AMD using bioreactors (Gusek et al. 1999; Reisinger et al. 2000; Reisman et al. 2003; Kuyucak et al. 2006). Bioreactors are responsible for generating alkalinity and raising pH levels using SRB. The role of alkalinity is to neutralise acidity in the AMD by dissolution. As reported by Novhe et al., (2016), RAPS 1 and 2 consisted at least 85% of $CaCO_3$ and 0.3 t of organic substrates which included chicken and cow manure, and powdered limestone. This enabled rapid generation of alkalinity, especially in the first few months. From November 2014 to April 2015, alkalinity averaged at 150 mg/L to 230 mg/L in RAPS 1 and 2 respectively. This increased the pH from the influent of 3.5 to 6 (RAPS 1) and 6.5 (RAPS2) (fig 2 & 3). Further alkalinity generation was observed in the cascading trench averaged at 300 mg/L. Consequently, pH was recorded to be 7.5 at the effluent (fig 5). Alkalinity decreased with time throughout the system. A sudden decrease in alkalinity could be due to clogging and depletion of materials. However, alkalinity maintained its integrity at 100 mg/L despite exhaustion of materials from May to August 2015.

Overall metal removal rates

There was substantial removal of contaminants > 90% throughout the system except for Mn. This could be due alkalinity generation from SRB and limestone dissolution which increased pH near neutral. Targeted contaminants includes: Fe, Al, Mn, Zn, Ni, Cd, Pd, Co, Cu and As. (Sheoran et al. 2010) reported that Fe forms iron sulphides and carbonates when pH is near neutral and in reducing conditions, and at pH ≥3.5 iron oxi(hydroxi)des are formed (Gilbert et al. 2005). ICP-MS and IC results showed a decrease of Fe concentration from ≈300 mg/L (inlet) to 0 mg/L (effluent) over time. Removal of Fe ranged from 15% to 70% from RAPS 1 and RAPS 2 respectively (fig 3 & 4). The low removal rate of 15% in RAPS 1 could be attributed to slow rate of H2S generation from microbial activities. Over time, Fe was further removed at 80% and 100% in the oxidation pond and the cascading trench respectively (fig 4 & 5). Generation of alkalinity by SRB reduced the concentration of metals and therefore precipitating them as metal sulphide.

With an increase of pH near neutral, Al was able to precipitate as $Al(OH)_3$ i.e. gibbsite and removed at 93% and 100% in RAPS 1 and 2 respectively (fig 2 & 3). There was a sudden decrease in Al removal rate in RAPS 1; however, the other units maintained the removal rate of 100%. Zn, and Ni were removed below detection limit (fig 2 & 3). Their removal in the system was due to microbial sulphate reduction (as metal sulphides) and co-precipitation with Fe and Al (oxy)hydroxides, (Gilbert et al., 2005). There was a sudden drop in April 2015 from RAPS1, however, the other units continued to remove contaminants (Zn, Ni and Al) at 100%. Other metals such Cd, Pb, Co, Cu and metalloid As showed similar trends and were also removed below detection limit. The non-removal of Mn was probably due to the presence of Fe in the oxidation pond and cascading trench. (Thomas and Romanek, 2002) documented that a high pH is required for Mn to precipitate and Fe must have been completely removed in the system. (Strumm and Morgan, 1996) revealed that in

AMD the oxidation of Mn is slow; however it can be stimulated by bacteria and catalysis by surfaces.

Effects of sulfate reduction on metal removal

The overall removal of sulphate in the system was 30% (fig 2 & 3). Sulfate reduction in this system was mainly due to microbial activities in RAPS 1 and 2 (anaerobic units). According to Sheoran et al. (2010) processes responsible for removing metals include adsorption, co-precipitation, biosorption and filtration. The success of this is determined by a reliable carbon source and a conducive environment for SO_4 reduction for microbial activity. Carbon source reduce sulphate to hydrogen sulphide which reacts with dissolved metals to form metal sulphide. In addition, materials should have enough pores to promote permeability. Locally, available treatment materials are preferred as they are readily available and inexpensive. The 30% sulphate reduction recorded in the first few months decreased with time as treatment materials get depleted and the system experienced clogging.

Conclusions

Generation of alkalinity by both SRB and limestone dissolution increased the median pH throughout the system from as low as 3 to an average of 7.5. The overall metal removal rate in the system was greater than 90% excluding Mn. The performance for this pilot plant has been adequate in generating alkalinity and removing contaminants such as Fe, Al, As, Zn, Cd, Co, Pb, Ni at 100% and below detection limit. Furthermore, there was substantial SO_4 removal rate of 30%. However, Mn was not removed as a pH of at least 9 and high oxidation rate are required. Microbial sulfate reduction which releases hydrogen sulphide contributed to removal of metals.

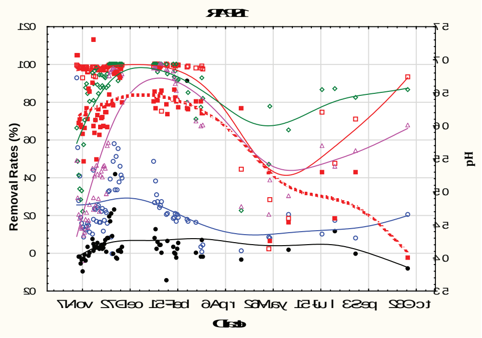

Figure 2 Contaminants removal rates against pH in the RAPS1.

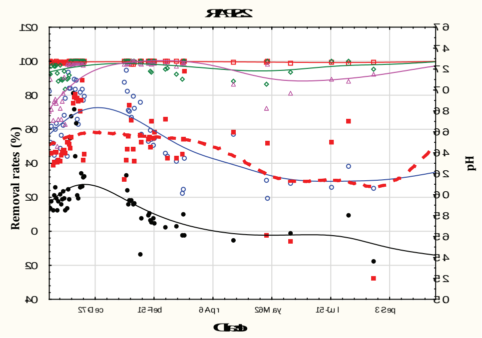

Figure 3 Contaminants removal rates against pH in the RAPS2.

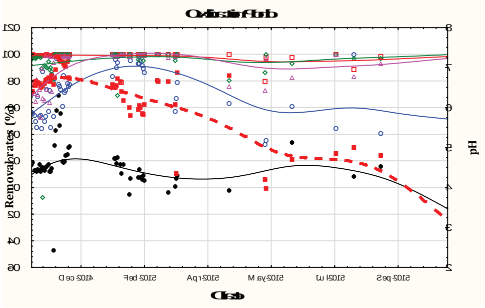

Figure 4 Contaminants removal rates against pH in the oxidation pond.

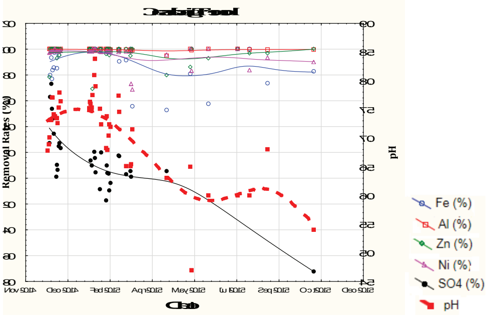

Figure 5 Contaminants removal rates against pH in the Cascading Trench.

For instance, the gradual decrease in Fe concentration from anaerobic units was due to microbial sulfate reduction which releases hydrogen sulphide and it further precipitates as hydroxides from oxidation pond and cascading trench. Depletion of treatment materials and clogging due to sludge (built-up) contributed to removal rate of metals being constant.

Recommendations

It is of paramount importance to select suitable organic materials to adsorb metals and encourage optimum microbial SRB. To prevent clogging and armouring from Al and Fe hydroxides, accumulated precipitates need to be flushed. Because Mn oxidation is slower than Fe oxidation, it is recommended that Fe must be removed completely before treating Mn.. To select the most suitable treatment materials for mine water, local available organic and alkaline substrates need to be characterised.

Acknowledgements

The authors thank Department of Mineral Resources for funding this project. Council for Geoscience colleagues are acknowledged for sample analysis and field assistance.

References

Gilbert O, Pablo de J, Cortiina, JL, Ayora, C (2005) Municipal compost-based mixture for acid mine drainage bioremediation:metal retention mechanism. Applied Geochemistry, 20(9), pp.1648–1657.

Gusek JJ, Wildeman TR, Miller A (1999) Design, construction and operation of a 1,200 gpm passive bioreactor for metal mine drainage. In: Phytoremediation and innovative strategies for specialized remedial applications, Battelle Press, Columbus, OH, pp.217–223.

Hedin RS, Nairn RW (1992) Designing and sizing passive mine drainage treatment systems - Online. Available at: http://wvmdtaskforce.com/proceedings/92/92HED/92HED.HTM.

Hedin RS, Nairn RW, Kleinmann RLP (1994) Information Circular 9389 : Passive treatment of coal mine drainage, pp.1–44.

Kleinmann P, Hedin RS (1993) Treat mine water using passive methods. Pollution Engineering, 25(August), pp.20–23.

Kuyucak N, Chabot F, Martschuk J (2006) Successful implementation and operation of a passive treatment system in an extremely cold climate. In Proc. of the 7th Int.Conf. on acid Rock Drainage (ICARD). St. Louis, MO, In: R.I. Barnhisel (Ed), American Society of Mining and Reclamation (ASMR), Lexington, KY, pp. 3132–3138.

Novhe NO, Yibas B, Coetzee H, Atanasova M, Netshitungulwana R, Modiba M, Mashalane T (2016) Long-term remediation of acid mine drainage from abandoned coal mine using intergrated (anaerobic and aerobic) passive treatment system in South Africa :A pilot study. Mining Meets Water -Conflicts and Solutions, (1), pp.668–675.

Reisinger RW, Gusek JJ, Richmond TC (2000) Pilot-scale passive treatment test of contaminated waters at the historic Ferris-Haggarty mine, Wyoming. In: Proc. of the 5th Int. Conf. on Acid Rock Drainage (ICARD), Denver, CO, pp. 1071–1077.

Reisman DJ, Gusek JJ, Bishop M (2003) A pretreatability study to provide data for construction of a demonstration bioreactor. In: The Proc. of the 10th Int. Conf. on Tailings and Mine Waste, Vail, CO, pp. 305–315.

Sheoran AS, Sheoran V, Choudhary RP (2010) Bioremediation of acid-rock drainage by sulphate-reducing prokaryotes: A review. Minerals Engineering, 23(14), pp.1073–1100, doi:10.1016/j.mineng.2010.07.001.

Strumm W, Morgan, JJ (1996) Aquatic chemistry, chemical equilibria and rates in natural waters 3rd edn., Wiley, New York.

Thomas RC, Romanek CS (2002) Passive treatment of low pH, ferric iron-dominated acid rock drainage in a vertical flow wetland II: Metal removal, American society of mining and reclamation, Lexington KY, pp.752–775.

Wieder RK (1993) Ion input/output budget for five wetlands constructed for acid coal mine drainage treatment. Water, Air and Soil Pollution, 71, pp.231–270.

Wolkersdorfer C (2008) Water Management at Abandoned Flooded Underground Mines, Heidelberg: Springer.

Younger PL, Banwart SA, Hedin RS (2002) Mine Water- Hydrology, Pollution, Remediation. Dordrecht: Kluwer.

Aeration via Renewable Energies Improves Passive Treatment System Performance

Robert W. Nairn[1], Nicholas L. Shepherd[1], Timothy Danehy[2], Cody Neely[2]

[1]*Center for Restoration of Ecosystems and Watersheds, University of Oklahoma, Norman, OK 73019, USA*
[2]*BioMost Inc. Mining and Reclamation Services, 434 Spring Street Ext., Mars, PA 16046, USA*

Abstract

Successful passive treatment requires effective aeration of mine waters to address both ecotoxic metals concentrations (e.g., removal via oxidation, hydrolysis, and precipitation) and nuisance constituents (e.g., sulfide and oxygen demanding substances produced by sulfate-reducing bioreactors). In the flat landscape of the Tri-State Lead-Zinc Mining District of the central United States, renewable energy-driven aeration technologies were implemented at two full-scale passive treatment systems with limited total relief. Solar-powered units, with the ability to store energy, provided consistent and effective aeration compared to wind-powered technologies. Off-the-grid aeration devices can enhance water quality improvement and may be especially attractive for use remote locations.

Keywords: Aeration, oxygenation, sulfide, iron, Tar Creek

Introduction

In passive treatment systems, effective aeration of mine waters is often needed to address elevated concentrations of ecotoxic metals and/or nuisance constituents produced by sulfate-reducing bioreactors. In many mining regions, substantial topographic variability provides site-specific opportunities for cascade aeration (Chen and Jiang 2012, Oh et al. 2016) and other related technologies relying on hydraulic head differences. At mine water sites in flat landscapes, differences in hydraulic head may be insufficient to provide effective aeration via these approaches. At derelict and abandoned mine water sites in these landscapes, where passive treatment may be an especially attractive option given its lesser long-term operation and maintenance commitments, aeration via traditional energy-intensive engineering technologies (e.g., fossil-fuel driven mechanical, bubble or pressure aerators) may not be a feasible economic or technical option. Utilization of renewable energy-driven aeration (e.g., solar- and wind-powered technologies) may offer a cost-effective and efficient option at these locations.

Solar- and wind-powered aeration technologies have been used in aquaculture, lake and reservoir management, and wastewater lagoon operations to promote mixing and increase dissolved oxygen (DO) concentrations (e.g., Westerman and Zhang 1997, Boyd 1998, DeMoyer et al. 2003). These systems are typically submerged and consist of a renewable power source that builds pressure in an air compressor or blower. The pressure is typically released through a valve and line to submerged diffusers at the bottom of the pond which produce "bubble plumes" that rise to the surface. The bubbles cause vertical and lateral circulation by entraining water as they rise, and the bubble interfaces help to transfer oxygen to the water. Further oxygen mass transfer may occur at the pond surface due to turbulence at the air-water interface created by the bubble plume.

In mine water passive treatment systems, effective aeration (and re-aeration) may drive several demonstrable water quality improvement processes. In ponds and wetlands, rates of iron oxidation are enhanced by the entrainment or addition of oxygen beyond passive diffusion or photosynthetic activity (Jageman et al. 1988, Hedin et al 1994, Kirby et al. 2009). In net alkaline mine drainage, degassing of elevated concentrations of carbon dioxide (CO_2) drives pH values upward, further enhancing iron oxidation rates (Kirby et al. 2009, Nairn 2013). Vertical flow bioreactors (VFBRs), designed to promote bacterial sulfate reduction and subsequent metal sulfide retention, often produce water with low oxidation-reduction potential (ORP) and DO concentrations, and elevated sulfide concentrations and biochemical oxygen demand (e.g., Yepez and Nairn 2012). Effective aeration helps to strip oxygen demand and sulfide and increase DO and ORP. In this preliminary study, the initial efficacy of renewable energy-driven aeration devices was evaluated for increasing DO and ORP, enhancing iron oxidation, and stripping sulfide and oxygen demand.

Methods

In the relatively flat landscape of the abandoned Tri-State Lead-Zinc Mining District of the central United States, off-the-grid aeration technologies were implemented at two full-scale passive treatment systems. Process unit designations, design functions and aeration status are summarized in Table 1. The Mayer Ranch system (Figure 1) has been in operation since late 2008 and the Southeast Commerce system (Figure 2) has been operational since early 2017. Each site has less than 1.8 m of total relief to facilitate gravity-driven treatment though multiple process units. Principal contaminants of interest are elevated concentrations of iron (138-192 mg/L), zinc (6-11 mg/L), lead (60-81 µg/L), cadmium (17-20 µg/L) and arsenic (40-64 µg/L) in net alkaline mine waters. Design volumetric flow rates are 1400 and 550 m^3/minute for Mayer Ranch and Southeast Commerce, respectively.

Aeration at Mayer Ranch includes two windmills powering vertical displacement air pumps and two solar units. In C1, a 6-m was installed including 12 1.85-m steel blades mounted on a self-governing upwind turbine with head-mounted vertical displacement compressor capable of producing 5 m^3/hour at 9000 Pa depending on wind speed, and dual rubber diaphragm bubble diffusers. In C4N, an additional 6-m windmill was installed including 12 1.78-m steel blades mounted on a self-governing upwind turbine with a Jet Stream direct drive compressor capable of producing 2.5 m^3/hour at 9000 Pa at wind speeds of 14-64 km/hour, and dual rubber diaphragm bubble diffusers. In C4S, a commercial solar lake bed aeration system was installed including a 120-W solar panel, high-volume compressor with air output of 8.5 m^3/hour, 30-amp charge control center, 210 amp-hour deep cycle solar battery, 12/24-volt smart box converter and dual rub-

__Table 1.__ Process unit designations, design functions and aeration type and capacity of the Mayer Ranch and Southeast Commerce passive treatment systems in the Tri-State Lead-Zinc Mining District, Oklahoma, USA.

	Design function	Aeration Type/Capacity (m3/ hour)
Mayer ranch passive treatment system		Wind/5
Initial oxidation pond (C1)	Oxidative Fe retention	---
Surface-flow wetlands/pond (C2N/C2S)	Trace metal sorption	---
Vertical flow bioreactors (C3N/C3S)	Additional Fe/ trace metals retention	C4N-Wind/2.5
	Trace metal sulfide retention	C4S-Solar/8.5
Re-aeration ponds (C4N/C4S)	Re-aeration and stripping of sulfide and	---
Horizontal flow limestone beds (C5N/C5S)	oxygen demand	Solar/0.5
Polishing pond/wetland (C6)	Polishing of Zn and addition of hardness	Solar/50
	Ecological buffering	---
Southeast Commerce passive treatment		Solar (OCS)/50
system		Solar/50
Initial oxidation pond (OX)	Oxidative Fe retention	
	Trace metal sorption	
Surface flow wetland/pond (WL)	Additional Fe/ trace metals retention	
Vertical flow bioreactors (VF)	Trace metal sulfide retention	
Final polishing unit (FP)	Re-aeration and stripping of sulfide and	
	oxygen demand	

ber diaphragm bubble diffusers. In C6, another commercial solar aerator system was installed including three 15-W solar panels, solar charge controller, 12-V deep cycle marine battery, 0.6 amp-hour pump house containing four compressors with air output of 0.5 m^3/hour, and a single rubber diaphragm bubble diffuser.

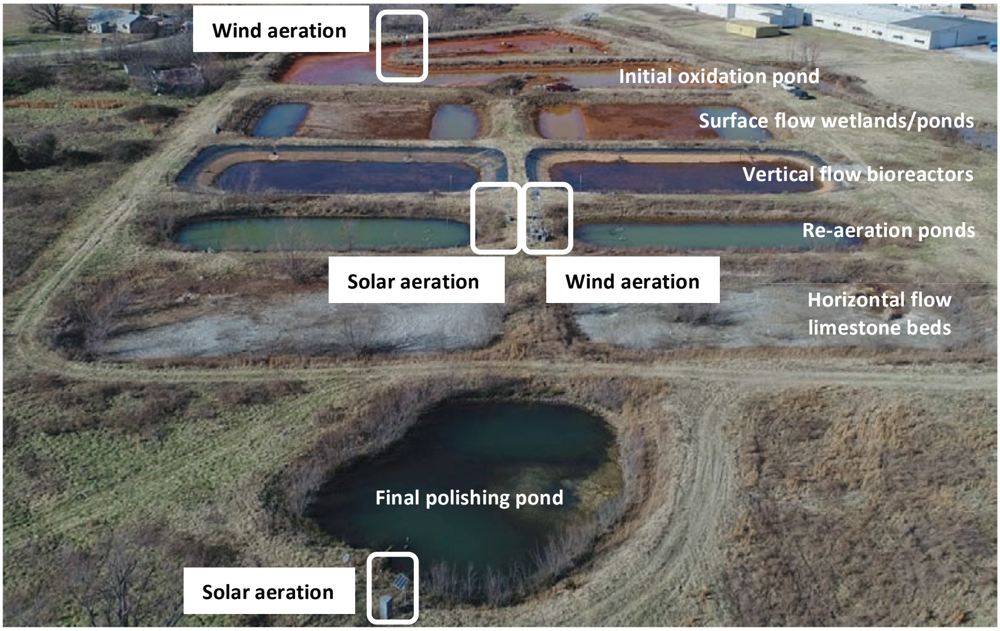

Figure 1 *Oblique aerial photograph of Mayer Ranch passive treatment system in December 2017 during a maintenance drawdown when water levels were decreased. Water flow paths are from top to bottom. Individual process unit designations and locations of aeration devices are shown. Image obtained via small Unmanned Aerial System.*

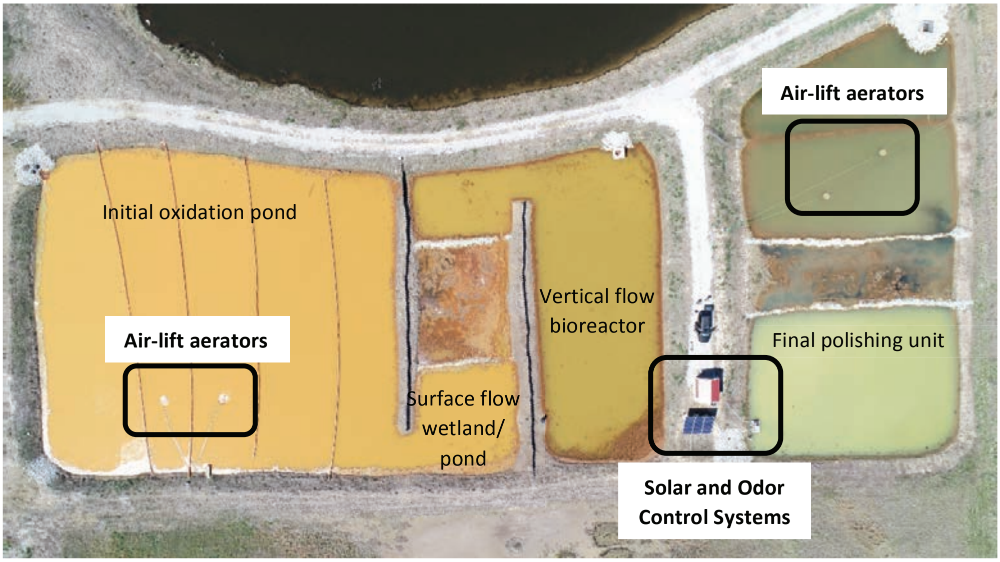

Figure 2 *Vertical aerial image of Southeast Commerce passive treatment system in April 2018. Individual process unit designations and locations of aeration and other devices are shown. Note directional baffle curtains in the initial oxidation pond. Image obtained via small Unmanned Aerial System.*

At Southeast Commerce, a custom-designed, solar-powered aeration and sulfide removal system was installed by BioMost Inc. This unique system includes a 3,180-W photovoltaic module, combiner box, two charge controllers, a bank of eight 6V/400 AH/20HR batteries, 1500-W 24V DC Inverter, two regenerative blowers with pressure kits and one regenerative blower with vacuum kit. This system drives four floating air-lift aerators (two in OX and two in FP) and a novel, closed Odor Control Structure (OCS) at the VFBR effluent. Gas (e.g., hydrogen sulfide) from the OCS outlets via suction through an Activated Carbon Filter (ACF) containing 180 kg of granular carbon media. This single combined system can provide air flows of more than 150 m^3/hour through the three subsystems (two sets of airlift aerators in OX and FP, and the OCS).

Water quality and quantity data were collected on a monthly (MRPTS: 2009-2013; SECPTS: 2017-2018) and quarterly (MRPTS: 2013-2018) basis and included volumetric flow rates, physical parameters (pH, DO, temperature, specific conductance, ORP, alkalinity, turbidity), sulfate, sulfide, and a full suite of total and dissolved metals and base cations (Al, As, Ba, Ca, Cd, Co, Cr, Cu, Fe, K, Li, Mg, Mn, Na, Ni, Pb, Si, Zn). Center for Restoration of Ecosystems and Watersheds (CREW) standard operating procedures follow US Environmental Protection Agency (USEPA) methods for all analyses.

Results

Both passive treatments systems addressed traditional mine water quality constituents, decreasing concentrations of targeted contaminants of concern (Table 1). Median annual mass retention values for Fe, Zn, Pb, Cd and As were 37000, 1670, 15, 3 and 13 kg/year, respectively, at Mayer Ranch. The Southeast Commerce system retained 24200, 1660, 5, 4, and 7 kg/year of Fe, Zn, Pb, Cd and As, respectively. Iron retention occurred in oxidative units (C1, C2N and C2S at Mayer Ranch, and OX and WL at Southeast Commerce) as well as substantial trace metal sorption to amorphous iron oxyhydroxide solids (Oxenford and Nairn 2010). Trace metals were further retained in the VFBRs (C3N and C3S at Mayer Ranch and VF at Southeast Commerce) by a suite of mechanisms including exchange, sorption, and sulfide precipitation (LaBar and Nairn 2018). Effluent Pb concentrations at Southeast Commerce were elevated, likely due to construction-related flow manipulations and are expected to decrease over time.

Table 3 presents selected data for passive treatment process units with renewable-energy driven aeration devices. Dissolved oxygen saturation and ORP increased significantly ($p<0.05$) in all units and sulfide, BOD5 and pCO2 decreased significantly ($p<0.05$). Sulfide and BOD5 were only evaluated for VFBR effluent reaeration. Increased dissolved oxy-

__Table 2.__ Influent and effluent water quality for the Mayer Ranch and Southeast Commerce passive treatment systems in the Tri-State Lead-Zinc Mining District, Oklahoma, USA. Values less than the practical quantitation limit (PQL) are reported as <PQL. The number of sampling events is reported as n.

	Mayer Ranch		Southeast Commerce	
	In (n=82)	Out (n=43)	In (n=80)	Out (n=22)
pH	5.95	7.02	6.06	7.02
Total alkalinity (mg/L CaCO3)	393	224	350	117
Total Fe (mg/L)	192	0.13	127	0.79
Total Zn (mg/L)	11	0.25	6.15	0.69
Total Ni (mg/L)	0.97	0.15	0.52	0.06
Total Cd (µg/L)	17	<PQL	18	<PQL
Total Pb (µg/L)	60	<PQL	80	26
Total As (µg/L)	64	<PQL	38	<PQL
Total SO4-2 (mg/L)	2239	2057	2102	1956

gen concentrations and degassing loss of CO_2 have direct positive effects on iron oxidation rates (Kirby et al. 2009). Sulfide and oxygen demand may be considered nuisance constituents, which are typically not present in the untreated mine drainage but are created during passive treatment in sulfate-reducing bioreactors. Elevated concentrations may be directly ecotoxic to aquatic life. In the two studied systems, oxygen demand was never problematic, but sulfide concentrations were often well above the aquatic life criteria of 0.002 mg/L (USEPA 2018) even after re-aeration, especially in hot summer months in Oklahoma when air temperatures are often above 35°C.

All parameters showed substantial seasonality due to temperature variability and subsequent effects on biological activity. In addition, these data represent median measurements for the full lifetime of each system. During initial startup, the Mayer Ranch passive treatment system VFBRs exported substantial concentrations of nutrients leading to algal blooms, of which subsequent decomposition decreased dissolved oxygen concentrations in downstream process units. However, once the system reached a quasi-steady state after the first two growing seasons, these issues were no longer present. It is likely that the Southeast Commerce passive treatment system VFBR is still in this initial startup phase.

In addition, at the Southeast Commerce system, the novel solar-driven OCS installation pulled gaseous sulfide from the atmosphere above the VFBR effluent into the ACF. Gaseous sulfide concentrations through the fall and winter of 2017 and early spring of 2018 were decreased by essentially 100% (all ACF effluent gaseous concentrations were below detectable limits with influent concentrations ranging from 17 to 78 ppm). In two sampling events in spring 2018, ACF effluent gaseous sulfide concentrations showed an increase to 2.7 and 142 ppm as temperatures increased and influent concentrations reached 490 ppm. The performance of this unique system is the subject of ongoing research as are the novel air-lift aerators in the oxidation pond and final polishing unit at Southeast Commerce.

Conclusions

Both passive treatment systems produced circumneutral pH effluent waters containing concentrations of trace metals meeting in-stream, hardness-adjusted aquatic life criteria. Aeration in initial oxidation ponds showed seasonal and spatial variability in effectiveness, mainly due to air temperature changes and subsequent changes in dissolved oxygen saturation concentrations. Degassing of carbon dioxide by active aeration helped to increase pH and had positive effects on iron

Table 3. *Median measured dissolved oxygen saturation, oxidation-reduction potential (ORP), sulfide (S^{-2}) and five-day biochemical oxygen demand (BOD_5) values and median calculated partial pressures of carbon dioxide (pCO2) in and out of process units which included solar- or wind-powered aeration devices. pCO2 was calculated using a modified Henderson-Hasselbach equation including temperature compensation for KH and K_1.*

	DO Saturation (%)	pCO_2 (atm)	ORP (mV)	S^{-2} (mg/L)	BOD_5 (mg/L)
Mayer Ranch passive treatment system					
C1 In	13	0.528	-116	---	---
C1 Out	37	0.189	+121	---	---
C4N In	11	0.038	-80	31	2.89
C4N Out	51	0.023	+78	1.9	1.11
C4S In	14	0.035	-73	38	2.44
C4S Out	38	0.023	+77	4.2	1.21
C6 In	10	0.025	+5	---	---
C6 Out	41	0.021	+97	---	---
Southeast Commerce passive treatment system					
OX In	10	0.364	-43	---	---
OX out	80	0.130	+130	---	---
FP In	10	0.074	-184	85	3.51
FP Out	73	0.023	+91	12	3.30

oxidation rates. However, it is likely that the effects were limited in scope given the large surface areas of the pond-like process units. Although sulfate-reducing bioreactors produced biochemical oxygen demand, especially in initial growing seasons, these values were not sufficiently elevated to be considered problematic. Sulfide concentrations, however, were often elevated enough (> 1000 µg/L) to be considered both a nuisance odor and an aquatic toxicant. Renewable-energy driven re-aeration decreased sulfide concentrations substantially with both wind- and solar-powered technologies. Overall, sulfide concentrations decreased by 94% and 86% using solar power at Mayer Ranch and Southeast Commerce, respectively, and by 89% using wind at Mayer Ranch. At least initially, the larger custom-designed solar-powered unit at Southeast Commerce has demonstrated more consistent and effective performance.

Off-the-grid aeration devices may enhance water quality improvement effectiveness in passive treatment systems, addressing both oxidative iron removal and nuisance constituent treatment, especially in regions lacking substantial topographic variability to sustain effective cascade aeration or other hydraulic head-driven technologies. They may be especially attractive for use remote locations and/or at abandoned or derelict sites where operation and maintenance budgets are limited.

Acknowledgements

This work was supported by the Oklahoma Department of Environmental Quality (Agreement PO 2929019163 SRA FY15-ORA4-14), the Grand River Dam Authority (Agreements GRDA 060910 and GRDA08272015), the Office of Surface Mining Reclamation and Enforcement (Agreement S11AC20000), and the U.S. Environmental Protection Agency (Agreement X7-97682001-0). Several private landowners provided access.

References

Boyd, CE (1998) Pond water aeration systems. Aquacultural Engineering 18(1): 9-40

Chen C-J and Jiang W-T (2012) Influence of waterfall aeration and seasonal temperature variation on the iron and arsenic attenuation rates in an acid mine drainage system. Applied Geochemistry 27(2012) 1966-1978.

DeMoyer CD, Schierholz EL, Gulliver JS, Wilhelms SC (2003) Impact of bubble and free surface oxygen transfer on diffused aeration systems. Water Research 37: 1890-1904.

Hedin RS, Nairn RW, Kleinmann RLP (1994) Passive Treatment of Coal Mine Drainage. U.S. Bureau of Mines Information Circular 9389. 37 pp.

Jageman TC, Yokley RA, Heunisch GW (1988) The Use of Pre-Aeration to Reduce the Cost of Neutralizing Acid Mine Drainage. In: Proceedings of the 1988 Mine Drainage and Surface Mine Reclamation Conference, Pittsburgh, PA, pp. 131-135.

Kirby CS, Dennis A, Kahler A (2009) Aeration to degas CO2, increase pH, and increase iron oxidation rates for efficient treatment of net alkaline mine drainage. Applied Geochemistry 24(7): 1175-1184.

LaBar JA, Nairn RW (2018) Characterization of trace metal removal products in vertical flow bioreactor substrates at the Mayer Ranch Passive Treatment System in the Tar Creek Superfund Site. *Chemosphere* 199(2018): 107-113

Nairn RW (2013) Carbon Dioxide Impacts Both Passive Treatment System Effectiveness and Carbon Footprint. Reliable Mine Water Technology: Proceedings International Mine Water Association, Golden, CO, USA, 6 pp.

Oh C, Ji S, Cheong Y, Yim G, Hong J (2016) Evaluation of design factors for a cascade aerator to enhance the efficiency of an oxidation pond for ferruginous mine drainage. Environmental Technology 37(19): 2483-2493.

Oxenford LR, Nairn RW (2010) Progressive Iron Removal Within the Initial Oxidation Cell of a Passive Treatment System. Proceedings of the 27th National Conference of the American Society of Mining and Reclamation, Pittsburgh, PA, pp. 767-779.

U.S. Environmental Protection Agency (2018) National Recommended Water Quality Criteria – Aquatic Life Criteria Table https://www.epa.gov/wqc/national-recommended-water-quality-criteria-aquatic-life-criteria-table

Westerman PW, Zhang RH (1997) Aeration of livestock manure slurry and lagoon liquid for odor control: a review. Applied Engineering in Agriculture 13(2): 245-249.

Yepez SA, Nairn RW (2012) Nutrient and Sulfide Export from a Mine Drainage Passive Treatment System. Proceedings of the 29th National Conference of the American Society of Mining and Reclamation, Tupelo, MS, pp. 539-556.

Valorisation of effluent from metal recovery plant

Marja Nappa[1], Kaisa Kiipula[2], Hanna Kyllönen[1], Tommi Kaartinen[1], Risto Pajarre[1], Petteri Kangas[1]

[1]VTT Technical Research Centre of Finland Ltd, P.O. Box 1000, FI-02044 VTT, Finland, marja.nappa@vtt.fi

[2]Terrafame Group, Aleksanterinkatu 17, PL 800, 00101 Helsinki, Finland

Abstract

Resource efficiency in a mine was assessed in this study. Two new process concepts were screened; (i) valorising metals from mine raffinate with selective precipitation with different alkalis and with possible CO^2 treatment and (ii) calcium removal through precipitation from neutralising pond water for improved performance of reverse osmosis. Both new concepts were evaluated with several alkalis. Concept screening was based on computational assessment and results were verified by experiments. Experiments showed qualitative agreement with findings from computational assessment and simultaneously promoted this computer-aided methodology for rapid screening of new processes.

Keywords: metal recovery, mine water, precipitation, concept development, process simulation; thermodynamic equilibrium

Introduction

There is a clear trend towards material efficiency and tightening environmental regulations, which has generated needs for valorising previously unutilized metals within mine waters. In addition, the limited availability of water in many regions has increased the reuse of water in the mining industry.

The case process in this study is a mining process based on bioheapleaching method to recover copper, zinc, nickel and cobalt present in the ore by first dissolving them into pregnant leach solution (PLS) as sulphates. The sulphates in the PLS are then stage wise recovered as sulphides through hydrogen sulphide precipitation. In addition to the aforementioned valuable metals, components with lower value are present in the PLS. The PLS containing these components is recirculated back to the heaps to maintain the water balance in the process. Rest of the remaining PLS needs to be neutralised before discharge. This is carried out through lime precipitation, which is the current BAT solution (see details in Geldenhuys et al., 2003). First step is to precipitate aluminium using limestone. Secondly, lime milk is used to precipitate iron, manganese and magnesium from the solution. With both of these steps, gypsum is formed and the sulphate level decreases. The precipitates from these stages are settled and the neutralizing pond (NP) overflow is further treated with reverse osmosis (RO).

According to current practice, the excess metals are precipitated simultaneously with gypsum, which is decreasing the possibilities of valorising these metals. In addition, the water recovery in the RO units can be quite low, i.e. 50-60%, due to scaling tendency (Kyllönen et al., 2016). When mine water contains a lot of sulphate and is treated with lime there is a great risk of gypsum scaling on the membrane (Kyllönen et al., 2017).

The aim of the present work was to study possibilities, using simulation as a method, to fractionate dissolved metals; magnesium (10000 mg/L), manganese (5000 mg/L), aluminium (4000 mg/L) and iron (20000 mg/L) from the residual raffinate of a metal recovery plant instead of precipitating these metals together with gypsum. Similar study has been previously conducted by (Kaartinen et al., 2017) for magnesium recovery from mine water. Besides valorisation of metals, the other target was to increase the amount of purified water and concentration of metal sulphates by reducing the scaling tendency in the RO plant occurring due to the calcium content of water (500 mg/L).

Methods

The screening and development of new process concepts was conducted based on process simulation. A thermodynamic multi-phase model describing the aqueous effluents and precipitated phases was developed. Thermodynamic simulations were applied to obtain the chemical equilibrium in the studied multiphase and multicomponent systems in this study. The chemical reactions taking place in multiphase systems were calculated with the Gibbs energy minimization method assuming that the reactions are fast and equilibrium assumption is valid in the aqueous solutions. The Gibbs energy minimization method does not entail assumptions of exact reaction paths between the chemical species but the equilibrium concentrations are obtained as the composition that gives the minimum Gibbs energy without violating the elementary mass balances. The aqueous phase describing mine water was based on the Pitzer formalism for solute interactions. (Pajarre et al., 2018) give detailed description of modelling aqueous solutions. The thermodynamic models have been applied using the VTT's Chemsheet program (Koukkari et al., 2000), which can be used in Microsoft's Excel. Key ions in the applied thermodynamic model were Na^+/K^+/H^+/Ca^{+2}/Mg^{+2}/Mn^{+2}/Fe^{+2}/Fe^{+3}/Al^{+3}/Ni^{+2}/Zn^{+2}/Cu^{+2} and Cl^-/OH^-/CO_3^{-2}/SO_4^{-2}. Similarly gaseous phase and tens of solid phases describing the precipitation were incorporated into the model, which can be used for modelling aqueous electrolyte solutions between temperatures 25-95 °C and ionic concentrations up to 6 mol/kg. The gaseous and aqueous phases include several compounds and ions. The solid phases were assumed to be pure stoichiometric phases comprising single precipitate. Examples of typical speciation of mine water are presented in (Pajarre et al., 2018).

The screening considered two mine water flows; raffinate and NP-water. The evaluated waters were obtained from Sotkamo mine, Finland and are described in Table 1. In the computational assessment, the anions were considered as sulphates and the pH of each solutions were adjusted by sodium hydroxide or sulphuric acid. Moreover, alkalis and acids were considered as pure components.

Figure 1 shows the flowsheets of screened concepts. In both concepts the solutions were treated with various alkalis and/or acids including sodium hydroxide, sodium carbonate, lime milk ($Ca(OH)_2$), limestone ($CaCO_3$) and carbon dioxide in the consecutive steps. The chemicals were dosed in such way that desired pH levels were achieved. Between steps, precipitates were removed. In the experimental work the most promising treatments, based on computational assessment were selected to be studied in laboratory scale. The experimental methods are not described here in detail but results are compared to the results of the computational assessment.

Results and discussion

Computational assessment - raffinate treatments

The screening of possible process concepts for recovering aluminium, manganese, iron and magnesium from raffinate solution was conducted. A list of screened chemicals is shown in Table 2, used raffinate (raffinate 1) composition is shown in Table 1. The study included tens of simulations with various combinations of chemicals.

Table 1. *Mine water compositions, mg/L, pH, and pH adjusting chemicals in computational assessment.*

Description	Al^{+3}	Ca^{+2}	Fe^{+2}	Fe^{+3}	Mg^{+2}	Mn^{+2}	Na^+	Ni^{+2}	Zn^{+2}	K^+
Raffinate 1	4411	637	19495	-	9665	5585	2415	76	1	-
Raffinate 2	4100	510	22000	-	12000	6300	2900	2800	54	-
NP-water	0.4	470	-	0.9	18	-	1300	-	-	41

Description	pH	H_2SO_4, mg/L	NaOH, mg/L
Raffinate 1/2	2.7/3	1913/1225	-
NP-water	10.4 / 9	-	42 / 6

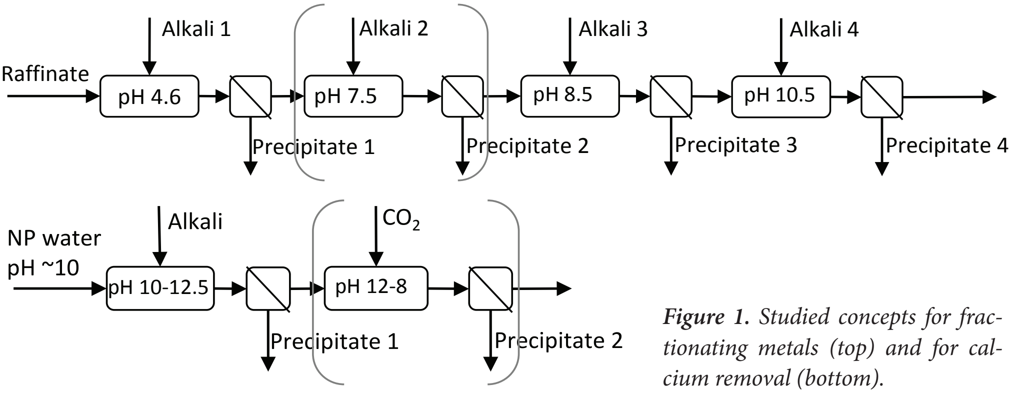

Figure 1. *Studied concepts for fractionating metals (top) and for calcium removal (bottom).*

Table 2. *Screened chemicals for metal fractionating concepts.*

Alkali 1 (pH 4.6)	Alkali 2 (pH 7.5)	Alkali 3 (pH 8.5)	Alkali 4 (pH 10.5)
$CaCO_3$ Na_2CO_3 NaOH	$CaCO_3$ Na_2CO_3	NaOH $Ca(OH)_2$ -	NaOH $Ca(OH)_2$

Based on analysis similar amounts of precipitates seemed to be formed in certain pH independently of previous steps, except gypsum in the last precipitate step. The precipitated phases and chemical consumption after treatments are illustrated in Figure 2. Based on analysis Na_2CO_3 and NaOH can be used in first step to selectively precipitate $Al(OH)_3$. Na_2CO_3 selectively precipitated $MnCO_3$ in second step. Further, NaOH can be used to precipitate $Fe(OH)_2$ and $Mg(OH)_2$ without simultaneous gypsum precipitation. The usage of lime and/or limestone as alkali caused simultaneous gypsum precipitation, always. However, the utilization of alternative alkalis (Na_2CO_3, NaOH) for recovering the metals may decrease the economic feasibility compared to the treatment with traditional alkalis, limestone and lime.

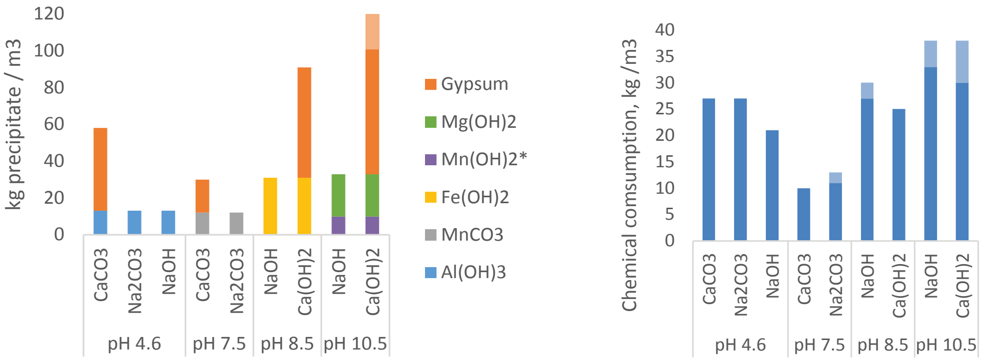

Figure 2. *Summary of screened concepts for metal recovery. Precipitates after each treatment, kg/m*^{3} *(left). * Mn*$(OH)_2$ *precipitates only if it is not precipitated as carbonate at pH 7.5. Chemical consumption in each treatment, kg/m*^{3} *(right). Light orange and light blue indicates range of gypsum precipitate and the range of chemical usage. Previous steps affect slightly on amounts of used chemicals.*

Computational assessment – NP water treatments

Similarly, the sequential treatments to minimize calcium concentration in NP water were screened. The pH of NP water was first raised with different alkalis; $Ca(OH)_2$, NaOH and Na_2CO_3 and the precipitate was removed. Next, carbon dioxide was fed to the solute aiming to precipitate calcium as $CaCO_3$. The CO_2 treatment simultaneously lowered the pH.

If $Ca(OH)_2$ was used (see Figure 3), the additional gypsum precipitate formed during pH rise, however dissolved Ca concentration started to rise near pH 12. During CO_2 dosing, Ca first precipitated as $CaCO_3$, and next dissolved again when the decrease in the pH continued. If NaOH was used (Figure 3), no gypsum formed during pH rise. During CO_2 dosing, Ca first precipitated as $CaCO_3$, and next dissolved again when the decrease in the pH continued, similar to $Ca(OH)_2$ + CO_2 treatment. However, when NaOH + CO_2 was applied, the possible pH ranges were larger than when $Ca(OH)_2$ + CO_2 was applied. This may affect the applicability of the method in the experimental work. With both alkalis, Mg precipitated as MgOH and Fe precipitated as $Fe(OH)_3$ during CO_2 dosing (Figure 4).

If Na_2CO_3 was applied (Figure 5), Ca precipitated as $CaCO_3$ with the alkali addition only and CO_2 treatment was not needed. Simulation was carried out with two initial pH levels (9 and 10.4) as the pH of water sample were lowered during storage. Very low calcium content (Ca < 10 mg/L) was reached before pH 10.1 or 10.5 depending on starting pH of solute.

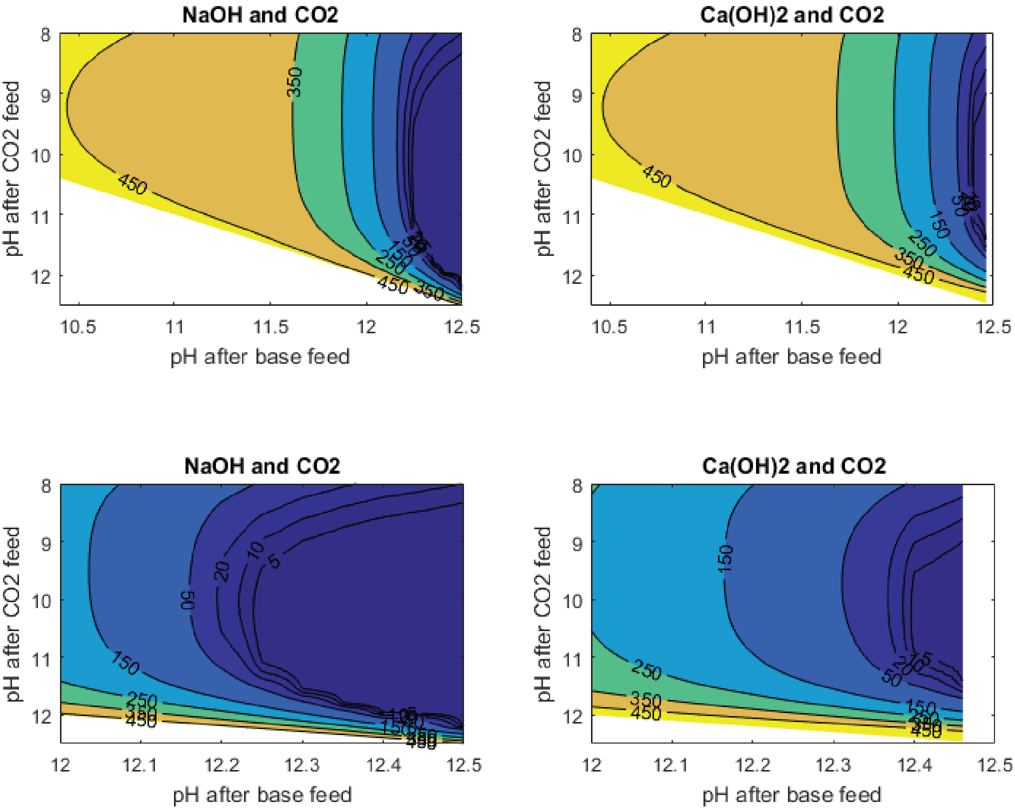

***Figure 3.** Treatment of NP overflow with base (NaOH left and $Ca(OH)_2$ right) and CO_2. Calcium ion concentrations in solute as function of pH after base feed and pH after CO_2 feed, mg/L. Bottom figures are enlargements of pH range 12-12.5.*

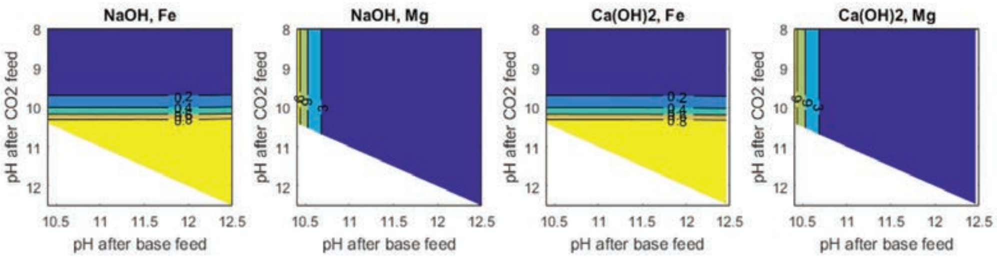

Figure 4. Treatment of NP overflow with base (NaOH left and Ca(OH)2 right) and CO2. Magnesium and iron ion concentrations in solute as function of pH after base feed and pH after CO2 feed, mg/L.

Based on simulation results Ca concentration in NP water can be decreased below 10 mg/L, with all studied options.

NaOH treatment, up to pH 5, of metal recovery treatments was performed experimentally. Composition of used water, raffinate 2, differed somewhat from the one used in simulation (see Table 1). NaOH treatment of raffinate 2 was also simulated to obtain comparable data. Figure 6 shows the results of the prediction and the experiment. Based on the results similar amount of NaOH was needed to reach pH 5, however the more rapid consumption of NaOH was predicted than what was obtained in the experiments. Moreover, computational assessment predicted that $Al(OH)_3$ precipitates selectively in the applied pH range, but in experiments precipitate seemed to contain also other phases and the amount of precipitate is significantly larger than predicted.

Experimental – NP water treatments

All three NP water treatments were carried out in experimental research. Figure 7 (left) shows the results of NaOH and $Ca(OH)_2$ treatments with CO_2 treatment. Alkali was first added to reach pH 12.2, and next CO_2 addition was carried out. Based on the experiments, dissolved Ca content first decreases during CO_2 dosing, and while continuing CO_2 dosing Ca dissolves again. When NaOH was used as alkali low (<10 mg/L) Ca content was achieved. When $Ca(OH)_2$ was applied, low Ca content was not achieved, but qualitatively similar phenomena occurred. The reason for this behaviour may be, that the pH was not raised high enough in the experiments, because based on computational assessment CO_2 dosing should be started after reaching pH of 12.4. Figure 7 (right) shows the results of Na_2CO_3 treatment. As predicted by modelling, Na_2CO_3 precipitation re-

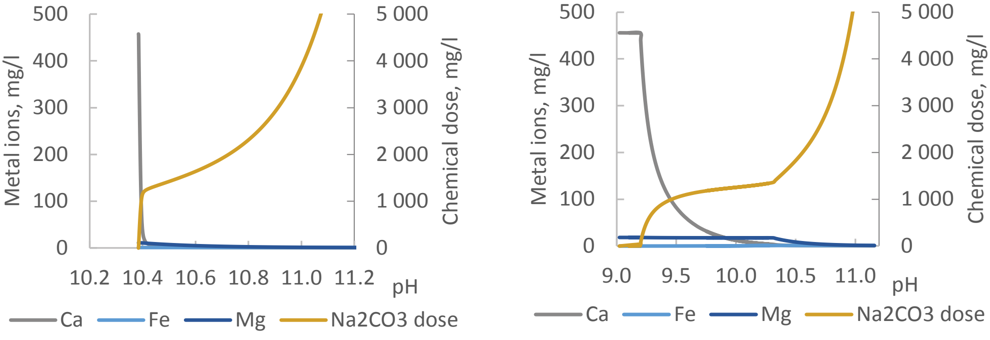

Figure 5. Treatment of NP water with Na_2CO_3. Metal ion concentrations and sodium carbonate feed as a function of pH, mg/L. Initial pH of NP water 10.4 (left) and 9.0 (right).

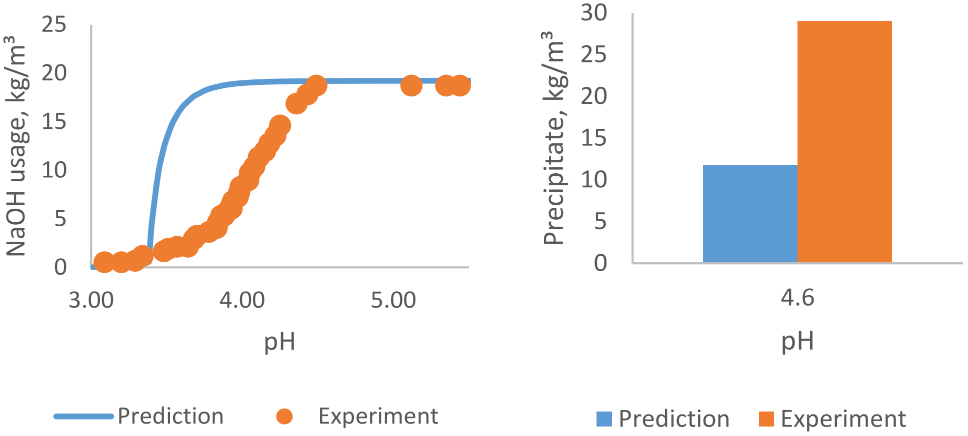

Figure 6. Treatment of raffinate 2 with NaOH. Alkali usage as a function of pH (left), and precipitate after treatment (right).

moves almost all dissolved calcium from water before pH reaches value 10.5.

Conclusions

From the results gained within this study, it can be deduced that computational methods can be utilized when surveying for new process concepts. They are useful tools especially in early stage evaluation of the feasibility of a new solution and in screening the most potential process options among several possibilities. However, the process options with the most potential still need validation with experimental studies. The simulations help guide also the experimental studies and reduce the amount of work needed.

NaOH and Na_2CO_3 can be used for fractionating metals from raffinate without simultaneous gypsum precipitation based on the computational assessment. However, the experimental validation of this concept was vague, and the topic is suggested to be studied in more detail. The other concept, the possibilities of calcium removal were assessed by simulation and later successfully confirmed with experimental results. Based on results NaOH + CO_2 and Na_2CO_3 can be used for calcium removal. Calcium removal with $Ca(OH)_2$ + CO_2 succeeded only in simulations. The process kinetics and super-saturations might result in variations between the predicted and validated results.

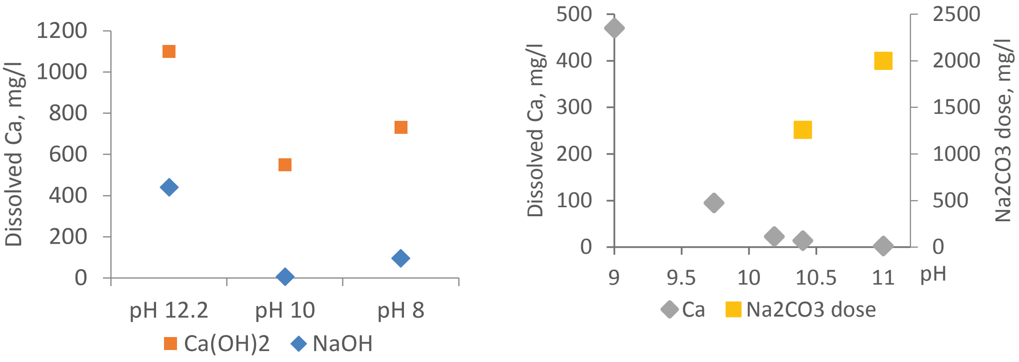

Figure 7. Dissolved calcium content after different experimental treatments. Sequential treatment with NaOH or lime up to pH 12.2 continued with acidification (left), Na_2CO_3 as treatment chemical (right).

Acknowledgements

The research was carried out in the MinePro project financed by Finnish Funding Agency for Innovation (Business Finland), VTT Research Centre of Finland Ltd (VTT) and the companies. The authors thank Business Finland, VTT, Terrafame Group, Aquaminerals, Teollisuuden Vesi, Sansox, Solenis, and Outotec for their support of the MinePro project.

References

Geldenhuys, A.J., Maree, J.P.P., de Beer, M., Hlabela, P., 2003. An integrated limestone/lime process for partial sulphate removal. J. South. African Inst. Min. Metall. 103, 345–354.

Kaartinen, T., Kangas, P., Arnold, M., 2017. Valorisation of Separated Solids from Mine Water Treatment. 13th Int. Mine Water Assoc. Congr. (IMWA 2017) 55–63.

Koukkari, P., Penttilä, K., Hack, K., Petersen, S., 2000. CHEMSHEET – An Efficient Worksheet Tool for Thermodynamic Process Simulation. Microstruct. Mech. Prop. Process. 3, 323–330. doi:10.1002/3527606157.ch51

Kyllönen, H., Grönroos, A., Järvelä, E., Heikkinen, J., Tang, C., 2016. Experimental Aspects of Scaling Control in Membrane Filtration of Mine Water. Mine Water Environ. 36, 193–198. doi:10.1007/s10230-016-0415-3

Kyllönen, H., Järvelä, E., Heikkinen, J., Urpanen, M., Grönroos, A., 2017. Emergent membrane technologies for mine water purification. IMWA 2017 Conf.

Pajarre, R., Koukkari, P., Kangas, P., 2018. Industrial and mine water chemistry Advanced aqueous database for modelling industrial processes. VTT Technology Report 321.

On-Site Pilot-Scale Demonstration of a Low-Cost Biological Process for the Treatment of High-Sulphate Mine Waters

John William Neale[1], Mariekie Gericke[2] and Ritva Mühlbauer[3]

[1]*Mintek, South Africa, JohnN@mintek.co.za*
[2]*Mintek, South Africa, MariekieG@mintek.co.za*
[3]*Anglo American Thermal Coal, South Africa, ritva.muhlbauer@angloamerican.com*

Abstract

This paper describes the commissioning and operation of a pilot-scale passive biological sulphate reduction (BSR) process, treating mine-impacted water from a South African coal mine. The pilot plant comprises three 7 m³ reactors, with a nominal feed rate of 245 L/d. The substrate comprises woodchips, wood shavings, hay, lucerne and cow manure. Process performance is evaluated relative to influent pH level, hydraulic residence time (HRT), ambient temperature variations, and substrate replenishment rate.

Early results demonstrate removal of sufficient sulphate to meet regulatory requirements for discharge or agricultural use. Benchmark capital and operating cost estimates of the process are discussed.

Keywords: passive treatment, biological sulphate reduction, mine waters, pilot plant

Introduction

The threat to the South African environment from acid mine drainage and mine-impacted waters is well documented. Effluents from the South African gold- and coal-mining industries can severely impact upon the quality of water supplies, both during the mines' operating lives and after their closure. Many such operations are nearing the ends of their operating life-cycles, and suitable processes for the post-closure treatment of decants and seepages are urgently required. These acidic, sulphate-laden and metal-contaminated waters are typically treated by lime neutralisation, which removes the metals and increases the pH level, but has little impact on the sulphate level. In South Africa, stringent regulations enforce low sulphate discharge limits of 200 600 mg/L. Biological treatment using sulphate-reducing bacteria is being investigated as an alternative to conventional technologies for the treatment of mine-impacted effluents. A passive process, with relatively low capital and operating costs, is ideally suited to post-closure applications, and laboratory-scale test work has demonstrated that it can meet the regulatory sulphate discharge limits.

Previous laboratory-scale test work (Neale *et al*. 2017) demonstrated that over 95 % of the sulphate in acidic mine-impacted waters laden with around 3 000 mg/L of sulphate could be removed in a passive BSR process, at an HRT of 4 days. The pH levels of the waters increased to around 7, residual metals were precipitated, and effluent sulphate concentrations of between 90 and 140 mg/L were achieved. It was also shown that residual sulphide and manganese in the BSR effluent could be removed using a two-stage process comprising an oxidation pond and a pebble-bed pond. Significant reductions in the ammonium, bicarbonate, phosphate and calcium levels, and minor reductions in the magnesium and potassium levels, were also achieved.

Based on these results, a pilot plant was designed and constructed. The plant was designed conservatively, with an HRT per stage of 6 days, at a feed rate of 245 L/d, giving a plant comprising three reactors with an active volume of around 7 m³ each. This paper describes the commissioning and early operation of the pilot plant, which was installed next to a raw water dam at a South African coal mine in Mpumalanga Province, South Africa. The acidic, sulphate-laden raw water from the dam is fed to the BSR plant, and the treated effluent is returned to the dam.

Pilot Plant Commissioning

To facilitate plant start-up, a suitable inoculum of around 6 000 L was prepared at Mintek. The substrate, consisting of a mix of woodchips, wood shavings, hay, lucerne and kraal manure, was blended at Mintek and loaded into 1 m3 bulk bags. These pre-prepared materials, together with the pilot plant equipment, were transported to the site, and the equipment was installed. Commissioning included loading of the vessels with a layer of pebbles and the pre-mixed substrate, and introducing the pre-prepared inoculum, which took place on 15 September 2017.

A crane was used to load the vessels. The pebbles were loaded first, by placing bulk bags in the open vessels, cutting the bags open, and then lifting the bags out. Each vessel was filled with 1 000 kg of pebbles, which was sufficient to cover the outlet box at the base of each vessel. The pre-mixed substrate was loaded in a similar way. Bulk bags containing the substrate were lifted by crane and positioned in the vessels, the bags were cut open, and then lifted out of the vessels.

In an attempt to promote rapid inoculation and start-up of the plant, some of the bags of pre-mixed substrate were contacted with inoculum prior to being transported to the site. The bags were dipped into one of the inoculum containers, and then lifted out and drained. The pre-wetted substrate was added to Reactor 1, since it was considered that a fast start-up in Reactor 1 would promote faster commissioning of the process once a feed was applied.

Following the loading of the substrate, a mixture of pre-prepared inoculum and raw water was pumped into the vessels, in an approximate ratio of 70 % inoculum to 30 % raw water. At the time of inoculating the plant, the pH level of the raw water was around 2.85, and so the 70:30 ratio of inoculum to raw water was chosen to ensure that the pH level was not too low. Small quantities of nutrients (ammonium sulphate and phosphoric acid) were added to the vessels to promote bacterial growth.

As the vessels were filled, it was discovered that there was a leak in the pipework of Reactor 2, and so the inoculation of Reactor 2 was postponed. In addition, it was noted that the quantity of substrate and fluid that had been added to Reactors 1 and 3 was not sufficient to completely fill the vessels. Following the loading and inoculation of the vessels, they were allowed to stand for a period of several weeks to enable the inoculum to take effect, and to observe whether any expansion or contraction of the substrate beds took place.

Two weeks after the loading and inoculation of the vessels, the first set of routine measurements was undertaken in Reactors 1 and 3 (on 29 September 2017), as summarised in tab. 1.

These results clearly show the beneficial impact of the pre-wetted substrate mixture in Reactor 1. The low redox potential and high pH level in that vessel indicated that bacterial activity had been established in Reactor 1, but was not yet apparent in Reactor 3. The much lower sulphate concentration of 1.36 g/L in Reactor 1 compared to Reactor 3 confirmed that biological sulphate reduction activity had been established in this vessel.

Table 1. *Initial routine measurements in Reactors 1 and 3, two weeks after inoculation*

Reactor	Temperature (°C)	Redox potential (mV, Ag|AgCl)	pH level	Electrical conductivity (mS/cm)	[SO_4^{2-}] (g/L)
1	20.0	333	6.85	10.60	1.36
3	19.7	190	3.02	10.82	5.11

On this day, the leak in Reactor 2 was repaired, in preparation for inoculating the vessel four days later, on 3 October 2017, when a mixture of inoculum, raw water and small amounts nutrients was introduced to Reactor 2. The ratio of inoculum to raw water was increased to 90:10, to try and alleviate the impact of the low pH level of the raw water. Additional quantities of inoculum and raw water were also added to Reactors 1 and 3. A second set of routine measurements was undertaken in Reactors 1 and 3, as summarised in tab. 2.

These measurements indicated that the conditions in Reactor 3 were improving, with the redox potential declining and the pH rising, albeit slowly. The increased sulphate concentration in Reactor 1 was caused by the introduction of a fresh quantity of raw water to this vessel.

The feed pump was commissioned, and recirculation from the bottom to the top of Reactor 1 was initiated, to facilitate mixing of the fluid in this vessel.

Three days later, on 6 October 2017, a further large quantity of inoculum was added to Reactor 2, together with a small quantity of raw water. The routine measurements are summarised in tab. 3.

Rapid biological sulphate reduction, facilitated by the introduction of fluid recirculation in the vessel, had occurred in Reactor 1, with the sulphate concentration declining to below 1 g/L. The sharp decline in the electrical conductivity also indicated to a high level of activity in this vessel. The benefit of introducing a smaller volume of raw water in Reactor 2 was apparent from the favourable redox potential and pH level measurements, indicating that biological activity had been initiated in this vessel within three days of inoculation. In Reactor 3, the redox potential was slowly declining, the pH level was slowly rising, but the sulphate concentration remained high.

Over the following weeks, intermittent feeding of the process was undertaken by periodically pumping 200 L batches of raw water into Reactor 1, and allowing it to overflow into Reactors 2 and 3 in order to fill them. This was done on three occasions between 27 October and 10 November 2017. By 15 November 2017, the conditions in the three vessels were as summarised in tab. 4, and on this day, 61 days after introduction of the first inoculum, continuous feed to the plant was initiated at a rate of 97.9 L/d, giving a HRT in each reactor of 15.8 d.

Table 2. *Second set of routine measurements in Reactors 1 and 3*

Reactor	Temperature (°C)	Redox potential (mV, Ag|AgCl)	pH level	Electrical conductivity (mS/cm)	[SO_4^{2-}] (g/L)
1	-	343	6.89	10.51	5.79
3	-	50	3.61	10.41	6.66

Table 3. *Third set of routine measurements in Reactors 1, 2 and 3*

Reactor	Temperature (°C)	Redox potential (mV, Ag|AgCl)	pH level	Electrical conductivity (mS/cm)	[SO_4^{2-}] (g/L)
1	20.8	345	6.68	8.94	0.912
2	20.3	275	6.32	10.81	1.83
3	18.9	34	3.93	10.56	6.70

Table 4. *Routine measurements in Reactors 1, 2 and 3 prior to start of continuous operation*

Reactor	Temperature (°C)	Redox potential (mV, Ag|AgCl)	pH level	Electrical conductivity (mS/cm)	[SO_4^{2-}] (g/L)
1	25.0	355	7.17	7.91	0.265
2	22.9	359	6.90	7.99	0.209
3	24.8	251	6.35	9.09	3.27

Figure 1 A view of the installed biological sulphate reduction pilot plant

The pH level of the raw water from the storage dam remained low, and so a mixing tank was installed to facilitate adjustment of the pH levels using lime. Raw water is pumped into the tank, where lime is added manually to raise the pH to the desired level. Once that is achieved, the mixing is stopped, the sludge is settled, and the clear water is pumped into the feed tanks.

The pilot plant is shown in fig. 1. This shows the feed vessels (partially obscured on the left), the three reaction vessels in the centre, a downstream treatment plant and the product collection vessels on the right, and the lime neutralisation tank at centre right, in front of Reactor 3

Pilot Plant Operation

Following the start of the continuous feed to the process on day 61, the objective was to increase the throughput to obtain a HRT in the first reactor of 7 days, and then to maintain that feed rate for some time. The feed rate to the plant, as well as the HRT in Reactor 1, is shown in fig. 2. The flow rate is shown in three ways: based on the feed pump setting, on the measured feed volume, and on the measured product volume. Occasional blockages were experienced in the feed line, which accounts for the scatter in the measured data.

Treated effluent first emerged on day 73 (27 November 2017). The feed flow rate was increased to the target of 220.3 L/d by 21 December 2017 (day 97), giving an HRT in Reactor 1 of 7.0 days.

The routine measurements that have been made since the start of the plant operations are shown in fig. 3, comprising the temperatures, pH levels, redox potentials, electrical conductivities and sulphate concentrations. The calculated sulphate removal levels are also shown in fig. 3.

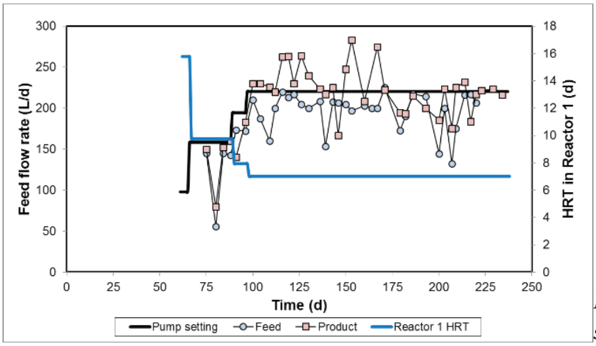

Figure 2 Feed flow rate to the on-site pilot plant

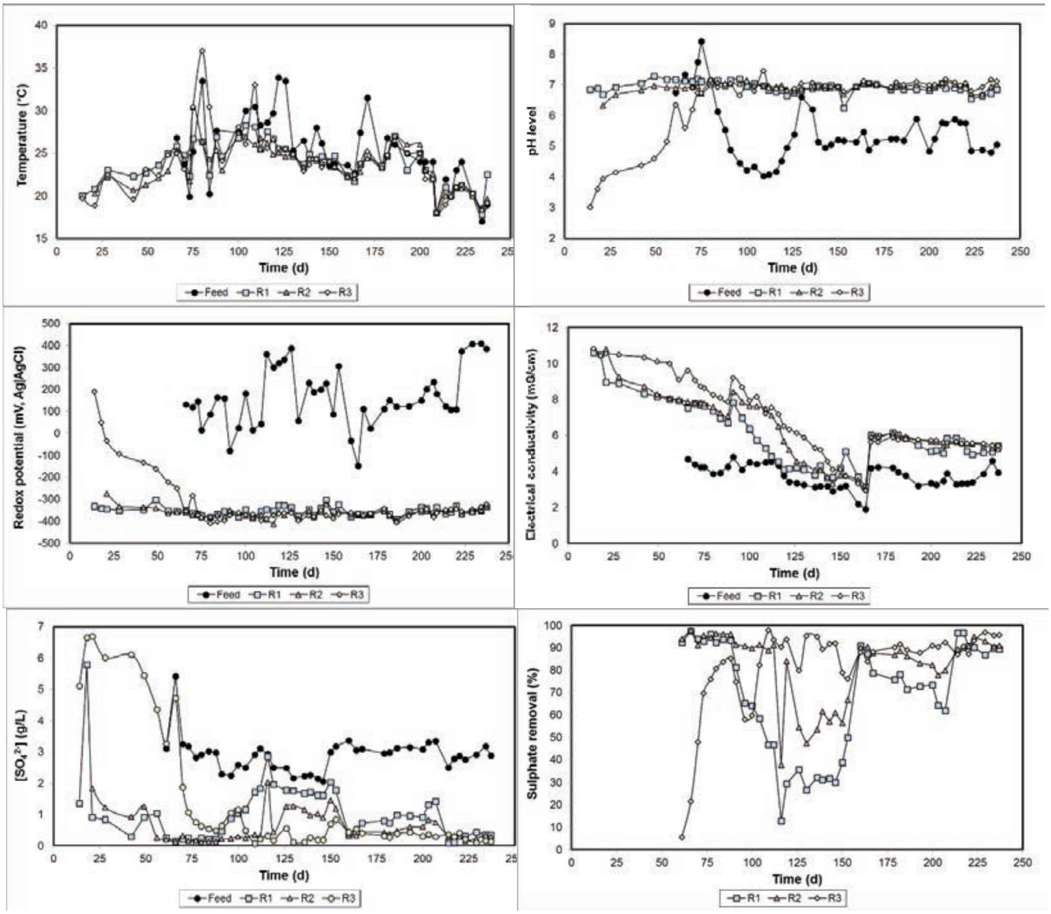

Figure 3 *Performance of the on-site pilot plant*

Following the introduction of continuous feeding on day 61, and the subsequent ramp-up of the feed rate between days 66 and 97, the following observations can be made:

- The temperatures varied quite widely, reflecting the warm conditions that are typical in summer. Generally, the temperatures remained between 25 and 30 °C through the summer months, but have begun to fall recently with the onset of autumn.
- The pH level of the feed was initially high, at around 7, owing to over-addition of lime in the pre-neutralisation tank. The current target for the pH level of the feed is 5.
- The pH levels in all three BSR reaction vessels have been maintained in the region of 7.
- The redox potentials in all three BSR reaction vessels have been maintained within a range of between 350 and 380 mV vs Ag|AgCl, which is considered ideal for the BSR process.
- The electrical conductivities in all three vessels continued to decrease after the continuous feed was applied, and the rate of decrease increased as the feed rate was ramped up. By this time, the substrate beds in all three vessels had expanded to such an extent that it was not possible to gain access to the water surface in Reactor 1 to initiate replenishment of the fast-reacting components of the substrate. Partial access to the surface was eventually possible on day 119 (12 January 2018), and substrate replenishment was initiated on that day. On day 150 (12 February 2018), the substrate replenishment regime was modified by reducing the quantity of

kraal manure being added, and introducing the addition of lucerne pellets, to mirror the substrate replenishment schedule that was implemented in the laboratory-scale test work. Limited availability of the substrates on site meant that the substrate replenishment regime was not steady during April 2018, but regular replenishment has now been instituted and will be maintained. The replenishment schedule is detailed in tab. 5.

On day 153, an increase in the electrical conductivity was observed, but it subsequently declined again. However, it is suspected that the electrical conductivity meter that was in use at that stage developed a fault, and so the measurements taken between then and day 167, when a new meter and probe were utilised, should be disregarded. The latest indications are that the electrical conductivities have stabilised in the region of 5–6 mS/cm in all three vessels.

- The average sulphate concentration of the feed to the plant has been around 3 g/L, and it has varied between about 2.0 and 3.5 g/L.
- Sulphate concentrations as low as 120 130 mg/L were recorded in Reactor 2 between days 80 and 88, corresponding to a sulphate removal of over 95 %. However, as the feed rate was increased, and prior to the introduction of a substrate replenishment regime on day 119, the sulphate concentrations in both Reactor 1 and Reactor 2 began to increase. Encouragingly, however, the sulphate concentration in Reactor 3 remained low, with the overall sulphate removal in the three-stage system remaining above 90 %.
- Following the introduction of substrate replenishment on day 119, there was a noticeable improvement in the overall performance, but this declined as the substrate replenishment was irregular. With more regular replenishment, the sulphate concentrations in all three vessels have stabilised at around 350 mg/L in Reactor 1 and about 130 mg/L in Reactor 3, corresponding to sulphate removal efficiencies of between 90 and 96 %. The system is now reaching a steady operating condition, which will enable the baseline performance under the current feed condition to be established.

The results of the on-site pilot plant operation presented here are preliminary, since the operation of the plant is still in the early stages. Future plans for the operation of the pilot plant include the following:

- Continuing the operation under the current feed rate to establish a baseline performance.
- Increasing the feed rate to establish the impact on the process performance.
- Reducing the feed pH to a level of around 4 to establish the impact on the process performance.
- Operation through the winter months to establish the impact of colder ambient temperatures on the process performance.
- Optimisation of the rate of replenishment of the fast-reacting components of the substrate. The possibility of utilising other solid and possibly liquid substrates may be investigated and evaluated with respect to the operating cost and operability of the passive BSR process.
- Evaluation of the microbiological components in the BSR process, to develop an understanding of how these components respond to changes in the feed conditions,

Table 5. *Schedule for the addition of fast-reacting substrate in the on-site pilot plant*

Day	Date	Kraal manure added (L)	Lucerne pellets added (L)
119, 130, 136, 143	12, 23, 29 January, 5 February 2018	240	0
150	12 February 2018	120	120
193, 200	27 March, 3 April 2018	120	0
207	10 April 2018	0	120
223	26 April 2018	120	0
243	16 May 2018	120	120

the ambient temperature, and changes in the substrate replenishment rates.

- Expansion of the assays performed on the samples to include the following: a wide range of metals, sulphide, ammonium, bicarbonate, sodium, potassium, magnesium, chemical oxygen demand (COD), and volatile fatty acids (VFAs).
- Commissioning of the downstream polishing plant to assess the impact on sulphide and manganese removal, and possibly on the reduction in the ammonium, bicarbonate, sodium, calcium, magnesium, phosphate and potassium concentrations, and also of any trace metals that remain in the treated effluent from the BSR process.

Benchmark Costing

A preliminary techno-economic evaluation of passive water treatments was undertaken, consisting of a "benchmarking exercise", by extracting capital and operating costs for passive and semi-passive BSR processes from the literature. Standard cost engineering techniques were applied to bring the costs to a common base of July 2017, and to scale them to a common treatment rate of 1 ML/d, which is envisaged for an industrial-scale operation. Based on this preliminary benchmarking study, the costs for a 1 ML/d passive water treatment plant are estimated to be:

- Capital cost: R25.5-million
- Operating cost: R4.45/m^3 of water treated

An in-house process design and costing package is being developed to produce more accurate costs for the specific passive BSR processes that are under development, utilising local cost data together with the process parameters obtained from the on-site pilot plant operation.

Conclusion

The successful demonstration of a low-cost, low-maintenance passive BSR process during an extended on-site trial will position it for consideration by the coal- and gold-mining industries for the treatment of mine waters emanating from existing processes, and especially after mine closure, producing effluents within regulatory limits specified for discharge or re-use.

Acknowledgements

This paper is published with the permission of Mintek. The work reported in this publication was conducted within the framework of the ACQUEAU-labelled project called MI-WARE (Mine water as a resource). Mintek's contribution to the project is funded jointly by Mintek and the South African Department of Science and Technology (DST), overseen by the Water Research Commission (WRC).

References

Neale JW, Muller HH, Gericke M Mühlbauer R (2017) Low-cost biological treatment of metal- and sulphate-contaminated mine waters. In: Wolkersdorfer C, Sartz L, Sillanpää M, Häkkinen A [Eds.] Proceedings of 13th International Mine Water Association Congress – Mine Water & Circular Economy, Volume 1. Lappeenranta University of Technology Scientific and Expertise Publications, Lappeenranta, Finland. p 453—460

Geochemistry and Mineralogy of Precipitates Formed During Passive Treatment of Acid Mine Drainage in the Ermelo Coalfield, South Africa

N.O. Novhe[1], B. Yibas[1,2], H. Coetzee[1], T Mashalane[1], M. Atanasova[1],
V.R.K. Vadapalli[1], C. Wolkersdorfer[3,4]

[1]*Council for Geoscience, 280 Pretoria Rd, Silverton, 0184, South Africa, onovhe@geoscience.org.za*
[2]*Department of Environmental Sciences, College of Agriculture and Environmental Sciences, University of South Africa, Florida Campus, Johannesburg, South Africa*
[3]*SARChI Chair for Mine Water Management, Department of Environmental, Water, and Earth Sciences Tshwane University of Technology Pretoria South Africa*
[4]*Laboratory of Green Chemistry, Lappeenranta University of Technology Mikkeli Finland*

Abstract

To optimise a passive treatment system for acid mine drainage, this study involved geochemical and mineralogical characterisation of resulting precipitates, using XRF, XRD and geochemical speciation modelling tools. Contaminants are removed as metal sulfides, sulfates and oxy-hydroxide in anaerobic units and as secondary oxides or hydroxides in aerobic units. The mineral phases formed are also responsible for attenuation of other trace elements such as Zn, Ni, Cu, Co, Pb, and REE (such as Ce, La, Nd, Y and Yb) and also control their mobility and fate in the environment. Accumulation of chemical constituents may present an opportunity for metal recovery.

Keywords: Anaerobic and aerobic passive treatment systems, XRF, XRD, Mineral phases, PHREEQC geochemical modelling

Introduction

Passive treatment is considered as a promising long-term solution for the management of polluted mine water in many parts of the world (Hedin et al. 1994; Ziemkiewicz et al. 2001). To contribute towards the development of sustainable mine water management solutions in South Africa, research is on-going to assess the applicability of passive treatment systems, evaluate their performance (to optimise the design criteria), and improve their efficiency and longevity.

Attenuation of contaminants during passive treatment of acid mine drainage is very complex and comprised of a number of reactions that occur under different redox conditions, such as formation and precipitation of metal hydroxides or oxides (due to oxidation reactions), microbial sulfate reduction forming metal sulfides, organic complexation reactions, ion exchange reactions and direct uptake of chemical constituents by living plants (phytoremediation) (Gusek et al. 2009). Some chemical constituents can be removed under both reducing and oxidising conditions (e.g. Fe, As, Al), whereas some can only be removed under oxidising conditions (e.g. Mn) or reducing conditions (e.g. sulfate, U, Co, Zn). Understanding these processes is important for proper design and optimisation of passive treatment systems.

This study involved geochemical and mineralogical characterisation of precipitates formed in a pilot-scale passive treatment plant designed to treat acid mine drainage discharging from an abandoned coal mine. The pilot-scale plant, which was operated for 15 months, successfully neutralised the water and substantially removed contaminants, such as Fe, Al, Co, Zn, Ni, As, Pb, V, and Cu but with minimal SO_4^{2-}-reduction.

Study area and methodology

The pilot plant is situated near Carolina in the Mpumalanga Province, South Africa. Geologically, the area forms part of the Ermelo coalfield. All of the coal seams occur within the Vryheid Formation of the Ecca Group, Karoo Supergroup. Sandstones with subordinate shales represent the bulk of the Vryheid Formation (Bell & Jeremy 2002).

A pilot-scale passive treatment plant consisting of integrated anaerobic and aerobic units was constructed to treat 1440 L of acid mine drainage per day from an abandoned underground coal mine (Fig. 1). The anaerobic unit used is a reducing alkalinity producing system (RAPS), which combines the mechanisms of anaerobic treatment wetlands and anoxic limestone drains, as developed by Kepler and McCleary (1994). Aerobic units consisted of an oxidising pond and a cascading trench. The pilot plant operated for 15 months, with regular monitoring of the water quality. After 12 months of operation, samples of precipitates were collected from the top and bottom of the units, air dried and analysed by means of X-ray fluorescence (XRF) for metal concentrations, as well as X-ray diffraction (XRD) and scanning electron microscopy (SEM) for mineralogical composition. The samples were sent to the Council for Geoscience's laboratory in Pretoria, South Africa, for analysis. To supplement the results obtained, geochemical modelling with PHREEQC code and the PHREEQC database (*Phreeqc.dat*) (Parkhurst and Appelo 2013) were also used to predict mineral phases that are likely to precipitate. Saturation indices for different mineral phases were determined from the water quality results. Species which are more likely to precipitate were determined using the saturation index (SI), where SI < 1 indicates an undersaturated solution, SI = 1 a saturated solution and SI > 1a supersaturated solution.

Results and discussions

Geochemical composition

From the results of the XRF analysis for both top and bottom layers, it can be seen that Fe oxides are dominant, especially in the oxidation pond and at the top of RAPS units (Fig. 2a). The Fe concentration decreases from the top to the bottom layers of the treatment units and this can be attributed to a decrease in oxygen ingress or oxidation rates with depth i.e. 54.46 to 28.52 wt%; 62.48 to 13.09 wt% and 78.10 to 65.08 wt% in the RAPS and oxidising units, respectively. Aluminium (expressed as Al_2O_3) is also dominant in the RAPS units, in addition to Fe and it increases with depth and depends on pH, i.e. 0.96 to 37.58 wt% and 11.35 to 18.30 wt%; 0.52–0.82 wt% (wt % expressed as oxides) for RAPS and aerobic units, respectively. Ca is also present in considerable amounts, especially in the RAPS units. Its concentration increases with depth, indicating dissolution of limestone in the RAPS units.

Concentrations of trace metals increase from the top to the bottom of the anaerobic

Figure 1 *Carolina pilot passive treatment RAPS and oxidation units*

units i.e. 33 to 8,839 mg/kg; 13 to 1,717 mg/kg; 7.6 to 1,569 and 102 to 118 mg/kg for Zn, Ni, Co and Cu respectively (Figure 2b and 2c). Metals, such as Co, Pb, V, Ni and Zn also precipitate in the aerobic units (oxidation pond). This is likely attributable to sorption/co-precipitation with oxy-hydroxides of Fe. Their concentration also increases with depth (from top to bottom) i.e. <1 to 12 mg/kg; 4.7 to 20 mg/kg, and 34 to 97 mg/kg for Co, Ni and Zn respectively.

Rare earth elements (REE) are also accumulated at the bottom of the RAPS units (Fig 2b). Their concentrations are highest in the first unit (RAPS 1) and slightly decrease in RAPS 2. i.e. Ce: 1035 to 1920 mg/kg, La: 300 to 555 mg/kg, Nd: 373 to 692 mg/kg, Y: 365 to 615 mg/kg, Yb: 31 to 60 mg/kg. These elements substantially accumulated at the bottom of the RAPS units, with minor amounts also accumulated on top of the RAPS2 and in the oxidation unit. The accumulation of REEs seems to depend on the pH and secondary mineral phases that are formed in the system. Al, Fe solid phases (oxides/hydroxides), and sulfate complexes have been reported as excellent sorbents for REE (Zänker et al. 2003, Ayora et al. 2016, Zhao et al. 2007). REEs are essential raw materials for various modern technological developments and are in high demand. Hence, accumulation of REE presents an opportunity for economic recovery, which could be used to help offset the costs of remediation.

Mineralogical composition

Mineralogical compositions of the precipitates were analysed by means of XRD and SEM (Fig. 3, 4, 5 and 6). Based on XRD, the top layer of RAPS 1 principally consists of goethite (FeOOH) (84.8 wt %), followed by jarosite $[KFe_3 (SO_4)_2(OH)_6]$ (8.3 wt %) and hematite (3.32 wt %), whereas the bottom layer consists of gypsum (23.15 wt %), jarosite (10.96 wt %) and sulfur (7.91 wt %). The mineralogical composition has been confirmed by SEM analyses (Fig. 3 and 4). The presence of high concentrations of iron hydroxide on the top layer of RAPS1 is indicative of a high rate of oxidation. The presence of jarosite is indicative of a low pH on top of RAPS1, which is the inlet to the system. However, since this is vertical flow system, the pH increases downwards; hence, the formation of gypsum at the bottom of the unit. Metals, such as Zn and Fe also precipitate as sulfides at the bottom of the RAPS units, which is attributed to microbial sulphate reduction (Fig. 3 and 5).

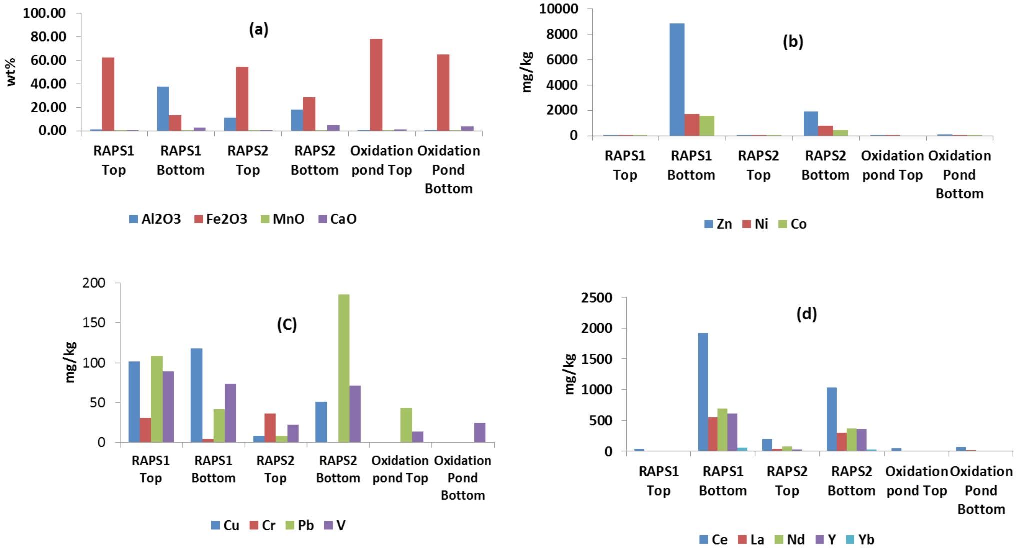

Figure 2 Major, minor elements as oxides (a) and trace elements composition (b, c and d).

The top layer of RAPS2 principally consists of amorphous contents (100 wt %) or poorly crystalline materials that do not contribute to diffraction peaks. Based on field observations, the top layer of RAPS2 consisted of white to orange slurry-like precipitates. The white is attributed to hydroxides of Al while the orange material is composed of hydroxides of Fe, as confirmed by SEM analyses (Fig. 3, 4 and 5). Gypsum (68.9 wt %) is predominant at the bottom of the RAPS2 unit, where the pH is higher and sometimes occurs as well-developed gypsum crystals (Fig. 6). Goethite is the dominant mineral species in the oxidation pond, especially in the top layer, and this is again attributed to a high rate of oxidation in the pond.

The mineral phases that formed in the passive treatment system are known to be excellent sorbents of trace metals (such as Co, Pb, Cu, Ni, and Zn) and also control their mobility, fate and transport in the environment (Dzombak and Morel 1990, Chapman et al. 1983, Carlson and Schwertmann 1981).

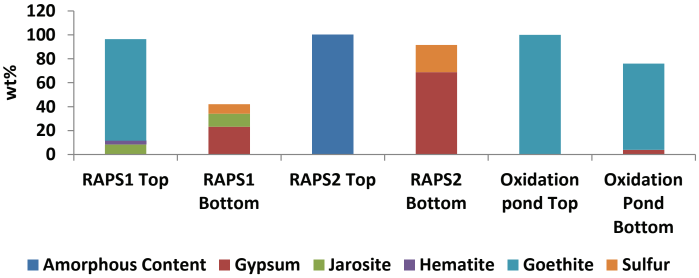

Figure 3 Mineralogical composition of the precipitates

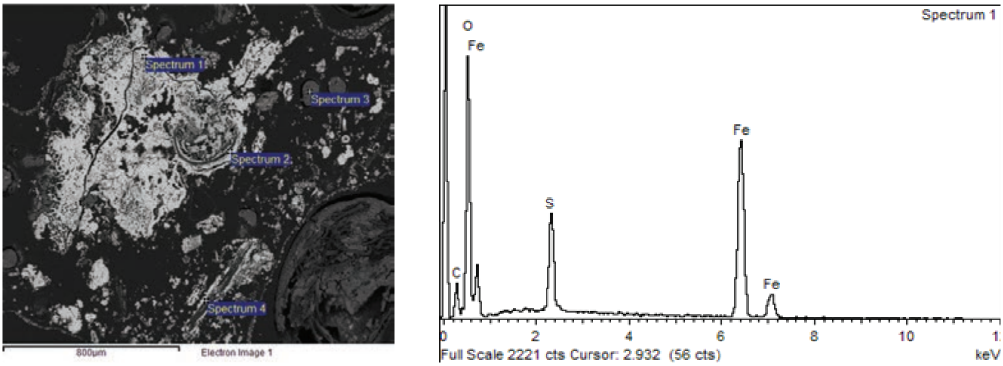

Figure 4 SEM image for the RAPS1 top layer, showing Fe-oxyhydroxide (Geothite) and Fe sufate (Jarosite) spectra

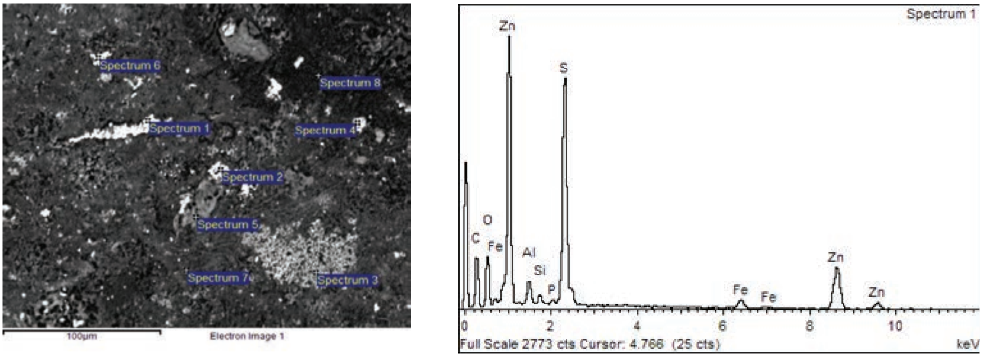

Figure 5 SEM image for the RAPS1 unit bottom layer, showing ZnS, FeS, Al-oxyhydroxide spectra

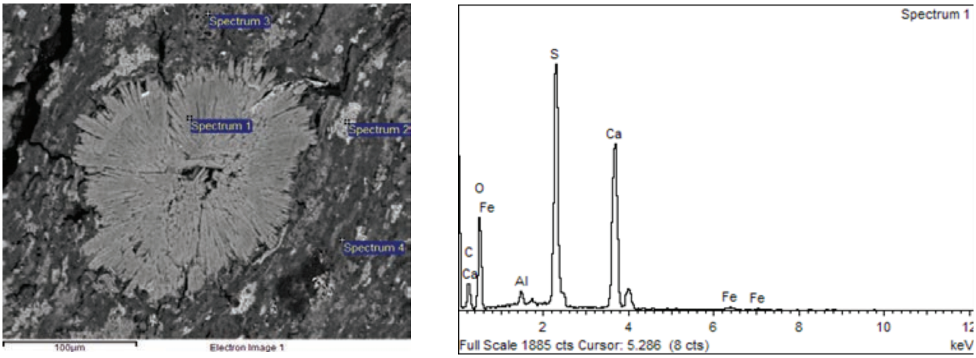

Figure 6 *SEM image for the RAPS2 unit bottom layer and associated spectra.*

Geochemical modelling

Saturation indices of mineral phases were calculated with PHREEQC code for the different treatment units (Fig. 7). The geochemical model confirmed the mineralogical and geochemical composition of the precipitates formed in the treatment units. The feed water or inlet is supersaturated relative to hematite and goethite and slightly saturated relative to jarosite and alunite ($KAl_3(SO_4)_2(OH)_6$. Their saturation indices increase throughout the treatment units, as the pH of water increases. In addition, the water also becomes supersaturated relative to gypsum ($CaSO_4{\cdot}2H_2O$) and gibbsite ($Al(OH)_3$) with increasing pH. Manganese-containing minerals, such as manganite (MnOOH) and pryrolusite, show saturation throughout the treatment units and this justified the minimal reduction of Mn ($MnO_2{\cdot}H_2O$) in the system.

Conclusions

The study revealed that chemical constituents (e.g. Fe, SO_4^{2-}, Al, Mn, Zn, Ni, Cu, Co, Cr, Pb, V, REE) precipitate in the units of the passive treatment system, dependent on various geochemical and biological conditions (such as pH, redox). Contaminants are removed as metal sulfides, sulfates and oxy-hydroxides in anaerobic units and as secondary oxides or hydroxides in aerobic units. The mineral phases formed are also responsible for attenuation of other trace elements such as Zn, Ni, Cu, Co, Pb, REE (e.g. Ce, La, Nd, Y and Yb) due to co-precipitation and control their mobility, fate and transport in the environment.

Accumulation of metals, especially REEs, may present an opportunity for economic metal recovery that can offset the cost of remediation. Sequential extraction is recommended to account for mineral phases responsible for the accumulation of REEs.

The results obtained from this study will enable development of predictive models for the type of precipitates that are likely to form in the passive treatment units, taking into considerations their environmental implications and economic potential. This will also be incorporated in the development of framework for acid mine drainage remediation in South Africa.

Acknowledgements

The authors thank the Department of Mineral Resources for their financial support.

References

Ayora C, Macías F, Torres E, Lozano A, Carrero S, Nieto JM, Pérez-López R, Fernández-Martínez A, Castillo- Miche H (2016) Recovery of Rare Earth Elements and Yttrium from Passive-Remediation Systems of Acid Mine Drainage. Environ. Sci. Technol., 50(15):8255–8262

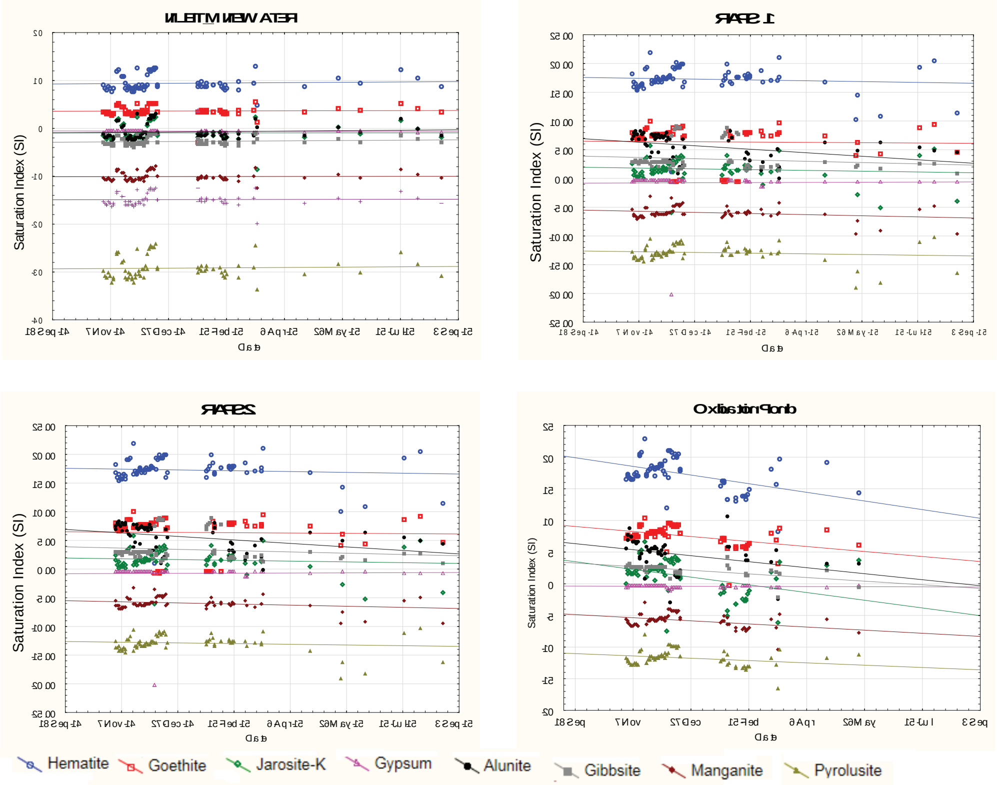

Figure 7 Saturation indices of mineral phases for different treatment units

Carlson L, Schwertmann U (1981) Natural ferrihydrites in surface deposits from Finland and their association with silica. Geochim. Cosmochim. Acta 45:421-429

Chapman BM, Jones DR, Jung RF (1983) Processes controlling metal ion attenuation in acid mine drainage streams. Geochim. Cosmochim. Acta 47:1957-1973

Dzombak DA, Morel FMM (1990) Surface complexation modeling – hydrous ferric oxide: New York, Wiley and Sons

Gusek JJ (2009) A Periodic Table of Passive Treatment for Mining Influenced Water. In R. Barnhisel, ed. 2009 National Meeting of the American Society of Mining and Reclamation. 3134 Montavesta Rd., Lexington, KY 40502: ASMR:550–562

Hedin RS, Watzlaf GR, Nairn RW (1994) Passive treatment of acid-mine drainage with limestone. J Environ Qual 23(6):1338-1345

Kepler DA, McCleary EC (1994). Successive Alkalinity Producing Systerm for the treatment of Acid Mine Drainage. In Pittsburgh, PA: International Land Reclamation and Mine Drainage Conference and the third International on the Abatement of Acid Drainage:195–204

Parkhurst DL, Appelo CAJ (2013) Description of Input and Examples for PHREEQC Version 3 – A Computer Program for Speciation, Batch-Reaction, One-Dimensional Transport, and Inverse Geochemical Calculations. US Geol Surv Tech Methods 6(A43):1-497

Zänker H, Richter W, Hüttig G (2003) Scavenging and immobilization of trace contaminants by colloids in the waters of abandoned ore mines. Colloid Surf. A-Physicochem. Eng. Asp. 217(1–3):21–31

Zhao F, Cong Z, Sun H, Ren D(2007) The geochemistry of rare earth elements (REE) in acid mine drainage from the Sitai coal mine, Shanxi Province, North China. Int. J. Coal Geol. 70(1–3):184–192

Ziemkiewicz P, Skousen J, Simmons J (2001) Cost Benefit Analysis of Passive Treatment Systems. Proceedings, 22nd West Virginia Surface Mine Drainage Task Force Symposium, 3-4 April, Morgantown, WV

The performance of nano-sized Banana Peels in the removal of vanadium from mine water

Opeyemi A. Oyewo[1], Christian Wolkersdorfer[2,3], Maurice S. Onyango[1], Amos Adeniyi[1]

[1]*Department of Chemical, Metallurgical and Materials Engineering, Tshwane University of Technology, Pretoria 0001, South Africa*

[2]*SARChI Chair for Mine Water Management, Department of Environmental, Water, and Earth Sciences, Tshwane University of Technology, Pretoria 0001, South Africa*

[3]*Lappeenranta University of Technology, Laboratory of Green Chemistry, Sammonkatu 12, 50130 Mikkeli, Finland*

Abstract

South African mine water might contain several harmful contaminants such as, but not limited to vanadium. Therefore, this study described the development and application of a newly developed banana peel nano-adsorbent (BPN) for the removal of vanadium from synthetic water. The adsorbent was characterized using scanning electron microscopy (SEM), Fourier transform infra-red (FT-IR), particle size distribution while the amount of rare earth elements (REEs) adsorbed were determined by ICP-OES. It could be shown that the milling process reduced the particle sizes from smaller than 65 µm to below 25 nm and the crystallite sizes from 108 to 12 nm. FT-IR analysis revealed that the coordination and the lanthanide removal results from amine and carboxylic groups with adsorption bands at 889 cm-1 and 1730 cm-1, respectively. Langmuir isotherms gave a good description of vanadium adsorption onto BPN with maximum adsorption capacity of 27.94 mg g-1. However, the matrix of the mine water to be treated substantially determines which sorbent needs to be used

Keywords: mine water, mechanical milling, batch adsorption, agricultural waste, rare earth elements

Introduction

South Africa economy might not survive without mining operation as it has become their source of income over the years. Toxic metals mined such Pb, Cr, and V are used industrially worldwide but also contaminates the surface and underground water due to their bioavailability. In addition, South Africa has been recognised as the second largest steel maker in which vanadium is an important additive in steel making. The contamination is significant therefore also finds its ways into the environment from the industries in which its usage is paramount.

Even though vanadium-laden water has been treated by many researchers via various techniques and mechanisms such as chemical precipitation, solvent extraction, micellar ultrafiltration, ion exchange and adsorption (Lynn and Kerry 2005 ; Srivastava 2006). It has been reported that the use of adsorption process remain the most cost effective method (Alimohammadi et al. 2016; Bakiya et al. 2012)

Adsorption process is highly economical and capable of removing contaminants even at trace level. The use of this technique in water and wastewater treatment due its simplicity, low cost of operation and wide end use is reported (Naeem et al. 2007). However, the success of the above mentioned process is highly dependent on the choice of appropriate media. As such, a number of sorbent materials have been investigated for the removal of vanadium from wastewater which include polymer composite, zeolite, clay and agricultural waste (Abollino et al. 2008; Kaczala et al. 2009; Kurniawan et al. 2006; Mariangela et al. 2012).

Agricultural resources considered as waste, such as sugarcane bagasse, pineapple peels, coconut coir, apple waste and banana peels have been employed to remove metals from waste water. This is possible due to the presence of useful constituents and acid groups such as cellulose, carboxylic and phenolic groups that are necessary for the effective treatment of industrial effluent. These materials can also be used in metal speciation, as in the case of Cr (VI) sorption by coconut coir (Gonzalez et al. 2008). Advances in nanoscience and nanotechnology have expanded the ability to develop nanomaterials with enhanced properties to solve the current problems involving water treatment. The main property that makes nanomaterials attractive is that they are extremely small in size (1-100 nm), which provides higher surface area per unit mass compared to their micron size counterparts (Arup and Jayanta 2015). In this study, nanostructured banana peels were developed in other to take advantage of their improved chemical and physical properties in vanadium removal from aqueous solution.

Experimental

Banana peels (*Musa paradisiacal*) were obtained, cut into chips and washed with deionized water to remove the adhering dirt and then sun dried for 10 days. The dried peels were crushed and screened to obtain a particle size of <65µm. The details of mechanical milling of crushed banana peels (<65µm) and all necessary characterization analyses was reported elsewhere (Oyewo et al. 2016).

Batch equilibrium experiments were performed to determine the performance of BPN on vanadium removal from aqueous prepared by decomposition of ammonium metavanadate in deionised water at around 200 °C (Crans 2005).

Firstly, the effect of solution pH was explored by varying pH from 2 to 10 using either NaOH (0.1 M) or HCl (0.1 M) for initial pH adjustment. The effect of sorbent loading was explored by varying the mass of the sorbent from 0.01 g to 0.2 g while the effect of concentration was explored by varying the concentration of the V synthetic solution from 20 to 200 mg/L. Finally, the effect of temperature was determined varying the temperature from 25 to 45 °C, with a 50 mg/L V solution at a pH of 2.10. The sorbent mass was fixed at 0.2 g for the latter experiments. For each experiment, the bottles were placed in a thermostatic shaker operated at 200 rpm for 24 h. At the end of the contact period, the samples were filtered using 0.2 µm pore size polypropylene syringe filters and the filtrate was analysed by inductive coupled plasma optical emission spectroscopy (ICP-OES) to determine the equilibrium concentration of V.

The percentage removal efficiency Rt was calculated (equation 1):

$$R_t = \frac{C_o - C_e}{C_o} \cdot 100 \qquad (1)$$

where C_o (mg·L^{-1}) is the initial lanthanides concentration, C_e (mg/L^{-1}) the concentration of lanthanides at equilibrium. All batch tests were performed in polypropylene tubes and sorbents separation as well as filtrate analysis was done accordingly.

Results and discussion

Characterization result

It was observed that as the milling progressed, the fracturing of the particles increased and more nanoparticles were formed as shown in Table 1. Clearly, mechanical milling gives a narrow size distribution of BPN which is a necessary precondition for a good adsorption media.

Adsorption results: Effect of pH

The nano-sized banana peels (BPN) removed very high concentration of V at pH 2 (Fig. 1.). A steep decrease in V uptake was observed

***Table 1.** Summary of TEM and particle size distribution analyses of milled banana peels*

Milling time (h)	Average particle size (nm)	Mean crystalline size (nm)	Lattice strain (%)
0	< 65000	108	0.24
10	< 300	71	0.63
20	< 65	20	0.64
30	< 25	12	0.69

with an increase in pH up to 8, indicative of the interaction of cationic V species with the surface hydrophilic of BPN. At low pH, positively charged V species predominant, therefore higher percentage removal observed might be due to hydrophobic interactions and hydrogen bonding since BPN is highly electronegative throughout the pH range (Oyewo et al., 2016). At pH 4–8, anionic V species predominate (Crans 2005) and this could explain the lower removal rates within this range. Crans (2005) reported that a higher pH causes a higher degree of protonation and polymerisation of V ions, which could limit removal of anionic V species, even at optimum pH. Therefore, adsorption of V onto BPN was pH dependent, and mainly occurred due to interaction between hydrophilic surface of BPN and the cationic V group.

Adsorption result: Sorption isotherms

The temperature dependence of V sorption from synthetic water was explored by varying the temperature from 25 to 45 °C (Fig.2). It was observed that an increase in equilibrium concentration increased V equilibrium uptake for all the temperatures studied. Moreover, the adsorption capacity increased as the temperature rose, indicating that V sorption on BPN is temperature dependent. The enhanced sorption at higher temperatures may have been due to a decrease in the thickness of the boundary layer surrounding the BPN. There is also a possibility that the increased movement of the molecules as the temperature rose increased the uptake. The data provided from sorption equilibrium are used to describe the interaction between adsorbate and adsorbent for effective design of an adsorption process. Furthermore, sorption equilibrium data are used in comparing the performance of different media for a given sorption process. Consequently, the experimental data were analysed using Langmuir and Freundlich models (Table 1).

The linear form of the Langmuir and Freundlich adsorption isotherm equations are given in equation (2) and equation (3), respectively:

$$\frac{C_e}{q_e} = \frac{1}{q_o b} + \frac{C_e}{q_o} \qquad (2)$$

$$\log q_e = \log K_F + \frac{1}{n} \log C_e \qquad (3)$$

where C_e (mg/L) is the concentration of V at equilibrium, q_e (mg/g) the V equilibrium uptake, b is the Langmuir constant and qo is the adsorption capacity of the monolayer; K_F and n are the Freundlich parameters related to adsorption capacity and adsorption intensity, respectively.

The Langmuir isotherm parameter q_o, which measures the monolayer capacity of the adsorbent, increased with an increase in temperature, as did the predicted K_F values

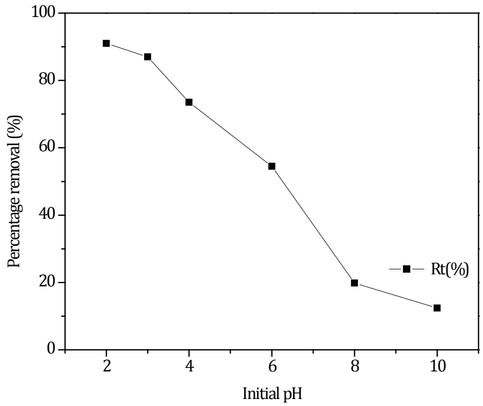

Figure 1 Effect of solution pH in the adsorption of vanadium in synthetic water onto banana peels nanosorbent (BPN)

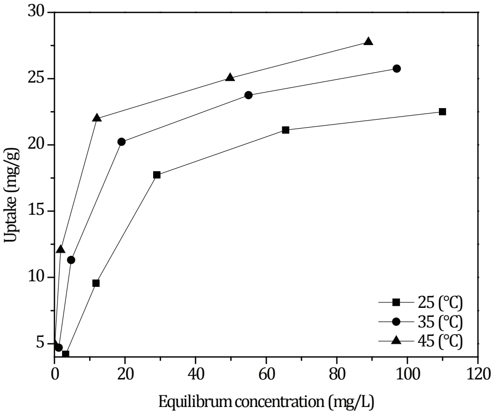

***Figure 2:** Isotherm for vanadium synthetic water onto BPN*

Table 1. Isotherms parameters for vanadium adsorption onto BPN

Temperature (°C)	Langmuir isotherm parameters			Freundlich isotherm parameters		
	q_m (mg/g)	*b* (L/mg)	R^2	K^F (L/g)	*1/n*	R^2
25	26.2	17.10	0.997	2.69	4.9×10^{-1}	0.946
35	27.2	6.62	0.999	5.27	3.8×10^{-1}	0.931
45	27.9	2.48	0.997	9.56	2.6×10^{-1}	0.968

from the Freundlich isotherm; an inconsistent pattern was noted for the Langmuir constant *b*. K_F is related to the sorption capacity, and its increase matched the enhanced sorption (Table 1). Comparing the Langmuir and Freundlich adsorption isotherm correlation values (R^2), the Langmuir isotherm gave a good description of V adsorption onto BPN. This was similar to the results reported by Manohar et al. (2005).

Conclusions

In this study, nanostructure formation of banana peels and its performance in Vanadium removal from aqueous solution has been demonstrated. The surface area increment of crushed banana peels powder (1.0694-4.5547 m^2/g) was observed as milling time increased (0 to 30 h) (Oyewo et al. 2016). The extent of adsorption was controlled primarily by pH and temperature. A solution pH of 2.10 was adopted for the sorption of Vanadium from synthetic water, which is consistent with the chemical interaction between the hydrophilic surface of BPN and the cationic Vanadium species. It was observed that a dosage of 0.2 g of BPN was required for 91 % removal of Vanadium from 100 mg/L initial concentration (aqueous solution). The Langmuir isotherm model gave a good description of Vanadium adsorption onto BPN compare to Freundlich isotherm model. Considering the availability of banana peels as a waste material, and the competitive sorption capacity achieved through milling, this material can be a potential candidate for treatment of vanadium-laden mine water.

Acknowledgement

The authors wish to appreciate National Research Foundation (NRF) for funding, Dr Modiu O. Durowoju, Dr Saliou Diouf, Dr Anthony Muliwa and Dr Olga Oleksiienko for their assistance in characterization and also for fruitful discussions.

References

Abollino O, Giacomino A, Malandrino M, Mentasti E (2008) Interaction of metal ions with montmorillonite and vermiculite. ApplClay Sci 38(3):227-236. doi:10.1016/j.clay.2007.04.002

Arup R, Jayanta B (2015) Nanotechnology in industrial wastewater treatment. IWA Publishing, 12 Caxton street, London

Alimohammadi Z, Younesi H, Bahramifar N (2016) Batch and Column Adsorption of Reactive Red 198 from Textile Industry Effluent by Microporous Activated Carbon Developed from Walnut Shells. Waste and Biomass Valorization 7(5):1255-1270. doi:10.1007/s12649-016-9506-4

Bakiya LK, Sudha PN (2012) Adsorption of Copper (II) ion onto chitosan/sisal/banana fiber hybrid composite. J Environ Sci 3(1):453. doi:10.6088/ijes.2012030131044

Crans DC, (2005) Fifteen years of dancing with vanadium. Pure Appl. Chem., 9(77):1497–1527. doi: 10.1351/pac200577091497.

Oyewo OA, Onyango MS, Wolkersdorfer C (2016) Nanostructure formation, characterization and application of banana peel in trivalent lanthanides removal from aqueous solution. Tshwane university of technology, p 1-17

Gonzalez MH, Araujo GCL, Pelizaro CB, Menezes EA, Lemos SG, de Sousa GB, Nogueira ARA (2008) Coconut coir as biosorbent for Cr(VI) removal from laboratory wastewater. J HazardMat 159(2-3):252-256. doi:10.1016/j.jhazmat.2008.02.014

Kaczala F, Marques M, Hogland W (2009) Lead and vanadium removal from a real industrial wastewater by gravitational settling/sedimentation and sorption onto Pinus sylvestris sawdust. Bioresource Technology 100(1):235-243. doi:http://dx.doi.org/10.1016/j.biortech.2008.05.055

Kurniawan TA, Chan GYS, Lo W-h, Babel S (2006) Comparisons of low-cost adsorbents for treating wastewaters laden with heavy metals. Science of The Total Environment 366(2–3):409-426. doi:http://dx.doi.org/10.1016/j.scitotenv.2005.10.001

Lynn EK, Kerry AK (2005) Treatment of produced water using a surfactant modified zeolite / vapour phase bioreactor system. Dept. of Civil, Architectural and Environmental EngineeringUniversity of TexasAustin, Texas 78712

Manohar DM, Noeline BF, Anirudhan TS (2005) Removal of vanadium (IV) from aqueous solutions by adsorption process with aluminum-pillared bentonite. Ind Eng Chem Res 44(17):6676-6684

Mariangela G, Gul K, Vincenzo B, Guisy L (2012) Removal of emerging contaminants from water and wastewater by adsorption process. In: Grassi M (ed) Emerging Compounds Removal from wastewater. vol 2, Via Ponte don Melillo, 84084 Fisciano (SA), Italy, p 15-24

Naeem A, Westerhoff P, Mustafa S (2007) Vanadium removal by metal (hydr)oxide adsorbents. Water Res 10:37-146

Srivastava VC (2006) Equilibrium modelling of single and binary adsorption of cadmium and nickel onto bagasse fly ash,. Chemical Engineering Journal 0315

A Review of Brine Treatment Technology for Mine Impacted Water (MIW) Plants

Brendan Petschel

Aveng Water, 1 Jurgens Road, Jet Park, Aveng Park, Gauteng, 1459, South Africa,
brendan.petschel@avenggroup.com

Abstract

Treatment of Mine Impacted Water using reverse osmosis (RO) technology has proven extremely effective. Most MIW water, however, cannot be treated to a zero-brine discharge with RO alone. The final reject produced has typically been stored in brine evaporation dams with the expectation of efficient natural evaporation. In practice it has been found that over time the natural evaporation has not been sufficient over the long term. That coupled with space constraints in new plants being designed, cost of new dams and the reluctance of environmental authorities to approve the construction of new brine dams, means alternative methods for dealing with the brine are required. More prevalently, it has also become a requirement to dispose of the brine off-site using approved waste disposal companies, thus incurring excessive operational costs for plant operations. An evaluation of available technologies suitable for treatment of brine was completed.

Keywords: Mine Impacted Water, Mine Water Treatment, Brine Treatment, ZLD, Evaporative Crystallisation, Freeze Crystallisation

Introduction

The treatment technologies considered fall into two main categories, evaporation technology and freeze technology. Evaporation technologies have been around for many years and have been optimised considerably in that time. Freeze technology is an up and coming solution showing promise and is currently being aggressively pursued in the industry.

The implementation requirements, capital costs and operational costs for various scenarios within these categories were considered as key factors to the technology selection.

An internal case study (with a complex brine) was used to explore different brine treatment scenarios, as presented. The scenarios evaluated includes a combination of RO with evaporation technology, evaporation technology on its own, freeze technology on its own and a combination of freeze and evaporation technologies

Basis

A typical complex brine composition was used as a basis for the comparison between scenarios. The feed water quality is defined in table 1 below:

Table 1. *Feed Brine Composition.*

Parameter	Unit	Value	Parameter	Unit	Value
Na	mg/L	7000	Al	mg/L	0.2
Ca	mg/L	1200	F	mg/L	1.2
Mg	mg/L	596	Fe	mg/L	4
K	mg/L	1480	Mn	mg/L	0.2
Cl	mg/L	1580	SiO2	mg/L	1.5
HCO3	mg/L	134	SS	mg/L	70
SO4	mg/L	19404	Temp	°C	22
NO3	mg/L	0.6	pH		8.1
Acidity	mg/L	8.8	TDS	mg/L	31401

The system is specified on the basis that a brine evaporation dam is in place and brine volume removal target of 12m^3/h is required for each scenario. The resultant brine/salt is required to be disposed of off-site.

Technologies

In developing the scenarios for evaluation, a screening of the technologies and their capabilities was completed. The first technology considered was *reverse osmosis technology.* This type of system would typically require an upfront softening step, followed by clarification, multi-media filtration and reverse osmosis separation. Due to the nature of the brine soda ash chemistry was selected for the softening system. Seawater desalination membranes were specified to maximise the brine reduction achievable in the system. This configuration can achieve a maximum recovery of 50%. The RO system will produce two reject streams, the clarifier sludge and the RO reject. The quantity of RO reject at this point will still be too high to feasibly consider off-site disposal and will be returned to the brine dam. As the RO system removes permeate the brine concentration in the dam will cycle up to a point where the brine concentration is above the operational limit of the RO System. An RO System would therefore not be the most suitable on its own. An additional treatment step is required to further reduce the brine volume and manage the TDS build up in the dam. At this point evaporative crystallisation and freeze crystallisation systems need to be considered for the further treatment of the RO Reject.

Evaporator technology is a well-developed, robust and mature technology. A number of suppliers can be found in industry, each with their own variations on the system and offering process guarantees on their systems. In principle evaporators are centred around either using steam to control temperatures or to use pressure (indirectly electricity) to control the temperatures. Modern optimisations on these systems include the use of solar power or waste heat available to minimise the energy requirement from external sources. It is unfortunate however that often the locations of water treatment plants in South Africa are not conveniently located to waste heat sources. Waste heat technology has been excluded in this evaluation. The solar systems available are too small to be considered for the industrial application of this brine treatment evaluation.

Steam dependant evaporator systems evaluated here include; multi-effect low temperature evaporation and thermal vapour recompression (TVR) systems. The multi-effect low temperature system offers the optimal solution in physical size, with the lowest power consumption in terms of electricity costs between the two systems. The TVR systems use more power and less steam, than the multi effect system to achieve the required separations. For the purposes of this evaluation the multi-effect low temperature system was used in the evaluation as the steam driven evaporator option. The Mechanical Vapour Recompression (MVR) system only requires steam for start-up. The energy required is supplied indirectly through electricity. The MVR system is more expensive and has a larger footprint than its steam dependant counterparts. It is included in the evaluation because of the lower operational costs associated with it not requiring steam.

To fully incorporate the evaporative crystalliser into an implementable solution, a boiler system, a cooling water circuit and chemical dosing systems are required. The evaporative crystalliser system will produce a salt slurry that requires dewatering. Installing decanters on the backend allows for the concentration of the slurry to a 25% moisture salt stream that can easily be disposed of off-site. All the required peripheral systems are included in the build-up of the capital costs determined in the evaluation. For the steam generation it has been identified that there is a significant cost difference in using various fuel sources for the boiler. Coal Boilers as well as Fuel/Gas Boilers have been included in the evaluation to indicate the impact of the cheaper (coal) versus the more expensive (fuel oil) boiler fuel. In terms of the evaluation, evaporation systems are considered as smaller systems following RO brine reduction as well as larger systems treating the full volume on their own.

Freeze technology is a much newer process that theoretically offers benefits in terms of operational costs in comparison to evaporator technology. There are not many suppliers able to offer freeze technology solutions and are also able to offer process guarantees without extensive test work before implementation. This technology currently has limited track record in actual treatment of complex brine streams. These factors are a serious drawback of the viability of freeze technology as a commercial option for brine treatment. The technology is, however, incorporated in this evaluation to show the merits it presents.

There are two operational stages to be considered with freeze technology. The first is the concentration of the brine by freezing of the water, retaining a concentrated brine. The second follows the first and is the combination of freezing the water and precipitation of salt crystals. The concentration step is extremely efficient, using far less power than an evaporator to achieve the same brine concentration. Investigations have, however, shown that for the complex brines produced by RO systems, the energy requirements to achieve the salt formation step is much less efficient than an evaporator system. The salt crystal formed have a higher value of waters of hydration, resulting in a greater mass of brine salt that needs to be disposed of in comparison to Evaporative Crystallisation.

The optimal solution based on the above is a combination of freeze technology to achieve the stage 1 brine concentration and an evaporator system to achieve the required salt formation and a final brine salt of 25% moisture for disposal. This combination is included as part of the evaluation. It was found that the most optimal split is for the freeze technology to remove 90% of the water from the brine and for an evaporator to treat the remaining 10%. This combination yields a 25% power saving over an MVR evaporator system treating the full capacity. All peripheral equipment for both the freeze and evaporator systems have been allowed for in the capital cost build up for these scenarios. The freeze system does not require additional chemical dosing.

Evaluation Procedure

The evaluation of the different scenarios will be done on a life cycle cost basis. The life cycle costs need to be considered in terms of Capital Costs and the Operations and Maintenance Costs.

The *Capital Cost* for each system has been compiled to include the design and implementation costs of a full turnkey scenario for each. The market has been engaged in preparing these costs to obtain an accurate budget cost for each scenario.

The *Operations and Maintenance (O&M)* have been calculated in terms of the variable costs only. It has been assumed that the labour requirements of each scenario will be similar and therefore bear no difference in comparison of the scenarios. The variable cost component includes the costs for; chemicals, electricity, other fuel sources and the brine disposal costs off-site. Each scenario is considered on the basis that the waste brine/brine salt will be removed off-site.

A summary of the assumption made in determining the life cycle is given in table 2.

Only present values have been used in the comparative calculation. No allowance has been made for funding or escalation of the costs as this would unnecessarily complicate the evaluation. The disposal costs also assume a proximity to available disposal sites. Cost for disposal will increase with distance to the disposal sites.

Table 2. *Evaluation Assumptions for O&M Costs*

Description	Assumption
Cost of Electricity	R1.03/kW.hr
Chemical Costs	Market Related Costs Q1 2018
Disposal Costs	Q1 Costs for rental of bins, periodic removal from site, disposal costs.
Labour and Maintenance Costs	Excluded
Life Cycle Costs	10 Years
Fuel Costs	Market Related Costs Q1 2018

Scenarios Compared

The following scenarios were considered as part of the case study:

Scenario 1 – Utilises an upfront RO brine reduction step that produces a portion of the treated brine. The side stream off the RO reject is then treated through an evaporator to produce a salt with a 25% moisture content and a clean water stream that is blended with the RO permeate. The balance of the brine stream is returned to the brine dam. The brine salt is disposed of offsite. The flowsheet for this scenario is given in figure 1. There are three sub-scenarios considered, each utilising different technology around the evaporation system:

1a. Multi-effect steam driven evaporator, coupled with a coal steam boiler;
1b. Multi-effect steam driven evaporator, coupled with a fuel oil steam boiler; and
1c. A MVR evaporator, that does not require steam for operation.

Scenario 2 – Utilises evaporative crystallisation technology to treat the raw feed from the brine pond. The brine is processed through the Evaporator to produce a salt with a 25% moisture content and a clean water stream that is taken away as product. The brine salt is disposed of offsite. The flowsheet for this scenario is given in figure 1. There are three sub-scenarios considered, each utilising different technology around the evaporation system:

2a. Multi-effect steam driven evaporator, coupled with a coal steam boiler;
2b. Multi-effect steam driven evaporator, coupled with a fuel oil steam boiler; and
2c. A MVR evaporator, that does not require steam for operation.

Scenario 3 - Utilises freeze crystallisation technology to treat the raw feed from the brine pond. The brine is processed through the freeze crystalliser to produce a concentrated brine having extracted 90% of the volume as clean water. The concentrated brine will need to be disposed of off-site. The flowsheet for this scenario is given in figure 1. There are no subcategories for this scenario.

Scenario 4 - Utilises a combination of freeze technology and evaporative crystallisation technology. The brine is processed through the freeze crystalliser to produce a concentrated brine scenario having extracted 90% of the volume as clean water. The concentrated brine scenario is then processed through the evaporator to produce a brine salt with a 25% moisture content and a clean water stream that is blended with the freeze crystallisation product water. The brine salt will be disposed of off-site. The flowsheet for this scenario is given in figure 1. There are two sub-scenarios considered, each utilising different technology around the evaporation system:

4a. Three stage multi-effect steam driven evaporator, coupled with a coal steam boiler;
4b. A mechanical vapour recompression evaporator, that does not require steam for operation.

Evaluation

Based on the evaluation criteria discussed above the comparison of each O&M cost is reported in table 3 on the next page for each of the scenarios and their sub-scenarios.

The results of the complete lifecycle costs of each scenario are summarised in table 4. The rand per cube rate calculated below is based on the $12 m^3/h$ product flow for uniformity in evaluation.

The best capital costs can be achieved with the RO brine reduction coupled with the smaller evaporators. However, the lifecycle costs, specifically due to the costs of chemicals and the clarifier sludge removal, put it amongst the most expensive over a full ten-year lifecycle. In South Africa steam production using coal is much more cost effective than gas/fuel oil.

The combination of freeze reduction and evaporative crystallisation yields the best overall lifecycle costs, but the investment cost is the highest. The freeze reduction solution also shows merit, offering efficient operating costs that are mainly dependant on the cost of disposal, which may vary depending on the site location.

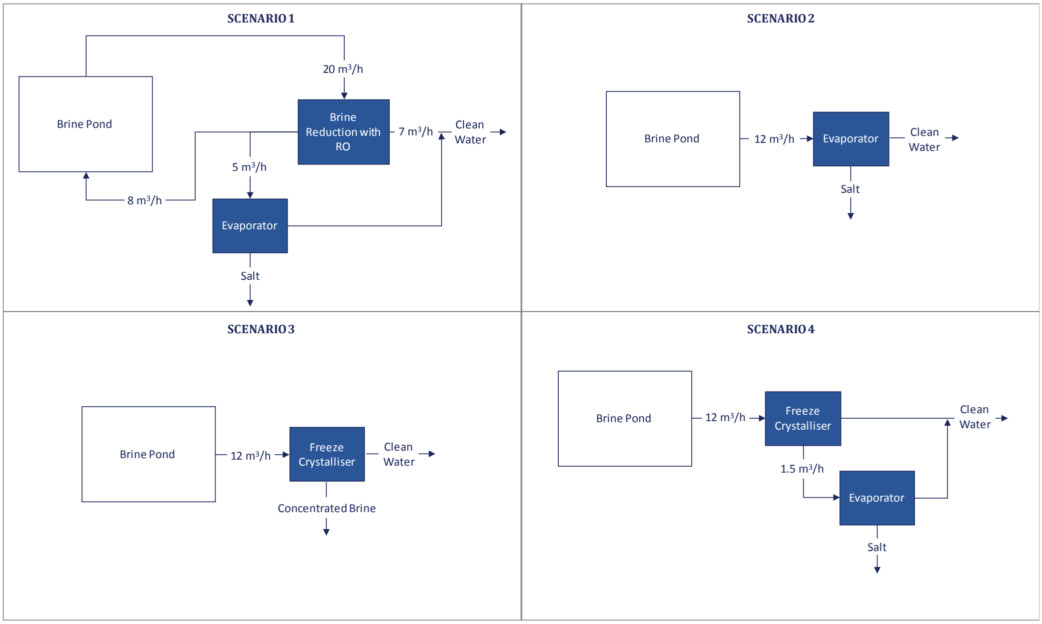

***Figure 1** Scenario Flowsheets*

***Table 3.** O&M Cost Breakdown Results*

Cost Description	1a.	1b.	1c.	2a.	2b.	2c.	3.	4a.	4b.
Power (R/m^3)	25.0	25.0	50.7	45.1	45.1	97.7	65.4	32.9	71.3
Chemicals (R/m^3)	99.4	99.4	99.4	5.0	5.0	5.0	0	1.9	1.9
Steam (R/m^3)	46.3	77.9	0	97.5	97.5	0	0	23.1	0
Disposal (R/m^3)	44.2	44.2	44.2	35.0	35.0	35.0	62.5	35.0	35.0
O&M Total (R/m^3)	215	246	194	183	249	138	122	93	108

***Table 4.** Overall Lifecycle Cost Summary*

Cost Description	1a.	1b.	1c.	2a.	2b.	2c.	3.	4a.	4b.
Capital Costs (R mil.)	75.2	74.3	82.7	83.3	80.0	95.8	115.0	138.5	143.0
O&M Costs (R mil.)	225.8	259.0	204.2	191.9	261.9	144.7	128.5	97.7	113.8
Life Cycle Total (R/mil.)	300.9	333.3	286.9	274.5	341.2	239.7	309.9	226.5	247.0
Total Averaged per m3	286	317	273	262	325	229	232	225	244

The MVR System without upfront brine reduction shows comparative lifecycle costs to the freeze and freeze/evaporator combination, specifically due to the lower capital costs associated with the system. Considering the access and availability of process guarantees from suppliers of Evaporator systems, the MVR System is the best choice for this application presented in the case study.

To better depict the results of the lifecycle costs evaluation, figure 2 is included below. The graph indicates the cost per cube of clean water produced for each scenario and their sub-scenarios.

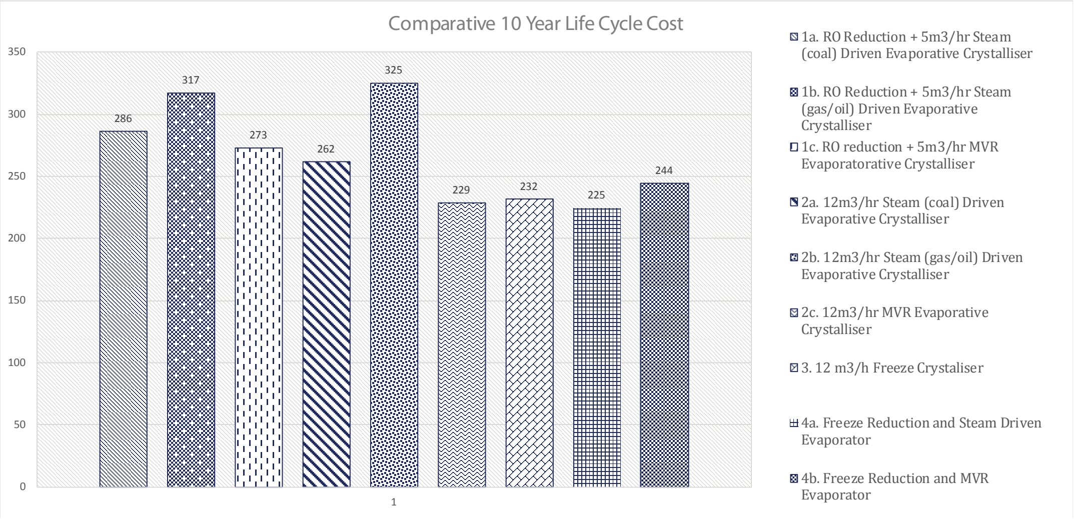

Figure 2 *Comparative 10-year lifecycle costs*

Conclusions

The comparative review from the case study showcases that the older more mature evaporation technology is still the best scenario for brine treatment. Comparable lifecycle costs coupled with performance security from suppliers outweighs the lower operational costs benefits of the freeze technologies. Evaporation technology often gets rejected due to the high upfront capital costs in favour of freeze technology or no solution at all. This should not be the standard outcome.

Water treatment systems are all singular in their requirements and need to be considered on a case by case basis. However, there are viable solutions to treatment of complex RO brine. Where applicable optimised evaporation systems using waste energy or solar energy are being developed and can have far cheaper life cycle costs than those presented in this case study.

Performance Evaluation of Orange Peels as Anti-Scaling Agent for Pretreatment of Water

Mashudu Ramakuela, Amos Adeniyi, Maurice Onyango,
Richard Mbaya, Opeyemi A. Oyewo

Department of Chemical, Metallurgical and Materials Engineering, Tshwane University of Technology (TUT), Private Bag X680, Pretoria 0001, South Africa. adeniyia@tut.ac.za, amosadeniyi7@yahoo.com

Abstract

This study described the development and application of efficient anti-scalant material using orange peels. Specifically, 2 g of dried orange peels screened up to 450 µm average particle, 10 mL of methanol was used to prepare 100 mL anti-scalant solution at room temperature. FT-IR analysis showed that the anti-scalant characteristics is similar to citric acid which is an indication for an efficient anti-scalant. At a dosage of 1 g/L based on the mass of dried orange peel powder, a solution containing calcium carbonate was found to increase the solubility from 14 mg/L to 60 mg/L at a pH of 6.2.

Keywords: anti-scalant, orange peels, extraction, pretreatment, membrane

Introduction

Fouling is a major hurdle that must be overcome for the implementation of membranes to water treatment worldwide (Bhattacharyya et al., 2000). Fouling is a phenomena whereby colloidal or particulate matter are deposited either on the membrane surface or right in the membrane pores which hinder transport through the membrane (Boerlage et al., 2002). Water flux and solute rejection performance are reduced when water containing foreign particles such as particulates, colloids, macromolecules, or microbes is treated using a membrane technology. In addition, the foreign material forms a cake layer which drastically reduces the overall performances of the membrane (Baker, 2004). Fouling causes flux declines and leads to high membrane operation cost because high energy is needed to obtain high flux through a fouled membrane. Also a fouled membrane need cleaning and eventually a total replacement (Basile et al., 2015). Fouling caused by inverse solubility salts are known as scaling or crystallization fouling (MacAdam and Parsons, 2004). Substances that caused scaling includes calcium carbonate, calcium sulphate, barium sulphate and silica. When water on the feed side becomes super saturated with these substances, scaling of the membrane is the result. Super-saturated salts can precipitate on the membrane surface building a thin layer, which hinders mass transfer through the membrane. Scaling always occurs at the membrane surface because of the increased salt concentration near the membrane caused by concentration polarization. Scaling can dramatically reduce permeate flux, and has to be avoided by all means. One of the methods to remove scale is by flushing the membrane with acid but a major issue with this method is the difficulty encounter when taking the crystalline mud out of the module. The best method is to pretreat the feed water and keep the concentration of the scale forming salt under saturation level by adjusting the pH or by preventing the precipitation using anti-scalant (MacAdam and Parsons, 2004). Commonly used chemical additives as anti-scale agents are solutions of low molecular weight polyacrylic acid, phosphoric acid, and phosphate esters (MacAdam and Parsons, 2004). Citric acid has been found to be an effective green scale inhibitor (Ghizellaoui et al., 2017). Orange peels are fruit wastes found in abundance in South Africa. Agricultural wastes such as banana peels, sugar cane baggase and orange peels has been proven highly efficient in wastewater treatment (Oyewo et al., 2016). Among the above listed, it has been reported that orange peels have the potential as an alternative raw material for citric acid fermentation (Rivers et al., 2008), it is hereby speculated that orange peels are highly efficient as anti-scalant. In this study, the evaluation of orange peels as natural anti-scalant was demonstrated due to its higher citric acid content using solubility method. The main aim was to use ecofriendly and highly economical anti-scalant material to optimize the commercially available anti-scaling agents in water pre-treatment.

Methods

Oranges peels obtained from Pretoria, South Africa, was carefully removed from its fruit and processed into powdered form as shown in Figure 1.

The dried solid powder was characterized using transform infrared spectroscopy (FT-IR) and Energy dispersive x-ray analysis (EDX) (Oyewo et al., 2016, Mafra et al., 2013). The anti-scalant was extracted from the orange peel powder as shown in Figure 2.

Extract prepared as a filtrate from adding 90 mL of deionized water and 10 mL of methanol to 2 g of the orange peel powered was used at different volumes of 5 mL, 10 mL, 15 mL, 20 mL, 25 mL and 30 mL for this investigation. Solutions of calcium carbonate were prepared using different masses of calcium carbonate which were 0.10 g, 0.15 g and 0.20 g in 100 mL of deionized water. The extract was added to each of the prepared solution at each of the volumes already stated in order to observe its effect on the solubility of calcium carbonate. The resulting solution was filtered. The pH of the filtrate was taken and the concentration of the calcium carbonate determined using ICP-OES.

Results and discussion

The discussion of results is divided into three parts. The first was on the characterization of the powder obtained after processing the orange peels. The aim was to discover the presence of elements and radicals that could indicate acidic properties in the orange peel powder. The second part was the extraction of the anti-scalant from the orange peel powder using a mixture of water and methanol. The third was the solubility test results whose aim was to confirm if the extract obtained from orange peel powder can actually increase the dissolution of the calcium carbonate and keep its concentration under saturation.

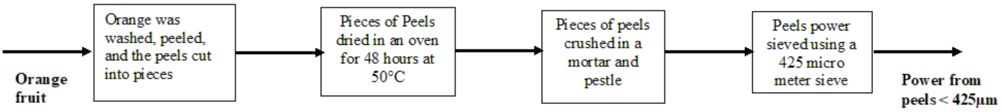

Figure 1 Flow diagram for the preparation of orange peels power from orange fruits.

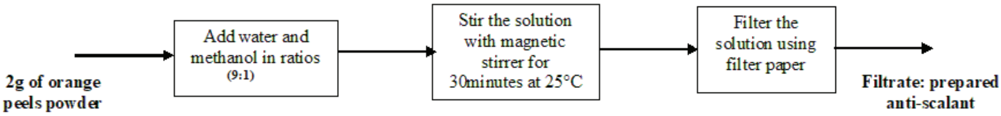

Figure 2 Chemical extraction method to extract anti-scalant from orange peels powder.

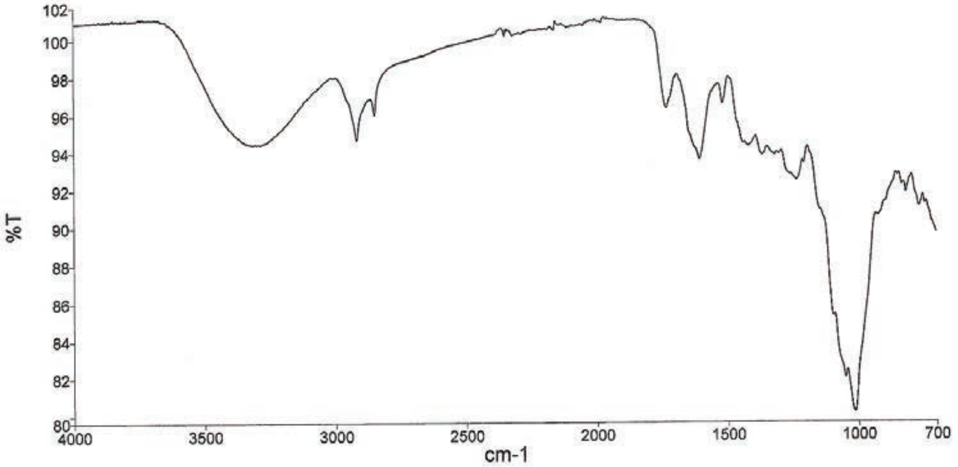

***Figure 3** FT-IR results of the orange peels powder.*

Figure 3 shows the FT-IR results of the orange peel powder. The FT-IR spectrum of the orange peel powder shows the complex nature of the powder, displaying a broad spectrum of adsorption peaks. The broad, intense absorption peaks around 3,400 cm-1 are indicating of is a strong presence of acid O-H, resulting from the O-H stretching mode of hydroxyl groups characteristic of citric acid as observed by Singh et al. (2014), who analyzed Fe_3O_4 coated with citric acid. The bands at 2,900 cm-1 and 2,850 cm-1 were due to the presence of C-H in the powder (Al-Qodah and Shawabkah, 2009). The peak around 1,635 cm-1 is due to the C=C stretching that can be attributed to the aromatic C-C bond, and the peak at 1,072 cm-1 can also be explained by the presence of either C-O symmetric or asymmetric stretching vibration (-C-O-C- ring) (Khaled et al., 2009).

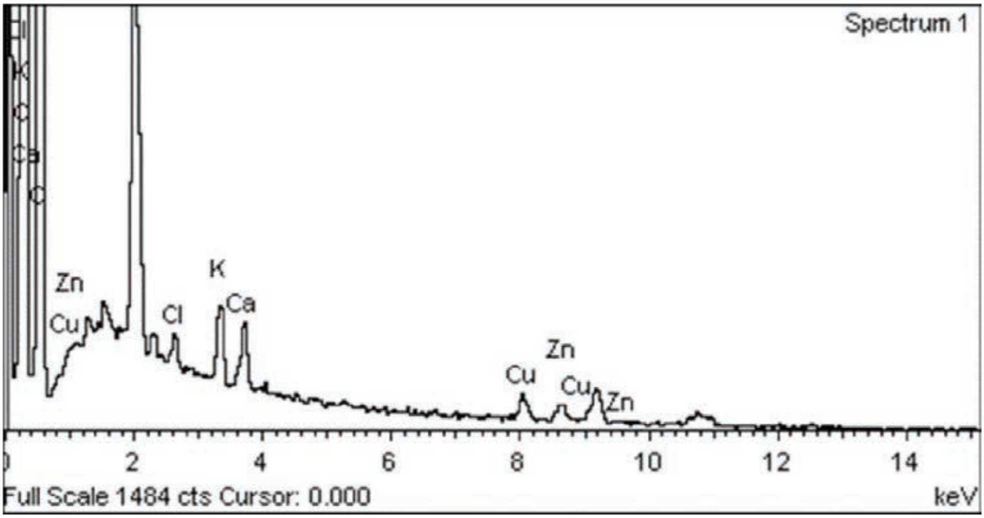

***Figure 4** EDX for the orange dried peels powder.*

The result was further confirmed by the EDX showing a significant presence of Carbon (67.86%) and Oxygen (31.62%) because they are organic materials. This is due to the fact that orange peels have tendency to demonstrate acid characteristics similar to citric acid.

Anti-scaling agents are a family of chemicals designed to inhibit the formation and precipitation of crystallized mineral salts that form scale (MacAdam and Parsons, 2004). It has been established that the tendency for scale formation is lower in an acidic environment (MacAdam and Parsons, 2004, Geise et al., 2010). The resulting extract (filtrate), obtained after adding water and methanol in ratios 3:1,4:1 and 9:1 to 2 g of the orange peel power and filtering, was tested for pH. Results are shown in Table 1. The extract prepared with the addition of water and methanol in the ratio 9:1 is more acidic than others at pH of 5.93., and was used for carbonate dissolution experiment. It is possible that the extract could have anti-scalant effect also due to threshold inhibition, crystal modification and dispersion but only dissolution effect was tested in this work.

Figure 5 shows the effect of addition of various volume of the extract to different concentration of calcium carbonate solution. The result shows that at a dosage of 5 mL, solubility of calcium carbonate increases from 14 mg/L to a minimum of 60 mg/L at room temperature for a solution with calcium carbonate concentration of 2000 mg/L. This is possibly due to higher solubility of calcium carbonate in acidic environment (MacAdam and Parsons, 2004) as the average pH of the resulting solutions was 6.2. However, in real situation, the concentration of calcium carbonate in not likely to get up to 1000 mg/L (Fritzmann et al., 2007). Extremely hard water is known to have concentration of 554 mg/L (Ghizellaoui et al., 2017) and the less the concentration the more effective the antiscalant. The estimated dosage is 1 g/L based on the mass of the dried orange peel powder used to prepare the extract and the volume added to the carbonate solutions.

Table 1. *Extraction of orange dried peels powder using distilled water and methanol at 25 °C.*

Mass (orange dried peels powder) (g)	Volume (distilled water and methanol) (ml)	pH
2	75 and 25	6.13
2	80 and 20	6.65
2	90 and 10	5.93

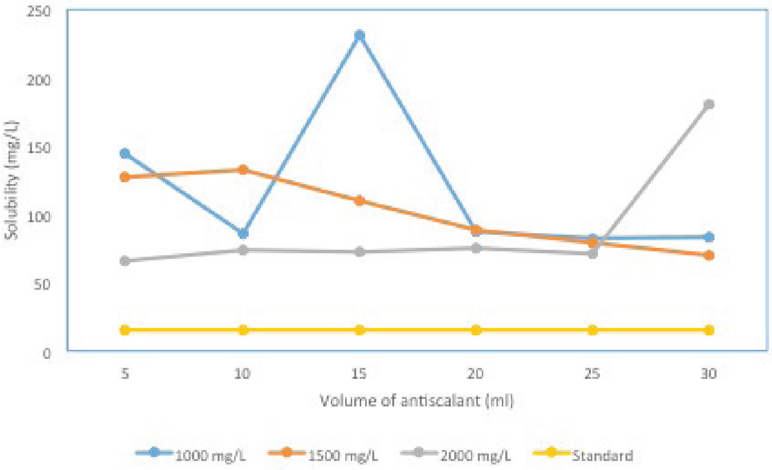

Figure *5 Effect of various volume of antiscalant on CaCO3 dissolution*

Conclusion

The following conclusions are drawn from this work:

1. Powder prepared by drying and grinding orange peels to 450µm average particle size demonstrated characteristics similar to citric acid which has been found to be an effective anti-scalant.
2. An extract prepared by adding 2 g of the dried powder to 100ml of solution containing 90ml of water and 10ml of methanol was found to have average pH of 5.95 at room temperature.
3. Addition of 5 ml of the extract to a solution containing calcium carbonate was found to increase the solubility from 14mg /L to an average of 60 mg/L at an average pH of 6.2 at room temperature.
4. At a dosage of 1 g/L based on the mass of dried orange peel powder, calcium carbonate scale formation can be effectively hindered.
5. Orange peels show a potential for anti-scalant preparation and can be a cheap alternative to commercially available anti-scalant and its use can also be advantageous for the environment in management of fruit wastes.

Acknowledgement

The authors acknowledge the Tshwane University of Technology for providing research facilities and laboratory equipment

References

Al-qodah Z, shawabkah R (2009) Production and characterization of granular activated carbon from activated sludge. *Brazilian Journal of Chemical Engineering*, 26, 127-136.

Baker RW (2004) Membrane technology and applications. John Wiley & Sons, Ltd, 96-103.

Basile A, Cassano A, Rastogi, NK (2015) *Advances in membrane technologies for water treatment: materials, processes and applications*, Elsevier.

Bhattacharyya D, Mangum W, Williams M (2000) Reverse osmosis. *Kirk-Othmer Encyclopedia of Chemical Technology*.

Boerlage SF, Kennedy MD, Bremere I, Witkamp GJ, Van Der Hoek JP, Schippers JC (2002) The scaling potential of barium sulphate in reverse osmosis systems. *Journal of Membrane Science,* 197, 251-268.

Fritzmann C, Löwenberg J, Wintgens T, Melin T (2007) State-of-the-art of reverse osmosis desalination. *Desalination*, 216, 1-76.

Geise GM, Lee HS, Miller DJ, Freeman BD, Mcgrath JE, Paul DR (2010) Water purification by membranes: the role of polymer science. *Journal of Polymer Science Part B: Polymer Physics*, 48, 1685-1718.

Ghizellaoui S, Ghizellaoui S, Semineras H (2017) Inhibition of scale formation by electrochemical means in the presence of a green inhibitor: citric acid.

Khaled A, El Nemr A, El-Sikaily A, Abdelwahab O (2009) Treatment of artificial textile dye effluent containing Direct Yellow 12 by orange peel carbon. Desalination, 238, 210-232.

Macadam J, Parsons SA (2004) Calcium carbonate scale formation and control. *Reviews in Environmental Science and Biotechnology*, 3, 159-169.

Mafra M, Igarashi-Mafra L, Zuim D, Vasques É, Ferreira M (2013) Adsorption of remazol brilliant blue on an orange peel adsorbent. *Brazilian Journal of Chemical Engineering*, 30, 657-665.

Oyewo OA, Onyango MS, Wolkersdorfer C (2016) Application of banana peels nanosorbent for the removal of radioactive minerals from real mine water. *Journal of environmental radioactivity*, 164, 369-376.

Rivas B, Torrado A, Torre P, Converti A, Domínguez JM (2008) Submerged citric acid fermentation on orange peel autohydrolysate. Journal of Agricultural and Food Chemistry, 56(7), pp.2380-2387.

Singh D, Gautam RK, Kumar R, Shukla BK, Shankar V, Krishna V (2014) Citric acid coated magnetic nanoparticles: synthesis, characterization and application in removal of Cd (II) ions from aqueous solution. *Journal of Water Process Engineering*, 4, 233-241.

A novel sampling technique using a sediment collector (SECO) to collect particles from suspended matter in mine water with regard to long term monitoring

Christoph Schabronath[1], Joachim Löchte[1], Patric Dibowski[1], Harald Rahm[2]

[1]RAG Aktiengesellschaft, Central Division Health Safety and Environment,
Im Welterbe 10, 44151 Essen, Germany, Christoph.Schabronath@rag.de Patric.Dibowski@rag.de
[2]Landesamt für Natur, Umwelt und Verbraucherschutz (LANUV) NRW, Auf dem Draap 25,44021
Düsseldorf, Germany, Harald.Rahm@lanuv.nrw.de

Abstract

In the year 2018 active hard coal mining in Germany, which requires water drainage, will cease and so do the last two active coal mines. Since RAG Aktiengesellschaft (RAG) will shut down the active mining process, mine water pumping for safety reasons won´t be necessary anymore and RAG has the opportunity for flooding in these areas. Nevertheless in some former mining areas mine water needs to be pumped for the next decades. RAG has to face major challenges regarding pumping technique for mine flooding, monitoring and reduction of environmental impacts caused by mine water. Different substances in mine water of either natural or anthropogenic origin can potentially influence the quality of surface water (Denneborg et. al. 2017). To quantify the impact of mine water on surface water a sampling technique is needed.

Since most of the organic substances in mine water are particle bound, a reliable, continuous and low cost sampling process for suspended matter is needed. One method accepted by the authorities is a sediment collector (LAWA-Expertengruppe „QHF" 1996, OGewV 2016). This article gives an overview of the challenges by transferring a standard monitoring method for surface water to an aggressive medium such as mine water. Furthermore effects of continuous monitoring in contrast to spot sampling with the centrifuge will be investigated.

Keywords: Monitoring, Sampling technique, Suspended matter, Water treatment, Mine Water, PCB, SECO

Introduction

In the year 2018 active coal mining in Germany will end. The last two active coal mines are managed by the RAG and will be shut down by the end of 2018. At the moment a huge amount of water is pumped from over −1000 mNN depth into surface waters to keep the mines dry. After a transition period for leaving the mines certain areas will be flooded. The positive side effects are that the pumped water volumes and the impact on surface waters will be reduced.

This is important because industrial residues which contained dioxins and furane were used for backfilling of voids. Certain substances were bound in concrete and used for construction in the mine. In addition for safety reasons, non-inflammable hydraulic liquids were used. Some ingredients are now known as toxic for example polychlorinated biphenyls (PCB). Due to leakage, certain areas can contain PCB. During the mine flooding process, mine water could get in touch with those areas and a resolving process of toxic compounds is possible.

Since most of those organic compounds are particle bound, concentrations were very small in mine water. This is why suspended matter in mine water needed to be collected.

A standard sampling technique to gather suspended matter is the centrifuge. RAG started a monitoring program in cooperation with the office for environmental protection (LANUV) to detect the amount of suspended matter in mine water. During a monitoring program in 2015 and 2017 problems with the sampling method centrifuge occurred, caused by the aggressive medium mine water. Several sealings needed replacing after a single day of sampling. This was in strict correlation to the high salt content of mine water up to 80.000 mg/L, which resulted in high maintenance costs after one single sampling. In addition there was a difference between active and closed mines regarding the amount of suspended matter in pumped mine water. At some plant sites, mainly the closed mines, sampling with the centrifuge didn´t collect enough suspended matter for analytics. Because of those reasons a resistant, long term period and cost effective sediment collector (SECO) should be tested.

As you can tell from Figure 1 the SECO was installed at five different locations, with different mine water compositions. Those were selected to represent two categories of mine water. Either the impact of mine water drainage of an active or closed mine on the surface water was evaluated. Therefore the last two active mines Ibbenbüren and Prosper Haniel as well as the closed mines Haus Aden, Zollverein and Walsum were selected. According to the different locations a variety of different mine water compositions with high salt concentrations and/or different loads of particles and sizes were given.

Materials and Methods

Since the mid-nineties the sediment collector with two chambers is a standard method to collect suspended matter from surface water (LAWA-Expertengruppe „QHF" 1996). The novel approach of RAG and LANUV is a continuous collection of suspended matter from the corrosive medium mine water. Adaptations were necessary to use this collector in mine water.

An improved sediment collector with three compartments is used to gather as

Figure 1: Five Locations including active and closed mines with a sediment collector

much sample material as possible. This is due to the amount of suspended matter, which can vary with the sampling point. With this adaption longer sampling periods can be tested, in contrast to single measurements with the centrifuge.

The SECO consists of a special plastic which is resistant against corrosion caused by salts. To guide the medium through the collector, several baffle plates were installed as shown in Figure 2.

To use the effect of sedimentation, the flow velocity is highly reduced by expanding the diameter of the flow channel in the chamber relative to the inlet pipe. Due to the reduction of flow velocity the suspended matter, symbolized by black dots in Figure 3, can sink down and be collected from trays.

To ensure stable operating conditions and to avoid varying flow velocities a flow control was installed and a flowmeter to measure the actual flow. This is necessary since the SECO operates best within flow velocities from 5 to 10 l/min. This also means it needed to be installed in bypass to the mine water mainstream. Furthermore the flowmeter is used to get the correlation to mine water volumes to identify the particle ratio see Figure 6.

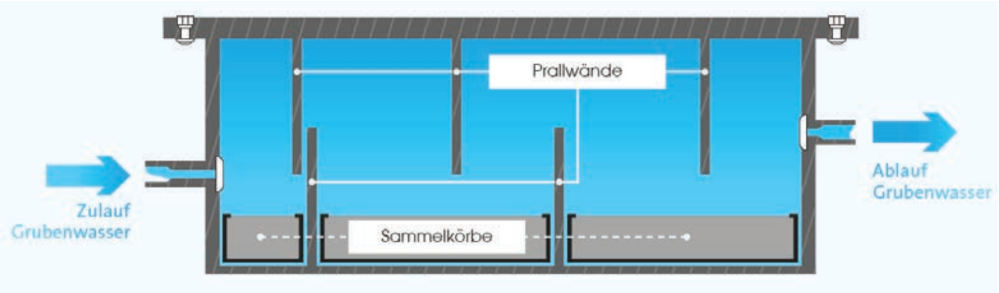

Figure 2: *Technical set-up sediment collector (SECO)*

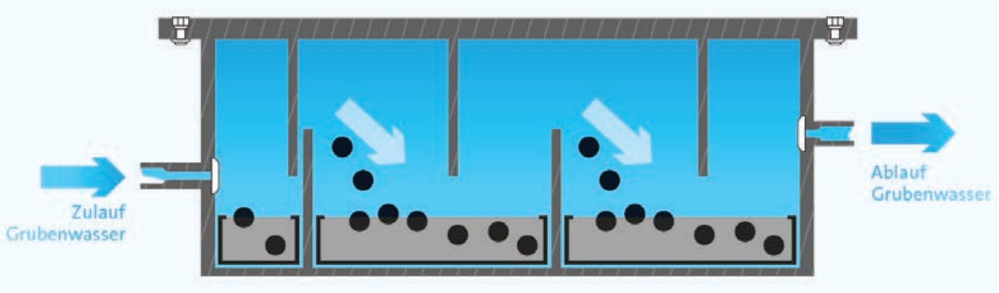

Figure 3: *Sedimentation process in SECO*

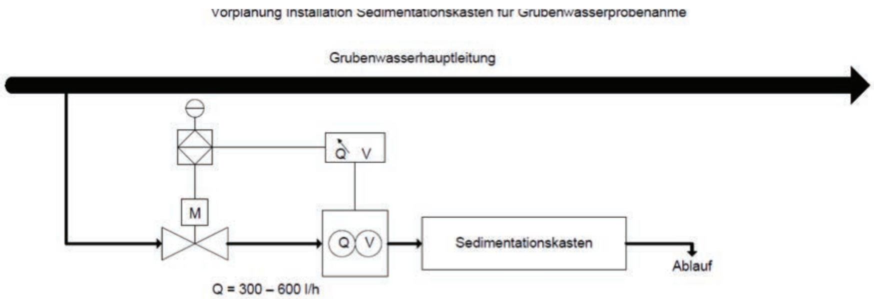

Figure 4: *Process flow diagram of a SECO installation*

Figure 5: Locations with installed SECO

According to the sampling points different installations had to be build. To avoid damages caused by rain or snow, the SECO and its environment was either protected by an isolation housing or if necessary installed in a container (see Figure 5). Beyond that the SECO required protection against vandalism, since some sampling points were located on public ground.

After four to twelve weeks of sampling an independent laboratory characterized the collected particles (Figure 6) concerning their amount and chemical composition. In addition the particle size distribution was determined. Results regarding PCB were compared to the corresponding results from suspended matter collected with the centrifuge.

Results

At five different plant sites, the sediment collector was able to capture suspended matter from aggressive mine water. Degrading effects to the synthetic housing material were not given. The sampling period, to collect enough matter for analysis, is highly depending on the investigated mine water and takes from four to twelve weeks as you can see in Table 1.

Figure 6: Collecting suspended matter

At all sites PCB were detected in the suspended matter during the first measurements. Several results for Ibbenbüren and Prosper Haniel are present and comparable. Exemplary results are stressed at the active mine Prosper Haniel. It could be shown that a correlation from the results of the SECO to the centrifuge

Table 1. Sampling periods

Location	Sampling period
Ibbenbüren	Sampling period
Prosper Haniel	6 weeks
Haus Aden	4 weeks
Zollverein	12 weeks
Walsum	8 weeks
	12 weeks

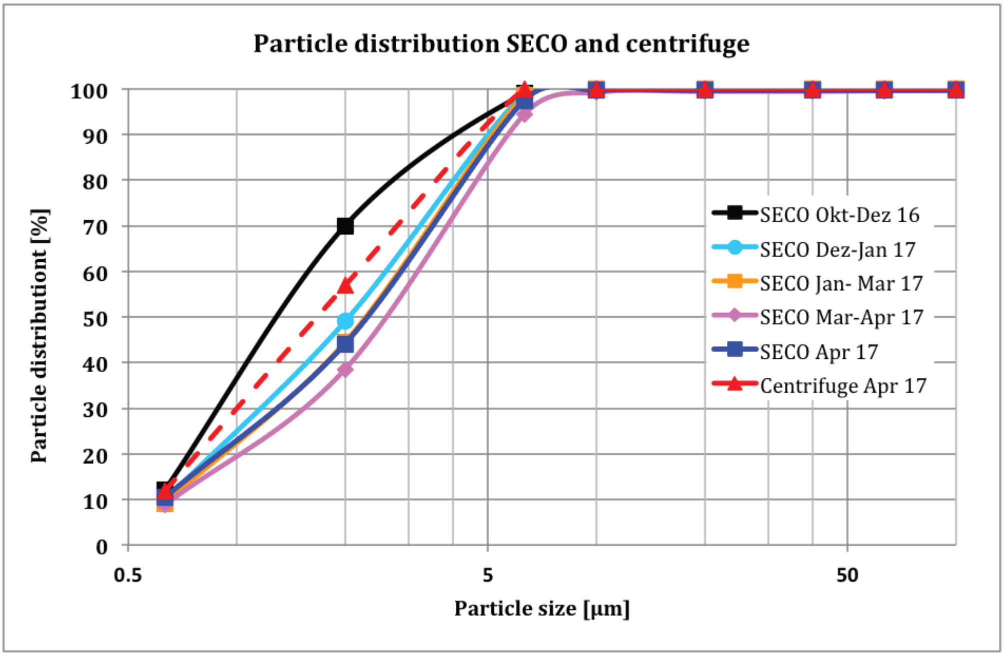

***Figure 7:** Comparison of particle distribution SECO and centrifuge*

was given (Figure 7 Rahm 2018). Both sampling techniques proofed to be abled to collect particles smaller than 63 µm. This was important for this investigation since organic matter like PCB can be found in this fraction.

As you can tell from Figure 8 (Rahm 2018) the solid content of PCB in collected suspended matter are comparable. PCB which were typically used in mining hydraulic liquids, meaning PCB 28 and PCB 52, were identified in all samples. The SECO enables long term integrative monitoring to accumulate suspended matter. This obviously takes a longer period to gather the same amount of suspended matter compared to the centrifuge. The SECO can collect for months without degrading effects to housing and without operating costs caused by an operator.

One side effect of this process while surveying water qualities at a high standard level is minimized costs. In comparison to the centrifuge the costs of invest are roughly 10 times smaller. Furthermore once installed the SECO is not as cost intensive as the centrifuge which needs an operator at all times.

Conclusion

The SECO is a reliable and comparable long term monitoring technique to collect particles from suspended matter in an aggressive medium such as mine water. It shows comparable results to the standard sampling method with the centrifuge and is not as cost intensive.

Process development took several steps. First the SECO was installed in free flowing

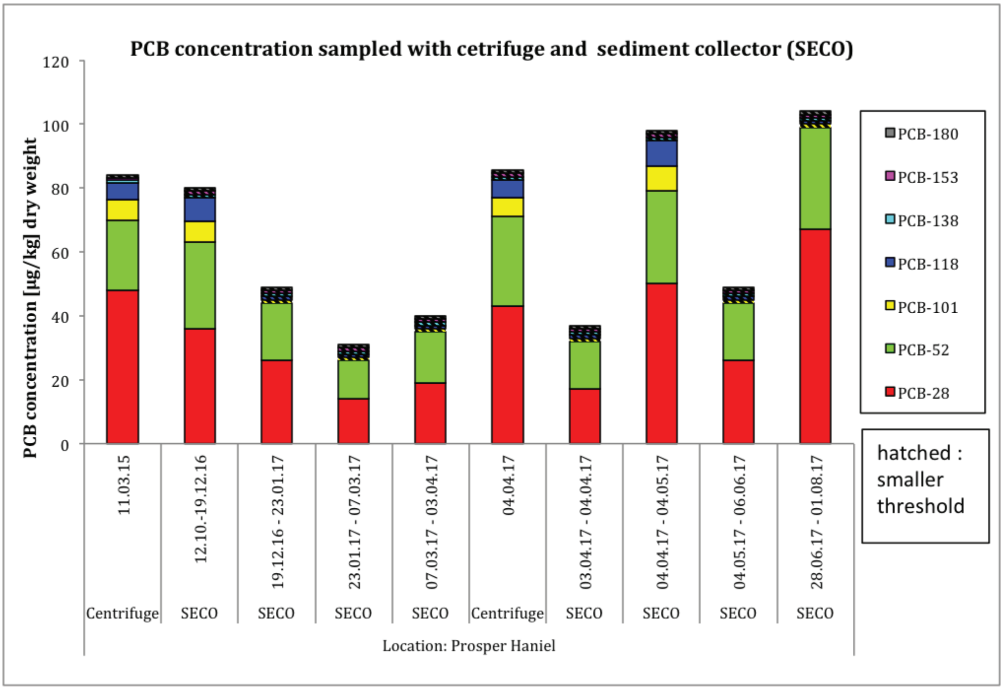

Figure 8: *PCB concentration in suspended matter sampled with centrifuge and SECO*

water than at a pipeline and in the end in a bypass of a high pressure mine water pipeline. The lessons learned can be read as follows.

1. Variation in water pressure caused pressure peaks hence a pressure relief valve needed to be installed. Maximum pressure is 0,5 bar, otherwise the SECO will burst.
2. The SECO needed to be resistant against cold temperatures and vandalism, so special housings and insulations were installed.
3. In high mineralised mine water the operating pump for the SECO needs to be replaced after three months, due to corrosion.
4. Depending on the sampling location, periods of four to twelve weeks were necessary to collect enough suspended matter for analysis.
5. With regard to installing, operating and maintaining the SECO is more stable than the centrifuge. Furthermore the SECO has proven to resist aggressive mine water in contrast to the centrifuge. Finally the SECO shows advantages with regard to costs.

In all industrial applications in which a continuous monitoring of suspended matter in harsh conditions is important, i.e. salt mining and ore mining, the sediment collector could be an appropriate sampling technique.

References

Denneborg et al. (2017) Gutachten zur Prüfung möglicher Umweltauswirkungen des Einsatzes von Abfall- und Reststoffen zur Bruchhohlraumverfüllung in Steinkohlebergwerken in Nordrhein-Westfalen Teil 1, Aachen, p 1; p 82; p 124.

Rahm, Obschernicat (2018) GDCh Jahrestagung p 4

OGewV (2016) Verordnung zum Schutz der Oberflächengewässer (Oberflächengewässerverordnung - OGewV), p 69

LAWA-Expertengruppe "QHF" (1996) Fließgewässer der Bundesrepublik Deutschland – Schwebstoffuntersuchungen-, Empfehlungen, p 21

In-lake neutralization of mine lakes – 15 years of continuous development

Oliver Totsche, Beate Lucke, Friedrich-Carl Benthaus

[1]*Lausitzer und Mitteldeutsche Bergbauverwaltungsgesellschaft mbH (LMBV), Knappenstraße 1,*
01968 Senftenberg, Germany, E-Mail: oliver.totsche@lmbv.de

Abstract

Due to acidic inflow from sulphur- and iron-rich groundwater into mine lakes in East Germany, the majority of the mine lakes and their run-off waters do not meet the national water quality requirements. Hence, water treatment is required either for the lake water bodies or the discharged waters. In-lake neutralization of the entire water body is the preferred option with regard to cost efficiency, water quality, and subsequent use. Over the last 15 years, LMBV and its partners has developed, tested and enhanced different in-lake neutralization techniques. Due to these efforts, the achieved state of technology will be presented. In East Germany, 17 acidic mine lakes have already been neutralized and need regular follow up treatments to stabilize the neutral conditions. At least five more lakes are to be neutralized in the next few years. This makes LMBV on of the most experienced organization in-lake technology for mine lakes.

Keywords: Lignite mining, contamination by sulphide minerals, active water treatment, in-lake neutralization of mine lakes

Introduction

Lignite mining in Germany has been carried out under soft rock conditions for about 150 years. In order to allow safe mining, the groundwater layers have been dewatered to a depth of about 50 – 80 m. To remove the overburden from lignite seam, the material has been displaced to outer damp sites. In the mined-out areas, large end lakes have been created with a volume of 20 – 450 mill. m^3 (LMBV 2017a).

In the phase of mine operation and closure, sulphide minerals (e.g. pyrite and marcasite) in the overburden had been oxidised. The minerals formed water-soluble iron- and sulphate ions, as well as small amounts of other heavy metal ions in some cases. When mining ceased, the groundwater layer outside the mining site was refilled and the sulphate and dissolved iron minerals were transported by the re-established groundwater flow. Due to acidic groundwater flow, the majority of the mine lakes and their run-off waters do not meet the national water quality requirements. Hence, water treatment is required either for the lake water bodies or the discharged waters. In-lake neutralization of the entire water body is the preferred option within regard to cost efficiency, water quality and subsequent use.

Water treatment principales

In order to comply with German water regulations §§ 27, 44 and 47 (WHG 2009) as well as Article 1 of the EU Water Framework Directive (WRRL 2000), the quality of surface and underground water may/must not be deteriorated by mining activities. To ensure the water from the mining lake as well as runoff waters do not adversely affect downstream biocenosis, a water treatment according pH values and iron components is necessary. Active water treatment is the most common form of water treatment in mining industry. Because the mine lake waters are slightly acidic (pH values from 3 to 7, iron levels from 1 to 150 mg/L), they require the addition of lime, limestone or soda to raise the pH value (LMBV 2017a). Once the pH value has been elevated, dissolved iron precipitates out of the solution and sinks to the bottom of the lake. As a result of the large amount of water being treated, techniques like ion exchangers, membrane filters or reverse osmosis are not suitable in this case.

In-lake neutralization involves the surface water body in the former opencast mining pit by mixing a neutralizing agent into the water. With this process, the total water body as well as sediment of the lake, erosion material and the water flowing into the groundwater aquifer must be neutralized. The main advantages compared to a run-off treatment are usually the following:

- the in-lake treatment is required just periodically, run-off treatments have to operate all the time,
- the degradation of ammonia by microbes in neutral water bodies,
- the iron sludge formed during neutralization settles on the lake bottom, and does not have to be disposed of elsewhere,
- the output of neutral lake water into the adjacent downstream groundwater aquifer and
- the higher usability of neutral waters (e.g. fishing, recreation, …)

Choice of in-lake procedure

Technically, not all treatment procedures are equally suitable for all types of lakes. Lake shore-based stationary water treatment plants would appear to be the preferable solution when continuous treatment cycles are required. They could be automated to a large extent so they can be both operated and monitored remotely. The lime should be introduced into the lake water body at an appropriate distance from the shore using pipes and subsurface turbulent jet technology. The required lime suspension is produced with lake water on the shore. Stationary plants of this kind are well-suited for relatively compact water bodies where good mixing as a result of the convective lake water currents can be expected (LMBV 2017b).

Some German mining lakes are heavily segmented and made up of several sub-basins. Here it is more likely that mobile plants (i.e. water treatment vessels) are capable of distributing the neutralization agent across the lake as required.

Water treatment vessels

The liming process of lakes has been long practiced in those regions in Scandinavia that have been affected by acid rain in soft water areas.

One such Swedish water treatment vessel, the *Brahe type*, was used for the first time on an eastern German post-mining lake in 2008. The lime-water suspension was spread across the lake surface by two water guns. The vessels could easily be transported by road on a trailer from which they can be launched to a lake. One disadvantage was that the relatively coarse-grained pulverised limestone being used was much less effective than in the soft water lakes of Scandinavia. Another ecological drawback is the risk of the fine lime particles drifting into the reed beds along the lake shore as they are unable, or only slowly able, to penetrate the air-water boundary. Therefore this vessel was changed over from over water to under water distribution.

In this context, the *Barbara* (Fig. 1) is another water treatment vessel, based on under

Figure 1 *Water treatment vessel Barbara in operation, and (bottom right) being lowered – showing the delivery system between the vessel's hulls (courtesy: LUG/LMBV)*

Figure 2 *LMBV water treatment vessel Klara during trial operation (courtesy: LMBV)*

water technology. The vessel is a catamaran with two tube mixers mounted between the hulls This allows additional mixing by the vessel's two propellers at the ends of the twin hulls. The vessel has two lime bunkers, each with a capacity of 12 m³, allowing material to be bunkered according to the bulk density of the lime.

Positive aspects of this new technology are high effectiveness of neutralization agent and economic mixing technology. This is due to the high turbulence and the low concentration of the solid matter with a suspension of way less than 1 %. The main disadvantage of this vessel is the long loading time of the on-board silo. A further step of development of particular relevance to LMBV is the water treatment vessel *Klara* (Fig. 2). It has been designed and built specifically for use at the Lausitzer Seenland, which are former mining pits.

The Lausitzer Seenland consists of nine former mining pits, which are connected by navigable canals, in the federal states of Saxony and Brandenburg (Fig. 3) between Senftenberg and Spremberg. AlthoughLake Senftenberg is nevertheless connected to the chain by the Koschen Canal. The water surface area of the entire lake chain exceeds 55 km², and it has a volume of more than 800 million m³.

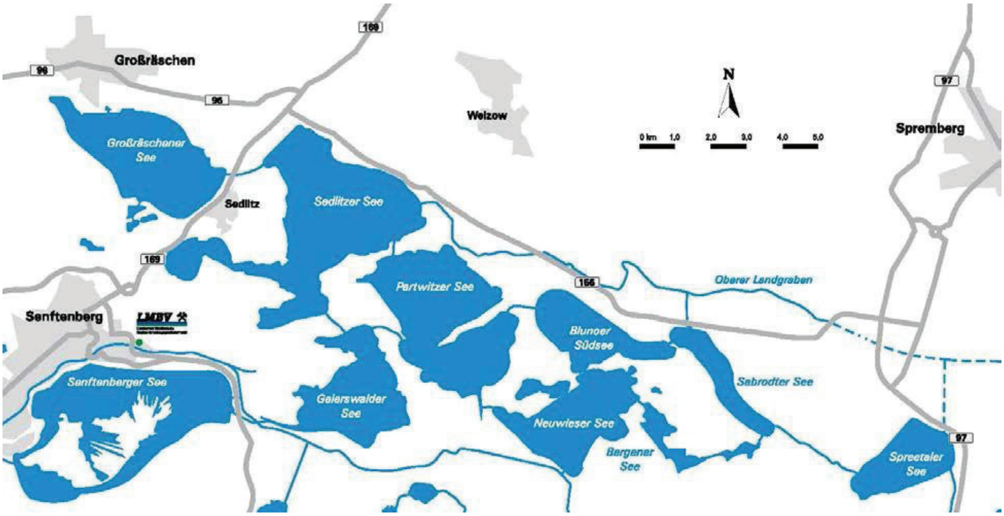

Figure 3 *Lausitzer Seenland, former mining pits and Lake Senftenberg – 9 interconnected post-mining lakes (courtesy: LMBV)*

The *Klara* dimensions were defined so that it would be able to pass through all canals, bridges, and locks. *Klara* vessel consists of a push boat with two barges with silos (Fig. 4).

The engine, generator, and the bridge are on the push boat. There are two lime silos on each barge, and beneath each of the barges, two discharge units have been mounted between the catamaran twin hulls.

This discharge unit arrangement of the water treatment vessel Klara has the advantage that while the first barge is on the lake with the push boat discharging neutralization agent, the second barge can be loaded. It reduces the time between two treatment cycles to about 5 minutes for changing the barges. *Klara* can distribute caustic lime, pulverised limestone, or calcium hydroxide, and is able to deliver neutralization very efficiently. It reaches high levels of dilution in lake water by boosting the agent by the vessel propellers. The vessel is dimensioned for the discharge of approximately 40,000 t of neutralization agent per year. Klara is therefore able to carry out both the initial neutralization as well as the follow-up for the entire Lausitzer Seenland (s. Fig. 3).

Choice of neutralizing agent

With regard to the neutralizing agents most frequently tested so far, the following statements can be made (LMBV 2017b). These are based on experience gathered over the past few years, regarding their efficient and effective use:

Caustic lime, pulverised calcium oxide CaO:
- high neutralization equivalent (approximately 30 to 35 mol/kg),
- reasonable price,
- high reactivity ensures a high kinetic rate of reaction, but can also cause locally high pH values in lake water

Calcium hydroxide, main ingredient: ground $Ca(OH)_2$
- neutralization equivalent of approximately Neq = 25 to 29 mol/kg,
- relatively high specific price due to the additional process steps involved in its production,
- supplied as a prepared lime water suspension is an advantage compared to the use of caustic lime.

Pulverised limestone, consisting of ground $CaCO_3$ (limestone or chalk)
- relatively low neutralization equivalent of Neq ≤ 20 mol/kg,
- efficient use, it needs to be finely pulverised (e.g. d90 < 40 µm),
- low specific costs, approximately 0.3 Euro cent per mole of alkalinity,
- ability to reach higher alkalinity more efficiently than when caustic lime is used, developing hydrogen carbonate buffer up to KS4.3 ≈ 0.5 mmol/l,
- ecological advantages due to the fact that over neutralization to pH-values of more than 8 are not possible.

Soda, main component: ground Na_2CO_3
- easily soluble in all pH ranges, does not require any complicated technology,
- comparatively expensive, and
- ecologically not ideal as it increases salinity (i.e. elevated sodium level).

Figure 4 *LMBV water treatment vessel Klara (right) coupled to barge 1 (right), barge 2 (left) at the loading site on the Koschendamm eastern bank (source: Totsche 2017)*

Although the specific prices per mole of alkalinity of caustic lime and of pulverised limestone are very similar, caustic lime is usually the more cost-effective option. Caustic lime would be preferred wherever neutralization does not require alkaline buffering of alkalinity > 0.25 mmol/l at $6 < pH < 7$. The focus of initial neutralization will therefore be on the use of caustic lime, while follow-up neutralization of post-mining lakes will focus on pulverised limestone. In coming years, when the initial neutralization will have been completed, this proportion/ratio will shift further towards finely pulverized limestone. Under certain circumstances, the use of chalk products as a specific form of pulverised limestone may become increasingly relevant.

Use of gaseous CO_2

The use of CO_2 to develop a hydrogen carbonate buffer decreases the need for follow-up treatments significantly. Generally, it can be stated that hydrogen carbonate buffering is a relevant follow-up treatment as well from the economic as from the ecological point of view (LMBV 2017b). It avoids the rapid neutralization during the treatment phase, and slower re-acidification during intervals without treatment. The pH fluctuations from $5 < pH < 9$ is assessed to be disadvantageous for biocoenosis in the water.

The use of CO_2 will remain of interest in the future, especially to prevent the pH value from sinking during the winter if the lakes freeze over. This had been the case at the Lake Drehna pilot project.

Here classic liming technology eight liming campaigns with caustic lime are necessary per year, and a pH-drop during the ice cover could not be avoided for sure. The use of CO_2 is limited to the fact, that over-dosage will harm biological species in the lake. Using CO_2, a three-month campaign is sufficient to keep the pH-value stable for more than a year.

Summary

A relevant example of a mobile plant used for neutralization is the LMBV water treatment vessel *Klara*. It was custom designed and built for the initial and follow-up neutralization of the Lausitzer Seenland, the mining lake. The *Klara* is the most powerful water treatment vessel built to date, which follows up the development of several in-lake treatment vessels. Other large treatment vessels such as the *Barbara* are suitable for post-mining lakes with relatively high demands for neutralization agent. They have proved their usefulness. However, hauling these large water treatment vessels from one lake to another by road is complicated. They also require suitable areas for launching the vessel and charging with neutralization agents. Small water treatment vessels such as the *Brahe* can easily be watered and hauled without requiring a heavy-load transport licence.

For initial neutralization, quicklime tends to be the most cost-efficient neutralization agent. For follow-up neutralization, finely ground limestone usually is the preferred agent due to health and ecological reasons. Under certain conditions the buffering of neutralized waters by the additional use of CO_2 gas can also be an appropriate method.

LMBV is able to carry out efficient and very effective in-lake neutralization measures using mobile water treatment vessels and stationary neutralization plants. By now, there are a number of well tested techniques available. The decision on technology and neutralization agent depends on both, technological and economic considerations. These decisions are usually made on a case-by-case basis.

References

LMBV 2017a Wasserwirtschaftlicher Jahresbericht, (LMBV Water Management Report) Senftenberg 2016,

LMBV 2017b Luckner L, Totsche O, Geller W, Grünewald U, Weiß H, Benthaus FC, (2017) In-Lake-Neutralization of Mining End Lakes in Lausitz and Mitteldeutschen Braunkohlerevier, State of the art and technical development, LMBV, 40 p

WRRL 2000 EU Water Framework Directive 2000, Directive 2000/60/EC of the European Parliament and the Council establishing the framework for the Community action in the field of water policy, Brussels 2000

WHG 2009 Gesetz zur Ordnung des Wasserhaushalts, Wasserhaushaltgesetz WHG (German Water Law) vom 31. Juli 2009 erschienen im BGBl. I S. 2585,

Totsche 2017 Totsche et.al. Wasserbehandlung und technische Entwicklung der In-Lake-Neutralisation von Bergbaufolgeseen, Proceedings DGFZ, ISSN 1430-0126, Heft 42

Treatment Of High Mn Concentrations At Waihi Gold Mine, New Zealand By Two Methods: A Limestone Leaching Bed And A Slag Leaching Bed

D. Trumm[1], H. Christenson[1], J. Pope[1], K. Watson[2],
K. Mason[2], R. Squire[2], G. McDonald[2], A. Mazzetti[2]

[1]CRL Energy, 97 Nazareth Avenue, Middleton, Christchurch 8540, d.trumm@crl.co.nz
[2]OceanaGold Corporation, 43 Moresby Avenue, Waihi 3610

Abstract

This work presents results of trial passive treatment systems at sites with up to 114 mg/L average Mn concentrations. Two parallel systems were trialled: one with a slag leaching bed and the other with a limestone leaching bed (LLB). Two types of slag were tested: melter slag and KOBM slag. The KOBM slag contained higher CaO content and outperformed the Melter slag, consistently removing over 97% of Mn and raising the pH to 8.6-12.9. The LLB removed an average of 32% of the Mn, and performance improved with time. Metal removal mechanisms for the two systems are discussed.

Keywords: passive treatment, manganese, steel slag leaching bed, limestone leaching bed

Introduction

The OceanaGold Waihi Gold Operation consists of the Martha open pit and the Favona, Trio, and Correnso underground gold mines located in Waihi New Zealand, North Island. Gold and silver are extracted from the ore and the barren tailings are pumped as a slurry into a tailings storage facility (TSF) containing two tailings storage ponds (TSF-1A and TSF-2). Waste rock from the open pit is utilised in the construction of the embankments for the TSFs. A network of drains collects seepage waters from tailings and waste rock in the TSFs. Some drains meet discharge requirements, but others are treated in an active treatment plant. In planning for eventual mine closure, OceanaGold would like to explore passive treatment options that could be used to treat all TSF drainage. The purpose of this work is to present the preliminary results of small-scale passive treatment systems treating two of the discharges from the TSFs at the Waihi Gold operations.

Methods

The tailings underdrain (TU site) for TSF-1A consists of three drainage lines installed under the tailings which join near the central part of the TSF and then flow underground through a common pipeline to the southwest into Manhole MH-11. Water quality data shows a water chemistry with neutral pH and elevated concentrations of Fe, Mn and, occasionally, Cu. Leachate drainage line L-10 (L-10 site) consist of two drainage lines installed under the northern embankment for TSF-2 which join near the northern edge of the TSF and then flow underground through a common pipeline to the north into collector sump T-13. Water quality data shows a water chemistry with slightly acidic pH and elevated concentrations of Fe, Al, Mn, Ni, Zn, Co and Cu.

Two different treatment systems were installed in parallel at each site: (1) a vertical flow reactor (VFR) for Fe removal followed by a steel slag leaching bed (SLB) for Mn and other trace element removal; and (2) a VFR for Fe removal followed by a limestone leaching bed (LLB) for Mn and other trace element removal.

VFRs are gravel filter beds which remove Fe at neutral and moderately-low pH through oxidation of Fe and precipitation and filtration of particulate and nanoparticulate ferric hydroxide precipitates (Sapsford et al. 2015; Blanco et al. 2018). VFRs are used here as a pre-treatment step prior to the SLB and the LLB systems. Each VFR was constructed using a 1 m^3 intermediate bulk container (IBC) mirroring the systems in Sapsford et al. (2007). Each tank was filled with 2-6 cm size gravel at a thickness of 280 mm (TU site) and 120 mm (L-10 site) which was overlain by 1 cm size stemming gravel at a thickness of 100 mm (both sites). Water flowed vertically down through the gravel bed, into a drainage pipe, and the exit point was outside the IBC through a riser to maintain water level in each tank at 830 mm (TU site) and 800 mm (L-10 site).

Both SLBs were constructed using IBCs filled to a height of 630 mm with waste slag from the electric arc furnace process at New Zealand Steel Limited. The material was Melter slag from iron making (10-20 mm size) and is dominated by TiO_2 (34-36%), AlO (18-19%), CaO (14-17%), and MgO (12.8-13.5%). Water flowed into the top of the SLB, vertically downwards through the bed, and out of the IBC through a riser to maintain water level in the tank at the top of the steel slag. After six months of operation, each SLB was taken off line and a new SLB was constructed at each site using Klöckner Oxygen Blowing Maximillanshuette (KOBM) slag (10-50 mm size). This slag is from steel making and is dominated by CaO (51-58%), FeO (16-23%), and MgO (9-13%).

Although the pH is not raised higher than 8 in an LLB, effective Mn removal has been shown to occur in these beds (Vail and Riley 1995; Tan et al. 2010; Christenson et al. 2016). Both LLBs were constructed using IBCs filled to a height of 900 mm of high-Ca limestone (15-25 mm size). Water flowed into the top of the LLB, flowed vertically downwards through the bed and out of the IBC through a riser to maintain water level in the tank at the top of the limestone.

Monitoring of the influent and effluent for the systems was conducted on an approximately fortnightly basis for 14 months. Samples from the TU systems were laboratory-analysed for pH, alkalinity, bicarbonate, Ca, Fe, Mn and Cu (dissolved), and Fe (total). Samples from the L-10 systems were laboratory-analysed for pH, alkalinity, bicarbonate, Ca, Fe, Mn, Ni, Zn and Co (dissolved), and Fe (total). Only a small percentage of the total flow at each site was treated. Influent and effluent flow measurements were taken during each site visit by timing the length of time to fill a measuring cylinder.

Results

TU Site

The inlet water pH was 6.0-6.5 and contained 17.4-25 mg/L Fe (total), 17.3-23 mg/L Fe (dissolved) and 7.3-10 mg/L Mn (dissolved). Cu concentrations were below detection limits. The flow rate through the VFR and SLB system ranged from 80 ml/min to 550 ml/min (224 ml/min average) and the flow rate through the VFR and LLB system ranged from 26 ml/min to 220 ml/min (129 ml/min average). The VFR preceding the SLB had an HRT of 18-124 h and removed 67-98% of the dissolved Fe and 25-93% of the total Fe. The VFR preceding the LLB had an HRT of 45-370 h and removed 57-98% of the dissolved Fe and 0-94% of the total Fe. Removal in both VFRs was proportional to HRT.

The HRT in the SLB (Melter slag) was 28-62 h (42 h average). Outlet pH was 6.9-7.9. Mn removal was as great as 11.5%, however, most of the data show negligible Mn removal and instead show net export of Mn from the slag (fig. 1). Longer HRTs in the SLB did not improve removal (fig. 2). For the KOBM slag, the HRT was 10-70 h (27 h average). Outlet pH from the SLB was 9.3-12.9 and Mn removal was >99.8% for all sampling events (figs 1 and 2).

The HRT in the LLB was 38-317 h (79 h average). Outlet pH was 6.5-7.8. Mn removal was between 5% and 86% (average of 23%) and showed a general decline in performance during the first three months, stabilising at removal percentages between 10% and 30% over the remaining 11 months (fig. 1). Longer HRTs in the LLB did not improve removal (fig. 2).

L-10 Site

The inlet water pH was 3.7-6.5 and contained 3.3-30 mg/L Fe (total), and 3.0-29 mg/L Fe (dissolved), 92-134 mg/L Mn, 0.94-1.54 mg/L Ni, 0.44-1.68 mg/L Zn and 0.37-0.71 mg/L Co (all dissolved). The flow rate through the VFR and SLB system ranged from 100 ml/min to 485 ml/min (213 ml/min average) and the flow rate through the VFR and LLB system ranged from 92 ml/min to 252 ml/min (150 ml/min average). The VFR preceding the SLB had an HRT of 22-95 h and removed 65-99% of the dissolved Fe and 0-94% of the total Fe. The VFR preceding the LLB had an HRT of 52-127 h and removed 67-99% of the dissolved Fe and 0-94% of the total Fe. Removal in both VFRs was proportional to HRT.

The HRT in the SLB (Melter slag) was 31-62 h (48 h average). Outlet pH was 6.2-7.6. Although net export of Mn occurred on two occasions, removal was documented on all other days (fig. 3). Removal of metals was 0-17% Mn (average of 5.6%), 2.1-64% Ni (average of 28%), 21-96% Zn (average of 46%) and 0-70% Co (average of 24%). Removal of Mn and all other trace elements was proportional to HRT (fig 4). For the KOBM slag the HRT was 11-51 h (25 h average). For all data points except one (an outlier), outlet pH from the SLB was 8.6-12.4 and Mn removal was 96.7% to >99.9%, with an average removal of 99.7% (figs 3 and 4). For all data points except one, the SLB also removed 99.0-99.9% of Ni (99.5% average), 96.2-99.7% of Zn (98.5% average), 99.0-99.9% of Co (99.6% average).

The HRT in the LLB was 31-85 h (57 h average). Outlet pH was 6.7-7.4. Mn removal was between 14% and 51% (average of 32%) and showed a general improvement in performance with time (fig. 3). The LLB also removed 12-58% of the Ni (average of 30%), 12-77% of the Zn (average of 49%) and 26-95% of the Co (average of 70%). Removal of Mn and all other trace elements was proportional to HRT (fig. 4).

Discussion

VFRs

The VFRs are removing Fe at percentages similar to that observed for other neutral Fe-rich mine drainage water in New Zealand and overseas (Sapsford et al. 2015; Trumm et al. 2015; Blanco et al. 2018). It is likely that Fe is removed through filtration of particulate and nanoparticulate Fe, microbial and heterogeneous oxidation of Fe(II), and heterogeneous precipitation of Fe(III) as ferrihydrite on the gravel substrate. VFRs should be used to remove Fe prior to treatment with either limestone or steel slag in LLBs and SLBs, otherwise, precipitation of iron hydroxides can plug the leaching beds and can armour the treatment media (limestone, slag) reducing treatment effectiveness (Ziemkiewicz et al. 1997; Skousen et al. 2000).

SLBs

The SLBs constructed using Melter slag showed variable removal percentages. At the TU site, increased HRT resulted in increased pH, however, this was unlikely to be high enough for effective removal of Mn as Mn oxides, carbonates or hydroxides. The maximum pH attained at TU was 7.9 and the lowest solubility for Mn is at a pH of 10.6 (INAP 2009).

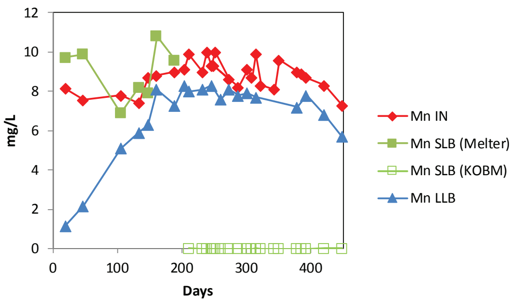

Figure 1 Concentrations of Mn for treatment systems at TU site. IN, into systems; SLB, slag leaching bed (using either Melter or KOBM slag); LLB, limestone leaching bed.

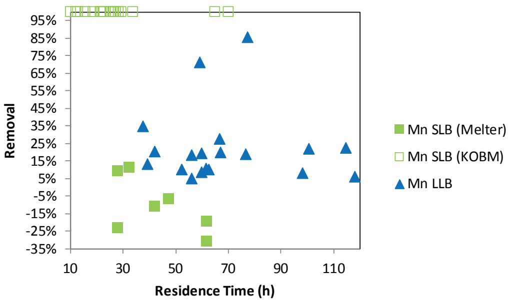

Figure 2 Percent removal of Mn by SLB and LLB for TU site. SLB, slag leaching bed; LLB, limestone leaching bed.

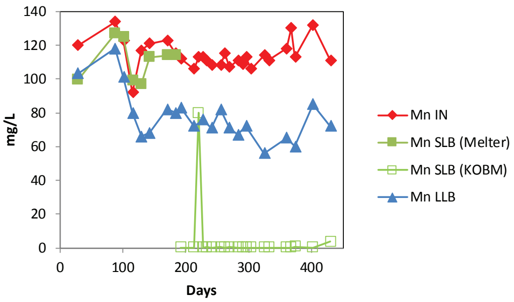

Figure 3 Concentrations of Mn for treatment systems at L-10 site. IN, into systems; SLB, slag leaching bed (using either Melter or KOBM slag); LLB, limestone leaching bed.

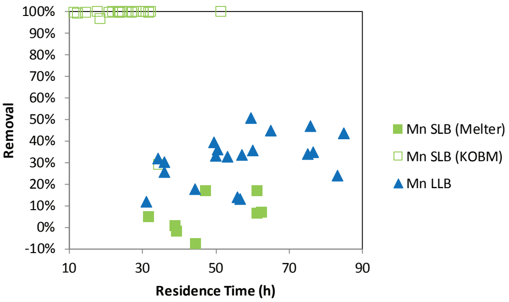

Figure 4 Percent removal of Mn by SLB and LLB for L-10 site. SLB, slag leaching bed; LLB, limestone leaching bed.

Removal of Mn by the SLB at the L-10 site was better than at the TU site. The pH was proportional to HRT and removal of Mn was proportional to pH, however, as with the TU site, the maximum pH attained (7.6) was far less than necessary for theoretical Mn removal. The inlet Mn concentration at L-10 was more than an order of magnitude greater than that at TU. Perhaps this very high concentration enhanced autocatalytic oxidation and precipitation of Mn or perhaps other conditions, such as the community of microbial Mn oxidisers or the oxidation states of Mn in the inlet water, favoured Mn removal at L-10. Regardless, the results at L-10 suggest that Melter slag can remove a proportion of Mn from solution (up to 17%). The percent removal of trace elements by the SLB was in the following order: Zn > Ni > Co. This is in the order of increasing pH of minimum solubilities for these metals (pH 8.5 for Zn, pH 9.3 for Ni, pH 11 for Co; Macdonald et al 1971; INAP 2009) and is also the order of increasing pH at which maximum adsorption of these metals occurs onto hydrous ferric oxide (Dzombak and Morel 1990). If the adsorption pattern onto Mn oxides is similar to that onto ferric oxide for these metals, either or both mechanisms may be removing these metals in the Melter slag SLB (precipitation or adsorption).

The results for the KOBM slag for both sites show exceptional performance in removal of Mn and other trace elements. Removal of these metals is likely to be due to minimum solubilities at the elevated pH achieved by the SLB, which is likely due to the higher CaO content compared to the Melter slag even though the effective surface area of the Melter slag was greater (due to smaller gravel size). Operation of the KOBM SLBs will continue at much shorter HRTs to determine potential operating parameters for a full-scale system.

LLBs

It is unlikely that elevated pH is a major factor in Mn removal in a limestone bed since the pH of minimum solubility for Mn is much greater than can be achieved by limestone alone. It is possible that microbial oxidation of Mn(II) is a primary mechanism and that autocatalytic oxidation and precipitation is enhanced with time as Mn oxides accumulate, as shown in the work by Christenson et al. (2016). Initial increase in pH in an LLB may help to initiate Mn removal. Limestone in both LLBs was coated with black precipitate.

At the TU site, longer HRTs do not result in higher pH, so percent removal of Mn is not affected by HRT (above the minimum 38 h in the trials). Removal percentage by the LLB at the L-10 site, however, has generally increased with time and is positively correlated with both HRT and pH. It is possible that due to the very high Mn concentrations at this site, autocatalytic oxidation and precipitation may be a much more important factor than at the TU site. The percent removal of trace elements by the LLB was in the following order: Co > Zn > Ni. Since cobalt has lowest solubility and maximum adsorption percentage onto ferric oxide at higher pHs than that of Zn and Ni, this high Co removal percentage is unexplained. However, it is possible that removal of these trace elements is by either or both mechanisms (precipitation and adsorption).

The advantage of an LLB over a SLB for treatment of Mn is that the pH will not increase much more than approximately 8, however, the advantage of an SLB over an LLB is that much lower concentrations of Mn and other trace elements can be achieved.

Conclusions

Two different passive treatment techniques were trialled at two different leachate drainages with elevated concentrations of Fe, Mn and a range of trace elements from the TSFs at the OceanaGold Waihi Operation. The systems consisted of (1) a VFR for Fe removal followed by an SLB (using Melter slag) for trace element removal, later replaced with an SLB using KOBM slag, and (2) a VFR followed by an LLB.

The VFRs in both systems at both sites were effective in removing up to 98% of the dissolved Fe. These systems removed Fe through filtration of particulate and nanoparticulate Fe, microbial and heterogeneous oxidation of Fe(II) and heterogeneous precipitation of Fe(III) as ferrihydrite on a gravel substrate.

Contrary to expectations, the SLBs did not increase the pH to levels high enough for substantial Mn removal. The maximum pH attained was 7.9 (TU site) and 7.6 (L-10 site). The maximum percent removal at the two sites was 12% (TU site) and 17% (L-10 site), and only the L-10 site showed consistent removal. It is possible that the very high concentrations at the L-10 site (112 mg/L Mn) resulted in autocatalytic oxidation and precipitation of Mn or perhaps other conditions, such as the community of microbial Mn oxidisers or the oxidation states of Mn in the inlet water, favoured Mn removal at L-10. In addition to Mn, trace elements were removed by the SLB at the L-10 site in the following order of decreasing effectiveness: Zn > Ni > Co. This is the order of increasing pH of minimum solubilities for these metals as well as the order of increasing pH at which maximum adsorption of these metals occurs, suggesting that removal was solubility-controlled and/or due to adsorption onto Mn oxides. Additional SLBs constructed at each site using steel slag with a higher CaO content (KOBM slag) raised the pH of the leachate to between 8.6 and 12.9 and showed consistent removal of >97% of Mn and other trace elements. Experimentation with different HRTs continue for the SLBs containing KOBM slag.

The LLBs were consistently better performers than the SLBs constructed with Melter slag. Percent removal averaged 23% (TU site) and 32% (L-10 site). Removal of Mn is possibly through microbial oxidation of Mn(II) and autocatalytic oxidation and precipitation as Mn oxides. Contrary to the SLB at the L-10 site, the percent removal of trace elements by the LLB was in the following order: Co > Zn > Ni. It is possible that removal of these trace elements is by the same mechanisms that may be occurring in the SLBs (precipitation and adsorption). The experiment will continue at both the TU and L-10 sites order to document performance of the LLBs over time.

Acknowledgements

This research was financed by OceanaGold and the Ministry for Business, Innovation and Employment, contract CRLE 1403. We thank Ngati Hako, Ngatiwai, Ngai Tahu, West Coast Regional Council, Waikato Regional Council, Northland Regional Council, Department of Conservation, Straterra, Minerals West Coast, OceanaGold, Solid Energy of New Zealand, Francis Mining Group and Bathurst Resources for their involvement and support for the research programme. More information on the Centre for Minerals Environmental Research (CMER), including research currently being undertaken, is available at: http://www.crl.co.nz/cmer/.

References

Blanco I, Sapsford DJ, Trumm D, Pope J, Kruse N, Cheong Y, McLaughlan H, Sinclair E, Weber P, Olds W (2018) International trials of vertical flow reactors for coal mine water treatment. Mine Water Environ 37(1): 4-17.

Christenson H, Pope J, Trumm D, Uster B, Newman N, Young M (2016) Manganese removal from New Zealand coal mine drainage using limestone leaching beds. In: Proceedings of the International Mine Water Association conference, Leipzig, Germany, 906-912.

Dzombak D, Morel FMM (1990) Surface complexation modeling. John Wiley & Sons. 393p.

INAP (International network for Acid Prevention) (2009) Global Acid Rock drainage Guide (GARD Guide). http://www.gardguide.com.

Macdonald DD, Shierman GR, Butler P (1971) The thermodynamics of metal-water systems at elevated temperatures. Part 3: The cobalt-water system. Whiteshell Nuclear Research Establishment, Pinawa, Manitoba ROE 1L0.

Sapsford D, Barnes A, Dey M, Williams K, Jarvis A, Younger P (2007) Low footprint passive mine water treatment: field demonstration and application. Mine Water Environ 26: 243-250.

Sapsford D, Florence K, Pope J, Trumm D (2015) Passive removal of iron from AMD using VFRs. Proceedings of the 10th International Conference on Acid Rock Drainage and IMWA Annual Conference. April 21-24, 2015. Santiago, Chile.

Skousen J, Sextone A, Ziemkiewicz PF (2000) Acid mine drainage control and treatment. In: Barnhisel RI, Darmody RG, Daniels, WL ed. Reclamation of drastically disturbed lands. Monograph Number 41. American Society of Agronomy, Madison, WI, USA. Pp. 131-168.

Tan H, Zhang G, Heaney PJ, Webb SM, Burgos WD (2010) Characterization of manganese oxide precipitates from Appalachian coal mine drainage treatment systems: Applied Geochemistry, v. 25(3), p. 389-399.

Trumm D, Sapsford D, Rubio I, Pope J (2015) Application of vertical flow reactors in New Zealand for removal of iron from AMD. Proceedings of the annual conference, New Zealand Branch of the Australasian Institute of Mining and Metallurgy, 31 September to 2 October 2015.

Trumm D, Pope J (2015) Passive treatment of neutral mine drainage at a metal mine in New Zealand using an oxidizing system and slag leaching bed. Mine Water Environ DOI 10.1007/s10230-015-0355-3. Published online at: http://dx.doi.org/10.1007/s10230-015-0355-3.

Vail WJ, Riley RK (1995) Process for removing manganese from solutions including aqueous industrial waste. U.S. Patent No. 5,441,641. 15 Aug. 1995.

Ziemkiewicz PF, Skousen JG, Brant DL, Sterner PL, Lovett RJ (1997) Acid mine drainage treatment with armoured limestone in open limestone channels. Journal of Environmental Quality 26: 1017-1024.

Development of a technical concept of spatial and temporal coordinated mine water recycling exemplified by a mining area with urban influence

Antje Ulbricht[1], Felix Bilek[1], Katrin Brömme[2]

[1]Groundwater Research Centre Dresden, Meraner Str. 10, 01217 Dresden, Germany, aulbricht@dgfz.de
[2]Ruhr University Bochum, EE+E Environmental Engineering and Ecology, Universitätsstraße 150,
44780 Bochum, Germany, katrin.broemme@rub.de

Abstract

A technical concept for an integrated mine water management regarding the spatial and temporal change and the strong seasonal weather variations was developed. The aim of the concept is the modification of the water infrastructure within the project area Hon Gai peninsula, Ha Long, Vietnam, to balance temporal water deficits. The adaption of the water treatment to the individual requirements of various users is also included in the concept. The methods and tools to identify the need for action and assess possible solutions are described.

Keywords: integrated water management, technical concept, mine water use, post-mining land use planning, Vietnam

Introduction

One of the hardcoal mining areas in Quang Ninh, Vietnam, is located on the Hon Gai peninsula next to Ha Long City. The mine water affects the surface water on the peninsula and the coastal water of Ha Long Bay, which was recognized as World Natural Heritage Site by UNESCO in 1994. For this region a concept for an integrated mine water management will be developed by the WaterMiner project, which is sponsored by the German Federal Ministry of Education and Research (BMBF). Due to spatial changes and the predictable change of the water demand caused by closure of mining and the socio-economic development, the concept includes the current stage as well as future stages of development of the region. The project combines the analysis from a material flow perspective (Brömme et al. 2018) and from an economic perspective (Do et al. 2018) with the technical perspective which is presented here. The final product is a spatial and temporal coordinated mine water management.

On the Hon Gai peninsula the mine water origins from the draining of the mines (pit water) and the surface runoff within the mining area. The pit water is characterised by moderate concentrations of iron and high manganese concentrations. Currently, this water is treated partly and reused for purposes like coal screening, truck wash, domestic use and watering plants. Due to the closing of open pit mines the process water volume will decrease in the future. Consequently the amount of water which can be reused for these purposes will decrease. The surface runoff contains high loads of sediment and coal dust. After heavy rain events the water and the sediments are transported by rivers to the urban area where the sediment and coal dust deposit. The amount of this water and the containing substances are currently not treated or reused.

Due to socio-economic changes of the region the water demand for domestic purposes will increase. Thus one of the major future challenges of this region is to cover the increasing water demand. The temporal fluctuating water quantity with water scarcity in dry season and flooding events in the rainy season is a major difficulty for the water management.

A technical concept is established which includes solutions to support the water infrastructure and balance water deficits and excess supply to guarantee a constant and long-term water supply for the whole region. The aim is to store, treat and supply surplus water to various users in the area according to their individual quality and quantity requirements.

Data acquisition

From 2005 to 2015 morphologic data, climatic data and data about the water quality of the project area were collected within RAME project (EE+E Environmental Engineering+Ecology 2016). These data were expanded and revised by the integration of new data which was collected during fieldtrips. Interviews with staff and managers of the mining companies and VINACOMIN (Vietnam National Coal – Mineral Industries Holding Corporation Limited) resulted in new information regarding the future territory planning. On the basis of this information the existing digital elevation models were updated (fig. 1) to get information about future morphology, catchment area borders and possible water storage volumes.

The geometry of the rivers (cross sections, slopes) was surveyed and water qualities were determined by taking water samples. The sediment samples were taken within the mining area and along the riverbanks to obtain knowledge of the sediment composition (grain sizes, share of coal dust).

Data about hydrological conditions of the rivers are currently not available. Due to this fact a monitoring concept was created to observe the river water levels and to measure the quality parameters pH, electrical conductivity, temperature and turbidity. For the monitoring multiparameter probes and cameras, which observe the water levels at water gauges, will be used. The water levels at various cross sections are required to calculate the water discharges. The knowledge of the discharge amount is the basis of the determination of the surface runoff within the mining area and the calibration of the precipitation-runoff model.

Methods

Due to the declining mining activities, the corresponding landscape transformation and the change of the water demand and water sources, the technical concept includes three stages of the project area. Stage 1 is the current stage with both open pit and underground mining. Stage 2 represents the near future when the opencast operations and partly underground operations will be stopped. Stage 3 describes the final situation of the area when the recultivation and landscaping is finished. For these stages the data was collected to identify the main difficulties of the water and sediment management and find solution approaches (tab. 1). Possible measures to improve the water quality and water management will be examined with the help of modeling tools (fig. 2).

The major uncertainty of the currently available data is the quantity of surface runoff and the sediment which is transported from the mining area into the rivers. The discharge data is necessary for planning technical measures to improve the water treatment and the water distribution system. It is also needed to estimate the effectiveness of future water storages. Information about the eroded sediment and coal dust will be used to plan the recov-

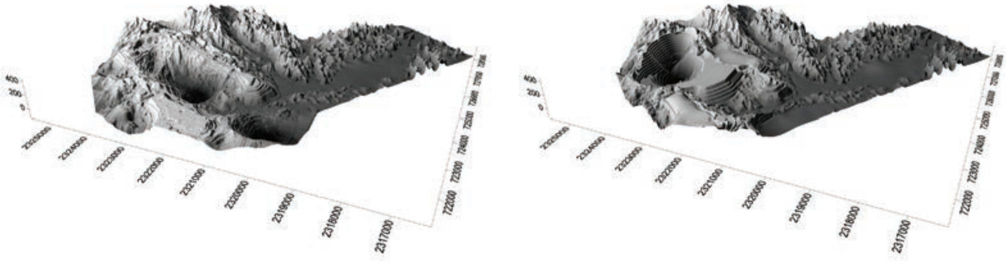

Figure 1 spatial change of the Ha Tu mining area (left: current stage, right: final stage) ery and separation of this material. To obtain these information the surface water runoff and the sediment transport will be calculated with the precipitation-runoff model HEC-RAS. The developed monitoring system will provide data to calibrate the model.

To determine the quantity of usable water in storages like lakes or aquifers the knowledge of water levels and the interactions between water and the geological structures is indispensable. The model ModelMuse (MODFLOW) will be used to simulate groundwater and lake water levels depending on the climatic conditions and different mining stages to identify the quantity of these storages. The influence of withdrawal rates will be analysed. Possible positions of wells and treatment plants will be planned.

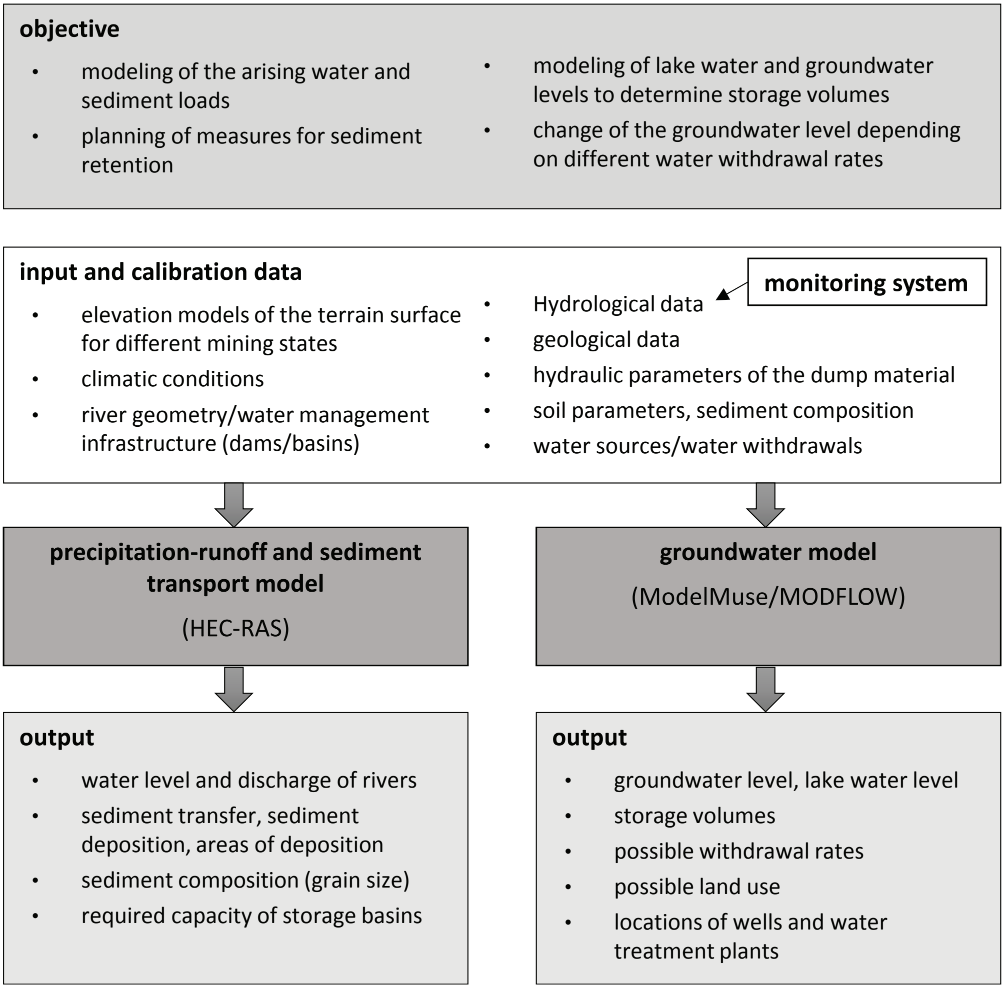

***Figure 2** modeling tools and data requirements for system analysis and the assessment of technical measures*

Results and Discussion

Several difficulties for the water management occur due to the high climatic seasonality, the socio-economic development of the region and the change of landscapes caused by the closing and restructuring of the mining areas (tab. 1). Currently, the greatest difficulty is the poor water quality in rainy season caused by the high sediment loads. To prevent the sediment deposition in the urban area and to retain the sediment within the mining area the technical concept includes the restructuring of the rivers and the installation of settling basins. Within the WaterMiner project those measures will be planned exemplary for a section of the Lo Phong River in the Ha Tu mining area. Depending on the needs of the Vietnamese partners the coal sludge and the clastic sediment can be either recovered and separated for later reuse or simply dumped together.

In the future the greatest difficulty will be the water deficit in dry season (tab. 1). On the annual average there is enough water to cover the increasing water demand. Consequently, storage possibilities are identified to guarantee the water supply in dry season.

When the coal dust and sediment loads will decrease due to the restructuring or the closing of open pit mines the settling basins will not be necessary anymore. Then the basins can be used as storage basins for water. Furthermore, a concept for the final stage was developed which includes the re-utilisation of the already existing pits and dumps as water storages (fig. 3). The water of the pit lakes and the groundwater which is accumulated in the porous material of the dumps can be used for several purposes. Depending on the quality requirements of the future water users the treatment process and the distribution system have to be adapted.

Table 1. *Difficulties and solution approaches depending on different mining stages*

	stage 1 – current stage	**stage 2 – near future**	**stage 3 – final situation**
difficulties	high water discharges with high sediment loads, sediment deposition along the river (rainy season)	increasing water deficit in the urban area (dry season) retention of floods is necessary (rainy season)	large water deficit in the urban area (dry season) retention of floods is necessary (rainy season)
solutions	installation of settling basins to retain sediment load, restructuring of the river	former settling basins can be used as retention basins, use of closed open pits as reservoir	use of the water of pit lakes, use of dumps as groundwater storage, adaptation of the water infrastructure and the water treatment
water sources	water from open pit and underground mining, precipitation	water from underground mining, precipitation	precipitation
treated water	base flow, water from open pit and underground mining	base flow, water from underground mining, water which is stored in open pits and basins	lake water, ground water
water use	truck wash, coal screening, watering plants, domestic use (mine internal)	agriculture, industry, domestic use (mining companies)	domestic use (city), agriculture, industry
possibilities to store water		settling basins, open pits	Lake, settling basins, aquifer
sediment retention		Settling basins, separation of coal sludge	(vegetation of dump sites)

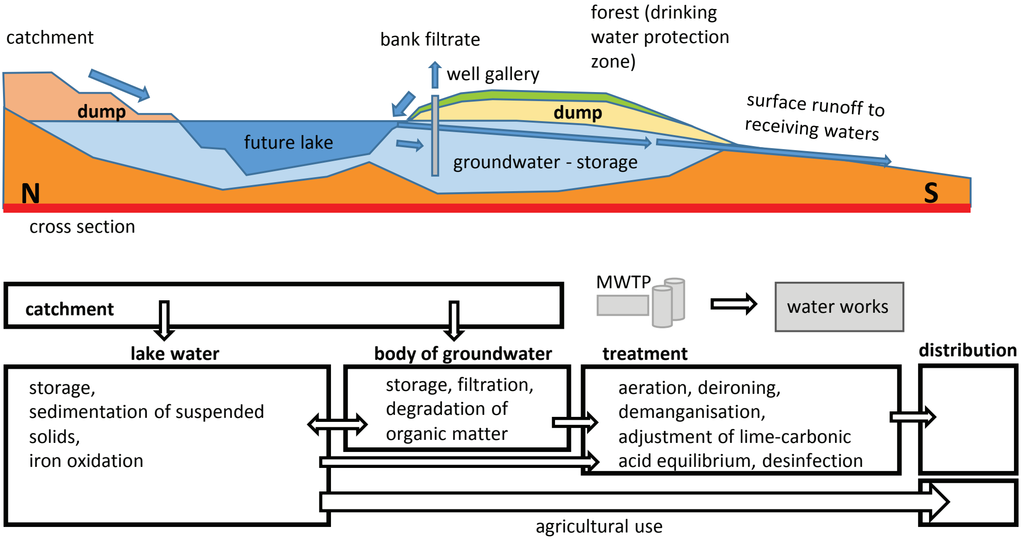

Figure 3 *concept for the use of pit lakes and adjoining aquifers as water sources and storages and necessary treatment steps for several purposes*

The developed technical concept is suitable for the water management of regions with open pit mining in areas characterised by strong seasonality of precipitation. In mining areas with underground mining problems like the salinization of groundwater occur, thus the water can not be used or has to be treated by cost-intensive technologies. In such cases a well-connected regional water distribution system and appropriate artificial water reservoirs are the basis for the prevention of local water deficits.

Conclusions

A general technical concept of spatial and temporal coordinated mine water recycling was developed. It will be used to identify suitable measures in a pilot area to improve the water management of the entire Hon Gai peninsula in its current and future stage. Precipitation-runoff, transport process, sediment and groundwater models will be used to quantify the volume of water and sediment resources which can be recovered. The concept will support the adaption of the water infrastructure to the future development and the increasing demands of residents, tourists and the industry.

Acknowledgements

The project is sponsored by the German Federal Ministry of Education and Research (Fkz. 02WAV1410A). The authors thank all contributors of the project partners Ruhr University of Bochum - EE+E Environmental Engineering and Ecology, VINACOMIN Vietnam National Coal – Mineral Industries Holding Corporation Limited, ribeka GmbH, disy Informationssysteme GmbH, LUG Engineering GmbH and University of Koblenz-Landau - Environmental Economy.

References

EE+E Environmental Engineering+Ecology (2016) Handbook on the results of the project „Mining and Environment in Vietnam 2005-2015". Bochum, 535 pp, doi: 10.2314/GBV:868016799.

Do, H.H., Trinh, V.Q., Frör, O. (2018) To invest or not to invest? – a valuation of mine water recirculation comprising private and public benefits in Halong, Vietnam. Proceedings of the International Mine Water Association Congress IMWA, 10-14 Sept. 2018. Pretoria, S_Africa (in publication).

Brömme, K., Trinh, V.Q., Greassidis, S., Stolpe, H. (2018) Material flow analysis for spatiotemporal mine water management in Hon Gai, Vietnam. Proceedings of the International Mine Water Association Congress IMWA, 10-14 Sept. 2018. Pretoria, S_Africa (in publication).

Are We Making Progress In The Treatment of Acid Mine Drainage?

Roxanne Naidoo, Kerri du Preez, Yageshni Govender-Ragubeer

Mintek, 200 Malibongwe Drive, Randburg, Gauteng, 2194A

Abstract

The formation of acid mine drainage (AMD) during the exposure of sulphide bearing material to oxygen and water, is of a major concern to the global mining industry and the environmental agencies of many nations. The recognition of AMD as one of the more serious current environmental problems internationally has resulted in its causes, prediction and treatment becoming the focus of a number of research initiatives commissioned by governments, the mining industry, universities and research establishments with input and support from environmental lobby groups.

Available literature contains a plethora of patented technologies and treatment techniques to address the growing concern of AMD. The High Density Sludge (HDS) process is cited as the most widely used process internationally to treat large quantities of polluted mine water. This is the most economical process available for the neutralisation of the acid content and the removal of the majority of metals from solution by lime addition. However it leaves between one and two grams per litre of sulfate in the product water and therefore ought to be followed by further treatment steps to reduce the sulfate content. For this, a number of options exist such as reverse osmosis, ettringite based precipitation and biological sulfate reduction.

AMD treatment requires (a) acid neutralisation, (b) metal removal and (c) sulfate removal. The HDS processes, whilst used extensively, addressed (a) and (b) only. This paper aims to provide a review of the current status of technologies aimed at (c) sulfate removal. This paper will also address why these technologies have not gained the same popularity as the HDS process for large scale implementation.

From this review it can be concluded that there are a number of factors that could hinder the technology transfer of treatment options from pilot to large scale implementation including (i) the quest for a "silver bullet" treatment approach versus intelligent solutions integration (ii) the impact of legislative framework and political systems on the selection of treatment options, (iii) the economic impacts of treatment costs and (iv) the treatment of secondary waste production.

Keywords: acid mine drainage, sulfate removal, water treatment technologies.

Introduction

Acid Mine Drainage (AMD) is produced when sulfide-bearing material is exposed to oxygen and water. This process can occur naturally, being mainly a function of the mineralogy of the local rock material and the availability of oxygen and water (Akcil, 2005). However mining can accelerate the process by exposing sulfide surfaces in mine waste rock, tailings and mine structures for example pits and underground workings. Naturally occurring bacteria promote AMD formation by catalysing the breakdown of sulphide minerals which they utilise as an energy source.

AMD is a historical problem that is worsened by present mining practices. It can potentially occur indefinitely and the long term environmental impact will continue long after mining activities have ceased. There are many abandoned, derelict and defunct mines which are a threat as gradually rising water is flooding these mines. This results in the contamination of shallow groundwater and surface water resources which is important for agriculture and human consumption.

A number of water treatment technologies have been proposed for AMD treatment, each producing a different quality of product water. It is important when choosing an AMD treatment technology that the end use of the product water has been identified first. For example some typical applications of treated water and the required sulfate levels thereof are given in Table 1.

The cost effectiveness of the process and the waste streams it will generate are also critical factors when choosing a suitable AMD treatment technology. The different technologies which have been evaluated can be divided into the following categories:

a. Chemical treatment processes with precipitation;
b. Biological sulfate reduction;
c. Physico-chemical treatment processes.

Background to AMD

AMD production

Typically AMD has a low pH, high conductivity, high concentrations of iron, aluminium and manganese, and low concentrations of toxic heavy metals. The reactions for acid production are best described by the oxidation of pyrite (FeS_2). The simplified pathway for pyrite oxidation is shown in Figure 1.

The equations described above have assumed that the oxidized material is pyrite and that the oxidant is oxygen. There are however other sulphide minerals such as pyrrhotite (FeS) and chalcocite (Cu_2S) which can also contribute to AMD generation.

Chemical treatment processes with mineral precipitation

SAVMIN^{TM}

SAVMIN^{TM} was patented by Mintek in 1998 for the treatment of AMD. A key feature of SAVMIN^{TM} is that it is able to decrease sulfate concentrations to less than 200 mg/L SO_4^{2-} via the addition of aluminium hydroxide to form the highly insoluble ettringite precipitate. A demonstration plant was recently run at Sibanye- Stillwater. An aerial view of the demonstration plant is shown in Figure 2.

Figure 2 *Aerial view of SAVMINTM demonstration site*

Table 1. Acceptable sulfate levels for potential applications of product water (Oelofse, 2012)

Product water application	Acceptable sulfate level in mg/L
Coal processing plant	1000
General industrial use	500
Discharge to public streams	500
Irrigation	200
Potable use	200
Cooling water in power station	20-40

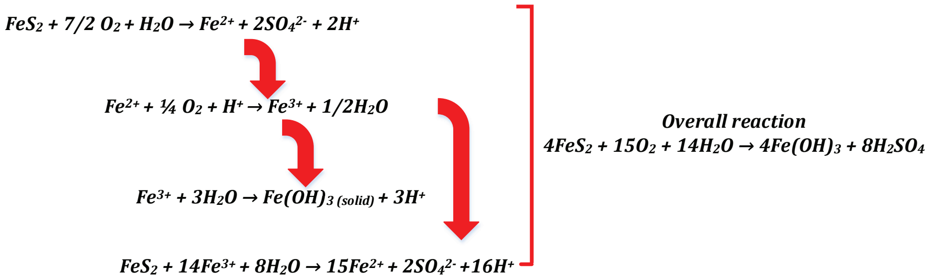

$$FeS_2 + 7/2\ O_2 + H_2O \rightarrow Fe^{2+} + 2SO_4^{2-} + 2H^+$$

$$Fe^{2+} + ¼\ O_2 + H^+ \rightarrow Fe^{3+} + 1/2H_2O$$

$$Fe^{3+} + 3H_2O \rightarrow Fe(OH)_{3\,(solid)} + 3H^+$$

$$FeS_2 + 14Fe^{3+} + 8H_2O \rightarrow 15Fe^{2+} + 2SO_4^{2-} + 16H^+$$

Overall reaction

$$4FeS_2 + 15O_2 + 14H_2O \rightarrow 4Fe(OH)_3 + 8H_2SO_4$$

Figure 1 *Simplified pathway for pyrite oxidation*

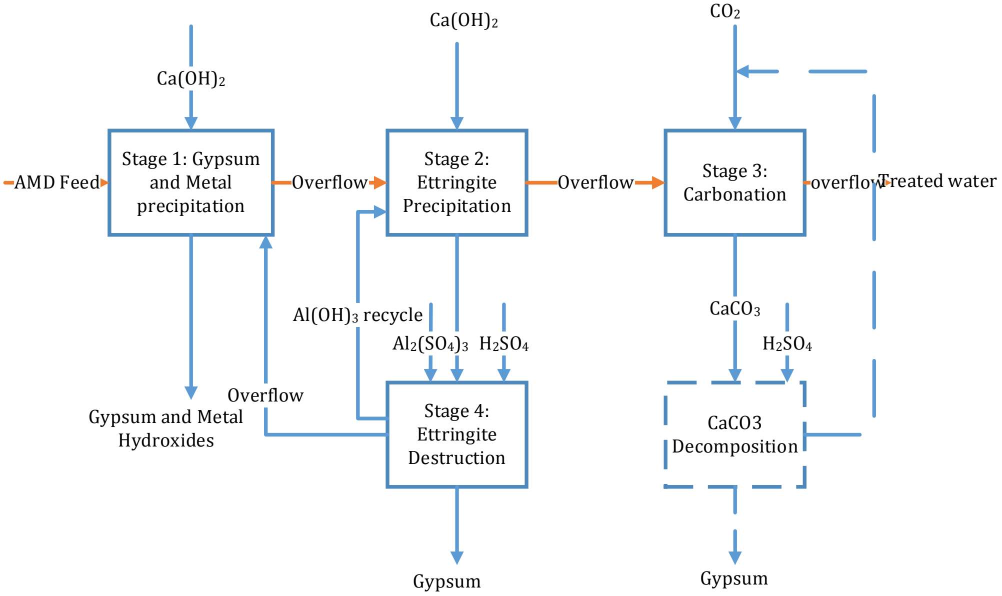

***Figure 3:** Simplified block flow diagram of SAVMINTM*

A simplified block flow diagram of SAVMIN^{TM} is shown in Figure 3. There are four stages in SAVMIN^{TM} which are as follows:

- Stage 1 – Heavy metal precipitation;
- Stage 2 - Ettringite precipitation;
- Stage 3 – Carbonation;
- Stage 4 - Recovery of aluminium hydroxide via ettringite decomposition.

SAVMIN^{TM} can recover >95 % of the water, reduce concentrations of trace metals and produce a non-saline effluent stream. The process is run at ambient temperature and pressure hence the electrical power consumption is also limited. However due to the high concentration of calcium sulfate in solution in parts of the circuit, gypsum scaling could be problematic without a proper management plan. The aluminium hydroxide can be recycled where relative costs of the reagents involved, warrant it. SAVMIN^{TM} does not address the monovalent ions, however this should not pose a problem for typical AMD solution compositions as it usually does not contain high concentrations of monovalent ions.

LoSO$_4$^{TM} process

The LoSO$_4$^{TM} process is similar to Savmin but requires large volumes of fresh water in the ettringite destruction stage to avoid solid gypsum formation. If the gypsum were to precipitate, it would contaminate the aluminium hydroxide in the ettringite precipitation stage thereby necessitating the Solid-Solid (S/S) separation step of SAVMIN^{TM}. A larger aluminium hydroxide recycle stream would be required if the recycled aluminium hydroxide is contaminated by gypsum. The use of HCl as an alternative means for ettringite destruction also introduces Cl-ions into the product water which complicates the system (Veolia, 2017).

ABC and MBA processes

The energy requirement for the ABC process would be relatively high due to the thermal reduction in the barium sludge processing step which is required for $BaCO_3$ recycling. The MBA process is an enhancement on the ABC process where magnesium hydroxide is also separated as a by-product. Barium carbonate is very toxic and if any unreacted barium carbonate were to pass through to the effluent stream it would have serious consequences (Beer, 2012).

Biological Sulfate Reduction

Mintek BSR

Biological treatment, using sulfate reducing bacteria (SRBs), can be used to purify effluent streams from the mining and metallurgical

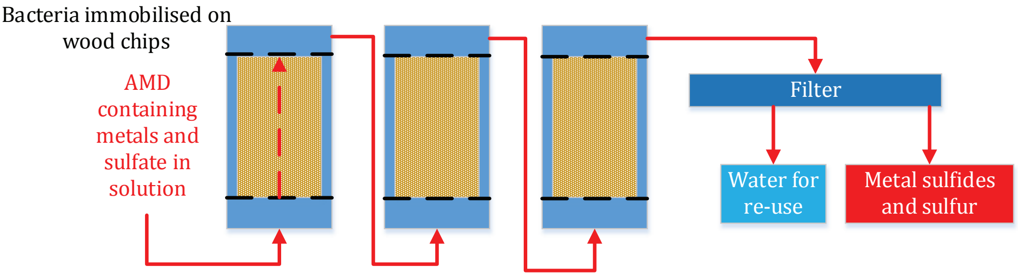

Figure 4: Schematic diagram of BSR process

industries. Biological sulfate reduction can be conducted in both passive and active systems. Passive systems maintain a large working inventory and operate slowly but require low maintenance, low operational input and use natural materials such as woodchips, gravel, manure and compost as substrate. In contrast the active treatment proceeds rapidly hence it requires a smaller inventory but requires frequent human intervention for maintenance and monitoring, requires external sources of chemicals, energy (electrical power) and labour, and incurs higher capital costs for infrastructure development. The active biological method involves the use of bioreactors which have the advantages of being compact and can offer more consistent performance and control while permitting the recovery of metals and sulphur as an added revenue stream to reduce the net operating costs.

Biological treatment of mine effluents and AMD offers a cost-effective and sustainable alternative to conventional treatment technologies. The process uses anaerobic SRB in the presence of organic substrates to remove sulfates and precipitate metals as metal-sulfides, while simultaneously producing alkalinity that raises the effluent pH.

A BSR pilot plant was commissioned at Sibanye-Stillwater, Randfontein on the West Rand of Johannesburg, as shown in Figure 5.

The BSR process removed more than 95% of the sulfates, and the treated water met the stringent South African discharge limits for sulfates (between 200 mg/L and 600 mg/L). The concentration of metals were reduced to trace amounts and the process produced considerably less solid waste, with decreased toxicity and increased stability compared to conventional chemical precipitation methods. The CAPEX is relatively low and the OPEX is reduced when using inexpensive carbon sources and/or a passive or semi-passive treatment design.

Figure 5: BSR pilot plant at Sibanye-Stillwater

Physico-chemical treatment processes

Electrocoagulation

The electrocoagulation system requires regular maintenance. There is the risk of electrode passivation over time which would reduce its efficiency. It is a relatively new technology compared to the typical water treatment processes (such as Reverse Osmosis (RO) and HiPRO) and limited information is available regarding the product water specifications. One of the main deterrents to the technology is the high electrical consumption, which directly impacts on the OPEX.

Membrane technology

Membrane technology cannot treat AMD directly. A pre-neutralisation step is required to remove the bulk of the metals from solution prior to purification. The membranes are prone to scaling and require regular maintenance which adds to the OPEX of the process. The membranes also have a limited lifespan which can further increase the OPEX (ENVIRONMENTAL, LORAX, 2003). The GYP-CIX process can tolerate relatively high concentrations of calcium, however the Total Dissolved Solids (TDS) needs to be less than 4000 mg/L SO_4^{2-}.

HiPRO process

The HiPRO process combines both precipitation and membrane technology. It produces potable water and requires relatively high maintenance of ultrafiltration and reverse osmosis membranes due to scaling. It also results in brine formation which cannot be discharged into rivers. The brine water is thus stored in large lined ponds at a high cost, and would need to be treated at some stage.

Secondary Waste production

Waste stream generation needs to be minimised to ensure that another potential hazard is not created. The amount of waste which is produced for the different processes are compared in Table 2.

Biological sulfate reduction would be the most favourable option as it does not produce a brine and the sludge generation is low to moderate.

Impact of legislative framework

Wastewater treatment plants in South Africa are regulated by the Constitution of the Republic of South Africa, 1996, the National Environmental Management Act 107 of 1998, the Water Services Act 108 of 1997, the National Water Act 36 of 1998, Provincial legislation, Municipal by-laws and other Government policies applicable to Local Government. However this comprehensive framework is applied retrospectively and cannot hold the current owners accountable for damages which were caused by AMD if the previous owners of the mines do not exist anymore. The AMD problem is mainly caused by defunct mines which are ownerless. Presently a comprehensive liability regime is required to prevent this disaster from occurring in the future. With regards to the current damage which was caused by AMD in the case of unidentifiable or non-existent liability, it would be up to the government and the taxpayer to pay for remediation and damages.

Conclusions

When choosing an appropriate AMD treatment technology, the following should be considered:

Table 2. *Waste by-products produced as a result of AMD treatment (Arnold, 2016), (ENVIRONMENTAL, LORAX, 2003)*

Chemical treatment processes with mineral precipitation	Sludge production	Brine production
Chemical treatment processes with mineral precipitation	Moderate-High	No
Biological sulfate reduction	Low-Moderate	No
Physico-chemical treatment processes	Low-moderate	Yes

- Composition of the inlet water;
- Specifications of product water;
- Infrastructure and space available;
- Waste generation.

These factors will identify possible pre-treatment steps required ahead of the chosen technology, and it also needs to be considered in calculating the OPEX and CAPEX of the technologies considered. Of course in general, costs can be expected to increase with increasingly demanding specifications of the product streams. Currently there is no ‘silver bullet treatment’ option but rather an integration of different solutions depending on the requirements of the product water. Storage/treatment of waste products also should be considered when calculating the OPEX. Secondary waste generation should also be carefully considered to ensure that additional environmental problems are not created. A concerted effort has gone into finding solutions to treat AMD over the last two decades which has resulted in a number of new developments. Progress has definitely been made and each technology is continually evolving to find the most economical and environmentally safe solution.

Acknowledgements

This paper is published with the permission of Mintek.

References

Akcil, A. K. (2005). Acid Mine Drainage (AMD):causes, treatment and case studies. Journal of Cleaner Production, 1139-1145.

Arnold, M. G. (2016). Technologies for sulphate removal with valorisation options. IMWA2016 Annual Conference.

Beer, M. M. (2012, March). Acid Mine Water Reclamation using the ABC Process. Pretoria, Gauteng, South Africa.

ENVIRONMENTAL, LORAX. (2003, October). Treatment of sulphate in mine effluents,.

Oelofse, R. d. (2012, March). Acomparison of the cost associated with pollution prevention measures to that required to treat polluted water resources.

Veolia. (2017, 01 11). LoSO4 TM Sulphate Reduction Technology for Mine Water. Pittsburg, USA.

Assessing biotic and abiotic conditions for understanding bioleaching processes in Zn-Pb-Ag tailings

Denys Villa Gomez[1], Patrick Botsch Cellette Gomes[1], Harald Hofmann[2], Chenming Zhang[1], David Williams[1]

[1]*School of Civil Engineering, The University of Queensland, 4072 QLD, Australia*
[2]*School of Earth and Environmental Science, The University of Queensland, 4072 QLD, Australia*

Abstract

The aim of this study was to assess biotic and abiotic conditions for a better understanding of the biological and chemical reactions in the bioleaching processes. For this, bioleaching experiments were carried out with Zn-Pb-Ag mine tailings using two column reactors, each operating under abiotic and biotic conditions, respectively. *Acidithiobacillus ferrooxidans, Leptospirillum ferroxidaans and Acidithiobacillus thiooxidans* were used to inoculate the biotic column. Both columns were equipped with moisture and oxygen sensors and build on top of two scales. A peristaltic pump ensured a constant medium inflow rate of 2.3 L/m²s. Oxidation-reduction potential, pH, oxygen, metals, moisture, sulfate and isotopes measurements were used analyze the composition of the leached material and to differentiate leaching from chemical and biological reactions. The pH behaviour was similar in both columns with an increase from 4.2 to 5.4 after 18 days of experiment, which may be due to the presence of carbonate shales and gangue mineral. The ORP decreased similarly in both columns, but slightly faster in the abiotic experiment. Oxygen concentration at the top of the columns was lower in the biotic column, denoting bacterial activity consuming oxygen. Sulfur and oxygen isotopic composition of formed sulfate might give relevant information about the processes involved on the sulfide mineral

Keywords: bioleaching, sphalerite, tailings, column reactor, sulfide mineral

Introduction

The increasingly decrease in the grade of the ore deposits has turned exploitation of minerals into a big challenge for the mining industries. This decrease has been generating bigger amounts of mining waste material (Falagán et al. 2006). Tailings are finely ground rock particles with a big reactive potential, which may contain metals in relatively high concentrations (Falagán et al. 2006). The high amount of these metals contained in the tailings has attracted a lot of attention of scientific and industrial areas on finding a profitable and environmental friendly technology of exploiting these lost resources. Since physical and chemical processes have shown many drawbacks like intensive energy consumption and secondary pollution (Ye et al. 2016), bioleaching have been gaining a lot of strength in processing sulfide minerals contained in the tailings. Bioleaching is a process in which acidophilic and chemolithotrophic microorganisms convert insoluble solids to soluble and extractable forms by oxidizing the reduced elemental sulfur and/or oxidizing ferrous iron as energy source (Heydarian et al. 2017). This technology can be utilized for a broad variety of different types of sulfide minerals, including: pyrite (FeS_2), chalcopyrite ($CuFeS_2$), arsenopyrite (FeAsS), sphalerite (ZnS), pentlandite ($(FeNi)_9S_8$) and pyrrhotite (FeS) (Mousavi et al. 2006).

From the bioleaching methodologies, heap bioleaching is widely applied due to its operational and economic advantages (Yin et al. 2018). Heap bioleaching consist of dumping low grade or mine tailings in a drained area, which is irrigated by a water-based inoculum of oxidizing microorganisms. While significant attention has been given to the geotechnical and hydraulic aspects of heap bioleaching, the optimal microbial conditions in the process is poor understood. In laboratory scale, heap bioleaching can be simulated by irrigated column reactors, once it is capable of reproducing one of the possible paths of a liquid percolating through a mass of material by gravity (Mousavi et al. 2006). This simulation enables a specific experimentation of different physicochemical and biological parameters and leaching conditions (Johnson, 2008; Manafi et al. 2013; Wang et al. 2014). Among the most important parameters and conditions cited are: pH, temperature, particle size, initial ferrous and ferric iron concentration (Pina et al. 2004; Haghshenas et al. 2011), dissolved oxygen, oxidation and reduction potential (ORP), bacterial strain and cell concentration (Hu et al. 2016). All these parameters and conditions are fundamental for a better comprehension of the biological activity and occurring mechanism in the reactor.

In order to achieve success and reduce the costs of heap bioleaching, it is crucial to improve our knowledge of the biological reactions existing in the process (Gericke 2012). Previous studies have proposed direct and indirect mechanisms to explain the solubilisation of sulfide minerals by oxidizing microorganisms. Direct mechanism describes the attachment of the microorganism and the oxidation of the mineral surface through enzymatic reactions. The indirect mechanism is summarized by the constant regeneration of the leaching agent through the bacterial enhanced oxidation of ferrous ions to ferric ions, whether by thiosulfate or polysulfide depending on the composition of the leached mineral (Ghassa et al. 2014). On the other hand, recent studies defend that the degradation of the sulfide mineral only happens because of the presence of the ferric ions oxidized by the bacteria in the glycocalyx or extracellular polymeric substance (EPS) created on the mineral surface by the attached bacteria (Gericke 2011; Ye et al. 2016). Regardless the mechanism, it is believe that the use of bacteria can considerably accelerate the dissolution rates of mineral sulfides (Pisapia et al. 2007 and Bruynesteyn and Hackl1982), but it is not clear at which extend. So a better understanding of the bio-oxidation mechanism in order to define more profitable heap leaching conditions is needed.

While Scanning Electron Microscopy (SEM) images of bacterial attachment to metal particles already proved that both mechanisms could happen at the same time in the same reactor it is still hard to compare the efficiency of each mechanism (Johnson 2010). Pisapia et al. (2007) studied the isotopic fractionations between sulfates and pyrite to constrain the oxidation pathways occurring during acid mine drainage formation. They found that at least two-pyrite bio-oxidation pathways occurred, which depend on the period occurring the oxidation process. This technique can help to explain the chemical and mineralogical nature and the oxygen isotopic composition of compounds formed on the mineral surface in bio-oxidation and compare it to the abiotic oxidation process. The information acquired with this comparison can be utilized in bigger scale heap bioleaching projects.

Therefore, the aim of this study is to assess biotic and abiotic conditions for a better understanding of the biological and chemical reactions in the bioleaching processes in fine-grained Zn-Pb-Ag tailing material.

Methods

Samples of tailings from Century Mine in north-west Queensland were used in this study, one of the largest Australia’s open cut zinc mine before its closure in August 2015. The sedimentary exhalative Zn-Pb-Ag deposit possessed average grades of approximately 10.2% Zn, 1.5% Pb and 36 g/t Ag. Mineralization comprises fine-grained sphalerite with minor galena and pyrite (Broadbent, Myers and Wright 1998). Scanning Electron Microscopy-Energy Dispersive Spectroscopy (SEM-EDS) showed abundant fine-grained and sub-µm-scale material, with silica and quartz phases, pyrite, jarosite, and sphalerite (Kerr 2017). Particle size distribution test was realized using ASTM sieves and hydrometer test resulting on a distribution of 7% clay, 76% silt and 17% sand in the tailing material. In virtue of the high amount of fine particles present in the material, a mixture of 40% tailings to 60% sterile sand on weight percentage was established to avoid permeability problems. Both materials were sterilized using a

200°C oven before being mixed. The pH of 4.9 of the sand tailing material mixture was defined using a ratio 1:2.5 to deionized water with a Sper Scientific benchtop pH meter. The bulk density of the mixed material was calculated and defined as 1.72 g/cm³.

Iron-oxidising bacteria (*Acidithiobacillus ferrooxidans and Leptospirillum ferroxidaans*) and sulphur-oxidising bacteria (*Acidithiobacillus thiooxidans*) were mixed and used in the bioleaching experiments at concentrations of $4x10^7$ cells/ml counted with a phase contrast microscope (Olympus EC-40) and a Hausser Scientific™ counting chamber. Bacterial growth was realized in 300ml Erlenmeyer flasks containing 100ml solution using a 9K modified medium containing: 20g $FeSO_4 * 7H_20$, 0.1 g KCl, 0.5 g K_2HPO_4, 0.5 g $MgSO_4.7H_2O$, 2.42 g $(NH_4)Cl$ and 3.22g $NaSO_4$ in 1 L of distilled water. The pH of the culture medium was adjusted to pH 2.0 with 1 M H_2SO_4, filtered (0.45 μm) and mixed with the bacteria on a 10 ml bacteria to 90 ml medium ratio. The bacteria were incubated in a 125 rpm shaker in a heating room at 30°C.

The experiments were carried out in two column reactors fabricated from 5mm thick acrylic cylinder glued on an acrylic plate and build on top of two Ohaus Navigator XL 20000 scales. The height of both columns is 50cm and the internal diameter 15cm. Special attention was given at the packing of the column in order to avoid preferential flow and clogging of the column. Therefore, the columns were dry packed carefully on 0.5cm layers and compacted and scarified after each layer to help integration of the fine particles. At the bottom of the columns, a sand layer of 4cm was packed with use of a geotextile between the two different soil materials to avoid the escape of the fine particles from the columns and also for filtering the collected leachate.

Before packing the columns, a set of six oxygen sensors from Presense GmbH and two EC-5 moisture sensors from ECHO equipped each of the two columns. Of the six spot oxygen sensors in each column, three were the SP-PSt-3 for a measurement range of 0-100% oxygen in dissolved or gaseous

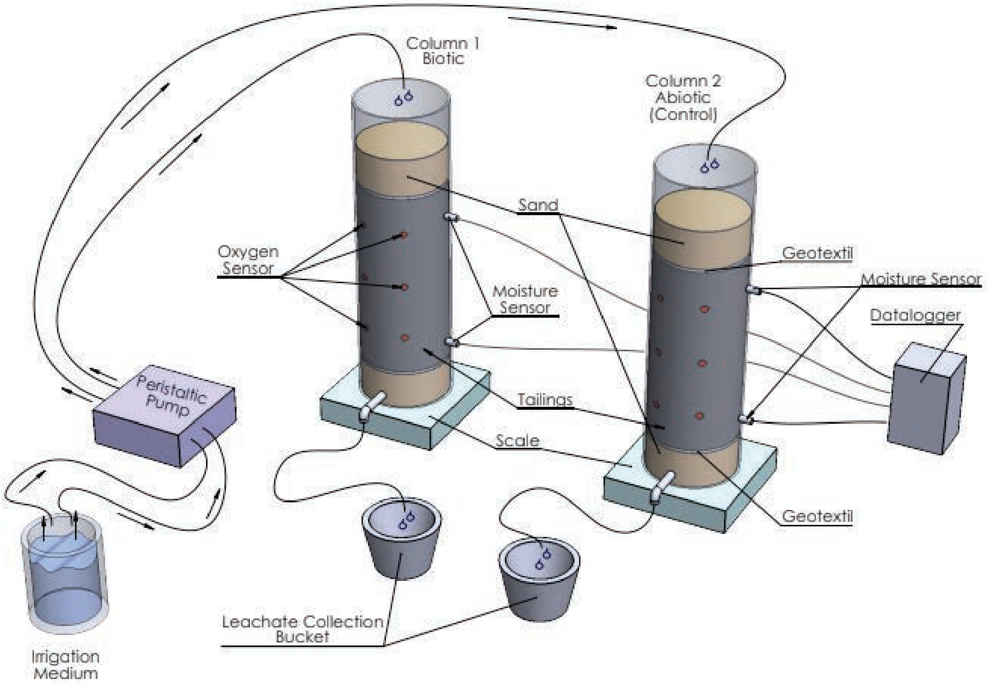

Figure 1 *Detailed scheme of the experiment.*

phase and three SP-PSt-6 for a low range of 0-5% oxygen content. The six optical sensor spots were attached to the inner wall of the cylinder and are being measured twice a week in a contactless and non-invasive way by the use of an optic fibre connected to a Fibox 4 oxygen meter. The two EC-5 moisture sensors were installed in each column using cable glands responsible for avoiding the leakage of the columns. All four sensors installed in both columns were connected to a HOBO datalogger and configured with a measurement interval of 10 minutes. The drawing below (Figure 1) helps to understand the set-up of the experiment.

The bioactive column was inoculated pouring 2.1 L of the modified 9K medium with the different strains of bacteria aiming to achieve the desired bacterial concentration. The control column was filled with 2.1 L of the modified medium and sodium azide (0.5g/L) to eliminate any remaining endemic species present in the tailing material. This bactericide was used in the control column every two weeks to ensure that no microorganism starts growing up again in the abiotic column. The columns were left closed for 36 hours inoculating. After this period they were leached and the leachate was recirculated to guarantee the attachment of the bacteria to the tailings.

After the inoculation, both columns were fed with an irrigation medium composed of 0,111 g NH_4Cl and 0,176 g K_2HPO_4 per liter with the use of a peristaltic pump (Watson Marlow™ 323) at a flow rate of 2,3 L/m^2s. This predominantly saturated condition had to be established in order to guarantee enough head pressure to maintain a constant outflow rate. Considering the inflow rate, the bulk density, the volume and the porosity of the tailing mixture material, a retention time of 60 hours was calculated. The solution was dripped on the top of a 5 cm sand layer packed on the top, which guaranteed a homogeneous distribution of the liquid through the tailing material. Two times a week samples have been collected from the leachate bucket of the two columns for the analysis of the liquid. The sampling interval was defined based on the retention time.

Ph and ORP (oxidation and reduction potential) is being measured using a Sper Scientific Benchtop pH/mV meter IC860031. Sulfate is going to be measured using a Thermo Fisher Dionex ICS-1100 Ion Chromatograph (IC). Metals are going to be measured with an Inductively Coupled Plasma Optical Emission Spectrophotometer (ICP-OES) Perkin Elmer Optima 7300DV after filtering and digesting the samples with nitric acid. SEM is going to be used to generate images in order to check the attachment of the bacteria to the mineral surface and to the metals precipitated. Samples were processed at the Centre for Microscopy and Microanalysis at the University of Queensland on a Hitachi TM3030 SEM. Isotope analysis of sulfur and oxygen isotope ratios of the leached sulfate are going to be determined by continuous flow isotope ratio mass spectrometry using an elemental analyser (δ_{34}S) or a Thermo-Finnigan TC/EA (δ_{18}O) coupled to a gas source mass spectrometer.

Results and discussion

Despite the low pH of 2.0 of the irrigation medium, the pH of the leachate increased similarly in both columns (Figure 2a). In column 1, the pH varied from 4.2 to 5.4, while in column 2 the variation during the 5 weeks was from 4.4 to 5.8. This increase may be due to the presence of carbonate shales and the gangue mineral siderite contained in the mine deposit, which has the capacity of buffering the acidity of the leachate (Broadbent, Myers and Wright 1998). The lower values of the pH in the bioactive column might be a result of the acidity produced by the microorganisms.

The ORP also decreased similarly in both columns, but slightly lower in the abiotic experiment (Figure 2b). After day 18, both pH and ORP displayed steady state conditions in both columns. The slight increase in ORP in the biotic column might be an indication of biological activity (Olson et al. 2003).

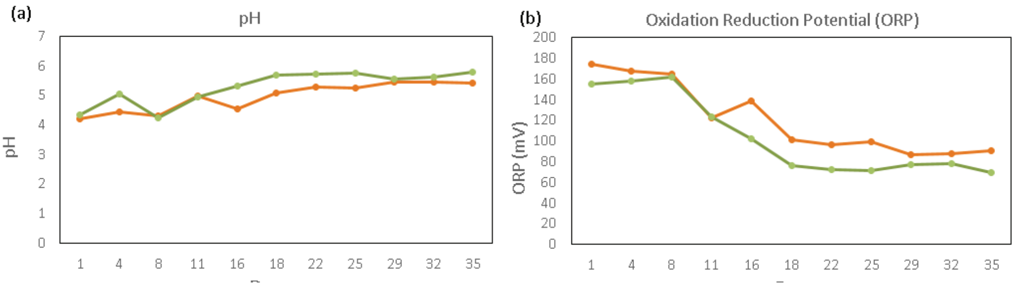

Figure 2 - *Parameters measured in the five weeks of the experiment: a) pH and b) ORP*

Figures 3 and 4 showed the data acquired by the 3 normal and 3 low range oxygen sensors in column 1 and 2. Both figures present a sharp decrease after the first day, which can be explained by the saturation of the tailings by the medium, pushing the trapped oxygen out of the columns. The only difference in oxygen concentration between the columns was observed at the top of the column in the abiotic experiment (Figure 4a), where a higher concentration might explain the lack of bacterial activity that can consume oxygen. The consumption of the oxygen by the aerobic microorganisms inoculated in the biotic column is key for the oxidation of ferrous iron into ferric iron and for the production of acids (Baba et al. 2011).

Comparable to the oxygen sensors, the moisture sensors have been delivering stable measurements with values between the range of 0.18 to 0.19 for the bottom sensors and 0.16 to 0.18 for the upper sensor showing that

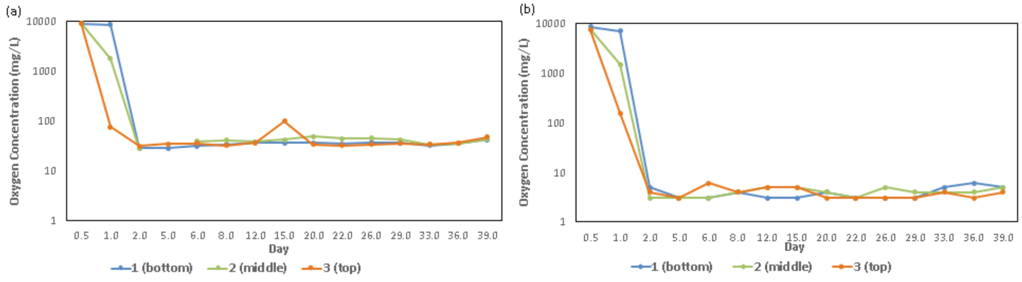

Figure 3 – *Oxygen concentration in Column 1 (biotic) with: a) normal range oxygen sensor (0-100% or 0-45mg/L) and b) low range oxygen sensor (0-5% or 0-2 mg/L) on a log scale with base 10 (Y-Axis)*

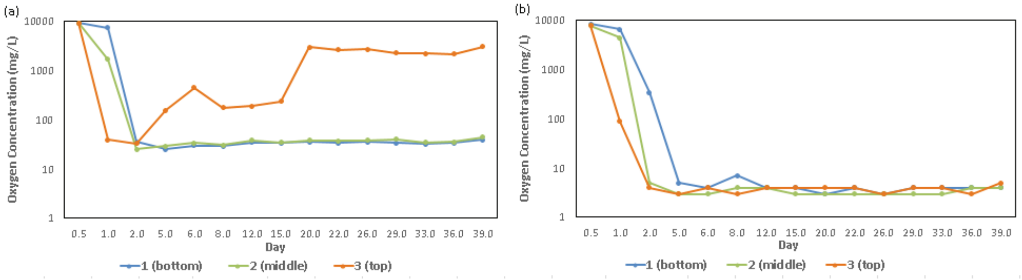

Figure 4 – *Oxygen concentration in Column 2 (abiotic) with: a) normal range oxygen sensor (0-100% or 0-45mg/L) and b) low range oxygen sensor (0-5% or 0-2 mg/L) on a log scale with base 10 (Y-Axis)*

the moisture conditions of both columns are equal and maintained constant with the in- and outflow rate (data not shown). Further analysis will support the results presented and will help us to clearly observe the differences between bioleaching under biotic and abiotic conditions. These analyses include metals content, and isotope analysis This analysis will also help to determine the relevance of the biological activity and better comprehend the bio-oxidation process at the mineral surface.

Conclusions

This study maintains a clear distinction between the biotic and the abiotic column aiming to understand the biological and chemical reactions existing in both columns and consequently, estimating the influence of using microorganisms through the metal leaching discrepancy between both columns. The outcome of the present study will provide clear evidence on the effect of bacterial activity in the dissolution of mineral sulfide contained in Zn-Pb-Ag tailing material in lab-scale simulations of heap leaching.

References

Baba AA, Adekola FA, Atata RF, Ahmed RN, Panda S (2011) Bioleaching of Zn(II) and Pb(II) from Nigerian sphalerite and galena ores by mixed culture of acidophilic bacteria. Transactions of Nonferrous Metals Society of China 21:2535-2541 doi: 10.1016/S1003-6326(11)61047-9

Balci N., Shanks III WC, Mayer B, Mandernack KW (2007) Oxygen and sulfur isotope systematics of sulfate produced by bacterial and abiotic oxidation of pyrite. 71:3796-3811 doi: 10.1016/j.gca.2007.04.017

Broadbent GC, Myers RE and Wright JV (1998) Geology and origin of shale-hosted Zn-Pb-Ag mineralization at the Century Deposit, Northwest Queensland, Australia. Economic Geology 93(8):1264-1294 doi: https://doi.org/10.2113/gsecongeo.93.8.1264

Bruynesteyn A and Hackl RP (1982) Evaluation of acid production potential of mining waste materials. Minerals and the Environment 4:5 doi: https://doi.org/10.1007/BF02093337

Brunner B, Yu JY,Mielke RE, MacAskill JA, Madzunkov S, McGenity TJ, Coleman M (2008) Different isotope and chemical patterns of pyrite oxidation related to lag and exponential growth phases of Acidithiobacillus ferrooxidans reveal a microbial growth strategy. 270:63-72 doi: 10.1016/j.epsl.2008.03.019

Falagán C, Grail BM, Johnson DB (2016) New approaches for extracting and recovering metals from mine tailings. Minerals Engineering 106:71-78 doi: http://dx.doi.org/10.1016/j.mineng.2016.10.008

Gericke M (2012) Review of the role of microbiology in the design and operation of heap bioleaching processes. The Journal of the Southern African Institute of Mining and Metallurgy 112:1005-1011

Ghassa S, Boruomand Z, Abdollahi H, Moradian M, Akcil A (2014) Bioleaching of high grade Zn-Pb bearing ore by mixed moderate thermophilic microorganisms. Separation and Purification Technology 136:241-249 doi: http://dx.doi.org/10.1016/j.seppur.2014.08.029

Haghshenas DF, Bonakdarpour B, Alamdari EK, Nasernejad B (2011) Optimization of physicochemical parameters for bioleaching of sphalerite by Acidithiobacillus ferrooxidans using shaking bioreactors. Hydrometallurgy 111:22-28 doi:10.1016/j.hydromet.2011.09.010

Heydarian A, Mousavi SM, Vakilchap F, Baniasadi M (2017) Application of a mixed culture of adapted acidophilic bacteria in two-step bioleaching of spent lithium-ion laptop batteries. Journal of Power Sources 378:19-30 doi: https://doi.org/10.1016/j.jpowsour.2017.12.009

Hu K, Wu A, Wang H, Wang S (2016) A New Heterotrophic Strain for Bioleaching of Low Grade Complex Copper Ore. Minerals 2016, 6, 12 doi: 10.3390/min6010012

Johnson DB (2008) Biodiversity and interactions of acidophiles: key to understanding and optimizing microbial processing of ores and concentrates. Transactions of Nonferrous Metals Society of China 18: 1367–1373 doi: https://doi.org/10.1016/S1003-6326(09)60010-8

Johnson DB, (2010) The biogeochemistry of biomining. Geomicrobiology; molecular and environmental perspective pp. 401-426 doi: 10.1007/978-90-481-9204-5_19

Manafi Z, Abdollahi H, Tuovinen OH (2013) Shake flask and column bioleaching of a pyritic porphyry copper sulphide ore. International Journal of Mineral Processing 119:16–20 doi: https://doi.org/10.1016/j.minpro.2012.12.010

Mousavi SM, Jafari A, Yaghmaei S, Vossoughi M, Roostaazard R (2006) Bioleaching of low-grade sphalerite using a column reactor. Hydrometallurgy 82:75–82 doi: 10.1016/j.hydromet.2006.03.001

Olson GJ, Brierley JA, Brierley CL (2003) Bioleaching review part B: Progress in bioleaching: applications of microbial processes by the minerals industries. Applied Microbiology and Biotechnology 63:249-257 doi: https://doi.org/10.1007/s00253-003-1404-6

Pina PS, Leao VA, Silva CA, Daman D, Frenay J (2004) The effect of ferrous and ferric iron on sphalerite bioleaching with Acidithiobacillus sp. Minerals Engineering 18:549-551 doi: 10.1016/j.mineng.2004.08.011

Pisapia C, Chaussidon M, Mustin C, Humbert B (2007) O and S isotopic composition of dissolved and attached oxidation products of pyrite by Acidithiobacillus ferrooxidans: Comparison with abiotic oxidations. Geochimica et Cosmochimica 71:2474-2490 doi: 10.1016/j.gca.2007.02.021

Wang Y, Zeng Weimin, Qiu Guanzhou, Chen X, Zhou H (2013) A Moderately Thermophilic Mixed Microbial Culture for Bioleaching of Chalcopyrite Concentrate at High Pulp Density. Applied and Environmental Microbiology 80:741-750 doi: http://dx.doi.org/10.1128 / AEM.02907-13

Ye M, Yan P, Sun S, Han D, Xiao X, Zheng L, Huang S, Chen Y, Zhuang C (2016) Bioleaching combined brine leaching of heavy metals from lead-zinc mine tailings: Transformations during the leaching process. Chemosphere 168:1115-1125 doi: http://dx.doi.org/10.1016/j.chemosphere.2016.10.095

Yin S, Wang, L, Kabwe E, Chen X, Yan R, An K, Zhang L, Wu A (2018) Copper Bioleaching in China: Review and Prospect. Minerals 2018,8,32 doi: https://doi.org/10.3390/min8020032

3

PRODUCED WATER

Application of a Coal Seam Gas Waste Product as part of the Rehabilitation Program for a Copper Heap Leach Operation

Alan Robertson[1], Greg Maddocks[1], Ben Kelly[2], Ian Sheppard[3]

[1]*RGS Environmental Pty Ltd, 123 Wynne Street, Sunnybank Hills 4109, Australia, alan@rgsenv.com*

[2]*Santos Ltd Level 19 Santos Place, 32 Turbot Street, Brisbane 4000, Australia*

[3]*Aeris Resources Ltd, Level 2 HQ Tower South, 520 Wickham Street, Fortitude Valley, 4006, Australia*

Abstract

There are few examples of successful collaboration between the mining industry and other industries in Australia, particularly where waste products have been used as part of mine rehabilitation activities to lower the risk of potential impacts to the environment. It is therefore important to highlight examples of where such successful collaboration is occurring.

From a near zero base, Australia has seen a massive growth in production of coal seam gas (CSG) since 1995 (Roarty, 2011). CSG production, requires the extraction of significant volumes of groundwater. The chemistry of the extracted water is a function of the geology in the region from which the water is extracted. The extracted water (produced water) is typically treated using RO to produce a treated water stream that can be used beneficially. The RO treatment process also produces a highly saline waste stream that can be further processed with thermal treatment processes to produce a highly saline stream and a dry salt material respectively. Managing the disposal or beneficially use of the salt product(s) ultimately produced, has been the subject of ongoing investigation. Over the past few years, a CSG producer has commissioned studies to investigate the potential for reusing the alkaline by-product in the mining industry to facilitate the remediation of acidic mine waste materials and acid and metalliferous drainage (AMD).

Preliminary studies have demonstrated the potential for the alkaline salt product to be successfully used in these activities. Further studies are now underway to look at the use of the alkaline salt by-product as part of rehabilitation plans for a copper heap leach facility. These studies involve both laboratory and field scale neutralisation trials, to harness the alkalinity from bicarbonate and carbonate species present in the produced water stream, to neutralise the acidity in the heap leach materials and immobilise dissolved metal species through precipitation.

The objective of the laboratory and field scale neutralisation trials is to reduce the risk of ongoing poor-quality seepage from the heap leach materials following the application of a soil cover system as part of rehabilitation activities. It is expected that the successful application of the alkaline CSG waste product at this mine site will lead to a positive outcome not only for the industry stakeholders and regulators, but for the environment.

Keywords: ICARD | IMWA | MWD 2018, Waste, Rehabilitation, AMD, Heap Leach, Collaboration

Introduction

AMD is an important environmental issue for the mining and mineral processing industries with reactive mine wastes generating acidic leachate, which can contain elevated concentrations of dissolved metals, metalloids and salts (INAP, 2009; COA, 2016). Neutralisation of AMD and precipitation of metals using alkaline reagents such as hydrated lime ($Ca(OH)_2$) remains the most widely used primary treatment process. The resulting neutralised waters can generally be recycled or may require secondary treatment (eg. reverse osmosis (RO)) prior to discharge to the environment. RO is expensive and can be subject to fouling through use of hydrated lime in the primary treatment step due to formation of insoluble gypsum ($CaSO_4$). Additionally, the mining of limestone and subsequent processing required to produce lime is not without environmental impacts as carbon dioxide (CO_2) is produced in the decomposition of limestone to produce lime and the combustion of fossil fuels used to facilitate the decomposition of limestone.

Coal seam gas (CSG) production in Australia has seen exponential growth in recent years and requires the extraction of large volumes of co-produced water, which commonly has high concentrations of dissolved salts dominated by Na^+, HCO_3^- and Cl^- (Davies et al., 2015). The co-produced water generally requires RO treatment to reduce the salt concentration and reclaim water for beneficial re-use. The RO treatment process also results in a much smaller volume of highly concentrated brine being produced which contains substantial alkalinity from bicarbonate and carbonate species. A dry alkaline salt can also be produced from the RO brine using evaporation and/or heating, which can contain a high concentration of sodium carbonate [Na_2CO_3]. The produced alkaline salt is typically transferred, and disposed of, to landfill and the overall process has substantial economic penalties, due to the energy required to generate the dry salt as well as transport and landfill costs.

Sodium carbonate offers some technical advantages over Ca-based neutralants, due to its high solubility with carbonate ions yielding high acid neutralising potential, and metal precipitation per unit mass. Also, unlike Ca-based salts, sodium carbonate will not exacerbate fouling of RO membranes by gypsum ($CaSO_4$). Carbonate-rich brines and salts generated from the CSG industry are an alternative source of sodium carbonate neutralant material, with the advantage that the waste output of one resource extraction industry has the potential to be converted into a valuable input for another industry.

Over the past few years, an Australian CSG producer has commissioned several studies to investigate the potential for reuse of an alkaline brine/salt by-product in the mining industry for the remediation of acidic mine waste materials and AMD (Chen et al., 2017; Cohen et al., 2017). These studies have demonstrated the potential for the alkaline brine/salt by-product to be successfully used in these activities.

This paper provides the findings from the first phase (laboratory scale neutralisation trials) of a study into at the planned use of the CSG alkaline brine/salt by-product as part of rehabilitation plans for a copper heap leach facility in NSW, Australia.

Methods

Heap Leach Samples

The methodology used to obtain representative samples of heap leach materials was undertaken in accordance with recognised industry guidelines. Existing technical guidelines for the geochemical assessment of mine waste materials in Australia (COA, 2016) were utilised as a framework for the sampling program. The sampling strategy was based on:

- An existing knowledge of the geochemistry of the heap leach materials of the site and potential for any significant environmental or health impacts;
- Size of operation and material volume;
- Sample representation requirements; and
- Level of confidence in predictive ability and cost

Site personnel collected 20 x 40 kg samples of heap leach materials and transferred the samples to ALS Brisbane laboratory (ALS) for static geochemical characterisation testing. The 20 samples represented composite High Sulfur (10 samples) and Low Sulfur (10 samples) heap leach materials taken from the three heap leach pads at the site. The sulfur content of the heap leach material varies due to the differing ore types that were progressively mined for placement on the heap leach pads over the project life. The samples were obtained using an excavator digging down to approximately 5 m depth and the operator collecting an approximate 40 kg sample by dragging the excavator bucket up the side of the hole. An approximate 2 kg sub-sample was collected and analysed for total sulfur using hand-held X-Ray Fluorescence (XRF) equipment during drilling to guide the field sampling program and indicate whether the samples were High Sulfur (HS) or Low Sulfur (LS). The XRF analyses were subsequently verified using a 2-acid digest to quantify the concentration of sulfur, major cations and metals and metalloids in each of the 2 kg sub-samples.

The 20 heap leach samples provided good lateral coverage of the 3 existing heap leach pads at the site and provided a reasonable statistical representation of the heap leach materials. The 20 heap leach samples were composited into four HS samples and four LS samples at ALS; each composite sample was approximately 75 kg; sub-samples of these eight composite samples taken and subjected to static geochemical characterisation and particle size distribution (PSD) tests at ALS.

Brine Sample

A 1,000L bulk sample of liquid brine from the CSG producer RO water treatment plant was obtained and a 20L sub-sample dried at 150°C and characterised as a dry salt at ALS. The bulk liquid brine sample was then used in dynamic neutralisation tests for the heap leach materials.

Neutralisation Tests

Following receipt and interpretation of the static geochemical characterisation results, six dynamic neutralisation tests were set up at the RGS in-house laboratory in Brisbane using the two bulk composite HS and LS heap leach samples from the site and the bulk liquid brine sample from the RO plant at Leewood.

The dynamic neutralisation tests involved six individual 60L open-top cone-bottom plastic tanks, each used to contain approximately 75 kg of heap leach material. The open-top vessels allowed heap leach materials and liquid brine to be easily added to the tank and the cone-bottom and stand also facilitated periodic leachate collection. The six tanks comprised:

- **Test 1:** Control test for LS heap leach material – ie no brine added – Test 1
- **Test 2:** Control test for HS heap leach material – ie no brine added – Test 2
- **Test 3:** Immersion in concentrated liquid brine LS heap leach material – Test 3
- **Test 4:** Immersion in concentrated liquid brine HS heap leach material – Test 4
- **Test 5:** Sprinkled with diluted liquid brine HS heap leach material – Test 5
- **Test 6:** Sprinkled with diluted liquid brine HS heap leach material – Test 6

The leachate data presented in this paper for the dynamic neutralisation tests covers the period November 2017 to March 2018. The tests were operated under various controlled conditions and leaching cycles, and leachate was tested for pH, conductivity, acidity, alkalinity, major cations and anions, and soluble metals/metalloids.

Results

Heap Leach Samples

The LS and HS composite samples are dominated by fine gravel and coarse sand. The results of the static geochemical tests on the composite HS and LS heap leach samples are provided in Table 1. The samples have low pH values, elevated conductivity and appreciable titratable actual acidity (TAA). Compared to the HS sample, the LS sample has very little inherent sulfide sulfur (as measured by Scr) remaining and therefore has little capacity to generate additional acidity through sulfide oxidation.

Multi-element results for the LS and HS heap leach samples show that some metal/metalloid concentrations are enriched compared to median values in un-mineralised soils (eg. As, Cd and Cu) (Bowen 1979). The enrichment of some metals/metalloids in the heap leach materials is expected, given that

Table 1 *Static geochemical characterisation results for heap leach materials.*

Sample	pH	EC (µS/cm)	TAA (mol H+/t)	S (%)	Scr (%)	MPA	ANC	NAPP	Classification
HS Comp.	3.3	4,800	139	4.45	2.950	90.3	<0.5	90.3	Acid Forming
LS Comp.	3.5	3,290	121	0.83	0.125	3.8	<0.5	3.8	Acid Forming

Notes: EC = Electrical Conductivity; TAA = Titratable Actual Acidity; Scr = Chromium Reducible Sulfur. MPA = Maximum Potential Acidity; ANC = Acid Neutralising Capacity and NAPP = Net Acid Producing Potential in kg H_2SO_4/t these materials were obtained from a mineralised ore body and are being heap leached under acidic conditions to obtain copper.

Brine Sample

The brine sample from the RO treatment plant was tested at ALS Brisbane and had a pH of 9.3, EC of 76,000 µS/cm, carbonate alkalinity of 27,700 mg/L (as $CaCO_3$) and bicarbonate alkalinity of 45,800 mg/L for a total alkalinity of 73,500 mg/L.

Table 2 provides the major ion composition of the brine from the RO water treatment plant as provided by the CSG producer.

The combined carbonate and bicarbonate content of the salt contained in the brine is between 53.3 % and 65.0 %. When the carbonate and bicarbonate salts contained in the brine react with acid (H^+) they form water and carbon dioxide gas according to the neutralisation reactions.

Carbonate neutralisation reaction;

$CO_3{}^{2-}{}_{(aq} + 2H^+{}_{(aq)} \Rightarrow H_2O_{(l)} + CO_{2(g)}$

Bicarbonate neutralisation reaction;

$HCO_3{}^{-}{}_{(aq)} + H^+{}_{(aq)} \Rightarrow H_2O_{(l)} + CO_{2(g)}$

The sodium, potassium and chloride ions (approximately 35 % to 46.7 % of the salts in the brine) that do not take part in the neutralisation reactions remain and have the potential to increase the salinity of a neutralised acidic material. However, at the copper heap leach site, groundwater is naturally highly saline and additional salt from brine neutralisation would not materially impact upon this level of salinity. Additional work is planned in future to verify that the potential impact of the proposed remediation activity and rehabilitation program, interms of salinity, is negligible.

Trace element analysis results for the brine sample indicate that the concentration of most of dissolved trace metals/metalloids is below the applied trigger values for moderately disturbed freshwater ecosystems (95 % species protection level). The exceptions are the concentrations of boron (5.6 mg/L) and fluoride (46.7 mg/L), which are elevated compared to the applied livestock drinking water guideline values for these elements (5 mg/L and 2 mg/L, respectively) (ANZECC & ARMCANZ, 2000).

Table 2 *Major ion composition in brine.*

Species	Minimum Mass (%)	Maximum Mass (%)
Sodium	32.7	35.5
Bicarbonate	39.8	44.8
Carbonate	13.5	20.2
Chloride	5.7	6.7
Potassium	0.2	0.4

Neutralisation Tests

Neutralisation tests were undertaken for LS and HS heap leach samples contained in six tanks subjected to different leachate compositions (deionised water and/or alkaline brine) and addition methods as detailed in previously in this paper. The pH results for the six samples over a period of four months is provided in Fig. 1. The results demonstrate that the brine has the potential to neutralise the titratable acidity in the heap leach materials but slow (sprinkled) addition of diluted brine provided a slower and more sustainable increase in pH than total immersion in concentrated brine. It is expected that addition of diluted brine to heap leach materials through a similar sprinkler system to that currently used at the site is the most practical and efficient method of adding alkalinity to the system. There is also the opportunity to physically disturb (turnover) the heap leach materials, where required, and to recycle collected leachate with excess alkalinity to promote efficient contact and neutralisation.

The quality of the leachate collected from the HS control sample (Test 2) is presented in Table 3 alongside the quality of leachate collected from the HS sample (Test 6) sprinkled with diluted brine (three-fold dilution to obtain sufficient leachate for analysis). The results show that addition of alkaline brine to the HS heap leach material has the potential to increase the pH and alkalinity of leachate, and reduce the concentration of acidity and several parameters/analytes in leachate (eg. Al, Cd, Co, Cu, F, Mn, Ni, and Zn), in some cases by several orders of magnitude. On the other hand, the concentration of some parameters (eg. EC, K, Na, Cl, Br, As, B, Mo and Se) have the potential to increase, to some extent, in leachate from heap leach materials neutralised with brine. It should be noted

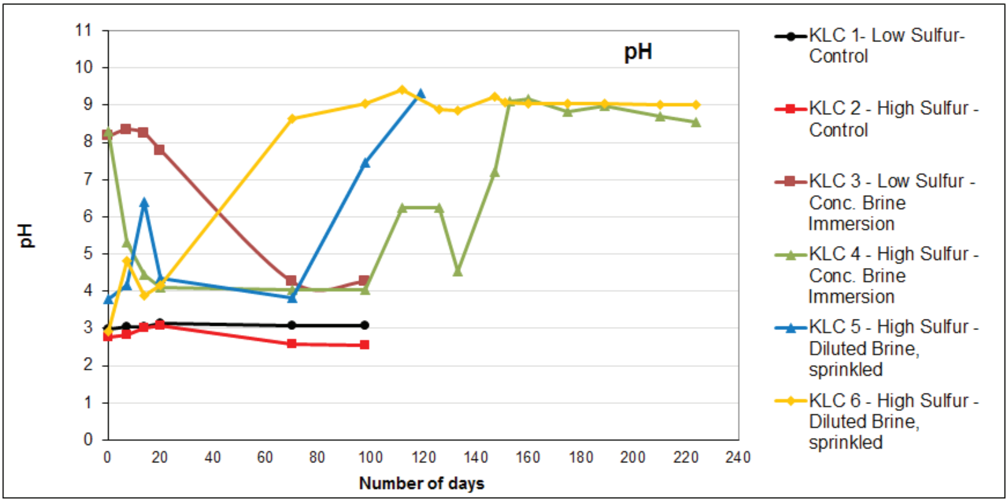

Figure 1 *pH results for heap leach neutralisation tests.*

that the CSG producer has the potential to remove some of these species from the final by-product by incorporation of additional treatment steps in water processing, should this be required. Additionally, a lower final end pH would also reduce the quantity of alkaline salt that needs to be added, which would in turn reduce the salinity in the treated neutralised material. Future work is proposed to optimise the dosing rate for both high sulfur and low sulfur ores found in the heap leach material taking into consideration the competing objectives of reducing dissolved metal concentrations, reducing the potential for re-acidification and minimising salinity in the treated neutralised material.

Table 3 *Leachate quality obtained from brine neutralisation Test 2 and Test 6*

	Test 2	**Test 6**		**Test 2**	**Test 6**
Parameter	Concentration (mg/L)		Parameter	Concentration (mg/L)	
pH (pH units)	3.06	9.41	Barium	<0.005	<0.005
EC (µS/cm)	15,840	47,550	Cadmium	2.3	0.0028
Acidity	21,800	<1	Cobalt	39	0.016
Alkalinity	<1	13,100	Chromium	0.33	<0.005
Calcium	136	4	Copper	320	0.596
Potassium	<1	71	Iron	734	<0.05
Magnesium	2,810	150	Mercury	<0.0005	<0.0005
Sodium	2	15,300	Manganese	99	0.36
Chloride	488	3,050	Molybdenum	<0.005	0.13
Fluoride	25	8.6	Nickel	12.5	<0.005
Sulfate	20,100	14,200	Lead	<0.005	<0.005
Bromide	<0.5	8.3	Strontium	0.036	<0.005
Aluminium	2300.00	0.22	Silicon	7.40	1.5
Arsenic	0.02	0.109	Selenium	0.1	1.19
Boron	<0.05	0.790	Vanadium	<0.05	<0.05
Beryllium	0.07	<0.005	Zinc	234	0.033

Conclusions

Laboratory scale neutralisation trials have been completed which demonstrate the potential to harness the alkalinity from bicarbonate and carbonate species in a CSG waste product, to neutralise the acidity in the heap leach materials from a copper heap leach operation and immobilise dissolved metal species through precipitation. Initial results from the study indicate that brine neutralisation has the potential to reduce the risk of ongoing poor-quality seepage from the heap leach materials following the application of a soil cover system as part of rehabilitation activities. However, there will be an increase in salinity and potentially in the concentration of some oxyanions in seepage under alkaline conditions

The laboratory-scale trials are continuing, and the sustainability of the water quality improvement is currently being investigated, by continuing the leaching of brine-neutralised HS materials with deionised water (with and without addition of agricultural limestone). It is planned that the findings of the laboratory-scale trials be used to inform the design of field scale trials planned to be constructed within the next 12 months. It is expected that the successful application of the alkaline CSG waste product at this mine site will lead to a positive outcome not only for the industry stakeholders and regulators, but for the environment.

Acknowledgements

The authors thank Tshwane University of Technology (TUT) for hosting the ICARD | IMWA | MWD 2018 Conference.

References

ANZECC and ARMCANZ (2000). Australian and New Zealand Guidelines for Fresh and Marine Water Quality. Australian and New Zealand Environment Conservation Council and Agriculture and Resource Management Council of Australia and New Zealand, Canberra, ACT (2000).

Bowen, H.J.M. (1979). Environmental Chemistry of the Elements. Academic Press, New York, USA.

Chen Q, Cohen DR, Andersen MS, Robertson AM, Jones DR, Kelly B (2017). Application of alkaline coal seam gas waters to remediate AMD from historical sulfide ore mining operation. In: Wolkersdorfer, C.; Sartz, L.; Sillanpää, M. & Häkkinen, A.: Mine Water & Circular Economy (Vol II). – p. 923 – 931; Lappeenranta, Finland (Lappeenranta University of Technology).

Cohen DR, Chen Q, Andersen MS, Robertson AM, Jones DR, and Kelly B (2017) Chemical and economic feasibility study of alkaline CSG waters in AMD Remediation. In 'Proceedings of the Ninth Australian Workshop on Acid and Metalliferous Drainage, Burnie, Tasmania. 20-23 November 2017. (Eds. Bell, L.C., Edraki, M. and Gerbo C.) pp. 231-238 (The University of Queensland: Brisbane).

COA (2016). Leading Practice Sustainable Development Program for the Mining Industry. Preventing Acid and Metalliferous Drainage. September, Commonwealth of Australia, Canberra ACT.

COA (2011). Background Note - The development of Australia's coal seam gas resources. July, 2011. Parliament of Australia – Department of Parliamentary Services, Commonwealth of Australia.

Davies PJ, Gore DB, Khan SJ. (2015). Managing produced water from coal seam gas projects: Implications for an emerging industry in Australia. Environ Sci. and Pollut. Res. 2015:22, 10981–11000.

INAP (2009). Global Acid Rock Drainage Guide (GARD Guide). Document prepared by Golder Associates on behalf of the International Network on Acid Prevention (INAP). June (http://www.inap.com.au/).

Roarty M. (2011). The development of Australia's coal seam gas resources. Science, Technology, Environment and Resources Section, Department of Parliamentary Services, Parliament of Australia. July 28.

4

SALINE AND NEUTRAL MINE WATER

Using a risk based, site-specific Decision Support System to determine the suitability of mine water for irrigation

John G Annandale[1], H Meiring du Plessis1, Phil D Tanner[1], Jo Burgess[2]

[1]*Department of Plant and Soil Sciences, University of Pretoria, Private Bag X20, Hatfield 0028, South Africa, john.annandale@up.ac.za*

[2]*Water Research Commission, Private Bag X03, Gezina, 0031, South Africa*

Abstract

Use of irrigation as a mine water management option often presents a cost-effective means of utilising poor quality mine-impacted waters that would otherwise need to be treated before release into surface water bodies. However, there are some waters that should not be considered for long-term irrigation, and site selection is critical. A newly developed risk based, site-specific irrigation water quality assessment tool defines key factors to consider when determining the viability and sustainability of irrigation with specific mine waters.

Keywords: Irrigation water quality, crop yield, crop quality, soil quality, Decision Support System

Introduction

There is much interest in the beneficial use of mine water for agricultural irrigation. Irrigation is often a cost-effective means for operating mines to manage surplus water. Upon closure, irrigation may present a sustainable means for communities to diversify away from mining, by producing food and fibre sustainably, and creating employment. Large savings in water treatment costs are also likely to follow. However, not all mine waters are suitable for irrigation, and support is necessary to make informed decisions on suitability.

An irrigation water quality Decision Support System (DSS) has recently been developed (du Plessis et al 2017). Fitness-for-use of water is presented as being 'ideal', 'acceptable', 'tolerable' or 'unacceptable'. The DSS is novel in a number of ways. Firstly, it is risk based, enabling the user to assess the implications of irrigating with a range of waters, including mining impacted waters on soil and crop resources, as well as on irrigation equipment. Secondly, the guidelines are structured in three tiers. Tier 1 provides generalised, conservative estimates of the suitability of water for irrigation. If mine waters are shown to be ideal or acceptable at this level, there may be no need to treat water or to utilise it through irrigation, and release into surface water bodies will likely be permitted and desirable. As this is unlikely with most mine-impacted waters, Tier 2 supplies more site-specific guidelines, enabling the user to design a crop production system to best accommodate the specific water quality. If there are still concerns about the usability of water for irrigation, then a Tier 3 assessment is indicated. This will require detailed expert input to assess whether or not irrigation is at all feasible, and if concerns highlighted by the Tier 2 assessment can be mitigated. Finally, the DSS is electronic and user-friendly, with colour coding to make the suitability of waters for irrigation intuitive. Help files provide information regarding the current state of knowledge for suitability indicators, and describe the approach and calculating procedures used in the DSS.

Methods

Water quality assessments at Tier 2 employ a scaled down version of the Soil Water Balance (SWB) crop growth and solute balance model (Annandale et al 2011), to dynamically simulate the interactions between irrigation water constituents and the soil-crop-atmosphere system. A simple cascading 11 layer soil water balance is used, with default parameters (field capacity, permanent wilting point, bulk density, and drainage characteristics) for predefined soil textures (clay, sandy loam, sand and coarse sand) populated in a database. A simple crop factor model is used (with many crop species parameters included in the database) to estimate water use, and a seasonal, root density-weighted profile salt content is estimated to predict yield reduction due to salinity using the Maas and Hoffmann (1977) approach. Soil profile chemical equilibrium reactions are modelled after Robbins (1991) in order to predict gypsum precipitation that reduces root zone salinity. Simulations are run over periods of 10 to 45 years in order to quantify the probability and severity of a specific effect occurring. Site-specificity is considered by means of populated databases that allow the user to select an appropriate weather station, soil texture, crop specie, irrigation management strategy, and irrigation system.

In this paper, the functionality of the DSS is demonstrated by simulating the effect on crop yield of 45 years of irrigation with five poor quality mine waters. The role of crop choice, climate and irrigation management on crop yield are also highlighted. In addition, nutrient supply to crops and trace element addition to the soil profile with irrigation water are demonstrated. Finally, the effect of mine impacted waters on corrosion and scaling of irrigation systems, and on soil physical properties are presented. Model predictions are discussed in the light of previous experience with irrigation using some of these waters.

Water qualities

Much research on irrigation with mine waters has been carried out in South Africa. Du Plessis (1983) modelled the advantage of sulphate rich waters over chloride dominated waters, suggesting that irrigation with gypsiferous mine waters would be feasible. This was proved correct by Jovanovic et al (1998), who showed that irrigation of a wide range of crops was feasible using lime treated acid mine drainage (AMD). Annandale et al (1999 and 2002) investigated the long-term sustainability of irrigation with gypsiferous mine waters, and demonstrated that gypsum precipitation in the soil kept soil solution salinity levels relatively low, thereby facilitating sustainable crop production, without negative consequences for soil resources. Beletse worked with sodium bicarbonate rich water from a coal bed methane operation (Beletse et al 2008) and showed this particular mine water to be problematic for irrigation due to the high levels of salinity and sodium, with no opportunity to precipitate gypsum and reduce soil salinity. Beletse also considered sodium sulphate rich waters on heavy clay soils, and although pastures did grow with this water, the sustainability of the practice was questioned (Beletse 2008).

For the demonstration of the irrigation water quality DSS, three mine waters that we have experience with for irrigation were considered (lime treated AMD, sodium bicarbonate rich and sodium sulphate rich waters). In addition, a chloride rich water was "generated" by keeping the properties of our actual lime treated AMD water, except that sulphate and chloride concentrations on a mol charge basis were swopped, to see if the DSS would come to the same conclusions that du Plessis (1983) did. Finally, because we are currently interested in investigating whether it is feasible to directly apply AMD to heavily limed soil (to negate the need for a liming plant), we also considered an acidic water of pH 3. These waters' analyses are presented in Table 1.

Relative crop yields

The DSS considers a relative crop yield above 90% to be ideal, between 80 and 90% is acceptable, between 70 and 80% is tolerable, and an unacceptable yield is below 70% of potential yield. Of course, in reality, this will depend on the grower and the profitability of producing a particular crop, but it is considered a useful guideline. Crops differ greatly in their sensitivity to or tolerance of salinity, but tend to show no yield penalty until a certain threshold salinity is exceeded, where after yield decline is linear, with the slope of this decline depending on the particular crop. The simulations presented are for a "Medium Sensitive" summer crop, maize, with a threshold saturation paste salinity of 170 mS/m and a 12% decrease in yield for each 100 mS/m increase in salinity, and two "Medium Tolerant" crops, soybeans, a summer crop with a threshold of 500 mS/m and slope of 20% and wheat, a winter crop with a threshold of 600 mS/m and slope of 7.1%.

Table 1 Composition of mine waters evaluated with the DSS

	Lime treated AMD	Chloride rich water	Sodium bicarbonate rich water	Sodium sulphate rich water	AMD
Major constituent					
Calcium (mg/L)	615	615	25	32	227
Magnesium (mg/L)	208	208	0	88	132
Sodium (mg/L)	10	10	2000	796	13
Bicarbonate (mg/L)	41	41	5000	450	0
Chloride (mg/L)	5	1500	375	18	3.5
Sulphate (mg/L)	2082	7	7	1647	2919
pH	5.7	5.7	7.5	8.9	3
EC (mS/m)	377	377	750	372	360
TDS (mg/L)	2961	2961	7407	3031	3295
SAR (mol/L)0.5	0.1	0.1	111	16.5	0.2
Trace elements					
Aluminium (mg/L)	2				158
Iron (mg/L)	31				233
Manganese (mg/L)	28				72
Nutrients					
Nitrogen (mg/L)	16				19.5
Phosphorus (mg/L)	0.4				0.5
Potassium (mg/L)	6				7

Relative yields were simulated for 45 years of irrigation with five different water qualities using weather data from Loskop Dam, which is reasonably representative of the coal fields of Mpumalanga in South Africa. The long simulation period is used to estimate the risk of irrigation with these waters, so that relative yields can be presented as the fraction of time they fall in a particular fitness for use category. The irrigation management practice for these simulations was to apply 20 mm every time the soil profile had a deficit to field capacity of 25 mm, thereby leaving room for at least 5 mm of rain. Results are presented in Table 2.

It is clear that production of a medium sensitive maize crop is only feasible with the gypsiferous lime treated AMD water. Soybean is clearly a summer crop that can be produced with a wider range of poor qual-

Table 2 Simulated % of time that yields of maize, soybean and wheat at Loskop would fall within specific fitness for use categories.

Fitness for Use	Relative crop yield	Lime treated AMD			Chloride rich water			Sodium bicarbonate rich water			Sodium sulphate rich water			AMD		
	%	Maize	Soybean	Wheat	Maize	Soybean	Wheat	Maize	Soybean	Wheat	Maize	Soybean	Wheat	Maize	Soybean	Wheat
Ideal	90-100	91	100	100		36	82			39		91	100			27
Acceptable	80-90	9				27	12		9	24	9					30
Tolerable	70-80					9	6		9	21	36	9				24
Unacceptable	<70				100	27		100	82	15	55			100	100	18

ity waters than maize, and wheat is able to be produced even with very poor quality waters. Clearly crop choice is one of the management practices available when assessing the feasibility of irrigating with a particular water quality. Directly irrigating with AMD does not look very promising, but initial pot trials undertaken at the University of Pretoria are encouraging when such waters are applied to highly buffered or limed soils.

The effect of location and irrigation management are illustrated in Table 3. Warmer, drier climates will be less suited to irrigation with saline waters than cooler wetter climates, where atmospheric evaporative demand is lower and a higher rainfall induced leaching environment is encountered. Simulations for Loskop are compared to those for Vaalharts, the biggest irrigation scheme in South Africa, which has a drier climate, with a far cooler winter. It is expected that maize will perform better in the more humid environment. In addition, two irrigation management strategies are compared. The "Deficit" irrigation strategy is designed to minimise leaching and use rainfall more efficiently. This is a wise strategy to follow when using good quality water, but irrigation is a salt concentrating practice, as crop roots extract water and exclude salts, and the higher the salinity, the greater the leaching requirement for sustainable irrigation. It is therefore not surprising that better yields are predicted for Vaalharts when effective leaching is increased from 5.7 to 7.5%.

Plant nutrient supply through mine water irrigation

Some mine waters are quite high in essential plant macro-nutrients, like nitrogen, phosphorus and potassium. Irrigation with nutrient rich waters can be beneficial for crop production, as this may represent a saving in the cost of buying fertiliser and the expenses incurred in applying it. However, some crops may be negatively affected by high concentrations of nutrients, through excessive vegetative growth and lodging, delayed maturity and reduced crop quality. High nutrient levels may complicate fertiliser management and limit control over nitrate leaching and P wash off. The rationale adopted in the DSS is that the higher the nutrient content and the greater the supply of nutrients to the crop, the harder it becomes to manage crop nutrient requirements. However, crops vary greatly in their nutrient requirements, and pasture crops in particular, will not easily be adversely affected by high nutrient loads, so crop selection is once again important when irrigating with mine impacted waters. Table 4 illustrates the nutrient supply to soybean and wheat from our treated and untreated AMD waters.

Table 3 *Demonstration of the effect of location (climate) and irrigation management (deficit irrigation vs a salt leaching strategy) on water requirements, effective leaching and relative yield.*

Fitness for Use	Relative crop yield (%)	Loskop Dam				Vaalharts			
		Deficit irrigation		Leaching requirement		Deficit irrigation		Leaching requirement	
		Maize	Wheat	Maize	Wheat	Maize	Wheat	Maize	Wheat
Ideal	90-100		100		100		100		100
Acceptable	80-90	9		9					
Tolerable	70-80	55		45		27		36	
Unacceptable	<70	36		45		73		64	
Irrigation	(mm)	731	557	763	560	978	523	1003	527
Effective Leaching	(%)	8.9	1.1	11.1	2.2	5.7	1.7	7.5	2.9

Simulations are for the sodium sulphate rich water on a maize-wheat rotation in the Loskop Dam area and at Vaalharts (drier region with cooler winters). The Deficit irrigation strategy is to irrigate with 15 mm whenever the deficit to field capacity reaches 20 mm, thereby leaving some room for rain. The leaching requirement strategy applies 15% more water than is required to return the profile to field capacity.

Table 4 Simulated plant nutrient (nitrogen) supply to a wheat-soybean rotation irrigated with lime treated AMD and AMD for Loskop weather data with irrigation leaving 5 mm room for rain once deficit to field capacity reaches 25 mm.

Fitness for Use	Contribution to crop N removal	Lime treated AMD				AMD			
		Soybean		Wheat		Soybean		Wheat	
		Time (%)	Applied (kg/ha)	Time (%)	Applied (kg/ha)	Time (%)	Applied (kg/ha)	Time (%)	Applied (kg/ha)
Ideal	0-10%								
Acceptable	10-30%	53	102			7	107		
Tolerable	30-50%	47	130	100	88	91	141	55	103
Unacceptable	>50%					2	191	45	114

Trace element accumulation in soil

A concern often raised with the use of mine water for irrigation is the fate of trace elements in the water. Especially with circumneutral waters this is usually not of great concern, but with lower pH waters this should certainly not be ignored. The DSS calculates how many years it will take to reach protective threshold soil values in the top 150 mm of the soil profile. Aluminium, iron and manganese are identified as the elements most likely to be flagged by regulators. However, the fact that they are found in abundance in natural soils raises the question whether or not these guidelines should be relaxed somewhat. To ascertain the real risk of detrimental food or forage safety due to trace element accumulation, more research needs to be done.

Corrosion and scaling of irrigation equipment and effect of mine water on soil physical properties

The DSS uses the Langelier Index to estimate corrosion or scaling of irrigation equipment. This may not be the best index for sulphate rich waters, as it was developed for carbonate rich waters. However, it can be seen in Table 6 that the sodium bicarbonate and sodium sulphate rich waters are predicted to be scaling, with the other waters indicated to be corrosive, especially the AMD. In addition, the DSS also predicts the effect of water quality on infiltration and hydraulic conductivity. Sodium is particularly problematic, but the negative effect is somewhat counteracted by high salinity levels.

***Table 5** Predicted effect of irrigation with different mine affected waters on corrosion (negative Langelier Index) or scaling (positive Langelier Index) of irrigation equipment, and the % of time soil physical properties will fall in specific fitness for use categories.*

Parameter	Fitness for Use	Lime treated AMD	Chloride rich water	Sodium bicarbonate rich water	Sodium sulphate rich water	AMD
Corrosion (-) Scaling (+) Langelier Index	Ideal					
	Acceptable			0.84		
	Tolerable	-1.62	-1.61		1.34	
	Unacceptable					-6
Surface Infiltration (% of time)	Ideal	92	92	92	92	92
	Acceptable	8	8	8	8	8
	Tolerable					
	Unacceptable					
Soil Hydraulic Conductivity (% of time)	Ideal	100	89	42	78	98
	Acceptable			28	2	
	Tolerable			17		
	Unacceptable		11	13	20	2

Conclusions

Not all mine waters are suitable for irrigation. However, the user-friendly DSS is able to assess site-specific factors that influence the suitability of mine waters for irrigation, and present the risk taken in using such waters, as far as crop yield and quality, soil factors and irrigation equipment is concerned. In some cases, a more detailed Tier 3 assessment is required, to ascertain if negative Tier 2 assessment issues, like for trace element loading in the simulations presented here, can be mitigated. This may require expert input by crop or soil scientists. The DSS will assist regulating authorities to make decisions on permitting mine water irrigation, and in consideration of mine closure options.

Future research should focus on the assessment of food and forage safety when using mine waters for irrigation, and improvements to algorithms for scaling and corrosion using gypsiferous waters. In addition, the need to discriminate against waters high in trace elements that are abundant in soils should be considered. Finally, an effort should be made to improve and expand parameters used in the model, especially for effects like scorching of foliage with low pH waters.

Acknowledgements

The authors thank the Water Research Commission for funding the development of the Irrigation Water Quality DSS.

References

Annandale JG, Jovanovic NZ, Benadé N, Tanner PD (1999) Modelling the longterm effect of irrigation with gypsiferous water on soil and water resources. Agric. Ecosyst. Environ. 76: 109-119.

Annandale JG, Jovanovic NZ, Tanner PD, Benadé N, du Plessis HM (2002) The sustainability of irrigation with gypsiferous mine water and implications for the mining industry in South Africa. Mine Water and the Environment, 21, 81-90.

Annandale JG, Stirzaker RJ, Singels A, van der Laan M, Laker MC (2011) Irrigation scheduling research: South African experiences and future prospects. Water SA. 37, 5, Special Issue, 751-763.

Beletse YG, Annandale JG, Steyn JM, Hall I, Aken ME (2008) Can crops be irrigated with sodium bicarbonate rich CBM deep aquifer water? Theoretical and field evaluation. Ecolog. Eng. 33(1), 26-36.

Beletse YG (2008) The environmental impact and sustainability of irrigation with coal-mine water. PhD thesis, University of Pretoria.

Du Plessis HM (1983) Using lime treated acid mine water for irrigation. Wat. Sci. Tech. 15, 145-154.

Du Plessis HM, Annandale JG, van der Laan M, Jooste S, du Preez CC, Barnard J, Rodda N, Dabrowski J, Genthe B, Nell P (2017) Risk based, site-specific, irrigation water quality guidelines. Water Research Commission Report No TT 727/17, ISBN No 978-1-4312-0910-1

Jovanovic NZ, Barnard RO, Rethman NFG, Annandale JG (1998) Crops can be irrigated with limetreated acid mine drainage. Water SA, 24(2), 113122.

Maas EV, Hoffman GJ (1977) Crop salt tolerance – current assessment. J. Irrig. Drain Div. ASCE 103(IR2), 115-134.

Robbins CH (1991) Solute transport and reactions in salt-affected soils. In: Hanks RJ, Ritchie JT (Eds) Modelling Plant and Soil Systems. Agronomy Monograph No. 31, ASA-CSSA-SSSA, Madison, Wisconsin, USA, p 365-395

Performance of passive systems for mine drainage treatment at high salinity and low temperature

Houssem E. Ben Ali[1], Carmen M. Neculita[1*], John W. Molson[2], Abdelkabir Maqsoud[1], Gérald J. Zagury[3]

[1]*Research Institute on Mines and Environment (RIME), University of Québec in Abitibi-Témiscamingue (UQAT), 445 Boul. de l'Université, Rouyn-Noranda, QC, Canada, J9X 5E4*

[2]*Department of Geology and Geological Engineering, Laval University, 2325 Rue de l'Université, Québec City, QC, Canada, G1V 0A6*

[3]*RIME- Polytechnique Montréal, Department of Civil, Geological, and Mining Engineering, Polytechnique Montréal, Montreal, QC, Canada, H3C 3A7*

Abstract

Low temperatures and high salinities can deteriorate the performance of passive biochemical reactors (PBRs) for mine drainage (MD) treatment. A 8-month parametric study was performed in eight 11 L PBRs using two mine drainage (MD) qualities (acidic and neutral), two salinities (0 and 20 g/L) and two temperatures (22 and 5°C) to select the optimal hydraulic retention times (HRTs) based on the PBRs' performance. HRTs of 1 and 5 days were required to efficiently treat acidic and neutral MD, respectively. The simultaneous effect of low temperature and high salinity decreased PBR efficiency by 30%-70%, especially for acidic MD.

Keywords: Saline mine drainage, passive treatment, cold climate, passive biochemical reactor.

Introduction

Passive treatment systems are considered as an essential complementary approach for successful mine site reclamation (USEPA, 2014). Their addition to conventional reclamation techniques prevents or improves the control of acid mine drainage (AMD) and contaminated neutral drainage (CND).

A passive biochemical reactor (PBR) is an efficient technology for the treatment of slightly contaminated MD in temperate or semi-arid climates (Neculita et al., 2011; Vasquez et al., 2016). However, PBR performance is less documented in northern climates, characterized by low temperatures (<4°C) and often high salinities (up to 40 g/L). In general, low temperatures reduce the efficiency of MD treatment by decreasing the kinetics of biogeochemical processes. The rate of sulfate reduction by sulfate reducing bacteria (SRB) decreased by over 50% when the temperature dropped from 16°C to 4°C (Benner et al., 2002). To improve PBR efficiency at low temperature, the addition of easily degradable substrate such as methanol, ethanol, lactate, acetate or glucose into PBR mixtures has been attempted (Gould et al., 2012; Nielsen et al., 2017). However, in these cases, the treatment system became semi-active rather than passive due to the occasional addition of substrate and, thus, operation costs increased.

High salinity represents another challenge, in addition to low temperature. Some of the main sources of salinity, which is an integrative measure of the major ions concentrations (Na^+, K^+, Ca^{2+}, Mg^{2+}, Cl-, SO_4^{2}- and HCO_{3-}) (Van Dam et al., 2014) are: (1) drainage water on mine sites (2) seawater intrusion at mines near the coasts, and (3) anthropogenic activities such as addition of de-icing agents (e.g. $CaCl_2$) (Feng et al., 2014; Kaushal et al., 2005; Nordstrom et al., 2015). Depending on the nature and concentration of the major ion components of salinity, PBRs have shown a good efficiency for sulfate reduction under high salinity (>40 g/L) at ambient and high temperature (70°C) (Vallero et al., 2005). At the same time, PBR effectiveness can decrease at high salinity due to the toxicity and osmotic stress on microorganisms, increases in metal solubility, as well as the competition of major ions with metals on sorption sites (Warrender and Pearce, 2007). Depending on the reactive mixture used in PBRs, a successful treatment of saline groundwater in semi-arid conditions (at 15-30°C) has been reported for periods varying from 260 days to more than 1,200 days (Degens, 2012; Biermann et al., 2014).

Nevertheless, the combined effects of high salinity and low temperature on alkalinity production (and acidity treatment) as well as on metal removal by PBR treatment are poorly documented and require further research. Thus, the present work aims to comparatively evaluate the effect of these two parameters on AMD and CND treatment using PBRs in column testing.

Methods

Mine drainage quality and column reactive mixtures

In the present study, two types of MD (AMD and CND) with two different salinities (0 and 20 g/L) were tested (tab. 1). The selection of AMD/CND chemistry was based on the compilation of surface water characterization data (pH, conductivity, sulfate and heavy metal concentrations) over 5 years of monitoring (2010-2014) for 2 sampling points at a nickel-copper mine located in a northern climate (average air temperature of -10.3°C).

Depending on the influent quality, columns were filled with two reactive mixtures (PBR#1 for AMD and PBR#2 for CND treatment) (tab. 2). All mixtures were fully characterized, before and after use (spent), and showed effective removal (>91%) of metals and sulfates during the treatment of highly contaminated MD in previous batch testing (Ben Ali et al., 2018).

Column design and experimental set-up

A parametric study was performed to evaluate the simultaneous effect of temperature and of salinity on sulfate reduction, metal removal, and acid neutralization. Experiments were performed with eight 11 L PBR columns (14 cm in diameter and 70 cm in height) for 8 months. Two types of MD (AMD and CND) with two different salinities (0 and 20 g/L) were tested at ambient temperature (22±0.5°C) during the first 3 months. The reactors were then transferred to a cold room at low temperature (5 ±1°C) for 5 months. Columns were operated at a HRT of 0.5 and 1 day for CND, and 2.5 and 5 days for AMD with vertically upward flow (fig. 1). For simplicity, columns were named according to the quality of the MD to be treated and the selected HRT (e.g., for saline AMD treatment with HRT of 2.5 days, column name is SAMD-2.5).

In each column, the mixture was placed between two layers of gravel (≈5 cm) and fine-mesh geotextiles, at the top and bottom, prior to being covered. All PBRs were saturated with the appropriate synthetic MD (tab. 2). Prior to starting the continuous feed of the columns, only the PBRs that treated acidic influent (AMD/SAMD) were incubated at room temperature for 1 week. Columns were fed with synthetic MD prepared weekly using peristaltic pumps (Masterflex).

Table 1 *MD quality used in PBR column reactors (all concentrations are in mg/L, except for pH)*

Parameters	AMD	Saline AMD	CND	Saline CND	Salt used
pH	2.8-3.5	2.7-3.6	5.1-7.8	6.1-7.5	-
Fe2+	27 ±3.5	24.2 ±4.2	9.0 ±2.1	8.2 ±2.6	FeSO4•7H2O
Ni2+	49 ±3.7	40.8 ±5.1	28 ±3.4	24 ±4.9	NiSO4•6H2O
Cu2+	3.2 ±0.5	2.8 ±0.7	1.1 ±0.2	0.9 ±0.3	CuSO4•5H2O
	1612 ±121	1615 ±157	519 ±53	546 ±76	Na2SO4
Ca2+	-	19 000 ±1100	-	20 000 ±2500	CaCl2

Table 2 *Components and proportions of reactive mixture composition*

Mixture	PBR#1	PBR#2
	(% dry weight)	
Carbon sources and porous material		
Wood chips / sawdust	48	0
Sphagnum peat moss	0	50
Nitrogen sources		
Leaf compost	10	20
Neutralizing agent		
Ash	30	20
Structural agent		
Sand	10	10
Inoculum		
Sludge from the Rouyn-Noranda WWTP*	2	0
Total	100	100

****WWTP: Wastewater*** *treatment plant*

Water sampling and analysis

Effluent water quality was monitored by weekly sampling and analysis of the physico-chemical parameters, including pH, redox potential (ORP), alkalinity, acidity, sulfate () and total metals. The pH and ORP were measured with an Orion Triode sensor coupled with a Benchtop pH/ISE Meter Orion model 920 (relative precision +/- 0.01 pH) and with a Pt/Ag/AgCl sensor linked to a Benchtop pH/ISE Meter Orion 920 (relative precision +/- 0.1 mV), respectively. The alkalinity and acidity were obtained by titration on non-filtered samples with a Metrohm Binkmann, 716 DMS Titrino titrator (APHA, 2012) (relative precision of 1 mg $CaCO_3$/L). Filtered samples (with a 0.45 µm filter) used to quantify metal content were acidified with 2% (v/v) of nitric acid (70%) before analysis. The techniques used to analyze metal concentrations were Inductively Coupled Plasma-Atomic Emission Spectroscopy (ICP-AES; Perkin Elmer

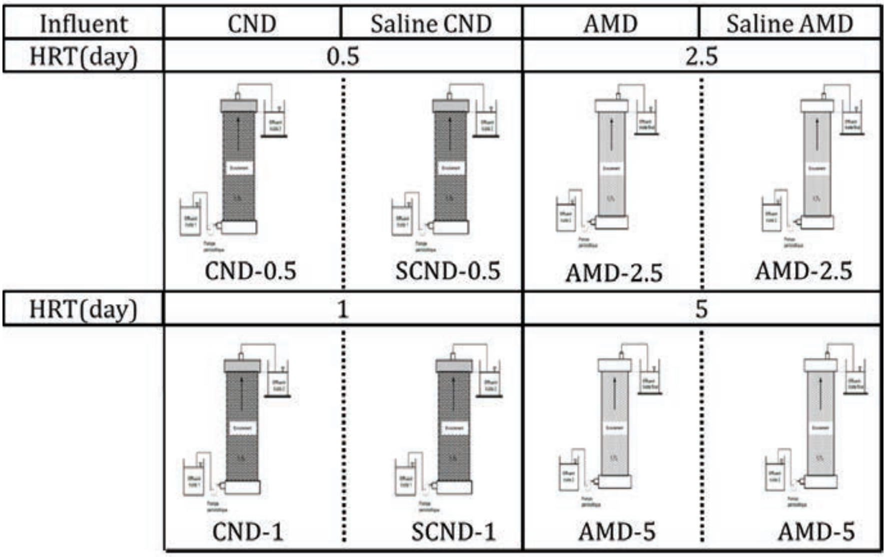

Figure 1 *Laboratory schematic representation of PBR column treatment scenarios*

3000 DV) and Inductively Coupled Plasma-Atomic Mass Spectrometry (ICP-MS; Agilent 7700X ICP-MS) for the non-saline and saline MD, respectively.

Results and discussion

The results will be discussed according to evolution of the treated water chemistry: 1) first period: 0-95 days, and 2) second period: 96-240 days, while highlighting the effect of temperature and salinity, as well as in combination for the treatment of each level of MD quality.

Influence of temperature on MD treatment

During the first period (0-95 days-22°C), pH increased from 5.5–6.2 to 6.4–8.2 in all CND columns which was essentially maintained when the temperature was decreased (to 5°C) during the second treatment period (96-240 days). For the AMD columns, pH increased from 2.8-3.5 to 7.3-8.4 at room temperature and then slightly decreased at 5°C (6.8-7.9). Oxidizing conditions (ORP between 200 and 414 mV) were found in the CND columns with low HRTs (0.5 and 1 day) at both tem-

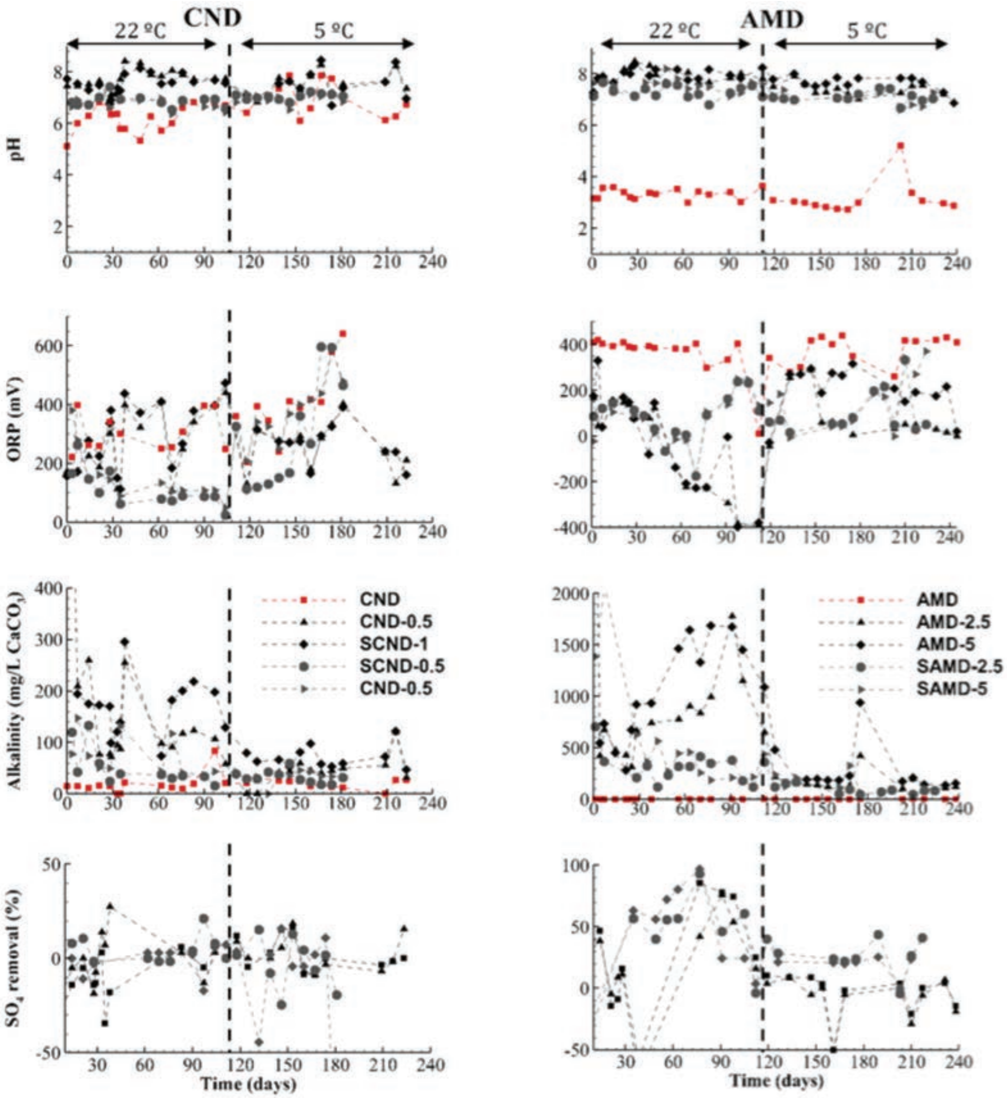

Figure 2 Evolution of pH, ORP, alkalinity and SO$_4$2- removal during CND/AMD treatment in column reactors

peratures. Nevertheless, for the AMD columns with 2.5 and 5 days of HRTs, anoxic conditions were noted (ORP from 200 to -400 mV) for 0–95 days, at room temperature, in contrast to the low temperature where slightly oxidizing conditions were maintained (>80 mV) (fig. 2). The lower HRTs used for CND treatment relative to AMD could explain these results.

Alkalinity increased from 0-20 to over 200 and 700 mg CaCO3 /L, for CND and AMD columns, respectively, at room temperature. However, alkalinity deceased significantly at low temperature to reach 100 mg CaCO3 /L (fig. 2). These findings are consistent with the evolution of acidity removal (results not shown). For SO42- removal, the results showed a release during the first three days, for both CND and AMD columns. A low removal efficiency (<27%) was noted for CND columns, regardless of the temperature and the HRT, as an indication of limited microbial reduction. However, for AMD reactors, better removal efficiencies were observed at room temperature, especially for AMD-5 (25-100%), contrary to low temperature, where efficiency decreased to <10%. One explication could be related to the low microbial activity at low temperature. For metal removal (Cu, Ni and Fe), results showed that, unlike copper which was efficiently removed (80%-99%) during the first and second periods, Fe and Ni removal was a function of HRT and temperature. Higher metal removal was found with 1-day HRT for the CND columns. More than 99% of Ni was removed in CND-1, at room temperature, relative to 70%, at 5°C. However, Fe removal was maintained at >95% for CND-1, regardless of the temperature. In the AMD columns, metal removal was better at room temperature (>97%) and no HRT dependent. Efficiency dropped to 80% for Fe but remained high for Ni at 5°C for AMD-5. Higher HRTs (1 day for CND and 5 days for AMD) showed better results for all parameters.

Influence of salinity on MD treatment

The effect of increased salinity will be dicussed only for the first period (0-95 days-22°C), period during which the pH and ORP showed similar evolution to non-saline CND and AMD columns. However, produced alkalinity was three times less. For SO_4^{2}- removal, only from saline AMD, efficiency significantly increased at room temperature (from 25% to 100% for AMD-5). This can be explained by sulfate microbial reduction, in addition to precipitation, especially of gypsum ($CaSO_4$), the formation of which is favored at sulfate and calcium concentrations greater than 1500 mg/L and 500 mg/L, respectively (Fernando et al., 2018). Metal removal from SCND-1 also showed less efficiency compared to CND-1 (65 and 70 % for Ni and Fe, respectively) at room temperature. The competition of major ions (especially Ca^{2+}) with metals on the sorption sites could be responsible for it (Warrender and Pearce, 2007). For the AMD columns, salinity has practically no effect on metal removal efficiencies which were even higher than 95% for AMD-5.

Combined effect of low temperature and high salinity on MD treatment

The evolution of the physicochemical parameters (pH, ORP, acidity and alkalinity) in the CND and AMD columns at low temperature and high salinity (96-240 days) were similar to non-saline MD over the same period. For SO_4^{2-} removal, no significant variation was noted for CND, but for AMD, SO_4^{2-} removal decreased significantly for SAMD-5 (<40%) and was absent for AMD-5. These results indicate that mineral precipitation takes over in the absence of any microbial activity. At low temperature, Ni, Fe and Cu removal did not change for SCND-1, whereas for SAMD-5 metal removal decreased to 74% and 80% for Ni and Fe, respectively.

Conclusion

The objective of the study was to evaluate the influence of temperature (22°C and 5°C) and salinity (0 g/L and 20 g/L as CaCl2) on the performance of PBR in the treatment of mine drainage (AMD and CND). Eight PBR columns were tested either at 2.5 and 5 days of HRT (for AMD) or 0.5 and 1 day of HRT (for CND), for a 8-month period. Results showed that, at room temperature, acidity neutralization and metal removal efficiency were maintained for saline/non-saline CND and AMD for more than 90 days, at HRTs of 0.5 and 2.5 days, respectively. However, better efficiency was found at a HRT of 1 day and 5 days for Ni, Cu, Fe and SO_4^{2-} removal from CND and AMD, respectively. At low temperature, metal removal efficiency decreased, especially for Ni, from 99% to 36% and 66% for the CND and the AMD, respectively. Regardless of the MD quality (CND vs AMD, saline vs non saline), biological sulfate reduction was severely hampered at low temperature. The simultaneous effect of low temperature and high salinity decreased the overall efficiency of the treatment system, especially when used to treat AMD. Moreover, metal and sulfate removal mechanisms depend on MD quality. Sorption could be the main mechanism for CND treatment, while precipitation as oxy-hydroxides, carbonates or sulfides and co-precipitation with iron oxy-hydroxides could be the main ones for AMD treatment with PBR. Nonetheless, a physicochemical (e.g. leaching) and mineralogical (e.g. scanning electron microscope and X-ray diffraction) characterization of the post treatment solids would allow a better understanding of the treatment mechanisms.

Acknowledgements

This research was supported by the Natural Sciences and Engineering Research Council of Canada (NSERC), the Canada Research Chairs Program, the Fonds de Recherche du Québec - Nature et Technologies (FRQNT, Québec’s Research Funds – Nature and Technologies), and the partners of the Research Institute on Mines and Environment (RIME-UQAT- Polytechnique): Agnico Eagle, Canadian Malartic Mine, Iamgold Corporation, Raglan Mine Glencore and Rio Tinto.

References

APHA (American Public Health Association) (2012) Alkalinity titration, standard methods for the examination of water and wastewater, 22nd ed. Greenberg A (Eds), Washington DC, USA

Ben Ali HE, Neculita CM, Maqsoud A, Molson JW, Zagury GJ (2018) Efficiency of batch biochemical reactors for mine drainage treatment at low temperature and high salinity. Appl Geochem (submitted).

Benner SG, Blowes DW, Ptacek CJ, Mayer KU (2002) Rates of sulfate reduction and metal sulfide precipitation in a permeable reactive barrier. Appl Geochem 17(3): 301-320.

Biermann V., Lillicrap AM, Magana C, Price B, Bell RW, Oldham CE (2014) Applicability of passive compost bioreactors for treatment of extremely acidic and saline waters in semi-arid climates. Water Res 55: 83-94.

Degens BP (2012) Performance of pilot-scale sulfate-reducing bioreactors treating acidic saline water under semi-arid conditions. Water Air Soil Pollut 223(2): 801-818.

Feng Q, Li T, Qian B, Zhou L, Gao B, Yuan T (2014) Chemical characteristics and utilization of coal mine drainage in China. Mine Water Environ 33(3): 276-286.

Fernando WAM, Ilankoon IMSK, Syed TH, Yellishetty M (2018) Challenges and opportunities in the removal of sulphate ions in contaminated mine water: A review. Miner Eng 117: 74-90.

Gould WD, Cameron R, Morin L, Bédard P, Lortie L (2012) Effect of lactate/acetate and glucose amendments on low temperature performance of anaerobic bioreactors treating simulated mine drainage. Proceedings of the 9th International Conference on Acid Rock Drainage (ICARD), Ottawa, Canada.

Kaushal SS, Groffman PM, Likens GE, Belt KT, Stack WP, Kelly VR, Band LE, Fisher GT (2005) Increased salinization of fresh water in the northeastern United States. Proc Natl Acad Sci USA 102: 13517-13520.

Neculita CM, Yim GJ, Lee G, Ji SW, Jung JW, Park HS, Song H (2011) Comparative effectiveness of mixed organic substrates to mushroom compost for treatment of mine drainage in passive bioreactors. Chemosphere 83(1): 76-82.

Nielsen G, Janin A, Coudert L, Blais JF, Mercier G (2017) Performance of sulfate-reducing passive bioreactors for the removal of Cd and Zn from mine drainage in a cold climate. Mine Water Environ 37(1): 42-55.

Nordstrom DK, Blowes DW, Ptacek CJ (2015) Hydrogeochemistry and microbiology of mine drainage: An update. Appl Geochem 57: 3-16.

Oren A (2011) Thermodynamic limits to microbial life at high salt concentrations. Environ Microbiol 13(8): 1908-1923.

Song H, Yim GJ, Ji SW, Nam IH, Neculita CM, Lee G (2012) Performance of mixed organic substrates during treatment of acidic and moderate mine drainage in column bioreactors. J Environ Eng 138(10): 1077-1084.

USEPA (United States Environmental Protection Agency) (2014) Reference guide to treatment technologies for mining-influenced water. EPA 542-R-14-001, 94p.

Vallero MV, Lettinga G, Lens PN (2005) High rate sulfate reduction in a submerged anaerobic membrane bioreactor (SAMBaR) at high salinity. J Membr Sci 253(1-2): 217-232.

Van Dam RA, Harford AJ, Lunn SA, Gagnon MM (2014) Identifying the cause of toxicity of a saline mine water. Plos ONE 9(9): e106857.

Vasquez Y, Escobar MC, Neculita CM, Arbeli Z, Roldan F (2016) Selection of reactive mixture for biochemical passive treatment of acid mine drainage. Environ Earth Sci 75(7): 576.

Warrender R, Pearce NJ (2007) Remediation of circum-neutral, low-iron waters by permeable reactive media. Proceedings of the International Mine Water Association (IMWA) Symposium, Cagliari, Italy.

Long-term Water Management of Saline Groundwater at the Ekati Diamond Mine

Michael Herrell[1], Jerry Vandenberg[2], John Faithful[2], April Hayward[3], Lukas Novy[3]

[1]*SRK Consulting (Canada) Ltd., Vancouver, British Columbia, Canada, mherrell@srk.com*
[2]*Golder Associates Ltd., Vancouver, British Columbia, Canada*
[3]*Dominion Diamond Ekati ULC, Calgary, Alberta, Canada*

Abstract

Deep groundwater in much of northern Canada is characterized by high concentrations of total dissolved solids (TDS) that can increase by orders of magnitude with depth. Mining in this region can result in upwelling of saline groundwater that needs to be managed during pit development during operations and in the mine closure/post-closure phases. Due to the pristine nature of the downstream receiving environment in northern Canada, direct discharge of high TDS water may not be acceptable and the remote location of the mine often makes water treatment not economically feasible. Therefore, alternate water management strategies often need to be developed to manage this water.

The proposed Jay open pit Project at the Ekati Mine in the Northwest Territories, Canada is expected to result in upwelling of high TDS groundwater that will have to be managed during mine operations. A water management strategy was developed to minimize TDS loads in the mine discharge through using an existing mined out pit (Misery Pit) to store mine water produced during the development of the Jay Pit. Water balance modelling indicates discharge to the receiving environment will be required during mining of Jay Pit for a period of time. To preclude discharge of peak TDS concentrations, which are predicted to increase through operations, water will be pumped to the bottom of Misery Pit allowing surface water in Misery Pit that meets regulatory criteria to be discharged. At closure, mine water will be pumped back from Misery Pit to Jay Pit, and Misery and Jay Pits will be capped with freshwater from a nearby lake to establish permanent meromictic conditions.

Evaluating the feasibility of the proposed water management strategy required the development and integration of several models that were linked at key times and nodes. These included a three-dimensional hydrogeological model to predict groundwater inflow rates and TDS loads to Jay Pit during operations, and a site mass balance water quality model and downstream lake hydrodynamic models to evaluate if the proposed water management strategy would result in an acceptable discharge water quality. For closure, the stability of meromixis was evaluated using pit lake hydrodynamic models.

This paper presents a case study of the Jay Project water management plan and an overview of modelling that is required to evaluate water management options for high TDS water.

Keywords: saline water, mine water management, pit lake water quality

Introduction

Groundwater in much of the Canadian Shield is characterized by high salinity that increases by orders of magnitude with depth (Fritz and Frape 1987). Mining in these areas has the potential to cause upwelling of deep seated groundwater containing elevated concentrations of total dissolved solids (TDS). This poses a challenge for developers since the pristine nature of the downstream receiving environment, which is characterized by very low (e.g., less than 20 milligrams per litre [mg/L]) concentrations of TDS (Vandenberg et. al, 2015), can preclude direct discharge of groundwater produced during mining.

Dominion Diamond ULC (Dominion Diamond) is currently constructing the Jay Project at the Ekati Mine, located in the Northwest Territories (Figure 1). The proposed Jay Pit is located below Lac du Sauvage, which contains an open talik. Hydrogeological modelling (Dominion Diamond 2014; Golder 2016) indicates that groundwater inflows and TDS concentrations will increase as mining progresses. To minimize the discharge volume of water containing high TDS, Dominion Diamond proposes to store saline mine water during operations and subsequently use this water to develop meromictic pit lakes, permanently isolating mine water from mixing with surface water during post-closure.

A detailed modelling evaluation of operational and post-closure water quality was completed for the Jay Project as part of the Developer's Assessment Report (DAR) (Dominion Diamond 2014) and the subsequent Water Licence Application (Golder 2016). There are several influences on water quality at the Jay Project (e.g., geochemical, hydrogeological, etc.) and accounting for all of these processes required several models to evaluate if the proposed water management strategy would be protective of downstream receptors.

This paper presents a summary of the modelling that was completed to validate the feasibility of the proposed saline water management strategy. A focus is given to the pit lake hydrodynamic modelling as the water management strategy takes advantage of the development of meromictic pit lakes during post-closure.

Project description

The Jay kimberlite pipe is located below Lac du Sauvage. Access to the pipe will require construction of a dyke around, and dewatering of, a small area of Lac du Sauvage (Figure 2). During mining of Jay Pit, mine water will be pumped to Misery Pit and subsequently discharged to Lac du Sauvage after the Misery Pit storage capacity is exceeded. Hydrogeological modelling indicates that TDS concentrations will increase as mining advances in Jay Pit. Dominion Diamond proposes to pump mine water from Jay Pit to the bottom of Misery Pit. This approach conceptually displaces water containing lower TDS concentrations vertically through the water column, precluding the discharge of water containing the highest concentrations of TDS that are produced later in the mine life.

At closure, mine water stored in the upper 50 m of Misery Pit will be pumped to the bottom of Jay Pit. Residual mine water in the Jay and Misery Pits will be covered with water pumped from Lac du Sauvage, catchment runoff and groundwater inflows. This approach will create a low-density, freshwater cap over the residual mine water and meromictic lakes in Misery and Jay pits. Following back-flooding, and after water quality monitoring confirms that water quality is suitable for discharge, the Jay dyke will be breached and the pit lake will be reconnected to Lac du Sauvage. Misery Pit lake will drain naturally to Lac de Gras.

Methods

To test the validity of the proposed water management strategy, several models (e.g., hydrogeological, water balance, site water quality, etc.) were developed that were linked at key times and nodes. This paper focuses on the pit lake hydrodynamic model developed in CE-QUAL-W2 (Cole and Wells 2008) to evaluate the vertical stratification potential within the pits during the first 200 years of the post-closure period (i.e., after the mined-out pits are entirely back-flooded). Initial conditions in the mixolimnion (upper layer) and monimolimnion (lower layer) of the pit lake were simulated using the site water quality model.

As part of the Water Licence Application, the stability of meromixis in Jay and Misery pits was evaluated for different density gradients between the mixolimnion and monimolimnion. These were referred to as the 1xTDS (low density gradient) and 2xTDS (high density gradient) scenarios. The reader is referred to Golder (2016) for additional details on the model scenarios as well as additional details on the pit lake model configuration and calibration.

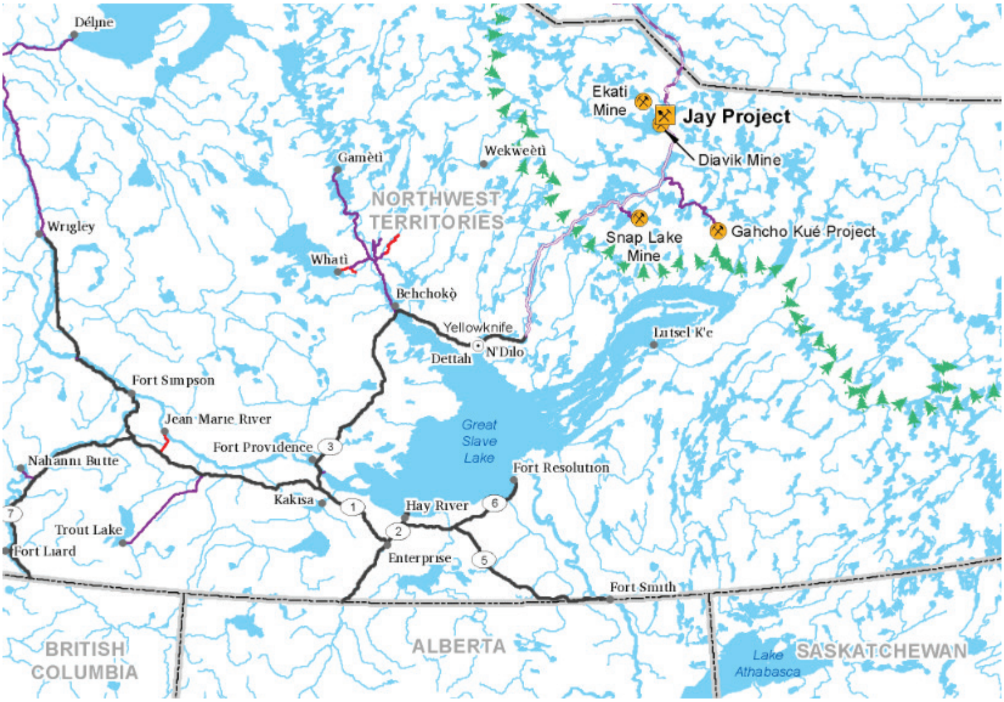

Figure 1 Location of the Jay Project

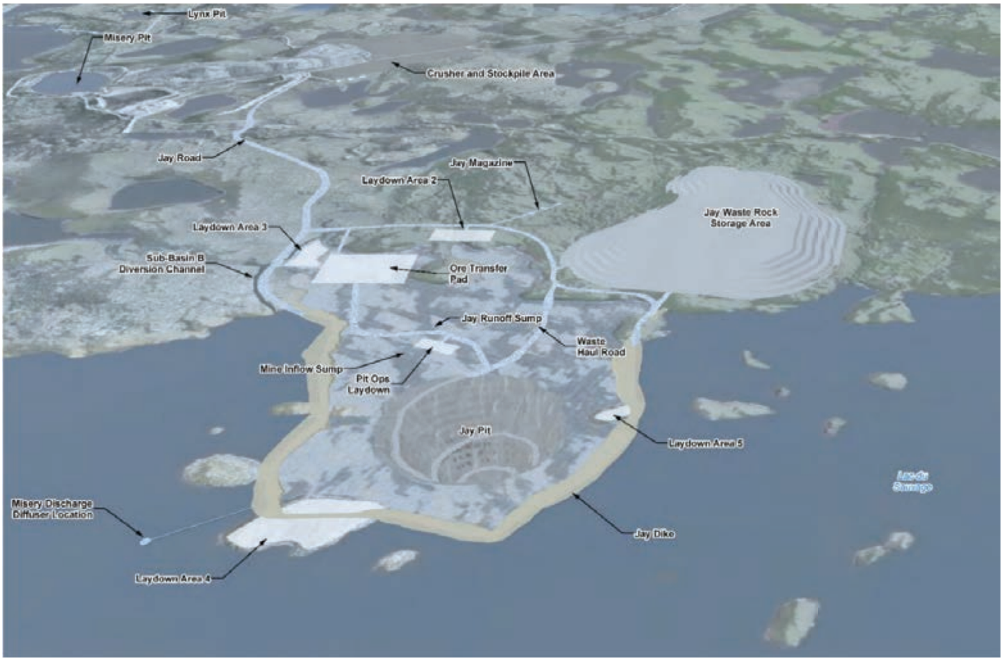

Figure 2 Proposed Jay Project Infrastructure

Results

Projected pit lake TDS profiles for the Jay and Misery Pit are presented in Figures 3 and 4, respectively. Predicted TDS concentrations for the Jay Pit indicated meromixis will be stable during the 200 year post-closure period. Concentrations of TDS in the mixolimnion increase to just over 100 mg/L for the 1xTDS and 2xTDS scenarios. For both scenarios, the transition layer gets thicker over time and the pycnocline migrates deeper into the pit lake creating a thicker freshwater cap.

Projected TDS concentrations for Misery Pit (Figure 4) also indicate this pit lake will remain meromictic throughout the 200 year modelled post-closure period for the 1xTDS and 2xTDS scenarios. For both scenarios, concentrations were predicted to increase in the mixolimnion until about 150 years into post-closure. This increase is mainly attributed to runoff from the high wall and other surface inflows. The model shows that the transition layer between the mixolimnion and monimolimnion will thicken over time but the elevation of the pycnocline is not expected to notably change. Concentrations in the monimolimnion remain unchanged because Misery Pit is developed in permafrost, which acts as a barrier to groundwater inflows. Similar to Jay Pit, there is a higher density difference in the long-term for the 2xTDS scenario in comparison to the 1xTDS scenario (Figure 4).

Discussion

The detailed water quality modelling completed as part of the Jay Project indicates that development of meromictic pit lakes is a viable solution for saline water management at the Ekati Mine. This saline water management strategy is considered feasible for the Jay Project for the following reasons;

- There is a location available (i.e., Misery Pit) to store saline water containing elevated TDS during mining of Jay Pit;
- There is an abundant source of water (e.g., Lac du Sauvage) available to develop a freshwater cap during closure;
- The pit geometry is favourable (e.g., low surface area to depth ratio) for the development of meromictic conditions (Pieters and Lawrence 2014); and
- The Jay dyke will act as a wave barrier, limiting the effective fetch and therefore limiting mixing in the Jay pit lake.

Use of mined out pit lakes as a viable saline water management strategy is therefore site specific and the above considerations would need to be evaluated as part of saline water management at other mine sites.

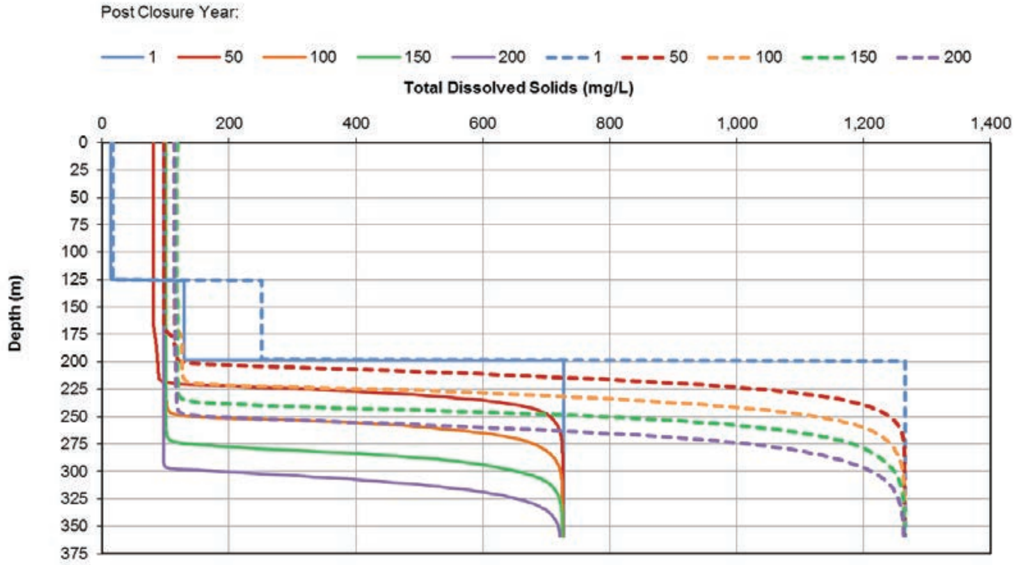

Figure 3 Predicted TDS Profiles for Jay Pit

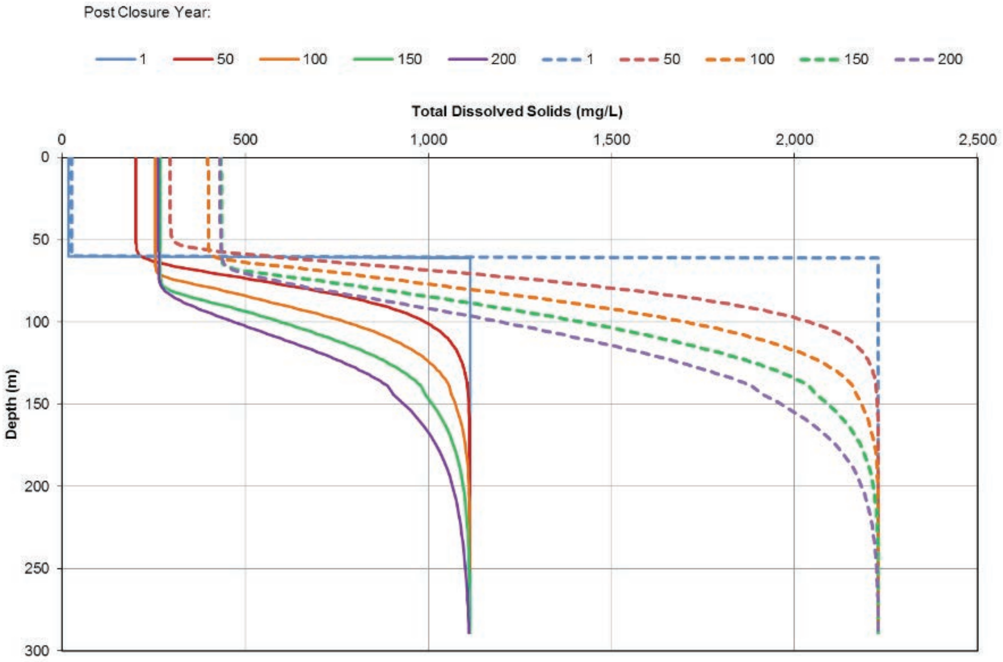

Figure 4 *Predicted TDS Profiles for Misery Pit*

As part of the Regulatory and Public review process, several other pit lake modelling scenarios were completed to evaluate the risk of a Jay Pit lake overturn in post-closure. These included a lower bound TDS scenario (Golder 2015a) and an extreme wind scenario (Golder 2015b). In all scenarios modelled, the Jay Pit was predicted to remain meromictic indicating there is a very low probability of a lake overturn. The additional model scenarios provided confidence to the Regulators and Public that use of mined out pit lakes the store minewater under established meromictic conditions was a viable saline water management strategy at the Jay Project, and the project was approved to proceed.

The Regulatory and Public review process was also valuable in "setting the bar" for the level of modelling that could be expected if use of pit lakes as a saline water management strategy were to be considered in Northern Canada. The feedback received clearly demonstrated the need to evaluate several model scenarios, included scenarios for upset conditions, to confirm the validity of using pit lakes as a proposed water management strategy.

Conclusions

Mining in Northern Canada poses several challenges. The baseline groundwater quality is characterized by high concentrations of TDS and mining in this region can produce saline water, which may not be able to be discharged due to the pristine nature of downstream receptors. In addition, the remote nature of the sites can make conventional treatment options impractical.

Use of mined out pit lakes to cap saline water with freshwater can produce meromictic pit lakes. These lakes contain a monimolimnion that is permanently isolated from mixing with the overlying mixolimnion, with the exception of a small amount of upward dispersion. If conditions indicate this is a feasible mine water management solution, it needs to be tested through a site-specific modelling exercise that accounts for all conditions, including upset conditions, that may be encountered.

References

Cole, T.M., Wells, S. 2008. CE-QUAL-W2: A Two-Dimensional, Laterally Averaged, Hydrodynamic and Water Quality Model, Version 3.6; User's Manual. Prepared for US Army Corps of Engineers Waterways Experiment Station. Washington, DC, USA.

Dominion Diamond (Dominion Diamond Ekati Corporation) 2014. Developer's Assessment Report for the Jay Project. Prepared by Golder Associates Ltd., October 2014. Yellowknife, NWT, Canada.

Golder (Golder Associates Ltd.) 2015a. Jay Project – Pit Lake Hydrodynamic Modelling – Lower Bound Scenario. Submitted to Dominion Diamond Ekati Corporation. July 3, 2015.

Golder 2015. Jay Project – Pit Lake Hydrodynamic Modelling – Extreme Wind Scenario. Submitted to Dominion Diamond Ekati Corporation. July 24, 2015.

Golder 2016. Jay Project – Water Licence Water Quality Model Updates. June 2016.

Fritz P, Frape SK (1987) Geochemical trends for groundwaters from the Canadian shield. In: Fritz P, Frape SK (eds) Saline water and gases in crystalline rocks, vol 33. Geological Association of Canada Special Paper, Ottawa, pp 19–38.

Pieters R and Lawrence G. Physical Processes and Meromixis in Pit Lakes Subject to Ice Cover. Canadian Journal of Civil Engineering. Vol 41. 2014.

Vandenberg J, Herrell M, Faithful J, Snow A, Lacrampe J, Bieber C, Dayyani S, Chisholm V. Multiple Modeling Approach for the Aquatic Effects Assessment of a Proposed Northern Diamond Mine Development. Mine Water and the Environment. DOI 10.1007/s10230-015-0337-5. March 26, 2015.

Bio-reduction of Selenium Oxyanions in the Presence of Nitrate in Neutral pH Coal Mining Influenced Water

Frank Nkansah-Boadu, Ido Hatam, Jon C. Taylor, Susan A. Baldwin

[1]*University of British Columbia, Department of Chemical and Biological Engineering, 2360 East Mall, Vancouver, British Columbia, V6T 1Z3, Canada*

Abstract

Biological treatment to remove dissolved selenium from coalmine-influenced water is inhibited by co-contaminants, especially nitrate. Consortia of bacteria capable of reducing selenate and nitrate were enriched from two sites impacted by coalmine waste seepage. Enrichments from a natural vegetated marsh removed both dissolved selenium and nitrate simultaneously, whereas tailings pond sediment enrichments reduced total dissolved selenium more effectively in the presence of nitrate but only once all nitrate was removed. When inoculated into actual mine water, the enriched tailings pond bacteria removed 40% selenium, whereas natural marsh enrichment bacteria achieved less selenium removal (10%).

Keywords: coalmining, selenium, nitrate, biological treatment

Introduction

Selenium is found in most coal waste rock (Lussier et al. 2003) and oxidative weathering can release the selenium into aquatic environments, together with other contaminants such as nitrate (by product of explosives used in mining) and sulfate. Selenium tends to biomagnify up the food chain leading to deleterious environmental effects (Janz et al., 2010). Active and semi-passive bioreactors have been developed for the removal of dissolved selenium from mine water (Tan et al., 2016). The success of these is dependent on seeding them with bacterial communities that can transform dissolved selenium in the presence of other contaminants to the less bioavailable elemental selenium. Nitrate is a competing anion often found in coalmine-affected water known to inhibit selenium reduction in previous attempts to biologically treat these waters (Steinberg et al. 1992). This study investigated the use of enrichments of bacterial consortia resident in sediments of ponds impacted by coalmine seepage, to remove total dissolved selenium in the presence of nitrate. We enriched bacteria from the sediments of both a vegetated natural marsh and a non-vegetated inactive tailings pond. Our results showed that the bacterial consortium enriched from the marsh reduced selenate and nitrate simultaneously in growth media. The tailings pond sediment bacteria reduced selenium more effectively in the presence of nitrate, but only once all nitrate had been consumed. Both enrichments were tested for their ability to remove selenium from actual mine waste seepage water. After transfer to the mine water both enrichment consortia changed in composition and comprised similar taxonomic groups. However the enrichment bacteria from the inactive tailings pond sediment were more efficient at removing selenate from the mine water than those from the marsh.

Materials and Methods

Preparation of selenate reducing enrichments

Sediment samples were collected from the water sediment interface from two aquatic environments located on two mine sites: A natural vegetated marsh (marsh) and a non-vegetated inactive tailings pond (pond). Measurements with an YSI Sonde model 600QS and probes indicated that, at sampling time, the sediments were anaerobic (dissolved oxygen < 2 mg/L), the pH was circum-neutral (≈7) and the temperature was 10-12oC. All samples were stored in a cooler with ice whilst en route to the laboratory for further experiments.

Organisms were enriched from the sediments in two types of growth media: one with selenate as the sole electron acceptor (GM1) and the second with both selenate and nitrate as electron acceptors (GM2). The enrichment medium was prepared according to (Stams et al. 1992), omitting selenite and adding 1 mg-Se-as-selenate/L instead, and using phosphate buffer instead of carbonate. Lactate was used as the carbon source and was added at a concentration of 600 mg/L. For the growth medium containing nitrate and selenate, 50 mg-N-as-nitrate/L was added also. Each growth medium was dispensed into two duplicate autoclaved 250 ml culture bottles for each sediment containing 25 ml of sediment slurry, which were then filled to the brim to remove any headspace. Thereafter, the bottles were sealed with butyl septa caps before subjected to static incubation at 30°C. Samples were collected at time intervals 0, 4, 8, 12, 24, 48 and 72 hr for analysis of total nitrite- plus nitrate-N (APHA method No. 4500 –NO_3^- E) and total dissolved selenium (ICP-MS at ALS Laboratory, Burnaby, BC). After 72 hours, culture bottles were decanted and 25 ml of biomass was transferred into freshly prepared growth medium and the culturing procedure repeated for three passages.

Removal of total dissolved selenium from actual mine water using the enrichments

Enrichments from the growth medium containing both selenate and nitrate were tested for their capability to remove dissolved selenium from actual mine water using triplicate batch culture bottles for five passages of three days each. The mine water was filtered through 0.45-µm nitrate cellulose membrane (GE Healthcare Life Sciences, USA) to remove suspended materials, including microorganisms. The actual mine water had the following chemical composition, total dissolved selenium (0.354 mg/L) and total nitrite-plus nitrate-N (54.9 mg/L), sulfate (2030 mg/L), sodium (14.4 mg/L), chloride (19 mg/L), calcium (404 mg/L), magnesium (390 mg/L) and CaCO3 (2610 mg/L). The major trace elements in the mine water were nickel (0.0327 mg/L) and strontium (0.250 mg/L). It was supplemented with phosphate buffer (K2HPO4 1 g/L / KH2PO4 0.2 g/L), 0.3 g/L ammonium chloride, and 600 mg/L lactate as essential nutrients. The pH of the nutrient amended mine water remained near neutral (6.8 – 7.04) throughout the duration of the experiment. Samples were collected daily for total dissolved selenium, total nitrate- plus nitrite-N and soluble chemical oxygen demand analyses, and for DNA extraction for bacterial population composition identification.

Bacterial community analysis

DNA was extracted using the FastDNA® SPIN kit for soil (MoBio Laboratories Inc. USA) according to the manufacturer's protocol. Sequencing and bioinformatics methods were the same as reported in Subedi et al. (2017). Read counts in each sample were normalized to 20,000 reads each.

Results and Discussion

Total dissolved selenium reduction in the presence and absence of nitrate

When sediments from the marsh were inoculated into growth medium containing selenate as the only electron acceptor, total dissolved selenium concentrations decreased with tiwme reaching almost complete removal within 48 hr (Figure 1a) indicating that these sediments contained bacteria capable of using selenate as an electron acceptor. No lag period was observed suggesting that the sediment bacteria were already adapted to grow on selenate. When the same sediments were inoculated into growth medium containing both selenate and nitrate, reduction in soluble selenium proceeded similarly with concomitant reduction in nitrate. Thus, the marsh sediments contained microorganisms capable of reducing selenate and nitrate simultaneously. In contrast, when equivalent amounts of sediment from the pond were inoculated in selenate-only growth medium, dissolved selenium was reduced more slowly (Figure 1b) suggesting that these sediments contained fewer or less capable selenate reducing microorganisms. In the growth medium with both selenate and nitrate, there was a lag period before dissolved selenium concentrations decreased, the duration of which was approximately the same as the time taken for complete denitrification. After this lag period, the rate of reduction in dissolved selenium was faster than that observed in the selenate-only growth medium. Thus, selenate reduction by the pond microorganisms was apparently stimulated by presence of nitrate. The results indicate that some selenate reducing bacteria from the marsh might be using a specific selenate reductase enzyme that is not competitively inhibited by the presence of nitrate, which resulted in simultaneous reduction of both nitrate and selenate. Whereas, the selenate reducing bacteria in the pond sediments that were enriched might have been denitrifying bacteria that increased in concentration first due to the presence of nitrate and then when nitrate was depleted, the non-specific nitrate reductases metabolized selenate. The bacteria enriched in the selenate plus nitrate growth medium from these two sediments represent two potentially different mechanisms of selenate reduction that were tested for their efficacy in removing dissolved selenium from actual coalmine affected water sourced from a mine site.

Total dissolved selenium removal from actual mine water containing nitrate and sulfate as well as selenium oxyanions

When inoculated into nutrient-amended mine water, the enrichment consortia were less efficient at reducing selenate compared to when grown in medium over the same period of time (3 days) (Table 1 & Figure 1). Unfortunately no data for total dissolved selenium were available for the first two passages. The extents of total dissolved selenium reduction increased with passaging, reaching in the final passage 8 ± 1% for the marsh enrichment inoculated mine water cultures and 40 ± 15 % for the pond enrichment inoculated mine water cultures. It is not known if these extents would continue to increase with further passaging as the microorganisms continue to adapt to the chemical environment of the nutrient-amended mine water. These results indicate that the microorganisms from the pond were more capable of reducing selenate in the mine water either due to their greater abundance or the metabolic traits of the species in that enrichment. It was not possible to measure the exact number or concentration of microorganisms in each enrichment that were inoculated into the mine water. Therefore, it is possible that there were more microorganisms in the pond enrichment cultures than in the marsh enrichment cultures at the beginning of the experiment. Similarly, although the same volume of suspended microorganisms was transferred into each new passage, the concentrations of microorganisms in that volume might have been different. The microorganism concentrations in these cultures were too low to capture with total volatile suspended solids analysis. Presence of particulates interfered with cell counts

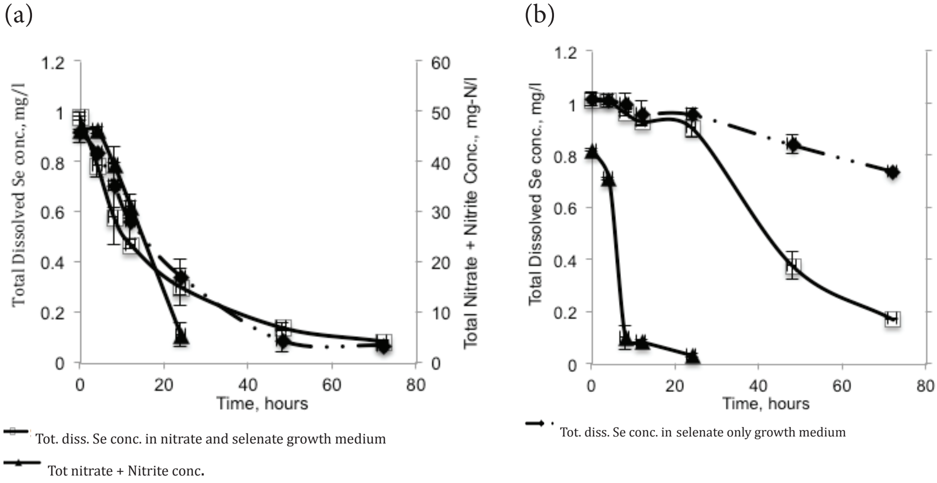

Figure 1: Total dissolved selenium (closed diamonds and triangles) and nitrate plus nitrite concentrations (mg/L) (closed triangles) versus time (in hours) measured in the selenate-only (black diamonds) and selenate plus nitrate (open squares and closed diamonds) growth media for sediment sourced from a) the natural vegetated marsh b) the inactive tailings pond. Data points are averages from duplicate culture bottles. Error bars represent the standard deviation.

Marsh	Passage1	Passage 2	Passage 3	Passage 4	Passage 5
Tot. diss. Se reduction (%)	n.d	n.d	3±2	8±2	8±1
Tot. NO2- + NO3-N reduction (%)	86±2	66±3	84±2	68±18	86±2
Δ SCOD concn. (mg/L)	1546 – 1337	1281 – 1186	1090 – 810	873-720	1407-956
Pond					
Tot. diss. Se reduction (%)	n.d	n.d	10±5	19±9	40±15
Tot. NO2- + NO3-N reduction (%)	88±1	86±8	91±1	87±4	78±1
Δ SCOD concn (mg/L)	1586-1373	1290-1055	1027-866	845-738	1467-1272

n.d not determined

Table 1: *Total dissolved selenium, total nitrite- plus nitrate-N reduction (%) and soluble chemical oxygen demand concentrations change (mg/L) measured over each passage for the mine water cultures inoculated with enriched marsh and pond microorganisms, respectively*

using flow cytometry.

One possible reason for less than expected dissolved selenium removal might be because the concentrations of active microorganisms inoculated into the mine water were low and more time would be required for them consume all of the selenate. However, presence of active microorganisms was confirmed by almost complete denitrification in the first passage (Table 1). Another possible factor that could have contributed to lower than expected dissolved selenium reduction might have been the availability of carbon source. However, this was not the case since soluble chemical oxygen demand (SCOD) concentrations suggested that not all carbon source was consumed (Table 1). Thus, contrary to the observations made in the growth medium enrichment experiments, nitrate might be inhibiting selenate reduction and removal of total dissolved selenium in the nutrient-amended mine water. It is possible that the microbial population composition of the enrichments changed when they were inoculated into the mine water due to differences in the chemical environment of the mine water compared to that in the growth medium. Indeed, tracking of the microbial community composition in the nutrient-amended mine water cultures indicated shifts in relative abundance of certain OTUs (species) with increasing adaption of the microbial community to the mine water environment. In fact, nine of the 20 dominant species in the pond enrichments declined in relative abundance, as did 14 out of 20 species from the marsh enrichments, with increasing passaging. A few dominant species continued to thrive in the mine water and some rare species not detected in the enrichments became dominant in the mine water microbial communities. For instance, a *Sulfurospirillum* species (OTU1) that was present in both enrichments increased in relative abundance in the nutrient-amended mine water to become the most dominant (Figure 2). A *Veillonella* species (OTU3) not detected in either enrichment, became dominant in most of the nutrient-amended mine water cultures. *Paracoccus* (OTU4) and *Macellibacteroides* (OTU6) dominated the nutrient-amended mine water cultures inoculated with the pond enrichments, but were absent from or rare in the marsh enrichment inoculated cultures. *Sulfurospirillum* species are members of the Epsilonproteobacteria and have been reported to grow on substrates such as selenate, as well as nitrate and S compounds (Goris & Diekert 2016), which explains its dominance of the nutrient-amended mine water cultures. *Veillonella* species are denitrifying bacteria and one species, *V. atypica*, produced elemental Se from reduction of selenite (Pearce et al. 2009). *Paracoccus* are well known denitrifiers. One species, *P. denitrificans*, was found to reduce selenite but not selenate. But when it was combined with a selenate-reducing bacterium (a *Pseudomonas* species) both selenate and nitrate reduction occurred simultaneously (Morita et al. 2007). Thus, a mixture of microorganisms performing different roles can contribute to simultaneous removal of multiple pollutants. The role of *Macellibacteroides* (OTU6) in the cultures is less clear since there is only one species that has been characterized and it was reported not to be able of using nitrate or S species as electron acceptors, and was a fermentative bacterium metabolizing sugars (Jabari et al. 2012). Taken together these observations suggest that both enrichment cultures had species with the potential to reduce selenate, with more of the pond enrichment bacteria persisting in the mine water.

The mine water contained high concentrations of some salts other than dissolved selenium and nitrate that might have influenced the metabolism of bacteria in the enrichments. For example, sulfate concentration in the mine water was 2030 mg/L. Even though sulfate is a less thermodynamically favourable electron acceptor than nitrate and selenate or selenite, its presence may have influenced the microbial community structure. Additionally, mine water was missing the essential minerals iron and molybdenum, which are required for enzymes involved in selenate and nitrate reduction (Sabaty et al. 2001). Additionally, the high concentrations of Mg^{2+} and Ca^{2+} in the mine water might have caused precipitation of the essential micro and macronutrients inhibiting microbial activity, as was seen in another study (Fernandez-Nava et al. 2008).

Conclusions

Bacteria with the capability to reduce both selenium oxyanions and nitrate can be enriched from native communities present in anaerobic sediments of both a natural marsh and tailings pond impacted by coalmine waste rock seepage. Even though species with the capability to reduce selenate survived when enriched bacteria from these two sites were inoculated into actual coalmine-affected water, the extents of total dissolved selenium removal were lower than those observed in

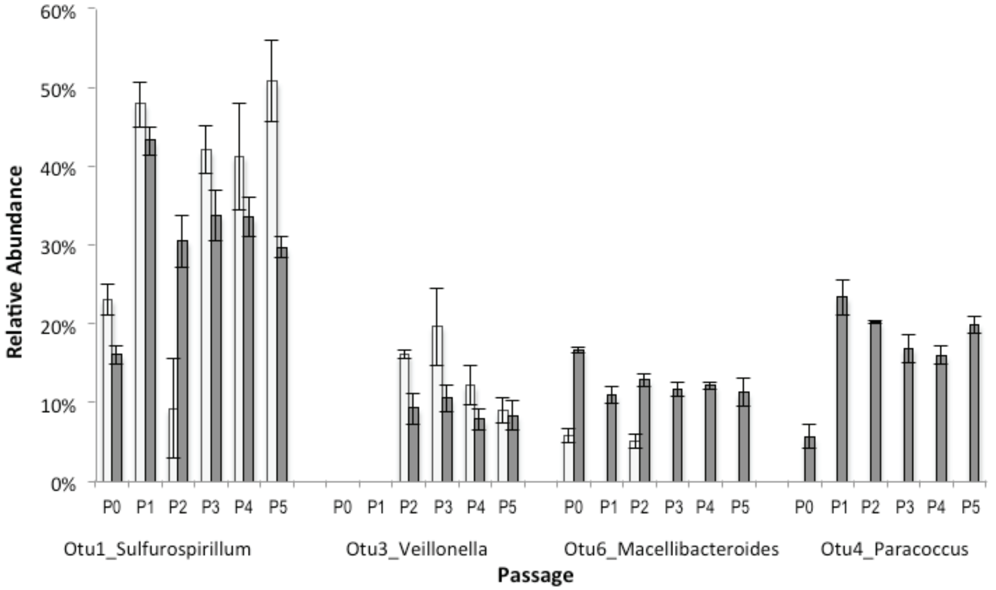

Figure 2: *Percentage relative abundance of selected dominant species (OTUs) and their genus-level taxonomic classification versus passage (P) in the nutrient-amended mine water cultures inoculated with enrichments from the (a) marsh, white filled with black border and (b) pond, grey filled with black border. Error bars represent standard deviations from the mean of measurements from triplicate culture bottles. P0 refers to samples taken at time zero at the start of the experiment.*

growth medium. Possibly other constituents of the coalmine-affected water negatively affected the selenium reducing bacteria or essential nutrients for selenium removal were missing from the coalmine-affected water although sufficient carbon source was provided.

Acknowledgements

Mine personnel are thanked assisting with sample collection.

References

APHA, AWWA and WEF (2017). Standard method for the examination of water and waste water 23rd edition. Edited by Baird, R.B., Eaton, A.D., and Rice, E.W. American Public Health Association, NW, Washington, 5.21-5.22.

Goris T, Diekert G (2016). The Genus *Sulfurospirillum*, in: Organohalide-Respiring Bacteria. Springer Berlin Heidelberg, Berlin, Heidelberg, pp. 209–234.

Fernández-Nava Y, Marañón E, Soons J, Castrillón L (2008). Denitrification of wastewater containing high nitrate and calcium concentrations. Bioresour. Technol. 99, 7976–7981.

Jabari L, Gannoun H, Cayol J-L, Hedi A, Sakamoto M, Falsen E, Ohkuma M, Hamdi M, Fauque G, Ollivier B, Fardeau M-L (2012). Macellibacteroides fermentans gen. nov., sp. nov., a member of the family Porphyromonadaceae isolated from an upflow anaerobic filter treating abattoir wastewaters. Int. J. Syst. Evol. Microbiol. 62, 2522–2527.

Janz DM, DeForest DK, Brooks (2010). Selenium Toxicity to Aquatic Organisms, in: Chapman, P.M., Adams, W.J., Brookes, M.L., Delos, C.G., Luoma, S.N., Maher, W.A., Ohlenforf, H.M., Presser, T.S., Shaw, D.P. (Eds.), Ecological Assessment of Selenium in the Aquatic Environment. Society of Environmental Toxicology and Chemistry, pp. 141–231.

Lussier C, Veiga V, Baldwin S (2003). The geochemistry of selenium associated with coal waste in the Elk Valley, Canada. Environ geology; 44; 905-913.

Morita M, Uemoto H, Watanabe A (2007. Reduction of selenium oxyanions in wastewater using two bacterial strains. Eng. Life Sci. 7, 235–240.

Pearce CI, Patrick RA, Law N, Charnock JM, Coker VS, Fellowes JW, Oremland RS, Lloyd JR (2009). Investigating different mechanisms for biogenic selenite transformations: *Geobacter sulfurreducens*, *Shewanella oneidensis* and *Veillonella atypical*. Environ Technol 30: 1313-1326.

Sabaty M, Avazeri C, Pignol D, Vermeglio, A (2001). Characterization of the reduction of selenate and Tellurite by nitrate reductases. Applied Microbioloby 67 (11) 5122-5126.

Stams AJM, Grolle KCF, Frijters CTM Van Lier JB (1992). Enrichment of thermophilic propionate-oxidizing bacteria in syntrophy with Methanobacterium thermoautotrophicum or methanobacterium thermoformicium. Appl. Environ. Microbiol. 58 (1), 346-352.

Steinberg NA, Blum JS, Hochstein L, Oremland RS (1992). Nitrate is a preferred electron acceptor for growth of freshwater selenate-respiring bacteria. Appl. Environ Microbiol 58, 426-428.

Subedi G, Taylor J, Hatam I, Baldwin SA (2017). Simultaneous selenate reduction and denitrification by a consortium of enriched mine site bacteria. Chemosphere 183, 536–545.

Tan CL, Nancharaiah YV, van Hullebusch ED, Lens PNL (2016). Selenium: environmental significance, pollution, and biological treatment technologies. Biotechnology Adv. 34; 886 – 907.

5

ELECTROCHEMICAL TREATMENT OPTIONS

Continuous electrocoagulation process for treatment of mining waters

Maria A. Mamelkina[1], Salvador Cotillas[2], Engracia Lacasa[2], Ritva Tuunila[1], Mika Sillänpää[1,4], Antti Häkkinen[1], Manuel A. Rodrigo[3]

[1] LUT School of Engineering Science, Lappeenranta University of Technology, P.O.Box 20
FI-53851, Lappeenranta, Finland

[2] Chemical Engineering Department, School of Indutrial Engineering University of Castilla-La Mancha.
Campus Universitario s/n, 02071 Albacete, Spain

[3] Chemical Engineering Department, Faculty of Chemical Sciences and Technologies, University of Castilla-La Mancha, Edificio Enrique Costa Novella. Campus Universitario s/n, 13005 Ciudad Real, Spain

[4] Florida International University, Department of Civil and Environmental Engineering

Abstract

This research is intendent to study the removal of sulfate and other anionic contaminants using continuous electrocoagulation (EC) with iron electrodes. Performances comparison of continuous EC with batch EC and conventional chemical coagulation was performed. Application of the continuous electrocoagulation process with a settler for solid accumulation resulted in a higher sulfate removal and almost complete nitrate elimination. Together with anionic contaminants removal, continuous electrocoagulation was found to be efficient in the depletion of NH^{4+}, Cu^{2+}, Ni2+ and Zn^{2+}. In addition, changes in pH were much lower than those observed in a batch mode.

Keywords: sulfate, continuous elelctrocoagulation, mining water, wastewater treatment

Introduction

Electrocoagulation is gaining recognition as an effective water treatment technique due to its successful application to remove metals, dyes, oil, suspended solids as well as anionic contaminants. When considering the comparison of electrocoagulation (EC) and chemical coagulation (CC), process performances are not always the same. The reasons for that can be the difference in their dosing methods, excess amount of OH- in the solution during EC and presence of negative counter ions during CC (Canizares 2009); (Harif 2012). Thus, during EC the coagulant is added to the system by electrolytic oxidation of an appropriate anode material when in CC a chemical coagulant is dissolved into solution. These different methods affect greatly the coagulation/flocculation mechanisms and the following floc formation resulting in possible difference in the removal mechanisms of the selected contaminants. Presence of counter ions may influence the formation of hydrolyzed species while excess amount of OH- will result in different pH conditions during EC and CC causing different coagulation mechanisms (Canizares 2009); (Demirbas 2017); (Harif 2012).

Meanwhile, EC operating modes has a great influence on the process performance. Batch EC process is always accompanied by an increasing pH up to the range of 8-10, when continuous EC has slight difference of initial and final pH making operation at the acidic conditions possible. Additionally, energy consumption of a continuous process is relatively low comparing to the batch process for the removal of the same amount of the contaminants. Moreover, operation at continuous mode allows treating of a larger volume of water and possible solid recirculation minimizing the formation of wastes.

Currently, great attention is given to EC as a possible method to treat mining waters. Mining waters are known to have sulfate concentration from hundreds to tens of thousands mg/L, containing nitrate, cyanide, ammonia and different metals. High sulfate concentration may lead to environmental issues such as excess water mineralization, soil and water acidification. Sulfate is toxic to aquatic environment and may be responsible for aggressiveness of water to concrete. Taking everything mentioned into account, high concentration of sulfate in mining water streams is one of the major environmental issues in many countries. Coming regulations and established limits made mining industry find and develop suitable and feasible sulfate treatment technologies.

Until recent years, relatively few papers have been devoted to the removal of sulfate by electrocoagulation. Drouiche (2007) reported on effective application of EC to decrease the sulfate concentration from 241.50 mg/L to 42 mg/L while performing tests with chemical mechanical polishing wastewaters. Murugananthan (2004) have studied the removal of sulfide, sulfate and sulfite from tannery wastewaters by electrocoagulation. The studied concentrations varied from 100 mg/L to 500 mg/L for all three components, and the removal efficiency for the sulfate of 500 mg/L was around 25%. Del Ángel (2014) have conducted electrocoagulation experiments by using aluminum electrodes, and achieved 53 % of sulfate removal from the drainage at an abandoned mine in Guanajuato, Mexico. Radić (2014) reported on over 86% removal efficiency of sulfate with combined CaO/electrocoagulation treatment. Nariyan (2017) affirmed 40.5 % of sulfate removal from mining waters using Al electrodes. However, information about the remediation of sulfate from mining water by electrocoagulation is rather scarce and studies on the continuous electrochemical removal of sulfate are non-existent.

To fill the gap the research on the performance evaluation of batch and continuous EC process for the removal of sulfate from mining waters was studied. Additionally, EC results were compared with those obtained during the chemical coagulation. This paper is dedicated to process performances, removal mechanisms and possible operation conditions for sulfate removal by CC and EC.

Methods

Electrocoagulation tests were performed in batch and continuous modes (Fig. 1). Batch EC tests were carried out in a lab scale plant described elsewhere (Lacasa 2011). During the continuous EC, the same plant with necessary modifications was used. Detailed setup and explanations are provided in (Mamelkina 2017). Iron electrodes connected in a monopolar arrangement were placed in between of two plastic plates (Lacasa 2011) The dimensions of electrodes with internal deployment were 100×100×2 mm (resulting in total anode area of 168 cm2). The current density used during the batch experiments was equal to 30 mA/cm2 and treatment time was 8 h. Continuous EC experiments were performed at 12.4 A h/dm^3. A proper mixing of treated water was provided by using a square blade impeller at a speed of 160 rpm (tip speed of 0.84 m/s) and by water circulation using a peristaltic pump at a speed of 90 ml/min.

Synthetic mining waters were prepared based on the average values provided by several Nordic mines. Treated eluent contained sulfate, nitrate, chloride, Cu, Zn and Ni. Levels of each contaminant can be found in the Table1. Treated water was used during the experiments with no conductivity adjustments. Solution pH was adjusted by 0.1 M NaOH and HCl. Metal contents were analyzed with an inductively coupled plasma spectrometer (Liberty Sequential, Varian). Anions concentrations were measured using ion chromatography with a Metrohm 930 Compact IC Flex coupled to a conductivity detector.

***Figure 1** Set-up for a continuous electrocoagulation*

Results and Discussion

Prior the electrochemical experiments chemical treatment was performed to find the most suitable range for EC process operation. Chemical coagulation was carried out with the synthetic solution at different pHs and iron coagulant doses. The maximum sulfate removal of 80% was achieved at pH 2 for iron dosage at the range 0.017-0.090 mol/dm. At neutral and alkaline conditions the increase in sulfate removal was observed with the increase in dose of iron coagulant and was as high as 60% at 0.537 mol/dm of iron. Taking into account the highest possible removal of sulfate and lowest possible amount of the coagulant used for elimination, EC operation at acidic conditions was suggested. Possible removal mechanism at acidic conditions during CC may be favored by sulfate precipitation with added iron not excluding other coagulation mechanisms. However, the detailed explanation of the sulfate removal mechanisms during CC is out of the scope of the paper and can be found elsewhere (Mamelkina 2017).

The current density for EC tests was selected based on the production of a specific iron concentration in the liquid face by the electrodissolution of the anode, i.e. a value that allow to generate at least 0.1 mol/dm3 of iron. Batch and continuous EC experiments were performed at pH 2, 5 and 7.

For batch EC, the maximum sulfate removal from synthetic mining waters was achieved at initial pH 2 and was as high as 20%. Comparing to the results obtained with CC, the significant decrease in the removal of sulfate at initial pH 2 can be explained by the pH increase to the vicinity of 10 during the first hour of treatment. Slight sulfate removal 10% was observed at pH 5, in this case the pH 10 conditions were reached even faster. At pH 7 the EC process was inefficient in terms of sulfate removal. A summary of sulfate treatment efficiencies for different processes and operation modes is given in the Table 1.

From the Table 1 it can be seen that removal of sulfate improved during the continuous EC treatment. One of the reasons for such a behavior is the possibility to maintain the pH almost constant without dropping from acidic to base conditions as it occurred during the batch EC. Among other parameters, affecting the sulfate removal is a dose of added iron that promotes the enmeshment of sulfate into iron hydroxide precipitates. To ensure the desired amount of solids added to the system a novel EC strategy was proposed. This was achieved through connecting a sedimentation tank to the EC cell, promoting the flocculation process. This modified electrocoagulation process was based on the coagulation processes typically applied in the treatment of surface water, in which the flocculation enhancement by concentration of coagulants is known to increase the efficiency of the technology.

The results obtained during the continuous treatment of mining waters at pHs 2,5 and 7 are shown in Fig. 2. In agreement with CC treatment the highest removal efficiency of over 60% was achieved at pH 2, illustrating the pivotal role of pH during the process. Accumulation and circulation of solids allowed providing higher solid concentrations ranging from 1.1 to 1.4 mol/dm3 that favored the enmeshment. Changes in pH profiles were not critical and very much lower then those during the batch EC, making the operation at acidic conditions possible even during the EC.

***Table 1** Removal of selected ions with chemical coagulation (CC), batch and continuous electrocoagulation (EC)*

	Mining ww, mg/L	R%, CC	R%, batch EC	R%, continuous EC
SO_4^{2-}	3000	80.0	23.0	63.0
NO_3^-	60	10.0	99.9	99.9
NH_4^+	30	68.0	99.9	99.9
Cu^{2+}	8	5.0	99.9	99.9
Ni^{2+}	8	64.0	99.9	99.9
Zn^{2+}	15	56.0	99.9	99.9

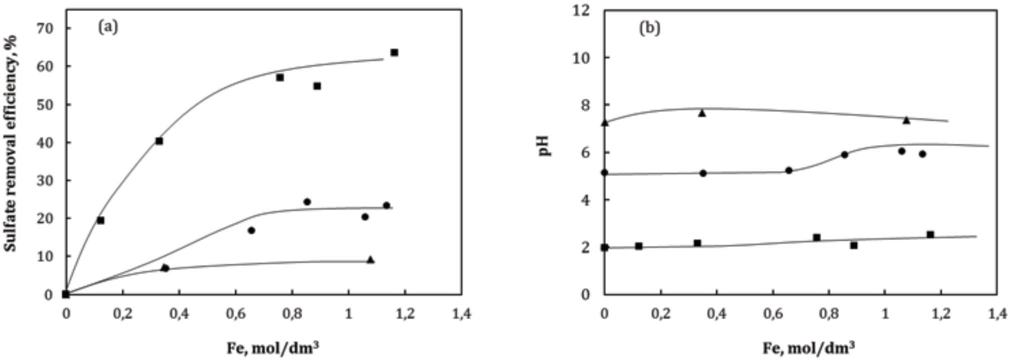

Figure 2 *Continuous EC treatment of mining waters*
a. sulfate *removal efficiency at ■ pH2, ● pH5, ▲ pH7 b. changes in pH*

Conclusion

New design of the EC process resulted in a better sulfate removal then during chemical coagulation and discontinuous EC treatment at the same dosage of iron. Changes in pH were not critical favoring higher sulfate removals obtained with the modified process. Differences in the performance of batch and continuous EC were due to the pH and iron dosing conditions. Continuous EC was found to be efficient because in addition to the elimination of sulfate, it also removed nitrate and selected cations. Moreover, opposite to chemical coagulation, chloride concentration was maintained almost constant, producing an effluent with a higher quality. Continuous operation provides the treatment possibility of sulfur-rich streams of a large volume. Solids recycling allows treatment of process mining water minimizing secondary pollution. Simultaneous removal of anionic and cationic contaminants by EC favours its application as one of the main technique at wastewater treatment plants.

Acknowledgements

This work was conducted as a part of Water Conscious Mining (WASCIOUS) project funded by the NordMin – A Nordic Network of Expertise for a Sustainable Mining and Mineral Industry. The authors acknowledge funding support from the Spanish Ministry of Economy, Industry and Competitiveness as well as European Union through the projects CTM2016-76197-R and FEDER 2007-2013 PP201010 (Planta Piloto de Estación de Regeneración de Aguas Depuradas) is gratefully acknowledged.

References

Cañizares P, Jiménez C, Martínez F, Rodrigo MA, Sáez C (2009) The pH as a key parameter in the choice between coagulation and electrocoagulation for the treatment of wastewaters. J Hazard Mater 163(1): 158-164

Del Ángel P, Carreño G, Nava JL, Martínez MT, Ortiz J (2014) Removal of arsenic and sulfates from an abandoned mine drainage by electrocoagulation. Influence of hydrodynamic and current density. Int J Electrocem Sci 9(2): 710-719

Demirbas E, Kobya M (2017) Operating cost and treatment of metalworking fluid wastewater by chemical coagulation and electrocoagulation processes. Process Saf Environ Prot 105: 79-90

Drouiche N, Ghaffour N, Lounici H, Mameri M (2007) Electrocoagulation of chemical mechanical polishing wastewater. Desalination 214(1–3): 31-37

Harif T, Khai M, Adin A (2012) Electrocoagulation versus chemical coagulation: Coagulation/flocculation mechanisms and resulting floc characteristics. Water Res 46(10): 3177-3188

Lacasa E, Cañizares P, Sáez C, Fernández FJ, Rodrigo MA (2011) Electrochemical phosphates removal using iron and aluminium electrodes. Chem Eng J 172(1): 137-143

Mamelkina MA, Cotillas S, Lacasa E, Sáez C, Tuunila R, Sillanpää M, Häkkinen A, Rodrigo MA (2017) Removal of sulfate from mining waters by electrocoagulation. Sep Purif Technol 182: 87-93

Muruganánthan M, Raju GB, Prabhakar S (2004) Removal of sulfide, sulfate and sulfite ions by electro coagulation. J Hazard Mater 109(1–3): 37-44

Nariyan E, Sillanpää M, Wolkersdorfer C (2017) Electrocoagulation treatment of mine water from the deepest working European metal mine – Performance, isotherm and kinetic studies. Sep Pur Technol 177: 363-373

Radić S, Vujčić V, Cvetković Ž, Cvjetko P, Oreščanin V (2014) The efficiency of combined CaO/electrochemical treatment in removal of acid mine drainage induced toxicity and genotoxicity. Sci Total Environ 466–467(0): 84-89

6

ACCEPTABILITY OF PROCESSED MINE WATER

Producing High Quality Drinking Water From Mine Imapcted Water At High Recoveries Using Reverse Osmosis Membranes

Andrew Hammond[1]

[1]*Aveng Water, 1 Jurgens Road, Jet Park, Aveng Park, Gauteng, 1459, South Africa, Tel: +27 10 205 1800*
Andrew.hammond@avenggroup.com

Abstract

Three Aveng Water designed HiPRO™ plants have been operating for a number of years. Each of these plants produce a product water that complies with the South African standards for drinking water (SANS241), two of which are currently supplying drinking water to the community. Key to producing this quality of water is the use of Reverse Osmosis Membranes. Management of these membranes is essential to maintaining consistent and reliable supply of water from the plant. The RO membranes on these plants are sensitive to inorganic scaling and biological/organic fouling due to the process and the feed water being reclaimed. The performance of these membranes is shown. The annual Salt Passage increase on the RO membranes is higher than the initial design but still within acceptable limits for potable water. A highly technical team is required to sustainably operate a plant of this nature.

Keywords: ICARD | IMWA | HiPRO™ | RO Membranes | Mine Water Treatment

Introduction

Water scarcity in South Africa and much of the world is becoming more pervasive. With a deficit in supply and demand of conventional sources, it is going to become paramount that alternate water sources are investigated as a way to augment the supply. It is estimated that there will be a shortfall of 83.3 Ml/day in the region around eMalahleni Mpumulang by 2030 (Coleman et al., 2011). Mine water reclamation presents one such augmentation strategy. It has estimated that mining activities in the upper Oliphants catchment area has created a need to treat between 200 and 250 Ml/day of Mine Impacted Water. These waters are complex and characterised by high levels of sulphate and a combination of balancing ions (Calcium, Magnesium, Acidity and monovalents) in various proportions, depending on the source. The resulting waters require rigorous treatment to remedy. One such active treatment process that can be used to remedy the mine impacted waters and produce potable water is Aveng Waters HiPRO™ process. This process combines chemical precipitation with advanced membrane processes allowing for large scale treatment of mine impacted waters. Currently four major installations use this technology and were all funded and owned by the senior coal miners in the Mpumalanga province. The four plants are the eMalahleni Water Reclamation Plant (EWRP) – (Phase 1 and Phase II), The Optimum Water Reclamation Plant (OWRP) and the Middleburg Water Reclamation Plant (MWRP). These four plants each are able to produce a product that complies with the regulatory requirements as specified by SANS241. Currently OWRP and EWRP produce water for the surrounding community.

Feed Water Quality

Table 1 summarises the design capacity of each plant, the year of commissioning, the plant owner, the plant designer and the typical feed water quality (major components only) currently being processed by the plant. It can be seen that the feed water quality differs between plants.

HiPRO™ Process

A detailed explanation of the process can be found Hutton et al (2009) so it will not be covered here, however Figure 1 shows the basic block flow diagram of the process.

The RO sections of the plant are the last

Table 1: *Summary of Major Aspects of the plant installations*

	EWRP Phase I	OWRP	MWRP
Plant Owner	Anglo American Thermal Coal	Optimum Colliery	South 32
Plant Designer	Aveng Water	Aveng Water	Aveng Water
Year Commissioned	2008	2011	2015
Design Capacity	25 Ml/day	15 Ml/day	25 Ml/day
Feed Water -Typical			
Calcium (mg/L)	520	414	460
Sulphate (mg/L)	2500	3000	3400
Magnesium (mg/L)	180	450	650
Sodium	130	160	60
Acidity (mg/L as CC)	80	0	0
Alkalinity (mg/L as CC)	10	180	180
pH	6	8.0	7.5
TDS (mg/L)	3500	5021.6	5000

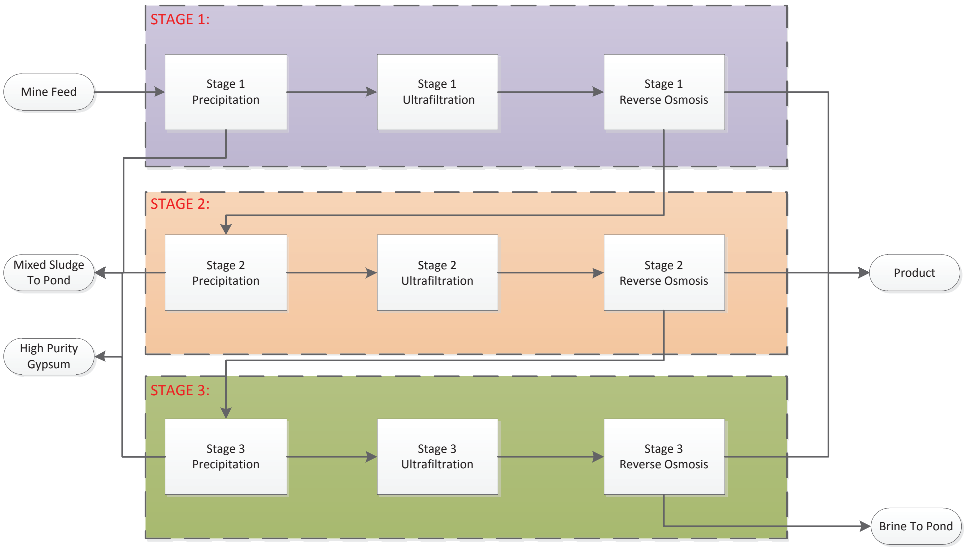

Figure 1: *Basic Process Flow of HiPRO™*

step in each stage of the process. Once an ultralow suspended solids water is produced from the UF membranes, the RO membranes desalinate the water and produce a low TDS product and a moderately high TDS brine. The brine from the RO then proceeds to the precipitation reactors. In these reactors, the salinity is reduced through chemical precipitation. Due the nature of the feed water, the main aim of the reactors is the sequential removal of sulphate from the feed. The effect of the inter-stage precipitation on the removal of sulphate is pronounced and can be seen in Figure 2.

When looking at the typical concentrations of sulphate through the plants (Figure 2) of EWRP Phase I, OWRP and MWRP, it can be clearly seen how efficient the precipitation steps are at removing sulphate. The Stage 2 precipitation removes the largest mass of sulphate relative to the feed (~70%) and the Stage 3 precipitation removes ~12.5% relative to the feed. The monovalents present in the feed water that cannot be precipitated

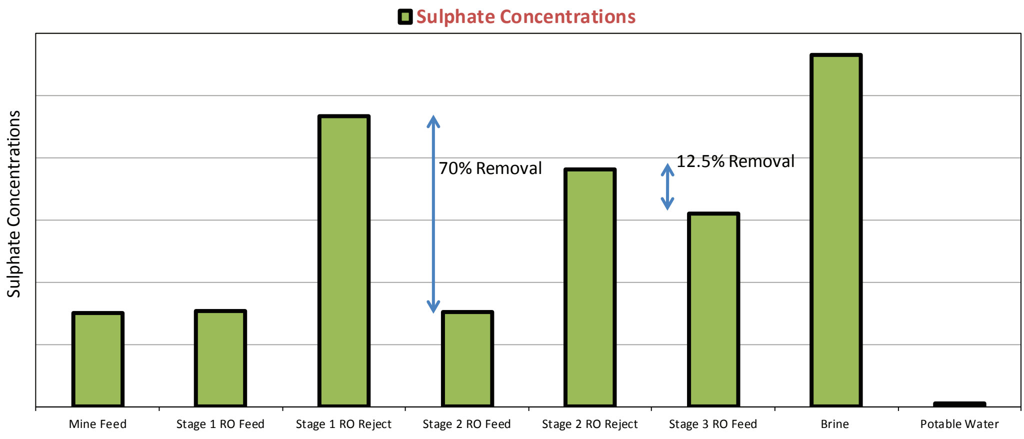

***Figure 2:** Effect of Inter-stage Precipitation on sulphate on OWRP*

are either permeated via the RO membranes or concentrated through the plant and discharged as a high salinity final reject stream. The secondary benefit of the staged precipitation is the recovery of water while minimising the required electrical power. The combination of targets to save energy on one hand and provide a well-controlled water quality on the other has been reached by employing this staged precipitation and high-rejection low energy RO elements. The average plant power consumption per m^3 of product ranges between 1.8 and 2.0 kWh/m3 while achieving water recoveries between 97% and 99% (water quality dependent).

Sustainable RO Operation

As with any membrane installation, the control and measurement of the feed water quality is paramount in maintaining sustainable operation. In these particular waters, this can be broadly be broken into control of the scaling potential and control of fouling.

Scaling Control

Antiscalant dosing and control is of essential importance in controlling scale formation within each stage of the process. Preventing the formation of calcium sulphate crystal formation on the membrane surface, key water quality parameters are measured a minimum

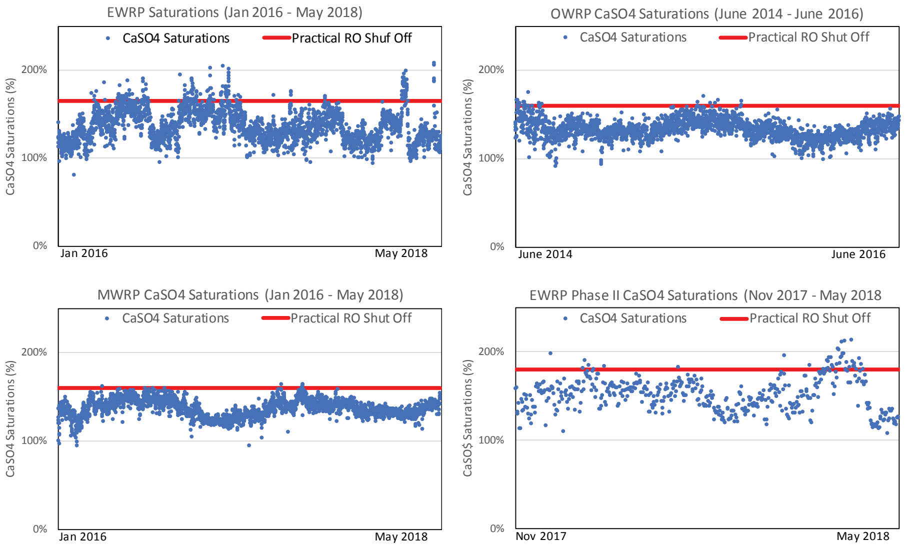
EWRP Saturations (Jan 2016 - May 2018)

OWRP CaSO4 Saturations (June 2014 - June 2016)

MWRP CaSO4 Saturations (Jan 2016 - May 2018)

EWRP Phase II CaSO4 Saturations (Nov 2017 - May 2018)

***Figure 3:** Scaling Potential at the various plants*

four times daily to ensure the scaling potential of the water is known at all time. Understanding the practical limitations of the antiscalant in terms of the water quality being processed and the RO unit configuration governs the practical RO recovery that can be managed in these complex scaling waters. The scaling potential is reduced by the precipitation reactors on each stage. Figure 3 shows the scaling potential as measured by the calcium sulphate saturations.

The horizontal lines indicate the practical maximum RO recovery that can be operated until scaling begins to occur. Should these boundaries be exceeded, rapid irreversible and severe scaling can results. However, the closer one operates to the maximum RO recovery, the greater instantaneous production that one can achieve from a given plant. It is apparent to see that the greater the standard deviation of the scaling potential, the greater the risk of scaling incidents. The precipitation steps in the process are able to reduce the scaling potential of the reject by between 3-5 times depending on the plant feed water quality. The impact of poor control of scaling potential is on the second bank of RO membranes installed. An increase in the DP without an increase in temperature indicates scaling. Figure 4 below shows the differential pressure increase on Bank 2 of one of the Stage 2 RO units at OWRP since the membranes were installed and the associated scaling potential of the water. The data has not been normalised. What one can see is that the rise in the DP is faster at the beginning period of the operation when there is greater variability of saturation data.

Fouling Control

Ultrafiltration membranes are utilised as a pre-treatment to the RO membranes. The selection of these membranes over conventional pre-filtration was due to the ability to process water of a high scaling potential and produce a filtrate that has very low suspended solids. Typically, the water that is produced from the UF membranes will have an SDI of below 3 and more generally below 2. It has been observed that the SDI will drift towards the 3 value as the membranes age. In general, a five year life can be obtained from the UF membranes in all of the installations. However, this is a function of the feed water being process and it UF fouling potential. However, if one looks at TOC profile within the plants, one can see that there in an increase through the plant. This is shown for OWRP graphically in the figure below. This increase can be observed through all the installations but the extent of the increase varies across the plants.

The implication of the increasing TOC through the plant is an increase in the fouling potential due to accelerated bacterial growth rates (as measured by change in weekly plate counts) and increased risk of organic fouling. What has in fact been observed is that higher fouling rates through Stage 3 are observed at MWRP and OWRP when one compares the cleaning frequency of Stage 1 and Stage 3 RO operation. However, this is not observed at EWRP where the reverse trend is observed.

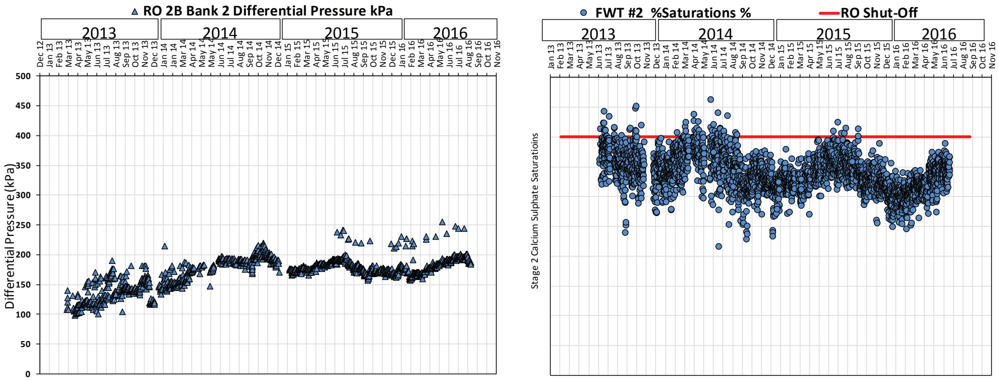

Figure 4: Demonstration of effect of Scaling Potential on Bank 2 DP Increase

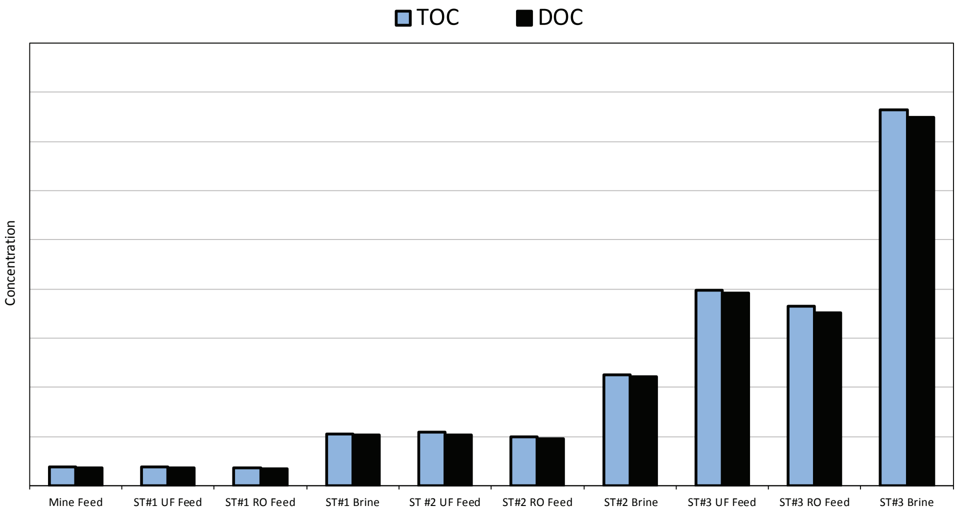

Figure 5: *TOC and DOC from feed to brine at OWRP. Similar trend observed on all installations*

This implies other factors besides just the levels of TOC are important when it comes to predicting fouling rate. It must be noted that the cleaning frequency is severe across all installations and is higher than what is expected through the industry for brackish water membranes. The current observed average cleaning frequency of the membranes across each plant is between 4 days and 14 days depending on the process Stage in operation and the time of year. The operational control of fouling on the plants is not elegant and combines a series of offline interventions (biocide, manual cleaning) done periodically to manage the situation. Further work is underway to better find better mitigation measures.

Salt Passage Increase

During the design phase of the plant, the default salt passage increase of the membrane supplier is used to determine the RO vectors within the plant. This results in an expected salt passage increase of 15% per year. However, the actual salt passage increase is substantially higher. What has been observed is that there is a much higher increase in the salt passage increase in the first few years of operation after which the salt passage increase flattens out. This can be seen in the figures below. Figure 6 shows the salt passage increase of a Stage 1 RO skid at OWRP from the first three years of operation and a second RO skid being the last three years of operation. For the new skid, the first years operation there was the greatest increase in permeate conductivity at 109% with this deterioration decreasing in years 2 and 3 from 89% and 59% respectively. This is compared to that of the skid of the last three years of operation where the last three years of salt passage increase can be seen at 4.27%. If one looks at a Stage 1 RO unit at MWRP (Figure 7) from new, the permeate conductivity increase over the first three years of operations is still higher than the design at 100% for the first year but only 2% in the second year and 23% after year three. It remains to be seen if MWRP Stage 1 RO skid will exhibit the same trends as the OWRP skid as the membranes age. However, even with this higher than expected salt passage increase, the product water produced from the RO skids is still well within the specification for SANS241. Showing that sustainable operation can be realised.

Figure 6 (Right) indicates that baring mechanical damage or scaling, there is a high deterioration of the permeate quality produced from the RO membranes in the early years of operation until it reaches a high point after which it flattens out. What is also interesting to note from the trends in Figure 6 is that the impact of temperature on the permeate quality is more pronounced as the

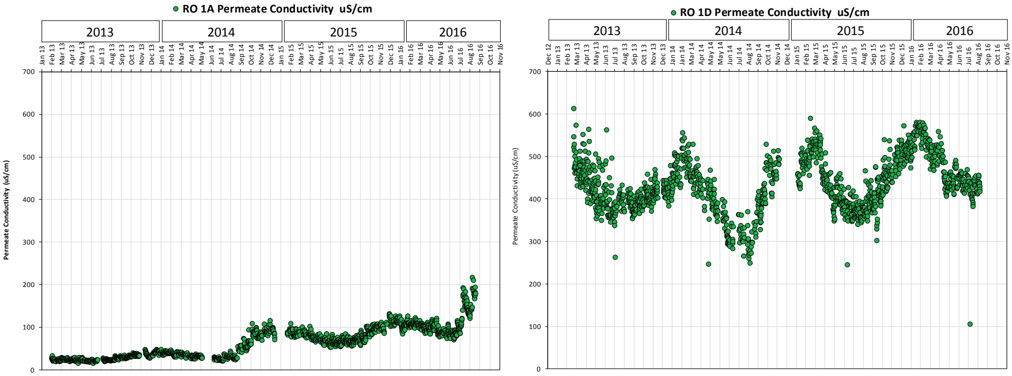

Figure 6: *Permeate Conductivity increase of New Membranes (left) and Old Membranes (right) at OWRP*

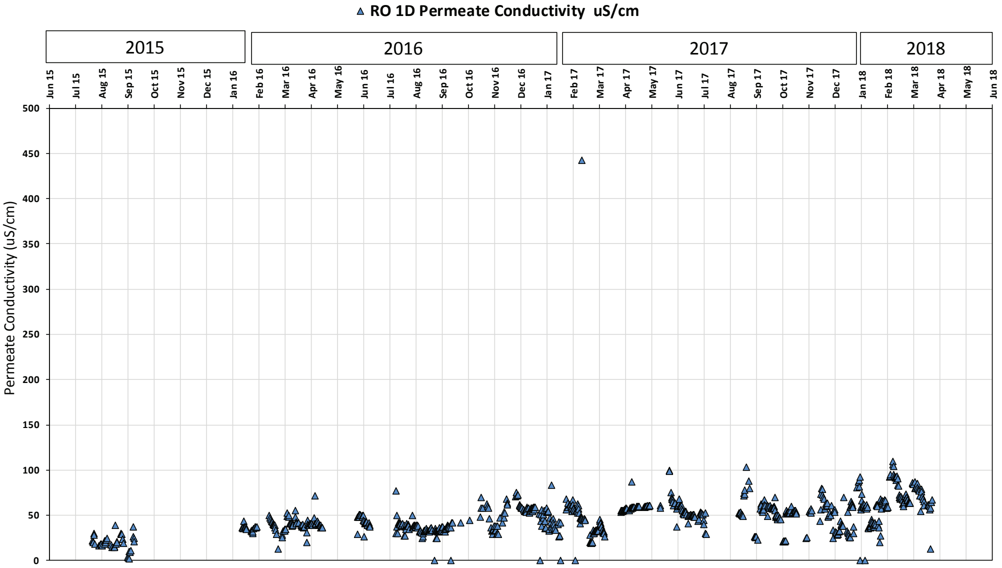

Figure 7: *Permeate conductivity increase of New Membranes at MWRP of New Membranes - Stage 1 RO Skid*

membrane ages. This can even be seen in the new membrane case, where in the first year, the difference between the permeate quality in the low temperature is not too dissimilar to the high temperature case but the cyclical variance becomes more pronounced in year 2 and year 3. The cyclical component on the older membranes is apparent. This is not only observed on the skids presented but on a number of skids of different ages within OWRP and EWRP but is not obviously seen at MWRP. The increased salt passage variability observed is due to the higher basic salt passage coefficient of the aged membrane, on which temperature acts as a multiplier.

Operations

The control of the upstream pre-treatment and the RO membranes requires careful management. Loss of control of any aspect of the plant will have a direct impact on the quality and quantity that can be produced from the plant. As a result, utilisation of this type of plant for the augmentation of water supply to the community will require a highly skilled team. In addition, continuous monitoring of the quality of the plant as well as the various process units require sophisticated control narratives and automation. Lastly, the operations team will need to be well versed in the operation of membranes specifically in terms of when it is required to take offline to clean as well as what cleaning recipes to use. These recipes fluctuate as the risk of both biological and inorganic foulants within the membrane are both present within these installations.

Conclusion

It has been shown that RO membranes can be used to produce a product water that complies with the required legislative parameters. This can be seen by the sustainable operation of three plants, each running for more than three years. The key to producing acceptable quality water is the use of RO membranes to desalinate the feed water. Sequential precipitation minimises scaling potential and energy costs associated with operations of the membranes and allows for high plant recoveries. Management of the scaling potential of the feed water with respect to Calcium Sulphate precipitation is paramount for sustained RO operation, failure of which will cause either a loss of membrane area or a loss of production. In addition to scaling, the levels of TOC increase substantially through the plants. This increases the risk of organic and biological fouling of the RO membranes. Salt passage increases of the ROs on these plants exceed the initial design expectation by a substantial factor. However, it is viewed that the initial sharp decline in permeate quality stabilises as the membranes age but there is an increased sensitivity of the permeate conductivity to temperature. The product water quality is still within the tolerances allowed for drinking water despite these challenges. The plants are operationally complex and require highly skilled staff to manage the various aspects of the membrane operation. The HiPRO™ plants that have been in operation for a number of years and all comply with the SANS241 specifications. Two of which are currently servicing the community for potable water showing that mine impacted water can sustainably be used to augment existing drinking water supplies.

References

Hutton B, Kahan I, Naidu T, Gunther P, (2009) Operating and Maintenance experience at the eMalahleni Water Reclamation Plant. IMWA 2009.

Coleman T.J., Usher B, Vermeulen D, Lorentz S, Scholtz N. Prediction of how different management options will affect drainage water quality and quantity in the Mpumalanga coal mines up to 2080. WRC Research Report No. 1628/1/11 , 2011

Achieving Sustainable Mine Closure Through the Use of Mine Water

Carla Hudson

NEPAD Business Foundation. P.O. Box 784144, Sandton, 2146

Abstract

Effective regional management is important in addressing the long-term effects of mine affected water, including acid rock drainage, acid mine drainage and saline drainage.

The Mine Water Coordinating Body (MWCB) has been established as a public-private platform for the mining industry and government to work together in identifying and implementing management options for water and closure for Mpumalanga Coalfields in South Africa. To date, the MWCB has attracted AngloCoal, Eskom, Exxaro, Glencore, Sasol and South32 as private sector partners and is working closely with the Department of Sanitation (DWS) and Department of Mineral Resources (DMR) who are key government bodies governing the mining sector. The MWCB is also engaging with other government departments to attract additional public sector support for their projects and initiatives. Currently, the MWCB projects include the Mine Water for Irrigation Project, The Green Engine and the Regional Post-closure Economic Study for the Coalfields.

The *Mine Water for Irrigation* project is a research study to investigate the use of saline water that meets agricultural quality standards in irrigating saline resistance crops such as wheat and soya. The study will extend over a total of 60Ha of both rehabilitated pits and nearby unmined land. The study will take place over 5 years to assess the longer term impact of irrigation on the local groundwater quality.

The *Green Engine* is an exciting project that, if successful, will change the way mine closure is viewed. It is aimed at demonstrating the viability of an integrated land stewardship model where mine owned land, renewable energy and treated mined water will work together in an integrated system to develop various business opportunities that will benefit local communities.

Regional Post-closure Economic Study for the Coalfields. Before regional closure can be successfully planned and implemented it is important to first understand what the potential economic opportunities for the region exist.

This study will investigate these opportunities, research implementing partners as well as ensure that government planning at national, provincial and local levels is integrated in the closure planning process. The study will identify sustainable projects which will in turn guide mining organisations with their rehabilitation and water management planning.

Lonmin Integrated Water Resource Management System

JJ van der Walt, I Pollard, H van der Merwe
PO Box 29, The Innovation Hub, Pretoria, 0087
wmias.vanderwalt@bigengroup.com

F Botha
Fanie@waterhunters.co.za

C Klopper, M Maynard
PO Box X508, Marikana, 0284
Charl.Klopper@lonmin.com

Abstract

Since the early late 1990's water shortages experienced in the Rustenburg area sparked considerable focus by all water users to find sustainable water solutions. Lonmin's approach followed the best practice guideline route by first exploring Water Conservation and Demand Management (WCDM) opportunities before introducing additional water supply into the region. A systematic approach was followed where water quality and demand requirements for various mining processes were used to develop first a static water balance model and then later followed by a dynamic water balance model. The dynamic water balance model incorporated detailed information of all the water circuits on the Lonmin mining area with time dependent water quantity and quality data. Based on the outcome of the dynamic water balance model numerous current and future operational and development scenarios were explored and compared with the current water use as a base case.

The dynamic water balance formed the basis of the resource management system and was constructed in such a way that water sources and points of consumption could be added in conjunction with various WCDM. It was shown that significant water use improvements were possible through the implementation of various WCDM strategies and that the incidental environmental overflows and the water purchases from external services providers could be reduced by as much as 46%.

This paper will demonstrate how the development of the integrated dynamic water balance was used to accurately model the *status quo* of the Lonmin network and establish the interventions required to achieve the significant improvements in water use efficiency and achieve Lonmin's key strategic objectives.

Keywords: Water use, water reuse, water conservation, mine water, integrated water resource

Introduction

During the late 1990's a number of water augmentation projects were developed and implemented to satisfy the increased demand for water to the growing platinum mining industry and the associated domestic water demand created by the influx of people into the area. At a very early stage it was realised that the water shortage cannot be addressed by individual mines, but that a collective effort will have to be made to address the water shortages in a coordinated manner. Municipalities, established a PPP to address some of the urgent water and sanitation issues. The mining industry also took hands and jointly sponsored a study exploring regional solutions to the water supply problems. This led to the establishment of the Western Limb Water Forum where planning of future water systems were coordinated between stakeholders. One action plan that was identified from these collaborations between the mines and stakeholders was the accelerated implementation of water conservation and demand management (WCDM).

The Lonmin water system spans a distance of about 30 km delivering water to and from numerous mines, concentrators, storage dams and pipelines. Not only does Lonmin supply and distribute water for their own needs, but Lonmin also act as a Water Services Intermediary by distributing water to surrounding communities. The burden to comply in all respects to the relevant legislation is significant and further complicated by the vast area covered by the Lonmin operation and complexity of the water systems. A primary aim of the project was to improve the legal compliance by implementing the basic principles contained in GN704 and the best practise guidelines and to improve overall water security.

Lonmin at the time took the lead in their approach by following best practise guidelines in exploring WCDM opportunities before introducing additional supply into the region. In 2012 Lonmin commenced with the development of a dynamic water balance and also exploratory drilling to establish the potential of local anthropogenic aquifers. This culminated in a detailed dynamic water balance indicating significant WCDM opportunities. The agreed strategic objectives of this WCDM programme was to ensure sustainable supply of water, strive toward sustainable water use, improve compliance and be a good neighbour. The WCDM results informed the development of the Lonmin integrated water resource management system.

Methodology

Overall WCDM development process

The development of the dynamic water balance model (DWBM) involved a number of clearly defined steps including; the establishment of water demand for specific mining plans, the identification of water sources and the development of various WCDM strategies. The DWBM was developed for each of the three mining areas in the Lonmin operation and later integrated into an integrated DWBM including the Karee, Western and Eastern areas. The initial DWBM was developed for a base case representing the status quo at the time as closely as possible. The gradually implementation of various WCDM strategies led to a number of WCDM scenarios. From these scenarios various WCDM projects were identified, scoped at a conceptual design level and prioritised based on return on investment and the strategic objectives of the WCDM programme.

Water demand assessment

The water demand projections, derived from the production projections formed the basis of the water DWBM. The mining production figures and the unit water consumption figures were used for each of the mining areas. The split between the water quality types required was estimated after the total water was determined. The split was determined from historical metering exercises and where metered information was not available informed estimates were made. After translating the mining production figures into water use figures a calibration was done using current mining and water use figures. There was general agreement between the figures apart from a few minor anomalies.

After defining the base case a number of scenarios were developed to assess the impact of various WCDM strategies. A unique water demand input set was developed for each model scenario based on different levels of internal recycle and grey water use. This resulted in a much reduced external top-up requirement from Rand Water. It was shown that a significant amount of potable water demand circuits could be substituted with grey water. Potable water circuits that were not changed to consume grey water are offices, ablution facilities and underground drinking water. The water circuits that were switched to grey water circuits included; gland service water, fire water, washwater, cooling water top-up, grout plant, workshop (washing),

Water sources

The Lonmin mining operation has evolved over time and has as a result sourced water from a number of different locations. Traditionally four sources have been recognised, but two additional sources have recently been quantified to be a significant local resource, i.e. anthropogenic aquifers and local water reuse. The key conventional water resources included Rand Water via the Barnardsvlei reservoir (~ 33 Ml/d), Buffelspoort irrigation canal (~2.5 Ml/d), Hartbeespoort canal in the Eatern area (~1 Ml/d) and Brits WwTW (~ 6.5 Ml/d). Each of these sources have their unique water quality and supply challenges. The more unconventional water sources included the potential yield from anthropogenic aquifers that have for many years been vastly underestimated (often accounted for as fissure or sub-surface environmental discharge). About 30 anthropogenic aquifer boreholes were identified with a potential yield of 12 Ml/d. The other unconventional source included the use of local water for reuse in a number of process that in the past used potable water.

WCDM strategies

The generally accepted principles of WCDM include: avoid, reduce, reuse, recycle and dispose. Lonmin interpreted and contextualised these principles and developed their own unique set of strategies based on the challenges and constraints. These strategies included; reduce losses through seepage and overflows, separate water circuits, regional integration of water systems in Karee, Western and Eastern mining areas and treatment of available dirty water to a higher standard to improve water reuse.

In order to assess the potential impact of the each of the WCDM strategies various infrastructure upgrade scenarios were developed. These infrastructure scenarios were captured in the DWBM and the outcomes tested against pre-determined success criteria. An example of the intricacies included in the DWBM is shown in Figure 1.

WCDM scenarios

The DWBM encapsulated time dependent elements of stochastic rainfall, water sources (quantity and quality), water demands (quantity, quality and timing), infrastructure capacity (eg. pipeline, pump and storage capacity) and operational rules currently practised by Lonmin. Using the above data the DWBM was developed to assess the entire Lonmin hydrological cycle for a 10 year planning horizon. The Base Case model primarily improves the basic understanding of the water cycle and also enables Lonmin to identify WCDM opportunities. The following scenarios were incorporated into the dynamic water balance model:

- Reduce spillage by de-silting RWDs and increase balancing storage (Scenarios 1a);
- Reduce seepage from RWDs and PCDs (Scenario 1b)
- Transfer water from water surplus areas to water deficit areas (Scenario 2a);
- Utilise borehole water from rehabilitated

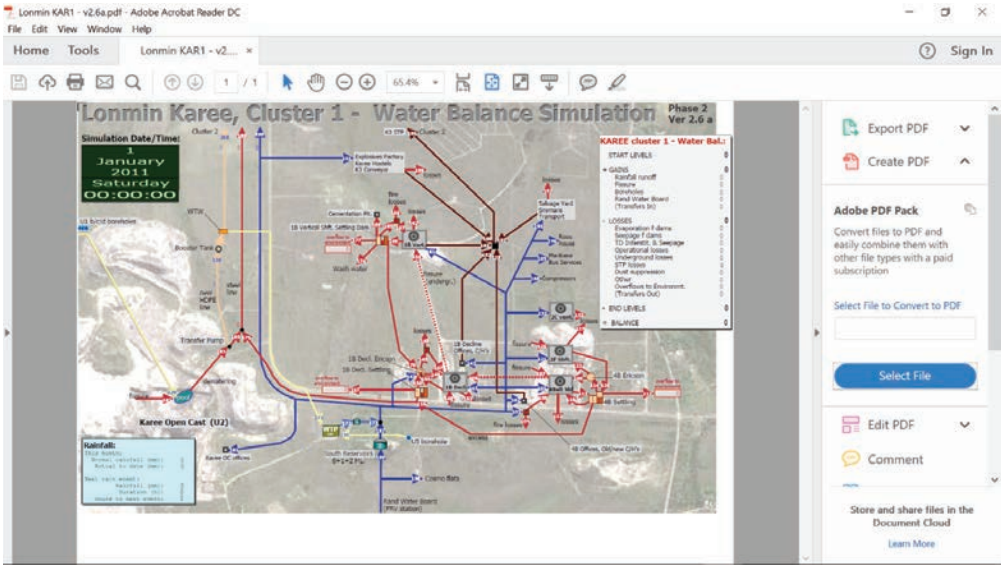

Lonmin Karee, Cluster 1 - Water Balance Simulation
Phase 2
Ver 2.6 a

Simulation Date/Time:
1
January
2011
Saturday
00:00:00

KAREE cluster 1 - Water Bal.:
START LEVELS 0
GAINS 0
Rainfall runoff
Fissure
Boreholes
Rand Water Board
(Transfers In)
LOSSES 0
Evaporation f dams
Seepage f dams
TD Interstit. & Seepage
Operational losses
Underground losses
STP losses
Dust suppression
Other
Overflows to Environmt.
(Transfers Out)
END LEVELS 0
BALANCE 0

Adobe PDF Pack

Convert files to PDF and easily combine them with other file types with a paid subscription

Select File to Convert to PDF

Store and share files in the Document Cloud

Figure 1 – Example of DWBM sub-areas water circuits

open cast areas for grey water (Scenario 2b);

- Import additional external grey water sources from Hartbeespoort Canal (Scenario 2c)
- Madibeng STW (Scenario 2d);
- Import from Buffelspoort canal and treat to potable standards (Scenario 3a);
- Import from Madibeng STW and treat to potable standards (Scenario 3b)

It became evident that no single scenario addressed all the success criteria determined earlier and that some of these scenarios may have to be implemented in a cumulative manner in order to achieve the strategic objectives. Based on the insight gained from scenarios 1 to 3, the following aspects were therefore added in the cumulative scenario:

- Buffelspoort water source was utilised for local potable water treatment
- Grey water use was enhanced through the development of selected open cast pit boreholes and grey water treatment facilities in the Eastern area.
- Replace potable water use at concentrator facilities with local grey water
- Complete development of the East to West transfer pipeline to address projected water shortages in the Karee area.
- Improvements to operational rules to prioritised grey water in areas where grey water can replace potable water use. Discharge surplus grey water into local storage for later use and to prevent Rand Water top-up with potable water.
- Lining of channels and dams to reduce losses.

The cumulative scenario demonstrated that a significant improvement can be realised in relation to the base case. It was evident as shown in **Table 1** that the Rand Water use could be reduced by a significant 4.2 million m3/a (~ 11.6 Ml/d) (a reduction of 46%). This was primarily as a result of the planned Buffelspoort WTW and the utilisation of boreholes for grey water instead of using external potable water. Apart from the reduced water use and water purchases, the environmental discharge could also be reduced significantly mainly as a result of the reduced external source import (via Rand Water) by approximately 0.6 million m3/a (a reduction of 39%). This was achieved through increased use of local ground water sources and the increased development of grey water sources.

The outcome of the optimised WCDM scenario was subsequently used as a new planning benchmark upon which the long term WCDM programme was based. A number of projects were identified, scoped, costed and prioritised based on project outcomes. Lonmin developed a long term WCDM programme to implementation of a number of these projects toward achieving the optimised WCDM scenario and improve the water security for the mining and neighbouring communities.

Conclusions

Through the development of the dynamic water balance it was possible to accurately model the *status quo* of the Lonmin network and establish the interventions required to achieve the key strategic objectives, demonstrate the effect of the interventions required and en-

***Table 1** – Optimised WCDM scenario*

Mining Area	Water use aspect	Base Case (m3/a)	Optimised Scenario (m3/a)	Change (m3/a)
Karee	Rand Water use	3 192 552	999 297	
	Environmental discharges	788 547	391 191	
Western	Rand Water use	3 446 155	2 205 578	
	Environmental discharges	328 292	220 307	
Eastern	Rand Water use	2 598 896	1 795 918	
	Environmental discharges	524 307	386 499	
Total	Rand Water use	9 237 603	5 000 793	4 236 810 (46%)
	Environmental discharges	1 641 145	997 997	643 148 (39%)

sure a sustainable water system meeting the long term mining demands. The potential water savings that could be realised through the optimised WCDM scenario would not only reduce Lonmin’s water use, but also the purchases from Rand Water (at the time estimated at about R 35 million per year). At the same time the water savings could also enable Lonmin and Rand Water to address community water supply needs as a result of the reduced potable water use. Last, but not the least the incidental environmental discharges that occurred primarily during the rainy season would also be contained to a much larger degree and reduce the environmental impact.

The project demonstrated how revisiting an existing mine water system and critically assessing historic practises can be turned around from a long term crisis into a long term opportunity and a win-win for stakeholders affected by the mining operation. It is hoped that all mines will in future follow the example of Lonmin.

Acknowledgements and disclaimer

The opportunity provided by Lonmin to participate on this interesting project is greatly appreciated. It should be noted that the mining quantities and water uses have changed significantly as a result of the institutional and structural changes implemented at Lonmin since the completion of the project. The focus of the paper was not on the quantum of water used, but the manner in which the water use could be improved. The input of Water Hunters in the development of the DWBM are also acknowledged.

Potential for Co-treatment of Mine Water and Waste Water in Waste Water Treatment Works

Christopher J. Satterley[1], Peter Thorn[1], Susan Davies[2]

[1]The Coal Authority, 200 Lichfield Lane, Mansfield, Nottinghamshire, NG4 3FT, UK. christophersatterley@coal.gov.uk
[2]Aqua Enviro, 8 Appleton Court, Calder Park, Wakefield, WF2 7AR, UK

Abstract

Tests on a range of mine and waste waters were conducted to investigate co-treatment of phosphate and iron. Using a molar dosing ratio of 6:1 Fe:P, the best performing mine water (53 mg/L of iron) removed 73% orthophosphate (excluding dilution) from waste water with 9 mg/l of orthophosphate. Treatability tests confirmed these results and showed iron levels in the final effluent were below 1 mg/L. Effluent sulphate and some metal levels were higher than is typical for waste water treatment. The results suggest primary co-treatment may be effective for higher iron mine waters and waste water, where these issues can be managed.

Keywords: Co-treatment, phosphate reduction, efficiencies, waste water, neutral mine water

Introduction

The Coal Authority is a UK non-departmental public body responsible for managing the effects of past coal mining including the treatment of coal mine water. The Authority operates over 70 coal mine water treatment schemes that treat nearly 100,000 megalitres of mine water from emerging discharges and protect important natural resources such as drinking aquifers from contamination by mine waters. Coal mine waters contain appreciable levels of iron that need to be removed prior to discharge into the receiving water course under permit. This is predominantly achieved by passive or semi-passive (pumped) treatment using aeration, settlement and reed-beds.

The waste water industry in the UK is currently faced with the addition of an annual average total phosphorus limit to be included in the discharge consents enforced by environmental regulators. To remove phosphorus from waste water during the treatment process the water utilities most commonly use chemicals such as ferric sulphate or ferric chloride. The iron in these chemicals reacts with the orthophosphate in the waste water to form a particulate compound which is settled out in either primary or secondary treatment.

Ochre is known in the literature for its potential to bind phosphate in water (e.g. Dobbie *et al*. 2009) however there are challenges related to the formulation of the ochre to enable effective treatment that required further work to overcome (e.g. Littler *et al*. 2013). Where mine water and waste water streams are co-located, direct co-treatment could offer an alternative to combine phosphate and iron removal that avoids some of these issues.

There are a number of areas where mine water and waste water treatment operations are located close to each other and may even discharge into the same receiving water course. Passive tertiary co-treatment has been demonstrated at Lamesley, Tyne and Wear, UK (Younger *et al*. 2014, Chamberlain *et al*. 2016) and indicates that the iron in mine water can reduce phosphate levels in the co-treated scheme, beyond simple dilution. There is potential that co-treatment at waste water treatment works may be more effective at phosphate removal, reducing the requirement for ferric chemical addition.

Methods

Samples of raw mine water were taken from four treatment schemes in the Yorkshire region of the UK. The samples were fully analysed for a range of metals (total and soluble), phosphate (total and orthophosphate), and a

***Table 1** Key analyses of coal mine waters and ochre chosen for the study*

Site	Total Iron	Soluble Iron	Total Phosphorus	Ortho-Phosphate	TSS	COD	Sulphate
	mg/L	mg/L	mg/L	mg/L	mg/L	mg/L	mg/L
Site 1	5.5	0.01	0.13	0.12	23.5	16	690
Site 2	52.7	56.8	0.46	0.14	4	19	370
Site 3	7.26	1.068	0.11	0.03	11.5	2	530
Site 4	28.3	26.76	0.23	0.09	16.5	4	720
Site 4 Ochre	59840	N/A	155	N/A	16% (Dry Solids)	N/A	200

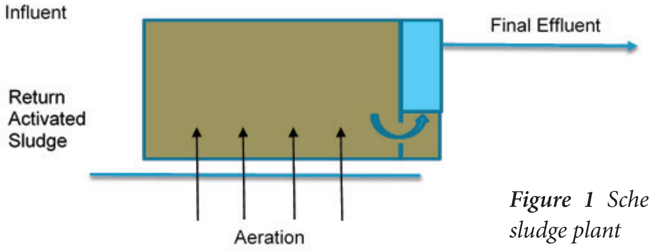

***Figure 1** Schematic of the bench-scale activated sludge plant*

range of physical parameters (including pH, electrical conductivity and dissolved oxygen (DO)). In addition, a sample of ochre from one site was also included as a comparison. The sites were selected to have a range of iron concentrations typical in UK coal mine waters. A summary of these analyses is presented in Table 1.

Raw waste water from two municipal treatment works in the Yorkshire region were sampled for use in the study. A summary of these analyses are shown in Table 2. The sites were chosen as examples of low and high phosphate waste water, however when the samples were analysed both appeared to have similar phosphate contents. This was not deemed critical for the study as both are considered typical of medium strength waste waters (Metcalfe & Eddy 2004).

All mine waters and ochre were individually combined with each waste water in a range of 1 litre jar tests using a series of Fe:P molar ratios of 2, 3, 4, 5 & 6. In addition a control of waste water alone was also run alongside. Each jar test was subject to the following regime considered representative of primary waste water treatment; a flash mix for 2 minutes with 100 rpm stirring; a flocculation step for 30 minutes with 30 rpm stirring and quiescent settlement for 30 minutes with no stirring. After this time a sample of the supernatant from each test was taken and analysed for pH, TSS, total phosphate, orthophosphate, total iron and soluble iron. In addition, control samples, the ochre and one of the mine waters that showed the best removal for each site were subject to detailed analysis of the supernatant and settled solids following repeat jar testing.

Treatability tests were undertaken on the best performing combination from the jar tests to simulate the downstream treatment process. Two bench-scale activated sludge reactors were set up and run for 7 days con-

***Table 2** Key analyses of waste waters chosen for the study*

Site	Total Iron	Soluble Iron	Total Phosphorus	Ortho-Phosphate	TSS	COD	BOD	Ammonia
	mg/L	mg/L	mg/L	mg/L	mg/L	mg/L	mg/L	mg/l
Site A	1.62	0.671	6.95	3.7	190	530	279.4	20.6
Site B	1.04	0.316	7.3	4.5	233	626	109.0	32.1

Table 3 *Activated Sludge rig operating parameters*

	Target BOD: MLSS ratio	Dissolved Oxygen (DO)	Feed Volume	Return Activated Sludge Volume	Hydraulic Residence Time
	Food:Mass	mg/l	l/d	l/d	hrs
Rig 1	0.08	2-3	20	13	8
Rig 2	0.1	2-3	8	5	19

tinuously. Each reactor had a capacity of 10 litres and diffused aerators to mimic fine bubble diffused aeration typically seen in an activated sludge plant (see Figure 1). The reactors were filled with mixed liquor (a combination of waste water/mine water and sludge) at a suspended solids concentration of 2000-3000 mg/L with DO maintained between 2-3 mg/L. The food to mass ratio (biological oxygen demand (BOD) vs mixed liquor suspended solids (MLSS)) and the hydraulic retention time (HRT) were used to determine the feed rates. For waste water alone a HRT of 19 hours was used as typical of a treatment plant of this type. A shorter HRT (8 hours) was required for the mine water blend due to the dilution effects of the mine water meaning more throughput was required to maintain a minimum organic loading of 0.08 kgBOD/kgMLSS. Test parameters are listed in Table 3. During the tests the final effluent and mixed liquor were sampled regularly and at the end of the trial detailed analysis was performed on the final effluent and mixed liquor suspended solids.

Results & Discussion

Jar testing results for all mine waters with Site A waste water are shown in Figure 2. Percentage orthophosphate removal is calculated exclusive of dilution effects by calculating the removal rate from the combined waste and mine water rather than waste water alone. This ensures that genuine removal is not masked by dilution effects. Mine water from Site 2 (52.7 mg/L total Fe) showed the best performance with increasing removal rates observed as the Fe:P molar ratio is increased to a maximum of 69% at a molar ratio of 6. This performance is higher than the comparator ochre sample for all molar ratios. Site 4 (28.3 mg/L total Fe) shows some positive removal at higher molar ratios, but this is relatively marginal. Both low iron sites (1 & 3) show negative removals in all cases. The negative removal rates observed are likely due to margins of error in analysis as orthophosphate levels for these tests are typically below 1 mg/L (due to the high mine water to waste water ratio for these sites). It is considered that negative removal rates are equivalent to

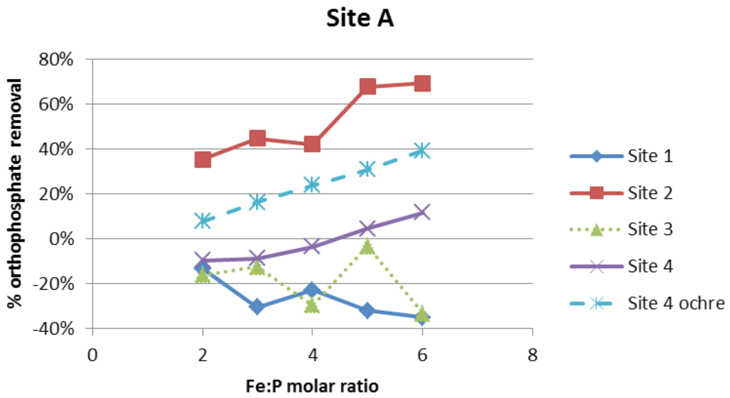

Figure 2 *Jar testing results for Site A with a range of mine waters and ochre.*

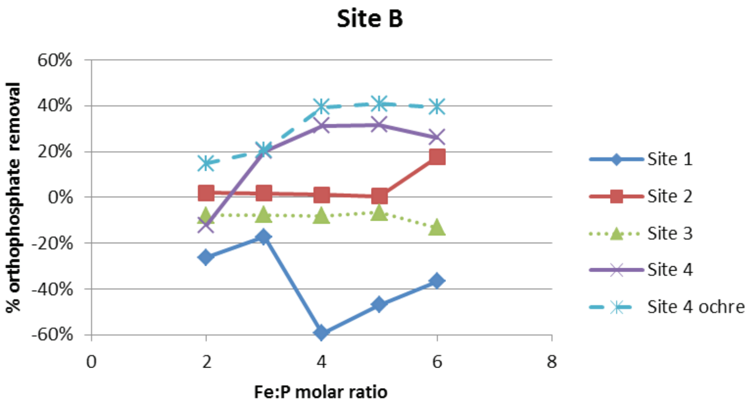

***Figure 3** Jar testing results for Site B with a range of mine waters and ochre.*

zero removal for the purposes of discussion.

Figure 3 shows the equivalent jar test results for Site B. The performance of the low iron site mine waters (sites 1 & 3) was similar to the results from Site A, with negative removal rates observed. The medium iron site (site 4) and the site 4 ochre also showed similar performance as for Site A but with a different trends in relation to molar ratio. The high iron site (site 2) showed a markedly different behaviour compared to Site A. This behaviour may be due to the interference of the increased BOD in the Site B waste water. This increased BOD could be indicative of increased levels of organic material with chelating properties that could reduce the availability of the iron to bind phosphate. If correct, it is plausible that this would affect the site 2 tests more than others due to the reduced dilution by mine water required to achieve the molar ratios. Alternatively, the Site B waste water had higher alkalinity, which could have impacted binding. This effect requires further investigation, which was not possible in this study due to time constraints.

Table 4 shows the relative volumes on mine and waste water used in all the jar tests performed with an Fe:P molar ratio of 6, where the most effective phosphate removal was observed. It can be seen that the relative volumes are strongly dependent on the iron concentration of the mine water and that higher iron concentrations are required to achieve a ratio of less than 1. The relatively high volumes of mine water required pose issues for co-treatment in existing WWTP where there is likely to be limited additional hydraulic capacity. This suggests that purpose built co-treatment facilities may be required; however these could still offer cost savings compared to separate treatment plants.

Repeat Jar testing with detailed analysis was performed on the best performing combinations and a control with waste water alone. This required further samples of waste water to be collected with Site A and Site B

***Table 4** Volumes and ratios of mine water and waste water added to achieve Fe:P of 6 for all sites*

	Site A			Site B		
	Waste water (ml)	Mine water (ml)	Mine water: waste water ratio	Waste water (ml)	Mine water (ml)	Mine water: waste water ratio
Site 1	109	791	7.26	91	809	8.89
Site 2	512	388	0.76	468	432	0.92
Site 3	138	762	5.52	117	783	6.69
Site 4	373	527	1.41	331	569	1.72

Table 5 Analytical results from jar retests of optimum phosphate removal combinations

		Site A Control	Site A + Site 2 Fe:P=6	Site A + Site 4 ochre Fe:P=6	Site B Control	Site B + Site 4 Fe:P=6	Site B + Site 4 ochre Fe:P=6
Ortho-phosphate, as P	mg/l	8	1.6	1.9	5.7	1.7	2.7
% ortho phosphate removal (exc. dilution)		11%	73%	79%	12%	25%	70%
Phosphorus, Total as P	mg/l	9.79	2.34	2.99	7.67	2.39	3.77
Iron , Total as Fe	mg/l	0.6	5.95	4.41	0.28	19.7	2.06
Iron, Filtered as Fe	mg/l	<0.23	0.85	1.11	<0.23	15	0.26
Arsenic, Total as As	mg/l	0.0012	0.0013	0.0015	<0.0010	0.0019	0.0012
Barium, Total as Ba	mg/l	0.026	0.011	0.019	0.062	0.023	0.041
Boron, Total as B	mg/l	<0.23	<0.23	<0.23	<0.23	<0.23	<0.23
Cadmium , Total as Cd	mg/l	<0.0006	<0.0006	<0.0006	<0.0006	<0.0006	<0.0006
Copper, Total as Cu	mg/l	0.013	<0.009	0.013	0.025	<0.009	0.01
Lead , Total as Pb	mg/l	<0.006	<0.006	<0.006	<0.006	<0.006	<0.006
Mercury, Total as Hg	mg/l	<0.00010	<0.00010	<0.00010	<0.00010	<0.00010	<0.00010
Nickel, Total as Ni	mg/l	0.01	0.026	0.011	0.008	0.051	0.006
Sulphate as SO4	mg/l	34.8	313	83.4	155	446	158
Zinc, Total as Zn	mg/l	0.07	0.03	0.05	0.07	0.04	0.02

samples having orthophosphate concentrations of 9 mg/L and 6.5 mg/L respectively. Repeat testing was undertaken on combinations of Site A with Site 2 mine water and Site 4 ochre and of Site B with Site 4 mine water and ochre, all at a Fe:P of 6.

Following mixing and settling, the supernatant was sampled from each test and analysed for phosphate removal and a range of metals (Table 5). For Site A orthophosphate removal was seen to improve for both Site 2 mine water and Site 4 ochre to 73% and 79% respectively. It is likely that the increased phosphate concentration in the new waste water samples accounts for this change, although the improvement in ochre performance is large and is likely to require further investigation. For Site B, a similar behaviour is observed; again the increased phosphate levels in the new samples are likely to account for this. Total phosphorous levels are above 2 mg/L in all cases suggesting that further treatment would be required to reduce phosphate to levels acceptable in the UK (<1 mg/L).

Iron levels are increased from the controls in all cases although with the exception of Site B with Site 4 mine water (19.7 mg/L total Fe) these would be considered reasonable (typical limits enforced in the UK are between 4-6 mg/L total iron). The high Fe levels in the Site B + Site 4 supernatant may arise from the relatively low removal rates resulting in reduced precipitation of iron phosphate. Sulphate levels are substantially increased in the mine water/ waste water blends compared to the controls and above typical maximum sulphate levels in UK waste waters (50 mg/L), this could lead to operational issues related to odour under anaerobic conditions and requires further investigation.

Metals levels in the supernatant of all tests are shown to be reduced by the addition of mine water or ochre with the exception of Ni (in mine water blends) and As (in all blends) where increases are observed. The levels observed are above Environment Agency recommended surface water levels in England (20 µg/L Ni and 10 µg/L As) indicating that the supernatant may not be suitable for final effluent discharge. Further investigation over a longer sampling period is recommended to confirm these results.

A further treatability study using a bench-scale activated sludge reactor was undertaken using a blend of Site A and Site 2 waters with a control with Site A waste water alone following pre-treatment as per the jar tests. The purpose of this study was to determine the impact of blending mine water with waste water on the downstream treatment process as well as providing some indicative results on potential sludge quality. The treatment performance of both reactors was generally good with BOD and COD removal found to be over 90% and 79% respectively. Orthophosphate removal in rig 1, fed with mine water was found to be an additional 68% beyond that achieved in the jar tests, compared to the control in rig 2, which showed 0% additional removal. Total Fe and P values in the rig 1 effluent were found to be below typical discharge limit values (4-6 mg/L and 1 mg/L respectively). Nickel levels in the rig 1 effluent were found to be marginally above recommended surface water levels at 22 µg/L. Sulphate levels in the final effluent for rig 1 were found to be high compared to rig 2 (330 mg/L and 94 mg/L respectively) in line with the jar test findings and similar levels were found in the biomass for both rigs implying the potential for odour issues if anaerobic conditions are present.

Due to the low % dry solids in the biomass in both rigs it was not possible to directly measure metals in the biomass. Conservative calculations indicate that if all the metals were associated with the dry weight, key metal concentrations would be 687 mg/kg Zn, 169 mg/kg Cu and 44 mg/kg Ni. Both Zn and Cu levels exceed the maximum permissible concentrations for sludge to land in England, Wales and N. Ireland at 200 mg/kg and 80 mg/kg respectively (Defra 2017). It is recommended further investigation is done into the fate of trace metals from mine water throughout the waste water process to determine metal concentrations in the final effluent and sludge.

Conclusions & Recommendations

The above results indicate that mine water does show some potential for the removal of orthophosphate from waste water during primary treatment, particularly for higher iron mine waters. Based on this study the substantial increase in hydraulic loading required for primary co-treatment means that this is most likely to find application where new treatment facilities are to be built or there is hydraulic capacity available in existing infrastructure. The impact of BOD levels, alkalinity, effluent and sludge metals and elevated sulphate also need to be considered before this option can be applied.

In addition, this study provides further data to indicate the potential for ochre to be used to treat phosphate in waste water. Ochre dosing would not present the same hydraulic issues as mine water co-treatment and if costs associated with transport and dosing are less than the OPEX costs of dosing ferric chemicals, this could be advantageous.

It is recommended that further investigations are undertaken on the impact of waste water quality, metals and sulphate on sludge and effluent in co-treatment. Also, further studies of the impact of ochre on secondary treatment should be undertaken to determine the impact on overall treatment and effluent quality.

Acknowledgements

The authors thank Yorkshire Water for their cooperation and support during this work. The Coal Authority would like to acknowledge the Department of Business, Energy and Industrial Strategy who have funded elements of this work.

References

Chamberlain S, Surdevan R, Smail I, Greenwell HC, Powell EJ, Moore A (2016) Co-treatment of iron and phosphorous in a wetland environment as an alternative to tertiary treatment using iron salts. 15th Int. Conf. of the IWA SG on Wetland Systems for Water Pollution Control, Gdansk, Poland.

Defra (2017) Guidance Sewage sludge on farmland: code of practice for England, Wales and Northern Ireland. Department of Environment, Food and Rural Affairs (Defra), 8 June 2017.

https://tinyurl.com/hag8tmh - accessed 3 May 2018

Dobbie KE, Heal KV, Aumonier J, Younger PL (2009) Evaluation of iron ochre from mine drainage treatment for removal of phosphorus from waste water. Chemosphere 75(6), pp 795-800.

Littler J, Geroni JN, Sapsford DJ, Coulton R, Griffiths AJ (2013). Mechanisms of phosphorus removal by cement-bound ochre pellets. Chemosphere 90(4), pp. 1533-1538.

Metcalfe & Eddy Inc. (2004). Waste water Engineering Treatment and Reuse, 4th Edition, McGraw Hill, New York.

Younger P, Henderson R (2014). Synergistic wetland treatment of sewage and mine water: pollutant removal performance of the first full-scale system. Water Research 55 pp. 74-82.

The Efficiency of Open Lime-Zeolite Channel System in Treatment of Acid Mine Drainage (AMD) Released from Sungun Copper Mine

Abdorreza Vaezihir[1], Fatemeh Safari[2], Hossein Javani[3], Nader Mazaheri4

[1] *University of Tabriz, Department of Earth sciences, 29 Bahman Blvd., Tabriz, Iran,* r.vaezi@tabrizu.ac.ir *and* vaezihir@yahoo.com

[2] *University of Tabriz, Department of Earth sciences, 29 Bahman Blvd., Tabriz, Iran,* safarifateme84@yahoo.com

[3] *Sungun Copper mine, Head of HSE ward, Varzaghan, Iran,* hossein_javani@yahoo.com

[4] *Sungun Copper mine, Head of environment office, Varzaghan, Iran,* mazaheri_nader@yahoo.com

Abstract

Sungun copper mine is located inside Arasbaran forest protected area of Iran and AMD drained from tailing dump of the mine is a big challenge between the mine authorities and the residents, NGOs and Iranian Environmental Protection Organization. As the first AMD treatment system in Iran, a passive open lime-zeolite channel was implemented in Sungun mine and the efficiency was evaluated.

Increasing of pH cannot decrease the concentration of heavy metal down to permissible level and need to be combined with another mechanism to increase the efficiency. A system with combination of zeolite and lime would be an effective treatment method for Cu removal of AMD. The zeolite omits Cu from aqueous phase by means of adsorption (2.86 mg/g based on Langmuir isotherm model) whereas increasing of pH with limestone is recognized as effective mechanism for precipitation of Cu from AMD. However, based on experimental data and site specifications, zeolite- limestone open channel stablished at site to use two mechanisms of buffering and adsorption for treatment of AMD. Combining open zeolite channel with routine open lime channel (OLC) increased the efficiency of AMD treatment system.

A few months after opening of AMD treatment system of Sungun copper mine, remediation efficiency of the system was evaluated using two rounds of sampling and comparing with the pre-treatment sampling results. The results showed that Cu concentration has been decreased from about 45 mg/L down to less than 4 mg/L implying a decrease of more than 91% percent in Cu concentration by lime part of the system. The second sampling which was done after complete installation of the system showed a complete restoration of the AMD related to the copper with decrease of concentration down to detection limit of the instrument (0.03 mg/L). The system also decreased Al concentration 69%, Fe concentration 55% and Zn below detection limit. Furthermore, the treatment system has increased pH value to neutral condition which has the main rule in immobilization of the metals.

Keywords: AMD, Treatment, Lime, Zeolite, Sungun mine

Introduction

Chemical precipitation, ion exchange, adsorption and ultra-filtration are common treatment processes to eliminate heavy metals from waste waters (Coulson et al. 1994). One of the most popular method for the removal of heavy metals from the waste waters is adsorption (Fala et al. 2006, Cui et al. 2006), especially when large quantities or certain wastes are released from mining, industrial or agricultural activities. Sorbents comprise a wide range of organic, inorganic and synthetic products. Among them, CaCO3, dead biomass, blast\ furnace slag, fly ash, clay, tree bark, tea leaves and natural zeolite have potential to remove heavy metals from waste water (Bhattacharyya and Gupta 2006, Günay et al. 2007, Bailey et al. 1999). Treatment systems provide a controlled environment in which natural chemical and biological reactions which help in the treatment of acid mine drainage can occur (DEP 1999). Open limestone channels (OLCs) are passive treatment systems that achieve remediation mostly through chemical means (Kalin et al. 2006). Other passive systems are anoxic limestone drains, aerobic and anaerobic wetlands, and biological and abiotic permeable, reactive barriers (Johnson and Hallberg 2005). Very often, an OLC is preferred due to its low building and maintenance costs. Generally, OLCs are used to treat AMD under conditions of very high flow, because continually-moving water may erode any armoring from the limestone (Pavlick et al. 2005).

In this research Acid Mine Drainage (AMD) samples taken from Sungun copper mine subjected to several treatments through lab scale experiments to find the best scenario of remediation. To optimize final scenarios, another series of treatments have been conducted in batch and semi continuous condition of water flow. The final goal of the study is finding a method or combination of methods to immobilize the heavy metals and decrease their concentration in AMD down to the standard values.

Methods

Water samples have been taken from AMD drained from the tails of porphyry copper mine located at the northwest of Iran (Fig. 1). Sungun deposit hosts 1200 Mt of ore at low grade 0.76% Cu and ~100 ppm Mo (Siahcheshm et al. 2014) so the mining processes produce a huge amount of waste materials and store in tailing dumps. Pore fluids of tailings can become acidic through reactions of surface waters with exposed sulfide minerals. Consequently, AMD can be formed which has low pH to solve heavy metals of the tailings and release them into a river beneath of the dump. The mine tailings are being dumped in a valley named Pakhir valley with an average flow rate of 25 L/s. In order to find the best method for remediation of the AMD a series of experiment were designed.

At the first step, the AMD samples were subjected to five remediation materials including granular activated carbon, natural zeolite, iron filing, lime, and poly aluminum chloride (PAC). All of these materials except PAC were prepared in the same of size between 1.4 to 2.3 mm and 1 g of each material was added to the 100 mL of drain and stirred for 2 hours in 20 OC in an incubator shaking with a rate of 200 rpm. Concentration of residual Cu in the treated drainage was measured by atomic absorption spectrometry (AAS) using a Novaa 400, Analytik-Jena machine.

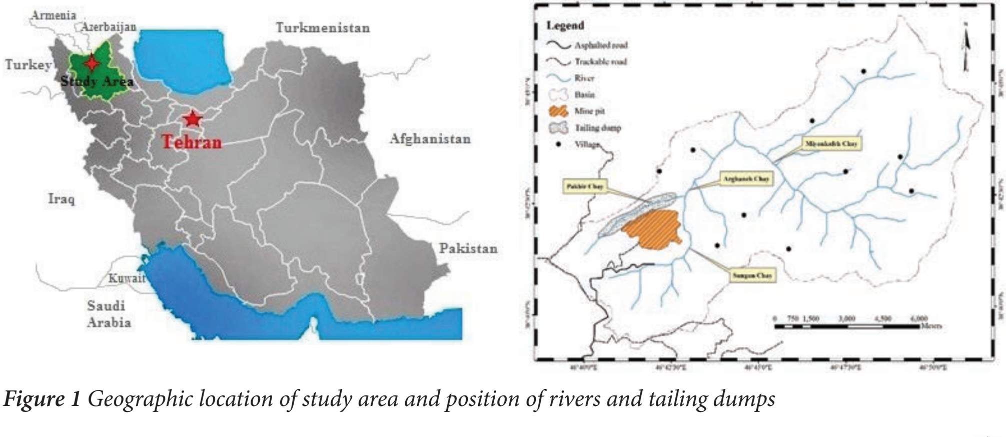

Figure 1 Geographic location of study area and position of rivers and tailing dumps

Table 1 *Physical properties and chemical composition parameters of AMD collected from "Sungun" mine*

Parameters	Unit	Value
pH	-	5.5
Total Dissolved Solid(TDS)	mg/L	1020
Cu2+	mg/L	34
Mn2+	mg/L	5.78
Ni2+	mg/L	0.51
Cd2+	mg/L	0.1
Al3+	mg/L	0.97
Fe3+	Mg/L	0.05

To evaluate the ability of PAC through coagulation-flocculation process on AMD treatment, 1.0 g of PAC and 100 mL of drainage sample were poured into an Erlenmeyer and the solution was stirred for 2 min in 20 oC in an incubator at a stirring speed of 200 rpm. Then it was kept for 30 min for efficient deposition of developed clots. Finally, Cu concentration in the treated drainage was determined. Two best options were selected according to the removal efficiency, cost and availability of materials and then the following batch and continuous tests were conducted on them.

To simulate the AMD treatment process, a physical model with dimension of 120 × 50 × 10 cm3 was made and placed on the bench with a slope of 2% to provide the necessary head for flow. To evaluate the performance of zeolite as one of the selected materials in AMD treatment under a semi continuous condition, the above mentioned reactor was filled up to 5 cm with zeolite grains of 2 to 5 mm. The drainage was entered to reactor with a flow rate of 7 L/h which caused a travel time about 21 min for the interred drainage through the model. Samples was taken with intervals of 30 min and assessment of Cu, Mn, Al and Ni concentration in the untreated and treated AMD samples were performed using AAS.

To evaluate the effect of solution pH on the ability of zeolite on copper removal from the drainage, 0.5 L drainage poured into a series of Erlenmeyer flasks and initial pHs were adjusted from 7 to 10 using NaOH. The treatments incubated for two days at room temperature to reach complete precipitation.

Results and Discussion

According to the chemical analysis of AMD sample collected from the toe of tailings of Sungun mine (Table 1), it is acidic with pH of 5.5 and present a high conductivity and high concentration of some heavy metal ions (Cu, Mn, Ni). These concentrations is higher than the permissible value recommended by WHO standard (1987-1999). The specific cyanic color of AMD and river bed is due to the high concentrations of copper in the solution. It is clear that this water drainage introduces sulphuric acid and toxic heavy metals (Cu, Mn and Ni) into the environment.

The initial concentration of Cu cations in the untreated AMD and its concentration in the treated samples have been shown in Fig. 2. All the treatment processes except coagulation and flocculation using PAC, can reduce

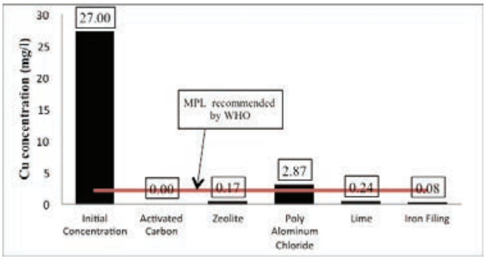

Figure 2 *Ability of various treatment processes on the decrease in copper concentration in batch scale model. (MPL: Maximum Permissible Level)*

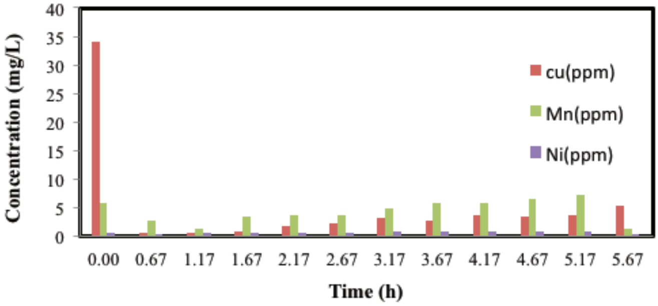

Figure 3 *Concentration of Cu, Mn and Ni heavy metals during semi continuous test using zeolite*

Cu concentration to reach permissible level. This indicates that the coagulation and flocculation process has lower efficiency than the sorption and pH reduction methods for Cu removal from AMD. Based on the results of this experiment and considering the local availability and low cost of zeolite and lime, these materials were selected for further investigations.

The results of treatment tests using zeolite (Fig. 3) revealed that concentrations of Cu, Mn and Ni ions in the initial and treated drainage sample indicate a good performance, especially in the removal of copper, but over time its performance decreased due of saturated of the surface active sites. In order to measure zeolite adsorption ability, a series of experiments were performed.

Through another test, AMD treatment using lime was investigated and the results demonstrated (Fig. 4) that the efficiency of lime for the removal of copper from solution is less than zeolite, and its ability decreases gradually during the test.

Treatment System Designing

According to the results of the experiments an open channel system was designed for treatment of Pakhir valley AMD in Sungun copper mine complex. To design this treatment system Pakhir valley discharge was measured for one year which show an average annually discharge of 0.025m^3/s. Also maximum instantaneous discharge with return periods of 25 and 50 years were calculated 20.5 and 6m^3/s, respectively.

The designed treatment system is including: initial box covered channel, diversion dam, limestone channel, zeolite channel and diversion channel. The initial box conveys AMD from the toe of the tailing to the diversion dam. Because every day new tailing was dumped into Pakhir valley, to prevent the contact of AMD with new tailings this concrete channel was designed as box and covered form. Limestone channel is a concrete one filling with limestone particles to increase pH which can precipitate heavy metal from equate phase. The particle size is 10 mm to increase contact area. According to the dimension of limestone channel (bed width is 80 cm and the depth is 40 cm) a length of about 120 m is necessary to decrease copper concentration down to 15 mg/L. So, AMD flowing through limestone particle precipitates a part of its copper due to increasing of pH and then inters to zeolite channel. The length of zeolite channel was optimized to be 250 m ac-

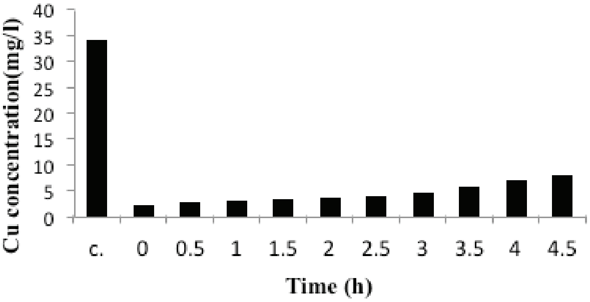

Figure 4 *Concentration of Cu during semi continuous test using lime*

Figure 5 *Open lime-zeolite channel system after construction*

cording to the results of the lab experiments which can provide enough time for absorption of copper. This channel can decrease Cu concentration down to 3 mg/L which is less than its MPL of irrigation water. To increase the resident time of AMD in limestone -zeolite channels several check dam were used in each25 meter.

One year after designing of AMD treatment system for Sungun copper mine, it was constructed and opened in late December 2016 (Fig. 5). In order to evaluate efficiency of system in remediation of AMD two rounds of sampling carried out one month after system opening (when only lime filter works) and three months after (when the both lime and zeolite filters work). The results showed that Cu concentration has been decreased from about 45 mg/L down to less than 4 mg/L implying a decrease of more than 91% percent in Cu concentration by lime part of the system. The second sampling which was done after complete installation of the system showed a complete restoration of the AMD related to the copper with decrease of that concentration down to detection limit of the instrument (0.03 mg/L). Table 2 also showed that this system more than Cu have decreased other metals like Al concentration decrease 69% percent, Fe concentration rate removal is 55% and Zn concentration reduced below detection limit.

Conclusion

The results of laboratory experiments showed that all the investigated compounds except the PAD could decrease the concentration of copper considerably. Due to feasibility of cost efficiency, lime and zeolite were selected to design a treatment system for Sungun copper mind AMD. Based on equilibrium experiments, lime has an ability to reduce the concentration of copper down to 15 mg/L, and changing the amount of lime has a little effect on the reducing of Cu concentration. Zeolite can decrease the concentration much more down to permissible value. Consequently, it seems a system with combination of zeolite and lime would be an effective treatment

Table 2 *System efficiency in terms of pollutant removal at Pakhir River (the values are in mg/L).*

pH	Zn	Pb	Mn	Fe	Cu	Cd	Al	Sampling Site	
6.1	1.92	ND	16.81	NM	44.49	0.31	2.26	Inlet of the system	Winter2017
7.3	1.43	ND	15.08	NM	3.84	0.29	1.25	Outlet of the limestone channels	
-	25.5	-	10.29	NM	91.36	6.45	44.7	Removing Percent	
5.4	3.06	0.38	8.315	1.024	46.35	ND	9.29	Before treatment system	Spring2017
7.1	ND	0.28	0.1450	0.507	ND	ND	2.85	Outlet of the Zeolite Channels	
-	100	26.3	98.2	50.5	100	-	69.3	Removing Percent	

NM: Not Measured ND: Not Detected

method for Cu removal of AMD. Based on experimental data and site specifications, it was recommended to use zeolite- limestone open channel to implement two buffering and adsorption agents for treatment of Sungun mine AMD. Construction of the designed system showed that the efficiency of the system is satisfactory, expectedly. Cu concentration was decreased from 45 mg/L down to less than detection limit (0.3 ppm) which is less than environmental permissible level for surface water. The treatment system also reduced concentration of some other metals like Zn, Al and Mn from 26 to near 100 percent of the initial value.

References

Bailey SE, Olin TJ, Bricka RM, Adrian DD (1999) A review of potentially low-cost sorbents for heavy metals. Water research, 33(11), p 2469-2479

Bhattacharyya KG, Gupta SS (2006) Kaolinite, montmorillonite, and their modified derivatives as adsorbents for removal of Cu (II) from aqueous solution. Separation and Purification Technology, 50(3), p 388-397

Coulson JM, Richardson JF, Peacock DG (1994) Coulson & Richardson's Chemical Engineering: Chemical & biochemical reactors & process control, Vol. 3. Elsevier

Cui H, Li LY, Grace JR (2006) Exploration of remediation of acid rock drainage with clinoptilolite as sorbent in a slurry bubble column for both heavy metal capture and regeneration. Water research, 40(18), p 3359-3366

DEP P (1999) The science of acid mine drainage and passive treatment. Bureau of Abandoned Mine Reclamation, Pennsylvania Dept of Environmental Protection

Fala O, Molson J, Aubertin M, Bussière B, Chapuis RP (2006) Numerical simulations of long term unsaturated flow and acid mine drainage at waste rock piles. In Proceedings of the 7th International Conference on Acid Rock Drainage and SME Annual Meeting, St. Louis, p 26-30

Günay A, Arslankaya E, Tosun I (2007) Lead removal from aqueous solution by natural and pretreated clinoptilolite: adsorption equilibrium and kinetics. Journal of Hazardous Materials, 146(1), p 362-371

Johnson DB, Hallberg KB (2005) Acid mine drainage remediation options: a review. Science of the total environment, 338(1), p 3-14

Kalin M, Fyson A, Wheeler WN (2006) The chemistry of conventional and alternative treatment systems for the neutralization of acid mine drainage. Science of the Total Environment, 366(2), p 395-408

Pavlick M, Hansen E, Christ M (2005) Watershed based plan for the north fork Blackwater River Watershed, West Virginia. Downstream Strategies, Morgantown

Siahcheshm K, Calagari AA, Abedini A, Sindern S (2014) Elemental mobility and mass changes during alteration in the Maher-Abad porphyry Cu–Au deposit, SW Birjand, Eastern Iran. PERIODICO DI MINERALOGIA, 83(1), p 55-76

7

Prediction

Lifetime Assessment of an Operating Tailings Facility through Modelling of the Unconsolidated Tailings Layer ◎

Samantha Barnes[1], Richard Martindale[2]

[1]*SRK Consulting (Canada) Inc, 1066 West Hastings Street, Vancouver, Canada*
[2]*SRK Consulting (UK) Ltd. 17 Churchill House, Cardiff, United Kingdom*

Abstract

The following paper presents a case study in which the remaining lifetime of an operating kaolin tailings facility in Southeast United States was evaluated. Due to the characteristics of the tailings, an unconsolidated tailings layer occupies a portion of the lake's capacity. The turbidity and total suspended solids in this layer exceeded the discharge criteria. The characterization of this layer was improved to predict how it could affect discharge compliance throughout the remaining life of the facility. A typical water balance approach to model tailings solids input to the lake was insufficient to model the movement and progression of the unsettled tailings layer. A more detailed investigation was developed to understand solids in this unconsolidated layer.

Introduction

Operational tailings facilities need to quantify the remaining pond capacity to manage large inflow events and plan for future expansions. Tailings reservoirs are often modelled through a mass balance and water balance based on known inputs and outputs, including precipitation, tailings deposition, pumped flows, seepage, reclaim and evaporation. In some cases, there are additional constraints to the facilities which are more complex and difficult to model. The additional factor limiting capacity in this case study is characterizing suspended solids in the interface between the open water and consolidated tailings.

Vertical mixing of unsettled tailings is often studied in pit lakes, where a freshwater cap is designed to isolate deposited tailings from turbulent surface mixing. Turbidity in water covers over oil sands tailings in Canada have been studied over the last 20 years, as described by Lawrence (2015). In these studies, seasonal and diurnal wind induced turbulent mixing were evaluated, and a minimum cover thickness was estimated to protect the tailings layer.

In this case, tailings are actively deposited on the north edge of the lake, producing a beach, with a partial and shallow water cover. Near the tailings deposition point, water depths range from 0.5 to 2.0 m and increase to a maximum depth of 8 m on the southern end of the facility. Discharge from the lake to the receiving environment is through a decant structure on the south end. Colour gradation observed from aerial imagery suggests that there is a highly turbid unsettled solids layer above the consolidated tailings (white) and a thicker freshwater cover near the south outlet (dark green). The uncertainty of how this transition layer between consolidated tailings and the overlying water layer behaves confounds management decisions regarding tailings deposition and expansion plans.

This study highlights the conceptual model, developed using limiting parameters to examine current and projected capacity of the tailings lake.

Model Parameters

Four limiting factors to the facility were identified and evaluated in this assessment.

1. The impact of discharging additional tailings into the lake and the projection of the beach;
2. Thickness and characteristics of the turbid unconsolidated tailings layer;
3. Mixing as a result of wind and wave action; and
4. Horizontal settling distance required for re-suspended particles to settle below the inlet of the decant structure.

1. Projected Tailings Surface

The bathymetry was surveyed at six-month intervals over five years. A total of nine surveys, complete with aerial imagery were compiled and analysed to evaluate the change in the lake bed surface. In comparing sequential surveys, some trends were observed in the beach delta area, however changes were offset by the larger inconsistencies in the remaining lake area to the south.

Kriging was used in ArcGIS Spatial Analyst tool (Environmental Systems Research Institute (ESRI), 2016) to interpolate and smooth the bathymetric surveys. After smoothing was complete, the first survey from September 2011 was compared with the most recent survey in December 2016 to assess the change in volumetric capacity of the lake. Figure 1 presents a comparison of volumetric losses and gains between the 2011 and 2016 surfaces, with gains in red and losses in blue.

The gains suggest a growing tailings beach, with more prominent increase in volume around the deposition point. The measured volumetric changes were used as a target in a back-analysis model, using the software Muck3D (MineBridge Software).

The bathymetry measured in September 2011 was used as the base surface upon which tailings deposition was modelled for comparison with the measured December 2016 bathymetry. Parameters included input location (as this varied during the period of modelled history) input tonnage rate and beach geometry. Profiles across the lake from north to south and from east to west were used to compare modelled results with the December 2016 survey and results were reasonably consistent accounting for modelling limitations.

A mass balance was generated to validate the deposition model and bathymetric survey results. Historic plant losses were evaluated from the process plant discharge to the lake where the total mass added over the period between surveys amounted to approximately 90% of the calibrated tailings rate input to the model. This suggests that 10% of reported tailings deposited over this period remained in suspension within the turbid layer.

2. Turbidity Layer Thickness

To understand the unsettled tailings layer in the lake, thickness and characteristics of the layer were assessed in two lake surveys. The surveys were designed to capture turbidity levels throughout the water column at various locations across the lake. Each survey included:

- Bathymetric survey by boat to estimate the lake volume and depths at the time of the investigation.

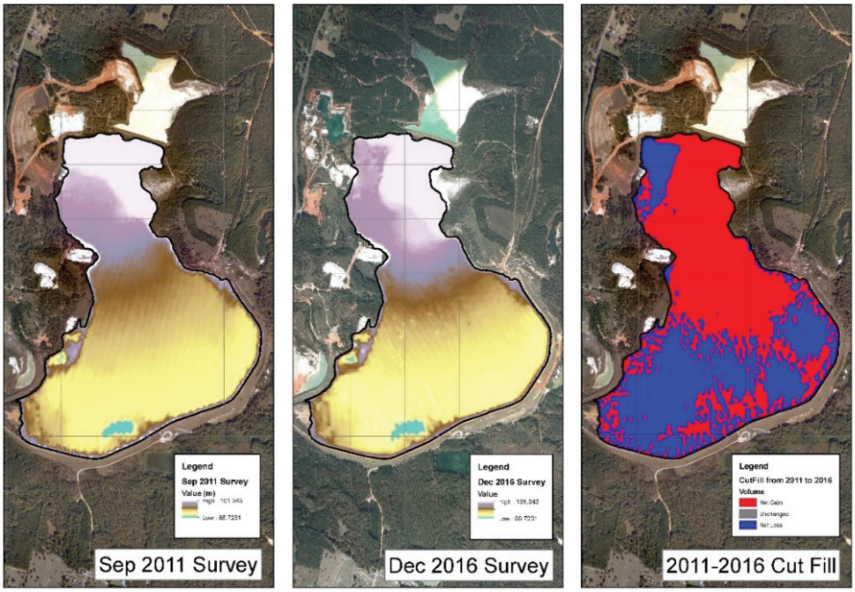

***Figure 1:** Comparison of Historic Bathymetric Surveys in terms of Net Gains and Losses*

- Turbidity readings throughout the water column using a YSI DSS Probe. A total of 83 profiles were collected in February 2017 and 84 profiles in March 2017. Profiles of the water column up to the tailings surface were obtained at every 0.1 m.
- A total of 20 grab samples from random profile locations, taken from the turbid tailings layer and the non-turbid upper layer of the lake to analyse total suspended and dissolved solids concentrations.

The surveys were performed approximately 1 month apart and were intended to assess if there was any short-term variance in lake behaviour. Future surveys will be undertaken at less frequent increments. Both completed surveys attempted to cover a similar distribution across the lake. Upper lake samples presented turbidity levels between 5 and 25 FNU. The transition between the upper, clear water and the lower, turbid layer was identified where a sudden change in turbidity was measured from the continuous readings on the probe. Turbidity levels in the unsettled tailings layer increased abruptly from 50 FNU, to between 1000 to 10,000 FNU. A reading of 50 FNU was inferred as the transition zone interface between the freshwater cover and the turbid layer.

Based on the lake bottom reading at each location from the boat survey equipment, the thickness of the turbid layer from the lake bottom to the transition depth was calculated for each point. Figure 2 presents the results of all turbidity data through the water column. Profile data are presented in order of total lake depth, and colours reflect the turbidity reading. The blue and purple points are readings within the turbid layer, while green points reflect depth within the transition zone.

As the depth of the lake increases, the clear cover layer begins to form, and the turbidity layer maintains a relatively consistent thickness. Both turbidity survey results are as follows:

- Average turbid layer thickness over both surveys was 1.0 m
- 95th percentile thickness was 1.9 m and 1.6 m in February and March 2017, respectively
- Maximum thickness was 2.7 m and 1.9 m in February and March 2017, respectively.

An offset of 2.0 m was selected for the capacity assessment. This offset is reflected in Figure 2 as a red dashed line, which highlights that most of elevated turbidity readings are below 2.0 m depth.

Results from the lab testing were used to estimate volume of sediment within the turbid layer. The average total suspended solids

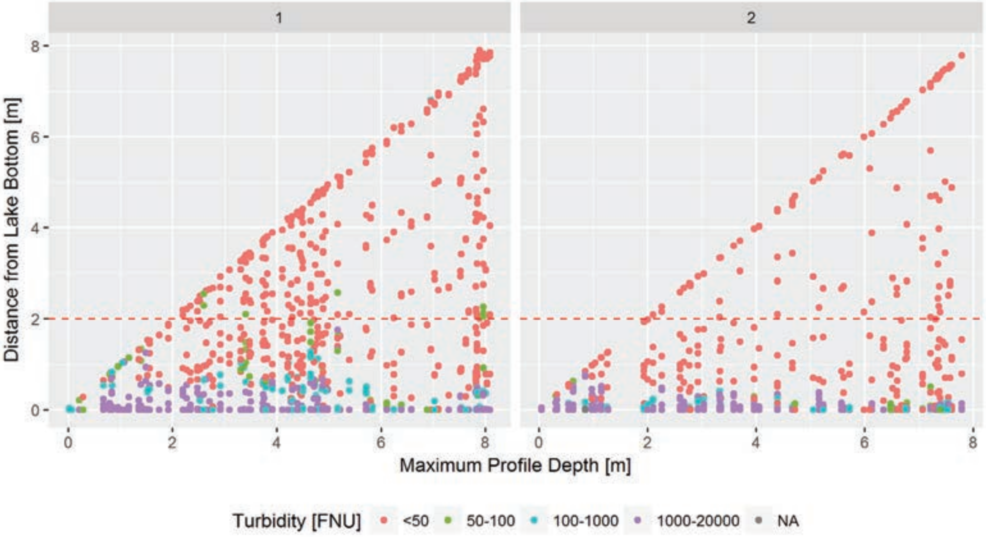

__Figure 2:__ Turbidity Readings through Water Column over two Separate Lake Surveys, for February (1) and March (2).

concentration from the samples collected in the turbid layer was approximately 900 mg/L. The mass of total suspended sediment was calculated by multiplying concentration by the volume of the turbid layer. Without additional snapshots, there is insufficient data to assess whether the mass of solids will change over time, and if change occurs, whether it will impact the density of the layer or the volume of space it occupies.

3. Wind Mixing Cover

According to the MEND Design Guide for Subaqueous Disposal of Reactive Tailings (MEND, 1998), a water cover design is required to ensure the consolidated bed of tailings is not entrained or remobilized. The report identifies five processes which may impact solids entrainment. Based on the surface area, lake depth, and climate of the region, wind waves are the sole process to be considered.

Inputs to the water cover design include median grain size, wind speed, fetch length, sediment density and water density.

Grain Size and Density: Particle size distribution analysis was performed by the client on composite samples from solids in the northern extents of the lake. The average of two sample sets presented a median grain size equal to 4.2 microns. A particle density of 2300 kg/m^3 was used based on review of literature for kaolin clays.

Fetch Length: Both west to east and north to south fetch lengths were modelled. The maximum was north to south. The maximum fetch length was used for this assessment.

Wind Speed: Wind speed was evaluated from regional analysis of available meteorological stations within 100 km of the site. The longest record consisted of 56 years of wind speed, including mean daily wind speed, daily maximum sustained wind speed, and daily maximum wind gust. According to Lawrence (2015), design wind speed needs to be sustained for a minimum duration. For this purpose, the maximum wind gust measurements were not considered.

Frequency analyses were performed on the annual maximum values for both the daily average and daily maximum wind measurement. Selection of the appropriate design criteria and type of wind condition to be used for the water cover calculations is typically based on risk tolerance and engineering judgement. Two wind speeds modelled were:

- Daily wind speed expected to occur once every 20 years.
- Maximum daily sustained wind speed expected to occur once every average year.

Sensitivity analyses were performed on the median grain size, particle density and fetch length as well as wind speed, which identified wind speed and fetch length as the more critical parameters. Based on the sensitivity to wind speed, two wind covers were included in the capacity assessment based on the wind conditions described above:

- Wind cover of 2.0 m, based on the 20-year daily average wind speed.
- Wind cover of 3.0 m, based on the average year maximum sustained wind speed.

These cover depths were applied to the surface of the lake in conjunction with the turbidity offset on the projected tailings surface, where sediment re-suspension would be expected to occur at the intersection of both offsets. This case study shows results for the larger wind cover of 3.0 m.

4. Particle Settling Distance

Tailings particles will be in suspension near the active deposition zone and could be mobilized in the lake until sufficient freshwater cover is maintained. The offset distance from the decant structure to the suspended tailings particles was estimated based on Stokes Law for terminal settling velocity (British Columbia Ministry of Environment, 2015). Effective flow area in the lake enabled calculation of the settling length required from the decant structure. Additional inputs included median grain size, particle density, discharge rate from the lake, and water viscosity.

Discharge rate from the lake was regularly measured at the weir in the decant. An average discharge rate was used for the purpose of the settling calculations. The same grain size and particle density values were used as in the wind cover design calculations. The geometry of the lake suggested that flow may short-circuit the system, resulting in a reduced effective flow width towards the decant structure. Sensitivity analyses identified effective flow width and particle diameter as the most sensitive parameters to settling distance.

A factor of safety of 2 was applied to the minimum settling distance result from a potentially reduced effective flow width, producing a minimum settling distance of 300 m.

The application of Stokes Law for particle settling assumes that turbidity levels will reduce with particle settlement. There is often a trend with turbidity and suspended sediment concentrations, however additional factors can also increase turbidity. For the purpose of this study, it is assumed that turbidity levels will be reflected in the particle settlement in the lake.

Conceptual Model

In combining the turbidity layer offset, water cover, and the calibrated deposition results, a model was developed to capture the lake behaviour after continued deposition. The 5-year, 10-year, 15-year and 20-year tailings volumes were deposited onto the most recent bathymetric survey from December 2016 to generate the projected consolidated tailings surface. The turbid layer offset of 2.0 m was applied to the top of the consolidated tailings surface, and the wind cover depth of 3.0 m was applied to the water surface. The conceptual model and its limitations to capacity are presented on a north to south cross-section in Figure 3, illustrating the projected 10-year tailings solids surface.

The distance from the intersection point of the wind cover and the turbidity offset to the decant structure was calculated from the combined model to evaluate the effective settling distance under each projected tailings scenario. The offset distance based on 10 years of tailings deposition was found to be 387 m, which is greater than the required settling distance of 300 m. From these results, there is good confidence that the tailings lake can continue to operate for a minimum of 10 years. Based on the limited survey information at the time of the study, capacity beyond 10 years was not guaranteed, however, the number of deposition years remaining to produce a 300 m settling distance with a 3 m wind offset is approximately 16 years. Continued monitoring and confirmation of turbidity layer behaviour through repeated surveys will be performed in late 2018 to update the capacity assessment.

Conclusions

A conceptual tailings deposition model was generated based on four limiting factors to

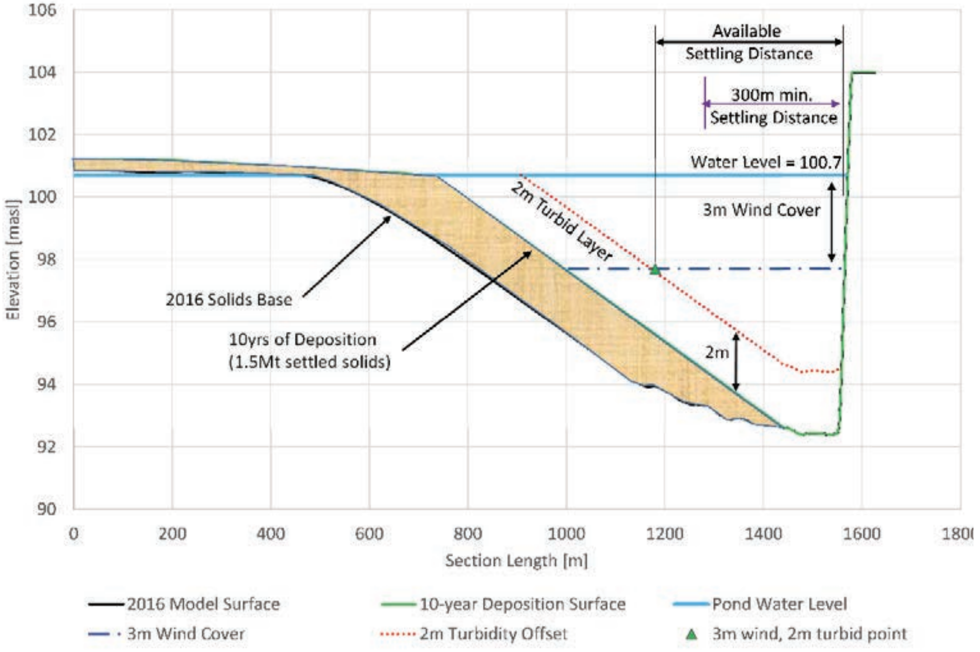

Figure 3: Conceptual Model along North-South Cross-Section of Tailings Lake

evaluate lake capacity. These include wave action, unsettled tailings, beach progression and settling distance. The model inputs were validated through two lake surveys to verify the lake was behaving in a predictable and consistent manner, as well as calibrated in a deposition software. Sensitivity analyses for model parameters, and the capacity of the structure in terms of remaining years of use, estimated there to be a minimum of 10 years based on currently available information.

The behaviour of the unsettled tailings layer was studied over a two-month period. These findings represent a snapshot of the tailings lake system, which does not capture potential seasonal variation. The projections assume that the system will continue to operate in a steady-state condition, with the underlying assumption that the unsettled tailings volume will not change over-time. Repeat surveys are required to confirm the turbidity layer thickness and total suspended solids concentrations to validate and model the tailings deposition over time.

Collection of particle size distributions for the material in suspension would provide greater confidence in the settling distance offset. A conservative factor of 2 was applied to account for this uncertainty, however in-situ testing, for example with tracer element monitoring, could be used to validate these calculations.

References

British Columbia Ministry of Environment. (2015). *Technical Guidance 7: Environmental Management Act. Assessing the Design, Size, and Operation of Sediment Ponds Used in Mining. Version 1.0.* Environmental Protection Division.

Environmental Systems Research Institute (ESRI). (2016). ArcGIS Spatial Analyst. Release 10.4.1. Redlands, CA.

Gregory A. Lawrence, E. W. (2015). Suspended Solids in an End Pit Lake: Potential Mixing Mechanisms. *NRC Research Press. Vol 43*, 211-2017.

MEND. (1998). *Design guide for the Subaqueous Disposal of Reactive Tailings in Constructed Impoundments. MEND Project 2.11.9.* Sponsored by Placer Dome Inc.

An integrated mineralogy-based modelling framework for the simultaneous assessment of plant operational parameters with acid rock drainage potential of tailings

Megan Becker[1,2], Edson Charikinya[1], Sithembiso Ntlhabane[1], Marcelene Voigt[1,2,4], Jennifer Broadhurst[1], Susan TL Harrison[1,3], Dee Bradshaw[1]

[1] *Minerals to Metals Initiative, Dept of Chemical Engineering, University of Cape Town, Rondebosch, 7700, South Africa, megan.becker@uct.ac.za*

[2] *Centre for Minerals Research, Dept of Chemical Engineering, University of Cape Town, Rondebosch, 7700, South Africa*

[3] *Centre for Bioprocess Engineering Research, Dept of Chemical Engineering, University of Cape Town, Rondebosch, 7700, South Africa*

[4] *Economic Geology Competency, Council for Geoscience, Bellville, 7530, South Africa*

Abstract

An integrated process modelling framework, underpinned by mineralogy, is under development at the University of Cape Town as a holistic approach towards addressing the multifaceted challenges currently faced in mining. This paper demonstrates application of this approach for the case of a polymetallic base metal sulfide flotation circuit. In this case study, the effect of potential design strategies and feed ore variability on net acid producing potential of the resulting tailings is assessed. The framework is underpinned by mineralogical calculations of acid potential and neutralising potential. Application of the framework allows for the identification of potential opportunities towards more sustainable mining practice.

Keywords: mineralogy, framework, ore variability, flotation

Introduction

The minerals industry is facing numerous multifaceted challenges ranging through the techno-economic, environmental and social domains, including increased ore variability, lower grade and more mineralogically complex ores, rising operating costs and lower profit margins, increased awareness and accountability of the environmental footprint of mining operations and the growing need to obtain and maintain a social license to operate. The generation of acid rock drainage (ARD) and the associated consequences of this heavy metal bearing, sulfate rich, acidic leachate on the surrounding environment is the key concern here. In order to address these challenges effectively and collectively, a holistic approach is required. In such an approach, the ability to compare scenarios, evaluating the various trade-offs between the techno-economic, environmental and social indicators, is needed (Tuazon et al. 2012).

Given the key role mineralogy plays in both valuable and deleterious metal deportment, metallurgical process design and optimisation and consequent environmental effects (Skinner 1976; Hochella 2002; Broadhurst et al. 2007; Becker 2018), it is an essential component in the design of the framework. In the context of ARD, it is the relative abundance of both acid forming and neutralising minerals, their mineral chemistries and the textural inter-relationships that play a pivotal role in determining whether ARD is generated, how much is generated, what is its composition and what are the relative time scales of the reactions.

The development of an integrated modelling framework is under development by researchers at the University of Cape Town which gives recognition to the critical role of mineralogy in the design of environmentally and socially responsible primary mineral beneficiation processes. The initial development of this modelling framework focused on a case study of a polymetallic sulfide ore flotation circuit (Ntlhabane et al. 2018). The circuit sequentially recovers the different metal sulfides to produce Cu (chalcopyrite), Pb (galena) and Zn (sphalerite) concentrates respectively. The final tailings are sent either to the tailings dam or used as backfill when required. This initial work focused on setting up a unique ore-specific element-to-mineral conversion (EMC) recipe to calculate mineral grades from chemical assays (Whiten 2008). Thereafter, a set of mineral distribution functions were developed for modelling and prediction of mineral grades across the flotation circuit under different scenarios. Mineralogical calculations of acid potential and neutralising potential were then performed to determine a theoretical 'mineralogical' net acid producing potential of the final tailings.

The objective of this paper is to further demonstrate the application of the integrated framework using the case study of Ntlhabane et al. (2018) on several different operating scenarios. Complementary static chemical tests are used to validate the mineralogical predictions of the acid producing potential of the tailings sample.

Methods

Full details of the initial sampling of the case study flotation circuit and associated chemical and mineralogical characterisation are provided in Ntlhabane et al. (2018). Mineralogical predictions of acid potential (APmin) and neutralising potential (NPmin) were calculated using the concepts of the approaches behind Paktunc (1999) and Lawrence and Scheske (1997). Laboratory chemical tests following the methods of Weber et al. (2004) and Miller et al. (1997) were used to determine the acid neutralising capacity (ANC) and net acid generation (NAG). Maximum potential acidity (MPA) was calculated from the Leco S assay after which the net acid producing potential (NAPP) was calculated.

A model describing the base case operations of the polymetallic base metal sulfide flotation circuit considered in this study was developed (Ntlhabane et al. 2018). HSC Chemistry 8 software was used as the platform to develop the integrated framework. Scenarios aimed at predicting the effects of improved concentrate recovery and the impact of ore variability on final tailings acid rock drainage potential were analysed. Monte Carlo simulation was used to evaluate each scenario.

Results and Discussion

The mineralogical composition of the sulfide ore to the flotation circuit and the final tailings as calculated using the EMC recipe of Ntlhabane et al. (2018) is given in Table 1. It is a massive magnetite - sulfide ore consisting of notable amounts of chalcopyrite, galena, sphalerite and pyrrhotite. Pyrrhotite is the dominant acid producing sulfide mineral with very minor pyrite present. The limitations of the EMC method are that the grades of both pyrite and pyrrhotite cannot be simultaneously calculated using solely chemical assays and therefore only pyrrhotite is reported. Quartz, biotite, garnet and magnetite are the dominant gangue minerals. No carbonate minerals are present. Following separation and concentration of chalcopyrite, galena and sphalerite by flotation, the tailings consist of only minor economic sulfides (0.6 wt. % in total), but with significant pyrrhotite (3.8 wt.%) with the potential to form ARD.

***Table 1** Mineralogy of the feed and final tails calculated using EMC (see Ntlhabane et al. 2018)*

Minerals (wt. %)	Feed Final tails
Chalcopyrite	2.3 0.2
Galena	5.1 0.2
Sphalerite	5.3 0.2
Pyrrhotite*	4.1 3.8
Garnet**	8.6 9.9
Biotite***	2.9 3.3
Quartz	21.1 24.3
Barite	0.9 1.0
Magnetite	49.6 57.2

* includes pyrite, ** almandine, spessartine and pyroxmangite, *** annite and chamosite

Based on both the knowledge of the mineral grades and chemistry, a theoretical acid producing potential (APmin) and neutralising potential (NPmin) can be calculated (Table 2). The AP is calculated directly from the sulfide mineral grades as 94.8kg H_2SO_4/t for the feed, and 47.4kg H_2SO_4/t for the final tails. Calculation of the NP considered all minerals with the potential to provide neutralising capacity, specifically those that are fast, intermediate or slow weathering, i.e. garnet, biotite and chlorite. This ore, however, has a notably strong Fe-Mn tenor which is reflected in the mineral chemistry of the silicates (Fe-rich biotite, Fe-rich chlorite, Fe-Mn-rich garnet). Consequently none of these silicate minerals were considered to provide neutralising capacity due to the presence of oxidisable cations and the NPmin was estimated at zero for both the feed and tailings. Both samples are classified as potentially acid forming based on their mineralogy.

The MPA calculated using the conventional approach (Table 2) directly from the S assay is considerably higher than the APmin. This is attributed to the assumptions of the standard method that the dominant sulfide is pyrite (a disulfide) and not pyrrhotite (a monosulfide). In this case the APmin is considered a more reliable estimate suitable for input to the modelling framework. The experimentally derived ANC indicates a potential neutralising capacity of 31 kg H_2SO_4/t. It is however recognised, that the harsh and aggressive chemical conditions of the ANC tests may overestimate neutralisation capacity. In this case the presence of silicate minerals containing oxidisable metal cations (Fe, Mn) are unlikely to provide any real long term neutralising capacity. The overall NAPP and NAG pH indicate both samples are classified as potentially acid forming.

Analysis of the base case based on measured plant data (Ntlhabane et al. 2018) showed a recovery of chalcopyrite of 77% with a mineral grade of 67 wt. % in the Cu bank. The copper (chalcopyrite) concentrate showed moderate dilution with pyrrhotite (26 wt. %), and minor dilution by sphalerite (2 wt. %) and galena (3 wt. %). Sphalerite (zinc) and galena (lead) achieved higher recoveries over 90% in the Zn and Pb banks, respectively. The following observations of the base case plant operation were key to formulating two scenarios for further investigation (see Figure 1): (a) The payable metal content of the Cu concentrate was only 95% due to significant dilution by pyrrhotite. An opportunity existed to further upgrade the concentrate and increase the payable metal content. (b) The final tailings consisted of over 50% magnetite and could be explored as a possible saleable magnetite product. The active intervention in formulating scenario I is the addition of an appropriate flotation reagent to depress pyrrhotite so it is recovered to the tailings instead of concentrate (chemical intervention). The active intervention in formulating scenario II is the installation of a magnetic separator to the final tailings of the existing circuit (Figure 2) to generate a magnetic fraction and a non-magnetic fraction (physical intervention). In both scenarios, the grade of pyrrhotite to the final tailings would be affected having a direct consequence on the estimated APmin of the final tailings. A sensitivity analysis was also conducted to assess the effect of feed ore variability on the two scenarios.

***Table 2** Summary of the chemical and mineralogical ARD characteristics.*

Parameter (units)	Plant feed Final tails
Total S (wt. %)	4.7 2.3
MPA (kg H2SO4/t)	143.8 70.4
ANC (kg H2SO4/t)	30.5 ±5.8 32.5 ± 7.1
NAPP (kg H2SO4/t)	113.5 37.9
NAG pH	2.88 ± 0.01 2.83 ±0.01
AP min (kg H2SO4/t)	145.3 47.4
NP min (kg H2SO4/t)	0 0
ARD classification	Potentially acid forming Potentially acid forming
ARD classification (min)	Potentially acid forming Potentially acid forming

When running the simulations it was assumed that: (a) recovery of pyrrhotite to the copper concentrate and consequent dilution of concentrate grade was not due to poor chalcopyrite liberation (recovery of com-

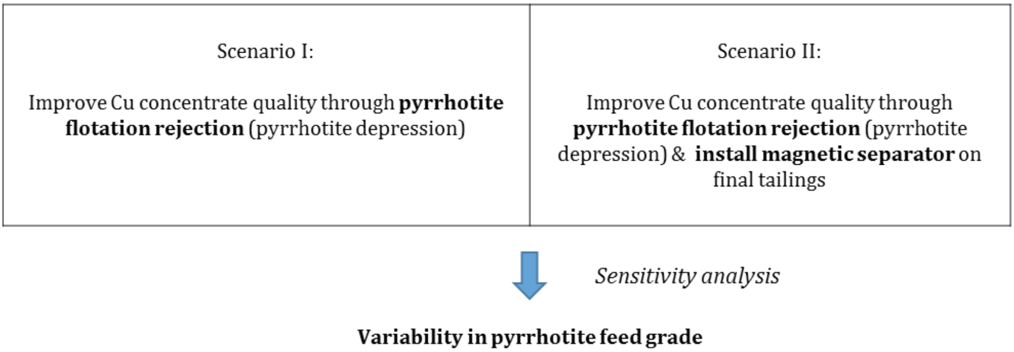

Figure 1 *Matrix of the different scenarios considered.*

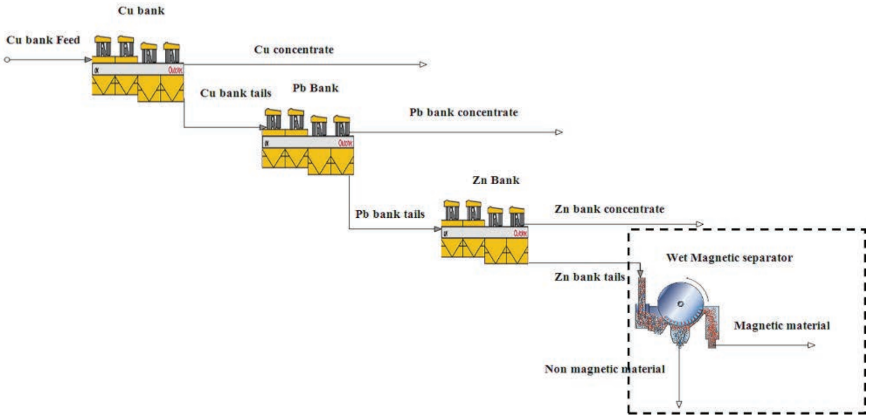

Figure 2 *Flotation circuit configurations considered for the scenario analysis. Boxed inset illustrates the circuit modification for scenario II.*

posite pyrrhotite-chalcopyrite particles) and (b) the pyrrhotite present was magnetic 4C pyrrhotite (Becker et al. 2010) that could be simultaneously recovered with magnetite using a wet magnetic separator. The sensitivity analysis only considered changes in pyrrhotite feed grade to the flotation circuit and other mineral recoveries remained constant.

The results of scenario analyses are illustrated in Figure 3. In scenario I, the effect of improving Cu concentrate grade by rejecting pyrrhotite to the tailings, resulted in a decrease in pyrrhotite recovery to the concentrate and a consequent increase in pyrrhotite tailings grade up 4.5 wt. % corresponding with an APmin of 53 kg H_2SO_4/t. In scenario II, where pyrrhotite is rejected to the flotation tailings and thereafter recovered by magnetic separation, resulted in a minimum APmin to 15 kg H_2SO_4/t for the final tailings (non-magnetic fraction). The sensitivity analysis of scenario I where pyrrhotite feed grade was varied (up to 8.1 wt. % in feed) resulted in an increase in pyrrhotite tailings grade corresponding with an increase in APmin to a maximum of 88 kg H_2SO_4/t. The sensitivity analysis of scenario II (up to 8.1 wt. % in feed), resulted in an overall decrease in pyrrhotite tailings grade with a maximum APmin of 29 kg H_2SO_4/t for the final tails (non-magnetic fraction).

Comparison of the absolute differences in APmin for the two scenarios and their sensitivity analyses (Figure 3) shows that the variability in pyrrhotite feed grade has the greatest effect on the modelled APmin. Ore variability therefore represents a significant challenge in both the processing of this ore and tailings management. Upfront knowledge of this variability on the scale of the geometallurgical block model ahead of mining and processing represents a significant opportunity of managing this variability and its consequent techno-economic and environmental effects (Wil-

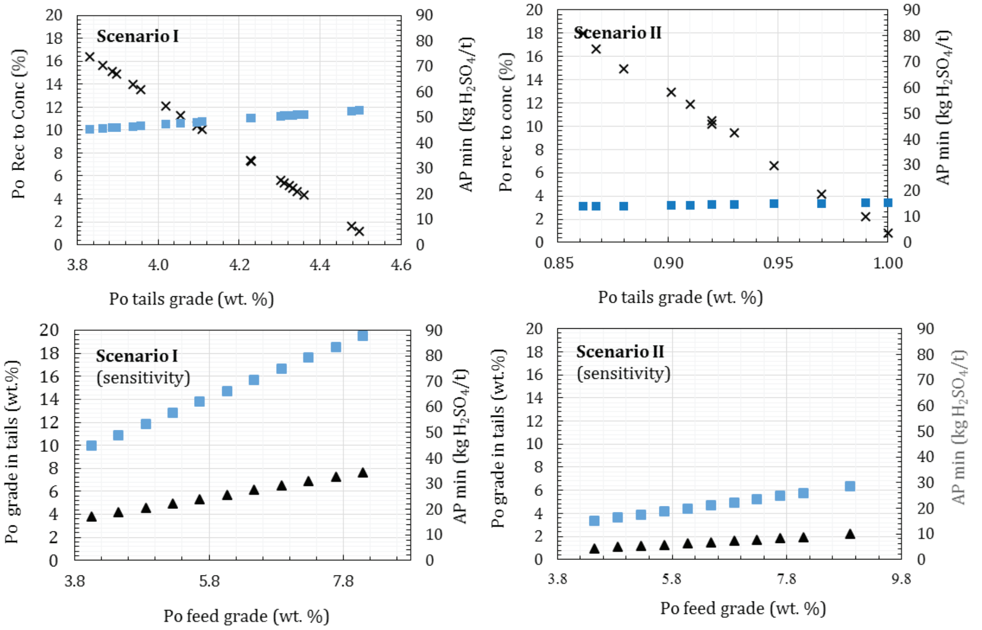

Figure 3 *Modelled AP min for the two scenarios analysed with their associated sensitivity analysis (see text for detail). ☐ indicates AP min, X indicates pyrrhotite (po) tails grade and Δ indicates pyrrhotite feed grade.*

liams and Richardson 2004). The consequence of upgrading payable metal content of the copper concentrate, by rejecting pyrrhotite to the flotation tailings has a notably smaller effect on the modelled APmin. With the installation of a magnetic separator in scenario II this could be partially alleviated. The viability of scenario II however, relies on two tailings products: a magnetic fraction containing both pyrrhotite and magnetite and a non-magnetic silicate rich product. With further processing the magnetic fraction could potentially be amenable for sale as a magnetite by-product, and the non-magnetic fraction could possibly become non-acid forming. In the case of scenario II, such a concept is consistent with a cleaner production approach similarly to that demonstrated by Hesketh et al. (2010) and Harrison et al. (2015).

Conclusions

This paper has demonstrated the first-order application of an integrated modelling framework to a polymetallic base metal sulfide ore. Mineralogical information provided a powerful input to the framework allowing the effect of ore variability and plant operating parameters on the acid potential of the resulting tailings to be evaluated.

The scenario analyses highlighted the opportunity to reduce the acid potential of the flotation tailings by actively rejecting pyrrhotite during flotation, and installing a magnetic separator to the final tailings. In both cases, a potential techno-economic advantage exists – to increase the payable metal content of the copper concentrate, and to produce a magnetite concentrate by-product. Further investigations should explore the viability of such interventions. The sensitivity analyses indicated that changes in pyrrhotite feed grade to the flotation circuit have a significant effect on the modeled acid potential of the tailings (almost double the APmin relative to the base case). Upfront knowledge of this variability ahead of mining provides an opportunity to manage these effects.

Development and application of such an integrated framework provides a new approach to addressing the multifaceted challenges faced as the industry strives for more sustainable mining practice.

Acknowledgements

Grateful thanks to Tolbert Golela for performing the ARD static characterisation tests.

This work is based on research supported in part by the South African Research Chairs Initiative (SARChI Chair in Minerals Beneficiation held by DB) of the Department of Science and Technology and National Research Foundation of South Africa. Any opinions, findings and conclusions or recommendations expressed in any publication generated by the NRF supported research is that of the author(s), and the NRF accepts no liability whatsoever in this regard.

References

Becker M (2018) Mineralogy: Underpinning sustainable processes and decision making. In: Digby C, Bradshaw D, Mostert H, Chicksen B (eds) Green Mining: Beyond the Myth. Juta, Cape Town, pp 32–33

Becker M, de Villiers J, Bradshaw D (2010) The mineralogy and crystallography of pyrrhotite from selected nickel and PGE ore deposits. Econ Geol 105:1025–1037

Broadhurst JL, Petrie JG, von Blottnitz H (2007) Understanding element distribution during primary metal production. Miner Process Extr Metall 116:1–16. doi: 10.1179/174328507X163751

Harrison STL, Franzidis JP, van Hille RP, et al (2015) Minimising the formation of acid rock drainage through management of the disposal of sulphidic waste rock and tailings, Water Research Commission Report 2015/1/13.

Hesketh AH, Broadhurst JL, Harrison STL (2010) Mitigating the generation of acid mine drainage from copper sulfide tailings impoundments in perpetuity: A case study for an integrated management strategy. Miner Eng 23:225–229. doi: 10.1016/j.mineng.2009.09.020

Hochella MF (2002) Sustaining Earth: Thoughts on the present and future roles of mineralogy in environmental science. Mineral Mag 66:627–652. doi: 10.1180/0026461026650053

Lawrence RW, Scheske M (1997) A method to calculate the neutralization potential of mining wastes. Environ Geol 32:100–106. doi: 10.1007/s002540050198

Miller SD, Robertson A, Donahue T (1997) Advances in Acid Drainage Prediction using the Net Acid Generation (NAG) test. In: 4th International Conference on Acid Rock Drainage. Vancouver, Canada, pp 533–549

Ntlhabane S, Becker M, Charikinya E, et al (2018) Towards the development of an integrated modelling framework underpinned by mineralogy. Miner Eng 116: 123-131. doi: 10.1016/j.mineng.2017.09.013

Paktunc AD (1999) Mineralogical constraints on the determination of neutralization potential and prediction of acid. Environ Geol 39:103–112

Skinner B (1976) A Second Iron Age Ahead? The distribution of chemical elements in the earth's crust sets natural limits to man's supply of metals that are much more important to the future of society than limits on energy. Am Sci 64:258–269

Tuazon D, Corder G, Powell M, Ziemski M (2012) A practical and rigorous approach for the integration of sustainability principles into the decision-making processes at minerals processing operations. Miner Eng 29:65–71. doi: 10.1016/j.mineng.2011.10.017

Weber PA, Thomas JE, Skinner W, Smart RS. (2004) Improved acid neutralisation capacity assessment of iron carbonates by titration and theoretical calculation. Appl Geochemistry 19:687–694

Whiten B (2008) Calculation of mineral composition from chemical assays. Miner Process Extr Metall Rev 29:83–97. doi: 10.1080/08827500701257860

Williams SR, Richardson JM (2004) Geometallurgical mapping: a new approach that reduces technical risk geometallurgical mapping. In: Proceedings of the 34th Annual Canadian Mineral Processors Meeting. Ottawa, Canada, pp 1–13

Geochemical assessment of Metal/Metalloid release by contrasting laboratory methods; The importance of secondary minerals

R.J. Bowell[1,2], D.J. Sapsford[2], B.M.Dey[2], K.P. Williams[2]

[1]*SRK Consulting, Churchill House, 17 Churchill Way, Cardiff, Wales, UK CF10 2HH rbowell@srk.co.uk*
[2]*School of Engineering, Newport Road, Cardiff, Wales, UK*

Abstract

Polymetallic arsenic-rich mineralized waste from Penberthy Croft, an abandoned copper-tin mine in South West England, hosts a unique assemblage of more than 200 oxide zone minerals. In addition, sulfide minerals, are also present in the exposed mine waste. Such material exposed to oxygen and water can generate acidic drainage with levels of metals/metalloids and present a potential environmental hazard. A challenge in the management of such waste is the prediction of long term future changes in the material with the most common method of humidity cell tests requiring a long lead period for prediction and uncertainty in the termination of the tests when they are considered complete.

The aim of the study was to assess different methods for the prediction of long term potential for metal/metalloid and acid release. This evaluation was achieved comparing results of agitated bottle roll tests and selective chemical extraction (SCE) to the results of humidity cell testwork on the sample material. Material characterization utilized mineralogy, whole rock geochemistry and aqua regia digest to select representative samples.

From the extraction results the agitated bottle roll tests provided a high concentration of metals and metalloids from the partly oxidized dominated samples to an aqua regia digest. By contrast, both the sulfide dominated samples and the pure oxide sample showed significantly lower concentration of metals in the bottle roll rinse tests compared to aqua regia. Utilizing selective extraction, the results can be interpreted in terms of potential mineral fractions showing release of highly soluble secondary forms but not iron oxides or sulfide mineral fractions.

Agitated oxygenated bottle roll tests could generate similar total release to standard humidity cells at various times for each material, particularly for reactive sulfide and partly oxidized sulfide samples but also consistent results for less reactive sulfides. The accelerated rate of oxidation within the cells provide a good determination of mineral reactions and a clear plateau in the results may be indicative of termination in reaction of available sulfides. Mass balance calculations from residue samples indicated similar release mass in the two tests. By comparison the oxide material showed similar release quantum to the sum of weeks 1-4 of the humidity cell results.

Keywords: ARDML prediction, laboratory testwork, secondary minerals

Introduction

Sulfide oxidation occurs when oxygen and water contact sulfide mineral surface and is catalysed by bacteria and ferric iron in nature (Nordstrom, 2011). The result is the potential generation of acidic sulfate-rich waters hosting variable concentrations of metals and metalloids. Dependent on the presence of minerals able to neutralize acid and attenuate metals and metalloids. The prediction of such reactions is an important aspect in the environmental assessment of mine waste (Blowes et al 2014; Williams and Diehl, 2014). Standard practice in the mining industry is the application of leach tests particularly humidity cells (Williams and Diehl, 2014). These are cells or columns executed with repeated cycles of alternating dry and humidified air cycles used to simulate element release under accelerated weathering conditions. They provide information on element release but limited speciation information inside the cell and in recent years these have come under scrutiny and may not always deliver the expected results and are sensitive to a number of potential artefacts in the operation and mechanism of the test undertaken (Sapsford et al 2009; Erguler and Erguler, 2015; Maest and Nordstrom 2017).

To assess the chemical and mineralogical changes in the weathering of sulfide material and thereby better understand their retention and release during weathering, selective chemical extraction was applied (Keon et al 2001). Unfortunately, the performance of such tests is prone to limitations due to incomplete dissolution of non-target phases (Tlustoš et al 2005) as well as incomplete removal due to re-adsorption or re-precipitation. In addition, another partial extraction method, bottle roll leaching was also assessed. These are a traditional metallurgical test used to determine "maximum" extractable metal in the presence of a reagent and like selective chemical extraction has limitations. The results were mass balanced and compared back to the whole rock geochemistry to assess quantum of elements mobilized over a given period of time and compared to mineral speciation to predict potential mechanisms of release in the cells. Although other factors such as particle size, frequency of sampling and presence of bacteria are important (Sapsford et al 2009; Erguler and Erguler, 2015; Maest and Nordstrom 2017) in this paper the focus is only on the mineralogical controls.

Site Description

Penberthy Croft is situated approximately 1.5 km northeast of the village of Goldsithney in the parish of St Hilary, Cornwall. It produced tin, copper and lead from a series of predominantly east-west lodes hosted by rocks of the Mylor Slate formation of Upper Devonian age. The mines were active in the 17th and 18th century (Betterton, 2000). Initially worked for high grade cassiterite lodes they were subsequently mined through to the mid-20th century for the rich copper supergene zone and the mixed copper-tin lower grade hypogene mineralization. The mineralisation is a multi-stage, polymetallic hydrothermal vein system and consists of several, but distinct overlapping assemblages: Minor, burial-related quartz-albite-anatase-monazite veins of a pre-tectonic, metamorphic origin; main-stage high-temperature hypothermal-mesothermal Sn-Cu-As-W veins; later lower-temperature epithermal Pb-Zn sulfide mineralisation; and a late-stage, low-temperature Fe-Mn mineralisation.

Subsequent supergene oxidation and weathering of lodes resulted in the formation of complex gossans with oxide and supergene enrichment zones. Post-mining formation of other minerals both underground and on the dumps, has resulted in a very large variety of mineral species in a small area. These in order of approximate abundance include arsenates, arsenate-sulfates and phosphates. The greatest diversity in terms of species has been located in five main areas of the old dumps: Three in the western and two in the eastern section of the workings. Most minerals here are found as good quality subhedral to euhedral microcrystals with occasional miniature specimens. Brecciation, fracturing, silicification, chloritization and carbonatization are abundant. The mineralisation formed over a very wide period of time extending from the Upper Palaeozoic through to the Cenozoic.

An extensive suite of supergene minerals has been found in the deposit and on the associated dumps including, in approximate order of abundance, arsenates, sulfates, arsenate-sulfates and phosphates with various oxide, carbonate, hydroxide and sulfide minerals also present (Betterton, 2000). The site has been listed as a SSSI by English Nature for its mineralogy in 1993.

Methods

Sample Description

For the purpose of this study, four samples were composited from surface material on the dumps at Penberthy Croft and these are summarised in Table 1.

Mineralogical identification was by fine powder X-Ray Diffraction (XRD). Samples were prepared from the testwork material as dry powders (for SEM). XRD analysis was carried out on pulverised samples of the precipitates. Bulk analyses were carried out on

Table 1. *Summary description of the four laboratory samples*

Sample	Sample Description	Major mineralogy
PC001	Reactive sulfides, no secondary minerals	Pyrite, marcasite, chalcopyrite, sphalerite, galena, tennantite, arsenopyrite, quartz, chlorite, siderite
PCCOO2	Low reactivity sulfides Minor secondary minerals	Chalcocite, sphalerite, galena, quartz, muscovite, calcite, siderite, ankerite, linarite, anglesite
PC003	Oxide ore	Goethite, quartz, scorodite, hidalgoite, kaolinite, monazite-La, duftite, dolomite, birnessite
PC004	Transitional oxide/sulfide	Balydonite, beudantite, pharmacosiderite, goethite, olivenite, annabergite, duftite, malachite, hidalgoite, stilpnomelane, carminite, pyrite, chalcopyrite, arsenopyrite, quartz, kaolinite, orthoclase, beaverite, brothanthite, mixite

the samples. Scans were run using the Philips PW1710 Automated Powder Diffractometer using Cu Kα radiation at 35kV and 40mA, between 2 and 70° 2θ at a scan speed of 0.04° 2θ/s. From the scans, phases were identified using Philips PC-Identify software and from the peak areas, semi quantitative analysis was performed and a percentage of each phase present calculated. Weighting factors were applied where necessary.

Two methods of Whole Rock Geochemistry were undertaken, analysis by X-Ray Florescence using a factory calibrated Olympus Delta hand held instrument and additionally in the laboratory utilizing an Aqua Regia digest comprised of 3:1 concentrated nitric and hydrochloric acid and adjusted to a 3M solution.

Selective Extraction

A selective extraction to a sub-split of each of the samples to determine them major mineral hosts for metals in the samples. This approach utilized a previously published scheme (Keon et al 2001; Bowell et al 2013). The method applied was completed to determine metal and metalloid speciation and mobility in the material. It utilizes a comprehensive 8-step extraction scheme (Keon et al. 2001), which includes the following extraction steps: (i) 1M $MgCl^2$ (for ionically-bound As); (ii) 1M NaH_2PO_4 (strongly adsorbed); (iii) 1M HCl (acid volatile sulphides, carbonates, Mn-oxides and very amorphous Fe oxyhydroxides); (iv) 0.2M oxalate/oxalic acid (amorphous Fe oxyhydroxides); (v) 0.05M Ti(III)–citrate-EDTAbicarbonate (crystalline Fe oxyhydroxides); (vi) 10M HF (As oxides and silicates); (vii) 16M HNO_3 (pyrite, arsenopyrite, tenantite, chalcopyrite, and pyrrhotite); and (viii) hot 16M HNO_3+ 1M HF +30% H_2O_2 (recalcitrant minerals such). This work was completed at the School of Engineering,Cardiff University and involved analysis by ICP-AES. Precision from standard solution analysis was ±5%.

Agitated Oxygenated Bottle Roll Tests

The bottle roll tests involved the placement of 3 kg charge of rock material into a 10 L barrel that was also filled with 3 L of water and had an air line into the barrel. This was placed on an agitated roller table and run continuously for 24 hours. The solution was then decanted and analysed.

Humidity Cell Test

The ASTM Procedure for humidity cell tests (ASTM D-5744-13e1) was applied in this study. The test follows a seven-day cycle during which water is trickled over the rock. After draining, dry air is circulated through the cell for 3 days followed by humidified air at 25°C for 3 days. On the seventh day, the sample is rinsed with an equal mass of distilled water and the extracted solution is collected for analysis. The leachate from the test is then chemically analysed by kone analyser for anions and ICPOES for metals and metalloids. Element release percentage was determined against a re-constituted head grade for the column utilizing released element concentrations and residue material concentration.

Results

Whole Rock Geochemistry

Selected results of Aqua Regia and XRF analysis of the four samples are provided in Table 2.

Table 2. *Whole Rock Geochemistry for As, Pb in ppm and Sulfide-S in wt%*

Element	Leco/XRF	Aqua Regia-ICPOES	Sample
Sulfide-S	3.76		PC001
	1.48		PC002
	0.09		PC003
	0.75		PC004
Arsenic	785	543	PC001
	46.7	23.4	PC002
	39.4	37.6	PC003
	553	497	PC004
Lead	13,300	11,800	PC001
	26,500	19,600	PC002
	350	298	PC003
	13,700	12,900	PC004

These show reasonable correlation in the oxide and partially oxidized samples but less so with the primary sulfide samples indicating a portion of the metals in these samples (and probably sulfide minerals) are encapsulated in resistant materials such as feldspar or quartz.

Selective Extraction

The selective extraction results demonstrate that in all samples some arsenic is present in secondary minerals (Figure 1) even in relatively apparent primary sulfide samples reflecting the challenge of sampling dump material. However, in the sulfide samples at least 60% or more of the arsenic is present as exposed sulfide minerals or as sulfides encapsulated in resilient silicate minerals.

By contrast lead is dominated by its presence in galena in the primary samples or by anglesite, cerussite and bayldonite in the secondary material. Although secondary in nature these minerals have low solubility compared to other secondary minerals and as such limit the mobility of lead in the environment.

Copper and zinc show a similar trend to lead but both contain a higher fraction in the amorphous oxide and strongly adsorbed fractions. Iron is dominated in the sulfides in PC001 and PC002 and as crystalline oxides in PC003. In PC004 it shows even distribution between carbonate fraction and crystalline oxide fraction.

Bottle roll tests

The four samples were subject to a 24-hour agitated oxygenated leach in a 1:1 mix with a reagent. In metallurgical work this is a common test using an acid leach, however in this study distilled water was used. The results for selected metals is shown in Table 3.

The addition of oxygen to an agitated leach certainly increases the potential to leach metals from the assemblages. The similarity in arsenic leaching levels in PC001, 002 and

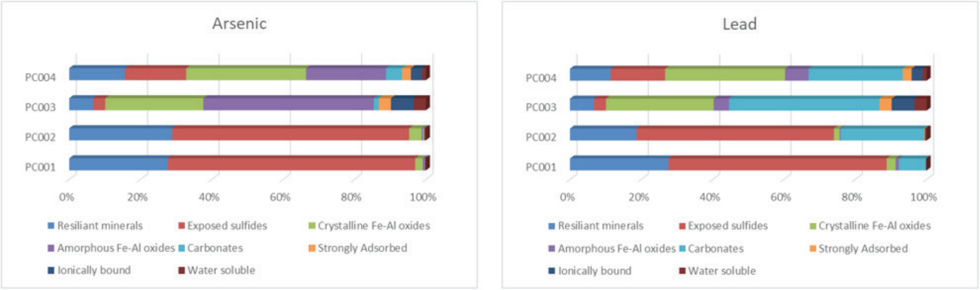

Figure 1 *Results of Selective Extraction Testwork for Arsenic and Lead*

Table 3. Results of Bottle Roll Tests (in mg/L)

Element	PC001	PC002	PC003	PC004
Arsenic	216	11.3	38.5	172
Copper	439	332	42.7	566
Iron	1070	238	334	411
Lead	89.7	130	5.6	17.8
Zinc	2100	2460	32.1	1760
Cadmium	71.4	65.4	11.4	26.7
pH	2.87	4.2	5.73	3.36

004 is perhaps a reflection of the dominant arsenic speciation in the crystalline secondary mineral fraction.

Humidity Cell Tests

Humidity cell tests were executed on the four samples for 100 weeks and during this time showed variable trend, consistent with typical humidity cells. Triplicates of the main cell were also run such that sacrificial cells could be terminated at weeks 4, 20 and 40 as well as week 100.

From the results in Table 4 it can be observed that utilising parts of the selective chemical extraction results it is possible to obtain similar mass balances for element release to those for different stages in the humidity cell.

The results indicate that by week 4 of the humidity cell most of the weakly held and water-soluble components are removed. This reflects benefit of flushing. Importantly the general held view that secondary minerals are flushed in early irrigation is not supported here and suggests secondary minerals are more complex. By week 20 of the humidity cell a portion of the secondary minerals are mobilized particularly soluble sulfates and simple salts. By week 40 only a small incremental amount of secondary minerals are mobilized and still no where near the balance of secondary minerals. For these samples the combination of cyclic irrigation and oxidation appear to mobilize much of the exposed sulfide in these samples as well as the majority of secondary minerals. The element release observed in the agitated leach bottles was not observed in week 40 and by qualitative estimate from leachate chemistry took until week 53 to see similar releases from the sulfide fraction. This indicates that for this material at least, a 52 week plus humidity cell program is required to leach the more reactive sulfide component and more than 100 weeks to leach the exposed sulfide component.

Discussion

Agitated oxygenated bottle roll tests were able to generate similar total release to standard humidity cells at various times for each material, particularly for reactive sulfide and partly oxidized sulfide samples but also consistent

***Table 4.** Mass Balance Release Rates, humidity cells, bottle rolls and prediction of labile load from SCE analysis for Arsenic*

Test	PC001	PC002	PC003	PC004
Water soluble (SCE)	0.2	0.5	9.8	4.2
Secondary Minerals	2.8	4.2	80.1	63
Exposed sulfides	69.4	66.4	3.4	17.2
Agitated Bottle Roll	27.6	24.1	97.7	31.1
Humidity cell, week 4	0.4	0.4	7.2	5.3
Humidity cell, week 20	2.6	3.7	90.2	34.7
Humidity cell week 40	3	4.1	92.3	36.4
Humidity cell week 100	65.7	68.3	93	82.6

results for less reactive sulfides. The accelerated rate of oxidation within the cells provide a good determination of mineral reactions and a clear plateau in the results may be indicative of termination in reaction of available sulfides. Mass balance calculations from residue samples indicated similar release mass in the two tests. By comparison the oxide material showed similar release quantum to the early weeks 1-4 of the humidity cell results.

All leaching tests, including HCTs provide only partial information about the redistribution of elements within the material being tested (Nordstrom and Maest, 2017). In this context, the protocols tested here appear complementary to each other and ideally if combined provide an integrated approach to characterizing geochemical weathering of mine waste and allow better conceptualization of the mechanisms dominating redistribution of chemical elements in weathering.

Conclusions

Mineralogy is an important control on water-rock interaction in the assessment of mine waste geochemistry. Artefacts in leaching protocols are not uniform with different mineral assemblages and understanding this is an important factor in the design of a laboratory program. Development of the understanding of mineralogy of a mine waste in critical not only in the interpretation but also the design of leaching tests and should be integral data collected prior to and during their execution.

Acknowledgements

The authors thank the David Howard of St Aubyn Estate, Marazion, Cornwall for access to Penberthy Croft and English Nature for approval to collect samples there.

References

Betterton J 2000 Famous Mineral Localities: Penberthy Croft mine, St Hilary, Cornwall, England. UK J.Mines Minerals, 20, 7-37

Blowes DW, Ptacek CJ, Jambor JL, Weisener CG, Paktunc D, Gould WD, Johnson DB 2014 Chapter 5: The Geochemistry of Acid Mine Drainage. In: volume 11, Treatise on Geochemistry, 2nd edition. 131-190.

Bowell RJ, Rees S, Barnes A., Prestia A, Warrender R, Dey, M. (2013). Geochemical assessment of arsenic toxicity in mine site along the proposed Mineral Tramway Project, Camborne, Cornwall. Geochemistry, Exploration, Environment, Analysis 13(2), 145-157

Diehl SF Williams RD (eds) 2014 Techniques for Predicting Metal Mining Influenced Water. SME, Colorado. 137p.

Erguler ZA, Erguler GK 2015 The effect of particle size on acid mine drainage generation: Kinetic column tests. Minerals Engineering 76, 154-167

Keon NE, Swartz CH, Brabander DJ, Harvey C, Hemond HF2001. Validation of an arsenic selective chemical extraction method for evaluating mobility in sediments. Environmental Science and Technology, 35, 2778–2784.

Maest AS, Nordstrom DK 2017 A geochemical examination of humidity cell tests. Applied Geochemistry 81, 109-131

Nordstrom DK 2011 Hydrogeochemical processes governing the origin, transport and fate of major and trace elements from mine wastes and mineralized rock to surface waters. Applied Geochemistry 26, 1777-1791.

Sapsford DJ, Bowell RJ, Williams KP, Dey BM 2009 Humidity cell tests for the prediction of acid rock drainage. Minerals Engineering 22, 25-36.

Tlustoš P, Száková J, Stárková A, Pavlíková D 2005 A comparison of selective chemical extraction procedures for fractionation of arsenic, cadmium, lead, and zinc in soil. Central European Journal of Chemistry, 3 830-851.

The Challenges of Predictive Numerical Calculation within Hypersaline Brines: Examples from Lithium Brines

Julien Declercq[1], Camilo de los Hoyos[2], Ruth Griffith[1] and Rob Bowell[1]

[1]*SRK Consulting (United Kingdom) 5th Floor, Churchill House, 17 Churchill Way, Cardiff, CF10 2HH, Wales, UK, jdeclercq@srk.co.uk*

[2]*SRK Consulting (Argentina), Av. Emilio Civit 404, (M5502GVR) Ciudad de Mendoza, Argentina*

Abstract

Lithium brines, today's main lithium source have been increasingly studied in recent years. Geochemical modelling can be used to predict the operational or underground brine lithium concentrations, but it can also be applied to ground stability prediction. However hypersaline systems are challenging to model due to the inaccuracies introduced by elevated ionic strength when using the extended Debye-Hückel theory. A different approach, such as Pitzer is required. However, while generally internally consistent, this database is limited in the number of phases and elements it contains and therefore has limited predictive power. To overcome this issue, a literature review was undertaken.

Keywords: Numerical Modelling, Pitzer, PHREEQC, Lithium, Brines

Introduction

Lithium is understood by many to be the "fuel of the future", as it is at the core of a post-fossil fuel economy. Along with several niche applications, such as technical grease, medication, lithium is now used essentially within batteries for electric vehicles and smart technologies, smartphone and wearable devices of all kinds. Lithium can be considered a fuel in the sense that, while electric car batteries will eventually be recycled, it is unlikely that the lithium contained in most wearables will be.

Lithium can be mined conventionally or extracted from naturally-enriched continental brines hosted within endorheic lakes (e.g. Evans 2014). It is currently understood that 60% of the global lithium resource is hosted in continental brines in South America (Bolivia, Chile and Argentina) with some appreciable lithium brine in the southwest USA, Australia and Israel. Owing to their preponderance as a source of lithium, brine formation has been increasingly studied in recent years (e.g. Evans 2014).

Numerical predictive calculations applied to lithium brines are mostly used to predict the operational concentrations or grade, of lithium being produced. However, it can be used as an optimisation tool for the lithium extraction process, and it can also be applied to the prediction of ground stability caused by changes in hydrogeological conditions or to the modelling of the lithium concentration within the underground brine. The high salinity of the brines produces a high ionic strength, generally above 3 compared to 0.72 for seawater (Nordstrom et al 1979) is a source of challenges for both the laboratory analysis and predictive numerical calculations. Many analytical methods are impacted by salt effects which can cause interferences with the analyses being carried out. Generally diluting the sample will allow reduce the salt effects and for the analysis to be carried out. However, dilution and *a fortiori* repeated dilution of the same sample introduces errors in the analysis and can cause matrix effects. Owing to the critical nature of lithium brine, efforts have been undertaken globally to determine thermodynamical parameters allowing its modelling.

The aim of this paper is to provide the readers with published lithium parameters to use within the Pitzer framework, including the reproduction of endorheic lake chemistry from the literature and an example of numerical modelling of lithium processing from brine via evapoconcentration.

Methods

Thermodynamic equilibrium calculations are based on the law of mass action to calculate mineral solubility and saturation indexes. However, the ionic strength of a solution has a significant effect on the thermodynamic properties of ions. For instance, with increasing ionic strength aqueous complexing will lower the activity of free ions. Illustrating the importance of aqueous complexing and activity corrections Appelo and Postma (2005) calculated the difference between activity and concentration for a 3.5% seawater at pH 8.22 and found differences of 30% for Na^+, 40% for Cl^-, 50% for SO_4^{2-},60% for Mg^{2+} and Ca^{2+}, and 15% for HCO_3^-. Using the extended Debye-Hückel theory to adjust the standard Gibbs energy and enthalpy to the desired ionic strength will perform well for solutions of ionic strength up to 0.7 mol/L or 2 mol/L if HCO_3^- and SO_4^{2-} are low (Parkhurst 1990). Brine and *a fortiori* lithium brine are far more concentrated, and to provide a semblance of approximation would require a different calculation method. The Pitzer equations (e.g. Pitzer 1981) have been developed for these ionic strengths.

These equations were first described by Pitzer to understand the behaviour of ions in high ionic strength. The parameters of the Pitzer equations, such as the osmotic coefficient, mixed ion activity coefficients, and salt solubility are derived from various experimental data. They are more rigorous than the equations of specific ion interaction theory, but also more numerous and difficult to determine experimentally.

Sets of those parameters have been measured and compiled since the 1970s, first by Kim and Frederick (1988) for single salts in aqueous solutions at 298.15 K. Then for some complex electrolytes, Ge et al. (2007) obtained a new set of Pitzer parameters. The Pitzer database for PHREEQC (Parkhurst and Appelo 1999). is built upon the formalism defined by Pitzer and derived from the database developed for the program PHRQPITZ (Plummer et al 1988). This database is build and extend on the compilations of Harvie et al. (1984), updated by the data for minerals from Deer et al. (1997), a temperature and pressure dependant volume of aqueous species, using parameters obtained from Johnson et al., 1992 and data compiled by Laliberté (2009).

Despite these efforts the Pitzer database for PHREEQC is extremely limited with 14 elements and 54 mineralogical phases compared to 29 elements and 71 different minerals for the PHREEQC database, by comparison the LLNL database has over 1000 phases described. This status signifies that the Pitzer database is internally consistent but has limited predictive power outside of the few elements and phases covered. In the context of lithium brine, only a few mixing parameters are defined, and no Li bearing phases are defined. To overcome this issue, a literature review must be undertaken to integrate lithium and lithium phases in the database.

Parameters and values from Monnin et al., 2002 and Meng et al., 2014, can be used to integrate lithium within the Pitzer database. Values for lithium bearing species can be found in other studies, e.g. Rard et al. (2007) and the entire work on the Yucca Mountain Project "data0.ypf.R2" (BSC 2007). While numerous Li bearing mineralogical phases are summarised in other Debuy-Huckel databases these phases are not described with the Pitzer formalism and analogue phases have to be used. This method introduces errors that are difficult to quantify. The parameters summarised (Table 1) in Song et al 2017 were used in this study.

In addition, oxygen was defined as a specie and several phases were recalculated from other databases distributed with PHREEQC version 3.4.0-12927. H_2O and $O_2(g)$ was recalculated from Minteq v4 database, distributed with PHREEQC while Li_2CO_3, LiCl, Lime and Hydrophilite ($CaCl_2$) were ported from the Lawrence Livermore National Laboratory (LLNL) database. It is understood that adding elements and phases in this manner reduces the degree of internal consistency of the database and introduces error that can only be corrected by recalculating all the parameters existing within the database.

Case Study

A brine is a solution containing high amount of dissolved salts of higher concentration than seawater (> 3.5%). Solutions of lower concentrations are defined as saline water (1-3.5%), Brackish water (0.1-1%) and fresh-

Table 1 *Compilation of Pitzer parameters used in this study.*

-B0			-PSI			
Li+	Cl-	0.20818	Cl-	SO4-2	Li+	-0.0124
Li+	SO4-2	0.14396	Cl-	SO4-2	Na+	0.0014
-B1			Cl-	SO4-2	Mg+2	-0.048
Li+	Cl-	-0.0726	Cl-	SO4-2	K+	-0.022
Li+	SO4-2	1.17736	Na+	Li+	Cl-	0.0057
-C0			Na+	Li+	SO4-2	-0.006
Li+	Cl-	-0.0042	Na+	K+	Cl-	-0.0074
Li+	SO4-2	-0.0571	Na+	Mg+2	Cl-	-0.0078
-THETA			Na+	Mg+2	SO4-2	-0.01
Na+	Li+	0.02016	K+	Li+	SO4-2	-0.0018
Na+	Mg+2	0.07	K+	Li+	Cl-	-0.012
Na+	K+	-0.012	K+	Mg+2	SO4-2	-0.015
K+	Li+	-0.0508	K+	Mg+2	Cl-	-0.008
K+	Mg+2	0	Mg+2	Li+	Cl-	-0.0059
Mg+2	Li+	0.0102	Mg+2	Li+	SO4-2	-0.0006
Cl-	SO4-2	0.02				

water (< 0.1%). Lithium brine are typically defined as hypersaline, with salinity ranging between 1.7 and 24 times that of seawater, with the Atacama high lithium brine reaching up to 3.1 g/L. Typical examples of brine chemistry are defined in Table 2. The ocean concentration is consistent with the chemistry defined by Nordstrom et al 1979.

The commercial production of lithium from brine, despite local differences in elemental composition, concentrations and physical parameters, follow generally the same processing methodology (Garrett, 2004). This methodology is used because they face the same issues of low concentrations and presence of potentially fouling components (such as magnesium). Most commercially exploited brine deposits are located in endorheic basins that are favourable to evapoconcentration. As a low-cost method, it is generally adopted and is represented in our idealized process route illustrated in Figure 1.

The first step in the process is to preconcentrate the brine via solar evaporation. Ideally up to 90% of evaporation occurs and the resulting brine is used in lithium production. This degree of evaporation corresponds to an ideal concentration of 6 wt.% of lithium in

Table 2 *Typical lithium brine chemistry (e.g. Evans 2014; Song 2017).*

Elements	Ocean	Clayton valley, USA		Salar de Atacama, Chile		Qarhan Salt Lake, China		Zhabuye Salt Lake, China	
g/L		min	max	min	Max	Min	Max	min	max
Li	0.0001	0.2	0.4	1.1	3.1	0.10	12.25	0.5	1
K	0.038	5.3	10	18	29.7	-	-	26.4	38.3
Mg	0.12	0.3	0.6	8.2	15.3	8	119	0	0.01
Ca	0.04	0.2	0.5	0.2	0.4	-	-	0	0.1
B	0.0004	0	0.1	0.6	0.7	-	-	2.9	14.6
Na	1.05	62	75	10.3	91.0	-	-	106.6	108.1
Cl	1.9	101	117	20.3	189.5	-	-	121.6	123.1

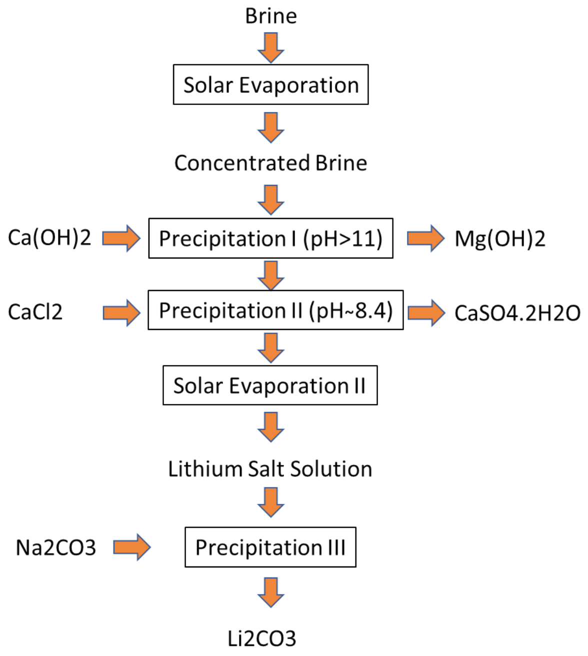

Figure 1 *Generalized Process for Lithium Bearing Brines (modified from Garrett, 2004)*

solution. This concentration has been defined as the "end point" or "drying-up point" (e.g. Galli et al. 2014).

The development of an increasingly saturated brine solution through evapoconcentration forces saturation with respect to lower solubility salts (e.g. anhydrite, halite) and a resulting brine solution that contains a progressively higher concentration of more soluble components such as lithium and boron. Lithium concentrations of 0.32 g/L to 2.75 g/L can be reached in such systems, however in carbonate rich brines lithium can settle as Li_2CO_3 crystals (Yu et al. 2015). While this allow for the recovery of some lithium, optimisation procedures consisting of removal of fouling elements (e.g. Mg, SO_4) will allow for an increase in efficiency. The formation of battery grade LiCl and Li_2CO_3 using an evaporation-precipitation-crystallization route requires the initial separation and precipitation of magnesium and calcium carbonates from the pre-concentrated brine (e.g. Boryta 2011; Galli et al. 2014). Although variations exist they typically use low cost reagents to precipitate calcium and magnesium as sulfate or carbonate salts at high alkalinity concentrations. Typically, solar evaporation has a recovery of approximately 50%, however the lithium carbonate process has a demonstrated recovery of above 80% (Pistilli 2013)

Calculations

The parameters defined in Table 1 were used to calculate elemental speciation, saturation indexes for different brines and reproducing the lithium extraction process described in Fig. 1.

The example of the Atacama brine, using maximum concentrations is illustrated in Fig. 2 and 3. Those figures illustrate the increase in concentration from the brine as evaporation occurs, from 0.16 g/L to 1.44 g/L. The addition of $CaCl_2$ and $Ca(OH)_2$ allows the precipitation of Mg and SO_4 trough the precipitation of brucite and gypsum. The ultimate step, addition of Na_2CO_3 allows the precipitation of $LiCO_3$ with a modelled recovery of 87.5%. Allowing $LiCO_3$ to precipitate without addition of Na_2CO_3 yield a predicted recovery rate of 39.6%. These values, are broadly in line with operating brine operations and indicate the validity of this numerical approach.

The use of less concentrated solutions, such as seawater and Zhabuye Salt Lake requires the second evapoconcentration step to allow suf-

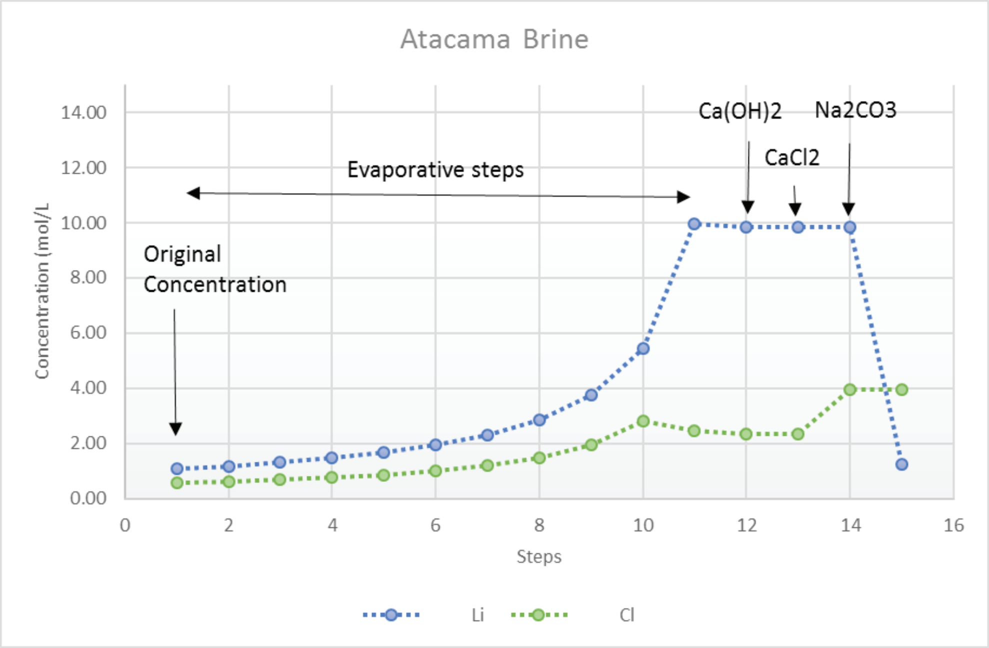

Figure 2 *Evolution of the Li and Cl concentrations in the Atacama brine as a function of the progress of the process*

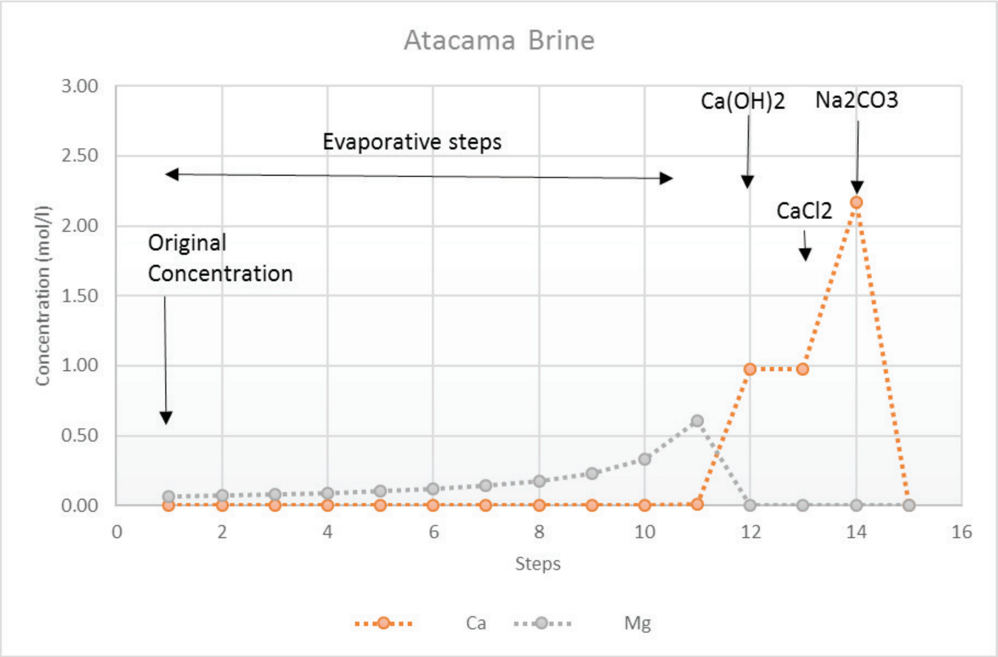

Figure 3 *Evolution of the Ca and Mg concentrations in the Atacama brine as a function of the progress of the process*

ficient for a sufficient increase in Li concentration to make this process economical.

Conclusions

The literature review and addition of Pitzer parameters of importance for the accurate modelling of lithium brine using the Pitzer formalism should allow for more accurate geochemical modelling of both lithium concentration within the brine, such as isopach calculations, but also, as exemplified in this study the calculation of lithium extraction processes. The predictions of Atacama brine showed therein illustrates the capacity of the model to reproduce the recovery rates of mentioned by Pistilli. While this result is encouraging, using the Pitzer formalism for more general predictions would still require a massive overall and update of the existing databases.

Acknowledgements

The authors thank SRK Consulting UK and AR for providing the financial support for this study.

References

Appelo, C.A.J. Postma, D. (2005). Geochemistry, Ground Water and Pollution. 10.1201/9781439833544.

Boryta, D.A. (2011). Production of Lithium Compounds Directly from Lithium Containing Brines. US Patent No. 8057764 B2.

BSC (Bechtel SAIC Company) (2007). In-Drift Precipitates/Salts Model. ANL-EBS-MD-000045 REV 03. Las Vegas, Nevada: Bechtel SAIC Company. DOC.20070306.0037.

Deer, W. A., Howie, R. A., & Zussman, J. (1997). Rock-forming minerals. Geological Society.

Evans, K. (2014). Lithium in: Critical Metals Handbook, Gunn, G (ed). Wiley & Sons Ltd, 230-260

Galli, D. E., Humana, D., de las Mercedes Otaiza, M., del Rosario Cachagua, C., & Santillan, R. E. (2014). U.S. Patent No. 8,641,992. Washington, DC: U.S. Patent and Trademark Office.

Garrett, D. (2004). Handbook of Lithium and Natural Calcium Chloride, first ed. Elsevier Academic Press, Amsterdam.Ge, X., Wang, X., Zhang, M., & Seetharaman, S. (2007). Correlation and prediction of activity and osmotic coefficients of aqueous electrolytes at 298.15 K by the modified TCPC model. Journal of Chemical & Engineering Data, 52(2), 538-547.

Harvie, C. E., Møller, N. and Weare, J. H. (1984). The prediction of mineral solubilities in nature waters: The Na-K-Mg- Ca-H-SO4-OH-HCO3-CO3-H2O system to high ionic strengths at 25 °C. Geochim. Cosmochim. Acta, 48, 723-751. Johnson, J. W., Oelkers, E. H., & Helgeson, H. C. (1992). SUPCRT92: A software package for calculating the standard molal thermodynamic properties of minerals, gases, aqueous species, and reactions from 1 to 5000 bar and 0 to 1000 C. Computers & Geosciences, 18(7), 899-947.

Kim, H. T., & Frederick Jr, W. J. (1988). Evaluation of Pitzer ion interaction parameters of aqueous mixed electrolyte solutions at 25. degree. C. 2. Ternary mixing parameters. Journal of Chemical and Engineering Data, 33(3), 278-283.

Laliberte´ M. (2009) A model for calculating the heat capacity of aqueous solutions, with updated density and viscosity data. J. Chem. Eng. Data 54, 1725–1760.

Meng, L., Li, D., Deng, T., and Guo, Y. (2014). Experiment and Pitzer Model Prediction for the Solid+ Liquid Equilibria of the Ternary System LiCl–CaCl2–H2O. Acta Geologica Sinica (English Edition), 88(s1), 356-358.

Monnin, C., Dubois, M., Papaiconomou, N., & Simonin, J. P. (2002). Thermodynamics of the LiCl+ H2O system. Journal of Chemical & Engineering Data, 47(6), 1331-1336.

Nordstrom, D. K., Plummer, L. N., Wigley, T. M. L., Wolery, T. J., BALL, J. W., Jenne, E. A., ... & Hoffman, M. (1979). A comparison of computerized chemical models for equilibrium calculations in aqueous systems.

Parkhurst, D. L. (1990). Ion-association models and mean activity coefficients of various salts.

Parkhurst, D. L., & Appelo, C. A. J. (1999). User's guide to PHREEQC (Version 2): A computer program for speciation, batch-reaction, one-dimensional transport, and inverse geochemical calculations.

Pistilli, M. (2013). POSCO's lithium brine processing technology could be a game changer: Vancouver, British Columbia, Canada, Lithium Investing News, April 4

Pitzer, K. S. (1981). Characteristics of very concentrated aqueous solutions. Physics and Chemistry of the Earth, 13, 249-272.

Plummer, L. N., Parkhurst, D. L., Fleming, G. W., & Dunkle, S. A. (1988). A computer program incorporating Pitzer's equations for calculation of geochemical reactions in brines. US Geological Survey Water-Resources Investigations Report, 88(4153), 310.

Rard, J. A., Clegg, S. L., & Palmer, D. A. (2007). Isopiestic determination of the osmotic and activity coefficients of Li2SO4 (aq) at T= 298.15 and 323.15 K, and representation with an extended ion-interaction (Pitzer) model. Journal of solution chemistry, 36(11-12), 1347-1371.

Song, W., Gang, H., Ma, Y., Yang, S., & Mu, B. (2017). Migration Behavior of Lithium during Brine Evaporation and KCl Production Plants in Qarhan Salt Lake. Minerals, 7(4), 57.

Yu, J., Zheng, M., Wu, Q., Nie, Z., Bu, L. (2015). Extracting lithium from Tibetan Dangxiong Tso Salt Lake of carbonate type by using geothermal salinity gradient solar pond. Sol. Energy 115, 133–144.

Hydrogeobotany in mine water studies

Gareth Digges La Touche[1], Freddy Brookes[2]

[1]*Golder, 20 Eastbourne Terrace, London, W2 6LG, United Kingdom, gdltouche@golder.com*
[2]*Golder, Cavendish House, Bourne End Business Park, Cores End Road, Bourne End, Buckinghamshire, SL8 5AS, United Kingdom*

Abstract

Geobotanical methods and application have a long heritage dating back centuries. Although there were minor peaks in the publishing of geobotanical studies, by Scandinavian and Canadian researchers, in the 1940s and late 1940s to mid 1950s respectively, the use of geobotanical methods only started to grow rapidly in the 1960s. This growth was principally driven by the need of the Soviet Union to establish the mineral resources of the state through a large scale programme of geological mapping (Brooks, 1972). While geobotanical methods became established, although they are far from mainstream, in mineral exploration their application in other geoscience fields has been limited. This paper will explore the application of geobotany to mine water studies.

Geobotany is currently very rarely used in the field of groundwater exploration due to the single discipline approach that is common in current practice. Geobotany, which in this instance may be better referred to as hydrogeobotany or ecohydrogeology, requires a holistic multi-disciplinary approach that draws not only on the disciplines of hydrogeology and hydrology, but also botany, soil science and chemistry. The most useful plants to the hydrogeologist are those whose presence or morphology can provide data about the hydrogeological setting. These indicator plants can be the source of information about the depth to groundwater, fluctuations in groundwater levels and groundwater chemistry.

The application of hydrogeobotany when integrated with conventional hydrogeological approaches has the potential to provide a valuable addition to conventional hydrogeological work flows. This paper will explore some of the concepts and the applications of hydrogeobotany as applied to mine water practice. For example: how it is possible to distinguish between plants that can tolerate high levels of certain metals (metallophyte) and plants that are wholly reliant on the presence of these metals (obligate metallophytes); and how certain plants may be used as indicators of groundwater depth or soil moisture conditions. The paper will conclude with some practical applications that can be readily applied to mine water studies.

Keywords: ecohydrology, geobotany, hydrogeobotany, ecohydrogeology

Introduction

The assessment of the impact of proposed mining operations on groundwater is often constrained by a lack of groundwater information beyond the immediate footprint of the proposed mine. So any information that can help develop a conceptual model of the hydrogeological regime is valuable.

Geobotanical methods have a long pedigree in geological studies, in particular in mineral exploration. Brooks (1972) reports minor peaks in the publishing of geobotanical studies, by Scandinavian and Canadian researchers, in the 1940s and late 1940s to mid 1950s respectively and that the use of geobotanical methods only started to grow rapidly in the 1960s. This later growth was driven principally by large scale mapping programmes in the Soviet Union that were needed to establish the mineral resources of the state (Brooks, 1972). While geobotanical methods became established, although they are far from mainstream, in mineral exploration their application in other geoscience fields has been limited.

In parallel to mineral exploration, or perhaps even preceding, it geobotany has played a role in groundwater studies with the Roman architect Vitruvius reporting on the use of plants to locate water sources (Gwilt, 1826) and the United States Geological Survey (USGS) publishing a water supply paper on the subject in the 1920s (USGS, 1927).

Geobotany in groundwater studies

While geobotany, or more aptly hydrogeobotany, in groundwater studies has clearly been established for some time it is not a commonly applied tool in modern groundwater studies. It has gained more recent prominence in Europe as a direct result of the European Commission Water Framework Directive 2000/60/EC (European Commission, 2000), which presents a requirement for a more holistic consideration of the water environment and impacts on ecological receptors as well as on the chemical quality of the water, however this ecohydrological approach has a focus on understanding groundwater supported ecosystems rather than using geobotanical methods as a tool for understanding groundwater.

Ecohydrological methods can however be equally be applied to determining the nature of the hydrogeological regime through application of the hydrogeobotanical method. The aim is to use plants to provide information regarding the groundwater regime in terms of depth to groundwater and or groundwater quality. What indicators are useful will vary depending on the environment, thought the common theme should be for the hydrogeologist to observe the environment in a holistic manner recording and taking note of floral assemblages as much as they record information relating to the geology or water features.

At the simplest level vegetation growth in arid regions can often indicate groundwater discharge zones as springs and oases (fig. 1 and 2), whereas in temperate regions the density of vegetation may indicate the depth to groundwater and the range of groundwater level fluctuation (fig. 3)

More subtly in tropical and subtropical regions the absence of trees and bushes may indicate the presence of calcrete horizons (fig. 4) indicative of differing soil conditions and vadose zone processes.

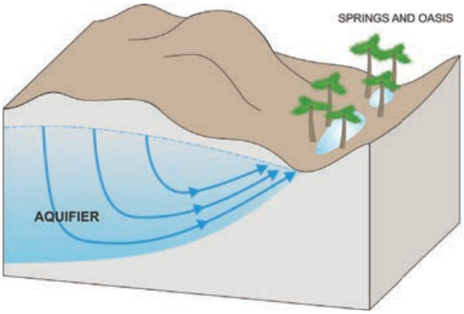

Figure 1 Vegetation around springs and oasis as indicators of groundwater discharge in arid regions (after International Association of Hydrogeologists, 2016).

Figure 2 Vegetation supported by perineal spring flow from a fracture conduit.

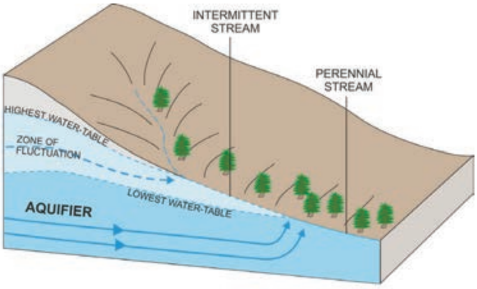

Figure 3 Vegetation density variation around a perineal stream in an area of fluctuating groundwater levels (after International Association of Hydrogeologists, 2016)

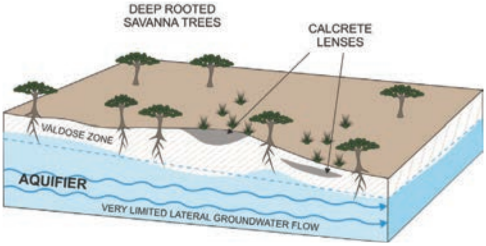

Figure 4 Tree growth controlled by the presence of calcrete lenses (after International Association of Hydrogeologists, 2016)

Direct indicators

Some plants are very direct indicators of particular geochemical conditions in the soil, for example the Alpine Pink (*Viscaria Alpina*) is an indicator of the prescence of copper (Brooks, 1972), hence the Viscaria Copper Mine in Sweden, and Milk Vetch (*Astragalus spp*) can be an indicator of selenium and uranium (Brooks, 1972), whereas others such as Couch Grass (*Agropyron repens*) typically indicate shallow groundwater and Marsh Marigolds (*Caltha palustris*) in wetland areas can be good indicator of a groundwater discharge into a surface water body (Rosenberry et al, 2000).

In more arid areas, such as for example the Sinai Desert, the height of a plant may also provide information regarding the groundwater regime. For example it is reported that the Manna tree grows to a mature height of approximately 1 m when groundwater is between 2 m and 5 m below ground level, but only to around 0.5 m tall when groundwater levels are deeper than about 8 m (Lewis, 2012). Similar controls on tree height are seen in eucalyptus (Bot, 2014) where maximum heights of greater than 25 m were recorded where groundwater depths were less than 5 m, but for example height was restricted to approximately 16 m where groundwater depths were greater than approximately 10 m (Zolfaghar *et al*, 2014).

An understanding of the types of tree present can also provide a constraint on the depth to groundwater as part of the development of a conceptual hydrogeological model. A number of studies have been published with regard to rooting depth (e.g. Stone and Kalisz, 1991) and while rooting depth does not necessarily indicate the depth to groundwater few trees develop well established root systems below the groundwater table. One reliable indicator of shallow groundwater is the presence of Mesquite (*Prosopis* spp) (Verma *et al*, 2015), native to the southern United States and northeastern Mexico but introduced and considered an invasive species in parts of Africa, Asia, and Australia. Another example is the Willow (*Salix* spp) which does not grow where groundwater depths are greater than approximately 3 m (Lewis, 2012).

Application

As outlined above the key is to establish what are the indicators present in the area of study. This may most readily be achieved through liaison and ideally working with biologists and ecologists familiar with the area and establishing the key indicators. The acquisition of hydrogeobotanical data should then be incorporated as part of reconnaissance and groundwater mapping studies. The benefit of such an approach was recognised by Tóth (1966) who recommended the inclusion of vegetation mapping as part of a groundwater mapping study commenting that it was, for a regional study, likely more cost effective than drilling a small number of boreholes.

The following general workflow is advocated:

- Establish indicator species and or assemblages for the area of interest;
- Incorporate vegetation mapping as part of the hydrogeological mapping or reconnaissance study;
- Formulate initial conceptual hydrogeological model constrained by the collated data;
- Acquire additional data as required (e.g. boreholes, spring surveys);
- Refine conceptual model and test using available geobotanical data and results of ecological surveys undertaken as part of environmental and social impacts assessment (ESIA) studies.

Conclusions

The application of hydrogeobotanical methods to groundwater investigations for mine impact assessments in areas with limited or no existing data has the potential to provide a valuable addition to conventional hydrogeological approaches. The use of hydrogeobotanical methods can facilitate the development of better constrained hydrogeological conceptual models at an earlier stage of study in the absence of conventional hydrogeological data acquired from drilling boreholes and monitoring groundwater levels and quality. In addition it may allow additional refinement when combined with conventional hydrogeological data, or at least constrain our conceptualisation of a groundwater system.

References

Zolfaghar S, Villalobos-Vega R, Cleverly J and Eamus C (2014) The influence of depth-to-groundwater on structure and productivity of *Eucalyptus* woodlands. Australian Journal of Botany, 62(5):428-437

Brooks RR (1972) Geobotany and biogeochemistry in mineral exploration. Harper & Row Publishers, 290 pp

European Commission (2000) Directive 2000/60/EC of the European Parliament and of the Council of 23 October 2000 establishing a framework for Community action in the field of water policy.

Gwilt J (1826) The architecture of Marcus Vitruvius Pollio in ten books. Translated from the Latin. Prestley & Weale. 413 pp

International Association of Hydrogeologists (2016) Ecosystem conservation and groundwater. Strategic Overview Series. https://iah.org/wp-content/uploads/2016/04/IAH-SOS-Ecosystem-Conservation-Groundwater-9-Mar-2016.pdf

Lewis J (2012) The application of ecohydrological groundwater indicators to hydrogeological conceptual models. Groundwater, 50(5), pp.679-689

Rosenberry DO, Striegl RG and Hudson DC (2000) Plants as indicators of focused groundwater discharge to a northern Minnesota lake. Groundwater, 38(2), pp.296-303.

Stone EL, Kalisz PJ (1991) On the maximum extent of tree roots. Forest Ecology and Management, 46, pp.59-102

Tóth J (1966) Mapping and interpretation of field phenomena for groundwater reconnaissance in a prairie environment, Alberta, Canada. Hydrological sciences Journal, 11(2), pp.20-68.

United States Geological Survey, 1927. Plants as indicators of groundwater. Water Supply Paper 577, 95 pp

Verma R, Jayanti T, Vinoda SK, Shivappa, Gowda ANS (2015) Tree species as indicators of ground water recharge and discharge. International JOuranl of Engineering and Technical Research, 3(11), pp.127-135

Bacterial ecology of biofilms sustaining pollution by acid mine drainage near mining areas in Mpumalanga Province – South Africa

E. Fosso-Kankeu and J. Redelinghuys

Water Pollution Monitoring and Remediation Initiatives Research Group, School of Chemical and Minerals Engineering, North-West University, South Africa, elvisfosso.ef@gmail.com; Elvis.FossoKankeu@nwu.ac.za

Abstract

The ecology of biofilms collected from sediments and efflorescent crusts along the AMD near coal mine in the Mpumalanga Province was determined using the 16S bacterial metagenomy.

The results revealed a dominating presence in the biofilms of selected acidophilic chemoautotrophs that are known to contribute to AMD formation. The water samples had low pH (2.4 to 3.5), total acidity as $CaCO_3$ (2440 to 7040 mg/L), high level of metals (Al, Ca, Fe, Mg and Ni) and sulphate (3899 to 8874 mg/L). PHREEQC model allowed to predict the dominance of free hydrated speciated forms of Fe and Ni in the AMD.

Keywords: AMD, biofilm, efflorescent crusts, metagenomy, acidophiles, PHREEQC

Introduction

Acid and metal tolerant microorganisms are likely to proliferate in the AMD through formation of chemoautotrophically-based biofilms which are sustained by electron donors from sulphide minerals as well as CO_2, O_2 and N_2 derived from air and phosphate liberated by water-rock interaction (Baker and Banfield, 2003). These microorganisms which are present in biofilms attached to coals at the bank of AMD have the potential to increase or sustain AMD formation. The most common acidophilic bacteria have been identified in the AMD worldwide and these include the first isolated microbe from AMD called *Acidithiobacillus ferrooxidans* (Colmer et al., 1950) and *Leptosprillum ferrooxidans*. Although the iron and sulfur oxidizing chemoautotrophic prokaryotes dominate primary production in acidophilic environment, other species of microorganisms such as iron-oxidizing heterotrophs, obligate-heterotrophs and moderate acidophiles have also been identified in AMD (Johnson, 2007; Hallberg, 2010). Acidophilic archaea have also been detected in AMD with the most common being the mesophilic *Ferroplasma acidiphilum*, while the other are mostly thermophilic (Colmer et al., 1950). A number of microorganisms found in AMD have been reported to grow with ferrous as electron donor and therefore consider as primary producers of AMD water while fixing CO_2 for the synthesis of organic matters. The acidophilic heterotrophs on the other hand benefit from these organic matters and in return produce CO_2 use by the autotrophs and also degrade the organic matters in the soil that can be toxic to the primary producers (Johnson and Hallberg, 2008). Acting in cooperation, the primary producers and heterotrophs continuously influence the geochemistry of the AMD through the production of acidity and mobilization of metals which increase the pollution of the environment. The geochemistry of acid mine drainage varies from site to site, implying that a diverse communities of acidophilic microorganisms with varying physiological properties can occur in AMD across geological areas. Spatial distribution at the local level may also consider the differentiation of the influence of microorganisms in planctonic state and in biofilms on metal sulphides. Biofilms are communities of microorganisms embedded in a matrix of extracellular polymeric substances (EPS) (Fosso-Kankeu et al., 2010). The attachment of chemoautotrophic leaching microorganisms at the surfaces of minerals plays a significant role in their dissolution and therefore on the generation of AMD (Bellenberg et al., 2012; Vera et al., 2013; Zhang et al., 2014). Study by Sanhueza et al. (1999) revealed that attachment of cells of *A. ferrooxidans* to pyrite correlated with the degree of pyrite crystallization.

The determination of the microbial ecology of biofilms found in AMD is therefore important to predict the persistence of acidification and release of toxic metals in the aqueous system.

Study area

Emalahleni is situated in Mpumalanga province in South Africa with geological coordinates [25.8728° S, 29.2553° E]. This area is 2 678 km^2 in size with a reported population of approximately 395,466 people in 2011 (Statistics South Africa, 2011), and is approximately 140 km from Johannesburg. Emalahleni is characterised as a semi-arid area with a grassland biome. The coal mining activities situated in this region feeds into the Olifants catchment area. Samples were collected near the mining areas and from a stream tributary of the Brugspruit River at 15 km to the east of the perennial Olifants River into which the Brugspruit River feeds (Figure 1). Upstream activities include an abandoned and operating underground coal mines as well as a ferrochrome processing plant, resulting in severe water pollution as reported by Netshitungulwana et al. (2013).

Methodology

Sample collection

Water samples along the AMD effluent from the mine canal and dam through the extended paths discharged in the nearby residential area, were collected, stored, transported and analyzed as discussed in our previous paper (Fosso-Kankeu et al., 2017).

Biofilms were collected at the surface of the efflorescent crusts and at the bank of AMD (attached to the rocks) using spatula. The dislodged biofilms were collected into sterile glass bottles and transported in a cooler box containing ice packs and stored in the fridge (4°C) in the water laboratory at the School of Chemical and Minerals Engineering at the North-West University. After 16 h the biofilms were used for molecular analysis.

Water analysis

At the sampling site, physico-chemical parameters such as pH, conductivity, redOx potential (ORP) and temperature were determined at each sampling point using appropriate probes and meters (Hanna Instrument Inc, USA): temperature (°C), pH, electrical conductivity (mS/cm) and redOx potential (mV). The pH meter was calibrated before analysis in the field, using reference buffer solutions. The analysis of cations and anions was performed by external accredited laboratory.

Molecular identification of microorganisms

The Genomic DNA was extracted from the biofilms using the ZR Soil Microbe DNA Mini Prep kit™ according to the manufacturer's instruction. DNA concentrations were determined spectrophotometrically with a Nano-Drop spectrophotometer (Thermo Scientific). Then extracted DNA samples were sent to Inqaba Biotechnical Industries (Pty) Ltd for sequencing. Briefly, genomic DNA samples were PCR amplified using a universal primer pair (341F and 785R - targeting V3 and V4 of the 16S rRNA gene). Resulting amplicons were gel purified, end repaired and illumina specific adapter sequence were ligated to each amplicon. Following quantification, the samples were individually indexed, and another purification step was performed. Amplicons were then sequenced on illumina's MiSeq platform, using a MiSeq v3 (600 cycle) kit. 20Mb of data (2×300bp long paired end reads) were produced for each sample. The BLAST-based data analysis was performed using an Inqaba in-house developed data analysis pipeline; 1) Data was trimmed and only >q20 (i.e high quality) reads were used; 2) Every read was BLASTED and the result file saved; 3) The top hit for every BLAST result (i.e genus and species name) was counted and a record was kept of how many times each species appeared as a hit.

Results and discussion

Microbial communities in the biofilms

Visible pellicles of biofilms of brownish to greenish colors were collected at four locations along the AMD. After DNA sequenc-

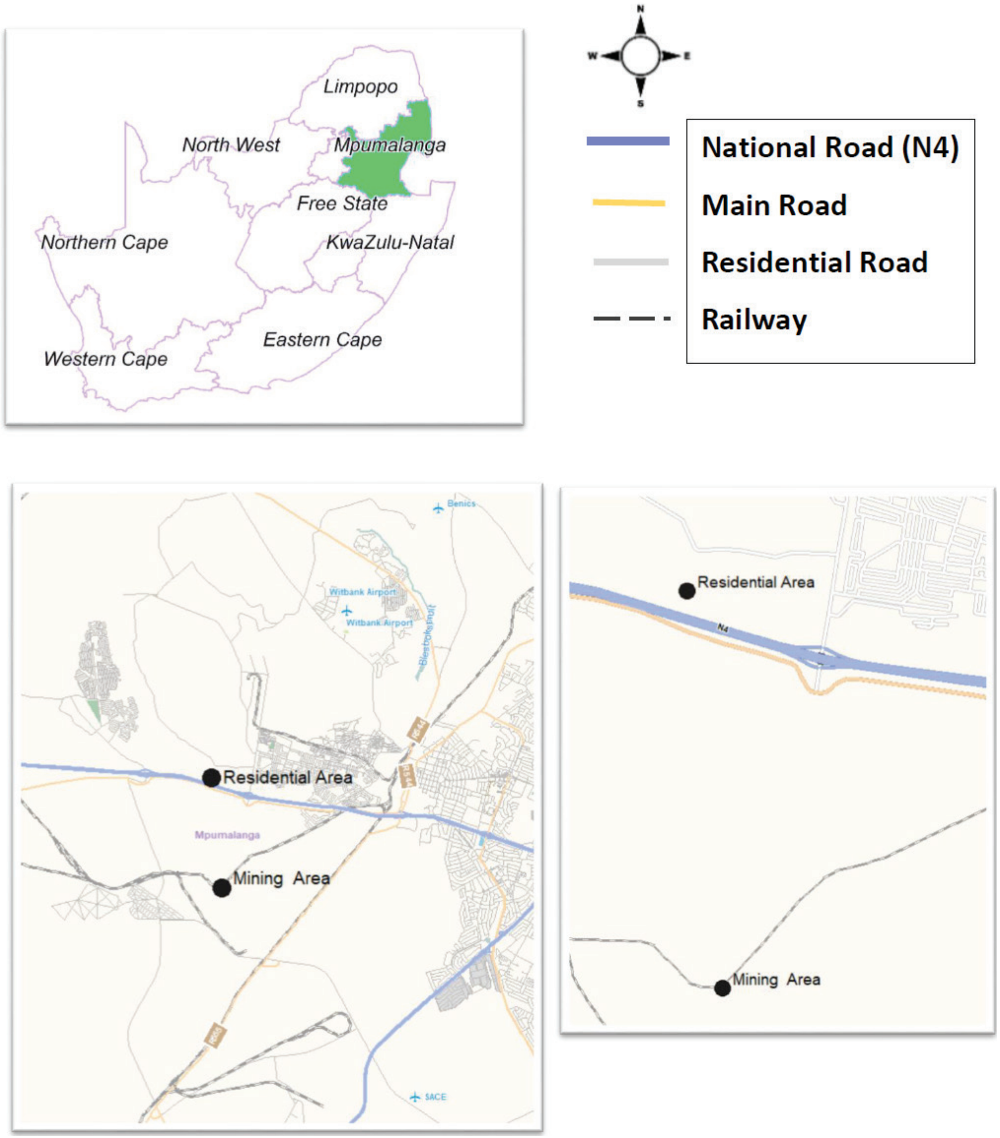

Figure 1 *Map of the sampling area in Emalahleni, Mpumalanga Province of South Africa*

ing, the results showed that the biofilms were harboring complex assemblages of microorganisms significantly dominated by bacterial community over the range of samples; previous reports have also shown that bacteria tend to dominate over archaea and eukarya in the mining wastes (Kock and Schippers, 2008). The abundant species were found to be acidophilic chemoautrophic bacteria such as *Acidithrix*, *L. ferrooxidans*, *A. ferrooxidans*, *Leptospirillum*, *Acidimicrobiaceae*, *Sulfobacillus*, *Acidiphilium* and *Acidithiobacillus* sp (Figure 2). These bacteria have been previously identified in environments of lower pH and higher ionic strength such as AMD (Bond et al., 2000). Acidophilic chemoautotroph bacteria group has been reported to dominate the community of bacteria in AMD, responsible of the acceleration of metal sulphide dissolution and formation or sustaining of AMD (Baker and Banfield, 2003). Sampling point Dt2 was found to contain most of the bacteria except *Sulfobacillus*, with *L. ferrooxidans* and *A. ferrooxidans* almost exclusively found in this sample. On the other hand, *Sulfobacillus* and *Acidithiobacillus* sp were dominants in sample D where they occur at 98.5 and 93% respectively. The last two species have been often detected in AMD and are known to enhance acid production in metal-leaching environments by oxidizing Fe^{2+} and replenishing the oxidant Fe^{3+} (Sand et al., 1995; Bond et al., 2000). *Acidimicrobiaceae* was found to be well represented in all the four samples. This is expected as it constitutes the family of *Acidimicrobiaceae* which harbors five monospecific genera, including *Acidimicrobium*, *Ferrimicrobium* and *Ferrithrix*, *Aciditerrimonas* and *Ilumatobacter* (Clark and Norris, 1996; Johnson et al., 2009; Matsumoto et al., 2009; Itoh et al., 2011; Stackebrandt, 2014). Although the profile of bacteria in the biofilms from all the different sites varied, all the sites had *Acidiphillium* and *Acidimicrobiacreae* in common, and most of them had at least one acidophilic chemoautotroph capable to oxidize sulphide minerals and generate acid. This could probably be the reason why water samples collected from sampling points Dt1, Dt2 and Dt3, located at few kilometers from the mine still had a very low pH. The involvement of iron-oxidizing chemoautotrophs in sulphide dissolution and acid generation has already been reported with implication on the environment. However, it was quite interesting to notice that the biofilms collected at the bank of the Dam's entrance (sample D) were mostly attached to the efflorescent crusts which is dominated by secondary minerals easily oxidizable. In our recent investigation (not published) it was shown that acidophilic chemoautotrophs from these biofilms accelerate the rate of oxidation of efflorescent crusts by several order of magnitude compared to the oxidation of coal tailings. This clearly shows that the presence of biofilms on efflorescent crusts at the bank of AMD can accelerate the process of acid generation therefore sustaining AMD pollution.

Water quality and metals speciation

After collection of water samples, some variables such as pH, electrical conductivity (EC) and redOx potential (Eh) were measured in-situ. The results (Table 1) show that all the samples were acidic with pH lower than 3.5, while high EC was also recorded indicating higher ionic strength which is characteristic of AMD. Although the sulphate content was high in all samples, higher concentrations were recorded in samples collected at the vicinity of the mine (PM and BB); this was also related to the large amount of minerals available at those points.

A multitude of metals were detected in the water samples at various concentrations. The major elements mainly included Al, Ca, Fe and Mg while those occurring in lower concentrations included Co, Cr, Ni and Zn among which Ni was the most abundant (Table 2). The concentration of Fe was ten times lowered

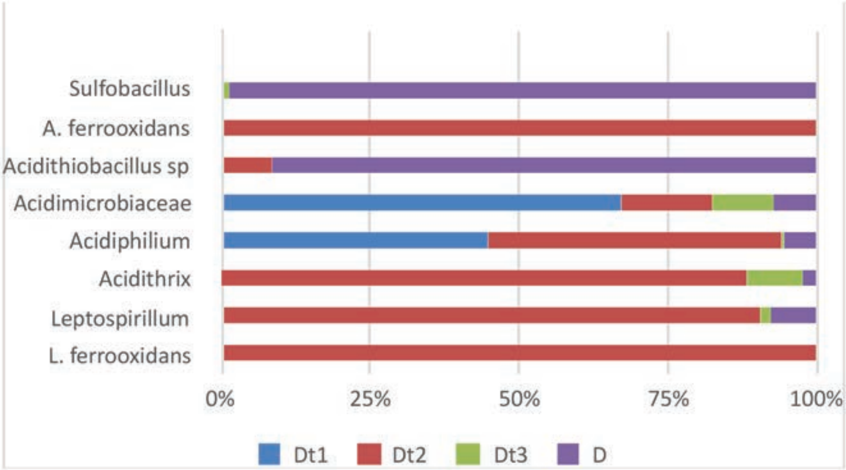

Figure 2 *Microbial profile in the biofilms collected from river bank and efflorescent crusts*

Table 1 Physico-chemical characteristics of water

Sampling points	In-situ variables			Major anions (mg/L)	
	pH	EC (mS/cm)	Eh (mV)	SO_4^{2-}	Cl^-
PM	2,7	750	220	8680	8
BB	2,7	718	220	8874	8
D	2,6	697	225	6776	11
AD	3,5	560	194	4911	29
UB	2,5	627	229	5624	14
Dt1	2,4	503	247	4069	14
Dt2	2,5	487	246	3899	13
Dt3	2,4	502	249	4008	14

when exiting the dam which implies that part of the Fe precipitated in the dam probably as a result of some form of treatment, but the concentration was increased further downstream, confirming that mobilization of metals is occurring along the AMD stream. It must also be noted that compared to Dt1, Dt2 and Dt3, higher concentration of Fe in the dam may have contributed to the growth of bacteria such as Sulphobacillus, Leptospirillum and Acidithiobacillus which required ferrous as electron donor. The continuous oxidation of minerals along the AMD stream can be partly attributed to the acidophilic chemoautotrophic bacteria present in the biofilms at the bank or attached to the efflorescent crusts.

To predict the potential of dispersion of mobilized metals from the coal tailings, the PHREEQC geochemical speciation model was used. The results of the prediction of metal species was presented in the form of free hydrated species or inorganic complexes (Table 3). It was observed that for both Fe and Ni, free hydrated species dominated over the inorganic complexes in all the water samples. The percentage range of the free hydrated speciated forms of Fe and Ni was between 68 to 74.8% and 52 to 61.8% respectively, while the percentage range of the inorganic complexes speciated forms of Fe and Ni was between 25.2 to 31.7% and 38.1 to 47.7% respectively. The free hydrated are likely to be bioavailable, while the inorganic complexes restrict the availability of free aqua metal ionic species to low concentration therefore reducing their bioavailability to the aquatic organisms which otherwise will be highly toxic (Korfali and Davies, 2004; Fosso-Kankeu et al., 2017). The dominance of free hydrated metal ionic species supported by lower pH contributed by acidophilic chemoautotrophic bacteria in the biofilms in this study therefore enhances the bioavailability and toxicity of metals to the aquatic life.

Table 2 Major and trace elements in water

Sampling points	Concentration of ions in water mg/L							
	Major elements				Trace elements			
	Al	Ca	Fe	Mg	Co	Cr	Ni	Zn
PM	261	461,8	2909	357,1	0,59	0,02	19,29	2,10
BB	261,7	454,6	2796	365,2	0,53	0,02	19,95	1,76
D	233,5	453,3	2514	387,7	0,52	0,02	17,63	1,52
AD	265,6	491,5	226,4	490	0,91	0,00	1,13	0,39
UB	208,7	453,6	1678	303,2	0,50	0,02	13,85	1,54
Dt1	110,1	402,8	598	227,8	0,27	0,01	5,70	1,01
Dt2	111,2	397,9	627,2	235,8	0,26	0,01	5,86	0,97
Dt3	114,1	401,3	582,9	238,7	0,27	0,02	5,76	1,00

Table 3 *Percentages of dominant speciated forms of metals in water*

Sampling point	% of species			
	Fe		Ni	
	Fe^{2+}	FeSO4	Ni^{2+}	NiSO4
AD	69	31	60.4	39.5
BB	71	28.9	52	47.7
D	74.8	25.2	59.4	40.5
Dt1	68	32	61	39
Dt2	68.5	31.5	61.8	38.1
Dt3	68.3	31.7	61.5	38.4
PM	72	28	53	46.8
UB	72.7	27.3	61	39

Conclusion

This study has demonstrated that the biofilms at the bank of AMD streams and those attached to the efflorescent crusts harbor complex assemblages of acidophilic chemoautotrophic bacteria with the potential to dissolve sulphide mineral and generate acid. The investigation of the quality of the AMD water along the stream further demonstrated that Fe was further mobilized downstream, clearly showing that the pollution is regenerated or sustain along the stream. The prediction of metals speciation revealed a dominance of free hydrated elements which are more likely to disperse across the stream and very importantly are bioavailable and more toxics.

Acknowledgements

The authors are grateful for the funding from the National Research Foundation (NRF) and the North-West University (NWU), and the contribution of Mr Nico Lemmer from the NWU.

References

Baker BJ and Banfield JF (2003) Microbial communities in acid mine drainage. Microbiology Ecology 44: 139-152.

Bellenberg S, Leon-Morales C-F, Sand W, Vera M (2012) Visualization of capsular polysaccharide induction in *Acidithiobacillus ferrooxidans*. Hydrometallurgy 129-130: 82-89.

Bond PL, Smriga SP, Banfield JF (2000) Phylogeny of microorganisms populating a thick, subaerial, predominantly lithotrophic biofilm extreme acid mine drainage site. Applied and Environmental Microbiology 66(9): 3842-3849.

Clark DA and Norris PR (1996) *Acidimicrobium ferrooxidans* gen. nov., sp. Nov.: mixed-culture ferrous iron oxidation with *Sulfolobus* species. Microbiology 142: 785-790.

Colmer AR, Temple KL, Hinkle ME (1950) An iron-oxidizing bacterium from the acid drainage of some bituminous coal mines. J. Bacteriol. 59: 317-328.

Fosso-Kankeu E, Du Preez H, Jagals P (2010) Health implication of lipopolysaccharide endotoxins in domestic container water used by rural households in South Africa. Journal of Water Health 80(4): 601-610.

Fosso-Kankeu E, Manyatshe A, Waanders F (2017) Mobility potential of metals in acid mine drainage occurring in the Highveld area of Mpumalanga Province in South Africa: Implication of sediments and efflorescent crusts. International Biodeterioration and Biodegradation 119: 661-670.

Hallberg KB (2010) New perspectives in acid mine drainage microbiology. Hydrometallurgy 104: 448-453.

Itoh T, Yamanoi K, Kudo T, Ohkuma M, Takashina T (2011) *Aciditerrimonas ferrireducens* gen. nov., sp. Nov., an iron-reducing thermoacidophilic actinobacterium isolated from a solfataric field. Int. J. Syst. Evol. Microbiol. 61: 1281-1285.

Johnson DB (2007) Physiology and ecology of acidophilic microorganisms. In: Gerday C, Glansdorff N. (Eds.), Physiology and Biochemistry of Extremophiles. ASM Press, Washington, D.C, pp. 257-270.

Johnson DB and Hallberg KB (2008) Carbon, iron and sulfur metabolism in acidophlic micro-organisms. Adv. Microb. Physiol. 54: 201-255.

Johnson DB, Bacelar-Nicolau P, Okibe N, Thomas A, Hallberg KB (2009) *Ferrimicrobium acidiphilum* gen. nov., sp. Nov. and *Ferrithrix thermotolerans* gen. nov., sp. Nov.: heterotrophic, iron-oxidizing extremely acidophilic actinobacteria. Int. J. Syst. Evol. Microbiol. 59: 1082-1089.

Kock D and Schippers A (2008) Quantitative microbial community analysis of three different sulfidic mine tailing dumps generating acid mine drainage. Apply and Environmental Microbiology 74(16): 5211-5219.

Korfali SI and Davies BE (2004) Speciation of metals in sediment and water in a river underlain by limestone: role of carbonate species for purification capacity of rivers. Adv. Environ. Res. 8: 599-612.

Matsumoto A, Kasai H, Matsuo Y, Omura S, Shizuri Y, Takahashi Y (2009) *Lumatobacter fluminis* gen. nov., sp. Nov., a novel actinoacterium isolated from the sediment of an estuary. J. Gen. Appl. Microbiol. 55: 201-205.

Sand WTG, Hallmann R, Schippers A (1995) Sulfur chemistry, biofilm, and the (in)direct attack mechanism – a critical-evaluation of bacterial leaching. Appl. Microbiol. Biotechnol. 43: 961-966.

Sanhueza A, Ferrer I, Vargas T, Amils R, Sanchez C (1999) Attachment of *Thiobacillus ferrooxidans* on synthetic pyrite of varying structural and electronic properties. Hydrometallurgy 51: 115-129.

Stackebrandt E (2014) The family of *Acidimicrobiaceae*. In The Prokaryotes. Eds. E. Rosenberg, E.F. Delong, S. Lory, E. Stackebrandt, F. Thompson. Springer. Pp 5-12.

Vera M, Schippers A, Sand W (2013) Progress in bioleaching: fundamentals and mechanisms of bacterial metal sulfide oxidation. Part A. Appl. Microbiol. Biotechnol. 97: 7529-7541.

Zhang R, Bellenberg S, Castro L, Neu TR, Sand W, Vera M (2014) Colonization and biofilm formation of the extremely acidophilic archaeon *Ferroplasma acidiphilum*. Hydrometallurgy 150: 245-252.

Snowmelt and Runoff Simulation at Mine Sites in Cold Climates using Probabilistic Methods

Hollie Garrick[1], Gareth Digges La Touche[2], Tomi Maksimainen[3], Romain Girard[4], Eoghan Hayes[2]

[1]Golder Associates, Attenborough House, Browns Lane Business Park, Stanton-on-the-Wolds, Nottingham. NG12 5BL, UK

[2]Golder Associates, 20 Eastbourne Terrace, London. W2 6LG, UK

[3]Boliden Kevitsa Mining Oy, Kevitsantie 730, FI-99670 Petkula, Finland

[4]Golder Associates, P.O. Box 20127, 104 60 Stockholm, Sweden

Abstract

A methodology for stochastic simulation of snowmelt and runoff for water balance modelling at mine sites in cold climates is presented in this paper. A stochastic climate model is combined with the Swedish Meteorological and Hydrological Institute's (SMHI) Hydrologiska Byråns Vattenbalansavdelning (HBV) model, which uses a degree-day method is applied to predict snow melting, and a simplified thermal analysis to predict ice formation and melting. The modelling objective is to represent random fluctuations in both precipitation and temperature as the main drivers in the rate and volume of spring meltwater generation. The model has been successfully implemented to support strategic decision making at the Kevitsa mine in Lapland, Northern Finland. The model performance and future model applications are discussed.

Keywords: snowmelt, mine water balance, stochastic simulation

Introduction

For mines in cold climates managing water supply and storage through the winter period, when precipitation falls as snow, and the seasonal meltwater influx in spring presents huge challenges. This carries associated risks to the mine operation, and potentially to the environment, if the spring peak flows cannot be managed. The prediction of snow and ice accumulation in winter and associated melt water generation in spring is critical to water balance calculations that facilitate the management of risks to mining operations.

It is generally recognised that good practice for water balance assessment for mine water management requires a holistic assessment of the side-wide water balance in dynamic modelling tools which are able to simulate interdependent system responses and responses to short term climate variability. For sites in cold climates, these hydrological models must incorporate the freeze and thaw cycle to be of value in understanding flood risk.

The primary goal of mine water balance studies is usually to predict conditions in future periods in the mine life. While models are often run by 'looping' or sampling historical data, to be truly predictive, stochastic climate generators are necessary to simulate the response of hydrologic systems beyond the limits of the historical record. Stochastic generators attempt to reproduce the statistical characteristics of the historical record in synthetic sequences of arbitrary length.

The model described in this study was developed to simulate the water balance of a site in artic Finland, where average temperatures are below freezing for 6 months of the year. This study implemented a hydrological model, the SMHI HBV model (Bergström, 1976, 1992) in GoldSim™, coupled with stochastic climate simulation to provide probabilistic simulation of snow accumulation, snowmelt and catchment runoff. This was further augmented by a model for ice formation and melting in water storages, driven by the stochastic temperature record.

Climate and Catchment Runoff Modelling Methodology

The most important element of the stochastic climate model is the stochastic precipitation simulator. The GoldSim model implements the Australian CRC for Catchment Hydrology's Stochastic Climate Library Daily Rainfall Model for a single site (Srikanthan and McMahon, 1985; Siriwardena et al., 2002) and has been previously described in O'Hara (2012). The model uses the State-Markov Transition Probability Matrix (TPM) method (lag-1 day) with shifted-gamma distributed top state rainfall. This type of model assumes that the climate state is binary, and is either wet or dry. Each state has an independent rainfall distribution, assumed to be Gaussian; transitions between states are governed by the TPM. Annual seasonality is imposed by computing separate transition probability matrices and gamma parameters for each calendar month. The TPM is developed by simple transition counting in the historical record; done separately for each calendar month to impose seasonality. A long period daily climate precipitation record is necessary to define the TPM.

The stochastic model for temperature is relatively simplistic, but is more sophisticated than a model based only on sampling statistical distributions derived from the historical record. The primary objective was to replicate short period correlation in temperature and seasonal variation in the degree of short range temperature fluctuation. The temperature model has two elements:

- A (non-stochastic) representation the seasonal temperature trend as a sinusoidal function fitted to mean average daily temperature.
- A stochastic temperature fluctuation modelled as deviation from the seasonal mean, represented as a probability density function (PDF) of deseasonalised temperature, with autocorrelation between daily values defined based the historical record.

The autocorrelation factor is determined by regressing daily deseasonalised temperature against the previous days' deseasonalised temperature. PDFs of deseasonalised temperature are derived based on observed data, seasonally or monthly depending on the degree of variability.

Evaporation is simulated according to the methodology described in the SMHI HBV model. Evaporation of each day is calculated from the seasonal mean value plus or minus an adjustment correlated to the deviation of temperature from the seasonal mean.

The HBV model is a catchment scale hydrological model for simulation of snow accumulation and melt, groundwater and surface water interaction and catchment runoff. While the model has been applied across

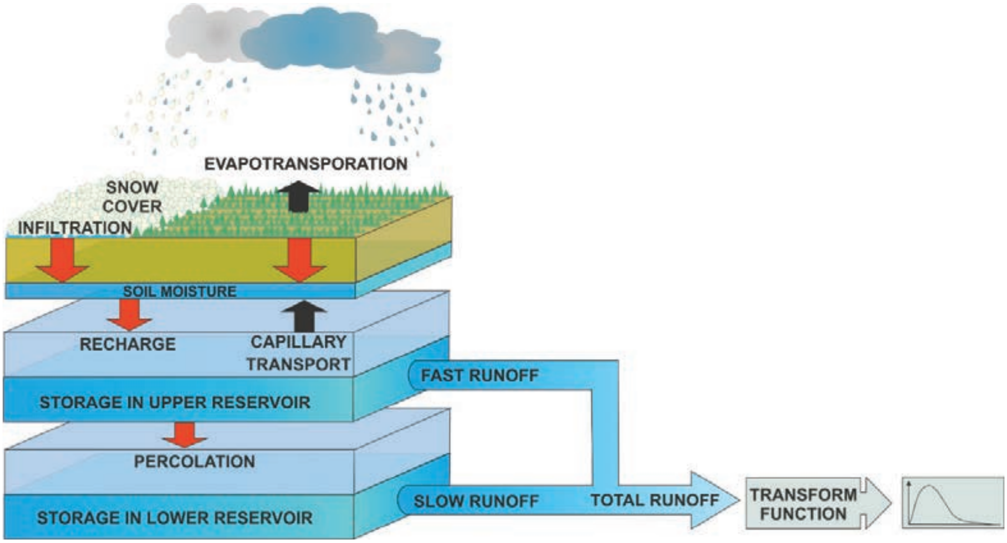

Figure 1 *Schematic representation of the HBV-96 model (modified from Lindström et al., 1997)*

the world, it is well suited for Scandinavian climatic and hydrological conditions. The HBV model comprises a number of routines for system components: snowmelt is calculated by a degree-day method; groundwater recharge and actual evapotranspiration are functions of the calculated soil-water storage; and runoff formation is simulated by linear reservoir functions. Daily values of storages and discharge are simulated using daily precipitation and temperature and long-term averages of potential evapotranspiration as inputs.

The model is calibrated through adjustment of empirical factors in each routine, including the snow melting rate and runoff recession coefficients.

Snow accumulation is defined by a threshold temperature, below which precipitation is snow and above which snowmelt occurs. Snowmelt occurs as a function of temperature based on a rate coefficient C_{FMAX} (mm/°C/day). Snowmelt is retained within the snowpack until meltwater exceeds a certain proportion of the snowpack, after which it is released. If the temperature falls below the threshold temperature, melt water refreezes based on a freezing rate coefficient. Sublimation, although not included in the HBV model, was included in our model as an additional loss from the snow water reservoir calculated as a proportion of snowfall based on calibration.

Ice formation is simulated using a simplification of the method proposed by Comfort and Abdelnour (2013). The method uses a heat-budget analysis based on a 'bulk' heat transfer coefficient which is suitable for application based only on available temperature, snowfall and rainfall data. Ice formation has been simulated as a combination of the following processes:

- Calculation of the lag in ice formation between air temperature reaching freezing and lake temperatures reaching freezing, allowing ice formation to start.
- Calculation of the rate of bottom ice growth through freezing at the basal surface of the ice sheet.
- Calculation of the rate of surface ice growth through:
  - Refreezing of slush in the snowpack following rainfall events; and
  - Freezing of surface ice following flooding events where snow loading results in submersion and flooding of the ice sheet.

The time lag for the onset of ice formation when air temperature falls below freezing has been calculated as in Leppäranta (2010) using an assumed atmospheric cooling rate. The rate of ice formation on the bottom of the ice sheet and surface ice growth is calculated using the following equation (Comfort and Abdelnour, 2013):

$$\frac{dh_i}{dt} = \frac{1}{\rho_i \lambda} \frac{(T_m - T_a)}{\frac{h_s}{k_s} + \frac{h_i}{k_i} + \frac{1}{H_a}}$$

Where subscript *i* represents ice and *s*, snow, *h* is thickness, *t* is time, T_m and T_a water and air temperature respectively (water temperature assumed to be 0°C), *k* thermal conductivity and H_a the heat transfer coefficient from the snow surface to the air. The water available to form surface ice is limited by two processes which may provide water for ice formation: rainfall events where precipitation falls as rain on existing snow and ice, and flooding events where snow loading results in submergence of the ice sheet.

The point at which the ice sheet becomes neutrally buoyant due to the overlying snow load is calculated as (Comfort and Abdelnour, 2013):

$$h_s = \left(\frac{\rho_w}{\rho_s}\right)\left(1 - \frac{\rho_i}{\rho_w}\right)h_i$$

Where definitions are as above, and ρ_w and ρ_s are the densities of ice and snow, respectively.

The resulting model is a simplified representation of ice formation and melting processes, neglecting some aspects of the Comfort and Abdelnour (2013) model as well as more sophisticated thermodynamically based models. It was found to perform well for ice growth, but not for ice melting.

Ice melting was simulated using Zubov's law (Zubov, 1945 in Leppäranta, 2010), a modification of Stefan's equation which includes an adjustment factor to allow for the insulating effect of the near-surface air-snow buffer.

Case Study: Kevitsa Mine

Kevitsa Mine is located near to Sodankylä in the Lapland region of Finland and is operated by Boliden Kevitsa Mining Oy. The Site lies north of the Artic circle and experiences average temperatures below freezing for more than 6 months of the year. At present, the ultimate catchment of the mine will be approximately 10.6 km^2. The catchment is gently undulating, lying at an elevation of between 200 m and 315 m above sea level, and is surrounded by areas of wetland. Groundwater is near to ground surface in many parts of the Site, which is underlain by superficial deposits comprising peat and glacial till, underlain by Paleoproterozoic basement rocks.

The mine is an open pit operation, with a waste rock dump, tailings storage facility, crusher (located underground) and processing plant, which began operation in 2012. The Site has a water reservoir for storage. Process water is taken from the water reservoir and also directly from the tailings decant pond. Water from all the mine facilities and small areas of catchment within the mine Site ultimately discharges to the water reservoir, from which excess water is treated and discharged under an Environmental Permit to the Kitinen River approximately 3.5 km west of the mine. A small amount of raw water is taken from the Kitinen River to augment the water supply.

Calibration was undertaken of the following aspects of the climate and runoff model in the Kevitsa study:

- Stochastic precipitation: mean and standard deviation, and predicted rainfall for the 1 in 10 year, 1 in 50 year and 1 in 100 year 24 hour events.
- Stochastic temperature: visual fit to observed, replication of 10%ile, 50%ile and 90%ile of observed record over an extended time period.
- Snow and ice thickness: snow accumulation as snow water equivalent, and ice thickness.

Historical data for surface flows at Kevitsa mine did not include runoff data for any natural catchment areas, and catchment runoff data for the region was not available from the Finnish Meteorological Institute. As such, the runoff model could not be directly calibrated to available data. The mine collects data for discharges from the major mine facilities, from the treatment plant and off site discharge location. The water balance was calibrated to these flows and to water inventory data where available. The model calibration therefore gives an indication of the accuracy of specific parts of the climate and runoff model, and of the site wide balance as a whole, but not of the runoff model directly. The HBV module incorporated into the model has been previously applied at site in Sweden and was found to perform well with calibration to a historical catchment runoff series.

Calibration of the stochastic precipitation module to 24 hour peak rainfall events is shown in Table 1. At the longer return periods, the model slightly over-predicts the rainfall intensity, but is within the 95%ile upper bound of the observed values. The daily, monthly and annual mean and standard deviation of simulated rainfall showed a good match to observed.

Predicted and observed snow pack thickness and ice thickness for the recent period are shown in Figure 2. The annual maximum snow pack was also calibrated over a much longer historical record. A degree-day method is unlikely to provide a good fit to observed conditions in all years as it neglects some key

Table 1: *Predicted and Observed 24-Hour Return Period Events, Stochastic Precipitation Module*

Return Period	Probability of Occurrence	Calculated Value (mm)	Observed Value, Average (mm)	Observed value, 95%ile Upper Bound (mm)
10 years	0.027%	41.8	39	45
20 years	0.014%	47.4	43	50
100 years	0.0027%	62.6	54	63

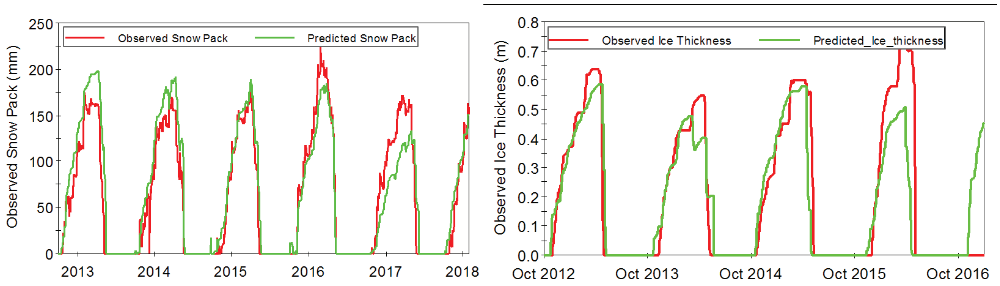

***Figure 2** Kevitsa Mine Model Calibration, Snow Depth (as Snow Water Equivalent) and Ice Thickness*

variables in terms of energy balance. However, an acceptable calibration was obtained through fitting of the threshold temperatures and adjustment of the observed record snow density within a defined range.

A good fit to observed temperature was achieved using the stochastic temperature module, but the extremes of the generated temperature record resulted in a poor calibration for snow and ice formation. The module was therefore modified to reduce the modelled extremes, resulting in a better calibration for snow and ice formation and melting.

The calibration of the Site's annual discharges is illustrated in Table 2. The normal operational demand for make up water is an input into the model: though the model can generate additional make up water if required, no additional make up water was generated in the calibration period. There are many factors in the calibration of the Site wide water balance that are unrelated to the climate and runoff model performance, and the overall model performance cannot be used to validate the climate and runoff model.

The water balance model has thus far been utilised to assist the mine in strategic decision making regarding the future water treatment requirements for the mine, and to evaluate the risk profile of the Site's major water storages. Golder continues to work with the mine to improve the water balance model performance and develop confidence in the model predictions. As further data is collected, this will include further calibration of the run off model.

Other Considerations

The catchment runoff and ice storage model described has the potential to provide a useful tool for stochastic generation of future runoff sequences for mine water balances, but is based on historical climate. While for operations, climate change impacts may be of little significance, for design of long term infrastructure and in particular for closure, climate change modelling results may significantly affect decision making and consideration of climate change factors is mandated.

A range of approaches to adopting modelled climate change impacts to support mine design and impact assessment can be found in literature; Fraser et al. (2017) includes a regionally appropriate example at a Boliden property in the region (Aitik Mine, Northern Sweden). In order to practically adapt this basis, Golder has previously presented a

***Table 2:** Observed and Predicted Annual Treatment and Off Site Discharge Volumes*

	Year	Calculated Volume (m^3/yr)	Recorded Volume (m^3/yr)	Variance (m^3)	Percentage Error
Off Site Discharge	2014	3 335 580	3 199 350	136 230	4.3%
	2015	3 624 740	3 652 090	-27 350	-0.7%
	2016	3 785 730	3 718 540	67 190	1.8%
ETP Flow	2014	2 709 200	2492560	216 640	8.7%
	2015	2 848 790	2 490 700	358 090	14.4%
	2016	2 553 870	2 406 890	146 980	6.1%

ETP – effluent treatment plant.

method which can be used to include climate change signals into future planning for water resource management within a GoldSim model (O'Hara et al, 2012).

The process of incorporating climate change scenarios can be summarised in 3 steps:

Analyse key parameters in Site and local historic and current baseline datasets, compare to longer term regional records and characterise anomalies to support selection of longer term future climate trend inputs.

Determine a regionally appropriate source of climate change scenario data. This may incorporate reference to industry and scientific best practice (e.g., IPCC publications, SMHI Report No. 116, 2014), technical experts and consultation with regulatory agencies and stakeholder groups. For the Kevitsa mine, the Rossby Centre (SMHI 2014) is a regional source for climate change scenario results which can provide downscaled, daily data for all required parameters, obtained via the CORDEX (COordinated Regional climate Downscaling EXperiment) system.

Derive seasonal and annual adjustments to precipitation and temperature for inclusion in the stochastic climate model from the future climate model data and adjust accordingly.

Conclusions

This paper presents a methodology for the stochastic simulation of snow and ice melting and runoff, implemented using the GoldSim^{TM} Monte Carlo simulation platform. Application of the model for the water balance at the Kevitsa mine has provided encouraging results regarding the model performance, though runoff rates have yet to be validated due to a lack of suitable data. The methodology proposed could be readily adapted to consider future climate scenarios, and as such has the potential to be valuable in long term planning.

Acknowledgements

Golder wishes to thank Boliden Kevitsa Mining Oy for their support throughout the water balance project, in sharing the data presented in this paper and for comments on the draft text.

References

Bergström S (1976) Development and application of a conceptual runoff model for Scandinavian catchments, SMHI RHO 7, Norrköping, 134 pp

Bergström S (1992) The HBV model – its structure and applications, SMHI RH No 4, Norrköping, 32 pp

Comfort G, Abdelnour R (2013) Ice Thickness Prediction: A Comparison of Various Practical Approaches, CGU HS Committee on River Ice Processes and the Environment, 17th Workshop on River Ice, Edmonton, Alberta, July 21-24, 2013

Fraser C, Martin A, Mueller S and Scott J (2017). Incorporating Climate Change Scenarios into Mine Design and Permitting Studies. 13th Annual International Mine Water Association Congress, Rauha Lappeenranta, Finland, June 25-30, 2017.

GoldSim (2017) GoldSim 12, Released February 2017.

Leppäranta M (2010) Modelling the Formation and Decay of Lake Ice in George, D.G. (Ed.), 2010. The Impact of Climate Change on European Lakes, Aquatic Ecology Series 4, Springer Science & Business Media BV, 507 pp

O'Hara C, Grobler, J, Hookey G and Vermaak J (2012). The Impact of Climate Change on a Mine Water Source, International Mine Water Association Symposium, Bunbury, Australia 2012

Srikanthan R, McMahon TA (1985) Stochastic Generation of Rainfall and Evaporation Data. Australian Water Resources Council, Department of Resources and Energy, Canberra, Technical Report 84.

Siriwardena L, Srikanthan R and McMahon TA (2002) Evaluation of Two Daily Rainfall Data Generation Models. CRC for Catchment Hydrology Technical Report 02/14.

Swedish Meteorological and Hydrological Institute (2014) CORDEX scenarios for Europe from the Rossby Centre regional climate model RCA4. – Report Meteorology and Climatology No. 116, Swedish Meteorological and Hydrological Institute, Norrköping, Sweden, 84 pp

Fe-Sulfide Liberation and Association as a Proxy for the Interpretation of Acid Rock Drainage (ARD) Test Results

Olga Guseva[1], Alexander K. B. Opitz[1], Jennifer L. Broadhurst[1], Susan T. L. Harrison[1,2], Dee J. Bradshaw[1], Megan Becker[1,3]

[1]*Minerals to Metals Initiative, University of Cape Town, South Africa, gsvolg001@myuct.ac.za*
[2]*Centre for Bioprocess Engineering Research, University of Cape Town, South Africa*
[3]*Centre for Minerals Research, University of Cape Town, South Africa*

Abstract

Acid rock drainage (ARD) characterisation and prediction protocols, comprising geochemical static, kinetic and biokinetic tests, sometimes fail to adequately assess the ARD potentials of sulfidic mine wastes. Several authors have partly linked this shortfall to the insufficient use of mineralogical and textural analyses. Mineral liberation and association data may inform the interpretation of the results of standard ARD tests and this study assesses these parameters for Fe-sulfide minerals in the feed material for humidity cell (meso-scale), static and biokinetic (micro-scale) tests. Results show that the dominating textural parameters on the meso- and micro-scales are association and liberation, respectively.

Keywords: mineralogy, texture, association, liberation, kinetic tests

Introduction

Acid rock drainage (ARD) occurs through complex mechanisms of acid formation and neutralisation reactions associated with metal sulfide oxidation and gangue mineral dissolution, respectively. The processes result in acidic drainage that often contains elevated levels of toxic elements. Due to its abundant occurrence with valuable minerals, pyrite is typically recognized as the main mineral contributing to ARD formation from mine wastes; however, it is well recognized that all mineral sulfides may be oxidized in the presence of oxygen and water (Nordstrom and Alpers 1999; INAP 2012). Mining and processing activities produce waste material ranging from coarse rocks to fine tailings. These waste fragments have a larger combined surface area exposed to oxidative conditions than the original undisturbed rock, exacerbating any naturally occurring ARD.

ARD characterisation and prediction techniques typically include a suite of geochemical static and kinetic tests (INAP 2012; Parbhakar-Fox and Lottermoser 2015). Static tests are relatively quick and inexpensive and are routinely performed on finely milled subsamples (particles passing 75μm) of the parent material, where the minerals are assumed to be fully liberated from one another. This accelerates reaction kinetics to gain an indication of the "worst case" scenario for ARD generation. In doing so, any textural relationships between acid forming and neutralizing minerals are destroyed (Brough et al. 2017). Kinetic tests (mainly humidity cell tests) are costlier and more time consuming, and are thus not explicitly performed on every sample, rather on those yielding uncertain or conflicting results in the characterisation stages. A coarser particle size distribution (particles passing 6.3mm) is used to provide an indication of the long-term weathering behaviour (Lengke et al. 2010; ASTM 2013). At this scale, textural and mineralogical relationships are thought to still be retained. As none of the above tests address the contribution made by naturally occurring microorganisms to ARD formation, the University of Cape Town (UCT) biokinetic test (Hesketh et al. 2010) was developed and makes use of finely milled material (passing 150μm).

Although recommended (Parbhakar-Fox et al. 2011; Becker et al. 2015; Brough et al. 2017; Dold 2017), thorough mineralogical and textural analyses are rarely undertaken for ARD assessment due to associated time and cost constraints (Jamieson et al. 2015). Textural factors influencing ARD formation include the grain size distributions, associations, reactivity, and the degree of liberation of the acid forming and neutralizing mineral phases present (Parbhakar-Fox et al. 2011) and may be assessed on three general scales, namely macro-, meso- and micro-texture. These scales may be linked to particle size, which has been found to affect metal recovery and drainage kinetics in heap leach systems due to the dependence of particle surface area on reactivity (Ghorbani et al. 2011). Finer particles consisting solely of the leachable material have been found to have an increased potential for reactivity as opposed to coarser particles where the leachable material was encapsulated (Ghorbani et al. 2011; Fagan-Endres et al. 2017). Liberation of minerals refers to mineral exposure to the reactive environment and may be classed into liberated, unliberated and locked/encapsulated categories (Evans and Morrison 2016). For humidity cell tests liberated material has been found to be more likely to produce acidic leachate than material with a lower degree of liberation (Brough et al. 2017). This phenomenon is well described in heap bioleaching studies (Fagan-Endres et al. 2017).

Mineralogy and textural analyses assess the mineral liberation, grade of a sample, mineral shape, size and interrelationships within the particles. A variety of tools exist for quantifying these parameters (Becker et al. 2016), but one that is frequently used is automated scanning electron microscopy with energy dispersive spectrometry (e.g. QEMSCAN, MLA, Mineralogic, TIMA). Challenges do still exist when quantifying textural measurements as there are no strict guidelines for quantitative texture in ARD test work. Representative sampling, quantifying the statistical implications thereof, obtaining the required number of particles of interest, as well as other factors associated specifically with two-dimensional measurements, are often overlooked or not fully quantified. Qualitative textural assessment is also frequently performed. The acid rock drainage index (ARDI) considers the texture and mineralogy for ARD formation through parameters such as sulfide content, associations, morphology, alteration (extent of weathering), and neutralising mineral content and association with sulfide minerals. It was developed as a semi-quantitative segment of a geometallurgy-mineralogy-texture (GMT) approach and was designed for the provision of rapid estimates of ARD potential for whole-rock samples at mine sites (Parbhakar-Fox et al. 2011).

Thorough mineralogical analyses and an awareness of mineral liberation and association may improve the interpretation of contradictory or unexpected results obtained from commonly used static and kinetic tests (Brough et al. 2013). The current study aims to assess the dominating textural parameters on the particle size scale of static and biokinetic tests (micro-scale) and humidity cell tests (meso-scale). Quantitative textural data is used to assess Fe-sulfide association and liberation on these scales, and potential implications of these results is addressed in the context of humidity cell test work for the meso-scale, interlinked with results published in Opitz et al. (2016) for the micro-scale.

Methods

This study was performed using a waste rock sample generated from the mining of a greenstone gold deposit. The static and biokinetic test feed material preparation is described in Opitz et al. (2016) and will be referred to as the standard characterisation test (SCT) feed. The meso-scale humidity cell test (HCT) feed material was prepared as per the ASTM D5744-13 method (ASTM 2013). Feed material larger than 150 µm was dry-screened, while material smaller than 150 µm was wet-screened to minimise particle agglomeration. Presentation of the results of the HCT feed material was split into six size fractions, while the SCT material is presented as the bulk.

Textural data was obtained using a FEI QEMSCAN 650F instrument with two Bruker XFlash 6130 detectors at the University of Cape Town. Suitably representative subsamples were obtained using eight- and ten-way rotary sample dividers and prepared into polished sample blocks for analysis. Standard blocks (30mm diameter) were prepared as vertical sections for all material smaller than 1mm. To allow for the measurement of sufficient particles of interest, HCT sample fractions larger than 1mm were prepared as

70×70mm square blocks. When analysing the data obtained from QEMSCAN, categorisers were set up to obtain the number of Fe-sulfide-bearing particles, Fe-sulfide grain size distribution, association and liberation data for the SCT and HCT feed material. Liberation categories were defined as liberated (>90% particle area for mineral of interest) and unliberated (< 90% particle area for mineral of interest).

Results

A pre-existing data set exists for the sample used in this study. Results for static and biokinetic tests, as well as the ARDI, mineralogical ANC and bulk mineralogy obtained via QEMSCAN are presented in Opitz et al. (2016), sample B. For the purposes of this study the pyrite and pyrrhotite were grouped into a general Fe-sulfide category, with other minerals being grouped into categories based on their relative reactivity as given by Lawrence and Scheske (1997). Bulk mineralogy indicated the dominance of pyrite in the Fe-sulfide category, while the dissolving, fast, intermediate and slow weathering, inert and other categories were dominated by calcite, olivine, biotite, plagioclase feldspar, quartz and apatite, respectively.

Table 1 shows the Fe-sulfide content and liberation of the sample by size for the HCT (columns 1-6) and SCT (column 7) feed material (as the bulk). Row one defines the Fe-sulfide content of each fraction as a percentage of the total Fe-sulfide content of the sample, for example, column 1 shows that 62% of all the Fe-sulfide present in the HCT feed is concentrated in the -6700/+2000µm size fraction. In column 7, however, the Fe-sulfide content and liberation are presented as the bulk, with the SCT feed having a total Fe-sulfide content of 7%. Rows two and three show the liberation of Fe-sulfide material, with the percentages representing the amount of liberated material (row two) and unliberated material (row three) in that size fraction. Fe-sulfides in the HCT feed predominantly occur as unliberated particles, with more than 50% of Fe-sulfides in size fractions greater than 425µm being unliberated and mineral association dominating over liberation (see Figure 2). For the SCT feed the liberation of the Fe-sulfide material is the dominating textural parameter, with only 10% unliberated Fe-sulfides.

Figure 1 below presents the corresponding false colour images for the size fractions listed in Table 1 and serves only as a visual representation of the Fe-sulfide-bearing particles that fall into the liberated and unliberated categories.

Figure 2 shows the Fe-sulfide liberation and association by size for the HCT feed and the bulk for the SCT feed material (see also Table 1). Fe-sulfide liberation increases as particle size decreases, with negligible Fe-sulfide liberation at size fractions above 1000µm, inferring unliberated texture (association dominated). The increase in liberation with size fraction is prominent for size fractions smaller than 1000µm, due to the largest Fe-sulfide grains not exceeding 600µm and the finest grains being under 3µm. Nonetheless, a small amount of liberated material does appear in the -1400/+1000 fraction, due to the massive sulfide texture. Fe-sulfide mineral association in all size fractions is dominated by inert, slow weathering and intermediate weathering material, followed by notably smaller associations to carbonate, fast weathering and other sulfides. The Fe-sulfide asso-

Table 1 *Row one: distribution by size represented as a percentage of the total Fe-sulfide in the sample (column 7 represented as the bulk). Rows two and three: Fe-sulfide liberation by size, with the percentages showing the portion of the Fe-sulfide in that fraction that is liberated or unliberated. Liberation for Fe-sulfide material is defined as liberated when 90% or more of its area is exposed to no other minerals and unliberated as having more than 90% of its area surrounded by other minerals. The size fractions of the HCT feed are 1: -6700/+2000; 2: -2000/+1400; 3: -1400/+1000; 4: -1000/+425; 5: -425/+150; 6: -150/+0 µm; and 7: SCT bulk feed (-150µm)*

Sample	1	2	3	4	5	6	7
Fe-sulfide	62%	6%	6%	7%	6%	13%	7%
Liberated	0%	0%	3%	18%	48%	81%	90%
Unliberated	100%	100%	97%	82%	52%	19%	10%

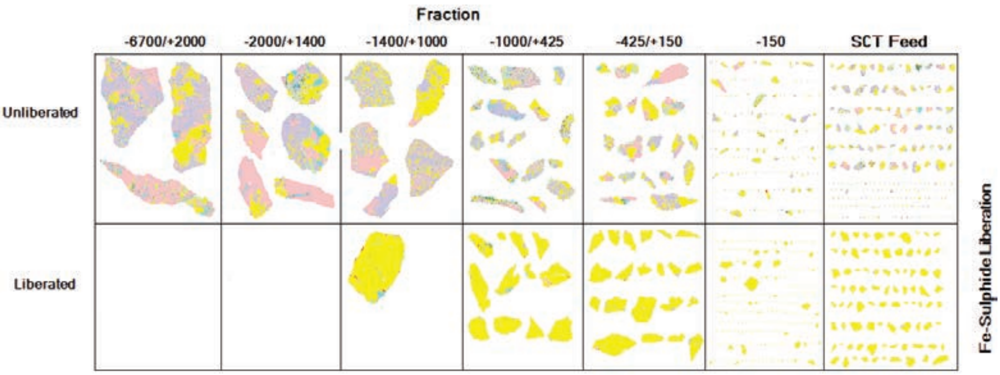

Figure 1 QESMCAN Image Grid categoriser set up by size fraction for Fe-sulfide-bearing particles. False colour images of Fe-sulfide-bearing particles correspond to the size fractions provided in Table 1. See Figure 2 for colour legend. The images are meant only to provide a visual representation of the Fe-sulfide liberation throughout size fractions and do not serve to display the relative abundance of particles in the categories or represent the "average" particle in each size fraction.

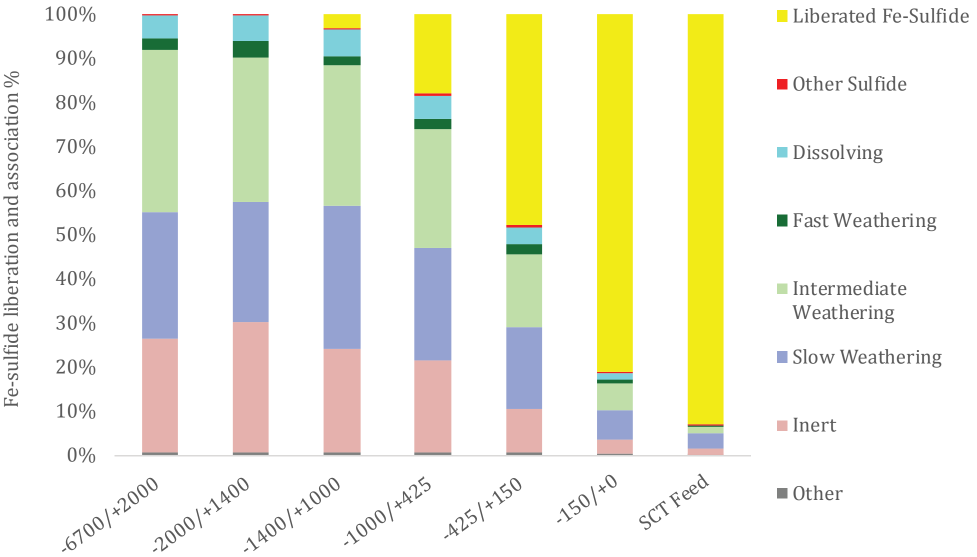

Figure 2 Fe-sulfide liberation and association for HCT and SCT feed material. The HCT feed is presented by size, while the SCT material is presented as the bulk. The major minerals contributing to the sub-groups are: Fe-Sulfide: pyrite, pyrrhotite; Other Sulfide: chalcopyrite, galena, sphalerite; Dissolving: calcite, dolomite, ankerite; Fast Weathering: olivine, diopside; Intermediate Weathering: epidote, pyroxene, amphiboles, chlorite, biotite; Slow Weathering: albite, orthoclase, muscovite; Inert: quartz, sphene; Other: apatite

ciation for the SCT feed is considerably lower than for the HCT feed material given the high liberation, but the unliberated material still shows Fe-sulfide association dominated by slow weathering, intermediate weathering and inert material.

Discussion

Liberated material comprises most of the Fe-sulfide mineral category in the SCT feed, as is expected for finely milled material. Consequently, this Fe-sulfide material is accessible for reaction under static and biokinetic test conditions. The very small association of Fe-sulfides with carbonate minerals indicates that the carbonate minerals may be liberated or associated with other phases. Static test results (Opitz et al. 2016) characterise the sample as potentially acid forming, which is expected as the Fe-sulfide content is comparatively larger (and predominantly liberated) than the dissolving mineral content. The biokinetic test results show a circumneutral final pH for this sample, which may be explained by reaction of the (potentially liberated) carbonate material, resulting in an initial rise in test pH to pH 7.0. Such conditions would hinder microbial metabolism and remove soluble ferric iron from solution, as may be observed by the corresponding low redox potential profile for sample B (Opitz et al. 2016).

The HCT feed association and liberation characteristics will have implications for humidity cell test results, as material that is liberated is readily susceptible to oxidizing conditions and will generate acidic leachate more rapidly than unliberated material (Brough et al. 2017). On this scale, most of the Fe-sulfide material is concentrated in size fractions above 1000µm, where association with intermediate weathering, slow weathering and inert mineral phases dominates. More than 70% of the Fe-sulfide material is found in size fractions above 1000µm (more than 90% of Fe-sulfides unliberated), thus the leaching behaviour of the HCT is likely to be dictated by this material. The Fe-sulfide material in the unliberated fraction, where it may be partially exposed, would still be accessible to oxidative conditions but a significantly longer time frame would be required to leach the Fe-sulfide grains completely, as opposed to more rapid leaching for liberated grains. This could have implications for the minimum specified duration for standard humidity cell tests (20 weeks) (ASTM 2013). Considering the potentially longer leach times due to predominantly unliberated material, it is expected that a longer test duration would be required for this sample to enable collection of meaningful leachate data. Additionally, the inert material associated with unliberated Fe-sulfides will not be susceptible to short-term weathering under the circum-neutral pH conditions within the humidity cell experiments. Physical breakage would be required to access these sulfides completely. Intermediate and slow weathering phases, however, would react over time and potentially expose the associated Fe-sulfide material to the oxidising environment, making acid formation over a longer period possible. Acid forming and neutralising minerals could also still be accessed through minor cracks or pores within the particles, but the net ARD formation from this pathway would be limited by mass transfer effects (Ghorbani et al. 2011). Fe-sulfide association with carbonate material may allow acid formed from these grains to be neutralised locally but the carbonate content is very small and would not offer sufficient neutralising capacity to label this sample as net non-acid forming, as shown by static test results (Opitz et al. 2016).

Conclusions

The Fe-sulfide material in the SCT feed was well liberated (dominating textural parameter), as expected for the determination of the “worst case” scenario for acid formation and neutralisation. For humidity cell tests the Fe-sulfide material in this sample is concentrated in the coarse size fractions where it is unliberated and associated predominantly with intermediate and slow weathering phases, which will not readily weather under circumneutral pH conditions. Over time these phases may weather, however, exposing the Fe-sulfide material. Fe-sulfides are also largely associated with inert minerals, making them accessible only through the exposed area in these unliberated categories or via minor cracks/pores. This will potentially extend the humidity cell test duration. Association of the Fe-sulfides with dissolving phases may offer local acid neutralisation but will be insufficient to buffer acid formation over time.

The knowledge gained from thorough textural and mineralogical analyses of waste samples could allow for an improved understanding of laboratory-based geochemical test results. This improvement will enable better characterisation and prediction of the ARD potential within waste deposits, and ultimately aid in the creation of reliable and accurate modelling frameworks.

Acknowledgements

Grateful thanks to the staff in the Department of Chemical Engineering at UCT who assisted with the mineralogical analyses. This work is based on the research supported in part by the National Research Foundation of South Africa (Grant Numbers 86054). The opinions, findings and conclusions or recommendations expressed in any publication generated by the NRF supported research is that of the author(s), and that the NRF accepts no liability whatsoever in this regard. This project is supported in part by the Water Research Commission (Project K5/2846/3).

References

ASTM (2013) Standard Test Method for Laboratory Weathering of Solid Materials Using a Humidity Cell. D5744-13 1–23. doi: 10.1520/D5744-13E01.2

Becker M, Dyantyi N, Broadhurst JL, et al (2015) A mineralogical approach to evaluating laboratory scale acid rock drainage characterisation tests. Miner Eng 80:33–36. doi: http://dx.doi.org/10.1016/j.mineng.2015.06.015

Becker M, Wightman EM, Evans CL (eds) (2016) Process Mineralogy: JKMRC Monograph Series in Mining and Mineral Processing: No. 6. Julius Kruttschnitt Mineral Research Centre, The University of Queensland, Queensland, Australia

Brough C, Strongman J, Bowell R, et al (2017) Automated environmental mineralogy; the use of liberation analysis in humidity cell testwork. Miner Eng 107:112–122. doi: 10.1016/j.mineng.2016.10.006

Brough CP, Warrender R, Bowell RJ, et al (2013) The process mineralogy of mine wastes. Miner Eng 52:125–135. doi: 10.1016/j.mineng.2013.05.003

Dold B (2017) Acid rock drainage prediction: A critical review. J Geochemical Explor 172:120–132. doi: 10.1016/j.gexplo.2016.09.014

Evans CL, Morrison RD (2016) Process Mineralogy: JKMRC Monograph Series in Mining and Mineral Processing: No. 6. In: Becker M, Wightman EM, Evans CL (eds)

Fagan-Endres MA, Cilliers JJ, Sederman AJ, Harrison STL (2017) Spatial variations in leaching of a low-grade, low-porosity chalcopyrite ore identified using X-ray μCT. Miner Eng 105:63–68. doi: 10.1016/j.mineng.2017.01.010

Ghorbani Y, Becker M, Mainza A, et al (2011) Large particle effects in chemical/biochemical heap leach processes - A review. Miner Eng 24:1172–1184. doi: 10.1016/j.mineng.2011.04.002

Hesketh AH, Broadhurst JL, Bryan CG, et al (2010) Biokinetic test for the characterisation of AMD generation potential of sulfide mineral wastes. Hydrometallurgy 104:459–464. doi: 10.1016/j.hydromet.2010.01.015

INAP (2012) Global Acid Rock Drainage Guide , INAP: The International Network for Acid Prevention

Jamieson HE, Walker SR, Parsons MB (2015) Mineralogical characterization of mine waste. Appl Geochemistry 57:85–105. doi: 10.1016/j.apgeochem.2014.12.014

Lengke MF, Davis A, Bucknam C (2010) Improving management of potentially acid generating waste rock. Mine Water Environ 29:29–44. doi: 10.1007/s10230-009-0097-1

Nordstrom DK, Alpers CN (1999) Geochemistry of acid mine waters. Environ Geochemistry Miner Depos 6:133–160

Opitz AKB, Becker M, Broadhurst JL, et al (2016) The Biokinetic Test as a Geometallurgical Indicator for Acid Rock Drainage Potentials. Perth, Australia, pp 183–191

Parbhakar-Fox A, Lottermoser BG (2015) A critical review of acid rock drainage prediction methods and practices. Miner Eng 82:107–124. doi: 10.1016/j.mineng.2015.03.015

Parbhakar-Fox AK, Edraki M, Walters S, Bradshaw D (2011) Development of a textural index for the prediction of acid rock drainage. Miner Eng 24:1277–1287. doi: 10.1016/j.mineng.2011.04.019

Metal Release from Acidic and Near-Neutral pH-Conditions in Historical W, Cu and F Skarn Tailings at Yxsjöberg, Sweden

Lina P.B. Hällström, Lena Alakangas, Olof Martinsson

Applied Geochemistry, Luleå University of Technology, 97187 Lulea, Sweden, lina.hallstrom@ltu.se

Abstract

Weathering products stored in the pore water and/or as easily soluble salts in historical skarn tailings containing Be, Bi, Cu, W, and Zn, were released in water soluble fraction in the upper-most acidic tailings, at the visual oxidation front (1.5m), and/or below 2.5m (pH>7). Thus, there is a risk that these metals can pollute receiving waters by neutral mine drainage. Re-mining the tailings could be a suitable remediation method that would both reduce the environmental impact and simultaneously support the supply of metals.

Keywords: Tungsten, Beryllium, Bismuth, Skarn tailings, water soluble fractions, Remining

Introduction

Tailings generated from mining activities in the ancient past can pose a risk to the water quality in the vicinity of the repository due to reckless disposal and long-term storage (Hudson-Edwards et al., 2011). This is if metals in high concentrations are released from their hosting minerals due to changing geochemical conditions (Lindsay et al., 2015). The extent of metal downward movement in the tailings is dependent on adsorption and (co-)precipitation processes (Lee et al., 2002). Elements captured in secondary minerals that are water soluble pose a high risk of being transported in the tailings along with the release from primary weathering processes, and leak out to the ground- and surface water in the vicinity of the repository. Most of the environmental studies related to mine waste have been focused on sulfidic deposits and acid mine drainage, while little attention has been paid to tailings from skarn ore deposits and neutral mine drainage. Skarn tailings can contain several elements of potential concern such as e.g. Be, Bi, Cu, W, and Zn, together with Fe-sulfides and carbonates (Meinert et al., 2005). The sulfides can enhance the mobility of metals in the tailings due to sulfide oxidation reducing the pH (Blowes et al., 2003), and the carbonates can form neutral mine drainage if the abundance is large enough to neutralize the acidity and immobilise metals generated from the sulfides (Lindsay et al., 2015). Studying the long-term effects of metal release in skarn tailings is of great importance. In Smaltjärnen's repository at Yxsjöberg, 2.8 Mt of tailings from a former W, Cu, and fluorite mine have been stored more than 50 years. The tailings are in direct contact with the atmosphere and Lake Smaltjärnen (Fig.1a). Total concentrations of 134 samples from four vertical cores through the tailings showed an average content of Be, Bi, Cu, Sn, Zn, W, and S in the tailings of 284, 495, 946, 559, 301, and 960 ppm, and 1.2 wt.%, respectively (Hällström et al., submitted). Pyrrhotite was the dominating sulfide in the tailings together with lower amounts of chalcopyrite and bismuthinite. The unusual mineral danalite ($Fe_4Be_3(SiO_4)_3S$) contained approximately 40% of all Be and Zn, and 2% of all Mn in the tailings (Hällström et al., submitted), and is considered to be more easily weathered than other Be-minerals (Taylor et al., 2003). Scheelite was the main W-mineral (Hällström et al., submitted). The long-term storage had resulted in pyrrhotite oxidation down to 2.5 m depth and depletion of calcite in the upper 1.5 m subsequent with formations of gypsum and hydrous ferric oxides (HFO). A distinctive change in color was found at 1.5m depth in the tailings (Fig.1c), which is referred to as the visual oxidation front. Hydrous ferric oxides (HFO) had colored the tailings reddish-brown above the oxidation front, and dark-grey tailings were present below. A detailed description of the site and mineralogy can be found in Hällström et al. (submitted). Earlier studies have shown that the groundwater has a pH in-between 7-9 and that the surface water has a pH around 6. Elevated concentrations of Ca, S, Be, and Zn has previously been found in the groundwater (Höglund et al., 2004).

In this study, the weathering products stored in the pore water and/or as easily soluble salts in the tailings of Yxsjöberg were analyzed with depth in one representative core (P4) from Hällström et al. (submitted), with emphasis on Be, Bi, Cu, W, and Zn. The results were coupled with the chemical composition and mineralogical studies from Hällström et al. (submitted) to evaluate the risk of elements leaching to receiving waters, and the suitability of re-mining as remediation method.

Method

The vertical core (P4) of 6 m has been sampled with percussion drilling through the tailings, and 50 subsamples of 10 – 30 cm were collected and analyzed for total concentrations (Hällström et al., submitted).

The water soluble fractions of 14 subsamples of P4 were analyzed according to the first step of Dold (2003). A sample of 2.5 g was mixed with 125 ml milliQ water (0.055 µS/cm) and shaken for 1 hour. The eluates were filtered through 0.22 µm cellulose acetate membrane filters, using a vacuum Sterifil® Aseptic System and Holder from Merck Millipore. The filters had been prewashed with 5% acetic acid for 72 h and left in milliQ water for 24 h (Ödman et al., 1999). Samples were sent to ALS Scandinavia, Luleå, for screening analysis of 71 elements with an inductively-coupled plasma sector field mass spectrometer (ICP-SFMS), and anion analysis of sulfate, fluoride, and chloride with ion chromatography (CSN ISO 10304-1, CSN EN 16192). pH in the eluates were measurements with pHenomenal MU 6100H and the electrode pHenomenal 111 (662-1157), which was calibrated prior to the measurements with standard buffer solutions 4, 7 and 10. The electrical conductivity (EC) electrode

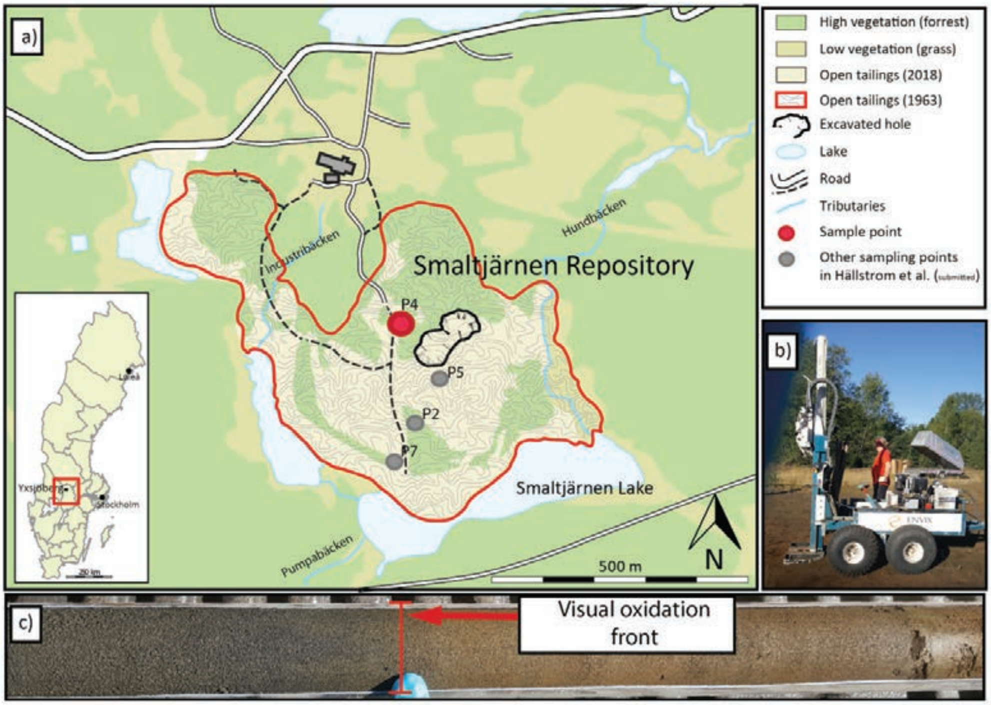

Figure 1. a) The water soluble fractions in tailings from Smaltjärnen Repository was studied with depth in one, out of four vertical cores (P4: marked in red) sampled with percussion drilling (b). c) The visual oxidation front in P4 was seen at 1.5m depth.

was controlled with a KCl-standard (1413 µS/cm) prior the measurements.

Results

In the water soluble fractions, pH was higher than 7 below the oxidation front (1.5 m) and less than 5 in the oxidized upper-most tailings (Fig. 2). The electrical conductivity (EC) was anti-correlated with pH, with a maximum of 0.88 mS/cm at 0.3 m depth. Calcium, S, and SO_4 in the water soluble fractions were highest in the upper-most samples, and the concentrations decreased with depth with an exception of a small increase at 3.6 m (Fig.2). The correlation between the molality of Ca and S (R^2=0.997), and between S and EC (R^2=0.993), showed that gypsum regulated EC in the water soluble fraction throughout the profile. Copper was released in highest concentrations in the upper-most samples (max: 780 µg/L) and a second peak of released at the visual oxidation front (Fig.2). Aluminum, Be, K, Mg, Mn, Na, and Zn were released in the highest concentrations at, or just above, the visual oxidation front (1.5 m, depth). Aluminum, Be and Zn were not re-

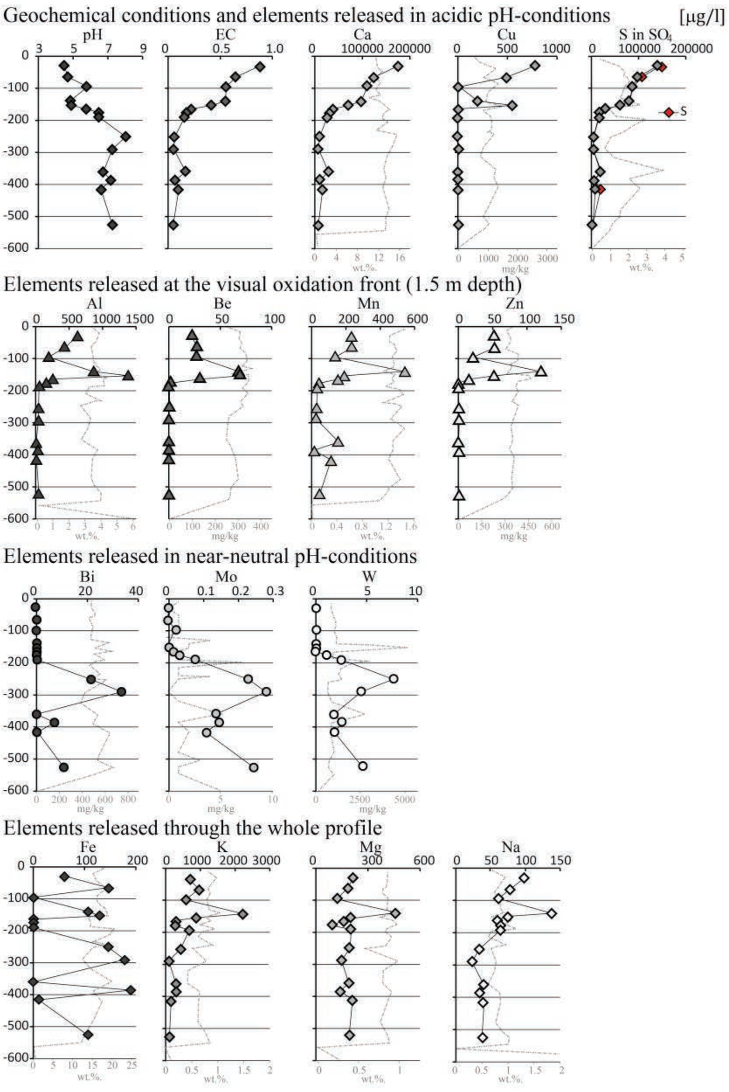

Figure 2. The water soluble fractions with depth in P4 is in µg/L and EC is in mS/cm. Total solid concentrations from Hällstrom et al. (submitted) are shown in grey dotted lines in mg/kg or wt.%.

leased below 2 m depth, whilst low concentrations of K, Mg, Na, and Mn was released through the whole profile. Manganese was water soluble at 3.6 m depth similar to Ca and SO_4. Bismuth, Mo, and W were released below 2.5 m depth. The highest concentrations were released between 2.5 – 3 m and lower concentrations were released between 3.5 – 4 m. Bismuth was released in the highest concentrations (max: 30 µg/L), followed by W (max: 10 µg/L). The released concentrations of Fe were varying through the whole profile with elevated concentrations in the upper-most samples, at the visual oxidation front and below 2.5 m depth. A maximum of 190 µg/L Fe at 2.5 m depth were released, which corresponds to a release of 9.5 mg/kg Fe from the tailings. This is only a small fraction compared to the total concentration in the tailings, 14.9 wt.% (Hällström et al., submitted).

Discussion

The long-term storage of tailings in ambient conditions has resulted in pyrrhotite oxidation down to 2.5 m depth, depletion of calcite and formations of HFO in the upper 1.5 m subsequent with reduced pH and increased electrical conductivity (Fig.2). At the visual oxidation front (1.5 m) pH was 4.9 and EC was 0.42 mS/cm. In the tailings, elements were released in elevated concentrations in either 1) the upper-most acidic tailings, 2) at the visual oxidation front (1.5 m), or 3) below 2.5 m in near-neutral pH-conditions (Fig.2). Only Fe was released in elevated concentrations in all three aforementioned settings. Gypsum dissolved by the water leaching test regulated EC throughout the profile, and the increase of water soluble Ca and S at 3.6 m combined with mineralogical studies revealed that a second oxidized layer occurred. Thus, pyrrhotite was partly oxidized, calcite was altered and crystalline HFO were formed (Fig. 3a), which shows that the tailings at 3.6 m depth have been exposed to oxygen during a longer period of time in the past.

Elements released in acidic pH-conditions in the upper-most samples

Oxidation of Fe-sulfides, subsequently decreased pH to 4.5, depletion of calcite and formations of gypsum and HFO has generated high concentrations of water soluble Ca, Cu, Fe, and S in the upper-most samples. Chalcopyrite is the main primary mineral for Cu and it was oxidized in the upper-parts of the tailings and covered with a thick rim of HFO (Hällström et al., submitted). Iron has previously been released from the oxidation of pyrrhotite, pyrite, and chalcopyrite, and has formed amorphous HFO around most mineral grains in the upper 1.5 m. The release of Cu and Fe are assumed to come from the pore water, or be loosely adsorbed to HFO or soluble Fe(II)salts. The total concentrations of Cu and Fe in the upper-most tailings are not decreasing considerably, which implies that released Cu and Fe in the acidic oxidizing conditions were not transported downwards.

The high concentrations of Ca and S in the water soluble fractions was due to the presence of secondary gypsum in upper-parts of the tailings. The occurrence was confirmed by mineralogical studies and gypsum had formed secondarily from the release of Ca from calcite and SO_4 from pyrrhotite oxida-

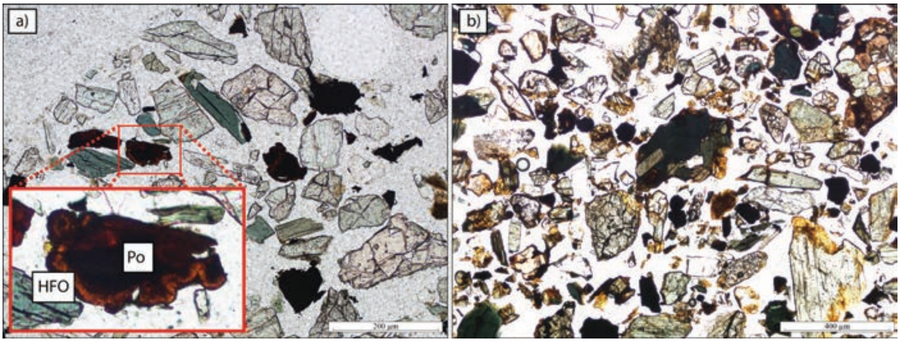

Figure 3. a) At 3.6 m depth, secondary hydrous ferric oxides (HFO) were found around grains of magnetite, pyrrhotite (Po), and scheelite. b) At the visual oxidation depth (1.5 m depth) amorphous HFO were present around almost all mineral grains in the tailings.

tion (Hällström et al., submitted). The formations of secondary gypsum have decreased the transport of Ca and SO_4 in the tailings, but high concentrations in the groundwater have, nevertheless, been found in previous studies (Höglund et al., 2004), and the solid content of Ca and S has both decreases from 1.5 m depth upwards (Fig.2). No other elements were following the same trends as Ca and SO_4 in the upper-most samples, which imply that no trace elements were co-precipitated with gypsum.

Elements released at the visual oxidation front (1.5m depth)

Weathering of silicates and danalite has generated water soluble Be, K, Mg, Mn, Na, and Zn in elevated concentrations at, or just above, the visual oxidation front (1.5 m, depth). In the unoxidized tailings, K was mainly found in biotite and orthoclase, Na in oligoclase, and Mg in biotite, chlorite, ferrohornblende, and hedenbergite. Beryllium, Zn, and Mn were all hosted by danalite ($Fe_4Be_3(SiO_4)_3S$), and the results indicated that ongoing weathering occurred at 1.5 m depth. Thus, the concentrations of Be had decreased stepwise with 40% from 351 mg/kg at 1.5 m to 250 mg/kg at 0.3 m, suggesting that danalite had already been weathered there. No strong accumulation peaks of Be were present deeper down in the tailings and Be, Zn, and Mn have previously been found in high concentrations in the groundwater of the repository (Höglund et al., 2004). The release of Al, K, Mg, and Na throughout the profile shows that silicate minerals have been weathered throughout the tailings profile but the most intense weathering occurred at the visual oxidation front. Weathering of silicates throughout the tailings was confirmed by mineralogical studies. Copper and Fe was also released in high concentrations at this depth. Compared to the release in the uppermost tailings, peaks of Cu of Fe were present at 1.6 m depth, coinciding with formations of blue secondary minerals, which is assumed to be a Cu-enrichment (Hällström et al., submitted). This implies that Cu has been transported downwards in the tailings due to low pH (4.5) and enriched when pH was above 5.5. Copper has not been found in high concentrations in the groundwater (Höglund et al., 2004), even though up to 780 µg/L were detected in the water soluble fraction in the tailings.

Elements released in near-neutral pH-conditions

A noteworthy downward transport of Bi, Mo, and W has occurred below 2.5 m depth where pH was higher than 7. Elevated concentrations in the water soluble fractions coinciding with low concentrations in the solid phases between 2.5 – 3.6 m for Bi, and between 2 – 3.6 m for Mo and W (Fig.2). The geochemical behaviors of Bi and W in tailings are poorly studied (Hällström et al., submitted), and their hosting minerals (bismuthinite and scheelite, respectively) has previously been considered as stable minerals (Bokii and Anikin, 1956; Jung et al., 2002). The few studies that exist about W, tentatively says that the release from scheelite in groundwater is due to anion exchange by CO_3^{2-}, OH^- (Atademir, 1979), or SiO_2 (Marinakis and Kelsall, 1987). The highest concentrations in water soluble phase of the tailings were found at 3 m depth, where secondary carbonates were formed (Hällström et al., submitted). Water soluble concentration of W and Mo were below the detection limit in tailings above 1.5m where HFO were present. Low concentrations of water soluble W and Mo were also coinciding with the oxidized layer of tailings at 3.6 were presence of HFO around grains of pyrrhotite, magnetite, and scheelite was observed (Fig.3a). Tungsten and Mo are known to form oxyanions with high affinity for HFO at pH <8 and remain in solution at pH >9 (Gustafsson, 2003). Bismuth is considered to be an immobile element due to its ion potential (Ball et al., 1982) but the element still showed similar trends as W and Mo.

Conclusions

This study showed that metals of potential concern (Be, Bi, Cu, W, and Zn) were released in both acidic and near-neutral pH-conditions of skarn tailings during long-term storage in ambient conditions. In the uppermost tailings, where pH was 4.5, Ca and S were released by gypsum dissolution, and Cu was tentatively desorbed from secondary minerals. At the visual oxidation front, silicate minerals such as orthoclase and oligoclase were being weathered together with the unusual mineral danalite ($Fe_4Be_3(SiO_4)_3S$), which released Be, Zn, and Mn into the water soluble fractions. In the deep tailings, pH was near-neutral (7 – 8) and Bi and W were found in elevated concentrations in the water soluble fractions, possibly due to anion exchange with carbonates, but this needs to be investigated further. Iron had an important role due to the formation of hydrous ferric oxides in the tailings capturing elements released in the water soluble fractions in both the upper-most samples and at 3.6m depth. The elements that were released at the visual oxidation front (Be, Mn, and Zn) were found in highest concentrations in the groundwater in previous studies. The transport of Cu, Bi, S, and W in the tailings and their retention by secondary minerals makes them to a potential concern since changes of geochemical conditions can release them to the groundwater. This makes re-mining to a more suitable remediation method than other more conventional options such as covers.

Acknowledgments

We want to thank our colleagues within the collaboration of the REMinE project from Luleå University of Technology (LTU) in Sweden, Porto University in Portugal and the National Institute for Metals and Radioactive Resources in Romania. This work was supported by Vinnova [Grant numbers 215 06 631] and co-funded by the Center of Advanced Mining and Metallurgy (CAMM^2) at LTU.

References

Atademir, M.R., Kitchener, J.A., Shergold, H.L., 1979. The surface chemistry and flotation of scheelite. I. Solubility and surface characteristics of precipitated calcium tungstate. Journal of Colloid and Interface Science 71, 466-476.

Ball, T.K., Basham, I.R., Blank, D., Smith, T.K., 1982. Aspects of the geochemistry of bismuth in South-West England. Proceedings of the Ussher Society 5, 376-382.

Blowes, D.W., Ptacek, C.J., Jambor, J.L., Weisener, C.G., 2003. The Geochemistry of Acid Mine Drainage. Treatise on geochemistry 9, 612. 150-195

Bokii, G.B., Anikin, I.N., 1956. Determination of the solubility of scheelite in water and aqueous solutions. Zhurnal Neorganicheskoi Khimii 1, 1926-1928.

Dold, B., 2003. Speciation of the most soluble phases in a sequential extraction procedure adapted for geochemical studies of copper sulfide mine waste. J. Geochem. Explor. 80, 55-68.

Gustafsson, J.P., 2003. Modelling molybdate and tungstate adsorption to ferrihydrite. Chem. Geol. 200, 105-115.

Hudson-Edwards, K.A., Jamieson, H.E., Lottermoser, B.G., 2011. Mine wastes: past, present, future. Elements 7, 375-380.

Hällström, L.P.B, Alakangas, L., Martinsson, O., 2018. Geochemical Characterization of W, Cu and F Skarn Tailings at Yxsjöberg, Sweden. *Submitted to Journal of Geochemical Exploration.*

Höglund, L.O., Jones, C., Lindgren, M., 2004. Förstudie för efterbehandling av sandmagasin i Yxsjöberg. Kemakta AR 2003-23.

Jung, M.C., Thornton, I., Chon, H., 2002. Arsenic, Sb and Bi contamination of soils, plants, waters and sediments in the vicinity of the Dalsung Cu–W mine in Korea. Sci. Total Environ. 295, 81-89.

Lee, G., Bigham, J.M., Faure, G., 2002. Removal of trace metals by coprecipitation with Fe, Al and Mn from natural waters contaminated with acid mine drainage in the Ducktown Mining District, Tennessee. Appl. Geochem. 17, 569-581.

Lindsay, M.B., Moncur, M.C., Bain, J.G., Jambor, J.L., Ptacek, C.J., Blowes, D.W., 2015. Geochemical and mineralogical aspects of sulfide mine tailings. Appl. Geochem. 57, 157-177.

Marinakis, K.I., Kelsall, G.H., 1987. The surface chemical properties of scheelite (CaWO4) I. The scheelite/water interface and CaWO4 solubility. Colloids and Surfaces 25, 369-385.

Meinert, L.D., Dipple, G.M., Nicolescu, S., 2005. World skarn deposits. Economic Geology 100, 299-336.

Taylor, T.P., Ding, M., Ehler, D.S., Foreman, T.M., Kaszuba, J.P., Sauer, N.N., 2003. Beryllium in the environment: a review. Journal of Environmental Science and Health, Part A 38, 439-469.

Ödman, F., Ruth, T., Pontér, C., 1999. Validation of a field filtration technique for characterization of suspended particulate matter from freshwater. Part I. Major elements1. Appl. Geochem. 14, 301-317.

Making Your Results Stick – Using General Likelihood Uncertainty Estimation (GLUE) In Water Quality Prediction From Coal Discard

Terry Harck

Solution[H+], Pretoria, South Africa, terry.harck@solutionhplus.com

Abstract

The GLUE methodology sets a "likelihood measure" in advance of modelling. Random realisations of uncertain values and input parameters are drawn from appropriate distributions during multiple model simulations. If the model results conform to the likelihood measure, the model is considered "behavioural", that is, one of a set of models that can replicate real-world observations.

We apply the GLUE methodology to a two-component ensemble geochemical model of a coal discard facility and one-dimensional transport in the underlying shallow groundwater system. The results indicate that our geochemical model was non-behavioural, that is, could not give an acceptable reproduction of observations, even with rather relaxed rejection criteria. This is probably due to the multitude of parameters required by the model.

This exercise illustrates that GLUE can be helpful in evaluating model results. However, random sampling can give rise to unrealistic sets of model inputs. These can generate noise in model results that may obscure whether the model is behavioural or not.

Keywords: ICARD, IMWA, MWD 2018, PHREEQC, geochemical model, coal discard, GLUE, uncertainty estimation

Introduction

Mine water management requires hydrological, hydrogeological, and geochemical models. These models are frequently "calibrated" against field and/or laboratory measurements. In general, agreement between the model and the observed measurements is considered an indicator that the model is a reasonable proxy for the system being considered. However, what constitutes "agreement" between observed and simulated data, and what does "agreement" actually mean in terms of simulating the system? Actually, the calibration process tells us nothing about whether the model is suitable for forecasting.

Uncertainty estimation in geochemical models is challenging when there are data available to evaluate model performance. The commonly-applied calibration approach can only be conditionally optimal as data errors will propagate through the model structure, which is itself a simplification of the reality generating the observations (Beven 2009). Therefore, there may be several different sets of parameters consistent with the data used for "calibration".

There are various statistical methods to address model optimisation including Bayesian and Monte Carlo methods. These are commonly applied with modern computing tools and technologies. However, these methods assume we have the correct model structure and only need to find the optimal input parameters. Beven (2009) considered the shortcomings of the calibration process and formulated the General Uncertainty Likelihood Estimation (GLUE) methodology as a means to provide more information on the suitability of a model for forecasting.

For any model there are many combinations of input parameters that may produce simulation results consistent with observations. However, there is no single "true" model. GLUE is an approach to model calibration that allows for the effects of model structural and data errors. "Model conditioning" is the descriptor used by Beven to describe a process that tries to find only those models that are acceptable from a theoretical set of all possible models.

The GLUE methodology is summarised as follows (from Beven 2009):

1. Before running the model, decide on a likelihood measure in evaluating each model run, including rejection criteria for non-behavioural model
2. Decide which model parameters and input variables are to be considered uncertain
3. Decide on prior distributions from which those uncertain parameters and variables can be sampled
4. Decide on a method of generating random realisations of models consistent with the assumptions in steps 1 and 2.

In this paper, we present the partial application of GLUE to an ensemble geochemical model of a coal discard heap. GLUE can provide insights into model structure not provided by other optimisation methods. While GLUE has been previously applied to hydrogeochemical models (eg. Zhang et al 2006), to our knowledge, it has not been applied to pyrite oxidation models.

Methods

The opportunity to apply the GLUE methodology arose while characterising a coal discard facility for environmental permitting. The facility is located in central Mpumalanga Province of South Africa. Satellite imagery (Google Earth) indicates the footprint topsoil was stripped during December 2007. Discard deposition commenced in January 2008.

Two boreholes "BH Shallow" (11 m) and "BH Deep" (30 m) monitor groundwater quality approximately 30 m downstream of the toe of the facility. The available monitoring data extends from November 2008 to June 2015. Groundwater quality monitoring indicates contamination by acid seepage from the discard in BH Shallow, while groundwater quality in BH Deep has remained relatively unimpacted (Figure 1). A marked increase in pH and decrease in sulphate concentration in early 2014 is considered anomalous.

Excluding the anomalous data, the shape of the monitored sulphate time series is reminiscent of a column breakthrough curve. The work in this paper attempts to model the groundwater quality at BH Shallow using the one-dimensional transport capability of PHREEQC (Parkhurst and Appelo 2013).

A two-component ensemble model was developed. The first component of the model simulated pore water quality due to sulphide oxidation in the coal discard using the relations of Williamson and Rimstidt (1994). Model parameters were determined from geochemical characterisation (Table 1) and physical characterisation of discard (Figure 2).

The second model component simulated one-dimensional transport in the shallow groundwater aquifer. The local hydrogeology consists of Karoo Sequence sedimentary units, including shaly sandstones and siltstones. BH Shallow samples groundwater in the weathered zone aquifer, while BH Deep is screened in the fractured zone aquifer. Groundwater velocity in the shallow aquifer, based on the data in Table 2, is 1.4 to 4.1×10^{-7} m/s.

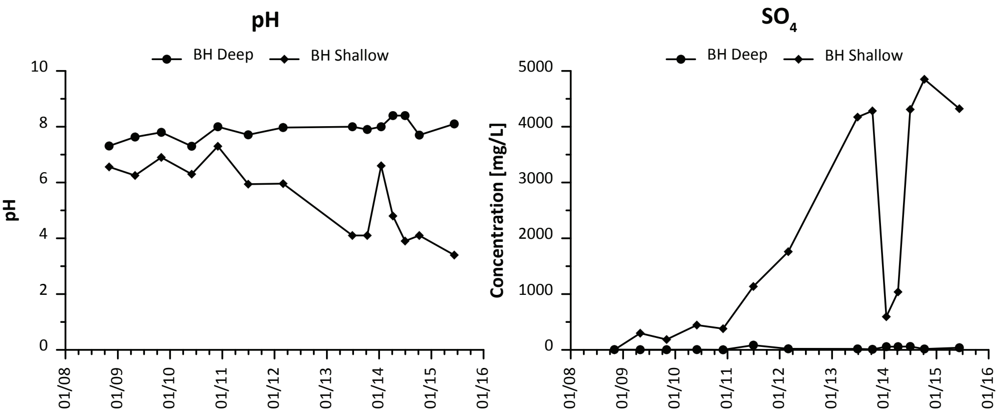

***Figure 1** Groundwater quality monitored downstream of discard.*

Table 1 *Geochemical characterisation of coal discard.*

Parameter	Unit	Value	Comment
Bulk density	kg/L	1.211	Mean of compacted bulk densities of three samples
Porosity	L/L	0.26	Estimated from particle size distribution
Pyrite	wt%	2.92	XRD on composite of three samples
Calcite	wt%	1.66	XRD on composite of three samples
Siderite	wt%	3.23	XRD on composite of three samples
Gypsum	wt%	--	not detected in sample
Particle density	kg/L	2.55	Calculated from mineralogy data
Porosity	L/L	0.48	Calculated from bulk density and particle size
Moisture content	wt%	48	Mean of three samples
Discard particle area	m^2/kg	30.12	Estimated from particle size distribution

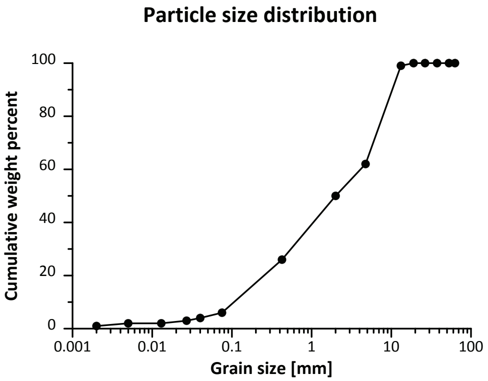

Figure 2 *Particle size distribution of discard.*

Applying Step 1 of the GLUE methodology to the first model component, the model results were “acceptable” if simulated pH at any time step was less than observed pH and if simulated SO_4 was higher than observed SO_4 at any step.

For the second model component an arbitrary likelihood measure of 80% of simulation results within one standard deviation was selected. That is, if 80% of the simulation results were within the field defined by one standard deviation of the mean parameter value (pH and SO_4), and one standard deviation of the mean period between successive monitoring events, the run would be considered “successful”.

Thirteen parameters/variables considered uncertain in the first model component were given prior distributions based on sample results, as indicated in Table 3. Table 4 shows eleven parameters/variables for the second model component. This comprised Steps 2 and 3 of the GLUE methodology.

Table 2 *Hydrogeology at coal discard facility.*

Aquifer	Depth	Estimated K	Estimated porosity
Weathered zone	±10	0.044 – 0.155	3%
Fractured zone	>10	0.015 – 0.04	0.4%

For Step 4 of the methodology, one hundred repetitions of the ensemble model were run using a Python 33 module and the IPHREEQC module (Charlton and Parkhurst 2011) called by the PhreeqPy method (Müller 2013). For each repetition, the Python code randomly selected values for each parameter from the relevant distribution and wrote the values to the PHREEQC input file, which was then executed using PhreeqPy to call IPHREEQC.

Results

For the first model component, simulated pH in the discard pore water was lower than observed pH at BH Shallow. However, simulated SO_4 was only higher than observed SO_4 in 9 out of 100 simulations (Figure 3).

The “acceptable” model results from the first model component were applied in the second model component. The model was run beyond the available observations to predict future groundwater quality at BH Shallow (Figure 4). The simulated time series of pH and SO4 bear some similarity to the real-world observations. However, the simulated pH values generally do not meet the criteria for a behavioural model, while the simulated sulphate values do. The prediction suggests

Table 3 *Uncertain model input parameters and values and the assumed distributions for the first model component (discard pore water quality).*

Parameter/ variable	Unit	Distribution	Distribution parameters^A	Comment
Initial pyrite	mol	Triangular	0.04, 0.15, 0.35	Range of XRD
Pyrite log A/V		Triangular	-0.94, -0.28, 0.1	Calculated (3 samples)
		Initial pore water:		
pH	pH unit	Triangular	8.0, 8.1, 8.3	Range of leach tests
Al	mg/L	Triangular	0.021, 0.032, 0.051	Range of leach tests
Alkalinity	mg/L as $CaCO_3$	Triangular	28, 51, 64	Range of leach tests
Ca	mg/L	Triangular	41, 60, 95	Range of leach tests
Cl	mg/L	Triangular	3, 5, 6	Range of leach tests
Fe	mg/L	Triangular	0.064, 0.110, 0.199	Range of leach tests
K	mg/L	Triangular	6.0, 7.1, 8.9	Range of leach tests
Mg	mg/L	Triangular	10, 15, 25	Range of leach tests
Mn	mg/L	Triangular	0.046, 0.086, 0.158	Range of leach tests
Na	mg/L	Triangular	8, 10, 15	Range of leach tests
SO_4	mg/L	Triangular	100, 155, 264	Range of leach tests

^{A} Left limit, mode, right limit

Table 4 *Uncertain model input parameters and values and the assumed distributions for the second model component (one-dimensional transport).*

Parameter/ variable	**Unit**	**Distribution**	**Distribution parameters^A**	**Comment**
		Background groundwater:		
pH	pH unit	Normal	7.6, 0.503	All distributions determined from 63 analyses of groundwater from several years of monitoring data
Al	mg/L	Lognormal	-1.98, 0.781	
Alkalinity	mg/L as $CaCO_3$	Normal	142, 50	
Ca	mg/L	Normal	22.7, 11.15	
Cl	mg/L	Normal	16.2, 6.632	
Fe	mg/L	Lognormal	-1.74, 1.500	
K	mg/L	Normal	1.63, 0.549	
Mg	mg/L	Normal	10.8, 4.492	
Mn	mg/L	Lognormal	-1.84, 1.012	
Na	mg/L	Normal	22.3, 7.516	
SO_4	mg/L	Lognormal	1.73, 0.299	

^{A} Mean, standard deviation

that SO_4 concentrations will continue to increase.

Discussion

The results of this application of GLUE to a geochemical model highlight several advantages and disadvantages of the methodology.

First, the criteria for acceptability or "likelihood measure" could have been more carefully selected. Figure 4 shows that the pH and SO_4 concentration of the source were too low to correspond well with observed values. In fact, the one-dimensional transport model results skirt the lower boundary of the "acceptable" field. More rigorous criteria for the first model component may have avoided this issue.

A challenging aspect of geochemical models is the large number of variables. If likelihood measures are set for several output variables, a condition may arise, as in our coal discard example, in which one output

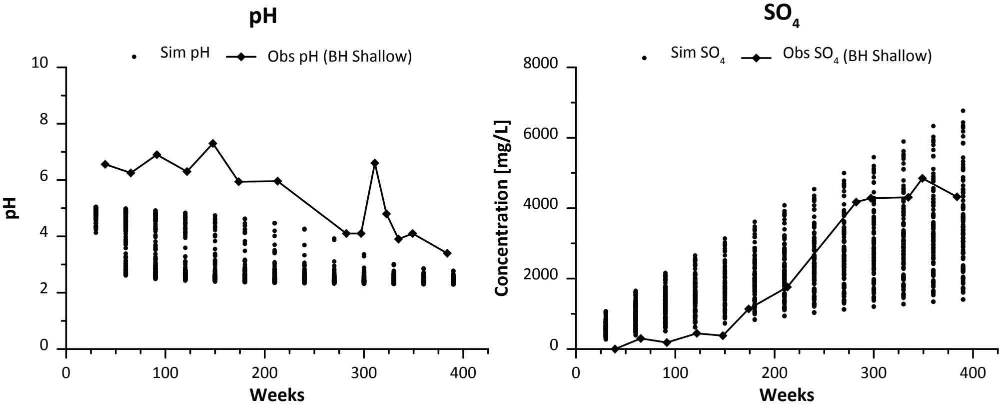

Figure 3 *Results of 100 simulations of discard pore water.*

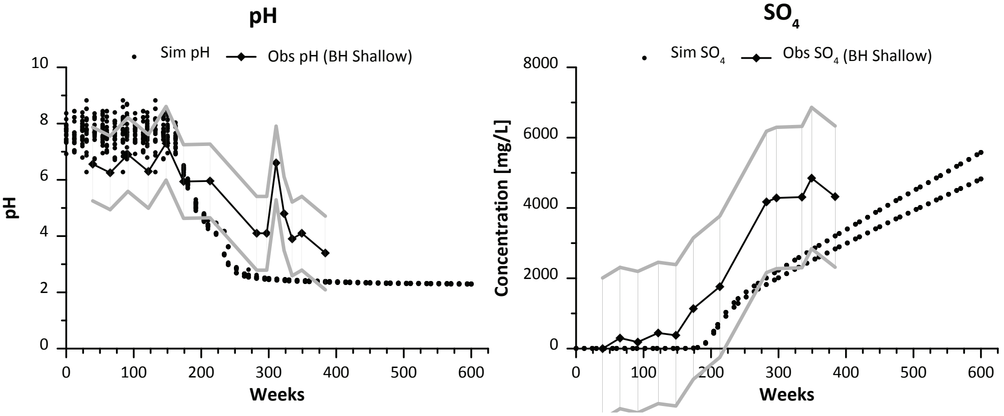

Figure 4 *Results of 100 simulations of one-dimensional transport. Grey lines indicate ±one standard deviation from observed values.*

variable indicates a behavioural model (SO_4 in this case), while another may not (pH in this case).

Second, and related to the above, the veracity of the discard pore water model component is called into question. Several possibly significant factors may have been excluded from the model, for example, a buffering mechanism resulting in a higher pH than modelled. Also, initial SO_4 concentrations in discard pore water were estimated from leach test results and did not consider evaporative concentration.

Third, the selection of uncertain parameters. Background groundwater concentrations were randomised in the one-dimensional transport model. However, the impact of this randomisation is only seen in the first 200 weeks of pH in Figure 4. Thereafter, the source concentrations appear to dominate the results. If other parameters were selected for random realisations, for example, groundwater velocity or dispersivity, the model results may have included more behavioural outcomes.

The above points may arise from the non-independence of model input variables. Therefore, random sampling from probability distributions can generate unrealistic sets of model inputs. These can generate "noise" in the model output, which may obscure useful results.

Last, development of this ensemble model was made possible with modern programming tools and techniques. However, the process was lengthy and complex as it required writing a custom code for the ensemble model. Multiple model simulations generate thousands of data points, which require extensive visualisation and interpretation.

Conclusions

The results indicate that our discard facility geochemical model was non-behavioural, that is, could not give an acceptable reproduction of observations, even with rather relaxed rejection criteria. This is probably due to the multitude of parameters required by the model, i.e. the model is probably too complex.

Selecting a likelihood measure is a critical aspect of the analysis. How closely should model results reproduce observations? Within one standard deviation of observed values seems reasonable given the uncertainties of geochemical and groundwater modelling. Rather than the wrong likelihood measure, it appears from this example, that the wrong model parameters and input variables were considered uncertain (eg. Background groundwater quality). Better results may have been obtained by considering variability in the pore water quality model.

The GLUE methodology, while somewhat cumbersome to implement, can deliver additional insight to the validity of geochemical models. Some form of filter is required for model inputs generated by random sampling to reduce "noise" in the output.

References

Beven K (2009) Environmental modelling: An uncertain future? Routledge, 310 pp

Charlton SR and Parkhurst DL (2011) Modules Based on the Geochemical Model PHREEQC for use in Scripting and Programming Languages. Computers and Geosciences, 37:1653-1663

Müller M (2013) PhreeqPy Documentation (Release 0.2). http://www.hydrocomputing.com

Parkhurst DL and Appelo CAJ (2013) User's Guide to PHREEQC (Version 3) – A computer program for speciation, batch reaction, one dimensional transport, and inverse geochemical calculations. U.S. Geological Survey Techniques and Methods, book 6, chap. A43, 497 p., available only at https://pubs.usgs.gov/tm/06/a43/

Williamson MA and Rimstidt JD (1994) The kinetics and electrochemical rate-determining step of aqueous pyrite oxidation. Geochimica et Cosmochimica Acta, 58:5443-5454

Zhang D, Beven K, and Mermoud A (2006) A comparison of nonlinear least square and GLUE for model calibration and uncertainty estimation for pesticide transport in soils. Advances in Water Research 29:1924-1933

Combining Predictive Modeling and a Full-Scale Analog to Reduce Uncertainty

Amy L. Hudson[1], Andrew Harley[2], Doc Richardson[3]

[1]*Tetra Tech, Inc. 1750 Kraft Drive, Suite 1503, Blacksburg, Virginia, USA, amy.hudson@tetratech.com*
[2]*Duraroot Environmental Consulting, 4626 WCR 65, Keenesburg, Colorado, USA*
[3]*Private Consultant, Montana, USA*

Abstract

A proposed project in the Northern Territory, Australia currently has a partially developed open pit that has filled with water and must be partially dewatered before the future operations can begin. The water quality of the pit lake is poor and predictive modeling of the future ultimate pit shell suggest that during operations and in post closure, the pit walls will be a source of acid rock drainage and metal leaching (ARD/ML), resulting in the need to treat water collected within the pit. To allow discharge of the water being removed from the existing pit lake, in pit treatment using micronized lime was considered with the goal of raising the lake water pH to greater than 7.0 and precipitating key metals from solution.

In-pit micronized lime addition began at this site in 2012, to allow dewatering of the pit and to move the project toward operations. The in-pit micronized lime treatment has been successful in producing circum-neutral water with decreased metals concentrations, which has allowed for dewatering to commence and for safe discharge to local rivers without adverse impacts. Even with pumping over the last five years, the pit lake level remains high enough that much of the potentially acid generating (PAG) rock units of the pit wall are submerged and are under oxygen limited conditions. Water quality data and lake profiling were completed prior to the treatment and have continued since implementation of an in-situ treatment approach. The combined predictive modeling and the information gained during the in-pit treatment and monitoring has allowed for a higher degree of confidence that closure options can be implemented successfully.

Keywords: pit lake, case-study, in pit treatment

Introduction

Predictive modeling is often the best tool at our disposal to assess impacts from mining facilities and to develop closure plans. However, these models can be challenging to calibrate since the facilities are not constructed and the data is from tests on small sample sizes that must be scaled up. Having a test cell or local analog can provide a means to validate the modeling, but these too are often not available. A proposed project in the Northern Territory, Australia currently has a partially developed open pit that has filled with water, and which has been monitored and treated with lime for more than five years. This has allowed discharge of the water, but also has resulted in the development of a much-needed dataset that can be used as a means to validate a commonly proposed treatment method for post closure pit lakes.

Current Conditions and In-Situ Treatment

The mine site is located 56 km by road northwest of Katherine, and approximately 290 km southeast of Darwin in NT, Australia. The Project contains a number of known occurrences of gold, which have been explored and/or exploited to various degrees. The largest and best-known are the Batman and Quigleys deposits, both of which have had historic mining by prior operators. The Batman deposit has produced and been explored more extensively than the Quigley deposit.

The Project is designed to be a conventional, large open-pit mining operation that will use large-scale mining equipment in a blast/load/haul operation. Ore is planned to be processed in a large comminution circuit over the expected 13-year mine life. An open pit currently exists onsite from past mining activities, which has filled with water that is not of sufficient water quality to directly discharge to local waters.

In order for the Project to re-start mining activities, the water in the pit lake must be lowered to a level below where mining is scheduled to occur. The quality of the water onsite was not suitable for continuous discharge year-round to nearby streams, which are tributaries to the Edith River. However, in situ treatment of the pit lake water was predicted to result in concentrations that are sufficient for discharge during the wet season under the Project's water discharge license.

Micronized Lime treatment was investigated by Micronised Mineral Solutions Pty Ltd (MMS) to determine the treatment methodology, expected effectiveness, and expected cost to implement the in-situ treatment full-scale. This treatment technology utilizes very finely ground calcium carbonate (< 150 µm) and quicklime to raise the pH of the impacted water and precipitate metals. Utilization of the finely ground calcium carbonate (limestone) is the key to the treatment effectiveness, as the small grain size serves to extend the reactivity time of the particles by extending the time in which they are suspended in solution prior to settling to the bottom of the pit lake. This is achieved by the reaction between sulphuric acid, a component of the pit lake water, and the calcium carbonate particles. This reaction results in the production of carbon dioxide gas, which in turn provides buoyancy to the calcium carbonate particles. This extended settling time allows for a more efficient use of calcium carbonate and quicklime to raise the pH to the required levels. The treatment methodology includes raising the pH of the water within the pit lake to greater than pH 7.0 using calcium carbonate and quicklime in succession to capitalize on the capabilities of the low-cost limestone and minimize the quantity of quicklime required to attain a pH sufficient to precipitate additional metals. Raising the pH to greater than 7.0 results in the precipitation of the key metals of concern, including iron, aluminum, chromium, copper, lead, nickel, cadmium, and cobalt.

As such, in-situ treatment of the pit lake has been conducted by use of limestone and quicklime. Treatment began in late 2012 with the goal of producing water that can be discharged at rates that continue to protect the quality of the Edith River. In-situ treatment is being conducted as it allows for discharge of treated water in a suitable timeframe to meet with project schedule requirements. As of August 2015, it was estimated that between 12.7 giga liters of impacted water are currently on site with 79.8% is contained within the pit lake and balance from other sources across the site.

Water quality within the pit lake has historically varied in the past due to inputs from other ARD/ML sources. However, current site conditions route water such that the pit lake receives primarily fresh water. The pit walls are still mostly submerged, limiting additional oxidation of the wall rock and that ARD/ML source to the pit lake. Table 1 provides a summary of the average water quality within the pit lake prior to and since the implementation of micronized lime treatment.

The treatment has been most successful in reducing the copper concentration and raising the pH. Cadmium and aluminum have also been reduced. As would be expected, the calcium concentrations increased, as did the zinc due to its solubility at neutral pH. Sulphate, magnesium, potassium, and sodium were not changed as a result of the treatment. These results provide a means to assess the full scale implementation of the effectiveness of the in-situ treatment. This can be applied to the closure design as an analog to develop more effective closure designs.

Prediction of Post Closure Conditions

After the cessation of mining, it is expected that the Project water will have a post closure pit lake, and based on geochemical modeling the water will be equal to or worse in quality than the water present in the pit lake prior to beginning treatment in 2012. To accurately predict the on-site water chemistry and how treatment options will affect it, it is imperative that detailed geochemical characterization be conducted to determine the affinity

***Table 1** Summary of Pit Lake Water Quality Prior to and Since Treatment Began*

Analyte	Units	May 2011	April 2013	October 2014	August 2016	February 2017
pH-Field	std units	3.49	7.26	7.1	7.1	6.8
Electrical Conductivity	µS/cm	2,852	2,661	290	2,820	2,845
Temp	°C	-	26.9	29.8	23.7	32.8
Dissolved Oxygen	% sat.	-	91.8	-	88.6	103.5
Calcium	mg/L	167	440	373	397	400
Potassium	mg/L	6.5		8.5	9.1	8.3
Sodium	mg/L	45.1	49	56.5	67.7	59
Magnesium	mg/L	224	110	210	216	200
Hardness mg $CaCO_3$/L	mg/L	-	1,600	1,723	1,886	1,800
Total Alkalinity as $CaCO_3$	mg/L	-	37	53	36	22
Sulfate	mg/L	1,870	1,500	1,534	1,771	1,800
Chloride	mg/L	5.6	8	6	7	7
Total Dissolved Solids	mg/L	-	1,200	-	-	1,500
Total Suspended Solids	mg/L	-	<5	-	-	<5
Aluminum	µg/L	62.5	230	10.3	10	30
Cadmium	µg/L	146	5.1	82	33.1	29
Cobalt	µg/L	-	57	53	39	80
Copper	µg/L	11,700	27	108	1	5
Chromium	µg/L	-	1	1	1	<1
Iron	µg/L	-	<10	-	-	21
Lanthanum	µg/L	-	-	25.8	1.43	-
Lead	µg/L	-	1	1	1	<1
Manganese	µg/L	-	1,500	7,293	208	660
Mercury	µg/L	-	<0.05	-	-	-
Nickel	µg/L	-	64	669	256	230
Zinc	µg/L	42.5	210	16,194	2,186	2,000

of ARD/ML for the various rock types at the mine site. The detailed Project geochemical characterization program provided the foundation for the predictive water quality modeling. The understanding of site water flows is also critical to predicting impacts to water quality. It was determined that due to fracturing of the pit wall from blasting and mining activities, the surface runoff will be exposed to sulphides with unlimited atmospheric oxygen and water, thus having a strong affinity for acid generation. The ARD/ML reactions will be accelerated due to the long contact times anticipated in the immediate surface of the pit walls.

For purposes of this geochemical model, the post closure pit lake effluent was determined using surface area ratios of the different non-potentially acid generating (non-PAG), uncertain, and PAG materials that constitute the ultimate pit surface (UPS). Figure 1 presents the UPS with the three geochemical classifications assigned based on the geochemical characterization program. Estimated runoff from each of the materials was based on humidity cell leachate. These runoff chemistries were the only source term inputs used in the geochemical model. A filling rate and evaporation/precipitation components were not incorporated; only a fully filled pit lake was considered.

Geochemical Modeling

The geochemical modeling was conducted using the computer code PHREEQC (Parkhurst and Appelo, 1999), a reaction path

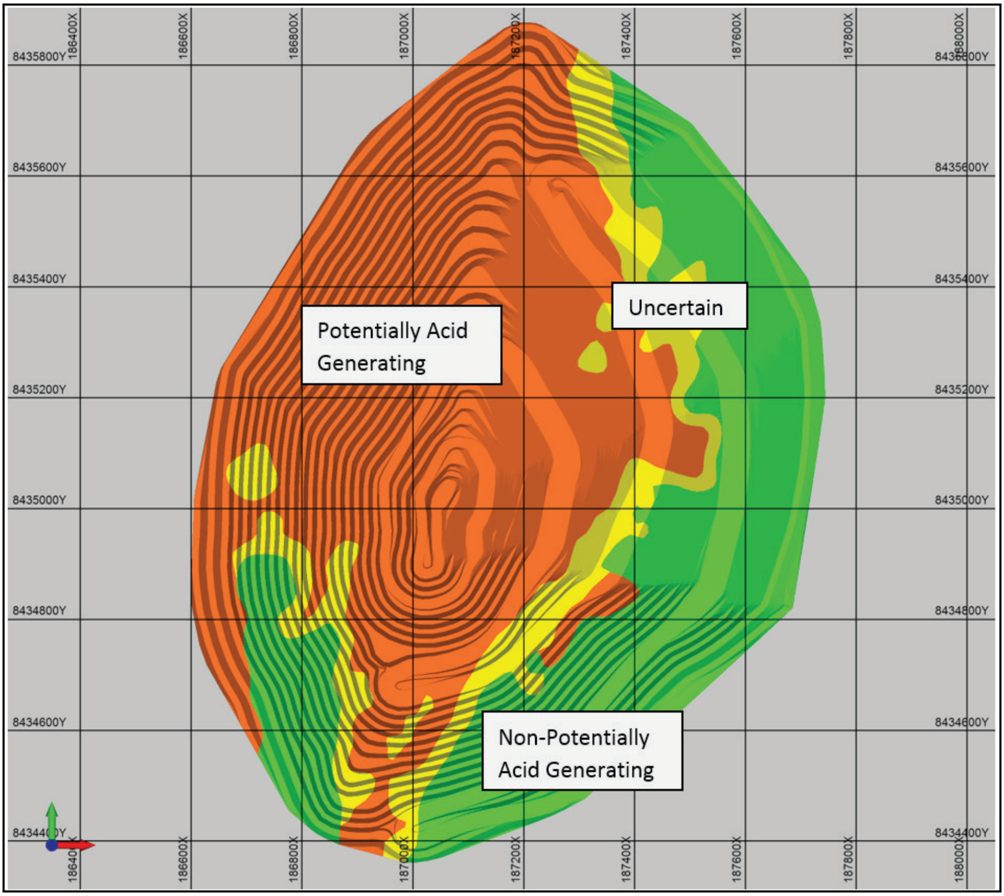

Figure 1 Ultimate Pit Surface with Color Coded ABA Criteria in Plan View. Orange represents potentially acid generating rock units, the yellow represents areas of uncertain acid generating potential, and the green represents the non-potentially acid generating rock units.

chemical equilibrium model supplied by the U.S. Geological Survey (USGS). PHREEQC is able to process multiple equilibrium and mixing reactions to produce the final chemical speciation. In addition to a computer code, geochemical modeling requires a database of the thermodynamic and kinetic parameters. For this study, the MINTEQ database (Allison et al, 1991) was chosen. However, this database does not include all of the relevant metals; therefore, to obtain a broader range of metals, data for Ti, Th, Bi were added from the Lawrence Livermore National Laboratory thermodynamic database (llnl.dat).

Some general assumptions were used throughout the geochemical modeling of the post closure pit lake. These general assumptions include:

- The precipitation source solution was limited to only hydrogen and oxygen, which were simulated as in equilibrium with atmospheric conditions;
- A six-month pyritic oxidation kinetic time step was used for the PAG wall rock units;
- Surface area proportions for the pit lake calculations were based on the UPS (i.e., the end of mine life); and
- Oxygen and carbon dioxide were assigned a steady-state concentration equal to atmospheric partial pressures.

Source Terms

To model the lithological units that comprise the UPS it was imperative to determine representative source terms for all the constituents. Source terms are stable leachate concentrations that represent long-term leachate quality. The selection of source terms was based on kinetic leachate concentrations.

Non-PAG source terms were based on the long-term kinetic metal leachate concentrations for each rock type. Several pertinent constituents were used in this determination. Each constituent's effluent concentrations were curve fitted, and assigned a point in time in which stable leachate concentrations were reached. Typically, stability was reached during the latter half of kinetic testing. Once stability ranges were acquired for the pertinent constituents, the curves were compared and a single flush (weekly) data point was chosen that represented the constant long-term leachate quality of the sample. The selection of a single flush (weekly) data point was necessary to satisfy the charge balance requirements for use in the geochemical modeling. This systematic process was repeated for each of the non-PAG rock types.

The uncertain source term was chosen based on the corresponding Round 2 humidity cell test sample results. Since this sample is trending towards acid generation after approximately two years, representative uncertain source terms were chosen before this onset. The most representative long-term leachate quality for the PAG lithologies is from the initial flush of the relevant humidity cells. These terms represent a higher metal load than the non-PAG samples. Unfortunately, only a single humidity cell has characteristics of ARD/ML generation and was terminated prior to reaching stable leachate concentrations. Thus, the most characteristic leachate quality for PAG material was from the initial flush. Its validity is due to the environmental conditions and subsequent extended contact time that water will have with PAG material in the UPS.

Surface area percentages and PAG classification for the rock types were based on the Project block model. Segregating the UPS based on lithologic composition and PAG criteria was accomplished by taking the individual pit slices from the block model and determining which blocks intersected the pit surface. When several blocks partially intersected the surface with the same x- and y-coordinates, the affected blocks were averaged and rounded up to the nearest ABA criterion (i.e., non-PAG, uncertain, PAG). These resulting blocks were used to contour the boundary strings and assign an ABA criterion to the UPS (Figure 1). Surface area ratios for the rock types and ABA designation were then calculated and used in the PHREEQC input file.

Figure 2 details the PHREEQC model construction for the post closure pit lake effluent. The chemical inputs for each of the lithologies from the non-PAG and uncertain material were mixed, respectively, based on their relative proportions of the UPS. The final PAG solution was developed by simulating the oxidation of pyrite for a six-month period. The three solutions (Solutions 8, 9, and 10 in Figure 2) were mixed in relation to their surface area percentages.

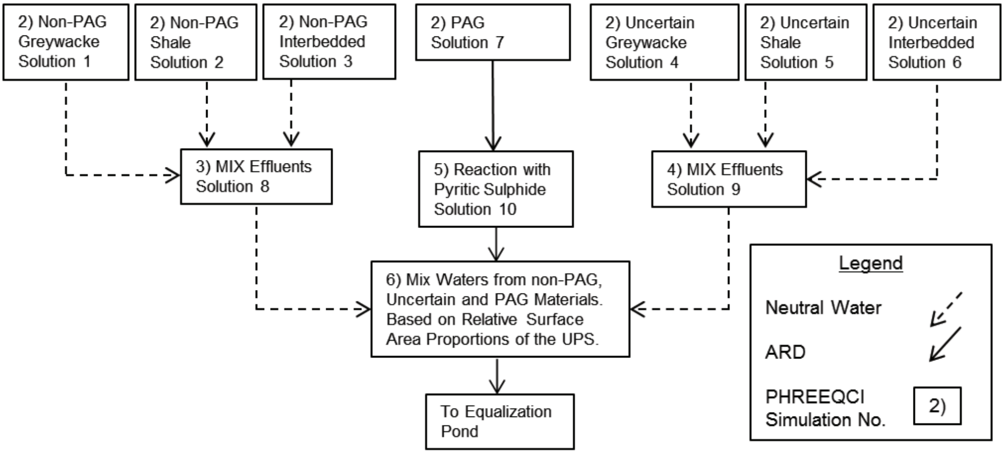

Figure 2 *Pit Lake Geochemical Model Construction*

Results and Conclusions

PAG material is estimated to compose approximately 55% of the UPS. As a result, the post closure pit lake is predicted to generate poor water quality. The predicted chemical effluent reporting from the post closure pit lake is similar to the poor water quality of the existing pit lake prior to treatment. The pH is predicted to be approximately 3.9, and the water will have elevated concentrations of most metals. Based on the experience and data gained from the in-situ treatment over the last five years of the existing pit lake, using a similar treatment option during closure will result in an increase of the pH and reduction of some key metals such as copper, iron, and aluminum, but may not result in full treatment of the water allowing discharge outside of the wet season. Raising the pH in the existing pit lake has resulted in an increase in the zinc concentration due to the solubility of this metal at pH 7 and has not changed the sulphate concentration, so other treatment options may be required if discharge is desired outside of the wet season. These issues may have been overlooked if the analog of the existing pit lake were not available for consideration as part of the Project closure planning.

References

Allison, J.D., Brown, D.S., and Novo-Gradac, K.J., 1991, MINTEQA2/PRODEFA2, A Geochemical Assessment Model for Environmental Systems: Version 3.0 User's Manual. EPA/600/3-91/021

Parkhurst, D.L. and Appelo, C.A.J., 1999, User's Guide to PHREEQC (Version 2)- A Computer Program for Speciation, Batch-Reaction, One-Dimensional Transport, and Inverse Geochemical Calculations, USGS WRIR 99-4259

Kinetic Investigation of Siderite Oxidation During Laboratory Neutralization Potential Determination

Robert J. Caldwell[1], Robert Irwin[2]

[1]*SGS Canada Inc., Lakefield, ON Canada, robert.caldwell@sgs.com*
[2]*SGS Canada Inc., Lakefield, ON Canada, rob.irwin@sgs.com*

Abstract

Accurate acid rock drainage (ARD) prediction is of major importance to any project that may expose potentially acid generating rock and mine waste to the atmosphere. One of the most important steps in any ARD evaluation is determination of neutralization potential (NP), which quantifies the material's ability to neutralize the acid produced through sulphide oxidation.

Siderite is a ferrous carbonate mineral which ultimately yields no net acidity on hydration, but can cause optimistically high values during NP determinations if it has been solubilized without oxidation of the associated Fe^{+2} ion. This paper documents a study of the Fe^{+2} and Fe total concentrations though-out the duration of standard Sobek and modified acid base accounting (ABA) NP determinations, with and without oxidation of Fe^{+2}.

Introduction

It is generally known that the presence of ferrous iron bearing minerals, especially carbonate minerals such as siderite ($Fe^{2+}CO_3^{2-}$), in mine wastes can lead to overestimation of NP values during standard Sobek and modified ABA evaluations. It is understood that the ferrous carbonate component of mine waste does not contribute to total NP due to oxidation of ferrous iron (Fe^{2+}) to ferric iron (Fe^{3+}), which releases an equivalent amount of acid through ferric iron hydrolysis (Skousen 1997). To correct for this during standard Sobek and modified ABA analyses, hydrogen peroxide is added as an oxidant to ensure the release of metal acidity from ferrous iron prior to the final NP titration. Often, the use of "siderite correction" during the modified NP determination of samples known to contain appreciable siderite may appear to have little or no apparent impact on the final NP value determined.

Use of the siderite correction is not universally considered to be warranted when completing the modified NP procedure due to the relatively low solubility of siderite at room temperature in comparison to the boiling temperatures used for the standard Sobek procedure. However, the procedure is generally of interest in ARD investigations regardless of method whenever the presence of siderite is identified.

To ascertain the efficacy of siderite correction, a kinetic investigation into the oxidation of ferrous iron was conducted on a not potentially acid generating (NPAG) waste rock high in siderite. The study was conducted over a range of dilutions using both the standard Sobek and modified NP methods, with and without hydrogen peroxide addition. Dilutions of the high siderite waste rock were prepared through mixing with an inert sand to provide insight into the impact different ranges of ferrous carbonate would have on final analysis. Solution samples were taken periodically to monitor total iron (inductively coupled plasma optical emission spectroscopy) and ferrous iron (discrete analyser - phenanthroline) concentrations to evaluate oxidation kinetics.

Materials

Testwork was conducted using a sample of waste rock collected from a Canadian iron mine known to have a high siderite concentration and a not potentially acid generating

(NPAG) ARD designation. Characterization of the samples siderite content was made by semi-quantitative x-ray diffraction (XRD) analysis using a Bruker AXS D8 Advance Diffractometer. XRD analysis determined the waste rock was predominantly quartz, with siderite making up 20.0 weight %, and pyrite making up 0.6 weight %.

Representative cuts of the pulverized waste rock were blended with pulverized Ottawa sand (85% passing 200 mesh) and sample cuts were riffled to provide representative waste rock to sand ratios of 300:300 and 180:420. In this manner samples of waste rock at 100%, 50%, 30% were prepared, plus a pure pulverized Ottawa sand sample provided to act as a control.

Methods

The standard Sobek NP determinations were made using the original US EPA acid base accounting method (Sobek 1978) by SGS at their Lakefield, ON Canada site. Only minor changes were made to the Sobek method with respect to equipment used. The modified NP determinations were completed using the Lawrence method from the Acid Rock Drainage Prediction Manual (Lawrence 1991), also at the SGS Lakefield site.

The hydrogen peroxide (H_2O_2) addition was made for the standard Sobek and the modified methods by adding 5 mL of 30% hydrogen peroxide to the suspension and boiling gently for one minute prior to the NaOH titration (Skousen 1997) to pH 7.0 for the standard Sobek, and to pH 8.3 for the modified NP.

Each of the three waste rock samples (100%, 50%, 30%) and the pulverized Ottawa sand were subjected to each method with and without siderite correction in triplicate. Samples were removed from each standard Sobek NP sample for Fe^{2+} and Fe total analysis after each step in the method. This included:

- 10 minutes after HCl acid addition,
- after the boil,
- after addition of hydrogen peroxide (siderite correction only),
- after hydrogen peroxide boil (siderite correction only), and
- after the titration to pH =7 with NaOH.

For each modified NP sample subsamples were removed for Fe^{2+} and Fe total analysis during each pH check in the method:

- Immediately after HCl acid addition (time zero),
- 0.5 hours after HCl acid addition,
- 1 hour after HCl acid addition,
- 4 hours after HCl acid addition,
- 22 hours after HCl acid addition,
- after hydrogen peroxide boil (siderite correction only), and
- after the titration to pH =8.3 with NaOH.

At each sampling point 1 mL of sample was removed and diluted into 50 mL of 2% HCl, using a 50 mL “digi-tube” and shaken well. The HCl served to preserve the Fe^{+2} concentrations. The 1 mL of sample removed was replaced with 1mL of deionized water.

The Fe total values were determined by trace level inductively coupled plasma, optical emission spectroscopy (ICP-OES) analysis. Because the Fe^{+2} and Fe total values were to be based on dissolved values, the Fe total samples were not digested prior to analysis. Hence, Fe total refers to the total Fe within the sample (Fe^{2+} and Fe^{3+}) rather than a total digestion.

The Fe^{2+} concentrations were determined using a Discrete Photometric Analyser running the Ferrous colourimetric Fe^{2+} method with phenanthroline. Prior to each use the Discrete Analyzer was calibrated with a freshly prepared calibration solution to ensure absence of Fe^{3+} due to oxidation.

The Fe^{2+} calibration solution was prepared by first diluting 5 mL of 1000 mg/L Fe stock solution into 10 mL of deionized water in a 50 mL centrifuge tube, then adding 2 ml of concentrated HCl. This results in the solution turning yellow which indicates that all the Fe present is Fe^{3+} iron. The solution was then heated to approximately 50°C by hot-block and stannous chloride was added carefully drop-wise until the solution cleared. Only sufficient stannous chloride required to discharge the yellow colour was used because excess Sn^{2+} can act as an interference for the colourimetric determination of Fe^{2+}. Once bulked to 50 mL with deionized water the solution was identified as the 100 mg/L Fe^{2+} stock solution.

The Discrete Analyzer was calibrated to run the Ferrous colourimetric Fe^{2+} method by loading the calibration standard, which was made by diluting 1 mL of the 100 mg/L stock solution into 50 mL of 2% HCl, resulting in a 2 mg/L Fe^{2+} calibrator (A-Fe2-2), and a blank solution of 2% HCl (A-Fe2-0) into one of the sample segments.

The following reagents were also required to be loaded into the Discrete Analyzer:

- FeBuffer: dissolve 12.5 g of ammonium acetate in 7 mL of deionized water, add 35 mL of glacial acetic acid and bulk to 50 mL capacity with deionized water and shake well.
- FeColour: dissolve 0.05 g of 1,10-phenanthroline into 50 mL of deionized water, add 2 drops of concentrated HCl, cap and shake well. If this solution darkens it needs to be freshly prepared.
- 2%HCl: dilute 1 mL of concentrated HCl into 50 mL of deionized water.

After the reagents and calibration solutions were loaded, the Ferrous Fe^{2+} method was selected and the calibration program initiated. Once the calibration sequence was complete, the NP samples could be immediately analyzed. To run the individual standard Sobek and modified NP samples, they were simply inserted onto one of the segments, the Ferrous method selected and the Discrete Analyzer analysis was initiated.

Because the linear range of the Discrete Analyzer Ferrous method is 0.02 mg/L to 20.0 mg/L Fe^{+2}, over-range samples had to be diluted using the 2% v/v HCl matrix in order stay in range of the method.

Results and Discussion

To reduce the data, the triplicate Fe^{2+} and Fe total results for each sample at each sampling point were averaged and then corrected by subtracting the average control value. The data for the standard Sobek NP Fe^{2+} values at each sampling point, and the average corrected NP value determined, are presented in Table 1, while the corresponding data from the Fe total analyses are given in Table 2. Similarly, the data for the modified NP are presented in Table 3 for Fe^{2+} and Table 4 for Fe total.

Data presented in Table 1 clearly illustrate that the concentration of Fe^{2+} in the standard Sobek NP solution increased dramatically after the boiling hydrochloric acid step. Although the Fe^{2+} concentration of the 50% Waste Rock sample was roughly 50% of the uncut sample, the same was not true of the 30% Waste Rock sample, which resulted in a concentration of roughly 10% of the uncut sample. After the addition of hydrogen peroxide the Fe^{2+} concentrations decreased dramatically, and there was generally some additional decrease after the hydrogen peroxide was boiled off prior to titration. After the titration for NP determination the siderite corrected samples Fe^{2+} concentrations were trending to zero after being corrected for the control. Without the siderite correction, the Fe^{2+} concentrations after titration were similar to those of the period 10 minutes after the initial hydrochloric acid addition.

Review of the Fe total data given in Table 2 indicated that essentially all of Fe in solution was in the form of Fe^{2+} up until the point where the hydrogen peroxide was first

Table 1 *Average corrected Sobek NP [Fe^{2+}] (mg/L) at time intervals with and without siderite correction.*

	10 min after acid addition	After Boil	10 min after H_2O_2 addition	After H_2O_2 boil	After titration	NP kg $CaCO_3$/tonne
Waste Rock	353	2182	---	---	424	393
50% Waste Rock	537	1012	---	---	301	178
30% Waste Rock	146	154	---	---	28.6	68.5
			With Siderite Correction			
Waste Rock	433	2139	43.2	6.79	-0.13	268
50% Waste Rock	359	1085	3.69	5.90	-0.16	176
30% Waste Rock	129	193	13.3	0.37	0.09	28.8

Table 2 *Average corrected Sobek NP [Fe] (mg/L) at time intervals with and without siderite correction.*

	10 min after acid addition	After Boil	10 min after H_2O_2 addition	After H_2O_2 boil	After titration
Waste Rock	380	2281	---	---	1055
50% Waste Rock	564	997	---	---	284
30% Waste Rock	157	159	---	---	28.4
		With Siderite Correction			
Waste Rock	476	2043	1626	1707	1.15
50% Waste Rock	397	1007	893	814	0.13
30% Waste Rock	141	197	146	151	0.85

Table 3 *Average corrected modified NP [Fe^{2+}] (mg/L) at time intervals with and without siderite correction.*

	Addition HCl Time Zero	Addition HCl 0.5 Hours	Addition HCl 1 Hours	Addition HCl 4 Hours	Addition HCl 22 Hours	After H_2O_2 Boil	After Titration	NP kg $CaCO_3$/ tonne
Waste Rock	517	564	461	635	767	---	21.4	94.9
50% Waste Rock	375	321	289	242	370	---	0.29	39.1
30% Waste Rock	358	253	195	165	145	---	0.10	10.9
				With Siderite Correction				
Waste Rock	505	493	437	601	732	7.31	0.09	70.3
50% Waste Rock	366	310	260	231	374	4.77	-0.02	50.4
30% Waste Rock	345	235	178	143	130	3.56	-0.05	20.9

introduced. Once the siderite correction was initiated the Fe total concentration was maintained, as Fe^{2+} was oxidized to Fe^{3+} and the metal acidity was released into solution. Without the hydrogen peroxide addition, the Fe total concentration was only marginally higher than the Fe^{2+}, indicating that little of the Fe^{2+} had oxidized to Fe^{3+}.

Returning to Table 1 we can see that the NP values were generally increased without the siderite correction step. The decrease in NP for the siderite corrected 50% Waste Rock was calculated to be only 2 kg of $CaCO_3$ per tonne, which is anomalous when compared with the 100% and 30% Waste Rock samples (125 kg and 39.7 kg of $CaCO_3$ per tonne, respectively).

Modified NP Fe^{2+} data, presented in Table 3, illustrates that the concentration of Fe^{2+} in the modified NP solution varied over time, but never increased dramatically in the manner observed after the standard Sobek NP boiling hydrochloric acid step. This indicated that the siderite was never brought into solution to the same extent when digested at room temperature, which was expected. However, it is notable that the Fe^{2+} concentrations in the higher siderite concentration samples increased over the 22 hours of the modified NP determination, while the 30% Waste Rock samples Fe^{2+} concentrations fell over 60% by the end of the digestion period. At the end of the modified NP digestion period the 100% Waste Rock sample's Fe^{2+} concentration was approximately double the 50% Waste Rock sample's Fe^{2+} concentration, while the 30% Waste Rock only represented about 20%. After the hydrogen peroxide addition and boiling off the hydrogen peroxide, the Fe^{2+} concentrations in the siderite corrected modified NP solutions decreased significantly. Again, after the titration for NP determination the siderite corrected sample's Fe^{2+} concentrations were trending to zero, as in the standard Sobek NP procedure, however in this case, the Fe^{2+} concentration was also relatively low without hydrogen peroxide addition.

A review of the Fe total data given in Table 4 indicated that essentially all of the iron in solution was Fe^{2+} up until the point where the hydrogen peroxide was first introduced. The Fe^{2+} concentrations were in many instances, marginally higher than the Fe total values, and as this was generally the case at higher concentration it may have been due to the higher dilutions required at high concentration to keep the Fe^{2+} measurements in range. As in the standard Sobek NP procedure, once the siderite correction was initiated, the Fe total concentration was maintained, as the Fe^{2+} was oxidized to Fe^{3+} and the metal acidity was released into solution. After titration, the drop in Fe total was apparent for all samples, regardless of whether the siderite correction had been made, and the highest value was that for the 100% Waste Rock sample without correction (21.4 mg/L). Although the siderite correction did have an impact on the modified NP Fe^{2+} concentrations, it was minimal when compared to the impact on the standard Sobek NP.

Calculated modified NP values for the Waste Rock materials are given in the final column of Table 3. Although the correction did reduce the NP of the 100% Waste Rock material, the 50% and 30% Waste Rock samples returned higher values after the correction.

Conclusions

In completing this study, it became readily apparent that the boiling step used in the standard Sobek ABA NP determination does put a great deal more Fe^{2+} into solution when compared to the room temperature modified ABA NP method. The standard Sobek ABA without the correction has a significant quantity of Fe^{2+} iron left in solution, and hence the potential metal acidity is not considered, and thus the siderite correction is quite valid. Although not unexpected, the study does illustrate that higher NP values are determined in general when using the standard Sobek ABA when compared to the modified ABA method due to the release of higher concentrations of minerals which would not have been solubilized without the boiling HCl digestion.

The study indicated that oxidation did not appear to impact the Fe^{2+} in solution over the course of the modified NP method's extended room temperature digestion period. For the 100% Waste Rock sample (20 wt% siderite) the Fe^{2+} concentrations in solution increased over the monitored 22-hour digestion period, while it decreased for the two samples with lower siderite concentrations. The Fe total concentrations mirrored these trends indicated that iron was almost entirely present in the lower oxidation state. For either method, hydrogen peroxide was necessary to oxidize soluble Fe^{2+} to Fe^{3+}.

The modified NP method puts less siderite into solution and hence has little need for correction. Results of the investigation clearly illustrate the benefit of siderite correction when completing the standard Sobek ABA method. Conversely, minimal real impact on NP determination was found through hydrogen peroxide addition when the modified ABA method was used.

Table 4 *Average corrected modified NP [Fe] (mg/L) at time intervals with and without siderite correction.*

	Addition HCl Time Zero	Addition HCl 0.5 Hours	Addition HCl 1 Hours	Addition HCl 4 Hours	Addition HCl 22 Hours	After H_2O_2 Boil	After Titration
Waste Rock	478	632	420	627	721	---	18.5
50% Waste Rock	350	230	259	180	345	---	0.60
30% Waste Rock	347	189	174	132	138	---	0.21
			With Siderite Correction				
Waste Rock	483	383	427	587	679	619	0.27
50% Waste Rock	362	302	235	235	342	360	0.06
30% Waste Rock	351	220	161	147	120	164	0.02

References

Sobek AA, Schuller WA, Freeman JR, Smith RM (1978) Field and laboratory methods applicable to overburdens and minesoils. Report EPA-600/2-78-054, U.S. National Technical Information Report PB-280 495. 203 pp.

Lawrence RW, Marchant PB (1991) Acid rock drainage prediction manual. MEND Project 1.16.1b, MEND Program, Natural Resources Canada, Ottawa, March 1991.) pp. 6.2-11 to 6.2-17.

Skousen J, Renton J, Brown H, Evans P, Leavitt B, Brady K, Cohen L, Ziemkiewicz P (1997) Neutralization Potential of Overburden Samples Containing Siderite. J Environ Qual 26:673-681

Mine water of abandoned coal mines for geothermal heat storage: Hydrogeochemical modeling and predictions

Felix Jagert, Florian Hahn, Roman Ignacy, Gregor Bussmann, Rolf Bracke

Bochum University of Applied Sciences, International Geothermal Centre (GZB), Lennershofstr. 140, 44801 Bochum, Germany, felix.jagert@hs-bochum.de

Abstract

Water samples from various hard coal mines (German Ruhr coal district, Dutch South-Limburg coal district) were modeled to evaluate a future mine thermal energy storage using the modeling software PHREEQC. Different thermodynamic databases had to be used for modeling. The geochemical reactions were simulated during charging up to 150 °C (at 5 bars).

The mineral phases calcite and anhydrite exceed the equilibrium during the operation and tend to precipitate as scaling. Depending on the redox potential, minerals like ferrihydrite, siderite and goethite tend to form deposits. A storage temperature up to about 90 °C is recommended to avoid intense scaling.

Keywords: storage, mine water, PHREEQC, scaling

Introduction

After the ending of hard coal mining in Germany in 2018, a large number of flooded galleries, shafts and converged gobs will remain in the subsurface, which are excellently suited as thermal energy storages due to the increased hydraulic permeability. A great potential for local low-temperature heating networks in cities, residential areas or industrial areas is given (compare Hahn et al. 2018). During summer it is possible to store industrial surplus heat via heat exchangers in the mine water of flooded galleries. In winter, the process is reversed and the heat is extracted with heat exchangers. Heat pumps can bring the temperature to the desired heating level. Figure 1 shows a sketch of a heat storage in a flooded Carboniferous hard coal mine. A lower flooded level is used as heat storage, whereby it is possible to use an upper flooded level as cold storage for cooling purposes.

The geology of the German Ruhr coal district and the adjacent Dutch South-Limburg coal district is dominated by typical Upper Carboniferous deposits composed of silt- and mudstones, intercalated with coal seams,

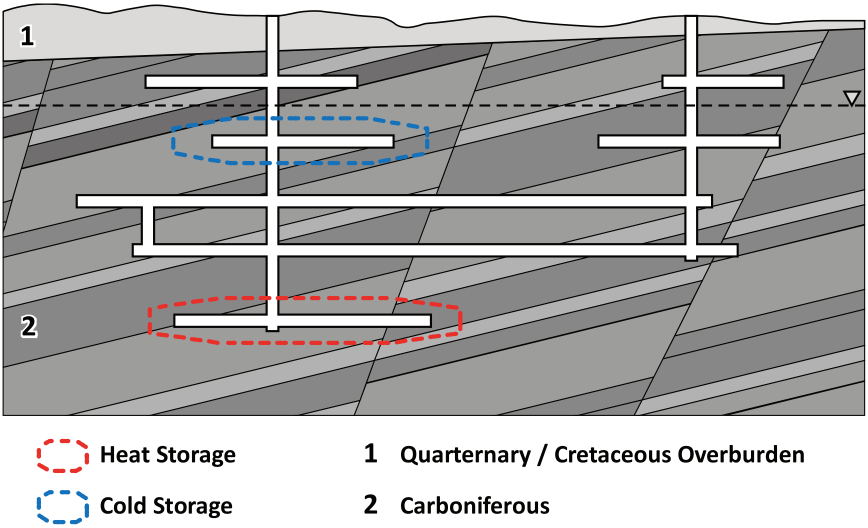

Figure 1 *Sketch of a heat storage in a flooded mine of the German Ruhr coal district (courtesy Felix Jagert).*

which can pass into sandstone beds (compare fig. 1). During the Variscan orogeny, the deposits were intensively folded. At the same time, the ductile-brittle rock tended to break and major faults were created. The resulting fault-systems are usually hydraulically effective. As a rule, the strata of the Upper Carboniferous are characterized by conjugate shear joint sets and therefore have only little hydraulic permeability. The Carboniferous deposits are superimposed by strata of the Upper Cretaceous as well as the Quaternary, which form the overburden.

Establishing a geothermal power plant for heating purposes with the ability to work as a seasonal heat storage as well in abandoned mines will cause certain hydrogeochemical reactions in the mine water. In general the mine waters of the Upper Carboniferous coal districts (Ruhr, Aachen, Ibbenbüren, Saar, South-Limburg) can be characterized as connate waters, influenced by mining activities (oxidation). The concentration of the main cations and anions (Na^+, K^+, Ca^{2+}, Mg^{2+}; Cl, SO_4^{2-}, HCO^{3-}) is rising with increasing depth from brackish waters (0.1 –1 % salinity) to brines (> 40 g/L, more than 4 % salinity). Heating mine water during charging of a thermal storage will cause precipitation and dissolution of certain mineral phases and also cause corrosion of pipes and heat exchangers. Figure 2 shows intense scaling of a historical dewatering pipe of a former hard coal mine in Bochum, obviously consisting of a mixture of different mineral phases.

Figure 2 A historical dewatering pipe of a former hard coal mine, Bochum shows the scaling potential of mine water (courtesy Felix Jagert).

Hydrogeochemical modeling of the thermodynamic behaviour and redox states of the mine waters enables qualitative and possibly quantitative predictions of scaling and corrosion during a future operation of a plant. In addition, a simulation of a hydraulic short circuit between mine levels or due to hydraulic active faults (mixing of waters) can help to estimate their hydrogeochemical effect on the storage.

Methods

Water analyses collected from various coal mines (table 1) were modeled to evaluate a future geothermal heat storage operation using the hydrogeochemical modeling software PHREEQC 3 (Parkhurst and Appelo 2013). Due to a large spread of ionic strengths, different thermodynamic databases had to be used for modeling. Freshwater to brackish waters were modeled with the PHREEQC or WATEQ4F databases, which are based on the Wateq-Debye-Hückel approach (theory of ion dissociation), whereas higher salinities up to brines are modeled with the PITZER approach (ion interaction theory) or the ThermoChimie database (specific ion interaction theory).

The criterion for accurate modeling is a complete, correct water analysis, which consists of the temperature, acidity as pH, the dissolved main constituents and secondary constituents (anions and cations). The redox state is also important, but it is rarely determined and often not measured correctly, because the redox electrode adjusts only slowly to a constant measurement result. It is possible to calculate the redox state via redox-couples using PHREEQC. Archives or various monitoring programs often already provide water analyses that can be used.

Most of the available databases contain hundreds of mineral phases, but often there is a lack of some desired elements (ions), species or mineral phases. In addition, many mineral solubilities were determined only under laboratory conditions at 25 °C and 1 bar. PITZER is more suitable for different pressure and temperature conditions, but it can be used to model rather few mineral phases.

Table 1 *Water analyses from various hard coal mines of Germany and the Netherlands.*

	Franz-Haniel 1/2	Robert Müser	Oranje Nassau III	Oranje Nassau III
location	Bottrop, Germany	Bochum, Germany	Heerlen, Netherlands	Heerlen, Netherlands
depth (m b.g.l.)	1148	570	692	229
temp. (°C)	20	20	28	16
pH	6.94	7.19	7.9	7.3
	cations / anions (mg/L)			
Na^+	12700	1180	1100	940
K^+	133	22	36	38
Mg^{2+}	304	54	47	100
Ca^{2+}	1050	120	62	160
Ba^{2+}	1.7	0.93	0.037	0.059
Fe(total)	5	15	3.1	6.1
Cl^-	20200	1630	850	530
SO_4^{2-}	510	76	480	1300
$HCO3^-$	160	995	940	1000
$NO3^-$	5	1	n.a.	n.a.
date	26.07.2013	14.08.2013	26.02.2016	18.09.2015
status	active mine dewatering	abandoned mine dewatering	Mijnwater-project 2.0	Mijnwater-project 2.0
source	BRA (2013)	BRA (2013)	Mijnwater B.V.	Mijnwater B.V.

Hydrogeological considerations

If shafts are already filled and the mine levels are inaccessible, the suitable gallery must be drilled into, using a directional drilling technique. An exploration borehole into the abandoned mine with appropriate water analyses and pumping tests is usually only available in later project phases. Therefore, before modeling, different hydrogeological scenarios should be considered.

The depth, extent and geometry of the galleries should be evident in the mine maps. With this information, the most suitable mine level for heat storage, cold storage and re-injection of the cooled water can be selected. Blind shafts, dams, gobs and faults increase the hydraulic permeability of the mine levels (fig. 1). In some cases, mine levels of adjacent mines were connected during the active mining phase so that the mine water flows from one mine to another.

Knowledge about the mine water level is important for further planning. Usually, in undisturbed formation waters, salinity and temperature increase significantly with depth. This is clearly documented in historical literature and in recent publications on the coal mines in the Ruhr region (e.g. Wedewardt 1995). However, the flooded mine levels are hydraulically connected via blind shafts or gobs on shallower mine levels, so that “communicating vessels” are created. Therefore, the salinity of the mine waters from deep galleries is not known exactly.

The mine dewatering of Ruhrkohle AG (RAG) provides insights into the composition of the abandoned mines (see table 1). The sodium chloride content, the sulphate content and the degree of hardness are significantly increased in comparison to groundwaters. Despite the pyrite oxidation caused by mining (air conditioning), the pH values remain in the neutral range. Barium is mostly dissolved in deep mine waters and points to deep, older formation waters, which enter the mine. High barium contents exclude sulphate contents and vice versa, because barium precipitates with sulphate as barite.

Hydrogeochemical modeling was carried out mostly with PITZER up to 150 °C. Other databases can also be used, for example, to calculate redox species, but the results are not reliable. The expected pressures will probably not exceed 50 bars since the maximum water column in the system will be around 500 m. Line pressures on the surface will barely exceed about 5 bars. The system is considered as closed. In the reality, however, air contact and a resulting shift of the redox state are expected near the pumps in the borehole or shafts.

Results

Significant changes in solubility occur in the carbonates and sulphates. Aluminium silicates were not taken into account for the modeling, since aluminium and silicon were seldom determined in water analyses and otherwise occur in very low concentrations. The pH values in the carbonate buffer range (pH 8.3 to 6.2) prevent the mobilization of certain metal ions, such as aluminium and others.

Thermodynamic Equilibria

The saturation index (SI) indicates whether a mineral phase in the solution is supersaturated at the appropriate pressure and temperature and tends to precipitate, or whether the solubility is undersaturated and the mineral remains in solution and is dissolved out of the rock respectively. Mineral phases are in equilibrium with the thermodynamic conditions at SI 0.0. Positive values, in particular values above 1 indicate a supersaturation and possibly a growth of crystals.

In general, a distinction is made between homogeneous and heterogeneous nucleation. Homogeneous nucleation describes the growth of a crystal directly from the supersaturated solution. For this spontaneous crystal formation, a high supersaturation of the corresponding mineral phase is necessary. The heterogeneous nucleation describes a much faster crystallization on already existing surfaces such as particles in the water. These existing surfaces then serve as a jump start for crystal growth.

Most mineral solubilities increase with rising temperature (e.g. Barite in fig. 3), which is beneficial for the life of the plant. However, the rapid decrease in the solubility (supersaturation) of calcite is remarkable. This also happens for mineral varieties, such as aragonite. It is evident that a temperature-induced decrease in CO_2-solubility shifts the lime-carbonic acid balance. A similar and less intense decrease in solubility is observed for gypsum / anhydrite. Modeling with PITZER shows that a pressure drop of up to 50 bars (500 m) has very little effect on the solubilities. Only very high pressure differences of a few thousand meters to the surface would induce a calcite precipitation.

In a closed system, without degassing, the pH remains stable. Though the temperature dependency of the self-ionization constant of water leads to small shifts in the pH (compare pH in fig. 3 and fig. 4).

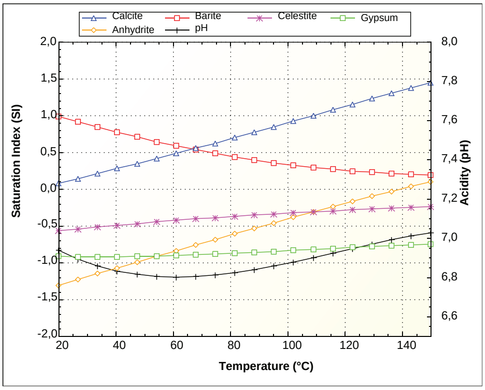

Figure 3 *Solubilities of certain mineral phases up to 150 °C (Mine water Franz-Haniel at 5 bars).*

Speciation and redox state

Some models showed that the redox state changes just due to the temperature increase. A redox-dependent specification has the consequence that different mineral phases are stable and therefore tend to precipitate. The model in fig. 4 was done with the ThermoChimie database, so the calculation of the redox state was possible. However, the database is less reliable for a temperature range above 90 °C and for acidities lower than pH 6.

Amorphous ferrihydrite is a mineral phase that forms rapidly in the presence of oxygen and then precipitates ("iron clogging"). The model in fig. 4 shows a significant increase in solubility (decreasing SI) with rising temperature due to a decreasing pE and pH. At the same time, the solubility of siderite (increasing

SI) decreases. This mineral phase generally is formed under reducing conditions. Goethite remains highly supersaturated and tends to precipitate, although its rate of formation is much slower than that of ferrihydrite.

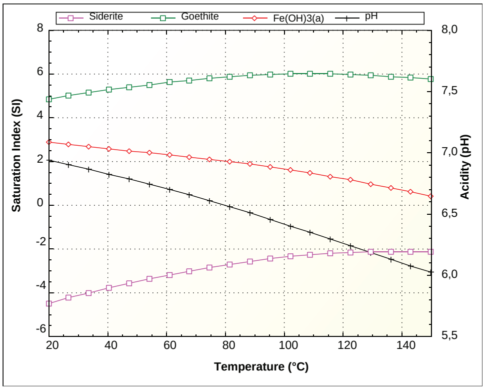

Figure 4 Solubilities of redox sensitive mineral phases up to 150 °C (Mine water Franz-Haniel at 5 bars).

Kinetics and rates of formation

The above-mentioned formation rates of minerals are of great importance in the calculation of precipitated quantities. Used mine water will only flow through the plant for a few hours and will stay in the storage for the most time. The saturation index is just a thermodynamic point of view and therefore time-independent. Plummer et al. (1978) described an approach obtaining reaction rates for the mineral phase calcite. The result adapted to the water analysis collected from Franz Haniel 1/2 is shown in fig. 5. The mine water was modeled up to 90 °C. About 55 mg/L will be precipitated after 200 hours to reach equilibrium with calcite.

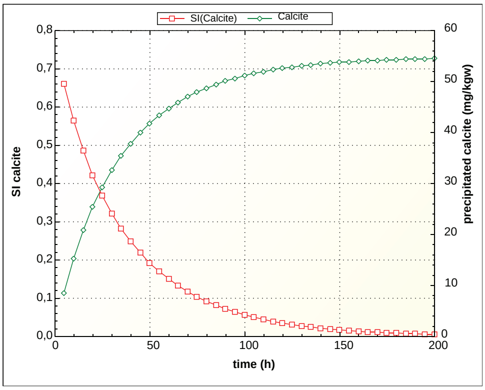

Figure 5 Kinetical reaction rates for calcite at 90 °C (Mine water Franz-Haniel at 5 bars).

Conclusions and outlook

The modeling has shown that a storage temperature only makes sense up to about 90 °C. Significantly higher temperatures in the system lead to high supersaturation, especially of the mineral phase calcite and further anhydrite. Corrosion due to high salt contents (high electrical conductivity) or due to hydrogen sulphide can hardly be described with PHREEQC. The dissolution of aluminium silicates (e.g. clay minerals like illite or smectite) or cation exchange processes on mineral surfaces are fields for further research.

In the Netherlands, galleries of the abandoned coal mine Oranje Nassau III have already been drilled for the Mijnwater-project and successfully used for geothermal installations (see Verhoeven et al. 2013 and references therein).

Acknowledgements

The authors thank Tshwane University of Technology (TUT) for hosting the ICARD | IMWA | MWD 2018 Conference. We thank Rene Verhoeven (Mijnwater B.V.) for the collaborative work and the release of the data. Florian Hahn provided critical comments on earlier versions of this text.

References

Bezirksregierung Arnsberg (BRA) Ergebnisse Sondermessprogramm Grubenwassereinleitungen 2013 Steinkohle Ruhrrevier. published open data: https://www.bezreg-arnsberg.nrw.de/themen/w/wasserwirtschaft_untertagebau/ [14.05.2018]

Hahn, F; Bussmann, G; Jagert, F; Ignacy, R; Bracke, R (2018) Reutilization of mine water as a heat storage medium in abandoned mines. Proceedings from the 11th ICARD | IMWA | MWD 2018 Conference (this issue), Pretoria, South Africa

Parkhurst, DL; Appelo, CAJ (2013) Description of Input and Examples for PHREEQC Version 3 — A Computer Program for Speciation, Batch-Reaction, One-Dimensional Transport, and Inverse Geochemical Calculations. http://wwwbrr.cr.usgs.gov/projects/GWC_coupled/phreeqc/

Plummer, LN; Wigley, TML und Parkhurst, DL (1978) The kinetics of calcite dissolution in CO2-water systems at 5°C to 60°C and 0.0 to

1.0 atm CO2. Am. Jour. Sci.: 278, 179-216, doi:10.2475/ajs.278.2.179

Verhoeven, R; Willems, E; Harcouët-Menou, V; De Boever, E; Hiddes, L; Op 't Veld, P; Demollin, E (2013) The EC REMINING-lowex project in Heerlen the Netherlands: development of a geothermal mine water pilot project to a full scale hybrid sustainable energy infrastructure Mine Water 2.0. European Geothermal Congress 2013. Pisa, Italy, 3-7 June 2013

Wedewardt, M (1995) Hydrochemie und Genese der Tiefenwässer im Ruhrrevier. DMT-Berichte aus Forschung und Entwicklung, 39, 250 pp, Bochum

Assessment of Silica Coating as a Technique for the Control of Acid Generation from Pyritic Tailings ©

Konstantinos Kollias, Evangelia Mylona, Katerina Adam, Nymphodora Papassiopi, Anthimos Xenidis

National Technical University of Athens, School of Mining & Metallurgical Eng., Laboratory of Metallurgy, 15780 Zografou, Greece, kkollias@metal.ntua.gr

Abstract

A promising strategy for the efficient management of sulfide mine wastes is related to the formation of Si-based coating on sulfides surface to prevent oxidation. In order to elucidate the coating technology, batch and column tests involving treatment of pyritic tailings with solutions consisting of SiO_4^{-4} and H_2O_2 were performed. To assess the stability of coatings, treated samples were leached with a solution of H_2O_2. Humidity cell tests on selected coated samples were also performed for 41 weeks. Based on the results, silica coating resulted in the reduction of sulfate release by up to 91%, compared to the non-treated sample.

Keywords: Acid Mine Drainage, sulfidic wastes, pyrite, oxidation, silica coating, humidity cells

Introduction

The environmental and financial impact of acid mine drainage (AMD) has challenged the global scientific community for decades in order to understand the evolution and the controlling parameters of AMD formation and thus to provide sustainable and cost-effective preventive technologies (Öhlander et al. 2012; Rimstidt and Vaughan 2014; Pozo-Antonio et al. 2014). A promising approach for the environmentally safe management of potentially acid generating mine wastes is aiming to passivate the sulfide mineral surface through the formation of a coating layer, which block the access of oxidants (oxygen, water)(BREF 2009; Sahoo et al. 2013).

Several inorganic and organic compounds have been used for the development of artificial coating including phosphates, iron hydroxides, humic acids, polyamines, organosilanes, siloxane etc. (Zhang and Evangelou 1996; Huminicki and Rimstidt 2009; Ačai et al. 2009; You et al. 2013; Diao et al. 2013; Ouyang et al. 2015; Kollias et al. 2015). Silicates have been also used for the formation of a protective layer around pyrite particles. Silica coatings are advantageous over other types due to the abundance of silicates in the crust as well as their inert nature and limited solubility (Iler 1979; O'Neill 1994). The methodology initially developed for the formation of silica coating included leaching of the pyritic waste using a solution containing hydrogen peroxide (H_2O_2), a silica source and pH adjustment in the range 4-6. Under these conditions, the pyrite is oxidized by H_2O_2 releasing mainly iron and sulfates in the presence of Si. The iron is hydrolyzed and iron hydroxides are precipitated on FeS_2 surface. Finally, an outer silica layer is formed on the chemically modified surface (Evangelou 1996). Later studies have shown that a coating layer containing Si and Fe can be developed on pyrite particles following treatment with solutions having variable Si concentrations (0.8-300 mM) at pH: 6-7 and variable L/S ratios (1-8600 mL/g). Silica coating was developed both in the presence and absence of H_2O_2 (Evangelou 2001; Kargbo and Chatterjee 2005; Bessho et al. 2011; Kang et al. 2017; Fan et al. 2017). However, the optimal conditions favoring the formation of coating as well as its stability are still under consideration.

Based on the above, the aim of this study is to optimize the conditions resulting in a stable Si-bearing protective layer around pyrite grains in order to increase the feasibility of the coating technology.

Materials and Methods

Pyritic tailings (Py) from Kassandra mines at Chalkidiki peninsula (Greece) were used in this study. The experiments were performed using the -2+0.074 mm and -0.125+0.074 mm size-fractions of particles. The secondary oxidation phases on the surface of pyrite grains were removed following treatment with a solution of 1 M HCl (Kollias et al. 2015). Thereafter, a representative amount of washed sample was finely ground and subjected to chemical and mineralogical analyses. Based on the results, the -2+0.074 mm and -0.125+0.074 mm size fractions contained 88% and 94% pyrite, respectively. The experimental methodology followed for the formation and characterization of silica coating is shown in Fig. 1.

For the development of silica coating, pyrite samples were treated with a solution consisting of 0.1 M H_2O_2 as oxidizing agent and 0.1-50 mM $Na_2SiO_3{\cdot}5H_2O$ as source of silicate ions. Hydrochloric acid (3 M HCl) was used to initially adjust pH to the selected values (pH: 5-8). Sodium acetate (0.2 M) was further used to buffer the coating solution to pH: 5-6, whereas Tris(hydroxymethyl) aminomethane (0.1 M) was used for adjusting pH at 7-8. Batch tests were conducted on the -0.125+0.074 mm-size sample, involving agitation on a rotary shaker (10 rpm). Based on the results of the batch tests, column tests with an up-flow mode involving continuous recirculation of the solution were conducted on the -2+0.074 mm size sample (Kollias et al. 2017). The variables studied in the batch and column tests are given in Table 1.

To investigate the coating effectiveness in suppressing oxidation, short- and a long-term tests were performed, i.e. oxidative leaching tests (24 hours) and humidity cell

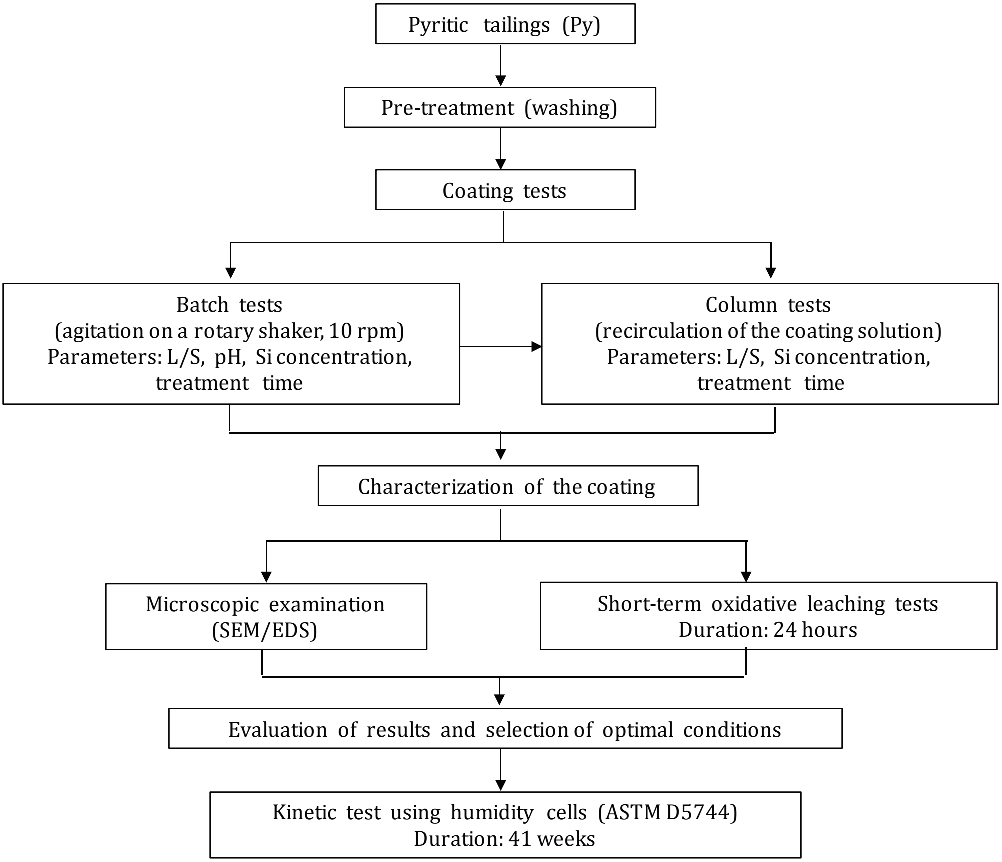

Figure 1 Methodology used for the development of silica coating on pyrite surface and the evaluation of coating effectiveness.

***Table 1** Experimental variables for the formation of silica coating.*

Parameter	Batch tests	Column tests
Particle size (mm)	-0.125+0.075	-2+0.075
Si (mM)	0, 0.1, 1, 5, 10, 25, 50	0, 0.1, 1, 5
pH	5, 6, 7, 8	6
L/S (mL/g)	5, 10, 20, 50, 100	5, 10, 20
Treatment time (h)	6, 24, 48	24, 48, 72

tests (41 weeks), respectively. The oxidative leaching tests were conducted on all the samples treated under the conditions examined in batch and column scale as well as on a "fresh" non-treated Py (i.e. washed Py sample without any coating treatment). The leaching test involved mixing of 1 g of solid samples with 100 mL of solution containing 0.1 M H_2O_2 under natural pH (≈5) in the absence of buffer. The suspensions were placed for agitation on a rotary shaker (10 rpm). At 24 hours, the suspensions were filtered through a 0.45 μm filter and the filtrate was analyzed for SO_4^{-2} and Si. The oxidative leaching tests were carried out in duplicate under controlled conditions (T=20±5°C).

Based on the experimental results, humidity cell tests were conducted on the coated Py samples with the best performance in comparison with the non-treated pyrite (control test). The humidity cell tests were performed on 1000 g sample following the procedure described in ASTM D5744 (Kollias et al. 2016).

In all cases, sulfate concentrations were measured gravimetrically (Rice et al. 2012), whereas the dissolved Si in the recovered solutions was measured using Atomic Adsorption Spectroscopy-Flame Emission (2100 Perkin Elmer). Furthermore, the coated samples were air dried and examined by SEM/EDS.

Results and Discussion

Based on the results of the oxidative leaching tests, the release of SO_4^{-2} from the treated Py samples under variable conditions as well as the non-treated Py (control sample) is shown in Fig. 2. The results can be categorized in three groups, i.e. Group "A", "B" and "C".

In Group "A", the released amount of SO_4^{-2} from the treated Py samples was reduced by 7-53%, compared to the control test. It includes batch tests involving pyrite treatment with zero or very high Si concentration (50 mM) and/or low L/S (5-50 mL/g) and/or short time (6 hours). Column tests involving pyrite treatment with Si: 0 and 1 mM, L/S: 5-20 mL/g for 24-72 hours are also categorized in Group "A". Based on SEM/EDS analysis, the above treatment conditions resulted in the formation of a partial coating layer around pyrite particles.

Group "B" includes treated Py samples, for which the dissolved amount of sulfates was reduced by 63-79% compared to the control test. The batch tests of this group were performed with solutions containing Si: 0-50 mM at pH: 6 and 7 and L/S: 50 and 100 mL/g for 24 hours. Column tests were conducted with solutions of Si: 5 mM and L/S: 10 mL/g for 48 hours.

In Group "C", a reduction of sulfate release by 83-91% as compared to the control test was observed. This group includes batch tests conducted with solutions of 0.1-50 mM Si at pH: 6-7 for high L/S ratio, i.e. 100 mL/g and treatment time equal to 24 hours. Column tests involved treatment with 0.1 mM Si for 48 hours and significantly lower L/S ratio, i.e. 10 mL/g as compared to the batch tests of the group. The SEM/EDS examination indicated that there was no cracking on the coating formed at the surface of group "C" samples.

Based on the batch test results, it is seen that the main parameters affecting the formation of an effective coating layer around pyrite particles is pH, treatment time and the liquid to solid ratio. The Py sample treated with Si: 1 mM, L/S: 100 mL/g at pH: 6 for 24 h (exp. No 30) exhibited the lower dissolved amount of sulfates (i.e. 10 mmol/kg) following the oxidative leaching test.

The effectiveness of coating formed under the above conditions to inhibit pyrite oxidation was further examined in humidity cells.

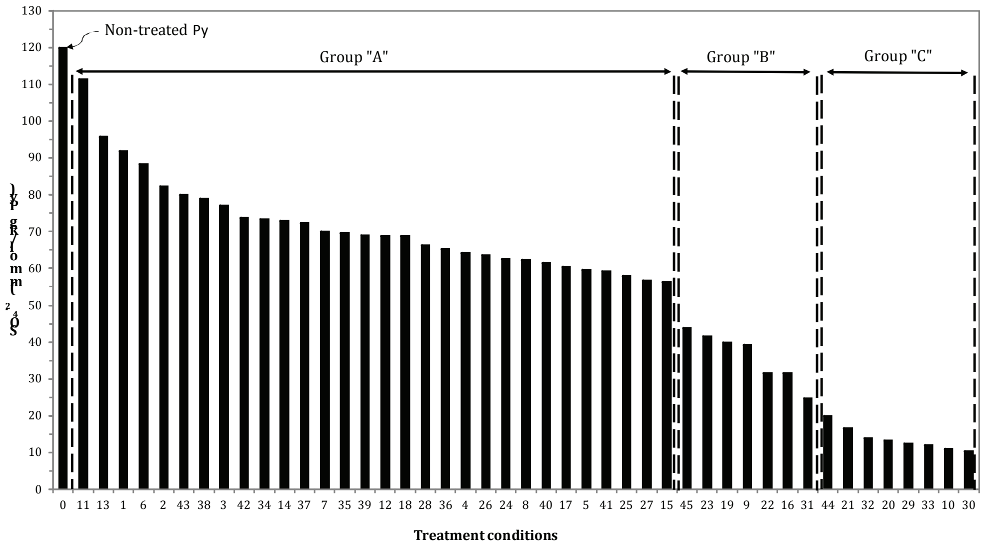

Figure 2 Comparative results of oxidative leaching tests carried out on treated pyritic tailings samples (Py) and "fresh" non-treated Py samples (mean values of duplicate tests).

The oxidation-reduction potential (ORP) versus pH of the leachates produced from the humidity cell tests is shown in Fig. 3a. pH of the leachates produced from the non-treated sample (control test) decreased from pH: 4.1 to pH: 2.7 at 4 weeks of testing. ORP values of the leachates were 400-490 mV. pH in the leachates of the Si treated sample was above pH: 4.1 after 4 weeks of testing, gradually decreased and stabilised to values 2.6±0.2 after 12 weeks of testing. The ORP values of the leachates were lower than the non-treated sample, i.e. 360-450 mV.

The cumulative amount of $S(SO_4)$ released from the Si treated and non-treated samples, expressed as a percentage of total sulfur content vs. time is shown in Fig. 3b. The evolution of dissolved $S(SO_4)$ can be distinguished in three periods, i.e. period I from 0 to 3 weeks, period II from 3 to 12 weeks and period III from 12 to 41 weeks. For the control sample, the initial dissolution rate (period I) was equivalent to 0.07% S per week, the rate was reduced to 0.03% during period II and finally the value became equal to 0.01% during period III. The observed decrease regarding the amount of S released from the non-treated Py may be attributed to the formation of a protective layer, probably consisting of iron oxyhydroxides, which suppresses the further oxidation process. The silica treated Py resulted in slower dissolution rates and the release of sulfur corresponded to 0.02, 0.01 and 0.006% per week for periods I, II and III, respectively. The cumulative amount of sulfur dissolved from the Si treated sample at 41 weeks of testing was 0.34% and was reduced by 60%, as compared to the non-treated sample (0.85%).

Based on SEM/EDS examination of the solid residues of humidity cell tests, Si concentration at the surface of treated pyrite particles ranged from 0.30 to 0.36% as compared to 0.37% for the coated particles before the test, indicating that pyrite coating remained stable under the conditions of the weathering test. This was in agreement with the chemical analyses of leachates of the Si coated sample, which showed that silica concentration was below detection limit after 3 weeks of testing.

Conclusions

Batch tests showed that the optimal conditions of coating formation involves treatment of pyritic tailings with solutions of low Si concentration (1 mM) and L/S equal to 100 L/kg at pH: 24 h. The release of sulfates from coated pyritic material was reduced by 91%, compared to the non-treated sample (control test). Humidity cell tests indicated that the coating formed using Si solution of 1 mM remained stable after 41 weeks of leaching re-

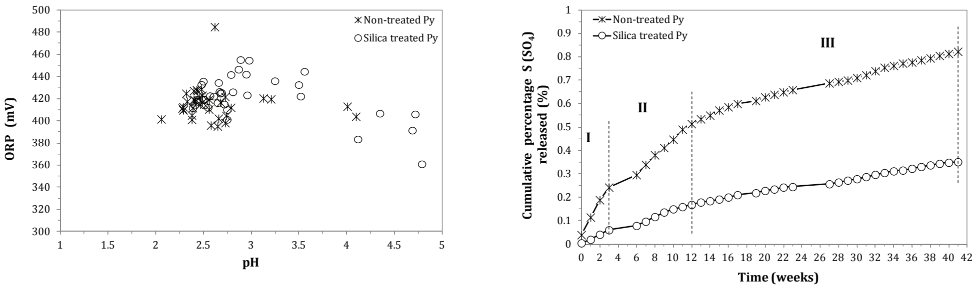

Figure 3 (a) ORP versus pH and (b) cumulative percentage of S(SO$_4$) released (%) vs. time in the leachates of treated and non-treated Py.

sulting in the reduction of SO_4^{-2} dissolution rate by 60%, compared to the control sample (non-treated sample). Column experiments indicated that an efficient coating can be also established using very low Si concentration, i.e. 0.1 mM and low L/S: 10 L/kg in case that coating solution is recirculated through the pyrite bed for 48 h. Under these conditions, the amount of S oxidized was reduced by 83% as compared to the non-treated sample. The coating technique could be applied in a mineral processing plant, after ore flotation and before the disposal of the tailings. For the efficient control of acid generation from pyritic wastes, the coating method should be combined with alkaline addition to neutralize the low amount of acidity still released from the coated material.

Acknowledgements

This research has been co-financed by the European Union (European Social Fund—ESF) and Greek national funds through the Operational Program “Education and Lifelong Learning” of the National Strategic Reference Framework (NSRF)—Research Funding Program: THALES. Investing in knowledge society through the European Social Fund [grant number MIS 380038]. The authors would like to thank Hellas Gold S.A. (Eldorado Gold Corporation) for providing the pyritic tailings as well as the anonymous reviewers for their constructive comments.

References

Ačai P, Sorrenti E, Gorner T, et al (2009) Pyrite passivation by humic acid investigated by inverse liquid chromatography. Colloids Surfaces A Physicochem Eng Asp 337:39–46. doi: 10.1016/j.colsurfa.2008.11.052

Bessho M, Wajima T, Ida T, Nishiyama T (2011) Experimental study on prevention of acid mine drainage by silica coating of pyrite waste rocks with amorphous silica solution. Environ Earth Sci 64:311–318. doi: 10.1007/s12665-010-0848-0

BREF (2009) Reference Document on Best Techniques for the Management of Tailings and Waste-Rock in Mining Activities. European Commission. http://ec.europa.eu/environment/waste/mining/bat.htm.

Diao Z, Shi T, Wang S, et al (2013) Silane-based coatings on the pyrite for remediation of acid mine drainage. Water Res 47:4391–4402. doi: 10.1016/j.watres.2013.05.006

Evangelou VP (1996) Oxidation proof silicate surface coating on iron sulfides. Plant Soil Sci Fac Patents 25:US Patent Number 5494703.

Evangelou VP (2001) Pyrite microencapsulation technologies: Principles and potential field application. Ecol Eng 17:165–178. doi: 10.1016/S0925-8574(00)00156-7

Fan R, Short MD, Zeng S-J, et al (2017) The Formation of Silicate-Stabilized Passivating Layers on Pyrite for Reduced Acid Rock Drainage. Environ Sci Technol 51:11317–11325. doi: 10.1021/acs.est.7b03232

Huminicki DMC, Rimstidt JD (2009) Iron oxyhydroxide coating of pyrite for acid mine drainage control. Appl Geochemistry 24:1626–1634. doi: 10.1016/j.apgeochem.2009.04.032

Iler RK (1979) The chemistry of silica: solubility, polymerization, colloid and surface properties, and biochemistry. John Wiley and Sons, New York, NY

Kang C-U, Jeon B-H, Kumar R, et al (2017) Stability of Coatings on Sulfide Minerals in Acidic and Low-Temperature Environments. Mine Water Environ 36:436–442. doi: 10.1007/s10230-017-0437-5

Kargbo DM, Chatterjee S (2005) Stability of Silicate Coatings on Pyrite Surfaces in a Low pH Environment. J Environ Eng 131:1340–1349. doi: 10.1061/(ASCE)0733-9372(2005)131:9(1340)

Kollias K, Mylona E, Adam K, et al (2016) Humidity cell test for evaluating the effectiveness of surface coating on pyrite particles. In: 6th International symposium of environmental issues and waste management in energy and mineral production (SWEMP 2016), October 5-7. Istanbul, Turkey,

Kollias K, Mylona E, Papassiopi N, Xenidis A (2015) Conditions favoring the formation of iron phosphate coatings on the pyrite surface. Desalin Water Treat 56:1274–1281. doi: 10.1080/19443994.2014.958537

Kollias K, Mylona E, Papassiopi N, Xenidis A (2017) Development of silica protective layer on pyrite surface: a column study. Environ Sci Pollut Res. doi: 10.1007/s11356-017-0083-2

O'Neill P (1994) Environmental Chemistry. Chapman and Hall, London

Öhlander B, Chatwin T, Alakangas L (2012) Management of Sulfide-Bearing Waste, a Challenge for the Mining Industry. Minerals 2:1–10. doi: 10.3390/min2010001

Ouyang Y, Liu Y, Zhu R, et al (2015) Pyrite oxidation inhibition by organosilane coatings for acid mine drainage control. Miner Eng 72:57–64. doi: 10.1016/j.mineng.2014.12.020

Pozo-Antonio S, Puente-Luna I, Lagüela-López S, Veiga-Ríos M (2014) Techniques to correct and prevent acid mine drainage: A review. DYNA 81:73. doi: 10.15446/dyna.v81n186.38436

Rice EW, Baird RB, Eaton AD, Clesceri LS (2012) Standard Methods for the Examination of Water and Wastewater, 22nd edn. American Public Health Association, American Water Works Association, Water Environment Federation

Rimstidt JD, Vaughan DJ (2014) Acid Mine Drainage. Elements 153–154.

Sahoo PK, Kim K, Equeenuddin SM, Powell MA (2013) Current Approaches for Mitigating Acid Mine Drainage. Rev Environ Contam Toxicol 1–32. doi: 10.1007/978-1-4614-6898-1_1

You G, Yu C, Lu Y, Dang Z (2013) Evaluation of the protective effect of polysiloxane coating on pyrite with electrochemical techniques. Electrochim Acta 93:65–71. doi: 10.1016/j.electacta.2013.01.098

Zhang YL, Evangelou VP (1996) Influence of iron oxide forming conditions on pyrite oxidation. Soil Sci 161:852–864. doi: 10.1097/00010694-199612000-00005

Effects of Variable Feeds in Wastewater Plants by Means of Process Simulation

E. Lahdenperä, T. Koiranen

Lappeenranta University of Technology, Laboratory of Green Chemistry, Skinnarilankatu 34, Lappeenranta, Finland, tuomas.koiranen@lut.fi

Abstract

Extreme weather conditions may cause heavy rain seasons or dry seasons which set new challenges to the wastewater plant operation. These challenges can be prepared for example by simulating the waste water treatment process (WWTP) at different inlet conditions. The feed stream flow rates may be exceeded up to the designed maximum values, and the compositions may vary a lot in extreme climate conditions. The goal of this study is to simplify the multivariate effect analysis of main weather specific variables. The WWTP operation is discussed from water quality viewpoint.

Keywords: Process simulation, steady-state, flooding, BOD, COD, extreme weather

Introduction

The increase of rain in Finland is estimated with different scenarios of RCP 2.6 (Representative Concentration Pathways) and RCP8.0 to be 6-20 % within this century compared to year 2000 rain level (Ruosteenoja et al. 2016). According to Lehtonen (2011) the heavy rain can strengthen 10-25 % from current average rain level within this century. The extreme weather conditions have clear impacts in wastewater treatment plants operations, as WWTP design specifications are exceeded.

Typically, WWTP main units consist of screening, primary clarification, aeration secondary clarification and filtration (Leino 2016). ASM models (IWA, 2000) from the International Water Association for activated sludge processes (ASP), are nowadays extensively used by the scientific community to model dynamic biochemical reactions of ASP reactors (Jeppson, 1996; Roeleveld, P.J., van Loosdrecht, 2002). The models are very complex, and non-linear which makes the use and optimization time-consuming. Additionally several model parameters need to be defined in order to start simulations (Keskitalo et al. 2010). Model parameter establishment is also needed for the use of WWTP specific simulation software (GPS-XTM by Hydromantis). Also multivariate-statistical methods and artificial neural networks modeling techniques have been studied in addition to white-box models (Gernaye 2004). In addition to activated sludge reactors the clarification section is also matter of modeling the WWTP essential parts (Hreiz et al, 2015).

In this study different feed conditions are simulated by solving steady-state mass balance equations using ASPEN+ (by AspenTech) process simulation tool and simplistic models without cumbersome determination of process parameters for this study. The example is from Kakolanmäki WWTP Year report (Leino 2016) in South-West Finland where the data has been extracted for WWTP model. The minimum and maximum inlet temperature values, and WWTP specific maximum flow rate are used in simulations which were designed to correspond extreme weather conditions. The simulation results are used for describing process sensitivity and thus the process behavior is better understood at limiting conditions. The combined effects of feed stream parameters are studied to the the quality parameters describing process operation.

Methods

The example wastewater treatment plant is activated sludge treatment with preliminary and secondary clarification, Fig 1. By-pass water circulation is included in the process with Actiflo® (Veolia 2018) purification

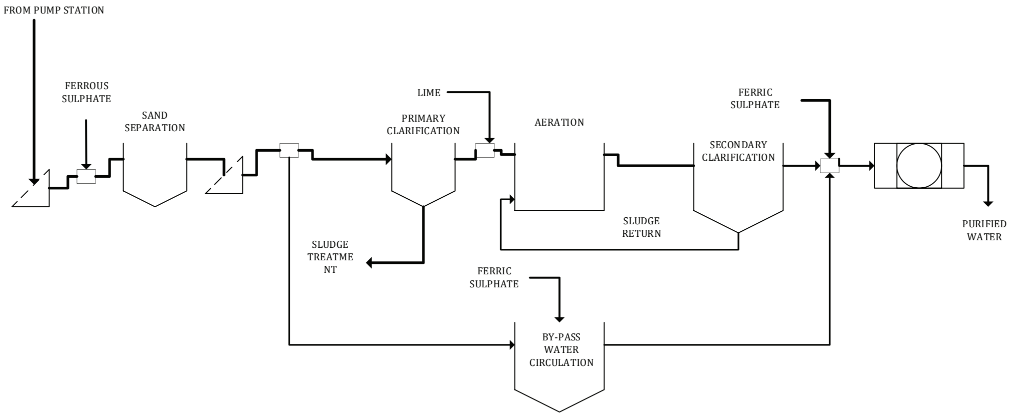

***Figure 1** Wastewater treatment plant (Leino, 2016). By-pass water circulation is Actiflo® unit supplied from Veolia.*

unit. It is used to equalize flow peaks to treat preclarified wastewater. Maximum allowed flowrate in WWTP is 275000 m^3/d and 2016 average is 77000 m^3/d whereas typical range is 74000-85000 m^3/d. In this study the evaluation of seasonal changes is based on correlating data from Kakolanmäki wastewater treatment plant (Leino, 2016).

WWTP is obliged yearly to report to Finnish environmental authorities the main purified water quality parameters. Acceptable limits are $COD_{Cr} < 60$ mg/L, $BOD_{7ATU} < 10$ mg/L, and total phosphorus $P_{tot} < 0.3$ mg/L, methods according to Leino (2016). In this study the main seasonal parameters affecting the water quality are inflow temperature and inlet flow rate. The report by Leino (2016) consists daily data of inflow and outflow water quality with flow rates and inlet temperature, seasonal variation in Table 1.

The purification efficiencies have been correlated to inlet flow rates and to inlet flow temperatures according to 2016 Kakolanmäki WWTP data by excluding outliers, such as reported process malfunctions.

$$1 - \frac{P_{TOT,out}}{P_{TOT,in}} = 0.9449 \left(\frac{T}{F}\right)^{0.0136} \qquad (1)$$

where F is inlet flow (m^3/s), $P_{TOT,in}$ and $P_{TOT,out}$ are total phosphorus in feed and purified streams, T is inlet temperature (°C). R^2 fit is 0.83.

$$1 - \frac{COD_{out}}{COD_{in}} = 0.9561 - 1.9977F/T^2 \qquad (2)$$

where COD_{in} and COD_{out} are Chemical oxygen demand using $K_2Cr_2O_7$ method in feed and purified streams, R^2 fit is 0.82

$$1 - \frac{BOD_{out}}{BOD_{in}} = 0.9977 - 0.0001F^3T \qquad (3)$$

where BOD_{in} and BOD_{out} are biological oxygen demand after 7 days using allyl thiourea method in feed and purified streams, R^2 fit is 0.98.

***Table 1** Minimum and maximum water quality during 2016 with inflow and temperature data.*

Parameter	Minimum	Maximum
COD_{Cr}, mg/L (inflow)	290	1300
BOD_{7ATU} (inflow)	120	610
P_{TOT} (inflow)	3.4	20
COD_{Cr}, mg/L (outflow)	20	54
BOD_{7ATU} (outflow)	1.2	15
P_{TOT} (outflow)	0.08	0.75
Temperature, °C	8.1	18.8
Inflow, m3/d	47200	247000

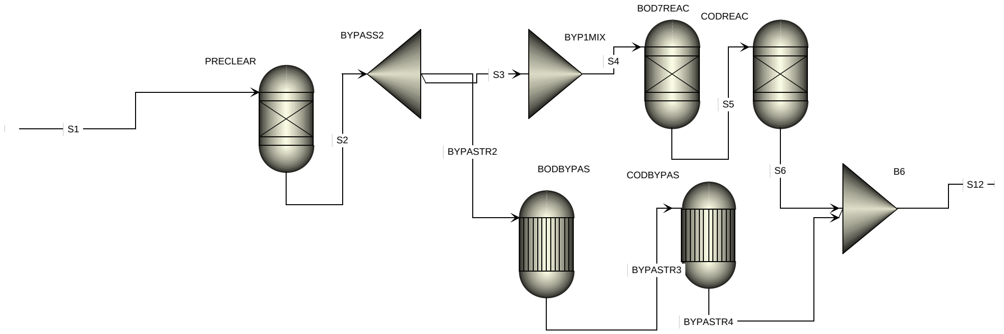

Figure 2 *ASPEN+ flow diagram from wastewater treatment process.*

The WWTP flow diagram used in ASPEN+ (v8.6) is presented in Figure 2. The preliminary clarification, aeration, Actiflo® (Veolia 2018) and secondary clarification have been simulated with RYIELD reactor models based on yields of remaining COD, BOD and total phosphorus values. These simplistic models have been selected to describe the complex wastewater treatment processes in the estimation of seasonal extreme conditions. Chemical dosings are assumed to be based on plant control systems and dosing system operation does not depend on external seasonal process parameters like temperature or inlet flow rates. Also solid separation, screening and sand separation are neglected in this process model. BODREAC and CODREAC are considered to model clarification and aeration units, CODBYPASS and BODBYPASS model Actiflo® unit in bypass water circulation.

Results

The simulation model can be adjusted to correspond correct actual outlet values by setting correct yield parameters for reactor units. The interesting part is the extreme conditions where correlation based yields are set in simulations. The WWTP year report did not include daily information about bypass water treatment efficiencies. The Actiflo® unit purification efficiencies were simulated with ASPEN+ to match the reported overall efficiencies (Table 2), and the difference between efficiencies at main stream and by-pass stream is minimal.

Table 2 *Simulated by-pass water treatment efficiencies, comparison to main stream efficiencies*

Inlet, t/d	Bypass t/d	Temperature °C	COD (Inlet)	COD (outlet)	Efficiency in COD removal (main process)	Efficiency in COD removal (by-pass)
73700	3395	15.3	750	39	0.948	0.948
89500	7841	17.7	660	47	0.929	0.925
165000	65037	14	550	54	0.902	0.9015
247000	100804	8.2	300	36	0.875	0,88
Inlet, t/d	Bypass t/d	Temperature °C	BOD (Inlet)	BOD (outlet)	Efficiency in BOD removal (main process)	Efficiency in BOD removal (by-pass)
73700	3395	15.3	390	5,9	0.985	0.982
89500	7841	17.7	260	4.3	0.983	0.989
165000	65037	14	220	13	0.941	0.941
247000	100804	8.2	120	15	0.875	0.875

The first simulations were performed for maximum flow rate 275000 m³/d. In simulations the maximum allowed BOD, COD and total phosphorus (P_{tot}) at outlet were set to estimate maximum loadings in inlet flow. The effect of temperature to BOD, COD and P_{tot} is presented in Fig. 3. P_{tot} yearly variation is 3.4-20 ppm, and maximum allowed amount is 6-8.5 ppm. Minimum COD was 290 ppm in 2016, which is exceeded at max. inflow even above 6.5 °C inflow temperatures. The calculated BOD and COD process efficiencies were 0.62-0.9 and 0.70-0.93 at 275000 m³/d, respectively. At average 77000 m³/d the BOD and COD efficiencies are 0.99-1.00 and 0.89-0.95. Minimum BOD was 120 ppm in 2016, which is not possible to achieve with 275000 m³/d inflow.

In the next set of simulations the effect of flow rate was estimated based on 15 °C temperature in inlet flow, Fig. 4. It can be found that at 120 ppm BOD inlet values BOD limit 10 ppm will be exceeded above 230000 m³/d inflows.

Conclusions

A wastewater treatment plant performance to seasonal effects has been studied, namely temperature and inflow loading. The actual plant data in this study has been used. The simulation set-up instead of complex reaction modeling was done using correlating the whole year daily data to determine purification efficiencies. The extreme seasonal changes at heavy rain seasons will be difficult to keep the BOD and COD quality within allowed limits while P_{tot} quality is possible to satisfy the limits by authorities. Also, simulations revealed BOD quality as most sensitive to inlet flow variations. Interestingly, at high flow rate loadings the wastewater temperature has a clear effect in purification.results.

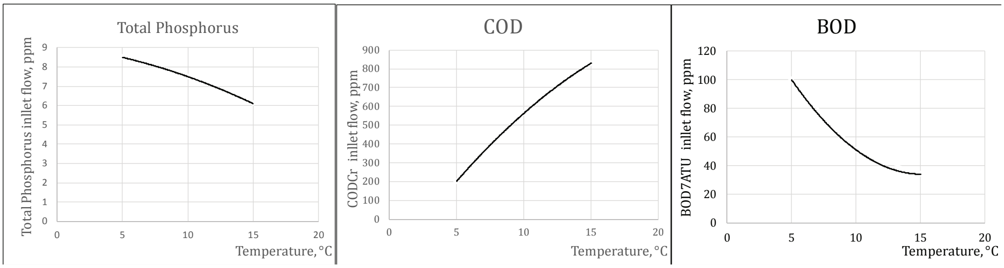

Figure 3 *Effect of temperature to maximum phosphorus, COD and BOD loadings in inlet at 275000 m³/d.*

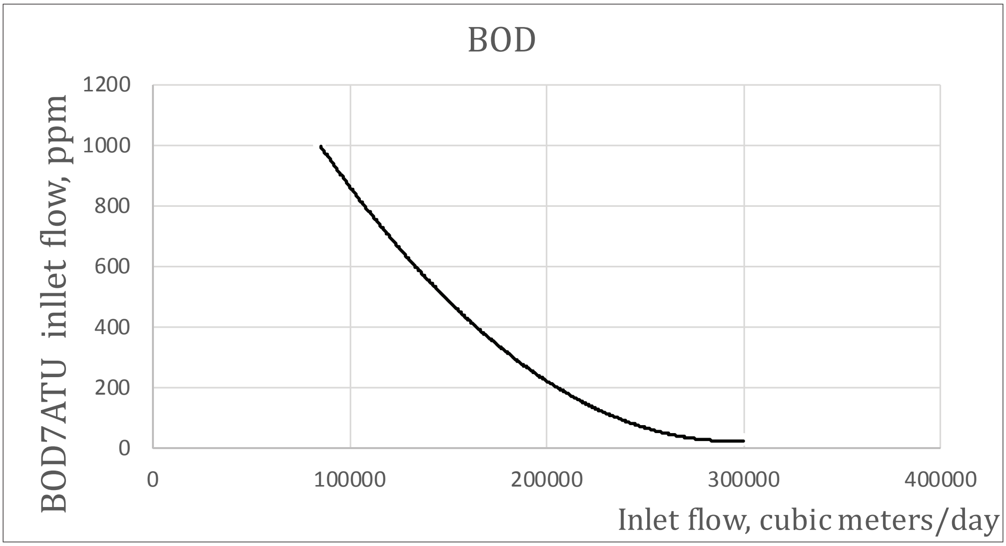

Figure 4 *Effect of inlet flow to maximum BOD loading in inlet at 15 °C inlet flow temperature.*

References

Gernaey KV, van Loosdrecht, MCM, Henze M, Lind M, Jørgensen, SB (2004). Activated sludge wastewater treatment plant modelling and simulation: state of the art. Environ Model Softw 19:763–783

Hreiz, R, Benyahiac, B, Latifi, M.A. (2015) Multiobjective optimal control of small-sizewastewater treatment plants. Chem Eng Res Des. 102: 345-353.

IWA task group on mathematical modelling for design and operation of biological wastewater treatment (2000). Activated sludge models ASM1, ASM2, ASM2d AND ASM3. IWA Publishing. Cornwall, UK, pp. 122.

Jeppsson, U (1996) Modelling aspects of wastewater treatment processes. Ph.D. Thesis, Lund Institute of Technology, Sweden. Available from http://www.iea.lth.se/publications/Theses/LTH-IEA-1010.pdf

Keskitalo, J, L Cur Janssen, J, Leiviskä, K (2010). Calibration and validation of a modified ASM1 using long-term simulation of a full-scale pulp mill wastewater treatment plant. Environ Technol 31 (5): 555-566. https://doi.org/10.1080/09593330903563802

Lehtonen, I (2011). Extreme precipitation changes in Europe according to worldwide climate models (In Finnish), Pro Gradu, University of Helsinki, Finland, 70 pp. http://urn.fi/URN:NBN:fi-fe201109052340

Leino, N (2017). Kakolanmäki wastewater treatment plant inspection report 2016 (in Finnish). Lounais-Suomen vesi- ja ympäristötutkimus Oy, 73 pp. https://www.turunseudunpuhdistamo.fi/wp-content/uploads/2017/03/Kakola8-vy2016-ID-35360-ID-14217.pdf

Roeleveld, PJ, van Loosdrecht, MCM (2002) Experience with guidelines for wastewater characterisation in The Netherlands. Water Sci. Technol. 45 (1): 77–87.

Ruosteenoja, K, Jylhä, K & Kämäräinen, M (2016) Climate projections for Finland under the RCP forcing scenarios. Geophysica 51: 17–50.

Veolia Water technologies (2018) - Actiflo-the ultimate clarifier, pp. 18. http://technomaps.veoliawatertechnologies.com/processes/lib/municipal/3329,Actiflo_brochure-7_datasheets_EN_09.pdf.

Acid Base Accounting (ABA) of mine tailings for the Potential of Acid Mine Drainage in the Sabie-Pilgrim's Rest Goldfields, South Africa

Lusunzi Rudzani[1, 3], Jabulani Ray Gumbo[2], Bisrat Yibas[1, 4], Obed Novhe[1]

[1]*Council of Geosciences, Environmental Geoscience Unit, 280 Pretoria Road, Silverton, 0184, South Africa,*

[2]*Department of Hydrology and Water Resources; University of Venda, P/Bag X5050, Thohoyandou, 0950, South Africa, jabulani.gumbo@univen.ac.za*

[3]*Department of Mining and Environmental Geology; University of Venda, P/Bag X5050, Thohoyandou, 0950, South Africa*

[4]*Department of Environmental Sciences, College of Agriculture and Environmental Sciences, University of South Africa, Florida Campus, Johannesburg, South Africa*

Abstract

The study noted that acid neutralising, calcite and dolomite bearing material was available at Glynn's mine tailings material that can be used to neutralise the acid generation capability of Nestor's mine tailings. The acid neutralising material would improve the acidic Nestor's mine tailings to an almost neutral pH, which is conducive for the growth of plants necessary for phytoremediation efforts.

The study however, noted that phytoremediation of Nestor mine tailings would not succeed because the plants could not grow in acidic soils. Nonetheless, the presence of acid neutralising material within Glynn's mine tailings can be used to neutralise the acid generation capability of Nestor mine tailings. Thus, the presence of acid neutralising material at a location less than a distance of 6 km would reduce transportation and material costs. This would ensure the success of phytoremediation efforts in saving the environment and the overall prevention of acid mine drainage.

Key words: Acid Base Accounting, Mine Tailings, Acid Mine Drainage, Net Acid Neutralizing Potential, Net Acid Potential

Introduction

Mining is one of the most important economic activities in South Africa. The country receives huge economic benefits from the mining industry. However, different kinds of mine residue deposits (herein referred to as mine tailings residue deposits) associated with the extraction and processing of metals stand out as sources of potential environmental pollution in specific mining areas and the country at large (McCarthy 2011). For coal and gold mining operations, these mine tailings are a continuous source of acid mine drainage (AMD) generation (Kleinman et al 1981; Oberholster et al 2013) and an environmental hazards (Rosner et al 1998; Nelushi et al 2013).

The Sabie-Pilgrim's Rest Goldfield, Mpumalanga, is one such area where gold mining activities occurred in the past. The area has numerous mine tailings of different ages and sizes. What is the key here is that a few or no environmental studies had been carried out on mine tailings; hence this study focused on the Nestor and Glynn's Lydenburg Gold mine tailings storage facilities. The main objective of this study was to determine the mineralogy and the geochemistry of mine tailings.

Location of the study area

The Nestor (NS) and Glynn's Lydenburg (GL) mine tailings, are located in the Sabie area of the Mpumalanga Province of South Africa (Fig. 1).

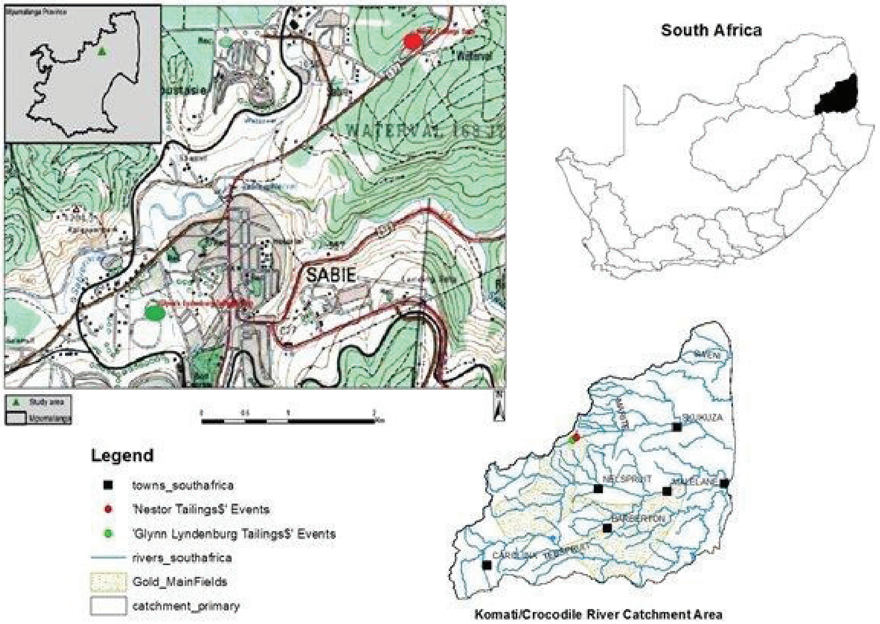

Fig. 1 *Location of the Study Area*

Methods

Sampling and Sample preparation

Thirty tailings profile samples and five grab samples were collected at mine tailings from 20 to 23 February 2015. A truck-mounted and a hand auger were used to collect samples up to the depth of 10 m at Glynn's Lydenburg tailings dam up to 3 m at the Nestor (drilling to 3 m) respectively. The samples were sent to the Council for Geoscience's laboratory in Pretoria, South Africa, for analysis.

The samples were then ground using milling pots made of carbon steel to minimize the level of contamination on a single swing mill (TM-SPR003) method which involved air drying, crushing and milling of samples to a size reduction of <75 µm,. In between milling, the equipment was washed using distilled water and wiped with the disposable paper towels wetted with ethanol and then allowed to dry to avoid the contamination of samples.

Acid base accounting have been determined in terms of paste/initial pH, reactive S (%), AP (as kg/ton $CaCO_3$), and NP (as kg/ton $CaCO_3$). The calculated parameters, namely, net neutralizing potential (NNP as kg/ton $CaCO_3$) and net potential ratio (NPR) have been used as criteria the acid potential of samples. Graphically, these results clearly show the dominant trends in results as shown in figures. The criteria used to classify the acid-producing potential of the samples analysed are those used by Usher et al (2003), and these should not be used in isolation, but in combination to categorise material from non-acid generating to acid generating with a slight grey area in between. The following criteria have been used: Paste pH (measure of sample's immediate acidity or alkalinity); net neutralizing potential (NNP=NP-AP); neutralizing potential ratio (NPR=NP/AP) as per Price (1995); and percent sulphide-sulphur and NPR.

Samples were analysed by X-ray diffraction spectrometry (XRD) in accordance with procedures of USEPA (1986). The XRD technique employed Bruker D8 HRXRD spectrometer, scanning from 2 to 70 ° 2θ Cukα radiation at a speed of 0.02 ° 2θ steps size 0.5 sec with a LYNXEYE detector and generator settings of 40 kV and 40 mA. Semi-quantitative approximations of the minerals present were based on the relative peak heights area proportion according to Brime (1985).

Data Analysis

Microsoft Excel 2013 was used for calculating of average, standard deviation and plotting of graphs.

Results and discussion

Acid base Accounting (ABA)

Fig. 2 below shows subdivision based on acid potential (AP), neutralisation potential (NP) (i.e. Neutralising potential ration, NPR) and paste pH of the tailings collected at Nestor and Glynn's Lydenburg mine tailings storage facilities. Based on this subdivision, Nestor mine tailings samples are characterized by high AP than NP, and its net potential ratio is less than 1 (NPR<1). Their AP ranges from 1.56-140.31 kg $CaCO_3$/ton while NP ranges from -57.75 to -0.3 kg $CaCO_3$/ton. However, Glynn's Lydenburg Mine Tailings which is associated with dolomite mineralization show no potential to leach any acidic drainage. Based on ABA results, the tailings have more NP than AP, and plot at NPR>2. Their AP ranges from 7.5 $CaCO_3$/ton to 56.56 $CaCO_3$/ton while NP ranges from 7.5 to 207.88 $CaCO_3$/ton to 190 $CaCO_3$/ton. The results of AP/NP (NPR) are also confirmed by paste pH of the samples (Fig. 2). Nestor tailings samples are characterised by low paste pH (2.7 to 5), which is indicative of presence of sulphides or sulfates that have reacted to form acid. On the other hand, Glynn Lydenburg tailings samples are characterised by high paste pH (7 to 8.8), which could be indicative of high neutralising minerals.

Gold tailings of Nestor Mine are characterized of very low NRP of less than one (NPR<1) with considerable percentage of sulphur and are having greater potential of acid production (Fig. 3). Glynn's Lydenberg Mine tailings are having a higher than four NPR (NPR>4) and most of them fall on the zone wherein no further testing is necessary (Fig. 3).

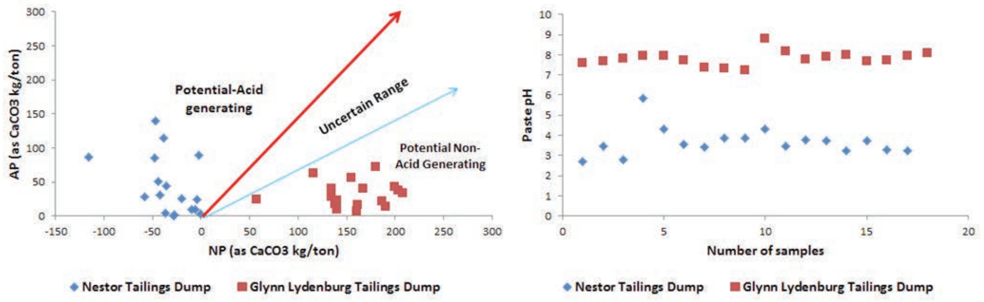

Fig. 2 Classification based on acid potential (AP), neutralising potential (NP) and paste pH.

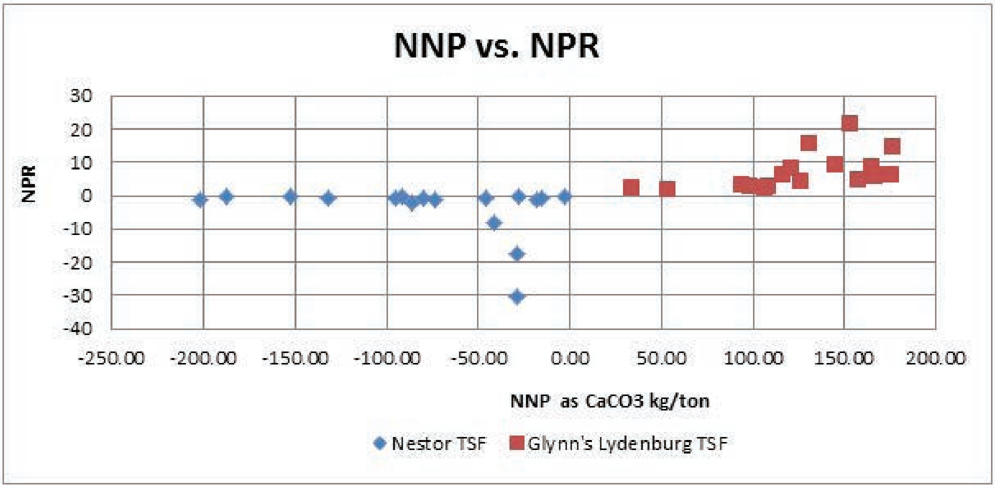

Fig. 3 NPR vs NNP of Nestor TSF and Glynn's Lydenburg TSF

Nestor Mine tailings have high sulphide concentration (in a range of 0.29 and 4.49 wt %) and negative NPR (ranging between -17.63 and 0), hence are potentially acid producing as their sulphur per cent exceeds 0.03 wt % described as acid producing (Fig. 4). On the other hand, Glynn's Lydenberg tailings have low sulphur concentration (ranging between 0.29 and 2.30 wt %) with high NRP values of up to 21.4, hence low AMD generating capacity. Sulphur percentage in Glynn's Lydenburg Mine tailings is less compared to Nestor Mine tailings (Fig. 4). Based on ABA results, NPR>2 in Glynn's Lydenburg Mine tailings, hence less likely to generate acid. This is confirmed by paste pH which ranges from 7.58 to 8.8 (Fig. 2).

Mineralogical Analysis of Mine Tailings

There is a wide range variation among the Nestor and Glynn's Lydenburg mine tailings' mineralogical composition based on X-ray diffraction (XRD) as expressed in weight percent (wt %) of bulk samples (Fig. 5). Both primary and secondary minerals were deduced from XRD mineralogical analysis.

In the Nestor TSF, predominant minerals include primary minerals: quartz (SiO_2) ranging from 64-87 wt%, followed by mica [$K(Mg, Fe)_3(AlSi_3O_{10})(OH)_2$], plagioclase ($NaAlSi_3O_8 – CaAl_2Si_2O_8$) and k-feldspar (Fig. 5A). Kaolinite is the secondary clay mineral which was found mostly on grab samples and on the depth of 2 m on one of handheld auger drilled holes, jarosite {$KFe_3(SO_4)_2(OH)_6$} and gypsum ($CaSO_4.2H_2O$) are secondary minerals which are dominant on top layers of the tailings of Nestor Mine. Goethite is a secondary oxide mineral absent in grab samples from Nestor tailings and is most concentrated in handheld auger samples. Gibbsite is not present in all Nestor TSF samples except for the one recorded at unoxidized 2 m depth in one of handheld auger samples. This indicates that the rate of sulphide oxidation is high in this saturated zone.

Quartz is the most dominant primary mineral and shows a constant trend from both grab samples and handheld auger samples with depth. This shows that it is less reactive in oxidizing conditions. Minerals such as quartz have no potential to neutralize acid, and this is mainly due to their physical property (hardness) and it has a relative reactivity of 0.004, which is twice slower than the relative reactivity of kaolinite (Sverdrup, 1990; Kwong, 1993). Pyrite (FeS_2) is the major acid producing mineral and hematite respectively. Mica is also common in high concentrations in both samples collected using handheld auger and grab samples. Calcite is absent in Nestor Mine tailings and dolomite was only found in two oxidized grab samples indicating that these tailings are acidic. The acidic nature of Nestor mine tailings would provide adverse conditions for growth of plants and grass that can be maybe used for revegetation of the tailings storage facility.

Tailings from Glynn's Lydenburg are com-

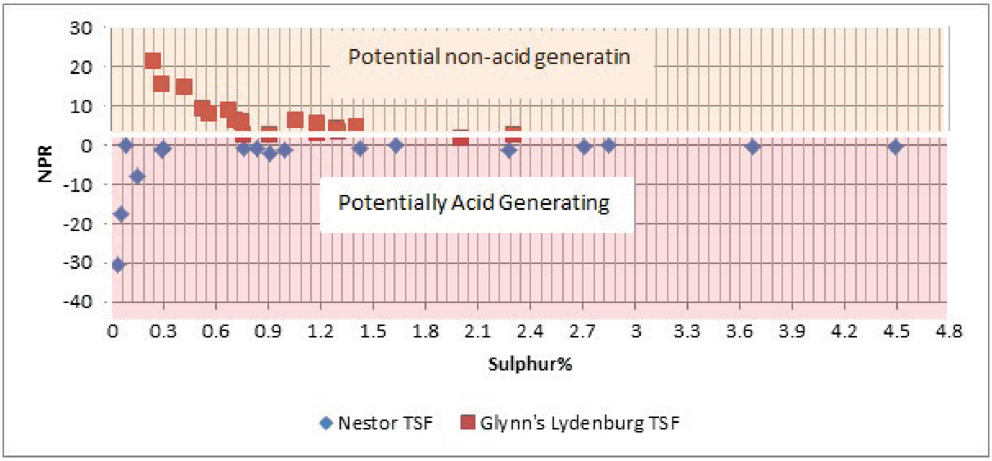

Fig. 4 *NRP vs Sulphur% in the Nestor TSF and Glynn's Lydenburg TSF*

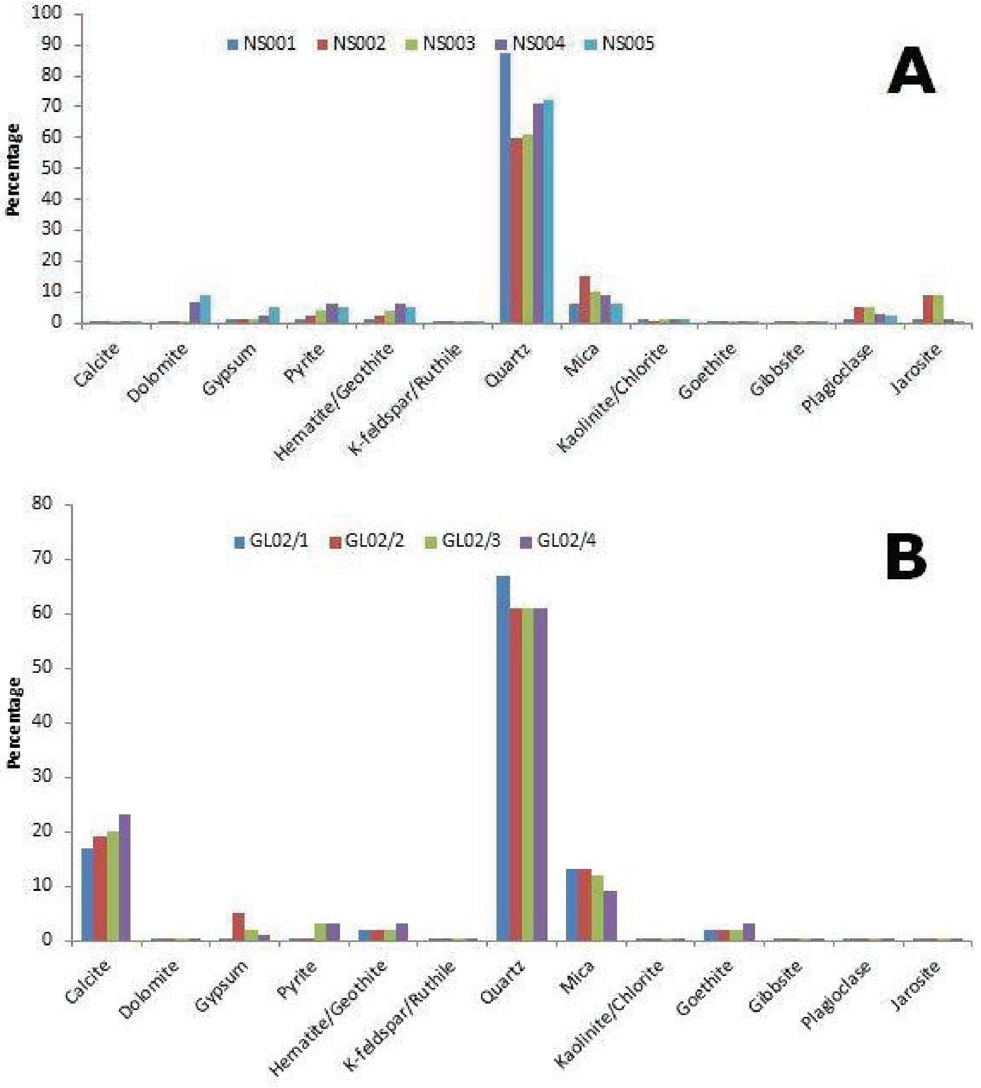

***Fig. 5** Mineralogical composition of (A) Nestor & Glynn's (B) Lydenburg TSFs samples as wt %*

prised of quartz and dolomite [CaMg (CO$_3$)] as major mineral assemblages (Fig. 5B). Quartz shows a constant trend with increasing depth (Fi. 5B). This shows that it is less reactive even under oxidizing conditions. Al_2O_3 and Fe_2O_3 show a slight constant trend with increasing depth and increases at depths. Cr_2O_3, K_2O, MnO and TiO_2 show a constant trend with depth.

Other primary minerals that are acid neutralizing include mica and plagioclase. Gypsum and goethite are also present as secondary minerals as neutralizing minerals, while the absence of jarosite in Glynn's Lydenburg Tailings dump could be attributed to less acidic conditions due to the presence of high concentrations of carbonates within the Malmani dolomite host rocks. Plagioclase was mainly found in truck-mounted auger samples and showed a constant trend of decreasing with depth. Mica being common in all three drilled holes including handheld auger samples also showed a decrease with depth trend. This can be attributed to low aid generation at unoxidized zones of the tailings dump (3-10 m) compared to semi-oxidized top part (0-2 m). Gypsum show a decreasing trend with depth in both handheld and truck-mounted augers drilled holes. The absence of dolomite in borehole GL 02/1-4 (Fig.

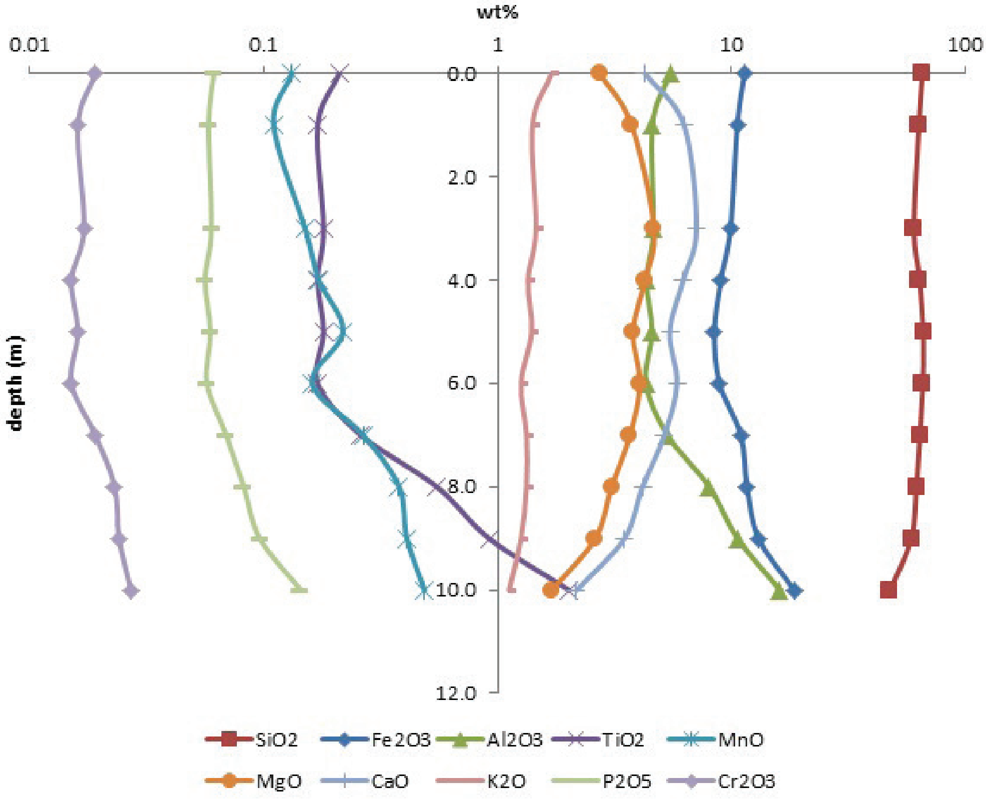

Fig. 6 *Depth profile for major oxides in Glynn's Lydenburg tailings storage facility (Log 10 scale on x-axis)*

5) can be attributed to oxidation that might be taking place within the top oxidized zone (0-2 m); however, the presence of calcite can add into neutralization potential to the acid that might be produced by primary mineral hematite. Gypsum is present in both truck-mounted auger samples and handheld auger samples showing a decrease with depth trend. Kaolinite was only found at unoxidized lower parts of the tailings dump between 8 and 10 m depth showing a rapid increase with depth (Fig. 5).

Conclusions

The study noted that acid neutralising, calcite and dolomite bearing material was available at Glynn's mine tailings material that was used to neutralise the acid generation capability of Nestor's mine tailings. The acid neutralising material would improve the acidic Nestor's mine tailings to an almost neutral pH, which is conducive for the growth of plants necessary for phytoremediation efforts. This interpretation of the geochemical and mineralogical data is also corroborated by the acid base accounting (ABA) which showed the relative acid and neutralization capacities and the resultant net acid generating capacity of the two tailings materials. The study further showed that the metal mobility was enhanced by the net acid generating capacity of the Nestor mine tailings. Whereas the alkaline conditions of the Glynn Lydenburg mine tailings lead to a non-acidic discharge. The presence of heavy metals, metal oxides, neutralizing oxides and acid-forming oxides in the mine tailings are likely to have negative impact on the environment.

Acknowledgements

The authors acknowledge the financial contribution to the study from both the University of Venda and Council for Geoscience, South Africa.

References

Alloway BJ & Ayres DC (1998) Chemical Principles of Environmental Pollution, BJ Alloway and

DC Ayres. Water, Air, & Soil Pollution, 102(1), 216-218.

Alpers CN, Blowes DN, Nordstrom DK, Jambor JL (1994) Secondary Minerals and Acid Minewater. In: J.L. Jambor and D.W. Blowes (eds). The Environmental Geochemistry of Sulphide Mine-wastes. Mineralogical Association of Canada. Short Course Series. Volume 22.

Brime C (1985) The accuracy of X-ray diffraction methods for determining mineral mixtures. Mineralogical Magazine, 49(353), 531-538.

Centeno JA, Tseng CH, Van der Voet GB, Finkelman RB (2007) Global impacts of geogenic arsenic: a medical geology research case. AMBIO: A Journal of the Human Environment, 36(1), 78-81.

Department of Environmental Affairs (DEA) (2013) National Norms and Standards for Remediation of Contaminated Land and Soil Quality in the Republic of South Africa

Department of Environmental Affairs and Forestry (DWAF) (1996) South African water Quality Guidelines. Second Edition. Volumes 1-8.

Harada M (1996) Characteristics of industrial poisoning and environmental contamination in developing countries. Environmental Sciences, 4(Suppl), 157-169.

Jambor JL (1994) Mineralogy of sulfide rich tailings and their oxidation products. In: Jambor JL, Blowes DW (Eds), The environmental geochemistry of sulfide mine wastes: Mineralogical Association of Canada, Short Course Handbook, v. 22, p103-132

Nelushi K., Gumbo JR, Dacosta, FA (2013) An investigation of the bioaccumulation of chromium and uranium metals by Cynodon dactylon: A case study of abandoned New Union Gold Mine Tailings, Limpopo, South Africa. African Journal of Biotechnology, 12(46), 6517-6525.

Kleinmann RLP, Hedin RS, Nairin RW (1998) Treatment of mine drainage by anoxic limestone drains and constructed wetlands. In: Geller A, Klapper H, Solomons W, editors. Acid Mining Lakes: Acid Mine Drainage, Limnology and Reclamation. Berlin: Springer. p.303-19.

Kneen MA, Ojelede ME, Annegarn HJ (2015) Housing and population sprawl near tailings storage facilities in the Witwatersrand: 1952 to current. South African Journal of Science, 111(11-12), 1-9.

Kwong YTJ (1993) Prediction and Prevention of Acid Rock Drainage from a Geological and Mineralogical Perspective. MEND Report 1.32.1. p.47.

Lapakko KA (2002) Metal mine drainage rock and waste characterization tools: An overview. *pubs.iied.org/pdfs/G00559.pd*

Luo X, Yu L, Wang C, Yin X, Mosa A, Lv J, Sun H (2017) Sorption of vanadium (V) onto natural soil colloids under various solution pH and ionic strength conditions. Chemosphere, 169, 609-617.

McCarthy TS (2011) The impact of acid mine drainage in South Africa. S. Afr. J. Sci. 107, 1-7.

Ngole-Jeme VM, Fantke P (2017) Ecological and human health risks associated with abandoned gold mine tailings contaminated soil. PloS one, 12(2), e0172517.

Oberholster PJ, Genthe B, Hobbs P, Cheng PH, de Klerk AR, Botha AM (2013) An ecotoxicological screening tool to prioritize acid mine drainage impacted streams for future restoration. Environ. Pollut. 176, 244-253.

Rosner T, Boer R, Reyneke R, Aucamp P, Vermaak J (1998) A preliminary assessment of pollution contained in saturated and unsaturated zone beneath mine residues deposits. Rep K5/797/0/1. Water Research Commission of South Africa, Pretoria.

Sverdrup HU (1990) The Kinetics of Base Cation Release due to Chemical Weathering, Lund University Press, Lund, p 246p.

United States Environmental Protection Agency (USEPA) (1986) Test Methods for Evaluating Solid waste, 3rd edition, Office of Solid Waste and Emergency Response, Report SW-846, volume 1, November 1986 with revisions to January 1995.

United States Environmental Protection Agency (USEP) (2009) National recommended Water Quality criteria. United States, Environmental Protection Agency, pp 1 -22.

Usher, B.H., Cruywagen, L.M., Necker.,E., and Hodgson, F.D.I., 2003. On-site and laboratory investigation of spoil in open cast collieries and the development of acid-base accounting procedures, WRC Report No. 1055/1/03, pp.627-638.

Developing a Flow-Through Biokinetic Test to Characterize ARD Potential: Investigating the Microbial Metabolic Activity on Pyrite-bearing Waste Rock Surfaces in an Unsaturated Ore Bed

Didi X. Makaula, Robert J. Huddy, Marijke A. Fagan-Endres, Susan T. L. Harrison

Centre for Bioprocess Engineering Research (CeBER), Department of Chemical Engineering, University of Cape Town

Abstract

ARD generation from mine waste rock associated with hard rock sulfide and coal mining poses environmental concerns over time. Therefore, it is important to characterise waste rock material for its acid-forming potential, prior to disposal. In this paper, column reactors simulating the flow-through, unsaturated packed bed environment of waste dumps were used to assess acid-forming potential of two pyrite-bearing waste rocks. Additionally, the activity of mineral-associated microbial populations was visualised and measured using isothermal microcalorimetry. The work forms the basis for development of a representative flow-through system, a modification of the UCT Biokinetic test that considers microbial-waste rock surface interaction.

Keywords: Acid rock drainage, metabolic activity, waste rock surface, microbial colonisation

Introduction

Current day mining operations typically generate large amounts of waste rock or pulverized mine tailings or both from the mining and metal extraction processes. These waste stockpiles may contain significant amounts of sulfidic minerals which undergo oxidation through contact with air and water (Dold et al., 2009). Their oxidation is exacerbated by the presence and activity of naturally occurring iron- and sulfur oxidizing microorganisms (Egiebor and Oni, 2007). These generate acid-laden liquid effluents stream, known as acid rock drainage (ARD), containing toxic metals and sulfates that pose a threat to surrounding water sources (Parbhakar-Fox et al., 2015).

To quantify the ARD risk, it is important to test mine waste for its potential to form acid prior to its disposal to ensure an appropriate disposal approach. This enables adequate control and management of ARD to minimise environmental impact and reduce costs associated with environmental remediation during life of the mine, through mine closure and persisting as legacy after life of mine (Parbhakar-Fox et al., 2015). A suite of tools is available to characterise the acid forming potential of waste material. These can be classified into laboratory, field-based and whole-rock geochemical assessments alongside mineralogical evaluations (Morin and Hutt, 1998). New or extended characterisation methods are sought to better address limitations caused by complex microbiological, hydrological, mineralogical, and geochemical processes and their interactions within a mine waste environment (Dobos, 2000). Characterising ARD generation potential of mine wastes through static and kinetic tests is critical for effective mitigation through treatment and disposal. Static tests are common and rapid, providing “snapshot” data under extreme conditions of acidity and oxidative potential to measure ‘net’ acid generation potential. However, they fail to account for relative rates of acid consuming and generating reactions or for the key role microorganisms play in ARD generation. Kinetic tests typically include humidity cell tests and field tests; these are slow and expensive (Hesketh et al 2010; Parbhakar-Fox et al 2013).

The UCT Biokinetic Test has been introduced to provide meaningful data on long term ARD generating potential of waste rock and tailings and its kinetics in a relatively short space of time (± 3 months) and is relatively inexpensive to operate (Hesketh et al., 2010; Broadhurst et al., 2013). It recognises the key role of microbial activity and microbial association and colonisation of the mineral surface by iron- and sulfur oxidizing microorganisms in the generation of ARD from waste rock dumps. However, limitations of the batch biokinetic test include poor representation of typical contacting mechanisms of liquid flow or leach solution with waste rock and failure to account for washout of neutralising capacity typical of a flow-through system such as a waste rock dump and the associated impact of differing kinetics of acid formation and neutralisation by ore components. Further development of the biokinetic test to provide a flow-through test is desired. The draw-and-fill flask based biokinetic test (Golela et al., in prep) addresses the first limitation while the flow-through biokinetic test under development here aims to remove both limitations.

In this study, we investigate the potential of a flow-through biokinetic test protocol, using two pyrite bearing low-grade waste rock fractions. Recognising the importance of microbial activity and its association and colonisation of the mineral surface in ARD generation, acidification potential, microbial activity and the community implicated in waste rock weathering and leaching were used as critical indicative variables for monitoring the potential of a flow-through system.

Methods

Waste rock samples

Two pyrite-bearing low grade or waste rock samples, namely low sulphur metapelite (PEL-LS) and high sulphur metapelite (PEL-HS) were used in this study. The samples were milled and wet sieved to obtain -75 µm particles. After air drying at 37 °C, representative samples were prepared by using a riffle splitter. The bulk mineralogical compositions of the waste samples were acquired using QEMSCAN and are shown in fig 1. Acid generating minerals present consist predominantly of pyrite (PEL-LS:13.99 wt. %, PEL-HS: 33.43 wt. %) and pyrrhotite (PEL-LS: 2.35 wt. %, PEL-HS: 3.9 wt. %). Acid consuming minerals consist predominantly of calcite (PEL-LS: 0.22 wt. %, PEL-HS: 0.03 wt. %), fast and intermediate weathering minerals predominantly contain garnet (PEL-LS: 2.83 wt. %, PEL-HS: 4.52 wt. %) and slow weathering minerals consist predominantly of muscovite (PEL-LS: 14.77 wt. %, PEL-HS: 12.42 wt. %). The waste rock samples contain approx. 35% inert quartz (PEL-LS: 36.67 wt. %, PEL-HS: 34.76 wt. %).

The pulverised waste rock samples were coated onto 6 mm glass beads, using Bostic glue (Africa et al. 2013), to provide a uniform and quantifiable surface area. The coated glass beads were air dried for a minimum of 24 hours before they were sterilised by irradiation at 45 kGy dosage.

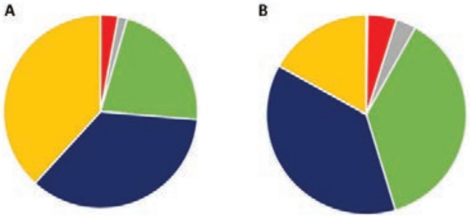

Figure 1 *Mineralogical analysis of the two waste rock samples acquired using QEMSCAN. A (PEL-HS) and B (PEL-LS) are results of the waste samples showing abundant acid forming minerals (pyrite and pyrrhotite; 🟡), dissolving mineral (calcite; 🔵), fast- (garnet; 🔴), intermediate- (Mn-Fe silicate and augite; ⚪) and slow-weathering (K-feldspar and muscovite; 🟢) respectively, and quartz as an inert mineral (🔵).*

Microbial cultures

A mixed mesophilic culture, comprising *Leptospirillum ferriphilum*, *Acidithiobacillus caldus* and archaea (*Ferroplasma acidiphilum* and *Acidiplasma cupricumulans*), was used in this study. The culture was grown on a 3% (w/v) pyrite concentrate in 0K basal salts medium (Kolmert and Johnson 2001)] in a 1 L batch stirred tank reactor at 35 °C. The stock reactor was maintained on a basis of a weekly draw and fill in which 15% (v/v) was replaced with fresh media and mineral concentrate. The culture was regularly assessed through direct microscopic cell counts (Thoma counting chamber; Olympus BX40 Microscope at 1500 fold magnification using phase contrast optics; detection limit of the Thoma counting chamber: 3 × 10^5 cells mL^1). Routine monitoring included measurement of the redox potential using a Ag/AgCl reference electrode connected to a Metrohm 704 pH/Eh meter and pH measurement. The microbial community in the reactor was maintained in the range of 1×10^9 to 4×10^9 cells mL^{-1} (Ngoma et al 2015).

Reactor operation

For the flow-through biokinetic test, twelve columns were operated, six of each waste rock sample. Each column was loaded with 300 waste rock mineral-coated glass beads and operated as a continuous flow-through system. Prior to inoculation, the loaded column reactors were washed and conditioned with 0K media (pH 1.6) at 1 mL min^{-1} for 24 h to remove readily leachable materials and create an environment conducive for microbial attachment to the ore surface by initiating neutralising reactions on the waste rock. One column of each waste rock type served as an un-inoculated control. The remaining 10 columns were inoculated by saturation (Tupikina et al., 2014) using up-flow of 100 mL 0 K media supplemented with 10^{10} mixed mesophilic microbial cells per kilogram of ore and 0.5 g L^{-1} of Fe^{2+} as $FeSO_4.7H_2O$ at 1 mL min^{-1} in closed circuit. The inoculum suspension was recycled for 18 h to allow microbial-mineral contacting and attachment. Thereafter, the columns were drained and the liquid fraction collected and analysed for planktonic cells by microscopic cell counts. A continuous down-flow of fresh feed containing sterile fresh 0 K media (pH 1.6) supplemented with 0.5 g L^{-1} Fe^{2+} ($FeSO_4.7H_2O$) was introduced at 1 mL min^{-1} and the columns operated as flow-through unsaturated beds for the duration of the experimental run for 20 days at 30 °C. Daily effluent pregnant leach solution (PLS) samples were taken and analysed for pH, using a Metrohm 704 pH metre and probe, calibrated at pH 7.0, pH 4.0 and pH 1.0 before use, redox potential, and Fe^{2+} and total Fe concentration using a colorimetric assay described by Komadel and Stucki (1988).

Individual columns were sacrificed on days 1, 7, 12, 15 and 20, respectively for each rock type. The microbial phase attached to the ore within these columns was analysed morphologically using electron microscopy, quantified and characterised by detachment and direct microscope cell counting, and characterised in terms of metabolic activity using isothermal microcalorimetry.

Microbial detachment and surface visualisation

A modified detachment protocol, described by Makaula et al. (2017), was used to recover microorganisms from waste rock surfaces on coated beads. In this current study the washing step was repeated 3 times to detach firmly attached microbial communities. For microbial-mineral surface visualisation, samples of colonised mineral surface obtained during each column sacrifice were processed as described by Makaula et al. (2017) prior to scanning electron microscopy.

Measurement of activity on mineral associated microbial populations

Isothermal microcalorimetry (IMC) was used to quantify the microbial metabolic activity of cells associated with the waste rock surfaces, as described by Makaula et al. (2017). Two microbially colonised waste rock coated beads from each sample were loaded aseptically into an IMC vial. Each sample was analysed in duplicate and maximum heat flow of each ampoule was recorded.

Results and Discussion

After the 24-hour conditioning period, the pH increased from pH 1.6 to 1.77 (± 0.025) for HS and 1.7 (± 0.012) for LS respectively. Following inoculation during which pH decreased, the pH of the experimental samples increased from pH 1.38 to 1.77 for PEL-HS and 1.6 for PEL-LS. The pH in the control samples increased from pH1.6 to 2.01 for PEL-HS and 1.69 for PEL-LS (fig 2A). The pH increase in the PLS suggests an initial dissolution of acid neutralising minerals such as calcite. During the complete flow-through operation phase, the average pH for the experimental PEL-HS and PEL-LS samples were 1.61 (± 0.035) and 1.59 (±0.011) respectively and the average pH for control samples was 1.63 (±0.024) for PEL-HS and 1.61 (± 0.022) for PEL-LS. These remained relatively stable and similar to the pH 1.6 media fed to the column reactors continuously in flow-through operation. This suggests that there was a depletion of readily available neutralising agents in the waste rocks or that the residence time in the column was too low to liberate these compounds significantly. The relatively constant pH also suggests a lack of effective activity in the leaching of the available sulfidic mineral in both waste rocks.

The redox potential of the experimental samples decreased from 499 to 401 mV for PEL-HS and from 504 to 430 mV for PEL-LS during the 18-hour inoculation period. The redox potential of the control samples remained the same at 301 mV for PEL-HS and increased from 301 to 335 mV for PEL-LS. The redox potential of both PEL-HS and PEL-LS experimental samples remained relatively low, circa 300 to 500 mV, throughout the continuous flow-through operation (fig 2B). This suggests either a lack of effective and detectable iron-oxidizing microbial activity that would result in the catalysed regeneration of Fe^{3+} and associated increased redox potential, or that the microbial activity generating Fe^{3+} is insignificant with respect to the ferric leaching of the mineral and the flowrate of the solution. This lack of effective activity corresponded with continued presence of Fe^{2+} (fig 2C) and no evidence of its conversion into Fe^{3+} (fig 2D). When the flow rate was lowered to 4 mL h^{-1} (within the industry standard), microbial activity was easily detectable from solution chemistry measurements (data not shown).

The SEM micrographs in fig 3 show leached waste rock surfaces sampled at day 1 and 20. On day 1, single cells were observed on the precipitate covered waste rock surfaces (fig 3A and B). On day 20 the surface of PEL-LS was pitted with microbial footprints (fig 3C). This indicates that microbially facilitated degradation took place and the cells detached. The microbial detachment may be caused by depletion of energy on the attached position or a high liquid flow rate (shear) or a combination of these factors. Cells of various morphologies were present, including spiral and rod-shaped cells that were consistent with the morphology of the microorganisms in the inoculum. Both single cells and colonies of embedded cells were also observed on the PEL-HS.

Cells on the waste rock mineral surfaces were mechanically detached and microscopically counted. Firmly attached cell numbers, as well as the percentage of mineral surface that is covered by these microorganisms in a monolayer are presented in fig 4A. Assuming a monolayer, the approximate number of cells required to saturate the surface is calculated at 1.32×10^{12} cells m^{-2}. After the 18-hour in-

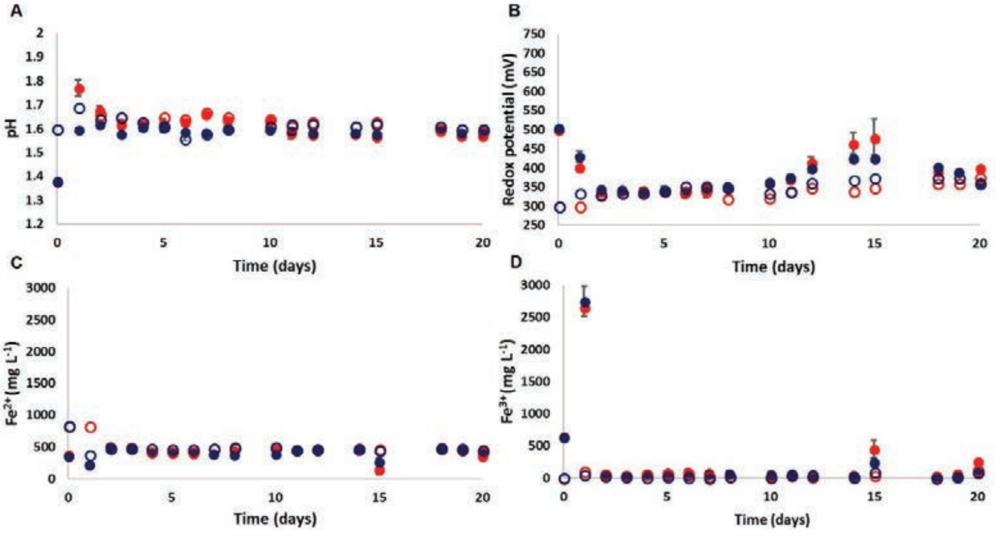

Figure 2 *A) pH, B) redox potential, C) Fe^{2+} and Fe^{3+} of the HS experimental (●) and LS experimental (●) and the HS control ( ) and LS control ( ) column PLS values over the course of the experimental period. Error bars represent the standard deviation from the mean pH across the experimental columns.*

oculation period, 9.21 × 10^{10} cells m^{-2} or approximately 7% coverage for PEL-LS and 1.08 × 10^{11} cells m^{-2} or 8.2% coverage for PEL-HS was achieved. Microbial growth was observed on the mineral surface and a total of 2.36 × 10^{11} cells m^{-2} (17.9% coverage) on PEL-LS and 2.85 × 10^{11} cells m^{-2} (21.6% overage) on PEL-HS were observed on day 20.

The observations of microbial growth on waste rock surfaces in terms of cell number was complemented by measurement of metabolic activity resulting from the oxidative processes, facilitated by the colonised cells (fig 4B). After 18 hours, the measured maximum heat output was 63 mW m^{-2} for PEL-LS and 123 mW m^{-2} for PEL-HS. At day 20 this increased to 157 mW m^{-2} for PEL-LS and 293 mW m^{-2} PEL-HS. This increase in metabolic activity corresponds with an increase in the active microbial populations associated with the waste rock surfaces.

Conclusions

This study thus far has demonstrated the feasibility of flow-through biokinetic system to provide a representation of microbial activity and leaching of liberated waste rock to provide an indication of acid generating potential. Solution chemistry analysis showed minimal changes regarding the performance of the system, owing to the high flowrate used which facilitated a stable oxidation environment. Through analysis of the mineral-microbe surface environment, progressive microbial growth on the mineral surface was shown through surface visualisation and mechanical cell detachment, together with increasing metabolic activity of surface associated microbial populations. This information is crucial in the understanding of microbial mineral interactions during characterisation of waste material for ARD and its ultimate mitigation. The results obtained provide a

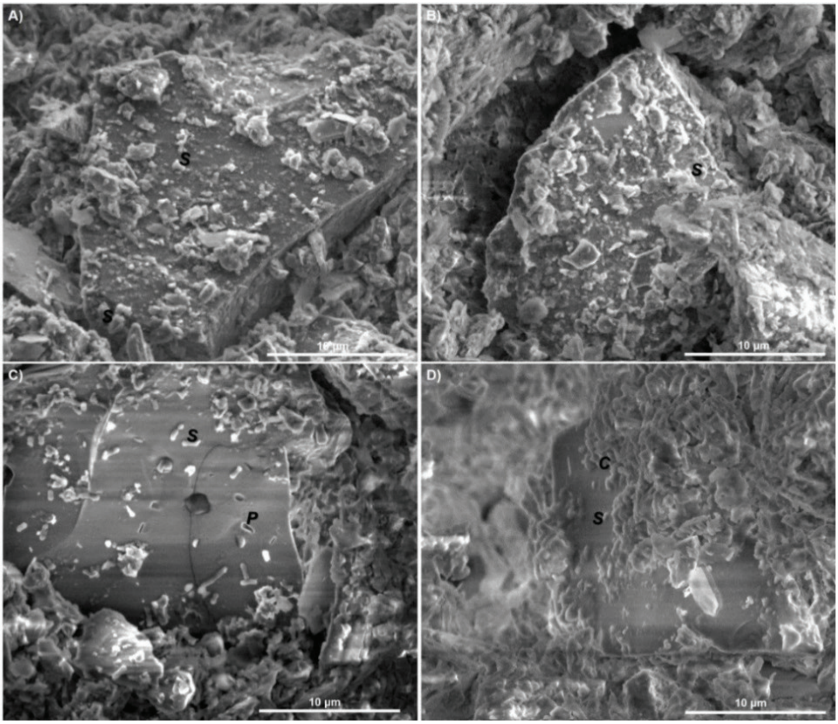

Figure 3 *SEM images of colonised pyrite bearing waste rock surfaces coated onto glass beads and leached over 20 days. Microbial mineral interactions on PEL-LS surfaces are shown in micrograph A (day 1, 18 hrs) and C (day 20) and interactions on PEL-HS surfaces are shown in micrograph B (day 1, 18 hrs) and D (day 20). Observed surface features including single cells (S), colonies (C) and pits (P), are labelled. A scale bar (10 µm) is shown on each image.*

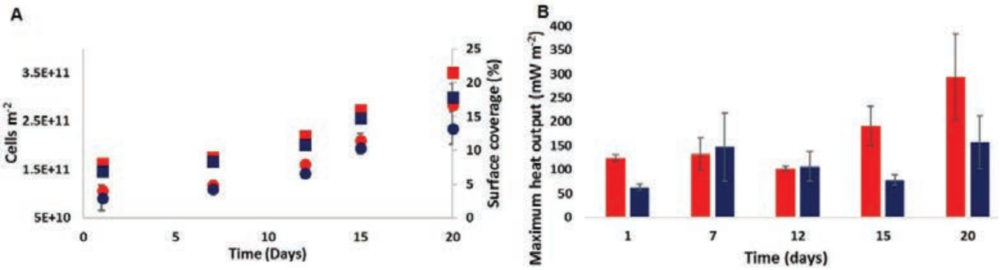

Figure 4 *A) Microorganisms firmly attached to the waste rock mineral surface of PEL-LS (●) and PEL-HS (●) at each time point, as well as the calculated percentage of surface microbial coverage for PEL-LS (○) and PEL-HS (○). The degree of surface coverage was determined from the number of cells firmly attached to the surfaces. Error bars represent the standard deviation from the mean of the mineral associated and firmly attached cells across the wash repeats. B) Maximum heat flow per unit surface area for PEL-LS (○) and PEL-HS (○) over 20 days measured using the IMC. Error bars represent the standard deviation from the duplicates of each material.*

platform on which to develop a standard protocol for the flow-through biokinetic test. This, together with acid-base accounting, mineralogy and data on dump hydrology, is proposed to provide improved insight into ARD characterisation and prediction.

Acknowledgements

The authors acknowledge DST, NRF of S.A for funding through the SARChI in Bioprocess Engineering (UID 64778) held by STLH. RJH is funded through a DST/NRF Research Career Advancement fellowship (UID 91465) and DXM is funded through CSIR DST-Interbursary. The technical support of Miranda Waldron of the EM Unit, UCT and Gaynor Yorath of CMR (QEMSCAN analysis) is greatly appreciated.

References

Africa, CJ, van Hille, RP, Harrison, STL (2013). Attachment of *A. ferrooxidans* and *L. ferriphilum* cultured under varying conditions to pyrite, chalcopyrite, low-grade ore and quartz in a packed column reactor. Appl. Microbiol. Biotechnol. 97 (3):1317–1324.

Broadhurst, JL, Bryan, CG, Becker, M, Franzidis J-P, Harrison STL (2013). Characterising the acid generating potential of mine water by means of laboratory-scale static and biokinetic tests. Proceedings IMWA 2013 (Wolkersdorfer, Brown and Figueroa (Eds)), Golden, Colorado, USA. pp 33 - 38.

Dobos, SK (2000) Potential problems with geologically uncontrolled sampling and the interpretation of chemical tests for waste characterisation and ARD prediction. In: Proc. 4th Australian ARD Workshop on Acid and Metalliferous Mine Drainage, Townsville. ACMER, Australia, p 25–29.

Dold, B, Wade, C, Fontbote, L (2009) Water management for acid mine drainage control at the polymetallic Zn-Pb-(Ag-Bi-Cu) deposit of Cerro de Pasco, Peru. J. Geochem. Explor., 100(2-3): 133-141.

Egiebor, N, Oni, B (2007) Acid rock drainage formation and treatment: a review. Chem Eng J, 2:47–62.

Hesketh, A, Broadhurst, JLB, Bryan, CG, van Hille RP, Harrison, STL (2010) Biokinetic test for the characterisation of AMD generation potential of sulfide mineral wastes, Hydrometall. 104: 459-464.

Kolmert, A, Johnson, DB (2001) Remediation of acidic waste waters using immobilised, acidophilic sulfate-reducing bacteria. J. Chem. Technol. Biotechnol. 76:836–843.

Komadel, P, Stucki, JW (1988) Quantitative assay of minerals for Fe^{2+} and Fe^{3+} using 1, 10-phenanthroline: III. A rapid photochemical method. Clay Minerals 36:379–381.

Makaula, DX, Huddy, RJ, Fagan-Endres, MA, Harrison, STL (2017) Using isothermal microcalorimetry to measure the metabolic activity of the mineral-associated microbial community in bioleaching, Minerals Engineering 106: 33 – 38.

Morin, KA, Hutt, NM (1998) Kinetic test and risk assessment for ARD. In: Proc. 5th Annual BC Metal Leaching and ARD Workshop, Vancouver, Canada.

Ngoma, IE, Ojumu, TV, Harrison, STL (2015) Investigating the effect of acid stress on selected mesophilic micro-organisms implicated in bioleaching. Miner. Eng. 75:6–13.

Parbhakar-Fox, A, Aalders, J, Lottermoser, B (2015) Effective field-based testing tools for rapid ARD prediction, 10th International Conference on Acid Rock Drainage & IMWA Annual Conference.

Parbhakar-Fox, A, Lottermoser, B, Bradshaw, DJ (2013) Cost-effective means for identifying acid rock drainage risks: integration of the geochemistry-mineralogy-texture approach and geometallurgical techniques, The Second AusIMM International Geometallurgy conference / Brisbane, QLD, 30 September - 2 October.

Tupikina, OV, Minnaar, SH, Rautenbach, GF, Dew, DW, Harrison, STL (2014) Effect of inoculum size on the rates of whole ore colonisation of mesophilic, moderate thermophilic and thermophilic acidophiles. Hydrometallurgy 149:244–251.

Coal Basins and the Environment

Nikolay Maksimovich[1], Sergey Pyankov[2], Vadim Khmurchik[1], Olga Berezina[2],
Artem Demenev[1], Alexey Sedinin[1]

[1]The Institute of Natural Science of Perm State University, Genkel st. 4, 614990 Perm, Russian Federation, khmurchik.vadim@mail.ru

[2]Perm State University, Bukirev st 15.,614990 Perm, Russian Federation

Abstract

One of the most serious ecological problems caused by coal mining is acidic mine water (AMW). Authors studied environmental condition on the territory of the Kizel coal basin (the Western Urals, Russia) using GIS-based environmental assessment, including catchment-based approach and methods of mathematical and cartographic modeling. Investigation revealed that the polluted territory in the basin was more large than previously reported. Applied GIS technologies will be used at engineering of remediation measures to determine optimal dimensions and location in situ of artificial geochemical barriers and develop environment monitoring system based on both remote sensing images and field observations.

Keywords: acid mine water, GIS-based technologies, land deforestation, river pollution, remediation strategy

Introduction

Mining is one of the most important sectors of the world economy. Coal-bearing formations occupy 15% in the earth's crust over all the continents. Total coal resources are estimated as 16–20 trln. tons, prospecting resources — 3,366 bln. tons; coal mining reaches 2,025 mln. tons annually. Coal industry has a significant and regionally negative impact on the environment. One of the most serious ecological problems caused by mining industry is the occurrence of acidic metal laden (e.g. Fe, Al, Mn, As, Cd, Zn, Cu, and Pb) mine water (AMW) from metal or coal mines. Coal mining also generate large amounts of wastes, which are deposited as waste piles or tailings. Conventional disposal methods that expose sulfidic mine wastes to atmosphere promote sulfide oxidation and the release of acidity, sulfate, and metals. Acidic effluents can migrate from storage areas to adjacent aquifers, surface water, and surrounding land, affecting the quality of water resources and soil and can inhibiting the growth of living organisms (Alekseenko et al. 2017; Blowes et al. 2014).

Abandoned, closed, or orphaned mine sites cover approximately 240,000 km^2 of the Earth's surface (Wolkersdorfer 2008). Closure and abandonment of mine sites usually results in a legacy of pollution of local environments that may persist for decades and even centuries after mining activity ceased (Younger 1997). Environmental pollution is a result of various sources and the costs for remediation, including environmental monitoring, can be substantial (Soni, Wolkersdorfer 2016). Over the past several decades, a number of researchers and reclamation practitioners have contributed to the development of AMW passive treatment designs and science. Robust, reliable and economically feasible technological solutions for treatment of AMW are available (Khayrulina et al. 2016; Skousen et al. 2017; Soni, Wolkersdorfer 2016; Tyulenev et al. 2015). Effective remediation of polluted sites requires extensive site characterization, including detailed spatial information about AMW sources, because AMW characteristics are site-specific and no single treatment would be effective and financially feasible for all AMW discharges (Pinto et al. 2016). It was found that the spatial distribution of the point and diffuse AMW sources was critical for spatially targeted, cost-effective remediation measures (Baresel et al. 2006). A critical activity in passive treatment is the selection of the proper system type for a given situation. Factors to be considered in selection include the quality and quantity of waters to be treated, water treatment goals, access, and the land resources available for use in system construction. Generally, larger land areas (relative to anticipated acid loads) enable more effective treatment, and essential design features for all systems include surface area and/or volume (Skousen et al. 2017).

GIS technology is considered as a powerful tool that supports environmental impact assessment and environmental management decision-making in coal mining districts as it allows to manipulate heterogeneous spatial data using a mathematical simulation and map-based modeling approach (Pyankov, Kalinin 2009). Synthetic geo-images integrating land survey and remote sensing data can be used to detect zones threatened by environmental crisis and disaster at regional and local scales, evaluate the result of reclamation strategies, and plan new in-situ and on-site treatment options in future.

The main objective of this study was to characterize AMW-impacted territory of The Kizel coal basin with GIS technology to better understand the current extent of the problem and develop remediation strategy.

Geological and Environmental Settings

The Kizel coal basin (the Western Urals, Russia) occupies area of 200 km^2 and is located within West Urals folding zone adjacent to the pre-Ural boundary deflection. Rocks of the basin are represented by sandstones, mudstones, siltstones, shales, limestones, dolomites, marls, coals, and others. Carbonate rocks are intensely karsted, especially in the upper part of geologic cross-section. Coal of the basin exhibits elevated content of sulfur (mainly as a pyrite) – 5.8%. Mines were closured in the 1990s, and 12 adits of abandoned mines have started to discharge acid mine water into 19 rivers. Several tones of sediments which consisted of amorphous iron and aluminum hydroxides and have a high content of Mn, Cu, Ni, Zn, Pb, and other metals have been accumulated in rivers' bottom. These sediments were washed downstream to the Kama river, where they become a secondary source of water pollution. Over 35 million cubic meters of waste rocks had been accumulated in more than 100 waste piles. Spontaneous combustion of waste piles, roasting and melting of their rocks, and fumarole processes within piles were detected. Rainfalls drained waste piles are enriched in soluble compounds and have a high salinity (up to 50 g L^{-1}). Infiltration of these waters into underlying grounds changes their physical-mechanical and filtration properties and pollutes groundwater (Khayrulina et al. 2016).

Methods

An integrated environmental assessment of each particular site in the Kizel coal basin was carried out using a set of spatial criteria, which include pH, total salinity of water or water extract, sulfate content, metal content, species composition of the surface-water bacterial community, and the area of degraded land. Seasonal sampling of AMW at about 200 sampling sites during more than 35 years of survey permitted collection of a large, multi-seasomal database of geochemical and hydrological values. SPOT-6 satellite images in the visible spectrum bands, as well as high resolution satellite images obtained from open source mapping services were used to determine the area of intensive soil pollution and land deforestation. LANDSAT-8 satellite images obtained during the summer low water level period were used to detect polluted and unpolluted river waters as they were differed in color — yellowboy coated plants and sediments in the polluted stream beds, so long stretches of 'dead' streams were easily visualized in images.

Results and Discussion

Integrating land survey database and remote sensing data allows to develope a cartographic and attribute GIS database of the Kizel coal basin consisted of the digital elevation models (DEMs) and catchment boundaries delineated from SRTM-90, and SRTM-X band's DEMs. Detailed DEMs were generated for waste rock piles and adjacent areas and used to determine waste piles' drainage water flow direction and delineate polluted land areas in the scale of 1:10,000. To compile the inventory of acid mine and drainage water flows over the entire coal basin area both the land survey database and satellite images were used. As a result, the determination of hydrographic characteristics on 1:100,000-scale digital topographic maps revealed more substantial rivers contamination with AMW than it was established earlier. One of the most polluted was the Poludennyi Kizel river, the tributary of the Yaiva river: the excess in metal Maximum Permissible Content (MPC) was 9,450 times for Fe, 1,188 times for Mn, 639 times for Al, and 56 times for Be (Fig. 1, sampling site no. 6).

As seen, surface water is contaminated along the rivers pathway: the Poludennyi Kizel, the Bol’shoi Kizel, the Severnaya Vil’va, the Yaiva rivers right up to the Kama reservoir. Investigation revealed that special attention should be paid to the Bol’shoi Kizel river basin as most polluters were located there. This river starts from the confluence of two rivers: the Poludennyi Kizel and Vostochnyi Kizel. Seven small rivers flow into the Bol’shoi Kizel and only one of them (the Severnyi Kizel) is not polluted by coal mining. This tributaries bring a lot of pollutants into the Bol’shoi Kizel: about 15,300 tons of sulfates, 6,000 tons of iron, 400 tons of aluminium and 57 tons of manganese come into the Bol’shoi Kizel annually. Moreover, the Bol’shoi Kizel is impacted by acid piles’ drainage water and mine water discharge. Piles’ drainage water has a high concentration of pollutants and is acid (pH<3). High concentration of iron, aluminium, beryllium and manganese comes into water as a result of rain water infiltration and leaching of pile’s rocks — the concentration of these elements 100-1,000 times exceeds MPC. Such metals as cadmium, cobalt, nickel were detected everywhere but in low quantity, lead and zinc were detected periodically and their quantity 2-70 times exceeds MPC. When the Bol’shoi Kizel flows into the Severnaya Vil’va river, the water of the latter changes the colour that is observed at the satellite image. Thus, the Yaiva river is greatly polluted by the sources located on its catchment area although they are tens of kilometers away from the river body and are restricted with watersheds.

LANDSAT images of rare flood events were used to detect and map potentially contaminated areas in river floodplains during flooding. Mathematical and map-based modeling of the river floodplains combined with the database on field survey was used to interpret remote sensing images. The results

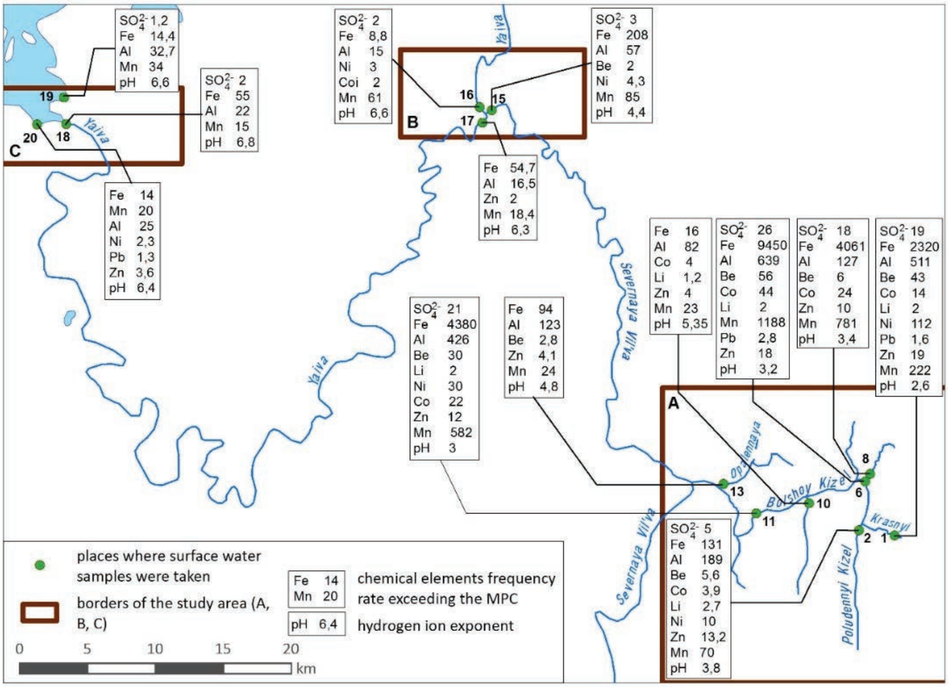

Figure 1 *Pollution of the Yaiva river basin with acid mine water.*

__Figure 2__ Deforestation of the Poludennyi Kizel river floodplain (left) and land area near the Kospashskaya shaft waste piles (right) as the result of acid water influence.

__Figure 3__ Satellite images of the Poludennyi Kizel river floodplain (left) and land area near the Kospashskaya shaft waste piles (right).

of the interpretation revealed that the polluted area in river floodplains was more large than previously reported. The total area of the river floodplains where near-stream vegetation could be affected by AMW during a peak flood event was estimated to be 9,642 ha.

High-resolution satellite images and field data were used to detect and map degradation in land areas affected AMW. Polluted land areas and river floodplains exhibited deforestation property (Fig. 2) and were easily observed in satellite images (Fig. 3).

Conclusions

GIS technologies applying to analyse environmental pollution at the territory of the Kizel coal basin had given more extensive its characterisation — more substantial pollution of lands and rivers with AMW than it was established earlier were revealed. Combination of field survey data and satellite images allowed to localize spotted sources of AMW, and delineate pollution boundaries and spatial distribution precisely.

AMW-impacted site remediation could be achieved either at the source of AMW or along the subsequent AMW pathway. Applied GIS technologies, combining data on the quality and quantity of waters to be treated, water treatment access, and the land resources available for use in passive treatment system construction, will be used at engineering of remediation measures in future.

The results of this investigation could be used to implement a complex remediation strategy in the Kizel coal basin, which will include both active and passive systems for AMW treatment. The construction of artificial geochemical barriers implies determination of their optimal dimensions and location in situ using GIS technologies. The development of an environment monitoring system based on both remote sensing images and field observations will be a constituent part of the strategy also.

Acknowledgements

This work was financially supported by the Ministry of Education and Science of the Russian Federation (Assignment No 5.6881.2017/8.9).

References

Alekseenko VA, Maximovich NG, Alekseenko AV (2017) Geochemical Barriers for Soil Protection in Mining Areas. In: Bech J, Bini C, Pashkevich MA (eds), Assessment, Restoration and Reclamation of Mining Influenced Soils, Elsevier Inc, p. 255–274. http://dx.doi.org/10.1016/B978-0-12-809588-1.00009-8

Baresel C, Destouni G, Gren IM (2006) The influence of metal source uncertainty on cost-effective allocation of mine water pollution abatement in catchments. J Environ Manage 78:138–148

Blowes DW, Ptacek CJ, Jambor JL, Weisener CG, Paktunc D, Gould WD, Johnson DB (2014) The Geochemistry of Acid Mine Drainage. In: Turekian HD, Holland KK (eds) Treatise on Geochemistry. 2nd edn. Elsevier, Oxford, p 131–190

Khayrulina E, Khmurchik V, Maksimovich N (2016) The Kizel coal basin (The Western Urals, Russia): Environmental problems and solutions. In: Drebenstedt C, Paul M (eds) Proc, IMWA 2016 Ann Conf. Freiberg/Germany (TU Bergakademie Freiberg), p. 766–771

Pinto PX, Al-Abed SR, Balz DA, Butler BA, Landy RB, Smith SJ (2016) Bench-scale and pilot-scale treatment technologies for the removal of total dissolved solids from coal mine water: A review. Mine Water Environ 35:94–112

Pyankov SV, Kalinin VG (2009) Methodological aspects of spatial analysis of the river runoff formation by using mathematical cartographical modeling. Russ Meteorol Hydro 34(1):58-61

Skousen J, Zipper CE,·Rose A, Ziemkiewicz PF,·Nairn R,·McDonald LM,·Kleinmann RL (2017) Review of Passive Systems for Acid Mine Drainage Treatment. Mine Water Environ 36:133–153

Soni AK, Wolkersdorfer C (2016) Mine water: policy perspective for improving water management in the mining environment with respect to developing economies. Int J Min Reclam Env 30(2)115–127

Tyulenev M., Zhironkin S., Litvin O (2015) The low-cost technology of quarry water purifying using the artificial filters of overburden rock. Pollut Res 34(4)825–830

Wolkersdorfer C (2008) Water Management at Abandoned Flooded Underground Mines – Fundamentals, Tracer Tests, Modelling, Water Treatment. Springer, Heidelberg

Younger PL (1997) The longevity of minewater pollution – a basis for decision-making. Sci Total Environ 194–195:457–466

Predicting natural attenuation for flooding of an ISL-uranium mine – potentials and limitations

Thomas Metschies, Wolfgang van Berk †, Ulf Jenk, Michael Paul

Wismut GmbH Jagdschänkenstraße 29 09117 Chemnitz Germany, t.metschies@wismut.de

Abstract

Flooding of a former ISL underground uranium mine situated in a sandstone aquifer inevitably results in mine waters entering the downstream aquifers influencing the groundwater quality. The mine water contains apart from elevated content of salts (e.g., sulfate, iron) also high concentrations of uranium exceeding the WHO guidance value for drinking waters by several orders of magnitude.

Especially uranium and other metals are of concern in terms of an impact on downstream groundwater quality. Even with high efforts to reduce the contaminant concentrations in the mine water by in-situ hydrochemical measures concentrations in the order of geogenic background conditions are to be achieved only in a time frame of decades. Complex technical efforts and consequently funding have to be assured. Effective and reasonable remediation solutions must consider groundwater-rock-gas interactions leading i) to a specific spatial and temporal development of pH/EH-conditions and ii) consequently to the immobilization and potential subsequent re-mobilization of contaminants (e.g., uranium) in the downstream aquifers. In combination with active remediation measures the contaminant retardation in the downstream aquifer could act as additional safety factor for a sustainable solution.

The paper outlines the approach followed to determine crucial processes of aqueous uranium mobility and related geohydraulic, geochemical, and hydrochemical parameters theoretically (by hydrogeochemical mass transport modeling) as well as in lab-scale experiments for a case study. Mineralogical and geochemical conditions within the affected aquifers were determined based on sampling from a number of boreholes. Using the findings of these studies a hydraulic and geochemical modelling concept was developed allowing predictions as scenario analysis. The concept for the hydrogeochemical model predictions is described with a number of limitations and constraints which mainly arise from limited data gathered on the field scale. The paper therefore especially focuses on the identification of representative parameter sets describing the potentially impacted part of the regional sandstone aquifer.

Keywords: mine flooding, geochemical modelling, parameterisation, contaminant retardation

Introduction

Uranium mining started at the Königstein mining site in 1964. The ore was first mined conventionally while in 1984 the winning technology was fully changed to an underground in-situ-leaching (ISL). The mined uranium ore is partly found in a 300 m deep sandstone aquifer with a considerable hydraulic conductivity. Ore in adjacent less permeable rocks was prepared for leaching by increasing the permeability by mining out compensation volumes followed by blasting of the ore containing rock. This generated additional flow paths for the drainage of the lixiviant. Sulfuric acid was used to leach the uranium from the sandstone and the ambient loosened host rocks. As a result the rocks in the underground mine contain pore water with high salt and metal concentrations and a low pH (tab. 1).

Presently the mine is flooded to a water level hydraulically not affecting the adjacent aquifers. A control drift surrounds the deepest downstream part of the mine. This control drift is separated by a safety pillar of sandstone rock from the flooded open mine workings.

Table 1 *Pore water concentration in leached sandstones of the Königstein mine.*

pH	EC [mV]	SO_4^{-2} [g/L]	Fe [g/L]	Zn [mg/Ll]	U [mg/L]	Al [mg/L]
2.0	700	10	3	200	200	300

Pumping water from the control drift creates a hydraulic depression and thereby assures that the mine water decant is fully collected, pumped out and treated in a water treatment plant. As a consequence the flooded mine is continuously washed resulting in decreasing contaminant concentrations and an increase of pH.

The remediation concept for the mine considers flooding to a natural level. The mine is mainly situated in a permeable sandstone aquifer which is the deepest in an interlayered system of sandstone aquifers and aquitards. Flooding the mine results in groundwater flowing through the mine workings and the leached sandstone block with finally entering the downstream surrounding aquifers. Especially the upper sandstone aquifer is a potential drinking water resource and needs to be protected against adverse effects from the mine flooding. Continuing flooding will lead to an outflow of mine water into this aquifer.

General modelling approach

The general modelling concept for the Königstein site consists of a number of separate modelling tools. A regional groundwater flow model was implemented based on the program code SPRING. It is used to describe the regional groundwater flow conditions in terms of potentiometric surfaces and water flow in the various model domains. Calibration and validation of the model was done using the extensive data set of groundwater monitoring results and mine water pumping. Modelling the different hydraulic states such as mine development, active mining and remediation the model uncertainty in predicting the regional hydraulic conditions was considerably reduced. Using this model the regional hydraulic conditions are described for various remediation options providing the boundary conditions for further modelling tools (Metschies et.al 2013). These additional tools comprise of reactive hydrogeochemical mass transport models describing the chemical conditions in different compartments such as the flooded mine or in the sandstone aquifers downstream of the mine.

The scope of the geochemical modelling is to evaluate the potential impact of mine water entering the aquifer. Even active remediation measures will not lead to contaminant concentrations at the natural background level for a fairly long time. Technical measures will be required as long as either a significantly elevated contaminant level in the surrounding aquifers compared to the natural conditions is accepted or potential retardation effects within a limited aquifer zone are taken into account. In any case model predictions of the dispersion of a contaminant plume resulting from the mine flooding are necessary.

Geochemical modelling approach and parameterisation

Without pumping out mine water balancing the natural water inflow to the mine contaminated water would enter the downstream aquifer which itself contains the remaining not mined ore body. This ore body forms a potential source for a groundwater contamination under specific milieu conditions. Apart from this flow path mine water could also enter the upper sandstone aquifer depending on the hydraulic conditions. In this case contaminants could spread in this at present hydrochemically unaffected aquifer. These two downstream paths are considered individually because the general flow direction in the two aquifers differs and there is no interaction of the potential plumes along these flow paths expected. Each of these two paths could be described in separate geochemical models.

The followed general approach in predicting the geochemical conditions focuses on identification of relevant geochemical processes influencing the fate of potential contaminants downstream of the mine. Due to the fact that the available baseline information concerning the geochemical and mineralogical conditions is limited the predictions are made as scenario analysis with a variation of several parameters based on their identified individual parameter ranges. The geochemical models are implemented using the transport option of the reactive modelling code PHREEQC (Parkhurst et. al. 1999). The thermodynamic model approach is used including the options of surface complexiation and ion-exchange. Such calculations are constraint by the principle laws of mass and charge conservation.

The identification of relevant processes is supported by laboratory experiments conducted in the conception phase. A step wise approach was followed with experiments on various scales including batch and column tests. The batch experiments represented single and combined reactions of the fluid solid mixtures containing elements and minerals relevant for the natural system to be modelled under the milieu conditions in the mine and the downstream aquifers. These batch experiments were reproduced and retraced by respective PHREEQC models to validate the general modelling concept.

For the parameterisation of the model mineralogical and geochemical analysis of rock samples from the relevant sandstone strata are available. Due to the depth of the modelled aquifers only a limited number of exploration drillings with relevant geochemical information are existent. Back in the 1960ies a vast number of drillings were made to explore the uranium ore body. Analysis of samples however were mainly focussed on the metal content with none or just limited data characterising the general mineralogical and geochemical conditions. In addition with the limited mineral content in the sandstones most relevant analysis data is below the detection limit at that time.

The respective sandstone aquifers have a thickness of several 10 metres. Due to the changing sedimentation conditions the characteristics of the rocks is variable over the depth. With saturated aquifer thickness of up to 50 m it is difficult to determine the zones of preferential groundwater flow. The variation of the vertical and lateral hydrogeological conditions, such as porosity and permeability, gives a high variety of the hydraulic and geochemical characteristics, as well. While average groundwater flow conditions could be well estimated using the calibrated and validated regional flow model the geochemical parameterisation is far more complex.

The mineralogical composition of the sandstone is dominated by the geochemically stable quartz but calcite, pyrite and goethite are to be considered as primary mineral phases even with their low concentrations influencing the geochemical conditions in the downstream of the mine outside of the ore body. Within the ore body uraninite, coffinite, sphalerite, orpiment and otavite are additional relevant mineral phases.

The mineral phase assemblage is defined based on the limited information from several new boreholes in the downstream area where more detailed analysis were made to gather a data set representative for the reactive transport modelling (tab. 2). The geochemical and mineralogical data show mostly local characteristics resulting in a high variability of the physical and geochemical properties. The values range several order of magnitude in vertical and lateral direction over short distances including the hydraulic conductivities, grain size distribution and mineral contents.

Apart from a plausible definition of the mineral content it has to be considered which share of the total content is reactive in terms of potential mass conversion in the natural system. This depends on preferential flow conditions as well as coating of surfaces or agglomeration inhibiting the access of potential reactants to the reactive minerals. It is practically impossible to derive values characterising the conditions in the regional flow system simply from the analysis of a limited number of rock samples. As an alternative approach just scenario calculations with varying shares of the mineral content considered as reac-

Table 2 *Range of measured geochemical content of sandstone relevant for geochemical transport modelling.*

Range	Carbonate-carbon [mass %]	Disulfid-S (pyrite) [mass %]	Non-sulfidic iron [mass %]	Potential cation exchange capacity [meq/100g]
min	<0.005	0.02	0.028	<0.02
max	0.02	2.6	0.65	3.4
mean (model)	0.01	0.4	0.19	1.5

tive are feasible. Thereby the reactive mineral content is changed over orders of magnitude in relation to an assumed mean concentration (tab. 2).

The uncertainty of the geochemical model parameterisation could not be simply reduced by additional sampling and analysis of sandstone material because under the given hydrogeological and sedimentological conditions a statistically safe parameter distribution could not be derived. Therefore, looking at the wide range of uncertainties in geochemical model parameterisation a full-scale 3D-reactive modelling seeming to give a biunique prediction is considered inadequate. In case of the Königstein mine it is instead preferred to make calculation under less complex geometrical assumptions to be able to investigate relevant effects and derive conclusion concerning the effect of specific geochemical parameter combinations. Here the 1D transport option of PHREEQC offers a volume based approach with a specified ratio of reacting pore water and solid. Implementing a simple transport model for a 1D-flow path allows a robust and reproducible scenario analysis for the wide range of parameter combinations. By negligence of effects on the groundwater flow due to spatial effects the focus can be put on the relevant processes. Otherwise PHREEQC allows to include diffusion und dispersion effects which can be characterised based on the results of the regional hydraulic modelling and are included accordingly in the geochemical transport model. This holds also for water balance considerations and groundwater flow velocities, as well.

Using this more generic modelling approach the geochemical conditions along the downstream flow path are predicted in close combination with the assumptions made concerning the availability of reactive minerals. Systematic calculation of various scenarios give valuable generalised information concerning the extent of a potential plume in the aquifer and the expected effect of retardation of mainly uranium along the flow path under the considered boundary conditions. It could be shown that the hydrochemical impact of mine flooding in terms of pH, uranium and other metal concentration is limited to a flow distance of a few 100 m downstream of the mine in the upper aquifer even under conservative parameter assumptions. As consequence, in case of the outflow of mine water during the final flooding a limited extend of the aquifer needs to be sacrificed for the retardation of the contaminants. In this part of the aquifer the use of the groundwater has to be restricted. However, with regard to the prohibition of deterioration defined by the EU water framework directive such a concept is difficult to be followed by the authorities in general under the given uncertainties.

Given the data base and the uncertainties of the various model parameters which could not be significantly further decreased by additional analysis or lab experiments a further improvement of the prediction accuracy is impossible unless first real data from the field scale is available. Field scale data would implicitly provide indications helping to better estimate the amounts of reactive minerals present along the groundwater flow path. It thereby leads to integral effective parameters which are more representative for the hydrogeological and chemical setting downstream of the mine than small drill core-derived data from local analysis.

It was agreed with the permitting authorities to make a test flooding of the mine by temporarily increasing the mine water level by another 10 m followed by an immediate lowering to the base level. As consequence, a limited volume of mine water enters the upper aquifer. By intensive monitoring of a number of groundwater observation boreholes along the expected flow path the propagation of the limited plume should be monitored. In a first step the conceptual model should be validated whereupon the low pH of the mine water is buffered and uranium is retarded in the aquifer. It is expected to detect only an increase of the salt content in the observation boreholes as signal for the breakthrough of the mine water.

Results

As figure 1 shows the limited outflow of mine water during the hydraulic test is expected to temporarily slightly decrease the pH-value in the groundwater close to the inflow. Depending on the acidity introduced and the available neutralisation potential the changes in the milieu conditions will be significant enough to be measured. However, an increase of the salt content as e.g. chloride should more clearly show the impact of the mine water. On the other hand uranium is expected to be retarded in any case. Even when the load of mine water entering the aquifer is doubled no measurable changes in concentration are expected. Based on such kind of predictions the mining and water authorities issued a permit for such a hydraulic test.

Presently the hydraulic test is ongoing accompanied by an intensified monitoring of the mine and groundwater composition in the mine and the downstream area. It is expected that first monitoring results showing the impact of the test on the surrounding aquifer will be available in 2019.

Conclusions

Predicting the impact of mine flooding on an adjacent aquifer is clearly constraint by baseline information concerning the geochemical and mineralogical composition. The mineralogical composition strongly affects the efficiency of retardation of certain contaminants. Due to the physical and chemical heterogeneity of the aquifer a representative parameterisation based on chemical and mineralogical analysis of selected drill-core based samples seems to be difficult to achieve. As a work-around scenario analysis allows to derive conclusions concerning general behaviour of the system allowing to make predictions considering the parameter uncertainties. Experiments on a laboratory scale allow to set up a

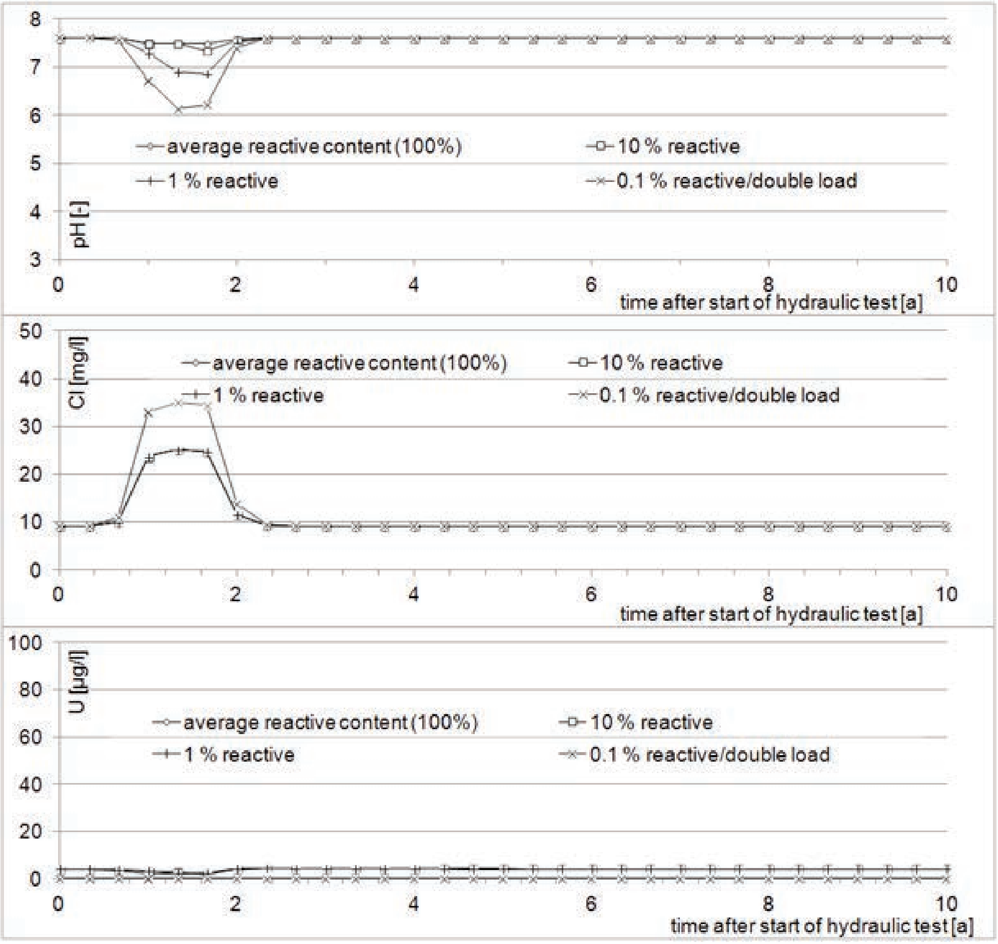

Figure 1 Predicted concentration curve in an observation borehole about 50 m downstream of inflow of mine water into the sandstone aquifer for selected scenarios varying the reactive mineral content and the load introduced during the hydraulic test.

conceptual model of the relevant geochemical processes and to validate the respective concept. For a reproducible prediction of the conditions downstream of a mine integral information on the field scale is essential to be able to up-scale the conceptual model and to derive a representative integral data set describing the reactive share of the available mineral content relevant for the retardation and other geochemical processes. This is a precondition to comprehensibly predict the effect of the natural attenuation of contaminants and thereby to include this effect in a sustainable remediation concept.

Outlook

Validating the conceptual geochemical model using the results of the hydraulic test in the Königstein mine will be fundamental to further decrease the uncertainty for predictions of the effect of mine water entering the surrounding aquifers. Using this confirmed and further improved understanding of the main geochemical processes and their interactions with groundwater flow an extension of the model from the column along the flow path to a model with a higher spatial resolution is the next step to improve the predictions for arbitrary points in the downstream flow path by better describing the influence of lateral dilution.

With regard to the final flooding of the Königstein mine a stepwise flooding with continuous monitoring will be necessary. This allows to further adapt the geochemical transport model to the effective conditions in the aquifer downstream of the mine. Only such an approach ensures to reduce the prediction uncertainties of the extent of a retardation of contaminants entering the aquifer with the mine water sufficiently.

Acknowledgements

The authors would like to acknowledge the work of our colleagues Martin Becker of delta-h Ingenieurgesellschaft mbH, Witten and Dr. Harald Kalka of UIT GmbH, Dresden in providing the necessary model basis to define the hydraulic and geochemical boundary conditions for the described transport model calculation.

References

Metschies T, Becker M, König C, Jenk U (2010) Modelling of the hydraulic behaviour of deep mines in regional aquifer systems. Proceedings of the International Mine Water Association Symposium 2010, Sydney/Canada. CBU Press. Cape Breton, p 495 - 498

Parkhurst DL, Appelo CAJ (1999) User's Guide to PHREEQC (Version 2)—A Computer Program for Speciation, Batch-Reaction, One-Dimensional Transport, and Inverse Geochemical Calculations. U.S. Geological Survey, Water Resources Investigations Report 99-4259, Washington DC.

Characterising the environmental risks of coal preparation wastes: A study of fine coal slurry waste and discards from South African collieries

Annah Moyo[1], Juarez Amaral Filho[2], Susan Harrison[1,2], Jennifer Broadhurst[1]

[1]Minerals to Metals, Department of Chemical Engineering, University of Cape Town, P/B X3, Cape Town, 7701, South Africa, jennifer.broadhurst@uct ac.za
[2]Center for Bioprocess Engineering Research, Department of Chemical Engineering, University of Cape Town, P/B X3, Cape Town, 7701, South Africa.

Abstract

In order to be effectively managed, the risks associated with wastes arising from the primary production of coal and other mineral resources first need to be well understood. This paper demonstrates the application of a combination of laboratory-scale tests and analytical methods to characterise the potential environmental risks associated with typical coal production wastes from South African collieries. The results indicate that the compositions and properties of these wastes are highly variable. The need to consider the time-related nature of the acid generating behaviour and the potential availability of metals and salts has also been highlighted.

Keywords: coal processing waste, environmental risks, acid rock drainage, metal contamination and salinization risks

Introduction

South Africa still relies heavily on its coal reserves for power generation, with around 70% of the country's primary energy consumption being based on coal. The preparation (also known as the cleaning or processing) of run-of-mine (ROM) coal, generates two different types of coal processing wastes: discards and ultra-fine slurry waste. These wastes are traditionally disposed of to landfill and pose a significant threat to the surrounding environment and local communities (Bosman and Kid 2009). Of particular concern is the long-term generation of acid rock drainage on exposure of the sulfide mineral, pyrite, to air and water in the presence of naturally-occurring microbial organisms (Oelofse 2008). The pollution risks associated with coal processing dumps are aggravated by the fact that coal wastes and associated environmental risks remain poorly characterised, making it difficult to identify and justify meaningful impact mitigation approaches. In particular, little attention has been given to the potential risks associated with metals and salts, or the role of microbial activity in the acid generating behaviour. To overcome these shortcomings, a generic protocol comprising a suite of laboratory-scale tests and analytical methods laboratory is proposed for characterising the risks typically associated with sulfidic mine wastes (Kotelo 2012; Opitz et al. 2015). This paper presents the key results derived from the application of such a protocol for characterising the environmentally significant properties of typical coal production wastes from South African collieries.

Methods

Application of the integrated characterisation protocol outlined in Figure 1 was demonstrated for the case of two fine coal slurry wastes and one coal discard, collected as fresh grab samples at collieries in the Witbank and Waterberg coalfields of South Africa. Environmentally significant properties investigated include: sulfur and its forms, total and available elements (including metals and semi-metals or metalloids), mineralogical composition, and the potential for acid rock drainage generation. Ash analysis was carried out using the SANS 131:2011 method, and analysis of inorganic elements was conducted by the University of Stellenbosch Central Analytical Facilities, using Wavelength-Dispersive X-Ray Fluorescence (WDXRF) and

Laser Ablation-Inductively Coupled Plasma-Mass Spectrometry (LA-ICP-MS). Total sulfur analysis was conducted by means of the standard Leco combustion method at the external ALS laboratories, and sulfur speciation conducted in-house, using the protocol developed by the Australian Coal Association Research Programme (ACARP) C15034 (Miller 2008). Semi-quantitative mineralogical analysis was also conducted using the relatively new QEMSCAN instrument acquired by the Centre for Minerals Research at UCT, in order to support interpretation of the chemical analytical data. Characterisation of the acid rock drainage potential was carried out using acid base accounting (ABA) and net acid generation (NAG) static chemical tests, as well as the standard batch biokinetic test developed at the University of Cape Town. Sequential chemical extraction (SCE) tests were carried out to assess the partitioning and potential availability of inorganic elements for release to the environment under different weathering conditions (Broadhurst et al. 2009; Opitz et al. 2015). On this basis, elements were ranked and scored according to their potential environmental risks (eq.1), using the protocol developed by Broadhurst and Petrie (2010).

$$RPFi = \frac{(ACi)^2}{ARCi \times BCi} \qquad \text{[eq.1]}$$

Where: AC_i is available concentration (mg/kg); ARCi environmentally accepted concentration (mg/kg), represented by drinking water standards as a proxy; and BC_i the natural background concentration (mg/kg), represented by average crustal abundance as a proxy.

Results and Discussion

Chemical composition of mineral matter

The relatively high ash content for the Witbank discard sample (tab.1) is consistent with the higher content of ash-forming minerals, such as quartz (SiO_2) and kaolinite ($Al_4Si_4O_{10}(OH)_2.H_2O$), identified by means of mineralogical analysis as being the major contributors to mineral matter in all three samples. The higher SiO_2:Al_2O_3 ratios in the Waterberg slurry relative to the Witbank slurry (tab. 1) is also consistent with the higher quartz: kaolinite ratio. The Waterberg coal slurry also has a higher content of CaO and MgO than the Witbank waste samples (tab. 1), which can probably be attributed to the higher content of acid neutralising calcite ($CaCO_3$) and amphibole ($Ca_2Mg_5Si_8O_{22}(OH)_2$) minerals, as identified by mineralogical analysis.

A comparison of sulfur speciation results indicates that the Witbank slurry has a lower content of sulfur and sulfur forms (sulfide sulfur, total soluble sulfate and organic sulfur) than the Waterberg slurry and Witbank discard wastes (tab. 1). Sulfide sulfur accounts for more than 50% of the sulfur in all the coal wastes samples, and, in accordance with mineralogical analysis, is mainly in the form of pyrite. Sulfate sulfur accounts for 17-20% of the total sulfur in the slurry wastes, but only 12% of total sulfur in the Witbank

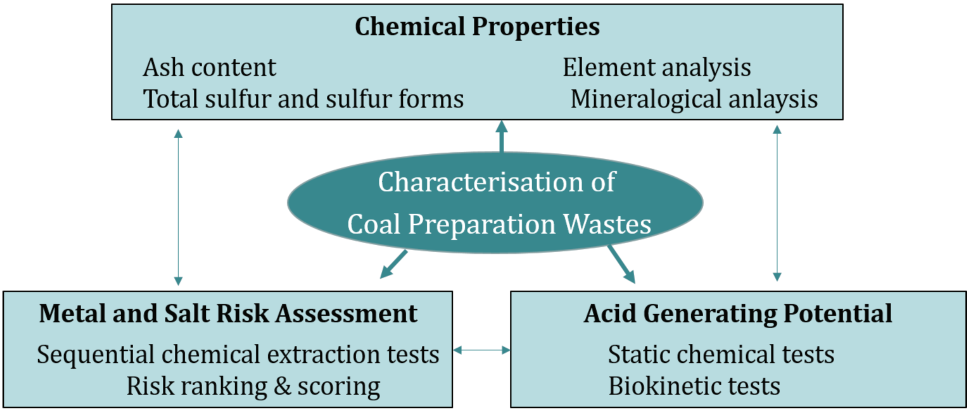

Figure 1 *Integrated characterisation protocol applied to the coal production wastes*

coal discards. Furthermore, whilst the soluble sulfate sulfur in the ultrafine slurry wastes is mainly in the form of non-acid generating minerals (e.g. gypsum, $CaSO_4.2H_2O$, and epsomite, $MgSO_4.7H_2O$), the majority of the sulfate sulfur in the Witbank discards is in the form of acid-generating sulfates (e.g. melanterite, $FeSO_4.7H_2O$). The contribution of the remaining sulfur, comprised mainly of organic sulfur, varies between 21% and 36%, with the proportion of organic sulfur being lower in the Waterberg slurry coal waste.

The concentration ranges of trace elements (< 100 ppm) were found to be similar across all the coal wastes, and also to those reported for the coal standard SARM 19. A comparison of trace element concentrations with average crustal abundance values indicated, however, that a number of trace elements are significantly enriched in the coal wastes relative to their average concentrations in the earth's crust. This pertains particularly to Bi and Se, the concentrations of which are more than 10 times higher than the average crustal abundance values. Other elements which are enriched by a factor of between 1 and 10 include Mo, In (discards only), Pb, Sn, As, Sb, Ge, Cs, Ce, U and Th.

Acid generating characteristics

MPA values obtained on the basis of acid-forming sulfur are significantly lower than those obtained on the basis of total sulfur, decreasing in the order Witbank discards ≥ Waterberg slurry >> Witbank slurry (tab. 2). On the other hand, the acid neutralising capacity (ANC) is significantly higher for the Waterberg coal slurry waste than for the Witbank coal wastes. This is consistent with the higher content of reactive neutralising minerals, calcite and amphibole, in the Waterberg slurry. Despite the relatively high sulfide sulfur content, the high ANC of the Waterberg slurry sample resulted in a negative net acid producing potential (NAPP), consistent with the circum-neutral final NAG pH. In contrast, the relatively low ANC of the Witbank discards resulted in positive NAPP values, consistent with the acidic NAG pH values. Although the Witbank slurry and discards wastes have similar ANC values, the lower MPA values for the slurry waste resulted in lower NAPP values, and a weakly acidic final NAG pH. Extended boiling of the NAG solution in the case of the Witbank slurry waste resulted in a decline in the final pH to 5.24, indicating that formation of soluble organic acids may be contributing to the acidity of the NAG solutions in the case of the standard single test (Stewart et al. 2009).

In accordance with universal classification criteria, the Waterberg sample is non-acid forming, regardless of whether the total or acid-forming sulfur contents are used to calculate NAPP (fig. 2). Similarly, the Witbank discards sample remains potentially

***Table 1** Major mineral components and sulfur forms in the coal processing wastes*

Characteristic	Composition (mass %)		
	Waterberg slurry	Witbank slurry	Witbank discard
Minerals matter			
Ash	49.20	40.90	63.00
SiO_2	28.49	22.58	47.21
Al_2O_3	3.83	13.16	15.39
Fe_2O_3	5.22	2.33	2.50
CaO	3.83	0.83	0.06
MgO	1.08	0.20	0.06
Sulfur speciation			
Sulfide sulfur	1.13	0.55	1.02
Acid soluble sulfur	0.00	0.01	0.23
Non-acid soluble sulfur	0.32	0.19	0.00
Organic sulfur	0.39	0.32	0.69
Total sulfur	1.84	1.06	1.94

Table 2 *Static acid rock drainage test results*

Sample	MPA (kg/t H_2SO_4)		ANC (kg/t H2SO4)	NAPP (kg/t H_2SO_4)		NAG pH	
	S(T)	S(AF)		S(T)	S(AF)	Single stage	Extended boil
Waterberg slurry	54.16	34.58	102.29	-48.12	-67.71	5.19	-
Witbank slurry	32.44	17.14	29.22	3.22	-12.39	3.97	5.24
Witbank discards	53.86	38.25	29.10	24.76	9.15	2.56	2.54

MPA = maximum potential acidity; ANC=acid neutralising capacity; NAPP = net acid producing potential; NAG=net acid generating; S(T)=Leco total sulfur; S(AF)=ACARP acid forming sulfur

acid-forming, even when only acid-forming sulfur is considered. In contrast, the classification of the Witbank slurry sample varies considerably, depending on whether the presence of non-acid forming sulfur compounds and formation of organic acids is taken into account.

The time-related pH profiles obtained in the biokinetic tests for the Waterberg slurry sample (fig. 3) confirm that this sample is net acid neutralising under the non-pH controlled biokinetic conditions, with the pH remaining above neutral for the duration of the test period. This is consistent with the NAF classfication in accordance with the static chemical tests.

The relatively low redox potentials (< 350 mV vs SHE) observed through the duration of this test are consistent with the absence of microbial catalytic activity. However, un-

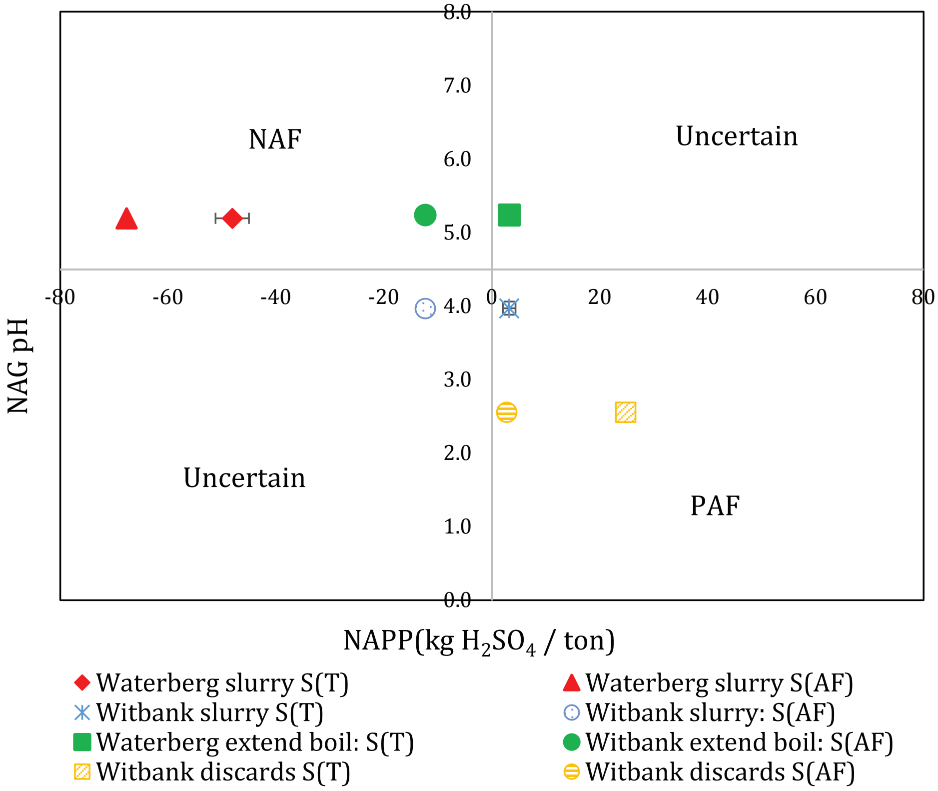

Figure 2 *Classification of acid generating potential of static test results (NAF=non-acid forming; PAF = potentially acid forming).*

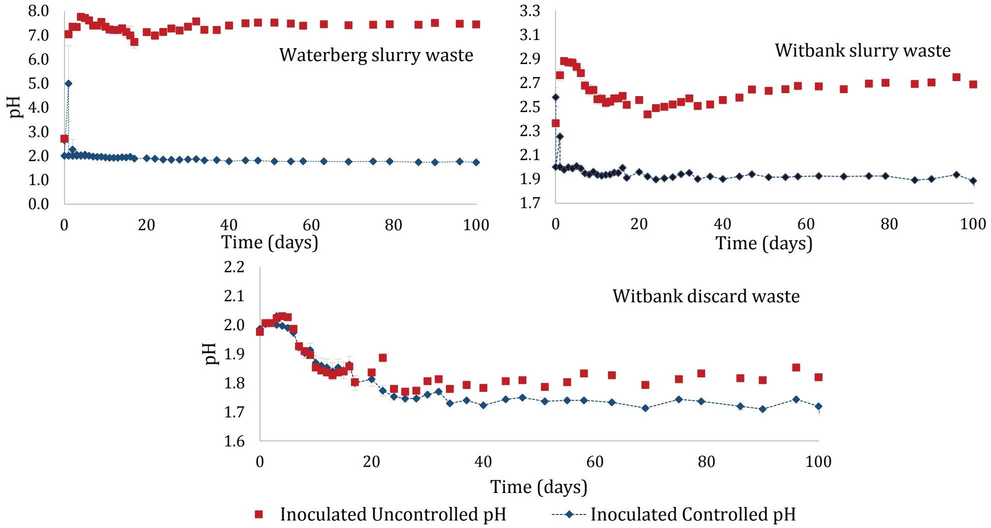

***Figure 3** Time-related pH profiles for the pH controlled and uncontrolled batch biokinetic tests.*

der conditions where the pH was controlled at a pH of 2.0, the acid neutralising capacity of the sample became depleted within 4 days, followed by an increase in the redox potential to 700 mV, indicative of microbial catalytic activity. This indicates that the sample could become net acid generating if exposed to acidic conditions. Consistent with the static tests, the time-related pH profiles for the biokinetic tests are indicative of the relatively low acid neutralising capacity of the Witbank coal wastes, with the pH increasing only slightly in the initial stages of the biokinetic tests (fig. 3). This neutralising capacity is, furthermore, rapidly depleted, with the sample becoming net acid generating over the 4-22 day period. A rapid increase in the redox potential to >700mV over this period is, furthemore, consistent with microbially assisted pyrite oxidation. In the case of the Witbank slurry, this was followed by a prolonged period (22-100 days) in which the pH gradually increased and the sample exhibited acid neutralising behaviour. These test results confirm that the acid generating behaviour of the Witbank slurry waste is likely to vary with time and be highly dependant on test conditions. In the case of the Witbank discards, there is very little evidence of long-term acid neutralising behaviour, with the pH remaining very acidic (<2) for the duration of the test period. This can be attributed to the higher content of acid-forming sulfur and is consistent with the potentially acid-forming (PAF) classification of the sample on the basis of static test results.

Potential metal contamination and salinization water-related risks

Ranking and scoring of the potential environmental significance of elements on the basis of sequential chemical extraction tests (tab. 3), indicates that no elements in the Witbank slurry waste are likely to pose a high risk under any leach conditions.

Iron poses a potentially high risk in the case of the Waterberg slurry and Witbank discard, and a moderate risk in the case of the Witbank slurry waste under oxidising conditions, as well as a moderate risk in all wastes under non-oxidising acid leach conditions. Other elements posing a moderate environmental risk include Mn (Waterberg slurry waste; all leach conditions), Pb (both non-oxidising and oxidising leach conditions for all coal waste samples), S (oxidising leach conditions for all coal waste samples), Sb (oxidising leach conditions for all coal waste samples); Al (Both coal slurry wastes; oxidising leach conditions) and Hg (Witbank coal slurry waste; oxidising leach conditions). Risks from Fe and Al relate largely to physical and aesthetic effects, whilst Mn, Pb, Sb and Hg are all potentially toxic to mammals and eco-systems. Salinization of water sources is mainly as a result of elevated concentrations of soluble sulphates.

***Table 3** Identification of significant elements on the basis of potential environmental risk under neutral, acid and oxidising leach conditions*

	Environmental risk potential (ERP)[1]		
	Low	**Moderate**	**High**
		Neutral leach conditions[2]	
Waterberg slurry	S, Ca, Sb, Pb	Mn	-
Witbank slurry	S, Sb	-	-
Witbank discards	S, Sb	-	-
		Acid leach conditions[3]	
Waterberg slurry	S, Sb, Ca, As, Ba, Se, Al	Mn, Fe, Pb	-
Witbank slurry	Mn, S, Sb, As, Al	Fe, Pb	-
Witbank discards	S, Sb, Al, Mo, Cr	Fe, Pb	-
		Oxidising leach condition[s4]	
Waterberg slurry	Se, Hg, Al, Ba, Ca, Ni, Mo, B, U, V, Cd	Mn, Pb, S, Sb, Al	Fe
Witbank slurry	As, Se, Ba, Mn, Ni, U	Fe, Pb, S, Sb, Al, Hg	-
Witbank discards	Hg, AS, Mo, Al, Se, Cr, Ni	S, Pb, Sb	Fe

1. Low= ERP/1000 of 0.1-1; Moderate= ERP/1000 of 1-10; High= ERP/1000 of 10-100
2. Accumulative concentration of elements in the water soluble and exchangeable fractions (1 and 2)
3. Accumulative concentration of elements in the water soluble, exchangeable, carbonate and oxide fractions (1-5)
4. Accumulative concentration of elements in all fractions except the residual fraction (i.e. 1-6)

Conclusions

The results of this study show that application of a combination of laboratory-scale tests and analytical methods is required in order to develop a comprehensive understanding of the key properties of coal preparation wastes on a case-by-case basis. In particular, biokinetic tests provide a rapid method for assessing the time-related behaviour of coal wastes under conditions of microbial activity, and can be used to compliment chemical static tests. Sequential chemical extraction tests can, furthermore, be combined with a relatively simple ranking and scoring method to identify elements of potential environmental significance under various weathering conditions. Elements identified as being of potential environmental significance under acid generating conditions for the wastes investigated include iron, sulfur, lead, antimony, and in certain cases arsenic, manganese and mercury. A more rigorous and quantitative analysis of mineralogical composition could provide further information on the components controlling the acid forming and neutralising reactions, thus further validating the outcomes of the static and biokinetic test results. It is also postulated that a flow-through biokinetic test would provide a more rigorous understanding of the acid generating behaviour under the type of conditions occurring in a disposal scenario.

Acknowledgements

The authors acknowledge the financial support of the South African Water Research Commission. The assistance of Megan Becker, Gaynor Yorath and Shireen Govender with the mineralogical analysis and sample preparation is also gratefully acknowledged.

References

Bosman C, Kidd M (2009) Water Pollution, Chapter 17 of Fuggle and Rabie's Environmental Management in South Africa. 2nd Edition. Juta Law Publishers

Broadhurst JL, Petrie J (2010) Ranking and scoring potential environmental risks from solid mineral wastes. Minerals Engineering 23:182–191

Kotelo LO (2012) Characterizing the Acid Mine Drainage Potential of Fine Coal Wastes. MSc. in Chemical Engineering Dissertation, Department of Chemical Engineering, University of Cape Town

Broadhurst JL, Malukele WJ and Von Blottnitz H (2009) Comparison and application of sequential chemical extraction techniques for metal speciation in sulfidic copper tailings. 8th International Conference on Acid Rock Drainage (ICARD 2009), Skellefteå, Sweden, June, 2009

Miller S (2008) ACARP Project C15034: Development of ARD Assessment for Coal Process Wastes, Environmental Geochemistry International Pty Ltd. Balmain NSW, Australia

Oelofse S (2008) Emerging Issues Paper : Mine Water Pollution, Environment & tourism. doi: ISBN NO: 978-0-9814178-5-1

Opitz AKB, Broadhurst JL, Harrison STL Harrison (2015) Assessing environmental risks associated with ultrafine coal wastes using laboratory-scale tests. Advanced Materials Research 1130: 635-639

Stewart W, Miller S, Kawashima N, Li J, Smart R (2009) Development of Prediction Methods for ARD Assessment of Coal Process Wastes. 8th International Conference on Acid Rock Drainage, pp. 1–14.

Understanding Mineralogy as a tool for Acid Rock Drainage (ARD) Characterisation

Alexander Opitz[1], Jennifer Broadhurst[1], Susan Harrison[1,2], Megan Becker[1,3]

[1]*Minerals to Metals Initiative, University of Cape Town, Cape Town, South Africa, optale001@myuct.ac.za*

[2]*Centre for Bioprocess Engineering Research, University of Cape Town, Cape Town, South Africa*

[3]*Centre for Minerals Research, University of Cape Town, Cape Town, South Africa*

Abstract

Accurate characterisation of ARD potentials is required for the development of suitable waste management strategies. Laboratory-scale static tests, provide information on the ARD capability of the waste, but not the behaviour of the individual minerals. This behaviour is dependent on the conditions within the static and Biokinetic tests. Dissolution of the carbonate and reactive silicates contributed to the neutralising capacity. Mineral behaviour within the static tests provided an indication of behaviour within Biokinetic tests. Elemental concentrations within leachate solutions supported the findings from the leach residues. The integration of the mineralogical and leachate analysis allows for better understanding of the ARD behaviour of sulfidic wastes.

Keywords: Mineralogy, Static Tests, Biokinetic Tests, Acid Rock Drainage

Introduction

Acid rock drainage (ARD) is one of the most serious pollution problems facing the mining of sulfidic ores. ARD pollution is characterised by acidic pH, and elevated concentrations of deleterious elements and soluble salts. The acidic nature of the pollution is due to the oxidation of sulfide minerals, which occurs naturally in the presence of water and oxygen. This oxidation, however, may be accelerated through the metabolic action of Fe- and S-oxidising micro-organisms. The accurate and reliable characterisation of the ARD potentials will allow for a more sustainable approach to waste management through the optimisation of cleaner production principles within the mining industry.

To limit the number of samples and the associated cost of analysis, a sequential approach is used in the characterisation and prediction of ARD hazards (Parbhakar-Fox and Lottermoser, 2015). The initial stage consists of acid-base accounting, with a balance of the acid-generating and acid-neutralising potentials of the waste providing an estimate of the net acid producing potential (NAPP). This assessment is performed using laboratory-scale tests. In addition, net acid generation (NAG) tests are performed, with the pH of the final solution indicating the potential for net acidity generation (Miller et al., 1997). Following static tests, potentially acid forming samples undergo kinetic testing to evaluate the rate of ARD generation and its potential composition. Samples which are found to be non-acid forming (NAF) are eliminated from the ARD protocol (Smart et al., 2002). A number of previous researchers have documented the various short-comings of this approach and the test methods involved (Dold, 2017, Parbhakar-Fox and Lottermoser, 2015).

However, the simplicity, speed and low cost of the laboratory tests ensures their continued use as the initial stage in the characterisation of potential ARD hazards (Smart et al., 2002). The reliability of these tests, therefore, remains a key parameter in the characterisation of the ARD hazards associated with mine wastes. In particular, studies have suggested the inclusion of sample mineralogy to provide understanding of the behaviour of individual minerals in the overall ARD generation process (Becker et al., 2015, Brough et al., 2013). Such information may be used directly for an estimation of the acid generating and acid neutralising capability of the wastes (Paktunc, 1999, Bouzahzah et al., 2014).

This study investigates the behaviour of individual minerals under the static and Biokinetic test conditions, through analysis of leach residues. This allowed for assessment of mineral reactivity as a function of test conditions, with a deeper understanding of the test results gained. Changes in sample mineralogy were supported through analysis of the elemental concentrations within the leachate solutions.

Materials and Methods

Two waste rock samples sourced from a greenstone belt gold deposit were used in this study. Statistically representative samples were prepared for use in the static and Biokinetic tests (Opitz et al., 2016). Mineral grades were quantified using QEMSCAN® analysis on an FEI QEMSCAN® 650F at the University of Cape Town and complimented by electron micro-probe analysis (EMPA) of various silicate minerals to accurately determine their end-member compositions.

Acid-generating sulfides included pyrrhotite (5.8 wt.%; 0.9 wt. %) and pyrite (1.2 wt.%; 6.0 wt. %) for the two waste samples, whereas the acid neutralising potential was due to fast-weathering calcite (0.9 wt.%; 2.8 wt. %), intermediate-weathering chlorite (1.4 wt.%; 0.7 wt. %) and biotite (1.7 wt.%; 15.5 wt. %), and slow-weathering magnetite (33 wt.%; 16 wt. %)(Opitz et al., 2016).Classification of the ARD potentials of both samples was performed using acid-base accounting. The acid neutralising capacity (ANC) was determined experimentally using the method outlined in Weber et al. (2004). Single stage Net acid generation (NAG) tests were performed using reaction of the wastes with a 15 % H_2O_2 solution (Miller et al., 1997). Further details are provided in Opitz et al. (2016), with a summary of the characterisation results presented in **Table 1**.

Biokinetic tests provided an understanding of the ARD generation under microbially-mediated conditions. Analysis of the solution pH with time (Figure 1) allowed for assessment of the relative rates of acid-neutralisation and acid-formation within the triplicate tests. For sample A, the rise in pH from reaction with calcite was followed by a decrease as a consequence of acidity formation. For sample B, however, the solution pH increased above conditions favourable for microbial growth and activity.

Leachate solution prior to the neutralisation step was recovered from the static tests, with liquid samples collected from the Biokinetic tests prior to commencement and daily thereafter. Solution analysis was performed for major elements (Al, Ca, Fe, K, Mg, Na) using induced coupled plasma optical emission spectrometry (ICP-OES) using a Varian 720 machine. Solid residues were collected upon the completion of the ARD laboratory tests, with mineralogical assessment performed using QEMSCAN. The extents of mineral reaction are presented as range, following the calculation presented in (Becker et al., 2015).

Results

Decreases in mineral content, as a percentage change from the feed material, are presented in **Table 2**. The reaction of the acid-consuming minerals was observed within all tests performed for both samples, while the depletion of the sulfides was predominately within the NAG and Biokinetic tests. The leach residues from the ANC tests from both samples confirmed the completion dissolution of calcite, as specifically targeted by the test conditions. In addition, dissolution of the reactive silicates (chlorite and biotite), and the Fe-oxyhydroxides were observed for both waste samples. The decreases in Fe-oxyhydroxides (1-30 %) and sulfides (1-30 %) (**Table 2**) are in agreement with Becker et al. (2015), where dissolution of these minerals was observed under similar test conditions. In particular, a reduction in pyrrhotite content was observed in the ANC residues for both samples, indi-

Table 1: *ARD characterisation results for the two waste rock samples indicating the overall acid generation classification of both samples. From: Opitz et al. (2016).*

Waste Sample	MPA [kg H_2SO_4 / ton]	ANC [kg H_2SO_4 / ton]	NAPP [kg H_2SO_4 / ton]	NAG pH	ARD Classification
Sample A	70.2 ± 0.7	53.2 ± 1.8	17.0 ± 1.9	2.5 ± 0	Potentially acid forming
Sample B	98.8 ± 1.4	95.7 ± 1.9	3.2 ± 2.4	2.7 ± 0	

cating fairly extensive dissolution under the relatively aggressive leach test conditions.

NAG tests are designed to provide an indication of net acidity generation upon simultaneous oxidation of the sulfide minerals and reaction of the neutralising minerals. For both samples, dissolution of pyrrhotite and pyrite was observed within the single stage NAG tests. Decreases in the calcite, chlorite and biotite content were due to reaction with the acidity produced from sulfide oxidation. The differences in extent of chlorite dissolution between ANC and NAG tests were due to the milder test conditions with respect to acid molarity.

In contrast to the NAG test conditions, oxidation within the Biokinetic tests was facilitated through microbial (re)generation of soluble ferric iron. The mineralogical changes as a consequence of the Biokinetic tests were different for the two samples, related to the acid neutralising content of the wastes (**Table 1**), which affected the pH conditions within the two experimental systems. The Biokinetic test results (Opitz et al., 2016) indicated a varied immediate response in solution pH for the two waste samples. Tests performed on sample A illustrated an initial dominance of acid neutralisation followed by acid generation. The favourable microbial conditions allowed for microbially-mediated oxidation of the pyrrhotite (>90 %) and pyrite (61-90 %), with the acidic environment leading to the dissolution of acid consuming minerals (> 90% calcite; 31-60 % chlorite). In contrast, the neutralisation content of sample B was sufficient to ensure pH levels rose to pH 7.0 over the initial 3 days. These pH levels were maintained for the duration of the experiment with limited acid generation observed. These unfavourable microbial conditions, limiting the solubility of the ferric iron oxidising agent. The pyrrhotite and pyrite oxidation observed within these residues were a result of initial reaction of the sulfides with ferric iron added as part of the inoculum solution. In addition, formation of iron-sulfate precipitates within both experimental systems occurred, as indicated by the increase in the sulfate composition of the test residues.

Analysis of the solution composition of the static and Biokinetic tests (Figure 2) supported the observations from the mineral residues. Greater concentrations of Al, Ca, K and Mg were observed in the ANC test solutions as compared to the NAG and Biokinetic tests. This is consistent with the greater dissolution of chlorite under the more aggressive leach conditions in the ANC tests. Differences in Fe concentrations between the tests are due primarily to differences in solution pH. Higher Fe concentrations were observed un-

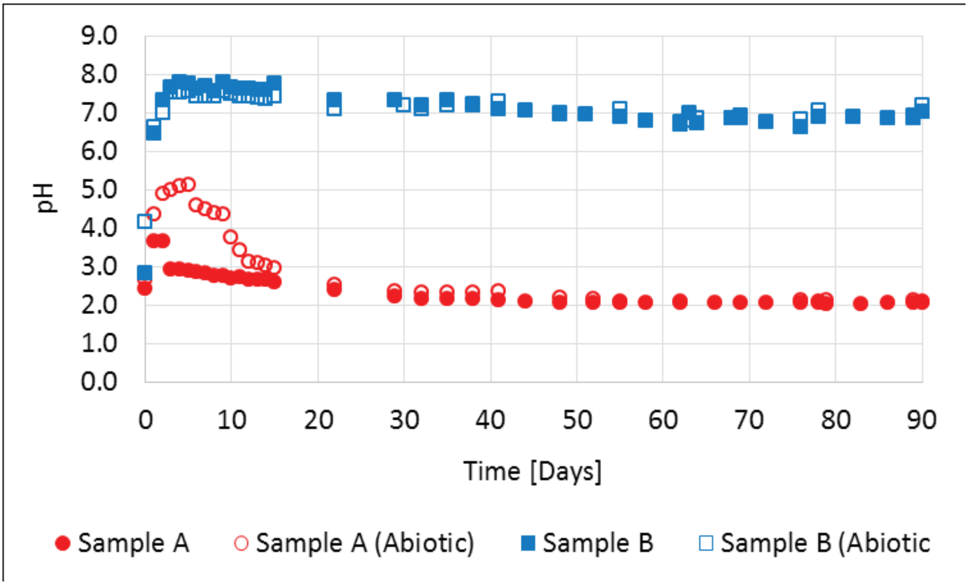

Figure 1: *pH profile of the Biokinetic tests performed on samples A and B, for biotic (closed symbols) and non-inoculated (open symbols) experiments (Opitz et al., 2016).*

der acidic conditions, with the formation of Fe-bearing sulfate precipitates at the elevated pH conditions within the Biokinetic test performed on sample B. Similar Mn concentrations were observed with all characterisation tests.

Discussion

The role of reactive silicates to the acid neutralising capacity of waste samples has been demonstrated previously (Becker et al., 2015, Lawrence and Scheske, 1997, Jambor et al., 2002). Such minerals, however, are not often included in estimations of the neutralising potential based on sample mineralogy. The dissolution of these minerals under ANC test conditions, however, indicates their inclusion in the experimental quantification of the acid neutralising capacity of the samples. In addition, dissolution of these silicates within the Biokinetic tests, with conditions similar to those within waste deposits, indicates the contribution of such minerals to ARD generation. Dissolution of pyrrhotite within the ANC tests highlighted the behaviour of sulfide minerals which undergo dissolution through proton attack. For pyrrhotite, the acid consumption upon dissolution within the ANC test may be offset by the acid released during precipitation of the ferric iron resulting from its dissolution. However, for non-ferrous sulfides such as galena (0.03 wt. %), this offset may not occur, with the potential for these minerals to contribute to acid-neutralisation and acid-generation estimates simultaneously.

The dissolution of the reactive silicates and Fe-oxyhydroxides within the NAG tests indicates the dissolution of these minerals by acidity produced through the oxidation of the sulfide minerals. The acid consuming behaviour, therefore, is accounted for through measurement of the NAGph upon completion of the single-stage NAG test. The lack of complete sulfide oxidation in the residue of this test, however, implies a remaining potential for acidity formation, and indicates the underestimation of the total ARD generation potential from the single-stage NAG test.

Quantification of the ARD potentials from mineralogical estimates and static characterisation tests provides an indication of the ARD potential of the wastes over geological time frames. No information on the relative rates of acid neutralisation and generation, however, is obtained. The importance of this knowledge is illustrated by the Biokinetic test results of the two samples. The greater calcite content in sample B led to a greater elevated in initial solution pH as compared to the tests performed on sample A. The resulting unfavourable microbial conditions limited the information gained on microbially-mediated sulfide oxidation for this sample. The suitable acidic and oxidative conditions within the Biokinetic tests performed on sample A, however, resulted in sulfide mineral oxidation, illustrated by the reduction in solution pH by day 3 (Figure 1) and the decrease in sulfide mineral content grade of this sample. In addition to the increase in acidity as a consequence of sulfide oxidation, the increase in sulfate content within the leach residues,

Table 2: *Changes in mineral composition presented as a percentage of the initial amounts as quantified from the leach residues following static and Biokinetic tests performed on waste sample A and B.*

Mineral Phase	Sample A [%]			Sample B [%]		
	ANC	NAG	Biokinetic	ANC	NAG	Biokinetic
Pyrrhotite	61-90 %	61–90 %	>90 %	1–30 %	31-60 %	1-30 %
Pyrite	0 %	61–90 %	61–90 %	0 %	61–90 %	1–30 %
Calcite	> 90 %	> 90 %	> 90 %	> 90 %	> 90 %	> 90 %
Chlorite	61-90 %	31–60 %	31-60 %	61-90 %	31–60 %	31-60 %
Fe-oxyhydroxides	1–30 %	1-30 %	1–30 %	1–30 %	1-30 %	1–30 %
Biotite	1–30 %	1–30 %	1–30 %	1–30 %	1–30 %	1–30 %
Actinolite	1-30 %	1-30 %	1-30 %	31-60 %	31-60 %	31-60 %
Albite	0 %	0 %	0 %	0 %	0 %	0 %
Quartz	0 %	0 %	0 %	0 %	0 %	0 %
Sulfates	31-60 %	31-60 %	< 0 %	31-60 %	31-60 %	< 0 %

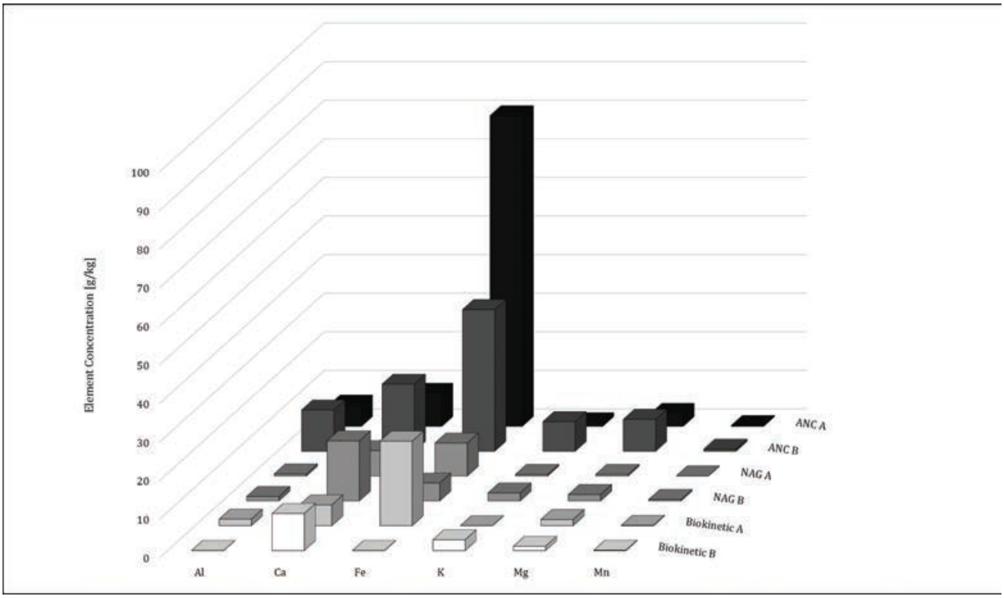

Figure 2: *Solution concentrations at test termination for the static ARD and Biokinetic tests performed on waste samples A and B. Tests were performed in triplicate (n=3)*

indicates the formation of Fe-precipitates within this test. The sustained presence of these precipitates over the duration of the Biokinetic tests is consistent with the formation of insoluble jarosite precipitate within the acid–sulfate system (Nordstrom, 1982). Although the static test residues provides an indication of the minerals which may contribute to the ARD generation within the Biokinetic tests, accurate prediction of the behaviour and contribution of the individual minerals may require decoupling of the rates of acid-consumption and acid-formation. In addition, while analysis of the Biokinetic test solutions allows for identification of the mobilised elements, fundamental understanding of individual mineral behaviour with time is necessary for more detailed knowledge on elemental deportment.

Integration of the static and Biokinetic test results allow for knowledge of the possible drainage characteristics under "worst case scenarios" and conditions more typical of waste deposits. The combination of the leach residue analysis and quantification of elemental concentrations allows for identification of the minerals responsible for acid-formation and acid-neutralisation, and an understanding of the behaviour of the individual minerals under these conditions.

Conclusions

Partial dissolution of reactive silicate minerals and pyrrhotite were observed within the ANC tests performed on both samples. Dissolution of the Fe-oxyhydroxides and reactive silicate minerals within the NAG tests suggests the dissolution of these minerals may be expected within acid-sulfate systems. An underestimate of the total sulfide oxidation potential within the single-stage NAG solution is suggested by the substantial sulfide grade of the NAG residues. Integration of the leach residue analysis and soluble elemental concentrations from the static tests allowed for identification of the minerals likely to contribute to the ARD behaviour under Biokinetic test conditions. The accurate contribution of the individual minerals within this test, however, requires further development of Biokinetic tests where test solution is replenished with time. The elemental concentrations within the leachate solutions supported the dissolution of identified minerals from the test residues. The deportment of deleterious elements within Biokinetic tests, however, may only be considered upon the formation of acidic and oxidative conditions. There remains a necessity for integrated knowledge of detailed sample mineralogy and solution chemistry, both under chemical and biological conditions, in understanding the ARD potentials of sulfide wastes. An approach which includes of both of these aspects is required to provide accurate and reliable ARD characterisation and prediction.

Acknowledgements

This work is based on research supported by the National Research Foundation (NRF) of South Africa (Grant Number 86054), and on research supported by the South African Research Chairs Initiative (SARChI Chair in Minerals Beneficiation). Any opinion, finding, conclusions or recommendation expressed in this material is that of the authors and the NRF does not accept any liability in this regard.

References

BECKER, M., DYANTYI, N., BROADHURST, J. L., HARRISON, S. T. L. & FRANZIDIS, J. P. 2015. A mineralogical approach to evaluating laboratory scale acid rock drainage characterisation tests. *Minerals Engineering,* 80**,** 33-36.

BOUZAHZAH, H., BENZAAZOUA, M., BUSSIERE, B. & PLANTE, B. 2014. Prediction of Acid Mine Drainage: Importance of Mineralogy and the Test Protocols for Static and Kinetic Tests. *Mine Water and the Environment,* 33**,** 54-65.

BROUGH, C. P., WARRENDER, R., BOWELL, R. J., BARNES, A. & PARBHAKAR-FOX, A. 2013. The process mineralogy of mine wastes. *Minerals Engineering,* 52**,** 125-135.

DOLD, B. 2017. Acid rock drainage prediction: a critical review. *Journal of Geochemical Exploration,* 172**,** 120-132.

JAMBOR, J. L., DUTRIZAC, J. E., GROAT, L. A. & RAUDSEPP, M. 2002. Static tests of neutralization potentials of silicate and aluminosilicate minerals. *Environmental Geology,* 43**,** 1-17.

LAWRENCE, R. W. & SCHESKE, M. 1997. A method to calculate the neutralization potential of mining wastes. *Environmental Geology,* 32**,** 100-106.

MILLER, S. D., ROBERTSON, A. & DONAHUE, T. Advances in Acid Drainage Prediction using the Net Acid Generation (NAG) test. 4th International Conference on Acid Rock Drainage, 1997 Vancouver, BC. 533-549.

NORDSTROM, D. K. 1982. *Aqueous pyrite oxidation and the consequent formation of secondary iron minerals*, Soil Science Society of America.

OPITZ, A. K. B., BECKER, M., BROADHURST, J. L., BRADSHAW, D. J. & HARRISON, S. T. L. The Biokinetic Test as a Geometallurgical Indicator for Acid Rock Drainage Potentials. The Third AusIMM International Geometallurgy Conference, 15-16 June 2016 Perth, Australia. AusIMM, 183-191.

PAKTUNC, A. 1999. Mineralogical constraints on the determination of neutralization potential and prediction of acid mine drainage. *Environmental Geology,* 39**,** 103-112.

PARBHAKAR-FOX, A. & LOTTERMOSER, B. G. 2015. A critical review of acid rock drainage prediction methods and practices. *Minerals Engineering,* 82**,** 107-124.

SMART, R., SKINNER, W., LEVAY, G., GERSON, A., THOMAS, J., SOBIERAJ, H., SCHUMANN, R., WEISENER, C., WEBER, P. & MILLER, S. 2002. ARD test handbook: Project P387, A prediction and kinetic control of acid mine drainage. *AMIRA, International Ltd, Ian Wark Research Institute, Melbourne, Australia*.

WEBER, P. A., THOMAS, J. E., SKINNER, W. M. & SMART, R. S. C. 2004. Improved acid neutralisation capacity assessment of iron carbonates by titration and theoretical calculation. *Applied Geochemistry,* 19**,** 687-694.

Wall Wash Samples to Predict AMD Longevity at Coal Mines in New Zealand

J. Pope, H. Christenson, N. Newman, K. Gordon, D. Trumm

CRl Energy Ltd, 97 Nazareth Ave, Christchurch, New Zealand. j.pope@crl.co.nz

Abstract

Wall wash samples were collected at man-made coal measures exposures between 3 days and 138 years old to understand to evolution of wall wash chemistry with time. Acidity in the wall wash solutions decreased rapidly from a maximum of >1000mg/L H_2SO_4 to <1mg/L H_2SO_4 as the age of the exposure increases. The composition of acidity also changes, at young exposures (≤1y) Fe Lewis acidity is the most abundant form of acid, at sites 3-18y old Al Lewis acidity is most abundant and at sites 45-130y old, proton acidity is most abundant. Trace element concentrations in wall wash (Zn, Ni, Co, Cd & Mn) also decrease 3-4 orders of magnitude with increasing age of exposure.

Keywords: Wall wash, AMD, Lewis acid, trace element.

Introduction

Wall wash samples were collected from man made Brunner Coal Measures exposures between 3 days old and 138 years old at mine sites on the West Coast of the South Island of New Zealand. The Brunner Coal measures are regionally extensive and contain high quality coking coal seams within PAF (potentially acid forming) mudstones and sandstones. There are several active mines and many abandoned mines hosted within these coal measures and the longevity of acid release related to mining disturbances is not quantified.

The solution chemistry of the acid mine drainage is from Brunner Coal Measures is well characterised, pH is low (2-4.5), Fe and Al are abundant Lewis acids, the most elevated trace elements Zn, Ni & Mn, and occasionally Cu, As or Co are present at elevated concentrations (Pope et al., 2010a; Pope et al., 2010b; Weber et al., 2006). However, the long term evolution of AMD chemistry is not well understood. Our objective is to measure changes in wall wash chemistry with the age of exposure and use this information to develop a predictive relationship for:

- decrease in acid release rate from pit walls with time and the time taken for acidity in pit wall run off to return to natural levels
- decreases in trace element release rate from pit walls with time
- evolution of mine drainage chemistry with time

Methods

Samples of wall wash were collected from Brunner Coal Measures outcrops at the high walls of 4 mine sites one road cutting and one rail cutting. Wall wash was generated by rapid (≈10 seconds) application of 500ml of distilled water to an area about 50cm by 50cm and collection of as much run off as possible in a large plastic sampling bag sealed to the outcrop with duct tape (Figure 1). About 40 to 80% of the wall wash was retrieved in the sampling bag with some lost due to rough surfaces and wetting. Wall wash samples were transferred into chilled 500ml sample bottles (unpreserved and un filtered) for subsequent processing in the laboratory. The samples often included a small amount of solid material (sediment, precipitates ± organic material). The sample collection process is similar to field conditions where solid material is washed off along with runoff mine drainage water and all material is discharged from the high-wall area with dissolved and suspended material included.

Application of this volume of water to ≈ $\frac{1}{4}m^2$ reflects a 6-10 mm rainfall event depending on the slope of the high-wall which is between 70° & 80° at the sites selected. This size of rainfall event was selected because it is relatively common on the West Coast (weekly) along with much larger rainfall events (annual rainfall 2-6m per year).

Sample sites

Site A is at a mine in the Buller Coalfield that has been operating for about 4 years where wall wash samples were collected from pit wall exposures that were 3 days old and 1 year old at the time of sampling.

Site B is an operational mine in the Garvey Creek Coalfield and includes a sequence of complexly folded and faulted Brunner Coal Measures. Pit walls where access was possible were between 3 & 5 y old at the time of sampling.

Site C is a road cutting through Brunner Coal Measures that occurs on the road close to the entrance of Stockton mine in the Buller Coalfield. The cutting was exposed about 10 years prior to the time of wall-wash sampling.

Site D is at a mothballed mine in Brunner Coal Measures within the Garvey Creek Coalfield. Access is available to the coal measures sequence in the mine high-wall which was 18 years old (pers. com. Phil Lindsay) at the time of sampling.

Site E is at a cutting for the portal of an abandoned underground mine in the Buller Coalfield. The cutting was about 62 years old at the time of wall wash sampling.

Site F is a cutting for historic rail operations near Denniston in the Buller Coalfield. The cutting was about 136 years old at the time of sampling and the surfaces were ≈60% lichen covered.

Laboratory methods

In the laboratory, the pH was measured in each sample using a calibrated (buffers 2,4 & 7) pH metre. Samples were filtered through 0.45µm syringe filters, then acid preserved using analytical grade HNO_3 and dispatched for element analyses. Analyses were conducted for major cations, and trace elements by APHA method 3125 B. The analysis suite included K, Na, Ca, Mg, Al, Fe, As, Sb, Cu, Cr, Co, Mn, Ni & Zn at Hills Laboratory by ICP-MS.

Results and Discussion

The chemistry of wall wash was variable at each site and between sites (Pope et al., 2018). However, in general the characteristics of wall wash at sites <60 years old match with previous studies of Brunner Coal Measures AMD, pH is commonly between 2.5 and 4, Fe and Al are typically abundant Lewis acids, and trace elements are enriched, Zn, Mn > Ni

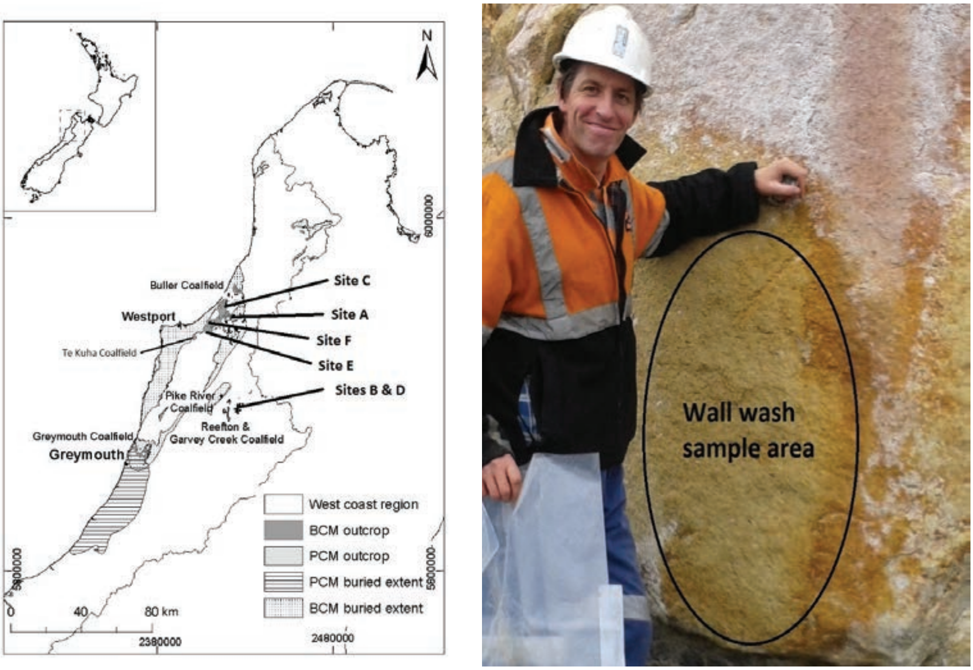

Figure 1 *Location map and example wall wash sample site.*

> Co, Cu, Cd > As, Sb and others (Pope et al., 2010a; Weber et al., 2006; Weisener and Weber, 2010). The total acidity (mg/L H_2SO_4) calculated from pH, Fe and Al concentrations is within the range between 0.05mg/L and just over 10000mg/L, similar to the range of acidity concentrations that occurs in leachate samples from Brunner Coal Measures column testing (Olds et al., 2016; Pope and Weber, 2013). The maximum concentration of trace elements in wall wash samples is often higher than the concentrations found in AMD or column leach analyses, Mn up to 90mg/L, Zn up to 31mg/L, Ni up to 43mg/L and Co up to 31mg/L (Pope et al., 2018). At sites < 60 years old the pH is often circumneutral and concentrations with low acidity, although trace element concentrations can remain relatively high compared to the acid load at some sites.

Acidity trends

The acidity data collected are variable and this reflects the nature of the sampling method and coal measures rocks that have been washed. The sampling method is difficult to standardise because each outcrop has a different slope, roughness and wetting characteristic. The rocks have variable lithology and secondary minerals that store acid and trace elements are not uniformly distributed. Despite the variability in acidity that can be washed from different sample sites, there are consistent trends in acid release compared to the age of the exposure.

There are two general trends in acidity released from the coal measures pit walls in this study. High acid loads are released for the first year and decreasing acid loads for subsequent years. When pit walls are fresh (3 days to ≈1 year in this study) the acid release rate is relatively rapid average 2032mg/L(H_2SO_4) from 3 day old pit walls, and 4187mg/L(H_2SO_4) from 1y old pit walls.

As pit walls age (1 year to 62 years in this study) the release rate of acid decreases with increasing age of pit exposure. Average acidity is 159mg/L(H_2SO_4) for 3-5y old exposures, decreasing to 79 and 55mg/L(H_2SO_4) for exposures 10 and 18y old respectively. Exposures that are 62y old produce wall wash average acidity with 4mg/L(H_2SO_4) and the exposure that is 138 years old produces wall wash with average acidity of 0.1mg/L(H_2SO_4). The changes in average concentration of acidity as a function of time can be fitted with a power law.

Different processes controlling acid release from mines at different times have been noted in other studies. In a long term study of closed underground coal mine drainage from the United Kingdom two phases of acid production also occur, vestigial acidity related to flushing of partial oxidation products in mine impacted areas and juvenile acidity related to ongoing pyrite oxidation in host rocks which decreases with time. (Younger, 1997). Although the hydrogeology in underground workings is very different to a pit wall, the concepts of juvenile and vestigial acidity can be applied. Wall-wash only measures vestigial acidity, acidity that can be rinsed off the pit wall by rainwater, juvenile acidity is released as pyrite oxidises this leads to the secondary minerals that store acid and build up on the pit wall until the next rainfall.

Chemical trends

In the wall wash samples the contribution of H^+, Fe^{3+} and Al^{3+} to the total acidity varies with the age of the pit wall. At the youngest pit walls (3 days and 1 year old) where acidity values are much higher dissolved Fe^{3+} is the largest component of acidity and Al^{3+} > than H^+. At the older pit walls (3 years to 18 years,) dissolved Al^{3+} is the most important component of acidity and H^+ is more significant than Fe^{3+}. At the oldest sites (62 years and 138 years), H^+ is the largest component of acidity, Al^{3+} acidity remains abundant and there is no detectable dissolved Fe^{3+}.

The contributions to acidity by pH, Fe & Al in Brunner Coal Measures AMD have previously been attributed to factors such as mine type with Al^{3+} typically considered the most important Lewis acid at open cut mines (Pope et al., 2010a). However, this previous study does not consider the evolution of AMD chemistry with time. At new seeps (McCauley et al., 2010) and early in column leach testing (Pope and Weber, 2013) Fe^{2+} and Fe^{3+} is often the most important component of total acidity regardless of whether mining occurs at surface or underground. At older seeps, in column leach samples from tests that proceed for >1 y and at a regional scale

Al^{3+} is the major component of Lewis acidity in Brunner Coal Measures AMD. At an active mine where pit walls might be cut back every few months to few years the pit wall chemistry will be a mix of Fe^{3+} and Al^{3+} rich AMD acidity.

Acid mine drainage from Brunner Coal Measures typically contain trace elements including Zn, Mn > Ni > Cu, Co, Cd > As, Sb and other trace elements. In the wall wash this pattern of enrichment is generally correct, however these samples contain some of the highest concentrations of trace elements occur that have been observed in Brunner Coal Measures AMD. Higher than previously recorded in seeps or leach tests (Pope et al., 2010a; Pope and Weber, 2013). In addition, the elevated concentrations of elements like Mn, Zn and Ni can occur in wall wash samples from either young or old pit walls. For example, the sample site D4 (18years old exposure) samples contains Zn 21mg/L, Ni 5.4mg/L and Mn 27mg/L. The reason for the elevated trace element concentrations in wall wash samples from both young and old pit walls is not clear.

Comparison to background

The power function correlation used to characterise the decay rate for acid release from pit walls can compared to the background acidity in streams draining Brunner Coal Measures. Background acidity concentrations are compiled from analyses of streams that drain only Brunner Coal Measures but are not impacted by mining disturbances. The range of acidity values at each site spans between 0.5 and 2.5 orders of magnitude and the total range of acidity in the data is almost 6 orders of magnitude. Extrapolating the data collected related to acid release with time indicates acid production at levels above maximum acidity level measured in streams will occur for between 10 and about 165 years. If a regression is applied to the average data, then the time taken for acid load from high walls to decline to similar levels found is streams is 45 years to meet the most acidic natural conditions and 130 years to meet low level natural acid conditions.

Conclusions

Wall wash samples from mine pit walls that range in age from 3 days to 138 years have been collected and show two trends in the concentration of acidity. Pit walls exposed to weathering for 3 days to 1 year release high concentrations of acid that is comparatively

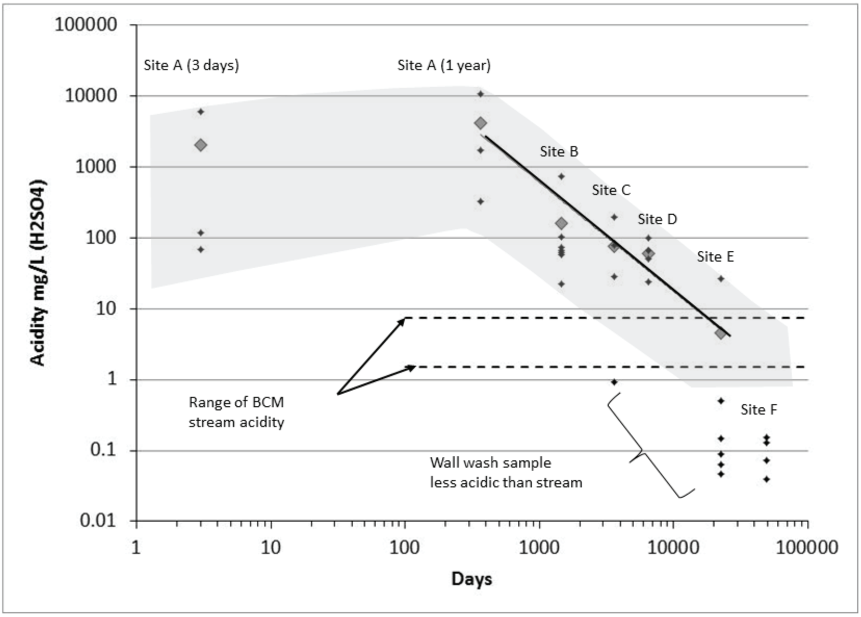

Figure 2 *Trends in acidity in wall wash at sites with different ages.*

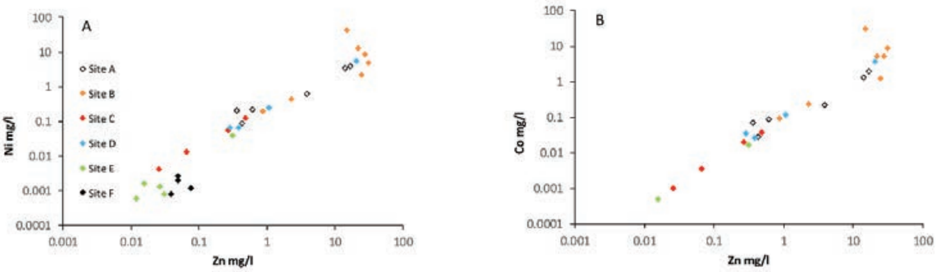

Figure 3 *Trends in trace element concentrations in wall wash at sites with different ages.*

Fe rich whereas older pit walls (3 – 18 years) release acid at lower concentrations and that is relatively Al rich. Pit walls that are older still release mostly proton acidity with some dissolved Al.

The average acidity concentration released from the pit walls greater than 1 year old decreases rapidly with time and can be fitted with a power function expression with data spanning 4 orders of magnitude. There is some uncertainty in the data related to the exact age of the pit wall samples and the nature of the sampling which is biased toward areas where samples can be collected easily (smooth with appropriate slope and limited debris). However, the correlation to the averaged data is relatively strong. The dataset indicate that acidic runoff from pit walls will continue at concentrations above background for a range between 10 and 165 years where background is defined by un-impacted streams draining only Brunner Coal Measures. If the averaged wall wash acidity data and power function fit is used for extrapolation, then the pit walls will release acid at concentrations above the maximum measured acidity in streams for about 45 years.

Maximum trace element concentrations in wall wash samples are higher than concentrations in AMD or column leach experiments on Brunner Coal Measures. Trace element enrichment is strongly cross correlated for elements that are typically abundant in Brunner Coal Measures AMD (Zn, Ni & Mn) as well as minor elements (Co, Cu, Cd), trace element concentrations are not as strongly correlated with acid release probably due to selective co-precipitation into different secondary minerals controlling acidity. In addition high concentrations of trace elements occur in wall wash samples from pit walls of all ages. The variability in trace element concentrations in wall wash samples indicates that the distribution of trace elements in Brunner Coal Measures is not uniform and trace elements could continue to be released as acidity declines.

This wall wash study can be used to predict acidity concentrations and loads from pit walls and other areas where unlimited oxygen and water are freely available to react Brunner Coal Measures. With this information, remediation, and treatment obligations for AMD from these types of sources can be predicted and built into mine operational and closure or rehabilitation plans.

Acknowledgements

This research is funded by the Ministry of Business Innovation and Employment under contract CRLE1403 – Mine Environment Life Cycle Guide. Access to field sites and data were made available by Solid Energy NZ Ltd, Bathurst Resources, New Zealand Coal and Carbon Ltd and Stevenson Mining Ltd.

References

McCauley, C., O'Sullivan, A., Weber, P., and Trumm, D., 2010, Variability of Stockton Coal Mine drainage chemistry and its treatment potential with biogeochemical reactors: New Zealand Journal of Geology and Geophysics, v. 53, no. Nos 2-3, p. 211-226.

Olds, W., Weber, P., Pope, J., and Pizey, M., 2016, Acid Mine Drainage analysis for the Reddale Coal Mine, Reefton, New Zealand: New Zealand Journal of Gelology and Geophysics, v. 59, p. 341-351.

Pope, J., Christenson, H., Gordon, K., Newman, N., and Trumm, D., 2018, Decrease in acid mine drainage release from pit walls in Brunner Coal Measures: New Zealand Journal of Geology and Geophysics.

Pope, J., Newman, N., Craw, D., Trumm, D., and Rait, R., 2010a, Factors that influence coal mine drainage chemistry, West Coast, South Island, New Zealand: New Zealand Journal of Geology and Geophysics, v. 53, no. Special Edition - Mine Drainages, p. 115-128.

Pope, J., and Weber, P., 2013, Interpretation of column leach characteristics of Brunner Coal Measures for mine drainage management, AusIMM Annual New Zealand Branch Conference: Nelson, p. 377-385.

Pope, J., Weber, P., MacKenzie, A., Newman, N., and Rait, R., 2010b, Correlation of acid base accounting characteristics with the Geology of commonly mined coal measures, West Coast and Southland, New Zealand: New Zealand Journal of Geology and Geophysics, v. 53, no. Special Edition - Mine Drainages, p. 153-166.

Weber, P. A., Skinner, W. M., Hughes, J., Lindsay, P., and Moore, T., 2006, Source of Ni in coal mine acid rock drainage, West Coast, New Zealand: International Journal of Coal Geology, v. 67, p. 214-220.

Weisener, C. G., and Weber, P. A., 2010 Preferential oxidation of pryrite as a function of morphology and relict texture: New Zealand Journal of Geology and Geophysics, v. 53, no. Nos 2-3, p. 167-176.

Younger, P., 1997, The longevity of mine water pollution: a basis for decision making: The Science of the Total Environment, v. 194/195, p. 457-466.

Model Simulations of the Layered Development of Waste Rock Stockpiles, Progressive Moisture Changes and Potential Seepage Generation in a Low Rainfall Environment: Case Study of an Australian Mine Development

Alan Anton Puhalovich

Golder Associates Pty Ltd, 1 Havelock Street West, Perth, Western Australia 6005, Australia

Abstract

Models simulating saturated-unsaturated flow processes have been developed and run to understand the potential risks of seepage generation from waste rock stockpiles in a low-rainfall, iron ore mining province.

The stockpiles are modelled within a holistic, waste rock stockpile - hydrogeological context. The temporal (staged) development of the stockpiles was modelled to reflect ongoing wetting-drying, with sensitivity testing undertaken to address data gaps.

The study results indicate that the nature of the staged development of waste rock stockpiles, low rates of rainfall and significant depth to groundwater make it unlikely that seepage fluxes to the underlying groundwater system would occur.

Keywords: hydrogeology, waste rock, seepage impacts

Introduction

SIMEC Mining is currently considering developing a new, hematite iron ore (open cut) mine at Iron Sultan, located at the Camel Hills ("Site"), approximately 45 km west of the town of Whyalla in South Australia, Australia (Figure 1). Two-dimensional modelling of saturated-unsaturated flow processes was undertaken of the progressive, layered development of the waste rock stockpiles to better understand seepage generation processes, taking account the underlying hydrogeological conditions and potential changes to groundwater conditions due to mining.

Site Setting

The Site is located in the Gawler Ranges district and to the west of the Iron Baron Mining Area (IBMA) (Figure 1) and within an arid to semi-arid climate, with potential evaporation substantially higher than rainfall (average rainfall and "Class A" pan evaporation are 270 and 2,550/annum respectively). The Site is located on the western flank of the regionally extensive, north-south trending Middleback Ranges (~350 m Australian Height Datum, mAHD).

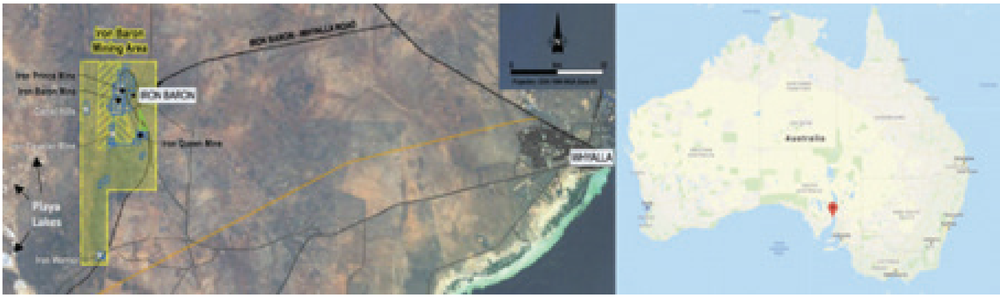

Figure 1 Site Location (adapted from information provided by SIMEC Mining)

Geology and Hydrogeology

The Site is situated in the Gawler Craton, a stable crystalline basement province containing Archaean to Mesoproterozoic rocks with thin overlying sediments of Neoproterozoic to Quaternary age overlying the basement rock (Rudd, 1094; Drexel et al., 1993; Parker and Flint, 2012). The basement rocks comprise Banded Iron Formation (BIF) and Granites/Schistose rocks. The regional hydrogeology is characterised by unconfined/confined, fractured rock hydrogeological units of the Middleback Ranges underlying unconfined aquifers in surficial Tertiary and Quaternary sediments located in lower areas of the landscape. The fractured rock units contain groundwater that are saline to brackish in water quality and have low yields. Groundwater of potable quality is mostly found in Quaternary limestone and Tertiary sand aquifers (Berens et al., 2011). Site-specific field investigations have been undertaken to understand site hydrogeological conditions at Camel Hills (Puhalovich, 2018).

Groundwater recharge occurs where basement rocks outcrop or sub-crop at or near the Ranges (Berens et al., 2011). Estimates of net groundwater recharge have been made using groundwater quality data and the CSIRO groundwater recharge-discharge calculation method (Leaney et al., 2011). Specific inputs included annual rainfall, annual rainfall chloride flux, groundwater chloride concentration, soil clay content, soil type, and vegetation type. Net groundwater recharge rates are estimated to range from 0.3 to 6.1 mm/year (or about 0.1 to 2.3 % of average annual rainfall).

Climate

The Site lies within an arid to semi-arid climate, with potential evaporation rates significantly greater than rainfall rates. Daily rainfall data are available from Bureau of Meteorology (BoM) Station 18117 (Whyalla – Moola, 1958 - present, located ~10 km from Site) and (“Class A”) pan evaporation data are available from the nearest BoM climate Station 18120 (Whyalla – Aero, 1983 - present, located ~38 km from Site). There exists a substantial, negative rainfall : evaporation deficit at the Site. The intensity of storm events typically range from 10 to 40 mm/day, occurring in both summer and winter months, with only 15 days each year when daily rainfall exceeded daily average evaporation between 1983 and 2013.

Development of Waste Rock Dump (WRD) and Low-Grade Ore Stockpile (LGOS)

The WRD and LGOS is currently planned to be constructed immediately to the west of the pit (Figure 2). The WRD will comprise 4.3 Mm^3 of rock / sediments and will be built using “end dumping” methods over a 4 ½ year (Life-of-Mine) period. Mining will occur above the water table and so it is expected that excavated materials will be dry.

It is not possible to define specific material zones within the WRD and LGOS as the placed materials will not be segregated. The deposit’s geology model has identified nine “geozones”. The WRD’s materials primarily comprise “Sediment Cover (sand, calcrete and clay/scree”)” (54.5%), “Scree Cover” (24.0%) and “BIF” / “Shear Zone” / “Clay Lenses” (19.4%).

The geotechnical properties of the above materials are untested, so are defined here as being equivalent to a medium to coarse grained sand. The “sand” component within the Sediment Cover materials will only be encountered at the near surface and so the “clay” component will likely dominate the waste materials in this Geozone.

There are also no data available relating to the saturated and unsaturated hydraulic properties of the WRD materials. It is therefore assumed that, given the above, the saturated (maximum) hydraulic conductivities and porosities of the waste rock materials are likely to range between 1 and 4 m/d and 0.1 to 0.3, respectively.

Study Objectives

The study objectives were to better understand the potential infiltration, saturation and seepage flux characteristics, and the sensitivity of various materials parameters, for the proposed WRD and LGOS in the operational period.

***Figure 2** Site Layout*

Conceptual Model

Rainfall will infiltrate into the WRD and LGOS structures, primarily in areas where uncompacted waste rock slopes exist and in active placement areas. Incident rainfall on compacted benches and haul roads is unlikely to infiltrate; ponded waters are likely to evaporate given the low rainfall – high evaporation climate.

During the operational period, wetting and drying phases will occur depending on the prevailing climate conditions. Seepage fronts from the WRD-LGOS will periodically occur and migrate vertically down through the waste materials, thereby increasing moisture levels and in-situ hydraulic conductivities. Seepage may reach the water table and potentially affect groundwater quality. In this scenario, were it to occur, seepage affected groundwater quality would migrate to the north-west, given the results of hydrogeological investigations (Puhalovich, 2018).

Modelling Approach

The approach followed comprised calculating potential infiltration fluxes to the WRD, followed by development of a saturated-unsaturated (flow process) model of the WRD using Feflow software.

Infiltration fluxes to the WRD were estimated by calculating the difference between measured daily rainfall and estimated daily evaporation (using monthly Class A pan data). A Pan factor of 0.8 was applied to the Class A Pan evaporation estimates. This approach is conservative since compaction of the upper surface of the WRD would likely result in significant runoff during peak storm events. The initial infiltration flux scenario tested was as follows: Scenario 1: "High Case" (1973 annual rainfall year, nearest to 5% annual exceedance of 450 mm/annum).

The unsaturated hydraulic conductivities of these materials are a function of maximum hydraulic conductivity (which occurs when the waste materials are saturated) and degree of saturation. The relationships assumed to exist between unsaturated hydraulic conductivities, pressure heads and degree of saturation can be replicated using the 'van Genuchten' model, as defined below.

$$se = (s - sr) / (ss - sr) = \left\{ \frac{[1 + (-\alpha\Psi)n]-m,}{1,} \quad \begin{matrix} \Psi < 0 \\ \Psi \geq 0 \end{matrix} \right.$$

$$Kr = se0.5[1 - (1 - se1/m)m]2$$

$$m = 1 - 1/n$$

$$\alpha > 0, n > 1$$

s	Saturation	(fluid volume per void volume)
sr	Residual saturation	(fluid volume per void volume)
ss	Maximum saturation	(fluid volume per void volume)
se	Effective saturation	(unitless)
Ψ	Pressure head	(units of length)
α	Fitting parameter	(units of length-1)
m, n	Fitting parameters	(unitless)
Kr	Relative conductivity	(unitless)

Model Development

A two-dimensional Feflow section model was developed along the section shown in Figure

2, interpreted to be a current (pre-mining) groundwater flow line from the Camel Hills site to Salt Creek (assumed discharge location to the north-west). The model comprises 16,303 elements and 8,516 nodes with boundary conditions and the pre-development heads applied presented in Figure 3.

Assumed hydraulic properties in the model were based on the results of single well permeability tests undertaken at the Camel Hills deposit and related interpretations (Puhalovich, 2018). Effective porosity and specific storage were assumed, based on experience elsewhere, to be 0.01 to 0.05 and 0.0001 m/m, respectively. Model boundary conditions comprised Dirichlet (“constant-head”) boundary conditions of 145 and 151 mAHD were set along the model’s western and eastern boundaries, reflecting groundwater flow gradients. Constant-head boundary conditions were also applied on the embankment slopes when pressure at a point on the slope is > 0 kPa (i.e. seepage faces). A Neumann Boundary Condition (Darcy “fixed flux”) was applied to the plateau of the WRD with the net infiltration (daily) fluxes calculated applied. The upper layer of the WRD, to which the net infiltration fluxes were applied, was increased by around 4.5 m each year.

Results of Model Simulations

The model simulated the progressive raising of lifts of the WRD by applying daily positive-negative fluxes to the uppermost surface of each layer (~4.5 m) of waste rock placed over the four and half years of operations. These fluxes are constrained such that pressures do not exceed the elevation of the upper surface of the waste rock and are not permitted to fall to below -200 kPa (given absence of fine silty/clayey materials within the waste rock).

Monitoring points 1 to 10 were set at the base of the WRD (Figure 3) to track whether groundwater pressures exceeded phreatic conditions (i.e. > 0 kPa), to indicate whether seepage fluxes are sufficiently high to result in saturated conditions beneath the WRD and seepage to the underlying water table. These points indicate increases in groundwater pressures and moisture contents. However, groundwater pressures do not exceed phreatic that would indicate vertical seepage and impacts to the underlying groundwater system, i.e. model predicted groundwater pressures (Figure 4) indicate that saturated conditions are not encountered. Model results indicate that model boundary inflows and outflows are low and remain unchanged, with groundwater outflows at Salt Creek (“model boundary outflow”) constant at around 0.1 to 0.2 $m^3/d/m$. Groundwater storage changes within the WRD are also presented in Figure 5. The figure shows significant infiltration fluxes in the first year of WRD operation, with ris-

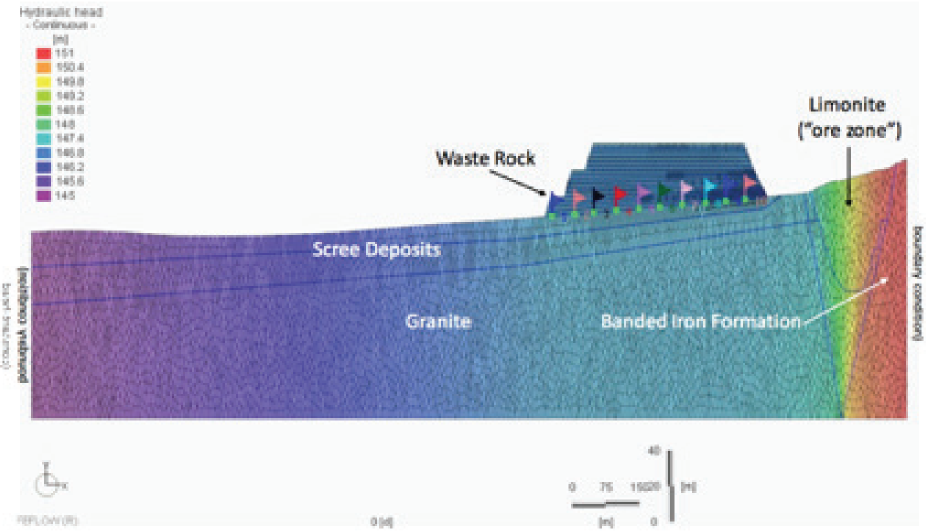

Figure 3 Model Design

ing groundwater storage. After the first year, however, groundwater storage is progressively lost due to net negative fluxes (due to evaporation) from years 1.0 to 4.5. The model results indicate that there no changes in groundwater storage beneath the WRD.

Sensitivity testing was undertaken to assess whether the properties (untested) of waste rock materials could significantly increase the likelihood of seepage fluxes. Table 1 presents the results of the sensitivity testing scenarios. It was found that the only scenario

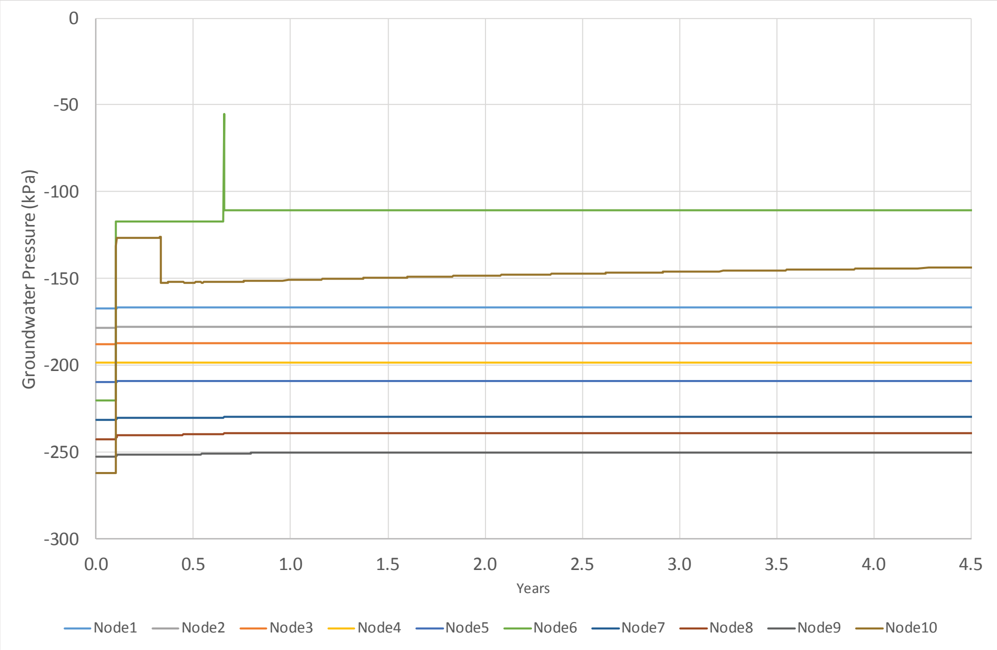

Figure 4 Model Predicted Groundwater Pressures (base of WRD)

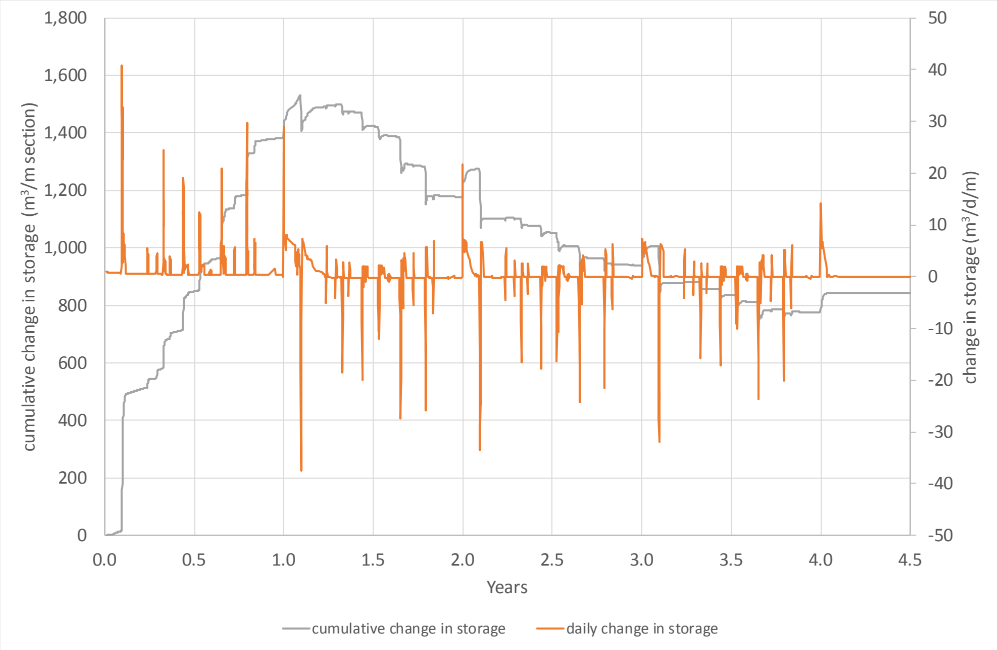

Figure 5 Model Predicted Groundwater Pressures (base of WRD)

***Table 1** Results of model sensitivity testing – groundwater pressures at base of WRD (kPa)*

Scenario	Min. Pressure	Average Pressure	Max. Pressure	Comment
Base Case	-261.76	-191.70	-55.58	
SENS1	-261.76	-190.52	-62.69	Anisotropy of waste rock materials increased from 0.1 to 1.0
SENS2	-97.79	-55.76	15.62	Saturation of three lowest layers in waste rock (4.5 m) changed from 0% to 100%
SENS3	-261.76	-180.18	-40.89	Reduce unsaturated porosity from 0.3 to 0.15
SENS4	-261.76	-105.05	-12.78	Reduce unsaturated porosity from 0.3 to 0.05
SENS5	-261.76	-204.41	-82.45	Increase unsaturated porosity from 0.3 to 0.4
SENS6	-262.18	-198.46	-56.42	Reduce saturated hydraulic conductivity (K) of waste rock from 4 to 2 m/day
SENS7	-261.76	-203.29	-149.91	Reduce saturated hydraulic conductivity of waste rock from 4 to 0.5 m/day
SENS8	-261.76	-191.70	-55.57	Modified Unsaturated Materials Properties (Pressure Head vs Rel. K): Abscissa min. increased from -10 to -1
SENS9	-261.76	-191.70	-55.57	Modified Unsaturated Materials Properties (Pressure Head vs Rel. K): Abscissa min. decreased from -10 to -200, max. increased from -0.0001 to -0.01
SENS10	-261.76	-191.82	-55.57	Modified Unsaturated Materials Properties (Saturation vs Rel. K): Abscissa min. increased from 0 to 0.001

that could result in seepage from the WRD (i.e. groundwater pressure at base of WRD > 0 kPa) would be a situation where initial waste rock layers were deposited in a saturated condition. Above water table mining makes this scenario unlikely.

Conclusions

The results of the study indicate that seepage fluxes from the waste rock dump and low-grade ore stockpile are unlikely to occur during the operational period. This is considered primarily due to the low rainfall, high evaporation environment and coarse nature of waste rock deposited.

Acknowledgements

The author thanks SIMEC Mining (Jennifer Gerard and Chris Smyth) for supporting the preparation of this paper and presentation of company information. Thanks are also given to Jennifer Levenick (Golder Associates) for model reviews.

References

Berens, V., Alcoe, D. and Watt E., 2011, Non-prescribed Groundwater Resources Assessment – Eyre Peninsula Natural Resources Management Region, Phase 1 – Literature and Data Review, DFW Technical Report 2011/16, Government of South Australia, through Department for Water, Adelaide.

Drexel, J.F., Preiss W.V. and Parker, A.J., (1993), The Geological Survey of South Australia. Vol. 1, The Precambrian. South Australia. Geological Survey. Bulletin, 54.

Leaney, F., Crosbie, R., O’Grady, A., Jolly, I., Gow, L., Davies, P., Wilford, J. and Kilgour, P., 2011, Recharge and discharge estimation in data poor areas: Scientific reference guide, CSIRO: Water for a Healthy Country National Research Flagship. 61 pp.

Parker, A.J. and Flint, R.B., 2012, Middleback 1:100,0000 Scale Geological Map, South Australian Department for Manufacturing, Innovation, Trade, resources and Energy, Adelaide.

Puhalovich (2018). Critical importance of conceptual model development when assessing mine impacts on groundwater dependent ecosystems: case study of an Australian mine development. Paper presented at IMWA-ICARD 2018, Pretoria, South Africa, September 2018.

Rudd, E.A., 1940, The Geology and Ore Reserves of the Middleback Ranges, South Australia. 26/2/40 1940.

Life-of-mine water management and treatment strategies

Tobias S. Rötting[1], Julia Dent[2], Rene Reyes[3]

[1]*WSP UK Ltd., Shrewsbury, SY1 2DP, UK, Tobias.Roetting@wsp.com*
[2]*WSP UK Ltd., 2 Queen St, Manchester, M2 5JB, UK*
[3]*WSP Peru, Av. Paseo de la República #5895, Miraflores, Lima, Peru*

Abstract

Water management, reuse and treatment are essential components of every mining operation. Integrated numerical models that represent the physical water balance and chemical mass balance of mine-water management systems can be used to predict water availability and chemical quality over the life of the mine.

Supernatant volume and water quality in a TSF during operation and closure was simulated using GoldSim and PHREEQC. Model results indicate that no treatment of TSF water during post-closure will be required, as long as ingress of seepage from the waste rock facility is effectively precluded after closure.

Keywords: Probabilistic models, predictive simulations, uncertainty, treatment costs, life of mine

Introduction

Water is vital for any mining operation. Water affects mineral extraction and processing, stability of pit slopes and mine workings, community relations and potential environmental impacts. Water management, reuse and treatment are essential components of every mining operation. The application of cost-intensive technologies such as reverse osmosis (RO) or nano-filtration is becoming increasingly common in mining operations—driven to a large extent by the requirement for low sulphate and total dissolved solids levels in both process waters and environmental discharges. As both capital expenditure (CAPEX) and operational expenditure (OPEX) of water treatment systems can be substantial (e.g. Dennis and Dennis 2017), adequate planning is essential to minimize costs. Moreover, ill-designed water treatment strategies may lead to compliance problems that are costly and can affect reputation, mine permits and social perception.

A thorough understanding of the site or process water balance and chemical composition at the different locations of the mine water management system (such as process ponds, tailings or waste rock storage facilities, discharge points etc.) is necessary to devise an efficient water reuse and treatment strategy. A major consideration that is frequently overlooked in the design of treatment systems is the long-term evolution of mine or process water quality, which can change dramatically due to either changing ore mineralogy or a progressive build-up of conservative solutes in process-reclaim circuits. Moreover, the volumes of water requiring treatment may also vary considerably with time. Retro-fitting treatment systems to resolve these problems can be more costly than designing for the long term from the outset.

Integrated numerical models to represent the physical water balance and chemical mass balance of mine-water management systems can constitute a powerful tool to avoid such issues and to proactively manage water on site and to design conveyance and treatment infrastructure. These models are used to predict water availability and chemical quality over the life of the mine. They can also be applied to simulate the performance of alternative treatment technologies or water management strategies, to size storage infrastructure and assess the benefits of blending or separating waters from multiple sources within an operation. This article outlines the methodology to construct these models and depicts applications in the mining sector.

Methods

Physical water balance model

The physical water balance model is constructed using the GoldSim software (GoldSim Technology Group, 2014). GoldSim is a flexible program which permits physical mass balance calculations to be performed at any specified point within a mine water conveyance system or a mineral processing circuit. For all such points, referred to as elements, graphic output can be generated with a high degree of self-documentation. Multiple elements performing different functions are also graphically represented and the inter-relationships between elements can be displayed such that it is generally easy to visualize the model structure.

The physical water balance model is focused on the volume of water moving through the system. The movement of chemical mass, associated with the movement of water, is addressed in the same model but as a parallel structure. With the exception of flow-dependent factors related to water quality (such as the calculation of dilution ratios), the physical water balance portion of the model is independent of the chemical mass balance. The chemical mass balance is described below.

Incorporation of uncertainty

A GoldSim model can be designed as a probabilistic, dynamic simulator, running continuously through the historical period and into future mine life in a sequence of time-steps with selected inputs permitted to vary within defined stochastic distributions. The model provides continuity in time through the use of stock elements that track the accumulation of water in the system and allow these to influence other components of the model. Additionally, the model can use a calendar to introduce or vary operational rules at specified points in time, or to simulate seasonal variation of inputs.

As a simulator of a complex system, the GoldSim incorporates uncertainty. Uncertain inputs can include for example future precipitation depths and operational factors such as pit dewatering flows. GoldSim addresses uncertainty by using Monte Carlo simulations to propagate uncertainty through the system. In a Monte Carlo simulation, each uncertain variable is input as a spectrum, based on a probability distribution. The Monte Carlo simulation repeatedly samples the value distribution and repeats the model evaluation with a different set of input parameters during multiple model reruns or 'realizations'. A Monte Carlo simulation will typically run up to 1000 realizations, resulting in a large number of independent results representing a probability distribution for the system.

An important fraction of the uncertainty within a mine site water balance model is often associated with the climatic inputs. Daily precipitation and pan evaporation can be stochastically sampled from probability distributions derived using historic climate data for the site. Other water balance components can also be modelled with stochastic elements, for example to represent the variable availability of pit sump pumps as a result of proximity to active mining areas.

Geochemical mass balance model

The geochemical mass balance model is constructed using the GoldSim Contaminant Transport Module (GCTM). The key inputs to the GCTM comprise concentration values for each parameter of concern or interest at each source-term, for example acid waters or process solutions, including pits, leach pads and waste rock facilities (WRF). The concentration inputs for each source-term are variably included as: (i) constants, (ii) flow-dependent variables, or (iii) partially flow-dependent variables.

Following the assignment of geochemical inputs to each source-term, the GCTM integrates the concentration values for each chemical parameter with flow volumes generated by the GoldSim water balance to yield a chemical mass load. During model execution, the movement of chemical load through the sequence of transport, storage and mixing stages of the model is simulated. At each point of mixing, the GCTM calculates an aggregate mass load for each chemical parameter. This is then divided by the gross water volume to produce an adjusted series of concentration values. Certain chemical reactions, for example precipitation of gypsum when saturation is reached, can also be integrated in the GCTM if these reactions are appropriately transcribed into the model by means of customised lookup tables.

The GCTM functions as an integral subcomponent of the GoldSim water balance model. Thus, the GCTM can perform water quality simulations for an infinite range of scenarios with respect to climatic inputs or facility discharge chemistry and flow permutations.

Presentation of model outputs

Following the execution of any model run, GoldSim can generate results for any model element within the water management system. Denominated 'reporting boxes' permit analysis of temporal trends with respect to virtually any variable within the model structure, for example the volume of seepage emanating from any individual WRF, pregnant solution volumes derived from heap leach pads, or projected variations of discharges from water treatment facilities. The chemical water quality results of the GCTM can also be visualized or exported at each of the 'reporting boxes'.

Typically, probabilistic time-series outputs are exported to Excel, formatted and graphed as flow rates, storage volumes or water chemistries through time. The median value (50% of all values calculated by the model), 5th and 95th percent values within the probabilistic range or even more detailed percentiles can then be easily plotted.

Case Study

The approach was applied at a mine in South America with a net-positive site water balance, where supernatant from the tailings storage facility (TSF) is fully re-used in the process plant during operation, but discharge of excess water to the environment will be necessary after closure (Figure 1). A physical water balance and chemical mass transport model was developed in GoldSim combined with PHREEQC (Parkhurst and Appelo 2013) to simulate and assess different strategies to ensure environmental compliance of any discharged water.

Results and Discussion

TSF Water Balance

Stochastic results for the TSF supernatant volume during operation and closure are shown in Figure 2. Water balance calculations indicate that during operation the supernatant volume fluctuates annually, responding to seasonal variations in rainfall and evaporation and reuse of water for mineral processing. During this period, the probability distribution displays a wide range of possible supernatant volumes, mainly due to the uncertainties associated with random climate input data. After closure, in absence of water abstraction for processing purposes, the stored volume rapidly increases to the maximum design value and any excess water is discharged towards the pit lake via the spillway. This is intended in the closure strategy to form a permanent water cover over the tailings which inhibits long-term sulphide oxidation. There is very little spread in the probability distribution during closure, because rainfall largely exceeds evaporation during most of the year and no other major sinks are affecting supernatant volume.

Water quality predictions

TSF supernatant water quality (pH and sulphate as examples) based on the 50th percentile flows from the TSF water balance is shown in Figure 3. During mine operation until 2022, supernatant pH fluctuates around values of pH 8-9, due to lime introduced with the tailings slurry. After closure in 2023, pH rapidly

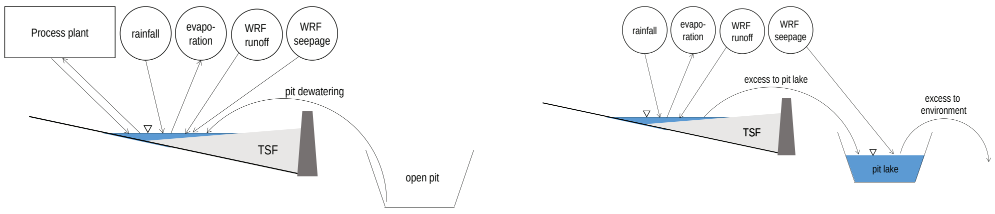

Figure 1 *Schematic case study TSF water balance during operation (left) and after mine closure (right).*

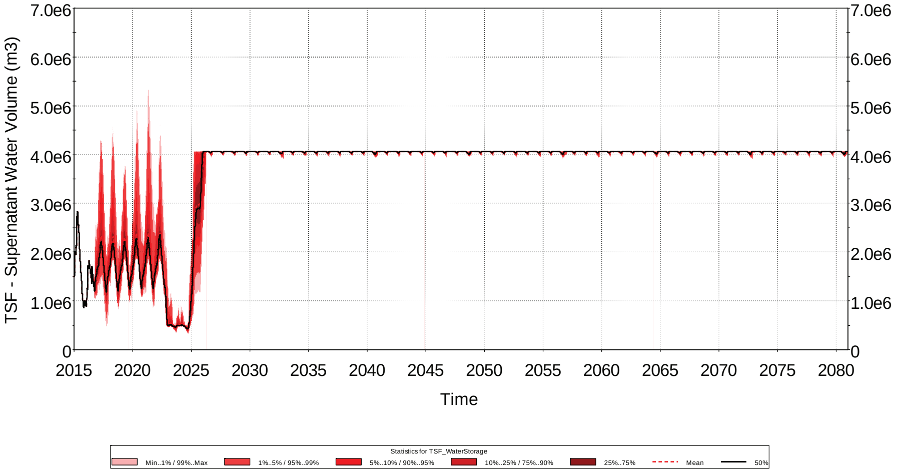

Figure 2 *Stochastic results for the TSF supernatant volume during operation and closure.*

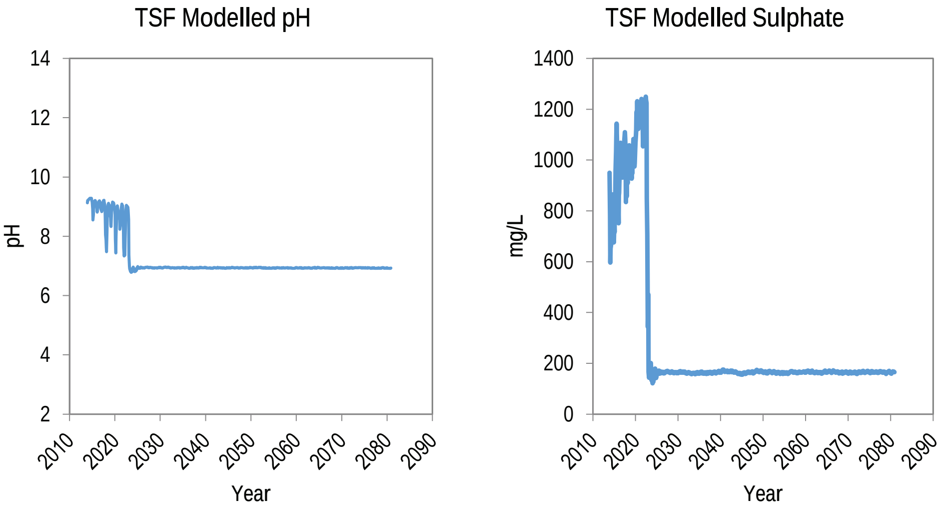

Figure 3 *TSF supernatant water quality predictions.*

stabilises near pH 7. Sulphate concentration increases continually during operation, mainly due to the loading from WRF seepage which grows proportionally to the deposited waste rock mass, plus inputs from the process plant. After closure, as WRF seepage and process waters are no longer routed to the TSF pond, sulphate concentration in the supernatant rapidly falls to less than 200 mg/L. Concentrations of dissolved metals (not shown) are also compliant with regulations after closure, and TSF supernatant is therefore apt for discharge to the pit lake or directly to the environment without treatment.

Conclusions

Water quantities and qualities within a mine water management system can change substantially during mine life as the mine configuration and ore mineralogy evolve. Mine water management, reuse, and treatment strategies that consider these changes result in a solution fit for purpose in the long term. More importantly, a strategic long-term solution avoids the consequences of inadequate planning, which include detrimental or even catastrophic water excess or shortage and costly retro-fitted solutions.

In our case study, results indicate that no treatment of TSF water during post-closure will be required, as long as ingress of seepage from the waste rock facility is effectively precluded after closure. The numerical model helps to define an optimized post-closure water management strategy, to reduce operational and closure risks, and in this case to avoid unnecessary investments (e.g. post-closure TSF water treatment infrastructure).

Integrated physical and chemical water balance models of a mine water management system assist the mining operation in day-to-day operation and strategic mine planning in the long term. Integrating technology and expertise early in the planning cycle can substantially reduce long-term cost.

References

Dennis I, Dennis R (2017) Financial Modelling for Mine Discharge Treatment Options, In: Wolkersdorfer C, Sartz L, Sillanpää M, Häkkinen A (eds.), Mine Water and Circular Economy, Lappeenranta University of Technology, p 649 – 655

GoldSim Technology Group (2014) GoldSim User Guide, GoldSim Technology Group LLC, Vol. 1+2.

Parkhurst DL and Appelo CAJ (2013) Description of input and examples for PHREEQC version 3—A computer program for speciation, batch-reaction, one-dimensional transport, and inverse geochemical calculations: U.S. Geological Survey Techniques and Methods, book 6, chap. A43, 497 p, available only at https://pubs.usgs.gov/tm/06/a43/

Evolving kinetic testing methods to incorporate key dynamic waste rock dump parameters

Ursula Salmon[1], Richard Marton[2], Michael O'Kane[3]

[1]*O'Kane Consultants, 1/11 Collingwood St, Osborne Park, Perth, WA 6017, Australia, usalmon@okc-sk.com*

[2]*BHP, Mineral Australia, 125 St Georges Terrace, Perth, WA 6000, Australia*

[3]*O'Kane Consultants, 200-1121 Centre St NW, Calgary, AB, T2E 7K6, Alberta, Canada, mokane@okc-sk.com*

Abstract

Kinetic testing of reactive mine waste material is a key step for characterising acid and metalliferous drainage (AMD) risk. The recently developed Advanced Customisable Leachate Columns (ACLCs) allow control of key parameters that significantly influence oxidation rates and pore water chemistry in the field. Gas flowrate and composition, temperature, and the water addition regime can be adjusted to better approximate conditions within a waste rock dump. Results of dynamic ACLC testing are compared to free draining leach columns using the AMIRA (2002) method. Data from ACLCs will better inform AMD risk assessment and optimisation of management strategies, while also limiting the need for scaling factors typically required when interpreting kinetic tests for predicting commercial scale seepage water quality.

Keywords: kinetic testing, acid and/or metalliferous drainage, waste rock dumps, geochemistry

Introduction

Exposure of sulfide-bearing mine waste material to atmospheric oxygen may lead to production of AMD. Risk assessment for a site's water quality typically involves subjecting site materials to a series of standardised tests, which focus on geochemical properties of the material, including the oxidation rate of the material (typically expressed in kgO$_2$/m^3/s). Results of such kinetic testing are used in both conceptual and predictive (quantitative) models of how water quality at mine sites will evolve over time.

The two main methods for estimating sulfide oxidation rates are the sulfate release method and the oxygen consumption method (Elberling 1993; Elberling et al. 1994; Hollings et al. 2001; Kempton et al. 2010):

- Sulfate release method – Utilises the relationship between measured sulfate production rate and the necessary oxygen required to enable stoichiometric oxidation of the sulfide mineral (usually pyrite) to estimate the oxidation rate (Elberling et al. 1994; Maest and Nordstrom, 2017).
- Oxygen consumption method – Estimates the sulfide oxidation rate by measuring the decrease in oxygen concentration over time (Hollings et al. 2001).

The sulfide oxidation rate determined by both methods is often presented as the intrinsic oxidation rate (IOR) of a material and is expressed in kg O$_2$/m^3/s.

Current standard kinetic testing methods (humidity cells, ASTM 2012; free draining leach columns, AMIRA 2002) involve assessment via the sulfate release method. However, there are a number of ways in which the experimental conditions for these tests can limit extrapolation of the results to field conditions:

- The reaction rates may be overestimated if there is accumulated sulfate present (e.g., gypsum) in the sample at the start of the experiment or underestimated if flushing events do not release all the sulfate generated (e.g., due to formation of jarosite-type minerals).
- A key control on the reaction is the availability of oxygen throughout the sample during the test; this is rarely measured or

controlled.
- The sample is crushed; this may alter water retention characteristics of the material, which in turn changes oxygen availability, as oxygen diffusion through water is four orders of magnitude slower than through air.
- Crushing of the sample also exposes more mineral surface area for reaction than would be otherwise be available.

Experimental conditions may therefore differ significantly to those that the material will be exposed to in the field, to a degree that is rarely monitored or even considered. Mine wastes at many sites also contain reactive organic matter, which may compete with sulfide minerals for oxygen. The standard testing methods do not allow assessment of this potentially ameliorating effect.

The alternative approach to assessing the reaction rate, through the measurement of oxygen consumption, is the basis of the newly developed Advanced Customisable Leachate Columns (ACLCs). The ACLC configuration specifically allows testing of how materials will respond with different oxygen concentrations and water flow. Irrespective of the way in which the rate is measured, the physical conditions of the kinetic testing can be as important as the geochemical properties of the material in controlling the overall reaction rate. This is because the physical material properties, combined with the water balance over the column, affect the water content in material porespaces, which in turn affects oxygen availability, which is the main driver of the geochemical processes. In ACLCs, physical properties such as the matric potential (suction), humidity, and airflow are controlled and monitored continuously, allowing interpretation with respect to physical as well as geochemical controls on the reaction rates. The ACLCs also have the capacity to hold a larger amount of material with larger particle sizes, which allows the tests to be run using material with hydraulic properties that are the same as, or closer to, those in the field.

This testing is highly relevant for assessing AMD management options for mine sites, as these typically involve altering the physical controls on the reaction rate, through reducing the availability of oxygen for reaction, for example through increasing the degree of water saturation of the material, and/or reducing water fluxes to reduce export of weathering products. In the field this can be achieved by altering waste rock dump (WRD) construction methods and drainage, or placing a cover system on the WRD to limit oxygen and/or water ingress. The information obtained from the ACLC method is therefore directly relevant for assessing impacts of different AMD risk mitigation strategies.

Key features of the flexible ACLC configuration include:
- Up to 25 kg of sample is placed in the column (Figure 1) with, or without, prior further particle size reduction, and flushed with water at a user-defined rate.
- The columns are run in a temperature-controlled enclosure; testing can therefore be performed at conditions that are relevant to the field.
- The gas phase composition in the column headspace/outlet is monitored over time, including for example O_2 and CO_2 concentrations.
- The columns can be flexibly configured to have constant or intermittent airflow, or reaction progress monitored under sealed conditions.
- Critical physical parameters such as the air flowrate, matric potential (suction), humidity, pressure, and temperature are continuously controlled and logged.
- Leachate collection allows assessment via the sulfate release method and oxygen consumption method in parallel. However, as the oxygen consumption method is not dependent upon leachate collection, experiments can be run at much lower liquid:solid ratios, with associated longer residence times, and greater potential for oxygen ingress into partially saturated porespaces, which more closely reproduces the conditions inside many WRDs.

Methods

For this paper, waste rock material (100 kg) was composited (2.9 wt% total S; 1.4 wt% acid soluble sulfate; 88 kg H_2SO_4/t maximum potential acidity; 10 kg H_2SO_4/t acid neutralising capacity) and then divided into ACLCs and AMIRA leach columns. Results in this paper are presented from ACLCs with varied

Figure 1 Advanced customisable leachate columns (ACLCs).

air flowrates as summarised in Table 1. The range of airflow values were selected to represent different oxygen availabilities inside a WRD, based on the WRD construction methodology, for example, low airflow represents lower WRD lift heights (e.g. less than 5 m to 10 m such that material segregation is reduced and/or density of the material is increased); the intermediate (control) airflow represents higher WRD lift heights where the propensity for material segregation increases and density can decrease; and, the high airflow represents relatively unrestricted oxygen supply.

Table 1 ACLC conditions tested

ACLC	Airflow (L/min)
ACLC_10	0.008
ACLC_11	0.06
ACLC_15	0.2

Temperature in the ACLC enclosure was maintained at 35-38°C. Water was added at the start of the experiments, with a target water content similar to that in the field (8-12 wt%). Additional flushing events occurred after 41 weeks and at the end of the experiment (≈65 weeks). Leachate was sent for analysis in order to facilitate geochemical equilibrium calculations, which give an indication as to whether typical secondary minerals are controlling aqueous concentrations. Detailed static geochemical characterisation was also completed on the materials before and after the kinetic tests (not shown).

During the first stages of the column tests the experimental conditions were adjusted as the methodology was fine-tuned, including adjustment of air flow rates and installation of a fan in the temperature-controlled enclosure to allow even heat distribution. Continuous monitoring of the physical and geochemical parameters allows responses to changing experimental conditions to be captured and analysed as the experiment progressed. The results presented below demonstrate that ACLCs can provide insight into how the material may behave under dynamic conditions in the field.

Free draining leach columns based on the AMIRA (2002) method were run on the same material, after crushing of the sample to < 6 mm, compared to 42% >6.7 mm in the original sample placed in the ACLCs. Airflow cannot be varied for AMIRA columns. The AMIRA columns were run at room temperature with heat lamps (150 W) operated for eight hours a day for five consecutive days each week.

Results

Oxygen consumption by organic carbon

In mine waste material that contains organic carbon (e.g., shale) the overall rate of oxygen consumption is a combination of consumption by pyrite and by organic matter. The organic matter oxidation releases CO_2, which was monitored in the control column. Assuming typical stoichiometry of 1 mole CO_2

produced for each mole of oxygen consumed, the CO_2 concentrations indicate that the rate of consumption of oxygen by organic carbon in these samples was more than an order of magnitude lower than the total oxygen consumption rate. For the purpose of this assessment, the oxygen consumption rate was therefore assumed to be predominantly due to pyrite oxidation.

Effect of varied air flowrate

The time series results of suction, oxygen concentration, airflow, and calculated IOR are shown in Figure 2. The suction in all three columns increased over time between wetting events. For these experiments the air entering the columns was passed through a moisture trap, and therefore there was a net export of moisture from the ACLCs. For future experiments, the moisture trap can be replaced with a humidifier, as required.

In the column with the lowest airflow, the water content was still sufficiently high that after the second wetting event, water pooled on the surface of the material in the column, until the standing water was carefully removed some weeks later (Figure 2). The oxidation rate was calculated on the basis of a mass balance over the column as a function of the air flow rates (oxygen resupply). The rate of oxygen consumption is also expected to be a function of the water content, as it affects the oxygen ingress into pore spaces. The causes of the low oxidation rate in the low air flowrate column are therefore likely twofold: low oxygen supply, and water-filled porespaces limiting oxygen transport to sulfide mineral surfaces. By comparison, in the ACLCs with higher airflow and less water in porespaces (as indicated by higher suction), the oxidation rates were higher.

The experiments revealed an unexpected control on the oxidation rate in the higher air flowrate experiment. The oxidation rate began to decease as the suction increased to around 1,000 kPa. Upon replenishment of moisture after the wetting event, the rate increased back to the maximum observed. The process of the rate decreasing as suction increased was repeated during the second drying cycle. Our experience indicates that the suction required to reduce the rate of oxygen consumption in this experiment was greater than those likely to exist in WRDs, which indicates that the rate limitation due to very low water availability (as indicated by high suction) is unlikely to occur in the field.

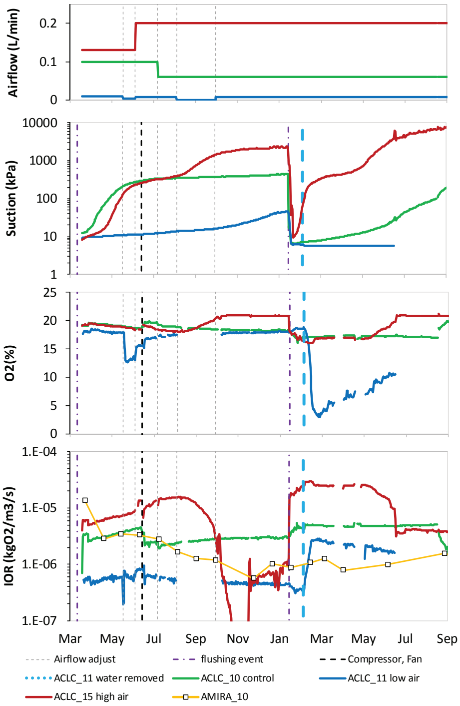

Figure 2 *Time series from (top): Air flowrate, suction, oxygen concentration, and oxidation rate (IOR) for the three ACLCs. Also shown is an oxidation rate for an AMIRA column with the same material (see text for explanation). Vertical lines indicate airflow adjustments, water flushing events, points where the compressor temporarily stopped and a temperature-levelling fan was installed in the enclosure, and when pooled water was removed from the top of ACLC_11 after the second flushing event.*

Comparison with AMIRA column oxidation rates

The oxidation rates determined from the AMIRA column are also show in Figure 2. Similar results were obtained for all AMIRA columns on this material. The decreasing rate over the first part of the experiment may be due to either a gradual release of pre-existing sulfate in the sample or the crushing process may have exposed fresh mineral surface area, the reactivity of which decreases over time (or as very fine particles are depleted); a commonly observed phenomenon in mineral weathering experiments.

For the majority of the duration of the experiment, the rate obtained from the AMIRA column was lower than the rates observed in the ACLCs with intermediate and high air flowrate, other than when the high flowrate experiment was limited by other factors. Given the higher surface area of the crushed material in the AMIRA column, with all else being equal, a higher oxidation rate would be expected in the AMIRA columns than in the ACLCs. However, there are a number of possible explanations for this, including:

- The AMIRA columns had a higher water content, and therefore less oxygen availability.
- Sulfate precipitation occurred within the column, leading to underestimation of IOR.
- Temperature as measured in one of the AMIRA columns varied considerably on a daily basis as a result of the heat lamp cycles, ranging from between below 20 °C to almost 50 °C. However, the daily average was 5-10 °C lower than the ACLC enclosure temperature; temperature is a key factor in geochemical rates.

Calculations with geochemical equilibrium software indicate that leachate from all AMIRA columns were close to solubility equilibrium, with the common sulfate mineral gypsum, indicating that this mineral may be dissolving or precipitating within the column. The oxidation rate, based on the assumption that the sulfate release rate is solely affected by the rate of pyrite oxidation, may therefore be over- or underestimating the true rate, respectively. Changes to the geochemical characteristics of the material before/after the experiment are being further investigated in order to elucidate the processes that have occurred.

Discussion and Conclusions

The new ACLC methodology can capture dynamic responses of geochemical process rates to physical controls (e.g., oxygen availability, water flushing rates) as well as geochemical controls (e.g., S content). The experimental methodology is being continually improved through OKC's R&D team. For example, experiments are currently being run at lower temperature (10°C) on materials from a site with a low annual average temperature; methods are being refined to allow accurate measurement of the correspondingly lower oxygen consumption rates. The flexibility of the ACLC allows experiments to be tailored to best approximate conditions relevant to the field in a range of different climate zones and under a range of different waste rock management options. The ACLC method therefore provides another powerful tool to complement existing methods of kinetic testing for assessment and mitigation of AMD risks.

References

AMIRA (2002) ARD Test Handbook - Project P387A Prediction and Kinetic Control of Acid Mine Drainage. AMIRA International Limited, Melbourne, Australia.

ASTM (2012) D5744 - 12 Standard Test Method for Laboratory Weathering of Solid Materials Using a Humidity Cell.

Elberling B (1993) Field Evaluation of Sulphide Oxidation Rates. Nordic Hydrology 24, 323-338.

Elberling B, Nicholson RV, Reardon EJ and Tibble P (1994) Evaluation of Sulfide Oxidation Rates - A Laboratory Study Comparing Oxygen Fluxes and Rates of Oxidation-Product Release. Canadian Geotechnical Journal 31, 3, 375-383.

Kempton H, Bloomfield TA, Hanson JL and Limerick P (2010) Policy guidance for identifying and effectively managing perpetual environmental impacts from new hardrock mines. Environmental Science and Policy 13, 6, 558.

Hollings P, Hendry MJ, Nicholson RV and Kirkland RA (2001) Quantification of oxygen consumption and sulphate release rates for waste rock piles using kinetic cells: Cluff lake uranium mine, northern Saskatchewan, Canada. Applied Geochemistry 16, 1215-1230.

Maest AS and Nordstrom DK (2017) A geochemical examination of humidity cell tests. Applied Geochemistry 81, 109-131.

Contribution of data analysis for the environmental study of post-closure coal ash landfill

Renata Santos[1], M. Cristina Vila[1,2], António Fernandes[1], Sara Guimarães[1], Diana Ferreira[1], António Fiúza[1,2]

[1]*Mining Engineering Department, Faculty of Engineering, University of Porto, Rua Dr. Roberto Frias, 4200-465 Porto, Portugal, rgsantos@fe.up.pt*
[2] *CERENA, Faculty of Engineering, University of Porto, Rua Dr. Roberto Frias, 4200-465 Porto, Portugal*

Abstract

To support future remedial decisions on a coal ash landfill a hydro-geochemical characterisation program assessing the metal leaching and acid rock drainage potential has been performed.

Several studies on the field and laboratory were carried out to characterise bedrock, soil, coal ashes and water in the landfill area.

The application of advanced data analysis tools allowed highlighting relationships between variables that contribute to the understanding of groundwater contamination, which is not possible to detect through the basic periodic monitoring procedures.

Keywords: Acid drainage, coal ash landfill, groundwater contamination, remediation solutions.

Introduction

During most of the 20th century, the burning of coal was the most important source of energy in Western Europe. The lack of environmental regulations allowed the disposal of the wastes from thermal power plants without any special precautions. The characteristics of ash landfills are very heterogeneous, since they depend on: a) the physical, chemical and mineralogical properties of the coal; b) burning conditions; c) disposal technologies; d) climate, geological and hydrogeological conditions of the region in which they are inserted (Dellantonio et al. 2008; Haynes 2009; Pen-Mouratov et al. 2014; Krgović et al. 2015; Voltaggio et al. 2015). Thus it is not possible a generalisation of the type of mitigation measures to be implemented. Nowadays, coal ash landfills constitute an environmental concern under current European legislation.

The present work deals with the evidence of groundwater contamination (acid drainage and high levels of sulfate, aluminium, manganese, zinc, iron and nickel) revealed by the periodic monitoring that has been carried out since the closure of a coal ash landfill in Portugal. Thus, an assessment plan was established to understand what measures should be taken to support future remedial decisions for coal ash landfill. A geochemical characterisation program assessing the metal leaching and acid rock drainage potential was also performed.

Materials and Methods

Study area

The Coal ash landfill area is located in the north of Portugal. Since the middle of 20th century, the area was extensively used to deposited coal combustion products without effective environmental care system to protect soils and groundwater. The landfill (confidential location) occupies about seven ha area and was built on hillside slope upon a water line that drains away to the main river. After the closure of the thermoelectric power plant, the landfill was sealed. It has been the target of environmental monitoring since then with the installation of a piezometric control network, comprising 5 piezometers (Pz1, Pz2, Pz3, Pz4, and Pz5), 1 discharge point at the base of the landfill (FC) and 1 monitoring point in the receiving river from the landfill (RD) (fig. 1).

The geological characteristics of the area consist of a unit of schist and greywackes. In hydrogeological terms this unit is essentially a homogeneous and impervious unit, consti-

Figure 1 *Location of the piezometers and core drills plotted in an aerial view of the study area.*

tuting an anisotropic fractured medium that does not define a regional aquifer. The coal burned in the thermal power plant was anthracite of variable composition, nevertheless with a high content on ash and sulphur.

Fieldwork

To better characterise bedrock, soil, coal ash, and surface and groundwater in the landfill area, new field works were needed. Thus, the fieldwork involved a drilling campaign of four boreholes (S1, S2, S3 and S4) to core sampling and the construction of two new piezometers (Pz6 and Pz7) (fig. 1). Water sampling campaigns in all the piezometers available (seven), periodic measurements of piezometric heads and permeability in situ tests were also done. The water samples were then sent to an independent laboratory for analysis.

Laboratory work

A total of 15 solid samples were taken from the cores at different depths (PZ6S, PZ6B, PZ7S, PZ7I, PZ7B, S1S, S1I, S1B, S2S, S2I, S2B, S3S, S3B, S4S and S4B); plus four composite samples representing the drilled cores (S1c, S2c, S3c and S4c) were submitted to several characterization laboratory tests, namely: elemental chemical analysis, total organic carbon content (TOC), particle size distribution, scanning electron microscopy (SEM-EDS), respirometry, natural dynamic and percolation leaching as well as static and kinetic acid generation potential tests. All the samples were oven dried at 105 ° C for 24 hours and after that partitioned with the aid of a Jones separator and stored in sealed containers for use in subsequent laboratory tests. Firstly, they were submitted to chemical analysis by X-ray fluorescence by dispersive energy, using INNOV-X-SYSTEM portable equipment, model α-4000S. Only the samples (S1S, S1I, S1B, S2S, S2I, S2B, S3S, S3B, S4S and S4B) from the drill cores reproduce the natural material as found in the landfill area were submitted to granulometric analysis by dry sieving. From the fractions passed on the 200 mesh screen, small samples were taken for analysis of fines on a Malvern Mastersizer 200 laser granulometer with Hydro 2000 G module.

Samples S1c, S2c, S3c and S4c were subjected to natural leaching tests according to NEN-EN 12457. The results of the short-time leach tests (24 and/or 48 h) in addition to allowing the identification of the fastest soluble components, complement the tests for the determination of acidic drainage (static and dynamic). In the dynamic leaching experiments performed, 100 g subsamples of the samples S1c, S2c, S3c and S4c were taken and were stirred for 24 h in distilled water, in a solid/liquid ratio of 1/10 (w/v). After 1, 3, 12 and 24 hours of agitation, the physicochemical parameters of the liquid phase (pH, conductivity, TDS and salinity) were measured. This procedure was also applied to subsamples from the samples PZ6B and PZ7B, and only continuous leaching was carried out without measurement of the initial parameters to produce leachate and to analyse its properties.

Static acid generation capacity (NAG) tests were performed for all solid samples, after milling until to have ≤ 75 µm in mean size. The Acid Generation (NAG) tests consist of oxidising 2.5 grams of sample. Due to the oxidation of the sulphides, sulfuric acid is formed assuming that all the acidity produced is due to this phenomenon and the neutralising particles reduce the acidity produced. After oxidation, a titration with NaOH is carried out to quantify the acidity produced in the form of kg of sulfuric acid per ton of sample (Stewart et al. 2006). In addition to NAG at pH 4.5 and 7.0, NAPP (Net Acid Producing Potential) was also determined for all samples. NAPP allows quantification of the neutralization capacity of the samples, although the NAG tests considering the neutralization effects of the sample, do not allow its quantification. The graphical representation of both allows to classify the products tested in one of three categories: NAF - Non Acid Forming for the case of a negative NAPP and a pH above 4.5 in the final NAG; PAF - Potential Acid Forming reveal acid generation in both tests - NAG pH below 4.5 and a NAPP positive; or UC - Uncertain to classify samples that the acid production is not clear). Typically, samples classified as UC require further analysis, and samples classified as PAF are likely to have a high sulfur concentration. Dynamic tests of acid generation potential in columns were also performed for the composite samples of the drilled cores (S1c, S2c, S3c and S4c). Dynamic tests are distinguished from static tests in that they attempt to simulate the natural oxidation reactions occurring in the field by using a larger amount of sample (ranging from 100 g to 2 kg) and the creation of several cycles of wetting and drying during the period of several days of the test to pattern the field meteorological conditions. The duration of these tests cannot be standardized due to the heterogeneity of the natural materials (mineralogical composition, porosity, permeability, *etc.*). The dynamic tests consisted of maintaining 100 grams of sample in an acrylic column, alternately submitting to 6 cycles of humidification and drying, for 12 days. In the humidification cycles, distilled water was percolated into the column, measuring the properties of the leachate at the end of the percolation. The drying cycles consisted of drying the solid material contained in the column immediately after a humidification cycle by injecting compressed air.

Data treatment and multivariate statistical methods

Exploratory data analysis and Principal Component Analysis (PCA) techniques were used to reveal the correlation structure of the variables allowing characterisation and interpretation of main processes affecting the study area.

Results

The field surveys made possible to identify three distinct layers in the landfill area: ash landfill, yellow schist and grey schist (fig. 2). The layer corresponding to the ash landfill is naturally thicker at the sites of Pz3, Pz4 and Pz7 because they are within the landfill area. The presence of ash in the Pz2 and Pz5 surveys, which are outside the landfill area, may be due to the various terrain modelling that have been performed over time in that area. Pz1 and Pz6 piezometers are located outside the landfill's influence zone, and their monitoring was carried out to know the regional background values of waters, soils and rocks. The values obtained were compared with other published studies of the hydrogeochemical background of the region. The water table is varied (fig 2). The recharge waters percolate the entire thickness of the landfill until they reach equilibrium in the yellow altered schist layer which is more permeable than the grey schist stratum that is underneath.

Particle size analysis allowed classifying the coal ashes as silt-sandy material (fig. 3a). Although the obtained grain-size curves show a well-balanced distribution of the particle diameter, in the surface samples is possible to verify the predominance of coarser grain size whereas the deeper samples possess much finer particle diameters.

The elemental composition obtained by XRF of the samples representative of the core drills (S1c, S2c, S3c and S4c) and the rock substrate (PZ6B and PZ7B) revealed the predominance of sulfur and iron (indicators of sulfides in the mineral matrix), besides the common elements of rock matrices such as K, Ca and Ti, must be noted. The samples have an identical average chemical composition regardless its depth and location. However, the values of arsenic and lead, which are an exception to this standard, are higher in ashes than those on the rock substrate.

Coal ash composition depends on parent coal rock and coal combustions' method (Valentim et al. 2018). SEM analysis performed on two samples - one representing the rocky substrate and the other the coal ash – recognise diverse morphotypes constituents. Coal ash sample has an elevated concentration of neoformation minerals like aluminosilicate glass (spheres or irregular shapes), glassy silica spheres and Fe-Ti oxides. Coal, which has not undergone combustion, has an irregular and angular shape, just like the primary min-

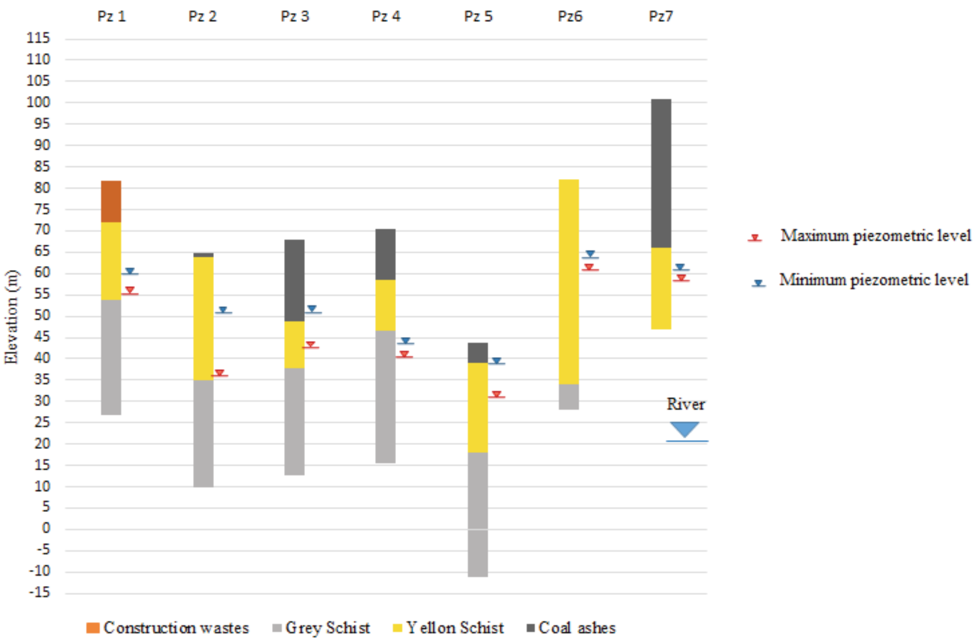

Figure 2 *Distinct layers identified in log core and maximum and minimum piezometric levels recorded during monitoring (years 2012-2016) for the piezometers.*

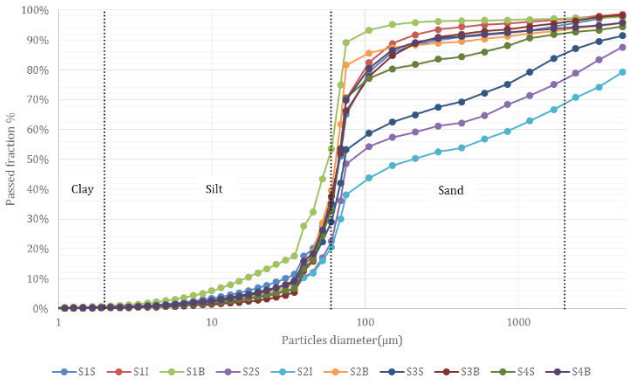

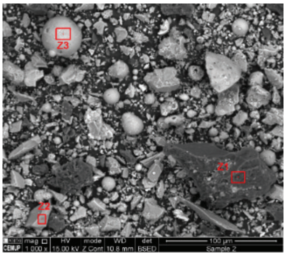

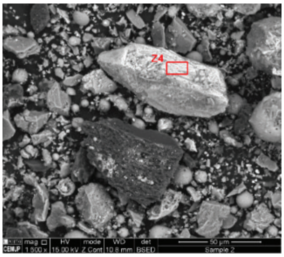

Figure 3a) *Particle size distribution. b) Microphotographs of the coal ash samples. 1: Z1 - Unburned carbon; Z2 - particle consisting essentially of aluminium, silicon, oxygen and iron; Z3 - Vitreous sphere consisting essentially of silica; 2: Z4 - titanium oxide.*

erals that have resisted combustion (fig. 3b).

The results of the TOC analysis of solid samples revealed a high percentage of organic carbon in the ashes as opposed to their absence on schists (samples PZ6S, PZ6B and PZ7B). The static NAG tests to which the 19 solid samples were submitted showed results that point to moderately acidic materials. From the results of ANC and MPA (Maximum Potential Acidity, based on the sulfur content of the samples), it was possible to calculate the NAPP (Neutralizing Acid Production Potential), whose comparison with the NAG allowed to classify the samples in the quadrant chart. All samples tested fell in the first quadrant of the graph that classified them as potentially acid forming (fig. 4).

The multivariate statistical analysis applied monitoring water parameters are summarized in figure 5. The left plot (fig. 5a) shows

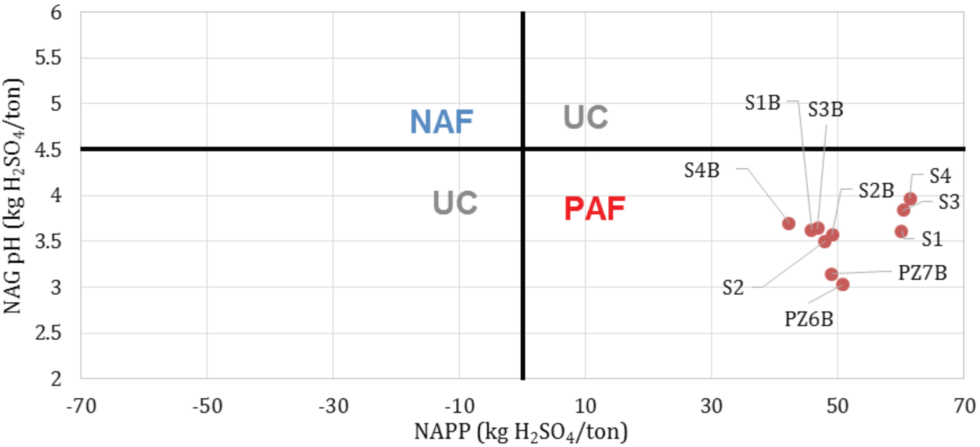

***Figure 4** Results of NAG and NAPP tests allowed to classify both ashes and schists as potentially acid-forming materials.*

the projection of variables on the first factorial plan. F1 represents 75% of the variation of the matrix data. This axis shows an opposition between electric conductivity (EC), SO_4^{2-}, Al, Fe, Mn, Zn, Cu and Ni (negative side) and pH (positive side). This negative correlation is typically observed between pH and concentrations of many metals and metalloids, base cations and sulfate in mine water (Banks 2004).

Figure 5b shows the projection of the water samples on the first factorial plane. It allows distinguishing different levels of contamination: groups A and B include the piezometers with higher contamination (Pz3 and Pz4); group C represent the variation of discharge point at the base of the landfill and group D contain the monitoring points were contamination is lower or does not exist. According to the interpretation of the 1st factorial plan, the contaminated sites are on the negative side of F1.

PCA results for the variables determined on solid samples are present in figure 6. In respect to variables (fig. 6a) is noticeable the group form by acid forming elements (S, Fe and Cr). Figure 6b it is possible to distinguish bedrock (Pz6B and Pz7B) from ashes (S1, S3 and S4).

Conclusions

The chemical characteristics of groundwater are strongly influenced by the presence of the landfill and the pathway through it. The highest anomalous concentrations are found in discharge point at the base of the landfill (FC) and in the piezometers located inside the landfill (Pz3, Pz4 and Pz7). The analysis by SEM-EDS allowed distinguishing the min-

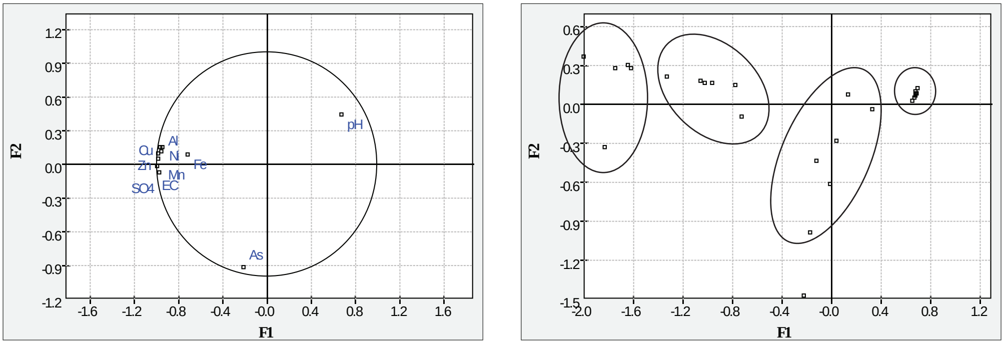

***Figure 5a)** Projection of variables on the 1st factorial plan; b) Distribution of different water samples on the 1st factorial plan*

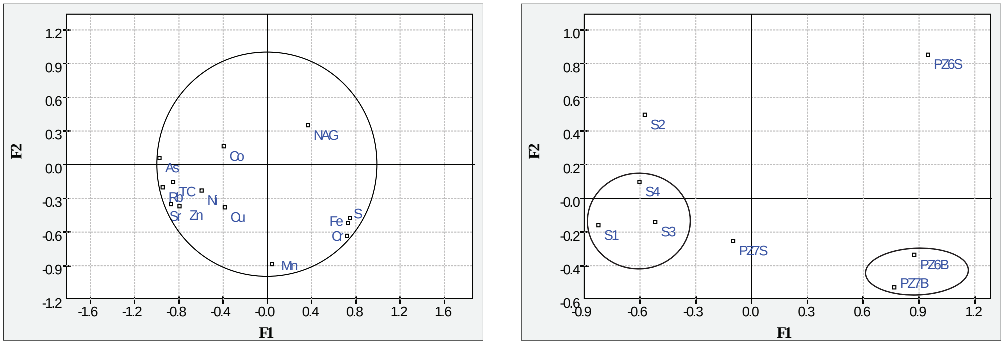

Figure 6a) *Projection of variables on the 1*st *factorial plan;* ***b)*** *Distribution of different solid samples on the 1*st *factorial plan*

erals of neoformation from the primary minerals and the unburned coal. The analysis of the total carbon and the inorganic carbon in the solid samples showed a high concentration in the ashes that contrasts with the low concentrations of the rocky substrate. The tests of acid generation potential performed on 19 samples show moderately acidic materials. Multivariate statistical techniques are a good approach to the identification of hydrogeochemical variations in a dataset.

This technique allowed to delimit the contamination of the waters by acid drainage spatially and to associate the elements that are related to the same one.

References

Banks D (2004) Geochemical processes controlling minewater pollution. In: Groundwater Management in Mining Areas. Proceedings of the 2nd IMAGE-TRAIN Advanced Study Course, Pécs, Hungary, Umweltbundesamt, Vienna, 17-44.

Dellantonio A, Fitz WJ, Custovic H, Repmann F, Schneider BU, Grünewald H, Gruber V, Zgorelec Z, Zerem N, Carter C, Markovic M, Puschenreiter M, Wenzel WW(2008) Environmental risks of farmed and barren alkaline coal ash landfills in Tuzla, Bosnia and Herzegovina. Environmental Pollution 153(3): 677-686.

Haynes RJ (2009) Reclamation and revegetation of fly ash disposal sites – Challenges and research needs. J. Environ. Manag. 90(1): 43-53.

Krgović R, Trifković J, Milojković-Opsenica D, Manojlović D, Marković M, Mutić J (2015) Phytoextraction of metals by Erigeron canadensis L. From fly ash landfill of power plant “Kolubara”. Environmental Science and Pollution Research 22(14): 10506-10515.

Pen-Mouratov S, Shukurov N, Yu J, Rakhmonkulova S, Kodirov O, Barness G, Kersten M, Steinberger Y (2014) Successive development of soil ecosystems at abandoned coal-ash landfills. Ecotoxicology 23(5): 880-897.

Stewart WA, Miller SD, Smart R (2006) Advances in Acid Rock Drainage (ARD) Characterisation of Mine Wastes. Proceedings of the 7th Int. Conf. Acid Rock Drain. 2006, ICARD, 3: 2098 - 2119.

Valentim B, Biatecka B, Gonçalves PA, Guedes A, Guimarães R, Cruceru M, Całus-Moszko J, Popescu L, Predeanu G, Santos A (2018) Undifferentiated Inorganics in Coal Fly Ash and Bottom Ash: Calcispheres, Magnesiacalcispheres, and Magnesiaspheres Minerals 8:140

Voltaggio M, Spadoni M, Sacchi E, Sanam R, Pujari PR, Labhasetwar PK (2015) Assessment of groundwater pollution from ash ponds using stable and unstable isotopes around the Koradi and Khaperkheda thermal power plants (Maharashtra, India). Sci. Total Environ. 518-519: 616-625.

Temporal Variability and Gas Transport Rates in Waste Rock ©

Mark Steinepreis[1], Richard T. Amos[2], David W. Blowes[3], Marek Stastna[3],
Ward Wilson[4]

[1]*Stantec Consulting Ltd., Waterloo, Ontario, Canada*

[2]*Department of Earth Sciences, Carleton University, Ottawa, Canada.*

[3]*Department of Earth and Environmental Sciences, University of Waterloo, Waterloo, Canada.*

[4]*Department of Geotechnical and Geoenvironmental Engineering, University of Alberta, Edmonton, Canada.*

Abstract

The production of acid mine drainage through the oxidation of sulfide minerals requires a constant supply of oxygen gas to proceed. Poor water quality on mine sites is therefore influenced by gas transport rates through mine waste, for which few studies currently exist. A field-based investigation was carried out into gas transport mechanisms and rates through a waste-rock pile with a low permeability till cover.

The results of the field monitoring of a waste rock pile at Detour Gold Corporation mine (Detour) in northern Ontario, Canada are presented. The relationship between external and internal gas pressure is indicated to be linear, indicating that advective flow is laminar through the cover and waste rock pile. Sub-atmospheric O_2 pore gas concentrations and super-atmospheric CO_2 concentrations were recorded within the pile, indicating that sulphide oxidation and carbonate neutralisation are occurring. Temperature monitoring in the pile indicates increased dampening of variations in ambient temperature inside the pile and some insulation from the frozen cover in the winter.

Introduction

Consumption of O_2 gas through acid producing reactions reduces the O_2 concentration in the pore gas of waste rock piles to sub-atmospheric levels, and advective (pressure driven) and diffusive (concentration driven) mechanisms contribute to the transport of O_2 from the atmosphere into the pile (Pantelis and Ritchie 1992; Amos et al. 2009; Chi et al 2012). It follows that a possible strategy to reduce the production of AMD and poor quality seepage from mine wastes could be to reduce O_2 gas ingress through low permeability covers.

A field based investigation into gas transport mechanisms and rates has been carried out for an historical waste-rock pile at Detour. Production at this mine was during 1983-1999 (recommenced in 2013) and a low permeability cover was installed on the test pile at the end of operations. The waste rock pile at Detour provides a unique opportunity to consider waste that has been oxidising for approximately 30 years.

Methods

The study site for the gas transport investigation was a waste rock pile from historic operations at Detour Gold Corporation mine, Ontario, Canada. Two boreholes (BH2011-3-1 and BH2011-3-2) were drilled on an approximately north-south axis on the crest of the waste rock pile during 2011. Soil moisture and temperature measurement probes (ECH2O probes and thermistors) were installed at several depths during the completion of the boreholes. In addition, ¼” LDPE tubing was installed to several depths for monitoring of pore-gas concentrations (Figure 1).

The magnitude of the pressure gradients, pore-gas concentration of O_2 and CO_2 as well as the wind speed and direction, barometric pressure and temperature were measured. The pile was instrumented to record exterior gas pressures and pore-gas concentrations at the surficial location of BH2011-3-1, and 12 locations around the pile. The ¼” tubing that was installed within the boreholes dur-

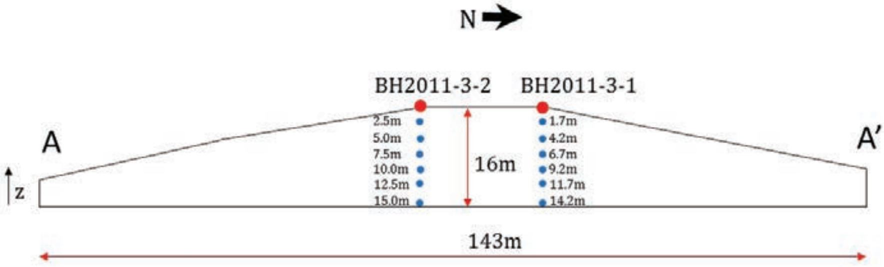

Figure 1 *Cross-section schematic of the waste rock pile and the monitoring locations for internal pressure and pore-gas concentrations.*

ing 2011 was used to record measurements within the pile.

A measurement of barometric pressure was taken on the crest of the pile, and the other pressure measurements were taken relative to this location (hereby referred to as differential pressure) (Figure 1). A wind sensor was mounted to the apparatus, and measurements of temperature within the pile were recorded using the ECH$_2$O probes and thermistors that were installed in 2011.

Measurements of wind vector and exterior and interior pressure were taken at 4 second intervals. The data capture program recorded average measurements at 1 minute intervals, to average out erratic data. These data were averaged to 10 minute and daily intervals to reduce the size of the data set. A measurement was recorded for gas O$_2$ and CO$_2$ once per day, and measurements for temperature were recorded every 6 hours. Data collection was from May 2014 - November 2015, however the quality of the data set is better during the summer months than the winter.

Results and Discussion - External and Internal Pressure

Mean wind speed over the monitoring period was 3.56 m s^{-1}, with a median of 3.32 m s^{-1} and a standard deviation of 1.97 m s^{-1}. The maximum observed wind speed was 15.55 m s^{-1}.

The relationship between wind speed and differential pressure measured on the pile surface is typically parabolic as predicted by Bernoulli's fluid flow principal (Bird 1960). Figure 4 presents a plot of the wind speed versus differential pressure at the southern toe; some outlying data is indicated, however the differential pressure was between 0 and 18 Pa at a wind speed of 5 m s^{-1} and was between 15 and 25 Pa at 10 m s^{-1}.

The mean barometric pressure over the monitoring period was 979.3 hPa. The barometric pressure data was noted to vary by up to 2000 Pa (20 hPa) over the course of a day, however differential pressures both around the exterior of the pile and within the pile was typically within ±10Pa at any time. Changes in barometric pressure are reflected within the pressure regime within the pile, even at depths beyond 15m.

Average external differential air pressures increase towards the toe of the pile. Average differential pressures was typically 0.5 Pa near the crest of the pile and 4-5.9 Pa at the toe. The exception was the western side of the pile, which had an average differential pressure of 2.4 Pa towards the middle of the batter and 1.7 Pa at the toe.

Positive and negative values were observed at internal monitoring points. Negative internal differential pressure indicated flow into the pile at that time, and positive internal differential pressure indicated outward flow. Positive internal differential pressure was indicative of decreasing barometric pressure. The differential pressure within the pile is positive for a greater amount of time during the winter (37.5% on average) than the summer (78% on average).

A linear relationship is typically observed for the external and internal pressures for summertime readings (Figure 5). The Pearson's correlation coefficient is typically higher for the comparison between an internal monitoring location and the exterior toe of the embankment versus towards the crest, and is also typically higher for the daily aver-

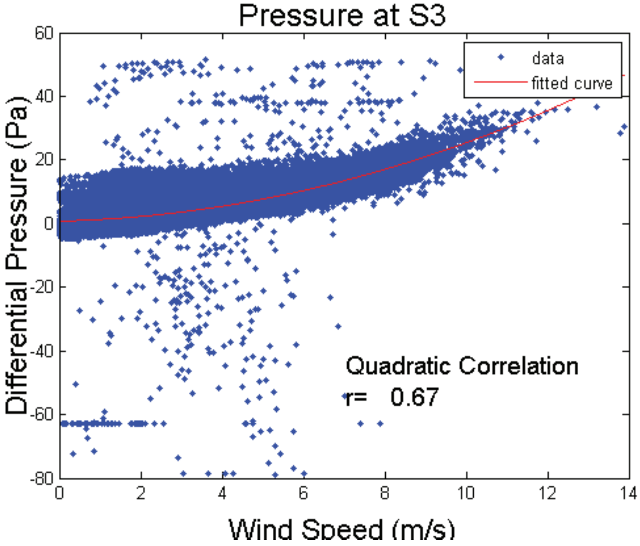

Figure 2 *Correlation between wind speed and differential pressure at the southern toe.*

aged data than the 10 minute averaged data. The linear relationships between external and internal pressure indicate that gas transport through the cover and waste-rock is laminar, and therefore Darcy's law is applicable. This observation is in agreement with the observations of Chi et al. (2013).

Pore Gas Oxygen Content

Pore-gas O_2 content was typically sub-atmospheric at all monitoring locations, indicating that sulphide oxidation is occurring and the rate of ingress of atmospheric O_2 is insufficient to return the pile to a fully oxygenated state. The pore gas concentration within the waste-rock fluctuated to a larger degree during the summer than the winter. Fluctuations in the O_2 content of up to 8% v/v were observed over the course of 24 hours during the summer (Figure 4). Trends in the time series of the different monitoring locations were similar in the summer, and a decreasing trend with depth was evident (Figure 4). The O_2 content at the base of the pile was relatively constant in the winter and summer, below 5% v/v, however this location was likely within the natural underlying peat and not the waste rock material.

A linear O_2 profile with depth has been described as an advective dominated system (Lefebvre et al. 2001). This profile was observed during the summer (Figure 5d), indicating that the permeability of the cover was insufficient to provide a barrier to advective transport. Particle size distribution test results provided in Cash (2014) indicate that the percentage of fines (passing the 75µm sieve) was less than 20% for most samples of the cover material, which is considered to be low for a mine waste cover. A typically diffusive profile was observed during the winter (Figure 5a and b) and the month of July is considered to be part of the transition months (Figure 5c).

Pore Gas Carbon Dioxide Content

Pore-gas CO_2 content was above atmospheric levels (effectively above zero in the context of this investigation) at all monitoring locations, indicating that carbonate neutralisation of acidic solution is occurring within the pile. The trends in pore-gas CO_2 content were similar to the O_2 in that they were variable during the summer (Figure 6a) and relatively constant during the winter (Figure 6b). However, an increasing trend with depth was indicated which is the contrasting observation for the O_2 content.

Temperature

Heat is transported within waste-rock piles through conductive and convective mechanisms, and advective flux of air/gas is in the di-

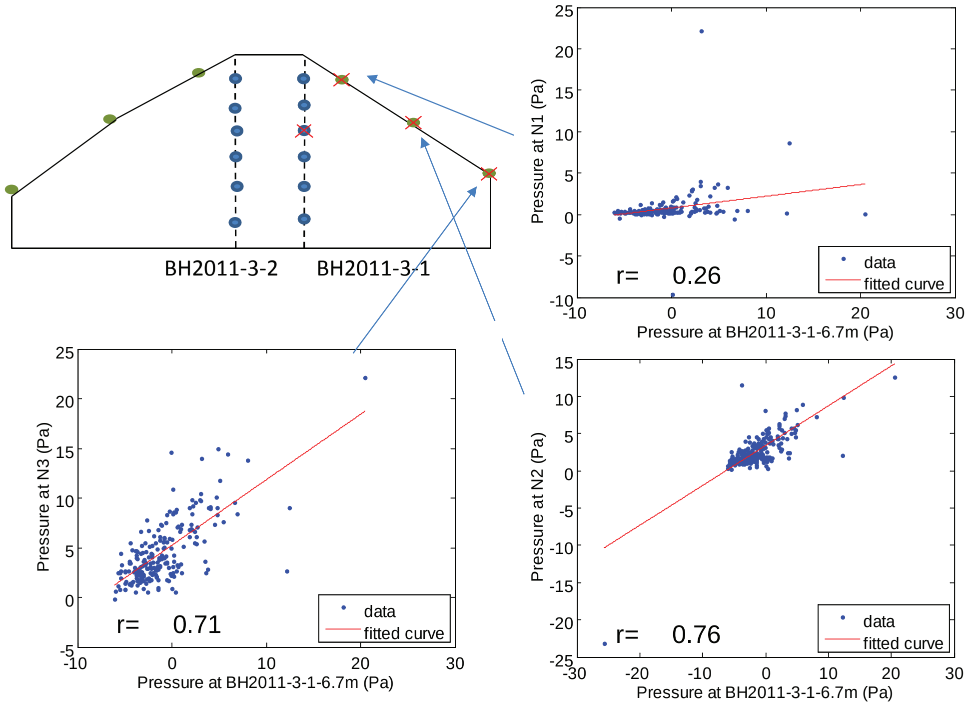

***Figure 3** Correlation between the internal pressure at BH2011-3-1-4.2m and a) external location N1 (crest), b) external location N2 and c) external location N3 (toe). Daily averaged data sets. The data sets are predominately summer-time data but does include winter-time data as well.*

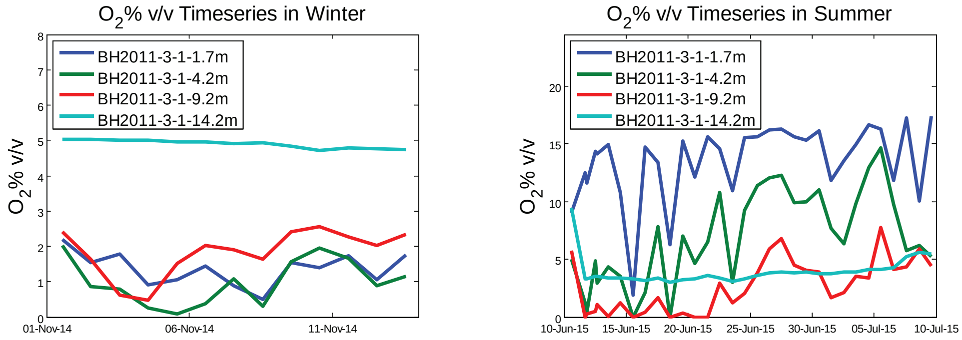

***Figure 4** Time series for pore-gas oxygen content during a) a period in the winter and b) the summer.*

rection of increasing temperatures. Soil covers are a poor conductor of heat in comparison to the waste-rock (Pham 2013), and will therefore reduce heat influx into the waste-rock pile during those times when the exterior temperature is higher than the internal temperature. Conversely, and undesirably, soil covers retain heat within the pile when the internal temperature is greater than the external temperature. The winter conditions at Detour and northern Canada in general are such that the cover will likely freeze and the permeability will subsequently reduce, thereby reducing the advective influx of air. Nonetheless, the timing of the maximum and minimum temperatures within the pile does not necessarily correspond with

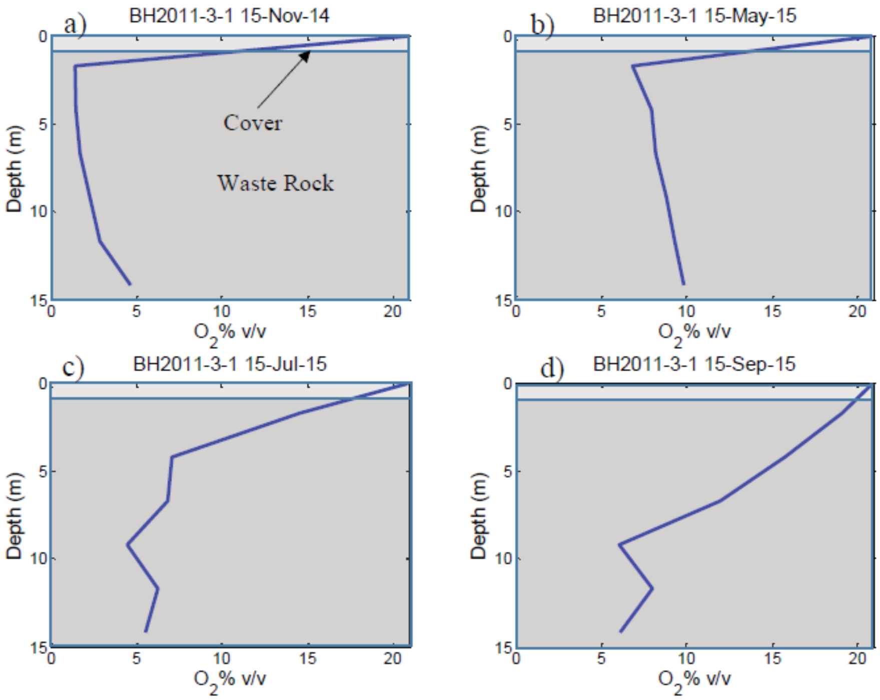

Figure 5 *Pore-gas oxygen content with depth for a) typical diffusive profile during the winter on a) 15t November, 2014, b) 15th May, 2015, c) transition period including both the advective and diffusive profile on 15st July, 2015 and d) typical advective profile during the summer on 15st September, 2015*

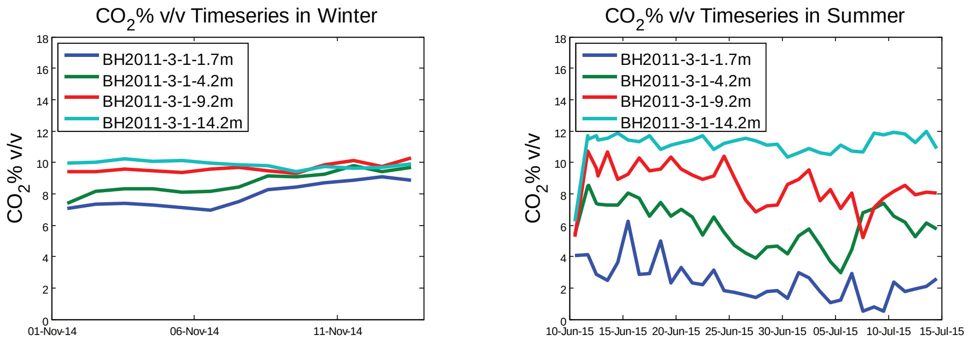

Figure 6 *Time series for pore-gas carbon dioxide content during a) a period in the winter and b) the summer.*

the summer and winter seasons due to time factors in heat transport and the insulating nature of the cover. The peak temperature at 9.18 m depth is around mid-January, which is in the middle of winter.

The temperature was monitored within the cover and the waste-rock at the test pile. The temperature profile of the locations within the cover indicates the magnitude of the seasonal fluctuations is reduced compared to the ambient temperature (Figure 7). This effect is greater during the winter as indicated by the lower rate of change of temperature. The frozen cover in the winter has a relatively

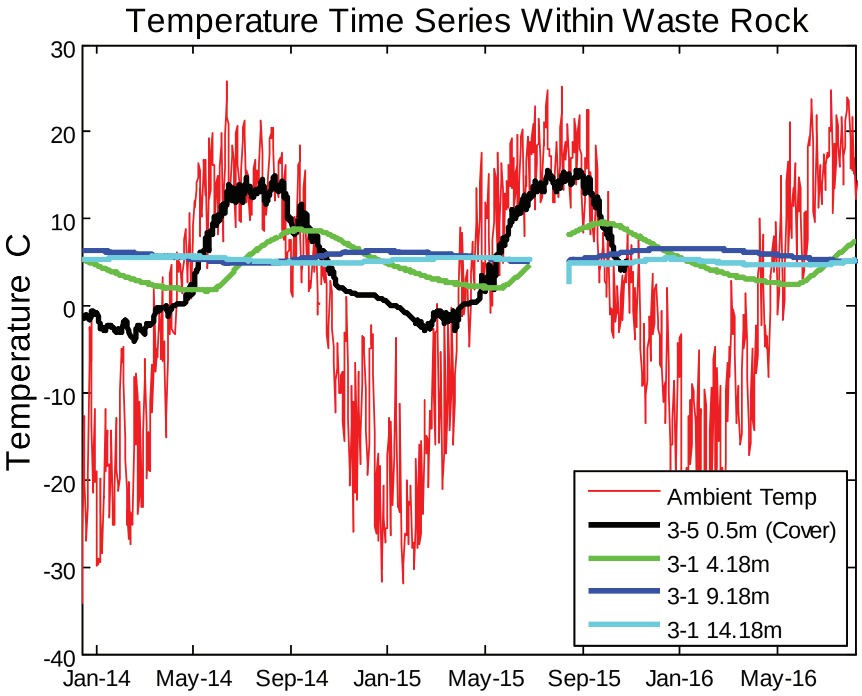

Figure 7 Time series for the ambient temperature and temperature within the cover and waste-rock at WRS#3.

higher insulating capacity and lower permeability. Within the waste rock, the amplitude of the temperature fluctuations reduces further into the pile (Figure 9).

The temperature regime in the pile affects gas pressures according to the ideal gas law. It follows that a complete understanding of the pressures and flow of gas through a waste rock pile cannot be achieved without concurrent temperature monitoring.

Conclusions

Field monitoring for gas transport through the covered waste rock pile indicates that laminar advective flow of gas is the dominant mechanism under summertime conditions, however diffusive flows prevail in the winter. Sulfide oxidation and carbonate neutralisation are occurring in the pile as indicated by sub-atmospheric O_2 contents and super-atmospheric CO_2 concentrations. Monitoring of pile internal temperatures indicates that dampening of fluctuations in ambient temperature occurs with depth, and the cover is likely reducing heat influx in the summer and insulating heat production in the winter.

Acknowledgements

A thank you is extended to Detour Gold Corporation for the funding contributions and the logistical assistance to allow me to collect my field data. I also thank the co-authors of this paper and the entire Earth Sciences team at the University of Waterloo. I express my gratitude to the Tshwane University of Technology (TUT) for hosting ICARD | IMWA | MWD 2018, and to all involved in the organisation of the conference.

References

Amos R, Smith L, Neuner M, Gupton M, Blowes D, Smith L. Sego D (2009) Diavik waste rock project: oxygen transport in covered and uncovered piles. In: Proceedings 2009 International Conference on Acid Rock Drainage (ICARD) Skellefteå, 8th, Sweden, p 22-26

Bird RB, Stewart WE, Lightfoot EN (1960) Transport Phenomena. John Wiley & Sons

Cash A (2014) Structural and Hydrologic Characterization of Two Historic Waste Rock Piles. M.Sc. thesis, Department of Civil and Environmental Engineering, University of Alberta, Edmonton, Alberta.

Chi X, Amos RT, Stastna M, Blowes DW, Sego DC, Smith L (2013) The Diavik Waste Rock Project: implications of wind-induced gas transport. Applied geochemistry 36:246-255

Lefebvre R, Hockley D, Smolensky J, Lamontagne A (2001) Multiphase transfer processes in waste rock piles producing acid mine drainage: 2. Applications of numerical simulation. Journal of Contaminant Hydrology 52(1):165-186

Pantelis G, Ritchie, AIM, (1992) Rate-limiting factors in dump leaching of pyritic ores. Applied Mathematical Modelling 16(10):553-560

Pham NH (2013) Heat Transfer in Waste-Rock Piles Constructed in a Continuous Permafrost Region. PhD thesis, Department of Civil and Environmental Engineering, University of Alberta, Edmonton, Alberta

Qualitative and Quantitative Decision-Making Model to Determine the Size of Safety Pillars for Mining Under Sand Aquifers

Wanghua Sui[1, 2], Binbin Yang[1], Jiawei Liu[1], Yong Liu[1, 2]

[1] School of Resources and Geosciences, China University of Mining and Technology, 1 University Rd, Xuzhou, Jiangsu, 221116, China
[2]Institute of Mine Water Hazards Prevention and Controlling Technology, China University of Mining and Technology, 1 University Rd, Xuzhou, Jiangsu, 221116, China

Abstract

A qualitative and quantitative decision-making model is proposed for determining the size of safety pillars under sand aquifers. The qualitative model is based on a fishbone chart, which includes hydrogeological and engineering geological conditions and their changes due to mining activities. The quantitative model is a decision-making model based on geographic information system and entropy values. The decision models are demonstrated using data from different coalmines in China. The qualitative model is simple and can be widely applied in determining the size of safety pillars under sand aquifers.

Keywords: Underground mining, Decision-making model, Geographic information system (GIS), Sand aquifers

Introduction

Sand and water inrush are major issues when mining under sand aquifers, greatly affecting the normal production of a coal mine (Sui and Dong 2008). The panel and the roadway may be clogged with silt, and the machinery equipment can be buried. Cleaning and recovery of the mine's production is difficult, and such incidents, therefore, cause serious economic losses. The conditions and mechanism of coal mine sand and water inrush are complicated, mostly related to the scale and characteristics of the overburden aquifers, the coal seam, the mining method, the thickness and strength of the overburden rock, and the failure form of the overburden rock (Sui et al. 2011). Sand and water inrush can occur under various conditions, such as fault conduction, direct mining and conduction (general thickness of bedrock is thinner), and borehole conduction (Figures 1(a), (b), and (c), respectively).

Therefore, the size of pillars left under aquifers is a key parameter for decision-making regarding the safety of mining under sand aquifers. This study proposes a qualitative and quantitative decision-making model for determining the size of safety pillars under sand aquifers which is proposed by Yang et al. (2017). The quantitative model is a decision-making model based on geographic information system (GIS) and entropy values. The decision models are demonstrated using data from different coalmines in China. The qualitative model is simple and shows great promise for applications in determining the size of safety pillars under sand aquifers. The quantitative method is effective and advantageous, as the influence of multiple factors has been quantitatively considered in accordance with the geological and mining conditions. The model provides more optimal direction on mining under sand aquifers. For further study in mines where the geological structure is more complicated, a three-dimensional (3D) quantitative model should be developed.

Methods

In accordance with China's regulations for coal pillar designs for main roadways and coal mining under buildings, water bodies, and railways (State Administrator of Work Safety, 2017) and the regulations for preventing water hazards for coalmines (State Administrator of Work Safety, 2018), there exist three types of safety pillars under aquifers as listed in Table 1.

***Table 1** Types of safety pillars under aquifers*

Types	I	II	III
Safety pillars	Water-proof	Sand prevention	Anti-collapse

The present qualitative model is based on a fishbone chart, which includes hydrogeological and engineering geological conditions and their changes due to mining activities. Four basic maps, including a specific capacity distribution map, an isopach map of overburden, a contour map of the elevation of the bedrock surface, and an isopach map of the bottom clay, are superimposed and analyzed. The bottom clay and the overburden thickness are beneficial factors for the safety of mining under sand aquifers. Next, the height of overburden failure, the flow rate through the fractured zone into the panel, and the quicksand risk assessment are predicted. A qualitative comprehensive model is finally proposed to determine the size of the required safety pillars under aquifers (Figure 2).

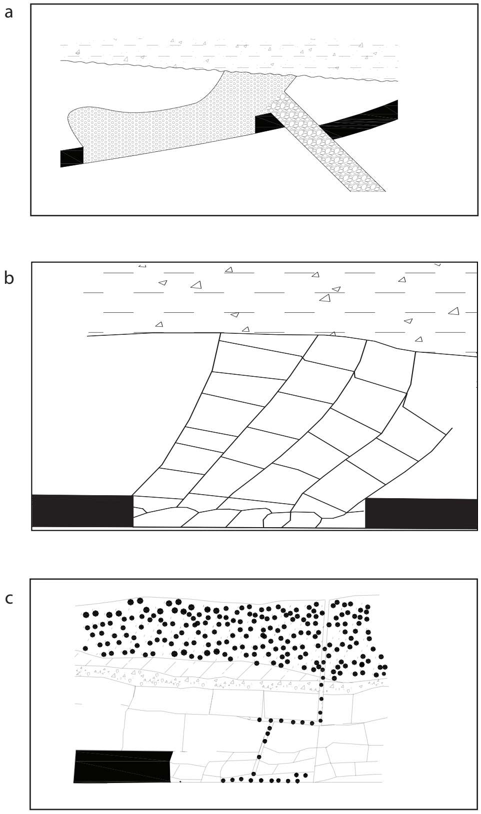

*(a) **fault** conduction;*

*(b) **direct** mining and conduction;*

*(c) **borehole** conduction*

***Figure 1** The conduction form of water and sand inrush*

With the rapid development of computer technology, space decision-making technology has also progressed significantly. The quantitative model is a decision-making model based on GIS and entropy values. An evaluation index system for controlling the mining safety under sand aquifers has been defined with reference to engineering geological and hydrogeological conditions. The factors included in the qualitative model are extensively and quantitatively defined and analyzed using GIS. Thematic map layers of the main factors that determine the safety of mining are generated based on geological data and other information. The risk index of mining under aquifers has been defined by Sui and Yang (2016) based on the weighted linear combination and information entropy. Figure 3 shows the flowchart of the quantitative model. First, the factor values are normalized according to the methodology proposed by Yang et al. (2017, 2018)

The entropy values of the thematic map layers are defined as follows.

$$e_j = \frac{1}{\ln(m)} \sum_{i=1}^{m} p_{ij} \ln(p_{ij}) \quad (k > 0, e_j \geq 0) \qquad (1)$$

The weights of the thematic map layers are calculated using formula (2).

$$\begin{cases} g_j = \dfrac{1-e_j}{j - \sum\limits_{j=1}^{n} e_j} (0 \leq g_j \leq 1, \sum\limits_{j=1}^{n} g_j = 1) \\ w_j = \dfrac{1-g_j}{\sum\limits_{j=1}^{n} g_j} (1 \leq j \leq n) \end{cases} \qquad (2)$$

Case Study

The Taiping Coalmine is located in the city of Jining, China. The study area falls within Panels S02 and S03, which are located in the southern region of the sixth mining area. The hydrogeological structure, which affects the mining of coal seam No. 3, comprises sandstone aquifers developed in Jurassic bedrock,

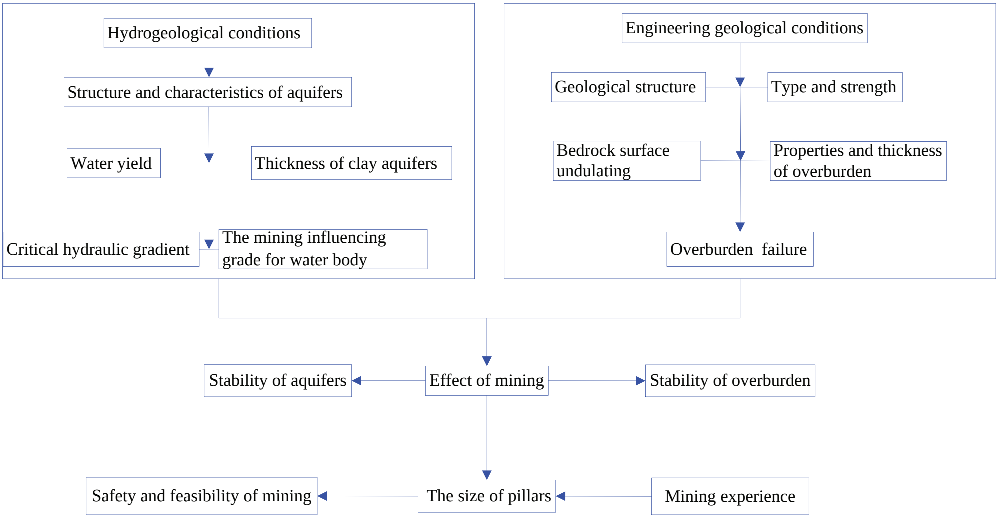

***Figure 2** Flowchart of qualitative decision-making for sand and water inrush*

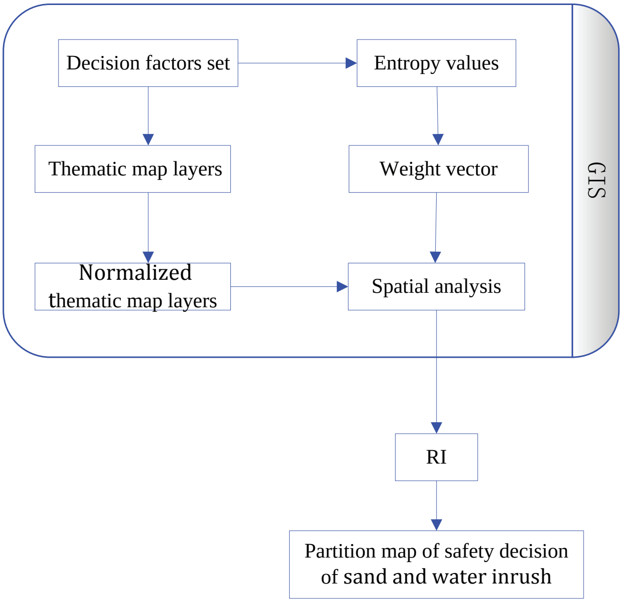

***Figure 3** Flowchart of quantitative decision-making for sand and water inrush*

clay aquifuge, and sand aquifer in unconsolidated Neogene sediments. Based on the data shown on the basic maps, the overburden isopach map, the contour map of the elevation of the bedrock surface, and the isopach map of the bottom clay are analyzed via superposition. Next, the height of overburden failure, the flow rate through the fractured zone into the panel, and the quicksand risk assessment are predicted. Figure 4 shows the size of the safety pillars under the aquifers determined by the qualitative comprehensive model.

Based on the GIS and entropy values, an evaluation index system including the water-yield property of the bottom aquifers, the height of overburden failure, the overlying strata thickness, the thickness of the bottom clay layer of the Neogene system, and the bedrock surface elevation are defined. The factors included in the qualitative model are extensively and quantitatively defined and analyzed using GIS. Figure 5 shows the risk assessment based on the thematic map layers of the main factors that determine mining safety.

Results and Discussions

Based on the results derived for different panels of the study area, the qualitative approach is simpler and presents great application potential for determining the size of safety pillars required under sand aquifers. The quantitative method is effective and advantageous, as the influence of multiple factors has been quantitatively considered in accordance with the geological and mining conditions. In accordance with the results of the qualitative model, the decision factors are classified and listed in Table 2.

Based on the results of the quantitative model, the relationship between risk index (*RI*) and decision factors is shown in Figure 6. When the water-yield property or the unit

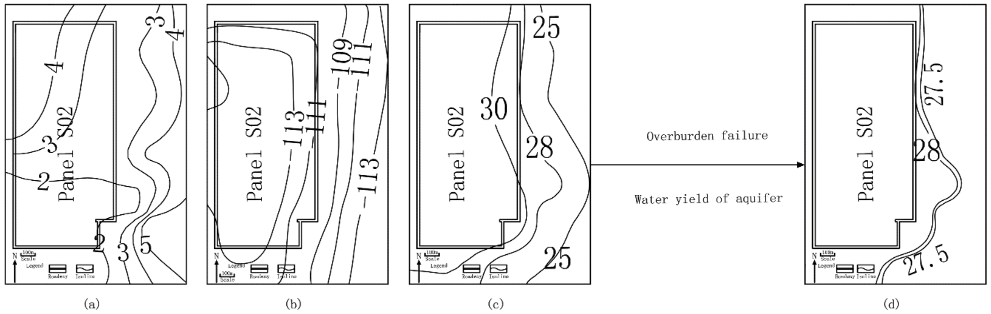

(a) ***isopach*** *map of the bottom clay; (b) contour map of the elevation of bed rock surface; (c) isopach map of overburden; (d) the size of safety pillars under aquifers*

Figure 4 *The flow chart of the qualitative comprehensive model of Panel S02*

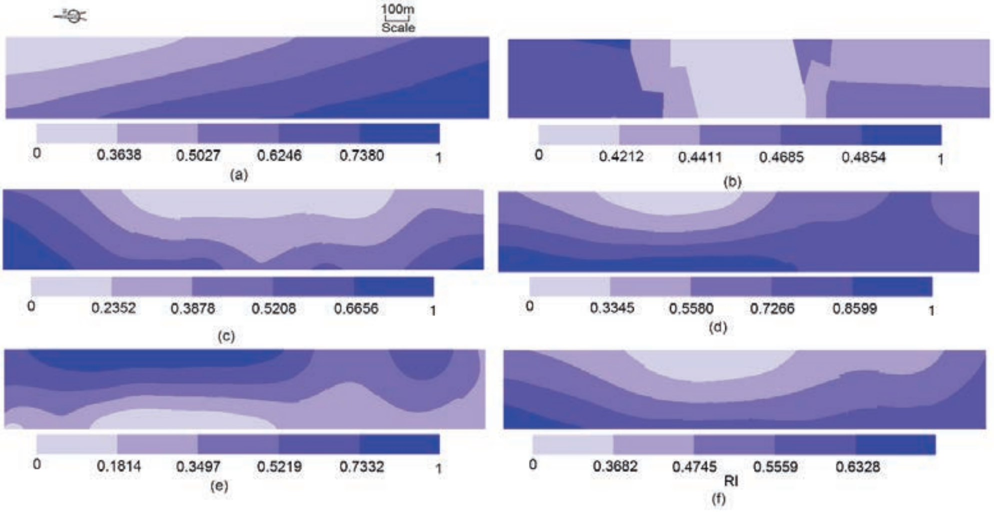

(a) water-yield *property of the lower aquifers; (b) height of overburden failure; (c) overlying strata thickness; (d) thickness of the bottom clay layer of the Neogene system; (e) contour map of the elevation of bedrock surface; (f) risk index of the quicksand*

Figure 5 *Flowchart of the quantitative model of Panel S03* water inflow (*q*) is greater than 0.1 L/s·m, *RI* increases rapidly.

Conclusions

The decision models are demonstrated using data from different panels (S02 and S03) of the Taiping Coalmine in China. The proposed qualitative approach is simple and has great potential for application in determining the size of safety pillars under sand aquifers. In this study, the influence of multiple factors has been quantitatively considered in accordance with the geological and mining conditions thereby making the proposed

Table 2 *Decision factors based on the qualitative model*

Decision factors	Classification	Remarks
Water-yield property of lower aquifers	Weak: $q \le 0.1$ L/(s·m)	q: Unit water inflow;
	Medium: 0.1 L/(s·m) $< q \le 1.0$ L/(s·m)	A: Mining thickness;
	Strong: 1.0 L/(s·m) $< q \le 5.0$ L/(s·m)	H_l: Thickness of overburden
	Extremely strong: $q > 5.0$ L/(s·m)	
Thickness of the bottom clay layer	Very good: $>7A$; Good: $5A \approx 7A$	
	Medium: $2A \approx 4A$; Poor: $<2A$	
Height of overburden failure(H_l)	Very good: $< 4A$; Good: $4A \approx 8A$	
	Medium: $8A \approx 16A$; Poor: $>16A$	
Thickness of overburden (H/H_l)	Very good: >1.4; Good: 1.4-1.2	
	Medium: 1.2-1.0; Poor: <1	

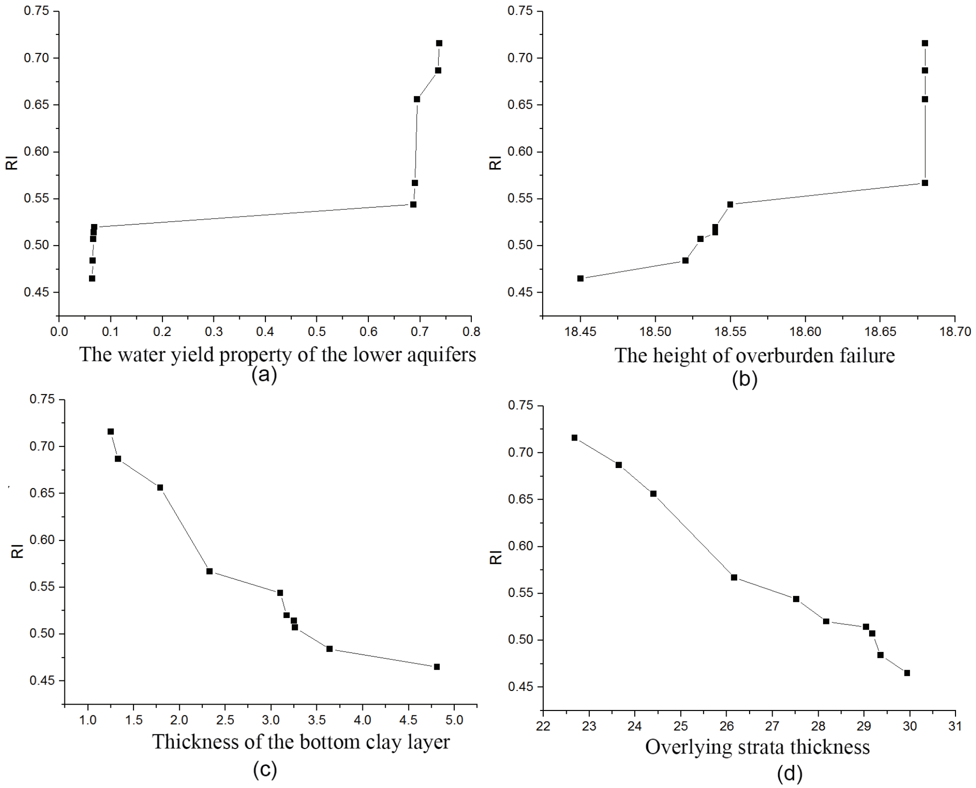

(a) ***Water-yield*** *property of the lower aquifers of the Neogene; (b) height of overburden failure; (c) thickness of the bottom clay layer of the Neogene system; (d) overlying strata thickness*

Figure 6 *The relationship between RI and decision factors* quantitative approach highly effective and advantageous. The proposed model provides optimal directions for mining under sand aquifers. For further study in mines where the geological structure is more complicated, a 3D quantitative model should be developed.

Acknowledgments

The authors are grateful for the financial support granted by the National Key R&D Program of China under Grant No. 2017YFC0804101, and the program, a Project Funded by the Priority Academic Program Development of Jiangsu Higher Education Institutions.

References

State Administrator of Work Safety (2017) Regulations of the coal pillar design for main roadway and coal mining under buildings, water bodies and railways. Coal Industry Press, Beijing(in Chinese).

State Administrator of Work Safety (2018) Detailed regulations of preventing water hazards for coalmines. Coal Industry Press, Beijing(in Chinese).

Sui WH, Dong QH (2008) Variation of pore water pressure and its precursor significance for quicksand disasters due to mining near unconsolidated formations. Chinese Journal of Rock Mechanics and Engineering 27:1908-1916

Sui WH, Liang YK, Zhang GL, Dong QH, Yang BB (2011) Study status and outlook of risk evaluation on water inrush and sand inrush mechanism of excavation and mining. Coal Science and Technology, 39(11):5-9

Sui WH, Yang BB (2016) Risk assessment of coal mining under sand aquifers. In: Drebenstedt, C. & Paul, M.: IMWA 2016 – Mining Meets Water – Conflicts and Solutions. p. 1092-1098; Freiberg/Germany (TU Bergakademie Freiberg).

Yang BB, Sui WH, Duan LH (2017) Risk assessment of water inrush in an underground coal mine based on GIS and fuzzy set theory. Mine Water and the Environment, 36(4), 617-627.

The Application of Hydropedological Surveys to Quantify Near-Surface Impacts of Mining Waste

Johan van Tol[1], Simon Lorentz[2,3]

[1]Department of Soil, Crop and Climate Sciences, University of the Free State, Bloemfontein 9300, South Africa, vantoljj@ufs.ac.za

[2]Centre for Water Resource Research, University of KwaZulu-Natal, Pietermaritzburg 3200, South Africa [3]SRK Consulting (SA), Pietermaritzburg 3200, South Africa

Abstract

Near-surface and lateral flow discharge comprise an often neglected pathway for contaminant movement from mine wastes toward downslope water resources. Contaminant loads moving through near surface pathways can exceed contaminant loading via surface water or groundwater fluxes. Hydropedological surveys to identify and quantify these near-surface fluxes provide an effective method to evaluate the potential impacts via this pathway. This paper describes the methodology of hydropedological surveys and their application in two hard-rock mining sites. Conceptual hydrological response models were developed which assisted with the understanding of mechanisms, modelling and monitoring of contaminant migration from the sites.

Keywords: Hydropedology, source-pathway-receptor, soil morphology, waste impacts

Introduction

Improving water quality through reducing the impacts of pollution, restoring water-linked ecosystems and implementing Integrated Water Resource Management (IWRM) are some of the key targets of the UN Sustainable Development Goal number 6. Achieving these targets necessitates a holistic approach which requires accurate analysis and characterisation of hydrological processes, especially in the highly variable water regimes of semi-arid areas (Savenije & van der Zaag 2008; Lorentz et al. 2003). Typically such an approach will involve the identification, conceptualization and quantification of the hydrological flowpaths, connectivities and residence times of water at different spatio-temporal scales. Capturing these processes in hydrological models can assist with water quality and quantity estimations and inform decision makers on best management practices to reduce the impacts of land-use change on water resources.

Efforts to characterise and quantify of these hydrological processes to determine the impact of mining waste are however often confronted with questions such as: '*where should measurements be conducted*?' and '*what is the extrapolation value of point measurements*'. Valid questions, as most hydrological processes are difficult to observe, dynamic in nature with strong spatio-temporal variation (Park & Van de Giesen 2004; Ticehurst et al. 2007). Conversely, soil properties are not dynamic in nature and their spatial distribution is not random (Webster 2000) and since water is the primary agent in the formation of soil morphological properties, the interpretation of these can illuminate the hydrological processes in the soil. In addition, soils are largely responsible for portioning of hydrological flowpaths (overland flow, subsurface lateral flow or groundwater recharge) and therefore act as a first order control on hydrological processes (Soulsby et al. 2006).

This interactive relationship between soil and water is the foundation of the relatively new interdisciplinary research field; hydropedology. Hydropedology recognizes that soils both control hydrological behaviour but their characteristics can also be used to predict hydropedological behaviour at various different scales (Lin 2003). In the South African context hydropedological studies have made contributions to the efficiency of hydrological modelling (e.g. Le Roux et al.

2011) and model development, identification of contaminant migration pathways from pit latrines (Lorentz et al. 2015) and industrial spills. A hydropedological survey is also now an informal prerequisite for application of a Water Use Licence for open-cast mining. In this paper we present two case studies where hydropedological surveys were conducted to conceptualise and quantify the near surface hydrological pathways, fluxes and contaminant loads from two hard-rock mining sites.

Background to case studies

The two case study sites (Mine A and Mine B are located in the Limpopo Province of South Africa. The names of the mines and the exact location cannot be disclosed due to client confidentiality agreements. The annual rainfall are approximately 700 and 500 mm for A and B respectively. A is underlain by basic to intermediate rock types (dolerite, norite and dunite), whereas B is underlain by granitic parent material.

The first case (Mine A) deals with a risk assessment of liner options for managing the water balance of a Tailings Storage Facility (Mine B). In order to assess the pollution risk associated with the various options the hydraulic properties of the soils and the hydrological flowpaths within and downslope of the tailings footprint had to be characterised.

In the second case study (Mine B), the water flow and contaminant migration from tailings impoundments, stockpiles and waste rock dumps of a mine had to be assessed to recommend appropriate monitoring, remediation and management actions. Previous work on Mine B focussed mainly on the potential contribution of polluted groundwater to a stream approximately 300 m downslope of the site. Contaminant loads in the groundwater could however not account for the increase in observed loads in the stream below the site. It was therefore hypothesised that the stream might be polluted through near-surface flowpaths and migration of contaminants.

Methodology

Hydropedological surveys were conducted in accordance with the methodology provided by Le Roux et al. (2011), on both A and B in order to characterise the dominant hydrological behaviour of the sites.

Dominant hillslopes/transects on each of the sites were identified from terrain analysis to ensure that the heterogeneity of soil distribution patterns in the landscapes are captured. Two transects were identified for A and three for B. Soil profile pits (23 and 9 for A and B respectively) were opened along these transects up to the soil/bedrock interface. Additional observations were made using hand augers and in erosion gullies or hillslope seeps. Soils were then classified in accordance with the South African Soil Classification System (Soil Classification Working Group 1991). All morphological properties and all soil horizons (including saprolite i.e. weathering rock) were described in detail, with particular emphasis to those properties influencing, or impacted by, the water regime of soils. These include *inter alia*, colour and colour variation, mottling, aggregation accumulation of iron, manganese and carbonate precipitates and the degree of saprolite weathering. The classified soils and associated properties were then interpreted grouped into one of six hydrological soil types, briefly summarised in tab. 1.

The dominant hydrological response for each of the sites were then determined based on the following considerations i) the occurrence of various hydrological soil types (tab. 1) in a hillslope, ii) the sequence of various soil types along the hillslope (distribution pattern), iii) the fraction of slope covered by different hydrological soil types and lastly iv) the dominant mechanism whereby water will reach the stream (van Tol et al. 2013).

The dominant hydrological responses of the various slopes are graphically presented as Conceptual Hydrological Response Models (CHRM). The CHRM's were validated and improved using measured soil physical properties and water levels in piezometers as well as through isotope analysis.

Results

Mine A The hydropedological survey of Mine A showed that shallow recharge soils dominate crest and midslope positions of this landscape (fig. 1-1). Vertical flow through the soil and into permeable rock and saprolite dominates. Slowly permeable bedrock below the saprolite restricts deeper drainage and

***Table 1** Hydrological soil types (adapted from Van Tol et al. 2013).*

Soil type	Description
Recharge (deep)	Deep freely drained soils without any morphological indication of saturation. Vertical flow through and out of the profile into the underlying bedrock is the dominant flow direction.
Recharge (shallow)	Shallow soils overlying permeable fractured rock. Vertical flow and out of profile is dominant with limited contributions to evapotranspiration (ET).
Interflow (A/B)	Duplex soils where the textural discontinuity facilitates build-up of water in the topsoil. Duration of drainable water depends on rate of ET, position in the hillslope, and slope with discharge in a predominantly lateral direction.
Interflow (soil/bedrock)	Soils overlying relatively impermeable bedrock. Hydromorphic properties signify temporal build of water on the soil/bedrock interface and slow discharge in a predominantly lateral direction.
Responsive (shallow)	Shallow soils overlying relatively impermeable bedrock. Limited storage capacity results in the generation of overland flow after rain events.
Responsive (wet)	Soils with morphological evidence of long periods of saturation. These soils are close to saturation during rainy seasons and promote the generation of overland flow due to saturation excess.

promotes lateral flow in the permeable rock (fig. 1-2). Evidence for this is frequent lime precipitations occurring on localised outcrops of hard rock in the midslope positions (fig. 1-3) where dissolved calcium-enriched water returns to the surface.

The lower midslope is covered by recharge soils (fig. 1-4). The soils are relatively shallow (< 500 mm) and overlies chemically weathered saprolite with signs of water logging on slowly permeable bedrock (> 1000 mm). Soil properties in the lower midslope (such as the chemically weathered saprolite and redoximorphic features) indicate that slope is hydrological connected as lateral draining water from upslope contributes to the water regime of this position. Again lateral flow in the saprolite is (at the fractured/hard rock interface) is significantly contributing to soils in lower lying positions (fig. 1-5).

Deep interflow soils occur in the valley bottom positions (fig. 1-6). Lime precipitations in the biopores and matrix of soils in these positions is an indication that there is a significant contribution of water via the saprolite/rock flowpath (fig. 1-5) from higher lying positions. These morphological properties forms in the capillary zone of a seasonal fluctuating water table. This is supported by the presence of manganese accumulations in the biopores indicating low degrees of reduction and some degree of stagnation/slow flow and biological impact. The signature implies an inflow of water from upslope that slowly drain through the toeslope soil with a controlled release to the streams. Grey matrix colours in subsoils also indicate long periods of saturation. Throughout the site, infiltration through fissures in the hard rock is possible, but this is considered to be sub-dominant flowpaths.

Mine B Vertical flow through recharge soils and into saprolite and fractured rocks is the dominant flowpath in the crest positions of slopes in Mine B (fig. 2). Solid granitic layers will however promote the generation of

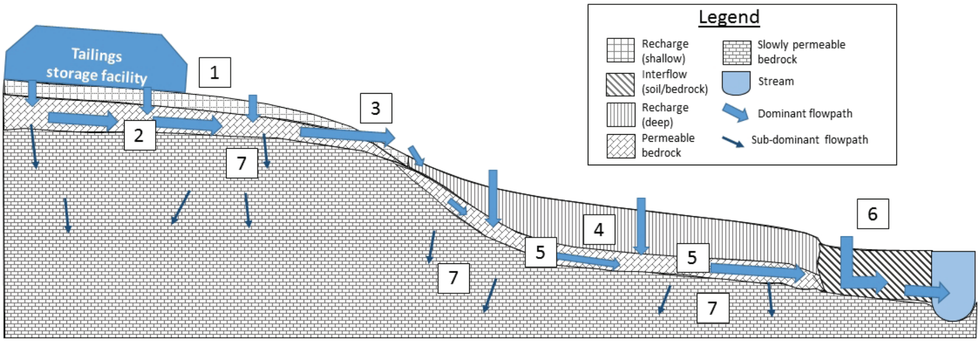

***Figure 1** Conceptual hydrological response model of hillslopes in Mine A.*

lateral flow within the saprolitic layer. With an increase in slope, the depth of the saprolite decrease, resulting in lateral flow at the soil/bedrock interface. At the lower midslope positions return flow to the surface is visible between fractured rock outcrops. This water re-infiltrates the soil and flows laterally at the soil bedrock interface resulting in long periods of saturation in the valley bottom positions.

The hydropedological study in combination with isotope analysis, numerical modelling and measured water quality indicators showed that, a relatively high percentage (> 70%) of mass loads are being transported through interflow to the river. Contaminants within the near-surface soils and preferential drainage paths are likely to be mobilised immediately following the first main rain event of the wet season, after which contaminants are then diluted with additional rain events ('typical' contaminant break-through curve). Cut-off trenches could therefore be successful implemented to intercept/treat contaminants.

Conclusions

The definition of the flow pathways based on the hydropedology studies, which included hydraulic characterisation of the materials, allowed for the estimation of water flux and solute load estimates from the vadose zone. Used in conjunction with hydrometric and isotope sampling, the hydropedology surveys were invaluable in characterising the fate of solutes in both sites.

Acknowledgements

The authors thank Digital Soils Africa for conducting the hydropedological surveys especially Prof. Pieter Le Roux and Dr. George van Zijl….

References

Le Roux PAL, Van Tol JJ, Kunene BT, Hensley M, Lorentz SA, Van Huyssteen CW, Hughes DA, Evison C, Van Rensburg LD, Kapangaziwiri E (2011) Hydropedological interpretation of the soils of selected catchments with the aim of improving efficiency of hydrological models: WRC Project K5/1748. Water Research Commission.

Lin H (2003) Hydropedology: bridging disciplines, scales and data. Vadose Zone J. 2, 1 – 11.

Lorentz SA, Hughes GO, Schulze RE (2003) Techniques for estimating groundwater recharge at different scales in Southern Africa. In: Xu, Y. and Beckman, H.E. (Eds) Groundwater Recharge Estimation in Southern Africa. UNESCO IHP

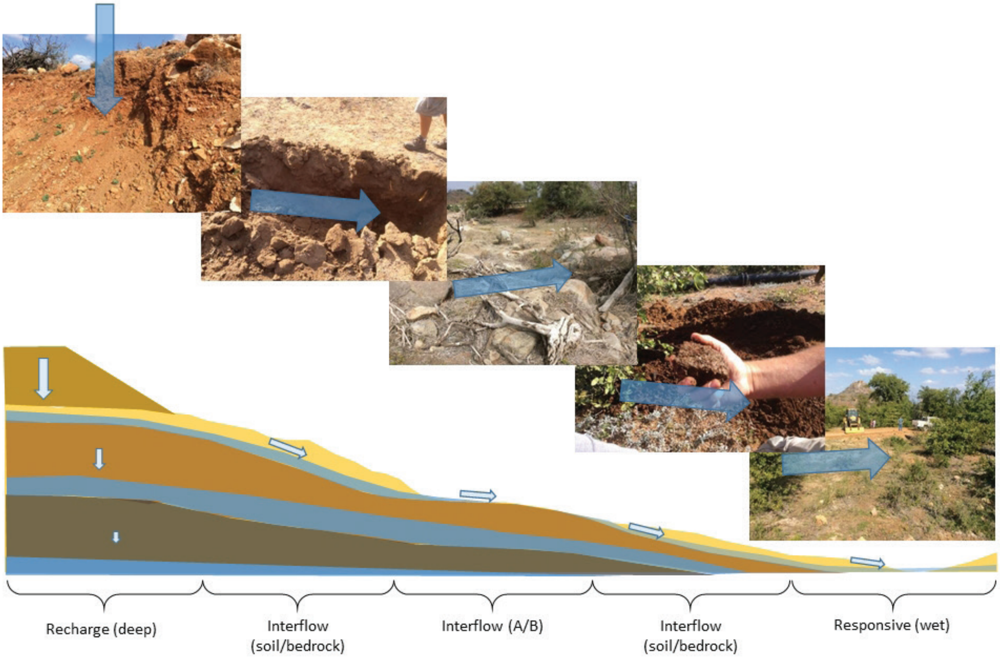

Figure 2 Soil distribution pattern and conceptual hydrological response model of hillslopes in Mine B.

Series No 64, UNESCO, Paris, France. ISBN 92-9220-000-3. Chapter 11, 149-164.

Lorentz SA, Wickham B, Still D (2015) Investigation into Pollution from On-Site Dry Sanitation Systems. Report No. 2115/1/15, Water Research Commission, Pretoria.

Park SJ, Van De Giesen N (2004) Soil-landscape delineation to define spatial sampling domains for hillslope hydrology. J. Hydrol. 295, 28 – 46.

Savenije HHG, van der Zaag P (2008) Integrated water resource management: Concepts and issues. Physics and Chemistry of the Earth, 33, 290 – 297.

Soulsby C, Tetzlff D, Rodgers P, Dunn S, Waldron S (2006) Runoff processes, stream water residence times and controlling landscape characteristics in a mesoscale catchment: An initial evaluation. J. Hydrol. 325, 197-221.

Soil Classification Working Group (1991) Soil classification: a taxonomic system for South Africa. Memoirs on the Agricultural Natural Resources of South Africa No. 15. SIRI, D.A.T.S., Pretoria.

Ticehurst JL, Cresswell HP, McKenzie NJ, Clover MR (2007) Interpreting soil and topographic properties to conceptualise hillslope hydrology. Geoderma 137, 279 – 292.

van Tol, JJ., Le Roux, PAL., Lorentz, SA. and Hensley, M. 2013. Hydropedological Classification of South African Hillslopes. Vadose Zone J. 12(4) – doi:10.2136/vzj2013.01.0007.

Webster R (2000) Is soil variation random? Geoderma 97:149–163. doi:10.1016/S0016-7061(00)00036-7

Risk-based Modelling of Soil Cover for Rehabilitation Planning of Coal Discard Facility in South Africa to Achieve Groundwater Quality Criteria

Albert van Zyl[1] Philip Barnard[2]

[1]*Terrasim CC, Suite 87, Private Bag X8, Elarduspark, 0047, South Africa, avanzyl@terrasim.co.za*

[2]*Golder Associates Africa (Pty) Ltd., P.O. Box 6001, Halfway House, 1685, Midrand, South Africa*

Abstract

Costly covers with a geo-synthetic liner system are required for discard facilities according to waste related legislation in South Africa. A risk-based approach is allowed to determine the requirements for an alternative pollution control barrier for mine residue facilities on a case-by-case basis.

Risk-based source-pathway-receptor modelling for an unlined discard facility optimised the soil cover design to achieve set groundwater TDS quality targets. It was concluded that thick soil covers can be a cost-effective alternative option that can outperforms a geo-synthetic liner with a growth medium in the long-term (>140 years) in mitigating seepage impact.

Keywords: Mine residue deposits, Outcomes based modelling**,** Store and release covers, **Source-pathway-receptor modelling,** Groundwater seepage impact mitigation

Introduction

Thick soil covers over coal discard facilities in arid and semi-arid regions are considered an important cost-effective measure to mitigate the impacts of leachate seeping into groundwater. With the National Environmental Management: Waste Amendment Act 26 of 24 of South Africa mine residue deposits and stockpiles were included in the definition of waste under the Waste Act. This results in a requirement for costly covers that include a geo-synthetic liner system for unlined discard facilities. In a statement released by the Department of Water Affairs and Sanitation of South Africa in June 2016, the Department conceded that they will consider a risk-based approach to determine the requirements for an alternative pollution control barrier for mine residue facilities on a case-by-case basis. When a soil cover is motivated as a cost-effective alternative option, the applicants must demonstrate that the influence of leachate on the receiving environment will be acceptable. This primarily points towards the achievement of a specified groundwater quality. An example of risk-based source-pathway-receptor modelling described in this article demonstrates a cover design process to meet a set quality target in the receiving groundwater at a discard facility.

The Mean Annual Potential Evaporation (Penman-Monteith equivalent (Allen et al. 1998)) of 1710 mm/yr. for the study area exceeds Mean Annual Precipitation (MAP) of 430 mm/yr by 4 times. Rainfall is highly seasonal with 95% of annual rainfall occurring during the October to April rainy season. According to INAP (2009), this climate is suitable for a store and release cover.

Qualifications and Limitations

Receiving Groundwater Environment is groundwater directly below and within 100 m of the final rehabilitated footprint of the discard facility, and includes the monitoring boreholes. TDS (total dissolved solids) concentrations represent leachate concentrations as it enters the receiving groundwater. Further dispersion, deposition or dilution of TDS in surrounding areas was not considered.

Acceptable Groundwater Quality was defined for TDS as the constituent of concern. Values of 1000, 2400 and 3400 mg/L as acceptable, tolerable and unacceptable concentrations were considered according to the upper limits of the DWAF (1999) water quality guidelines for domestic use. In general the background water quality was not good. Some monitoring boreholes showed natural TDS concentrations exceeding the 1000 mg/L target for acceptable drinking water quality. Hence the target value used for this study was the tolerable level of 2400 mg/L TDS.

Stable Climate Conditions were assumed for this study. While, on a regional level, there are indications that the 430 mm MAP used in this study has decreased, and is likely to decrease further due to climate change, there was not sufficient local data available to accurately model changes in precipitation, evaporation and temperature into an uncertain future.

Assumptions

*Spatial Representativeness***.** Moisture and contaminant flow profiles are spatially representative of the flows and contaminant leaching that would occur in the rehabilitated discard facility. Numerical vadose zone profiles defined from six monitoring boreholes immediately surrounding the facility and other available information represented moisture and contaminant flows that would occur through the vadose zone below the discard facility.

*Material Representativeness***.** Hydraulic and geochemical properties of materials used for modelling are spatially representative of the cover materials and of the coal discard. This is a fair assumption as a wide range in cover materials, coal discard and coal samples were collected, and analysed.

*Material Hydraulic Properties***.** Water retention and permeability of the cover materials and coal discard were determined by the particle size distribution and not by the formation of clods or cracks. Proposed cover materials and discard are not prone to the development of soil structure (clods).

*Preferential Flow***.** Simulated matrix flows through the cover assumed no preferential flows, such as flow through cracks. Proposed cover materials are not prone to the development of desiccation cracks and have a low risk for increased percolation rates associated with preferential flows through desiccation cracks.

*Geochemical Controls***.** Geochemical solubility controls within the dump were determined in laboratory kinetic tests (Naicker *et. al* submitted).

*Interstitial Water Contaminant Concentrations***.** Interstitial (pore water) TDS concentrations remained constant during active discard. Concentrations will initially vary post-closure, increasing with reduced percolation rates.

*Declining Source-term***.** With limited aeration below a cover layer, the generation of contaminant loads will decrease and contaminant TDS in interstitial water will become leached out with infiltrated rainwater over the long post closure period simulated in this study. TDS concentrations (and TDS loads) were simulated to decline over time.

Synthetic liner degradation. Ambient temperatures of above 40 degrees Celsius decrease the half-life of the impermeable characteristic of the liner to 70 years. This combined with the presence of hot areas on the discard facility, due to spontaneous combustion, reduces the long term suitability of a synthetic liner to the extent that perpetual replacement could be required.

Methods

Integration of a number of models and processes was required for this study, in an iterative process that repeatedly refined the design to achieve a desired long-term water quality impact with the most cost effective cover design (Figure 1).

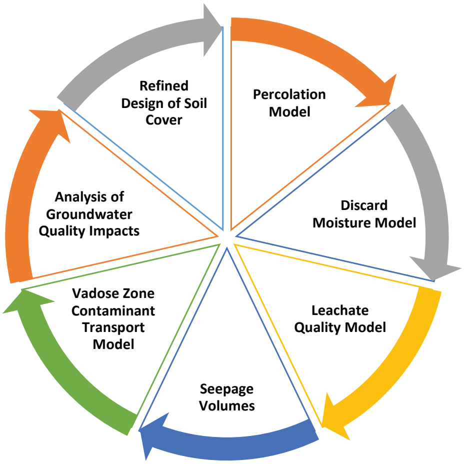

Figure 1 *Work Flow Chart.*

Percolation Modelling used the SVFlux finite element unsaturated flow model developed by SoilVision Systems (2016) to predict net percolation (moisture ingress) rates into the discard facility. Percolation was modelled for an uncovered discard facility, store-and-release soil covers and for a geo-synthetic liner system with a growth medium layer, and predictions were based on rainfall, climate, material hydraulic properties, vegetation characteristics and cover configuration. Climate model inputs included 40 years of daily rainfall recorded at site and available daily climate data. Hydraulic properties of soil cover materials and growth media available on site and of the discard were used as model input, as well as expected vegetative cover characteristics. Outputs of the model are net percolation rates into the discard facility.

Liner Leakage Modelling used the Landsim probabilistic liner leakage model (Golder Associates 2007) to predict the leakage rates from the cover with a geosynthetic liner system. Liner leakage was predicted based on predicted net percolation rates for the 30 cm growth medium, properties of the geo-composite drain, base slope and length of the upper surface and outer wall, as well as the defect rates, onset and rate of degradation of an installed geomembrane in ambient temperatures exceeding 40 degrees Celsius during summer. Predicted liner leakage rates were used as net percolation rates into the discard facility for the geosynthetic cover.

Discard Moisture Modelling used predicted net percolation rates together with information on the age, depth and profile of discard material. Moisture contents determined for samples collected from test pits at the upper surface and outer wall of the facility provided a base-line of gravimetric moisture contents within discard profiles. This provided some validation of the moisture contents predicted by the unsaturated flow model.

Leachate Quality Modelling used the ChemFlux finite element unsaturated contaminant transport model developed by SoilVision Systems (2016a) interactively coupled with SVFlux unsaturated flow model was used to predict a time series of interstitial/pore water TDS concentrations in the coal discard. Inputs included analytical results of humidity cell kinetic tests (Naicker *et. al* submitted) and of predicted time series of moisture content in discard profiles.

Seepage Volumes reporting to the base of the facility were derived from the predicted net percolation rates, facility height and footprint area, including incremental increase in the discard footprint. Flow through the facility is retarded due to discard moisture retention, which was accounted for in the modelling.

Vadose Zone Contaminant Transport Modelling simulated seepage through the unsaturated pathway (represented by the soil profile and by the weathered- and fractured zones between the base of the discard facility and the groundwater table). Model results predict a time series of TDS loads that report to the groundwater over time. Model verification used hydraulic properties of materials, predicted seepage rates, contaminant loads and vadose zone characteristics as inputs into ConSim (Golder 2005) and ChemFlux contaminant transport models. The predictions of these models were compared to measured groundwater TDS concentration at six monitoring boreholes immediately surrounding the facility.

Analysis of Receiving Groundwater Quality Impacts was limited to the comparison of the results of vadose zone contaminant transport models with groundwater quality objectives, represented by target TDS values. For the risk based (or outcomes based) approach, the cover design was revised and the facility re-modelled until the quality objectives were met.

Design or Re-design of the Soil Cover was the central element of all modelling. Initial cover design options included rain/water-shedding covers as previously regulated in South Africa, and store and release covers composed of the wide range of soils available on site. In this arid to semi-arid climate, design options became limited to thick single- and dual-layer store and release covers constructed with soils that have a low risk of undesirable structure development.

Results

Time series of TDS seepage loads were generated (modelled) for:

- Conditions prior to discard placement based on natural groundwater recharge rates and background TDS loads.
- Progressive discard placement over the footprint of the facility.

- Post closure conditions with the following cover scenarios:
  - Base case representing an uncovered facility
  - Store-and-release cover, and
  - Cover that includes a 30 cm growth medium and geo-synthetic liner system.

The TDS seepage loads time series into the receiving groundwater were used to predict the impact of discard leachate on:

- Six monitoring boreholes immediately surrounding the facility, for both the pre-discard placement conditions and the period of discard placement.
- Facility footprint for both the pre-discard placement scenarios and period of discard placement, as well as for post closure with various cover scenarios.

Predictions of Groundwater TDS Concentrations at Monitoring Boreholes closely matched monitored TDS concentrations and minimum refinement of the models was required. The break-through of discard leachate into the receiving groundwater was retarded by 6-8 years at the footprint area underlain by basalt with a shallower (10-12 mbgl) resting groundwater table. Discard placement commenced in these areas providing sufficient time for leachate to seep through the vadose zone. Peak TDS concentrations have been reached at areas where discard placement started. TDS interstitial water concentrations of the vadose zone have equilibrated to discard leachate concentrations.

Break-through of leachate through the vadose zone was not predicted for the area underlain by sandstone by 2016, which is confirmed by monitored TDS concentrations. This can be ascribed to the long travel time for the discard leachate through the thick (8-9 m) soil horizon and relatively thick weathered zone (8 to 20 mbgl) to the relatively deep (22-41 mbgl) groundwater table. Future leachate break-through was predicted.

Predictions for the cover that includes a geo-synthetic liner show that water quality initially improve comparable to natural (ambient) TDS concentrations, which indicate an over-design (Figure 2). The geo-synthetic liner will, however, degrade due to high ambient temperatures. Increased TDS concentration in the groundwater is delayed for at least 120 years, but not significantly mitigated over the longer period of seepage impact (centuries).

Predictions for thick store and release cov-

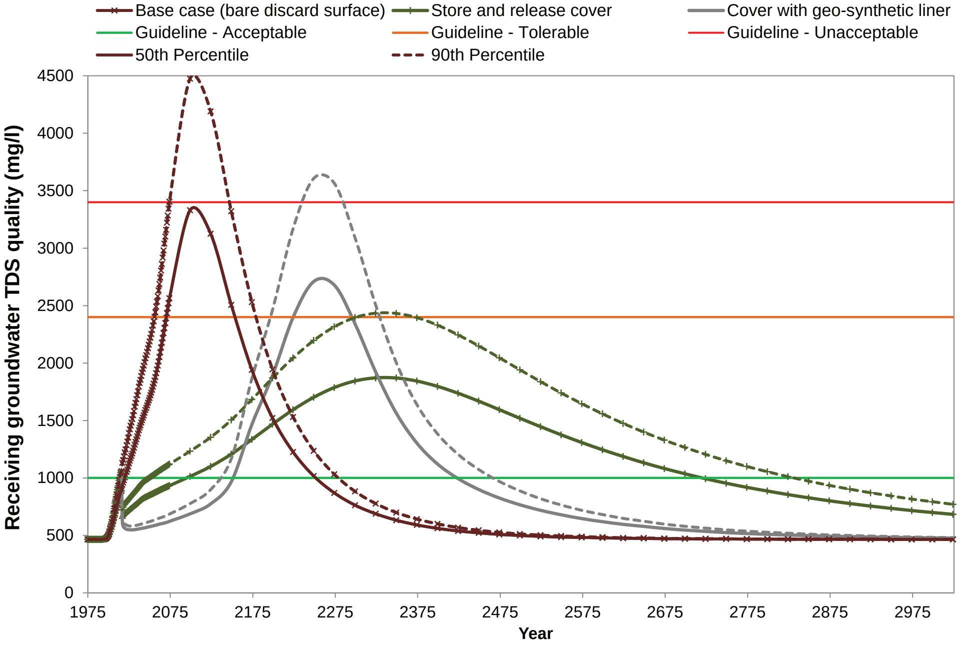

***Figure 2** Likely groundwater TDS concentrations with various covers.*

ers showed that the soil cover outperforms the costly cover with a geo-synthetic liner from about 140 years when liner degradation becomes significant (Figure 2). The thick store and release cover mitigates the impact of the facility to target groundwater quality levels over the full period of seepage impact.

At an effective mean annual seepage rate of 16 mm/yr (3.2% of MAP), source-pathway-receptor modelling indicated that groundwater quality targets can be met. Covers were designed to achieve this target net percolation rate. The modelling of covers showed that the required cover thickness is determined by soil characteristics, level of rehabilitation and probability that good vegetation cover will be established and maintained in the long-term.

Conclusions

The recommended cover with a geo-synthetic liner may improve the groundwater quality to better than natural (ambient) TDS concentrations for the first 120 years, which indicates an over-design. For this facility, a thick store and release cover outperforms a cover with a costly geo-synthetic liner over the long period (centuries) that seepage impact must be mitigated. Construction of store and release covers instead of covers with geo-synthetic liner also represents a substantial cost saving (> 50%).

Source-pathway-receptor modelling, based on site- and facility specific conditions, is necessary to demonstrate that the required groundwater quality criteria can be met.

Acknowledgements

The authors thank Leon Bredenhann for guidance on relevant legislation in South Africa.

References

Allen R. G., Pereire L.S., Raeas D. & Smith M. (1998) Crop evapotranspiration - Guidelines for computing crop water requirements. FAO Irrigation and drainage paper 56, Food and Agriculture Organization of the United Nations, Rome, Italy.

Department of Water Affairs and Forestry (1999) Quality of domestic water supplies. Volume 1: Assessment Guide (second edition), Water Research Commission Report No.: TT 101/98, Water Research Commission, Pretoria, South Africa.

Golder Associates (2007) LandSim Version 2.5.17. Golder Associates UK Ltd.

Golder (2005) Contamination Impact on Groundwater: Simulation by Monte Carlo Method. UK Environment Agency R&D Publication 132.

Naicker K, van Zyl A and Barnard P (Submitted). Prediction of Seepage Quality from Coal Discard Facility in a Semi-Arid Climate, ICARD | IMWA | MWD 2018 Conference, Pretoria, South Africa.

INAP 2009. The International Network for Acid Prevention. Gobal Acid Rock Drainage Guide (GARD Guide), http://www.gardguide.com.

SoilVision Systems 2016. SVFlux Saturated / Unsaturated Finite Element 1D/2D/3D Seepage Modelling Software. SoilVision Systems Ltd., Saskatoon, Canada.

SoilVision Systems 2016a. ChemFlux Saturated / Unsaturated Finite Element 1D/2D/3D Seepage Modelling Software. SoilVision Systems Ltd., Saskatoon, Canada.

Evaluation and Comparison of Kinetic Tests Performed with the Humidity Cell, Column and Funnel Methods and Proposition of a Model with the Disposition Way

Fernando Vilela[1-2], Geraldo Lima[2], Jéssica Macniks[2], Juliene Ferreira[2] and Mark Le Petit[2]

[1] *University of Brasília, Brazil. Chemistry Institute. Brasília –DF – Brazil – e-mail: fernando.vilela@campoanalises.com.br*

[2] *CAMPO ANÁLISES Lab, Center of Agricultural and Environmental Technology, Paracatu – MG, Brazil*

Abstract

With the growing importance recognition of acid mine drainage evaluation, the prediction studies are becoming more frequent and more important. There are scientific consensus methods and interpretation of static test results, however, there are still doubts in the indication and interpretation of kinetic assays.

In this study, were assessed three samples with different potential acid drainage, using the kinetic three methodologies the most recognized and used in all regions of the world, being the Humidity Cell (ASTM D5744-B,) Column test (EPA 1627/2011) and Funnel test (AMIRA, 2002) during a 20-week cycle. The tests were conducted simultaneously and under controlled conditions, exactly as required by the methodology. Static tests were carried out in the ANC and NAG. Petrography analysis was done and assessed the parameters pH, alkalinity, and sulphate in the leachate.

The final results demonstrated that the same samples submitted to different methods of kinetic tests result in different amounts of cations, pH and Alkalinity in the leachate. The variations in results were mainly related to the amount of interstitial water in each method, which influenced on the solubility of species with neutralizing power.

These results are important and fundamental for the choice of which kinetic test should be performed, in prediction studies or remediation programs. With the correct choice of the most appropriate test for each type of use, we will have a higher quality of results and savings for businesses.

Keywords: ARD Prediction, kinetic assays, metal leaching.

Introduction

Acid mine drainage is the name given to the process resulting from the oxidation of sulfide compounds from the mining process. Sulfide compounds when exposed to the weather in the form of tailings, dam or any other forms of exposure, can suffer an oxidation and result in the generation of an acid effluent, mainly with a high content of sulphate. The low pH of the effluent from the acid mine drainage increase the dissolution of metals, causing significant environmental damage when released in water bodies without proper treatment.

Acid drainage is one of the major environmental problem of mining and due to the complexity of the factors to which the process of acid mine drainage is related, the process of treatment is usually expensive and long-term. Thus, is necessary that the acid drainage generation potential of a disposal material been known prior to the implementation of the operational activities.

In Brazil, the disposal of mining waste is regulated by ABNT 13029 (2017), which features on the guidelines for elaboration and presentation of the mining waste disposal project design. In this standard, evaluation is required of the potential acid drainage and neutral leaching of tailings, however, there is no a standard that regulates which tests must be performed to attend this requirement.

Among the various stages of ARD prediction, there are tests performed in laboratories. These tests to assess the acid drainage potential are divided into 2 groups: Kinetic and static.

The static tests are essay where are evaluated the potential for acid generation and neutralization. One of the first classic method for this evaluation and worldwide used is the Sobek method (1978) Acid-Base Accounting (ABA) that was later modified by Lapakko (2002) (MABA). Another test used is the NAG (Net acid Generation) proposed by Stewart (2003). This method presents the balance between the acid production and acid consumption of the mine solidwaste. Besides the balance between the acid-base production, others considerations are important, as the DRX and SEM analysis to give support to the data interpretation.

Kinetic tests are essay conducted usually in columns or funnel where a quantity of sample (some kilograms) are exposed to wet and dry cycles. The effluent leached of these extracts are usually collected and analyzed for pH, EC, Sulphate, Alkalinity and metals content. Among the various kinetic tests available in the literature, the most used are the humidity cell tests (ASTM D5744), column test (EPA 1627/2011) and funnel test (AMIRA, 2002). Although of this three kinetic test, have the same principle, some specifics procedures can result in a data with large variance.

Thus, considering the variety of testing methods for evaluation of acid drainage potential available, as well as seeking to provide subsidies to a standardization of kinetic assays in Brazil, this study aimed to evaluate the results of three samples with different acid generation potential submitted to different kinetic tests and to compare the results obtained.

Methods

Three samples were selected from mining sites with different acid drainage generation potential, using the NAPP criterion: A low potential to acid generation (NAF), the second with acid generation potential uncertain (UAF) and a third with high acid generation potential (HAF). The samples were collected in the State of Minas Gerais-Brazil, in a region of a gold mine. Was collected a total of 100 kg. The samples were crushed to 6 mm for the kinetic and ground tests for static tests.

Were prepared three columns of each type of material (NAF, UAF and HAF) for each one of the three evaluation methods: Humidity Cell (ASTM D5744-B), column test (EPA 1627/2011) and funnel test (AMIRA, 2002), as shown in Figure 1.

The procedures were performed exactly as described in the methods listed and details below:

Humidity Cell – ASTM D5744-B: This test requires that temperature and relative humidity be maintained within a constant range

__Figure 1__ Picture of the three Kinetic test: a (column), b (humidity cell) and c (funnel)

by storing the cells in an environmentally and controlled enclosure during the 6 days following the weekly 500- or 1000-mL leach. After this period, a new leaching cycle is started.

Column test – EPA 1627: This test is carried out using 2-inch columns with material less than 6 mm. Once the column has been drained after initial procedures, the humidified gas mixture with 10% of CO_2 at a rate of 1 L/min is introduced continuously through the gas at the bottom of the column. The column is allowed to sit for a period of 6 days during the humidified air cycle. This cycle is repeated after each saturation cycle. After each humidified air cycle, reagent water is introduced at the bottom of the column and after a 1 day of contact time, the leach is collected.

Funnel test – Amira (2002): This test consists in expose the crushed sample in a funnel and hold weekly cycles of addition of reagent water. Heat lamps are installed to ensure that the columns dry-out between watering. The leached are collected weekly.

For all leached, after each completed cycle, leachate collected volume was recorded. The pH was measured with Hanna HI 221-pH meter that was calibrated against commercial buffer solutions (pH 4, pH 7 and pH 10) and electrical conductivity using a conductivity meter. Leachate was filtered through a filter paper cellulose nitrate of 0.45 µm. Samples were collected and acidified with nitric acid for ICP-OES (Agilent, 5100) analysis of Al, as, Ca, Cu, Fe, Mg, Pb, and Zn. Sulphate concentrations were determined by ion Chromatography (Metrohm IC-801). The environmental conditions in the lab were kept at 20 ± 1° C.

Results and discussion

Static Tests

The selected samples were analyzed in order to verify the acid drainage generation potential using static tests. The results are presented in Table 1.

As it can be seen on table 1, the results of the static testing have indicated that the sample NAF have not presented an acid drainage generation potential, since the value of the NPP was at 156.9 kg $CaCO_3$/t, as well as the NAG value presented was <1 kg H_2SO_4 and NAG pH of 4.6, due to the high presence of carbonates in the sample. Moreover, the UAF sample has presented an uncertain potential acid drainage generation, given that the NPP was -1.2 $CaCO_3$/t and the NAG in 16.5 H_2SO_4/t and a NAGpH of 4.3. The sample HAF has already presented an acid drainage generation potential, once the value of NPP was -63.1 $CaCO_3$/t and NAG of 44.8 H_2SO_4/t and a NAG pH of 3.1.

Furthermore, it was carried out a petrographic analysis was carried aiming at evaluating the different stages of sulfides present in each sample. The results are shown in Figure 2.

The results of petrographic analyses can be seen on Figure 2 and they corroborate the static tests that had been done, once in the sample NAF was found carbonate, just as pyrite was found in the sample HAF, conversely it was found a fraction of chalcopyrite in the UAF sample. The analysis of the results of the static testing endorse the sample selection, once it has shown different acid drainage generation potential.

Each sample underwent 3 diffferent tests, that were replicated 3 times. The statistical analysis had a confidence level of 95%.

Kinetic Tests

The results of the kinetic tests are shown in the tables 2 and 3 and Figure 3.

The final pH values (week 20) are presented on table 2 covering all three samples (NAF, UAF and HAF) and the three methods evaluated (Funnel test, Humidity cell and Column test).

Regarding the NAF sample, the three methods of kinetic tests have assessed that

***Table 1** The results of the static tests*

Sample	pH 1:1	PA	PN	NPP	NAG	NAG pH
	Kg $CaCO_3$/t	Kg $CaCO_3$/t	Kg $CaCO_3$/t	Kg H_2SO_4/t	Kg H_2SO_4/t	Kg H_2SO_4/t
NAF	8.22	28.4	185.3	156,9	<1	4.6
UAF	6.37	18.4	17.2	- 1.2	16.5	4.3
HAF	5.16	93.7	30.6	- 63.1	44.8	3.1

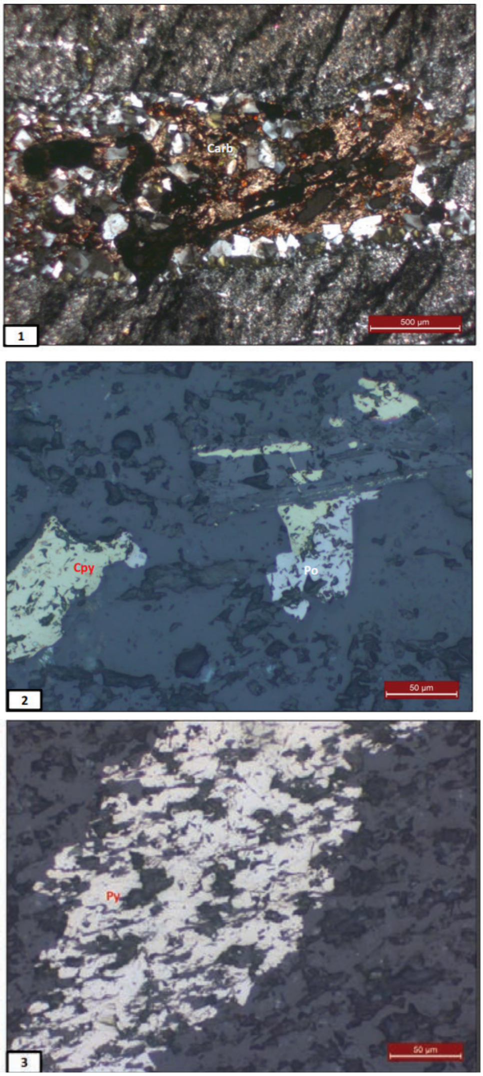

***Figure 2** Petrographic analysis images: 1 (NAF), 2 (UAF), 3 (HAF)*

***Table 2** Final pH in the 20 weeks*

	Final pH		
Samples	Funnel Test	Humidity cell	Column Test
NAF	6.91 a	6.75 a	6.89 a
UAF	6.39 a	6.67 a	6.49 a
HAF	3.38 a	6.89 b	4.62 c

there was no statistical difference in the pH value, all results are above 6, thus they endorse the static test results that indicate a sample without acid drainage generation potential during the evaluted period.

Means followed by the same letter in the lines do not differ according to t's test at 95% confidence level.

Futhermore, the UAF samples had a similar behavior, once the value of pH have not showed any statistical difference in the three methods evaluated. In fact, all pH values are above 6, what indicates that the sample UAF did not present a potential for generating acidic drainage during the period of analysis.

Finally, the HAF samples have shown a significant difference between the final pH concerning the three chosen methods. The Funnel test resulted in a final pH of 3.38, by the other hand , the Column Test restults show a pH of 4.62, at last the Humidity cell test presented a final pH of 6.89, thus, all of them are statistically different from each other. This result indicates that the chosen method in the kinetic test might be decisive for the assessment of potential acid drainage from a sample. The outputs show that the test of the funnel and the column test resulted in a leached with low pH, meanwhile the humidity cell test resulted in a leached with neutral pH.

Means followed by the same letter in the lines do not differ according to t's test at 95% confidence level.

Then, Figure 3 shows pH measurement results of the leachate during the 20 weeks the experiments were performed. It can be seen that for the samples NAF and UAF there are no differences between the pH values, however, when it concerns the HAF sample, after the 10th week, the pH of the leached obtained from the Funnel Test started to decrease, which was sustained until the 13th week, therefore it stabilized in pH around 3. The same effect can be seen in the leached obtained from the

***Table 3** Accumulate amount of Alkalinity and Sulphate in 20 weeks*

	Alkalinity – mg $CaCO_3$			Sulphate mg SO_4		
Sample	Funnel Test	Humidity cell	Column Test	Funnel Test	Humidity cell	Column Test
NAF	163.0 a	615.0 b	656.3 b	1,879.9 d	1,323.1 e	2,472.4 f
UAF	120.8 a	219.5 b	269.6 b	809.0 d	668.1 e	1,218.5 f
HAF	58.8 a	431.2 b	270.9 c	4,429.6 d	4,329.9 d	4,377.6 d

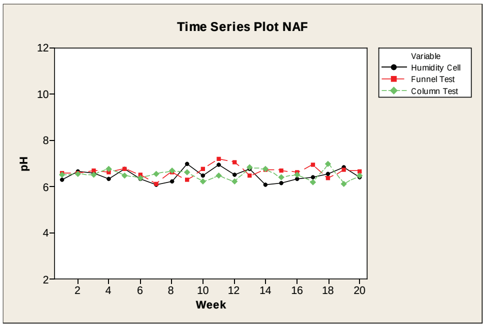

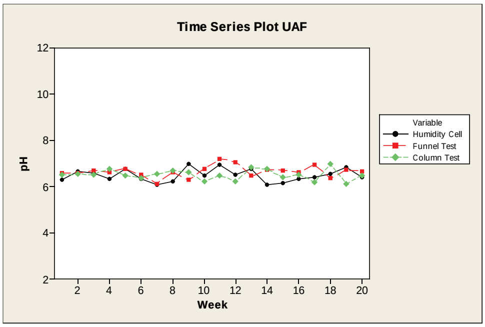

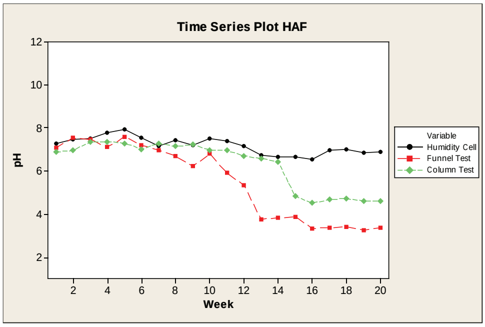

***Figure 3** Evolution of pH in the NAF, UAF e HAF samples*

Column Test, in which after the 14th week it started a trend of decrease in pH values, it stabilized the pH around 4. These results indicate that the process of weathering had different rate for each test. In order to better assess these results, it is important to determine the alkalinity and sulphate leached over the 20 weeks, as shown in table 3.

Thereby, table 3 shows that the HAF sample had a quantity of sulphate in leachate statistically equal in each of the three methods, whereas the value of alkalinity was lower concerning the funnel test, it is followed by the method of the column, the highest value of alkalinity was obtained for the leached from the test with humidity cell. It is important to point out that the amount of alkalinity in the leachate was always greater in the humidity cell and column methods, when they were compared with the method of the funnel. This result probably is related to a greater amount of interstitial water in humidity cell and Column methods, what can increase the solubility of the cations of carbonate formation, consequently, it resulted in a higher alkalinity in leachate. The impact of the increased solubilization of sulphate can be minimized because of the high solubility of these chemical species.

As a matter of fact, this observation is really relevant considering the samples that showed leaching sulfides potential and carbonates, what led to produce a self-neutralization. In this case, choosing the method of the kinetic assay can be decisive. Once the geologic formation of samples may change the solubility of some chemical species, as for example during the testing of NAF and UAF the amount of leachate sulphate was different for each of the three methods.

That way, depending on, the choice of the method used in the kinetic assay, it can reproduce the conditions of disposal of the solid waste, both in the presence or not of interstitial water, or direct exposure to sunlight, what can be a decisive factor to the process of weathering this material.

During the tests the metals concentration in the leachate have been evaluated, which will be discussed in an upcoming paper.

Conclusions

The results data have shown that the kinetic assay method can lead to different chemical results for the same sample, mostly due to the amount of surface and interstitial water and the time of contact of water and the sample, which increases the solubility of cations and consequently it can influence the leachate pH. Moreover, studies are being carried out in order to develop a mathematical model that will be able to relate the results of the different kinetic assays methods and the way of disposing solid waste, thus, the best method for each sample will be chosen.

Acknowledgements

The authors would like to thank CAMPO ANÀLISES for providing the structure of the laboratories for the carry out the tests.

References

ABNT NBR13029 - Mineração - Elaboração e apresentação de projeto de disposição de estéril em pilha. Associação Brasileira de Normas Técnicas, 2017. Brasil

Mineração - Elaboração e apresentação de projeto de disposição de estéril em pilha

AMIRA Project P387A Prediction & Kinetic Control of Acid Mine Drainage, Project P387A Prediction & Kinetic Control of Acid Mine Drainage, 271 William Street Melbourne 3000 Australia.

ASTM D5744 – 13. Standard Test Method for Laboratory Weathering of Solid Materials Using a Humidity Cell, 100 Barr Harbor Drive, PO Box C700, West Conshohocken, PA 19428-2959. United States

Lapakko, K. 2002. Metal Mine Rock and Waste Characterization Tools: An Overview. Minnesota Department of Natural Resources, US. April 2002 No. 67.

Environmental Protection Agency, Method 1627: Kinetic Test Method for the Prediction of Mine Drainage Quality (2011). EPA, U.S.

Stewart, W., Miller, S., Smart R. Gerson, A., Thomas, J.E., Skinner, W., Levay, G., and Schumann, R. 2003a. Evaluation of the Net Acid Generation (NAG) Test for Assessing the Acid Generating Capacity of Sulphide Minerals. p. 617-625. I: Proceedings of the Sixth International Conference on Acid Rock drainage (Cairns, 12-18th July 2003).

Sobek, A.A., Schuller, W.A., Freeman, J.R. and Smith, R.M. (1978), Field and Laboratory Methods Applicable to Overburden and Minesoils, EPA 600/2-78-054, 203pp.

Diavik Waste Rock Project: A Mechanistic Approach To The Prediction Of The Geochemical Evolution Of Sulfidic Waste Rock

David Wilson[1], Richard T. Amos[2], David W. Blowes[1], Jeff B. Langman[3], Leslie Smith[4], David C. Sego[5]

[1]*Department of Earth and Environmental Sciences, University of Waterloo, Waterloo, Canada.*

[2]*Deptartment of Earth Sciences, Carleton University, Ottawa, Canada.*

[3]*Department of Geological Sciences, University of Idaho, Moscow, U.S.A.*

[4]*Department of Earth, Ocean and Atmospheric Sciences, University of British Columbia, Vancouver, Canada.*

[5]*Department of Civil and Environmental Engineering, University of Alberta, Edmonton, Canada.*

Abstract

Prediction of the geochemical evolution of mine-waste rock is of critical importance to mining companies and regulators because the impacts of mining activities on the local environment must be considered as part of mine-life planning. Prediction is often achieved by using the results of small-scale kinetic tests in conjunction with scale factors in a process commonly referred to as scale-up. One of the overall goals of the Diavik Waste Rock Project was the development of a mechanistic scale-up technique for the prediction of the geochemistry of mine-waste effluent. The project consisted of laboratory and field experiments to investigate the geochemical evolution of waste rock at different scales in support of scale-up research. The laboratory study consisted of long-term (9 years) humidity cell (0.1 m) experiments; the field studies consisted of medium scale (2 m) lysimeter experiments and large-scale test pile (15 m) experiments.

A conceptual model of the geochemical evolution of the Diavik waste rock was implemented at the humidity cell scale using the multicomponent reactive transport model MIN3P. The humidity cell experiments were conducted with replicate cells under three different sulfide mineral contents and two temperature conditions (5 and 22 °C). Mass- and temperature-dependent rate parameters for reactions involving sulfide content, host mineralogy, and secondary minerals were calibrated by simulating the effluent geochemistry of the humidity cell experiments. The resulting calibrated model of the geochemical evolution of Diavik waste rock was then implemented for the field-scale experiments, using site measured temperature and hydrological parameters that provided conditions representative of the experiments. Only the sulfide and carbonate mineral contents of the field simulations were changed from the humidity cell simulations; initially, no other calibration was conducted.

Results of the simulations at the three experiment scales indicated that carbonate mineral availability was likely more limited in the field experiments when compared to the humidity cell experiments. Otherwise, the geochemical evolution of the field experiments was captured well by the scaled model.

These simulations indicated that a reactive transport model, calibrated using results of humidity cell experiments, has the potential to predict the geochemical evolution of mine-waste rock at the large scale without the use of scaling factors. Site specific measurements of physical parameters including precipitation, temperature, hydraulic conductivity, and mineralogy would be required to conduct the appropriate simulations at other sites.

Keywords: scale-up, reactive transport, sulfide oxidation, waste rock

Introduction

The assessment of environmental impacts due to waste rock stockpiling is a critical component of the mine planning process. The potential for acidity and elevated solute concentrations from waste-rock are often assessed by conducting laboratory-scale humidity cell experiments (Lapakko, 2003; Ardau, Blowes & Ptacek, 2009; Sapsford et al., 2009). Solute release rates from the small-scale experiments are typically extrapolated using scale factors to make predictions about waste-rock effluent chemistry (a process commonly referred to as scale-up). Parameters understood to influence effluent chemistry, including pH, particle size, moisture content, temperature, oxygen availability and mineral surface area, (Kempton, 2012; Amos et al., 2015) are some of the scale factors that are typically considered for a scale-up assessment. These empirical scale factors often do not take in to consideration site specific heterogeneities and variability in flow and temperature regimes that can make it very difficult to approximate the geochemical and physical behaviour of a waste-rock pile in a realistic manner. Mechanistic approaches to scale-up, specifically the use of reactive transport models, may be able to address these complexities and provide a quantitative approach to scale-up that more closely approximates the geochemical conditions at a waste-rock pile.

The Diavik Waste Rock Project (DWRP) consists of small-scale laboratory (0.1 m), and medium-scale (2 m) and large-scale (15 m) field experiments conducted to address issues related to scale-up. The Diavik Diamond Mine (Diavik) is located approximately 300 km northeast of Yellowknife, NT, Canada. Simulations of the geochemical evolution of low-sulfide waste rock produced at Diavik were conducted using the reactive transport code MIN3P (Mayer, Frind & Blowes, 2002). This article presents the implementation of a conceptual model of sulfide mineral weathering, developed at the laboratory scale, to simulate the geochemical evolution at the two field-scale experiments. Further detail on each stage of the modelling can be found in Wilson et al., (2018a), Wilson et al., (2018b), and Wilson et al., (in prep). The simulations are intended to demonstrate a mechanistic method of scale-up of laboratory-scale experiments for the assessment of the geochemical evolution of waste rock at the large scale.

Methods

Waste rock used in the experiments exhibited similar mineralogy consisting of approximately 75% granite (primarily quartz, K-feldspar, and albite), 14% pegmatitic granite, 10% biotite schist, and 1 % diabase (Blowes & Logsdon, 1998; Langman et al., 2014). The biotite schist was composed primarily of albite (35–55%), quartz (20–50%), and biotite (10–25%). The dominant sulfide mineral, pyrrhotite with minor substitution of Ni and Co for Fe following an approximate ratio of [$Fe_{0.852}Ni_{0.004}Co_{0.001}S$] (Jambor, 1997), was contained primarily in the biotite schist component of the waste rock. Other sulfide minerals present in the waste rock included minor amounts of chalcopyrite [$CuFeS_2$], sphalerite [ZnS], and pentlandite [$(Ni,Fe)_9S_8$]. The waste rock at Diavik is sorted into three streams according to S content (Type I < 0.04 wt.%, Type II 0.04 to 0.08 wt.%, and Type III > 0.08 wt.% S) (Smith et al., 2013a).

Each of the 4 humidity cell experiments (small-scale laboratory) discussed here was conducted over a 9 year period. The humidity cells were each constructed with 1 kg of Type III waste rock with mean S content of 0.18 wt.%. The weathering cycle for the humidity cells was based on a weekly schedule of flooding the cells with 500 mL deionized water (first week of the experiment included three flooding events then twice weekly flooding events for the second and third weeks), dry air, and wet air per the ASTM D5744 (ASTM, 1996) protocol and the Lapakko and White (2000) modification of the protocol (Langman et al. 2014). The humidity cell experiments were conducted in duplicate at two temperatures (22 °C and 5 °C).

The Type III active-zone lysimeter (AZL) experiments (medium-scale field) were conducted over 11+ years at Diavik and consisted of two HDPE vessels (2.2 m in diameter × 1.7 m in height). Duplicate experiments were constructed with Type III waste rock with mean S content of 0.053 wt.%. Flow volume from the AZL experiments was measured using rain gauge tipping buckets connected to drains. Samples for geochemical analysis were collected from the drains every 2-3 days during periods of flow. Temperature was measured at the AZL experiments at depths of 0.3, 0.6, and 1.0 m below ground surface.

The Type III test pile experiments (large-scale field) were conducted over a period of 11+ years at Diavik and included a waste-rock pile constructed of Type III material measuring 50 m × 60 m × 15 m high with mean S content of 0.053 w.t.% (Smith et al., 2013b). Flow volume from the interior of the test pile experiment was measured using rain gauge tipping buckets connected to lysimeter drains at the base of the pile. Samples for geochemical analysis were collected from the drains every 2-3 days during periods of active flow. Temperature was measured at the interior of the test pile at intervals of ≈0.5 m through the top 11 m of the experiment and below the liner of the test pile (≈14-16 m below the pile crest).

Samples collected from each of the experiments were analysed for a suite of 42 inorganic and general parameters, which included Fe, Ni, Co, Cu, Zn, Al, Si, Ca, Mg, K, Na, and SO_4, pH, and alkalinity. Thorough descriptions of the humidity cell, AZL, and test pile experiment sampling procedures are provided by Langman et al. (2014), Bailey et al. (2015), and Smith et al. (2013c), respectively.

Conceptual Model

An integrated conceptual model for sulfidic mine waste-rock weathering developed to simulate the geochemical evolution of Diavik waste rock in a humidity cell experiment (Wilson et al., 2018a) was scaled to simulate the geochemical evolution at the Diavik field experiments. Similar mineralogy was used for the simulations with the exception of S and C mineral contents which differed between the laboratory and field experiments. Temperature and infiltration rates were constant for the humidity cell simulations. The temperature for the field experiment simulations were based on the measured daily values at the AZLs and test pile experiments. Infiltration of water through the field experiments was calculated on a daily basis from measured precipitation data using the FAO Penman-Monteith (FAO P-M) method described by Neuner et al. (2013).

Simulations of the Type III humidity cell effluent were conducted to facilitate calibration of the model using S and C mineralogy specific to the laboratory experiments. Specific calibration parameters included diffusion coefficients for the sulfide minerals, surface area for the host minerals and equilibrium constants for the precipitation and dissolution of secondary minerals. Calibration of the influence of temperature on rate constants was also conducted for the humidity cell simulations. Simulation of the Type III AZL and Type III test pile experiments were conducted by adjusting the S and C content to match the measured S and C content of the field experiments. Physical parameters including hydraulic conductivity and soil hydraulic values were also adjusted to represent the field experiments. Only the matrix portion (material < 5 mm diameter) of the field experiments was considered in the simulations. The temperature of the AZL simulation was uniform throughout the simulation domain; the temperature for the test pile simulation varied with depth within the simulation domain consistent with measured values. Temperature within simulations of the field experiments fluctuated daily and flow and reactions within the test pile simulation stopped when T<0°C.

The integrated conceptual model of sulfidic mineral weathering is based on oxidants $O_{2(aq)}$ and Fe^{3+} being dominant drivers of sulfide mineral oxidation (Nordstrom & Southam, 1997; Blowes et al., 2003). The stoichiometry for generic pyrrhotite can be used to describe the overall reaction of oxidation by $O_{2(aq)}$ (Nicholson and Scharer, 1998; Janzen et al., 2000; Belzile et al., 2004):

$$Fe_{(1-x)}S + (2 - 0.5x)O_{2(aq)} + xH_2O \rightarrow (1 - x)Fe^{2+} + SO_4^{2-} + 2xH^+, \quad (1)$$

Versions of equation 1 for $CuFeS_2$, ZnS, and $(Fe,Ni)_9S_8$ were included in the simulations to approximate oxidation of the remaining sulfide minerals by $O_{2(aq)}$.

To simulate the oxidation of sulfide minerals by Fe^{3+}, three parallel reactions were used, following a reaction mechanism proposed by Schippers and Sand (1999). The oxidation of Fe^{2+} was kinetically controlled and was included because it of its role in the supply of Fe^{3+} to the geochemical system (Singer and Stumm, 1970; Schippers and Sand, 1999; Rohwerder et al., 2003).

$$Fe_{(1-x)}S + (2-2x)Fe^{3+} \rightarrow (3-3x)Fe^{2+} + S^{0}, \quad (2)$$

$$S^{0} + 1.5O_{2(aq)} + H_2O \rightarrow SO_4^{2-} + 2H^{+}, \quad (3)$$

$$Fe^{2+} + 0.25O_{2(aq)} + H^{+} \leftrightarrow Fe^{3+} + 0.5H_2O, \quad (4)$$

Site specific host minerals were included based on host rock mineralogy. Host minerals biotite, muscovite, albite, calcite, and dolomite were represented by mineral specific rate expressions coupled with reaction stoichiometry. Secondary minerals were included based on the results of speciation modelling which indicated that Fe(III)(oxy)hydroxide, jarosite, gypsum, siderite, gibbsite, and amorphous silica could all be present at one or more of the experimental scales. Secondary minerals were allowed to precipitate or dissolve according to mineral specific equilibrium-controlled rate expressions coupled with reaction stoichiometry.

All simulations were conducted using 1-D domains sized to the experiment (e.g. the test pile simulation domain was a 1 m × 1 m × 12.5 m column). Physical parameters such as hydraulic conductivity and van Genuchten soil hydraulic parameters were obtained from Neuner et al. (2013).

Results and Discussion

The simulated effluent concentrations for the humidity cell experiments indicated that the conceptual model as implemented captured the measured effluent concentrations well for parameters SO_4, Fe, Ni, and pH over the course of the 9 year simulation period (fig. 1). The simulated effluent concentrations for the AZL and test pile experiments (fig. 1) indicated that the calibrated model captured the measured effluent concentrations well for parameters SO_4, Fe, Ni, and pH over the course of the 5 year simulation period; however, pH was slightly over-estimated in later years in both cases. Additional simulations for the AZL and test pile experiments indicated that carbonate mineral availability may be reduced at the field-experiment scale (calibrated pH shown in fig. 1).

The effluent concentrations of Fe, Ni, Co, Cu, Zn, Al, Si, Ca, Mg, K, Na, and SO_4 were influenced in the simulations by multiple processes including primary and secondary mineral precipitation and dissolution, sorption, and temperature. For example: i) SO_4 concentrations were influenced by sulfide mineral oxidation and precipitation and dissolution of jarosite and gypsum, ii) Ni, Co, Cu, and Zn concentrations were influenced by sulfide mineral oxidation and sorption to Fe(III)(oxy)hydroxide minerals, and iii) Fe and Al concentrations were influenced by the dissolution of multiple host minerals (biotite, muscovite, sulfides (Fe only)) and precipitation and dissolution of Fe(III)(oxy)hydroxide and gibbsite respectively.

Conclusions

This reactive transport code implementation of a conceptual model of sulfide oxidation developed at the laboratory scale indicated that a mechanistic approach to scale-up can result in a reasonable assessment of expected waste-rock effluent. The core scale-up parameters used in these simulations are routinely measured at mine sites and include mineral content, temperature, and rainfall. It is suggested that there is good potential for implementation of this approach at other sites because of the use of the relatively small number of readily available parameters required for the simulations.

Acknowledgements

Funding for this research was provided by a Collaborative Research and Development Grant from the Natural Sciences and Engineering Research Council of Canada (NSERC) awarded to D.W. Blowes, Principal Investigator; Diavik Diamond Mines, Inc.; the International Network for Acid Prevention; and the Mine Environment Neutral Drainage Program. The authors would like to thank our colleagues Carol Ptacek, Jeff Bain, Sean Sinclair, Colleen Atherton, Steven Holland, Lianna Smith, Andrew Krentz, Jordan Zak, David Barsi, and the many other graduate and undergraduate students who contributed to this project, and Diavik personnel Gord Macdonald, David Wells, Darcy Bourassa, Dianne Dul, Justin Grandjambe, and Kyla Gray for their assistance with this research.

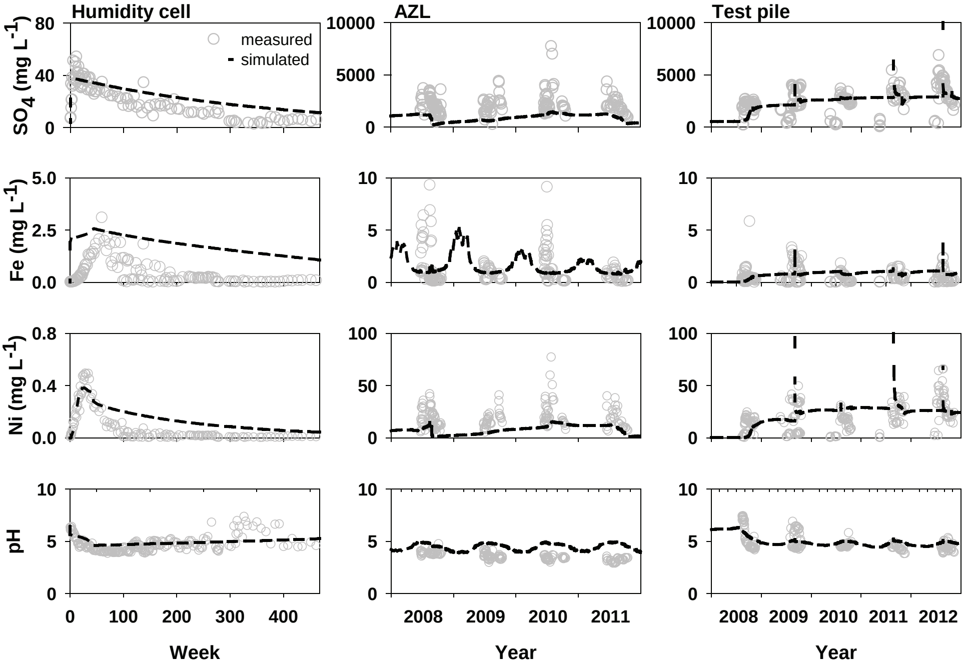

Figure 1 *Concentrations of mineral weathering products SO4, Fe Ni, [mg L-1] and pH versus time [weeks, year] measured in Type III warm temperature humidity cell, Type III AZL, and Type III test pile effluents compared to aqueous concentrations exiting the simulation domains.*

References

American Society for Testing and Materials. *Test Method for Laboratory Weathering of Solid Materials Using a Humidity Cell*; ASTM International, 1996; p. 19.

Ardau, C., Blowes, D.W., Ptacek, C.J. (2009) Comparison of laboratory testing protocols to field observations of the weathering of sulfide-bearing mine tailings. J. Geochem. Explor. 100, 182-191.

Amos, R.T., Blowes, D.W., Bailey, B.L., Sego, D.C., Smith, L., Ritchie, A.I.M. (2015) Waste-rock hydrogeology and geochemistry. Appl. Geochem. 57, 140-156.

Bailey, B.L., Blowes, D.W., Smith, L., Sego, D.C. (2015) The Diavik Waste Rock Project: Geochemical and microbiological characterization of drainage from low-sulfide waste rock: Active zone field experiments. Appl. Geochem. 62, 18-34.

Belzile, N., Chen, Y.W., Cai, M.F., Li, Y. (2004) A review on pyrrhotite oxidation. J. Geochem. Explor. 84, 65–76.

Blowes, D.W., Logsdon, M.J. (1998) Diavik Geochemistry Baseline Report. Prepared by Sala Groundwater, Inc. and Geochimica, Inc. for Diavik Diamond Mines and submitted to Canadian Environmental Assessment Agency, 121 p.

Blowes, D.W., Ptacek, C.J., Jambor, J.L., Weisener, C.G. (2003) The geochemistry of acid mine drainage. In: Lollar, B.S. (Ed.), Environmental Geochemistry, 9, Treatise on Geochemistry, Elsevier-Pergamon, pp. 149–204.

Jambor, J.L. (1997) Mineralogy of the Diavik Lac de Gras kimberlites and Host Rocks. Prepared by Leslie Investment, Ltd. for Diavik Diamond Mines and submitted to the Canadian Environmental Assessment Agency, 187 p.

Janzen, M.P., Nicholson, R.V., Scharer, J.M. (2000) Pyrrhotite reaction kinetics: reaction rates for oxidation by oxygen, ferric iron, and for nonoxidative dissolution. Geochim. Cosmochim. Acta 64(9), 1511-1522.

Kempton, H. (2012) A review of scale factors for estimating waste rock weathering from laboratory tests. In: *Proceedings of Ninth International Conference on Acid Rock Drainage*; Ottawa, Ontario, 2012.

Langman, J.B., Moore, M.L., Ptacek, C.J., Smith, L., Sego, D., Blowes, D.W. (2014) Diavik Waste Rock Project: evolution of mineral weathering, element release, and acid generation and neutralization during a 5-year humidity cell experiment. Minerals 4(2), 257–278.

Lapakko, K.A., 2003. Developments in humidity-cell tests and their application. In: Jambor, J.L., Blowes, D.W., Ritchie, A.I.M. (Eds.), Environmental Aspects of Mine Wastes: Mineralogical Association of Canada Short Course Series. Economic Geology Publishing Company, pp. 147-164.

Lapakko, K.A., White, W.W., 2000. Modification of the ASTM 5744-96 kinetic test. In: *Proceedings of Fifth International Conference on Acid Rock Drainage*; Society for Mining, Metallurgy, and Exploration: Littleton, Colorado, 2000; pp. 631-639.

Mayer, K.U., Frind, E.O., Blowes, D.W. (2002) Multicomponent reactive transport modeling in variably saturated porous media using a generalized formulation for kinetically controlled reactions. Water Resour. Res. 38(9), 13-1–21.

Neuner, M., Smith, L., Blowes, D.W., Sego, D.C., Smith, L.J.D., Fretz, N., Gupton, M. (2013) The Diavik Waste Rock Project: water flow though waste rock in a permafrost terrain. Appl. Geochem. 36, 222–233.

Nicholson, R.V., Scharer, J.M. (1998) Laboratory Studies of Pyrrhotite Oxidation, MEND Project 1.21.2.

Nordstrom, D.K., Southam, G. (1997) Geomicrobiology of sulfide mineral oxidation. Rev. Mineral. Geochem. 35, 361-390.

Rohwerder, T., Gehrke, T., Kinzler, K., Sand, W. (2003) Bioleaching review part A: progress in bioleaching: fundamentals and mechanisms of bacterial metal sulfide oxidation. Appl. Microbiol. Biotechnol. 63, 239-248.

Sapsford, D.J., Bowell, R.J., Dey, M., Williams, K.P. (2009) Humidity cell tests for the prediction of acid rock drainage. Minerals Engineering, Vol. 22, pp. 25-36.

Schippers, A., Sand, W. (1999) Bacterial leaching of metal sulfides proceeds by two indirect mechanisms via thiosulfate or via polysulfides and sulfur. Appl. Environ. Microbiol. 65(1), 319-321.

Singer P.C., Stumm, W. (1970) Acidic mine drainage: the rate-determining step. Science, New Series, 167(3921), 1121-1123.

Smith, L.J.D., Moncur, M.C., Neuner, M., Gupton, M., Blowes, D.W., Smith, L., Sego, D.C. (2013a) The Diavik Waste Rock Project: Design, construction, and instrumentation of field-scale experimental waste-rock piles. Appl. Geochem. 36, 187-199.

Smith, L.J.D., Blowes, D.W., Jambor, J.L., Smith, L., Sego, D.C., Neuner, M. (2013b) The Diavik Waste Rock Project: Particle size distribution and sulfur characteristics of low-sulfide waste rock. Appl. Geochem. 36, 200-209.

Smith, L.J.D., Bailey, B.L., Blowes, D.W., Jambor, J.L., Smith, L., Sego, D.C. (2013c) The Diavik Waste Rock Project: Initial geochemical response from a low sulfide waste rock pile. Appl. Geochem. 36, 210-221.

Wilson, D., Amos, R.T., Blowes, D.W., Langman, J.B., Smith, L., Sego, D.C. (2018a) The Diavik Waste Rock Project: A conceptual model for temperature and sulfide-content dependent geochemical evolution of waste rock – laboratory scale. Appl. Geochem. 89, 160-172.

Wilson, D., Amos, R.T., Blowes, D.W., Langman, J.B., Smith, L., Sego, D.C., (2018b). The Diavik Waste Rock Project: Scale-up of a reactive transport conceptual model for temperature and sulfide-content dependent geochemical evolution of waste rock. Appl. Geochem. 96, 177-190.

Wilson, D., Amos, R.T., Blowes, D.W., Sinclair, S.A., Smith, L., Sego, D.C., (in prep). The Diavik Waste Rock Project: Simulation of the geochemical evolution of large-scale test piles using a scaled temperature and sulfide-content dependent reactive transport conceptual model.

A New Approach to Validate a Mixing Zone Study of a Gold Mine Effluent

Caroline Sant'Ana Zanetti, Flávio de Morais Vasconcelos

Hidrogeo Engenharia e Gestão de Projetos, Rio Grande do Norte street, 1.164, room 501, Belo Horizonte, Brazil

Abstract

This study was conducted in a gold mining located at the city of Conceição do Pará/MG. This study aims to validate the theoretical dimension of a mixing zone with field physical chemical parameter data and to verify the impact of the effluent discharge of this gold mine into the Pará river. Water quality data of parameters such as: arsenic, copper, iron and sulfate were also used for the development of mixing zone dimension. Mathematical modeling of mixing zone was done in accordance to the methodology recommended by the EPA, 1991.

Introduction

Due to the relevant difference between the water quality criteria for effluent discharge and the water quality criteria for receiving water, the national and state environmental regulation for water quality in Brazil (CONAMA 430/2011 and DN-COPAM/CERH-MG 01/08) allow the development of a study to determine the "Mixing Zone". This type of study is very important and applicable for the mining industries that need to discharge its effluent in receiving water.

In order to enlarge the security level of the mining water dam in terms of the increase of the free board and decrease of the probability of untreated water discard disposal, this study was made to determine the mixing zone of the Pará River generated by the Effluent Treatment Plant (ETP) treated effluent in the proportion of 48 m^3/h from the dam and 50 m^3/h from the underground mine. The water that is inside the dam has high concentrations of arsenic, total cyanide, copper, iron, sulfate, and total dissolved solids (water that is not pumped to the ETP).

The objective of the present study is to define the geometry of a mixing zone generated by a mining effluent discharge into Pará River, for the following parameters: arsenic, total cyanide, copper, iron, phosphorus, nitrate, total dissolved solids (TDS) and sulfate. The study area is located in Conceição do Pará, Minas Gerais, Brazil, where a gold mine discharge its effluent into Pará River.

Dam Water Balance: The dam receives 3 m^3/h from the Oil-Water Separator (OWS), 69 m^3/h annually from the gold ore processing plant and 31,7 m^3/h annually from average rainfall (total income of 103,7 m^3/h). The dam loses 26 m^3/h of water by evaporation due to the use of sprinklers, 18,87 m^3/h in solar evaporation and 105 m^3/h by feeding the ore processing plant (total water 149,87 m^3/h). At the end there is a negative balance of 46,17 m^3/h (free board of 1,5 m is very concerning, since torrential rains can make this board even smaller).

There is an Effluent Treatment Plant where aluminum sulfate and flocculants are added to the suspended solids in the water, and then it passes though columns of activated carbon. This ETP works with water from the underground mine, and it directs the effluent to the Carneiro stream.

The current study was developed to calculate the mixing zone in Pará River in a situation where the ETP starts to receive water from the mine and the tailing water dam (approximately 98 m^3/h) and discharge into the river. Furthermore, the study aims to confirm that the treated effluent discharge is environmentally acceptable, increases the free board of the water dam and reduces the need for emergency discharge in case of torrential rains.

Technical Background

To understand the mixing zone of a receiving water, it is necessary to know the water quality of both the effluent and the receiving drainage (at the discharge point), each flow rate and the cross-section geometry of the receiving channel. This data was found throughout the study and made it possible to calculate the geometry and extension of the mixing zone. Furthermore, after the effluent discharge, the river starts the self-attenuation process, where the effluent flow dilutes in the river water.

Methodology

Sample collection: The ETP should operate at least 24 hours before the sample collection to ensure that the effluent gets to the receiving body (effluents flow velocity is unknown). The sample collection was made in 4 different points such as three samples in Pará River (one upstream, one downstream and one at the discharge point) and one last sample in the effluent, right after the ETP treatment.

The samples collected in the Pará River were obtained using a boat in order to better characterize the physical dimension of the mixing zone. The ETP effluent sample was collected on a reservoir where the treated water is stored before being discharged into the river. The temperature, pH, dissolved oxygen (DO), electrical conductivity (EC) and redox potential (Eh) were measured *in situ*.

Chemical analysis: The parameters that were analyzed are: major cations (Ca, Mg, Na, K), trace metals (Fe, Al, Cu, Pb, Ni, Zn, Cd, Mn, Co), non-metal (As), anions (sulphate, carbonate, bicarbonate, total alkalinity, nitrate, nitrite, chloride, phosphorus and cyanide).

Flow rate estimation on the river: The flow rate was estimated using data from the fluviometric station named Velho do Taipa #40330000, which is located downstream in the river in relation to the discharge point. In order to have a conservative analysis in terms of parameters dilution, the study used the minimum monthly flow recorded by the fluviometric station.

Mass balance for the ETP effluent discharge into the Pará River: The arsenic, total cyanide, copper, iron, phosphorus, nitrate, TDS and sulfate concentration on the receiving body were determined through the application of a mass balance between the parameters concentration in the discharged ETP effluent and the concentrations recorded upstream in the Pará River, following the equation (Equation 01):

$$C_{final} = \frac{\left(C_1 \cdot Q_1\right) + \left(C_2 \cdot Q_2\right)}{Q_1 + Q_2} \qquad (01)$$

Where:

C_{final}: final concentration;
C_1: upstream concentration;
Q_1: receptor flow rate;
C_2: concentration in the ETP effluent;
Q_2: effluent flow rate.

Mathematical modeling of the mixing zones physical length: the physical dispersion of the sulfate was used as basis to model the mixing zone length, since this parameter falls within the category of "inert" elements, and faithfully represents the physical advance of the parameters inside the drainage. Elements which are labeled as "not inert" will dissipate faster in the water and will have a shorter mixing zone when compared with the "inert" ones. In other words, the sulfate dilution depends only on physical processes, while the other elements also depend on chemical processes (adsorption, absorption or simple precipitation). Therefore, the end of the mixing zone of the sulfate shows that all other parameters are already diluted in the receiving water.

The geometric characteristics of the water drainage is determined by using some parameters in the calculation model of the mixing zone (section width, river slope and river depth for the specific flow rate). The water level determination was made by the HidroWIN software, and the input data were: geometric characteristics of the section, average slope and the Manning's Roughness Coefficient.

The mathematical modeling of the sulfates physical dispersion after the effluent discharge is obtained through the following equation (Equation 02):

$$C_x = \frac{C_e Q_e W}{Q_s \left(\pi \cdot D_y \, X/u\right)^{1/2}} \qquad (02)$$

Where:

C_x: maximum pollutant concentration distance X from the outlet;
C_e: effluent concentration;
Q_e: design effluent flow;
W: stream width;

Q_s: design stream flow;
D_y: lateral dispersion coefficient;
X: distance from the outlet;
u: flow velocity for the design flow.

The Equation 02 is recommended by the *Environmental Protection Agency of United States* (EPA, 1991) for situations where the effluent dispersion is ruled by the receiving body's turbulence (*ambient-inducted mixing*), in other words, when the flow rate of the receiving body is substantially higher than the effluent flow, as showed in this study.

The lateral dispersion coefficient is calculated through the following equation (Equation 03):

$$D_y = 0.6 \,.\, d \,.\, u^* \pm 50\% \qquad (03)$$

Where:
d: water depth at the design flow;
u^*: shear velocity.

For calculating the shear velocity, the following equation should be used (Equation 04):

$$u^* = (g \,.\, d.\, s)^{1/2} \qquad (04)$$

Where:
g: acceleration due to gravity;
s: slope of the channel;
d: water depth.

***Table 1** Results obtained with the mixing zone's mathematical modeling using a flow rate of 31,7 m³/s.*

Medium flow rate of 31,7 m³/s and Q effluent =0,028 m³/s = 100 m³/h		
Acceleration due to gravity (g)	9.81	m/s²
Slope of the channel (s)	0.0005	m/m
Shear velocity (u*)	0.41	m/s
Water depth (d)	7.0	m
Lateral dispersion coefficient (Dy)	1.740215	
Effluent concentration (SO_4)	3,229.16	mg/L
Design effluent flow (Qe)	0,028	m³/s
Stream width (W)	60	m
Design stream flow (Qs)	31.7	m³/s
Flow velocity for the design flow (u)	0.12	m/s

Results

Physical-chemical parameters results: The effluent electrical conductivity on the ETP was high. However, these values decrease rapidly when the effluent is discharged into the river and equals with the conditions measured upstream. The other parameters were not so different from the reference values (upstream situation). This is the most important physical-chemical parameter to determine the geometry of a mixing zone in the field

Chemical analysis result: The parameters used for the determination of the mixing zone, in this situation, are: arsenic, total cyanide, dissolved copper, dissolved iron, phosphorus, nitrate, TDS and sulfate. The results were compared with the Brazilian state norm DN COPAM 01/08-Effluent discharge.

Flow rate calculation of the wanted section of the Pará River: This calculation can be done through a maximum, medium and minimum flow analysis, using data collected from the Fluviometric Station Velho do Taipa, which is located downstream in the same river of the ETP effluent discharge. The minimum monthly flows were measured between 1938 and 2016, and its drainage basin is approximately 7,350 km². However, the effluent discharge point is located upstream in the river compared to the fluviometric station, and a ponderation between the two drainage areas must be done. Using a drainage area of 5695 km² for the effluent discharge point, a correction factor of 0.77 was found. After the calculations, the minimum monthly flow (conservative analysis) was 31.7 m³/s (analysis was made in September, which is a month that the ETP doesn't discharge the effluent on the river since it's when the river has the smallest flow rate).

Mass balance and definition of the effluent discharge mixing zone at the ETP of the Pará River: According to the following table, it becomes clear that one of the most important factors in the mass balance calculation to obtain the final concentration after the dilution is the flow of the receiving water, which is 114,120 m³/h (31.7 m³/s). As mentioned earlier in this study, this flow rate is calculated using a conservative method and represents the minimum monthly flow in the Pará River.

Mathematical modeling of the mixing

***Table 2** Discharge effluent and receiving body's quality data*

Parameter	Unity	DN COPAM 01/08-Effluent discharge	ETP Effluent	DN COPAM 01/08- Class II	Pará River (upstream)
Total Arsenic	mg/L	0.2	0.686	0.01	0.0157
Free Cyanide	mg/L	0.2	0.134	0.005	0.003
Dissolved Copper	mg/L	1.0	0.705	0.009	0.003
Dissolved Iron	mg/L	15	9.73	0.3	1.328
Total Phosphorus	mg/L	-	0.41	0.2	0.23
Sulfate	mg/L	-	3,229.160	250	21.958
TDS	mg/L	-	4,919	500	157
EC	µS/cm	-	6,013	-	92
Nitrate	mg/L	-	30.500	10	1.198

***Table 3** Parameter concentration in the mixing zone considering the mass balance concept*

Parameter	ETP Effluent		Pará River		Mixing zone's effluent	DN COPAM 01/08- Class II
	C (mg/L)	Q (m^3/h)	C (mg/L)	Q (m^3/h)	(mg/L)	
Total Arsenic	0.686	100	0.016	114,120	0.016	0.01
Free Cyanide	0.134	100	0.003	114,120	0.003	0.005
Dissolved Copper	0.705	100	0.003	114,120	0.004	0.009
Dissolved Iron	9.730	100	1.328	114,120	1.335	0.3
Total Phosphorus	0.412	100	0.230	114,120	0.230	0.2
Sulfate	3,229.16	100	21.958	114,120	24.766	250
TDS	4,919.00	100	157.00	114,120	161.169	500
Nitrate	30.50	100	1.20	114,120	1.224	10

zones physical length: the mixing zone calculation confirms the in situ evaluation of the water electrical conductivity data, showing a quick parameter dilution in a small distance. With the calculations and analysis of the previous table, it was concluded that the Pará River establishes its original characteristics approximately 3 meters downstream the effluent discharge.

In this modeling the parameter sulfate was used in all the calculations. That way, to calculate the physical length of the mixing zone it was used a concentration of 22 mg/L, as suggested by the laboratory analysis of the superficial water of the Pará River.

In other words, a 3 meters long mixing zone is enough to reduce 3,229.16 mg/L of sulfate being discharged with a flow rate of 0.028 m^3/s (100 m^3/h) to 22 mg/L (upstream value) in the Pará River, therefore, making it possible to use this discharge alternative. This length is consistent with the electrical conductivity values obtained in the river at the time of the discharge, consequently validating the mathematical value calculated (Figure 1).

Therefore, as it was mentioned before, the mixing zone calculation is confirmed by the *in situ* evaluation at the discharge point, showing a quick recovery of the original river parameters after a small distance. At the discharge point, the river water electrical conductivity was slightly elevated (274 µs/cm), and about 3 meters downstream this value decreased to 92 µs/cm (upstream original value).

Conclusions

The study showed the results of an estimated and field measured mixing zone of a treated ETP effluent discharge into the Pará River. The procedure was made with the mass balance calculation and the mathematical modeling to estimate the physical length of the receiving body's mixing zone.

The mathematical modeling of the mixing

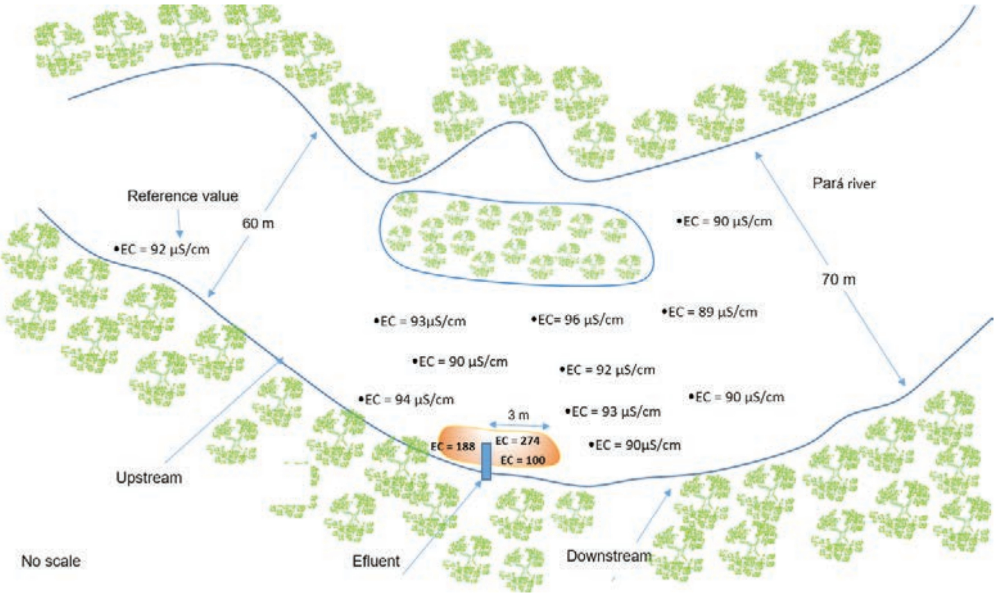

Figure 1 *Schematic drawing of the mixing zone.*

zone's length was made in agreement with the EPA norms, and an extension of 3 meters was found for it. In other words, the parameters concentration returns to the values collected upstream approximately 3 meters after the effluent launching point (the river reestablishes its original physical-chemical condition).

With all the calculations and analysis made it is safe to say that the discharge of the ETP effluent does not imply in consequences to the receiving body, since the parameters concentrations are quickly diluted due to the high flow rate of the receiving body.

References

ABNT – NBR 9897 (1987). Planejamento de amostragem de efluentes líquido e corpos receptores. Rio de Janeiro RJ.

ABNT – NBR 9898 (1987). Preservação e técnicas de amostragem efluentes líquidos e corpos receptores. Rio de Janeiro RJ.

Agência Nacional das Águas - ANA. Inventário das Estações Pluviométricas da Agência Nacional das Águas. Available in <www.ana.gov.br>

AMERICAN PUBLIC HEALTH ASSOCIATION (APHA) Standard Methods for the Examination of Water and Wastewater. 2005. 21st ed., Baltimore, Maryland.

Deliberação Normativa Conjunta COPAM/CERH-MG nº 01, de 05 de maio de 2008. Provides the classification of water bodies and the environmental guidelines for their classification, as well as establishing the effluent launching conditions and standards, and provides other measures, 2008.

US EPA. 1991. Technical Support Document for Water Quality-based Toxics Control. EPA 505-290-001. U.S. Environmental Protection Agency, Office of Water, Washington, DC.

8

MIGITATION

Remediation options for wind-remobilised Pb-Zn old tailings: An example from an 80-year Pb-Zn-Ag mine in NW-Argentina

Camilo R. de los Hoyos[1], Diego A. Marrero[1], Juan M. Sitjá y Balbastro[2], Julien Declercq[3], Robert J. Bowell[3]

[1]*SRK Consulting (Argentina), Av. Emilio Civit 404, (M5502GVR) Ciudad de Mendoza, Argentina*

[2]*National Direction for Water Politics and Federal Coordination, Secretary for Water Politics and Infrastructure, Ministry of Interior. Esmeralda 255, office 1106, (C1035ABE), Ciudad Autónoma de Buenos Aires, Argentina*

[3]*SRK Consulting (United Kingdom), 5th Floor, Churchill House, 17 Churchill Way, Cardiff, CF10, Wales, UK*

Abstract

This article describes remediation options for wind-remobilised old tailings at an 81-year Pb-Zn-Ag mine in NW-Argentina. Long-term exposure of the dry surface of the older impoundments to wind led to spread of tailings over 2.5km^2. Scoping-level geochemical characterisation included grain-size analysis, ICP-MS whole-rock geochemistry, XRD mineralogy, ABA and SPLP tests, and sequential extraction. Results suggested that high Pb-Zn contents are restricted to remobilised waste material and no leaching to the underlying soil occurred. Thus, the thickness was the driving factor to define remediation options. For sectors with up to 0.3m (22%), excavation and mobilisation was suggested. For thicknesses between 0.3 and 0.6m (78%), re-vegetation without impermeabilization was considered the best option. For in-situ old tailings (0.1km^2), surface impermeabilization and re-vegetation was strongly suggested.

Keywords: Pb-Zn tailings | wind remobilisation | scoping-level study | remediation options

Introduction

Pb-Zn-Ag mining has an over 80-year history at Mina El Aguilar in Jujuy province, NW-Argentina, where more than 20Mt ore has been processed since 1936. Tailings have been disposed in seven impoundments covering 5km^2. Most of the exposed surface of the older impoundments has been covered and remediation tasks are ongoing. Long-term exposure of the dry surface of the older impoundments to strong wind has led to remobilisation of tailings with deposition in dunes and layers spread over 2.5km^2. Only the most recent TSF is lined, in line with current international standards internally adopted by the company and progressively being required by regulators. Progressive closure of the old TSFs started in 2006 by means of geophysics and drilling surveys to determine thickness and material type for remediation purposes. Closure of the two major old TFSs 4 and 5 (≈70% of the TFS area) consisted of a low-permeability cover underlying a layer of soil for revegetation. These closure tasks were concluded in 2014. The same remediation method was planned to be applied for TFS 6 once construction of TFS 7 was complete in 2015/16.

At the starting time for operation at Mina El Aguilar and further decades, virtually no environmental standards were applied and tailings were normally disposed over the natural soil and were not covered after their lifespan. As part of the measures taken by the new owner to upgrade the operation to international environmental standards, a remediation program was undertaken. The challenge was not only to eradicate or minimise health and safety risks, but to optimise the expenditure in terms of environmental conservation and protection.

SRK was commissioned to undertake a scoping-level study for the remediation of the areas covered by remobilized old tailing. The

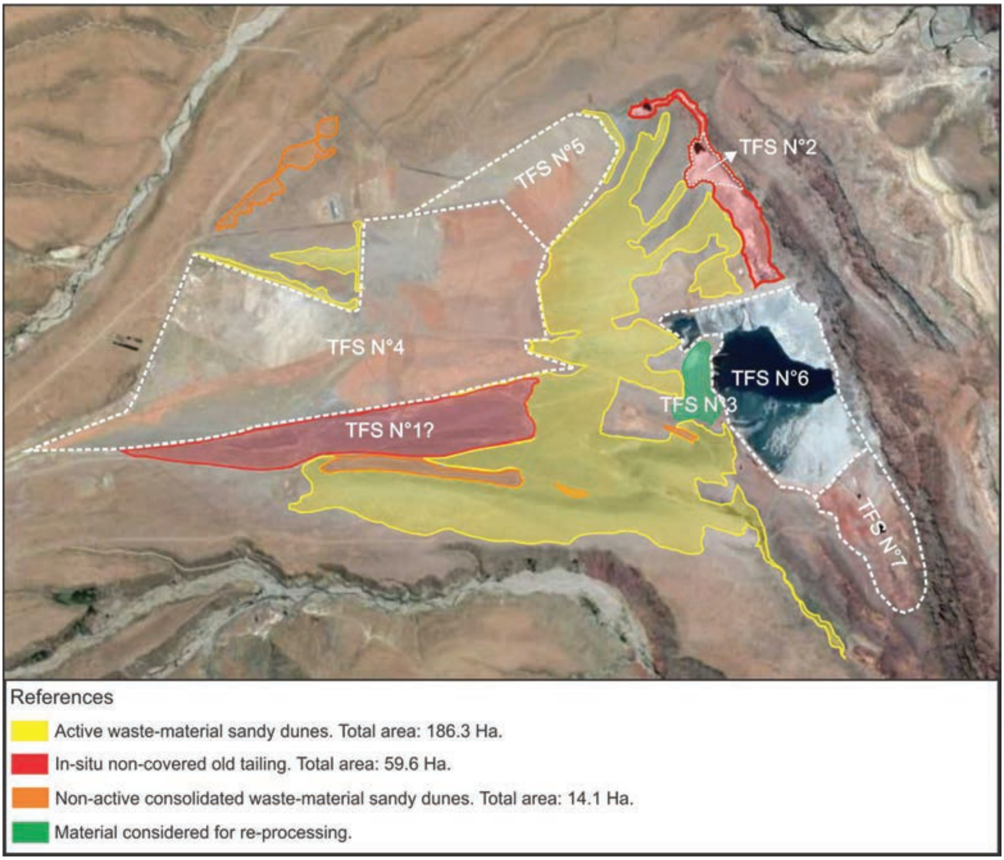

***Figure 1** Main lithotypes for wind-remobilized tailings.*

study included an initial geochemical characterization of the waste material, estimation of the volume of each waste-material category and recommendations for conceptual remediation options.

Project background

The region of Mina El Aguilar is characterized by arid climate, scarce rainfall, (<300mm a year) and strong wind most part of the year. The TFSs and wind-remobilized tailings area is composed of fossil alluvial fans where virtually no drainage network is present. These alluvial deposits end against an outcrop called "Espinazo del Diablo", mainly composed of Cretaceous/Tertiary sandstones and shales. Average alluvial sediments thickness in the study area is between 30 and 50m and they are mainly composed of conglomerates with a red-coloured matrix formed by silt/clay and minor sand.

Five groundwater monitoring wells were installed in the TFSs area and surroundings until 2013 (Ausenco-Vector, 2013), three of which are located in the study area itself. The water level measured during the drilling campaign at these two wells was 33 and 50m below surface. Hydraulic testing at these wells yielded hydraulic conductivity values between 10^{-7} and 10^{-9} m/s for the hosting sedimentary aquifers, suggesting low permeability. Physic-chemical analyses were performed on water samples collected in three wells. Groundwater is neutral to slightly alkaline (pH 7-8) and electrical conductivity suggests fresh water in the periphery (EC 850-1,500 µS/cm) and brackish (EC up to 4,000 µS/cm) in the central area. However, further hydrogeological studies are required to distinguish different aquifers. Metals such as Pb, Zn, Cd, Fe, Mn and Cu are below maximum limits for drinking water (DR N° 5980/06, Government of Jujuy Province, Argentina) and frequently below detection limits (LODs). This suggests

Figure 2 *(a) Active waste-material sandy dunes; (b) Non-active waste-material sandy dunes; (c) In-situ old tailings.*

that metals possibly leached from overlying TFSs and remobilized tailings might be retained in the waste material itself and/or the pre-mining sediments. However, further sampling and static/kinetic geochemical testing together with further data from hydrochemical monitoring is necessary to assess chemical leaching from sediments to groundwater.

SRK distinguished three main types of remobilized waste material (Figure 1).

Active sandy dunes (ASD) are the most widespread waste material cover an area of 1.86 km^2 and are composed of fine and medium-grained grey-coloured sand with no cementation. Non-active sandy dunes (NASD) are present in relatively small patches which cover 0.14 km^2 all together. This material is characterized by fine and medium-grained dark grey sand slightly cemented and more stabilized against wind. In-situ old tailings (IOT) possibly corresponding to the oldest TFSs were identified immediately southwards from TFS 4 and to the northwest of the study area, covering a total area of 0.6 km^2. This material is composed of strongly cemented layered fine sediments partially covered by aeolian sand. TFS 3 was found to host economic Ag, Pb and Zn contents and is being considered for reprocessing. Examples for the mentioned lithologies are shown in Figure 2.

Methods

The owner carried out the first sampling campaign in 2012 which consisted of 90 samples from 30 sampling soil pits, where sediments were collected each 0.3m for whole rock chemical analyses. Results showed that the highest Pb, Zn and Cd total contents occur in the upper sediments, although no relationship between chemistry and lithology was assessed. For this reason, SRK carried out a complementary sampling at a scoping level.

18 new soil pits were excavated to sample the identified lithologies in surface and up to about 1.5 m. Material types were first distinguished and 3 to 5 samples were collected from each pit according to the described lithotypes. Special care was taken to avoid sample contamination of pre-mining sediments from the overlying waste material. 63 new samples were collected to perform the following static geochemical tests:

- Whole-rock chemistry: 63 analyses by the ICP-MA-39 method. Maximum LODs were 10,000 ppm for Pb, Zn and As and 2,000 for Cd.
- X-Ray diffractometry: 23 samples without previous heavy mineral separation.
- Acid-Base Accounting (ABA): 12 samples to assess overall acid rock drainage (ARD) potential from disulfides, including pH-paste tests. The modified ABA test (Lawrence and Wang, 1997) was preferred.
- Synthetic Precipitation Leaching Procedure (SPLP): 13 samples to assess short-term metal mobility.
- Sequential extraction: 9 samples to assess metal speciation. The method designed by Renella et al. (2004) was used to assess Cd speciation, which consists of a preliminary step of sample exposure to ammonium nitrate to optimize separation of Cd-bearing soluble species.

Additionally, thickness of the waste-material was measured in 229 points to assess volume estimation of each lithotype for engineering purposes.

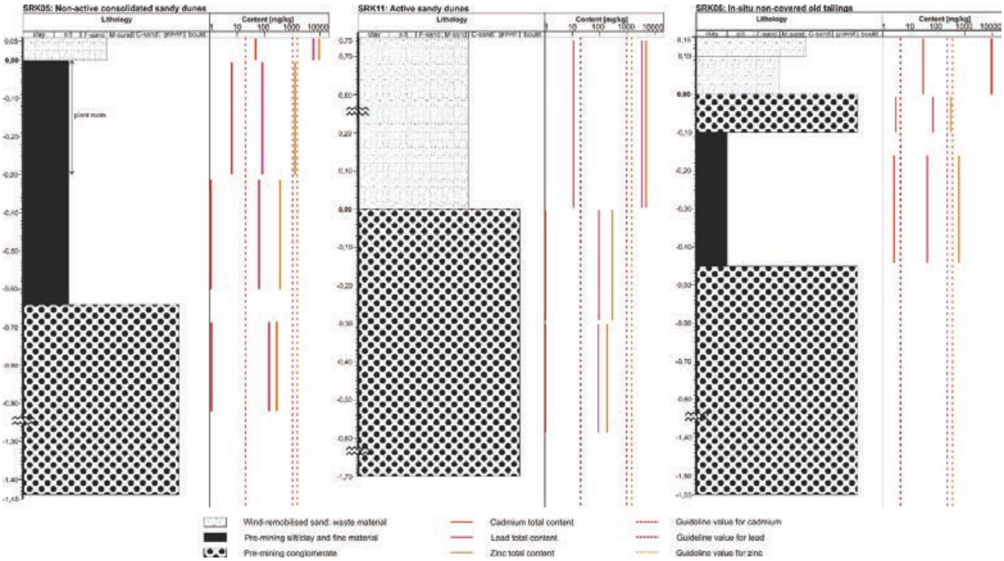

Figure 3 *Chosen examples to represent NASD, ASD and IOT-type waste material sites.*

Results

Figure 3 shows one typical example representing each waste-material type and the total Zn, Pb, Cd contents sampled in depth and related to lithology. As no baseline control limits are available, maximum reference limits based on the guidelines (DR N° 5980/06, Government of Jujuy Province, Argentina) for industrial use of soil for Zn (15,000 ppm), Pb (10,000 ppm) and Cd (30ppm) are also plotted in Figure 3. Whole-rock chemistry showed that high total contents of Zn, Pb and Cd are restricted to the waste material in the ASD (pit SRK11), suggesting poor to virtually absent leaching to the underlying PMS. In the typical example of NASD (pit SRK05), high contents in the mentioned metals exceeding the reference values are also restricted to the waste material. However still high Zn concentrations were measured up to 30cm depth, suggesting leaching of this metal at shallow depths. The example representing the IOT sites (pit SRK06) shows high contents in Zn, Pb and Cd in the tailing material although Zn is virtually exceeding its reference value until 0.5 m depth, suggesting relatively strong leaching of this metal to the underlying PMS.

A summary of results for each lithotype is shown in Table 1, which includes Zn, Pb and Cd total contents, total vs sulphide S and neutralization vs acid potential (NP/AP) from ABA testing. Pre-mining underlying sediments and paleo-soils (PMS) are added to Table 1 for comparison with the waste material. Overall, Zn, Pb and Cd total contents in the waste material are much higher than those in the PMS. The PMS are richer in Zn, Pb and Cd only in the close vicinity of

Table 1 *Summary of results for total contents, ratios and ABA testing.*

Lithotype	St	S2-/St	Zn	Pb	Cd	NP/AP	pH-paste
ASD	2.02 to 2.91	0.71 to 0.91	3,341 to >10,000	2,031 to >10,000	13 to 55	0.01 to 0.70	7.0 to 7.8
NASD	2.33	0.68	9,164 to >10,000	4,166 to 6,561	27 to 44	1.04	7.2
IOT	1.98 to 6.67	0.55 to 0.70	4,337 to >10,000	3,398 to >10,000	163 to 361	0.01 to 1.27	7.2 to 7.8
PMS	N/A	N/A	40 to 2,546	17 to 299	<1 to 13	N/A	6.0 to 7.8

the IOT, specially that one possibly related to an ancient TFS (TFS 1?). Among the waste-material lithotypes, the IOT are the highest in total S although it generally in the oxidized form as the total-S/sulphide-S tend to be relatively low. The neutralization potential ratio (NP/AP) is very low in the waste material (0.01 to 1.27), which combined with the sulphide S contents (>1%) would classify this material as potentially acid producing. However, this result show inconsistency with high paste-pH values (7.0 to 7.8), suggesting that either sulphide S is somehow encapsulated or speciated in monosulfides that do not produce ARD when oxydized (e.g. galena, sphalerite). Unfortunately, NAG testing was not performed to assess directly acid producing by disulphide rapid oxidation due to tight budget and schedule. NAG testing is strongly recommended for a forthcoming PFS level of remediation engineering.

The most abundant minerals identified by X-Ray diffractometry were quartz, muscovite, plagioclase, K-feldspar and gypsum. Chlorite is frequent in the NASD whereas dickite and muscovite are more frequent in the ASD. The most frequent sulphide is sphalerite and galena was not detected in this sample batch, which possibly requires a previous separation from light minerals. A Pb-carbonate was identified as shannonite in the ASD, which forms in strongly oxidized environments from further oxidation of cerussite. However, further mineralogical studies should be performed to identify Pb and Zn carbonates and sulphates that might be present in the waste material.

Results from SPLP testing showed concentrations below the maximum limits of the method for the majority of the analysed material. Waste material collected from the NASD resulted in 1.098 mg/L for Cd and 5.141 mg/L for Zn in the leachates, strongly exceeding the respective limits of 0.03 and 0.084 mg/L. The sample representing the IOT showed even stronger exceedances in the produced leachate, containing 4.108 mg/L of Cd and 6.251 mg/L of Zn.

The total accumulated concentration of metals released in the four stages of the chosen sequential extraction methodology (Renella et al., 2004) is difficult to check against total contents for QC purposes, as the maximum LOD of ICP-MA-39 is 10,000 mg/L for Zn and Pb. Overall, 40-65% of the Pb content is released in the first stage of soluble exchangeable cations. Contrastingly, very high Pb contents are released in the second stage when Fe-Mn oxi-hydroxides are attacked. An even higher proportion (around 75%) is released in the third stage when sulphides and sulfosalts are attacked, suggesting that Pb is speciated in these reduced minerals and might be released in oxidizing conditions. Geochemical kinetic tests simultaneous with mineralogical studies should be performed to assess metals speciation and release into solution. Very high Zn contents were released in the first step of soluble cation exchange. Cd was not extracted during the previous exposure to ammonium nitrate at pH 3 and 7, suggesting that it is not speciated in calcium carbonate. The sample representing the IOT released about 80% of Cd during the third stage (secondary sulphides) although this metal also shows positive correlation with Zn.

Discussion

Results from static geochemical studies and mineralogical assessment were conclusive enough to perform a preliminary classification of the wind-remobilized waste material. These results together with detailed lithological mapping and thickness measurement allowed for a scoping-level assessment on remediation options based on geochemical characterization and volume estimation of each lithotype. The three waste-material types shown Zn, Pb and Cd contents much higher than the underlying pre-mining sediments. However, the IOT released these metals in exceedance during the short-term leaching tests, suggesting that important metal release is highly possible during long-term leaching in natural conditions, despite of the dry climate at the study area. Indeed, the underlying pre-mining sediments were affected by release of metals (mainly Zn) from the overlying IOT until at least 0.5 depth. Thus, characteristics and volumes for the studied waste materials can be summarized as follows:

- Active sandy dunes: 619,797 m^3 distributed in 1.86 km^2. Metal leaching potential is considered to be low. About 30-50 samples to complete static geochemical characterization at a PFS level. 3 to 5 samples necessary for kinetic testing.

- Non-active sandy dunes: 15, 129 m^3 distributed on 0.14 km^2. Metal leaching potential is low to medium, the latter especially in the vicinity of in-situ old tailings. About 20-30 samples to complete static geochemistry al PFS level. 3 to 5 samples to perform kinetic testing.
- In-situ old tailings: 264,506 m^3 distributed in 0.60 km^2. Metal leaching potential is considered to be high and short-term with enough rainfall. About 25-40 samples to complete static geochemistry at a PFS level. 8-10 samples for kinetic testing.

Conclusion

At a conceptual level, only economic factors were considered for the ASD as they are not geochemically reactive. Given their small area and volume, as well as their low to medium leaching potential the NASD were incorporated to the ASD until further studied are performed. Thus, the thickness was the driving factor to define conceptual remediation options for the both mentioned units. For sectors with up to 0.3m (22%), excavation and mobilisation was suggested. For thicknesses between 0.3 and 0.6m (78%), re-vegetation without impermeabilization was considered the best option. For in-situ old tailings (0.60km^2), surface impermeabilization and re-vegetation was strongly suggested, regardless the thickness of these deposits. To upgrade the level of this study to PFS or higher, further geochemical assessment consisting of volumetrically representative sampling for static tests to complete waste-material characterization and kinetic testing running at least 40 weeks to assess chemical reactivity are recommended.

Acknowledgements

The authors thank Compañía Minera Aguilar S.A. for providing critical comments on the preliminary verions of this article and for the proper permits to publish some results from the SRK´s geochemical and engineering study.

References

Ausenco-Vector (2013a) Perforación e instalación de freatímetros – Complejo Minero Aguilar (FR-01, FR-02 y FR-03). Report N° ARVC-00304-00-000. February 2013.

Ausenco-Vector (2013b) Perforación e instalación de freatímetros – Complejo Minero Aguilar (FR04 y FR-05. Report N° ARVC-00304-00-000. June 2013.

Lawrence, R.W., Wang, Y. (1997). Determination of neutralization potential in the prediction of acid rock drainage. Proc. 4th International Conference on Acid Rock Drainage, Vancouver, BC: 449-464.

Renella, g., Adamo, P., Bianco, M.R., Landi, L., Violante, P., Nannipieri, P. (2004). Availability and speciation of cadmium added to a calcareous soil under various managements. European Journal of Soil Sciences 55: 123-133.

Water Ingress Mitigation Programs for Underground Mines – Hydrogeological and Rock Mechanical Demands on Grout Properties

William Goodman, Deon Van Dyk, Nico Grobler, Antony Osborne

Sovereign Hydro Pty Ltd, Box 999, 6951 South Perth, Australia, wgoodman@sovereignhydro.com

Abstract

Many grouting programs designed to manage mine water ingress involve high pressure injection into water-bearing fractures to reduce/eliminate inflows. Optimal grouts for durable mine water control 1) exhibit low viscosity and very small particle size (suspension grouts) or no particles (solution grouts) to permit deep penetration into water-bearing fractures; and 2) set up as an insoluble, chemically inert, flexible or self-healing solid that maintains adhesion to wet rock surfaces and concrete despite recovering formation pressure and continued blasting, mining-induced subsidence and stress redistribution.

Keywords: grout, water ingress, fractures, cementitious, solution, bitumen, precipitate, polymer-based emulsion

Introduction

Underground mines commonly combat water ingress into shafts, declines and production areas. Depending on a region's hydrogeology, a mine may have to manage significant water inflows simply to maintain operation. Grouting is one means of managing mine and tunnel leaks. Grout types used for water ingress control vary widely but can be generally categorized as cementitious, solution, bituminous, precipitate and polymer-based emulsion.

Each type of grout has strengths and weaknesses for water sealing. Some grouts are used in combination to improve efficacy and to control costs. For example, low-cost Ordinary Portland Cement (OPC) is commonly used with more expensive specialty grouts. OPC is used to fill a significant percentage of void space, and the specialty grout with superior wash-out resistance and penetrability is the principal means of sealing off the water.

This paper is a review of grout types commonly used for water ingress control. Applicability of different grouts depends on pore space aperture, differing inflow rates, hydrostatic pressures, water geochemistry and rock movement.

Hydrogeologic Considerations

High compressive strength of many rock types permits mining at considerable subsurface depths. Given a hydrostatic pressure gradient of 9.8 kPa/m in freshwater systems, pressures at practical mining depths (greater than 3500 m in South Africa, for example) can be very high.

Many mines use active dewatering in advance of mining to increase the cone of depression (reduce hydrostatic pressures) and thereby reduce the rate at which water enters the mine through exposed fractures in shafts and production areas. Still, inflow rates can be significant, and very large water volumes require management unless routine grouting programs are part of the mine's operation and maintenance plan.

Even small leaks in salt mines can lead to dissolution of halite and failure of shafts and engineered systems such as at the Belle Isle Salt Mine in Louisiana (Kupfer 1998). Even though some mines have pumping systems capable of handling large volumes of mine water, large inflows can be erosive to both cement and country rock (Momber and Kovacevic 1994; Banghua et al. 2018).

Grouts for Water Ingress Control

Grout types used for water control vary widely but can be generally categorized as cementitious (suspension), chemical (solution), bituminous, precipitate and polymer-based emulsion. Each category of grout has strengths and weaknesses relative to its application to water ingress control as summarized below.

Cementitious Grouts: Cements are a type of suspension grout – they contain solid particles suspended in a liquid (typically water). Cementitious grouts are differentiated based on particle size as Ordinary Portland, Microfine and Ultrafine.

Ordinary Portland Cement (OPC) has historically been widely used grout for leak control, but exhibits performance limitations without additives. OPC will permeate fissures with apertures as small as 70 microns (Henn 2017), but intragranular pore space in many permeable sedimentary rocks is often smaller. Furthermore, OPC washes out when injected into high pressure, high rate inflows. Additives (e.g. Type F fly ash, slag, silica fume, pumice, bentonite, $CaCl_2$) are needed to combat washout, control bleed, and resist pressure filtration (Naudts et al. 2003). Dispersants, water reducers, and superplasticizers are used to improve mixing, and viscosity modifiers, retarders, and stabilizers are commercially available and can be incorporated into the mix. Grouters may use other additives to neutralize adverse effects of H2S (present in some limestones and evaporites) and improve set up in saline water environments.

Microfine and ultrafine grouts are milled finer (particle size about 30 microns and 10-15 microns, respectively) to penetrate smaller fissures. Some microfine grouts are slag-based. Plasticizers and viscosity modifiers are often added. Ultrafine grouts are composed of Portland cement, pumice and dispersant (Magill and Berry 2007). Although finer, microfine is still mostly applicable to fracture injection and much less so to permeation grouting of intragranular porosity in rock. Ultrafine can be used for permeation grouting although hole spacing on the order of 1-2 meters is required because of limited penetrability. Ultrafine has also been used to grout fractures in salt to reduce leaks into crude oil storage caverns at Weeks Island, Louisiana, USA (Magill and Berry 2007) and at the Waste Isolation Pilot Plant in Carlsbad, New Mexico, USA.

Cementitious grouts are brittle when set up. Consequently, in evaporites (salt and potash) that exhibit high creep rates, these types of grout can crack allowing inflows to restart. Hence, there has been considerable experimentation with, and commercialization of, alternative grouts that are either flexible or self-healing and that can also penetrate very fine aperture fractures and pores.

Solution (Chemical) Grouts: In contrast to cementitious (suspension) grouts, solution grouts do not contain particles. As such, they can penetrate very small fissures and pore space (Naudts 2003). Commonly used solution grouts include polyurethanes, acrylamides, and acrylates among others. Ideal solution grouts exhibit an initial, stable and very low viscosity followed by a sudden increase in viscosity immediately prior to gelation or curing. Gelation and set times can be controlled through the use of catalysts or inhibitors. Solution grouts are also generally chemically resistant.

Polyurethanes are commonly used to grout shafts and tunnels, and to further reduce seepage from residual wet zones after grouting with other products. Naudts (2003) categorizes polyurethane grouts as 1) water reactive; 2) two component foaming grouts (polyol-isocyanides combination); and 3) two component polyurethane elastomers. Water reactive grouts use available water to create a foam or gel. Naudts (2003) differentiates hydrophobic and hydrophilic sub-categories, and notes that hydrophilic grouts are not ideal for water ingress control. Hence they are not considered further here.

Hydrophobic polyurethane grouts repel water after the amount needed for curing is used. Hydrophobic polyurethanes penetrate, expand and fill cracks as fine as 8 microns. Different hydrophobic polyurethane grouts set up as a flexible solid (for crack injection – injectable tube applications), a semi-rigid solid (stopping large water inflows), and a rigid solid (for soil injection). In saline water environments, large mine inflows can be grouted by injecting both brine and polyurethane. The cured grout can accommodate movement along fractures (Magill and Berry 2007).

Hydrophobic polyurethanes are pH, pressure and temperature sensitive (Magill and Berry 2007). Neutral pH produces the most ideally cured grout; quality degrades in water above a pH of 8-9, and reactivity slows as the pH decreases below 7. Extremely acidic waters may preclude reactivity. These grouts react most efficiently at temperatures above 10° C. At 100 kPa pressure, reaction time, expansion and swelling begin to decrease and at 1000 kPa, no expansion or swelling occurs. Grouts may also fail to react in the presence of high concentrations of hydrocarbons. Groundwater TDS may affect gel time through chemical reaction or pH buffering. High water salinity may promote flocculation, which limits grout penetrability.

Acrylamide is a monomer used as an aqueous solution in geo-technical grouting applications for over 50 years (Magill and Berry 2007). Catalysts, activator and inhibitors are mixed together to obtain a gel grout that is impervious to water. Grout constituents include acrylamide, methylene-bis-acrylamide, acrylic acide, triethanolamine, and ethylene glycol (Spalding et al. 1987).

Acrylamide ranks high among solution grouts for water ingress control because of its extremely low viscosity (about 2 centipoise [cP]), high penetrability, controllable gel time (from 3 seconds to 10 hours), long half-life (>300 years) after injection, and resistance to shrinkage and microbiological degradation (Gentry and Magill 2012; Babcock 2016; Spalding et al. 1987). Acrylamide grout can also be used with cementitious grouts, and can withstand exposure to nuclear waste. Acrylamide grout can be mixed with brine for use in salt mines (Magill and Berry 2007).

One notable concern with use of acrylamides is health and safety during the mixing process. Mono-acrylamide is a neurotoxin that can enter the body by inhalation, ingestion or absorption through skin (Magill and Berry 2007). Grouters using acrylamide must receive special safety training. In gel form, it is non-toxic, however.

Magill and Berry (2007) also note that acrylamide is susceptible to shrinkage and premature polymerization if subjected to constant UV rays, and the grout will degrade if exposed to continual freeze-thaw and wet-dry cycles. Acrylamide does not adhere to concrete surfaces and will not stretch in a moving crack. Acrylamide also reacts more slowly in the presence of petroleum hydrocarbons.

Acrylate grouts were developed to be a less toxic alternative to acrylamide grouts. Similar to acrylamide, acrylates require a base resin to be mixed with a catalyst in order to set up a flexible gel-type grout; set times range from about one minute to one hour (Babcock 2016). United States Army Corps of Engineers (1995) describes the gelling reaction to be catalyzed by the addition of triethanolamine and ammonium or sodium persulfate to a metal acrylate (usually magnesium acrylate). Methylene-bis-acrylamide is used as a cross-linking agent. Potassium ferricyanide is used as an inhibitor if long times of setting are required. Adhesion to concrete is reportedly good, and lab testing indicates that acrylate grout can cure in the presence of extremely hot water (82°C), making it feasible for deep mining applications. (Sunder 2015). These grouts have been used in salt mine settings by balancing grout chemistry with brine.

Some acrylates physically absorb vast amounts of water and swell, thereby losing their strength (Magill and Berry 2007). The life span of acrylate grout is about 50 years, which is considerably lower than acrylamide (Babcock 2016).

Precipitation grouts: $CaCl_2$ injections have long been used to seal mine leaks at the K2 potash mine in Esterhazy, Saskatchewan (Ziegenbalg and Crosby 1997). Injected $CaCl_2$ reacts with the brine in an overlying aquifer to precipitate NaCl that clogs flow paths connecting the aquifer to the mine workings. Although somewhat successful, timing of NaCl precipitation cannot be controlled, and the finely crystalline halite precipitate does not always extend beyond the boundaries in a plug flow situation. Continued research led to development of a second precipitation grout using solutions supersaturated with gypsum (Ziegenbalg et al 2009). Supersaturation is achieved using $NaSO_4$ and $CaCL_2$ solutions as inhibitors.

Achieving an effective seal using precipitation grouts (or any grout for that matter) requires that enough solids block the flow conduit and exhibit enough strength to hold against rebounding formation pressure. Secondly, flow must be sufficiently turbulent to induce gypsum precipitation.

Hot Bitumen: When injected into a water-saturated medium, hot bitumen cools quickly at the interface with water; the viscosity increases rapidly (Naudts and Hooey 2003). Steam is created at that point, however, thus decreasing the viscosity of the bitumen and serving to draw the bitumen into pore space. The faster the water flows, the faster the bitumen cools off. The skin prevents washout while the "sheltered" hot bitumen behind the skin penetrates void space in similar fashion as solution grouts. Naudts and Hooey (2003) cite a case study involving a Saskatchewan potash mine where hot bitumen was able to temporarily seal a 7000 lpm mine inflow.

Bitumen's good insulating characteristics allow it to be injected for a very long time (days - even weeks) into the same grout hole without risk of either premature blockage or wash-out (Naudts and Hooey 2003). The width of the fissures accessible to hot bitumen varies with the duration of the grouting operation. The longer the grouting operation, the finer the apertures the bitumen will penetrate. Naudts and Hooey claim that hot bitumen will penetrate 100 micron fractures.

When hot bitumen cools it is subject to significant thermal shrinkage (Naudts and Hooey 2003). Cement-based suspension grout is often injected in conjunction with hot bitumen to compensate for the thermal shrinkage of the bitumen; to make the bitumen less susceptible to creep; and to increase the mechanical strength of the end product.

Besides safety considerations in the application of hot bitumen, injection of hydrocarbons into the ground raises environmental concerns. There are, however, many types of bitumen available with a wide range of characteristics. Naudts and Hooey (2003) recommend use of a "hard" oxidized environmentally friendly type of bitumen with a high solidification point.

Polymer-Based Emulsion (PBE): PBE is a suspension of polymer emulsoids colloidally dispersed in a solution of additives that promote flow and adhesion (Gancarz and Yilmaz 2017). PBE is injected in a fluid state and remains a fluid until activated. The grain size of the particles in the polymer is less than one micron, and the viscosity of the polymer is 2.5 cP. Hence, the dilatant polymer solution at the time of injection is extremely penetrable and will go where water travels.

PBE was developed in the 1970s and first applied to high pressure-high rate inflows into deep South African mines. The grout has sealed discrete inflows of up to 12,000 lpm at pressures up to 20,000 kPa (Gancarz and Yilmaz 2017).

Inhibitors and activators are used to change the characteristics of the polymer, enhancing the control over direction of flow and resulting in greater penetration. The polymer remains stable in its fluid state until activated. Activation may also be achieved through agitation when the polymer is subjected to shear action as it passes through an orifice of a fissure. Once activated, the dispersed colloidal compound coagulates to form a mass of linked and tethered rubberlike laths.

When first formed, the activated polymer transforms to a hydrated jelly–like plug of matted laths. As pressure is applied to the activated polymer, the water is expelled and the laths adhere to each other to form a denser and more competent plug that is both impermeable and flexible.

PBE is non-expanding, non-toxic and user friendly. PBE is not exothermic – no heat is generated during the curing process.

At present, PBE is available only through a single entity that holds the patent. The grout cannot be purchased for use other than by license holders. The grout is primarily used for sealing fissures (consolidation grouting). PBE has not yet been extensively used for sealing intragranular pore space (permeation grouting).

Conclusion

Optimal grouts for durable mine water control 1) exhibit low viscosity and very small particle size (or no particles in the case of a solution grout) to permit deep penetration into water-bearing fractures; 2) set up as an insoluble, chemically inert, flexible or self-healing solid that maintains adhesion to wet rock surfaces and concrete despite continued blasting, mining-induced subsidence and stress redistribution; and 3) withstand high formation pressures. Precipitation grouts can be useful but only where mine waters are highly saline. Ultrafine cement satisfies the first and third criteria, but is brittle and may fracture in rocks that are prone to shifting or creep. Polyurethane grouts satisfy the first and second criteria, but may be pushed out of fissures under high fluid pressures. Acrylamide satisfies the first and second criteria, but does not adhere to rock/concrete. Hot bitumen and PBE grouts satisfy all three criteria. Hot bitumen and PBE have proven ability to stop large mine inflows. Hot bitumen poses environmental and safety issues whereas PBE is environmentally safe. Hot bitumen may not seal water-transmissive pore space smaller than 100 microns, whereas the particle size for PBE is less than one micron. Hot bitumen is commercially available and can be applied by appropriately trained grouting crews, whereas PBE is a patented product that can only be applied by users under license. Low-cost OPC can be used in combination with any of the above-referenced grouts to fill larger voids and to provide strength.

References

Babcock, BN (2016) Cement Grout vs. Chemical Grout: Which One to Use, When, and Why. Tunnel Business Magazine. May 26, 2016, 4 pp

Banghua Y, Zhongwei C, Jianping W, Tianhang B, Shumin L (2018) Predicting Erosion-Induced Water Inrush of Karst Collapse Pillars Using Inverse Velocity Theory. Geofluids, vol. 2018, Article ID 2090584, 18 pp doi:10.1155/2018/2090584

Gancarz PM, Yilmaz A (2017) Curtain Grouting for Leak Mitigation in Tunnels. Underground Grouting and Ground Improvement Short Course, Colorado School of Mines, May 1-5, 2017, Golden, Colorado, 148 pp

Gentry J and Magill (2012) Acrylamide grouting: successfully controlling groundwater from Canada to South America. American Society of Civil Engineers. Grouting and Deep Mixing 2012, New Orleans, Louisiana, p 1562-1568

Henn RW (2017) Grouting of Underground Structures. Gancarz PM, Yilmaz A (2017) Curtain Grouting for Leak Mitigation in Tunnels. Underground Grouting and Ground Improvement Short Course, Colorado School of Mines, May 1-5, 2017, Golden, Colorado, 52 pp

Kupfer DH (1998) Geology and History of the Belle Isle Salt Mine, The Southernmost Five Islands Salt Dome, St. Mary Parish, Louisiana. Louisiana Geological Survey Geological Pamphlet No. 11, Baton Rouge, Louisiana, 34 pp

Momber A, Kovacevic R (1994) Fundamental Investigations on Concrete Wear by High Velocity Water Flow. Wear. 177. 55-62. 10.1016/0043-1648(94)90117-1.

Magill D, Berry R (2007) Comparison of Chemical Grout Properties, Which Grout Can be Used Where and Why. Geo-Denver 2007 Congress, Denver, Colorado 11pp

Naudts A, Landry E, Hooey S, Naudts W (2003) Additives and admixtures in cement-based grouts. Grout 2003, Deep Foundations Institute/Geo-Institute of the American Society of Civil Engineers, New Orleans, Louisiana 14 pp

Naudts A (2003) Irreversible changes in the grouting industry caused by polyurethane grouting: an overview of 30 years of polyurethane grouting. Grout 2003, Deep Foundations Institute/Geo-Institute of the American Society of Civil Engineers, New Orleans, Louisiana 17 pp

Naudts A, Hooey S (2003) Hot bitumen grouting: the antidote for catastrophic inflows. Grout 2003, Deep Foundations Institute/Geo-Institute of the American Society of Civil Engineers, New Orleans, Louisiana 17 pp

Spalding BP, Lee SY, Farmer CD, Hyder KL, Supaokit P (1987) In Situ Grouting of Transuranic Waste with Polyacrylamide. Oak Ridge Model (CONF-871075) Conference Proceedings, Volume I, Part 3. Martin Marietta Energy Systems, Inc., Oak Ridge, Tennessee, p 39-76.

Sunder, S (2015) Acrylate Resinous Grout Systems: New Solutions for Stabilizing Soil and Sealing Leaks. Trenchless Technology, October 8, 2015, Trenchlesstechnology.com

United States Army Corps of Engineers (1995) Engineering and Design, Chemical Grouting. Engineering Manual EM 1110-1-3500, Washington, D.C., 34 pp

Ziegenbalg G, Crosby KS (1997) An Overview of a Pilot Test to Reduce Brine Inflows with Controlled Crystallization of Gypsum at the IMC Kalium K2 Brine Inflow. Mineral Resources Engineering vol. 6, no. 4, p 173-184

Ziegenbalg G, Gosselin J, Johnson CS (2009) Grouting by Controlled Gypsum Crystallization From Supersaturated Solutions – A New Way to Reduce Brine Inflows Into Salt and Potash Mines. Proceedings, 9th International Symposium on Salt, Gold Wall Press, Beijing, p 657-667

Horizontal scavenger borehole system for plume containment

Martin Holland[1], Kai Witthüser,[1,2]

[1]Delta-h Water Systems Modelling (Pty) Ltd, Pretoria, South Africa, info@deltah.co.za

[2]Affiliated Professor, Institute for Groundwater Studies, University of Free State. Bloemfontein 9300, South Africa

Abstract

While scavenger boreholes have been proposed for groundwater remediation for a number of Mine Residue Deposits throughout Southern Africa, a limited number of case studies are available. Furthermore, the use of horizontal scavenger boreholes for site remediation is common in the northern hemisphere but is an emerging technology in South Africa. This paper presents results and lessons learnt from implementing the first horizontal scavenger borehole system for the hydraulic containment of a seepage plume emanating from an unlined Tailings Storage Facility (TSF).

Keywords: ICARD | IMWA | MWD 2018, hydraulic plume containment, horizontal scavenger boreholes.

Introduction

The Horizontal Directional Drilling (HDD) Industry in South Africa is largely focused on the installation of underground utilities mainly within the overburden. As a result, directional drilling companies are not familiar with the drilling and equipping of horizontal boreholes for hydraulic plume containment, just as very few hydrogeologists have experience in the design and installation of horizontal boreholes. In this case study, two horizontal scavenger boreholes were drilled, screened and commissioned to intercept a seepage plume emanating from a Tailings Storage Facility (TSF) and associated Return Water Dam (RWD). The study area is located in the eastern limb of the Bushveld Igneous Complex, 25 km south west of Steelpoort in the Limpopo Province, South Africa. The area is underlain by massive to poorly layered pyroxenites and norites of the Rustenburg Layered Suite, intruded by numerous dykes. In-situ weathered and unconsolidated transported overburden covers most of the valley bottom and lower and mid slopes of the valley sides, forming a typical Basement aquifer system. Tailings deposition (from a Platinum Group Metals Concentrator) onto the TSF started in October 2006 and surface- and groundwater monitoring data showed a deterioration of water qualities downstream of the TSF and RWD. Highly elevated nitrate, ammonia, sulphate and sodium concentrations in the seepage water from the TSF contribute to a saline mine drainage chemistry. The current plume (represented in fig. 1 by sulphate) emanating from the 60 Ha TSF migrates preferentially in zones of deeper weathering along 'pre-facility' drainage courses to the east and south-east towards a large perennial river. The vertical plume migration is limited by the underlying fresh bedrock with significantly lower permeability compared to the upper weathered overburden with associated higher flow rates. Results from a site specific numerical groundwater flow and transport model indicated that the plume could be intercepted before reaching the receptors, in this case regarded as the southern tributary and the perennial river to the east. The sulphate concentration limit for the river is 70 mg/L based on the instream flow requirement. Scenario modelling concluded that two horizontal wells could in theory be more effective than 10 conventional boreholes, reducing the Capex and eventually the long-term Opex cost for the predicted minimum pumping rate of 15 years post-closure (expected for 2019).

Methods

Following an initial plume characterisation study, additional monitoring boreholes were drilled during the plume interception study to establish sub-surface conditions along the

Figure 1 *Simulated sulphate plume extent.*

proposed horizontal borehole path. The drilling was preceded by ground geophysical surveys, including earth resistivity imaging, and electromagnetic and magnetic traverses adjacent and downstream of the TSF. The main aim of the survey was to:

- confirm dyke positions inferred from regional aeromagnetic data,
- investigate geological structures and deep weathering zones as potential preferential flow paths,
- optimize the selection of drilling sites for scavenger wells.

Ultimately a total of nine geophysical traverses were conducted with a total length of 1 918 m. Based on the resistivity survey results, the resistive basement (bedrock) varies in depth from 4 m to approximately 18m below surface. Overburden and soil cover varies from absent (rock outcrops) to 1-2 m thickness. The resistivity results were also used to delineate areas associated with deep seepage, indicating saturated conditions immediately downstream of the TSF and RWD.

Boreholes drilled along the proposed horizontal borehole paths were used to confirm

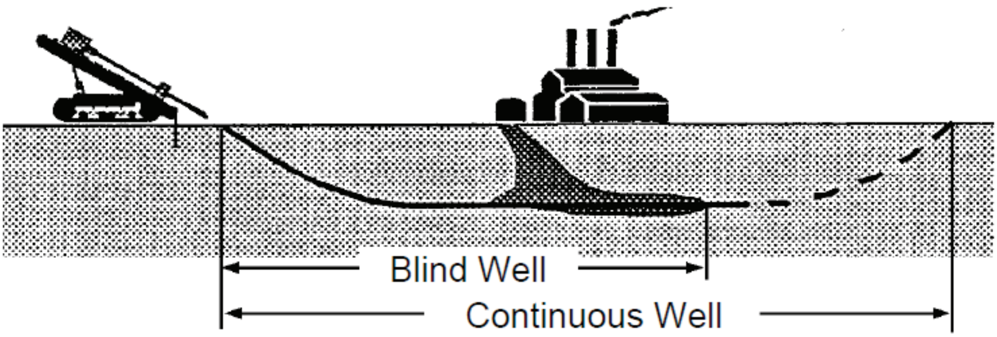

Figure 2 *Horizontal well used to intercept a plume. The solid line represents a blind well; the solid line plus the dashed line represents a continuous well. (EPA, 1994).*

the depth to bedrock, likely lithologies and groundwater qualities to optimise the horizontal borehole profile. These observation boreholes also aid in assessing and monitoring the drawdown of the water levels during testing and commissioning. Additional monitoring boreholes were drilled further downstream of the horizontal boreholes to assess the effectiveness of the hydraulic containment system. Based on hydraulic test results, the hydraulic conductivity varies from 0.1 to 0.8 m/d for the area with the highest contaminant concentrations (south of the TSF and RWD).

The information was used to establish a horizontal profile to be followed during the horizontal drilling process. The target depths were essentially the weathered-bedrock interface zones perpendicular to the preferential groundwater flow path. Directional drilling methods use specialized bits to curve bores in a controlled arc which enables bores to be initiated at a relatively shallow angle from the ground surface and gradually curve to horizontal (EPA, 1994). While blind horizontal boreholes terminate in the subsurface, in most cases the borehole is turned back towards the surface and returns to the ground to form a continuous well (Figure 2).

A summary of the pre-drilling design criteria is provided in Table 1, while the initial design considerations are given below:

- The original aim was to drill the horizontal boreholes from surface to surface along the pre-planned path so that the well screen portion of the borehole is flat or inclined at a specified grade at the desired location.
- Once the drill head (with a diameter of 165 mm) has re-emerged at the surface, it is removed from the drill string and the 110 mm OD sleeves (screened and solids) are attached directly behind the drill head and pulled into the borehole.
- A walk-over system consisting of a radio beacon-receiver measures surface location up to a depth of 16 to 18 mbgl to ensure the boreholes follow the correct path.

Results

Drilling was carried out using an American Augers DD-10 percussion rig with an air percussion hammer head. Each drill entry point was excavated to around 1 m below surface. Steering of the drill head remained below 2 % per 6 m rod length, which prevented the borehole being completed back to surface. As a result, the two horizontal boreholes were

Table 1 *Design criteria of the horizontal scavenger borehole system*

Borehole	Deepest target depth (m)	Length to target depth (m)	Total length (m)	Sulphate (concentrations)
HWELL-B1	18	70	140	450
HWELL-B1	9	50	110	96

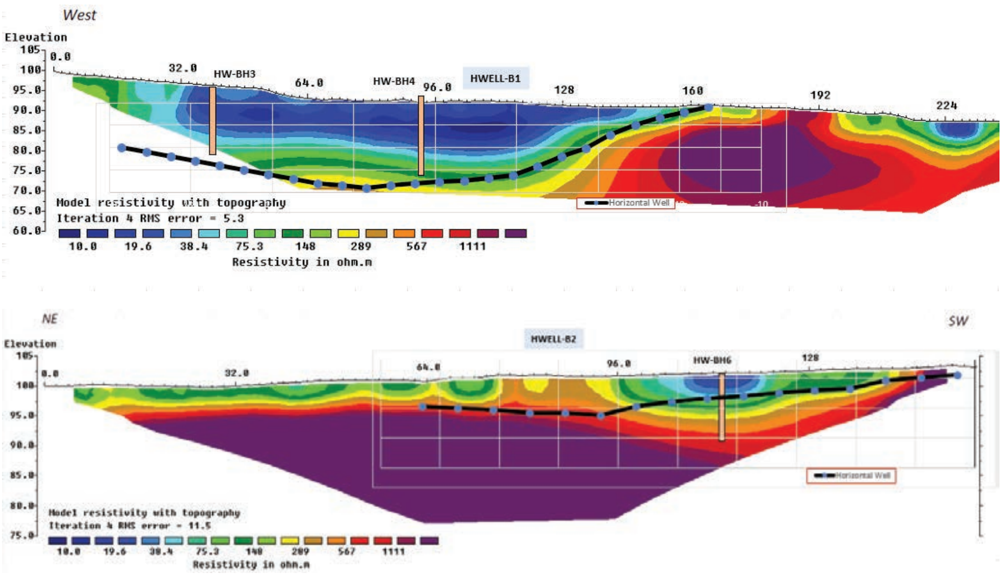

***Figure 3** Horizontal borehole profiles in relation to the closest resistivity results.*

completed as blind wells. The final drilled horizontal borehole profiles, in relation to the closest geophysical profile and vertical monitoring boreholes, is shown in fig. 3.

After a horizontal borehole was drilled it was developed using a smaller reamer forcing air and water into the horizontal borehole, flushing soft sandy overburden material from the open hole. The drill rods were moved back and forth along the entire screened section until the discharged water was relatively free of suspended material. The HDPE sleeve was pushed into the hole with the screened sections installed along the target area. Solid sleeves were used in the upper overburden. The hole opening with the protruding starter sleeve fitting over the riser HDPE pipe was sealed with a bentonite-based cement block.

The preliminary pumping tests of the horizontal boreholes included limited step tests and constant discharge tests followed by a recovery monitoring period, mainly to determine the potential yields of the boreholes and to determine the specifications for the submersible pumps for the installation. The detailed schedule of the constant discharge tests is provided in Table 2.

Based on the results, the horizontal boreholes were equipped with 3-inch submersible pumps which run through an inverter, allowing for variable discharge rates. Based on the tests conducted and the limitation of the 3-inch pump diameter, the following ranges are obtainable form the current installation.

- HWELL-B1: 0.1 L/s to 0.9 L/s (at 75 m horizontal distance)
- HWELL-B2: 0.1 L/s to 0.6 L/s (at 60 m horizontal distance)

During the time of the study, the reticulation system to the Pollution Control Dam was yet to be installed. Although no formal monitoring programme was implemented yet, the time was used to test the pumps and reticulation up to a transfer dam. Two piezometric data loggers were installed within the

***Table 2** Pumping test summary*

Borehole	Screened section (m)	Pump intake (horizontal) distance (m)	Constant discharge rate (L/s)	Time (m)	Max. drawdown (m) at pump intake
HWELL-B1	102	47	0.84	480	4.23
HWELL-B1	66	45	0.54	960	5.05

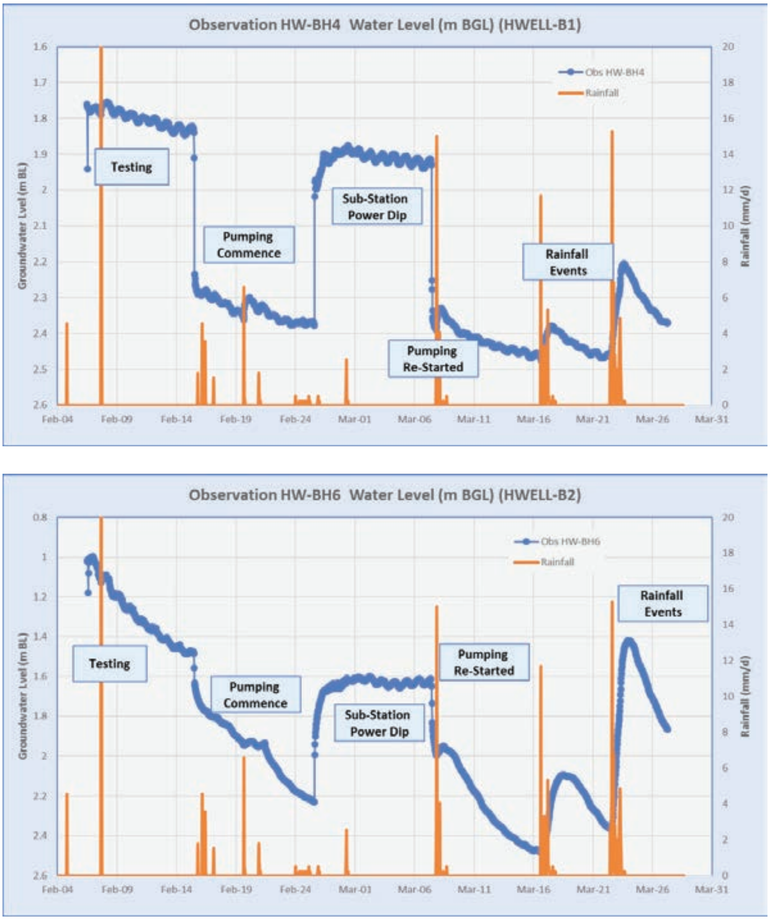

Figure 4 *Drawdown results from longer term tests.*

observation boreholes closest to the completed horizontal boreholes. Pumping rates were commissioned on preliminary licensed abstraction figures (established pre-drilling of the horizontal boreholes), namely 0.54 L/s for HWELL-B1 and 0.23 L/s for HWELL-B2. The drawdown results for the longer-term testing period are shown in Figure 4. No continuous pumping of the horizontal boreholes was possible due to power surges in the substation providing electricity to the pumps, resulting in a recovery of water levels during down-time. The system is currently being investigated to ensure an uninterrupted power supply to the pumps. While the results indicate drawdowns within the perimeter of the horizontal borehole, the larger zone of influence will only be determined once the site-specific monitoring programme becomes operational.

Updated post-closure model predictions indicate that pumping should continue beyond 15 years post closure, until source depletion (i.e. reduction of seepage rate once active deposition onto the TSF cedes and the TSF is rehabilitated) and natural attenuation of the remaining plume after pumping ceased prevents unacceptable plume concentrations reporting to the receptor (tributary). Figure 5 depicts the seepage plume with a cut-off value of 70 mg/L after 15 years post closure with the commissioning of the two existing horizontal wells. While it appears that the distribution and pumping rates assigned are sufficient to limit the plume migration, it's only with ongoing monitoring and post-audits that model predictions can be verified.

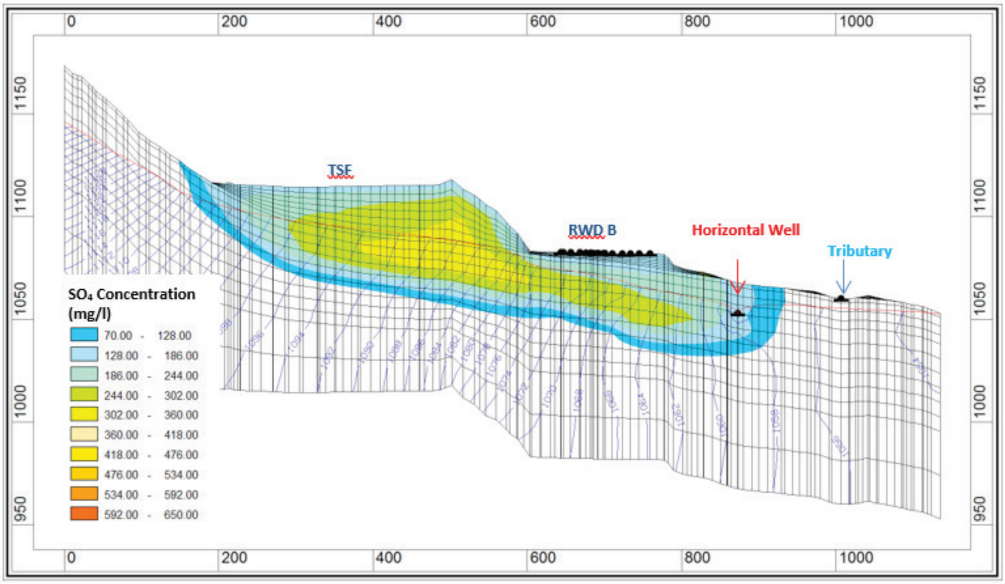

Figure 5 *Cross section showing simulated plume extent 15 years after hydraulic plume containment using horizontal boreholes commenced.*

Conclusions

Hydraulic containment of seepage plumes emanating from an unlined TSF and RWD in the eastern limb of the Bushveld Igneous Complex was required to prevent impacts on a downstream river and ensure legal compliance. Detailed geophysical and intrusive investigations as well as numerical modelling assisted in the delineation of zones of preferential weathering and ultimately groundwater flow and transport pathways. These were intercepted using two horizontal scavenger boreholes. Current pumping rates are based on licensed abstraction limits, but will be adjusted once a site-specific monitoring programme is initiated to delineate the zone of influence and to determine the effectiveness of the scavenger system.

References

EPA (1994) Alternative Methods for Fluid Delivery and Recovery. EPA/625/R-94/003. U.S. Environmental Protection Agency (EPA). Ohio, United States of America.

Mine Design for In-Situ Control of Selenium and Nitrate

Soren Jensen[1], Jennifer Foster[1], Marie-Christine Noel[1], Mike Bartlett[2]

[1]*SRK Consulting, 1066 West Hastings Street, Vancouver, British Columbia, Canada, sjensen@srk.com*
[2]*Millennium EMS Solutions Ltd. Suite 325, 1925 18 Avenue NE, Calgary, AB T2E 7T8*

Abstract

This paper describes an approach for designing and developing a coal project for in-situ control of selenium and nitrate in contact water from the mine as an alternative to engineered water treatment plants. The design integrates water management, pit design and sequencing such that completed open pits can be backfilled and used as in-situ bioreactors for attenuating selenium and nitrate. The attenuation process is well established and proven at different scales but the hydraulic design of the backfilled pit and operational control of carbon dosing will have to be developed through phased field tests carried out concurrently with full-scale design. Results of the initial on-site pilot test are presented.

Keywords: coal, selenium, nitrate, in-situ, biological, treatment, suboxic, anaerobic

Introduction

Selenium (Se) is a naturally occurring substance and an essential element required for the health of humans, animals, and some plants. However, selenium has also become a contaminant of potential concern throughout the world. Mining, power generation and agriculture are among the largest emitters of selenium world-wide (Lemly 2004).

Selenium management at mining operations typically involves:

- Source control measures to limit release from oxidizing sulphide minerals such as subaqueous disposal and low permeability covers; and
- Interception and collection of contact water for passive or active selenium water treatment.

Selenium concentrations in mine water are project specific and vary widely. Concentrations can approach 1 mg/L at sites with pronounced selenium leaching (Dockrey 2012). In comparison, the freshwater ambient chronic water quality criterion for selenium recommended by the United States Environmental Protection Agency is 0.0031 mg/L for lotic (flowing) waters (US EPA 2016). In some cases, the recommended water quality criterion for selenium could therefore be exceeded if seepage or discharge from a mine exceeds 0.5% of the total streamflow. The orders-of-magnitude difference between selenium concentrations in mine water and receiving water quality criteria means that some mining projects are required to achieve near-complete capture and treatment of all mine water from a project area to comply with instream selenium criteria.

Over the last three decades, the growing understanding of ecological effects that can be caused by selenium in aquatic environments has prompted industry to develop better and more reliable selenium water treatment technologies. Historically, selenium water treatment processes have relied on chemical reduction of selenate to selenite or elemental selenium using reducing agents such as zero-valent iron followed by ferric-coprecipitation for removal of residual selenite (CH2M Hill 2013). However, chemical processes are costly and tend to increase concentrations of dissolved components, which must subsequently be removed. In addition, the processes were not able to reliably achieve effluent concentrations required by discharge permits (Golder 2009). In the 1990s, several selenium water treatment technologies that rely on biological reduction for removal of selenium were developed and have been adopted by the mining industry (CH2M Hill 2013).

Biological removal of selenium from water relies on anaerobic microorganisms, which reduce oxidized forms of selenium, such as selenate, to more reduced forms (selenite) or to elemental selenium, which can then be removed from water by co-precipitation or precipitation. The process occurs naturally in wetlands and in suboxic lake sediments and has also been observed to occur in backfilled open pits at a closed coal mine (de Souza 1999, Bianchin 2013). The biological water treatment process also removes nitrate, which is another water quality parameter of potential concern for the mining industry. Nitrate in mine water is primarily due to dissolution of ammonium nitrate-based explosive residuals.

Although biological treatment has been proven on an industrial scale, the treatment process is relatively costly to implement and operate, particularly since water treatment often is required in-perpetuity. Lower cost treatment options, such as gravel reactors or in-pit anaerobic biological treatment, are emerging as real alternatives to mechanized treatment plants. In addition to lower cost, the in-situ treatment systems may also improve treatment performance.

This paper presents the approach used for integrating mine design and in-situ selenium management for the proposed Grassy Mountain Coal Project located in Southern Alberta and discusses design and operational control of in-situ treatment systems.

Methods

Geochemical characterization of the coal deposit and host rock at the Grassy Mountain Coal Project identified oxidizable and leachable selenium and a high likelihood of selenium concentrations exceeding water quality targets in waste rock seepage at the proposed mine. Located on a mountain ridge near the headwaters of Blairmore Creek and Gold Creek, the Project area occupies a sizable portion of the local catchment areas (Figure 1). Therefore, the capacity of the creeks to assimilate mine water discharge is limited. From the inception of the Project, it was clear that efficient collection of mine water and selenium water treatment would be required to meet receiving water quality guidelines in the downstream environment.

In a traditional approach to mine design, mine engineers are tasked with development, and later optimization, of an economic mine design that includes an open pit or under-

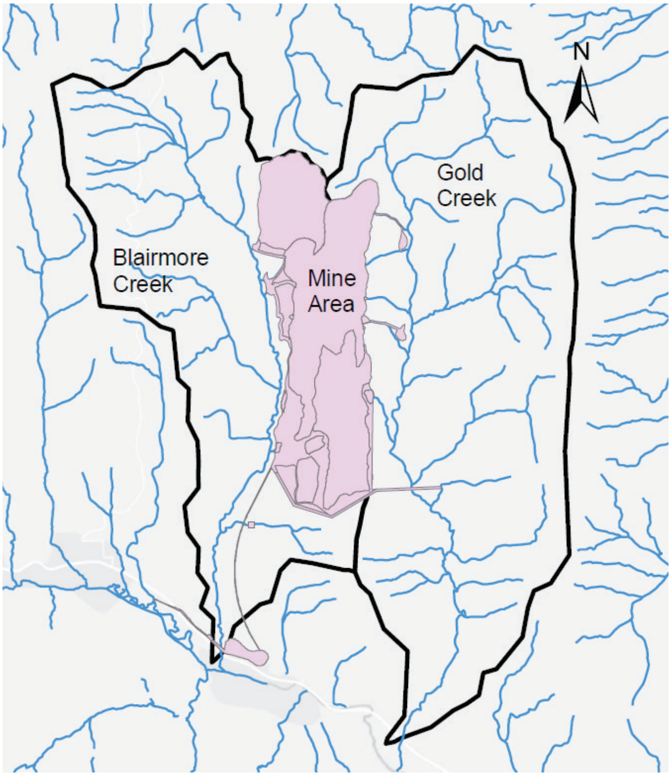

Figure 1 Ultimate Mine Footprint and Adjacent Catchments

ground mine development schedule and design of waste rock storage areas. Water management features are then designed to accommodate the most economic mine design. However, the high efficiency capture and water treatment required to manage selenium for the Project meant that the mine design had to accommodate water collection and water treatment for the project to be feasible. Selenium mitigation measures that were incorporated in the mine design included:

- A mining sequence that allowed for timely conversion of mined-out open pits to saturated in-situ anaerobic bioreactors to allow for attenuation of selenium and nitrate.
- Maximizing in-pit placement of waste rock to facilitate seepage capture.
- Design of ex-pit waste rock area foundations for seepage collection.

The conversion of mined-out open pits to anaerobic bioreactors for removal of selenium and nitrate is the key aspect of the proposed mine design and water management approach and therefore the focus of the discussion in this paper. Suboxic conditions in pit water promote the conversion of soluble selenate ions (SeO_4^{2-}) to selenite (SeO_3^{2}) or elemental selenium metal (Se^0). Selenite is less soluble and tends to adsorb to mineral surfaces. Elemental selenium is insoluble. Therefore, the conversion of selenate causes the reduced selenium species to become attenuated. Nitrate (NO_3^-) is reduced to nitrogen gas (N_2) (Martin 2009). A key requirement is the presence of dissolved organic carbon that provides electrons for these processes. The carbon in turn is oxidized to carbonate as bicarbonate and dissolved carbon dioxide.

In-situ attenuation of selenium using suboxic or anaerobic biological processes is well researched and has been demonstrated at different scales in various configurations. Luek (2012), for example, describes a pilot-scale biological reactor with a media comprising mulch, manure and gravel. In-situ biological treatment was used in a batch configuration for removal of dissolved selenium and uranium from a pit lake at the Sweetwater Mine in Wyoming in 1999 (Paulson 2004). However, there are to date no publicised examples of backfilled open pits that have been specifically designed and operated as biological reactors for removal of selenium. For the Grassy Mountain Project, the approach was therefore to develop an understanding of the process kinetics and process control strategy in parallel with the mine development by implementing on-site field trials at increasing scales.

Conversion of the open pits to anaerobic bioreactors involves some of the same design considerations as in mechanical reactor design used for active water treatment plants:

- At least one pit with sufficient hydraulic retention time must be available for water treatment early in the mine life by the time selenium and nitrate impacted mine water is produced on site.
- Subsequent open pits should ideally be hydraulically connected to the downstream-most open pit such that selenium and nitrate treatment can occur in a series of in-situ pit reactors with a single discharge point.
- The combined volume of the in-situ bioreactor (i.e. open pits backfilled with waste rock) must provide sufficient residence time for complete selenium and nitrate attenuation to occur for a range of flow and temperature conditions.
- Placement of backfilled waste rock should be planned in a way that would facilitate hydraulic control of mine water passing through the in-situ bioreactors in the open pits.

Suboxic conditions required for the attenuation process are generated by microorganisms that consume oxygen and other electron acceptors such as nitrate as they metabolize carbon. Therefore, unless existing concentrations of dissolved organic carbon are sufficient, addition of organic carbon and nutrients in the mine water is required for the process to work and is also the main process variable for controlling in-situ bioreactors. Molasses and methanol are readily available and relatively low-cost sources of organic carbon that have been used in similar in-situ treatment applications and in active water treatment plants (Martin 2009). The dose of organic carbon required depends primarily on the concentration of dissolved oxygen and nitrate in the mine water. Approximately 3 g of methanol is stoichiometrically required to attenuate 1 g of nitrate.

The rate at which suboxic conditions develop determines the time required for attenuation and consequently the hydraulic residence time required for the in-situ bioreactor. In an active water treatment plant, the residence time required is in the order of hours. The residence time required to achieve complete attenuation of selenium and nitrate in an in-situ bioreactor at the Grassy Mountain site is unknown; however, case studies of full-scale treatment systems using similar processes indicate that the hydraulic residence time required is on the order of a few weeks (Poulson 2004, Martin 2009).

Implementation of in-situ bioreactors requires an understanding of the process stoichiometry, kinetics and performance response to varying carbon types and doses. The goal of the first small-scale field trial was to evaluate these factors.

The first field test was conducted in the summer of 2017 and was intended as simple, small-scale reactors that would yield basic information on the stoichiometry and kinetics of the treatment process for a limited set of conditions. Another objective was to establish and test operating and monitoring procedures that could be transferred to subsequent larger-scale tests and eventually to full-scale operations.

Seven 45-gallon (170 Litre (L)) plastic barrels were used as small-scale reactors. Each barrel was filled with coarse waste rock and coal reject from historical mining activities in the project area. No organic material or microbial seed was added. A 1,000 L tote elevated above the barrels was used as a feed tank for the test. Feed water flowed by gravity through the test barrels. Feed flow rates were controlled by adjusting drip valves installed at the inlet on each barrel. The test setup required no power.

The barrel setup was first tested hydraulically by feeding a sodium chloride tracer solution through each barrel and monitoring the conductivity of the effluent. The tracer test demonstrated that feed flow could be controlled reliably to yield a hydraulic retention time of approximately two weeks. Reactive tests were conducted next. The feed water tote was filled with water and charged with nitrate (80 mg/L as nitrate-N) and selenate (1.3 mg/L as sodium selenate). Pails with dissolved carbon or water (for the controls) were connected to the feed water inlet of each barrel. The flow of dissolved carbon or water from the pails were also controlled by drip valves. Flow from the feed tote and from the carbon (or water) totes were approximately equal, which resulted in a combined feed with approximately 40 mg/L nitrate-N and 0.650 mg/L of selenium.

Pails containing carbon solution were replaced weekly to prevent degradation of the organic carbon in the pail. Each barrel was equipped with three inlet ports, which allowed operators to switch ports in the event biofouling blocked the flow of influent – a common problem in fixed-bed bioreactors.

Table 1 shows the test conditions used for the seven barrels. The control barrel (1) was filled with waste rock and received feed from the tote but no carbon (only water) was added to the pail. Barrels 2 through 5 received low (75% of stoichiometric demand) or high (110% of stoichiometric demand) doses of either methanol or a 50:50 mixture of methanol and molasses (by weight). In barrels 6 and 7, 5% and 20% the waste rock had been replaced by coarse coal material. The purpose of these barrel tests was to evaluate whether organic carbon leaching from coal would be sufficient to generate suboxic conditions.

Results of the reactive test are illustrated in Figure 2. Chloride concentrations in the barrel effluent (residual from the tracer test) decreased relatively uniformly for all barrels, except for the control barrel, which saw higher feed flow from the feed tote than the other six barrels. Selenium concentrations in the effluent from the four barrels that were dosed with methanol or methanol and molasses were reduced to less than 0.015 mg/L compared to a concentration of 0.200 mg/L in the control after approximately two weeks. The barrels with coal reject (6 and 7) appeared to show some attenuation when compared to the control barrel (1). However, a concentration increase in the control barrel was considered a consequence of the greater rate of flow from the feed tote as evidenced by the greater nitrate and selenium concentration. When normalized for flow, the reactive response of the coal reject barrels is the same as the response of the control barrel. Nitrate-N concentrations in the barrels dosed with carbon were less than 0.1 mg/L after two weeks compared to approximately 20 mg/L in the control barrels. The dose or type of organic carbon did not appear to affect the rate or extent of degradation.

Table 1 Test Barrel Carbon Type and Dose

Barrel #	Carbon Type	Carbon Dose
1	Control	None
2	Methanol	Carbon 1, Low Dose
3	Methanol	Carbon 1, High Dose
4	Methanol + Molasses	Carbon 2, Low Dose
5	Methanol + Molasses	Carbon 2, High Dose
6	Coal Reject	5% of Barrel Volume
7	Coal Reject	20% of Barrel Volume

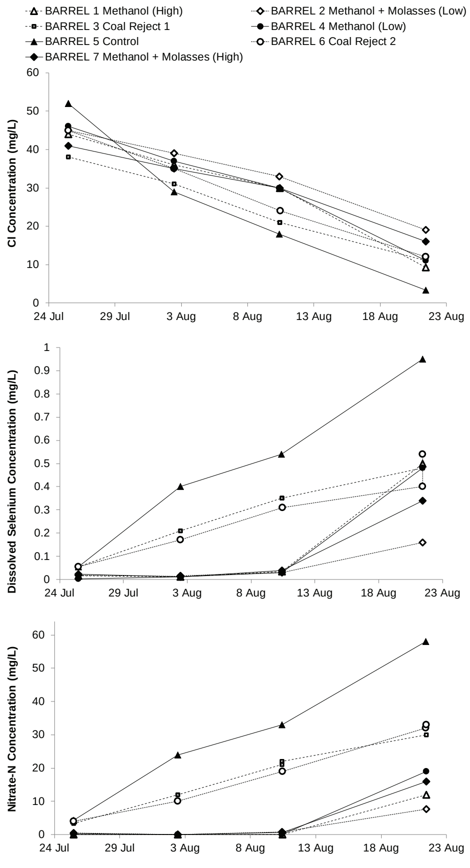

Figure 2 Chloride, Diss. Selenium and Nitrate-N Concentrations in Test Barrel Effluent

Attenuation of selenium and nitrate was sustained in the barrels for approximately two weeks after which concentrations of selenium and nitrate rebounded. This occurred due to a loss of carbon in the feed solution. Despite efforts to prevent carbon degradation in the pails with carbon solution, a biofilm formed on the inside of the tubing that supplied carbon to the barrels. The biofilm likely metabolized the readily degradable carbon before it reached the barrel inlet. This unintended loss of organic carbon illustrates the importance of maintaining anaerobic conditions in the in-situ bioreactors. Subsequent, larger-scale tests will use 100% methanol as a carbon source, which in its pure form is toxic to microorganisms, to circumvent this problem.

The barrel test demonstrated that attenuation of selenium and nitrate can be accomplished in a simple flow-through reactor using a rock media and a simple organic carbon source. The test also validated the operability of the bioreactor system, demonstrated that two weeks of resident time is a reasonable starting point for future tests and showed the importance of maintaining sufficient carbon supply to sustain suboxic conditions. Larger-scale field-tests are required to evaluate process kinetics and control at a wider range of temperatures and residence times.

Conclusions

Selenium management for the Grassy Mountain Coal Project requires that mine water capture and treatment considerations are integrated in the mine design. The conversion of mined-out open pits to anaerobic bioreactors for attenuation of selenium and nitrate is the key aspect of the proposed mine design and water management approach. The attenuation process is well established and proven at different scale but the hydraulic design of the backfilled pit and operational control of carbon dosing will have to be developed through phased field tests carried out concurrently with full-scale design.

Acknowledgements

The authors thank the Riversdale Resources Limited and Millennium EMS Solutions Ltd. for their support and cooperation in the planning and execution of the work presented in this paper.

References

Bianchin M, Martin A, Adams J (2013) In-Situ Immobilization of Selenium within the Saturated Zones of Backfilled Pits at Coal-Mine Operations. BC Mine Reclamation Symposium, September 2013.

CH2M Hill (2013a) Review of Available Technologies for the Removal of Selenium from Water – Addendum. Prepared for North American Metals Council. Prepared by CH2MHILL, March 2013.

de Souza M, Huang C, Chee N (1999) Rhizosphere bacteria enhance the accumulation of selenium and mercury in wetland plants. Planta 209: 259. https://doi.org/10.1007/s004250050630 DOI

Dockrey J, Martin A, Stockwell J (2012) Potential Rose of Nitrate in the Release and Attenuation of Selenium in Coal-Mine Environments. Proceedings of 19th Annual BC MEND ML/ARD Workshop, presentation 25, 2012.

Golder Associates (2009) Literature Review of treatment Technologies to Remove Selenium from Mining Influenced Water. North American Metals Council, http://www.namc.org/docs/00057713.PDF

Lemly DA (2004) Aquatic selenium pollution is a global environmental safety issue. Ecotoxicology and Environmental Safety 59, 2004, p. 44-56

Martin A, Jones R, Buckwalter-Davis M (2009) Passive and Semi-Passive Treatment Alternatives for the Bioremediation of Selenium from Mine Waters [C]. doi:http://dx.doi.org/10.14288/1.0042571

Paulson O, Harrington J (2004) Bioremediation of the Sweetwater Pit Lake – Four Years Following Treatment. Proceedings of the US EPA Meeting: Pit Lakes 2004, November 16 – 18, Reno, Nevada, Washington, D.C.

Luek A, Brock C, Rowan D, Rasmussen J (2014) A Simplified Anaerobic Bioreactor for the Treatment of Selenium-Laden Discharges from Non-acidic, End-Pit Lakes. Mine Water Environment, 2014, 33:295–306. DOI 10.1007/s10230-014-0296-2

United States Environmental Protection Agency (US EPA) (2016) Aquatic Life Ambient Water Quality Criterion for Selenium – Freshwater. EPA 822-R-16-006, June 2016, Washington, DC, USA.

Yanfolila Gold Mine Open Pit Slope Depressurisation, Mali

Gareth Lottreaux[1], Karen Nicole King[2], Angus Errol Rowland3

[1] *WSP, Hydrogeologist, Water Services Unit, 33 Sloane Street Bryanston, 2191 South Africa*

[2] *WSP, Hydrologist, Water Services Unit, 33 Sloane Street Bryanston, 2191 South Africa*

[3] *Piteau Associates, Hydrogeologist, Operations Manager, 25 Rudd Road, Illovo, South Africa 2196*

Abstract

WSP carried out a risk mitigation and dewatering implementation programme for the Yanfolila Gold Project in southwestern Mali. The project centred on the development of two open pits; the Komana East and Komana West pits. The main tasks associated with the project included a risk mitigation study of the Komana West pit in order to determine whether the pit was hydraulically connected to the Sankarani River – approximately 200 meters from the pit – and to install a network of peripheral dewatering/depressurisation boreholes around the two pits in order to depressurise a 60 meter thick saprolite layer by dewatering the underlying fractured rock aquifer.

Long-term (14-day) pump testing of boreholes between the Sankarani River and the Komana West pit was undertaken. Water levels in the pumping borehole and a network of monitoring boreholes were monitored throughout the test to identify indications of the system reaching steady state flow conditions, which would indicate water being drawn in from the river. Electrical conductivity and pH values were measured at regular intervals in the river upstream of the pumping well and in the pump discharge water in order to determine any similarities in quality, which would further indicate inflow from the river. Pump testing also indicated potential efficacy of depressurising the saprolite through pumping from the underlying fractured aquifer. Following this, drilling and pump testing of 27 dewatering boreholes around the perimeters of the two pits was undertaken in order to recommend a pumping regime for the mine.

The study found that there was no hydraulic link between the Sankarani River and the Komana West pit, thus significantly decreasing risks to mining in this area. It was further determined that the saprolite could be effectively depressurised through dewatering the underlying fractured rock aquifer.

The main applications of this study are that the Komana West pit can be developed without risk of flooding from the Sankarani River. Furthermore, effective depressurisation of the saprolite means that the open pits can be designed with 'dry' slopes, resulting in steeper slope angles, minimised stripping ratios and thus improved overall profit margins for the mine, as well as reducing the risk of collapse within the pits.

Keywords: Yanfolila, dewatering, slope depressurisation, hydraulic connectivity

Introduction

WSP carried out a risk mitigation and dewatering implementation programme for the Yanfolila Gold Project in southwestern Mali. The project centred on the development of two open pits; the Komana East and the Komana West Pits. The area shows a typical tropical weathering profile with hard laterites present at the surface in many areas. A virtually ubiquitous saprolite unit exists across the area, with a typical thickness of approximately 60 meters across the site. This is underlain by a weathered, saprock zone, which exhibits abundant hard rock zones with extensive relict fractures, many of which are open. The saprock transitions downwards into fresh bedrock, which is typically fractured in its upper 20-30 meters, with the frequency and intensity of fracturing reducing rapidly below this.

The site is bound to the west and north by the Sankarani River, which forms the international border between Mali and Guinea. The Komana West pit is located approximately 200 meters to the east of the Sankarani River. The site setting of the Komana West pit re;ative o the Sankarani River is shown in Figure 1, with a West-East cross section, including the interpreted groundwater surface, is shown in Figure 2.

The purpose of the investigation was to:

- Determine whether the Sankarani River is hydraulically connected to the area to be exposed during development of the Komana West pit, which could pose a flooding risk to the pit, as well as have an impact on slope stability;

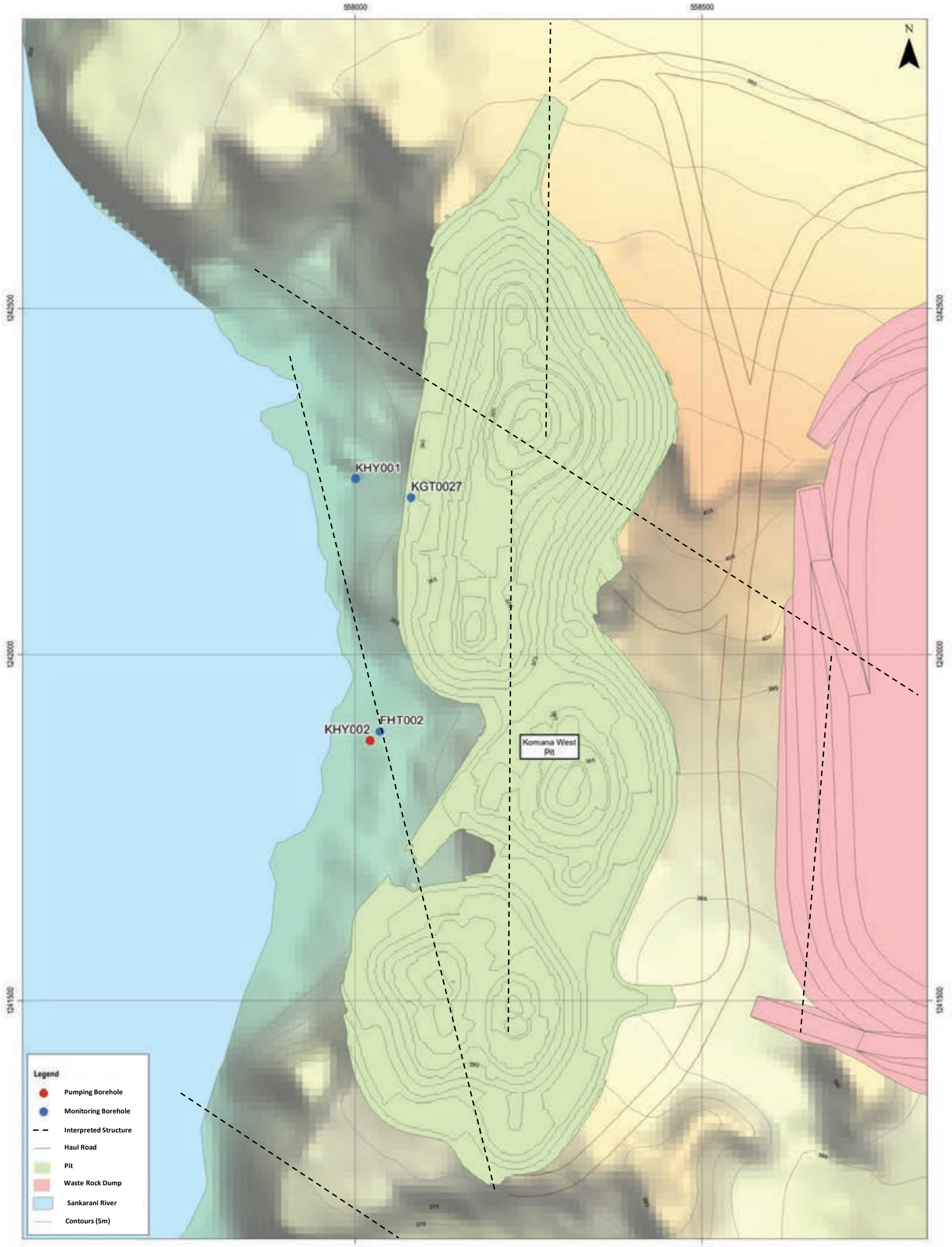

Figure 1: *Location of pump testing boreholes relative to Komana West pit and Sankarani River.*

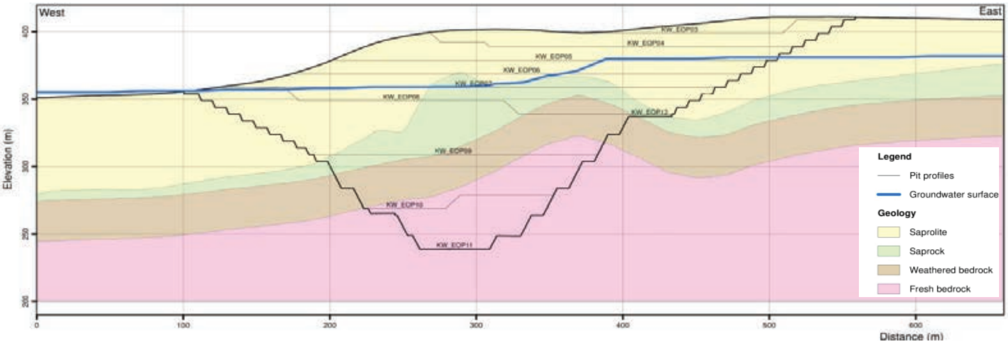

***Figure 2:** West-East cross section through the Komana West Pit*

- Determine whether the approximately 60 meter thick saprolite layer could be successfully depressurised through dewatering the underlying fractured rock aquifer, effectively under-draining the saprolite; and
- Use the information gathered to design and implement a network of peripheral dewatering boreholes around the perimeter of the two pits.

Methodology

A long-term pump test was conducted on borehole KHY002, shown in Figure 1, located between the Sankarani River and the Komana West pit footprint, over a period of 14 days at a constant rate of 3.7 litres per second. Water levels in the pumping borehole were monitored throughout the pump test in order to determine whether steady state flow conditions were reached, which would indicate water being drawn into the borehole from the Sanakarani River. Throughout the pumping test, pH and electrical conductivity (EC) measurements were taken simultaneously in both the borehole discharge water and in the Sankarani River at the closest possible location upstream of KHY002. The two sets of pH and EC values were compared against each other in order to determine whether the groundwater abstracted from KHY002 displayed any hydrochemical affinity to that of the river water, as might be anticipated under circumstances in which drawdown of water at KHY002 induced ingress or increased recharge from the river.

Water levels in three monitoring boreholes; FHT002, KGT0027 and KHY001, also shown in Figure 1, were also measured throughout the pump test. The monitoring boreholes were located between 15 and 380 meters from the pumping borehole, and were drilled into both the saprolite (FHT002 and KGT0027) and saprock (KHY001). The aim of monitoring the water levels in these three boreholes was to determine the efficacy of pumping from the fractured rock aquifer to depressurise the overlying saprolite.

Final dewatering borehole locations were selected in order to intercept structural features in the fractured rock aquifer identified through geological mapping and geophysical investigations. Preference was given to areas with lower basal saprock elevation in order to target potential local groundwater ‘sumps’, enabling the dewatering boreholes to underdrain a larger portion of saturated saprolite and saprock.

Results and Discussion

Table 1 provides a summary of the boreholes used during the pump test, the lithology into which they were drilled, the maximum drawdown achieved and their distance from the KHY0002 pumping well. Table 2 provides the hydraulic conductivity and storativity of the saprolite and saprock units, as calculated from the aquifer testing conducted. The drawdown observed in all boreholes is shown graphically in Figure 3, with the EC data recorded throughout the test at both KHY002 and in the Sankarani River shown in Figure 4.

Table 1: *Summary of pump test data*

Borehole ID	Maximum Drawdown (m)	Distance from KHY002 (m)	Lithology
KHY002	12.77	0	Fractured rock
KHY001	4.43	380	Saprock
FHT002	6.18	15	Saprolite
KGT0027	0.70	360	Saprolite

Table 2: *Summary hydraulic properties of saprolite and saprock*

Lithological Unit	Hydraulic Conductivity (K – m/s)	Storativity (S)
Saprolite	4.78 x 10-8	1.21 x 10-2
Saprock	8.89x 10-7	5.76 x 10-6

From the data presented in Table 1 and Figure 3 it is evident that substantial (and continuous) drawdown was achieved both at KHY002 and in all monitoring wells, with no steady state flow-recharge condition observed. No excursions from the drawdown curve were noted, which may potentially indicate the presence of a recharge boundary. The lack of any obvious recharge boundary indicates limited hydraulic connection of the Sankarani River to the underlying aquifer. Figure 4 shows that the EC profiles of KHY002 and the Sankarani River water remained markedly different throughout the test, with minimal variability in the KHY002 conductivity measurements observed over the period of the test. Furthermore, no geological structures were detected linking the River to the Pit (Figure 1). This supports the interpretation that no tangible ingress of water from the river towards the KHY002 borehole occurred in response to the drawdown induced by pumping.

The drawdown observed in the monitoring boreholes indicates that dewatering within the fractured rock aquifer can have a laterally extensive impact on local water levels, with water levels in the saprolite showing a relatively rapid response to dewatering. It can thus be concluded that dewatering in the fractured rock aquifer can be effectively used to lower water levels and thus reduce pore pressures in the saprolite across the mining area by underdraining the saprolite. Consequently, the open pits can be designed with 'dry slopes', allowing for steeper slope angles and thus minimised stripping ratios, which will result in improved overall profit margins, as well as reduced risk of collapse within the pits.

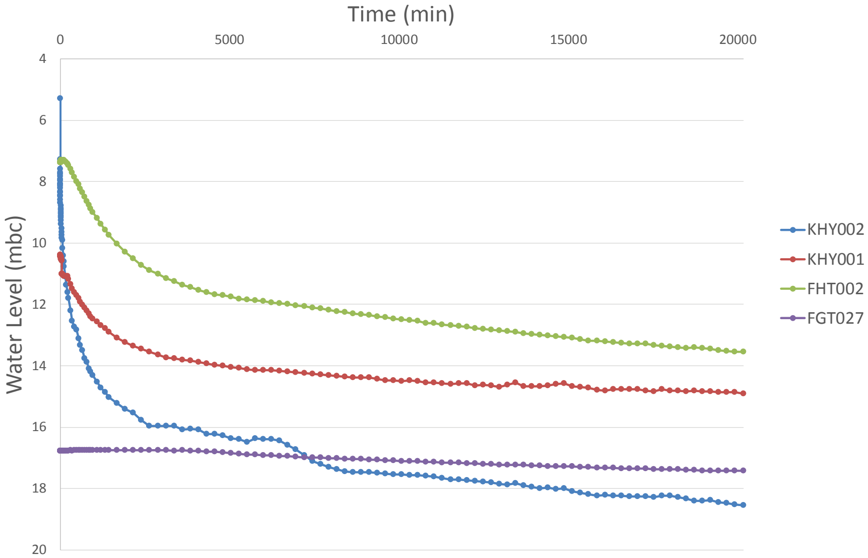

Figure 3: *Water level comparison between pumping borehole and observation boreholes.*

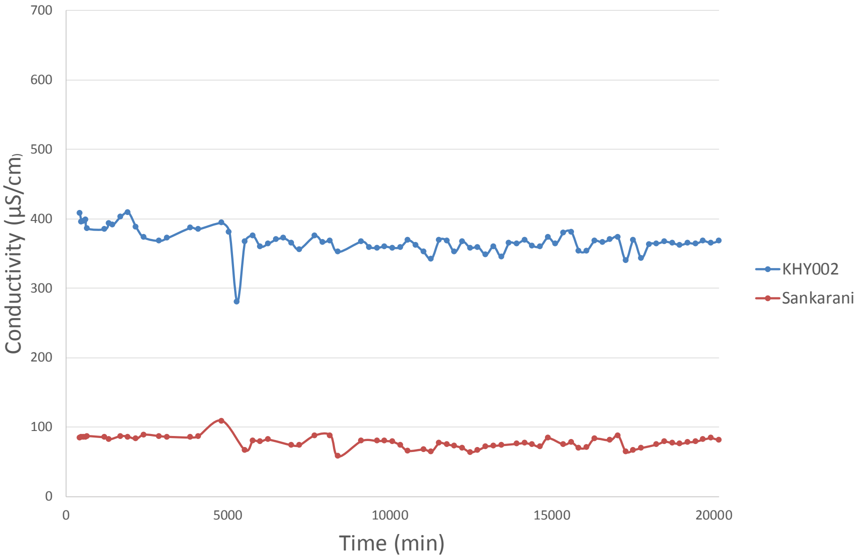

***Figure 4:** Electrical conductivity comparisons between pump test borehole and Sankarani River water.*

Following the initial investigations, a network of 27 dewatering boreholes were drilled across the site, 13 at Komana East and 14 at Komana West. Pump tests were carried out on all boreholes in order to recommend optimal dewatering rates for each borehole in order to achieve sufficient dewatering and slope depressurisation across each pit.

Conclusions

The following key findings were made:

- Significant drawdown was achieved and sustained over pumping for the duration of the pump test at borehole KHY002. This drawdown extended through both the saprolite and saprock units and was observed to propagate to boreholes located up to 380 m from the pumping well;
- No evidence of steady state pumping conditions or recharge was observed throughout the testing period, with water levels in the pumping borehole continuing to draw down for the duration of the test;
- No evidence of hydrochemical modification of the abstracted water from KHY002 was observed throughout the testing period. At all times, abstracted water appeared distinct from that of the Sankarani River with respect to EC, with no evidence of any ingress of river water through the saprolite or saprock units;
- Theseresults indicate that there is unlikely to be any significant hydraulic connection between the Sankarani River and the groundwater system in the Komana Pit area.

The lack of hydraulic connectivity between the Sankarani River and the underlying aquifer results in a low risk of water ingress from the River into the Komana West pit. Additionally, the pump testing indicated that dewatering of the fractured rock unit can effectively underdrain the above lying saprolite.

Active dewatering through the use of boreholes completed in the fractured rock will likely be effective as both a dewatering and upper slope depressurization method for both the Komana East and Komana West pits. As a result, a network of 27 dewatering boreholes were drilled into the fractured rock aquifer across the Yanfolila site.

References

Schlumberger Water Services (2013) Yanfolila Gold Mine Hydrological and Hydrogeological De-risking Study. Report Number 52674/R1.

Schlumberger Water Services (2015) Yanfolila Optimisation Study: Supplementary Investigations Addendum. Report Number 52674/R4.

WSP (2017) Yanfolila Gold Project Dewatering Implementation Plan. Report Number 48555/R01.

Use of Residues Generated from Construction and Fish Industries to Remediate Mine Drainage in Greenland

Morten Birch Larsen[1], Yu Jia[1], Sigga Joensen[1]

[1]*Greenland Institute of Natural Resources, Department of Environment and Mineral Resources, Kivioq 2, 3900 Nuuk, Greenland*

Abstract

This study focuses on the development of low-tech remediation methods using local residue materials – shrimp shells from the fishing industry and crushed concrete from the construction industry. The mobility of selected trace elements was compared based on batch and column leaching studies, where the waste rock was mixed with the residue materials. The batch leaching results showed that both concrete and shrimps were able to decrease the leaching of Pb and Zn. The column study showed that concrete was not a satisfactory candidate to immobilize Pb and Zn from a long-term of view.

Keywords: Batch leaching test, Column leaching test, Concrete, Heavy metals, Mine Drainage, Shrimps, waste rock

Introduction

Cryolite has the chemical formula Na_3AlF_6 (sodium hexafluoroaluminate) and is used in the Hall-Héroult process for production of aluminum, where it works as a catalyzer and lowers the melting point of aluminum oxides from 2072 °C to 1012 °C. Ivittuut in southern Greenland had the biggest known cryolite deposit, which was mined from the middle of the 18th century until 1962, where the mine was closed, since artificial cryolite took over the market.

The mine pit is placed adjacent to a large fiord system, and a series of environmental site investigations in the early 80's revealed high concentrations of particularly lead and zinc in sediments, sea weed, blue mussels, dust and lichens, but not in samples of fish and shrimps. The most significant increases were found for lead and zinc in organisms living in the tidal zone (sea weed and blue mussels). The investigations showed, that waste rock used for building the quay area was the main source of leaching of metals. The area is highly influenced by tidal water with an amplitude of more than 4 m, and at each tidal cycle sea water is sieving through the quay area and dissolving lead and zinc minerals in the waste rock and leaching the metals to the fiord system. It was estimated that 1-3 kg of lead was entering the fiord every day giving an annual impact of the fiord of 400-1000 kg lead (Johansen et al. 1995; Bach et al. 2014).

In Greenland, logistics is challenging, due to climatic conditions and very limited road network. It also means that the mining industry in Greenland can be economically challenged, due to high transport costs, and the fact that most goods are shipped to Greenland from Denmark.

Shrimp shells generated from the Greenlandic fishing industry have been either discharged with the waste water, used for animal feed production or production of shrimp flour. Shrimp shells contains 40-50% proteins and 15-25% chitin. Chitin is a polysaccharide and is considered to be one of the most abundant renewable biopolymers (Anastopoulos et al. 2017). Several studies have shown that shrimp shells are capable of removing metals from aqueous solutions either by adsorption on chitin (Karthikeyan et al. 2005; Forutan et al. 2016; Karthik et al. 2015) or by precipitation with sulfide, where the chitin work as substrate for microbial reduction of SO_4^{2-} to S^{2-} which may precipitate a number of heavy metals: Me^{2+} (aq) + S^{2-} (aq)   MeS (s) (Daubert & Brennan 2007, Robinson-Lora & Brennan 2008, Sinziana et al. 2001).

Concrete residue is generated from the construction industry when demolishing buildings, concrete structures etc. The concrete waste product is a basic material due to the presence of hydroxide ions, and its immobilization of heavy metals in the waste rock by the increase of pH due to cement amendment is well documented (Sephton and Webb 2017).

The purpose of this study was to investigate the use of local residue materials to minimize the leaching of metals from mining waste products. It was tested if amendment of waste rock with shrimp shells could decrease the leaching of metals, and it was tested if amendment of waste rock with crushed concrete would decrease the mobility of some metals.

Methods

Waste rock (WR) material was collected at the quay area in Ivittuut. The material was air dried and crushed to <4 mm. Shrimp shells were delivered by a local shrimp factory. The shells were freeze-dried. Crushed concrete was obtained from a recycle center in Denmark. The leachant was sea water collected from the Nuuk fiord system. Water was collected every 2 weeks at the same site and at a depth of 50 m. After collection the water was filtered to 1.2 µm and stored at 5°C with continuously air supply.

Batch leaching tests were performed as 24-h shake flask tests according to a modified ASTM D3987 method, using 250 mL PE bottles with 100 ml sea water and 10 or 10+1 g solid. The bottles were placed on a shaking table at room temperature (21 °C). Column leach tests were performed according to a modified ISO/TS 21268-3 standard method. The columns were constructed from acrylic plastic tubes (PPMA) with an internal diameter of 50 mm and a length of 35 cm. The leachant flowrate was set to 12 ml/h. pH, redox, conductivity, dissolved oxygen (DO) and temperature was measured using a YSI professional Plus multiparameter instruments. See table 1 for composition of the tests.

Chemical analysis were performed at an accredited laboratory (Eurofins, DK)

The directly measured elemental values in mg/L for the batch and column leaching results was converted to be mg/kg WR taking into account of the L/S ratio for further mass balance calculation.

The X-ray diffraction analysis (XRD) analysis was performed on a Panalytical X'Pert Pro diffractometer at a commercial laboratory Actlabs, Canada. The XRD analysis was performed for the raw WR, raw concrete, and 6 residues obtained from the column test (WR–C01, C02; shrimps amended WR samples – C03 vs C04; concrete amended WR samples – C05 vs C06. Top and bottom indicate the position in the column where the samples were taken for XRD analysis). A portion of each pulverized sample was mixed with corundum (as an internal standard). The amount of the crystalline minerals were recalculated based on a known percent of corundum.

Results and discussion

Raw materials

The chemical analysis showed that in the raw WR, Pb and Zn level was 0.06 % and 0.53 % of dry weight (DW), respectively (Table 2). The variation of these trace elements was typically high representing the heterogeneous of the waste rock. In shrimps the Pb and Zn level accounted for only <0.0003 % and 0.002 %, respectively when compared with that of the raw WR. The content of total organic carbon (TOC) in the shrimps was 22 %, which was more than 3000 times higher than that in the WR. The TOC level in the WR and concrete was low (0.4–0.7 %).

***Table 1** Composition of batch tests (n=3) and column test.*

Batch	W_{WR} (g)	$W_{shrimps}$ (g)	$W_{concrete}$ (g)	Column	W_{WR} (g)	$W_{shrimps}$ (g)	$W_{concrete}$ (g)
B01	10	-	-	C01+C02	1250	-	-
B02	-	1	-	C03+C04	660	70	-
B03	-	-	1	C05+C06	1120	-	125
B04	10	1	-				
B05	10	-	1				

***Table 2** Chemical composition of raw waste rock, shrimps and concrete samples.*

	DW (%)	Pb (mg/kg DW)	Zn (mg/kg DW)	TOC (%)
Waste Rock	100.0±0	600±286	5257±6798	0.68±0.09
Shrimps	91.3±0.6	3.0±0.0	20.0±1.7	22.0±0.0
Concrete	91±0	7.8±0.7	500±61	0.4±0.1

Batch leaching results

The eluate from WR was of neutral pH (B01), however the eluate from the shrimps and concrete was slightly alkaline (8.7–9.2) (Table 3). The eluate from amended samples (B04, B05) had slightly higher pH than that from the WR sample. Dissolved oxygen (DO) was much lower in the tests containing shrimps, which implies that degradation of organic matter was going on. The EC values in the raw samples was in quite similar level with respect to WR, shrimps and concrete.

The leached Pb and Zn from the WR samples was 13.3 mg/kg and 2.8 mg/kg, which accounted for 2.2 % and 0.053 % of the total content of Pb (600 mg/kg) and Zn (5257 mg/kg) in the WR (Table 1), respectively. The leached Pb and Zn from the raw shrimps and concrete was much lower than that from the raw WR. The leached Pb level from the raw WR was more than 200 times that of the Pb leaching from the shrimp amended WR sample and more than 300 times that of the concrete amended WR sample. Similarly, the leached Zn level from the raw WR was 15 and 44 times the leached zinc level from the shrimps- and concrete amended WR samples. The batch leaching results revealed the dramatic effect of shrimps and concrete in immobilization of Pb and Zn.

Column leaching results

The column tests showed that the cumulated level of Pb at L/S ratio 10 (v/w) in WR (C01 vs C02), shrimps amended (C03 vs C04) and concrete amended (C05 vs C06) samples was 42–55, 0.48–2.4 and 67–98 mg/kg, respectively (Figure 1).

The cumulated level of Zn at L/S 10 in the WR, concrete amended- and shrimps amended samples was 57–64, 2.4–7.6 and 140–220 mg/kg, respectively (Figure 1). The results clearly demonstrated a trend and plateau when the leachant was going through the materials packed in each individual column. Based on the column leaching test, amendment of the WR with shrimps showed a large effect on the immobilization of Pb and Zn. In contrast, the concrete amended WR samples showed higher leached level of Pb and Zn. Opposite to the batch leaching results, the column results suggested that the WR amended with concrete was not a promising method in the immobilization of Pb and Zn in the WR. An average leached Pb at L/S 10 in the columns was calculated to be 48.5, 1.44 and 82.5 mg/kg for the sole WR, shrimps amended WR and concrete amended WR sample, respectively, which was corresponding to 8.1 %, 0.24 % and 13.8 % of the total content of 600 mg/kg Pb (Table 1) in the raw WR. Similarly, the average leached Zn at L/S 10 was calculated to be 60.5, 5.0 and 80 mg/kg for WR, shrimps amended- and concrete amended sample, respectively, which was corresponding to 1.1 %, 0.1 % and 1.5 % of the total content of 5257 mg/kg Zn (Table 2) in the raw WR.

Eluate from the shrimp amended columns had a very low DO content and a very low ORP (Figure 2), compared to the other

***Table 3** Physicochemical characterization and mobilized elements in eluate from batch test.*

	pH	DO (mg/L)	EC (µS/cm)	Pb (µg/kg) (n=3)	Zn (µg/kg) (n=1)
B01 WR	6.5±0.0	5.1±0.1	42931±266	13333±577	2800
B02 Shrimps	8.7±0.1	0.2±0.3	44316±474	61.3 ± 51.1	200
B03 Concrete	9.2±0.0	4.0±0.3	44877±400	36.7±8.3	200
B04 WR + shrimps	7.7±0.4	0.0±0.1	37618±6122	209.4 ± 178.4	63.6
B05 WR + concrete	8.0±0.0	5.1±0.3	42904±674	136.4 ± 53.7	190.9

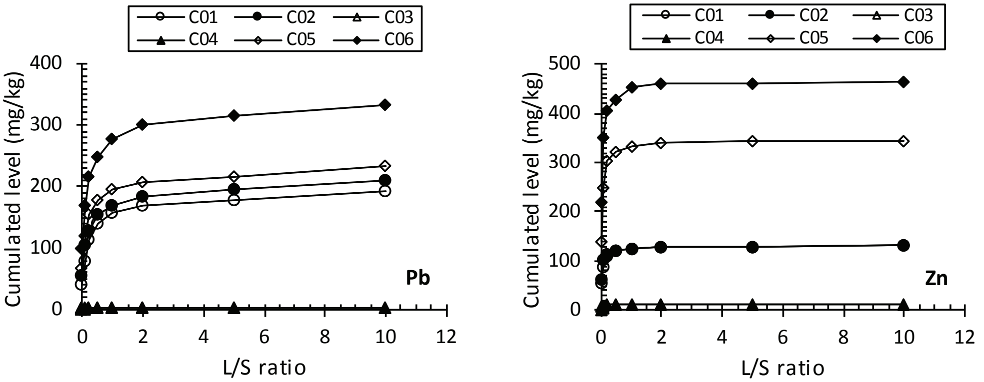

Figure 1 Cumulated leaching of Pb and Zn from the column test

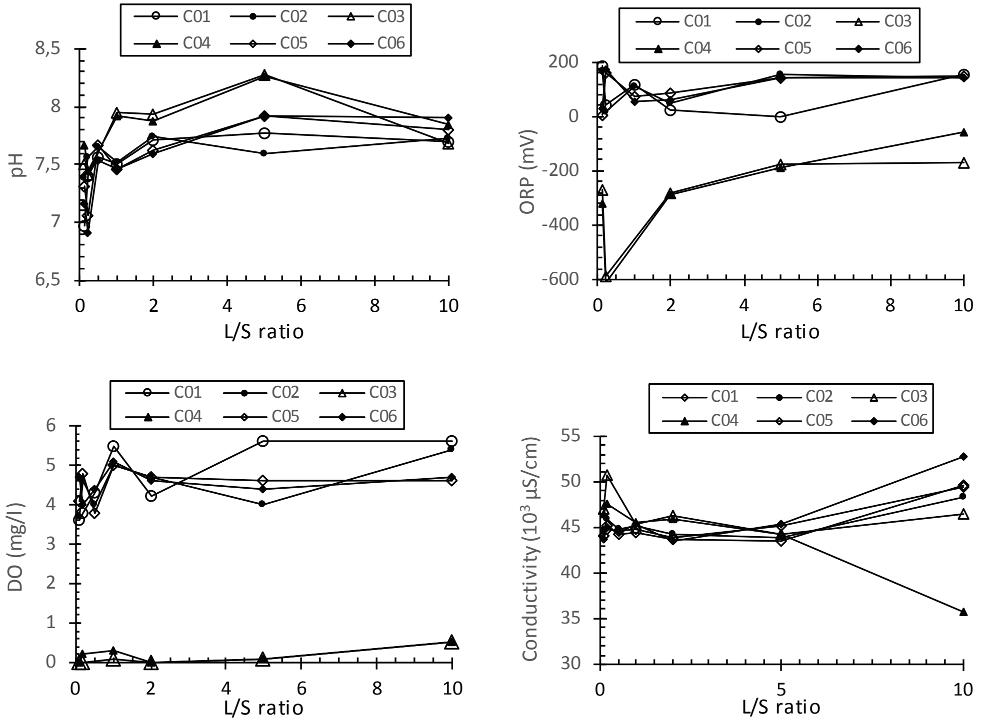

Figure 2 Physical/chemical parameters from the column test

columns, which as it was the case in the batch test implies degradation of organic material. For most of the measurements, the highest pH was found in the shrimp amended columns, while the amendment with concrete only had limited effect on the pH compared to the sole WR. The conductivity in the eluate was high, due to the use of sea water as leachant, and generally the measurements were relatively stable with a minor increase at L/S 10.

XRD results

The XRD analysis revealed that quartz (SiO2) (44.3–61.3 %, data not shown) and cryolite (31.2–41.9 %) were the most abundant minerals in all the tested samples. Siderite was detected in most samples (4.4–7.3 %) (Table 4). Muscovite $(KF)_2(Al_2O_3)_3(SiO_2)_6$ (0.9–2.0 %) was identified in the raw WR and a few amended samples. Plagioclase (3.0-6.9 %) was not detected in the control, shrimp- and con-

***Table 4** Mineral abundances (%) for the raw materials and residues from column leaching test*

Mineral	Cryolite	Siderite	Plagioclase	Sphalerite	Galena
Chemical formula	**Na3AlF6**	**FeCO3**	**NaAlSi3O8 to CaAl2Si2O8**	**ZnS**	**PbS**
Columns after L/S10					
CO1	39.3	7.1	n.d.	0.2	0.2
CO2	41.5	6.9	n.d.	0.2	0.1
CO3 top	37.5	7.3	n.d.	0.2	n.d.
CO3 bottom	36.3	7.1	n.d.	n.d.	n.d.
CO4 top	36.7	4.4	n.d.	n.d.	0.4
CO4 bottom	31.2	4.8	n.d.	n.d.	n.d.
CO5	34.6	6.2	3.0	trace	n.d.
CO6	38.2	6.5	3.2	n.d.	n.d.
Raw material					
WR	41.1	6.9	5.6	trace	n.d.
Concrete	n.d.	n.d.	6.9	n.d.	n.d.
WR + concrete	41.9	6.8	4.4	n.d.	n.d.
WR + shrimp	35.1	7.2	n.d.	0.2	n.d.

WR= waste rock. n.d. = not detected

crete amended WR. Sphalerite (≤ 0.2 %) and galena (≤ 0.4 %) was detected only in few samples. Amorphous mineral (26.1 %) was solely detected in the raw concrete sample (data not shown). Apatite $Ca_5(PO_4,CO_3)_3(OH,F)$ (≤ 2.8 %) was detected only in one of shrimp amended column (data not shown), implying that microbial activities were on-going in the column, similar to that described by Briggs and Kear (1994). Calcite ($CaCO_3$) (6.4 %) was detected only in the raw concrete.

General consideration

Previously Johansen et al. (1995) reported that the WR in the mining area consists of trace amount (0.29 %) of pyrite (FeS_2), ZnS (0.3 %) and PbS (0.25 %). In the present study, however pyrite is not detectable in the raw WR. The sulfur containing minerals are ZnS and PbS (Table 4), which are non-acid producing sulfide minerals while pyrite is acid generating (Dold 2003).

At pH 6–8.5 and E_h in the range of -0.6 to 0.2 v (Figure 2) which are measured in the present study, following the geochemical behavior of elements between aquatic and solid phases (Takeno 2005), it finds that the predominant Pb species is Pb^{2+} or $Pb(OH)^+$, and the predominant Zn species is Zn^{2+} and $Zn(OH)_2(aq)$.

The addition of nutrients e.g. P to WR due to amendment of shrimp with WR led to the formation of minerals, e.g. apatite, similar to that mechanism described by Porter et al. (2004). Ca compounds are abundant in concrete. The high level of Ca compounds is generally considered to be efficient for the Pb immobilization (Kumpiene et al. 2008). However, this was not the case for the concrete amended WR in the column test, and the reason remains unclear.

This study has shown, that shrimps can minimize the leaching of metals from waste rock. It was not determined, if it was due to adsorption on chitin or due to precipitation with sulfide, but the work is still ongoing. Future work will also investigate long-term capacity of the shrimp amended waste rock.

Conclusions

The batch leaching results showed that both concrete and shrimps were feasible to use in immobilizing of Pb and Zn. The column leaching results demonstrated clearly that shrimps was a good candidate in immobilization of Pb and Zn. However, the column study showed that concrete was not a satisfactory candidate to immobilize Pb and Zn from a long-term perspective, which might be due to the change of pH value in the system. The total chemical content of Pb (0.06 %) and Zn (0.52 %) in the raw WR sample agreed well with the XRD results, of which the mineral abundance of galena and sphalerite for the raw WR sample was undetectable, while it was in trace amount in some of the amended samples, which clearly showed a low level of these minerals. Low dissolved oxygen in the shrimps amended batch, and the formation of apatite in a column with shrimps amended sample implied that microbial activities were involved in the leaching process, though a more specific investigation is needed to confirm this.

Acknowledgements

The authors thank Environmental Agency for Mineral Resource Activities, Greenland, and Ministry of Education, Culture, Research and Church, Greenland, for funding of the project.

References

Anastopoulos I, Bhatnagar A, Bikiaris DN, Kyzas GZ (2017) Chitin adsorbents for toxic metals: A review. Int. J. Mol. Sci 2017, 18, 114, doi: 10.3390/ijms18010114

ASTM D3987-12 (2012) Standard Practice for Shake Extraction of Solid Waste with Water, ASTM International, West Conshohocken, PA, 2012, www.astm.org, DOI: 10.1520/D3987-12

Bach L, Asmund G, Riget F (2014) Environmental monitoring in 2013 at the cryolite mine in Ivittuut, South Greenland. Aarhus University, DCE – Danish Centre for Environment and Energy, 32 pp. Scientific Report from DCE – Danish Centre for Environment and Energy No. 105. dce2.au.dk/pub/SR105.pdf

Briggs DEG, Kear AJ (1994) Decay and Mineralization of Shrimps. Palaios 9:431-456, doi: 10.2307/3515135

Daubert LN, Brennan RA (2007) Passive Remediation of Acid Mine Drainage Using Crab Shell Chitin. Env. Eng. Sci. 24 (10), 1475-1480.

Dold B (2003) Basic concepts of environmental geochemistry of sulfide mine-waste, in: Geochemistry and geomicrobiology of mine water formation. Universitė de Genève, Lisbon, pp 1–36

Forutan R, Ehsandoost E, Hadipour S, Mobaraki Z, Saleki M, Mohebbi G (2016) Kinetic and equilibrium studies on the adsorption of lead by the chitin of pink shrimp (Solenocera melantho). Entomol. Appl. Sci. Lett. 2016, 3, 20–26.

Johansen P, Asmund G, Riget F (1995) Environmental investigations at Ivittuut 1982-1992. Report no. 7, Greenland Environmental Investigations, March 1995. (In Danish)

Karthik R, Meenakshi S (2015) Chemical modification of chitin with polypyrrole for the uptake of Pb(II) and Cd(II) ions. Int. J. Biol. Macromol. 2015, 78, 157–164.

Karthikeyan G, Andal NM, Anbalagan K (2005) Adsorption studies of iron(III) on chitin. J. Chem. Sci. 2005, 117, 663–672.

Kumpiene J, Lagerkvist A, Maurice C (2008) Stabilization of As, Cr, Cu, Pb and Zn in soil using amendments – A review. Waste Manage 28:215–225, doi: 10.1016/j.wasman.2006.12.012

Porter SK., Scheckel KG, Impellitteri CA, Ryan JA (2004) Toxic metals in the environment: thermodynamic considerations for possible immobilisation strategies for Pb, Cd, As, and Hg. Crit Rev Environ Sci Technol 34:495–604, doi: org/10.1080/10643380490492412

Robinson-Lora MA, Brennan RA (2008) Evaluating crab-shell chitin, lactate, and spent mushroom compost for acid mine drainage remediation in Central Pennsylvania. Proceedings America Society of Mining and Reclamation 2008, 911-926, doi: 10.21000/JASMR08010911

Sephton MG, Webb, JA (2017) Application of Portland cement to control acid mine drainage generation from waste rocks. Appl Geochem 81:143-154, doi: 10.1016/j.apgeochem.2017.03.017

Sinziana VM, Werth CJ, Sanford RA (2001) Evaluation of Different Polymeric Organic Materials for Creating Conditions That Favor Reductive Processes in Groundwater. Bioremediation Journal 5(1):1-13, doi: 10.1080/20018891079267

Takeno N (2005) Atlas of Eh-pH diagrams. Intercomparison of thermodynamic databases. Geological Survey of Japan Open File Report 419

Vermiculite Covers on Mining Wastes in a Semi-Arid Environment in South Africa

Johann McDonald[1,2], Simon Lorentz[2,3]

[1]*SHEQ MS & Environmental Department, Palabora Copper, Phalaborwa, 1390, South Africa,*
johann.mcdonald@palabora.co.za

[2]*Centre for Water Resource Research, University of KwaZulu-Natal, Pietermaritzburg 3200, South Africa*
3SRK Consulting (SA), Pietermaritzburg 3200, South Africa

Abstract

Deposition of large quantities of mining waste can have negative impacts on surface and ground water resources. These impacts necessitate amelioration of the wastes through various measures, but primarily through a cover system. These covers are designed to restrict percolation of rain water through the waste material, and thereby restrict moving contaminants to groundwater, either through retention and subsequent evapotranspiration, or by water shedding. Cover systems in semi-arid areas require particularly careful design and performance evaluation in order to provide a sustained first defence to impacts. This study assesses the performance of covers comprising vermiculite material over waste rock and tailings.

Keywords: Mine waste covers, vermiculite covers, mine waste water balance

Introduction

Deposition of large quantities of mining waste can have negative impacts on surface and ground water resources. These impacts necessitate reclamation and amelioration of the wastes through various measures, but primarily through a first level of remediation in the placing of cover systems over the waste. These covers are designed to restrict or detain percolation of rain water through the waste material and thereby moving contaminants into the groundwater or surface water receptors. Covers also protect waste materials from water and wind erosion, thus contributing to the sustainability of vegetation, which can further restrict the ingress of rain. Moreover, cover systems located in semi-arid areas require particularly careful design and performance evaluation in order to provide a sustained first defence to impacts.

The aim of this study is to evaluate a vermiculate material in a waste rock and tailings cover in a mine in the Limpopo province of South Africa, where the Mean Annual Precipitation (517 mm) is considerably less than the Mean Annual Potential Evaporation

***Figure 1** Sampling site layout*

(1774 mm). Performance of this type of material in cover systems in semi-arid environments has not been quantified heretofore. Observations include percolation fluxes in two large lysimeters in waste rock material, with a vermiculite cover as well as runoff from an automated runoff plot on the Waste Rock Dump (WRD). On a copper tailings storage facility (TSF), top surfaces and side slopes runoff was observed, together with the monitoring of soil water content and soil water tension at various depths in the cover and tailings waste. In addition, the hydraulic characteristics of the cover and waste materials were measured through in-situ and laboratory testing.

This study provides a rare set of physical observations, simulations and assessment of the water balance resulting from the use of a vermiculite material in waste covers in a semi-arid environment. The detailed observations and assessments lend value to cover design using other materials in semi-arid climates.

Methodology

Although some research has been conducted on the use of exfoliated vermiculite in hydroponics, no documented research has been discovered on un-exfoliated vermiculite in the mineral state, as a cover for mine wastes (Abate & Masini, 2005). The hydraulic characterisation of vermiculite may also be very site specific as this will depend on the mineral waste materials that were mined with the vermiculite (Van der Nest & Kuit, 1993; Wates, et al., 2006). Cover types and material properties of the covers have a specific influence on the water balance mechanisms and these need to be identified and quantified to determine an accurate water balance.

Setting

The study area is located in the North-Eastern part of the Limpopo Province of the Republic of South Africa, some 5km southeast of the town of Phalaborwa and adjacent to the Kruger National Park

Eight (8) sampling sites (fig.1) were identified that were seen as representative of the location. A Davis Weather station was used to obtain continuous climatic data at the site. Additional climatic data were also obtained from at least 2 other local weather stations. The sampling sites included 5 runoff plot sites on the TSF, with 2 Lysimeters as well as a runoff plot on a WRD. In the selection of the runoff plot sites consideration was given to slope, aspect, vegetation and cover materials. Runoff- plots 1, 2, 3 & 4 have been established on the side slopes (1:3) of the TSF. Runoff plot 5 has been established on a top surface of the TSF, whereas runoff plot 6 was established on a very steep slope of the WRD (fig. 1).

Lysimeters

Lysimeters 1 and 2 were established on the WRD on top surfaces by excavating and shaping an 8x8x2m cavity in the waste rock (fig. 2). The base and sides of the lysimeter were lined with a plastic liner and an aggregate drain was placed at the bottom centre.

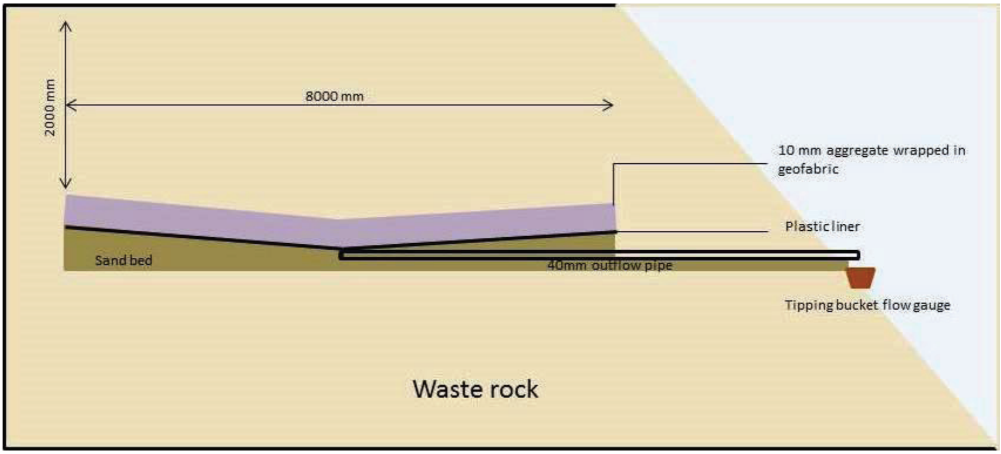

***Figure 2** Lysimeter design*

The base of the lysimeter sloped towards the centre where a drain led the seepage water to a tipping bucket approximately 6 meters away from the lysimeter. The tipping bucket was placed in an excavation lower than the drain to allow for gravity flow from the lysimeter drain to the tipping bucket (fig.2).

Soil Water Monitoring

Next to each sampling site Time Domain Reflectometry (TDR) probes were installed at 100mm, 500mm and 1000mm below the surface. These served as volumetric water content sensors which were read periodically using a TDR100 wave generator. The volumetric water content record was used to calibrate the water balance modelling and to assess water transfers between cover and waste.

Runoff Plots

Event based infiltration and run-off was measured in plots (2m wide x10 m long), isolated from surrounding runoff by sheet metal inserted into the surface. Each plot was equipped with a collection gutter at the down slope end, from which runoff was discharged into a tipping bucket and tips recorded with an event logger. The soil moisture measurements were used to assess subsequent evaporation and transpiration of the water infiltrated into the cover and waste.

Material characteristics

Cover and underlying waste hydraulic characterisation was completed in-situ using Tension Infiltrometers, Double Ring Infiltrometers as well as Guelph Permeameters and samples were extracted for laboratory water retention tests. The tests were performed on surface and at depths of 100mm, 500mm and a 1000mm at each of the eight sampling sites. The surface measurement represented the cover material, the 100mm depth observation represented the cover-waste and the 500 mm and 1000 mm measurements represented the tailings materials.

Evaporation and seepage

Potential evapotranspiration was estimated using temperature, humidity, wind speed and solar radiation data. Lysimeters were also used to estimate the actual evapo-transpiration released by vegetation and soils.

Results

Hydraulic characteristics

Typical hydraulic characteristics at two sites are compared here. The hydraulic conductivity characteristic of the materials at runoff plot 3, on a steep TSF side slope (1:3), and runoff plot 5, on a flat TSF surface, reveal significant differences between the materials (fig. 3). The hydraulic conductivity (both saturated and unsaturated) of the flat surface runoff plot 5 has unsaturated hydraulic conductivities an order of magnitude lower than at runoff plot 3, on the 1:3 side slope. The saturated hydraulic conductivities at runoff plot 5 are also lower than those at runoff plot 3, but by less than an order of magnitude. The differences in hydraulic conductivities of the tailings material may also be attributed to the method of tailings deposition. Runoff from the flat surface at plot 5 could be expected to exceed

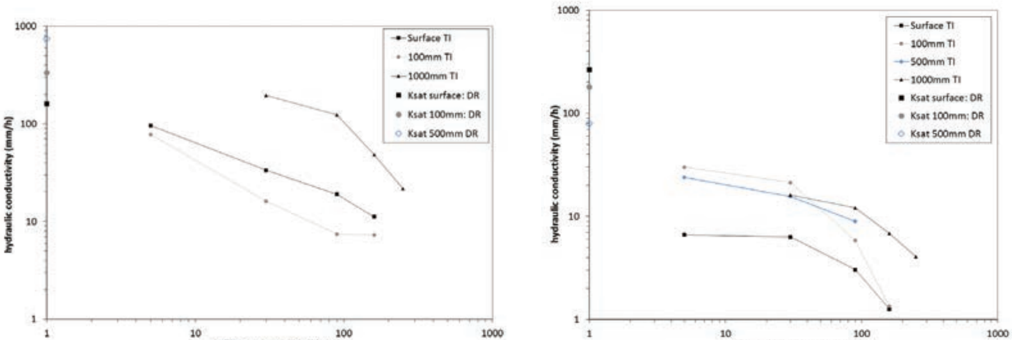

Figure 3 *Hydraulic conductivity characteristics at runoff plot 3 (left) abd runoff plot 5 (right).*

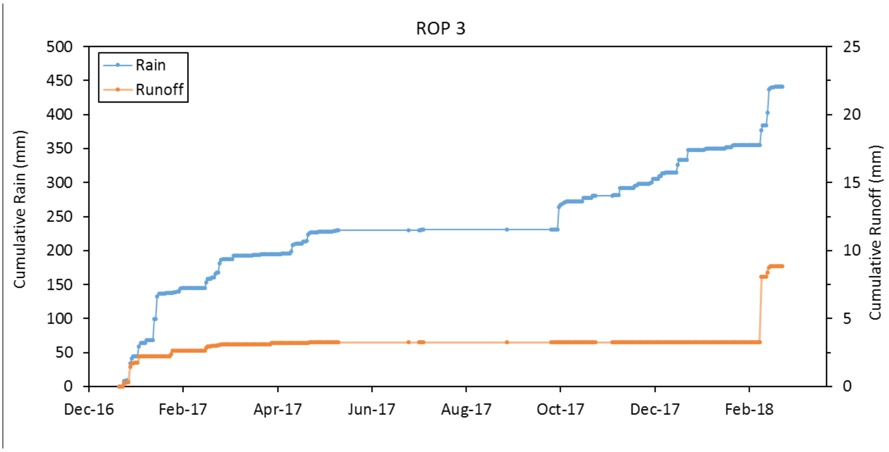

***Figure 4** Rainfall and runoff at TSF runoff plot 3 (side slope 1:3)*

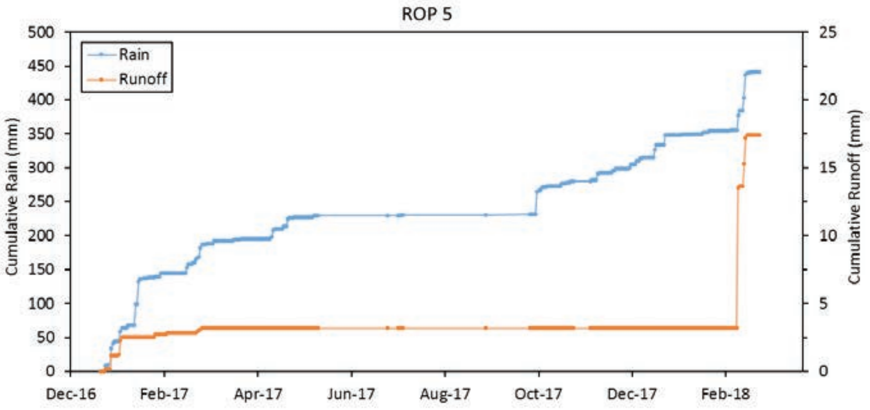

***Figure 5** Rainfall and runoff at TSF runoff plot 5 (slope ≈ 0).*

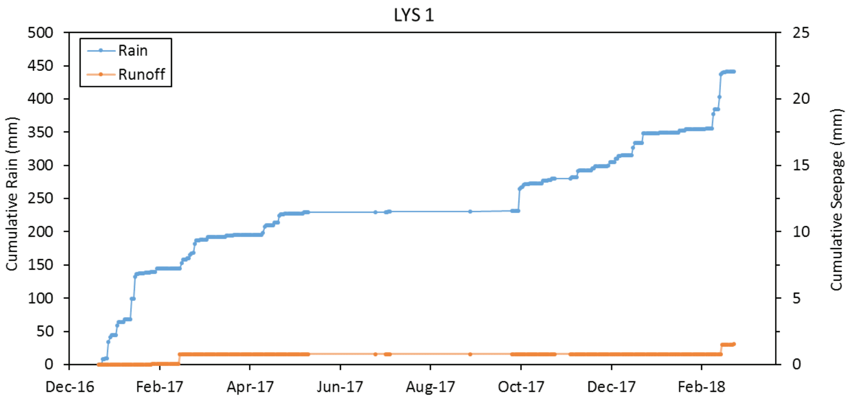

***Figure 6** Rainfall and seepage at a WRD lysimeter plot (similar for both plots)*

Table 1 *Summary of the water balance*

Component	Runoff Plot 3		Runoff Plot 5		WRD Lysimeter	
	(mm)	(%)	(mm)	(%)	(mm)	(%)
Rain	441.4	100	441.1	100	441.4	100
Runoff	8.8	2	17.4	4	0.0	0
Infiltration	432.6	98	424.0	96	441.4	100
Evaporation	156.9	36	156.9	36	169.3	38
Transpiration	250.9	56	250.9	56	270.7	61
Seepage	25.0	6	16.4	4	1.5	0.3

that of the sloped site due to the low hydraulic conductivities at plot 5, limiting the ingress of water. The materials in the plot 5 profile are more compacted than at the side slope site, resulting in these low conductivities.

The hydraulic conductivities within the cover materials are generally lower than in the tailings, although at the flat site (plot 5), the saturated conductivity in the cover material is higher than in the tailings, but the unsaturated characteristic of the cover material falls below the tailings material, at least on surface, and particularly at capillary pressure heads lower than 100 mm. The higher conductivities in the tailings compared to the vermiculite cover materials is indicative of the fine nature of the tailings, retaining water at low capillary pressures, while the coarser nature of the vermiculite material loses water, even at low capillary pressures, resulting in low hydraulic conductivities.

Runoff and Seepage

The time series of runoff over 14 months of observation at plot 3 (sloped), (fig. 4) and runoff plot 5 (flat), (fig. 5) reveal that the steeper slope yields less runoff (9 mm) than the flat TSF area (17 mm). This surprising difference in the runoff volumes suggests a high infiltration capacity in the side slope profile and a lack of deeper wetting, indicated by the deep soil water probes, supports the high water retention in the vermiculite cover. At the WRD lysimeters, on the other hand, the infiltration at both sites yielded just 0.7 mm of seepage at 2m below surface, indicating that the vermiculite fines in the cover and within the waste rock matrix are highly effective in retaining the ingress of rainfall (fig. 6).

Observations of the water contents over a long time series indicate that these infiltrated volumes are released to evapotranspiration demands after the events.

Water balance

The water balance in the tailings and waste rock have been estimated using a combination of simulations with the HYDRUS-2D soil physics model, (Šimůnek et al., 2006), and confirmed against the observations. The surface runoff in the TSF and the seepage in WRD were confirmed through observed fluxes.

The resultant water balance is summarised in Table 1, showing volumetric water balance components in mm and as a percentage of total rainfall during the observation period from 21 December 2016 to 2 March 2018. The total rainfall observed during the period was very low (441 mm) and produced very little runoff or seepage. This is typical of the savanna in which the site is located.

In the TSF, runoff varies from 2% (sloped surface) to 4% (flat surface) of the rainfall. Seepage varies from 6% to 4% of the rainfall for the sloped and flat surfaces, respectively, while the evapotranspiration losses comprise 92% of the rainfall.

In the WRD lysimeters, no runoff was observed, while seepage comprised only 0.3% of the rainfall recorded during the observation period. Here, the evapotranspiration is estimated to comprise over 99% of the rainfall. This is deemed feasible as rooting systems were observed in the entire 2 m of the WRD upper profile.

Conclusions

Preliminary examination of the 14 months of monitoring the tailings and waste rock sites indicate that the vermiculite cover materials over the tailings and within and over the waste rock provides an excellent medium for allowing infiltration of rainwater at the surface, but also provides an effective storage medium for later release of water to evapotranspiration demands.

Water content observations within the cover and tailings materials in the TSF sites indicate the tailings below the cover is a significant component of the store and release fluxes of the cover system.

Continued monitoring is recommended so that rainfall seasons yielding higher annual precipitation can be observed, since the 14 year observation period in this study coincided with a significantly low precipitation period.

References

Abate G, Masini J (2005) Influence of pH, ionic strength and humic acid on adsorption of Cd(II) and Pb(II) onto vermiculite. Colloids and Surfaces A: Physicochem. Eng. Aspects, Volume 262, pp. 33-39.

Van der Nest L, Kuit, H (1993) The use of exfoliated vermiculite in mining-waste materials for rehabilitation purposes, Potchefstroom: Research Institute for Reclamation Ecology-PU.

Wates JA, Lorentz SA, Marais H, Baxter BJM, Theron M, Dollar L (2007) An evaluation of the performance and effectiveness of improved soil cover designs to limit through-flow of water and ingress of air. WRC report 1350/1/06. Water Research Commission, Pretoria, South Africa.

Yibas B, Pulles W, Lorentz S, Maiyana B, (2011) Development of water balances for operational and post-closure situations for gold mine residue deposits to be used as input to pollution prediction studies for such facilities. WRC Report no. 1460/1/11. Water Research Commission, Pretoria, South Africa.

Development of Co-Disposal Methods for Fine Coal Waste and Coal Waste Rock to Facilitate the Prevention of Acid Mine Drainage

Donald Mjonono, Sue T.L Harrison, Athanasios Kotsiopoulos

Centre for Bioprocess Engineering Research (CeBER), Department of Chemical Engineering, University of Cape Town, Rondebosch 7701, Cape Town, South Africa

Abstract

Co-disposal of coal waste rock (WR) and fine coal waste (FW) offers the potential to mitigate the generation of acid mine drainage. ARD is generated when sulfide minerals in WR are exposed to aqueous oxidants. In this study, geochemical and geotechnical characterisation of mixtures of coal WR and FW in dry mass ratios of 3:2 and 2:3 (WR: FW) was conducted. Results indicated that FW dominated samples are effective in delaying the generation of acidity when co-disposed with coal WR whereas WR dominated samples result in incompressible and impermeable beds. This provides insight to developing detailed ARD prevention strategies.

Keywords: packing methods, drainage, compressibility, acid mine drainage, mitigation

Introduction

With increasing mining and processing of coal in South Africa, large volumes of coal waste rock and fine waste are generated (Pujado, 2006). The accumulation of these coal wastes creates an environmental burden as metals in high concentrations are released and acidic sulfur-rich waste waters are formed (Johnson and Hallberg, 2005). Sulfidic minerals, which may predominate as pyrite, react with natural elements to initiate these acid producing reactions and are accelerated by the presence of acidophilic microorganisms (Hesketh et al., 2010). This leads to the proliferation of acid rock drainage (ARD) which is a major pollutant of the limited underground and surface water sources and poses a threat to the survival of surrounding flora and fauna.

Preventing the occurrence of ARD from its source is critical. Success has been demonstrated in the coating of sulfidic waste rocks (Shu et al., 2013). These coatings, that include phosphate and silica compounds, limit the access of oxygen and water to sulfide mineral surfaces (Descostes et al., 2002; Johnson and Hallberg, 2005; Kollias et al., 2014). The efficacy of these synthetic coatings in long term ARD prevention can, however, be compromised by excessive degradation over time (Shu et al., 2013). ARD remedial options have also been developed. Addition of phosphates such as apatite can lead to the formation of ferric phosphate precipitates that limit the amount of ferric ion available for oxidation. However, this approach can be resource intensive, especially at large scale (Johnson and Hallberg, 2005).

In prevention studies, the repurposing of fine desulfurised coal waste from a two-step flotation process has been investigated, with various methods being developed to dispose of the fine environmentally benign component effectively (Kotsiopoulos and Harrison, 2018; Mbamba et al., 2012). The co-disposal of sulfidic waste rock and fine benign waste provides an alternative solution to sustaining neutral conditions over long periods (Kotsiopoulos and Harrison, 2015, 2017). Acid consuming components that contain relatively high bicarbonate concentrations, such as sand and clay, offset the net acidity of the mixture thereby delaying the acidification of the waste water. Covers with capillary barrier effects have shown effectiveness in preventing ARD by forming impermeable layers that restrict acidic runoffs (Bussière et al., 2003; Kotsiopoulos and Harrison, 2017).

Co-disposal of coarse coal waste rock and fine-grained coal wastes offers potential environmental benefits over conventional disposal operations, particularly in the prevention of ARD. However, to gain an informed perspective of the geochemistry and geotechnical properties of the waste, it is essential that the ARD potential (Alakangas et al., 2013) and packing behaviour (Li et al., 2017; Shokouhi and Williams, 2017; Wickland et al., 2006) of the samples are determined prior to codisposal application. The geochemical characterisation of individual waste rock and fine waste samples has been previously investigated with success (Hesketh et al., 2010; Kotsiopoulos and Harrison, 2017; Mbamba et al., 2012). However, the use of geochemical indicators to determine the acid producing potential of mixtures of sulfidic waste rock and benign fine waste has rarely been practised. Further, an integrated geochemical and geotechnical approach when developing packing procedures of coal mine waste is essential for successful co-disposal practices.

In this study, blended samples of coal waste rock and fine coal waste were analysed for their ARD generating potential over time, their packing behaviour and consistency. Bench-scale coal waste handling approaches were developed to impede the flow of oxidants in packed beds. Geotechnical properties such as void ratio, packing density, compressibility and slump, were investigated when developing packing procedures. This work demonstrates opportunities for the sustainable management of mine wastes and ARD mitigation through mechanisms that are applicable in the field.

Materials and methods

Acid base accounting tests and biokinetic tests

Two coal waste samples were used in this study. These included coal waste rock (WR) and fine coal waste (FW) samples from mines in the eMalahleni region in Mpumalanga, South Africa. LECO sulfur analyses of the individual WR and FW samples and blended ratios of 3WR:2FW and 2WR:3FW of the waste samples indicated sulfur contents of 1.32%, 0.50% ,0.97% and 0.81 %, respectively. To characterise the ARD potential of the two coal waste samples, static acid-base accounting (ABA) tests were conducted according to methods presented elsewhere (Miller et al., 1997; Skousen et al., 1997; Stewart et al., 2006) . The biokinetic test developed by Hesketh et al., (2010) was used to analyse the blends of coal waste rock and fine coal waste with respect to their relative acid producing and acid neutralising potentials over time. In these tests, 7.5 g of the blended waste samples (particle size < 150 μm) were introduced into 150 mL autotrophic basal salts solution at pH 2 in a 250 mL Erlenmeyer flask. Test samples were inoculated with equal proportions of *Leptospirillum ferriphilum* and *Acidthiobacillus caldus* dominant cultures (10^9 cells/mL) while control samples were similarly prepared but were not inoculated. The flasks were continuously agitated and incubated at 37 °C at 150 rpm for 90 days. The pH, redox potential, ferrous iron, total iron and sulphate concentrations of the sample solutions were monitored daily. Sample volumes were corrected for evaporation gravimetrically by adding distilled water as required over the test time frame.

Packing density and slump tests

Packing protocols, as stipulated in the American standard test method ASTM:C29/C29M-09 (2009), were applied when performing both dry and wet packing density tests. In the dry packing tests, the blended sample was introduced into a polyvinyl chloride (PVC) (H/D=1; H=0.19 m) mould in three equal portions using both assisted and un-assisted packing protocols. In the assisted packing approach, rodding and levelling was performed on each portion prior to the introduction of the following fraction. Wet packing tests were conducted according to procedures developed by Wong and Kwan (2008). The weight of the packed sample was measured to compute the packing density (ø) as the ratio of the solid volume (V_S) to the bulk volume (V). The unconfined flow potential of the mixed coal samples WR and FW was evaluated in terms of flow spread using a modified standard testing method (ASTM Committee C09.47, 2009) by using a cylindrical mould instead of the conventional Abrams cone (Clayton et al., 2003). For these tests, assisted and un-assisted packings were evaluated in which the PVC mould (H/D = 1), open at both ends, was placed vertically on a flat surface and loaded with the well-mixed samples. After loading the test sample, the PVC mould was slowly and steadily lifted vertically to ensure minimal disturbance of the packed contents upon release. The flow spread, an indication of lateral flow of the sample during deposition, was then determined by measuring and averaging the liberated diameters of the formed heap.

Results and discussion

Acid base accounting test results for blended samples of waste rock (WR) and fine waste (FW)

The WR sample was found to be potentially acid forming (PAF) with a NAPP of 10.88 kg_{H2SO4}/t and a pre-boil NAGpH of 1.98 while the FW sample was non-acid forming (NAF) with an ANC of 56,55 kg_{H2SO4}/t, a NAPP of -41.21 kg_{H2SO4}/t and a pre-boil NAGpH of 6.04 (Table 1). The 3WR:2FW sample demonstrated acid producing tendencies (pre-boil NAGpH of 2.85), with an ANC of 32.04 kg_{H2SO4}/t comparable to the MPA of 29.76 kg_{H2SO4}/t. In contrast, the 2WR:3FW sample had an ANC of 45.86 kg_{H2SO4}/t that was significantly greater than the MPA of 24.82 kg_{H2SO4}/t indicating that it was not acid forming. This suggested that the higher fine waste fraction in the 2WR:3FW samples was responsible for the observed low acid producing characteristics with a pre-boil $\text{NAGpH}_{2WR:3FW}$ = 5.37. Comparison of these blended samples showed similar acid producing behaviour with after-boil $\text{NAGpH}_{3WR:2FW}$ = 2.61 and $\text{NAGpH}_{2WR:3FW}$ = 2.73 over time.

Effect of coal waste rock (WR) and fine coal waste (FW) mixture ratios on ARD prevention: reactivity analysis

Two sets of three shake flasks containing WR and FW in dry mass ratios of 3:2 and 2:3 (WR: FW) were investigated for combined acid producing and neutralising potential. With a maximum pH of 2.8 and 3.0 from a pH 2.0 at initiation of the tests, coupled with a decrease in redox potential from 500 mV to *ca.* 420 mV and from 473 mV to 395 mV recorded for the 3WR:2FW inoculated and uninoculated samples respectively, dissolution of acid neutralisers such as carbonates was evident in the first 3 days of the biokinetic test (Figure 1 a & b).

Thereafter, the pH gradually decreased to 2.4 as acid producing reactions dominated in both the inoculated and uninoculated samples. In the uninoculated 2WR:3FW sample, an increase in the pH from pH 3.0 to pH 4.9 with corresponding drop in the redox potential from 305 mV to 280 mV in the first 6 days was noted indicating a significant buffering effect of the fine waste component. By day 40, some acidification was observed in all samples, with the increased redox potential of *ca.* 700 mV indicating the facilitated regeneration of ferric ions by the microorganisms, whether added by inoculation or occurring naturally on the coal samples. However, acidification was not sustained in the uninoculated 2WR:3FW sample, with pH returning to pH 3.5 by day 55 (Figure 1a).

These results indicate the limitation of the benign low sulphur component in sustaining near neutral conditions when mixed with the acid producing waste rock component. Given

Table 1 *Acid base accounting test results showing the total sulphur (S), maximum potential acidity (MPA), acid neutralising capacity (ANC), net acid producing potential (NAPP), and the pre-boil, after-boil and extended boil net acid generating pH (NAGpH) of the WR, FW, 3WR:2FW and 2FW:3WR samples.*

Sample name	Total S	MPA	ANC	NAPP	Pre-boil	After-boil	Ext - boil	ARD classification
	%		kg H_2SO_4/t		NAGpH	NAGpH	NAGpH	
WR	1,32	40,39	29,51	10,88	1,98	2,54	2,57	PAF
FW	0,50	15,34	56,55	-41,21	6,04	5,18	5,21	NAF
3WR:2FW	0,97	29,76	32,04	-2,28	2,85	2,61	5,14	NAF
2FW:3WR	0,81	24,82	45,86	-21,04	5,37	2,73	5,45	NAF

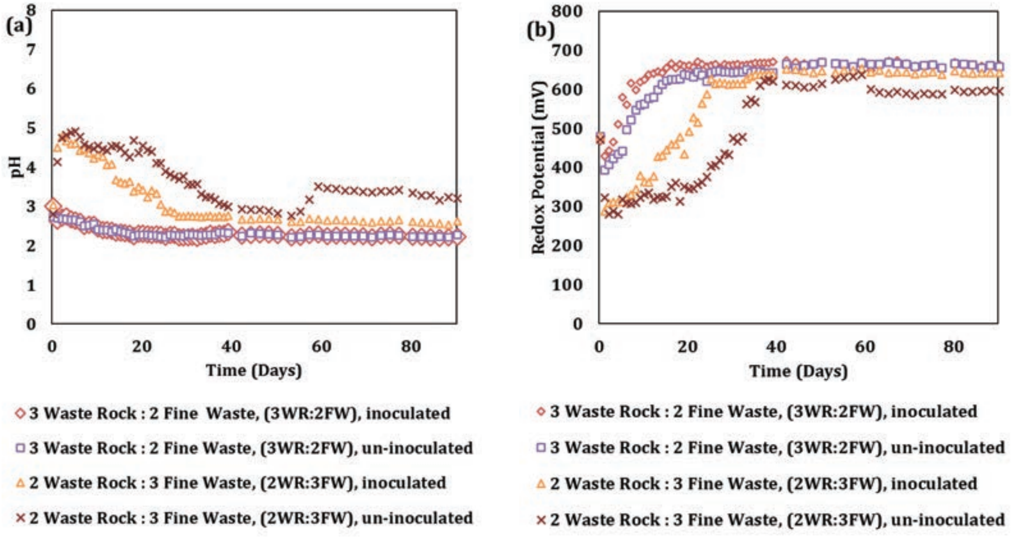

***Figure 1** Biokinetic pH and redox potential profiles for tests performed on waste rock (WR) and fine waste (FW) blends*

that these experiments were conducted in a batch system where acid neutralisers are sustained in the reaction environments, highly acidic environments are more rapidly likely to ensue in flow-through systems with the continual dilution and washout of generated neutralisers. The proliferation of preferential flow paths and unrestricted access of oxidants to the acid generating fraction would further worsen this phenomenon. Developing improved packing protocols to minimise voids within ore beds and reducing the permeability thereof therefore is an important limiting factor in ARD post dissipation of the neutralising components. To achieve this, the homogeneity of co-disposed blends is investigated to improve deposition techniques that increase the packing density and bed stability of mine waste sites.

Effect of packing methods on packing density and flow spread

The packing density is influenced by the water/solid (W/S) ratio (Figure 2a). Under dry conditions (W/S = 0), the packing density is equal to the solids concentration. The increase in W/S ratio beyond 0.08 (v/v) in both the 3WR:2FW and 2WR:3FW blended samples resulted in an increase in the packing density suggesting a reduction in voids. The maximum packing density was reached at the W/S ratio of 0.089 with a corresponding spread of 0.330 m as shown in Figure 2b for the 3WR:2FW sample whereas in the 2WR:3FW sample, the maximum packing density was reached at W/S = 0.170 with a corresponding spread of 0.351 m. This suggests a relationship between blend proportion and the W/S ratio needed to achieve maximum packing density and the associated unconfined flow potential of the sample during deposition. At a specific WR to FW ratio, typically 3WR:2FW, the fine waste just fills the voids of the waste rock skeleton promoting effective occupation of the bulk volume by the solid particles, and enhancing particle-particle interaction between the coarse and fine grains hence the lower spread (Wickland et al., 2006).

The addition of fine coal waste to fill the voids between waste rock particles improves the packing density of the bed. The void content ϵ, defined as the ratio of the volume of voids ($V - V_s$) to the bulk volume V of the granular material, decreased with an increase in solid content (Figure 3). The void content is higher in the fine waste dominated sample (2WR:3FW) than in the waste rock dominated sample (3WR:2FW). This indicates that voidage is reduced as the blend approaches

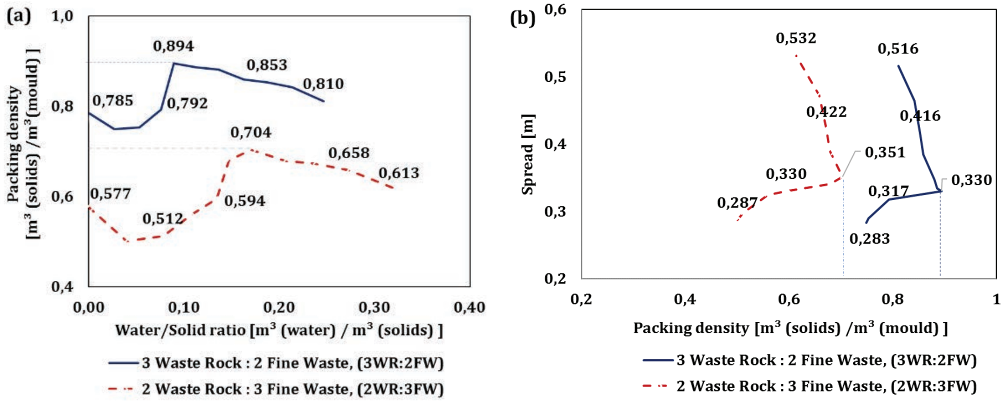

Figure 2 *(a) The effect of water/solid (W/S) ratio on the solid concentration and (b) the relationship between packing density and spread*

the 'just filled in' state (*viz.* 3WR:2FW in Figure 2 & 3a). Comparatively, the 3WR:2FW packing results in a more compact structure.

Compact beds are less susceptible to volume change under the action of compressive loads, particularly in coarse particle dominated samples (Li et al., 2017; Shokouhi and Williams, 2017). The load-bearing waste rock skeleton limits the total axial strain and increases the stability of the bed (Wickland et al., 2006). Such stress-strain behaviour shows the significance of mix proportions in developing packing protocols for ARD prevention.

Conclusions

The suitability and packing behaviour of co-disposed coal waste rock (WR) and fine coal waste (FW) in preventing the generation of ARD was demonstrated. ABA and biokinetic tests were used to evaluate the ARD potential of the coal WR, FW and the co-mingled blends of these samples (3WR:2FW and 2WR:3FW). The packing behaviour of these mixtures was analysed using packing density tests and slump tests.

The FW dominated blended sample (2WR:3FW) showed higher neutralisation characteristics than the WR dominated blends (3WR:2FW). Consistent with ABA tests, FW samples showed potential in delaying the generation of acidity when blended with sulfidic coal WR. The limited neutralising effect of FW over time calls for the development of packing methods that would enhance the prevention of ARD by restricting access of aqueous oxidants to acid generating coal waste fractions. The WR dominated sam-

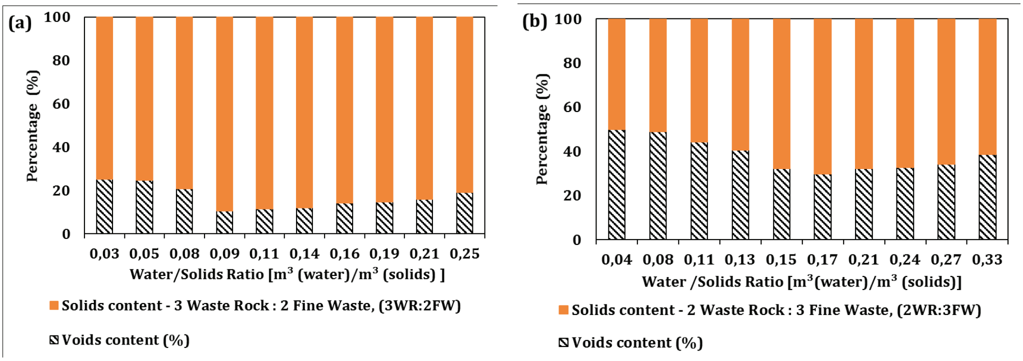

Figure 3 *Relationship between solids and voids content for blends in dry mass ratio (a) 2WR:3FW (b) 3WR:2FW*

ple (3WR:2FW) displayed favourable packing densities (0.89 $\text{m}^3_{\text{solids}}/\text{m}^3_{\text{mould}}$) with low void content (10.6%) relative to the FW dominated blends. Compressibility tests are expected to validate that with decreasing void content, minimum axial strain will be observed under constant rate loads; thereby providing insight into the engineered design of geochemically and geotechnically stable packed beds.

Acknowledgements

The authors thank the South African Water Research Commission (WRC) through WRC 2761, as well as the technical input of the steering committee to this project. Further funding and support through the DST-NRF SARChI chair in Bioprocess Engineering (UID 64788), held by STLH, is gratefully acknowledged.

References

Alakangas, L., Dagli, D., Knutsson, S., 2013. Literature Review on Potential Geochemical and Geotechnical Effects of Adopting Paste Technology under Cold Climate Conditions 1–36.

ASTM:C29/C29M-09, 2009. Standard Test Method for Bulk Density (" Unit Weight ") and Voids in Aggregate. ASTM Int. i, 1–5. https://doi.org/10.1520/C0029

ASTM Committee C09.47, 2009. ASTM C1611-09 Standard Test Method for Slump Flow of Self-Consolidating Concrete. Annu. B. ASTM Stand. Vol. 04.02 1–6. https://doi.org/10.1520/C1611

Bussière, B., Aubertin, M., Chapuis, R.P., 2003. The behavior of inclined covers used as oxygen barriers. Can. Geotech. J. 40, 512–535. https://doi.org/10.1139/t03-001

Clayton, S., Grice, T.G., Boger, D. V., 2003. Analysis of the slump test for on-site yield stress measurement of mineral suspensions. Int. J. Miner. Process. 70, 3–21. https://doi.org/10.1016/S0301-7516(02)00148-5

Descostes, M., Beaucaire, C., Mercier, F., Savoye, S., Sow, J., Zuddas, P., 2002. Effect of carbonate ions on pyrite (FeS2) dissolution. Bull. Soc. geol. Fr. 173, 265–270. https://doi.org/10.2113/173.3.265

Hesketh, A.H., Broadhurst, J.L., Bryan, C.G., Van Hille, R.P., Harrison, S.T.L., 2010. Biokinetic test for the characterisation of AMD generation potential of sulfide mineral wastes. Hydrometallurgy 104, 459–464. https://doi.org/10.1016/j.hydromet.2010.01.015

Johnson, D.B., Hallberg, K.B., 2005. Acid mine drainage remediation options: A review. Sci. Total Environ. 338, 3–14. https://doi.org/10.1016/j.scitotenv.2004.09.002

Kollias, K., Mylona, E., Adam, K., Papassiopi, N., Papassiopi, N., Xenidis, A., 2014. Suppression of Pyrite Oxidation by Surface Silica Coating. J. Geosci. Environ. Prot. 02, 37–43. https://doi.org/10.4236/gep.2014.24006

Kotsiopoulos, A., Harrison, S.T.L., 2018. Co-disposal of benign desulfurised tailings with sulfidic waste rock to mitigate ARD generation: Influence of flow and contact surface. Miner. Eng. https://doi.org/10.1016/j.mineng.2017.03.003

Kotsiopoulos, A., Harrison, S.T.L., 2017. Application of fine desulfurised coal tailings as neutralising barriers in the prevention of acid rock drainage. Hydrometallurgy 168, 159–166. https://doi.org/10.1016/j.hydromet.2016.10.004

Kotsiopoulos, A., Harrison, S.T.L., 2015. Enhancing ARD Mitigation by Application of Benign Tailings to Reduce the Permeability of Waste Rock Dumps. Adv. Mater. Res. 1130, 560–563. https://doi.org/10.4028/www.scientific.net/AMR.1130.560

Li, L.G., Lin, C.J., Chen, G.M., Kwan, A.K.H., Jiang, T., 2017. Effects of packing on compressive behaviour of recycled aggregate concrete. Constr. Build. Mater. 157, 757–777. https://doi.org/10.1016/j.conbuildmat.2017.09.097

Mbamba, C.K., Harrison, S.T.L., Franzidis, J., Broadhurst, J.L., 2012. Mitigating acid rock drainage risks while recovering low-sulfur coal from ultrafine colliery wastes using froth flotation. Miner. Eng. 29, 13–21. https://doi.org/10.1016/j.mineng.2012.02.001

Miller, S.D., Robertson, A., Donahue, T., 1997. Advances in acid drainage prediction using the Net Acid Generation (NAG) test, in: 4th International Conference on Acid Rock Drainage. Vancouver, BC, pp. 533–549.

Pujado, P.R., 2006. Economic analysis. Statistics South Africa, Pretoria. https://doi.org/www.statssa.gov.za/publications/Report-04-05-20/Report-04-05-202014.pd

Shokouhi, A., Williams, D.J., 2017. Volume change behaviour of mixtures of coarse coal reject and tailings. Min. Technol. 126, 163–176. https://doi.org/10.1080/14749009.2016.1277649

Shu, X., Dang, Z., Zhang, Q., Yi, X., Lu, G., Guo, C., Yang, C., 2013. Passivation of metal-sulfide tailings by covalent coating. Miner. Eng. 42, 36–42. https://doi.org/10.1016/j.mineng.2012.11.010

Skousen, J., Renton, J., Brown, H., Evans, P., Leavitt, B., Brady, K., Cohen, L., Ziemkiewicz, P., 1997. Neutralization Potential of Overburden Samples Containing Siderite. J. Environ. Qual. 26, 673. https://doi.org/10.2134/jeq1997.00472425002600030012x

Stewart, W.A., Miller, S.D., Smart, R., 2006. Advances in Acid Rock Drainage (Ard) Characterisation of Mine Wastes. J. Am. Soc. Min. Reclam. 2006, 2098–2119. https://doi.org/10.21000/JASMR06022098

Wickland, Wilson, G.W., Wijewickreme, D., Klein, B., 2006. Design and evaluation of mixtures of mine waste rock and tailings. Can. Geotech. J. 43, 928–945. https://doi.org/10.1139/t06-058

Wong, H.H.C., Kwan, A.K.H., 2008. Packing density of cementitious materials: Part 1-measurement using a wet packing method. Mater. Struct. Constr. 41, 689–701. https://doi.org/10.1617/s11527-007-9274-5

The WIN-WIN solution to the clean-up of mine residue - An innovative and cost-effective method to reduce acid drainage from mine residue in Southern Africa that can also provide social upliftment.

Kym L Morton PhD MBA[1],

[1]*KLM Consulting Services, Johannesburg, South Africa, kmorton@klmcs.co.za*

Abstract

South Africa's heritage of over 150 years of gold mining in the Witwatersrand area is continuous exposure of sulphide rich soils and mine dump residue to rainwater. Rainwater increases the acidity in the soils and ground water contributing to the acid mine drainage problem prevalent across 120km of semi-urbanised land. Many of the easily accessible dumps have been removed by mechanised hydro-mining leaving behind thick skins of toxic sediments and contaminated soils. Collection and clean-up of the residual soils requires manual labour. Polluted land has a reduced value despite being very close to fast growing nodes of urbanisation. This short paper describes how the South Africa Government's Working for Water Programme (WfW) can be adapted to create a WIN WIN programme where training and employment can be used to remove polluted sediments and pay for itself by selling the valuable metals and increasing the value of the land. The paper concludes by listing the advantages of the WfW clean up to social development, water protection and economic development of the Witwatersrand. Implementation in other polluted areas is a possible add-on.

Keywords: ICARD | IMWA | MWD 2018, WIN-WIN, water protection, ground water protection, land values and social upliftment

Introduction

The Witwatersrand is an arc of mining activity centred on Johannesburg that has a history of gold mining dating back to the late 1800's. Gold and other metal ores such as Silver and Copper were mined from reefs that were then crushed and processed, using an increasingly efficient refining process. Millions of tons of processed, crushed rock have been deposited as mine waste dumps and Tailings Residue Facilities (TSF's), collectively known as mine dumps. The residues from the hydro-mining of the dumps often contain high concentrations of Gold, Silver, Cadmium, Cobalt, Uranium and other metals.

Johannesburg is one of the few cities in the world that is not located on a river. The water needed for mineral processing came originally from underground, (e.g. Zuurbekom pumping station near Soweto) and distant surface water supplies such as the Vaal dam. As Johannesburg grew, the urban nodes and water distribution system occupied the sites of the original mining villages which then became towns and coalesced into the Witwatersrand urban conurbation. The Witwatersrand has over 120km of land running East-West that is contaminated by mining activities including and dominated by re-processed mine dump residue. Acidic runoff and ground water base flow enters the streams and rivers which then contaminate the water supply system.

Figure 1 shows the Rand Water pipeline network and its proximity to mine waste dumps.

Many people live close to the old gold mine dumps; often in informal settlements with very high unemployment and are affected by the pollution emanating from mine dumps in the form of seepage water and polluted ground water. Figure 2 shows the proximity of informal settlements to the gold mining areas.

The proximity of people to the mine dump areas means their health is compromised. The

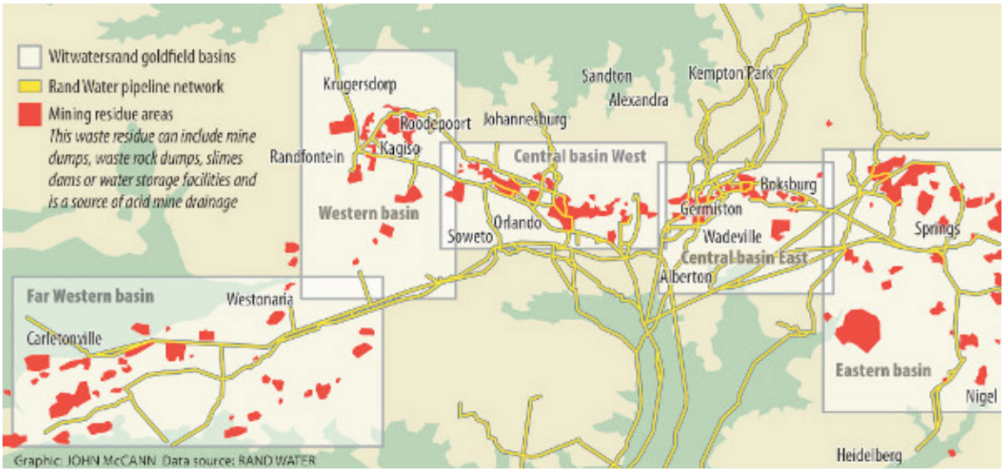

Figure 1 *Rand water pipeline and proximity to mine waste dumps on the Witwatersrand. (Source John McCann).*

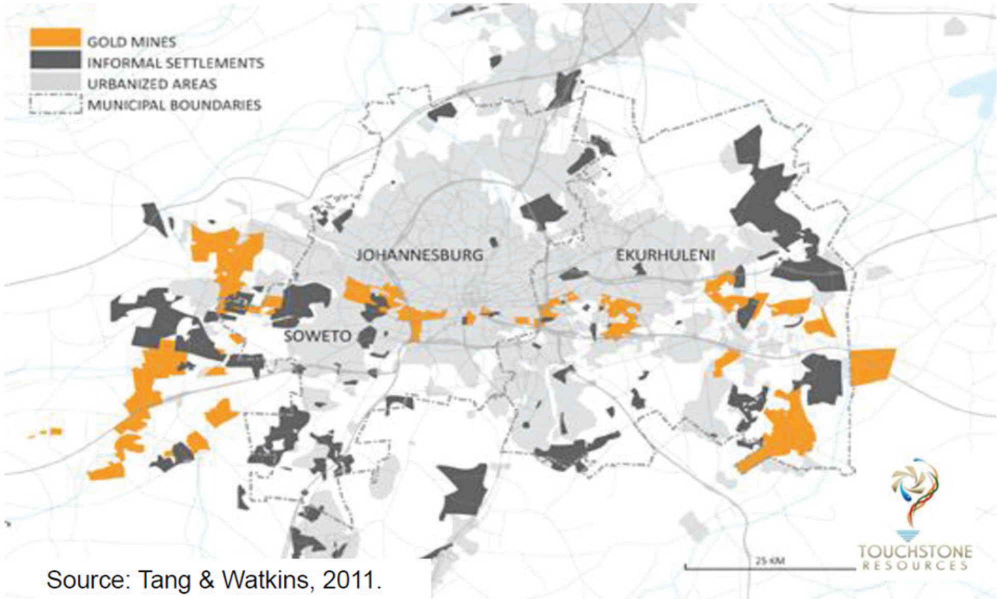

Source: Tang & Watkins, 2011.

Figure 2 *Proximity of gold mines and informal settlements.*

Tudor Shaft settlement near Krugersdorp on the West Rand has been occupied for over 15 years with people living on top of old mine dumps where children are exposed every day to polluted soils and water, which are often radioactive. Naidoo (2017) gives a comprehensive list of the polluted areas and social impacts.

Figure 3 shows the Tudor Shaft settlement and Figure 4 shows the proximity of Grootvlei Snake Park settlement in Soweto to an eroding mine dump.

The soils and sediments comprise pyritic rock, which creates acidic runoff whenever it rains. This adds to the acidic seepage from underground sources of abandoned mines that are now decanting. The United Nations estimated cost of conventional clean-up is US$60Bn. This cost is beyond the mining rehabilitation fun, the government and NGO's.

***Figure 3** Tudor Shaft settlement on mine dump residue (Source M Liefferink)*

All the polluted water flows into river systems used for drinking water. If contaminated soils and sediments are removed and the land rehabilitated, the water pollution will decrease and the cost of water treatment in the catchment reduced. Radioactivity levels will also decrease when the source material is removed.

***Figure 4** Grootvlei Snake Park settlement, Soweto (Source M Safodien)*

Figure 5 shows the location of the major streams draining the Witwatersrand

A lot of the mine dumps along the Witwatersrand have been reprocessed, but often the roots of the mine dumps have been left behind. The roots and bases of the old mine dumps have the highest value in terms of unprocessed metals. Early mineral processing techniques were inefficient and therefore the lower layers of the mine residue dumps have high concentrations of gold, silver and other valuable metals. May 2018 prices were:

Gold	US$ 1291.10/Oz (ZAR16,220/Oz)
Cadmium	US$ 1.85/Kg
Cobalt	US$ 91.49/Kg
Silver	US$ 16.19/Oz
Uranium	US$ 44.38/Kg
Potassium nitrate	US$ 7.82/Kg

Source: www.metalprices.com

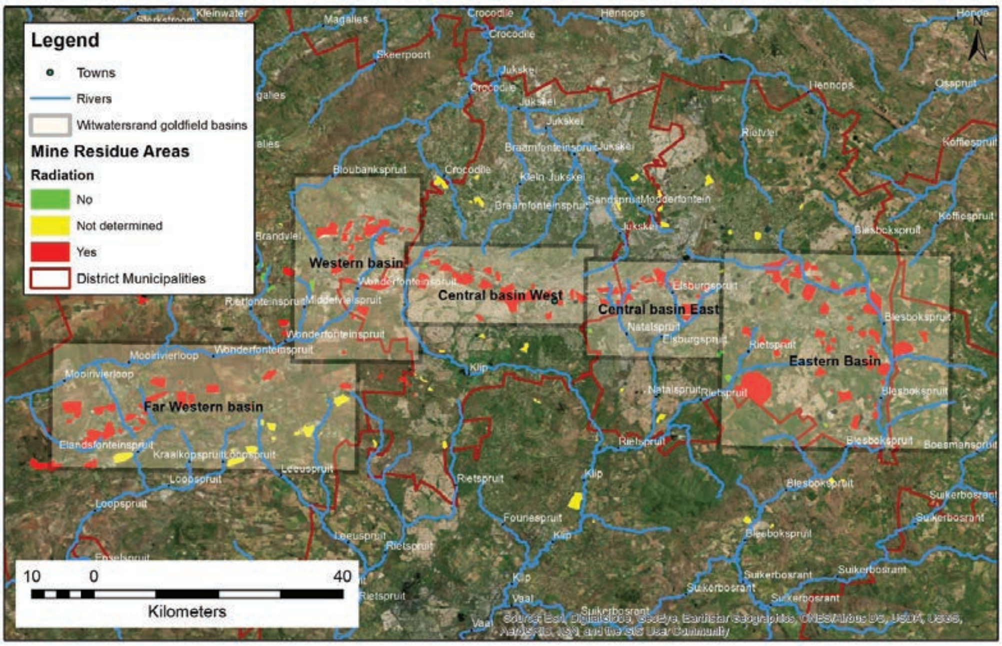

Figure 5 Drainage basins and drainage streams affected by mine dumps in the Witwatersrand (Source John McCann and Rand Water)

Solution

There is opportunity to collect the mine residue and extract value. The main cost is labour. The reason the roots of the mine residue dumps were not collected for reprocessing, was the difficulty of using machinery to collect the soils and sediments. Many deposits are inaccessible, except through shovelling and sweeping. Both activities are labour intensive.

There is a will amongst people living next to the dumps to clean up and create employment. The proximity of informal settlements to mine dumps means, with proper training in hazardous material clean up, local labour is available to collect the soils and sediments machinery is unable to collect.

When people are trained in waste clean-up and the use of appropriate Personal Protection Equipment (PPE), then the soils and sediments can be bagged, collected, transported to refineries and the metals extracted. The revenue from the metals can be used to reinvest in training and expansion of the work programme into other areas requiring clean-up. This programme has been called a WIN -WIN solution for mine dump clean up and acid drainage reduction.

The WIN-WIN programme imitates the very successful Working for Water (WfW) programme initiated by the South African Government.

Since 1995, WfW has cleared more than one million hectares of invasive alien plants providing jobs and training to 30 000 people from among the most marginalized sectors of society per annum. 52% are women. WfW, through the Department of the Environment, has 300 projects in all nine of South Africa's provinces.

WfW is globally recognized as one of the most outstanding environmental conservation initiatives on the continent. It enjoys sustained political support for its job creation efforts and the fight against poverty. WfW considers the development of people as an essential element of environmental conservation. Short-term contract jobs created through the clearing activities are undertaken, with the emphasis on endeavouring to recruit women (the target is 60%), youth (20%) and disabled (5%). (Department of Water and Sanitation web site July 2017).

WIN-WIN aims to build on this success and develop a skilled work force in environmental monitoring, Hazardous waste clean-up, Human Resources Management , training, logistics and management.

The WIN-WIN solution for clean-up of mine residue, requires the consultation and co-operation of the affected parties and land owners, Environmental and Water departments and mine processing plant owners. It also requires the development of a funding, Human Resources and logistics plan.

Conclusions

The programme is called WIN-WIN because not only will it result in the clean-up of the polluted mine waste land around the Witwatersrand there are other advantages:

- Unemployed become trained, skilled and employed
- Contaminated land is cleaned up
- Living areas become habitable
- Land becomes valuable and sales can pay for rehousing and further clean up
- Valuable metals are collected which funds further clean up
- Costs of water treatment for water supply are reduced saving Rand Water money
- Health care costs reduce
- Healthier work force and healthier children
- Boost to the economy

The next steps and work in progress comprises:

- Public Private Partnership (PPP)
- Planning and obtaining seed money
- Linkage of communities, trainers, permit experts, land owners to process plant owners
- Agreement with the Department of Environment and Department of Water and Sanitation to plan and permit the Win-Win solution
- Implement a pilot site – suggested Tudor shaft area

Acknowledgements

The author thanks Dr Guy Preston of the Department of Environment for his contributions to the planning of the implementation of the WIN-WIN Solution and the financial support of the Water Research commission (WRC) with advice and guidance from Dr Jo Burgess.

References

J McCann (2014) The Witwatersrand's toxic time bomb. Graphic

Lieferrink M (2012) Environment risks and hazards pertaining to Acid Mine drainage and radioactivity within the Witwatersrand Goldfields. Power Point presentation Federation for a sustainable Environment

M Plaut (2014) South Africa's toxic acid mine water a threat to 12 million. https://martinplaut.wordpress.com

Naidoo S (2017) Acid Mine Drainage in South Africa Development, actors, policy impacts and broader implications Springer pp128

Safodien M (2018) https://www.news24.com/SouthAfrica/News/joburg-suffocates-in-the-shadow-of-mine-dumps-20180103

Passive Underground Mine-water Purification System (PUMPS): a conceptual geo-engineering model for the treatment and management of acid mine water in the Witwatersrand gold mines, South Africa

Thakane Ntholi [1,2], Maarten deWit[2]

[1]Council for Geoscience, Pretoria, South Africa, thakane.ntholi@gmail.com

[2]AEON and Nelson Mandela University, Port Elizabeth, South Africa

Abstract

The Passive Underground Mine-water Purification System (PUMPS) is a hybrid geo-engineering model based on the mimicry of natural systems integrated with modern technologies designed for semi passive *in-situ* remediation of acid mine water in the Witwatersrand gold mines using sulfate reducing bacteria and driven by geothermal energy. The model simulates reactions that occur at deep sea hydrothermal white smokers. The mimicry of a hydrothermal system is achieved by combining three components: a low enthalpy geothermal energy system, a reaction (bioremediatiom). chamber in which bioremediation takes place through sulfate reduction and a water reservoir which together form PUMPS.

Keywords: Acid mine water, Geo-engineering, *in-situ* bioremediation, Geothermal energy, Witwatersrand gold mines

Introduction

Acid mine drainage, is one of the biggest threats to South Africa's water quality and one of the biggest socio-economic and environmental liabilities to result from the gold mining industry (de Villiers & de Wit 2010). Acid mine drainage refers to the acidic, metal and sulphate rich water (herein referred \to as acid mine water (AMW) resulting from chemical and/or biological oxidation of sulphide minerals (Gray 1998; Wolkersdorfer 2008; Nordstrom 2011).In the Witwatersrand gold mines, pyrite is the most common sulphide mineral associated with gold, and is excessively exposed to water and oxygen as a result of mining activities (Van der Walt, I. J.; Roer 2006; Akcil & Koldas 2006; McCarthy 2011). The gold mines extend to depths up to 4km, far below the water table, and are subject to continuos inflow of groundwater (Naicker et al. 2003), which then reacts with pyrite and generates acid mine water (AMW). In active mines, inflowing ground water is continuously pumped out to enable safe and efficient mining (Naicker et al. 2003), consequently retarding the formation and/or accumulation of AMW. Therefore increased generation and accumulation of AMW is more prevalent in abandoned and/or disused mines where pumping of inflowing groundwater has stopped (McCarthy 2011). Absent owners and high treatment costs have led to most of the AMW in these disuded mines being left untreated and flood levels rising towards the surface (Akcil & Koldas 2006; Coetzee et al. 2010). Structural interconnectivity of the mines occasionally results in seepage of AMW from flooded, abandoned mines into neighbouring active mines (McCarthy 2011), placing an extra burden of pumping and treating the AMW on the latter (Winde & Stoch 2010; Coetzee et al. 2010).

In this paper, a conceptual geo-engineering model PUMPS (Passive Underground Mine-water Purification) (Fig. 1) is presented as a potential long term, solution for localised and regional AMW mitigation in disused gold mines. PUMPS is a semi-passive *in-situ* AMW purification system, that uses sulphate reducing bacteria for bioremediation of large volumes of AMW. PUMPS is designed to draw its operational energy from geothermal heat extracted from mines below the mines and to eventually convert the mines into clean water reservoirs.

Background of the PUMPS Model

As a geo-enginering model, PUMPS is based on mimicing natural systems to remediate anthropogenically created environmetal problems. Specifically, PUMPS is modelled after chemical and biological reactions observed at white-smokers of deep sea hydrothermal vent systems. At these system, sea water percolates through the surface and is circulated through the subsurface rocks (Douville 2002). During circulation, the sulphate-rich sea water dissolves and entrains high concentrations of metals and the sulphate undergoes thermochemical sulfate reduction, leading to a decrease in pH. The resultant fluid, with similar chemistry to that of AMW, is then emitted through black or white smokers. White-smoker, which can be found on their own or as divergent chimneys of black smokers, emit fluid at temperatures up to 150^{0}C. Upon emission, part of the fluid immediately precipitates metal sulfides. The remaining fluid is subjected to biogenic sulphate reduction by sulphate reducing bacteria (SRB), resulting in further precipitation of metal sulphides (German, C.; Baker, E.; Klinkhammer 1995; Tarasov et al. 2005). This process decreases the metal and sulphate concentrations in the fluid and increases the pH, similar to what is required for AMW remediation. Geoengineering of white smoker was found to be fitting for the Witwatersrand gold mines because successful implementation of this system will demonstrate the viability of *in-situ* semi-passive bioremediation, a treatment option that was believed not be viable in these mines.

To mimic this system, the floor of PUMP system in mines is equated to the sea floor, the flooding AMW is equated to the sea water and the rocks below the base of the mines are equivalent to the subsurface rocks. In order to achieve optimum conditions for sulphate reducing bacteria, they are hosted in a closed reaction chamber (similar to bioreactors) in which the AMW can flow in and flow out once bioremediation is complete. The circu-

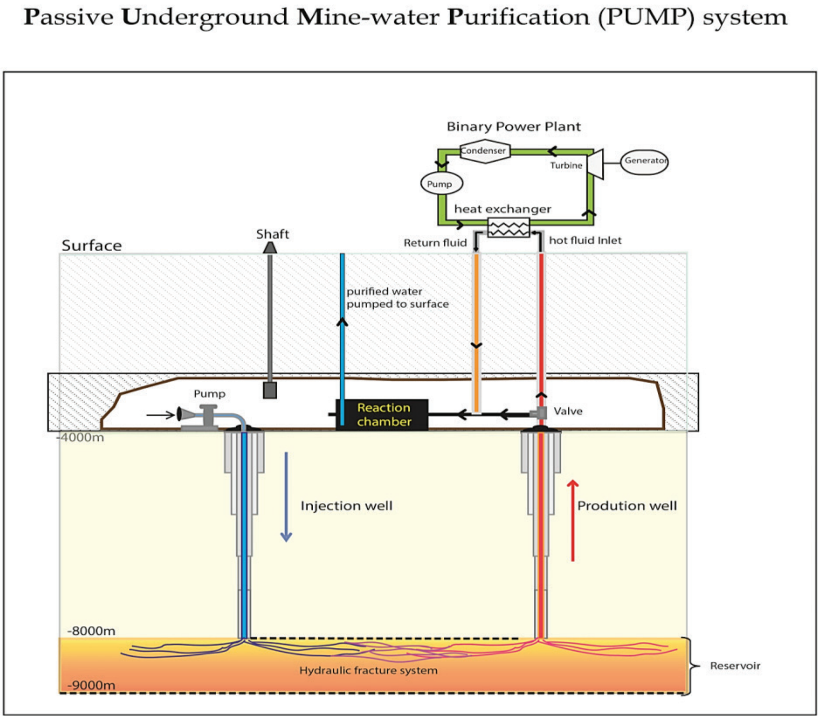
Passive Underground Mine-water Purification (PUMP) system

Figure 1 Schematic representation of the Passive Underground Mine-water Purification System (PUMPS) when installed in a mine.

lation of water for harvesting heat from the rocks is modelled according to known geothermal energy sysytems and the surplus heat harvested through circulating AMW through the hot rocks will be used to generate electricity for the energy needs of PUMPS. The treated water will circulate back into the mine voids, and this will continue until the voids converted into clean water reservoirs.

In essence PUMPS is made up of three components; the geothermal energy system, the reaction chamber and the 'water reservoir'. Here, we present the first of a series of proof of concept investigations carried out for each of the components of PUMPS. We present bench experiments for bioremediation of the mine water, and desktop studies of the geothermal potential of the Witwatersrand Basin and the total volume of the underground mines to be converted into water reservoirs.

Methodology for emperical and technical analysis of PUMPS

Sampling and analyses

Mine water (AMW) samples were collected from an abandoned shaft of an old mine in the West Rand. Relevant onsite measurements such as pH, electrical conductivity and RedOx were recorded and samples preserved with nitric acid. Analysis of cations concentrations was performed with ICP AES (Varian VISTA-MPX, axiales Plasma) at GFZ-Potsdam, Germany

Bench-scale bioremediation with D. kuznetsovii

The *Desulfotomaculum kuznetsovii* strain 17T (VKM B-1805; DSM 6115) was selected as the test sulfate reducer for PUMPS (Tourova 2001). For this experiment, one strain was used in order to constrain the experiment and prevent variability that results from using a consortium. The experiments were carried out in 100 ml serum vials sealed with butyl rubber stoppers secured with aluminium crimp seals. 50ml of AMW/ DSMZ medium M63 was added to the vials which were then flushed with nitrogen to eliminate air and dissolved oxygen. Pressure in the vials was adjusted to 1bar before autoclaving at 121^{o}C for 15 minutes to eliminate pre-existing bacteria. After cooling to room temperature, the AMW vials were enriched with 10mM lactate electron donor, same concentration as in DSMZ M63. Lactase is a good electron donor partcicularly for *Desulfotomaculum*. A fresh 24 hour anaerobic culture (10% v/v) of *D. kuznetsovii* was used as inoculum for both AMW and DSMZ M63 and the vials were incubated at 40^{o}C, 63^{o}C and 80^{o}C. Parallel uninoculated vials were added as blanks for each temperature condition. The experiment was carried out for a duration of four weeks and samples were taken at weekly intervals for analyses of pH and sulphate concentration. The sulphate concentrations were measured using photospectrometry. Final cation concentrations were measured at the end of the experiment. All experiments and controls were performed in duplicates.

Geothermal energy potential of the Witwatersrand Basin

Thermal distribution in the Witwatersrand was determined using 2D modelling of a geological cross section (Fig. 2) taken along the WNW-ESE (A-B) profile. The 2D model uses a MATLAB code development by Norden, (2010), which incorporates both vertical and lateral temperature variations taking into account the contribution of heat producing elements and heat sinks. For input

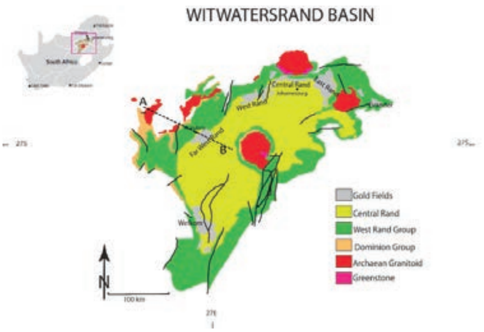

Figure 2: *Geological map of the Witwatersrand Basin showing the formations from the base of the basin to the Witwatersrand Supergroup. The Gold Fields lie between the West Rand and Central Rand groups. Normal faults on the boundaries of the basin control the depth distribution of the gold deposits. Modified from Frimmel and Minter (2002). Section A-B reveals a thermal profile across the basin as summarized in Fig. 3.*

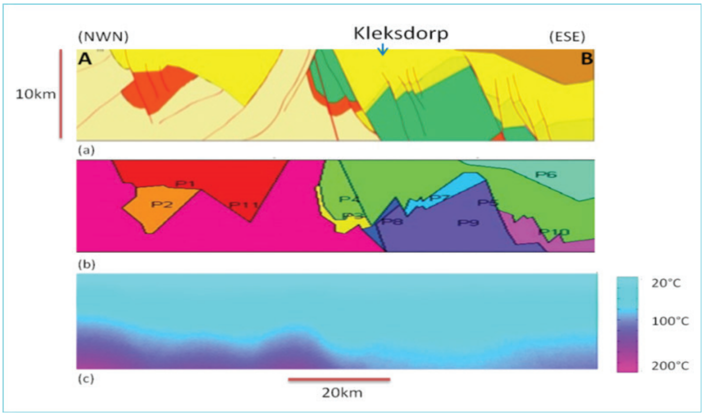

Figure 3 (a) Simplified lithologic cross-section of the transect A-B (see Fig. 2), used to model a 2D geothermal profile of the Witwatersrand Basin. The variable lithologies have different thermal properties that affect both lateral and vertical heat transfer. (b) Model polygons of lithologies with their thermal properties linked to their adjacent lithologies. Polygons are further divided into mesh triangles to derive (c), a final 2D thermal profile.

into the model, the section is translated into vectors that delineate structural and lithology boundries (Fig. 3a). The model uses heat conductivity, and heat capacity of the different lithologies as inputs. It then generates polygons defined by thermal and structural properties (Fig. 3b). It further divides the polygons into mesh triangles and the final output is a 2D thermal colour gradient (Fig. 3c).

Water Reservoir capacity

The total residual volume of underground voids were estimated using two independent methods that quantify the volume of rock exhumed and processed during gold mining, derived from: (1) the volume of mine tailings and (2) from the total gold production based on an estimated average grade of 3.5g /ton (see below). The tailings volume was calculated by measuring the area of the tailings in GIS and using an estimated average height of 50m. The gold production data was aquired from Depatment of Minerals and Energy, Goldsheetlinks and Goldcoin websites in 2012. It is estimated that the mine tailings represent the total 120 years, whilst gold production data is only available for the past 30 years. Although backfilling, which involves the re-insertion of processed material back into the mines, has been practiced recently (Winde 2006; Ngcobo 2006) and advanced technology has minimized the amount of barren rock brought to surface during mining, these practices are assumed to be negligible.

Results and discussion

Bioremediation

Mine water sampled from the discharge point wad found to be circum-neutral with average pH of 5.6. At 40°C and 80°C, the pH increases form 5.6 to 6.5 and 29% iron removal was achieved, with sulphate concentrations decreasing from 4300mg/L to 1692mg/L and 1882mg/L, respectively. At the optimum temperature of 63°C, pH increased from 5.6 to 8 and iron concentration of 758mg/L decreased to below detectable limits. Sulphate concentrations decreased from 4300mg/L to 1200mg/L *i.e.* by 70% removal. The resuling precipitates were identified using SEM imagery and were identified as armophous iron sulphides and calcium sulphates.

Thermal profile of the Witwatersrand

The thermal profile (Fig 3c) shows that the maximum temperatures at 8km along this profile is ca. 200°C, in areas where the basement granitoids are closer to the surface. The goldfield region around Kleksdorp, reach a maximum range of 100-120°C. These maximum temperatures are consistent with the geothermal gradient of 12°C/km and more inportantly, they are sufficient for the simulation of white smoker reactions within the gold mines.

Total volume of mine voids

Mine volume calculations indicate that the total volume of the mine voids is at least 5.60E+9 m^3 which is more than twice the volume of the Vaal Dam, South Africa's fourth largest reservoirs. This volume is more than sufficient for an underground fresh water reservoir and will make a significant contribution towards water security in the Gold field regions.

Conclusion and future work

The PUMPS model is a multi-faceted long term solution to the acid mine drainage challenge in the Witwatersrand Basin. It explores the potential for *in-situ* remediation, driven by renewable energy and provides post-mining use for the mine voids.

Results show that bioremediation using *D. kuznetsovii* SRB was successful. Total removal of iron, a significant removal of sulphate and an increase in pH are a good indication that bioremediation in an all-encompassing option for the gold fields mine water. The necessary temperatures for low enthalpy geothermal energy are found at approximately 8km below the surface. However, taking advantage of the deep gold mines will reduce the necessary drilling depth to reach 8km. Storing treated water in the mine voids provides a good post-mining alternative for the voids, and more importantly storage capacity that is protected from evaporation.

These results are first of a series of proof of concept investigations and provided sufficient confidence on which subsequent investigations were based.

The innovative nature of PUMPS requires extensive technical analysis, therefore focus of the subsequent investigations focused on the following technical aspects of the PUMPS components:

- Design and drilling parameters of the geothermal system
- The amount of energy that can be generated from the the geothermal system
- Behaviour of acid mine water in the PUMPS geothermal system
- The ability of the sulphate reducing bacteria to survive high pressure condition
- The economic model/implications of PUMPS

Results of the technical analysis will lay a solid foundation for an on-site pilot plant and will be presented in future contributions.

Acknowledgements

The Authors would like to thank the NRF for research funding throuth Inkaba ye Afrika (now Iphakade). We woul also like to thank the GFZ –Potsdam, Germany for technical assistance. Finally, we would like to thank all the colleaques that contributed to this work.

References

Akcil, A. & Koldas, S., 2006. Acid Mine Drainage (AMD): causes, treatment and case studies. *Journal of Cleaner Production*, 14(12–13), pp.1139–1145.

Coetzee, H., Hobbs, P.J., Burgess, J.E., Thomas, A. & Keet, M., 2010. *Mine water management in the Witwatersrand gold fields with special emphasis on acid mine drainage: Report to the Inter-ministerial Commitee on acid mine drainage.*,

Douville, E. et al., 2002. The rainbow vent fluids (36 °14' N, MAR): the influence of ultramafic rocks and phase separation on trace metal content in Mid-Atlantic Ridge hydrothermal fluids. *Chemical Geology*, 184, p.37–48.

German, C.; Baker, E.; Klinkhammer, G., 1995. Regional setting of hydrothermal activity. In Hydrothermal Vents and processes. *Geological Society, London, Special Publications*, 87, pp.3–15.

Gray, N.F., 1998. Acid mine drainage composition and the implications for its impact on lotic systems. *Water Research*, 32(7), pp.2122–2134.

Lottermoser, B., 2010. *Mine Wastes*, Berlin Heidelberg: Springer Berlin Heidelberg.

McCarthy, T.S., 2011. The impact of acid mine drainage in South Africa. *South African Journal of Science*, 107(5/6), pp.1–7.

Naicker, K., Cukrowska, E. & McCarthy, T.S., 2003. Acid mine drainage arising from gold mining activity in Johannesburg, South Africa and environs. *Environmental pollution (Barking, Essex : 1987)*, 122(1), pp.29–40.

Ngcobo, T.A., 2006. The risks associated with mines in dolomitic compartments. *Geology*, (April), pp.251–264.

Nordstrom, D.K., 2011. Applied Geochemistry Hydrogeochemical processes governing the origin , transport and fate of major and trace elements from mine wastes and mineralized rock to surface waters. *Applied Geochemistry*, 26(11), pp.1777–1791.

Tarasov, V.G. et al., 2005. Deep-sea and shallow-water hydrothermal vent communities: Two different phenomena? *Chemical Geology*, 224(1–3), pp.5–39.

Tourova, T.P. et al., 2001. Heterogeneity of the Nucleotide Sequences of the 16S rRNA Genes of the Type Strain of Desulfotomaculum kuznetsovii. *Micobiology*, 70, pp.678–684.

de Villiers, S. & de Wit, M., 2010. *H2O-CO2-Energy equations for South Africa: PRESENT STATUS , FUTURE SCENARIOS AND PROPOSED SOLUTIONS Abstract*, Available at: www.aeon.uct.ac.za.

Van der Walt, I. J.; Roer, K.D., 2006. Hydrologic impact of rewatering of the Gemsbokfontein dolomitic western subcompartment on the Wonderfonteinspruit , South Africa. *Physical Geography*, 27, p.316–332.

Winde, F., 2006. Challenges For Sustainable Water use in Dolomitic Mining Regions of South Africa—A Case Study of Uranium Pollution Part II: Spatial Patterns, Mechanisms, and Dynamics. *Physical Geography*, 27(5), pp.379–395.

Winde, F. & Stoch, E.J., 2010. Threats and opportunities for post-closure development in dolomitic gold-mining areas of the West Rand and Far West Rand (South Africa) - A hydraulic view Part 2: Opportunities. *Water SA*, 36(1), pp.75–82.

Wolkersdorfer, C., 2008. *Water Management at Abandoned Flooded Underground Mines: Fundamentals, Tracer Tests, Modelling, Water Treatment* illustrate., Heidelberg: Springer Science & Business Media,.

Evaluation of the Use of Sulphide Paste Rock as Cover Material in Mine Reclamation

Sandra Pouliot[1], Bruno Bussière[1], Anne-Marie Dagenais[2], Ward Wilson[3],
Yanick Létourneau[4]

[1]RIME UQAT, Rouyn-Noranda, Quebec, Canada
[2]Golder and Ass., Montreal, Quebec, Canada
[3]University of Alberta, Edmonton, Alberta, Canada
[4]LaRonde Mine, Agnico Eagle Mines Ltd, Rouyn-Noranda, Quebec, Canada

Abstract

Today's mining industry faces challenges related to mine site reclamation with increasing impacted footprints and the quantity of materials required to put covers in place. This research is complementary to other technical pre-reclamation studies to evaluate the application of paste rock, a mixture of waste rock and mill tailings, available at the LaRonde mine (Agnico Eagle Mines Ltd), with or without a limestone amendment and/or compaction. This study on the use of paste rock presents the results of various material characterizations, as well as hydrogeological and geochemical data from laboratory-based column tests.

Keywords: Mine site reclamation, reclamation covers, paste rock, cover with capillary barrier effects

Introduction

Tailings deposited in surface impoundments are prone to oxidation when they contain sulphide minerals and are exposed to water and atmospheric oxygen. In many cases, this can lead to the formation of acid mine drainage (AMD), and thus, appropriate measures must be taken to mitigate the associated environmental impacts. Covers with capillary barrier effects (CCBEs) can be used to control oxygen migration and, as a result, AMD generation (Aubertin et al.1995; Bussière et al. 2003). This type of cover relies on a phenomenon called the capillary barrier effect, which occurs when a fine-grained material overlies a coarse-grained material due to the contrast between the materials' unsaturated hydrogeological properties. In a CCBE, capillary barrier effects allow for one of the layers, i.e., the moisture-retaining layer (MRL), to be maintained at a high degree of saturation, thereby limiting the diffusion of oxygen from the atmosphere into the reactive mine wastes.

Cover systems used to limit acid generation in tailings storage facilities (TSF) are often comprised of natural materials. However, when the required volume of such materials is significant, concerns can arise related to the availability of suitable materials, as well as land preparation and transportation costs. As a result, the use of mined materials in covers has become an interesting, more sustainable alternative to natural soils. One such alternative is paste rock, which is a homogeneous mixture of waste rocks and mill tailings that are generated by routine mine operations. This mixture is offers significant environmental advantages because it retains both the geotechnical characteristics of waste rock and the hydrogeological characteristics of mill tailings (Wickland 2006; Wilson 2008).

LaRonde mine (Agnico Eagle Mines Ltd) is a polymetallic mine located in the Abitibi region of Québec (Canada). The mine has more than 180 hectares of TSF that contain sulphide-rich, acid-generating tailings. Because of the TSF area and the low availability of suitable natural soils, paste rock is currently being evaluated as a potential cover material for the reclamation the TSF, with or without a limestone amendment and/or compaction.

This study presents an assessment of paste rock (made with mined materials available at LaRonde mine) as a cover system for controlling the generation of AMD. More specifically, the performances of limestone-amended and unamended paste rocks were assessed using laboratory-based column tests. Four columns were mounted and monitored for their hydrogeological and geochemical behavior over a period of eighteen months. Permeability tests, hydrogeological behavior (suction, ψ; volumetric water content, VWC, profiles), and effluent water quality were used to assess the paste rocks' performances.

Materials and Methods

Both the waste rocks and tailings used in this study were sampled at LaRonde mine. The grain-size of the waste rock samples was truncated to 50 mm before being transported to the laboratory. Based on studies by Wickland (2006) and Wilson (2008), the ideal ratio in dry weight to make an efficient paste rock mixture should be between approximately 4:1 and 5:1 (waste rock: tailings). Several tests with ratios ranging from 3.6:1 to 5.1:1 were produced in the laboratory using a small cement mixer. Permeability tests, as described below, were used to select 4.3:1 as the optimal ratio for the LaRonde materials.

Material Characterization

The grain-size distribution (GSD) of the tailings was obtained using a Malvern Mastersizer laser particle size analyzer. Grain-size distributions for the waste rock and paste rock were determined by sieving for the coarse fraction (according to ASTM standard D422; ASTM, 2007), and by the laser particle size analyzer for the fine fraction (< 0.425 mm). The specific gravity (G_S) of each material was determined using an immersion basin for particles over 5 mm and with a helium pycnometer (according to ASTM standard D854-10; ASTM, 2012) for smaller particles.

The saturated hydraulic conductivity (k_{sat}) was determined for the tailings, the paste rock mixture, and waste rocks. For the tailings, the k_{sat} was evaluated using a rigid-wall permeameter (according to ASTM standard D5868-95; ASTM, 2007), then compared to values predicted by a model described by Mbonimpa et al. (2002a). Because of their GSDs, k_{sat} values for the waste rock and paste rock were evaluated through variable-head permeability tests in large high-density polyethylene (HDPE) columns (80 cm in height and 30 cm in diameter; see Peregoedova et al. 2013 for more details) as per standard ASTM D2434-68 (ASTM, 2006). The values were then compared to values from the predictive models proposed by Shepherd (1989) and Chapuis et al. (2004). The tailings' water retention curve (WRC) was determined using a pressure cell (Tempe Cell) following ASTM standard D6836-02 (ASTM,). A larger pressure cell test, which uses the same mechanism as a Tempe Cell and follows a similar protocol to ASTM standard 6836-02 (ASTM,), was developed to determine WRCs for coarse-grained materials that contain fine, silt-like particles, as is the case for paste rock mixtures. The materials used in this study were also tested for their geochemical and mineralogical characteristics. Total sulfur (S) and carbon (C) contents were measured using an induction furnace; these values were used to estimate the acid generation and neutralization potential of the tailings and waste rocks. Concentrations of metal(oid)s (As, Be, Bi, Sb, Se, and Te) were measured using ICP-AES following complete digestion. Semi-quantitative estimates of the tailings' and waste rocks' mineralogical compositions were obtained using X-ray diffraction (XRD). For further details on material characterization methods, see Kalonji et al. (2017).

Column Construction and Instrumentation

Column tests were used to assess the performance of the paste rock cover in controlling AMD generation in the LaRonde tailings. Each column was constructed using black HDPE with an internal diameter of 0.30 m and a height between 0.9 and 1.2 m, depending on the thickness of the cover system. A 0.1 m headspace was left at the top of each column to allow for oxygen consumption (OC) tests and monthly wetting-drying cycles. These OC tests allowed for the in-situ estimation of diffusive oxygen fluxes migrating through the cover to the LaRonde tailings; results related to these tests can be found in Pouliot (2019). At the base of the columns, a ceramic plate was installed that connected to a flexible tube and a bottle; this produced suction by simulating the water table level below the base of the column.

The parametric settings of the four laboratory columns (C1, C2, C3, and C4) are

Table 1 - *Parametric settings for the experimental columns.*

Column	C1	C2	C3	C4
Limestone amendment	No	Yes	Yes	Yes
Compaction	Yes	Yes	Yes	Yes
Drainage layer (0.3 m)	Waste rock (0 - 50 mm)			
Moisture-retaining layer (0.5 m)	Paste rock (4.3:1, waste rock:tailings)			
Capillary break layer (0.4 m)	Waste rock (0 - 50 mm)		No	No

summarized in Table 1. The moisture retaining layer of each cover was comprised of paste rock, with a ratio of 4.3:1 waste rock to tailings used in all columns. Two of the columns (C1 and C2) assessed the paste rock cover in a CCBE configuration with a waste rock capillary break, while the other two columns (C3 and C4) tested a bilayer cover configuration. Because of the high sulfur content of the LaRonde materials, the paste rock used as an MRL in columns C2 and C3 was amended with a fine limestone gravel as a neutralizing agent. The waste rocks used for the top draining layer were identical in all four columns (0 - 50 mm) and were all compacted.

Various instruments were installed throughout the experimental columns, including: GS-3 probes to determine the VWC in each layer, and Watermark probes and tensiometers to measure ψ values. Further details on the use of these instruments in covers are available in Kalonji et al. (2016).

Results

Material Characteristics

Table 2 shows the important characteristics of the LaRonde tailings, paste rock mixture, and waste rocks that relate to their hydrogeological and geochemical behaviors. The materials' G_s values are influenced by their sulphide contents, with the tailings (3.29) showing higher values as compared to the waste rocks (2.73). Based on the grain-size distribution, the tailings are classified, according to the USCS classification system, as a plastic silt (ML) and the waste rocks as a well-graded sand (SW) with variable proportions of fine particles. The tailings' k_{sat} varied between 3.9 × 10-^{8} and 5.7 × 10^{-8} m.s-1, while k_{sat} values for the waste rock varied between 1.6 × 10^{-5} and 7.1 × 10^{-4} m.s^{-1}, and the k_{sat} of the paste rock was 2.8 × 10^{-8} m.s^{-1}. The air entry value (AEV) of the two tested tailings samples were approximately between 20 to 30 kPa (Tempe Cell measurements). The AEV

Table 2 - *Chemical, physical, and hydrogeological properties of materials used in experimental columns.*

Properties	Tailings	Paste rock	Waste rock
%S	19.08		1.065
%C	< 0.05		0.44
D_{10} (mm)	0.00437	0.180	0.11
D_{50} (mm)	0.02526	20	9.11
D_{60} (mm)	0.03475	24	13.50
C_U (D_{60}/ D_{10})	0.00795	0.133	122.73
k_{sat} (m.s^{-1})	3.9 × 10^{-8} to 5.7 × 10^{-8}	2.8 × 10^{-8}	1.6 × 10^{-5} to 7.1 × 10^{-6}
Porosity	0.42 - 0.46		
Gs	3.29		2.73
AEV, ψ_a (kPa)	20-30	n.d.	0.4*

* Kalonji et al. (2017)

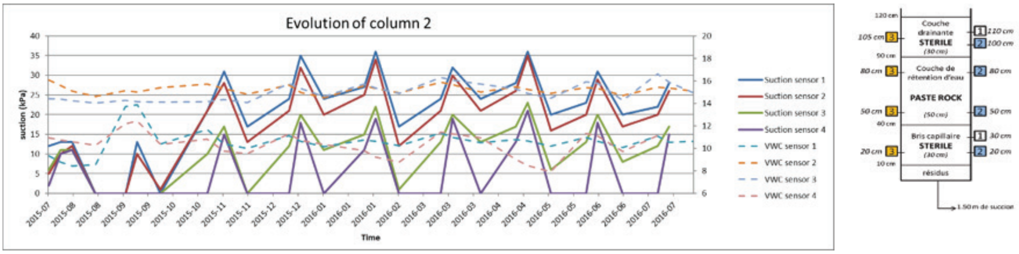

Figure 1 - *Volumetric water content and suction for column 2 (amended CCBE)*

for the waste rock was measured at 0.4 kPa in a prior study (Kalonji et al., 2017).

Using the measured total S and C values, the net neutralization ratio (NP/AP) was calculated at 0.007 for the tailings and 1.1 for the waste rock, demonstrating that both materials are potentially acid-generating (PAG; NP/AP < 2). For this reason, a 6 mm limestone gravel was added to the paste rock mixture in columns C2 and C3 to increase the neutralization potential and make the material non-acid-generating. Semi-quantitative XRD analyses showed that the tailings are mainly composed of silicates such as quartz (42%), albite, and muscovite, but also included 30% pyrite. Analyses of the waste rocks demonstrated that it is rich in quartz (50%), carbonates (4.6%), and sulfides (1.35%).

Hydrogeological Results

Figures 1 and 2 show the evolution of the VWC (θ) and suction for two amended columns, C2 and C3, respectively. Data for the unamended columns, C1 and C4, are not shown because the hydrogeological results were similar to the amended columns. For the CCBE columns (C1 and C2), suction and VWC sensors were placed at 100 cm, 80 cm, 50 cm, and 20 cm from the base of the column. For bilayer columns (C3 and C4), suction and VWC sensors were placed at 70 cm, 50 cm, and 20 cm from the base of the column.

In columns C1 and C2, which had CCBE configurations, higher VWCs were observed in the moisture-retaining layer made of paste rock. Suction values in the moisture retaining layer (MRL) were below the paste rock's AEV; this allowed for the material to maintain saturation (Figure 1). For the bilayer columns without a capillary break, C3 and C4, the VWCs measured near the top of the MRL were lower than those measured near the bottom. Additionally, suction values at the top of the MRL in the bilayer columns were slightly higher than in the CCBE columns, rising close to 40 kPa (Figure 2).

When the results for the amended columns are compared to the unamended columns (not shown here), lower VWC values and higher suction values were observed in the unamended scenario. This can likely be explained by the fact that the addition of the limestone amendment increases the density and decreases the porosity of the paste rock mixture. This improves water retention characteristics and allows for higher VWCs for a given suction.

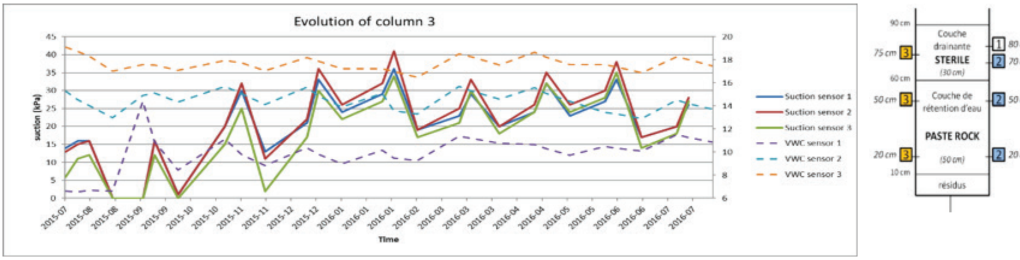

Figure 2 - *Volumetric water content and suction for column 3 (amended bilayer).*

Geochemical Results

The leachate samples from each column following each monthly rinse cycle were analyzed for pH, Eh, electrical conductivity, alkalinity, acidity, total sulfur, and several metals. The objective was to assess the capacity of each cover configuration to limit AMD generation and metal leaching. Some of the results, which were representative of the overall trends observed, are shown in Figure 3.

The unamended columns, C1 and C3, drop in pH and alkalinity over time. Column C1 performed slightly better than C3; this was likely due to its CCBE configuration more efficiently reducing oxygen migration. The amended columns, C2 and C4, maintained pH values above the limits set by the Canadian Mining Metal Effluent Regulation (MMER), however, a downward trend developed at around 400 days. Leachates from all columns showed negligible alkalinity by 500 days. This suggests that, at that point, the limestone amendment in columns C2 and C4 was not able to counterbalance the acidity generated by the tailings materials.

Concentrations of nickel (Ni) and zinc (Zn) were lower in the amended columns up to 400 days. Because of the limestone amendment, there was a downward trend in Ni and Zn for both columns C2 and C4. Concentrations of Ni were below the regulatory limit following the first flush, while concentrations of Zn decreased until 325 days, but did not fall below the regulatory limit. After alkalinity was depleted and the pH began to drop, the concentrations of both Ni and Zn started to increase.

Conclusions

An experiment using laboratory-based columns was performed to evaluate the use of paste rock as a cover material for the prevention of acid mine drainage. Hydrogeological monitoring of the columns demonstrated that the paste rock cover in a CCBE configuration that was amended with limestone was most successful in maintaining adequate volumetric water content and suction levels to limit the migration of oxygen through the cover. However, geochemical monitoring of the leachates showed that the limestone amendment was able to maintain a circumneutral pH for a period of approximately 325 days in the tested column.

To further interpret the results obtained in this study, data obtained from the columns will be compared to a full season of results from a field-scale experimental cell (CR4) with a paste rock cover that was constructed at LaRonde mine; this cover was designed

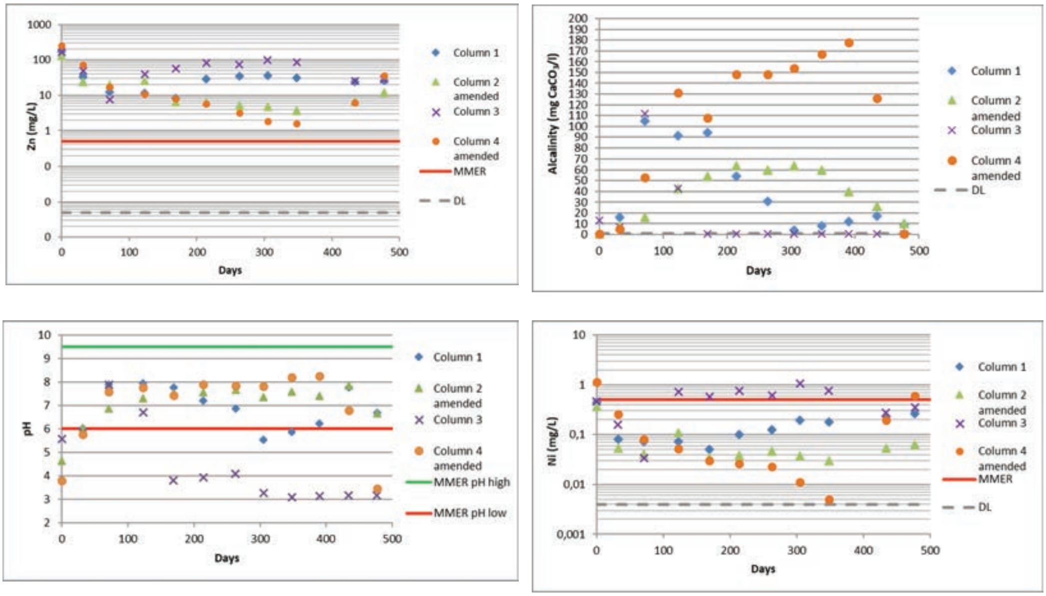

Figure 3 - Results for pH, alkalinity, Ni, and Zn measured from the leachates of the four laboratory columns.

based on previous work by Bussière et al. (2007). The field cell is instrumented with volumetric water content sensors and suction sensors positioned in each of the different layers of material. A pore gas sampler was also installed and connected to oxygen sensors in each of the cell’s layers; this will allow for the measurement of vertical oxygen concentration profiles. A comparison between the covered cell and a control cell will be performed to assess the efficiency of the system. Results will be presented in Pouliot (2019).

Acknowledgements

The authors would like to acknowledge the partners of the UQAT-Polytechnique Research Institute on Mines and the Environment (RIME) for their financial support. The collaboration of the LaRonde – Agnico Eagle team is greatly appreciated. The authors would also like to thank the URSTM staff for their assistance in the laboratory.

References

ASTM 2006, D2434-68 Permeability of granular soils (constant head) ASTM standard D2434. In ASTM Annual CDs of standards, vol. 04.08. ASTM, West Conshohocken, Pa

ASTM 2012, D854-10 Standard Test Methods for Specific Gravity of Soil Solids by Water Pycnometer. In ASTM Annual CDs of standards, American Society for Testing and Materials (ASTM), West Conshohocken, Pa

ASTM 2007, D422 Standard Test Method for Particle-Size Analysis of Soils (D422). ASTM International, West Conshohocken, Pa

ASTM 2007, D5856-07 Standard Test Method for Measurement of Hydraulic Conductivity of Porous Materials Using Rigid-Wall, Compaction-Mold Permeameter. West Conshohocken, Pa 19428-2959

Aubertin M, Chapuis RP, Aachib M, Bussière B, Ricard JF, Tremblay L (1995) Evaluation en laboratoire de barrières sèches construites à partir de résidus miniers. École Polytechnique de Montréal, NEDEM/MEND Projet 2.22.2a

Bussière B (2007) Colloquium 2004: Hydrogeotechnical properties of hard rock tailings from metal mines and emerging geoenvironmental disposal approaches. Canadian Geotechnical Journal, 44(9): 1019–1052

Bussière B, Aubertin M, Chapuis RP (2003) The behaviour of inclined covers used as oxygen barriers: Canadian Geotechnical Journal, 40: 512–535

Kalonji Kabambi A, Bussière B, Demers I (2017) Hydrogeological behaviour of covers with capillary barrier effects made of mining materials. Geotech Geol Eng, 22p. doi: 10.1007/s10706-017-0174-3

Peregoedova A, Aubertin M, Bussière B (2013) Laboratory measurement and prediction of the saturated hydraulic conductivity of mine waste rock. GeoMontreal 2013: Geosciences for Sustainability, 66th CGS Conference, Montreal, QC, 6p.

Wickland BE et al (2006b) Design and evaluation of mixtures of mine waste rock and tailings. Canadian Geotechnical Journal, 43 (9): 928-945. doi: 10.1139/T06-058

Wilson GW et al (2008) Design and performance of paste rock systems for improved mine waste management. Proceedings of the 1st International seminar on management of rock dumps, stockpiles, and heap leach pads, Perth, Australia. 5-6 March 2008

Re-purposing of Acid Generating Fine Coal Waste: An Assessment and Analysis of Opportunities

Helene-Marie Stander[1], Susan T.L. Harrison[1], Jennifer L. Broadhurst[1]

[1]*Minerals to Metals, University of Cape Town, P/B Rondebosch, 7700, Cape Town, South Africa, STN-HEL008@myuct.ac.za*

Abstract

This paper focuses on opportunities for the re-purposing of separated sulfide-rich coal tailings. The approach used in this study was based on the innovation value chain and included identification and preliminary analysis of alternatives, multi-criteria performance assessment of selected alternatives, and a scenario analysis of the two preferred options to achieve a better understanding of the implications of these applications in the South African context. This analysis indicated that whilst cemented paste backfill and soil amelioration were the preferred options, further developmental work would be required to establish efficacy, particularly in the case of the less promising cemented paste backfill option.

Keywords: sulfidic coal tailings, waste re-purposing alternatives, decision-support analysis

Introduction

The coal industry in South Africa is currently both imperative for South Africa's immediate energy security and a contributor to South Africa's significant acid rock drainage (ARD) problems. ARD in coal mining is generated in the mines themselves, and in deposits of coarse discards and ultra-fine tailings produced in coal washing operations. Researchers at the University of Cape Town's Department of Chemical Engineering have developed a two-stage separation process which separates ultra-fine coal tailings into a recovered coal stream, a sulfide-lean stream which is non-acid generating, and a sulfide-enriched stream (fig. 1). The sulfide-enriched stream, which has a relatively low volume and is acid generating, can potentially be re-allocated as feedstock for other uses. In this way, the long-term pollution risks associated with ARD generation from the coal tailings deposits are effectively eliminated, whilst simultaneously increasing recovery of mined resources.

The selection and implementation of the preferred options for the re-purposing or utilisation of wastes, such as the separated sulfide-rich coal tailings fractions, is, however, not a trivial exercise and needs to be based on a comprehensive understanding of the alternatives available and the consequences of these alternatives (Zeleny 1982; Cano-Ruiz and McRae 1998). In this regard, an approach for the identification and analysis of opportunities for the re-purposing of mine wastes has

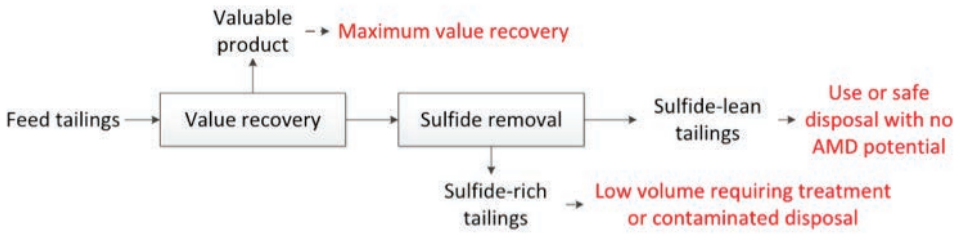

Figure 1 *Two-stage separation process developed by UCT researchers (Hesketh et al. 2010; Kazadi Mbamba et al. 2012).*

Figure 2 The innovation value chain (Dervitsiotis 2010).

been developed, which is based on the innovation value chain (fig. 2). This is an iterative process, with increasing articulation of detail on progressing from the early to later project development stages.

The focus of this paper is on the identification, selection and pre-feasibility assessment of potential re-purposing opportunities for the specific case of sulfide-enriched coal tailings fraction, consistent with the early project stage application of the first three steps of the innovation chain. The methodological approach and key outcomes are summarised in the sections below.

Stage 1: Alternative identification

The innovation value chain (fig. 2) starts with idea generation. The set of identification activities are both creative and systematic (Douglas 1985; Cano-Ruiz and McRae 1998; Sinnott 2005). These solutions are represented using block flow diagrams and mass balances and, if information permits, energy balances to ensure technical rigor (Cano-Ruiz and McRae 1998). In the case of our sulfide-enriched coal waste the application alternatives (box 1) were identified through a combination of literature survey and first principles, based on a preliminary characterisation of the stream. It comprised of residual coal, ash and a significant sulfur component in the form of pyrite (Kazadi Mbamba et al. 2012). A sulfur content of up to 16% has been achieved experimentally (Howlett and Marsden 2013).

Stage 2: Alternative selection

Alternative selection requires a clear indication of what constitutes a superior outcome. A conception of this 'superior outcome' is usually defined using several different, and often conflicting, criteria. Alternative selection therefore normally entails the trade-off between different processes based on relative performance in accordance with multiple project criteria. In this study, analysis and selection of alternative options for the sulfidic coal tailings was carried out in two stages: screening and multiple criteria decision analysis.

Step 1: screening analysis

The first step entailed preliminary screening of the 14 identified alternatives (box 1), to make the process of multiple criteria analysis less onerous. In the case of the sulfide-enriched coal waste, the screening criterion was whether the application alternative would be effective when it was only 20% enriched in pyrite. On this basis seven alternatives were identified for further analysis: sulfuric acid production, ferric sulfate production, ferrous sulfate production, Cr(VI) reduction, soil ameliorant, facilitating heap leaching, and cemented paste backfill production.

Step 2: multiple criteria decision analysis

Multiple criteria decision support tools are commonly used to evaluate the trade-offs between, and facilitate the selection of, alternative process or product options (Cano-Ruiz

***Box 1** Potential application alternatives for the sulfide-enriched stream, where sulfide is mainly in the form of pyrite.*

Sulfuric acid production
Sulfuric acid & paint pigment
Glass pigment production
Ferric sulfate coagulant
Ferrous sulfate heptahydrate
Iron production
Secondary lead refining
Copper smelting
Chrome(VI) reduction
Soil ameliorant
Facilitating heap leaching
Cemented paste backfill
Photovoltaics production
Use in nano- and micro-linear actuators

***Box 2** Steps used in Value Function Decision Analysis (Von Winterfeldt and Edwards 1986).*

1. “Define alternatives and value-relevant attributes”
2. “Evaluate each alternative separately on each attribute”
3. “Assign relative weights to the attributes”
4. “Aggregate the weights of attributes and the single-attribute evaluations of alternatives to obtain an overall evaluation of alternatives”
5. “Perform sensitivity analyses and make recommendations”

and McRae 1998). In this study multiple-criteria analysis of the 7 potentially viable alternatives was conducted using the Value Function Decision Analysis framework (box 2) and tools, as these are relatively easy to understand and can be used effectively by non-experts in the field (Edwards and Barron 1994).

In line with the first stage of the value-based decision analysis framework, several criteria were developed for the technical, social, economic and environmental categories (tab. 3) to make sure that the application alternatives perform well over a range of important considerations, and not just techno-economics.

The alternatives were subsequently scored by design professionals based on the identified criteria (stage 2 of the framework outlined in box 2). To make the scoring process consistent between design professionals, a scoring scale was developed for each criterion. This allowed the design professionals to score an application alternative from 0 to 4 based on descriptions for each score. The semi-quantitative nature of the scoring scale was consistent with the early design stage requirements in terms of uncertainty. The design experts also rated their level of certainty in the score they assigned, to reflect their experience and knowledge of the specific application alternative.

The scores were then aggregated to arrive at a single, comparable number for each application alternative, which would indicate a level of preference. The aggregation process was conducted in two steps. Scores for each criterion were first aggregated across the different design experts, using the levels of certainty to weight their scores. This achieved a single score per criterion per alternative. Then the criterion scores were aggregated using a weighted average. Some criteria are more important than others to decision makers, taking into account the ranges in which they are found and the variability between the alternatives, and should therefore be assigned heavier ‘weights’ when aggregating the scores (Von Winterfeldt and Edwards 1986; Belton and Stewart 2002). Decision makers are required to indicate their preferences by assigning criteria weights. In our case the academics choosing which application alternative to invest research in were the decision makers and weighted the criteria. As outlined by Belton and Stewart (2002), there are several different ways to do this. In this study three different weighting methods were used: Indifference Weighting, Swing Weighting and a modified version of the Analytical Hierarchy Process.

Whilst the different weighting methods did give rise to slightly different aggregated score, in all cases soil amelioration and cement paste backfill were ranked as the pre-

***Table 1** The criteria used to assess the suitability of the application alternatives for sulfide-enriched coal waste.*

Technical	Social	Economic	Environmental
• System complexity • Simplicity of process control • Technical maturity • Conversion efficiency	• Job creation • Operating health & safety • Community health & safety • Skills development potential • Entrepreneurship	• Expected profitability • Availability on the local market • Local deficit • Scale of use	• Waste generation • Mineral recovery • Energy consumption • Water consumption

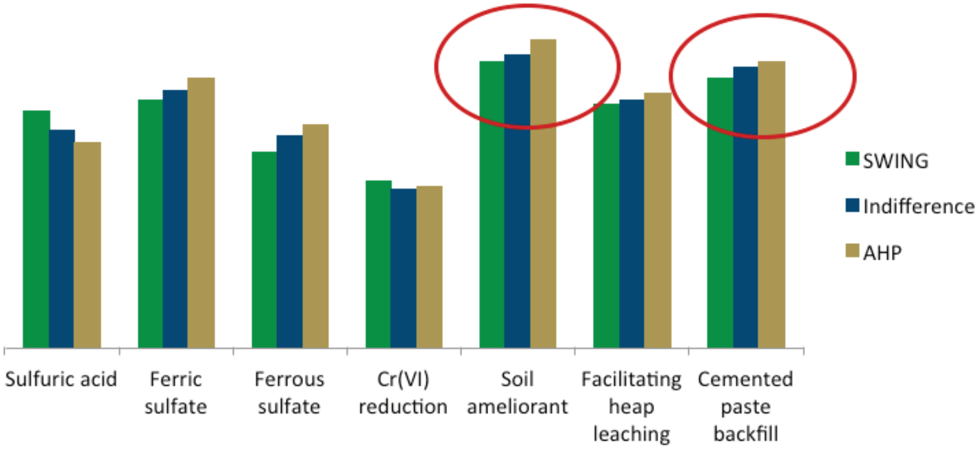

Figure 3 *Relative performance of the alternative options for the repurposing of sulfide-rich coal tailings based on Value Function Decision Analysis using three different weighting methods. (Since the alternatives are ranked relative to each other, a y-axis scale is not necessary. The abbreviation AHP stands for Analytical Hierarchy Process.)*

ferred options for the repurposing of sulfide-rich coal tailings (fig. 3).

Stage 3: Pre-feasibility assessment

For early stage development, a scenario study is done to understand some of the context-specific issues associated with the preferred options that will need to be addressed if a solution is to be developed further and ultimately implemented. This enhances understanding of the implications of implementing an alternative within a specific context, in this case the South African coal industry. In the case of the sulfide-enriched coal waste, soil amelioration and cemented paste backfill were considered. The assessment included an in-depth literature survey on the alternative and the science and technology that enables it. This was followed by an assessment of the economic, environmental, social and technical feasibility of the application in the South African context. Issues such as market location, application efficacy compared to competitor products and pollution potential were considered. As such, information sources such as local agricultural co-ops, government-published regional agricultural production reports, as well as company annual reports were consulted.

Cemented paste backfill, a mixture of tailings, water and binder, is used to fill underground mine workings and in so doing enhance the stability of underground mines (Belem and Benzaazoua 2004; Kesimal et al. 2005). This improves the stability of operating mines, reduces surface waste disposal of tailings and prevents problems like ground subsidence in derelict mines (IIED 2002; Jung and Biswas 2002; Lu and Cai 2012). The preliminary assessment of the cemented paste backfill option showed that sufficient sulfide-enriched material is unlikely to be produced in South Africa for this alternative to be considered viable. The material is also potentially reactive and long-term stability has not been proven. Therefore, it is uncertain whether this approach will be environmentally beneficial over the course of many years.

Soil amelioration is the improvement of the physical and chemical characteristics of soil through the application of an ameliorating substance (Bradshaw 1997; Liebenberg-Weyers 2010). In the case of the sulfide-enriched stream this means application to alkaline soil to reduce the soil's pH (Castelo-Branco et al. 1999). This improves the soil's chemical and physical characteristics by precipitating sodium, reducing the availability of boron ions and increasing the availability of nitrogen, phosphorus, iron and manganese

(Vlek and Lindsay 1978; Somani 1986; Foth and Ellis 1996; Castelo-Branco et al. 1999). Sulfide-enriched coal waste will also improve sulfur availability in soils. Preliminary assessment indicated that this application shows some promise, since it should be effective in improving alkaline soil conditions in arid regions in South Africa and there is enough alkaline farmland to absorb the material stream. The solution may not be profitable, though, since the material will have to travel large distances from coal mines to regions with alkaline soil. For example, the distance between Upington, where table grapes are grown, and the Emalahleni (Witbank) coal fields is around 930km (Google and AfriGIS (Pty) Ltd 2016). The suitability of this solution will also be impacted by the safety of the material for agricultural applications. This will depend on the coal content as well as the trace element content of the material.

Concluding remarks

This study showed that there are several potential applications for sulfidic coal tailings, with cemented paste backfill and soil amelioration being the preferred options. However, a more detailed scenario analysis showed that cemented paste backfill is unlikely to be viable in the South African context, whilst further developmental work would be required to establish economic feasibility of the soil amelioration option.

The approach presented here for the identification, selection and preliminary assessment of options for the downstream application or re-purposing of sulfidic materials can be applied to a diverse range of mine wastes and supports waste management approaches which remove the ARD generating risk and long-term liability associated with land disposal of these materials. Such waste management approaches are also consistent with the principles of sustainable development and the circular economy and have the potential to contribute to local social and economic development, by stimulating additional business opportunities.

It is, furthermore, recognised that technology transfer is an important activity in the development of environmental technologies for the mining industry, since improving the industry's tangible environmental footprint is the objective. Obtaining commitment and buy-in from potential industrial partners is an important part of the innovation chain and should be undertaken in the early-stages of project development.

Acknowledgements

This work is based on research supported by the South African Research Chairs Initiative (SARChI Chair in Minerals Beneficiation) of the National Research Foundation (NRF) of South Africa. Any opinion, finding, conclusions or recommendation expressed in this material is that of the authors and the NRF does not accept any liability in this regard.

References

Belem T, Benzaazoua M (2004) An overview on the use of paste backfill technology as a ground support method in cut-and-fill mines. In: Villaescusa, Potvin (eds) Proceedings of the 5th International Symposium on Ground support in Mining and Underground Construction. Tayler & Francis Group, London, Perth, pp 637 – 650

Belton V, Stewart TJ (2002) Multiple Criteria Decision Analysis. Kluwer Academic Publishers, Boston

Bradshaw A (1997) Restoration of mined lands—using natural processes. Ecol Eng 8:255–269. doi: 10.1016/S0925-8574(97)00022-0

Cano-Ruiz JA, McRae GJ (1998) Environmentally conscious chemical process design. Annu Rev Energy Environ 23:499–536

Castelo-Branco MA, Santos J, Moreira O, et al (1999) Potential use of pyrite as an amendment for calcareous soil. J Geochemical Explor 66:363–367

Dervitsiotis KN (2010) Developing full-spectrum innovation capability for survival and success in the global economy. Total Qual Manag Bus Excell 21:159–170. doi: 10.1080/14783360903549865

Douglas JM (1985) A Hierarchical Decision Procedure for Process Synthesis. 31:353–362

Edwards W, Barron FH (1994) SMARTS and SMARTER: Improved simple methods for multiattribute utility measurement. Organ Behav Hum Decis Process 60:306–325

Foth HD, Ellis BG (1996) Soil Fertility, second. Lewis Publishers, New York

Google, AfriGIS (Pty) Ltd (2016) Locations of South African coal mines that produce coal for beneficiation

Hesketh AH, Broadhurst JL, Harrison STL (2010) Mitigating the generation of acid mine drainage from copper sulfide tailings impoundments in perpetuity: A case study for an integrated management strategy. Miner Eng 23:225–229. doi: 10.1016/j.mineng.2009.09.020

Howlett N, Marsden A (2013) Desulphurisation of coal by two-stage froth flotation. Cape Town

IIED (2002) Mining for the Future Appendix A: Large Volume Waste Working Paper. London

Jung SJ, Biswas K (2002) Review of current high density paste fill and its technology. Miner Resour Eng 11:165–182. doi: 10.1142/S0950609802000926

Kazadi Mbamba C, Harrison STL, Franzidis J, Broadhurst JL (2012) Mitigating acid rock drainage risks while recovering low-sulfur coal from ultrafine colliery wastes using froth flotation. Miner Eng 29:13–21. doi: 10.1016/j.mineng.2012.02.001

Kesimal A, Yilmaz E, Ercikdi B, et al (2005) Effect of properties of tailings and binder on the short- and long-term strength and stability of cemented paste backfill. Mater Lett 59:3703–3709. doi: 10.1016/j.matlet.2005.06.042

Liebenberg-Weyers D (2010) A multidisciplinary approach for the assessment of rehabilitation at asbestos mines in South Africa. North-West University

Lu Z, Cai M (2012) Disposal methods on solid wastes from mines in transition from open-pit to underground mining. Procedia Environ Sci 16:715–721. doi: 10.1016/j.proenv.2012.10.098

Sinnott RK (2005) Chemical Engineering Design, 4th edn. Elsevier Butterworth-Heinemann, New York

Somani LL (1986) Use of pyrites as a soil amendment. Sulphur Agric 10:16–20

Vlek PLG, Lindsay WL (1978) Potential use of finely disintegrated iron pyrite in sodic iron-deficient soils. J Environ Qual 7:111–114

Von Winterfeldt D, Edwards W (1986) Decision Analysis and Behavioral Research. Cambridge University Press, Cambridge

Zeleny M (1982) Multiple Criteria Decision Making. McGraw-Hill Company, New York

Lagniappe

Author Index

Volume 1 pages 1-570

Volume 2 pages 571-1142

Keyword Index

Volume 1 pages 1-570 **Volume 2** pages 571-1142

INAP

IMWA

WISA
MINE WATER
DIVISION

11th International Conference on Acid Rock Drainage
International Mine Water Association
WISA Mine Water Division (MWD)

Pretoria, South Africa
September 10 – 14, 2018

Mine water, and especially acid rock drainage (ARD) or acid and metalliferous drainage (AMD) is considered one of the most serious threats to the environment in a mining context. Yet, researchers, practitioners and regulators as well as mining companies constantly aim to prevent damage to the environment and receiving water. The 11th ICARD | IMWA | WISA MWD 2018 conference in Pretoria, South Africa, brings together nearly 350 experts from around the world. It provides an invaluable opportunity for sharing information on current good practice, emerging technologies, on-going research, and developments in regulation. The conference also helps to highlight advances in our knowledge as well as gaps and challenges.

187 peer reviewed papers, which can all be freely downloaded from the IMWA web site (www.IMWA.info), are collected in this proceedings volume. Seventeen topics, covering an extensive range of mine water related subjects are included – mitigation and geochemistry having attracted the largest interest. This proceedings volume represents the most current developments in the field and cover different experiences from around the world and can be considered the state-of-the-art in mine water management and mitigation.

AngloAmerican

WATER RESEARCH COMMISSION

SMI Sustainable Minerals Institute

Sovereign

Klohn Crippen Berger

aqualytic
laboratory & environmental

GEOSLOPE

GCS
Water & Environmental Consultants

ITASCA
Africa (Pty) Ltd.

srk

Council for Geoscience

3SMEDIA

Tshwane University of Technology
We empower people

South Africa
Inspiring new ways

ISBN 978-0-620-80650-3